Proceedings of the 15th Congress of the International Colour Association 2023

Chiang rai, Thailand
28th November - 2nd December 2023

This publication includes invited, keynote, oral and poster papers presented at the 15th Congress of the International Colour Association 2023. The congress was organized by the Colour Society of Thailand (CST), held in Chiang Rai, Thailand from November 28th - 2nd December, 2023

More information at www.aic2023.org

© 2023 International Colour Association - Multidisciplinary Association in the field of Colour
www.aic-color.org

All rights reserved.

Disclaimer
Matters of copyright for all images and text associated with the papers within the Proceedings of the 15th Congress of the International Colour Association 2023 are the responsibility of the authors. The AIC and the Colour Society of Thailand do not accept responsibility for any liabilities arising from the publication of any of the submissions.

Copyright
Reproduction of this document or parts thereof by any means whatsoever is prohibited without the written permission of the International Colour Association - Multidisciplinary Association in the field of Colour.
All copies of the individual articles remain the intellectual property of the individual authors and/or their affiliated institutions.

ISSN: 2617-2410
eISSN: 2617-2429
ISBN: 978-0-6484724-5-2

How to cite this book
AIC (International Colour Association - Multidisciplinary Association in the field of Colour). 2023. Proceedings of the 15th Congress of the International Colour Association 2023. Chiang Rai, Thailand.

How to cite an article included in this book
Author's name. 2023. Title of the article. In: Proceedings of the 15th Congress of the International Colour Association 2023. Chiang Rai, Thailand, page numbers of the article.

Organized by the Colour Society of Thailand (CST)
Published by the International Colour Association - Multidisciplinary Association in the field of Colour(AIC)

Table of Contents

Committee **7**

Organizing Institutions **10**

Co-Organizing Institutions **11**

AIC Members **12**

AIC 2023 Sponsors **15**

Welcome from the AIC 2023 Organizing Chair **16**

Welcome from the AIC President **17**

JUDD & CADE Award **18**

Schedule **36**

Study Group **56**

Invited Speakers

What Color is Thai? **62**
Piyanan Prasarnrajkit

Colour, Machine learning and Creativity **63**
Stephen Westland

Digital Color Literacy, Media Arts and Design Education **64**
Petronio Bendito

Keynote Speakers

Invariance of Color Constancy Models to Complex Lighting Conditions **66**
Alain Tremeau

On why the nature of color is spatial **75**
Alessandro Rizzi

Cone Fundamentals, Colour Matching Functions and Individual Differences **76**
Andrew Stockman

Can we change the colour education to an attractive and inspiring choice of subject in design and architecture? **77**
Berit Bergström

The Concept of Cesia (Visual Appearance other than color): Antecedents, Development, and Applications **85**
Jose Luis Caivano

Advanced Colorimetry for Imaging Colour Reproduction 93
Ming Ronnier Luo

Managing Museum Collections, Climate and Colour Change 94
Nicole Tse

Physical and Perceptual Worlds of Material Appearance 95
Takahiko Horiuchi

The Choices of Color: Exploring Color Selection from Maslow to AI 102
Tien Rien Lee

The Pink Tax 103
Vien Cheung

Oral Papers

Session 1 - Doi Tung - 28 November 2023

Optimization of Spectral Sensitivity for Multispectral Imaging Based on Adaptive Noise Levels 106
Xu, Peng*; Xu, Haisong

A Low-Cost Portable Spectrophotometer 112
Trentini, Andrea; Bini, Lorenzo; Rizzi, Alessandro*

Spectrofluorimetry – a New Paradigm in the Assessment of Color Appearance 118
Ladson, Jack A*; Lategano, Charles

Display Enhancement for HDR Contents Under Ambient Lighting 127
Huang, Yiming; Xu, Haisong*; Li, Yuemin; Yang, Minhang

Estimating Spectral Transmittance of Translucent Media from An Opacity Value and Known Spectral Reflectance 131
Safdar, Muhammad*; Emmel, Patrick

Modelling Colour Appearance of Images Under HDR Viewing Conditions 137
Shi, Xinye*; Zhu, Yuechen; Luo, Ming Ronnier

The Influence of Background on the Color Difference Evaluation of Multicolored Material 143
Wu, Jiaying; Shamey, Renzo*

Session 2 - Doi Tong - 28 November 2023

Colour Processing of Architectural Finishes in Historic Townscapes Units 150
Diaz-Ramos, Isolina*; Artioli, Gilberto

The Nature of Redness 156
O'Connor, Natalie A*

Aesthetic Characteristics of the Buddhist Cuisine Shojin Ryori Served in Contemporary Japan: From the Perspective of SDGs 164
Yoshimura, Kohji*; Shrader, Stephen; Yamada, Yuko

From Digital Colour to Circular Colour. The Colour of Architectural Surface in the Circular Economy. A Review 170
Gasparini, Katia*

The Effects of Chroma on Designers' Intellectual Abilities in An Immersive Virtual Environment 177
Xia, Guobin*; Henry, Phil; Queiroz, Francisco; Westland, Stephen; Yu, Luwen; Cheng, Qian; Yang, Jie

Colour Palette Generation from Virtual Fashion Images 184
Lai, Peihua*; Pan, Qianqian; Hemingray, Caroline; Westland, Stephen

Production of Functional Inks from Natural Colorant Anthocyanin for Meat Spoilage Indication 190
Siangyai, Rattachai; Katemake, Pichayada ; Hongrattanavichit, Intatch*

Stability of Pigments and Binders to Narrow-Band Wavelength LEDs 191
Dethsuphar, Duantemdoung*; Katemake, Pichayada ; Westland, Stephen

Coral Reefs in Uncertain Seas 199
Ingoldsby, Joseph E.*

Session 3 - Doi Wawee - 28 November 2023

Web Users' Attitude Towards the Size and Position of Sidebar Ads on Websites 206
Meeusah, Natchaphak*; Torsabsinchai, Kamonthip; Tangkijviwat, Uravis

A Study of the User's Eye Movement Behavior on Different Colored Banners of the Commerce Website Using Eye Tracking Technology 212
Torsabsinchai, Kamonthip*; Meeusah, Natchaphak

Hue Polarity Selectivity in a Color Contrast-Contrast Phenomenon 218
Kamegawa, Shohei*; Sato, Hiromi; Motoyoshi, Isamu; Mizokami, Yoko

Effect of Display Technique on Simultaneous Color Contrast 224
Mepean, Janejira*; Phuangsuwan, Chanprapha; Ikeda, Mitsuo

Color Analysis and Consumer Preferences of Sinom and Kunyitasam Drinks, Traditional Drinks from Indonesia 230
Mardhiyyah, Yunita Siti*; Sari, Lisa Risfana; Noviasri, Rizky; Cholilie, Irvan Adhin; Rahmat, Anni; Cahyono, Hadi; Kurniati, Yuni; Nugraheni, Roostikasari

Customer Perspectives and Preferences for the Color in Sorghum Cookies Caused by Different Types of Sugar 236
Laily Rahmadina Azzahra

Colour Design and Conservation of Gummer and Ford Libraries in Auckland, New Zealand: Guidelines and Comparison with Notable Buildings (1923-33) 242
Premier, Alessandro*; Rennie, Julian

The Image of Paris: Development of Colour Harmony on the Banks of the Seine. 248
Noury, Larissa*

Color for Hospitals: Color Design Vs Artworks 253
Schindler, Verena M.*

Towards a Future Holistic Interior Design Considering Color and Lighting Together 254
Rossi, Maurizio*

Color Spatial Layering in Architectural Interiors After Josef Albers' Homages to the Square at RIT 260
Serra, Juan*; Murdoch, Michael

Color, the Soul of Sketching 267
Moreira Da Silva, Ana M S*

Session 4 - Doi Tung - 29 November 2023

Colour Matching Functions Measured in 30 Young Colour-Normal 274
Observers Shi, Keyu*; Luo, Ming Ronnier; Rider, Andy; Stockman, Andrew

Effect of Spatial Distribution of Chromaticity and Luminance on Chromatic Adaptation 280
Li, Siqi*; Ma, Shining; Liu, Yue; Wang, Yongtian; Song, Weitao

Color Constancy and Visual Perception 286
Moreira Da Silva, Fernando J C*

Relationship Between Softness/Hardness Evaluation and Movement Characteristics of Black Fabric Using Fabric'S Rotating Video - Comparison of Engineering and Clothing Students - 292
Kawamata, Takumi*; Ishikawa, Tomoharu; Maehara, Takashi; Yanagida, Yoshiko; Ayama, Miyoshi

Identification of Natural Indigo Dyed Fabrics by Color Image Analysis 298
Kamolrat, Kannikar*; Phongsuphap, Sukanya

Contrast Impression Between Upper and Lower Garments in Terms of Lightness, Influence on Sensibility Evaluation, and Application to Image Analysis 304
Murakami, Shiho*; Ishikawa, Tomoharu; Okuda, Shino; Ayama, Miyoshi

Natural Hair Color Appearance and Classification Analysis 310
Abebe, Mekides Assefa*; Hardeberg, Jon Yngve; Hafslund, Bente; Asghari, Sahara Smith

Performance Analysis of the Ishihara Test Based on Individual Colorimetric Observer Model 317
Sun, Lijia*; Ma, Shining; Liu, Yue; Wang, Yongtian; Song, Weitao

Color Rendering Indexes for Color Blind Observers 323
Huertas, Rafael*; Machado, Pedro; Zapata, Lucia; Valero, Eva M.; Martínez-Domingo, Miguel Ángel; Gómez-Robledo, Luis; Galindo, Jose Luis; Hernandez-Andres, Javier

Colour Discrimination for Visually Impaired People Under Mixed Light LEDs and White LEDs 329
Plerksophon, Ektawat*; Katemake, Pichayada ; Tremeau, Alain; Dinet, Eric

The Effect of Changes in Melanopsin Stimulation of the Surrounding Light on Brightness and Color Perception 335
Shibata, Wakana*; Tokunaga, Rumi; Tsujimura, Sei-Ichi

Session 5 - Doi Tong - 29 November 2023

Is Color Preference Affected by Personality? 342
Cheng, Wen-Hsin*; Ou, Li-Chen

Examination of the Color Image Scale for Contemporary Western Culture: Phase One of a Multiphase Approach 348
Lamarra, Julie K*

The Effects of Colour in Human Fabric Perceptions 354
Han, Xu*; Yu, Luwen; Li, Liting; Xiao, Kaida; Mao, Ningtao; Xia, Guobin

Rosé De Provence Colour Choice in Young Adults 360
Bonnardel, Valerie*; Pouzalgues, Nathalie; Chevallier, Aurélie; Lorey, Thierry; Masson, Gilles

A Study on the Relationship Between Clothing Preference and Color Cognition 366
He, Shuang*; Yue, Longxin; Sun, Pei; Li, Liting

Effects of the Colors of Sanitary Masks on Facial Attractiveness and Impression 375
Sakurai, Masato*; Takeda, Ena

Prerogatives for Teaching Color 380
Souza, Pedro Felipe P*

Teaching Material Design and Education Ractices of Color Education for Children in China 385
Huang, Qian*; Li, Anni

Exploring the Effects of Background Colours of Digital Materials on Learners' Comprehension in Higher Education 392
Gong, Zhe*; Henry, Philip; Queiroz, Francisco; Lee, Soojin; Xia, Guobin

Effects of Classroom Wall Color on University Students' Performance and Attention 399
Baniani, Mahshid*

Pigments Applied in Phra Dhevabhinimmit (Chai Thiamsilpajai)'S Painting Analyzed by Portable Micro X-Ray Fluorescence 404
Kaew-on, Nawarat*; Kaewkong, Thanaporn

Chromatic Bio-Indicators of Biofilm Community Structure on Stone Heritage 412
Sarti, Beatrice*; Villa, Federica; Cappitelli, Francesca; Rizzi, Alessandro

Beauty of Colour in the Light and the Shade of Japanese Traditional Noh Costume 418
Osumi, Masayuki*

Session 6 - Doi Wawee - 29 November 2023

Augmenting Colour Communication in English, Greek and Thai 425
Mylonas, Dimitris*; Koliousis, Alexandros; Stutters, Jonathan; Katemake, Pichayada ; Stockman, Andrew; Eskew, Rhea T.

"Geometry" of Color Harmony in the CIELAB Color Space: Evidence from An Online Experiment Across Countries 431
Griber, Yulia A.*; Samoilova, Tatiana; Al-Rasheed, Abdulrahman S.; Bogushevskaya, Victoria; Cordero Jahr, Elisa; Gouaich, Yacine; Manteith, James; Mefoh, Philip; Odetti, Jimena Vanina; Politi, Gloria; Sivova, Tatiana

Colour Specification for an English-Chinese Colour Names Dictionary 437
Li, Qinyuan*; Hutchings, John; Chang, Kaiping; Ye, Yuxin; Luo, Ming Ronnier

The Origin and Development of Colour Names and Categories, and the Biological Basis for Colour Categories 443
Dedrick, Donald*

Session 7 - Doi Tung - 1 December 2023

Color Afterimage Appearance Measured with Natural Color System **452**
Sun, Vincent*; Peng, Ching-Wei; Fu, Ming Chuan

Developing CCT and Luminance Correction Functions for High Dynamic Range Based on Real-World Scene **458**
Zhu, Yuechen*; Luo, Ming Ronnier

New Vividness and Depth Equation Developed by CAM16 Q, M **464**
Li, Molin*; Luo, Ming Ronnier

Colour, Form and Product - Form Ghosts in Design Education **470**
Bäckström, Eva-Lena*

Colour Design for Facade Integrated Photovoltaics Systems in Campus- a Case Study in Hong Kong **476**
Wang, Wanting; Xu, Kaiyan; Xiang, Changying*

Applying a Colour Value Framework for Colour Design of Lifestyle Products **485**
Dubey, Nijoo*; Damodaraswamy, Sudhakar

A Colour Rendering Chart for Preferred Colour Reproduction **491**
Luo, Ming Ronnier*

TM-30-20 and CIE-CRI Ra: Investigation of Colour Rendering of White Pc LEDs **496**
Bieske, Karin*; Schierz, Christoph

A Set of Optimal Reflectance Curves to Detect and Reduce Inter-Instrument Differences Between Spectrophotometers **502**
Nilsson, Anders*; Seymour, John

The Spectral Reflectance Ratio and Deterioration Simulation of Toyohara Kunichika'S Japanese Woodblock Print **512**
Taguchi, Satoko*; Okuda, Shino; Okajima, Katsunori

Session 8 - Doi Tong - 1 December 2023

Gaudi'S Chromatology in Park Güell As Case Study **517**
Durão, Maria João*

A Colour Story: How Designers Use Colour As a Visual Storytelling Tool in Sneaker Design **518**
Jackson, Kel*; Choi, Youngmi Christina

The Unique Color Worlds of Painters with Color Vision Deficiency **532**
Muraya, Tsukasa*; Taniguchi, Yunoka; Ichihara, Yasuyo G.; Sunaga, Shoji

Achieving Color Richness in Painting – Concepts & Techniques of Conventional & Digital Paintings **538**
Ng, Woon Lam*; Chan, David, Kw; Ngai, Carey

Color Standards in City Planning and Shop Facade Design Changes: Field Survey of Two Urban Landscape Formation Districts in Nagoya City, Japan and Analysis of Corporate Identity Elements **544**
Mukaiguchi, Takeshi*; Harada, Masayuki; Terashima, Toshiharu; Ono, Tomoka

The Impact of Chromatic Palettes in Social Neighborhoods' Environments: Cause and Consequence of Human Interactions **550**
Caramelo Gomes, Cristina *

A Study on the Impression Difference Between Facechart and Actual Makeup Looks **557**
Hsu, Chi-Ying*; Lee, Wen-Yuan

Influence of Lighting Spectra on Facial Appearance in Static Images, Movies, and Real Environment **563**
Iwasaki, Takuma*; Sato, Hiromi; Mizokami, Yoko

Exploring Relationships Between Skin Tone and Personal Colour **569**
Sueeprasan, Suchitra*

Continuous Skin Color Classification of Warm-Netural-Cool **574**
Park, Yungkyung*

Apparatus to Study Total Appearance **578**
Lin, Jinyi*; Luo, Ming Ronnier

Optical Measurements of Sparkle and Graininess **585**
Basic, Nina*; Blattner, Peter; Aebischer, Cyrill

Session 9 - Doi Wawee - 1 December 2023

Auto-White Balance Algorithm of Skin Colour Based on Asymmetric Generative Adversarial Network **587**
Zhou, Sicong*; Li, Hesong; Sun, Wenjun; Zhou, Fanyi; Yang, Yang; Xiao, Kaida

A Study of Image Features and Colour Classification in Tongue Diagnosis in Traditional Chinese Medicine **593**
Qingmei, Huang*; Shen, Zhang; Ziyuan, Wei; Rong, Liang; Lingyan, Wang

To Perform White Balance Using Skin Memory Color **601**
Wang, Liqing*; Luo, Ming Ronnier; Zhu, Yuechen; Liu, Xiaoxuan

Image Statistics and the Perception of Summary Color of Natural Materials 607
Zhang, Yan*; Motoyoshi, Isamu

Reliable Uncertainty Evaluation of Measurements of Color Quantities 611
Ikonen, Erkki*; Rezazadeh, Yasaman; Maham, Kinza

Poster Papers

Relationship Between Color Preference and Personality Trait in Selecting Clothing 618
Nakamura, Shinji*

Differences in the Impressions of Professional Women'S Makeup Looks on Different Genders and Age Levels 624
Hsu, Chi-Ying*; Lee, Wen-Yuan

The Impact of Goalkeeper Uniform Color on Penalty Kick Performance in a Video Game—Using Fifa22 for the Experiment 630
Lu, Yi-Chan*; Lee, Wen-Yuan

Examine the Universal Color Emotion Models and Additive Theory by the Color Emotions Evoked by Two-Color Combinations on 3D Color Configurations 634
Gong, Shi Min *; Lee, Wen-Yuan

Local Color, Constancy and Illusion 638
De Lucas Tron, Alfonso*

Color Characteristics of Korean Purple-Based and Green-Based Natural Dyeing Fabric 643
Shukla, Anshika*; Yang, Junghee; Park, Hyewon

Korean Experts' Empirical Perceptions of the Personal Color System 649
Ham, Dakyeong*; Park, Hyewon

Comparison of Colors in Metaverse and offline Space of Fashion Brands 654
Ahn, Kyuhee*; Choi, Gyoungsil

Recognition of Smartphone Buttons According to Size and Shape 659
Yeo, Jiwon*; Park, Yungkyung

Pigments Applied in "Autumn (1956)" Painting of Fua Haripitak, the First and Most Outstanding Artist of Thai Contemporary, Analyzed by Portable Micro-Xrf 664
Kaew-on, Nawarat*; Kaewkong, Thanaporn

Multiband Imaging with Smartphone Cameras for Spectral Reflectance Estimation **671**
Nishi, Shogo*; Ohtera, Ryo; Tominaga, Shoji

Automatic Color Calibration Without Color Chart **676**
Muselet, Damien*; Cortes Jaramillo, Felipe; Colantoni, Philippe; Tremeau, Alain

Pakistani Truck Art Colors: Inspiring Fashion Designers by Reflecting Local Heritage on the Global Stage **681**
Ume Farwa, Syeda*; Yu, Jinsang; Park, Hyewon

A Reflection on the Korean Colorist and Color Qualification Over the Past Three Decades **687**
Lee, Gyeonghwa*; Cheung, Vien

Text Mining Analysis on Korean Perception of Personal Colors **694**
Kim, Se Jin; Kwon, Minseo*

Color Quality Control of Multicolored Fabrics Containing Color Gradients Based on Spectral Imaging and Unsupervised Segmentation Method **699**
Xiong, Nian; Shamey, Renzo*

Effect of Color Purity of LED Light on Taste Threshold **705**
Takahashi, Hiroshi*; Tsuchida, Kento; Asaga, Sota

Measurement of RGB-LMS Color Space Transformation Function for Dichromat **710**
Zhang, Yuhang*; Shinoda, Hiroyuki

The Influence of Spot Varnishing on the Color Appearance of Print Typefaces in Uv Inkjet Printing **716**
Nilmanee, Somporn*

Investigating the Effect of Lipstick Colour on Skin Colour Perception for Chinese Female **722**
Chen, Yifei*; Xiao, Kaida; Rigout, Muriel.

Color Change of the Ten Symbols of Longevity Cadets in the Late Joseon Dynasty **729**
Lhi, Wona* ; Choi, Gyoungsil

Effect of Color Quantization on Color Harmony **735**
Sharma, Shreeniwas*; Tandukar, Jyoti; Bista, Rabindra

Influence of Color Appearance on Dichromats' Superiority in the Visual Search Task with Color — 741
Palomo, Héctor A*; Muraya, Tsukasa; Sunaga, Shoji

Researching of Costume Featured in the K-Movie, <The King'S Letters(나랏말싸미 naramalsami)> — 747
Hee, Bae Mi*; Park, Hyewon

Effect of Narrow-Band Primary Colors on Observer Metamerism of Anomalous Trichromats — 752
Inoshita, Taiju*; Muraya, Tsukasa; Sunaga, Shoji

Automatic Colour Palettes from Mood Boards — 758
Westland, Stephen; Angharad, Sally*; Lai, Peihua

The Environmental Color Imagery Survey Via Virtual Reality \ — 764
Wei, Robert Y.C.*; Kuo, Monica; Kuo, Ya-Ping

Redness Perception of Dichromats for Short-Wavelength Lights — 771
Asakura, Suzuka S*; Inoshita, Taiju; Muraya, Tsukasa; Sunaga, Shoji

Influence of Lighting Source Direction on Color Perception and Texture Impression of Fabrics — 777
He, Shuilan*

Steady State Pupil Response Elicited by Independent Stimulation of Melanopsin and Cone Photoreceptors — 783
Ito, Tomoe*; Takikawa, Mizuki; Takasu, Aoi; Fujita, Yuno; Tsujimura, Sei-Ichi

Contribution of Melanopsin Photoreceptors to Brightness Perception by Steady Light Stimulation — 789
Fujita, Yuno*; Takasu, Aoi; Ito, Tomoe; Tsujimura, Sei-Ichi

Dynamic and Responsive Color in Fashion Design — 795
He, Shuang*; Lan, Cuiqin; Song, Jiajia

A Study on Additivity of Psychological Stress by Mixed Color Lighting of Three Primary Colors — 801
Oe, Yuki*; Miura, Yukie; Onai, Miku; Yoshizawa, Nozomu

A Comparative Study on Impressions of Clothes Withheld Brand Names in Japan, China, and Thailand — 807
Sakamoto, Takashi*; Sakamoto, Takashi; Hattri, Nanako; Takahashi, Naoki; Kato, Toshikazu

An Investigation into the Variability of Hair Colour Measurements — 811
Wang, Haoyu*; Xiao, Kaida

Effect of Modality on the Efficacy of Light Exposure on Mood **818**
Chen, Mengyuan*; Westland, Stephen

An Image Quality Evaluation Dataset for Atmosphere Quality Modeling **824**
Xu, Nanlin; Zhu, Yuechen; Luo, Ming Ronnier*

Color Preference of Thai Tea Photo **830**
Saksirikosol, Chanida*; Rattanakasamsuk, Kitirochna

Red and Blue – Abstract and Cultural Issues **835**
Asano, Akira*; Asano, Chie Muraki; Ogura, Genki; Chida, Emi

Qualia Change Phenomenon Related to Color Vision Diversity **841**
Hiramatsu, Chihiro*; Yamada, Anna; Ishii, Mochine; Baba, Yasuhito

Worldwide Survey of the Association Between Color and Temperature **847**
Ndeye Meissa Koura Sow, Sow*; Saksirikosol, Chanida; Shamohammadi, Mina; Rattanakasamsuk, Kitirochna; Phuangsuwan, Chanprapha; Hiramatsu, Chihiro

Impact of Colour on Recognition of Cultural Landscape Images **852**
Griber, Yulia A.*; Paramei, Galina

Appearance of Fluorence in Architectural Spaces: Quantification of the Influence of Size Angle and Luminance Gradient **858**
Noguchi, Hidetoshi*; Yoshizawa, Nozomu

Tinted Interior Spaces with the Daylight Reflecting off the Outside Greenery **864**
Kitamura, Kaoruko*; Makino, Kanoko; Oe, Yuki; Yoshizawa, Nozomu

Appearance of Objects Seen Through Coloured Low-E Glasses: Application of An Edge Detection Algorithm for Visibility Judgment **870**
Okamura, Akane*; Yoshizawa, Nozomu; Kitadani, Yukie; Suzuki, Hirotaka

Visualizing Health Status Using Face Color Analysis and Its Application to Smart Mirrors **876**
Moriyama, Tsuyoshi*; Tsunashima, Nobuhiro

The Appearance Characteristics of the Textile Material and Color Tint of the Ainu Costume – the Differences Between the Attus of Sakhalin and Hokkaido **880**
Asano, Chie Muraki*

Color Naming and Constancy of 3D Translucent Objects **886**
Gigilashvili, Davit*; Amirkhanashvili, Ana

Effect of Lip Colours on Colour Appearance and Preference of Facial Skin 893
Okuda, Shino*; Jonai, Riho; Okajima, Katsunori

Individual Colour Preference Change Over Time: A Three-Month Study 897
Lee, Soojin*; Westland, Stephen; Rodski, Stan

Colour Design and Spatial Quality- A Critical Analysis of the Mosaic Colours in Hong Kong Mass Transit Railway Stations 904
Liang, Jiaxin; Chang, Raine Marie; Wang, Wanting; Xiang, Changying*

Effect of Wall Color on Comfort of Indoor Space 914
Azuma, Yoshihiko*

Improving Abandoned Pet Detection in Natural Spaces Through Adaptive Single-Coloured Image Augmentation Techniques 920
Akinwehinmi, Oluwakemi; Pedro, Arnau Del Amo; Francesc, Xavier Solsona Tehas

A Methodological Approach to Colour Construction for Island Fishing Village Community Based on “Social Lifestyle” 927
Mao, Xue*

Emotional Responses to Images of the Same Scene with Different Colours 933
Sueeprasan, Suchitra*

Concentration Dependency on the Identification of Pigment 939
Khampaeng , Sureeporn*; Katemake, Pichayada ; Tse, Nicole

The Question of Color / the Color in Question: Cathedral of Portalegre, Portugal 940
Duarte, Rui B*; Pinheiro, Ana Paula

Petrological Characteristics of Natural Pigments from Rayong, Eastern Thailand 946
Meethum, Jinnawat; Fanka, Alongkot*; Hattagee, S.; Katemake, Pichayada; Ngamukot, Passapol; Noppakundilograt, Supaporn; Assawincharoenkij, Thitiphan

Influence of Illumination Spectrum on Visual Comfort 953
Liu, He*; Shinoda, Hiroyuki

Pigment Analysis in Three Paintings (1966-1967) by Pratuang Emjaroen by Portable Micro-X-Ray Fluorescence 959
Kaew-on, Nawarat*; Kaewkong, Thanaporn

Influence of Illumination Color on Person Tracking Based on Deep Learning and Its Compensation **966**
Doi, Motonori*; Ishikawa, Yoshiki; Nishi, Shogo; Kimachi, Akira

Effect of Color on Gender Identification in Thailand and Japan **971**
Rattanakasamsuk, Kitirochna*; Saksirikosol, Chanida

The Influence of Color on Short-Term Memory **972**
Tangkijviwat, Uravis*; Meenorn, Methawee; Yamprasai, Porntip

Data Analysis of Regional Aesthetic Factors on "Colorscape" in Japan **973**
Yamashita, Ryoma*; Nagaya, Shoma; Hanari, Takashi; Kawasumi, Mikiko

Color Index Development of Nagoya Cochin Eggshell **978**
Nagaya, Shoma*; Yamashita, Ryoma; Akao, Mika; Miyakawa, Hiromitsu; Nakamura, Akihiro; Tsukada, Toshihiko; Kawasumi, Mikiko

Red Background Enhances Dominance Judgement of Geometric Shapes **983**
Yang, Yidie*; Chen, Na; Kobayashi, Maiko; Nakamura, Koyo; Watanabe, Katsumi

A Study on Improving Efficiency of Color Matching Function Measurement Using Selection Techniques **989**
Okuda, Akito*; Yamauchi, Yasuki

Effect of Lighting on Wristwatch for Advertising Photography **995**
Jarernros, Jarunee *; Srisuro, Ploy

The Analysis of Eye-Catching on Thai Movie Posters **1001**
Srisuro, Ploy*

Congenital Red-Green Colour Deficiency: Study of the Efficacy of Commercial Color Filters **1007**
Huertas, Rafael*; Jimenez Molina, María; Martinez-Navarro, Carlos; Lopez-Jabalera, Maria De Los Angeles; Martin-Sevilla, Arturo; Valero, Eva M; Gomez-Robledo, Luis; Martinez-Domingo, Miguel Angel; Hernandez-Andres, Javier

Data Scientific Colour Comparison Among Five Ethnic Townscapes in Singapore **1011**
Kawasumi, Natsuko*; Phuangsuwan, Chanprapha; Kawasumi, Mikiko

Unveiling Emotions and Meaning Through Colour Significant Experiences **1016**
Conte, Veronica*

Optimised Wavelengths for Displaying Coloured Materials with Cinnabar and Red Coral Pigments 1022
Katemake, Pichayada *; Ariyavarapong, Airin; Leewatchararoongjaroen, Kasama; Noppakundilograt, Supaporn; Fanka, Alongkot

Tone Mapping Operator Based on Just Noticeable Difference of Luminance 1023
Kasidet Kanthong*; Jakkarin Singnoo

BAGIS Session

The Comparison of the Light Distribution Characteristics of External Flash Accessories 1030
Puenpa, Suwat*; Rattanakasamsuk, Kitirochna

Visual Perception Experiment and Analysis of Metamorphosis for Object Appearance by Change-Detection Task 1034
Iwase, Kota*; Matsufuji, Momoka; Tanaka, Midori; Horiuchi, Takahiko

Perceptual Collation Method for Colour Halftone Images Based on Visual Saliency 1039
Baba, Taiga*; Tanaka, Midori; Imaizumi, Shoko; Horiuchi, Takahiko

Analysis of Harmony Between Coloured Light and Fragrance by the Reaction of the Left-Right Orbitofrontal Area 1045
Oba, Toshinori*; Tanaka, Midori; Horiuchi, Takahiko

Relationship Between the Observer Metamerism of Color Vision Diversity and the Spectral Bandwidth of Primary Color Spectrum 1051
Nakayama, Rei*; Sato, Hiromi; Mizokami, Yoko

The Linear Scale Between Chromaticness and Lightness Axis on the Polar Diagram 1056
Chitapanya, Phubet*; Phuangsuwan, Chanprapha; Ikeda, Mitsuo

Quantifying the Hue Components of Fa and Blue Using the Elementary Color Naming Method 1061
Phuangsuwan, Chanprapha*; Phuangsuwan, Chanprapha; Tokunaga, Rumi; Mizokami, Yoko; Likitpunyawat, Kusuma

Influence of Skin Color Change on Facial Expression Recognition Among Asian Observers 1066
He, Yuanyuan*; Michishita, Ryo; Sato, Hiromi; Mizokami, Yoko

Author Index 1072

Appendix 1077

Committees

AIC Executive Committee 2022 - 2023

President	Leslie **Harrington,** United States
Past President	Vien **Cheung**, United Kingdom
Vice President	Maurizio **Rossi**, Italy
Secretary/Treasurer	Maria João **Durão**, Portugal
Ordinary Members	Robert **Hirschler**, Hungary
	Valérie **Bonnardel**, France
	Ingrid **Calvo Ivanovic**, Chile
	Pichayada **Katemake**, Thailand
Auditors	Tien-Rein **Lee**, Taiwan
	Javier **Romero Mora**, Spain

AIC 2023 Organizing Committee (Thailand)

Organizing Chair	Pichayada **Katemake**
Technical Chair	Kitirochna **Rattanakasamsuk**
Publication Chair	Boonchai **Waleetorncheepsawat**
Communication Chair/ Secretary	Chanprapha **Phuangsuwan**
Local Organizing Chair	Waiyawut **Wuthiastasarn**
Special Events Chair	Kornkanok **Nindum**
Financial Chair	Uravis **Tangkijviwat**
Fund Raising Chair	Chawan **Koopipat**
Committee	Mitsuo **Ikeda**
	Supawadee **Theerathammakorn**
	Suchitra **Sueeprasan**
	Anan **Tanwilaisiri**
	Somporn **Nilmanee**
	Suwat **Puenpa**
	Natwipa **Sinsuwarn**

Committee	Ploy **Srisuro**
	Chanida **Saksirikosol**
	Jarunee **Jarernros**
	Akaradet **Tongsawang**
	Supannika **Younsue**
	Sakuntala **Saijai**
	Paripan **Keawnet**
	Sermsiri **Nindum**
	Pappim **Chuenjai**

AIC 2023 Technical Committee (Thailand)

Chair	Kitirochna **Rattanakasamsuk**
Committee	Mitsuo **Ikeda**
	Pichayada **Katemake**
	Supawadee **Theerathammakorn**
	Natwipa **Sinsuwarn**
	Chanprapha **Phuangusuwan**
	Uravis **Tangkijviwat**
	Boonchai **Waleetorncheepsawat**
	Waiyawut **Wuthiastasarn**
	Suchitra **Sueeprasan**
	Chanida **Saksirikosol**

AIC 2023 Publication Committee (Thailand)

Proceedings Editor	Kitirochna **Rattanakasamsuk**
Editorial Team	Boonchai **Waleetorncheepsawat**
	Supawadee **Theerathammakorn**
	Duantemdoung **Dethsuphar**
Graphic Design	Duantemdoung **Dethsuphar**
AIC 2023 Website Maintenance	Pappim **Chuenjai**
	Sureeporn **Khampaeng**

AIC 2023 Scientific Review Committee

Akira **Asano**, Japan
Alain **Tremeau**, France
Alessandro **Rizzi**, Italy
Andrew **Stockman**, United Kingdom
Berit G. **Bergstrom**, Sweden
Boonchai **Waleetorncheepsawat**, Thailand
Brian **Funt**, Canada
Chanida **Saksirikosol**, Thailand
Chanprapha **Phuangsuwan**, Thailand
Chihiro **Hiramatsu**, Japan
Damien **Muselet**, France
Dimitris **Mylonas**, United Kingdom
Eric **Dinet**, France
Haisong **Xu**, China
Hideki **Sakai**, Japan
Hirohisa **Yaguchi**, Japan
Javier **Hernandez-Andres,** Spain
Jean Baptiste **Thomas**, France
Jon Yngve **Hardeberg**, Norway
Jose Luis **Caivano**, Argentina
Juan Luis **Nieves**, Spain
Katsunori **Okajima**, Japan
Kine **Angelo**, Norway
Kitirochna **Rattanakasamsuk**, Thailand
Manuel **Melgosa**, Spain
Maria João **Durão**, Portugal
Maurizio **Rossi**, Italy
Mikiko **Kawasumi**, Japan
Ming Ronnier **Luo**, China
Miyoshi **Ayama**, Japan
Natwipa **Sinsuwarn**, Thailand
Nawarat **Kaew-on**, Thailand
Nicholas **Harkness**, Australia
Pichayada **Katemake**, Thailand
Rafael **Huertas**, Spain
Raju **Shrestha**, Norway
Robert **Hirschler**, Hungary
Robert Y.C. **Wei**, Taiwan
Robin **Kingsburg**h, Canada
Rumi **Tokunaga**, Japan
Sakuntala **Saijai**, Thailand
Seyed Ali **Amirshahi**, Norway
Shinji **Nakamura**, Japan
Shino **Okuda**, Japan
Shoji **Tominaga**, Norway
Somporn **Nilmanee**, Thailand
Supawadee **Theerathammakorn**, Thailand
Taiichiro **Ishida**, Japan
Takahiko **Horiuchi**, Japan
Tetsuya **Sato**, Japan
Ulrich **Bachmann**, Switzerland
Uravis **Tangkijviwat**, Thailand
Valerie **Bonnardel**, France
Verena M. **Schindler**, Switzerland
Vien **Cheung**, United Kingdom
Vincent **Sun**, Taiwan
Waiyawut **Wuthiastasarn**, Thailand
Wen-Yuan **Lee**, Taiwan
Yoko **Mizokami**, Japan
Yulia A. **Griber**, Russia

Organizing Institutions

The International Colour Association (AIC), also known as Association Internationale de la Couleur or Internationale Vereinigung für die Farbe, is an academic society with a mission to promote research in all aspects of color. They strive to share the knowledge gained from this research and apply it to solve problems in the fields of science, art, design, and industry on a global scale. Additionally, AIC collaborates closely with established international organizations like the International Commission on Illumination (CIE), the International Organization for Standardization (ISO), and the International Commission for Optics (ICO) on color-related issues.

Website: www.aic-color.org

Color Society of Thailand is a group of academics, researchers, and people interested in the fields of color such as color science, technology, social sciences, art, architecture, and applications. In addition, the Color Society of Thailand is also an ordinary member of the International Color Organization. (International Color Association) on behalf of Thailand. From the day when the Thai color group was founded, the members have started various activities. We hope that it will create a learning community, continue to be a platform that inspires and supports academic development and research in the field of color as well as be a channel for exchanging knowledge with various sciences related. We set resolutions to be a small cog that drives various sectors of the country to have advancement to those of other civilized countries

Website: www.colorsocietythailand.com

Co-Organizing Institutions

AIC Members

GRUPO ARGENTINO DEL COLOR, Argentina
grupoargentinodelcolor.blogspot.com.ar

COLOUR SOCIETY OF AUSTRALIA, Australia
www.coloursociety.org.au

INTERDISCIPLINARY COLOUR ASSOCIATION - BELGIUM, Belgium
www.ica-belgium.org

ASSOCIAÇÃO PRÓ-COR DO BRASIL, Brazil
www.procor.org.br

COLOUR GROUP – BULGARIA, Bulgaria
www.bgcolorgroup.org

COLOUR RESEARCH SOCIETY OF CANADA, Canada
www.colourresearch.org

ASOCIACIÓN CHILENA DEL COLOR, Chile
www.asociaciondelcolor.cl

COLOR ASSOCIATION OF CHINA, China
chsxu@zju.edu.cn

HRVATSKA UDRUGA ZA BOJE, Croatia
www.hubo.hr

SUOMEN VÄRIYHDISTYS SVY RY, Finland
www.svy.fi
CENTRE FRANÇAIS DE LA COULEUR, France
www.centrefrancaisdelacouleur.fr

DEUTSCHER VERBAND FARBE, Germany
www.dfwg.de www.deutsches-farbenzentrum.de

THE COLOUR GROUP (GREAT BRITAIN), Great Britain
www.colour.org.uk

HUNGARIAN NATIONAL COLOUR COMMITTEE, Hungary
aic.kee.hu

GRUPPO DEL COLORE - ASSOCIAZIONE ITALIANA COLORE, Italy
www.gruppodelcolore.org

COLOR SCIENCE ASSOCIATION OF JAPAN, Japan
www.color-science.jp

KOREAN SOCIETY OF COLOR STUDIES, Korea
www.color.or.kr

ASOCIACIÓN MEXICANA DE INVESTIGADORES DEL COLOR, Mexico
www.amexinc.mx

STICHTING KLEURENVISIE: Het Nederlands Platform voor Kleur, The Netherlands
www.kleurenvisie.nl

FORUM FARGE Norway
www.forumfarge.no

ASSOCIAÇÃO PORTUGUESA DA COR, Portugal
www.apcor.org

SLOVENSKO ZDRUZENJE ZA BARVE, Slovenia
www.szb.si

COMITÉ ESPAÑOL DEL COLOR, Spain
www.sedoptica.es/SEDO/color

STIFTELSEN SVENSKT FÄRGCENTRUM, Sweden
www.colourspot.org

PRO COLORE, Switzerland
www.procolore.ch

COLOR ASSOCIATION OF TAIWAN, Taiwan
www.color.org.tw

COLOR SOCIETY OF THAILAND, Thailand
colorsocietythailand.com

INTER-SOCIETY COLOR COUNCIL, United States
www.iscc.org

AIC Associate Members

INTERNATIONAL ASSOCIATION OF COLOR CONSULTANTS/DESIGNERS, North America
www.iaccna.org

COLOR MARKETING GROUP, United States
colormarketing.org

AIC Individual Members

Lia Margarita **Tapis** - Colombia
Martina **Vikova** - The Czech Republic
Jaqueline **Carron** - France
Yannis **Skarpelos** - Greece
Yulia **Griber** - Russia
Andrea **Urland** - Slovakia
Kazim **Hilmi Or** - Turkey

AIC 2023 Sponsors

IMAGING & PRINTING
CHULALONGKORN
UNIVERSITY

TCEB
THAILAND CONVENTION
& EXHIBITION BUREAU

Chula
The Second Century Fund (C2F)

BAGIS

NCS®

CENTASIA

Welcome from the AIC 2023 Organizing Chair

Welcome, all esteemed participants and distinguished guests to the AIC2023, the 15th Congress of the International Colour Association. We are thrilled to host this remarkable event in the enchanting city of Chiang Rai, Thailand.

In these extraordinary times, we find ourselves on the threshold of a new beginning. The shadows of the global pandemic have receded, granting us the privilege of reuniting as color artists and scientists in the flesh, following two years of virtual AIC conferences. We stand here today with hope, resilience, and a belief in the incredible advancements of medical technology and the dedicated pursuit of sanitation management.

At the closing ceremony of AIC2022, 'Sensing Colour,' we unveiled our intentions to bring the AIC community to Chiang Rai, not fully certain of the state of the world. Yet, here we are, fueled by the optimism of a brighter future. Our commitment to fostering invaluable connections through workshops, welcoming ceremonies, engaging oral and poster presentations, inspiring excursions, and convivial banquets remains unwavering. The opportunities that lie before us are beyond measure.

The AIC Congress is more than just a professional congregation; it is a family reunion of individuals who speak the same universal language—the language of color. We share a profound and mutual fascination with the world of color, and this shared passion makes our AIC gatherings truly unique.

The meticulous planning of AIC2023 was set in motion in December 2019, just before the onset of the COVID-19 pandemic. It was originally intended to be the AIC Midterm meeting, allowing us to better manage the event given our resources within the Colour Society of Thailand. Now, it stands as a formidable challenge for our organizing team, one that we embrace with steady dedication and enthusiasm.

In closing, I extend my heartfelt gratitude to all our esteemed participants, invited speakers, and keynote speakers who have contributed to this symphony of knowledge exchange, through their engaging oral and poster presentations. Your dedication to the arts and science of color is the very essence of the AIC, and we are profoundly grateful for your presence.

Welcome, once again, to AIC2023. Let us come together, explore the infinite spectrum of color, and paint a brighter future for the world of colour art and science.

Pichayada Katemake
AIC 2023 Organizing Chair

Welcome from the AIC President

Welcome to AIC 2023! It is time, once again, to meet for our annual meeting. This meeting is particularly special as it marks the first in- person meeting since 2019 when Covid forced us to move to a virtual format. I am sure many of us are excited to be able to meet face-to- face again as there is nothing quite like it.

I would like to express my sincere gratitude to the Colour Society of Thailand (CST) organizing committees for their hard work hosting the AIC 2015th Congress in Chiang Rai, Thailand. It was 20 years ago that CST hosted the 2003 Mid-term meeting, I know we are all excited to revisit this beautiful country. A special thanks to the congress sponsors; the Department of Imaging and Printing Technology, NCS, TCEB, the BAGIS program, Chulalongkorn university: the second century fund (C2F), and Centasia. We know that the support of our industry partner helps to elevate the conference experience.

Some of the conference highlights include:

• The awarding of the Judd Award sponsored by RIT to Prof. Rolf Kuehni who has spent most of his life dedicated to color science and the CADE award to Clino Trini Castelli for his contribution to environmental and industrial design.

• There is great excitement around the two special workshops, Calm and Focus: NeuroArt as a Gateway for Understanding the Mind by Petronio Bendito and Tim Korb and Water Color Painting by Suphawat Hiranthanawiwat.

• The excursion to visit four meaningful locations in the Chiang Rai area: Way Phra Knew, What Song Suea ten, Was Hauy Play Kang, and Was Wrong Khun, and for many of us is a trip of a lifetime.

In 2023, we had to deal with some important and critical issues that impacted the organization's future. This year, we were able to complete the relocation of AIC to Austria. This process has been complicated as it impacts most of the organizations operational's touch points. To everyone involved, thank you for your support and dedication, it was not an easy journey.

2023 will also mark the end of my term as AIC president. I would like to thank the 2022-23 EC for their tireless dedication to a very busy two years. It always amazes me how many twists and turns there are in a journey and how quickly time passes. 2024 will usher in a new EC Committee that will be elected at this 2023 Congress, and I am confident now that we have settled into our new environment they will lead AIC into a growth phase.

Finally, I would be remiss if I did not recognize those who have submitted papers, the Review Committee, the session chairs, and the AIC Study Group chairs for hosting the workshops. Most of all thank you to all that attended AIC 2023.

Cheers,
Leslie Harrington
AIC President | 2022/23

JUDD & CADE Award

JUDD Award

AIC JUDD AWARD CITATON FOR PROFESSOR ROLF GEORG KUEHNI

Renzo Shamey[1*], Paula J. Alessi[1] and Roy S. Berns[1]

[1]*The Inter Society Color Council (ISCC).*

*Corresponding author: rshamey@ncsu.edu

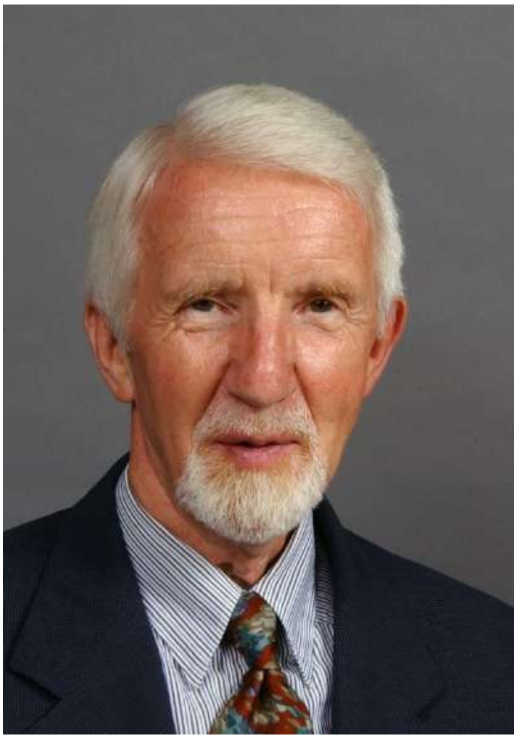

BIOGRAPHY

Rolf Georg Kuehni is a member of an old family of citizens in Switzerland. He received his basic education in the town of Schoenenwerd, where his father worked as a shoe designer in the Bally Shoe factory. He then moved to Krefeld in Germany for his education and obtained a degree in textile chemistry from Fachhochschule Niederrhein in 1961.

Dr. Paul Ulrich, a research chemist at CIBA in Basel, Switzerland, became Kuehni's supervisor after college in 1962. Ulrich had a deep and broad interest in color and at the time was working on color literature and he encouraged Mr. Kuehni to read some early psychological papers which he later said did not mean much to him at the time. Kuehni was more interested in strength determination of dyes by transmittance and reflectance to make his job easier and more productive. He quickly learned their limitations at a time when instrumentation was still in rapid development. He moved to the United States in 1963 where he eventually became a dual citizen. Being specifically involved in the subject of color matching of textiles he became interested in color technology. In 1965 he joined Verona Dyestuffs, owned by Bayer Corporation, as a Manager of Development and Color Physics. Part of his job responsibility was to try to make use of a Color Eye®. Sometime later he talked the management into acquiring an IBM 1130 computer and thereby began his involvement in computer formulation. Color quality control, and color difference, became other subjects of interest. A color course at Davidson and

Hemmendinger and meeting Ralph Stanziola were important elements in steering him deeper into color technology.

In 1967 Kuehni became a member of the Inter-Society Color Council (ISCC). Over the course of his employment, he advanced to Vice President Marketing/Textile Products for Bayer Corp. in the USA and also was Vice President in the successor company Dystar Corp. from which he retired in 2001.

During these years he maintained a solid interest in color science, being active in the Inter-Society Color Council and in research committees of the American Association of Textile Chemists and Colorists (AATCC). From 2002 to 2018 Professor Kuehni served as an Adjunct Professor of color science at North Carolina State University in Raleigh, NC.

CONTRIBUTIONS TO THE FIELD OF COLOR SCIENCE AND TECHNOLOGY

Rolf Kuehni has spent most of his life dedicated to color science. His major research contributions include color tolerances, indices of metamerism, theoretical bases of metamerism, and modeling hue perception. From 1987-89 he was the editor of the journal 'Color Research and Application' (CR&A). He translated seminal articles by German scholars including J. H. Lambert, A. Koenig, W. Ostwald, R. Luther, E. Schrödinger, and P. Runge into English, published in CR&A. He has written or co-authored nine books on diverse subjects such as computer colorant formulation, introductory color science and technology, and color order systems. During his industrial career at Bayer, he authored approximately 80 peer-reviewed scientific and technical articles as well as encyclopedia articles about color.

Professor Kuehni has mentored numerous color scientists, including Professors Roy S. Berns and Renzo Shamey. At North Carolina State University alongside Professors Shamey and Hinks, he mentored students, delivered lectures on the science of color and visual perception, and oversaw several student projects. Additionally, he co-authored several articles on unique hues and other color topics.

Professor Kuehni has actively participated in the International Commission on Illumination (CIE) as a member or advisor on technical committees, such as TC 1-55 *Uniform Colour Space for Industrial Colour Difference Evaluation*, TC 1-56 *Improved Colour Matching Functions*, and TC 1-76 *Unique Hue Data*. His expertise in the history of various developments has proved invaluable and assisted members of technical committees in successfully completing their tasks. Kuehni's pointed and precise questions, along with his constructive feedback, have often provided members with a fresh perspective on the problem at hand.

In 1986 he received the Armin J. Bruning award from the Federation of Societies for Coatings Technology in recognition of his significant contributions to the development of the science of colorimetry in the paint and coatings industries.

Professor Kuehni was also heavily involved in the AATCC, and chaired the RA36, Color Measurement Test Methods Committee. He regularly provided detailed information and precise answers to questions and comments related to color and associated test methods. He received the association's most prestigious scientific award, the Olney Medal, in 2005, in recognition of his significant contributions.

The Inter-Society Color Council has recognized his many achievements. He received the Godlove Award, the ISCC's most prestigious award honoring long-term contributions in the field of color in 2003, the Nickerson service award in 2015, and the Munsell Centennial Award for Science in 2018.

The breadth of his expertise and scholarship goes beyond the list of Kuehni's accomplishments as evidenced by his book publications. We will highlight several of these.

Professor Kuehni's second book was *Computer Colorant Formulation*, written in 1975. This was the first book that explained what is "under the hood" of formulation systems used in coloring industries and paint stores to produce custom colors. Kuehni believed that a better understanding of the underlying science and engineering would enable colorists to be more successful in formulating recipes that matched a standard. He introduced the term “colorant formulation” rather than “color matching” that remains in use today.

Color: An Introduction to Practices and Principles is in its third edition. Its table of contents indicates Kuehni’s breadth as a color scientist, technologist, and historian:

1. Sources of Color
2. What Is Color and How Did We Come to Experience It?
3. From Light to Color
4. Color Perception Phenomena
5. Orderly Arrangements of Color
6. Defining the Color Stimulus
7. Calculating Color
8. Colorants and Their Mixture
9. Color Reproduction
10. The Web of Color 187
11. Color (Theory) in Art
12. Harmony of Colors

Appendix: Timetable of Color in Science and Art

Chapters 1 – 9 are typical color technology topics. Chapters 10 – 12 are not. These seem to be subjects addressed in color design and color and art books. Only a single author can combine these topics into a cohesive and compelling story.

Color Ordered: A Survey of Color Systems from Antiquity to the Present, cowritten with Andreas Schwarz, is, arguably, the definitive book about color order systems. Its excellence is revealed by Chapters 2 – 4:

2. Linear Systems
3. Color Diagrams and Color Circles
4. From Two to Three Dimensions

For centuries, color ordering was based on a single scale or described in two dimensions on a single page. However, it is now widely recognized that color ordering requires at least three dimensions. Explaining the evolution and understanding of color from one to three dimensions is a remarkable achievement.

Professor Kuehni can also be described as an expert in the history of color science and its developments. In *Pioneers of Color Science*, co-authored with Renzo Shamey and published in 2020, the achievements, and significant contributions of some 100 historic figures in the field of color science are discussed. He was also the section editor for Vison Phenomena, and Vision Physiology as well as authoring multiple entries in the *Encyclopedia of Color Science and Technology*, Shamey R. (Ed.), Springer International (2023).

Professor Kuehni has also served as an editor, editorial board member, and reviewer of several scientific journals, providing prompt and precise feedback to colleagues and guidance to the younger generation of color scientists and enthusiasts.

ISCC NICKERSON SERVICE AWARD

The 2015 ISCC Nickerson Service award was presented to Professor Rolf Kuehni on Oct 21, 2015, at the North Carolina State University College of Textiles Color Science Laboratory. The Nickerson Service Award is presented for outstanding, long-term contributions towards the advancement of the Council and its aims and purposes. The contribution may be in the form of organizational, clerical, technical or other services that benefit the Council and its members. Professor Kuehni was nominated to receive the 2015 Nickerson Service Award on the basis of his substantial contributions to color education that have been posted to the ISCC website. Under Historic Translations on that website, he contributed many translations of color articles and books from German and French to English, biographical information on the authors, and often technical introductions as well. (These authors include J. H. Lambert, A. Koenig, W. Ostwald, R. Luther, E. Schrödinger, and P. Runge, as well as an anonymous French author.) In addition, Kuehni edited the ISCC-posted manuscript by I. H. Godlove entitled "The Earliest People and their Colors". Rolf Kuehni has touched virtually every part of the ISCC electronic presence, including a column on A. H. Munsell that he wrote for Hue Angles several years ago.

The presentation was made by Professor Renzo Shamey and Ms. Ann Laidlaw (ISCC representatives). Professor Kuehni provided an overview of the important contributions of Dorothy Nickerson, for whom the award is named. Professor Kuehni also provided a lecture for students on "How many colors are distinguishable?"

Figure 1. Professor Kuehni receiving the 2015 ISCC Nickerson Service Award, with Professor Shamey, and Ms. Laidlaw.

MUNSELL CENTENNIAL AWARD FOR SCIENCE

The recipient of the 2018 ISCC Munsell Centennial Award for Science was Rolf G. Kuehni. Here are some excerpts from the citation given by Paula J. Alessi:

> After more than 30 years working in color for Bayer and BASF in the United States, Rolf retired and became more active than ever in the science of color. As a matter of fact, during his retirement he feels that "involving himself in color saves his sanity". One of the passions that Rolf Kuehni pursued in retirement is understanding why color space metrics like CIELAB did not always agree with visual experience. Kuehni has studied color, color differences, uniform color spaces, unique hues and color order systems both from a current technological standpoint and from a historical perspective. Throughout his career, Kuehni

has been a proponent of closer ties between industrial scientists studying and applying color technology and academic scientists studying color vision and developing the foundational principles of color science. Kuehni also has a strong belief in color education as evidenced by his commitment to being an adjunct Professor at North Carolina State University in Raleigh.

In his 2008 Hue Angles article, ‘150th Anniversary of Albert Henry Munsell’s Year of Birth’ Rolf stated: ‘In 1918, the year of Munsell’s death, the Munsell Color Company was founded, and the rest is history. Munsell’s landscapes and portraits are curiosities today; his color order system is a lasting contribution to our understanding of the world of color’.

Figure 2, Rolf G. Kuehni early career years.

ISCC GODLOVE AWARD

Rolf G. Kuehni was presented with the prestigious Godlove Award during the ISCC Annual Meeting in Chicago, IL in 2003 This coveted ISCC Award was presented to Kuehni for his career-long commitment to color science. For more than two decades Kuehni has been a strong proponent of closer ties between the industrial scientists studying and applying color technology and the academic scientists studying color vision and developing the bases of color science. Below are excerpts from Professor Kuehni’s acceptance speech.

> The Godlove award is clearly prestigious because among its winners are some of the most important names in color science. When looking recently at the work of Dr. Godlove, I found we have a number of common interests.
>
> …I remember fondly Max Saltzman teaching me the ropes of this [ISCC] organization. Among many other things I also remember the sharp red pen of Deane Judd correcting our draft for a test procedure on dye strength determination.
>
> As I advanced in managerial rank, the practical side of color more and more retreated to the background. My 3-year stint as the editor of *Color Research and Application* in the later 1980's was an effort to remain involved and knowledgeable. A general interest in color grew in the areas of culture and art, as well as its history, philosophy, and its role in consciousness.
>
> During my last few months of employment at DyStar and my stint as consultant, I had relatively little meaningful work to do and involving myself in color saved my sanity. I decided to delve again into the mysteries of color space and its divisions, an effort resulting in a series of papers and now a just published book (*Color Space and its Divisions*, Wiley, 2003). As an Adjunct Professor at NCSU, I can share some of my experience with students and help establish color science as a solid part of the curriculum.
>
> In the last couple of years, I have come to believe that we know in reality considerably less about color perception than is generally assumed. I have recently come

across some experimental facts that are very puzzling and make me wonder how much we really know about the variability of trichromatic color perception. The first has to do with standard observers. Using an idea of mine from 1979 a student calculated what we call the transition wavelengths of gray metamers where one is maximal in terms of the square root difference from the other. These three wavelengths are independent of linear transformation of the underlying observer data and are convenient identifiers for observers. The point is that in published observer data we seem to have two distinct groups of observers. It seems important for CIE Committee TCI-56 to arrange for additional experimental data to determine the effect of methodology on the results and separately the variability of observers.

I also looked at ten sets of published unique hue data. These have been established under several different experimental paradigms, from sub-second exposure to lights with black surround to indefinite exposure to arrays of color chips. There is, in my view, no pattern in regard to experimental paradigm detectable in the results. What struck me most, however, are the surprisingly large ranges of individual unique hues. Three of these in fact overlap. That is, unique blue for one observer can be unique green for another and unique green for one can be unique yellow for another. Most of the papers from which the data have been taken have been published in Vision Research and JOSA and I am not about to doubt their veracity. The findings raise serious questions about the meaning of unique hues as well as the usefulness of color appearance and color difference formulas. Finally, studying past large-scale efforts of determining constant chroma and constant hue differences in global color space I found that the three largest efforts have produced considerably different results. All three involved more than 10,000 observations. I would not want to claim that one of these results is more accurate. We do not know what causes these differences. It is evident that we do not have reliable, replicated global scaling of color space. The same applies to small color differences.

I think this is good news for the younger people. There is a lot that we do not know about color perception and color science still offers many and large challenges to those wanting to take them on.

CADE Award

THE *"COLOR FEVER"* CHROMA SURVEY 1973

Clino Trini Castelli[1]*
*Castelli Design; memo@castellidesign.it

BIOGRAPHY

Clino Trini Castelli (Civitavecchia, 1944) industrial designer, artist and design theorist lives and works in Milan. Internationally known for *CMF design* (Color, Material and Finishes) of which he was the initiator, Castelli introduced the "No-form" renewal of plastic languages applied to industrial products through the tools of *Design Primario*.

As opposed to traditional compositional methods, Castelli has focused on the design of the more intangible aspects of figuration, like material and color, light and sound, emphasizing the virtues of a sensorial approach to art and design. Since the early 1970s this has made him a pioneer in research on the emotional identity of products in the industrial sector.

From 1978 to 1983 he conceived and directed *ColorTerminal IVI* in Milan, the first center of research and services on the new RGB additive technologies. In 1983, alongside his activities of research and design, he was one of the founders of Domus Academy.

Clino Castelli has continued his work in education, teaching in many international design schools and universities, including the Milan Polytechnic. He has published several writings and book on design culture, including articles for leading international magazines of art and design. His work has received important European, American and Japanese prizes, including two ADI Compasso d'Oro awards.

(Read the entire paper The "Color Fever" Chroma Survey 1973 *in the appendix)*

Schedule

Date	November 27, 2023	November 28, 2023		
	Monday	Tuesday		
		Day 1		
Room		Doi Tung	Doi Tong	Doi Wawee
Morning (8:30-12:00)		Opening Ceremony and Group Photo (9:00-10:15)		
		Invited Lecture: What Color Is Thai? Prasarnrajkit, Piyanan (10:30-11:45)		
Afternoon (13:00-17:30)	Registration open **Workshop 1:** Cultivating Calm and Focus by Petronio Bendito **Workshop 2:** Water Color Painting by Suphawat Hiranthanawiwat	Keynote Lecture: Rizzi, Alessandro Color Technology and Applications	Keynote Lecture: Cheung, Vien Color and Culture	BAGIS Session (Sponsored by JSPS)
		Keynote Lecture: Luo, Ming Ronnier Color Technology and Applications	Color Technology and Applications / Color in Nature	Color in Art and Design
				Study Group on Environmental Colour Design (16:15-17:30)
Evening (18:00~)	Welcome Party (18.00-20.00)			

<table>
<tr><th rowspan="3">Date</th><td colspan="3">November 29, 2023</td><td>November 30, 2023</td></tr>
<tr><td colspan="3">Wednesday</td><td>Thursday</td></tr>
<tr><td colspan="3">Day 2</td><td>Day 3</td></tr>
<tr><th>Room</th><td>Doi Tung</td><td>Doi Tong</td><td>Doi Wawee</td><td>Doi Tung</td></tr>
<tr><th rowspan="2">Morning
(8:30-12:00)</th><td colspan="3">Invited Lecture:
Digital Color Literacy, Media Arts and Design Education
Bendito, Petronio
(9:00-10:15)</td><td>General Assembly
(8:30-10:30)</td></tr>
<tr><td>Keynote Lecture:
Stockman, Andrew
Color Vision</td><td>Color Psychology</td><td></td><td>Poster Session
(10:45-11:45)</td></tr>
<tr><th rowspan="3">Afternoon
(13:00-17:30)</th><td>Keynote Lecture:
Horiuchi, Takahiko
Color Technology and Applications</td><td>Keynote Lecture:
Bergstrom, Berit
Color and Education</td><td></td><td rowspan="3">Excursion
(13:00-17:00)</td></tr>
<tr><td>Color Vision</td><td>Keynote Lecture:
Tse, Nicole
Color Applications</td><td>Color Naming</td></tr>
<tr><td></td><td></td><td>Study Group on Language of Color
(16:00-17:15)</td></tr>
<tr><th>Evening
(18:00~)</th><td colspan="3">Banquet
(18.00-22.00)</td><td></td></tr>
</table>

<table>
<tr><th rowspan="3">Date</th><th colspan="3">December 1, 2023</th><th>December 2, 2023</th></tr>
<tr><th colspan="3">Friday</th><th>Saturday</th></tr>
<tr><th colspan="3">Day 4</th><th>Day 5</th></tr>
<tr><th>Room</th><th>Doi Tung</th><th>Doi Tong</th><th>Doi Wawee</th><th>Doi Tung</th></tr>
<tr><td rowspan="2">Morning (8:30-12:00)</td><td>Keynote Lecture:
Tremeau, Alain

Color Appearance</td><td>Color in Art and Design</td><td></td><td>Invited Lecture:
Colour, Machine Learning and Creativity
Westland, Stephen
(9:00-10:15)</td></tr>
<tr><td>Keynote Lecture:
Lee, Tien Rien
Color Designs</td><td>Color and Beauty</td><td>Color Technology</td><td>Closing Ceremony
(10:30-11:30)</td></tr>
<tr><td rowspan="3">Afternoon (13:00-17:30)</td><td>Color Technology</td><td>Keynote Lecture:
Caivano, Jose
Color Appearance</td><td></td><td></td></tr>
<tr><td colspan="3">Judd Award Citation
CADE Award Lecture
(14:45-16:00)</td><td></td></tr>
<tr><td>Study Group on Art and Design
(16:00-17:15)</td><td></td><td></td><td></td></tr>
</table>

ORAL SESSION

Doi Tung		
Start - End	**28 November 2023**	
09:00 - 10:15	Opening Ceremony	
10:15 - 10:30	Coffee Break	
10:30 - 11:45	What Color Is Thai? Prasarnrajkit, Piyanan	Invited Lecture
12:00 - 13:00	Lunch	
13:00 - 13:30	On Why the Nature of Color Is Spatial Rizzi, Alessandro	Keynote Lecture
13:30 - 13:45	Optimization of Spectral Sensitivity for Multispectral Imaging Based on Adaptive Noise Levels Xu, Peng*; Xu, Haisong	
13:45 - 14:00	A Low-Cost Portable Spectrophotometer Trentini, Andrea; Bini, Lorenzo; Rizzi, Alessandro*	
14:00 - 14:15	Spectrofluorimetry – a New Paradigm in the Assessment of Color Appearance Ladson, Jack A*; Lategano, Charles	
14:30 - 14:45	Coffee Break	
14:45 - 15:15	Advanced Colorimetry for Imaging Colour Reproduction *Luo, Ronnier Ming*	Keynote Lecture
15:15 - 15:30	Display Enhancement for HDR Contents Under Ambient Lighting Huang, Yiming; Xu, Haisong*; Li, Yuemin; Yang, Minhang	
15:30 - 15:45	Estimating Spectral Transmittance of Translucent Media from An Opacity Value and Known Spectral Reflectance Safdar, Muhammad*; Emmel, Patrick	
15:45 - 16:00	Modelling Colour Appearance of Images Under HDR Viewing Conditions Shi, Xinye*; Zhu, Yuechen; Luo, Ming Ronnier	
16:00 - 16:15	The Influence of Background on the Color Difference Evaluation of Multicolored Material Wu, Jiaying; Shamey, Renzo*	

Doi Tong		
Start - End	**28 November 2023**	**Paper ID**
09:00 - 10:15	-	
10:15 - 10:30	Coffee Break	
10:30 - 12:00	-	
12:00 - 13:00	Lunch	
13:00 - 13:15	Colour Processing of Architectural Finishes in Historic Townscapes Units Diaz-Ramos, Isolina*; Artioli, Gilberto	
13:15 - 13:30	The Nature of Redness O'Connor, Natalie A*	
13:30 - 13:45	Aesthetic Characteristics of the Buddhist Cuisine Shojin Ryori Served in Contemporary Japan: From the Perspective of SDGs Yoshimura, Kohji*; Shrader, Stephen; Yamada, Yuko	
13:45 - 14:00	From Digital Colour to Circular Colour. The Colour of Architectural Surface in the Circular Economy. A Review Gasparini, Katia*	
14:00 - 14:30	The Pink Tax Cheung, Vien	Keynote Lecture
14:30 - 14:45	Coffee Break	
14:45 - 15:00	The Effects of Chroma on Designers' Intellectual Abilities in An Immersive Virtual Environment Xia, Guobin*; Henry, Phil; Queiroz, Francisco; Westland, Stephen; Yu, Luwen; Cheng, Qian; Yang, Jie	
15:00 - 15:15	Colour Palette Generation from Virtual Fashion Images Lai, Peihua*; Pan, Qianqian; Hemingray, Caroline; Westland, Stephen	
15:15 - 15:30	Production of Functional Inks from Natural Colorant Anthocyanin for Meat Spoilage Indication Hongrattanavichit, Intatch*; Katemake, Pichayada ; Siangyai, Rattachai	
15:30 - 15:45	Stability of Pigments and Binders to Narrow-Band Wavelength LEDs Dethsuphar, Duantemdoung*; Katemake, Pichayada ; Westland, Stephen	
15:45 - 16:00	Coral Reefs in Uncertain Seas Ingoldsby, Joseph E.*	

Doi Wawee		
Start - End	**28 November 2023**	**Paper ID**
09:00 - 10:15	-	
10:15 - 10:30	Coffee Break	
10:30 - 12:00	-	
12:00 - 13:00	Lunch	
13:00 - 13:15	Web Users’ Attitude Towards the Size and Position of Sidebar Ads on Websites Meeusah, Natchaphak*; Torsabsinchai, Kamonthip; Tangkijviwat, Uravis	
13:15 - 13:30	A Study of the User’s Eye Movement Behavior on Different Colored Banners of the Commerce Website Using Eye Tracking Technology Torsabsinchai, Kamonthip*; Meeusah, Natchaphak	
13:30 - 13:45	Hue Polarity Selectivity in a Color Contrast-Contrast Phenomenon Kamegawa, Shohei*; Sato, Hiromi; Motoyoshi, Isamu; Mizokami, Yoko	
13:45 - 14:00	Effect of Display Technique on Simultaneous Color Contrast Mepean, Janejira*; Phuangsuwan, Chanprapha; Ikeda, Mitsuo	
14:00 - 14:15	Color Analysis and Consumer Preferences of Sinom and Kunyitasam Drinks, Traditional Drinks from Indonesia Mardhiyyah, Yunita Siti*; Sari, Lisa Risfana; Noviasri, Rizky; Cholilie, Irvan Adhin; Rahmat, Anni; Cahyono, Hadi; Kurniati, Yuni; Nugraheni, Roostikasari	
14:15 - 14:30	Customer Perspectives and Preferences for the Color in Sorghum Cookies Caused by Different Types of Sugar Azzahra, Laily Rahmadina; Mardhiyyah, Yunita Siti	
14:30 - 14:45	Coffee Break	
14:45 - 15:00	Colour Design and Conservation of Gummer and Ford Libraries in Auckland, New Zealand: Guidelines and Comparison with Notable Buildings (1923-33) Premier, Alessandro*; Rennie, Julian	
15:00 - 15:15	The Image of Paris: Development of Colour Harmony on the Banks of the Seine. Noury, Larissa*	
15:15 - 15:30	Color for Hospitals: Color Design Vs Artworks Schindler, Verena M.*	
15:30 - 15:45	Towards a Future Holistic Interior Design Considering Color and Lighting Together Rossi, Maurizio*	
15:45 - 16:00	Color Spatial Layering in Architectural Interiors After Josef Albers’ Homages to the Square at RIT Serra, Juan*; Murdoch, Michael	
16:00 - 16:15	Color, the Soul of Sketching Moreira Da Silva, Ana M S*	

16:15 - 17:30	**Study Group on Environmental Colour Design** Schindler, Verena M.	Study Group

Doi Tung		
Start - End	**29 November 2023**	**Paper ID**
09:00 - 10:15	**Digital Color Literacy, Media Arts and Design Education** **Petronio Bendito**	Invited Lecture
10:15 - 10:30	Coffee Break	
10:30 - 11:00	Cone Fundamentals, Colour Matching Functions and Individual Differences Stockman, Andrew	Keynote Lecture
11:00 - 11:15	Colour Matching Functions Measured in 30 Young Colour-Normal Observers Shi, Keyu*; Luo, Ming Ronnier; Rider, Andy; Stockman, Andrew	
11:15 - 11:30	Effect of Spatial Distribution of Chromaticity and Luminance on Chromatic Adaptation Li, Siqi*; Ma, Shining; Liu, Yue; Wang, Yongtian; Song, Weitao	
11:30 - 11:45	Color Constancy and Visual Perception Moreira Da Silva, Fernando J C*	
12:00 - 13:00	Lunch	
13:00 - 13:15	Relationship Between Softness/Hardness Evaluation and Movement Characteristics of Black Fabric Using Fabric'S Rotating Video - Comparison of Engineering and Clothing Students - Kawamata, Takumi*; Ishikawa, Tomoharu; Maehara, Takashi; Yanagida, Yoshiko; Ayama, Miyoshi	
13:15 - 13:30	Identification of Natural Indigo Dyed Fabrics by Color Image Analysis Kamolrat, Kannikar*; Phongsuphap, Sukanya	
13:30 - 13:45	Contrast Impression Between Upper and Lower Garments in Terms of Lightness, Influence on Sensibility Evaluation, and Application to Image Analysis Murakami, Shiho*; Ishikawa, Tomoharu; Okuda, Shino; Ayama, Miyoshi	
13:45 - 14:00	Natural Hair Color Appearance and Classification Analysis Abebe, Mekides Assefa*; Hardeberg, Jon Yngve; Hafslund, Bente; Asghari, Sahara Smith	
14:00 - 14:30	Physical and Perceptual Worlds of Material Appearance Horiuchi, Takahiko	Keynote Lecture
14:30 - 14:45	Coffee Break	
14:45 - 15:00	Performance Analysis of the Ishihara Test Based on Individual Colorimetric Observer Model Sun, Lijia*; Ma, Shining; Liu, Yue; Wang, Yongtian; Song, Weitao	
15:00 - 15:15	Color Rendering Indexes for Color Blind Observers Huertas, Rafael*; Machado, Pedro; Zapata, Lucia; Valero, Eva M.; Martínez-Domingo, Miguel Ángel; Gómez-Robledo, Luis; Galindo, Jose Luis; Hernandez-Andres, Javier	
15:15 - 15:30	Colour Discrimination for Visually Impaired People Under Mixed Light LEDs and White LEDs Plerksophon, Ektawat*; Katemake, Pichayada ; Tremeau, Alain; Dinet, Eric	
15:30 - 15:45	The Effect of Changes in Melanopsin Stimulation of the Surrounding Light on Brightness and Color Perception Shibata, Wakana*; Tokunaga, Rumi; Tsujimura, Sei-Ichi	

Doi Tong		
Start - End	**29 November 2023**	
09:00 - 10:15	-	
10:15 - 10:30	Coffee Break	
10:30 - 10:45	Is Color Preference Affected by Personality? Cheng, Wen-Hsin*; Ou, Li-Chen	
10:45 - 11:00	Examination of the Color Image Scale for Contemporary Western Culture: Phase One of a Multiphase Approach Lamarra, Julie K*	
11:00 - 11:15	The Effects of Colour in Human Fabric Perceptions Han, Xu*; Yu, Luwen; Li, Liting; Xiao, Kaida; Mao, Ningtao; Xia, Guobin	
11:15 - 11:30	Rosé De Provence Colour Choice in Young Adults Bonnardel, Valerie*; Pouzalgues, Nathalie; Chevallier, Aurélie; Lorey, Thierry; Masson, Gilles	
11:30 - 11:45	A Study on the Relationship Between Clothing Preference and Color Cognition He, Shuang*; Yue, Longxin; Sun, Pei; Li, Liting	
11:45 - 12:00	Effects of the Colors of Sanitary Masks on Facial Attractiveness and Impression Sakurai, Masato*; Takeda, Ena	
12:00 - 13:00	Lunch	
13:00 - 13:30	Can We Change the Colour Education to an Attractive and Inspiring Choice of Subject in Design and Architecture? Bergstrom, Berit	Keynote Lecture
13:30 - 13:45	Prerogatives for Teaching Color Souza, Pedro Felipe P*	
13:45 - 14:00	Teaching Material Design and Education Ractices of Color Education for Children in China Huang, Qian*; Li, Anni	
14:00 - 14:15	Exploring the Effects of Background Colours of Digital Materials on Learners' Comprehension in Higher Education Gong, Zhe*; Henry, Philip; Queiroz, Francisco; Lee, Soojin; Xia, Guobin	
14:15 - 14:30	Effects of Classroom Wall Color on University Students' Performance and Attention Baniani, Mahshid*	
14:30 - 14:45	Coffee Break	
14:45 - 15:15	Managing Museum Collections, Climate and Colour Change Tse, Nicole	Keynote Lecture
15:15 - 15:30	Pigments Applied in Phra Dhevabhinimmit (Chai Thiamsilpajai)'S Painting Analyzed by Portable Micro X-Ray Fluorescence Kaew-on, Nawarat*; Kaewkong, Thanaporn	
15:30 - 15:45	Chromatic Bio-Indicators of Biofilm Community Structure on Stone Heritage Sarti, Beatrice*; Villa, Federica; Cappitelli, Francesca; Rizzi, Alessandro	
15:45 - 16:00	Beauty of Colour in the Light and the Shade of Japanese Traditional Noh Costume Osumi, Masayuki*	

Doi Wawee		
Start - End	**29 November 2023**	**Paper ID**
09:00 - 10:15	-	
10:15 - 10:30	Coffee Break	
10:30 - 12:00	-	
12:00 - 13:00	Lunch	
13:00 - 14:30	-	
14:30 - 10:45	Coffee Break	
14:45 - 15:00	Augmenting Colour Communication in English, Greek and Thai Mylonas, Dimitris*; Koliousis, Alexandros; Stutters, Jonathan; Katemake, Pichayada ; Stockman, Andrew; Eskew, Rhea T.	
15:00 - 15:15	"Geometry" of Color Harmony in the CIELAB Color Space: Evidence from An Online Experiment Across Countries Griber, Yulia A.*; Samoilova, Tatiana; Al-Rasheed, Abdulrahman S.; Bogushevskaya, Victoria; Cordero Jahr, Elisa; Gouaich, Yacine; Manteith, James; Mefoh, Philip; Odetti, Jimena Vanina; Politi, Gloria; Sivova, Tatiana	
15:15 - 15:30	Colour Specification for an English-Chinese Colour Names Dictionary Li, Qinyuan*; Hutchings, John; Chang, Kaiping; Ye, Yuxin; Luo, Ming Ronnier	
15:30 - 15:45	The Origin and Development of Colour Names and Categories, and the Biological Basis for Colour Categories. Dedrick, Donald*	

16:00 - 17:15	**Study Group on Language of Color** Mylonas, Dimitris	Study Group

Doi Tung		
Start - End	**30 November 2023**	**Paper ID**
08:30 - 10:30	**General Assembly**	
10:30 - 10:45	Coffee Break	
10:15 - 11:45	**Poster Session** (at Doi Tung Foyer)	
11:45 - 12:45	Lunch	

12:45 - 17:00	Excursion	

Doi Tung		
Start - End	**1 December 2023**	
09:00 - 09:30	Invariance of Color Constancy Models to Complex Lighting Conditions Tremeau, Alain	Keynote Lecture
09:30 - 09:45	Color Afterimage Appearance Measured with Natural Color System Sun, Vincent*; Peng, Ching-Wei; Fu, Ming Chuan	
09:45 - 10:00	Developing CCT and Luminance Correction Functions for High Dynamic Range Based on Real-World Scene Zhu, Yuechen*; Luo, Ming Ronnier	
10:00 - 10:15	New Vividness and Depth Equation Developed by CAM16 Q, M Li, Molin*; Luo, Ming Ronnier	
10:15 - 10:30	Coffee Break	
10:30 - 11:00	The Choices of Color: Exploring Color Selection from Maslow to AI Lee, Tien Rien	Keynote Lecture
11:00 - 11:15	Colour, Form and Product - Form Ghosts in Design Education Bäckström, Eva-Lena*	
11:15 - 11:30	Colour Design for Facade Integrated Photovoltaics Systems in Campus- a Case Study in Hong Kong Wang, Wanting; Xu, Kaiyan; Xiang, Changying*	
11:30 - 11:45	Applying a Colour Value Framework for Colour Design of Lifestyle Products Dubey, Nijoo*; Damodaraswamy, Sudhakar	
12:00 - 13:00	Lunch	
13:00 - 13:15	A Colour Rendering Chart for Preferred Colour Reproduction Luo, Ming Ronnier*	
13:15 - 13:30	TM-30-20 and CIE-CRI Ra: Investigation of Colour Rendering of White Pc LEDs Bieske, Karin*; Schierz, Christoph	
13:30 - 13:45	A Set of Optimal Reflectance Curves to Detect and Reduce Inter-Instrument Differences Between Spectrophotometers Nilsson, Anders*; Seymour, John	
13:45 - 14:00	The Spectral Reflectance Ratio and Deterioration Simulation of Toyohara Kunichika'S Japanese Woodblock Print Taguchi, Satoko*; Okuda, Shino; Okajima, Katsunori	
14:00 - 14:15	Coffee Break	
14:15 - 14:45	**AIC Judd Award Citation** Kuehni, Rolf Georg	Judd Award
14:45 - 16:00	**AIC CADE Award Presentation** **AIC CADE Award Lecture: The "Color Fever" Chroma Survey 1973** Castellli, Clino Trini	CADE Award Lecture

16:00 - 16:15	**Study Group on Art and Design** Durão, Maria João	Study Group

Doi Tong		
Start - End	**1 December 2023**	**Paper ID**
09:00 - 09:15	Gaudi'S Chromatology in Park Güell As Case Study Durão, Maria João*	
09:15 - 09:30	A Colour Story: How Designers Use Colour As a Visual Storytelling Tool in Sneaker Design Jackson, Kel*; Choi, Youngmi Christina	
09:30 - 09:45	The Unique Color Worlds of Painters with Color Vision Deficiency Muraya, Tsukasa*; Taniguchi, Yunoka; Ichihara, Yasuyo G.; Sunaga, Shoji	
09:45 - 10:00	Achieving Color Richness in Painting – Concepts & Techniques of Conventional & Digital Paintings Ng, Woon Lam*; Chan, David, Kw; Ngai, Carey	
10:00 - 10:15	Color Standards in City Planning and Shop Facade Design Changes: Field Survey of Two Urban Landscape Formation Districts in Nagoya City, Japan and Analysis of Corporate Identity Elements Mukaiguchi, Takeshi*; Harada, Masayuki; Terashima, Toshiharu; Ono, Tomoka	
10:15 - 10:30	The Impact of Chromatic Palettes in Social Neighborhoods' Environments: Cause and Consequence of Human Interactions Caramelo Gomes, Cristina *	
10:30 - 10:45	Coffee Break	
11:00 - 11:15	A Study on the Impression Difference Between Facechart and Actual Makeup Looks Hsu, Chi-Ying*; Lee, Wen-Yuan	
11:15 - 11:30	Influence of Lighting Spectra on Facial Appearance in Static Images, Movies, and Real Environment Iwasaki, Takuma*; Sato, Hiromi; Mizokami, Yoko	
11:30 - 11:45	Exploring Relationships Between Skin Tone and Personal Colour Sueeprasan, Suchitra*	
11:45 - 12:00	Continuous Skin Color Classification of Warm-Netural-Cool Park, Yungkyung*	
12:00 - 13:00	Lunch	
13:00 - 13:30	The Concept of Cesia (Visual Appearance Other Than Color): Antecedents, Development, and Applications Caivano, Jose	Keynote Lecture
13:30 - 13:45	Apparatus to Study Total Appearance Lin, Jinyi*; Luo, Ming Ronnier	
13:45 - 14:00	Optical Measurements of Sparkle and Graininess Basic, Nina*; Blattner, Peter; Aebischer, Cyrill	
14:00 - 14:15	Coffee Break	
14:15 - 16:00	-	

Doi Wawee		
Start - End	**1 December 2023**	
09:00 - 10:15	-	
10:15 - 10:30	Coffee Break	
10:30 - 10:45	Auto-White Balance Algorithm of Skin Colour Based on Asymmetric Generative Adversarial Network Zhou, Sicong*; Li, Hesong; Sun, Wenjun; Zhou, Fanyi; Yang, Yang; Xiao, Kaida	
10:45 - 11:00	A Study of Image Features and Colour Classification in Tongue Diagnosis in Traditional Chinese Medicine Qingmei, Huang*; Shen, Zhang; Ziyuan, Wei; Rong, Liang; Lingyan, Wang	
11:00 - 11:15	To Perform White Balance Using Skin Memory Color Wang, Liqing*; Luo, Ming Ronnier; Zhu, Yuechen; Liu, Xiaoxuan	
11:15 - 11:30	Image Statistics and the Perception of Summary Color of Natural Materials Zhang, Yan*; Motoyoshi, Isamu	
11:30 - 11:45	Reliable Uncertainty Evaluation of Measurements of Color Quantities Ikonen, Erkki*; Rezazadeh, Yasaman; Maham, Kinza	
12:00 - 13:00	Lunch	
13:00 - 16:00	-	

Doi Tung		
Start - End	**2 December 2023**	
09:00 - 10:15	Colour, Machine Learning and Creativity Westland, Stephen	Invited Lecture
10:15 - 10:30	Coffee Break	
10:30 - 11:30	Closing Ceremony	

POSTER SESSION

Doi Tung Foyer	30 November 2023
	Title and Authors
	Relationship Between Color Preference and Personality Trait in Selecting Clothing Nakamura, Shinji*
	Differences in the Impressions of Professional Women'S Makeup Looks on Different Genders and Age Levels Hsu, Chi-Ying*; Lee, Wen-Yuan
	The Impact of Goalkeeper Uniform Color on Penalty Kick Performance in a Video Game—Using Fifa22 for the Experiment Lu, Yi-Chan*; Lee, Wen-Yuan
	Examine the Universal Color Emotion Models and Additive Theory by the Color Emotions Evoked by Two-Color Combinations on 3D Color Configurations Gong, Shi Min *; Lee, Wen-Yuan
	Local Color, Constancy and Illusion De Lucas Tron, Alfonso*
	Color Characteristics of Korean Purple-Based and Green-Based Natural Dyeing Fabric Shukla, Anshika*; Yang, Junghee; Park, Hyewon
	Korean Experts' Empirical Perceptions of the Personal Color System Ham, Dakyeong*; Park, Hyewon
	Comparison of Colors in Metaverse and offline Space of Fashion Brands Ahn, Kyuhee*; Choi, Gyoungsil
	Recognition of Smartphone Buttons According to Size and Shape Yeo, Jiwon*; Park, Yungkyung
	Pigments Applied in “Autumn (1956)” Painting of Fua Haripitak, the First and Most Outstanding Artist of Thai Contemporary, Analyzed by Portable Micro-Xrf Kaew-on, Nawarat*; Kaewkong, Thanaporn
	Multiband Imaging with Smartphone Cameras for Spectral Reflectance Estimation Nishi, Shogo*; Ohtera, Ryo; Tominaga, Shoji
	Automatic Color Calibration Without Color Chart Muselet, Damien*; Cortes Jaramillo, Felipe; Colantoni, Philippe; Tremeau, Alain
	Pakistani Truck Art Colors: Inspiring Fashion Designers by Reflecting Local Heritage on the Global Stage Ume Farwa, Syeda*; Yu, Jinsang; Park, Hyewon
	A Reflection on the Korean Colorist and Color Qualification Over the Past Three Decades Lee, Gyeonghwa*; Cheung, Vien
	Text Mining Analysis on Korean Perception of Personal Colors Kim, Se Jin; Kwon, Minseo*
	Color Quality Control of Multicolored Fabrics Containing Color Gradients Based on Spectral Imaging and Unsupervised Segmentation Method Xiong, Nian; Shamey, Renzo*
	Effect of Color Purity of LED Light on Taste Threshold Takahashi, Hiroshi*; Tsuchida, Kento; Asaga, Sota
	Measurement of RGB-LMS Color Space Transformation Function for Dichromat Zhang, Yuhang*; Shinoda, Hiroyuki

Doi Tung Foyer	30 November 2023
	Title and Authors
	The Influence of Spot Varnishing on the Color Appearance of Print Typefaces in Uv Inkjet Printing Nilmanee, Somporn*
	Investigating the Effect of Lipstick Colour on Skin Colour Perception for Chinese Female Chen, Yifei*; Xiao, Kaida; Rigout, Muriel.
	Color Change of the Ten Symbols of Longevity Cadets in the Late Joseon Dynasty Lhi,Wona* ; Choi, Gyoungsil
	Effect of Color Quantization on Color Harmony Sharma, Shreeniwas*; Tandukar, Jyoti; Bista, Rabindra
	Influence of Color Appearance on Dichromats' Superiority in the Visual Search Task with Color Palomo, Héctor A*; Muraya, Tsukasa; Sunaga, Shoji
	Researching of Costume Featured in the K-Movie, <The King'S Letters(나랏말싸미naramalsami)> Hee, Bae Mi*; Park, Hyewon
	Effect of Narrow-Band Primary Colors on Observer Metamerism of Anomalous Trichromats Inoshita, Taiju*; Muraya, Tsukasa; Sunaga, Shoji
	Automatic Colour Palettes from Mood Boards Westland, Stephen; Angharad, Sally*; Lai, Peihua
	The Environmental Color Imagery Survey Via Virtual Reality Wei, Robert Y.C.*; Kuo, Monica; Kuo, Ya-Ping
	Redness Perception of Dichromats for Short-Wavelength Lights Asakura, Suzuka S*; Inoshita, Taiju; Muraya, Tsukasa; Sunaga, Shoji
	Influence of Lighting Source Direction on Color Perception and Texture Impression of Fabrics He, Shuilan*
	Steady State Pupil Response Elicited by Independent Stimulation of Melanopsin and Cone Photoreceptors Ito, Tomoe*; Takikawa, Mizuki; Takasu, Aoi; Fujita, Yuno; Tsujimura, Sei-Ichi
	Contribution of Melanopsin Photoreceptors to Brightness Perception by Steady Light Stimulation Fujita, Yuno*; Takasu, Aoi; Ito, Tomoe; Tsujimura, Sei-Ichi
	Dynamic and Responsive Color in Fashion Design He, Shuang*; Lan, Cuiqin; Song, Jiajia
	A Study on Additivity of Psychological Stress by Mixed Color Lighting of Three Primary Colors Oe, Yuki*; Miura, Yukie; Onai, Miku; Yoshizawa, Nozomu
	A Comparative Study on Impressions of Clothes Withheld Brand Names in Japan, China, and Thailand Sakamoto, Takashi*; Sakamoto, Takashi; Hattri, Nanako; Takahashi, Naoki; Kato, Toshikazu
	An Investigation into the Variability of Hair Colour Measurements Wang, Haoyu*; Xiao, Kaida
	Effect of Modality on the Efficacy of Light Exposure on Mood Chen, Mengyuan*; Westland, Stephen

Doi Tung Foyer	30 November 2023
	Title and Authors
	An Image Quality Evaluation Dataset for Atmosphere Quality Modeling Xu, Nanlin; Zhu, Yuechen; Luo, Ming Ronnier*
	Color Preference of Thai Tea Photo Saksirikosol, Chanida*; Rattanakasamsuk, Kitirochna
	Red and Blue – Abstract and Cultural Issues Asano, Akira*; Asano, Chie Muraki; Ogura, Genki; Chida, Emi
	Qualia Change Phenomenon Related to Color Vision Diversity Hiramatsu, Chihiro*; Yamada, Anna; Ishii, Mochine; Baba, Yasuhito
	Worldwide Survey of the Association Between Color and Temperature Ndeye Meissa Koura Sow, Sow*; Saksirikosol, Chanida; Shamohammadi, Mina; Rattanakasamsuk, Kitirochna; Phuangsuwan, Chanprapha; Hiramatsu, Chihiro
	Impact of Colour on Recognition of Cultural Landscape Images Griber, Yulia A.*; Paramei, Galina
	Appearance of Fluorence in Architectural Spaces: Quantification of the Influence of Size Angle and Luminance Gradient Noguchi, Hidetoshi*; Yoshizawa, Nozomu
	Tinted Interior Spaces with the Daylight Reflecting off the Outside Greenery Kitamura, Kaoruko*; Makino, Kanoko; Oe, Yuki; Yoshizawa, Nozomu
	Appearance of Objects Seen Through Coloured Low-E Glasses: Application of An Edge Detection Algorithm for Visibility Judgment Okamura, Akane*; Yoshizawa, Nozomu; Kitadani, Yukie; Suzuki, Hirotaka
	Visualizing Health Status Using Face Color Analysis and Its Application to Smart Mirrors Moriyama, Tsuyoshi*; Tsunashima, Nobuhiro
	The Appearance Characteristics of the Textile Material and Color Tint of the *Ainu* Costume – the Differences Between the *Attus* of Sakhalin and Hokkaido Asano, Chie Muraki*
	Color Naming and Constancy of 3D Translucent Objects Gigilashvili, Davit*; Amirkhanashvili, Ana
	Effect of Lip Colours on Colour Appearance and Preference of Facial Skin. Okuda, Shino*; Jonai, Riho; Okajima, Katsunori
	Individual Colour Preference Change Over Time: A Three-Month Study Lee, Soojin*; Westland, Stephen; Rodski, Stan
	Colour Design and Spatial Quality- A Critical Analysis of the Mosaic Colours in Hong Kong Mass Transit Railway Stations Liang, Jiaxin; Chang, Raine Marie; Wang, Wanting; Xiang, Changying*
	Effect of Wall Color on Comfort of Indoor Space Azuma, Yoshihiko*
	Improving Abandoned Pet Detection in Natural Spaces Through Adaptive Single-Coloured Image Augmentation Techniques Akinwehinmi, Oluwakemi; Pedro, Arnau Del Amo; Francesc, Xavier Solsona Tehas
	A Methodological Approach to Colour Construction for Island Fishing Village Community Based on "Social Lifestyle" Mao, Xue*
	Emotional Responses to Images of the Same Scene with Different Colours Sueeprasan, Suchitra*
	Concentration Dependency on the Identification of Pigment Khampaeng , Sureeporn*; Katemake, Pichayada ; Tse, Nicole

Doi Tung Foyer	30 November 2023
	Title and Authors
	The Question of Color / the Color in Question: Cathedral of Portalegre, Portugal Duarte, Rui B*; Pinheiro, Ana Paula
	Petrological Characteristics of Natural Pigments from Rayong, Eastern Thailand Meethum, Jinnawat; Fanka, Alongkot*; Hattagee, S.; Katemake, Pichayada; Ngamukot, Passapol; Noppakundilograt, Supaporn; Assawincharoenkij, Thitiphan
	Influence of Illumination Spectrum on Visual Comfort Liu, He*; Shinoda, Hiroyuki
	Pigment Analysis in Three Paintings (1966-1967) by Pratuang Emjaroen by Portable Micro-X-Ray Fluorescence Kaew-on, Nawarat*; Kaewkong, Thanaporn
	Influence of Illumination Color on Person Tracking Based on Deep Learning and Its Compensation Doi, Motonori*; Ishikawa, Yoshiki; Nishi, Shogo; Kimachi, Akira
	Effect of Color on Gender Identification in Thailand and Japan Rattanakasamsuk, Kitirochna*; Saksirikosol, Chanida
	The Influence of Color on Short-Term Memory Tangkijviwat, Uravis*; Meenorn, Methawee; Yamprasai, Porntip
	Data Analysis of Regional Aesthetic Factors on “Colorscape” in Japan Yamashita, Ryoma*; Nagaya, Shoma; Hanari, Takashi; Kawasumi, Mikiko
	Color Index Development of Nagoya Cochin Eggshell Nagaya, Shoma*; Yamashita, Ryoma; Akao, Mika; Miyakawa, Hiromitsu; Nakamura, Akihiro; Tsukada, Toshihiko; Kawasumi, Mikiko
	Red Background Enhances Dominance Judgement of Geometric Shapes Yang, Yidie*; Chen, Na; Kobayashi, Maiko; Nakamura, Koyo; Watanabe, Katsumi
	A Study on Improving Efficiency of Color Matching Function Measurement Using Selection Techniques Okuda, Akito*; Yamauchi, Yasuki
	Effect of Lighting on Wristwatch for Advertising Photography Jarernros, Jarunee *; Srisuro, Ploy
	The Analysis of Eye-Catching on Thai Movie Posters Srisuro, Ploy*
	Congenital Red-Green Colour Deficiency: Study of the Efficacy of Commercial Color Filters Huertas, Rafael*; Jimenez Molina, María; Martinez-Navarro, Carlos; Lopez-Jabalera, Maria De Los Angeles; Martin-Sevilla, Arturo; Valero, Eva M; Gomez-Robledo, Luis; Martinez-Domingo, Miguel Angel; Hernandez-Andres, Javier
	Data Scientific Colour Comparison Among Five Ethnic Townscapes in Singapore Kawasumi, Natsuko*; Phuangsuwan, Chanprapha; Kawasumi, Mikiko
	Unveiling Emotions and Meaning Through Colour Significant Experiences Conte, Veronica*
	Optimised Wavelengths for Displaying Coloured Materials with Cinnabar and Red Coral Pigments Katemake, Pichayada *; Ariyavarapong, Airin; Leewatchararoongjaroen, Kasama; Noppakundilograt, Supaporn; Fanka, Alongkot
	Tone Mapping Operator Based on Just Noticeable Difference of Luminance Kanthong, Kasidet * and Singnoo, Jakkarin

	BAGIS Session
	The Comparison of the Light Distribution Characteristics of External Flash Accessories Puenpa, Suwat*; Rattanakasamsuk, Kitirochna
	Visual Perception Experiment and Analysis of Metamorphosis for Object Appearance by Change-Detection Task Iwase, Kota*; Matsufuji, Momoka; Tanaka, Midori; Horiuchi, Takahiko
	Perceptual Collation Method for Colour Halftone Images Based on Visual Saliency Baba, Taiga*; Tanaka, Midori; Imaizumi, Shoko; Horiuchi, Takahiko
	Analysis of Harmony Between Coloured Light and Fragrance by the Reaction of the Left-Right Orbitofrontal Area Oba, Toshinori*; Tanaka, Midori; Horiuchi, Takahiko
	Relationship Between the Observer Metamerism of Color Vision Diversity and the Spectral Bandwidth of Primary Color Spectrum Nakayama, Rei*; Sato, Hiromi; Mizokami, Yoko
	The Linear Scale Between Chromaticness and Lightness Axis on the Polar Diagram Chitapanya, Phubet*; Phuangsuwan, Chanprapha; Ikeda, Mitsuo
	Quantifying the Hue Components of Fa and Blue Using the Elementary Color Naming Method Phuangsuwan, Chanprapha*; Phuangsuwan, Chanprapha; Tokunaga, Rumi; Mizokami, Yoko; Likitpunyawat, Kusuma
	Influence of Skin Color Change on Facial Expression Recognition Among Asian Observers He, Yuanyuan*; Michishita, Ryo; Sato, Hiromi; Mizokami, Yoko

Study Group

Study Group
Environmental Colour Design

2023 Meeting of 'the Study Group on Environmental Colour Design (SG ECD)' of the International Colour Association (AIC)

Date: Tuesday, 28 November 2023
Time: 4:15 PM - 5:30 PM
Location: 15th AIC Congress 2023, Chiang Rai, Thailand
Chair: Verena M. Schindler

The role of theory and practice in environmental colour design

This ECD meeting will focus on the discussion of the different roles and relationships between theory and application. We will inquire into what theory is in environmental colour design and what application means. Is theory completely detached from practical experience? Or, is it an ideal abstraction of observations that emerge from practice and experience? In other words, is theory fundamental to the practice of environmental colour design? What is applied theory? Do we apply a methodology, rules or regulations? Is it merely a matter of conducting an investigative analysis of a natural and urban environment? Or is it more about carrying out an analysis and synthesis to create colour palettes and colour schemes for the application in a space or on mobile devices? That is, can practice be completely detached from theory? Does practice entail entirely different concepts that have nothing to do with the application of academic models and theoretical frameworks? The aim of this meeting is to disentangle the complexity and understand the different roles that theory, application, and practice hold.

Study Group

Exploring the Language of Colour Beyond Primary Colours in the Age of AI

2023 Meeting of the Study Group on 'the Language of Colour' of the International Colour Association (AIC)

Date: 29 November 2023
Time: 04:00 PM - 05:15 PM
Location: 15th AIC Congress 2023, Chiang Rai, Thailand
Chair: Dr Dimitris Mylonas

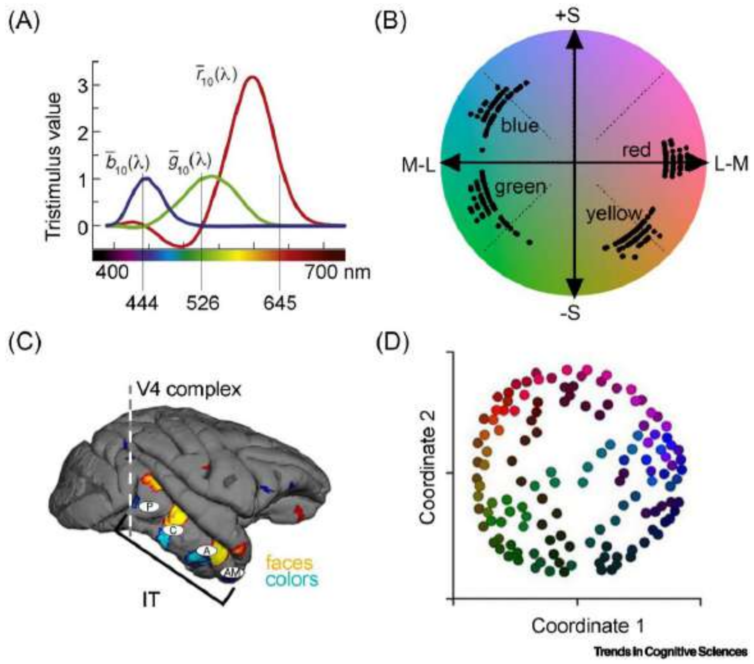

Figure 1. Colour encoding and neural representation. (A) Colour matching functions. (B) Distribution of unique hue settings. (C) Lateral view of the macaque brain showing functional domains biased for colours and faces. (D) Geometry of the neural represention of colour for neurons. (Source: Conway et al., 2023, Figure 2, CC BY-NC-ND 4.0 Deed; https://doi.org/10.1016/j.tics.2023.06.003)

The longstanding notion of primary colours has been foundational in colour studies. However, extensive research into their very existence has produced inconclusive results. Compelling neurobiological evidence from Conway et al., 2023 now suggests that it is time to move beyond traditional paradigms (Fig 1). Added to this, advancements in Artificial Intelligence (AI) can offer us large language models to explore this relatively uncharted colour domain in different languages (Fig 2).

Figure 2. Image generated on DALL-E 2 using the prompt: 3D render of a pink balloon dog in a violet room.

In this meeting of the Study Group on the Language of Colour (SGLC), we will open a discussion on the implications of this new understanding for future research on the language of colour beyond primary colours, as well as related challenges and opportunities that the rise of AI presents for our field. This meeting is open to SGLC members and all AIC 2023 attendees who are interested in this topic and joining our study group.

Benefits of joining the SGLC meeting

- Connect with a community of scholars and practitioners who are passionate about the cognitive aspects of colour
- Learn about the latest research in the field
- Share your own insights and perspectives

Anticipating a vibrant exchange of knowledge and ideas!

Study Group
Arts and Design

2023 Meeting of the Study Group on ‘the Arts and Design’ of the International Colour Association (AIC)

Date: Friday, 1 December 2023, 16:00-17:15
Time: 04:00 PM - 05:15 PM
Location: 15th AIC Congress 2023, Chiang Rai, Thailand
Chair: Maria João Durão, David Briggs

Program

1. Invited lecture: **Colour research impacts in Design praxis: An analysis of academia and industry approaches to colour.** By Cristina Caramelo Gomes

2. Presentation of 2nd SGAD Virtual Exhibition of Arts and Design

In collaboration with the Colour and Light Research Group-CIAUD-School of Architecture, University of Lisbon, the Portuguese Colour Association, and the Colour Society of Australia.

3. Discussion within the group.

Invited Speakers

What Color is Thai?

Piyanan Prasarnrajkit

Abstract

Colorants, techniques, believes and inspirations that create the exotic colors used in Thai Architecture, costumes and handicrafts.

Biography

I was born in 1956, groomed up in an artistic family. I was fascinated by arts and architecture since my early childhood. After graduated with highest honor and gold medal in Art-education from Chulalongkorn University in 1978, I pursued my Master's Degree in Interior Design from Syracuse University and Florida State University, USA in 1981. Started my career as full-time lecturer & instructor in Interior Design courses at Department of Industrial Design and Interior Design in the Faculty of Architecture, Chulalongkorn University.

Assigned to teach color as an element in basic design, I further researched in color at the Royal College of Art, London in 1990 and wrote a book, Color in Interior Design, funded by CU book program in 1991.

Joined the NCS color workshop in Sweden in 2005.Founded an elective course, Color Study and Design, 2006 and left the full-time teaching career from CU to work for TOA paint company as Color design consultant till 2019.

During 1982-2020 I have done over 50 Interior and Color design projects: houses, offices, medical clinics, hospitals, temples, commercial displays and exhibitions. And also done research on color trend, and color seeing: Simultaneous contrast in 3Ds.

I have occasionally attended Color meetings: AIC in Thailand, Switzerland, Spain, Sweden, and Portugal. CMG in England, Thailand and Malaysia.

At the moment I enjoy painting both watercolor and acrylic and creat printing products from my painting under my brand Piyananta.

Color Knowledge is essential for everyone who cares upon its effects and affects. Therefore, I am still active and enthusiastic in seeking color knowledge and pleased to be a giver to everyone including my beloved 3 grandchildren.

Color was, is and always will be in my soul forever.

Colour, Machine learning and Creativity

Stephen Westland

Abstract

We are going through a period of almost unparalleled technological change that is dominated by advances in machine learning. This talk will look at developments in machine learning and how they change the way we think about colour research. Research findings increasingly rely on very large amounts of data and machine learning helps us to derive valuable insights from the data. Recent research to use machine learning in two areas - colour meaning and colour forecasting - will be described with examples. Some thoughts on future developments will be presented including the question of whether creativity is unique to humans or might be possible using machine learning.

Biography

Stephen Westland is Professor of Colour Science and Technology at the University of Leeds (UK), a position he has held since 2003. During his academic career, Westland has published over 275 refereed books, book chapters, journal papers and conference papers in areas of colour measurement, colour vision and colour design. He holds visiting professorships at University of East Anglia (UK), University of Texas (USA) and Huazhong University of Science and Technology (China).

He has made a notable contribution to the use of computational methods in various areas of colour application. He was first author of Computational Methods in Colour Science (Wiley) that was first published in 2004 with a second edition published in 2012. He was one of the first people to use artificial neural networks in colour science during the first AI era when he showed that multi-layer perceptrons could be used to map between colorant recipe data and spectral or colorimetric data. He has since continued to use machine learning to predict colour from recipe data for textile fibre blends using neural networks and to automatically extract key colours from images. He also applied computational methods for colorimetry in dentistry where he developed an optimised whiteness index for dentistry that has been widely used worldwide in clinical trials to develop whitening products. Recently he explored the relationship between whiteness and yellowness in dentistry and developed a yellowness index for use in dentistry.

Westland has also made a sustained contribution to colour education, particularly through his long involvement with the Society of Dyers and Colourists (SDC) since 1983 where he served for many years on the colour measurement committee and, more recently, chairs the Society's Examinations, Qualifications and Examinations Board. He also held the honour of being President of the Society of Dyers and Colourists in 2019/2020. At the universities of Derby and Leeds, he has supervised 66 PhD students (40 as first supervisor). He founded a new journal with the SDC entitled Colour: Design and Creativity which later became the Journal of the International Colour Association (JAIC) of which he continues to be chief academic editor. He is a member of the Colour Literacy Project (supported by ISCC and AIC) and publishes on issues of colour education. He is co-author of the textbook 100 Principles of Color in Art and Design which addresses many contemporary issues in colour theory.

Digital Color Literacy, Media Arts and Design Education

Petronio Bendito

Abstract

Integrating art, science, and technology in color design education paves the way for innovative tools and methods for creating color palettes for art and design applications and teaching. This invited paper introduces the author's methodology for teaching color design in the context of media arts education. Fundamental to the methodology is the science of color vision and how it informs the exploration of the most commonly used three-dimensional color systems of the digital age—RGB (Red, Green, and Blue), CMYK (Cyan, Magenta, Yellow, and Black), and HSB (Hue, Saturation, and Brightness). An examination of the potential and limitations of these color models are crucial to digital color literacy. Traditionally, color wheels are predictors of color mixing and are also used as a tool for creating color combinations. The author's RGB/CMY digital color wheel aims to provide a framework for promoting essential digital color literacy proficiency by 21st Century learners. Fundamentally, a digital color wheel needs to function as a visual aid to foster an understanding of the digital color spectrum based on Red, Green, and Blue color mixing. The RGB/CMY digital color wheel offers a broader color spectrum than traditional color wheels based on red, yellow, and blue color mixing, such as Johannes Itten's 12-step color circle, which does not include the color Magenta. In this presentation, the implications of using science-based RGB LED color blocks and microscopes in the classroom to introduce color at the pixel level are discussed. In this methodology, learning how to create colors using a digital color mixer and generating a digital color wheel from scratch are considered two of the essential skills of digital color literacy. Finally, the paper introduces a perceptual analysis of the HSB color model and how to use it to teach the fundamental concept of generating color palettes based on tonal relationships—another important 21st Century digital color literacy foundation.

Biography

Petronio Bendito is a designer, artist, and professor. He teaches digital media design in the Visual Communication Design program at Purdue University in the Rueff School of Design, Art, and Performance (USA). His creative and scholarly works investigate digital color design methodologies and the intersection of art, design, science, and technology.

Keynote Speakers

Invariance of Color Constancy Models to Complex Lighting Conditions

Alain Tremeau

Abstract

Color constancy is the ability of human vision to recognize a stable color in objects under varying lighting conditions. When it comes to computer vision, color constancy is not as accurate as in human vision. Computer vision aims at “seeing” and “understanding” visual data (content of images and videos) in order to provide decision-support for many applications. It is a multi-disciplinary approach which seeks to get closer to human visual perception and understanding in order to automate tasks that the human visual system can do. In this quest, color constancy is a prevalent issue in every discipline associated with computer vision. The results of computer vision models deeply depend on the point of view and lighting conditions. The task of computational color constancy is to estimate the scene illumination and then perform the chromatic adaptation in order to remove the influence of the illumination and the camera sensor on the colors of the objects in the scene. Removing the influence of the illuminants, of the camera sensor, and of the optical effects is of primordial importance in computer vision to make sense of digital videos and images. This is how, for example, most digital cameras use color constancy methods in their camera Image Signal Processing (ISP) Pipeline. In this presentation we will survey the most recent models/methods dealing with color constancy and will discuss the following research questions: - How might we make computer vision more robust against complex illumination/ viewing conditions? - How to make materials and colors appearance, optical and photonics models consistent with human perception when using new image sensors (eg. multispectral sensors) and display devices (eg. AR/XR)? - How might we improve the deployment of smartphones and low-cost sensors in professional uses? We will also discuss some areas of improvements using machine learning methods.

Biography

Alain Trémeau is Professor at University Jean Monnet (UJM), France and member of the laboratory Hubert Curien (CNRS - UMR 5516). He is also affiliated as Affiliate Researcher at Chulalongkorn university, Thailand. His research activity covers various fields, such as Human Perception of visually impair people, Color Appearance of materials, Color Constancy in computer vision, 3D human body pose estimation in performing arts, etc. He wrote numerous scientific papers and book chapters, in the domain of Color Imaging and Computer Vision in the highest ranked journal and conferences in the domain. He is member of the COSI consortium, at UJM his teaching activities cover Color and Multispectral Image Processing, and Computer Vision. Homepage: http://perso.univ-st-etienne.fr/tremeaua/.

INVARIANCE OF COLOR CONSTANCY MODELS TO COMPLEX LIGHTING CONDITIONS

Alain Trémeau[1]*, Felipe Cortes Jaramillo[1], Damien Muselet[1], Philippe Colantoni[1]

[1]*Université Jean Monnet – Laboratoire Hubert Curien - UMR5516, France*

*Corresponding author: Alain Trémeau, alain.tremeau@univ-st-etienne.fr

ABSTRACT

Color constancy is the ability of human vision to recognize a stable color in objects under varying lighting conditions. When it comes to computer vision, color constancy is not as accurate as in human vision. Computer vision aims at “seeing” and “understanding” visual data in order to provide decision-support for many applications. It is a multi-disciplinary approach which seeks to get closer to human visual perception and understanding in order to automate tasks that the human visual system can do. In this quest, colour constancy is a prevalent issue in every discipline associated with computer vision. The results of computer vision models deeply depend on the point of view and lighting conditions. The task of computational color constancy is to estimate the scene illumination and then perform the chromatic adaptation in order to remove the influence of the illumination and the camera sensor on the colors of the objects in the scene. Removing the influence of the illuminants, of the camera sensor, and of the optical effects is of primordial importance in computer vision to make sense of digital videos and images. This is how, for example, most digital cameras use color constancy methods in their camera Image Signal Processing (ISP) Pipeline. In this paper we will survey the most recent models/methods dealing with color constancy and will discuss the following research questions: - how might we make computer vision more robust against complex illumination/viewing conditions? - how to make materials/colors appearance, optical/photonics models consistent with human perception when using new image sensors (e.g. multispectral sensors) and display devices (e.g. AR/XR)? - how might we improve the deployment of smartphones and low-cost sensors in professional uses? We will also discuss some areas of improvements using machine learning methods.

Keywords: Color Constancy, Illumination Estimation, Color Correction, Multi-Views, Multi-Illuminants

INTRODUCTION

Color constancy is the ability of human vision to recognize a stable color in objects under varying lighting conditions. Usually, when we look at some objects the Human Visual System (HVS) [1, 2] unconsciously removes the influence of the lightning, then the color of the objects is perceived as if they were illuminated by a neutral white light. In computer vision, we can mimic this complex human system with different approaches that try to solve these under-constrained challenges related to the color constancy problem, and the solutions can be used in multiple fields like object recognition, tracking, color calibration, pattern recognition, etc.

Generally this problem is solved with a function ρ(x,y) depending on three important factors [3]: illuminant distribution I(x, y, λ), surface reflectance R(x, y, λ), and the camera sensitivity S(λ), where (x, y) is the pixel position and λ is the wavelength. See Figure 1. We can express this function for each RGB channel as, i.e., (Eq. 1):

$$\rho(x, y) = \int_{\lambda} I(x, y, \lambda) R(x, y, \lambda) S(\lambda) d\lambda \qquad (1)$$

If we assume that the scene is illuminated by a single light source and that the lighting field is uniform on the surface of the object, and that the surface is Lambertian and flat (i.e. R(λ) is constant whatever the pixel location), then the goal of color constancy is to estimate the light source color I(λ) independently of the pixel position. See Figure 2. In real world the lighting conditions are various, especially in indoor environment, so conventional approaches based on single illumination assumption cannot apply, see Figure 3.

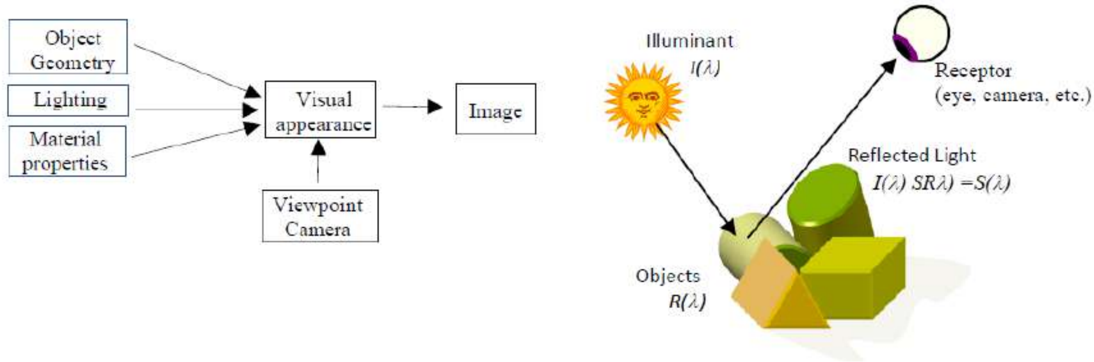

Figure 1: Visual appearance depends on geometry, materials reflectance, lights

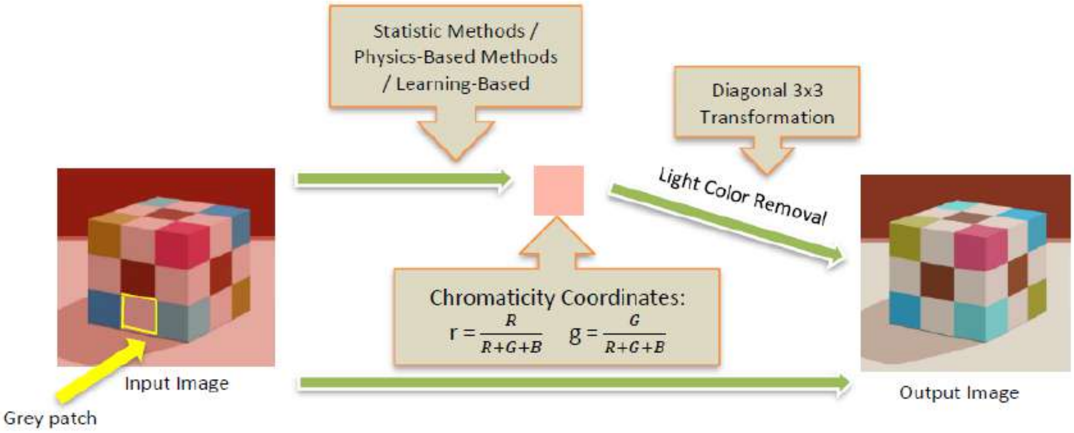

Figure 2: White balance of a scene lighted by a single illuminant based on the average grey computation. One solution consists to extract a grey patch, next to perform white balance from the color of this patch. Another solution consists to use a color chart, next to perform white balance from the colors of this chart.

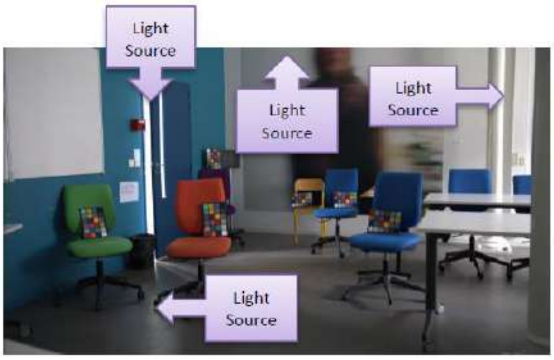

Figure 3: Example of scene lighted by various light sources (direct & indirect illumination). Six color charts are located in different areas (depths, orientations).

SHORT SURVEY OF THE STATE OF THE ART

Color constancy methods are generally classified into three main categories [3]: statistic-based, physics-based, and learning-based methods. The first group of solutions uses different low-level image statistics and empirical assumptions to achieve the color estimation, all of them can be unified with the framework proposed by van de Weijer et al. [4] as i.e., (Eq. 2):

$$\left(\int \left| \frac{\partial^n \mathbf{f}^\sigma(\mathbf{x})}{\partial \mathbf{x}^n} \right|^p d\mathbf{x} \right)^{\frac{1}{p}} = k\mathbf{e}^{n,p,\sigma} \tag{2}$$

where: n is the parameter (the order of the image structure) determining if the method is a Grey-World or a Grey-Edge algorithm; p (the Minkowski norm) determines the relative weights of the multiple measurements from which the final illuminant color is estimated. A high Minkowski norm emphasizes larger measurements whereas a low Minkowski norm equally distributes weights among the measurements; σ determines the scale of the local measurements. For first or higher order estimation, this local scale is combined with the differentiation operation computed with the Gaussian derivative.

Most of the grey patch -based methods do the assumption that to estimate the scene illumination, it is only required to extract one grey patch from the surface reference. However, in [5] it was proven that the prediction of a set of 19 patches (18 color and 1 grey among the 6 grey-level patches of the MacBeth color checker) from a reference surface is much more accurate in terms of light estimation and color correction. Considering that the illumination fields are not equally distributed in a scene (as example see Figure 4) and that they depend on multiple factors, we suggest to predict locally the color of these 19 patches in the scene using a deep learning -based approach, as if the color checker would have been there during the acquisition. Predicting multiple color checkers captured in the same image would enable to train a model able to predict illumination conditions, and to insert a synthetic color checker at any image location in order to prove that color pixel values change when we change color chart position.

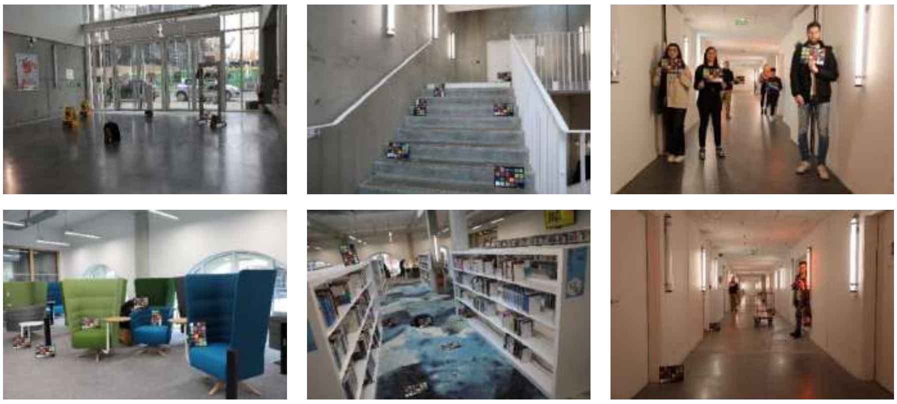

Figure 4: Examples of indoor images captured with the same Canon camera, taken under multi-illuminant conditions. In each image six color charts were put in various positions.

The second group of solutions exploits the dichromatic reflections principle and they require to detect grey surfaces, specularities, or segments from the image. As example, a segmentation-based method for mixed-illuminant scene images was proposed in [6]. On the other hand, a dichromatic reflection -based method for multiple illumination estimation was proposed in [7]. This method is based on a grayness index.

Lastly, the third group of solutions focuses on learning algorithm methods based on gamut mapping, patch-based approaches, or deep learning frameworks to model illumination estimation and related problems. One of the first paper addressing the problem of multiple illumination estimation was proposed in [8]. This paper is based on the concept of exemplar-based learning. It consists, first to apply a mean-shift segmentation of the input image (with unknown illuminant), next to generate surface models for each surface, then to find the nearest neighbour surface model in training surface models (from a dataset of images with known illuminants), and lastly for each nearest neighbour surface model to estimate the illuminant. Until recently most of state-of-the-art methods rely on single illuminant, complex features, and have long evaluation and training times. However, the paper proposed in [9] suggests a learning-based method based on four simple color features (average color chromaticity, brightness color chromaticity, dominant color chromaticity, and palette chromaticity mode), and an ensemble of regression trees (based on basic decision rules) to estimate the illumination. This method only works for a single illuminant but was extended to two illuminants in [10]. On the other hand, the CNN-based estimator, followed by a local-to-global regressor, approach proposed in [11] works for multiple illuminants. A multiple illuminant detector is used to determine whether or not the local estimates of the network must be aggregated into a single estimate. The GAN-based approach proposed in [12] incorporates a discriminator loss and a conventional color constancy loss. This method requires ground truth illumination data which may not be available in a common case. It does not need to estimate an illumination color map, as it is based on an image-to-image transformation. Another GAN-based approach was proposed in [13]. Using an image-to-image domain translation (domain transfer) learning approach this method estimates a multi-illumination probability map. The most relevant illumination estimation methods are based on pixel-wise approaches. Very recently, several pixel-wise / patch-by-patch approaches have been proposed in the literature, such as [14, 15, 16, 17]. Pixel-wise approaches are more efficient than patch-based methods to estimate illuminant conditions when multiple light sources illuminate the scene.

Another approach consists to “colorize” color images, as in [18], or to “white balance” color images, as in [19]. The colorization method proposed in [18] is based on training a deep neural network to learn the connection between the colors in an “improperly balanced” image and those in a “properly balanced” one. This method does not explicitly estimate the chromaticity of the illumination, however it handles spatially varying illumination conditions. The Automatic White Balance (AWB) method proposed in [19] is based on a camera imaging pipeline dealing with a small set of predefined white-balance settings. Given a set of rendered images, this method learns to estimate weighting maps to generate the final corrected image. This method does not require illuminant estimation. It generates spatially varying weighting maps that allows to correct for mixed lighting conditions in the captured scene.

To evaluate the accuracy of a color constancy method various standard metrics may be used [20, 21]: the Misclassification Rate, the Average or Median Angular Error (MAE), the Peak-Signal-to-Noise-Ratio (PSNR), the Root Mean Square Error (RMSE), etc.

ILLUMINATION ESTIMATION IN THE FIELD OF VR/AR/XR

Very few papers investigated chromatic characterization issues in VR, and color reproduction and calibration issues with VR. The first experiment done with a VR head mounted display (HMD), reported in [22, 23], consists of an indoor scene (office environment) rendered by the Unreal Engine (a gaming engine software). The office room contains matte and glossy objects, and two light sources: one on the ceiling, and a dimmer one at the back of the room. This study demonstrated that colour constancy performance in an immersive realistic VR environment is similar to what is reported for natural scenes. More investigations are necessary to extend the promising results obtained in the color vision domain with VR to the computer vision domain (to more realistic real-world scenarios) with AR and XR (as example see [24]).

Very recently, few image editing solutions based on Neural Rendering and Relighting (NeRF) have been proposed in the literature to estimate light sources and their direction in each pixel using implicit radiance fields, as for example in [25, 26, 27, 28]. With these solutions, it is now possible to insert virtual objects in an indoor or outdoor scene from a single color image and also to add or remove light sources. To the best on our knowledge till now none of these papers used explicitly these solutions for color constancy, but this would make sense.

COLOR CONSTANCY IN SPECTRAL IMAGING

Very few papers investigated the influence of camera spectral sensitivities (with varying spectral resolutions) and number of channels on color constancy. Some promising results were obtained in [29, 30]; in [30] the authors claimed that the spectral dimension is more important than the spatial dimension for estimating the illuminant white points. However, to the best on our knowledge, till now, spectral color constancy models were only developed for single illuminant case.

SHORT SURVEY OF COLOR CONSTANCY DATASETS

Very few real-world images datasets with multiple light sources have been proposed in the state of the art. One of the first datasets with real world images was introduced in [20]. It only contains 68 images (59 were taken in laboratory environments and 9 were real-world images) but it also contains their corresponding illuminations. The one proposed in [31] contains 197 images of faces taken with a varying number of color charts (most of images contains only one color chart) and captured with 4 different cameras. The MIMO public dataset introduced in [32] contains 58 indoor images (10 scenes, with complex scenes with multiple reflectances and specularities, lighted by 2 lights) and 20 outdoor images (with shadow, sun light, and in some cases with additional direct light); it provides pixel-level illumination images (for each light the illumination map is provided; images are taken with and without a color chart). This dataset was extended in [33] with high-resolution multi-view images (5 scenes acquired with 6 cameras) of complex multi-illuminant scenes (4 single-illuminant, 11 multi-illuminant, and 5 specular multi-illuminant) with precise reflectance and shading ground-truth. However, these data sets are both small and mainly consist of images of quite constrained single-object scenes [34].

The Cube++ illumination estimation dataset contains 4890 real world images (indoor and outdoor) with known illumination colors as well as with additional semantic data [35]. A Spyder cube color target (with white faces, grey faces, black patch and chrome ball) provides for every image two ground-truth illumination records covering different directions. In the dataset proposed in [36], the illumination for each scene was determined at once at many different points using a flying drone (carrying a grey ball); it contains multiple images (indoor and outdoor) taken from multi-view taken during the flight (150 images per scene, 30 scenes). According the authors “expanding the dataset further to include many more scenes would make it more useful for training machine learning methods; the range of illumination chromaticities could also be increased by recording scenes at sunrise/sunset, during different seasons, and different parts of the world”. The two equipment used to build these datasets are less convenient than the use of color charts; the use of only one Spyder cube can be insufficient to estimate complex illumination fields; the use of a flying drone can be too low to estimate rapid illumination changes.

The large-scale multi-illuminant (LMSI) dataset is the biggest dataset publicly available; it contains 7,486 raw format images of realistic scenes, captured with three different cameras (on more than 2,700 scenes), captured under two or three illuminants (natural light, indoor light) [37]. It provides the ground truth illumination map from multiple images of the same scene taken under different combination of the lights. For each scene, 3 Macbeth color charts were arranged in places that are well affected by each light source in the scene. Even though the LSMI dataset contains a variety of images with various lighting settings, the diversity is still limited compared to real-world lighting conditions. To evaluate the relevance of a deep learning architecture trained and tested, we suggest to use the LMSI dataset (as it is the biggest one) and to train the network from a subset of images (e.g. images acquired with the Sony camera) and to test the network from another subset of images (e.g. images acquired with the Samsung Galaxy camera), independently from the training step; we also suggest to use 3-fold cross-validation separating both training and testing sets by the number of unique scenes that we have in total.

The NUS-8 dataset contains 1736 outdoor and indoor images taken with 8 different high-end consumer cameras (approximately 250 images per camera) [38]. For each image, the coordinates of the color-checker put inside the image are provided, as well as small region masks for every color patch. The ground truth illuminants provided were obtained from the difference of the two brightest achromatic patches. Despite having only one color checker in the scene, this dataset can be used to compare the performance of illumination estimation methods with past approaches for predicting one single color estimation per scene. As with the LMSI dataset, we suggest to train single illuminant estimation networks from a subset of images (acquired with only one camera) and to test the network from another subset of images (acquired with another camera), independently from the training step; we also suggest to use 3-fold cross-validation separating both training and testing sets.

CONCLUSION

Traditional color constancy algorithms consist of two steps: light color estimation and color correction. Till recently, most of papers in the state-of-the-art proposed solutions to estimate the lightning condition under a single illuminant. Since few years, several papers (mainly based on machine learning methods) proposed solutions to face multi-lighting conditions. Some of these methods outperform others, but there is still a room for improvement. Firstly, the training process should be improved from a large and well-balanced images dataset. Secondly, a good trade-off should be found between the efficiency of a method and its computational cost (e.g. if we want to embark it on a camera ISP hardware). Lastly, a good trade-off should be found between the efficiency and the relevance of a global/local estimation method and a pixel-wise estimation method; this could be managed using additional loss functions.

There is still a lack of relevant color constancy datasets with pixel-wise ground-truth. Datasets with more realistic scenarios (including linear mixtures of light sources; shadows and specularities; mixing ambient, direct light and natural light; no fully controlled lighting conditions) and a higher number of images (including multi-view of the same scene, multi-images from various cameras, multi-illuminant) are still needed to train and test color constancy methods. More reliable ground-truth (i.e. accurate estimation of the illumination map, not a estimation from a grey sphere, color chart, chrome ball, uniform diffuse grey spray paint) is still needed, for outdoor images taken under daylight condition only, for images of indoor scenes captured under multi-illuminant, for outdoor images combining natural light and light sources. We assume that using several color charts could improve the local illumination estimation (depending on their location in a scene); it could also improve grey-patch -based methods and single color chart -based methods when dealing with multi-illuminant. The first experiments we did confirmed this assumption; we created a new dataset satisfying the conditions above (as examples see images shown in Figures 4 and 5) in order to perform our evaluations. As future work, we will increase the number of real-world images (of acquisitions from various cameras and viewing directions) in this dataset before making it publicly available.

Figure 5: Outdoor images captured with the same Canon camera, taken under multi-illuminant conditions (eg. shadows, daylight shifts, etc.). In each image six color charts were put in various positions and distances to the camera.

In computer vision, in some study cases, color changes induced by shadows and illumination fields (as illustration see Figure 6) can impact object detection and tracking in videos, 3D scene analysis and understanding, 3D pose trajectories estimation of moving objects, etc. However, thanks to the progress made in the computer vision domain after the start of the deep learning area, many computer vision tasks (such as human body pose detection in complex lighting environments) are nowadays robust to illumination changes, shadows, object's reflectance, etc. Color constancy and illumination estimation are nowadays less problematic for computer vision tasks, up to complex situations involving multi-views and multi-illuminations.

Figure 6: (top images) Indoor images of the same scene captured from various points of view using a set of GoPro cameras, (bottom images) Indoor images of the same scene captured from the same point of view. From left to right different light sources have been used to make the multi-illumination estimation (resp. object detection) more challenging.

ACKNOWLEDGEMENT

This work was partially supported by HORIZON-CL2-2021-HERITAGE-01-04 grant. Project: 101061303 — PREMIERE.

REFERENCES

1. Agarwal V., Abidi B. R., Koschan A., *et al*. (2006). An overview of color constancy algorithms, *Journal of Pattern Recognition Research*, vol. 1, no. 1, pp. 42–54.
2. Laakom F., Passalis N., Raitoharju J., *et al*. (2020). Bag of color features for color constancy, *IEEE Transactions on Image Processing*, vol. 29, pp. 7722–7734.
3. Das P., Liu Y., Karaoglu S., Gevers T. (2021) Generative models for multi-illumination color constancy, *IEEE/CVF International Conference on Computer Vision*, pp. 1194–1203.
4. van de Weijer J., Gevers T., and Gijsenij A. (2007) Edge-based color constancy, *IEEE Transactions on Image Processing*, vol. 16, no. 9, pp. 2207–2214.
5. Dubuisson I., Muselet D. *et al.* (2022) Predicting the colors of reference surfaces for color constancy, I*EEE International Conference on Image Processing*, pp. 1761–1765.
6. Hussain M., Sheikh Akbari A. (2018) Color Constancy Algorithm for Mixed-Illuminant Scene Images. *IEEE Access*. 6. 1-1. 10.1109/ACCESS.2018.2808502.
7. Qian Y., Nikkanen J., Kämäräinen, J. Matas J. (2019) On Finding Gray Pixels*, IEEE/CVF Conference on Computer Vision and Pattern Recognition (CVPR): 8054-8062.*
8. Joze H.R., Drew M.S. (2014) Exemplar-Based Color Constancy and Multiple Illumination. *IEEE Trans Pattern Anal Mach Intell*. 36(5):860-73. doi: 10.1109/TPAMI.2013.169.
9. Cheng D., *et al.* (2015) Effective learning-based illuminant estimation using simple features, *IEEE Conference on Computer Vision and Pattern Recognition* (CVPR), pp. 1000-1008.
10. Cheng D., *et al.*. (2016) Two Illuminant Estimation and User Correction Preference, *IEEE Conference on Computer Vision and Pattern Recognition* (CVPR), pp. 469-477.
11. Bianco S., Cusano C., *et al.* (2017) Single and Multiple Illuminant Estimation Using Convolutional Neural Networks, *IEEE Trans. on Image Processing*, vol. 26, 9, pp. 4347-4362.
12. Sidorov O. (2019) Conditional GANs for Multi-Illuminant Color Constancy: Revolution or yet Another Approach? *IEEE/CVF Conference on Computer Vision and Pattern Recognition Workshops (CVPRW)*, pp. 1748-1758, doi: 10.1109/CVPRW.2019.00225.
13. Das P., Liu Y., Karaoglu S. and Gevers T. (2021) Generative Models for Multi-Illumination Color Constancy, *IEEE/CVF International Conference on Computer Vision Workshops* (ICCVW), pp. 1194-1203. doi: 10.1109/ICCVW54120.2021.00139
14. Domislović I., *et al.* (2023) Color constancy for non-uniform illumination estimation with variable number of illuminants. *Neural Comput. & Applic.* 35, pp 14825–14835.

15. Wang F., Wang W., Wu D., *et al.* (2022) Multi illumination color constancy based on multi-scale supervision and single-scale estimation cascade convolution neural network. *Frontiers in Neuroinformatics*, 16. 953235. 10.3389/fninf.2022.953235.
16. Li S., Wang J., Brown M., Tan R. (2022) TransCC: Transformer-based Multiple Illuminant Color Constancy Using Multitask Learning, 10.48550/arXiv.2211.08772.
17. Hemrit G., Meehan J. (2022) Revisiting and Optimising a CNN Colour Constancy Method for Multi-Illuminant Estimation, 10.48550/arXiv.2211.01946.
18. Zhu L., Funt B. (2018) Colorizing Color Images, *IS&T Int'l. Symp. on Electronic Imaging: Human Vision and Electronic Imaging*, pp 1-6.
19. Afifi M., Brubaker M. A., Brown M. S. (2022) Auto White-Balance Correction for Mixed-Illuminant Scenes, *IEEE/CVF Winter Conference on Applications of Computer Vision (WACV),* pp. 934-943, doi: 10.1109/WACV51458.2022.00101.
20. Gijsenij A., Lu R., Gevers T. (2011) Color Constancy for Multiple Light Sources, *IEEE Transactions on Image Processing*, 2011. 21, pp 697-707. 10.1109/TIP.2011.2165219.
21. Hao X., Funt B., Jiang H. (2019) Evaluating Colour Constancy on the new MIST dataset of Multi-Illuminant Scenes, *Color Imaging Conference*, pp 108-113.
22. Gil Rodriguez R., Toscani M., Guarnera D., *et al.* (2020) Color constancy in a Virtual Reality environment. *Journal of Vision*, 20 (11):1226. https://doi.org/10.1167/jov.20.11.1226.
23. Gil Rodriguez R., Bayer F., Toscani M., *et al.* (2022) Colour Calibration of a Head Mounted Display for Colour Vision Research Using Virtual Reality. *SN Computer Science*. 3, 10.1007/s42979-021-00855-7.
24. Murdoch M. J. (2022) Keynote: Color from Real Reality to Extended Reality, *3rd International Symposium for Color Science and Art*, Tokyo Polytechnic University (Online).
25. Li Z., Shafiei Rezvani Nezhad M., *et al.* (2020). Inverse Rendering for Complex Indoor Scenes: Shape, Spatially-Varying Lighting and SVBRDF From a Single Image. *IEEE/CVF Conference on Computer Vision and Pattern Recognition* (CVPR), pp 2472-2481.
26. Li, Z. *et al.* (2022). Physically-Based Editing of Indoor Scene Lighting from a Single Image. *European Conf. on Computer Vision (ECCV). Lecture Notes in Computer Science*, vol 13666.
27. Weber H., Garon M., Lalonde J.F. (2022) Editable Indoor Lighting Estimation. *European Conference on Computer Vision (ECCV),* 10.48550/arXiv.2211.03928. 2022.
28. Reza Karimi Dastjerdi M., Eisenmann J., *et al.* (2023) EverLight: Indoor-Outdoor Editable HDR Lighting Estimation, *IEEE/CVF International Conference on Computer Vision* (ICCV).
29. Ahmad Khan H., Thomas J. B., Hardeberg J. Y., Laligant O. (2017) Illuminant estimation in multispectral imaging. *Journal of the Optical Society of America A*. 34. 1085.
30. Koskinen S., Acar E., Kämäräinen J.K. (2023) Single Pixel Spectral Color Constancy. *International Journal of Computer Vision*. Pp 1-13,10.1007/s11263-023-01867-x.
31. Bianco S., Schettini R. (2014) Adaptive Color Constancy Using Faces. *IEEE Trans. Pattern Anal. Mach. Intell.* 36(8): pp 1505-1518.
32. Beigpour S., Riess C., van de Weijer J., *et al.* (2014) Multi-Illuminant Estimation With Conditional Random Fields, *IEEE Trans. on Image Processing*, vol. 23, no. 1, pp. 83-96.
33. Beigpour S., Ha M., Kunz S., Kolb A., Blanz V. (2016) Multi-view Multi-illuminant Intrinsic Dataset. *British Machine Vision Conference*, pp 10.1-10.13, 10.5244/C.30.10.
34. Laakom F., Raitoharju J., Nikkanen J., Iosifidis A., Gabbouj M. (2021) INTEL-TAU: A Color Constancy Dataset. *IEEE Access*. pp. 1-1. 2021,10.1109/ACCESS.2021.3064382.
35. Ershov E., Savchik A., Semenkov I., *et al.* (2020) The Cube++ Illumination Estimation Dataset, *IEEE Access*, pp (99):1-1, 10.1109/ACCESS.2020.3045066
36. Aghaei H., Funt B. (2020) A Flying Gray Ball Multi-illuminant Image Dataset for Color Research. *Journal of Imaging Science and Technology*. 64. 50411-1.
37. Kim D., Kim J., Nam S., Lee D., *et al.* (2021) Large scale multi-illuminant (lsmi) dataset for developing white balance algorithm under mixed illumination, *IEEE/CVF International Conference on Computer Vision*, pp. 2410–2419.
38. Cheng D., Prasad D. K., Brown M. S. (2014) Illuminant estimation for color constancy: why spatial-domain methods work and the role of the color distribution, *Journal of the Optical Society of America A*, vol. 31, no. 5, pp. 1049–1058.

On why the nature of color is spatial

Alessandro Rizzi

Abstract

Everybody knows the spatial nature of color and how its appearance can change as context changes. We usually think about color in the same way we measure color, but our visual system is not a spectrophotometer and the world we look at is observed in a context, whatever it could be. Nevertheless, in our mind color is mainly pointwise, and we are used to think at it like a physical quantity. But it is not. Color is formed and exists only in our brain, not at the point or on the surface.

This talk aims at discussing these two alternative approaches, starting from the biological bases of our vision. It reviews some old and new experimental findings on how color sensation is formed in our visual system. From these sets of data, it emerges not only the spatial nature of color, but most important, how this is a mandatory characteristic that has developed to overcome the optical limitations of the human eye. Our visual system has come up with smart methods to extract as much visual information as possible, given the constraints of the visual input. It therefore appears that the next challenge in color science is to incorporate the spatial nature of color in all future metrics and to move from the color at the point to the chromatic appearance in everyday contexts.

Biography

Alessandro Rizzi is Full Professor at the Computer Science Department of the University of Milano. He is researching since 1990 in digital imaging with a particular interest on color, visualization, photography, HDR. He is Senior Editor of Color Research and Applications and Associate Editor of Journal of Electronic Imaging. He has been Topical Editor of the Journal of Optical Society of America A, Secretary of CIE Division 8, IS&T Fellow and Vice President. In 2015 he received the Davies medal from the Royal photographic Society.

Cone Fundamentals, Colour Matching Functions and Individual Differences

Andrew Stockman

Abstract

Colour perception depends on a complex sequence of serial and parallel processes but at its initial stage it is relatively simple. At its input it depends on the activations of just three photoreceptor types: the long- (L), middle- (M) and short- (S) wavelength-sensitive cones, each of which responds to light univariantly (i.e., with regard only to the number of photons absorbed). Consequently, a knowledge of how well each type responds to different wavelengths—the three cone spectral sensitivities—allows us to predict pairs of lights that should appear the same to the normal or "standard" human observer. The CIE has sanctioned the cone spectral sensitivity estimates of Stockman and Sharpe (2000) and their associated measures of luminous efficiency (Sharpe et al., 2005, 2011) as "physiologically-relevant" standards for colour vision (CIE, 2006). These discrete tabulated cone spectral sensitivities—often referred to as "cone fundamentals"—are specified for 2 and 10-deg vision for the mean "standard" observers with wild-type (normal) photopigment genotypes and with average ocular transparencies. The LMS fundamentals can be easily transformed into colour matching functions (CMFs) for any other sets of primaries, such as XYZ (CIE, 2015) or RGB.

While it is important to be able to define the mean CMFs, it is becoming increasingly important in colour applications to be able to predict the CMFs of individual observers many of which differ substantially from the mean functions. Partly to facilitate this computationally, we have developed formulae that account for the three cone spectral sensitivities, their underlying photopigment spectra and the macular and lens pigment optical density spectra as continuous functions of wavelength from 360 nm to 850 nm with minimal error. These continuous functions enable individual differences to be easily calculated and allow the straightforward generation of non-standard cone spectral sensitivities (and other colour matching functions) with different macular, lens and photopigment optical densities, and with spectrally shifted L- and M-cone photopigments such as those found in red-green colour vision deficient observers. In a recent series of experiments, we have successfully used these continuous functions to analyse colour matching data obtained with a new 11-primary LED-driven colour matching device (LEDMax) and have been able to identify the causes of the individual variations in the matches.

References: Stockman and Sharpe, Vision Research (2000) 40, 1711-1737. Sharpe et al., Journal of Vision (2005) 5, 948-968; Color Research & Application (2011) 36, 42-46. CIE (2006) 170-1:2006; (2015) 170-2:2015.

Biography

Andrew Stockman is the Steers Professor at the Institute of Ophthalmology at University College London and is a part-time Qiushi Chair Professor at the College of Optical Science and Engineering, Zhejiang University. His research areas include color vision, rod vision, visual adaptation, temporal sensitivity, and clinical psychophysics. He may be best known for his work with Ted Sharpe on spectral sensitivities and luminous efficiency. He runs the widely used colour database at http://www.cvrl.org and is Editor-in-Chief of Color Research and Application. In 2016 he received the Colour Group GB Newton medal, and in 2018 the Inter-Society Color Council Macbeth Award.

Can we change the colour education to an attractive and inspiring choice of subject in design and architecture?

Berit Bergström

Abstract

What can we do to inspire, engage, and increase interest in colour knowledge and education? Colour education must be more than just learning the colour theories. We need more practical training and assignments where colour theory is put into practice to understand the importance of colour knowledge. We must deepen the knowledge of colour to become more practical and hands on. The colour of an object is not constant. It changes depending on among other things, the observation situation, viewing distance, surrounding colours and lighting conditions. We should highlight colour as an important design factor for creating good environments and products for people. Colour is a crucial design factor that affects spatiality, function, and aesthetics.

Colour is one of the strongest factors in the experience of a building, a room, or a product. Colour and light are so obvious, they are just there, and we take them for granted. We trust that the architect, designer and colourist have a genuine knowledge of the impact of colour on us humans and how colour affects the perception of the building and the room. This applies to both the aesthetic experience and the function of the colour. We need beautifully coloured environments to feel good and we also need the colour's ability to distinguish and clarify our surroundings, for example to facilitate orientation in a building.

The background of my lecture is the importance to spread the knowledge and experience that exists in the science of colour. It can provide both support and inspiration for colour choices and selection in colour schemes and design, of both products and the colouring of our surroundings and finally colour education. Colour education can develop creative environments where creativity, communication, and exchange of experiences between different disciplines are the central point. In this respect, colour science is unique in the field of education. There is no other branch of science which concerns so many different disciplines and can involve students in working together with colour in the same creative project but from different starting points.

The lack of colour education: How can you use colour to create the feeling that you strive for in different environments? Unfortunately, at many of our design and architecture schools around the world, colour has taken on a secondary importance. You like to think that colour doesn't need to be learned anything about "because it's so easy to choose a colour on a product or a house; it is just to pick a colour". Colouring is much more complicated than that. Spatial design is a complex task with many different factors that have to be considered and work together to get the desired effects in a room. The old knowledge of colour is disappearing because the teaching of colour and colour and lighting is no longer compulsory in architectural and design programs. Colour teaching is also an important factor in creating interest in further colour research!

In nature's there is a natural and appreciated flora of colour and light contrasts. Colours and contrasts that touch our senses. Can we find this variation in our built environments? Very often we find office rooms with grey floors, beige walls, white ceilings, dreary furnishings, and lack of accents that

catch your eyes; this creates a lack of engagement. We need more knowledge and inspiration to create a consistent and harmonious colour scheme which will be used for clarifying functions and underscoring different types of information.

Biography

Berit Bergström is a Colour Specialist & Educator in colour theory and colour scheme working in her own business, Berit ColourTalks, since 2016. She was employed by NCS Colour AB from 1990 to 2016. She was the Managing Director for NCS Colour Academy between 1991 and 2012. She has long experience of giving international colour design courses and presentations and has conducted colour studies at university level worldwide for more than 30 years. This has newly resulted her new book "Colour Choices. A practitioner's guide to designing colour schemes" in both English and Swedish. She was the secretary of the Colour Science Foundation (1991-1997) and was responsible for granting funding for different colour research projects within the field of colour. She is the secretary of the Swedish Colour Centre Foundation since 1991. She has been a member of the AIC Executive Committee between 2006 – 2021. She was the President of AIC 2010 to 2013 and the chairperson of the AIC Study Group on Colour Education between 1998 and 2009.

CAN WE CHANGE THE COLOUR EDUCATION TO AN ATTRACTIVE AND INSPIRING CHOICE OF SUBJECT IN DESIGN AND ARCHITECTURE?

Berit Bergström

Berit Bergström, Swedish Colour Centre Foundation/NCS Colour AB, Stockholm, Sweden
Berit Bergström, e-mail: bergstrom.berit@gmail.com/beritcolourtalks@gmail.com

ABSTRACT

What can we do to inspire, engage, and increase interest in colour education and knowledge? Colour education must be more than just learning the colour theories. We need more practical training and assignments where colour theory is put into practice to understand the importance of colour knowledge. We must deepen the knowledge of colour to become more practical and hands on. The colour of an object is not constant. It changes depending on the actual conditions. We must highlight colour as an important design factor for creating good environments and products for people. Colour education is about our colour perception, colour communication, the colour design process, significance of colours, colour changes and a lot of practical colour exercises and practical colour projects. To learn different ways of working and using colour in the way you experience colours.

Keywords: colour education, colour communication, colour design process, colour pedagogy.

INTRODUCTION

The Importance of Colour in the Design of our Surroundings

Colour is one of the strongest factors in the experience of a building, room or product. Colour and light are so obvious, and they are just there, and we take them for granted. We trust that the architect, designer and colourist have a genuine knowledge of the impact of colour on us humans and how colour affects the experience of the building and the room. This applies to both the aesthetic experience and the function of the colour. We need beautifully coloured environments to feel good and we need the colour's ability to distinguish and clarify our surroundings, for example to facilitate orientation in a building.

The Lack of Colour Education

Unfortunately, at many of our design and architecture schools around the world, colour has taken on a secondary importance. You like to think that colour doesn't need to be learned anything about "because it's so easy to choose a colour on a product or a house; it is just to paint the house". Colouring is much more complex than that. Spatial design is a complicated task with many different factors that must work together to get the desired effects in a room. How can you use colour to create the feeling that you strive for in different environments, on products etc.? The old knowledge of colour is disappearing because the teaching of colour and colour and lighting is no longer compulsory in architectural and design programs. Colour teaching is also an important factor in creating interest in further and more colour research!

THE IMPORTANCE OF CONSTRUCTIVE AND CREATIVE COLOUR EDUCATION

Colour education can develop creative environments where creation, communication and an exchange of experiences between different disciplines are the central point. In this respect, colour science is unique in the field of education. There is no other branch of science which concerns so many and can involve students in working together with colour in the same creative project but from different starting points. Colour education is about perception, communication, compositions, associations, colour changes and a lot of practical colour exercises and practical colour projects. A good colour scheme in the built environment is often considered to be of minor importance. This is sometimes because of a lack of insight of the importance and weighty arguments for pushing through the scheduled colour scheme proposal. The colour question can also be neglected because it has not been timed in the construction planning process.

Colour Perception – a mental phenomenon

"What is colour?" is a good question when starting the colour education. The word colour can mean pigment, paint, wavelength energy, chromatic surface among other things. Colour can be unequivocally defined, if you make clear in what sense you are using the word. A strict combination of pigments can give a paint which can be reproduced repeatedly. A spectral reflection curve can convey a full description of the reflective properties of the painted surface. The visual colour impression created by that surface is a different matter. The subjective observation, however, must be viewed as the primary meaning since colour only exists as a mental phenomenon. A colour is what it looks to be and nothing else. Accordingly, man's perception of colour has played the principal role for putting all colours into a system. Colours are created in the psyche, in the very moment *we perceive them*, and as long as *we look at them*. It is important in colour science to distinguish between physical colour (physics) and perceptual colour (psychology), what we see as colour.

Colour Communication – the need for a colour language

In the past, when the paint materials were made of plants and minerals, the colour scale was very limited. Objects received the natural colour scale, which were determined by the availability of natural pigments found in nature. Today we have access to a much larger range of colours. The increasing use of colour in every imaginable context has created a need for clear verbal and written communication about colours – not just their chemical and physical properties, but what they look like, how you perceive them. Several colour systems and colour atlases have been developed in response to this need. In a colour system based on physical properties of the colour material, the colours are ordered. They can be ordered according to the quantity of pigment included or the composition of the reflective radiation.

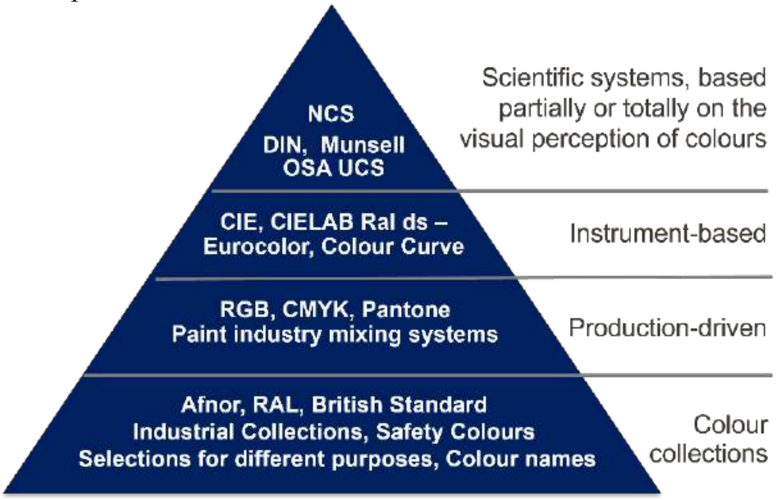

Figure: The colour pyramid shows the most common systems and their uses. At the top we find visually-based systems followed by instrument-based systems. Then we find production-driven systems and at the bottom colour collections.

The visually-based systems are the ones that facilitate communication in different contexts like the NCS system which is based entirely on the way in which human beings see and perceive colours. People choose colours by the look of them. The way in which a colour is mixed, or its physical quantitative data are, for the most part, only of interest to producers and manufacturers.

The NCS colour notation represents a specific colour percept and says nothing about what pigments, light rays or nerve signals that give rise to this perception. NCS will be used in colour communication in this presentation.

The Colour Design Process – colour choices and compositions

A visual colour system helps us to study the expressive potential of different colour compositions. The concept of different colour categories indicates that several colours are perceived as similar in one way, although they may in another way be very different.

Colour categories: NCS Colour Category Scheme divides the world of colour into 8 hue categories (vertical) and 7 nuance categories (horizontal), giving a total of 56 characteristic colour fields. This gives possibilities of identifying characteristic similarities and relations between colours and referring all the colours of the colour space to a limited number of colour categories.

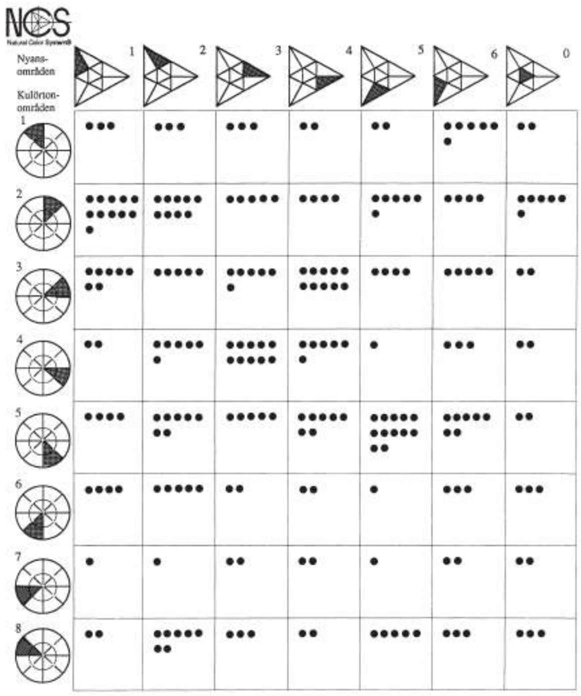

Figure: With the NCS Colour Category Scheme you can easily find the distribution of colours in a colour range. Here is a sewing thread colour range analysed. (Bergström 2008)

This way of placing and arranging the colours can be used to sort and analyse a colour selection for a product or a collection, such as ceramic tiles, knitting wool, or cosmetics. You can see in which colour areas colours are lacking and in which ones there is already a good distribution or too many colours. Is it necessary to have so many colours right here? Which nuances and hues are the most common? Which colours serve as markers or exclamation marks, and which break out of an otherwise coherent pattern?

Colour similarities: Studying the NCS Colour Space, one finds a number of properties which are easily identifiable as similarities in hue, nuance, blackness, chromaticness, whiteness, saturation, lightness, and complementary colours. One can easily study how these similarities between the colours affect the expressive quality of a colour composition. These visual colour attributes have become important tools in the colour design process. Swedish research studies (Hård/Sivik 2001 & Sivik/Hård 1994 & Sivik/Hård 1989) have found that compositions of colours with one or more of these NCS similarities also tend to be more highly appreciated (more harmonious) than others.

With a visual colour system you can quickly find these harmonious colour combinations which can bring some order to the infinite number of possible combinations of colours. It does not take away intuition or creativity, which needs some systematically way of working when investigating different colour combinations. A colour system does not necessarily give pretty colour combinations, but it does provide a tool for experimenting with different colour harmonies.

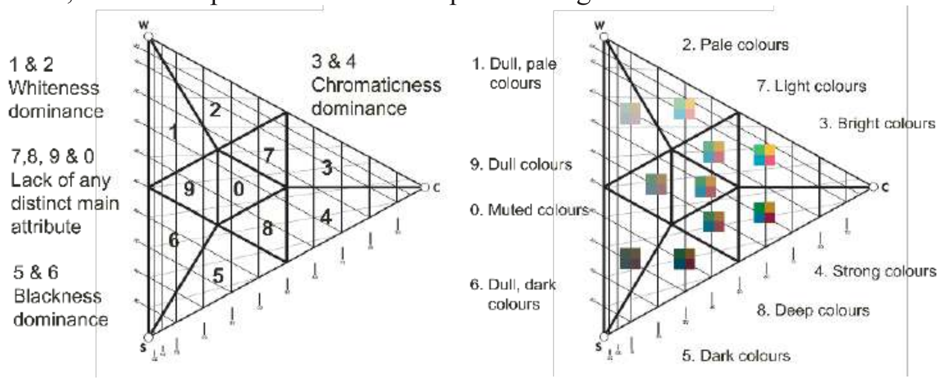

Figures: The different nuance categories shown in the triangle and a verbal description of nuance colour areas (Green-Armytage P. & Bergstrom B. 2018.)

Lightness contrast: Lightness or contrasting lightness is highly important in the patterning context. Great contrast in lightness gives a clearly distinguishable pattern and a small difference in lightness makes for an indistinct pattern. A great difference in lightness between the colours in a pattern makes for a distinctly articulated pattern. To determine the lightness position of a colour, one compares it with a reference scale of lightness, usually a series of colour samples from white to black (greyscale). By placing the chosen colour sample side by side with the different grey samples on the reference scale one sees the boundary between the samples appearing more or less clearly, depending on which sample on the reference scale one includes in the comparison. Where the boundary is least distinct, we have the lightness or contrast position.

Significance of colours – associations & human impact

What do we associate with different colours? Which colours appeal to us in certain connections? What effect does the colour of a room have on people in it? How are we affected by colours? Which colours are "good for us" in hospital wards, waiting rooms and workplaces? Can the colour design support older people's ability to orient themselves? There are many questions to be asked, but are there any straightforward answers to them? One thing is clear: colour makes an important difference to our surroundings, as witness all that is said and written about it in the media. Colour is a popular subject which seems to interest everybody. Unfortunately, there are many beliefs about how colours affect us, but many of these does not hold up for a scientific review. All colours cannot be investigated, most of them can be answered by common sense.

In our nature there is a natural and appreciated flora of colour and light contrasts. Colours and contrasts which touch our senses and are self-evident in our nature. Nature's different colour scales and seasons in colours create different feelings. A richness and variety of colours that we all value highly. If you compare this with our constructed environments – can we find this variation that we need?

Human impact in workspaces: Very often we find office rooms with grey floors, beige walls, white ceilings, dreary furnishings, and lack of accents that catch your eyes; this creates a lack of engagements. We also need windows which create a sense of freedom and space. In public spaces where many people must get on together under similar conditions, a balance needs to be struck between a calm, harmonious background and more colourful room elements and furnishing details. We need more knowledge and inspiration to create a consistent and harmonious colour scheme which can be used for clarifying functions and underscoring different types of information. Colour and contrasts that we so badly need to function and feel good in our environments.

Caring environments: Several international studies emphasize the relationship between quality of life and a thoughtful design for the elderly. The way the rooms are planned, the sound environment and the choice of lighting and colour scheme are just a few factors that have a major impact on well-being and quality of life, not least for people with dementia. A sufficient lightness- and colour contrast in the interior is a thoughtful colour scheme that will facilitate orientation, recognition and attention. The colouring of the patients' doors, for example, demands attention and leads people in the right direction, at the same time as staff doors are "camouflaged". A good lightness contrast between wall and flooring and most colours that meet in a room should have different light contrast to be seen in their surroundings. A well-thought-out environment can help to reduce anxiety.

Changeability of Colour Impressions

The colour of an object is not constant. It changes depending on the observation situation, viewing distance, surrounding colours, light conditions etc. Everyone is doubtless aware of the difference between the small colour sample and the way the colour "turned out" when the paint is applied on an entire wall in a room. Then the saying usually goes, "that colour is not the colour I thought it would be". The colour of the sample and the resulting colour of the wall is not the same.

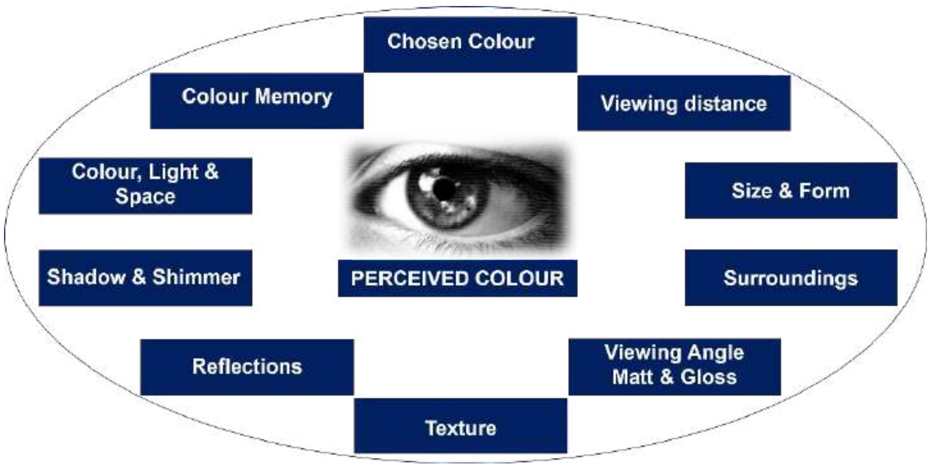

Looking at an object, we perceive it as having a particular colour. We ascribe to objects colours which we normally see in them, colours which we regard as constant and unaffected by outward circumstances, and which are here referred to as the inherent colour of objects, i.e., the "true" colours of objects, colours which can be established in a standardised viewing situation or with a colour measuring instrument. The changes we can nevertheless see are called wrong, because it is the colours we see, and are often called optical illusions. Understanding of these phenomena is made easier by thinking of colour as what we see, and thus incapable of being an optical illusion. To avoid misunderstandings, we distinguish between inherent colour and perceived colour. Inherent colour can also be termed local, material, or nominal colour.

Practical Colour Exercises and Projects

The whole colour education program for the students should combine an informative lecture and several practical exercises about the actual subject. The program should be completed with an overall colour project where they can use the new colour knowledge and understand how it can be used in their future professional practice. Then you get a better understanding and insight how important it is to practice the colour issues and what colour can accomplish in a professional design process.

Colour analysis: An inspiring and learning colour exercise or project is to analyse colours and colour combinations. You can analyse historical colours in genuine environments where we have a good representation of historical colours. The NCS System can be used to analyse the colours and to find the typical colour areas for different time periods. You can analyse how colours change in distance, analyse a colour scale you like and so on. Visual assessments can be made through comparison with colour samples parallel with a wireless colour reader/scan.

CONCLUSION

Above all my paper is intended to inspire, engage and increase interest in colour education, but also to deepen the knowledge about colour and show the importance of colour knowledge. It will highlight colour as an important design factor in creating good environments and products for people. Colour is a valuable design factor that affects spatiality, function and aesthetics. How can I use colour to get the desired effects on my product or my surroundings? What should I keep in mind? How can colours work together to create a harmonious overall experience of a building or a product? During my presentation a lot of inspiring and creating projects will be showed.

REFERENCES

1. Bergstrom, B. (2022). *Colour Choices: A practitioner's guide to designing colour schemes.* Studentlitteratur AB, Lund, Sweden.
2. Bergstrom, B. (2008). *Colour Choices – A practitioner's guide to colour scheming and design.* Forskningsrådet Formas T7:2008, Stockholm, Sweden.
3. SS 19102:2022 (2022). *NCS Colour Atlas.* SIS, Swedish Institute for Standards, Stockholm, Sweden.

Further reading:

4. Bergström B. & Sivik L (2013) *Colour Harmony or not.* Proceedings of the 12th Congress AIC 2013, 8-12 July 2013, Newcastle upon Tyne, UK, edited by Lindsay MacDonald, Stephen Westland and Sophie Wuerger. ISBN 978-0901623027. Organizer: The Colour Group (Great Britain), 417-420.
5. Hård A. & Sivik L. (2001) *A theory of colors in combination – A descriptive model related to the NCS Color Order System.* An offprint from Color Research & Application, Volume 26, No 1, 4-28.
6. Hård A. & Sivik, L. & Tonnquist G. (1996) *Natural Color System-from Concept to Research and Applications. Part I and Part II.* Color Research & Application, Volume 21, No 3.
7. Sivik L. & Hård A. (1994) *Some Reflections on Studying Colour Combinations*. Color Res. App. 19, 286-295.
8. Sivik L. & Hård A. (1989) *On studying Color Combinations. Some Reflexions and Preliminary Experiments*, Göteborg Psychological Reports 19, No 2.
9. Sivik L. & Taft C. *(1989) Semantic Variables for Judging Color Combinations: An Analysis of Semantic Dimensions*, Göteborg Psychological Reports 19, No 5.

The Concept of Cesia (Visual Appearance other than color): Antecedents, Development, and Applications

Jose Luis Caivano

Abstract

Cesia is the name given to the visual perception of different spatial distributions of light. It encompass sensations of transparency, opaque appearance, translucency, matte appearance, gloss, mirrorlike appearance, etc., in addition to sensations of lightness and darkness (which are the direct link between cesia and color). Cesia and color are complementary to each other. In short terms, we could define color as the visual perception of the different spectral distributions of light. A parallelism can be noted in both definitions: spectral properties of light, in one case, spatial distribution of light, in the other.

While color sensations span from red/green and blue/yellow oppositions (in terms of hue), from grays to vivid or saturated colors (in terms of chromaticity or saturation), and from light to dark (in terms of lightness), cesia sensations span from transparent to opaque (in terms of the perceived permeability to light), from diffuse to regular or clear (in terms of perceived diffusivity), and also from light to dark (in terms of darkness, as we call the variable that cesia shares with color). Hence, all the appearances included in color and cesia combined can be defined by five dimensions: the classical three color variables plus permeability and diffusivity. There are, thus, five kind of scales that can be developed. We may think in the CIELAB color space (or any other 3D color space) being expanded with the additional dimensions of permeability and diffusivity; or either in the CIE chromaticity diagram (or any color circle) being expanded with the dimensions of lightness, permeability and diffusivity. Any color may appear as a transparent layer or volume, which can vary between crystal clear and translucent or turbid media. Colors may also appear as opaque surfaces, either with matte or glossy finish, which can even reach a mirrorlike appearance (with maximum gloss). And all these appearances may occur at different levels of darkness.

The presentation will make a basic chronological survey of antecedents of the concept, with bibliographical references to authors who have dealt with these aspects of visual appearance before the name "cesia" was proposed to designate them. After that, a brief review of the developments that started after the adoption of that term will follow. Here, a recent proposal for the amplification of the concept of cesia will be explained, which is intended to include also primary sources of light. We originally considered that cesia was only applied to secondary sources of light, those that absorb, reflect or transmit light coming from primary sources. But a recent doctoral thesis by an author who have greatly contributed to the development of cesia, has made the point that some primary sources (extended ones) can also be perceived in particular cesias. And finally, some applications or uses of the concept by different authors will be shown in different fields: visual arts, architecture, design (graphics, textiles, fashion), sensory evaluation of food, etc.

Biography

Dr. Jose Luis Caivano is a research fellow at the National Council for Research, Argentina, and professor at Buenos Aires University, in the School of Architecture, where he also leads the Color Research Program. He holds a degree in architecture, a PhD in theory and history of art, and the highest category in the national research system of Argentina. He was a research associate at the Center for Language and Semiotic Studies, Indiana University, United States, president of the International Color Association (AIC), the International Association for Visual Semiotics (IASV), and the Argentine Color Group (GAC). Caivano has been appointed as honorary member of Ad Chroma (France), the Portuguese, and Mexican Color Societies. He serves in the editorial board of various international journals and is a senior editor of Color Research and Application. He has more than 190 publications, most of which are freely available at https://colorysemiotica.wordpress.com/publicaciones/

THE CONCEPT OF CESIA (VISUAL APPEARANCE OTHER THAN COLOR): ANTECEDENTS, DEVELOPMENT AND APPLICATIONS

José Luis Caivano

Universidad de Buenos Aires, and Conicet (National Council for Research), Argentina

caivano@fadu.uba.ar

ABSTRACT

Cesia is the name given to the visual perception of different spatial distributions of light. It encompass sensations of transparency, translucency, opaque and matte appearance, gloss, mirrorlike appearance, etc., in addition to sensations of lightness or darkness. Cesia and color are complementary to each other. We could define color as the visual perception of the different spectral distributions of light. A parallelism can be noted in both definitions: spectral properties of light, in one case, spatial distribution of light, in the other. While color sensations span from red/green and blue/yellow oppositions (in terms of *hue*), from grays to vivid or saturated colors (in terms of chromaticity or *saturation*), and from dark to light (in terms of *lightness*), cesia sensations span from opaque to transparent (in terms of the perceived *permeability* to light), from regular or clear to diffuse (in terms of perceived *diffusivity*), and from light to dark (in terms of *darkness*, as we call the variable that cesia shares with color). Hence, all the appearances included in color and cesia combined can be defined by five dimensions: the classical three color variables plus permeability and diffusivity. We may think in any 3D color space being expanded with the additional dimensions of permeability and diffusivity. Any color may appear as a transparent layer or volume, which can vary between crystal clear and translucent or turbid media. Colors may also appear as opaque surfaces, either with matte or glossy finish, which can even reach a mirrorlike appearance (with maximum gloss). And all these appearances may occur at different levels of darkness. This paper presents a basic chronological survey of antecedents of the concept, with bibliographical references to authors who have dealt with these aspects of visual appearance before the name *cesia* was proposed. Then, a review of developments after the adoption of that term follows, including a recent proposal for the amplification of the concept of cesia, which is intended to include primary sources of light. Also, some applications or uses of the concept by different authors are mentioned in various fields: visual arts, architecture, graphic, textile and fashion design, sensory evaluation of food, etc.

Keywords: visual appearance, cesia, transparency & opacity, gloss, darkness

INTRODUCTION: DEFINITION OF CESIA

The name *cesia* has been proposed to account for the aspect of visual appearance that is related to the perception of different spatial distributions of light. Light that is not absorbed by an object may be reflected or transmitted either regularly or diffusely. These interactions of light with matter are perceived as more or less glossy (from a mirror to a matte surface as the two extremes), more or less transparent, translucent or opalescent, in different levels of darkness (according to the light-dark axis). It is the same kind of phenomena that other authors have called "geometric attributes of appearance" or "quality of surfaces", with attributes such as transparency, translucency, turbidity, gloss, matte appearance, mirrorlike appearance, etc. The advantage is that the concept of cesia encompasses all the involved aspects in a single word, and that all cesias have been arranged in a 3D order system according to three axes of variation: transparent-opaque, diffuse-regular (or sharp), and light-dark (Figure 1).

Cesia can also be understood as different modalities of color appearance, in the sense that any color can be seen on an opaque surface (which is usually the most common situation) with a greater or lesser degree of gloss, but the same color can also appear in a transparent or translucent object. In Figure 1b, a yellow color appears on four types of surfaces: matte, mirrored, translucent and transparent, and all of them are different visual sensations. To account for these variations we can add two dimensions (permeability and diffusivity) to the three classical variables of color (hue, saturation, lightness). For this reason, all the appearances included in color and cesia combined can be defined by five dimensions. There are, thus, five kind of basic scales that can be developed. We may think in the CIELAB color space (or any other 3D color space) being expanded with the additional dimensions of permeability and diffusivity; or either in the CIE chromaticity diagram (or any color circle or triangle) being expanded with the dimensions of lightness, permeability and diffusivity. Any color may appear as a transparent layer or volume, which can vary between crystal clear and translucent or turbid media. Colors may also appear as opaque surfaces, either with matte or glossy finish, which can even reach a mirrorlike appearance (with maximum gloss). And all these appearances may occur at different levels of darkness.

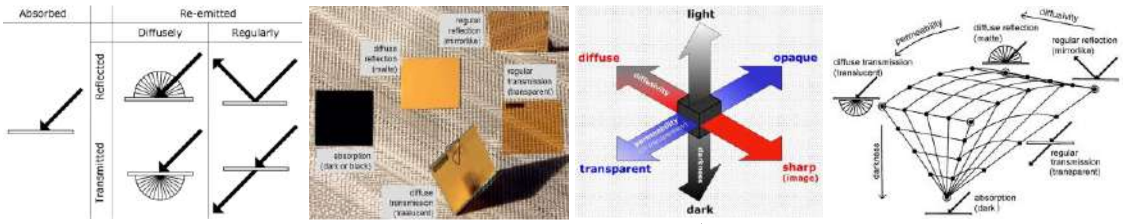

a) b) c) d)

Figure 1. a) Basic interactions of light with matter. b) Basic visual sensations of cesia. c) Three axes of variation. d) Solid of cesias.

AUTHORS WHO HAVE WRITTEN ABOUT SIMILAR PHENOMENA BEFORE 1990

Before the term *cesia* was invented around the 1980s and an international publication about cesia appeared in 1991, various authors have been concerned with phenomena similar to those included in this concept, at least since the beginnings of the 19th century. Probably we could go earlier in the search of antecedents, but let's take just the last two centuries.

In 1810 Philipp Otto Runge published his color sphere, the first model that can be regarded as a modern 3D color order system. But between 1809 and 1810, he wrote a short essay entitled "On the dual nature of color" (in German, "Von der Doppelheit der Farbe"), not included in his book of the color sphere. In that essay, Runge considers how color is modified by the material in which it appears. The "dual nature of color" means the possibility of being transparent or opaque. He also realizes (as Wittgenstein will do much later) that white cannot be transparent, and differentiates between blackness (a quality of opaque surfaces) and darkness (which can refer also to transparent colors). Runge also conceives the possibility of an order system for transparent colors, besides his color sphere, meant for opaque colors [1]. One century later, in 1911, David Katz published a monograph entitled *The modes of appearance of colors* (in German, *Die Erscheinungsweisen der Farben*), whose second edition of 1930 (*Der Aufbau der Farbwelt*) was translated into English as *The world of color* in 1935. Katz analyzes the various kinds of phenomena that always accompany the perception of color. He describes different modes of color appearance: surface color, which is essentially opaque, film color and volume color, which have the attribute of transparency, specular colors, perception of luster, etc. [2].

By the middle of the 20th century, Arthur Pope realized that in order to define a color with accuracy, i.e., giving account for different modes in which a color may appear, more than the three usual variables (hue, saturation, and lightness) are needed [3]. In his *Remarks on color*, published posthumously in 1951, Ludwig Wittgenstein is concerned, among other aspects, with the different types of white, yellow and golden, gray and silver, "black" mirrors, etc., and affirms that "opaqueness is not a property of the white color; any more than transparency is a property of the green" [4]. In 1953, the Committee on Colorimetry of the Optical Society of America (OSA) published a book in which visual perception is classified into eleven attributes of modes of appearance: 1) brightness or lightness, 2) hue, 3) saturation, 4) size, 5) shape, 6) location, 7) flicker, 8) sparkle, 9) transparency, 10) glossiness, 11) luster [5]. The last three attributes are included in our concept of cesia. In addition to the perception of color, Sven Hesselgren includes the perception of shape, illumination, texture and movement, as other visual categories [6]. He observes that visual sensations such as luster, reflection, and gloss are not perceived as belonging to the color of an object but as something separate from color [7]. Like Arthur Pope, Ralph Evans also realized that the three variables normally used to define color are not enough to characterize color under different modes of appearance. Evans concluded that it would be necessary to define at least five variables [8].

Richard Hunter proposed a classification of the geometric attributes of visual appearance. He defined six different types of gloss and developed instruments for the measurement of some of these phenomena: goniophotometers, diffuse-reflection and specular-reflection meters, glossmeters, diffuse- and specular-transmission meters, etc. [9, 10]. The American Society for Testing and Materials (ASTM) has standardized the measurement of various physical aspects related to visual appearance [11-13]. John Hutchings emphasized the importance of visual appearance in food, and particularly studied the phenomenon of translucency among other visual qualities of food [14-16].

THE EMERGENCE OF THE CONCEPT OF CESIA

Sometime before 1980, César Jannello, a professor at the University of Buenos Aires, mainly influenced by the publications of Pope, Hesselgren, Evans, and the Optical Society of America, coined the term *cesia* in order to encompass with a single word the visual appearances elicited by different spatial distributions of light [17]. I heard for the first time about this in 1980 and 1981, when I was a student of Jannello at the School of Architecture of Buenos Aires University [18]. A couple of years after my graduation I got a research grant, and between 1987 and 1988 I decided to investigate more about cesia, particularly trying to develop an order system for the variation of the involved aspects [19]. After a paper that appeared in Spanish in a journal at my Faculty in 1990, I published the first article on cesia in *Color Research and Application* [20].

It was a coincidence that by 1989 Paul Green-Armytage was doing a similar research and proposed a 3D model to organize what he called "qualities of surfaces" [21]. He did not know about me and I was also totally ignorant of his work. After reading my article in *Color Res. Appl.*, Paul wrote me a letter and we started an interchange of ideas on the subject. Our first personal meeting was in 1993 in the AIC congress in Budapest, where I also met John Hutchings and Osvaldo da Pos (who was introduced to me by Paul as "the king of transparency"). In his paper presented to the AIC 1993 conference, Green-Armytage already mentions the term "cesia". Subsequently, he introduced the term "tincture," borrowed from heraldry, to encompass color, texture, and cesia [22, 23].

In 1992, I started to produce scales of variation of cesia employing spinning disks and mixing five materials: transparent air, translucent polyester film, opaque polyester film with specular finish, black matte cardboard, and white matte cardboard. My paper presented to the AIC 1993 conference was precisely about this, and in 1994 I published a more detailed article [24].

DEVELOPMENTS AFTER THE INTRODUCTION OF THE TERM *CESIA*

In 1996, Leo Oberascher included the concept of cesia in his paper on environmental color design presented to the AIC Interim Meeting 1996 in Gothenburg, Sweden [25]. In Argentina, artist and professor Varinnia Jofré, from the University of Córdoba, worked on ceramic tiles with different cesias and presented her results in the 3rd Argentine Color Conference [26]. Since 1996, with the help of designer Patricia Doria, we started to produce a prototype of an atlas of cesia made with pieces of glass, in the Optics Laboratory of the National Institute of Industrial Technology. This atlas includes 5 plates, each one with a different degree of *permeability* to light, from opaque (0% permeability) to transparent (100% permeability). Within each plate a scale of 5 steps in *darkness* and 5 steps in *diffusivity* (from matte to specular, in different degrees of gloss) are developed. It was presented in the AIC 1997 conference in Kyoto, Japan [27]. There, Leo Oberascher also spoke about cesia in his paper on “The role of color in the 21st century” [28].

Other scholars that started to use the concept of cesia, making some developments or applications in their fields of specialty in the 1990s, have been: Fernanda García Gil, Jesús Díaz Bucero and Justo Romero Torres (University of Granada, Fine Arts), Mabel A. López (University of Buenos Aires, Communication in Design), Diana Varela (University of Buenos Aires, Textile Design), María M. Avila (University of Córdoba, Architecture), and Monica Billger (Chalmers University of Technology, Sweden). See their publications in ref. [29], section 1990-1999.

A chronology of publications

Let’s now review what happened after the turn of the millennium:

2000 to 2009: In the first decade of the new millennium, we find the concept spread out in different fields, taken and amplified by other authors. At the University of Buenos Aires: Rodrigo Amuchástegui (philosophy), Julieta Garavaglia (graphic design), Paulina Becerra (industrial design). At the University of Litoral, in Santa Fe: Susana Cariola, Luis Curubetto (architecture). The concept of cesia is also quoted in the following books or monographic publications: *Modern concepts of color and appearance*, by Asim Choudhury (2000), *Understanding color*, by Giordano Beretta (2003), *A framework for the measurement of visual appearance*, by the CIE Technical Committee 1-65 (2006), *Figures de la figure: semiotics and general rhetoric* (chapter by Tiziana Migliore, 2008), as well as in articles or papers by Lucia Ronchi (2002), Berit Bergström (2004), B. Roullet et al. (2005). See these publications in ref. [29], section 2000-2009.

Roberto Daniel Lozano, deals extensively with cesia in a paper entitled “A new approach to appearance characterization”, published in 2006 in *Color Res. Appl.* [30], and in his paper presented to the CIE Experts Symposium on Visual Appearance [31]. Nuria Acevedo, Pilar Buera and others apply the concept to the analysis of food appearance [32]. With the help of Ingrid Menghi and Nicolás Iadisernia, working at the laboratory of Sherwin Williams paint company in Buenos Aires, we developed a new prototype of atlas of cesias, in this case produced with painted samples. By mixing three kinds of paints (white enamel, black enamel and transparent varnish) in three different finishes (matte, satin and glossy), we were able to build scales of cesia with five steps each, covering the whole ranges from opaque to transparent, bright to dark, and matte to glossy, making a total of five charts with 25 samples each, i.e., 125 samples. This work was presented to the AIC 2004 Interim Meeting on Color and Paints, in Porto Alegre, Brazil [33].

2010 to 2019: In 2010, the AIC Interim Meeting on Color and Food was held in Mar del Plata city, Argentina, and five papers dealing with cesia in food or food packaging were presented by Becerra et al., Castillo and Becerra, Giglio, Lozano, Prause and Cariola (see ref. [29], year 2010). Also in 2010, Francis Édeline, one of the three authors of Groupe μ, who wrote the famous *Treatise on visual semiotics*, devoted a section of an article of his authorship to explain cesia, pointing out its importance for camouflage purposes [34].

In the AIC Meeting 2011 on Color and Light, in Zurich, I presented a paper on color and cesia, the interaction of light and color [35], and Green-Armytage described a new model to link different modes and aspects of appearance, which extends the solid of cesias towards texture, on one side, and towards the illuminant mode, on the other side [36]. In a similar vein, in 2014 Varinnia Jofré introduced the new hypothesis of *luminous cesia*, the idea that these kinds of visual appearances are not limited to secondary sources of light but can be also produced in primary light sources [37]. Taking examples and applications from the visual arts, she will further develop and amplify this idea in her doctoral dissertation presented to the University of Córdoba in 2017, whose title is *Aspects of cesia in the artistic image* and deals entirely with the concept of cesia throughout its six chapters [38]. See Figure 2.

In 2015, 2016 and 2018 Tien-Rein Lee, Vincent Sun and Ming-Kang Lan presented papers dealing extensively with cesia in the AIC Meetings 2015 (Tokyo) and 2016 (Santiago, Chile), as well as in the Munsell Centennial Symposium in Boston [39]. In this period, we can also find mentions and citations in doctoral and master thesis in Spain and Argentina by Raúl Parada

(2016), María Lambana (2016), and Carlos Jones (2017). Also, in the book on *Visual appearance and its measurement* by Lozano (Argentina, 2015), in the book on *Color in industrial design* by Gallardo Frade (Mexico, 2016), as well as in the compendium on color words in the English language by John Hutchings et al. (United Kingdom, 2019). See these publications in ref. [29]. The first edition of the *Encyclopedia of Color Science and Technology*, published in 2016 by Springer, includes an entry on "Appearance" by Caivano and Green-Armytage [40].

2020 to nowadays: In 2021 I published a new article in *Color Res. Appl.*, dealing with the role of cesia in color mixtures and the consequences on the shape of color order systems [41]. The 2nd edition of Springer's *Encyclopedia of Color Science and Technology*, published in 2022, includes also a new version of the entry on "Appearance" by Caivano and Green-Armytage. Finally, at the beginning of 2023, with two students of design in Buenos Aires University, we arranged a website entirely devoted to cesia, featuring a homepage with a definition, a short introduction and some graphic and photographic material, a chronology with access to more than 120 publications, references to scientific societies, conferences, programs of seminars, calls for papers in which the concept of cesia is used, videos of recorded lectures, and other materials [42].

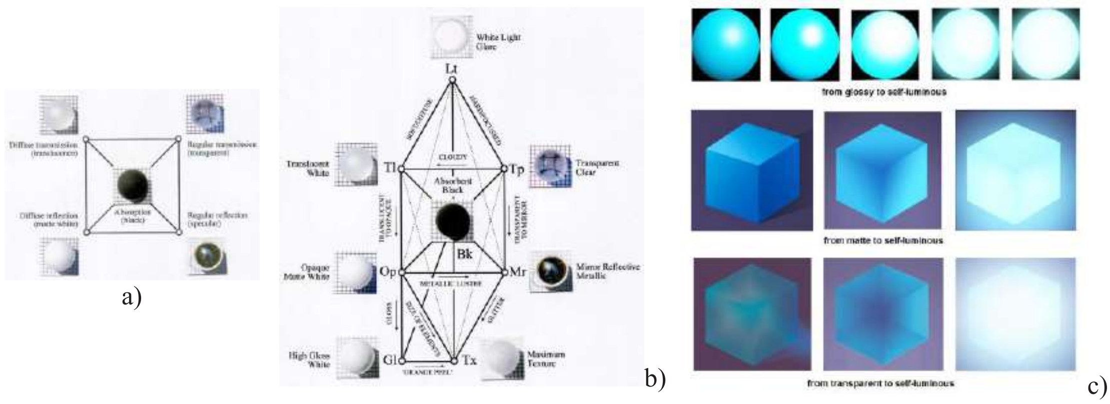

Figure 2. a) Model of cesia in 2D. b) Green-Armytage amplification. c) Jofré: glossy-luminous, matte-luminous, and transparent-luminous scales.

CONCLUSION

The notion of cesia has evolved in at least three stages. The initial conception was rather linked to the nature of the physical stimuli, i.e., the interaction of luminous radiation with matter. Later we understood that, without leaving the physical stimulus aside, what is important is the visual sensation produced in the observer, which can vary not only in relation to the materiality of objects but also with the type of light source, the mode and conditions of lighting and observation (visual angle, distance, contextual situation, etc.). Finally, proposals for expanding the model of cesia have appeared with the aim of integrating the different modes of appearance, including not only the surface mode (typical of opaque objects), the volume and film modes (typical of transparent objects) but also the illuminant mode (for primary sources). An additional idea is that, instead of understanding these modes of appearance as situations separate from each other, we can see them related or linked through gradual transitions or intermediate steps.

REFERENCES

Note: References [17] to [41] are available at https://cesiapage.wordpress.com/chronology.

1. Runge, P. (1809). Von der Doppelheit der Farbe. In *Hinterlassene Schriften*. Hamburg: Perthes, 1840, 141-146. Transl. R. Kuehni, On the dual nature of color. In *P. O. Runge's color sphere*, 2008, 72-75.
2. Katz, D. (1911). *Die Erscheinungsweisen der Farben*. 2nd ed. *Der Aufbau der Farbwelt*. Leipzig: J. A. Barth, 1930. Transl., *The world of color*. London: Kegan, Paul, Trench, Trubner & Co., 1935.
3. Pope, A. (1949). *The language of drawing and painting*. Cambridge, MA: Harvard Univ. Press, p. 28.
4. Wittgenstein, L. (1951). *Remarks on colour*. Berkeley: University of California Press, 1977.
5. OSA, Committee on Colorimetry. (1953). *The science of color*. New York: Crowell, ch. 2.

6. Hesselgren, S. (1954). *Arkitekturens uttrycksmedel*. Stockholm: Almquist & Wiskell. Transl. B. Dahlbäck, revis. C. Jannello, *Los medios de expresión de la arquitectura*. Buenos Aires: Eudeba, 1964, ch. 2.
7. Hesselgren, S. (1967). *The language of architecture*. Lund, Sweden: Studentlitteratur, ch. 3.
8. Evans, R. (1974). *The perception of color*. New York: Wiley.
9. Hunter, R. (1969). Geometric and color attributes of object appearance. In *AIC Color 69, Proceedings*. Göttingen: Muster-Schmidt, 1970, vol. 1, 525-529.
10. Hunter, R. (1975). *The measurement of appearance*. New York: Wiley.
11. ASTM. (1974). Standard recommended practice for selection of geometric conditions for measurement of reflectance and transmittance. Standard E, 179-173.
12. ASTM. (1990). Standard guide for selection of geometric conditions for measurement of reflection and transmission properties of materials. Standard E, 179.
13. ASTM. (1990). Standard test method for visual evaluation of gloss differences between surfaces of similar appearance. Standard D, 4449.
14. Hutchings, J. (1977). The importance of visual appearance of foods to the food processor and the consumer. *Journal of Food Quality* 1, 267-278.
15. Hutchings, J. (1977). Colour and translucency as food attributes. In *AIC Color 77, Proceedings*. Bristol: Adam Hilger, 1978, 467-470.
16. Hutchings, J., & C. Gordon. (1981). Translucency specification and its application to a model food system. In *AIC Color 81, Proceedings*. Berlin: DfG, section C4.
17. Jannello, C. (circa 1980). La cesía como materia conceptual. In G. Carvajal, *Diseño como poética*. Buenos Aires: Acad. Nac. Bellas Artes, 2005, 112-115.
    Unpublished drawings and schemes on cesia. FAU-UBA.
18. Jannello, C. (1980-1981). Handwritten notes on cesia taken by Caivano in two classes. FAU-UBA.
19. Caivano, J. (1988). Cesía. In *Trabajo de investigación*. Buenos Aires: UBA, reports.
20. Caivano, J. (1991). Cesia: a system of visual signs complementing color. *Color Res. Appl.* 16, 258-268.
21. Green-Armytage, P. (1989). Colour and other aspects of appearance. 2nd Confer. Colour Society Australia. In *Spectrum* 6 (3), 1992, 1-11. Available at https://cesiapage.wordpress.com/antecedents.
22. Green-Armytage, P. (1993). Beyond colour. In *Color 93, Proceed.* vol. A. Budapest: HNCC, 155-162.
23. Green-Armytage, P. (1993). Tincture – A new/old word for the appearance of things. *Journal of the School of Design* (Perth) 2, 16-23.
24. Caivano, J. (1994). Appearance (cesia): construction of scales by spinning disks. *Color Res. Appl.* 19, 351-362.
25. Oberascher, L. (1996). Environmental colour design. Simulating real world complexity. In *Colour and psychology. From AIC Interim Meeting 96*. Stockholm: SCI, 1997, 49-55.
26. Jofré, V. (1996). El color cerámico y la cesía. In *ArgenColor 1996*. Buenos Aires: GAC, 1998, 92-102.
27. Caivano, J., & P. Doria. (1997). An atlas of cesia with physical samples. In *AIC Color 97,* vol. I. Kyoto: Color Science Association of Japan, 499-502.
28. Oberascher, L. (1997). The role of color in the 21st century. In *AIC Color 97,* vol. I. Kyoto: CSAJ, 83-89.
29. Chronology of the concept of cesia: https://cesiapage.wordpress.com/chronology.
30. Lozano, R. (2006). A new approach to appearance characterization. *Color Res. Appl.* 31, 164-167.
31. Lozano, R. (2006). A new look into perception of appearance. In *Proceedings of the CIE Experts Symposium on Visual Appearance*. Paris: CIE, 23-27.
32. Acevedo, N., et al. (2008). Integrating spatial and chromatic properties for a better definition of food appearance, 1st International ISEKI_Food Conference, Porto, Portugal.
33. Caivano, J., et al. (2004). Cesia and paints: an atlas of cesia with painted samples. In *AIC 2004*, 113-117.
34. Édeline, F. (2010). Énoncés dénoncés. *Visible* 7, 9-33.
35. Caivano, J. (2011). Color and cesia: the interaction of light & color. In *AIC 2011.* Zurich: pro/colore, 225-228.
36. Green-Armytage, P. (2011). A model to link different modes and different aspects of appearance. In *AIC 2011.* Zurich: pro/colore. Further developed in: More than colour – dimensions of light and appearance. *Journal of the AIC* 17, 2017. See also ref. [40].
37. Jofré, V. (2014). La cesía luminosa en el arte. In *ArgenColor 2014*. Buenos Aires: GAC, 2016, 110-119.
38. Jofré, V. (2017). *Aspectos de la cesía en la imagen artística*. Univ. of Córdoba, Artes, PhD thesis.
39. Lan, M. (2015). Influence of surface properties on material appearance. In *AIC 2015.* Tokyo: CSAJ, 1217-1220.
    Lee, T. (2016). Material perception and surface properties. In *AIC 2016.* Santiago, Chile: ACC, 254-257.
    Lee, T., & V. Sun. (2018). An order system based on material perception", Munsell Color Sympos. Boston.
40. Caivano, J., & P. Green-Armytage. (2016). Appearance. In *Encyclopedia of Color Science and Technology*. New York: Springer.
41. Caivano, J. (2021). Color order systems, color mixtures and the role of cesia. *Color Res. Appl.* 46, 1169-1179.
42. Cesia: https://cesiapage.wordpress.com.

Advanced Colorimetry for Imaging Colour Reproduction

Ming Ronnier Luo

Abstract

A status quo of colour science will be firstly introduced, such as colour matching function, uniform colour space and colour appearance model. Their use to achieve different types of colour imaging reproductions, including spectral, colorimetric, appearance, preferred. However, there are still limitations. New technologies have been developed to address these problems.

Biography

Ronnier is a Professor at the College of Optical Science and Engineering, Zhejiang University (China). He received his PhD from the Bradford University (UK) on colour science in 1986. He has published over 750 peer reviewed papers in the fields of colour science, imaging science and illumination engineering. He is a Fellow of Society of Dyers and Colouists (SDC) and of Imaging Science and Technology (IS&T). He has been an active member of International Commission on Illumination (CIE), ex-Vice President, ex-Division Director on Colour and Vision, Technical chairs, etc. He has received the Judd 2017 Award from the International Colour Association (AIC), and the Newton 2020 Award from the Colour Group of the Great Britain for his contribution in colour science research.

Managing Museum Collections, Climate and Colour Change

Nicole Tse

Abstract

States of material change are intrinsic and objective material properties, but how we interpret that change and perceive damage is reliant on custodian knowledge, localised contexts and the cultural environment. In conserving collections, museum standards have evolved to manage change. Thresholds for temperature, relative humidity, air quality and specifically lighting to control colour change exist, but have evolved out of universal museum practices from the global north.

T his paper examines current lighting guidelines to manage colour change of museum collections such as illumination levels, total light budgets and just noticeable fading. It considers their applicability to Southeast Asian collections, where higher temperatures, relative humidities and potentially pollution, alter the lifetime of the material fabric of collections, and thereby their fading rates and colour changes. How then can the principles of optimum illumination levels and just noticeable fading be applied to museums in tropical climates? Although there maybe colour changes due to the physical fabric of collections and climate, what levels of fading are acceptable over a given period of time? These questions of colour change and acceptability will be examined in the context of Southeast Asia, what collections should look like, their situated contexts and values, and history of care.

Biography

Dr Nicole Tse is a Senior Lecturer at the Grimwade Centre for Cultural Materials Conservation, The University of Melbourne and has a long-standing record of research in Southeast Asia. Her research focuses on regionally relevant conservation approaches for material culture in tropical Southeast Asia, under the auspices of APTCCARN (Asia Pacific Tropical Climate Conservation Art Research Network, www.aptccarn.com). With a strong commitment to cultural materials conservation in tropical climates, she has a PhD and Post-Doctoral studies on canvas paintings and modern paints in tropical environments and has co-convened four international meetings in Malaysia, Thailand, Taiwan the Philippines and Indonesia since 2009. Since 2013, she has been the Chief Editor of the AICCM Bulletin, the Australia Institute for Cultural Materials Conservations', peer reviewed journal published by Routledge Taylor and Francis.

Physical and Perceptual Worlds of Material Appearance

Takahiko Horiuchi

Abstract

When we observe objects in our surroundings, various perceptions and emotions are evoked within us. For example, the sight of a beautiful glittering jewel leads to the perception of luster, which evokes feelings of admiration and luxury. The feelings may further influence our behaviour by motivating us to purchase the jewel. Although the relationship between colour and emotion has been the subject of many studies over the years, research on visual appearance cues other than colour is still in its early stage. For example, our experiments have shown that physical gloss measured by a gloss meter does not necessarily correlate with the glossiness perceived by the human eye. However, the relationship between them has not been elucidated. In this talk, I will introduce our efforts to elucidate the relationship between physical properties (physical gloss, surface roughness, etc.) and perceptual attributes (perceptual gloss, perceptual roughness, etc.) of material objects. In addition, applications based on those analyses will be presented.

Biography

Prof. Takahiko Horiuchi is a professor at the Graduate School of Engineering, Chiba University, Japan. He is a chair of Department of Imaging Sciences. He has made several important contributions to colour image science and technology. His contributions, spanning over the past quarter century, range from the fundamentals of colour imaging to its computer image applications. He has contributed in particular, to advancements in colour image processing, spectral imaging, and colour perception. From 2018 to 2021, he served as the Executive Committee of the International Colour Association (AIC). He has published more than 320 scientific papers on international journals or conferences in the field of colour sciences and engineering.

PHYSICAL AND PERCEPTUAL WORLDS OF MATERIAL APPEARANCE

Takahiko Horiuchi

[1]Graduate School of Engineering, Chiba University, Japan

*Corresponding author: Takahiko Horiuchi, horiuchi@faculty.chiba-u.jp

ABSTRACT

The process of observing objects in our surroundings evokes various perceptions and emotions. For example, the sight of a beautiful, glittering jewel leads to the perception of lustre, which evokes feelings of admiration and luxury. These feelings may further influence our behaviour by motivating us to purchase the jewel. Although the relationship between colour and emotion has been the subject of many studies, research on visual cues other than colour is still in its infancy. For example, our experiments have shown that physical gloss measured using a gloss meter does not necessarily correlate with the glossiness perceived by the human eye. However, the relationships between these factors have not yet been elucidated. In this talk, I will introduce our efforts to elucidate the relationship between the physical (physical gloss, surface roughness, etc.) and perceptual (perceptual gloss, perceptual roughness, etc.) attributes of material objects. In addition, applications based on these analyses are presented.

Keywords: Gloss, roughness, material appearance, surface quality

INTRODUCTION

In addition to colour perception, evolution has given us various other abilities to instantly recognise object features through sight. The assessment of an object based on perceptual information is known as *shitsukan* in Japanese [1]. Despite *shitsukan* being a key element of human behaviour, academic efforts to answer questions such as how to perceive, measure, calculate, or reproduce it have proven elusive. Colour information strongly contributes to *shitsukan*, which, however, uses not only RGB three-channel signals but also higher-order colour features based on spatial and temporal distributions.

The study of material appearance and perception based on *shitsukan* is an established field of research in Japan, and various projects have been launched worldwide. We are interested in the relationship between physical features and perception with respect to the appearance of materials. This study explores the relationship between the physical and perceptual worlds using gloss and roughness as examples.

WORLD OF GLOSS

Measurement of Perceptual Gloss

Gloss refers to the lustre or sheen that an object's surface emits when exposed to light and is an important element of product appearance. The gloss measurement method, which expresses the gloss numerically, is standardised in ISO [2] and is determined by the amount of reflected light at a measurement angle corresponding to the surface gloss. However, it has been reported that such ‘physical gloss’ differs from ‘perceptual gloss,’ which is a human sensory value. Therefore, gloss has been defined and used independently in various industries; however, there is still no standardised gloss-evaluation method, and discussions on standardisation have just started [3]. Subsequently, we experimentally investigated a method to stably measure the perceived amount of gloss.

A total of 30 objects made of 9 materials (fabric, glass, paper, wood, ceramics, metal, plastic, rubber, and leather) were used as samples for evaluation. Lustre is affected by colour; thus, we decided to primarily use samples of achromatic colours in this experiment. As shown in Figure 1(a), in a sunny outdoor natural environment, five observers were each given a tray with one material (three or four samples), as shown in Figure 1(b), and asked to fill in the perceptual gloss scores for all samples on an evaluation sheet. The evaluation time for each material was set at 10 seconds, allowing the observers to intuitively evaluate the glossiness.

The following scores were considered as evaluation methods: (1) free scale, (2) range from 0 to 100, and (3) comparison with a reference sample (diameter: 50 mm, shape material: copper, plating: mirror polished, lustre nickel 15 µm + hard gold 1 µm) defined as 100 (see Figure 1(b)). In Method (3), the reference sample was placed at the centre of five observers, as shown in Figure 1(c); subsequently, the observers were asked to evaluate the reference sample by comparing it with the sample for evaluation. To evaluate the stability of the responses, two sessions each were conducted for the three methods.

(a)

(b)

(c)

Figure 1. Perceptual evaluation condition

The inter- and intra-observer variances of the glossiness scores are summarised in Table 1, and those for each evaluation sample are shown in Figure 2. The order of the evaluation samples on the horizontal axis shown in Figure 2 is the same for all three graphs (in descending order of the mean of the scores in Method (3)). As shown in Table 1, the inter-observer variance was the smallest for Method (3), and the evaluation was reproducible. The intra-observer variance was stable for Methods (2) and (3). The score of Method (3) was slightly higher than that of Method (2); however, this was because Method (3) did not have a limit on the maximum score, resulting in a larger range of scores. As shown in Figure 2, Method (3) is generally suitable as an evaluation method because the inter-observer variance for each sample is relatively small. However, when the glossiness was felt more strongly than the reference sample, the inter-observer variance was smaller than that of Method (1) but slightly larger than that of Method (2), revealing a tendency for the evaluation to be scattered.

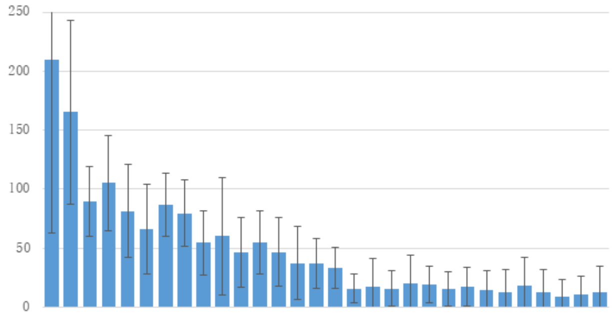

(a) Method (1)

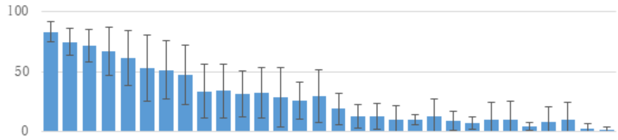

(b) Method (2)

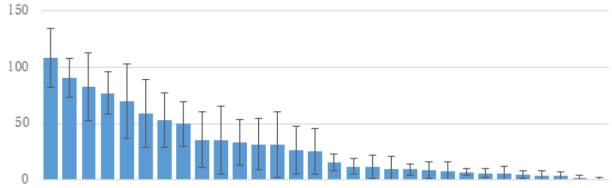

(c) Method (3)

Figure 2. Evaluation score (horizontal axis: sample; vertical axis: score)

Table 1. Inter- and intra-observer variances for glossiness score

	Method (1)	Method (2)	Method (3)
Inter-observer variance	204.4	30.1	18.6
Intra-observer variance	1537.3	263.8	327.2

The illuminances at the beginning of the evaluation from Methods (1) to (3), respectively, were (1) 99,040 lx, (2) 41,470 lx, and (3) 9,263 lx (illuminance in the horizontal plane in Methods (1) and (2)). The illuminance in Method (3) was that in the vertical plane; this is because the illuminance in the horizontal plane exceeded 100,000 (lx) and was outside the measurement range of the measuring instrument (Konica Minolta's CL-500A). During the experiment, the sample visibility changed owing to changes in the outdoor lighting environment. However, Method (3) was robust to changes in lighting because it was compared with a reference sample.

Modelling of Perceptual Gloss

Leloup et al. summarised years of research on perceptual gloss, physical gloss, and their measurements, indicating the future direction of gloss research [4]. Ged et al. investigated the changes in perceptual gloss under different lighting conditions [5]. The investigation of perceptual gloss in conventional studies has generally been limited to discussing objects with uniform and progressively different glosses, such as coated paper samples developed using the Natural Colour System (NCS). We conducted visual evaluations and physical feature analyses of gloss, transparency, and roughness for 34 real object materials consisting of 10 types (i.e., stone, leather, fabric, paper, metal, resin, glass, rubber, wood, and ceramic) and attempted to model these 3 perceptual quantities [6]. However, when modelling the perceptual gloss, high accuracy was not achieved when only physical gloss was used. This may be because people acquire and process complex scattering information on the object surface, and the modelling of perceptual gloss with physical features is not a simple process. To improve the accuracy of modelling real objects with complex optical properties, it is necessary to introduce other physical features independent of physical gloss. In Ref.[7], we constructed an improved prediction model for perceptual gloss with higher accuracy using various measured physical features other than physical gloss and conducted experiments to evaluate perceptual gloss. Experimental samples with different levels of physical gloss were prepared to consider minute changes in perceptual and physical gloss. For these samples, we analysed the data of physical features and perceptual gloss from evaluation experiments and proposed an accurate prediction model to derive perceptual gloss from physical features.

In Ref.[7], we prepared 28 types of NCS-coated papers with gradually varying base colours and glosses. These NCS samples have been used in conventional studies of gloss perception [5]. In addition, we used 99 Japan Industrial Design Association (JIDA) samples (JIDA Standard Samples, n.d.) with different glosses (lustre, sparkle, etc.) and gloss levels. The shapes of the JIDA samples were flat, with their surfaces forming planes or embosses. The smooth gloss of the lustre was presented on the surfaces of the resin and plating metal, and a sparkle was generated with radiant materials, such as pearl and lame, into the resin base. Therefore, three types of sample materials (paper, resin, and metal plating) were used. The total number of experimental samples was 127 (28 NCS, 99 JIDA). Examples of these samples are shown in Figure 3.

Figure 3. Test samples

We performed physical measurements to determine the physical characteristics of the experimental samples. We measured the features representing the sample’s surface, such as reflectance, transmittance, and texture. To select physical features, we referred to the following six types of gloss proposed by Hunter [8]: specular (brilliance of secularly reflected light, shininess), sheen (shininess at grazing angles), contrast (contrast between secularly reflecting areas and other areas), absence-of-bloom (absence of smear or excess semi-specular reflection adjacent to reflected highlights and images), distinctness-of-reflected-image (distinctness and sharpness or reflected images), and absence-of-surface-texture (surface evenness, absence of surface). Our study hypothesised that these gloss types can be satisfied by the following physical features: physical gloss (gloss unit), haze, distinctness of image, transmittance, and features of the two-dimensional luminance distribution obtained from captured luminance images.

We analysed the physical features, evaluated the data, and proposed a prediction model to derive perceptual gloss. Several combinations of explanatory variables were examined and analysed using regression analysis. Consequently, in the model using multiple physical features on a logarithmic scale, the coefficient of determination was determined between 0.3 and 0.6. We confirmed that perceptual gloss could be predicted within approximately 1σ of the standard deviation of the evaluation values between the observers (see also Ref. [7] for more details).

WORLD OF ROUGHNESS

The measurement of object surface roughness has been standardised by ISO [9] and others and is specified as a change in the depth direction. However, 'physical roughness' is different from 'perceptual roughness', which is a human sensory quantity, and these have not been sufficiently investigated. Consequently, we modelled the physical and perceptual properties of the leather surface.

In a study mentioned in Ref. [10], the author examined the construction of a perception model of authenticity, that is, *shitsukan*, using various leather samples under tactile and visual-tactile conditions. The perception model consisted of three layers and was constructed by correlating each layer, as in the previous section. To obtain the properties and impressions of each layer, the author conducted measurement and subjective evaluation experiments. In the measurement experiment, 3 types of measurements were performed, and 14 tactile-related physical properties were acquired. The subjective evaluation experiments were performed by both groups of observers. Under tactile conditions, they evaluated using their hand and finger to rub the samples without observing them. However, under visual-tactile conditions, they evaluated by rubbing the curved sample while observing it.

The following important findings were obtained from the above attempts:

1) Neither group was able to construct an authenticity model under tactile conditions. The author theorised that this was because even familiar groups rarely touched leather with their vision blocked. Therefore, the authenticity evaluations of both groups showed large variability, and the evaluations could not be scaled to a single dimension.

2) Under visual-tactile conditions, an authenticity model could be constructed for both groups. In the familiar group, the author estimated that vision was superior to the perception of leather because it could also be constructed under visual conditions. However, the unfamiliar group could not be constructed under visual and tactile conditions. Thus, the author considered that–all the tactile conditions could be constructed by the cross-modal phenomenon.

Similar to visual conditions, the shitsukan perception step can be explained only by the sensory attribute step. Based on the results under visual, tactile, and visual-tactile conditions, the author inferred that the perception of the familiar group followed a visually-dominant weighted average rule. That is, it can also be interpreted as an optimal Bayesian integration. In contrast, the results for the unfamiliar group did not seem to follow certain rules (see also Ref. [10] for more details). Despite the limitations and issues mentioned above, the results of this study can contribute to the production of artificial leather with stronger authenticity.

CONCLUSION

In this study, gloss and roughness were presented as examples of the relationship between physical features and perception. Achromatic objects were used; however, it is evident that colour is highly involved in the real world. In future, modelling that includes colours will be necessary.

ACKNOWLEDGEMENTS

I am grateful to Assistant Professor Dr. Midori Tanaka of Chiba University for helpful discussions. I also gratefully acknowledge the work of past and present members of my laboratory. This work was supported by JSPS KAKENHI (Grant Number 20H05958).

REFERENCES

1. Horiuchi, T. (2018). Challenges in Shitsukan Imaging. *Proc. 4th conference of the Asia Color Association ACA*, 30-32.

2. ISO 2813:2014 Paints and varnishes ― Determination of gloss value at 20°, 60° and 85°.
3. CIE JTC 17 (D1/D2/D8), Gloss Measurement and Gloss Perception.
4. Leloup, F. B., Obein, G., Pointer, M.R. & Hanselaer, P. (2013). Toward the Soft Metrology of Surface Gloss: A Review. *Color Res Appl., 39* (6), 559-570.
5. Ged, G., Rabal-Almozor A.M., Himbert, M. E. & Obein, G. (2020). Assessing Gloss under Diffuse and Specular Lighting. *Color Res Appl., 45* (4), 591-602.
6. Tanaka, M., Osumi, M. & Horiuchi, T. (2019). Physical Indices for Representing Material Perception with Regard to Glossiness, Transparency, and Roughness. *Proc. 29th CIE Session,* 1102-1107.
7. Amari, S., Tanaka, M. & Horiuchi, T. (2021). Modelling of Perceptual Gloss by Physical Measurement of Flat Surface. *Proc. CIE Midterm Meeting*.
8. Hunter, R.S. (1937). Methods of Determining Gloss. *J. Res. Natl. Bur. Stand., 18* (1), 19-41.
9. ISO_25178-2:2012 Geometrical Product Specifications (GPS) Surface Texture: Areal 2: Terms, Definitions and Surface Texture Parameters: British Standards Institute.
10. Watanabe, S. & Horiuchi, T. (2021). Perception modeling based on vision and touch: "authenticity" of leather defined through observational experience. *Textile Res. J., 91* (17-18).

The Choices of Color: Exploring Color Selection from Maslow to AI

Tien Rien Lee

Abstract

Colors are ubiquitous in our daily lives, surrounding us at every turn, and we frequently find ourselves making decisions about them. Whether consciously or unconsciously, with or without a specific purpose, we engage in the process of color selection. How can we satisfy our psychological needs when it comes to choosing colors? Is it a challenging task? Can we simply defer this decision to the currently popular artificial intelligence systems that determine color choices for us? This article delves into the various methods we employ to select colors in our daily lives and raises questions about our reliance on existing tools like AI to make these decisions on our behalf.

Biography

Dr. Tien-rein Lee, who holds a Ph.D. in Culture and Communication from NYU and a Master's degree in Electronic Imaging from UCLA, currently serves as a Chair Professor at the Chinese Culture University. His areas of instruction include color theory and its applications, communication technology, visual communication, and image arts, among other subjects. Dr. Lee has held distinguished roles such as the president of both the Chinese Culture University and Huafan University. He has also fulfilled duties as the Dean of the School of Communication, Chief of General Affairs, Director of the Information Center, and Head of the Department of Information Communication. From 2019 to 2020, Dr. Lee served as the chairman of the International Color Association (AIC). He organized the AIC 2012 conference in Taiwan and has been an active participant in the Asia Color Association (ACA) activities. As the founding president of the Color Association of Taiwan (CAT), he has made significant contributions to the field. Dr. Lee has pursued in-depth research in areas such as color preferences, color psychology, and the Chinese Five Element colors. Apart from academia, he is passionate about photography, pottery, and printmaking arts. He has further extended his talents to film, creating experimental films that have won him two Golden Harvest Awards.

The Pink Tax

Vien Cheung

Abstract

Colour is a powerful vehicle which latches significantly onto perceptions through its extensive associations with culture, history, symbolic meanings, psychological effects and many others. Gendered colours have been an established part of societies and engrained within consumers for a long time due to their use as navigators, identifiers and differentiators. Today, the colour pink stands for femininity, in all its positives and otherwise, while a century ago was it viewed as masculine. The term "pink tax" refers to gender-based pricing disparities – specifically an upcharge on products and services intended for female consumers. What is the connection between pink and binary? Could debate such as 'nature versus nurture', which considers particular aspects of thinking and behaviour are outcomes of either inheritance or learning, shed light on the answers? This talk discusses the history and coding of the colour pink, and presents a philosophical analysis on the gender equality, diversity and inclusion.

Biography

Vien Cheung, an academic in the UK, has authored more than 100 refereed publications in the areas of color vision, color science, color imaging and color design. Her ethos on integrity and diversity takes her to explore how colour can be used as a vehicle to shift our 'black and white' judgements into a more variegated and expansive perception of the world. Vien is also active in charitable and educational colour organisations including the International Colour Association (AIC) and the Colour Group Great Britain in which she is the Immediate Past President and Chairman respectively.

Oral Paper

Session 1

Doi Tung
28 November 2023

OPTIMIZATION OF SPECTRAL SENSITIVITY FOR MULTISPECTRAL IMAGING BASED ON ADAPTIVE NOISE LEVELS

Peng Xu[1]* and Haisong Xu[2]

[1]Department of Engineering and Technology, Jiyang College of Zhejiang A&F University, China.
[2] College of Optical Science and Engineering, Zhejiang University, China.

*Corresponding author: Peng Xu, xsjzxp@163.com

ABSTRACT

The spectral sensitivity of multispectral imaging influences the generation of multichannel responses and further impacts the colorimetric and spectral accuracy of spectral estimation. This study focuses on optimizing the spectral sensitivities of multiple channels through simulation, to improve the performance of multispectral imaging. Noise generally interferes with the formation of multichannel responses, and therefore noise is commonly added to the channel responses when spectral sensitivity is optimized. The shot noise is usually considered to predominate over other noise types. The adaptive noise levels were proposed in this paper, and the shot noise was produced on the basis of the magnitude of the multichannel responses. Cooperative cooperation was employed to optimize the spectral sensitivities of multiple channels simultaneously. Besides, to improve the generalization of optimized spectral sensitivity, the uniform target samples were selected and served as the target samples in the optimization. The optimization was performed toward different objective functions, including one colorimetric objective and one spectral objective. The results show that the peak wavelengths and bandwidths of optimized spectral sensitivities vary under different levels of light intensity. The bandwidth of the spectral sensitivity becomes wider under high noise levels in colorimetric optimization for the illuminant D65, which is inconsistent with the results derived under fixed noise levels. It is indicated that there is a balance between the bandwidth and SNR for reaching an accurate spectral estimation when shot noise is considered.

Keywords: Multispectral imaging, Spectral sensitivity, Optimization, Noise level

INTRODUCTION

For multispectral imaging, the spectral sensitivities of spectral channels drive the formation of multichannel responses of objects, and further the recovered colorimetric and spectral values. Much research has been directed at the problem of optimization of spectral sensitivity to improve the colorimetric or spectral accuracy. One way to optimize spectral sensitivity is to minimize the colorimetric or spectral error between the recovered target samples and the original ones by optimizing the spectral sensitivity. However, the optimized spectral sensitivity might vary significantly from one set of target samples to another [1]. So, if the target samples are skewed toward a specific color region, the resulting spectral sensitivity based on this set of target samples will not apply to samples outside of that color range.

Different optimization algorithms can be employed to search for the optimal spectral sensitivity. López-Álvarez et al. adopted the simulated annealing (SA) algorithms to optimize the spectral sensitivity for measuring skylight [2]. Shen et al. selected a set of optimal channels for a multispectral camera through the differential evolution (DE) algorithm [3]. The adaptive genetic algorithm was used to select the most appropriate filters for a multispectral camera under different light sources [4]. Such optimization algorithms can obtain a good result when the number of decision variables is small, while the optimization results will become unstable as the number of decision variables increases.

The performance of multispectral imaging is also influenced by the noise present in the devices besides the spectral sensitivity [5]. The fixed noise levels were commonly added to the multichannel responses when the spectral sensitivity was optimized [2,5]. The shot noise is considered to be the dominant component of noise [6,7]. The shot noise can be calculated as the square root of the signal [6]. To simulate the shot noise, the adaptive noise levels are designed and adopted in the formation of multichannel responses in this paper. Besides, the uniform target samples are selected from a larger number of real objects, to suppress the bias of the optimized spectral sensitivity. Moreover, the cooperation coevolution (CC) [8] is employed to attain better and more stable results when the number of decision variables is large.

METHODOLOGY

Optimization of spectral sensitivity with cooperative coevolution

To optimize the spectral sensitivities of multiple channels, the cooperative coevolution is embedded in the complete process of multispectral imaging and spectral estimation, as illustrated in Figure 1. For improving the generalization ability of the optimized spectral sensitivity, that is any object can be accurately acquired by the optimized spectral sensitivity, the uniform target samples (UTS) are selected. The objective of optimization is to minimize the error between the recovered spectral reflectance of the UTS and the ground truth data. The multichannel responses of UTS can be simulated by the integration of the SPD of illuminant, the spectral reflectance of UTS, and the spectral sensitivity of the multispectral imaging system. Thereupon, the spectral reflectance of UTS can be recovered with the spectral estimation algorithm.

The cooperation coevolution modulates the spectral sensitivity to improve the accuracy of the recovered spectral reflectance of UTS. Since a multispectral imaging system usually comprises multiple channels, and the spectral sensitivity of each channel is characterized by several parameters, the optimization of spectral sensitivity can be formulated as an issue of multivariable optimization. Compared to conventional optimization algorithms, CC optimizes one subcomponent each time rather than the whole variables. This strategy can reduce the size of solution space and is beneficial to approach the best solution. Any evolutionary algorithm (EA) can be used in the framework of CC.

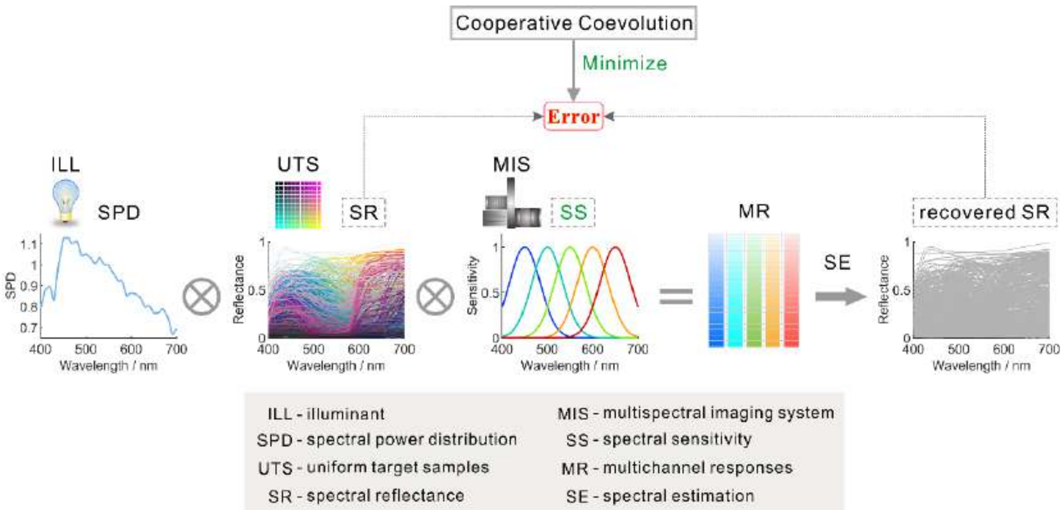

Figure 1. The schematic diagram of optimizing spectral sensitivity

The type of spectral sensitivity for one spectral channel is formulated as the Gaussian curve. This type of spectral sensitivity is dominated by two parameters, i.e., peak wavelength and bandwidth. The bandwidth means the full width at half maximum. Hence, the variables to be optimized are the peak wavelength and bandwidth for the spectral sensitivity of one channel. In other words, two variables will be optimized for one channel. The uniform target samples (UTS) are selected from the spectral reflectances of a large number of real objects. The uniform target samples comprise 2035 samples, including 1980 color samples and 55 neutral samples.

Adaptive noise levels

Since the shot noise is considered to be dominant in all types of noise, the shot noise is added to the multichannel responses during the process of optimizing the spectral sensitivity. The shot noise can be calculated as the square root of the signal, as displayed in Eq. (1).

$$\begin{cases} n = \sqrt{p} \\ \mathrm{SNR} = 10\log_{10}(\frac{p^2}{n^2}) = 20\log_{10}(\frac{p}{n}) \\ \mathrm{SNR} = 20\log_{10}(\frac{p}{\sqrt{p}}) = 20\log_{10}(\sqrt{p}) \end{cases} \tag{1}$$

In Eq. (1), n denotes the noise, and p represents the multispectral image signal which is the multichannel responses of the UTS for the designed optimization process. As a result, SNR is proportional to the square root of p. Therefore, the SNR is changed as the variation of the multichannel responses, and adaptive to the magnitude of the multispectral image signal. In detail, SNR is high when the multispectral image signal is strong, and conversely, SNR is low when the multispectral image signal becomes weak. The magnitude of the image signal is largely influenced by the light reaching the image sensor. In this paper, the magnitude of the image signal is supposed to be impacted by the intensity of the light source. Figure 2 illustrates three intensity levels of one light source which is virtually the CIE illuminant D65. The relative spectral power distribution (RSPD) of the light source at each intensity level is presented. Level L1 can generate a strong image signal of multispectral imaging and produce a high SNR, while level L3 will lead to a weak image signal and thus result in a low SNR.

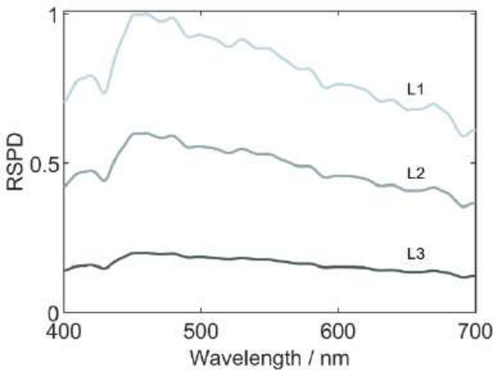

Figure 2. The relative spectral power distributions of one light source at three intensity levels.

Experiment setup

The peak wavelength of each channel will be searched between 400 nm to 700 nm. The bandwidth of each channel will be explored from 5nm to 400 nm. The number of channels to be optimized is 3 to 16. The CIE illuminant D65 is used to generate the multichannel responses. The spectral estimation algorithm PI (Pseudoinverse) [9] recovers the spectral reflectances from the multichannel responses. Six optimization algorithms are employed to search the optimal spectral sensitivity under the framework of cooperative cooperation, including SA, genetic algorithm (GA), AGA[10], particle swarm optimization (PSO), DE, and one kind of adaptive DE (ADE) [11]. Two objective functions are adopted, containing one spectral objective function RMSE and one colorimetric objective function ΔE_{00}. They correspond to spectral optimization and colorimetric optimization, respectively.

RESULT AND DISCUSSION

Performance of cooperative cooperation

The above six optimization algorithms were used to search the optimal spectral sensitivity toward the spectral objective function. The performance of these algorithms with and without

CC is shown in Figure 3 in which each chart displays the RMSE of the optimal spectral sensitivity obtained by one optimization algorithm. When the number of channels is small, the performance of optimization algorithms without CC is very close to that with CC. So, the optimization algorithm without CC can get good results if the number of decision variables is less. Nevertheless, the performance with CC begins to surpass that without CC as the number of channels increases. When the number of channels increases, more decision variables are produced because one channel will generate two variables, i.e., peak wavelength and bandwidth. Therefore, the advantage of CC is manifested in dealing with a large number of decision variables. Moreover, the GA algorithm obtains the best results among the six algorithms when the CC is used. In the next section, the optimized spectral sensitivity with the GA algorithm under CC is shown and analyzed.

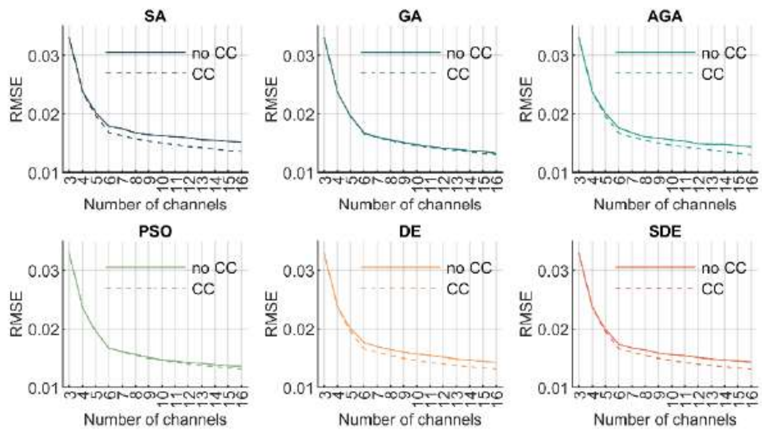

Figure 3. Spectral estimation errors for six optimization algorithms

Optimized spectral sensitivity under adaptive noise levels

Figure 4 illustrates the optimized spectral sensitivity toward the spectral objective function under adaptive noise levels and fixed noise levels, respectively. The peak wavelengths are almost evenly distributed throughout the whole spectral range for fixed noise levels. However, this kind of distribution is not obvious under adaptive noise levels. Under fixed noise levels, the bandwidths for different channels are very close for a certain number of channels, while there is a larger difference in bandwidth between different channels under adaptive noise levels. Under fixed noise levels, the bandwidth tends to decline when SNR becomes lower. However, the bandwidth obtained under adaptive noise levels is still wide and even wider when SNR decreases. Since the low SNR is generated by the weak light intensity under adaptive noise levels, it is indicated that a wider bandwidth is needed to increase the magnitude of the multichannel responses and thus to improve the SNR. In other words, wider bandwidth is preferred under low light intensity. In the case of fixed noise, for reaching a low SNR, a narrow bandwidth is produced to reduce the magnitude of the multichannel responses and lower the SNR. Moreover, the first channel and the last channel get wider bandwidths under adaptive noise levels. In Figure 2, it can be observed that the spectral power at both ends of the wavelength is weaker than the middle ones, therefore, the SNR of the first and the last channels will be improved if wider bandwidth is obtained. However, the bandwidths of middle channels are not as wide as the first and the last channels, indicating too wide bandwidth is not helpful to accurately recover spectral reflectances. The mean bandwidth for different numbers of channels is shown in Figure 5. Under adaptive noise levels, the mean bandwidth is generally higher at lower levels of light intensity, and this phenomenon is more obvious in colorimetric optimization. It is suggested that improving the SNR is more beneficial to spectral estimation than finding a proper bandwidth when the light intensity is weak. However, it is the reverse case under fixed noise levels that the mean bandwidth gets narrow under low SNR.

Figure 4. Optimized spectral sensitivity. (a), (c) and (d) correspond to the results in light intensity levels L1, L2, and L3. (b), (d) and (e) show the results under three corresponding fixed noise levels.

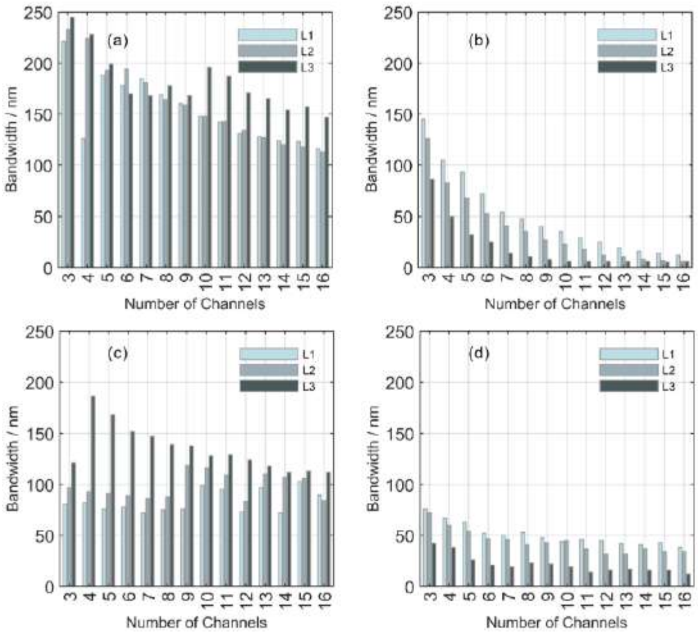

Figure 5. The mean bandwidth for different numbers of channels. (a) and (c) show the results for spectral and colorimetric optimizations under adaptive noise levels. (b) and (d) show the results for spectral and colorimetric optimizations under fixed noise levels.

CONCLUSION

The adaptive noise is designed and considered in the process of optimizing spectral sensitivity for multispectral imaging. Under low levels of light intensity, the bandwidths of spectral channels become wider to improve the SNR and thus the spectral estimation accuracy. However, too wide bandwidth is not helpful to spectral estimation. It is indicated that a balance exists between the bandwidth and SNR for obtaining high accuracy of spectral estimation. Besides, the bandwidth of each channel is influenced by the spectral power at the corresponding wavelength of the employed light source. In addition, cooperative cooperation can more efficiently optimize spectral sensitivity for more channels.

ACKNOWLEDGEMENT

Supported by the National Natural Science Foundation of China (Grant No. 62005246) and the Scientific Research and Development Fund of Jiyang College of Zhejiang A&F University (Grant No. JY2018RC02).

REFERENCES

1. Nie, S., Gu, L., Zheng, Y., et al. (2018). Deeply learned filter response functions for hyperspectral reconstruction. *In: Proceedings of the IEEE Conference on Computer Vision and Pattern Recognition*(2018), pp. 4767-4776. https://doi.org/10.1109/CVPR.2018.00501
2. López-Álvarez, M. A., Hernández-Andrés, J., Valero, et al. (2007). Selecting algorithms, sensors, and linear bases for optimum spectral recovery of skylight. *Journal of the Optical Society of America A*, 24(4), 942-956. https://doi.org/10.1364/JOSAA.24.000942
3. Shen H., Yao J., Li C., et al. (2014). Channel selection for multispectral color imaging using binary differential evolution. *Applied Optics*, 53(4), 634-642. https://doi.org/10.1364/AO.53.000634
4. Xu, P., &Xu, H. (2016). Filter selection based on light source for multispectral imaging. *Optical Engineering*, 55(7), 074102. https://doi.org/10.1117/1.OE.55.7.074102
5. Shimano, N. (2006). Optimization of spectral sensitivities with Gaussian distribution functions for a color image acquisition device in the presence of noise. *Optical Engineering*, 45(1), 013201. https://doi.org/10.1117/1.2159480
6. Braun D., Alperovich V., Berger M. J. (2000). Performance analyses for multispectral imaging systems. *Proc. SPIE 4029, Targets and Backgrounds VI: Characterization, Visualization, and the Detection Process*. https://doi.org/10.1117/12.392537
7. Haneishi H., Hasegawa T., Hosoi A., et al. (2000). System design for accurately estimating the spectral reflectance of art paintings. *Applied Optics*, 39(35), 6621-6632. https://doi.org/10.1364/AO.39.006621
8. Potter M. A., & De Jong K. A. (1994). A cooperative coevolutionary approach to function optimization. *International conference on parallel problem solving from nature*, 249-257.
9. Shen, H., Xin, J. H., Shao, S. (2007). Improved reflectance reconstruction for multispectral imaging by combining different techniques. *Optics Express*, 15(9), 5531-5536. https://doi.org/10.1364/OE.15.005531
10. Srinivas M., & Patnaik L. M. (1994). Adaptive probabilities of crossover and mutation in genetic algorithms. *IEEE Transactions on Systems, Man, and Cybernetics*, 24(4), 656-667. https://doi.org/10.1109/21.286385
11. Yang Z., Tang K., Yao X. (2008). Self-adaptive differential evolution with neighborhood search. *2008 IEEE Congress on Evolutionary Computation (IEEE World Congress on Computational Intelligence)*, 1110-1116. https://doi.org/10.1109/CEC.2008.4630935

A LOW-COST PORTABLE SPECTROPHOTOMETER

Andrea Trentini, Lorenzo Bini and Alessandro Rizzi*

Department of Computer Science, University of Milano, Italy.

*Corresponding author: Alessandro Rizzi

ABSTRACT

In this work we present an electronic open hardware project for building a low-cost portable contact spectrophotometer. The project is based on a low-cost, pre-cabled on-board spectral sensor designed for device embedding. It is an off-the-shelf "low cost" component based on the AS7265x Smart Spectral Sensor chip family which consists of three sensor devices: AS72651 with master capability, AS72652, and AS72653. This integrated sensor is capable of measures on 18 spectral channels, ranging from 410nm to 940nm. Each AS7265x component has two integrated LED drivers with programmable current and can be timed for electronic shutter applications. Features include UART or I2C slave digital interface, 16-bit ADC with digital access, and programmable LED drivers. The device prototype we have built has also a GPS and a DHT (temperature and humidity) sensor to collect data to factor from the environment when measuring spectral information. Here we describe its main characteristics and present some preliminary tests and calibration.

Keywords: Color Measure, Color Measurement devices, Spectrophotometer

INTRODUCTION

This article describes the development of an affordable portable spectrophotometry device using off-the-shelf components, based on the AS7265x Smart Spectral Sensor chip family [4]. It has been designed for studying phototrophic biofilms that grow on outdoor surfaces like statues. These biofilms can damage structures and heritage sites, and their early detection is crucial. Unlike current methods that are costly, time-consuming, and destructive, the proposed device offers non-destructive, on-site, and inexpensive analysis by measuring color changes associated with the quantity of microorganisms in the biofilm. Biofilms consist of microorganism-secreted polymers and cells that are resilient to environmental stressors and antimicrobial agents. Existing techniques include culture-based methods, microscopy, and indirect approaches like measuring biofilm mass or ATP levels. Scanning Electron Microscopy provides detailed images but requires high vacuum and sample preparation, limiting its use on living samples. The spectrometer-based [1] methods present an advantage by only needing spectrophotometric data, addressing the limitations of existing techniques [2,3]. The use of this low-cost device introduces a cost-effective spectrometer-based method for analyzing phototrophic biofilms, offering non-destructive on-site analysis with potential applications in heritage preservation and antimicrobial treatment evaluation.

THE DEVICE

The device is a prototype assembled on a breadboard and enclosed in a plastic box (Figure 1), with a separate spectrometer probe connected via a cable. It can be worn around the neck or hung on a hook when not in use. The device has two use modes:

- **Field Use**: users can press the Record button to initiate data recording, which includes spectrometry, temperature, humidity, time, and GPS location. The display indicates the recording process, and once completed, it shows the recorded spectrometer data briefly before entering idle mode. The device allows users to switch between different information display modes by turning a dial. Pressing the Record button in a specific mode enters Detail Mode, enabling browsing of individual band data from the last capture using a scrollbar controlled by a knob (a potentiometer, used a monodimensional joystick). Exiting Detail Mode is done by pressing the Record button again.

- **Downloading and Managing Data**: users connect to the device's Wi-Fi access point and access a designated web page on the local network to manage data. The interface presents four buttons:
  - Edit Comment: allows users to modify comments stored alongside each capture
  - Download Data: enables the downloading of the data file (in CSV format) from the spectrometer device to the connecting device
  - View Data: displays all data in a table format, though memory limitations could cause visible errors
  - Delete Data: deletes all recorded data on the spectrometer after a confirmation prompt.

In summary, the prototype device is designed for field use and data management. It records various data including spectrometry and environmental parameters, offers display modes and Detail Mode, and provides a data management interface accessible through Wi-Fi for downloading, viewing, editing comments, and deleting data.

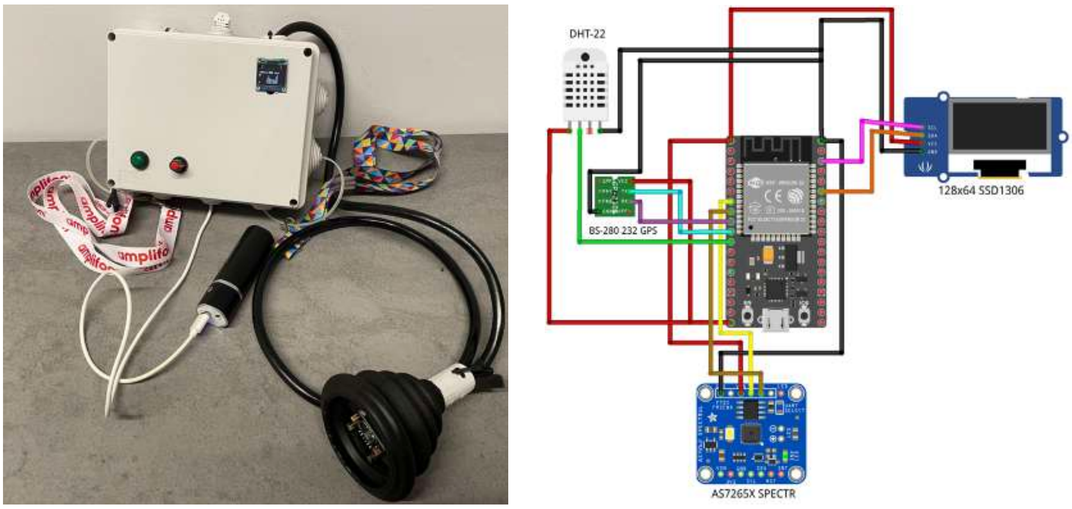

Figure 1. Device prototype and internal diagram

IMPLEMENTATION

The hardware implementation consists of the following components with specific functions:

1. ESP32, a microcontroller with GPIO, UART, and I2C connections
2. DHT-22, a temperature and humidity sensor
3. BS-280, a GPS sensor operating connected through the UART
4. SSD1306, an OLED display connected using the I2C protocol
5. AS7265X, the actual spectrophotometer sensor connected through the UART.

Some details about the chosen components:

- the temperature and humidity sensor (the DHT-22 is an enhanced and more sensitive version of the DHT-11) readings showed variations due to factors like the physical presence of the user in the immediate proximity of the sensor, heat from the circuit board that the sensor is mounted on, and heat from nearby electronic equipment (e.g. a PC display), i.e. sensor positioning on the box must be carefully thought.

- the display (SSD1306) is connected via I2C, it has a resolution of 128x64 pixels. The chosen library is ThingPulse OLED SSD1306 due to its simplicity and alignment capabilities.
- The GPS sensor (BS-280) is connected via UART, capable of providing location data outdoors after a short initial period, but (obviously) less reliable indoors.
- The spectrophotometer (AS7265X) is connected via UART, the proper UART port (i.e. hardware instead of software) is crucial for accurate readings, the software based serial port (implemented via bit banging) may miss data due to timing.

As for the file system for the ESP32, LittleFS (over SPIFFS) was preferred due to its compatibility and fault-tolerance in case of power loss. The default partitioning on the ESP-32 devices included a partition for the file system. Mounting the LittleFS file system required setting the proper flag for automatic formatting in case of mount failure.

In summary, the hardware implementation involves a range of components with specific connections and voltage requirements. Testing and configurations were performed for each component, addressing potential issues related to UART signaling, data accuracy, and power loss. The choice of LittleFS as the file system provides reliability and compatibility for the prototype device.

Declared channel spectral sensitivity is shown in Figure 2.

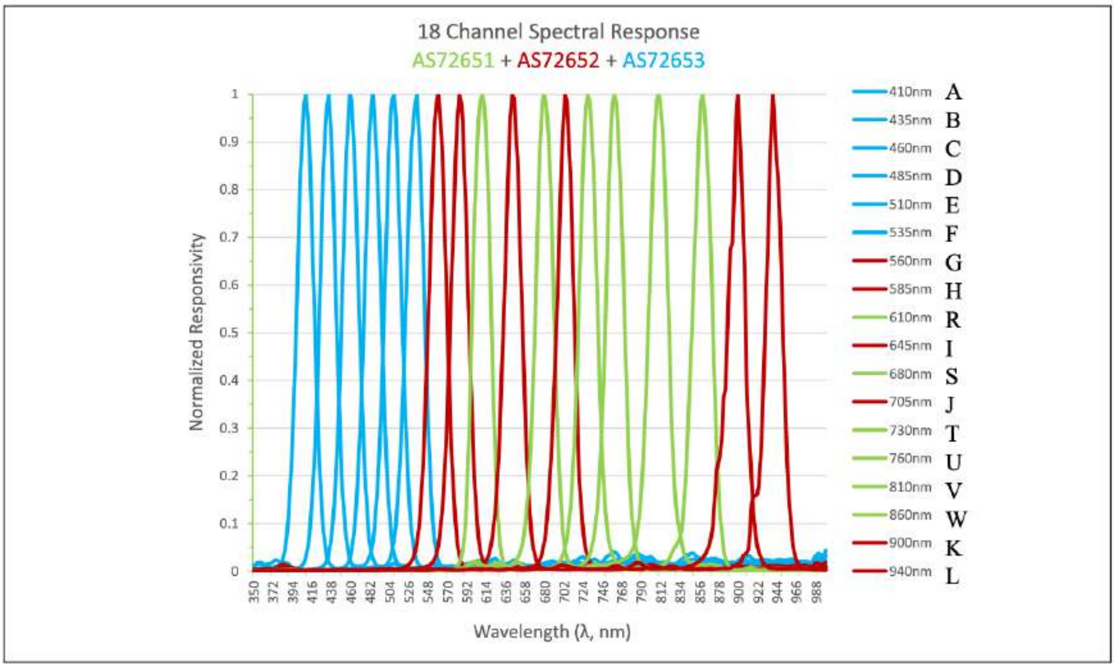

Figure 2. Declared 18-Channel Spectral Responsivity [4]

FIELD TEST

During the development of the prototype spectrometer device, thorough verification was conducted to ensure that external factors wouldn't significantly impact its readings. Three key factors were examined:

1. Temperature: the prototype was tested under different temperature conditions (30°C exterior, 25°C interior with air conditioning, and 22°C interior with air conditioning). The results showed minimal impact on the device's readings, indicating temperature stability.
2. Environmental Light: the prototype was tested under various lighting conditions (direct sunlight, shade, LED-lit room, complete darkness) to assess if external lighting affected the readings. The findings demonstrated that external lighting had negligible influence on the device's performance.
3. Long-Term Fluctuations: a stability test was conducted, where the prototype continuously collected spectrometer readings over an hour. The initial anomalies in readings quickly stabilized, and occasional minor fluctuations occurred. However, these anomalies rarely manifest in real-world use, suggesting acceptable stability.

To assess the device precision some tests and comparisons have been performed:

- Synthetic Comparison: colored card stock was used to perform synthetic tests on both the prototype and a professional spectrometer (Minolta CM2600D). The card stock used for this comparison was an Architetto Album Colore product, with a paper weight of and size of 24x33cm. The colors used were yellow, green, blue, red and black, measured in this order. A single measurement was performed on each colored card stock with each of the devices. For the CM2600D device, which allows both Specular Component Included (SCI) and Excluded (SCE) modes, the measurements were made in SCE mode only, as the prototype device has no ability to measure SCI. The data showed that the prototype's measurements were "generally similar" (see comparison below) to the professional device. However, the prototype occasionally produced noisier and differently scaled data in certain wavelength bands, particularly on higher-frequency wavelengths.
- Comparison on Real Monuments (first trial): tests were conducted on actual tombs in the main Milano cemetery (Monumentale). The prototype and the professional device (Minolta CM2600D) were used to measure the same surfaces. The results indicated that the prototype's larger sampling area and lower luminosity led to discrepancies in readings compared to the professional device. While some targets showed satisfactory similarity, others displayed significant differences due to the prototype's limitations.
- 2022 Trial: a second trial was carried out a year later with a different spectrophotometer sensor of the same model and maker. The results were similar to the first trial, suggesting that the prototype's limitations stem from its illuminant quality and the low-cost sensors. Despite efforts to sample even areas, the prototype's performance did not notably improve.

Overall, the verification process and field tests revealed that the prototype spectrometer device generally provides readings that are competitive, considering the cost, with those of a professional device in certain conditions. However, limitations related to the prototype's larger sampling area, illuminant quality, and sensor performance affect its accuracy on uneven and varying surfaces (Figure 3 and 4).

As can be seen from the plots in Figure 3 and 4, the data obtained from the prototype device is generally similar to what the professional device produces. However, it must be noted that the prototype often produces data which is noisier and, sometimes, which shows a different scale in some wavelength bands compared to the professional one, especially on higher-frequency wavelengths. Notably, this is not the case with all targets, but only with those presenting high values over these bands.

Unusually, the black card stock showed an inverse correlation between the two devices. This is almost certainly the result of random noise, as black produces extremely low readings that are easily influenced by small variations.

Target	Color	Corr.
0	Yellow	0.86
1	Green	0.94
2	Blue	0.20
3	Red	0.98
4	Black	-0.85

Table 1. target colors and correlation

For more detailed data, correlation plots, and results, refer to the provided directories and files within the FieldTests section. The project's code and documentation are available in an open GitLab (https://gitlab.di.unimi.it/lorenzo.bini/spettrometro-da-campo) repository for further analysis.

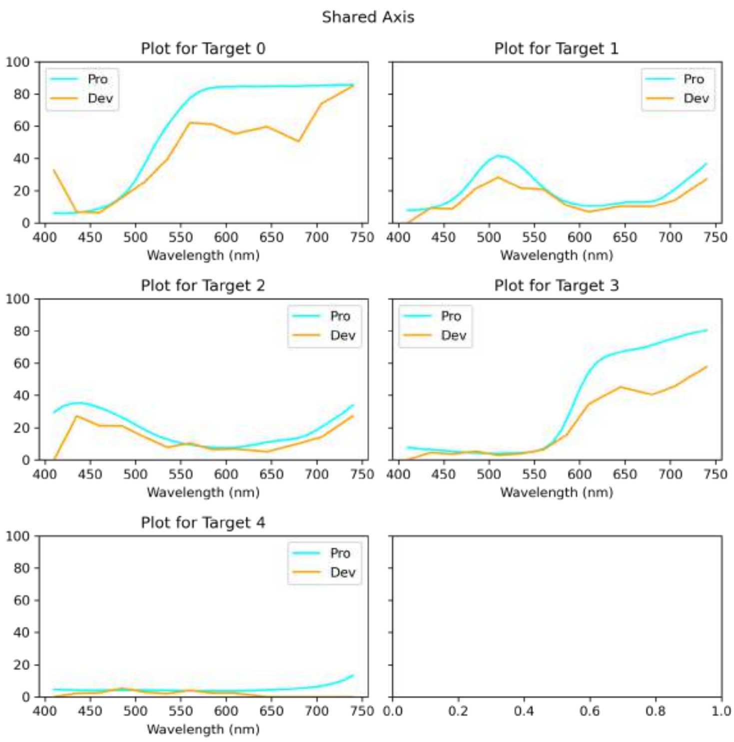

Figure 3. Plots of spectrometer data from professional and prototype devices

CONCLUSIONS

The prototype spectrophotometer exhibited good accuracy in synthetic tests on evenly-colored samples, indicating reasonable accuracy of the sensor packages. However, when tested on real targets at the Monumentale Cemetery (Milan, Italy), significant differences between the prototype and the professional machine were observed (Figure 3 and 4). Possible explanations for these differences include variations in aperture between the devices, positioning of the professional device, specific sensor settings on the prototype, and poor illumination provided by the prototype.

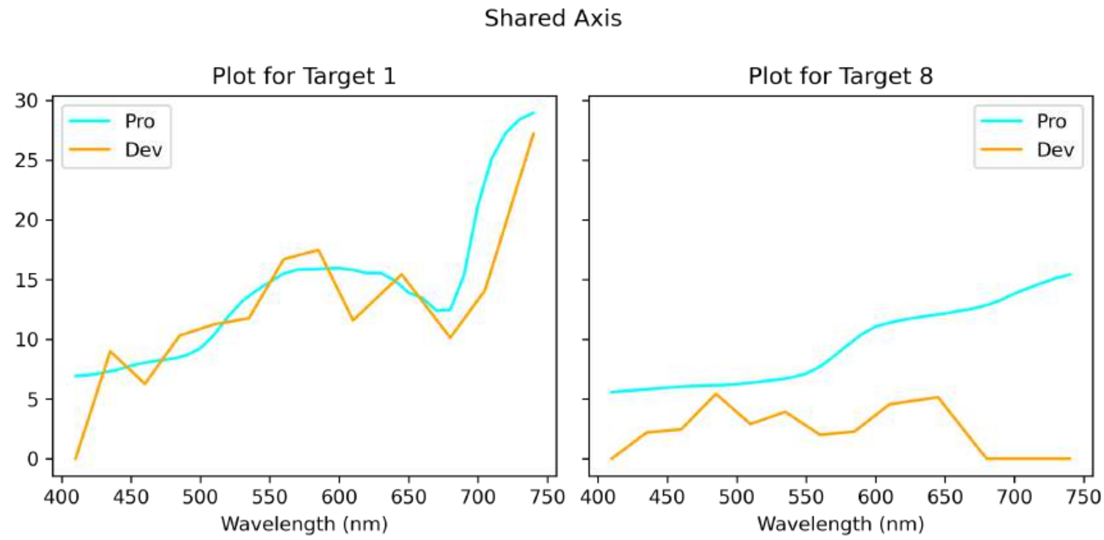

Figure 4. An example of good and bad similarity between prototype and professional data on a real target

The substantial difference in aperture size between the professional device (3mm) and the prototype (60mm) resulted in the prototype measuring a larger area, potentially leading to color differences averaging out due to the larger sample. This may suggest that a larger measuring area could provide more reasonable results for biofilm measurements.

Regarding the prototype's sensor settings, future research could explore adjusting gain, integration time, and sampling interval to optimize results and compare with the professional device's parameters.

The prototype's illuminant, consisting of three white LEDs, proved to be less powerful compared to the professional device's xenon-based flash. The prototype's LEDs were sensitive to power delivery conditions, flickering with slight movements. Investigating the use of a more powerful illuminant, like a camera-grade flash, could enhance performance, especially on dark surfaces. An external light source can be easily embedded in a further version of the device.

Although the prototype's performance was lower compared to the professional device, its cost-effectiveness and additional features make it noteworthy. The overall cost is around 100 EUR to build, the prototype offers GPS location recording, temperature and humidity recording, a user-friendly web interface, and full data visualization (vs. a clumsy proprietary interface for the professional device). The web interface facilitates data download to any Wi-Fi-enabled device without complex hardware interactions. The prototype's portability, usability, and affordability present advantages over the professional device.

REFERENCES

1. Prieto, Beatriz, Patricia Sanmartín, Benita Silva, and Francisco Martínez-Verdú. 2010. “Measuring the Color of Granite Rocks: A Proposed Procedure.” *Color Research & Application* 35 (5): 368–75. https://doi.org/10.1002/col.20579.
2. Sanmartín, Patricia, Federica Villa, Andrea Polo, Benita Silva, Beatriz Prieto, and Francesca Cappitelli. 2014. “Rapid Evaluation of Three Biocide Treatments Against the Cyanobacterium Nostoc Sp. PCC 9104 by Color Changes.” *Annals of Microbiology* 65 (2): 1153–58. https://doi.org/10.1007/s13213-014-0882-3.
3. Sanmartín, P., F. Villa, B. Silva, F. Cappitelli, and B. Prieto. 2010. “Color Measurements as a Reliable Method for Estimating Chlorophyll Degradation to Phaeopigments.” *Biodegradation* 22 (4): 763–71. https://doi.org/10.1007/s10532-010-9402-8.
4. https://ams.com/en/as7265x#tab/documents

SPECTROFLUORIMETRY – A NEW PARADIGM IN COLOR APPEARANCE

Jack A Ladson[1]* and Charles Lategano[1]

[1]HunterLab, 11491 Sunset Hills Rd, Reston, VA 20190

*Corresponding author: Jack A Ladson, Jack.Ladson@HunterLab.com

ABSTRACT

Surface luminescence, or fluorescence as it is more commonly called, is used in various materials to enhance an object's apparent whiteness and colorfulness. These materials or coatings contain fluorescent dyes and colorants that enhance these unique color appearance properties. The color appearance attributes of materials, including fluorescence, is essential in accurately evaluating coatings, detergents, textiles, pens & markers, plastics, and fluorescent safety colors.

A spectrofluorometer provides the only standardized way in colorimetric spectrometry to measure and quantify the photoluminescence of calibration standards and materials.

Technical advancements in Fluorescent Whitening Agents, FWAs, require an accurate assessment of the samples' luminescent character. The bi-spectral method is the only precise way to determine the Bi-Spectral Luminescent Radiance Factor (BSLRF). The values obtained by measuring the BSLRF are independent of instrument characteristics. This feature allows the samples' total radiance properties to be calculated. These data allow the critical parameters of color appearance properties to be calculated for any illumination spectrum of interest. These data are a vital component in determining product success.

The instrument geometry is significant in the determination and characterization of fluorescence. The CIE recommends the bi-directional geometry, of 0o illumination: 45o detection, for the measurement of fluorescence. This is the referee method for the characterization of the fluorescence phenomenon. The sphere geometry, which is more prevalent in color appearance industries, generates ambiguous and inferior results.

The accurate characterization of the specimens' color appearance depends upon the content of illumination on the specimen. The equipment, methodologies, and procedures were developed to produce and evaluate demonstrated conformance to daylight illumination in the instrument's sample plane. This realization is a first in the color appearance industry and allows us to visualize samples differently.

INTRODUCTION

In color spectrophotometry, we characterize materials by their reflectance spectra. In color appearance spectrofluorometry, the color appearance of opaque materials is determined not only by reflectance spectra but also by the fractionated component of photons reflected or emitted at each wavelength from the near UltraViolet, UV, through the visible, and into the near Infrared, IR. In the component of color attributable to fluorescence, we have photons' absorption, excitation, and emission. The quantity of interest is $\beta_\tau(\lambda)$. This parameter is the sum of the spectral radiance factor, $\beta_R(\lambda)$, and the spectral luminosity factor, $\beta_L(\lambda)$. The equation is given by:

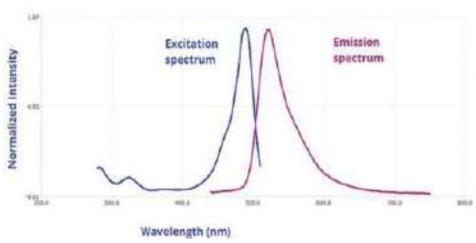

Figure 1-Typical Fluorescence Spectra

$$\beta_\tau(\lambda) = \beta_R(\lambda) + \beta_L(\lambda) \tag{1}$$

The spectral range of emission is at a different frequency (wavelength) band and outside the frequency band than the excitation. Here is a working definition[1] of fluorescence. The classical description of fluorescence describes the spontaneous emission of luminescence radiation from an excited molecule. Remember that fluorescence is the process of an excited molecule relaxing to the ground state by the emission of a photon at a higher charge. In colorimetry, fluorescence light has a longer wavelength and lower energy than the absorbed light. This phenomenon is termed Stokes Shift and occurs because of the energy loss between the time, t, that a photon is absorbed and the time a new one is emitted, typically less than 10^{-6} to 10^{-8} seconds[2]. The Stokes shift is named after British scientist Sir George G. Stokes, who first described fluorescence in 1852. A definition of standards includes the physical requirements and chemical basis of standards. Instrument and standards characterization significantly affects values used for transfer calibration. This subject is discussed in the following paragraphs. Phosphorescence is another species of photoluminescence. The understanding of phosphorescence is similar, except that the initial and final states have different spins termed multiplicity. The time, t, is greater than 10^{-6} seconds. The entire molecular fluorescence lifetime, from excitation to emission, is measured in billionths of a second; the phenomenon is the interaction between light and matter. This is the basis for steady-state fluorescence, time-resolved fluorescence spectroscopy, and the basis of this paper. The time difference is the phenomenological difference between these two species. A Jablonski diagram[3] illustrates the mechanism and the effect of fluorescence and phosphorescence. Chemiluminescence is another phenomenon of photoluminescence that includes energy from chemical reactions occurring within living organisms, such as glowworms and fireflies.

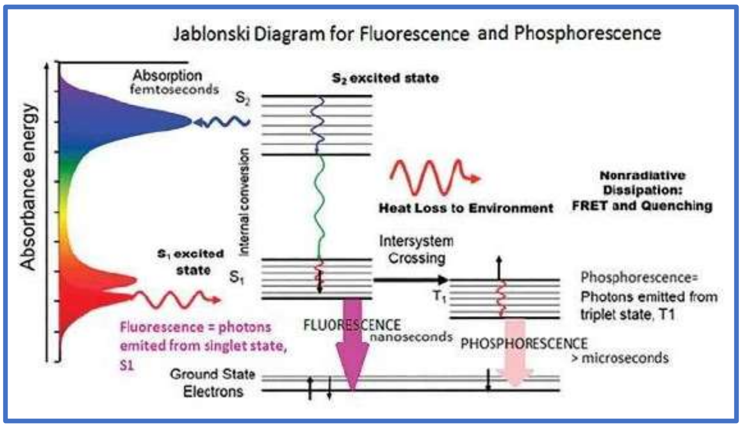

Figure 2-Jablonski Diagram

APPLICATIONS OF FLUORESCENCE MEASUREMENT

Assessing fluorescence can be viewed into two different categories; The first is analytical applications. These applications are found in the science fields, such as; biochemistry, medical diagnostics, and biotechnology. Another broad application addressed primarily in this paper is colorimetric fluorescence spectrometry. The measurement and quantification of photoluminescence in materials, such as coatings, detergents, inks, paper, plastics, and textiles, are inherently flawed and neglected. Users of these measurement techniques neglect the imprecisions that cause unreliable and poor-quality assessments. These poor-quality measurements are due primarily to incorrect instrumental optical geometry, inadequate calibrations, improper measurement methods, and other instrumental effects. Ineffective

[1]https://chem.libretexts.org/Bookshelves/Physical_and_Theoretical_Chemistry_Textbook_Maps/Supplemental_Modules_(Physical_and_Theoretical_Chemistry)/Spectroscopy/Electronic_Spectroscopy/Radiative_Decay/Fluorescence
[2] In the literature, this value ranges between 10^{-5} and 10^{-12} s.
[3] HORIBA Scientific. "*Fluorescence Spectroscopy - Applications and Principles*". *AZoM*. 10 July 2022. <https://www.azom.com/article.aspx?ArticleID=16086>

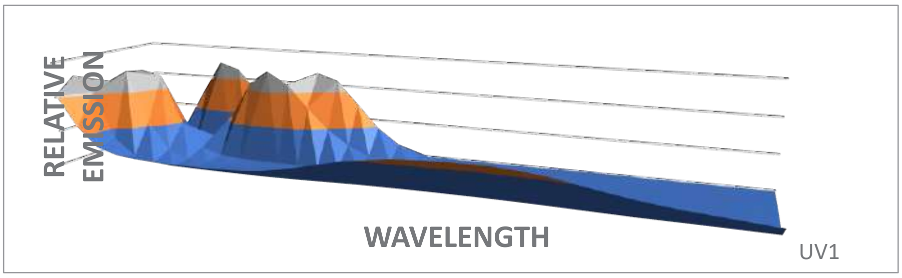

Figure 3- Typical Emission of LEDs

instrumental error corrections are unaccounted for by most colorimetric spectrometer manufacturers. Purchasers of said equipment are frequently ignorant on how to proceed. The confusion is further manifest by different terminology between these two general areas, quantifying results in terms of photons and radiometric quantities.

SPECTRAL BANDWIDTH

The spectral bandwidth required to accurately measure luminescence, fluorescence, and phosphorescence is specified in multiple sources as 5 nanometers (nm) bandwidth. The requirements are specified in ASTM E-388[4], *Spectral bandwidth and wavelength accuracy of fluorescence spectrometers*.

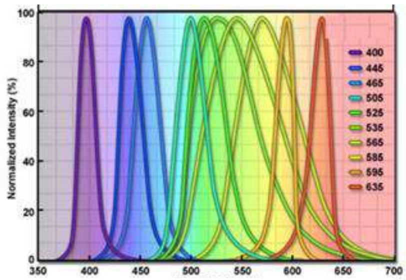

Figure 4 Typical LED Spectral Power Distribution

Some manufacturers use LEDs as a pseudo-narrow-band monochrometer. The full width specifies fluorescence spectrometers' spectral bandwidth and wavelength accuracy at half maximum (FWHM; bandwidth). A typical LED bandwidth, when used as a quasi-monochrometer, varies between 20 and 70 nanometers (see Figure 2).

The issue with a system with a large FMWH is that the spectral difference in excitation and emission wavelengths may be equal to or less than the bandwidth of the measuring device. For instance, a commonly used fluorescent yellow dye in 2- ethoxy ethyl acetate has a spectral difference between the excitation and emission wavelengths of approximately 17 nm[5]. There are several issues of concern when the instrumental bandwidth specification exceeds the requirement. First, the excitation frequency of the fluorescent compound can not be determined. Secondly, since the frequency of excitation is not known, neither can the relative energy known that caused the excitation. Thirdly, the quantum efficiency of the fluorescent compound in the vehicle cannot be determined. Hence, the efficacy cannot be quantified. In this paper, we define quantum efficiency as the percentage of molecules in an excited state that decay to the ground state by fluorescent emission in the spectral range of 380 to 560 nm. Fourthly, it is unknown if the total reflectance component, including the radiance from the fluorescent component, can be quantized. All this goes to say as a result of these unknowns, an indeterminable difference between the excitation and the emission cannot be resolved; hence, fluorescence cannot be reliably detected.
The conceptual arrangement of the emission of LEDs in a spectrofluorometer is presented as shown in Figure 3.

---

[4] ASTM E 388-04. "*Spectral bandwidth and wavelength accuracy of fluorescence spectrometers*", in Annual Book of ASTM Standards, Vol. 03.06, ASTM International (2004, original version 1972).
[5] *Tutorial on Fluorescence and Fluorescent Instrumentation*, Section_2, Washington.edu.

COLORIMETRY

In object color colorimetry, we assess the object's overall color appearance by quantifying the emitted fluorescent component and the spectrally diffuse reflectance factor, known as the body color, under a broad-band illumination source. These reflected radiations are responsible for determining the color appearance properties of the material being characterized. Typical materials are coatings, detergents, markers, paper, pens, plastics, textiles, and fluorescent safety colors. These numerical values convolved with the values for the desired illuminant-Observer condition produce colorimetric values used for analysis. These tables and convolution mathematics are specified in ASTM E 308, Standard Practice for Computing the Colors of Objects using the CIE System[6]. Most all colorimetric spectrometers incorporate these computations and tables. Additionally, the instrument must conform to the geometries recommended by the International Commission[7] on Illumination. There are two geometries recognized and specified by the CIE. These geometries are D:8° , Diffuse : Detection, known as the sphere or hemispherical geometry. An additional notation associated with this geometry denotes the inclusion, i, or the exclusion, e, of the specular reflectance component. The other CIE-recognized geometry is 45° illumination, 0° Detection, known as the bi-directional geometry. The standardizing authorities realize and approve reciprocal geometries for the integrating sphere or bi-directional geometries. As referenced in this article, the notations for these reciprocal geometries are 8°:D or 0°:45°, respectively.

GEOMETRIES

Spherical Geometries

Most colorimetric spectrometers sold and utilized worldwide are of the sphere geometry, D:8°. Regrettably, the measurement error of the fluorescence component is exacerbated in this geometry and, therefore, not satisfactory for the characterization of fluorescence. Alman and Billmeyer8 demonstrated that this geometry is less than ideal for fluorescence characterization. This is because the sphere geometry alters the source spectral irradiance on the specimen, and the emitted fluorescence contributes to the measurement values of the diffuse reflectance component. This means that the diffuse reflectance component depends upon the emitted fluorescent component's magnitude and the integrating sphere's efficiency. Additionally, the initial fluorescence radiance impinges again on the specimen, causing an additional excitation and emission, creating erroneous values. Therefore, this geometry is unsuitable for quantifying the emitted fluorescent component in object color characterization.

Bi-directional Geometries

For the reasons cited in the preceding paragraphs, the recommended reference geometry for measuring fluorescence materials is bi-directional. Reducing the variation caused by irregularities and non-homogeneities in the surface structure and the uniformity of the colorant distribution, the annular circumferential geometry minimizes errors and is preferred. This geometry carries the notation 0°:45°c. The letter c in the instrumental geometry notation refers

[6] Available from ASTM International,100 Barr Harbor Drive, West Conshohocken, PA 19428, www.ASTM.org.
[7] Commission Internationale de l'Elcairage (CIE), https://www.techstreet.com/cie/?,
[8] D.H. Alman, F.W. Billmeyer, *Integrating Sphere Errors in the colorimetry of fluorescent materials*, Color Research and Application, 1976. 141-145

to circumferential detection. This design reduces the error contribution attributable to the imprecise positioning of the non-homogenous specimen on the instrument's sample port. The notation for this bi-directional geometry is: 0º:45ºc. This circumferential viewing geometry (Detection) at 45 degrees and the standard illumination normal (Illumination) geometry minimizes the error contribution attributable to surface defects, structure, or patterns. A fluorescent specimen used in the safety industry is shown in Figure 2. Note the stripes and a wire mesh pattern incorporated in the design. This sample is approximately one hundred millimeters (4 inches) square. The sample port is fifty-one millimeters (2 inches) in diameter.

Figure 5 Geometric Patterns on an Orange Fluorescent Specimen

Sampling the surface of the fluorescent specimen over its surface using a cartesian coordinate method and including rotating the specimen about its geometrical axis 12 times shows no significant change in the deviation of the colorimetric readings larger than the measurement uncertainty made under reproducibility conditions[9]. This is attributable to the excellence in the design of the optical system.

It is well known and recognized that competent high-level measurement of fluorescent specimens could only be made using a two-monochromator method illuminating the specimen under a standard illuminant condition. The methodology we chose uses near monochromatic illumination and polychromatic detection. Because the spectrofluorometer optical design conforms to known, referenced, international standards for colorimetric spectrometers, a specific, trustworthy colorimetric answer can be realized.

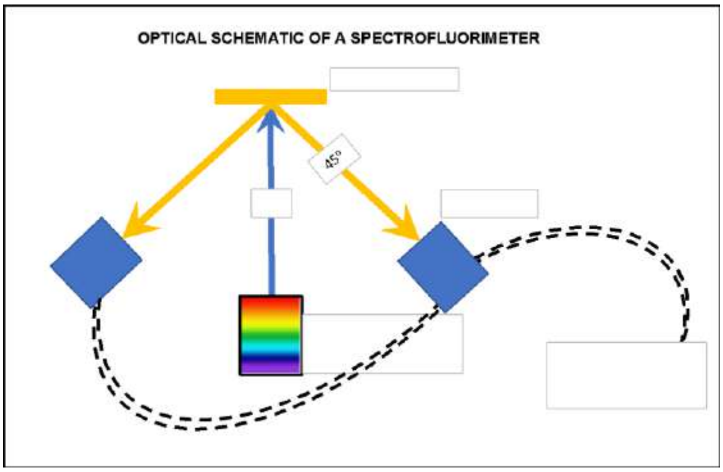

Figure 6-Optical Schematic

Conceptually, a bi-directional spectrofluorometer operates in this manner. First, the illumination monochrometer is set to the beginning wavelength, 380 nm. Then the specimen is illuminated with this spectrally selective illumination. The sample's spectral reflectivity and fluorescent radiance are captured and measured with a low bandpass, 5 nm, monochrometer over the spectral range of measurement from 390 to 700 nm. The illumination wavelength increments a step, say 5 nm, to 385 nm, and the collection of the sample's spectral radiance is collected over the visible range of the specimen's excitation. This process continues over the defined spectral range within the visible spectrum of the specimen's emission range.

This procedure is known as the bi-spectral method of fluorescent measurement. The bi-spectral, 45º:0º, measurement is the referee method used to study fluorescence measurements' colorimetry. A spectrofluorometer for color measurement of opaque fluorescent materials must conform to the geometry specified by the CIE. This method allows the complete separation of the two

[9] REF ASTM E-XXX, ASTM International,100 Barr Harbor Drive, West Conshohocken, PA 19428, www.ASTM.org.

components – the spectral reflectance factor and the fluorescent radiance. This is the definition and the meaning of the term spectrofluorometer.

CALIBRATION

Typically, spectrally diffuse reflectance specimens are calibrated by substitution or comparison measurements. The idea here is that specimens nominated to serve as standards must have the following:

1- Similar spectral reflectance factors,
2- Similar bi-directional reflectance distribution functions (BRDFs),
3- Lambertian radiator properties,
4- Short-Term stability,
5- Long-Term stability,
6- Reflectance uniformity, and
7- Non-photoluminescence property.

Photoluminescence is the singular most significant error in the calibration of material standards. In the industry, it is well known that most materials produce photoluminescence upon exposure to UV radiation. Most all commercial color spectrometers employ UV-CUT filters to eliminate or minimize the UV radiation that causes sample photoluminescence. Little attention has been paid to this kind of photoluminescence. Our system is dual-beam and quite sensitive. Therefore, we detect the existence of photoluminescence on materials previously not thought to be photoluminescent. A dual or double-beam spectrometer operates faster and provides more reproducible results. The system provides automatic correction for any change in the light intensity of the sample measurement beam attributable to the light source by measuring the power of the reference beam.

There are a few studies on the fluorescence properties of opal glasses[10] and ceramic tiles and even fewer studies on visible activated fluorescence. Analyzing calibration plaques of popular suppliers of spectrometers in Asia, China, Europe, and the US reveals errors of several percent in the assigned values. This is attributable to photoluminescence in the instrument calibration plaques that adversely affect the spectrally diffuse reflectance measurements.
These calibration plaques are known as physical transfer standards. These standards link the fluorescence measurements and the radiometric (colorimetric) scales. We used standards calibrated by a national metrology institute, such as National Research Council[11], NRC.

ILLUMINATION

For colorimetry of fluorescent materials, Illuminant D65 is the essential condition for irradiating a specimen under test or calibration of a spectrofluorometer. The spectral power distribution measured in the sample plane using an Ocean Optics 2000+ Fiber Optic Spectroradiometer[12] reveals that the spectral content of the illumination closely conforms to the definition of Illuminant D65. Another complementary method is specified by CIE 51.2, *A method for assessing the daylight quality of simulators*. We adapted this method and developed a protocol for the spectrofluorometer under test. The conformance demonstrated to CIE 51.2 is a B rating. The high-quality B rating, with A rating as the highest, is required for the accurate instrumental

[10] *Photoluminescence from White Reference Materials for Spectral Diffuse Reflectance upon Exposure to the Radiation Shorter than 400 nm*, H. Shitomi, I. Saito, National Metrology Institute of Japan, National Institute of Advanced Industrial Science and Technology (NMIJ/AIST), 1-1-1 Umezono, Tsukuba, Ibaraki, 305-8563, JAPAN
[11] https://nrc.canada.ca/en
[12] https://www.oceaninsight.com/globalassets/catalog-blocks-and-images/manuals--instruction-old-logo/spectrometer/usb2000-operating-instructions1.pdf

colorimetric assessment of fluorescent specimens. Additionally, since the spectral power distribution illuminating the specimen is known, and the fluorescence component is known, then the colorimetric properties of the specimen under a different illuminant can be determined. This attribute is essential in understanding how the specimen will appear under other spectral power distributions (illuminants) and the conspicuity of the specimen. These values are crucial to understanding safety colors. We believe this is the first colorimetric spectrometer to realize the spectral power distribution of illuminant D65 in the instrument's sample plane. This feature represents a significant milestone in the science of color appearance.

Color instrument manufacturers that do not accurately simulate a daylight illuminant in the sample plane of the measuring instrument cannot accurately access a fluorescent color component. This is particularly true of those manufacturers that use optical filters to modify the spectral power distribution of continuous or pulsed xenon sources. These manufacturers measure in one, two, or more conditions, often called UV-IN and UV-OUT. The difference in the spectral content of these sources has significant non-compliance with the spectral power distribution of Illuminant D65. These systems do not warrant a rating under this system. This causes substantial uncertainties[13] in the measured total radiance factors. Additionally, this is a considerable factor negatively influencing inter-instrument agreement for fluorescent specimens.

SPECTRAL ACCURACY

The classical CERAM[14] standards and others were used to assess colorimetric performance. Measuring the instrument standard 30 times under repeatability (r) conditions, we achieved a performance of 0.15 CIELAB DE*2000(1:1:1) units. Over the 12 CCSII standards under reproducibility (R) conditions, we achieved a performance of less than 0.50 CIELAB DE*2000(1:1:1) units. The initial production run is small, and these data may not be statistically significant; however, the inferred batch r & R statistical results are commensurate with those values presented.

COLORIMETRIC RESULTS

We conventionally acquired data after calibrating, as discussed above. The spectral reflectance factor and the radiance data are obtained as each LED(s) are individually and sequentially activated. A narrow bandwidth, high-precision polychromator collects the data for analysis. This process is continued and repeated over the visible spectrum. The collected data are arranged, thereby providing the data for a Donaldson Matrix[15].

A numerical example of the Donaldson Matrix is shown below in Table 1. The spectral reflectance factor is shown on the diagonal. It is highlighted and in bold. The data in blue presented above the diagonal is anti-Stokes data. Anti-Stokes data are not discussed here. We are interested in the data below the diagonal. These data, shown in yellow, represents the fluorescence data. The range of these data is from 380 to 700 nm.

[13] Zwinkels, JoAnn, et.al, *Design and Testing of a two-monochrometer reference spectrofluorometer for high accuracy total radiance factor measurement*, National Research Council, Applied Optics, Vol. 36, No 4, 1 February 1997

[14] Lucideon Limited, Queens Road, Penkhull, Stoke-on-Trent, Staffordshire ST4 7LQ, UK

[15] Donaldson, R. (1954). Spectrophotometry of fluorescent pigments. British Journal of Applied Physics, 5(6), 210.

Table 1- Illustrative Donaldson Matrix

Illustrative Donaldson Matrix

EMISSION \ EXCITATION	380	385	390	395	400	405	410	415	420
380	**1.03E-03**	0.00E+00	4.84E-04	7.87E-05	5.14E-04	1.02E-03	1.58E-04	4.99E-04	5.08E-04
385	0.00E+00	**1.29E-03**	2.88E-04	0.00E+00	2.16E-04	2.67E-04	3.18E-04	2.60E-04	2.37E-04
390	2.56E-04	1.39E-04	**1.47E-03**	2.01E-04	2.30E-04	3.10E[illegible]	ANTI-STOKES LAND	[illegible]4	1.46E-04
395	1.30E-04	2.84E-04	9.83E-05	**1.72E-03**	2.85E-05	1.34E-04	2.56E-04	2.99E-04	2.09E-04
400	0.00E+00	7.16E-05	5.91E-04	5.05E-04	**5.02E-03**	3.65E-05	1.92E-04	4.87E-05	7.71E-05
405	0.00E+00	1[illegible]	FLUORESCENSE LAND	[illegible]-03	1.82E-03	**1.97E-02**	0.00E+00	0.00E+00	5.06E-05
410	0.00E+00	2[illegible]	[illegible]	[illegible]-04	3.41E-03	3.38E-03	**2.71E-02**	0.00E+00	0.00E+00
415	2.45E-04	1.17E-04	1.09E-04	1.46E-04	4.89E-04	3.08E-03	3.43E-03	**2.39E-02**	0.00E+00
420	7.73E-05	1.32E-04	5.31E-05	0.00E+00	8.62E-05	4.20E-05	2.17E-03	1.93E-03	**1.77E-02**
425	7.95E-05	6.59E-05	5.65E-05	0.00E+00	0.00E+00	0.00E+00	1.10E-04	1.32E-03	1.30E-03 ...

Estimating the bi-spectral Donaldson matrix provides the spectral characterization data of fluorescent objects. The Donaldson matrix represents the spectral radiance factor that consists of the sum of two components: a reflectance factor and a luminescence radiance factor. The luminescent radiance & luminescence is separable into the emission and excitation wavelength components; hence a complete understanding of the phenomenon of fluorescence can be assigned to the specimen being characterized. In the Donaldson Matrix, the diagonal is the reflected component, and the data below the diagonal is the fluorescent component.

Measuring highly fluorescent specimens, as shown in Figure 2, used in safety applications, we achieved the following results, as shown in Table 2.

Figure 7 Fluorescent Standards

We favorably compare our values to those reported by the National Physics laboratory, NPL and the "Gold Standard" in the industry, a Model BFC- 450, produced by Labsphere[16].

This separation of the luminescence radiance factor from the spectral reflectance factor allows investigations to occur that describe the color appearance of the specimen under different illuminants. One can discern the effect of illumination by LEDs, horizon light, another illuminant, or any source of illumination where the spectral power distribution is known, LEDs. Understanding the product's color appearance in different lighting conditions is invaluable for product designers. The success or failure of a product can be determined by understanding the product's color appearance.

[16] Labsphere, Inc., 231 Shaker St., North Sutton, NH 03260, (603) 927-4266, https://www.labsphere.com/

Table 2 Data Fluorescent Standards

Flo -Yellow-Green						
Sensor	**Yr**	**Yt**	**Yf**	**Yf/Yt**	**Max %R**	**λ nm at Max**
BFC-450 Report 3M 2deg	58.13	113.58	55.46	49%		
HL Solve Donaldson 5nm D65/2	58.13	106.29	48.16	45%	156.8	540
HL Solve Donaldson 10nm D65/2	58.05	106.33	48.28	45%	157.3	540
Spectrofluorometer D65/2	76.56	136.44	59.89	44%	209.2	540
Flo -Yellow						
Sensor	**Yr**	**Yt**	**Yf**	**Yf/Yt**	**Max %R**	**λ nm at Max**
BFC-450 Report 3M 2deg	31.01	76.79	45.78	60%		
HL Solve Donaldson 5nm D65/2	31.01	69.44	38.43	55%	166.7	580
HL Solve Donaldson 10nm D65/2	30.85	69.36	38.51	56%	168.3	580
Spectrofluorometer D65/2	42.82	80.22	37.40	47%	169.5	580
Flo -Orange						
Sensor	**Yr**	**Yt**	**Yf**	**Yf/Yt**	**Max %R**	**λ nm at Max**
BFC-450 Report 3M 2deg	13.92	33.63	19.72	59%		
HL Solve Donaldson 5nm D65/2	13.92	29.24	15.32	52%	113.4	620
HL Solve Donaldson 10nm D65/2	13.85	29.15	15.30	52%	113.8	610
Spectrofluorometer D65/2	19.82	32.77	12.95	40%	129.0	630

DISCUSSION

We observe that some CERAM-colored standards are fluorescent. We are confirming the work of Koo[17], et.al. and concluding that more work is required to fully understand the implication of fluorescence in color instrument standardization, color measurement, and assessment.

CONCLUSIONS

We discovered that a new, novel, high-accuracy spectrofluorometer can be used to measure and characterize industrial specimens' fluorescent components and the spectral reflectance factor of the specimen. The spectral range of characterization is 380 to 700 nm. The illumination LEDs are deployed to produce a close match, a B rating, to CIE Illuminant D65 in the sample plane and provide the spectral selectivity in concert with a classical monochrometer to create an effective two-monochrometer system using 45° circumferential detection and normal illumination conditions. This design follows recommendations in ASTM & CIE colorimetric standards.

Designers are always looking for notable effects to increase sales, and manufacturers are looking for ways to characterize optical properties, thereby reducing the cost of goods sold, COGS. This product offering is unique in the color appearance market and offers colorists and stylists valuable information not previously or currently available.

[17] Koo, A., *Fluorescence of ceramic color standards*, https://doi.org/10.1364/AO.49.002376

DISPLAY ENHANCEMENT FOR HDR CONTENTS UNDER AMBIENT LIGHTING

Yiming Huang, Haisong Xu*, Yuemin Li, and Minhang Yang

College of Optical Science and Engineering, Zhejiang University, Hangzhou 310027, China.

* Corresponding author: Haisong Xu, chsxu@zju.edu.cn

ABSTRACT

High dynamic range (HDR) could enhance the contrast and gradation of the image, and it is recommended to be watched in darkrooms for the best viewing experience. However, the practical lighting conditions are much more diverse, making the images displayed under a high illumination level appear dull and washed out. In this work, we propose a method to enhance the display quality for HDR contents under ambient lighting. Specifically, the perceptual luminance is first quantified based on the contrast sensitivity of the human visual system (HVS). Then, the luminance mapping operator is constructed by treating the target as a transcoding problem between the quantified luminance and the HDR display model. Finally, the mapping operator is implemented to the luma channel of the image in $Y'C_B'C_R'$ format, and the chromatic components are scaled accordingly. The results of psychophysical experiment indicate that the proposed method could significantly improve the image quality under different ambient lighting levels.

Keywords: Display enhancement, HDR contents, ambient lighting

INTRODUCTION

By enriching the shadow and highlight details, high dynamic range (HDR) could enhance the image, delivering a more vivid visual experience to users than standard dynamic range (SDR) system. In order to attain the best image quality, the recommended surround luminance for viewing HDR contents is below 5 cd/m^2 [1]. However, the practical ambient illumination is much more diverse, including dim living rooms, bright offices, outdoor environments, and etc., resulting in the loss of image details and contrast. Due to the absolute luminance mapping characteristics of the perceptual quantization (PQ) curve [2], increasing the peak luminance of the display would not improve the overall brightness perception of the HDR images. Therefore, the pixel-level enhancement methods are required. In recent years, both Dolby laboratories and Samsung have separately introduced specialized solutions based on their respective standards [3], yet they are unable to encompass the dynamic range requirements for mobile display usage scenarios.

In this work, we propose a display enhancement method to offer "viewing consistency" across various ambient illuminations for HDR images. The proposed method is image contents independent, considering both the display characteristics and the perception of the human visual system (HVS).

METHODOLOGY

As one of the standard electro-optical transfer function (EOTF) of HDR, the PQ curve is obtained by integrating minimum detectable contrast from Barten's contrast sensitivity function (CSF) [4]. However, the luminance of the experimental data in Barten's model is lower than 500 cd/m^2, and it also does not account for the influence of the lighting environment. In light of this, the proposed method could be divided into two stages, i.e., surround-aware perceptual quantization and luminance mapping.

Surround-aware Perceptual Quantization Recently, a surround-aware CSF was modified on a state-of-the-art HDR display with the peak luminance over 4000 cd/m^2 [5], which was derived based on Barten's model as:

$$S(L,u,L_s)=R\left(L^*;a,b(u),c(u)\right)\cdot S_B(L,u) \tag{1}$$

where $L^*=L_s/L$ and L_s is the adapted luminance. The function R is the relative sensitivity and S_B represents Barten's model. The details of Eq. (1) could be found in [5]. Therefore, the minimum detectable contrast for each luminance L could be calculated as:

$$C_t(L,L_s)=\frac{1}{S_{\max}(L,L_s)}\times\frac{2}{1.27} \tag{2}$$

where $S_{max}(L, L_s)$ is the peak sensitivity to luminance L. The constant 2 is used for the conversion from modulation to contrast, and 1/1.27 is used for the conversion from sinusoidal to rectangular waves. In addition to the adaptation of the HVS, the reflected luminance on the screen would also affect the image quality under ambient lighting. Therefore, the total luminance of an HDR display under ambient illumination E_{amb} can be represented as:

$$L_{total}(Y,E_{amb})=L_d(Y)+L_{refl}(E_{amb})=\mathrm{PQ}(Y)+L_B+\frac{r}{\pi}E_{amb} \tag{3}$$

where Y is the pixel value, L_B is the black level, L_{refl} is the reflected luminance, and r is the reflectivity of the display. According to Eqs. (1) and (2), we set the minimum detectable contrast as the contrast between each pair of consecutive codes of the display, thereby quantifying the perceptual luminance as:

$$L_d(Y)=\begin{cases}L_B & Y=0\\ L_d(Y-1)\dfrac{1+1.27\cdot S_{\max}(L_{i-1},L_s)}{1-1.27\cdot S_{\max}(L_{i-1},L_s)}-\dfrac{r}{\pi}E_{amb} & Y\geq 1 \text{ and } L_d(Y)\leq L_W\end{cases} \tag{4}$$

A functional form of PQ could be adopted to fit the iterative luminance from Eq. (4) for further image enhancement, which we refer to as surround-aware perceptual quantization (SA-PQ) curve.

Luminance mapping The construction of the mapping operator is regarded as a transcoding problem, which aims to produce the identical image appearance as that from the ideal signal of SA-PQ when the transcoded signal is reproduced on the HDR display in a bright environment.

Figure 1 illustrates the concept of transcoding from the SA-PQ to the PQ curve, in which V_{clip} is the pixel value of the display's peak luminance, V and V′ are the normalized PQ encoding values before and after transcoding, and L_{PQ} and L_{SA-PQ} are their corresponding display luminance, respectively. Therefore, the luminance mapping operator can be modeled as:

$$V'=\begin{cases}\mathrm{PQ}^{-1}\left(\text{SA-PQ}\left(\dfrac{V}{V_{clip}}\right)\right) & 0\leq V\leq V_{clip}\\ V & V_{clip}<V\leq 1\end{cases} \tag{5}$$

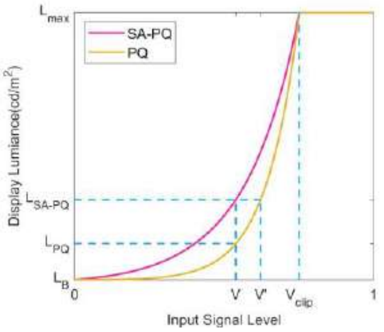

Figure 1. The schematic of transcoding from SA-PQ to PQ

In order to balance the efficiency and performance of the proposed method, the luminance mapping operator is implemented to the luma channel of the Y'C_B'C_R' color space, and the chromatic component is scaled according to the enhanced luminance as:

$$C'_d = C' \cdot \left(\frac{Y'_d}{Y'}\right)^s \tag{6}$$

where *Y'* and *Y_d'* are luma channels before and after the enhancement, respectively, *C'* and *C_d'* are the scaled chromatic values, and *s* is a constant, which is set to 0.4 in this study.

EXPERIMENTAL RESULTS

A series of visual evaluations were conducted to compare the performance of our method with the other two ones, namely Song et al.'s [6], and Borer et al.'s [7]. A panel of 11 participants (5 females and 6 males) participated in the psychophysical experiment, and they were all confirmed to have normal color vision. A smartphone of iphone13 was employed as the test device, with a peak luminance of 825 cd/m^2 and a display surface reflectance of approximately 4.6%. The experiment was conducted in three lighting conditions, i.e., 500 lx, 5000 lx, and 10000 lx, simulating the environments of a bright office, shadows in a cloudy day, and an overcast day, respectively. The psychophysical technique of categorical judgement was adopted, and the observers were asked to give their judgments on the overall quality of the test images and their enhanced results by 3 different methods. A total of 8 HDR video frames [8] were selected as the test images, so we obtained 1056 classification levels, i.e., 11 observers × 8 test images × (1 original version + 3 enhanced results) × 3 lighting levels. These raw visual data were further converted to interval scales as shown in Figure 2, together with Figure 3 presenting some enhanced results, indicating that our method obtained the best performance among the tested methods.

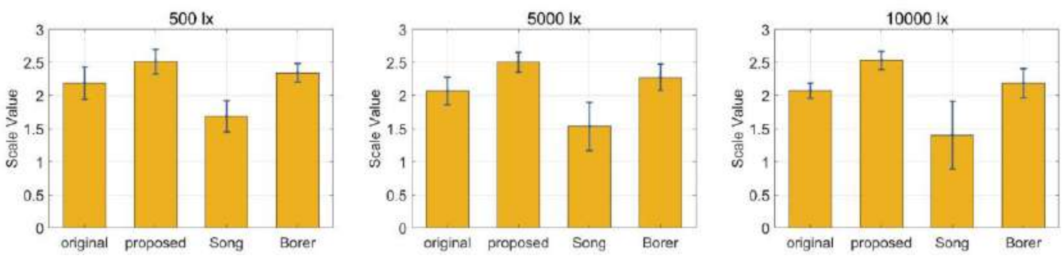

Figure 2. The scale values of different methods in the test lighting environments

Figure 3. The original images and the enhanced results by different methods under three ambient illumination levels. From top to bottom rows: 500 lx, 5000 lx, and 10000 lx

The runtime of the proposed method was also tested, which took approximately 0.032 s to enhance a 2K HDR image on a PC with Intel(R) Core (TM) i5-3470 CPU @ 3.20GHz. This means that the processing speed of our method could easily exceed 30 fps, implying its potential for real-time applications.

CONCLUSION

In this work, we propose a method to enhance the displayed HDR images under ambient lighting, considering the display characteristics as well as the perceptual luminance of the HVS. The experimental results demonstrate that the proposed method outperforms the existing algorithms and could significantly improve the perceptual quality of HDR images in the bright environment. The proposed method is image contents independent and requires a short time consumption, so it has the potential to be implemented for the video applications.

REFERENCES

1. ITU-R BT.2100-2 (2018). Image parameter values for high dynamic range television for use in production and international programme exchange.
2. Vo, D., Liu, C., Nelson, M., Mandel, B., & Hyun, S. (2022). HDR10+ Adaptive Ambient Compensation using Creative Intent Metadata. *IEEE Transactions on Consumer Electronics*, *68*(2), 149-160.
3. Miller, S., Nezamabadi, M., & Daly, S. (2013). Perceptual signal coding for more efficient usage of bit codes. *SMPTE Motion Imaging Journal*, 122(4), 52-59.
4. Barten, P. G. (2003). Formula for the contrast sensitivity of the human eye. In *Image Quality & System Performance*, *5294*, 231-238.
5. Yi, S., Jeon, D. S., Serrano, A., Jeong, S. Y., Kim, H. Y., Gutierrez, D., & Kim, M. H. (2022). Modelling Surround-aware Contrast Sensitivity for HDR Displays. *Computer Graphics Forum*, *41*(1), 350-363.
6. Song, Q., & Cosman, P. C. (2018). Luminance enhancement and detail preservation of images and videos adapted to ambient illumination. *IEEE transactions on image processing*, *27*(10), 4901-4915.
7. Borer, T. (2017). Display of high dynamic range images under varying viewing conditions. In *Applications of Digital Image Processing XL*, *10396*, 48-60.
8. Froehlich, J., Grandinetti, S., Eberhardt, B., Walter, S., Schilling, A., & Brendel, H. (2014). Creating cinematic wide gamut HDR-video for the evaluation of tone mapping operators and HDR-displays. In *Digital photography X*, *9023*, 279-288.

ESTIMATING SPECTRAL TRANSMITTANCE OF TRANSLUCENT MEDIA FROM AN OPACITY VALUE AND KNOWN SPECTRAL REFLECTANCE

Muhammad Safdar[1]* and Patrick Emmel[2]

[1]*Avient Corporation, Avient Colorants Singapore Pte Ltd, 618684 Singapore, Singapore.*
[2]*Avient Corporation, Avient Switzerland GmbH, Hauptstrasse 30, 4127 Birsfelden, Switzerland.*

*Corresponding author: Muhammad Safdar, muhammad.safdar@avient.com

ABSTRACT

An ill–posed problem of estimating spectral transmittance of a translucent scattering–material from known spectral reflectance and an average opacity was solved in the current study. Plenty of methods are available to reconstruct spectral curve of reflectance or transmittance from a given colorimetric measurement. Hitherto, no study is known to the authors that recovers transmittance spectrum from a value of opacity and known reflectance. Even though spectral reflectance is known or can be accurately recovered from colorimetric values, estimating transmittance curve from a given value of opacity (average–transmittance) is an ill–posed problem. The problem was solved using Kubelka–Munk model. The prediction model was tested using a large dataset consisting of over 100,000 plastic samples measured in Reflection/Transmission mode using a sphere–based benchtop spectrophotometer. The estimated transmittance curves were compared with the measured ones in terms of average–transmittance difference, root mean square error (RMSE), and color difference (in units of the CIEDE2000). The difference of the average–transmittance was kept at zero. Results showed that the predicted transmittance curves fall in the acceptable range of error as the plastic samples are mostly viewed in the direction of the incident light flux and not from the transmission side.

Keywords: Transmittance, Reflectance, Translucent Media, Spectral Recovery, Ill–posed Problem

INTRODUCTION

To accurately reproduce color appearance of translucent media, two measurements either reflectance–over–light & reflectance–over–dark or reflectance (over–light) & transmittance are required. In most of the practical scenarios (outside of laboratory), to reproduce a color sample, we are given either trichromatic colorimetric values or spectral curve measured from the reflection side and an opacity value (e.g., average–transmittance, contrast–ratio or hiding–power). Spectral measurements are crucial in surface color industry to avoid metameric matches of the colors being formulated as they are independent of the illumination and observer/camera responses. Transmittance curve is important to have in some applications e.g., spectral color matching, [1] scene rendering, [2] agriculture, [3] medical, [4] color appearance, [5] etc.

Different spectral reconstruction methods are used to obtain spectral information when only colorimetric information of the sample colors is given [6]. The problem of spectral reflectance reconstruction from colorimetric/camera measurements has been intensively studied over the past few decades [6–12]. Comparatively, reconstruction of transmittance has been little researched as it is required in fewer applications [13–15]. Bell and Baranoski [13] used a novel piecewise PCA approach (PPCA) to reconstruct reflectance and transmittance curves for herbaceous and woody specimens aiming at a root mean square error lower than 1%. Aghanouri *et al.*, [14] reconstructed spectral transmission from the RGB color values of colored solutions captured using a digital camera. They assembled a capturing box and gathered a spectral data set from colored solutions and employed principal component analysis (PCA), pseudoinverse, and matrix R methods to reconstruct the spectral transmission of clear solutions from their RGB data. They found that matrix R method gave the best performance. Such methods reconstruct spectral transmittance curves from measured colorimetric values. Moreover, the accuracy of the spectral curves reconstructed by means of above approaches, especially the kinds of training–based estimation approaches, highly depends on the amount, coverage of the gamut, and representativeness of valid samples in the training dataset. Generally, a larger sample set would help to improve the reflectance estimation accuracy. Whereas an analytical approach for reconstruction of spectral transmittance for translucent scattering–media from a single value of opacity (*defined as average–transmittance in the current study*) along with the reflectance spectra, used in the current study, is hitherto undiscovered as per author's knowledge.

An analytical model derived based on Kubelka–Munk theory is proposed in this study [16]. Kubelka and Munk derived relations for reflectance and transmittance as [16]:

$$\boldsymbol{R}_{KM} = \frac{1-\boldsymbol{R}_g\left(\boldsymbol{a}-\boldsymbol{b}\left(\mathrm{ctgh}(\boldsymbol{bS}X)\right)\right)}{\boldsymbol{a}+\boldsymbol{b}\left(\mathrm{ctgh}(\boldsymbol{bS}X)\right)-\boldsymbol{R}_g}, \tag{1}$$

and

$$\boldsymbol{T}_{KM} = \frac{\boldsymbol{b}}{\boldsymbol{a}\left(\sinh\,(\boldsymbol{bS}X)\right)+\boldsymbol{b}\left(\cosh(\boldsymbol{bS}X)\right)}, \tag{2}$$

respectively, where $\boldsymbol{R}_{KM}$, $\boldsymbol{T}_{KM}$, $\boldsymbol{R}_g$, X and $\boldsymbol{S}$ are KM reflectance (the reflectance of a specimen of thickness X mm placed over a backing of reflectance $\boldsymbol{R}_g$) and KM transmittance, reflectance of the backing, thickness of the specimen in *mm* and scattering coefficient per mm, respectively. And $\boldsymbol{a}$ and $\boldsymbol{b}$, respectively, can be written as follows:

$$\boldsymbol{a} = \frac{1}{2}\left(\frac{1}{\boldsymbol{R}_\infty} + \boldsymbol{R}_\infty\right), \tag{3}$$

and

$$\boldsymbol{b} = \frac{1}{2}\left(\frac{1}{\boldsymbol{R}_\infty} - \boldsymbol{R}_\infty\right), \tag{4}$$

where $\boldsymbol{R}_\infty$ represents the reflectance of the specimen at a thickness approaching infinity.

The rest of the paper is organized as follows. Test dataset is introduced in the next section, followed by the method implemented to reconstruct spectral transmittance. Results are then discussed, and conclusions are drawn in the final section.

Test Dataset

Measured reflectance and transmittance curves of more than 100,000 plastic samples historically produced at Avient Corporation were used as test dataset. The test samples were measured in Reflection/Transmission mode using a sphere–based bench–top spectrophotometer (Instrument: DataColor 850). Reflectance was measured using diffuse: eight–degree geometry, specular component included (di: 8^o) and *UV* (M_0 mode) included [17]. Transmittance was measured using diffuse/normal geometry, regular component included (di: 0^o) [17]. The measurements covered the spectral range between 400 *nm* to 700 *nm* with 10 *nm* intervals. The CIE L*a*b* values for all the test samples are plotted for reflectance and transmittance as shown in Figure 1. As a few examples, reflectance and transmittance curves of a few typical plastic samples are shown in Figure 2. Note that reflectance and transmittance of a given sample can sum to a value greater than 1.0 (see Cyan (dotted) curve at 650 *nm in Figure 2*) at a given wavelength due to the way they are measured. The sum of reflectance and transmittance at a given wavelength (λ) can go up to $R_{g,\lambda}$+0.923, where $R_{g,\lambda}$ is the reflectance of the light background used to measure reflectance of the specimen at wavelength λ and 0.923 is the theoretical maximum transmittance for a media with refractive index of 1.5 [1].

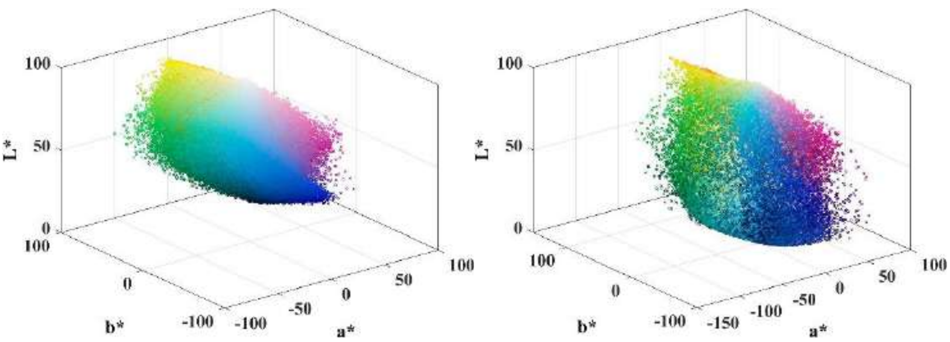

Figure 1. Color distributions of the test samples in the CIE a^*b^* chromaticity coordinates computed from: (left) reflectance, and (right) transmittance.

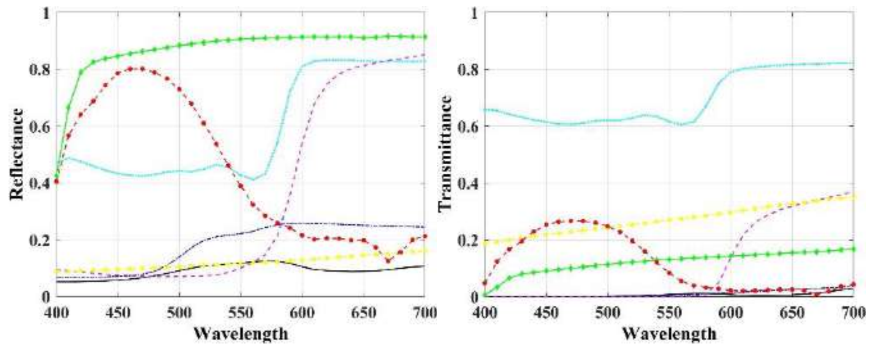

Figure 2. Some typical measured spectral curves from the test set: (left) measured reflectance, and (right) measured transmittance.

METHODOLOGY

The Kubelk–Munk (KM) reflectance ($\boldsymbol{R}_{KM}$) can be computed from measured reflectance ($\boldsymbol{R}_m$) using famous Saunderson's correction [18]:

$$\boldsymbol{R_{KM}} = \frac{\boldsymbol{R_m - r_1}}{\boldsymbol{1 - r_1 - r_2(1 - R_m)}}, \tag{5}$$

where r_1 and r_2 are the fraction of the incident light which is reflected from the front surface of the sample, and the fraction of the light incident upon the surface of the sample from the inside, which is reflected, respectively. Eq. (5) was also used to apply surface correction on the measured reflectance of the background. Kubelka, [16] derived a list of practical formulas from Eqs. (1) and (2) where transmittance ($\mathbf{T}_{\mathrm{KM}}$) can also be written as:

$$\boldsymbol{T_{KM}} = \sqrt{(\boldsymbol{R_{KM}} + \boldsymbol{R_0})\left(\frac{\boldsymbol{1}}{\boldsymbol{R_g}} + \boldsymbol{R_0}\right)}, \tag{6}$$

where $\boldsymbol{R}_0$ is reflectance of the specimen over a dark background with zero reflectance. Now if we assume specimen with zero scattering, $\boldsymbol{R}_0$ approaches zero and Eq. (6) reduces to:

$$\boldsymbol{T_{KM}} = \sqrt{\frac{\boldsymbol{R_{KM}}}{\boldsymbol{R_g}}}, \tag{7}$$

Though the assumption of zero scattering is not practically true in the current application, it helps to simplify the problem, and a curve for KM transmittance can be obtained. Now, using refractive–index correction, external transmittance can be written as [18]:

$$\boldsymbol{T}_{ext} = \frac{\boldsymbol{(1 - r_1)(1 - r_2)T_{KM}}}{\boldsymbol{1 - r_2^2 T_{KM}^2}}, \tag{8}$$

The reconstructed transmittance curve ($\boldsymbol{T}_{rec}$) can then be obtained by scaling transmittance computed in Eq. (8) in a way that average–transmittance equals the desired opacity ($\boldsymbol{T}_{avg}$).

$$\boldsymbol{T_{rec}} = \boldsymbol{T_{avg}} \frac{\boldsymbol{T_{ext}}}{\boldsymbol{mean(T_{ext})}}, \tag{9}$$

In case, measured spectral reflectance is not given but measured colorimetric values of the color are given, spectral reflectance can be reconstructed using any suitable method for reflectance reconstruction [6–12], and then above method can be used to estimate spectral transmittance.

Surface reflectance (r_1) was set to 0.04 assuming average refractive index (n) of 1.5 for plastic materials [19]. Coefficient of internal reflection (r_2) would be same as r_1 in case of a transparent (zero optical thickness i.e., $d(\mu_s+\mu_a)$ where d is thickness, μ_s is scattering coefficient and μ_a is absorption coefficient [20]) media, and otherwise it would be a function of optical thickness ($d(\mu_s+\mu_a)$) as found by Gautheron *et al.*, [20]. Since we didn't have access to the optical thickness in the current scenario, we derived an expression for r_2 being a linear function of the opacity (i.e., average–transmittance) so that it attains a value between 0.04 (in the case of purely transparent media and totally collimated incident flux) and 0.6 (theoretical value for a perfectly diffused media [21]). Allen [18] proposed that a more practical value for the upper limit of r_2 would be 0.4 (instead of 0.6) that was also considered as a case in the current study. The currently driven relationship between r_2 and opacity value assumes that when the specimen is fully opaque it acts as a perfectly diffused media.

RESULT AND DISCUSSION

Measured and reconstructed spectral transmittance curves were compared in terms of Root Mean Square Error (RMSE) and the CIEDE2000 color difference under three different illuminants (the CIE standard illuminant D65, the CIE standard illuminant A, and the CIE illuminant F11) [17,22]. Note that before computing RMSE, measured and reconstructed spectra were multiplied by sum of the CIE 1931 color matching functions. Numerical values of the median, mean, and 95th percentile of RMSE and the CIEDE2000 are listed in Table 1. Around 30% test samples were opaque (i.e., average–transmittance <= 10%) and other 70% translucent (i.e., average–transmittance from 10% to 80%). Results showed that average error values in terms of both RMSE and the CIEDE2000 are relatively smaller by a factor of four for opaque samples compared to translucent ones. Note that when a practical value (40%) of the coefficient if internal reflection was considered instead of the theoretical value of ~60%, the prediction error improved in both units of the CIEDE2000 and RMSE (see Table 1). The mean results in units of the CIEDE2000 and RMSE remained below 5.0 and 1%, respectively, when $r_2 = 0.4\text{-}0.39^*Opacity$. Results also showed that 95% of the test samples give RMSE of less than 3% that falls within the threshold of acceptability in many applications of transmissions spectral especially when the specimen is being viewed from the reflection side only. Results were slightly worse when $r_2 = 0.6\text{-}0.6067^*Opacity$. These results are acceptable in the plastics industry as the plastic samples are generally viewed from reflection side. More importantly the difference of average–transmission remained zero that may be crucial in some plastics applications where transmission of light through the material is a concern e.g., food packaging, chemical packaging, medical usage, etc.

The variation in the color difference under the three selected illuminants is within the threshold of ±0.1 that means the current model's performance does not vary much with the change of illumination. The equation $r_2 = 0.4\text{-}0.39^*Opacity$ is recommended to be used as it represents a more practical solution [18].

Authors did not find any previously reported research results for the same problem to compare with. Under given conditions, current results can be acceptable for some applications as the average–transmittance of the measured and reconstructed spectral transmittance are exactly same though there is some different in the spectral shape mainly caused due to the assumptions made.

Table 1: Transmittance prediction results

r_2	Metric	Median	Mean	95th Percentile
*0.6-0.6067*Opacity*	DE_{00} (D65)	4.04	4.94	13.36
	DE_{00} (A)	3.89	4.89	14.33
	DE_{00} (F11)	3.83	5.12	14.56
	RMSE (%)	0.57	0.92	3.02
*0.4-0.39*Opacity*	DE_{00} (D65)	3.83	4.78	13.19
	DE_{00} (A)	3.69	4.76	14.16
	DE_{00} (F11)	3.64	4.98	14.44
	RMSE (%)	0.56	0.86	2.66

CONCLUSION

An analytical method is proposed to determine spectral transmittance of translucent scattering–media from minimal known information regarding transmission (i.e., average–transmittance) and for a known reflectance curve of the specimen. Kubelka–Munk model was used with some assumptions to reconstruct spectral transmittance with average value exactly matched to the given opacity value and spectral curve plausibly close to the measured curve. Data based on above 100,000 real plastic samples were used to test the method. The results showed that the spectral transmittance determined with the current method has median and mean color difference 4.0 and 5.0, respectively, in units of the CIEDE2000 under three different illuminants, and mean RMSE less than 1%. With these results, the current method can be useful for many applications e.g., plastics, paper etc.

ACKNOWLEDGEMENT

The authors would like to thank Avient associates who helped to collect, refine and filter the test data, and other members of the ColorNow™ team for their support and feedback during this study.

REFERENCES

1. Safdar, M., & Emmel, P. (2023). Matching target color in polyolefins by estimating pigment concentrations using a four–flux model. *Applied Optics*. DOI: 10.1364/AO.497213.
2. Vicini, D., Jakob, W., & Kaplanyan, A. (2021). A non–exponential transmittance model for volumetric scene representations. *ACM Transactions on Graphics (TOG)*, 40(4), 1-16.
3. Baranoski, G. V., & Rokne, J. G. (1997, September). An algorithmic reflectance and transmittance model for plant tissue. In *Computer Graphics Forum (Vol. 16, pp. C141-C150)*. Oxford, UK and Boston, USA: Blackwell Publishers Ltd.
4. Durmuş, H. O., & Seyidov, M. Y. Determination of microscopic optical properties of agar and Zerdine phantoms at 635 nm using Kubelka–Munk function approach: a numerical study. *Int J Adv Appl Sci* ISSN, 2252(8814), 8814.
5. Safdar, M., Hardeberg, J. Y., & Luo, M. R. (2021). ZCAM, a colour appearance model based on a high dynamic range uniform colour space. *Optics Express*, 29(4), 6036-6052.
6. Safdar, M., & Emmel, P. (2022). Toward non–metameric reflectance recovery by emulating the spectral neighborhood using corresponding color information. *JOSA A*, 39(6), 1066-1075.

7. Lin, Y. T., & Finlayson, G. D. (2021). On the optimization of regression–based spectral reconstruction. *Sensors*, 21(16), 5586.
8. Bianco, S. (2010). Reflectance spectra recovery from tristimulus values by adaptive estimation with metameric shape correction. *JOSA A*, 27(8), 1868-1877.
9. Babaei, V., Amirshahi, S. H., & Agahian, F. (2009). Reflectance reconstruction by adapting Wiener restoration method: using color difference values as weighting matrix. In *11th Congress of the International Colour Association* (pp. 252-1).
10. Shen, H. L., Cai, P. Q., Shao, S. J., & Xin, J. H. (2007). Reflectance reconstruction for multispectral imaging by adaptive Wiener estimation. *Optics Express*, 15(23), 15545-15554.
11. Safdar, M., Luo, M. R., Wang, Y., & Liu, X. (2015, May). Multispectral imaging system based on tuneable LEDs. In *Conference: Multispectral Color Science (MCS) Symposium*, At Tokyo, Japan (pp. 130-134).
12. Zuffi, S., Santini, S., & Schettini, R. (2008). From color sensor space to feasible reflectance spectra. *IEEE Transactions on Signal Processing*, 56(2), 518-531.
13. Bell, I. E., & Baranoski, G. V. (2004). Reducing the dimensionality of plant spectral databases. *IEEE Transactions on Geoscience and Remote Sensing*, 42(3), 570-576.
14. Aghanouri, A., Amirshahi, S., & Agahian, F. (2010). Reconstruction of spectral transmission of colored solutions using a conventional digital camera. *J. Imaging Sci. Technol.*, 54, 010508.
15. Funamizu, H., Tokuno, Y., & Aizu, Y. (2016). Estimation of spectral transmittance curves from RGB images in color digital holographic microscopy using speckle illuminations. *Optical Review*, 23, 535-543.
16. Kubelka, P. (1948). New contributions to the optics of intensely light-scattering materials. Part I. *JOSA*, 38(5), 448-457.
17. CIE (2004). Colorimetry. *Commission Internationale de l'Eclairage (CIE)*, Vienna, Publication 15:2004.
18. Allen, E. (1987). Refractive-index correction for translucent films. *Color Research & Application*, 12(2), 106-107.
19. Hébert, M., Hersch, R. D., & Emmel, P. (2015). Fundamentals of optics and radiometry for color reproduction. *Handbook of Digital Imaging*, 1-57.
20. Gautheron, A., Clerc, R., Duveiller, V., Simonot, L., Montcel, B., & Hebert, M. (2022, January). Light scattering in translucent layers: angular distribution and internal reflections at flat interfaces. In *Electronic Imaging* 2022 (EI 2022) (Vol. 34, No. 15, pp. 221-1).
21. Judd Deane, B., & Gunter, W. (1975). *Color in Business, Science and Industry*. New York: Wiley.
22. Luo, M. R., Cui, G., & Rigg, B. (2001). The development of the CIE 2000 colour-difference formula: CIEDE2000. *Color Research & Application*, 26(5), 340-350.

MODELLING COLOUR APPEARANCE OF IMAGES UNDER HDR VIEWING CONDITIONS

Xinye Shi[1], Yuechen Zhu[1] and Ming Ronnier Luo[1]*

[1]*State Key Laboratory of Modern Optical Instrumentation, Zhejiang University, China.*

*Corresponding author: Ming Ronnier Luo, m.r.luo@zju.edu.cn

ABSTRACT

HDR imaging technology has received great attention recently. Most of the mobile imaging devices include the HDR function with an aim to achieve successful colour reproduction. The present work is designed to conduct psychophysical experiment using images and the results were used to test the effectiveness of these functions. In the present work, the data were used to evaluate colour appearance model, CIECAM16, the latest CIE colour appearance model recommended by CIE. CAM16-UCS is an extension of CIECAM16 and is one of the most uniform colour spaces reported. CAM16-UCS was used here to present experimental data due to its uniformity and capability of predicting corresponding colors in different viewing conditions. Firstly, different oil paintings in the light box (six different illumination levels from 15 lux to 32000 lux) were captured by a camera. The images obtained were input into the CAM16-UCS model with different parameters to obtain the corresponding color data on the display. The results showed small difference between the images under different illuminations, but differences from the real environment were significant, mainly reflected in the brightness and saturation of the images. Subsequently, ten observers took part in an experiment to adjust the overall lightness (J') and colorfulness (M') of the image in the J'M' space to match the real scene. The results showed that in low illuminance environments, the visual results indicate a great reduction of J' and M' to achieve a higher level of restoration on the display and in the light box. In contrast, in high illuminance environments, the display could not achieve the corresponding brightness level. Observers' results showed that J' and M' needed to be raised to achieve color match while avoiding overexposure distortion. This phenomenon also indicated that as illumination increased, both colorfulness contrast and brightness contrast increased. The colorfulness and brightness of the color stimulus obviously changed with the change of the adapting illuminance of an illuminant, which were known as Hunt effect and Stevens effect. These two effects jointly affect color appearance, and with increasing illumination, color shifts are reflected in the direction of vividness. Therefore, this study derived new formulas from J' and M' to the original CAM16-UCS model to correct its application in image restoration. In the validation experiment, new 6 illuminations and 5 images were used to test the effectiveness of the new formulas. The CAM16-UCS original model and the modified CAM16-UCS model generated 30 scene images each. Observers rated the image restoration on a scale of -3 to 3, where -3 represented "very dissimilar" and 3 represented "very similar". The experimental results were converted into Z-scores. At six different luminance levels, the new model performed better than the original model by a factor about 71%. The results showed that the modified CAM16-UCS model had better performance in image scene reproduction.

Keywords: Color appearance model, CAM16-UCS, HDR viewing condition

INTRODUCTION

High Dynamic Range (HDR) imaging technology has recently gained widespread attention, particularly with the integration of HDR functions into mobile imaging devices. This technological advancement aims to achieve more accurate color reproduction in images. Therefore, it is necessary to obtain a good color appearance model for high dynamic scenes, such as the CIECAM16, which is the latest CIE colour appearance model recommended by CIE [1]. CAM16-UCS [2] is the uniform color space of CIECAM16 to predict accurate color differences. Its output attributes are lightness (J'), colorfulness (M') and hue angle (h), which were the modifications of CIECAM16 J and M. Note J', M' and h were the best combination of attributes to give most accurate color difference predictions [3]. In our previous work [4], we collected the corresponding color data set of color blocks in a high dynamic observation environment, and focused on testing the accuracy of color appearance restoration in the CAM16-UCS space. In present study, in order to test the effect of CAM16-UCS on color reproduction of images, a psychophysical experiment using images was conducted to evaluate the effectiveness of the CAM16-UCS model in HDR viewing condition.

METHODOLOGY

In this study, camera-captured images were used to assess CAM16-UCS model, following this methodology: a) Various oil paintings were placed in a lightbox, and the camera photographed them under different illumination conditions, specifically, at six different illuminance levels: 15, 100, 1,000, 3160, 10000, and 32000 lx. b) Then a polynomial camera characterization model [5] was applied to convert the captured RGB data into XYZr values (where 'r' represents the real scene). c) The obtained XYZr values, along with environmental parameters, were input into CAM16-UCS model, resulting in the generation of XYZd values (where 'd' represents the display) based on display condition parameters. d) By employing a Gain-Offset-Gamma (GOG) display model [6], the XYZd values were transformed into the RGB color space and rendered on the display. This allowed for the observation and comparison of the similarity between the displayed image and the real scene. The specific process flow is showed in Figure 1.

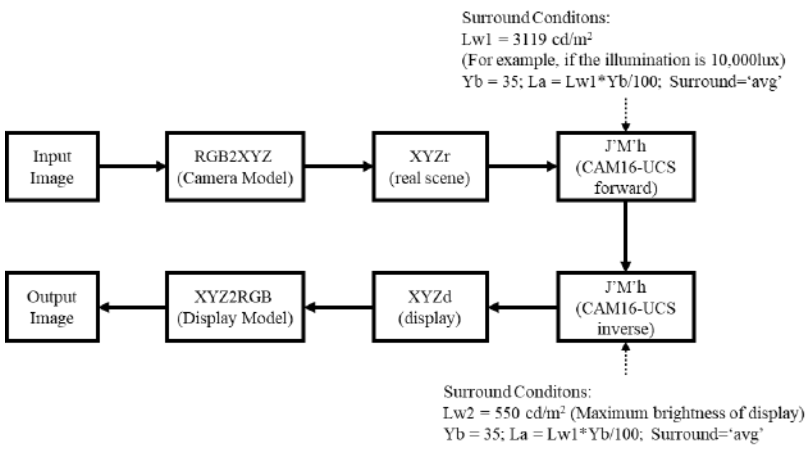

Figure 1. Imaging Processing Flow Chart

The results of image processing are shown in Figure 2, with an example presented herein. The six images illustrate the outcome generated under varying illuminance conditions, following the image processing methodology described earlier. First and foremost, besides the difference in colorfulness, discerning variations in the image under different illumination levels proves to be quite challenging. Nevertheless, upon comparing these results with the actual scene, it becomes apparent that they do not meet the desired level of fidelity. Therefore, a psychophysical experiment was conducted within a high-dynamic observation environment created using three light boxes. The primary objective was to rectify the outcomes obtained from CAM16-UCS concerning the image and to identify the trends in lightness and colorfulness changes.

To establish a high dynamic range environment, three illumination boxes (IBs) were utilized specifically, IB1, IB2, and IB3. Positioned at the center-top, IB1 boasted an adjustable luminance range spanning from 15 to 200,000 lx. Meanwhile, IB2 and IB3 were situated at the bottom-left and bottom-right positions, respectively, with fixed illuminances set at 10 lx and 200,000 lx. During the experiment, paintings were placed within IB1, while two X-Rite Macbeth Color Checker Charts (MCCC) were positioned in IB2 and IB3, so that observers did observe colors on the both charts, resulting a high-dynamic range environment.

Figure 2. Groups of images generated in different illuminance

The display used to match was an Apple Pro Display XDR display with 2560×1440 pixels, which was set to a peak luminance of 550 cd/m2. The display was characterized using a Gain-Offset-Gamma (GOG) model. By using 24 colors form X-Rite Macbeth ColorChecker Chart (MCCC) to test the GOG model, the mean accuracy was 0.63 ΔE^*_{ab} (SD = 0.52).

Ten observers participated in the experiment, with 5 females and 5 males, aged between 22 and 29 years, averaging 24.7 years (standard deviation is 2.1). Each observer in the experiment passed the Ishihara color vision test.

Figure 3. Three paintings selected for the experiment

Three images were selected as shown in Figure 3. Each image generated six images under different illuminations through the CAM16-UCS model as the initial point of adjustment, i.e., the 6 images in Figure 2.

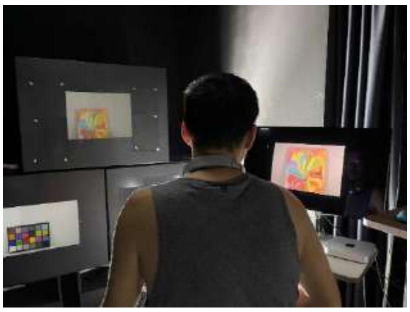

Figure 4. colour image experiment environment

The experiment was conducted in a dark room. The overall environment of the experiment was shown in Figure 4. The observer adjusted the overall brightness and saturation of the image to match the painting in the real scene. In the experiment, the RGB value of the image was first converted into XYZ value through the camera model, and then entered the CAM16-UCS model to obtain the J'M'h' value, and all J' and M' were multiplied by the coefficients FJ' and FM' to change the lightness and colorfulness of the image. The observer adjusted the size of FJ' and FM' through the keyboard, and the initial value of FJ and FC is 1.00. The adjustment process involves modifying factors to align the display image with the real scene, and this adjustment is categorized into coarse and fine adjustments. The experimental results were used to build an image-specific model.

RESULT AND DISCUSSION

Improve CAM16-UCS model

Table 1 shows the results of parameters FJ' and FM'. The results of 10 observers were very close, which was reflected in the low standard deviation. In addition to this, images need to greatly adjust its lightness and colorfulness to match the real environment, especially in low luminance conditions. Since the maximum brightness of the display is only 550 cd/m^2, which cannot be numerically close to the actual environment, the adjustment coefficients FJ' and FM' will not increase all the time.

Table 1: The results of Colour Imaging Experiment, the mean and standard deviation for FJ' and FM' factors under different illuminations

Illumination (lx)		15	100	1000	3160	10000	32000
FJ'	Avg	0.05	0.27	0.92	1.10	1.16	1.10
	Std	0.01	0.04	0.07	0.08	0.02	0.06
FM'	Avg	0.39	0.78	1.03	1.08	1.05	0.99
	Std	0.04	0.06	0.06	0.05	0.08	0.05

Obviously, FJ' and FM' are related to the ambient luminance. At the same time, the matching experiments were only performed on XDR monitors, and the maximum brightness of different monitors were different. The final model should be able to reflect the difference of the display. So, a parameter p was set, its value is the ratio of the display background brightness to the adaptation field brightness, as shown in the Eq. (1). Take the logarithm of p to fit FJ and FM respectively, and obtain the Eq. (2)(3).

$$p = \frac{L_{display}}{L_{adapting}} \tag{1}$$

$$FJ' = a1 \times \frac{1}{a2 + e^{-a3 \times log10(p) + a4}} + a5 \tag{2}$$

While $\mathrm{a1} = 0.97, \mathrm{a2} = 0.86, \mathrm{a3} = -2.68, \mathrm{a4} = -2.35, \mathrm{a5} = 0.02;$

$$FM' = b1 \times \frac{1}{b2 + e^{-b3 \times log10(p) + b4}} + b5 \tag{3}$$

While $\mathrm{b1} = 1.45, \mathrm{b2} = 2.20, \mathrm{b3} = -5.27, \mathrm{b4} = -6.51, \mathrm{b5} = 0.38.$

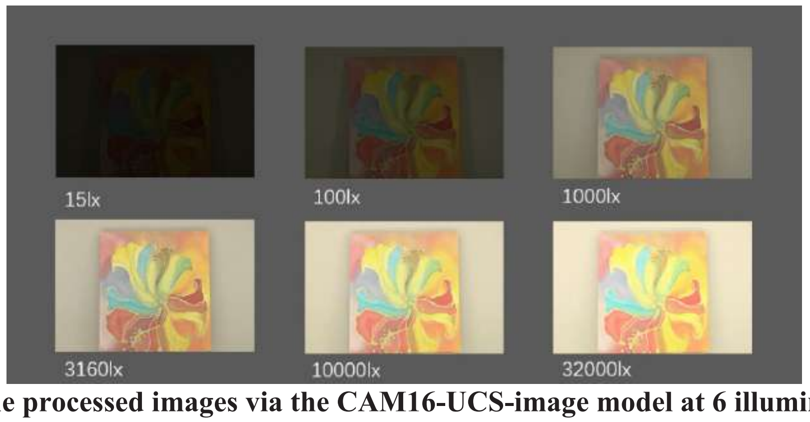

Figure 5. The processed images via the CAM16-UCS-image model at 6 illumination levels

Figure 5 shows the images generated by the improved CAM16-UCS model under various illumination levels, using the same example as depicted in Figure 2. These images more effectively capture the distinctions between different illuminance conditions and closely approximate the appearance of paintings within real scenes, particularly at illuminance levels of 15 lx and 100 lx.

Image Verification Experiment

To assess the image restoration capabilities of the CAM16-UCS image model across various content types and different lighting conditions, we conducted a verification experiment involving five scenes and six illumination levels (Figure 6). Both the original and improved CAM16-UCS models were used to create a total of 60 images. Notably, the illumination levels for IB1 differed from those used in the color patch experiment. For this verification experiment, we selected illuminance levels of 15, 34, 100, 316, 10,000, and 32,000 lux. We chose these levels because at the intermediate illumination level, the image closely resembled the real scene, with differences primarily noticeable in low and high illumination conditions. Therefore, we included two low illumination levels for assessment. Ten observers, including 5 females and 5 males, participated in the verification experiment. The display presented the images generated by the two models for the current scene in a random order. Observers provided scores ranging from -3 to 3 based on the degree of match between the real scene and the display screen, with higher scores indicating better alignment and a score of 3 indicating almost perfect agreement.

Figure 6. 5 scenes and 6 illumination selected for the verification experiment (these images were generated by the improved CAM16-UCS model)

The results for Image Verification Experiment

First, negative scores were added by 4, while positive scores were added by 3. Consequently, the original scale of -3 to 3 was transformed into a range of 1 to 6. The Standardized Residual Sum of Squares (STRESS) was employed to assess variations among both intra-observer and inter-observer measurements. The value of STRESS is ranged from 0 to 100, zero means perfect agreement and higher STRESS value indicates a larger dispersion. The results showed that the intra-observer variations ranged from 21.34% to 41.79% (mean=30, SD=7) and inter-observer variations ranged from 21.49% to 32.91% (mean=28, SD=4).

Table 2 shows the mean scores of the two models under different illumination levels. It is evident that the enhanced CAM16-UCS model significantly outperforms the original CAM16-UCS model. Furthermore, it can be observed that under an illumination level of 316 lx, the average score of the image model reached 4.96, suggesting that the improved CAM16-UCS model exhibited superior performance under moderate illumination conditions. However, under an illumination level of 32000 lx, the average score of the improved CAM16-UCS model was only 4.02. In this scenario, the display brightness is notably lower than that of the real scene, which objectively leads to an inability to achieve a high level of matching. These results effectively reflect this situation. The validation experimental findings indicate that the CAM16-UCS image model exhibits a greater enhancement in image restoration compared to the original CAM16-UCS model.

Table 2: The mean z-score of the three models under different illumination levels

Illumination (lx)	15	34	100	316	10000	32000	Mean
Original Model	1.60	1.88	2.08	3.04	3.82	3.36	2.63
Improved Model	4.52	4.66	4.32	4.96	4.54	4.02	4.50

CONCLUSION

The primary objective of this research was to conduct a psychophysical experiment using images to assess the efficacy of CAM16-UCS in image restoration under HDR viewing condition. The research involved capturing images of different oil paintings under six different illumination levels ranging from 15 lux to 32,000 lux. These images were then processed using the CAM16-UCS model with varying parameters to obtain color data for display. The findings revealed minor differences between images under different illuminations, but significant disparities compared to the real environment, primarily in terms of lightness and colorfulness. Subsequently, a psychophysical experiment engaged ten observers to adjust the overall lightness (J') and colorfulness (M') of the images in the J'M' space (CAM16-UCS) to match the real scene. The results indicated that in low illuminance environments, significant reductions in J' and M' were required to achieve faithful reproduction on the display. Conversely, in high illuminance conditions, the display fell short of reaching the corresponding brightness level, necessitating increases in J' and M' to achieve color accuracy while avoiding overexposure distortion. Consequently, new formulas were derived from J' and M' to enhance the original CAM16-UCS model's performance in image restoration. In the validation experiment, the improved CAM16-UCS model outperformed the original model by approximately 71% across six different luminance levels, showcasing superior image scene reproduction capabilities. Overall, this research highlights the importance of modifying color appearance models such as CAM16-UCS to adapt different lighting conditions, which contributing to more accurate and effective image restoration in various real-world scenarios.

REFERENCES

1. CIE 248. (2022). The CIE 2016 colour appearance model for colour management systems: CIECAM16.
2. Li, C., Li, Z., Wang, Z., Xu, Y., Luo, M. R., Cui, G., ... & Pointer, M. (2017). Comprehensive color solutions: CAM16, CAT16, and CAM16-UCS. Color Research & Application, 42(6), 703-718.
3. Luo, M. R., Cui, G., & Li, C. (2006). Uniform colour spaces based on CIECAM02 colour appearance model. Color Research & Application: Endorsed by Inter-Society Color Council, The Colour Group (Great Britain), Canadian Society for Color, Color Science Association of Japan, Dutch Society for the Study of Color, The Swedish Colour Centre Foundation, Colour Society of Australia, Centre Français de la Couleur, 31(4), 320-330.
4. Xinye, S., Yuechen, Z., & Luo, M. R. (2021, November). A new corresponding color dataset covering a wide luminance range under high dynamic range viewing condition. In Color and Imaging Conference (Vol. 29, pp. 184-187). Society for Imaging Science and Technology.R. S. Berns, 1996. 'Methods for characterizing CRT displays', Displays.
5. Berns, R. S. (1996). Methods for characterizing CRT displays. Displays, 16(4), 173-182. Stevens J C, Stevens S S. Brightness function: Effects of adaptation[J]. JOSA, 1963, 53(3): 375-385.
6. Hong, G., Luo, M. R., & Rhodes, P. A. (2001). A study of digital camera colorimetric characterization based on polynomial modeling. Color Research & Application: Endorsed by Inter-Society Color Council, The Colour Group (Great Britain), Canadian Society for Color, Color Science Association of Japan, Dutch Society for the Study of Color, The Swedish Colour Centre Foundation, Colour Society of Australia, Centre Français de la Couleur, 26(1), 76-84.

THE INFLUENCE OF BACKGROUND ON THE COLOR DIFFERENCE EVALUTION OF MULTICOLORED MATERIAL

Jiaying Wu[1] and Renzo Shamey[1]*

[1]*Color Science and Imaging Labs, TECS Dept., North Carolina State University, Raleigh, USA.*

*Corresponding author: Renzo Shamey, rshamey@ncsu.edu

ABSTRACT

It is well-known that the perception of a color is impacted by its surround. However, the color quality control of multicolored materials is often conducted by evaluating each of the colors separately and in isolation, despite the fact that this may not correspond with the actual perception of the overall pattern. The color quality evaluation of camouflage substrates is a prime example of this type of evaluation and was the motivation behind this study. The initial focus of the work was on the color quality assessment of a military camouflage pattern called MARPAT, which is employed by the United States Marine Corps. This is a multicolored pattern composed of a range of low chroma colors. The main goal of the study was to analyze the assessment results of each of the MARPAT colors when surrounded by a simplified background composed of averaged neighboring colors. A set of sample pairs consisting of two images was thus produced using the center-background paradigm. The central squares of each pair were either the same color or had a lightness difference of 0.5 or 1.0 unit against each other. Three kinds of backgrounds were tested, including a checkerboard background consisting of the MARPAT colors, a single-color background based on the spatial averaging of the colors of the checkerboard pattern, as well as a gray background, which was used as reference. Monitor based psychophysical assessments were conducted to test the influence of these backgrounds on the perceived color difference of the central color pairs. Twenty color normal observers participated in this study. For all tested color combinations observers noted a visual difference between central patches surrounded by a checkerboard background or the associated color-averaged background. For identical central patches the average visual difference was found to be from 0.2 to 1.2 $DE_{00(1:1:1)}$ for all combinations. Results were significantly different from zero, which indicates a color-averaged background does not replicate, nor should be considered equivalent to the visual processing of a complex background. It was found that color combinations employed have a significant impact on the perceived visual difference of the central stimuli, which may be due to differences in the center-surround contrast. When the lightness contrast between the central color and the background was approximately one, observers reported a larger difference between the central colors surrounded by a checkerboard background compared to the color-averaged homogenous background. Results have an impact on color quality control of multicolored stimuli and can be utilized to model the effect of background on perceived color differences.

Keywords: Color perception, MARPAT camouflage pattern, multicolored stimuli, background.

INTRODUCTION

When assessing multicolored stimuli, the visual signal at each point, and the perception of the color in the region of interest, is affected by the neighboring regions. This may alter the appearance of the point of interest compared to its isolated form due to induced color shifts. Instead of assessing colors one after another, the color difference of a pair of stimuli within a complex scene may be assessed by incorporating the influence of the background. The so-called "color in context" phenomenon has been extensively studied in psychophysics for decades and observed in simple uniformly inducing backgrounds [1-3], as well as geometrically more complex ones [4-6].

The concept of "functionally equivalent surrounds" has been considered by several researchers. Attempts have been made to use a simplified algorithm to determine the color appearance of complex scenes. This typically includes the prediction of color appearance based on the mean light reflected from the background [7-10]. Although an average background is implied in many popular color models [11-15], it is debatable whether the effect of a complex background on assessments can be accurately represented by an average homogenous background. The fundamental aspects of color induction that take place when viewing complex scenes remain unclear. Some studies support [4,16,17] while others refute [5,18-22] the use of a uniform background in place of a complex background.

The focus of this study was the color quality assessment of a common military camouflage pattern (MARPAT), which is a multicolored material containing a range of low chroma colors, used by the United States Marine Corps. The hypothesis was that the perceived differences between MARPAT colors on an average homogeneous background are different from those on more complex backgrounds. Psychophysical experiments were thus designed and conducted to test the above hypothesis.

METHODOLOGY

Preparation of samples

The stimuli consisted of a color square subtending a 2-degree field of view placed within a checkerboard background composed of two MARPAT colors subtending a 10-degree field of view. Other backgrounds of identical size were also tested: one was gray and the other was the average of the colors of the checkerboard pattern (see figure 1). Three different checkerboard patterns were examined, whereby the background mosaic of identical size was divided into 16×16, or 8×8, or 4×4 squares. Six color combinations were utilized. Three colors were selected from the MARPAT pattern and the other three were higher chroma colors which were included to expand the range of colors tested in the psychophysical experiment. The majority of the central squares among the tested stimuli pairs were identical. However, to assess the observer's ability in estimating small color differences under complex surround conditions, a lightness difference (ΔL^*) of either 0.5 or 1.0 unit was applied to several sample pairs which were also displayed on different backgrounds for comparison. The central squares, containing the preset lightness difference, were either connected on one side or had a distance from their centers subtending a 10-degree field of view size. Hence three categories of sample pairs with preset color differences were tested. Figure 1 shows an example stimuli pair in each of the tested appearance settings.

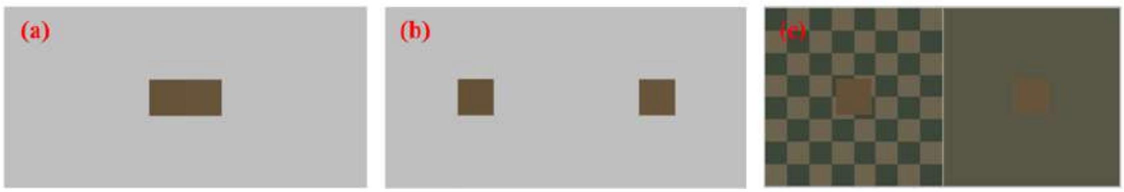

Figure 1. A sample pair with a preset lightness difference tested in three appearance settings: a-connected side by side, b- with a 10º distance, both against a gray background, and c- with a 10º distance against a checkerboard and a color-averaged background.

Visual assessment procedure

A psychophysical experiment was conducted with a group of 20 color-normal volunteers. An EIZO ColorEdge CG277 LCD color calibrated display was used to present the sample images to the observers in a dark room. Observers performed a two-step visual experiment to evaluate each sample pair. The first step determined whether the colors of the central squares were a "match" or "not match". If a "not match" response was obtained, the observer then proceeded to the second step and rated the magnitude of the visual difference between the two patches according to a 7-step (0 to 2.3 $DE_{00(1:1:1)}$) linear grayscale. Each observer assessed sample pairs a total of five times in three separate trials and overall, 4200 assessments, including replicates, were completed by all observers.

RESULTS AND DISCUSSION

Linear regression was performed to transform grayscale ratings to visual differences (VD) described in terms of $DE_{00(1:1:1)}$. The variability in visual differences of the same sample pairs on the checkerboard versus color-averaged background is shown in Figure 2 using box plots. The "4", "8", and "16" indicate different checkerboard patterns. The "KC_G", "GK_C", and "CG_K" denote combinations of colors selected from the MARPAT pattern. For all color combinations, observers claimed to have perceived differences of up to 2.4 $DE_{00(1:1:1)}$ when no differences were actually present between the central patches. The average perceived difference, expressed in $DE_{00(1:1:1)}$, ranged from 0.2 – 1.2 units for all six color combinations. Single-factor analysis of variance (ANOVA) was performed, and results showed no significant differences between different patterns (4×4, 8×8, or 16×16) at a significance level of 0.05 for the majority of cases. Color combinations were found to play an important role in observer ratings regardless of the checkerboard pattern employed ($p < 0.001$).

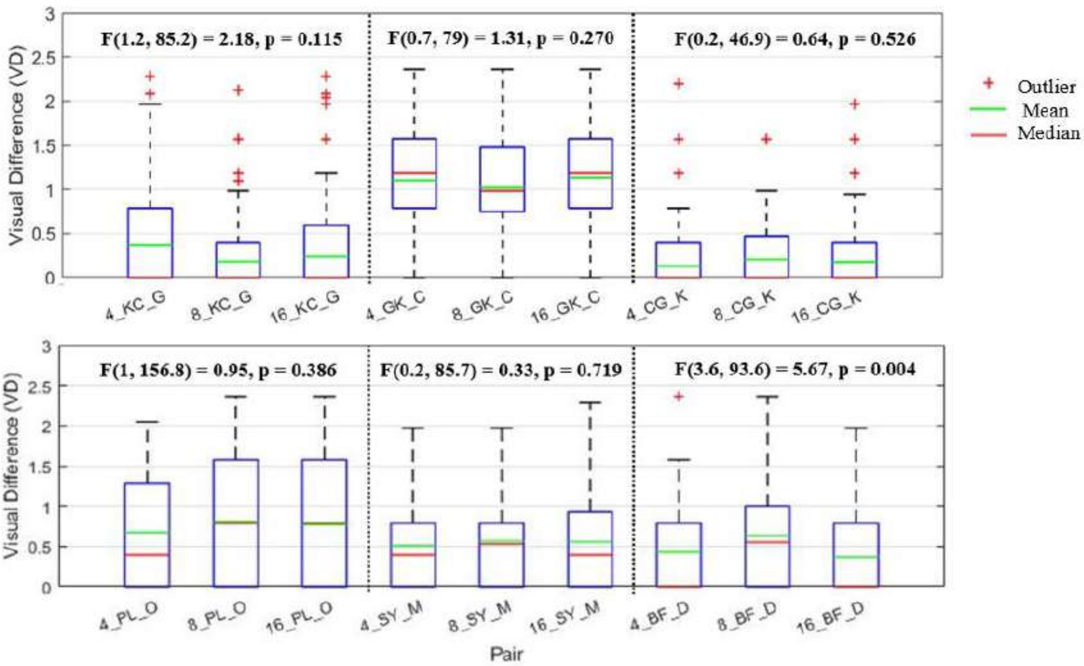

Figure 2. Variability in visual differences for the same sample pairs presented against the checkerboard vs. color-averaged backgrounds for three different checkerboard patterns.

Visual differences among the same colors, when used in different arrangements in the checkerboard patterns, are also distinctly different. According to the Tukey test, the average visual difference for the "GK_C" color combination is significantly higher than that for the "KC_G" and "CG_K" combinations for all patterns. In the case of the latter two combinations, more than half of the participants observed no visual differences between the central squares, and 60% to 80% of reported visual differences were below 0.4 $DE_{00(1:1:1)}$ units. Meanwhile for the "GK_C", the highest frequency of the visual difference was 0.8-1.2 $DE_{00(1:1:1)}$ units. It should be noted that the lightness contrast between the color-averaged background and the central square color for the "GK_C" combination was close to 1 unit. Thus, since in this case the induction effect caused by the color-averaged background would be larger the observers may have detected larger visual differences for these sample pairs compared to other color combinations. This aligns well with the prior studies [23,24] which have reported that the magnitude of the chromatic induction effect is greatest when there is no brightness contrast between the test area and the inducing field.

Small lightness differences were also added to the central squares of color pairs "GK_C" and "KC_G". Visual difference results for the sample pairs containing lightness differences for the three appearance settings are shown in Figure 3 using box plots. The four boxes from left to right in each section (separated by dotted lines) show the data for the sample pair with approximately -1, -0.5, +0.5, and +1 ΔL^* difference from the reference color, respectively. The reproduced ΔL^* values, as determined by a PR-670 spectroradiometer, are listed on top of each box. ANOVA results indicate the visual differences are significantly different among sample pairs with the same lightness difference for both reference colors in each of the three appearance settings. For sample pairs with the "Coyote" reference color the differences were significant in all cases ($p < .001$). For sample pairs with the "Green" reference color, the visual differences were more significant at -1 or +1 ΔL^* level ($p < .001$) compared to -0.5 or +0.5 ΔL^* level ($p = 0.004$).

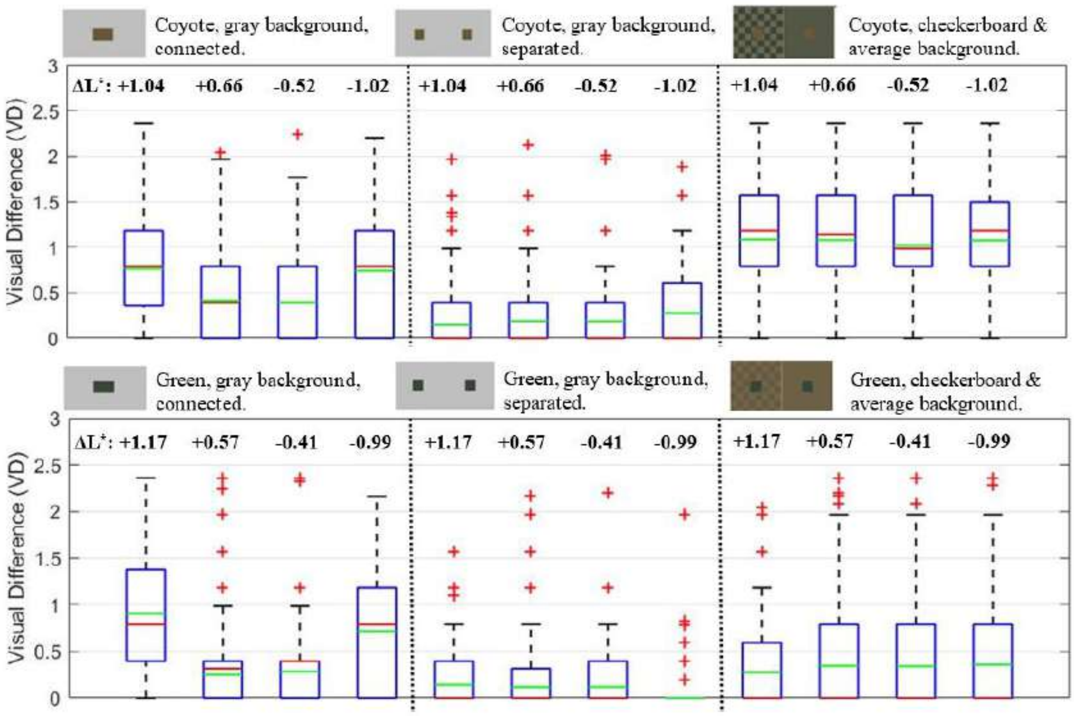

Figure 3. Variability in visual assessment results for sample pairs containing preset lightness differences for the three appearance settings.

For both reference colors when the central patches were connected side by side, observers were able to distinguish color differences. The four boxes on the left side of Figure 4 clearly show a "V" shape corresponding to the magnitude of the difference applied. However, by adding a 10º distance between the pairs, the observers' ability to quantify the same color differences seems to have been suppressed since more than 60% of responses were rated as "match". For sample pairs with checkerboard backgrounds, the perceived differences were similar regardless of the magnitude of the color difference present. However, differences were relatively larger compared to those for separated samples against the gray background especially for pairs with a "Coyote" reference color. This is possibly due to the larger induction effect of the "GK_C" compared to the "KC_G" combination. These observations indicate that the visual difference of samples against checkerboard backgrounds are largely affected by the color induction effect and that most observers may not be able to detect small color differences under such appearance configurations.

CONCLUSION

The main goal of this study was to determine whether color difference assessments of a pair of stimuli within a complex pattern can be replicated by assessments against a color-averaged background. In addition, the role of the background pattern and the magnitude of the small difference between the stimuli as well as the combination of colors used in the pattern were tested. Despite the large variations observed, most of the participants were able to distinguish color differences when the stimuli had a 0.5 or 1.0 lightness difference, shared a border, and were displayed against a gray background. Meanwhile, observers were not able to determine lightness differences between the stimuli up to one unit when the stimuli were separated by a 10º distance. The changes in the checkerboard pattern had an insignificant impact on the mean visual difference of stimuli, while a change in colors resulted in a significant effect. The color combination with a center-background lightness contrast ratio of approximately 1 had the largest visual difference, likely due to a strong induction effect. For all color combinations, the average visual difference for identical stimuli displayed in different appearance settings was found to be significantly different from zero, ranging from approximately 0.2 to 1.2 CIEDE2000(1:1:1) units for different color combinations. This indicates a color-averaged background does not fully represent the perception of the complex checkerboard background when assessing color differences.

ACKNOWLEDGEMENT

The authors thank all volunteers who took part in the visual experiment, and Professor Joel Trussell for his helpful comments.

REFERENCES

1. Valberg, A., (1974). Color induction: Dependence on luminance, purity, and dominant or complementary wavelength of inducing stimuli. *Journal of the Optical Society of America, 64*(11), 1531-1540.
2. Shepherd, A. J. (1999). Remodelling colour contrast: implications for visual processing and colour representation. *Vision Research, 39*(7), 1329-1345.
3. Bosten, J. M., & Mollon, J. D. (2012). Kirschmann’s Fourth Law. *Vision Research, 53*(1), 40-46.
4. Valberg, A., & Lange-Malecki, B. (1990). “Colour constancy” in Mondrian patterns: A partial cancellation of physical chromaticity shifts by simultaneous contrast. *Vision Research*, *30*(3), 371–380.
5. Brown, R. O., & MacLeod, D. I. A. (1997). Color appearance depends on the variance of surround colors. *Current Biology*, *7*(11), 844–849.
6. Brenner, E., Ruiz, J. S., Herráiz, E. M., Cornelissen, F. W., & Smeets, J. B. J. (2003). Chromatic induction and the layout of colours within a complex scene. *Vision Research, 43*(13), 1413-1421.
7. Helson, H. (1938). Fundamental problems in color vision. I. The principle governing changes in Hue, saturation, and lightness of non-selective samples in chromatic illumination. *Journal of Experimental Psychology*, *23*(5), 439–476.
8. Helson, H., & Jeffers, V. B. (1940). Fundamental problems in color vision. II. Hue, lightness, and saturation of selective samples in chromatic illumination. *Journal of Experimental Psychology*, *26*(1), 1–27.
9. Buchsbaum, G. (1980). A spatial processor model for object colour perception. *Journal of the Franklin Institute*, *310*(1), 1–26.
10. Fairchild, M. D., & Lennie, P. (1992). Chromatic adaptation to natural and incandescent illuminants. *Vision Research*, *32*(11), 2077–2085.
11. Zhang, X., & Wandell, B. A. (1996). A spatial extension of CIELAB for Digital Color-image reproduction. *Journal of the Society for Information Display*, *5*(1), 61-63.

12. Hunt, R. W. G. (1991). Revised colour-appearance model for related and unrelated colours. *Color Research & Application*, *16*(3), 146–165.
13. Hunt, R. W. G. (1994). An improved predictor of colourfulness in a model of colour vision, *Color Research & Application*, *19*(1), 23–26.
14. CIE 159 (2004). A colour appearance model for colour management systems:CIECAM02. Central Bureau of the CIE, Vienna: Commission Internationale de L'Eclairage.
15. Li, C., Li, Z., Wang, Z., Xu, Y., Luo, M. R., Cui, G., Melgosa, M., Brill, M. H., & Pointer, M. (2017). Comprehensive color solutions: CAM16, CAT16, and CAM16-UCS. *Color Research & Application*, *42*(6), 703–718.
16. Brenner, E., Cornelissen, F., & Nuboer, J. F. W. (1989). Some spatial aspects of simultaneous colour contrast. *Seeing contour and colour*, 311-316.
17. Brenner, E., & Cornelissen, F. W. (1998). When is a background equivalent? sparse chromatic context revisited. *Vision Research*, *38*(12), 1789–1793.
18. Jenness, J. W., & Shevell, S. K. (1995). Color appearance with sparse chromatic context. *Vision Research*, *35*(6), 797–805.
19. Schirillo, J. A., & Shevell, S. K. (1996). Brightness contrast from inhomogeneous surrounds. *Vision Research*, *36*(12), 1783–1796.
20. Bruno, N., Bernardis, P., & Schirillo, J. (1997). Lightness, equivalent backgrounds, and anchoring. *Perception & Psychophysics*, *59*(5), 643–654.
21. Shevell, S. K., & Wei, J. (1998). Chromatic induction: border contrast or adaptation to surrounding light?. *Vision research, 38*(11), 1561-1566.
22. Barnes, C. S., Wei, J., & Shevell, S. K. (1999). Chromatic induction with remote chromatic contrast varied in magnitude, spatial frequency, and chromaticity. *Vision Research*, *39*(21), 3561-3574.
23. Kirschmann, A. (1891). Ueber die quantitativen Verhältnisse des simultanen Helligkeits- und Farbencontrastes, *Philosophische Studien*, *6*, 417–491.
24. Shapley, R., & Gordon, J. (2006). Brightness contrast inhibits color induction: Evidence for a new kind of color theory. *Spatial Vision, 19*(2-4), 133–146.

Session 2

Doi Tong
28 November 2023

COLOUR PROCESSING OF ARCHITECTURAL FINISHES IN HISTORIC TOWNSCAPES UNITS

Isolina Díaz-Ramos[1]* and Gilberto Artioli[1]

[1]*Department of Geosciences, University of Padua / Interdepartmental Research Centre for the Study of Cementitious Materials and Hydraulic Binders, Italy.*

*Corresponding author: Isolina Díaz-Ramos, isolinadelpino.diazramos@unipd.it

ABSTRACT

The original aesthetic of historic townscapes is a fundamental knowledge to retain the important heritage value of authenticity. This implies the identification of colour layers in buildings. The authors have studied 314 samples removed from 28 historic dwellings dating from the 16th to 20th centuries and located on the historic artistic units of Vegueta and Triana in Las Palmas de Gran Canaria, Spain. Buildings have been designed mostly in Traditional (16th, 17th and 18th centuries), Neoclassical (19th century), Academic and Eclectic styles (20th c.). The aim is to obtain an overall picture of the current hues and the past colour palette of the historic city, contributing to determine how the paintwork of the buildings changes over time. Using a wireless digital colour reader Colourpin SE, we identify the different colour layers in the samples. Colours are given in the NCS notation. The large data set obtained will be interpreted to observe patterns and tendencies in larger data. Results for the samples analysed display 220 colours coming from walls, ornaments, plinths, stonemasonry, carpentry and metal works in façades. The trend is a yellow hue with 30% red. This is displayed in 61% of the buildings studied. The prevailing nuance in 21% of the buildings has 5% of blackness, 2% chromaticity and 93% whiteness. This is found in the current walls and in ornamental colour layers. The NCS S6005-Y notation is visible on 14% of the buildings surveyed. Although there is apparently a chromatic continuity, this is lost as the buildings get older, and this is evident in the Traditional style dwellings. We believe that this study can be useful for interpreting and processing the chromatic history of historic urban landscape units and serve as a reflection on key concepts related to aesthetics, identity and authenticity in built heritage.

Keywords. Colour notation, building heritage, Natural Colour System (NCS), architectural finishes

INTRODUCTION

When studying the colour in buildings located in large historic units[1] [1], multiple analytical techniques can be used to determine the nature of the material. This work shows the initial procedures carried out to have a map of colours of the historic centers of Vegueta and Triana, in Las Palmas de Gran Canaria, Spain, listed as historic units in years 1973 and 1993 consecutively (Figure1).

Vegueta and Triana were planned by Spanish conquerors during 16th and 17th centuries. Until the 18th century, buildings follow a Traditional style, with sober asymmetrical façades and remarkable carpentry works [2]. In the 19th century, the predominant aesthetic sense of the time was Noclassicism, and the façades were decorated with pilasters, plinths, balusters, and other elements. The profusion of ornamentation in this and future architectural styles can be painted or adorned in stonemasonry. At the end of 19th, birth of the 20th centuries, the first Spanish-trained architects arrived in the city, and the Eclectic and Academic styles predominated [3].

[1] Spanish Historical Heritage Law defines a historical unit as "a group of immovable properties forming continuous or dispersed unit of settlement, […] representing the development of a human community in that it testifies to their culture or constitutes a value […]. A historical unit is also any individualised group of properties in a larger population unit having the same characteristics and that can be clearly delimited".

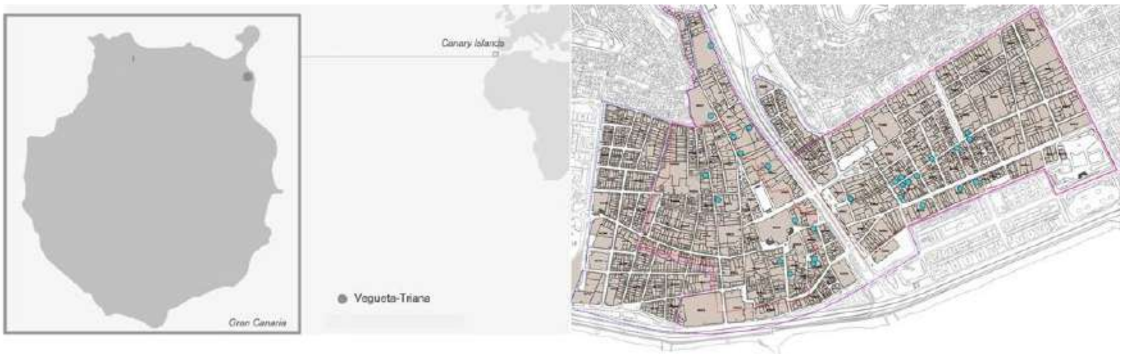

Figure 1. Location of the study site (left) and plan of the historic units of Vegueta and Triana. The study buildings are marked in blue. Credits: Ayto. LPGC & GEURSA

Last century, at the end of the 80's and beginning of the 90's decades, many façades were renewed due to an economic uprise [4]. However, renovation works were carried out without a critical conservative approach, and colour palettes and materials used to rehabilitate the image of the historic city were derived from new materials used in construction industry such as cements and modern plastic colours, equating historic buildings with modern ones, leading to a loss of the value of authenticity [5]. The lime colours washed by the passage of time and the specific textures given by the materials and mineral pigments used, disappeared.

Today, in spite the efforts committed to protect these ensembles, no enough attention is paid to the original aesthetic of the buildings, stablishing vague recommendations on the colour palette to be used when restoring the historic exteriors.

In this paper, we explain the procedures carried out to get knowledge on the hues that make up the buildings today and the image that the dwellings may have had in the past.

METHODOLOGY

A correct protocol for the selection of the buildings that include an appropriate sampling methodology and analysis is relevant. The creation of three different databases to store the information extracted was one of the first steps. We outlined a design of a robust rationale that allowed us to analyse a subset of data related to the historical buildings and the collection of samples in 3 work phases.

Phase I. Building selection. Local heritage catalogues were used to identify the buildings to be included in our research [6]. They display around 600 protected housing, half of them are in Vegueta and the rest are located in Triana. Our aim was to get a general picture of the most representative domestic buildings. Combining this review with an on-site evaluation, we established the housing that had original features preserved in good condition. A data sheet was designed and it was composed by several headings: a code (acronym to identify the building), historical unit, building construction date, architect name's, architectonic style, date of restoration, restorer name, number of floors and spatial situation.[2]

Phase II. Sampling. In order to systematise the data collected, a sample identification code (SIC) was designated in the following way: Street name and number, a hyphen separating a capital letter that corresponds to the location from which the sample was taken: W for wall, P for plinth, O for ornament, and a number indicating the sequency of the samples (Figure 2).

[2] The spatial situation refers to the location of the building in relation to other buildings and to the historic space. Three types are included: side-attached, corner and free-standing.

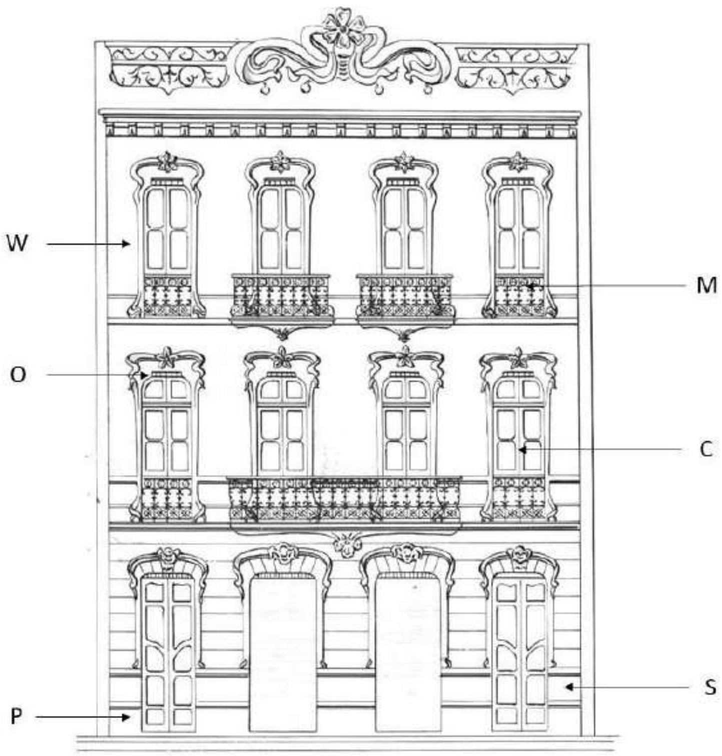

Figure 2. Elevation of the dwelling T98 (98, Triana Street), and different elements that constitute the buildings (P, plinth; O, ornament; W, walls; S, Stonemasonry; C, Carpentry, M, metalworks). Credits: AHP de LP: 1908 exp. 617-4 leg. 7

A total of 314 samples were collected. 80% were taken from walls, 15% from ornamentation and 5% from the plinth. The elements that couldn't be sampled as stonemasonry (S), metal works (M) and carpentry (C) were pinned on site. Data collected allowed us to create 3 different and individual blanks for every building, providing information about the dwellings, samples and analysis to be done [7].

Phase III. Colorimetric analysis. All samples were carefully documented at the CIRCe laboratory in Geosciences Department at University of Padova. The tool used was a wireless digital colour reader Colourpin SE, supplied with a tri-stimulus XYZ sensor and full spectrum white LEDs. The measurement capacity of 4mm diameter area and 45/0 measuring optics. Colours were given in RGB, CIE Lab, CMYK and lightness value and translated to the NCS notation [8]. The technical specification outlines an accuracy of 99% match on NCS fan decks, short term repeatability <0.1 $\triangle$E (CIE2000) and an inter-instrument agreement <0.3 $\triangle$E (CIE2000). Connected via Bluetooth to a smartphone application, colour differences in the collected samples were pinned. To individualise the different colour layers in a sample, the SIC was followed by a sequence of numbers, where 0 referred to the external layer, and roman numerals in lower case were used to the inner colour layers. By the use of multiple samples and measurements, reliable results were provided [9]. 885 colour notations were displayed, in the matrix generated, the absolute maximum frequency in each of the different colour layers was taken into account.

RESULT AND DISCUSSION

Twenty-eight buildings were sampled: 14 belonged to the neighbourhood of Vegueta and 14 were located in the Triana district. 47% were described by the catalogues as being in the Traditional style. These dwellings were built between the 16th and 18th centuries with no authorship. 25% of the buildings dated from the 19th century, and 28% were from the 20th. Buildings from 19th were represented in the Neoclassical style, with Manuel Ponce de León and Francisco de la Torre as representative authors, and housing built in the 20th century were designed in the Academic (15%) and Eclectic styles (13%). Laureano Arroyo and Fernando Navarro were the most active architects in that century, the latter also being the one who was to restore 10% of the houses studied. 61% of the buildings had two floors, with a maximum height of three storeys for 11%. Most of them were side-attached (43%), followed by corner buildings (39%).

Table 1 shows the maximum absolute frequency in all building elements, from the external or current colours to the past layers. Half of the buildings studied have more than one colour notation per element, as the samples collected or measured in-situ provided different colours in the same layer. Therefore, all notations have been included in the table.

Table 1: Colour layers in buildings at Vegueta (V) and Triana (T) neighborhoods

N	Style	SIC	W0	Wi	O0	Oi	P0	Pi	C	S	M
V	Traditional	BA12	S1510-R20B	S1505-R30B	S0804-Y10R	S0601-Y			S8000-N	S4502-Y20R	
V	Traditional	BA15	S0502-Y80R	S0804-Y70R					S9000-N	S6005-Y	S7005-G50Y
V	Traditional	CAS 10	S1515-Y80R	S1010-Y50R					S5030-Y40R	S6502-G50Y	
				S3030-R							
V	Neoclassic	CAS/JQ	S2030-R20B	S1005-Y10R					S4050-Y50R	S4502-Y50R	
V	Traditional	DV/LB	S0502-Y20R	S0907-G60Y			S2002-G	S2010-Y30R	S7010-Y50R	S5502-Y50R	
V	Neoclassic	D4	S1030-R80B	S0502-Y50R	S2020-Y40R				S7020-Y70R		
V	Traditional	H8	S3010-Y30R	S2010-Y40R	S3030-Y40R	S1515-Y60R			S7010-Y70R	S6005-Y	
			S3005-Y50R	S2010-Y20R	S4010-Y30R						
			S2020-Y30R		S2005-Y40R						
V	Academic	JQ30	S0507-G	S0505-G80Y	S0505-G	S2010-Y			S0502-Y		
					S3005-Y20R						
V	Traditional	LB29	S1020-Y30R	S4010-Y10R			S1010-R70B		S8010-Y70R	S6502-Y20R	S4020-B90G
									S8010-B90G	S5502-Y50R	
V	Neoclassic	PSA/F	S0515-Y20R	S0505-Y20R					S5020-Y70R	S7005-Y50R	S4020-Y30R
									S0300-N	S4005-Y20R	
									S7020-Y40R		
									S5040-Y50R		
V	Traditional	PSAA2	S0804-Y70R	S4010-Y30R			S1002-Y20R	S0502-Y50R	S8010-Y70R	S6005-Y	S8500-N
			S0300-N								
V	Traditional	PSAA3	S0502-Y20R	S0505-Y					S7502-R		
V	Neoclassic	RC1	S0515-Y30R	S2010-Y30R					S7020-Y60R	S6005-Y80R	S8502-G
V	Traditional	SM	S0507-Y20R	S1515-Y30R							
T	Eclectic	A/CA	S6010-G30Y	S1505-G80Y	S1510-Y10R	S0603-G80Y			S4550-Y50R	S5005-G80Y	S7005-G50Y
T	Traditional	CA10	S0505-Y30R	S1515-Y30R					S8010-Y70R	S5005-Y50R	
T	Traditional	CA/TO	S1515-Y20R	S2020-Y30R	S6502-Y	S5005-Y			S6010-Y70R	S7005-Y20R	
T	Neoclassic	CA5	S1010-Y20R	S1510-Y20R					S7020-Y80R	S6502-Y20R	
T	Neoclassic	CA9	S0507-Y	S0520-Y20R					S6030-Y50R	S6005-Y	
T	Eclectic	DRG	S1005-R90B	S1015-Y40R	S5010-Y90R	S0507-Y40R			S4550-Y50R	S5502-Y	
					S0502-Y						
T	Eclectic	MA20	S1000-N	S2002-Y	S0603-Y60R	S2000-N	S4000-N		S0804-Y30R		
									S0603-Y60R		
T	Neoclassic	P/R	S0520-Y10R	S2005-B20G					S5030-Y40R	S5005-Y	
									S0502-G50Y		
									S7010-Y70R		
T	Neoclassic	T/FG	S0300-N	S2020-Y90R					S5020-Y60R	S6005-R	
				S1515-G80Y							
				S3010-Y							
T	Academic	T56	S1510-R20B	S0804-Y30R					S5020-Y20R		S2502-G50Y
				S0804-Y70R							
T	Academic	T98	S3005-Y	S3005-G80Y					S4040-Y30R	S5502-Y50R	S7502-G
T	Traditional	TR/CA	S0502-Y	S2020-Y30R	S0907-Y50R		S6000-N		S7020-Y70R	S6010-G90Y	
			S0510-Y20R								
			S0515-Y30R								
T	Academic	VC/PSB	S0505-Y	S0510-Y40R	S4000-N		S4502-G50Y	S6502-R	S7502-G		
					S4502-Y						
T	Eclectic	CO/VC	S4020-Y90R	S3020-G30Y	S0502-B	S0300-N	S6020-R10B	S1502-Y80R	S7020-Y70R		
					S4502-Y						

W0, O0, P0 show the current colours in terms of walls, ornaments and plinths. Past colours are considered to be those found in the last columns of each element, and are referred on this table as Wi, Oi, Pi. Consecutively, the last three rows show the measurements made on site on carpentry (C), stonemasonry (S) and metal elements (M). 39% of the studied buildings are ornamented, 25% of them have coloured plinths meanwhile 71% have stonemasonry decorations, and only 29% hold metal works. White, brown and green colours are often combined in the carpentry of the same building in 14% of the cases.

The NCS notation S6005Y is found in 14% of the walls of buildings surveyed as well as in stonemasonry, and the prevailing nuance in 21% of the buildings has 5% of blackness, 2% chromaticity and 93% whiteness. This is found in the current walls and in ornamental colour layers. Apparently, in many buildings there is a colour continuity. However, current hues are mostly reddish and whitish in dwellings built until 19th centuries, but in earlier times the wall backgrounds were painted in ochre and green. Moreover, the Traditional style is the architectonic feature that shows remarkable colour differences in buildings.

The representative hue is Y30R [Table 2]. It is displayed in the past wall backgrounds in all architectural styles. This hue was also found in the metal elements of Neoclassical houses.

Table 2: Prevailing hues in buildings (T, Traditional; N, Neoclassical; A, Academic and E, Eclectic style)

	W0		Wi		O0		Oi		C		S		M		TOTAL	
	Unit	*Style*	*Unit*	*Style*	*Unit*	*Style*	*Unit*	*Style*	*Unit*	*Style*	*Unit*	*Style*	*Unit*	*Style*	*Unit*	*%*
Y	2/2/1	T/E/N			1/2	T/E	2/1	T/A			2/2/1	T/N			16	57
N	1/1/1	T/E/N					2	E	2/1	T/N					8	29
Y20R	4/2	T/N	1/3	T/N							3/2	T/N			15	53
Y30R	5/1	T/N	5/2/1/1	T/A/E/N									2	N	17	61
Y40R			1/1/1	T/A/E	2/1	T/N			1/2	T/N					9	32
Y50R									1/3/2	T/N/E	3/2/1	T/N/A	1/1/1	T/A/E	5	17
Y70R									6/3/1	T/N/E					10	36
G80G			2/1	A/N											3	11
R20B	1/1/1	T/E/N													3	11

Y30R and Y20R are the characteristic hues in wall backgrounds in Traditional and Neoclassical buildings. A combination of yellow and neutral hues are displayed in the ornaments of Traditional, Academic and Eclectic buildings, and there are no representative hues on the plinths.

CONCLUSION

We understand that colour is an essential part of the history of buildings that reflects not only the aesthetic appreciation of each period, but also an aspect of critical analysis. For this reason, we pursue to have a collection of historical finishes to conserve and retain the original colour and materiality of historic units. This initial map invites us to reflect on the changes in materials and techniques used throughout history.

ACKNOWLEDGEMENT

This work was undertaken within the framework of project CLEA (Reviewing and integrating methods for the Conservation of European architectural finishes in urban heritage townscapes), funded by the EU through the Marie Skłodowska-Curie actions. H2020 grant agreement 101024606. https://cordis.europa.eu/project/id/101024606

REFERENCES

1. Law 16/1985 on the Spanish Historical Heritage. 25 June 1985. (Official State bulletin of 29 June1985).https://en.unesco.org/sites/default/files/spa_ley_16_1985_spaorof.pdf [17.04.2022].
2. Gago Vaquero, J. 1998. *Desmedievalización arquitectónica de Vegueta*. Las Palmas de Gran Canaria: Cabildo de Gran Canaria. Servicio de Patrimonio Histórico.
3. Alemán Hernández, S. (2008). *Las Palmas de Gran Canaria. Ciudad y Arquitectura (1870-1930).* Las Palmas de Gran Canaria: Cabildo de Gran Canaria.
4. Fierro, F. (1999). *Guia del color de Las Palmas de Gran Canaria.* Las Palmas de Gran Canaria: Ayuntamiento de Las Palmas de Gran Canaria.

5. INTERNATIONAL COUNCIL ON MONUMENTS AND SITES (1994). «The Nara Document on Authenticity». https://www.iccrom.org/sites/default/files/publications/2020-05/convern8_01_hstovel_ing.pdf [28.02.2021].
6. AYUNTAMIENTO DE LAS PALMAS DE GRAN CANARIA Y GEURSA (2017). «Planos de formación. Plan especial de protección Vegueta-Triana». https://www.laspalmasgc.es/export/ sites/laspalmasgc/.galleries/documentos-urbanismo/DOC.3_VT_Mem_Inf_Planos_1.pdf [30.06.2022].
7. Díaz-Ramos, I., Ferrazza, L., Manzano Cabrera, J., Melica, D., & Borrelli, E. (2023). Aplicación de métodos científicos de análisis en el estudio de los acabados arquitectónicos de una vivienda doméstica en la ciudad de Las Palmas de Gran Canaria. *Ge-Conservacion*, *24*(1), 43-55. https://doi.org/10.37558/gec.v24i1.1187
8. Hard, A, Sivik, L. (1981). NCS-Natural Color System: A Swedish Standard for Color Notation. *Color Research & Application* *6*, 3. 129-138. https://doi.org/10.1002/col.5080060303
9. Johnston-Feller, R. (2001). Color science in the examination of museum objects: nondestructive procedures. *Tools for Conservation*. Los Angeles: Getty Conservation Institute.

THE NATURE OF REDNESS

Natalie Anne O'Connor

UNSW Sydney, Australia
Art, Design & Architecture

ABSTRACT

Colour has long been a commodity, and the instructional information once developed for professional artists with a 'cultivated eye' is now more centred on the mass market. Critical information about an artist's colour pigment name, permanency, and access to hand colour charts can be absent or highlight manufacturing inconsistencies. The experience of artists' pigments and their inner workings are separate from the guise of marketing on digital platforms from the colourmaking industry. Through my practical inquiry of red pigments as an exemplar of all colours, I examined the contemporary artists' palette using the nineteenth-century colourmaker George Field's characterisations of the inherent qualities of good pigments to contribute a new perspective, bringing to light the genealogy of red's nature and working properties. This provided a framework for observing and the autoethnographic study of a 100,000-year-old red in the deepest layer exposed at Lake Mungo in a remote arid area of Australia. By scrutinising redness in artists' pigments, a sensory engagement is explored with material colours, offering valuable perspectives for painters. It also encourages colour-making chemists and industries to re-evaluate prevailing standards and explore novel possibilities. This study provides a deeper understanding of colour's agency, materiality, and sensory attributes through a series of time-based observations. The incorporation of George Field's characterisations allows for a nuanced exploration of red pigments, revealing their unique working properties in the contemporary artistic context, enriching the discourse on colour to inspire further inquiry among art, science, and industry.

Keywords: AIC2023, Colour, Pigments, George Field, Red, Practice-based research.

INTRODUCTION

My practice-based research is an invitation to immerse oneself experientially within a place of inquiry and the practice of observing red. I purposefully examine the coloured pigments on my palette and consider their relationship to a unique place for a new understanding of material colour. This research reveals transformations on the artist's palette since the nineteenth century and exposes the historical construction of pigments. This paper examines material colour on the contemporary palette and its transformation since the early nineteenth century. It investigates the histories, strategies, and new potentials for observing artists' colours within contemporary painting practice. It acknowledges that artists understood material colour in Britain before the early nineteenth century, but with industrialisation came the commercialisation and an explosion of colours (Skira Editore, 2009, p. 59). Colourmaking chemists met the demands of artists for an extended colour palette that used more robust and permanent coloured pigments. Colour became a commodity, and the differing quality of artists' colours and pigments offered by each colourmaker resulted in a necessity for colourmakers and purveyors to communicate their innovations and the attributes of colours to artists via technical guides and catalogues.

Figure 1. Artist, Natalie O'Connor walking and observing the ancient red layer of the Gol Gol unit, at the Mungo Lunettes, Willandra Lakes Region World Heritage Area.

My autoethnographic, creative and reflective research (Candy, 2020) is situated in multiple paradigms that stem from my background and experience as an art practitioner, art educator, and former technical and educational adviser for the commercial colourmaker Winsor and Newton (W&N). An eclectic methodological approach was employed to understand the materiality of colour and the transforming artists' palettes as a 'painterly idea' (Gage, 1993, p. 177), representing conventions of historical painting practice. In considering multiple paradigms, questions emerged as I engaged with the notebooks of the nineteenth-century chemist George Field, the archives of W&N, and the unique environment of Lake Mungo, Willandra Lakes Region in far southwestern New South Wales (NSW), Australia (see Figure 1).

My practice-based research primarily rests on a series of observational studies, documented on an external website www.natalieoconnorartist.com under the webpage #redresearch. My research conveys the experience of 'real' material artists' colours. I argue that associating colour with its chemical composition has eroded artists' concept of colour, making it so vague that it no longer communicates technical expert knowledge. Nearly two hundred years since this transition began, the production of more colours for artists by commercial colourmakers has disconnected many artists from manufacturing processes. The chemical and unique behavioral properties of pigments available to the contemporary painter are underused and misunderstood. Reframing Field's inherent qualities of pigments as understood through my series of observational studies could offer a new understanding for painters, resulting in an expansion and re-purposing of the artist's palette.

METHODOLOGY

My interdisciplinary autoethnographic approach to studying red pigments is an inquiry through practice (Frayling, 1993), whereby my art practice and its procedures constitute the research methodology. The methodological approaches are outlined below as I describe the multiple paradigms of place and the colourmakers archive. My method to investigate this proposition has been an inquiry that singles out red pigments as analogous to all coloured pigments. The research identified three domains on the artist's palette of red pigments: advancing warm reds, receding cool reds, and earth reds, and considered three corresponding case studies of Cadmium Red, Rose Madder and Burnt Sienna. Each case study explored three of Field's 'inherent qualities of good pigment' to evidence my research aims and address the central research question: How can the study of red pigments offer a new understanding of material colour?

Field characterised the inherent qualities of pigments as possessing beauty of colour, transparency and opacity, keeping their place, and durability. Field used this characterisation to assist painters in knowing their materials. My observational studies focus on three of the key 'inherent qualities': beauty of colour, transparency or opacity, and durability. My research reveals that W&N, which acquired Field's notebooks, has continued to develop colours today with consideration of Field's characterisations of colour pigments. By conducting a series of observational studies, evidence was gathered about each red-coloured pigment over time, which developed into questions that are a personal reflection and an interpretation of my creative processes.

Connection to Redness

My art practice contextualises the artist's palette by recognising my place in this world and my cultural origins. Life brought some challenges that I would never have anticipated throughout my research journey, and in retrospect, these challenges also provided a new perspective for reflection. A more profound interconnectedness developed between my practice, what I made art with (colour), and where I made art (place). I connected a history of commercial colourmakers' innovations and changes to artists' palettes to my personal response to the world I live in and make art about.

Connection to Place

My art practice engages with the remote and unique area of Lake Mungo as I navigate ideas of place and its connection to my palette. I frequently return to this remote arid area of Australia to reflect on the ideas and theories interconnected with the artist's palette.

Figure 2. Natalie O'Connor at the Mungo Lunettes site with the dry state paper samples of earth red pigments from Gol Gol Layer Colour Observation (GGLCO) 6 to observe the pigments in situ. Photo by Nicole Walton. Acknowledgement of permission by NSW National Parks, Aboriginal Advisory Group and Three Traditional Tribal Groups.

As a practice-based researcher, I have had to recognise not only where I make art but how I am influenced by these places and what histories I take to them. I have used the term 'place' as it is more closely aligned with the First Nations Australian concept of 'country'. I avoid the terms 'land' and 'landscape' as I felt they had colonial connotations, and presently in Australia they carry an implication of possession. In addition, I do not work as a painter in the tradition of landscape as subject matter.

My initial research did not start in Mungo; it began in the colourmakers' labs. But my questions about material colour came from the many visits and walks on country. My connection to place and colour came through my interactions, conversations, and consultation with the communities of Mungo and staff from NSW National Parks & Wildlife Service. After reading about the red ochre laid over the cremated body of Mungo Man in a ritual so many tens of thousands of years ago, I had a sense that if I was to learn about the materiality and nature of redness, it might happen in this place.

From there, I developed artworks that comprise of a series of observations that identify the behavioural properties of red pigments and characterised innovations in colourmaking since the early 1800s. I refer to these as the Gol Gol Layer Colour Observations (GGLCO). They investigate the behaviour of red-coloured artists' pigments as a response to the Gol Gol unit (see Figure 1 and Figure 2), the 100,000-year-old red layer found beneath layers of sand and clay to form the base of the Mungo Lunettes. It was first described to me as a demarcation layer of life and I wanted to know what red on my palette, could express this extraordinary place.

Each GGLCO study involves submerging paper into vessels of colourant, pigment (classified as pigment red PR) and water. Each vessel of red colourant is observed in a wet state with changes documented over time. Finally, the paper is removed and allowed to dry, revealing the inherent qualities of each pigment. See figure 3, 5 and https://www.natalieoconnorartist.com/red-research.

Ultimately, this procedure of observation interrogates each red pigment and the act of close observation over time, provides a new experience of interpreting colour that is about seeing and tactility.

Figure 3. GGLCO5 with red pigments and paper in wet state.
Installation at Lakebed exhibition, Concordia Gallery. 2018

Connection to the Colourmaker's Archive

As an artist, I engage with a place, the contemporary artists' palette, and have inherited the histories and strategies of the nineteenth-century colourmaker, George Field. In my role as resident artist for W&N, I developed a unique perspective of the inner workings of the colour manufacturing industry, and this extended to privileged access to rare books, catalogues, and materials from the company's historical archives. During my encounters at W&N's archive with Field's notebooks (see Figure 3), a structure and language of colour were discovered that became the cornerstone of my investigations and observations. My research reveals that an understanding and identification of artists' colours, adopted from George Field's notebooks by W&N, became significant to their development (Pavey, 1984) and an understanding of material colour in painting practice today.

Figure 4. George Field's notebooks from the Winsor & Newton Archive.
Image courtesy of Colart Pty Ltd.

My practice-based research examines Field's characterisation of the inherent qualities of the 'good' artist pigments, as written about in *Chromatography* (1835). In my thesis, I refer most frequently to this 1835 edition of *Chromatography*, along with the original text, *Chromatics* (1817), and a concise version of *Rudiments of The Painter's Art* (1850). I expose that despite the noteworthy developments to expand the palette of colours for artists, George Field is not well accounted for in more recent literature on colour.

As explained by historian John Gage, Field's anti-Newtonian approach to colour distanced him from his scientific and artistic contemporaries, who questioned his theories. After his death, the subsequent omission of his colour theories in later editions of *Chromatography*, edited by J. Scott Taylor, further confirmed the unpopularity of his ideas. Gage has written the most comprehensive accounts of Field's contribution to colour in *A Romantic Colourman: George Field and British Art* (2001), in which he retraces the life and work of Field. Gage claims that Field 'contributed to the visual transformation of British painting in the first half of the nineteenth century' (2001, p. 1) and suggests Field's influence continued into the twentieth century thanks to his condensed technical handbook (Field, 1850), which travelled across the globe to the Americas in art and design schools. I propose that this popular guide by Field for students cemented his characterisations of colour as the 'inherent qualities of good pigments' in schools. It gave authority for the identification of pigments in the colourmaking industry, and this requires further investigation.

I re-interpret and critically engage primarily with Field's 1835 edition of *Chromatography, or A treatise on Colours and Pigments, and of Their Powers in Painting* to form an inquiry that provides new multimodal insight that can confirm, challenge, or change our understanding of artists' colours for the contemporary painter. 'Artists' colour' is a term frequently used by the commercial colourmaking industry to imply a standard of quality of paint specific to the needs of artist practitioners, as opposed to student colours or industrial paint. Artists' colours are also referred to as artists' paints and are often known by their binder, for example, artists' oil colours, artists' acrylic colours, and artists' watercolours.

My research concentrates on one artists' colour manufacturer to enable consistency and specificity when describing colour systems and pigment names. Many contemporary brands have adopted historical systems of classification. Still, they have also created their own specific brand language, as each colourmaker endeavours to create distinction and differentiation in the commercial market. As I reviewed the colours currently made available by chemists at the W&N Innovation and Development labs, I reflected on the constructs of the nineteenth-century colourmakers, whose principles, theories, and knowledge of colour pigments characterised them and determined labelling systems still used globally by manufacturers and artists. In the W&N

1892 catalogue, the introduction declares they make artists' colours 'to endow the fleeting aspects of nature and the ephemeral creations of imagination with the "living hues of art"' (Winsor & Newton Pty Ltd, 1892). In this same year, W&N was the first commercial colourmaker to publish the composition of pigments they had prepared (Pavey, 1984).

RESULT AND DISCUSSION

This reflective art practice is an examination of red pigments that connects historical archives (George Field's notebooks, Mary Gartside's notebooks, the W&N pigment, artists' tools library and catalogues), and most significantly the interactions with the chemists and the Colart organisation (the contemporary colourmakers). The act of observation and qualitative accounts of Field's inherent qualities of red pigments, within the W&N Professional Watercolour range, encompass a series of experimental colour observational studies extending from 2016–2022.

In developing a framework for examining red pigments, I adopted Field's phrase 'inherent qualities of pigments' (Field, 1810; 1835). Field suggested that a selection of pigments that possess the desired qualities provides a reliable and expansive palette for artists. The qualities were: Beauty of Colour; Body; Transparency or Opacity; Working Well; Keeping their place; Drying well; and Durability. He explained that a pigment might exhibit certain inherent qualities but not possess all qualities entirely, which is why we must understand the complete palette available and allow the artist to create a palette with a purposeful selection of colours.

These inherent qualities describe what Field believed to be the essential attributes and characteristics of coloured pigments, which predicate their potential behaviours when used by artists. From these seven qualities, my art practice examines three to observe: the beauty of colour, transparency or opacity, and durability. The inherent quality of Field's (1850) beauty of colour is the pigment's sureness, brightness and depth, as examined in GGLCO 5 and 6 (Figures 3, 5 and 7). Field states sureness to be a condition whereby the pigment is reliable and without doubt. Brightness was identified as the quality of being and reflecting light. A coloured pigment's depth is its intensity, which today's artist could understand as saturation, and defines its relationship to the coloured pigment's tinting strength.

My art practice is a procedure that interrogates and examines the inherent qualities of red-coloured pigments, establishing a connection between Field's understanding of the materiality of colour and, in my painting, a connection to place.

Figure 5. Installation of Gol Gol Layer Colour Observation 5, red pigments in dry state on paper (on the right) and Gol Gol Layer Colour Observation 6, test tubes holding red pigments on paper in wet state (on the left). Finalist in Art on Paper Exhibition 2018 at Hazelhurst Arts Centre. 5.5 x 3m approx.

CONCLUSION

The GGLCOs are visual, autoethnographic accounts that involve a process, product, and method that reveals 'my personal experience and insider knowledge' (Ellis & Adams, 2014), as well as existing knowledge and histories. I could be accused of building anecdotal proof supporting my view about colour and its materiality. Still, my practice (written and visual) does not generalise but offers a systematic reflective inquiry with a uniquely positioned voice. My thesis and the digital documentation of the observational studies on the webpage #RedResearch evidence the visual and written autoethnographic approach taken in my research that is presented as a method or tool to explore and represent the inherent qualities of pigments, which requires evaluation and self-evaluation.

A sensorial response to place has been made through a practical time-based examination of red pigments (see Figure 3,5,6 and 7). I enact methods of observation and reflection to engage with the materiality and phenomena of colour. The 100,000-year-old red in the deepest layer exposed at Lake Mungo is the cornerstone of my contemporary analysis of pigments as an exemplar of colour, examining the genealogy of red's nature, behaviour, and working properties. This work contributes a new perspective for contemporary painters as I bring Field's characterisations of pigments and their inherent qualities to light through observations in my art practice.

My research argues that the contemporary artist's palette is a construct inherited from nineteenth-century colourmakers. Field's inherent qualities of 'good' pigments continue to be the characterisations retained by W&N and, more broadly, the colourmaking industry today. Through my art practice, I extend existing research on colour by examining colour innovations and identifying new challenges in comprehending the creations on the contemporary artist's palette.

Figure 6. Gol Gol Layer Colour Observation 7. 2020 during Covid Lockdown at UNSW research studios. Test tubes with earth red pigments after 1250 hours.

ACKNOWLEDGEMENT

This research would not have been possible without the support of many people. I would like to sincerely thank UNSW and my supervisors, Dr Livia Lazzaro Rezende, Professor Paul Thomas, and Associate Professor Kim Snepvangers.

Words cannot express my deepest gratitude to the communities of Mungo. I acknowledge and respect the Elders of the Three Traditional Tribal Groups (3TTGs) and the Aboriginal Advisory Group (AAG). They welcomed me onto their country and shared this ancient place and its stories with me. I also thank the management and staff of New South Wales National Parks and Wildlife Service, Willandra Lakes Region World Heritage Area.

I would also like to acknowledge the support from Jasco Australia Pty Ltd and Colart International Pty Ltd and I am indebted to their management, artists, and scientists who provided an incredible perspective of the world of colourmaking.

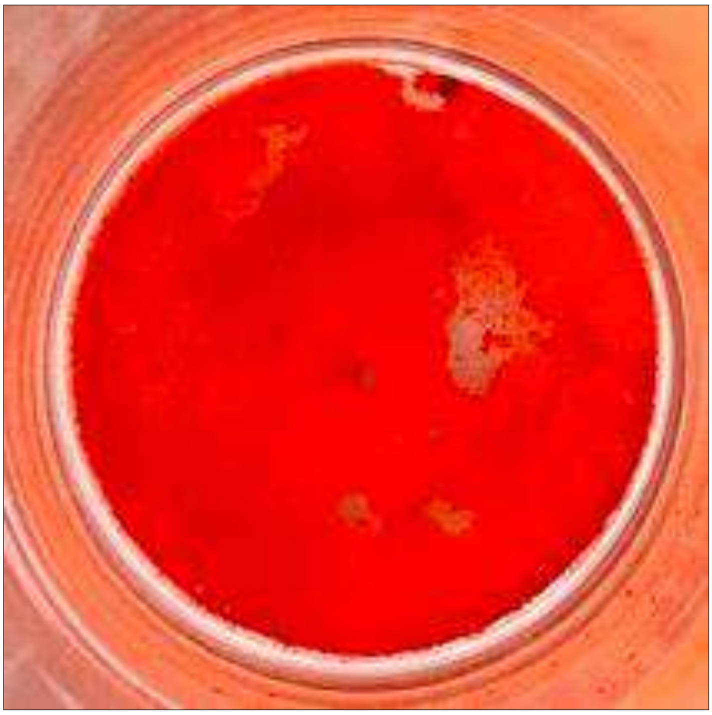

Figure 7. Cadmium Red pigment after 25000 hours from Gol Gol Layer Colour Observation 5. 2020. By artist Natalie O'Connor.

REFERENCES

Barad, K. (2003). Posthumanist Performativity: Toward an Understanding of How Matter Comes to Matter. *Signs, 28*(3), 801 - 831.

Candy, L. (2020). *The Creative Reflective Practitioner. Research Through Making and Practice.* Routledge Taylor & Francis Group.

Ellis, C., & Adams, T. E. (2014). *The Purposes, Practices, and Principles of Autoethnographic Research.* (P. Leavy, Ed.) Retrieved June 2019, from Oxford Handbooks Online.

Fairburn, L. (1982). Paint & Painting. *Paint & Painting:- An exhibition and working studio sponsored by Winsor & Newton to celebrate their 150th anniversary*, 118. Tate Gallery Publications.

Field, G. (1817). *Chromatics, Or, An Essay on the Analogy and Harmony of Colours.* (Harley, Ed.) Retrieved from Linda Hall Library.

Field, G. (1835). *Chromatography, or , A Treatise On Colours And Pigments, and of Their Powers In Painting.* Charles Tilt.

Field, G. (1850). *Rudiments of The Painters' Art;or a Grammar of Colouring, Applicable to Operative Painting, Decorative Architecture, and The Arts.*

Frayling, C. (1993). Research in Art and Design. *London Royal College of Art Research Papers, 1*(1), 1-5.

Gage, J. (1993). *Color and Culture- Practice and Meaning From Antiquity to Abstraction.* California: University of California Press.

Gage, J. (2001). A Romantic Colourman: George Field And British Art. *The Volume of The Walpole Society, 63*, 1-73.

Kincholoe, J. L., & Berry, K. S. (2004). *Rigour and Complexity in Educational Research: Conceptualizing the Bricolage.* Open University Press.

Pavey, D. (1984). *The Artists' Colourmens Story.* London: Winsor & Newton.

Skira Editore. (2009). *Painting Light - The Hidden Techniques of the Impressionists.* Skira.

TATE. (2021). *https://www.tate.org.uk/art/art-terms/p/palette*. (L. Tate, Producer, & Tate, London) Retrieved October 2021, from www.tate.org: http://www.tate.org.uk

Aesthetic Characteristics of the Buddhist Cuisine *Shojin Ryori* Served in Contemporary Japan: From the Perspective of SDGs

Kohji Yoshimura[1]*, Stephen Shrader[2], and Yuko Yamada[3]

[1]*Kansai Gaidai University, Emeritus Professor, Japan.*
[2] *Notre Dame Seishin University, Japan.*
[3]*Yuko Yamada, Colour Instructor, Illustrator, Japan.*

*Corresponding author: Kohji Yoshimura, yoshicolor@earth.zaq.jp

ABSTRACT

Even today, the Buddhist cuisine in Japan, *Shojin Ryori*, uses the fundamentals of five flavors, five colors, and five cooking methods. The five cooking methods are simmering, grilling, frying, steaming, and food served uncooked. This way of cooking food served raw reflects the aesthetic sense of Japan, which aims to blend with nature. It aims to produce a menu that uses five colors: red, white, yellow, green, and black. Although the five colors, red, white, yellow, blue, and black are used in the doctrine of Yin-Yang and the Five Agents or Elements (metal, wood, water, fire, and earth) in Chinese cosmology, green is used instead of blue in contemporary Japan. The basic six tastes are the five flavors (sweet, sour, spicy, salty, and bitter) that are used for seasoning, and the light taste (淡味：*tanmi*) to bring out the natural flavors of the ingredients. Its focus on maintaining a light taste that brings out the flavor of the ingredients reflects the Japanese aesthetic of valuing things in their natural state, as they are, and with a kind of casual presentation. *Shojin* is a Buddhist term that means "avoiding gourmet food and the consumption of meat, and instead purifying oneself by eating simple vegetarian food." *Shojin Ryori* was originally a cuisine for Buddhist monks who followed the precepts of Buddhism. Dairy products such as butter, cheese, and milk were basically not used, but nowadays butter is sometimes added to complement flavor. Some families prepare it as an offering for the *Bon* festival, and even while preserving the characteristics of traditional Japanese fare, the preparation and presentation of vegetables has evolved into a more modern version, attracting attention as "healthy food (soul food) using only vegetables." It is used as a main dish. *Shojin* cuisine in contemporary Japan reflects a variety of Japanese aesthetics, such as the spirit of hospitality. Therefore, from the perspective of SDGs, we will consider the aesthetic characteristics of *Shojin Ryori* in contemporary Japan. For example, *kenchin-jiru*, a feast with lots of ingredients, uses leftover vegetables, making it an eco-friendly dish. It is made with vegetables which are easily available at hand. Peeled vegetable skins and leftover vegetables from other dishes are also finely chopped and added to create a rich flavor and at the same time fully utilize the life of the vegetables.

Keywords: aesthetic characteristics, *Shojin Ryori* (Buddhist cuisine), Contemporary Japan, SDGs, the ultimate hospitality cuisine, mock dishes (*Modoki* cuisine)

1. INTRODUCTION: *The fundamentals of five flavors, five colors, and five cooking methods*

Even today, the Buddhist cuisine in Japan, *Shojin Ryori*, uses the fundamentals of five flavors, five colors, and five cooking methods. The five cooking methods are simmering, grilling, frying, steaming, and food served uncooked. This cooking method of food served raw reflects the aesthetic sense of Japan, which aims to blend with nature. For seasoning, the five flavors of "sweet, sour, spicy, salty, and bitter" are used, and the six flavors are based on the addition of the light taste (*tanmi*) that makes it lighter to make the most of the inherent flavor of the ingredients. The fact that the taste of the ingredients is made thin reflects the Japan's aesthetic sense of "natural, as it is, and casually."[1)] In addition to sugar, soy sauce, salt, vinegar, and mustard, miso and sake are also used as seasonings. "*Shojin*" is a Buddhist term that means "avoiding gourmet food and the consumption of meat, and instead practicing spiritual improvement (purification) through coarse food and vegetarian diets."[2)]

Shojin Ryori was originally a cuisine for Buddhist monks who followed the precepts of Buddhism, and it also means a dish made only with plant-based ingredients such as vegetables and grains, avoiding killing and the use of animal ingredients. It is a monastic dish that developed mainly in Buddhist temples. That is, it is based on the "command to abstain from taking life or harming living things." Dairy products such as butter, cheese, and milk were basically not used, but nowadays butter is sometimes added to complement flavor. In addition, some families prepare it as an offering for the *Bon* festival (the Buddhist All Souls' Day), and even while preserving the characteristics of traditional Japanese fare, the preparation and presentation of vegetables has evolved into a more modern version, attracting attention as "healthy food (soul food) using only vegetables." The Buddhist Cuisine served in Contemporary Japan also reflects the traditional aesthetic sense of Japan. Therefore, from the perspective of SDGs, we will consider the aesthetic characteristics of *Shojin Ryori* in contemporary Japan.

2. MEANING OF *SHOJIN*: *Part of the Noble Eightfold Path or Six Waves of Honey*

Shojin is a Chinese translation of the Sanskrit word *vīrya*, meaning to control evil deeds and practice good deeds.[3)] It is one of the eight practical virtues that form the basis of training in Buddhism, the Noble Eightfold Path (*Hasshodō*：八正道).[4)] The Noble Eightfold Path is *Shoken* (正見：to see correctly with one's heart that recognizes impermanence), *Shoshiyui* (正思惟：to protect life without harming people, living things, or nature by thinking and judging correctly; that is, not to get angry even if one doesn't get what one wants; not to be greedy), *Shogo* (正語：to use the right language that makes people happy and beneficial; that is, not to lie, speak ill of others, or flatter others), *Shogyo* (正業：to do the right thing without killing or stealing), *Shomyo* (正命：to do work that can contribute to human life; to live in a righteous manner), *Shoshojin* (正精進：to continue to strive with sincerity; to strive without neglect so that there will be no evil in the future, and so that a good deed that has not yet arisen will arise), *Shonen* (正念：to see things without including our likes or dislikes and a sense of values; to keep the essence of things in our mind as they are, and never forget always to seek the truth), and *Shojo* (正定：to meditate to unify and stabilize the mind; to perfect the correct concentration). All these eightfold paths work in harmony with each other. *Shojin* is also closely related to other virtues of the Noble Eightfold Path, as if it were two sides of the same coin.

In addition, *Shojin* is also included in the Six Waves of Honey (*Rokuharamitsu*：六波羅蜜), which indicates the six types of ascetic virtues that bodhisattvas practice to attain nirvana (the state of Buddha's enlightenment). The six virtues of the Six Waves of Honey are *Fuse* (布施：the act of generosity, that is, kindness to those in need without asking for anything in return; the three kinds of giving of goods, the practice of teaching the truth, and the sense of security that is reassurance), *Jikai* (持戒： self-discipline; to have commandments that are good habits for oneself; consistency in words and deeds), *Nin-niku* (忍辱：to endure hardship; patience to endure even when one is angry), *Shojin* (精進： perseverance; to keep working with all one's heart; to work tirelessly and practice), *Zenjo* (禅定：to unify the mind through meditation, stabilize the mind, and practice self-reflection), and *Chie* (智慧： wisdom; the practice of awakening to the great work of life; the practice of believing in the law of fate of causality, to stop doing bad things and to do good things; the cognitive ability to grasp things as they are and discern the truth). The perfection of these six virtues is called the Waves of Honey.

According to its literal sense, *Shojin* means to go forward with diligence, "to devote oneself to things and to devote oneself to oneself" (Nishikawa 1997: 3). *Shojin Ryori* is "a simple meal of one soup and one dish originally eaten by monks of Zen temples" (*op. cit.*, 1), which means a dish that is made with all one's heart and effort.

3. MEANING OF *SHOJIN RYORI*: *"Zen heart" that makes use of ingredients*

Shojin Ryori refers to vegetarian cuisine that does not use animal ingredients such as meat, fish, and eggs, but uses only plant-based ingredients such as edible wild plants, root vegetables, grains, legumes, tofu (bean curd), marine products such as seaweed, fruits, seeds, and dried foods such as *Koya-tofu* and *Campyo* (dried strips of the flesh of a variety of gourd), with a focus on seasonal vegetables that match the season. As practiced in a temple, it is a "diet to preserve the body" (Fujii 1993: 188), which means not to eat enough just to be full, but to overcome hunger to the extent that it does not interfere with the practice and to do what needs to be done today (cf. T.E.N. 2000: 62). Odorous irritant vegetables such as garlic, Chinese chives (*nira*), and leek are excluded because they interfere with practice, but *Shojin Ryori* is an ancient vegetarian food that values a sense of unity with nature.[5)]

Today, new ingredients such as avocado, kiwi, green asparagus, and bok choy (a green vegetable of the mustard family originating in China) are also used (cf. Fujii 1992: 26).

Shojin Ryori is a simple cuisine, and it is important to use seasonal ingredients which are easily available at hand and make the most of their unique flavors so that they are not wasted. In addition to the color and seasoning of the dishes, the buds of trees and green perilla are decorated to make use of the aroma of the season in the dishes, just like Japanese flower arrangement, *ikebana*. We value the feeling of the seasons of spring, summer, autumn, and winter so that it feels cool in summer and warm in winter. The people who eat it are young and old, men and women, and each person has different tastes, so we also value the kindness of caring for that person. In modern times, weddings / funerals, happiness / misfortune, etc., are planned to be suitable for the occasion. In other words, it has evolved into the ultimate hospitality cuisine.

In *Shojin Ryori*, it is considered that all the ingredients have life. Therefore, it is devised so that scraps, skins, and leaves of vegetables that are not normally used are not wasted. They are salted and pickled in an instant pickle, shredded vegetable tempura (*kakiage*), finely chopped and boiled or fried in yuba or thinly fried rolls. Finely cut vegetables and kelp are kneaded with tofu and yam and fried in oil to make "*gan-modoki*" (*gan* means a wild goose and -*modoki* represents imitation), which is deep-fried bean curd containing bits of various kinds of vegetables. The name of this food comes from the fact that the taste resembles goose meat. "*Gan-modoki*" is also called "flying dragon head" or "*gammo*" (the shortened form of *gan-modoki*).

4. A KIND OF VERBAL PLAYFULNESS CALLED "MITATE or MODOKI"

A dish made by grating potatoes, spreading them on grilled seaweed, and deep-frying them is called "*kabayaki modoki*." *Kabayaki* means eel broiled and basted with a sweet sauce. This kind of "*modoki* (imitation)" and "*mitate* (likening)" can be seen in *Shojin* cuisine. This is also a kind of wordplay and a sense of Japan aesthetic. In Koyasan's "*Shojin Kabayaki*", grilled seaweed, lotus root, yam, starch syrup, etc. are used, and in the dish name "*unagi* (eel) *no kabayaki modoki*", coarse-grained tofu, Japanese yam, nori seaweed, Shishito pepper, *Hajikami* ginger, etc. are used (cf. Japan Food Thinking Association 2009: 28, 116-117).

In curry and rice, pickled plum-sized konjac jelly is used as a meat substitute (cf. Fujii 1996: 98-99). In eggplant *oden* dishes, the color, lapis lazuli blue, of the eggplant is beautiful, and when it is divided vertically into two, it is reminiscent of Japanese lute, *biwa*. Eggplant *oden* is made by cutting an eggplant in the shape of a *biwa* fried in oil, kneading miso paste kneaded with sake and sugar, sprinkling it with yuzu, and serving it on a plate.

In addition, we can also see "*yaki chikuwa Modoki"* (*yaki* means "toasted", *chikuwa* "a kind of fish paste", and *modoki* "imitation") using coarse-grained tofu and Japanese yam, and "*kamaboko modoki*" using long potatoes (cf. Japan Food Thinking Association 2009: 118-119). *Kamaboko* means white fish meat formed onto a wooden board. In addition, "bite-sized cutlets" using *kurumabu*, one of the baked light cakes made from wheat gluten, are also made (cf. Fujii

1996: 132-133). Since the main ingredient of wheat-gluten breads is protein (gluten) obtained from wheat flour, it is said that "there is no fat and it becomes a fine cutlet" (*op. cit.*, 134).

5. FEATURES OF SOUPS SUCH AS "*KENCHIN-JIRU*"

Kenchin-jiru, a feast with a lot of ingredients, uses leftover vegetables and is an ecological dish. A variety of vegetables which are easily available at hand are used, and the peels of peeled vegetables and the scraps of vegetables from other dishes are finely chopped and added, resulting in a rich flavor, and at the same time fully utilizing the life of the vegetables.

Kenchin-jiru is written in kanji as "建長汁" or "巻繊汁." The notation, "建長汁", indicates that *kenchin-jiru* is a *Shojin* and local dish that originated at the *Kenchoji* Temple in Kamakura City, and that "*Kenchoji-jiru*" is accented as "*kenchin-jiru*." The notation, "巻繊汁" shows that *kenchin-jiru* is derived from *Kenchan* (巻繊), a type of *Fucha* cuisine that is a Chinese *Shojin* dish. It was in the Kamakura period that the *Kenchoji* Temple was built and Zen Buddhism was introduced from China to Japan. There is also a belief that the Kamakura Zen meal is the origin of the taste of modern Japan (cf. Japan Food Discussion Group 2009: 55-59).

In this way, *Shojin Ryori* makes full use of all the ingredients and produces almost no food waste, which is the starting point of *Shojin Ryori*.

Even with the same *Shojin Ryori* name, Kyoto and Kamakura may have different cooking methods and tastes. In Kamakura's *kenchin-jiru*, the main ingredients are "bite-sized slightly large slices", while in Kyoto they are "shredded long thin strips" (cf. Fujii 1996: 90). *Shojin* cuisine is also affected by the climate and natural features of the region (cf. Fujii Sotetsu and Fujii Mari 2017: 105).

6. SEASONAL CUISINE THAT VALUES THE SENSE OF THE SEASON

It is said in Japan that eating "seven herbs porridge" on the seventh day of the New Year will ward off evil spirits and eliminate all diseases. The porridge is cooked with the seven spring herbs, *seri* (Java water dropwort), *nazuna* (shepherd's purse), *gogyō* (*hahakogusa*: cudweed), *hakobera* (chickweed), *hotkenoza* (henbit), *kabu* (turnip), and *daikon* (Japanese radish, giant white radish). In addition, the custom of eating rice cakes with red bean porridge (adzuki-bean gruel) on the morning of the 12th to the 31st of the New Year is held in Zen temples and other places (cf. Nishikawa 1997: 9).

It is believed that summer vegetables have a cooling effect and winter vegetables have a warming effect on the body. It is also considered that eating seasonal vegetables during the season is in accordance with the laws of nature (cf. Fujii 1996: 17-25). In addition, it is pointed out that tasting seasonal ingredients, which express a sense of the seasons, represents "gratitude for the workings and blessings of nature and becoming one with nature" (Masuno 2016: 29).

Shojin Ryori is made according to the season. For example, in January "a dish of lotus root boiled in miso", in February "*yuzu* tempura", in March "*udo-no Kishu-ae*", in April "fertile shoot of field-horsetail boiled in soy" and "bracken rice", in May "horse bean rice" and "butterbur leaf walnut-ae", in June "daikon pickled in cherry blossoms" and "shredded newly-picked-tea tempura", in July "crispy pickle" and "perilla seeds rice", in August "salted eggplant" and "stir-fried cucumber", In September "steamed fig skewered, roasted over coals, and coated with miso", in October "*yukari* rice ball" and "rice ball steamed together with wild plants", in November "fried edible chrysanthemums", and in December "boiled pumpkin in oil" and "dried persimmons dressed with white sesame, tofu, and white miso" (cf. Fujii 2004: 11-280).

7. RICE PORRIDGE, THE BASIS OF THE DIET OF TRAINEE MONKS

In the diet of Zen trainee monks, in the morning "rice porridge, yellow pickled radish, and pickled plums", in the afternoon "barley rice, miso soup, yellow pickled radish", and at night "porridge of rice and other ingredients, yellow pickled radish" are served. The basic meal of the trainee monks is said to be barley rice, miso soup, and pickles, i.e., a meal consisting of one soup and one main dish besides rice (cf. Fujii 1996: 98, Hosokawa 1997: 4).

The monks' tableware consists of five layers of black-painted bowls, which are called "*jihatsu*" (持鉢: bowls that each monk brings to the Zen meditation hall) or "*ōryō-ki*" (応量器: bowls which are supplied according to the amount of food that each monk can eat). It is customary to use rice in the bottom bowl, miso soup in the second bowl from the bottom, simmered food in the third bowl, deep-fried food in the second bowl from the top, and vegetables dressed with miso, sesame, or vinegar in the top bowl (cf. Fujii 1996: 99). The color, black, of black-painted bowls indicates that Zen monks are not influenced by popular taste.

The spirit of "hospitality" means "to think about the other person, as though it were a once-in-a-lifetime opportunity" (cf. Masuno 2016: 64).

8. CONCLUSION: *Shojin cuisine, the ultimate slow food*

Shojin Ryori also continues to evolve. The unique "acrid taste in the throat" of edible wild plants as a spring flavor (cf. Fujii Sotetsu and Fujii Mari 2017: 105) and "*umami* or *jimi* (滋味：dainty)" that represents nourishment and good taste is also taken into consideration (cf. Abe 1998: 78). In addition to the five colors, "brown" such as "*hōji-cha* (toasted tea)" that gives "peace of mind" is also taken into consideration. In terms of cooking methods, "stir-frying" is also emphasized in addition to the five methods.[6)]

What is important in *Shojin Ryori* is to use authentic seasonal ingredients, to spend time and effort generously, and to make the most of the original flavor, taste, texture, and color of the ingredients (cf. Nishii 1992: 9). It is extremely important to make the most of the color of them. It is considered that the decisive factor in any dish is the quality of the broth, and it is usual to soak various vegetables such as shiitake mushrooms, kelp (*konbu*), Chinese cabbage, and carrots in water from the night before to make the broth. *Shojin Ryori* is the ultimate slow food.

When we consider the vegetarian cuisine in contemporary Japan from the perspective of the Sustainable Development Goals (SDGs), which consist of 17 goals and 169 targets, we can point out that it is an effective means of achieving these goals. The phrases such as "to make the most of the ingredients", "enough is as good as a feast", "disordered food is disorder of the mind", "as they are", and "light taste" express the spirit of hospitality in *Shojin Ryori* and are effective.

NOTE

1) The word "*tan* (淡)" of "*tanmi* (淡味)" refers to the middle way in Buddhism and Confucianism, that is, to be extremely unbiased, and is referred to as "a so-called casual way of life" (cf. Fujii Sotetsu and Fujii Mari 2017: 104).
2) *Shojin Ryori* is by no means considered to be a plain dish, but a simple dish. Zen's characteristics of being "simple and refreshing" have been highly evaluated. Sotetsu Fujii and Mari Fujii (2004: 5) believe that *Shojin Ryori* is characterized by "*tan*", which is synonymous with "*wa*: harmony, peace", and that *Shojin* represents "living hard with harmony." *Tanmi* is interpreted as "a balanced state that encompasses all tastes" (Fujii 1996: 19).
3) It has been pointed out that the original meaning of the Chinese word for *Shojin* is "to further enrich the pure and fulfilling mind and body, and to strive for self-enforcement" (Fujii 1993: 187). When Buddhism was introduced to Japan in the early sixth century, *Shojin* was called "*sōjimono*: 精進物" (*op. cit.*, 189), and it is believed that the form of *Shojin Ryori* was established from the *Kamakura* period to the early *Muromachi* period, when Zen Buddhism was introduced to Japan. The Zen monk of the early *Kamakura* period, Dogen (1200-1253) who is the founder of the Sōtō sect of Zen Buddhism, preached on dietary etiquette in the *Tenzo Kyo-kun* (『典座教訓』established in 1237; the mindset of a person who prepares a meal) and the *Fushoku Hanpo* (『赴粥飯法』established in 1246: the attitude of a person who eats a meal). These two books are still practiced by Zen monks as the only "Book of Food" in Zen Gate.
4) *Syugyo* (修行：training, practice, ascetic practices) means "cleansing the unclean mind" and driving away the three poisons (greedy mind, anger, and complaints) (cf. Yoshimura 2019: 93).

The three poisons are greed (貪り), short temper (怒り), and complaints (愚痴; ignorance of the truth) and is considered to be the four fundamental disturbing emotions by adding arrogance (慢心：conceit) to the three poisons. The purpose of training is enlightenment (*Satori*: 悟り), but enlightenment is "attaining the purest mind at the bottom of one's heart", which means "becoming aware of and becoming that mind."

5) There are also five types of irritating vegetables that emit odors and have an intense taste. They are called "*goshin* (五辛)." In addition to garlic, Chinese chives, and leek, it contains *rakkyō* (Japanese scallion) and *hajikami* (Japanese pepper and ginger) (cf. Abe 1998: 174). These were forbidden as vegetables that increased lust and rage.

6) The cooking method of stir-frying is a way of cooking that did not exist in the Japan ancient diet. It is considered that it was introduced to Japan when Zen monks returned to Japan during the Kamakura period and when Chinese monks came to Japan.

ACKNOWLEDGEMENT

In finalizing this paper, we were instructed by Emeritus Prof. George Hlawatsch of Kansai Gaidai University. We would like to express our deepest gratitude for his support.

REFERENCES

Abe, Jien (ed.) (1998). *Shojin Ryori Nyumon: Kokoro-to Katada-wo Iyasu Hotoke-no Chie* (*Introduction to Shojin Cuisine: Buddha's Wisdom to Heal the Mind and Body*). Tokyo: Daihorin-Kaku.

Fujii, Sotetsu (1992). *Zendera-no Shokutaku: Sotetu Osho-no Shojin Ryori* (*The Zen Temple Table: Shojin Cuisine of Buddhist Priest, Sotetsu*). Tokyo: Suzuki Publishing.

Fujii, Sotetsu (1993) *Bukkyo Gogen Sansaku Jiten* (*Buddhist Etymological Strolling Dictionary*). Tokyo: Sotaku-Sha.

Fujii, Sotetsu (1996). *Otoko-ha Damatte Shojin Ryori: Nichiyōbi-no Asobikata Sotetsu-ryu, Sosyoku-no Susume* (*Men, Shut Up and Shojin Cuisine: How to Play on Sundays, Sotetsu-ryu, Recommendation of Simple Dishes*). Tokyo: Yukisha.

Fujii, Sotetsu (2004). *Zendera-no Shojin Ryouri Jyuni-ka-Getsu* (*Twelve Months of Zen Temple Shojin Cuisine*). Chikuma Bunko Fu 33-1, Tokyo: Chikuma Shobo.

Fujii, Sotetsu and Fujii, Mari (2017). *Kamakura, Fuorian, Sotetsu Osho-no Shojin Resipi: Syun-no Yasai-de Shinshin-wo Yashinau* (*Kamakura, Fuorian, Buddhist Priest Sotetsu's Shojin Recipes: Nourishing the Mind and Body with Seasonal Vegetables*). Tokyo: Kawade Shobo Shinsha.

Hosokawa, Atsushi (ed.) (1997). *Koto-de Ajiwau Shojin Ryori: Yumei Jiin-kara Senmonten-made* (*Shojin Cuisine in the Ancient Capital: From Famous Temples to Specialty Restaurants*). Ars Books 40, Tokyo: Fujingaho-Sha.

Japan Food Thinking Association (supervised) Three Seasons (planning and editing) (2009). *Meisatu-ni Tutawaru Yasasii Shojin Ryori: Subete-no Sozai-wo Mudanaku Tukaikiru Shojin-no Kokoro* (*Easy Shojin Cuisine Transmitted to a Famous Temple: The Spirit of Shojin to Use All Ingredients without Waste*). Tokyo: Gakken Publishing.

Masuno, Shunmyo (2013, 2016). *Zen-to Shoku: "Ikiru"-wo Totonoeru* (*Zen and Food: Preparing "Living"*). Shogakukan Bunko Ma 6-1, Tokyo: Shogakukan.

Nishikawa, Genbo (ed.) (1997). *Dare-nidemo Dekiru Shojin Ryori: Sozai-wo Ikasita Herushii-na Okazu* (S*hojin Cuisine That Anyone Can Do: Healthy Dishes That Make the Most of the Ingredients*). Kyoto: Tanko-Sha.

T.E.N. (ed.) (2000). *Karada-ni Kiku Oisii Shojin Ryori: Syun-wo Ajiwau & Syokutaku-wo Irodoru Resipi-syu* (*Delicious Shojin Cuisine for the Body: A Collection of Recipes to Taste the Seasons & Decorate the Dining Table*). Tokyo: Oizumi Shoten.

Yoshimura, Shōyō (2019). *Shojin Ryori-ko* (*Shojin Cuisine*). Tokyo: Shunju-Sha.

FROM DIGITAL COLOUR TO CIRCULAR COLOUR. The color of architectural surface in the circular economy. A review

Katia Gasparini

[1]*Department of Architecture, Design and Planning, University of Sassari, Italy*

*Corresponding author: Katia Gasparini, kgasparini@uniss.it

ABSTRACT

Nowadays, circular economy principles have persuasively entered architectural design and façade covering, transforming their visibility. Previously, the facade was "covered" by paint or a flashy and super-colored digital screen; now, the final layer is neutral, typical of recycled materials. The facade has now lost its role as the superficial identity of the building, instead becoming a sacrifice surface for new experimentations. The aim of the paper is to describe the transformation of textures and colors of contemporary architecture, within the circular economy paradigm, through the analysis of some case studies of the last years and the perceptive and social repercussions. Where before the facade was "covered" by a bright and colorful digital screen, now the overlade of layers is neutral color, like the recycled materials. Today the façade is no longer considered an identifying surface of the building, but as a surface of sacrifice for new experiments. The new architectural façades therefore adopt green, grey, carbon-neutral solutions and more, with a focus to circularity and resilience of the contemporary construction system. At the same time, the new environmental demands of the circular economy are leading us to use technical elements made with recycled or natural materials, which completely change the perception of architectural surfaces, in this Era characterized by speed. The colors are the natural ones of the materials, which can then be recycled, or the neutral colors of recycled materials, maybe as 3D printed powder blends. With this new paradigm, do buildings lose their identity and look all the same or do they re-appropriate the identity of the original materials of the place? What is the impact of these new hypo-colored surfaces within urban landscapes? Will the genius loci [1] of urban spaces survive the changes due to the new circular paradigms?

Keywords: circular colour; architectural surface; digital colour; neutral colour; hypo-coloured surface

INTRODUCTION

In the second half of the 20th century, we witnessed the construction of colored and luminous architectural façades, thanks to industrial research and technology transfer, which have brought materials and technologies with high visual impact to the construction field. Silica, acrylic, and siloxane paint in ordinary construction and experimentation with digital technologies in tall buildings (in the late 20th century) transformed the perception of architectural façades and the skyline of big cities and peripheral hamlets. In major European and international cities, building façades were turned into large TV screens, catching the attention of passers-by with luminous colors, saturated and brilliant, moving images, and super-colored advertisements (urban screens). In residential and social housing, long-lasting synthetic colors have subverted historical buildings' tendency toward soft ones, covering houses with bright tones. Saturated and brilliant colors, which can resist any weather, have transformed suburbs into colored mosaics: façades are neon green, cherry red, lemon yellow, light blue, purple, and so on. At the same time, the parable of urban screens concluded in little more than 15 years, leaving room for a revived environmental awareness oriented toward the realization of green façades. Living walls started to invade some of the most famous contemporary architectures and some residential buildings, albeit to a smaller extent. Following the same revived environmental consciousness, contemporary façades have been equipped with new green, grey, carbon-neutral and other solutions, in a perspective of circularity and resilience. The new environmental needs of the circular economy are leading us to use technical elements realized with recycled materials, whether natural or artificial. They often lose their original color during recycling, moving toward more neutral (achromatic) shades. At the same time, the contemporary construction of Italian suburbs is subjected to a generalized chromatic flattening, with new buildings indistinctly painted in grey shades. Nowadays, circular economy principles have persuasively entered architectural design and façade covering, transforming their visibility. The paper aims to describe the transformation that has invested contemporary architecture's textures and colors within the circular economy paradigm. This will be accomplished by analyzing case studies from recent years for both building typologies. Now, the colors of façades are the natural or neutral colors of recycled materials, sometimes as 3D-printed powder mixes or shades of grey in the suburbs. This leads buildings to lose identity and visibility. What is the impact of these new hypo-colored surfaces in urban landscapes? Will the genius loci [1] of urban spaces survive the modifications of circular paradigms?

METHODOLOGY

This paper employs the descriptive analysis method by combining a literature review with a case study analysis to identify the relevant items for studying the color of contemporary façades. A state-of-the-art analysis was made, including both case studies with materials deriving from a "circular" design and constructive approach (20 case studies) and the color of façades built in the last years in urban suburbs (50 case studies). When possible –in peripheral residential buildings – a survey with an NCS Colourpin II colorimeter (or color survey tool) has been performed [2]. In internal case studies, it was impossible to survey building colors directly; hence, a photographic sample provided by designers or obtained from journals was used. Images have been processed with the Adobe Photoshop software (pixilation method). Color conversion from RGB to NCS has been performed with the conversion tool from e-paint.co.uk [3] to identify the closest NCS value to the RGB hexadecimal one. The analyzed buildings have been built relatively recently: 2008-2022 for the 20 international case studies and 2020-2023 for the 50 Italian case studies. Color variations due to different natural light conditions, artificial lighting, reflections, and other environmental factors were not considered, as they were negligible. The paper will present the first analyses inferred from the case studies, which will have to be further studied and substantiated with multi-disciplinary research in the future. The paper is articulated into 3 items: historical-circular excursus on the colors on the façade, with a focus on contemporaneity; chromatic scales found in the case studies and façade materials in the circular economy; results and conclusions.

THE COLOUR OF FACADES: "CIRCULAR" EVOLUTION

In the past, buildings were made with local materials. Some regions used bricks, others used stone, and in others, the wall had a lime plaster. Colours were composed of local pigments in a solution of water and lime. For this reason, in most urban and periurban historical centres, façades have the colour of natural materials and soils. In broad outline, five different phases of façade colours can be recognised in history (fig. 1):

- The first is the longest one, preceding the Industrial Revolution, where colours were determined by the materials used and by the frescoes and decoration in prestigious buildings;
- The second one is the phase between the two industrial revolutions when the development of glass and steel buildings led to the construction of high-rise buildings with innovative materials;
- The third phase is the post-war phase, that of the reconstruction of large residential complexes (social housing) and the diffusion of synthetic paint;
- The fourth one started in the '80s, with the production of artificial light envelope (overcladding systems) made with coloured components and any type of material, with digital panels (urban screens) and innovative materials that change colour and form, etc.;

- The fifth is the contemporary age, gradually shifting from the construction of living walls to a new type of sustainability, which reuses construction materials and is called "circular economy".

Figure. 1: Circular evolution of the colour of the façade.

It can be inferred that the productive and cultural system's evolution has influenced the built environment's colour. Which colours have characterised these five phases? In small urban centres, the colours of less affluent classes and bourgeoises' houses used to derive from locally obtainable materials and components: the colour of bricks (which could be red, grey, or red-yellow according to the place), the colour of local trees (Fig. 2) or stones. In ancient times, plastered houses could be left in their natural colour: in Florence, it was a white grey, which became yellow over time; in Rome, it was pinkish grey, obtained from pozzolana. Throughout the 17th and 18th centuries, façades were painted yellow, red, green, or bicolour, like in Naples [4]. For example, in Tuscany, the 14th and 15th centuries are characterised by the pictorial use of low tones, without flashy colours, due to the practice of frescoes on lime, requiring the use of earth colours (oxides) [5]

Figure 2: Facades of small historical centres built with local materials. On the left, Storo (I), with its typical constructions in stone and timber. On the right, Buddusò (I), with houses built in grey granite blocks.

In the second post-war period, has brought about an unconfined transport of goods. Architectures can no longer age and must always appear flawless and impervious to time. Artisanal techniques have disappeared, and artificial materials are used. Saturated and bright colors are preferred, especially as their visual properties are unaltered by the sun and weather over time. This leads to the employment of synthetic paint with improbable neon green or yellow tones, blue and purple, and so on. This is true for residential construction in general. Then tall buildings, constructed of steel and glass, mainly have neutral, reflective colors or colored ceramic or marble cladding. Consider, for example, the buildings Giò Ponti designed and covered with three-dimensional colored ceramics or think to Aldo Rossi and the "Postmoderns." In the late twentieth century, there was the spread of artificial coatings: colored or grey metal panels, polycarbonates, up to the bright, saturated digital layers (Fig. 3) with an initial environmentalist sensibility that took the form of living walls.

Figure 3: Madrid. Left, a façade with coloured metal panels (social housing on the outskirts of Madrid); right, the digital façade of MediaLab Prado.

Ideally, the circle completes again in contemporary times. The colours of recycled materials and components are mixed to give rise to natural/artificial powder mixtures, which 3D printing transforms into living components or cells. They are the colours of Pla, marble powders, and soils. That is, basically neutral colours. What happened?

THE COLOUR OF CONTEMPORARY FACADES

The analysis of buildings constructed in recent years revealed a trend toward achromatic or low-saturation facades: grey and beige scales. The study focused on two types of buildings: diffuse housing in suburbs (expansion areas) and large architectural projects of office centres, exhibition halls, installations, tall buildings, etc. As for the latter, the colour tends to come from the components of the cladding or exterior walls, often made from recycled materials. Reintroducing materials into the production process usually involves their transformation into another form than the source material, which can lead to colour variation. In this case, this involves reusing stone waste, which can be turned into powder to make blends with other materials (geopolymers) [6] for 3D printing or components from recycled polymers, more colourful, or metals. The case of current residential construction is different. Our contemporary urban environment seems to have mutated into a monochromatic world with a limited spectrum of tones. Examples of this kind of architecture and urbanism are found in large residential projects in the suburbs [7]. Today, variations of grey and beige (Fig. 4) are widely used instead of the saturated colours used until recently. Sometimes, grey colours are also proposed in in historic centres. Thus, while historically, the grey colour of facades was typical of poor suburbs, where the wall face was barely plastered (the grey colour of the mortar plaster) and not painted, now grey is deliberately chosen as a valuable finish. Concerning this aspect, it would be appropriate to investigate the reasons through sociological and anthropological analysis. According to Weber's recent research [7], the reason for the contemporary monochromatic orientation is solely commercial. Neutral colour loosens attention and distracts from imperfections and design errors, "It is [even] believed that there might be a higher margin of error with grey and white tones." And for that reason, "visual impoverishment is the accepted consequence."

Figure 4: Some case study of newly built residential buildings in different suburbs. All new buildings are painted with gray variants.

FAÇADE MATERIALS AND TECHNOLOGIES IN THE CIRCULAR ECONOMY

In the analysed case studies of international architectures, the façades were almost all made by recycling building components: bricks, tiles, and stones salvaged from other demolished buildings and reused with more innovative textures than the historic building.

The result is colours that tend to be neutral and darker than the same new product, with hues ranging from grey scales to beige and brown scales (for terracotta components) (Fig. 5).

Figure 5: color palette obtained from contemporary architectural projects, built with recycled components

These colors belong to components originally made from natural materials (the soils or stones), but their tones have turned darker and less vivid. Examples include the Ningbo Historic Museum project and Kengo Kuma's China Academy of Arts' Folk Art Museum, both in China. The former is constructed from building waste of different shapes and materials, and this identity is left exposed on the facade of the building. The general color is grey, with a few bands of brick colour. Recycled materials are deliberately left exposed. Kengo Kuma's project is grey, too, in a dark shade, and it is interesting because the surfaces are covered with old tiles from local houses but laid at right angles to the vertical wall, set on a metal mesh. In this way, they form a kind of brise-soleil. The innovation in almost every project is in the design process: parametric design and sinuous shapes. Thus, the colors of the circular economy take us back to the basics, to the pre-industrial revolution building tradition, because components made of natural materials are reused in their entirety. There are also plastic wrappers, whose colors tend to be from light blues to whites, reusing recycled plastic components, too. There are still few case studies in which recycled components are crushed or melted and reinserted into a new production process. Then, they are usually used for 3D printing housing components or cells. The colors do not change much from the above, whether polymers or natural materials. In the case of Tecla from Wasp (Fig. 6), the mixture of soils substitutes the beige-brown color of the recycled material. Also, in cases of digital polymer printing such as Killa Design's of the Future Pavilion or the EU Pavilion by Dus Architect, the colors are white or light blue. In the People Pavilion the colored tiles that make up the Pavilion's upper facade are made from plastic household waste materials (Fig.7).

Figure 6-7: Left, Tecla by Wasp (ph. WASP); right, People Pavilion (ph. Pretty Plastic)

In the color analysis of residential buildings, the color palette is drastically reduced to grey scales (Fig. 8). In this case, it is not the reuse of waste material but newly produced synthetic paints that somehow "mimic" the color scheme of houses built between the wars. In that period, houses remained plastered with grey cement mortar without a layer of colored paint. The phenomenon almost exclusively occurs in new construction.

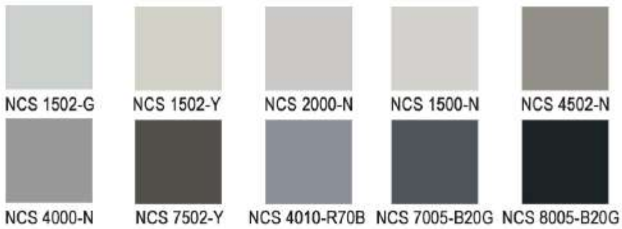

Figure 8: Colour palette derived from residential building plans

RESULT AND CONCLUSION

The findings of this study highlight that, in the time of the circular economy, even architectural facades are adapting their appearance to the increased environmental sensitivity. The reuse of building components and materials in the construction process affects the color of façades at the level of large-scale architecture. It is well known that architecture represents its own time. This is perhaps the time for the recovery of a more honest relationship with the environment and the resources available to us. This new approach manifests itself through facades with duller, more opaque colors. These are the colors of recycled materials that, for that reason, have been ageing due to exposure to the elements over many years. In fact, the color palette derived from the 20 case studies (Fig. 6) reveals the original materials: the beiges/reds of bricks, the grey tones of concrete, and the white/blue tones of polymers. However, they are decidedly low-saturation colors. In the case studies shown, only one (Tecla) was built by 3D printing with a local soil-based mixture that influenced its final color. However, other non-structural components made with marble powder binder-jetting technology are being tested. In this case, the color will not realistically match the source stone but be more similar to a mixture of stone and other materials, fading the color. The other analysis, performed on residential construction, from the material point of view, is apparently unrelated to the logic of circular economy and recycling. The new buildings are all grey; the materials are newly manufactured paints. What is the reason for this generalized color flattening? Weber cites purely commercial reasons. Maybe other explanations are more related to environmental sociology and anthropology, which would be worth exploring. The grey color does not draw attention to either the object or the design flaws, is welcomed by most people (how many grey cars do we see along the streets?), and keeps the profile low compared to the quality of the building. However, interventions with recycled materials and those with grey paints are strongly self-referential, prioritizing experimentation, economy, and emulation. In the era of Industry 5.0, with even the European community issuing documents on the importance of a Human-Centered (HCD) approach to manufacturing [8], we are going in the diametrically opposite direction, regardless of urban color plans and the valorization of the identity of historical centers and suburbs.

REFERENCES

1. Norberg-Schulz, C. (1980). Genius loci. Towards a phenomenology of architecture. Milan (I), Rizzoli.
2. https://ncscolour.com/product-category/shop/digital-colour-tools/ (access on 20.07.23)
3. https://www.e-paint.co.uk/compare-colours.asp (access on 20.07.23)
4. Quaroni, L. (1977). Progettare un edificio. Milan (I). Mazzotta, pp.196-197
5. Zennaro, P. (2002). Il colore degli edifici. Florence (I). Alinea, pp. 27-29
6. See research on 3D printing of geopolymers made from stone dust: Gobbin, F. et al. (2021). Large scale additive manufacturing of artificial stone components using binder jetting and their X-ray microtomography investigations. Open Ceramics, 7: 1-1, https://doi:10.1016/j.oceram.2021.100162; Elsayed, H. et al. (2022). Additive manufacturing of inorganic components using a geopolymer and binder jetting. Additive Manufacturing, 56:, https://doi:10.1016/j.addma.2022.102909.
7. Weber, R. (2023). Monochromatic design in a polychrome world. Why our cities have become increasingly gray: A dichotomy between production and reception in architectural color design. Color research and Application, https://doi.org/10.1002/col.22876
8. Breque, M., De Lars, N., Petridis, A. (2021), "Industry 5.0. Towards a sustainable, human-centric and resilient European industry, European Commission. https://research-and-innovation.ec.europa.eu/knowledge-publications-tools-and-data/publications/all-publications/industry-50-towards-sustainable-human-centric-and-resilient-european-industry_en (Access 02 August 2023).

THE EFFECTS OF CHROMA ON DESIGNERS' INTELLECTUAL ABILITIES IN AN IMMERSIVE VIRTUAL ENVIRONMENT

Guobin Xia[1]*, Phil Henry[2], Francisco Queiroz[2], Stephen Westland[2], Luwen Yu[3], Qian Cheng[2], and Jie Yang[4]

[1]*School of Textiles and Design, Heriot-Watt University, United Kingdom.*
[2]*School of Design, University of Leeds, United Kingdom.*
[3]*School of Computational Media and Arts, Hong Kong University of Science and Technology, China.*
[4]*Department of Journalism Studies, The University of Sheffield, United Kingdom.*

*Corresponding author: Guobin Xia, g.xia@hw.ac.uk

ABSTRACT

Immersive virtual reality (VR) technology has gradually found its place within the fashion and creative design industries, aiming to stimulate creativity, imagination, and engagement. However, it's important to note that limited systematic research has delved into the intricate design of immersive VR environments to effectively evoke positive emotions and enhance cognitive performance, particularly with regards to nurturing designers' logical and lateral thinking abilities. Colour, as a pervasive visual design element, has shown that a deliberate approach to hue design can elicit favourable cognitive responses and intellectual capabilities. This research, therefore, endeavours to reignite the exploration of interactions between colour and cognitive performance in VR, focusing on the impact of chroma on intellectual abilities of design students within immersive VR environments. The study employed green-coloured backgrounds across seven chroma levels (90%, 75%, 60%, 45%, 30%, 15%, and 0%), all with equal luminosity settings. Thirty designers and students (15 males and 15 females), ranging from 20 to 28 years old, participated in a series of psychrometric experiments. Their logical and lateral abilities, along with attention to detail, were assessed through a sequence of single-choice tests delivered via an HTC Vive VR system. Data obtained from the experiment were analysed using a multivariate analysis of variance (MANOVA). The findings from this experiment indicate that varying levels of chroma significantly influence the logical and lateral thinking abilities of design students, as well as their attention to detail within immersive VR environments. The outcomes of this research offer potential encouragement for VR researchers to incorporate and maximize the use of advanced immersive computing technologies. The fresh insights gleaned from this study underscore the potential of selective colour application in enhancing intellectual abilities and refining the design of immersive VR experiences. Practical implementation could involve crafting VR applications tailored specifically to stimulate users' creativity, imagination, and logical thinking skills. However, it's important to acknowledge that this experiment's scope was limited to a diverse cultural and age range, necessitating a more comprehensive exploration in the future. Furthermore, extrapolating the effects of chroma on arousal and impulsiveness across the entire colour spectrum based on these selected samples remains a challenging endeavour.

Keywords: Virtual Reality, Chroma, Colour Design, Intellectual Abilities

INTRODUCTION

In the contemporary era, immersive virtual reality (VR) technology has revolutionized various industries, notably fashion and creative design. These sectors have adeptly harnessed VR's capabilities to amplify creativity, imagination, and user engagement. For instance, Tao et al. (2021) emphasized the potential of immersive VR health games to support long-term engagement with therapeutic interventions, suggesting the profound impact of VR on user engagement in health contexts. Similarly, Škola et al. (2020) demonstrated that modern immersive VR applications, when combined with 360° storytelling, can sustain high levels of presence, immersion, and general engagement. Fröhlich et al. (2018) introduced a unique VR-sandbox system, highlighting the potential of VR to foster creativity and exploration by allowing users to design landscapes through haptic interactions. Furthermore, Elor et al. (2021) showcased the effectiveness of a VR game in maintaining engagement and motivation for physical rehabilitation, emphasizing the versatility of VR applications. Yet, as the adoption of immersive VR environments grows, a significant knowledge gap persists regarding their optimal design to foster positive emotional and cognitive outcomes. A particularly uncharted territory is the potential of VR to enhance designers' logical and lateral thinking abilities.

Central to the visual landscape and design process is the ubiquitous element of colour. Emerging research has illuminated the profound impact of colour, specifically hue, chroma, and brightness, on cognitive responses and intellectual capacities (Xia et al., 2021a, Xia et al., 2021b, Xia et al., 2022, Xia et al., 2023). This litany of research outputs, although prolific, beckons for a more scrutinizing assessment of their methodologies and implications. Take, for instance, Xia et al.'s (2021c) endeavours, which purportedly dissect the intricacies of how colour stimuli wield influence over lateral and logical abilities. Their assertions of heightened arousal and impulsiveness induced by certain colours in individuals' cognitive processes are tantalizing, yet warrant a closer examination of the broader ecological validity of such conclusions. Moreover, the ambitious assertions put forth by Xia et al. (2023), delving into the domain of colour attributes' impact on cognitive performance within immersive virtual environments, although intriguing, demand a cautious interpretation. The revelation of colour's influence on thinking and abilities, within the context of virtual experiences, while undoubtedly provocative, necessitates further consideration of the multifaceted factors at play. In essence, while these studies offer preliminary glimpses into the potential interplay of colour and cognition, they beckon for more rigorous exploration and nuanced understanding before we can fully embrace their implications. As such, this study embarks on a novel exploration, aiming to reinvigorate the discourse surrounding the interaction between colour and cognitive performance within the immersive context of VR, with a focus on exploring the potential to positively trigger designers' cognitive responses and intellectual capacities.

In a deliberate focus on the effects of chroma, the study investigates its influence on the intellectual capacities of design students and professionals, thereby providing fresh insights into the untapped potential of selective colour application in immersive VR experience design.
To address these inquiries, the research engaged a cohort of twenty-eight designers and students, encompassing an equal distribution of 15 males and 15 females. Ranging in age from 20 to 32 years old, this diverse group participated in a meticulously designed series of psychrometric experiments, facilitated by an HTC Vive VR system. Through these experiments, the study evaluated participants' logical and lateral thinking abilities, along with their attention to detail, across varying levels of chroma. The ensuing analysis, conducted via a multivariate analysis of variance (MANOVA), uncovers nuanced relationships between chroma, cognitive

performance, and intellectual capacities within the immersive VR environments. The ensuing sections delineate the methodology, results, and implications of this pioneering research endeavor. By shedding light on the intricate interplay between chroma, cognitive faculties, and intellectual capacities within the context of immersive VR, this study lays the foundation for harnessing advanced immersive computing technologies to enhance intellectual capabilities and craft more impactful VR applications tailored to nurture creativity, imagination, and logical thinking abilities. However, it is pertinent to acknowledge the preliminary nature of this study's scope, urging further comprehensive exploration across diverse demographics and broader colour spectrums.

METHODOLOGY

Materials

Chroma trials were conducted utilizing the Unity platform in conjunction with the HTC Vive Pro head-mounted display.

Colour Conditions

The experiments involving chroma employed green backgrounds across seven different chroma levels (90%, 75%, 60%, 45%, 30%, 15%, and 0%), all with uniform luminosity settings. The specific green hue utilized for these experiments is designated as the 90% chroma within this investigation. The attributes of the background colors on both the monitor and the VR headset are detailed in Table 1.

Table 1: The attributes of the background colors within the VR headset.

Colour Conditions	R	G	B	L	a*	b*	C*	h (°)
Green_90%_chroma	23	229	171	81.38	-58.92	15.62	60.946	165.15°
Green_75%_chroma	57	229	181	82.00	-53.80	11.26	54.96	168.18°
Green_60%_chroma	92	229	190	83.00	-46.42	8.00	47.10	170.23°
Green_45%_chroma	126	229	200	84.30	-36.81	4.85	37.13	172.50°
Green_30%_chroma	161	229	210	86.12	-25.26	2.45	25.38	174.46°
Green_15%_chroma	195	229	220	88.36	-12.84	0.66	12.86	177.07°
Green_0%_chroma	229	229	229	90.94	-0.00	0.00	0.00	270.00°

Psychometric Tests

The psychophysical study was carried out to explore how chroma impacts individuals' cognitive capabilities through the use of a Head-Mounted Display (HMD) Virtual Reality (VR) headset. Six distinct types of psychometric tests were employed to evaluate participants' cognitive capacities: logical ability (logic rule test, mathematics sequence test), lateral ability (spatial structure test, rotation test), and detail ability (odd one out, same detail test). Within each test category, seven questions were presented, with each question featuring a distinct coloured background. Consequently, the total number of questions reached 42 (6 test types multiplied by 7 coloured backgrounds), with each participant tasked with responding to the entire set. The assignment of coloured backgrounds to questions and the sequence of question presentation were randomized for each participant. It's important to note that while every participant encountered each question with the seven coloured backgrounds within a given test, the specific colour allocations varied among participants. This approach aimed to mitigate bias, ensuring that if a question proved slightly more challenging, its association with any particular background for a participant was equally probable. The primary data collected from the experiment encompassed response time and error rates. These metrics will be utilized in the Results section to gauge participants' levels of arousal and impulsiveness, serving as an indirect means to elucidate the influence of colour on individuals' lateral and logical abilities.

Participants

A cohort comprising 30 individuals (15 males and 15 females), aged between 20 and 32 years, was enlisted for the chroma experiment phase. In light of potential cultural influences and to mitigate variations in logical tendencies, the participant pool exclusively consisted of Chinese design students and professionals for this experimental segment.

Experimental Procedure

Prior to commencing the experiments, every participant underwent the Ishihara colour vision test to ensure their normal colour recognition capability. Once participants successfully completed the test, they were provided with a comprehensive explanation of the experimental instructions. Following this, participants engaged in a set of practice tasks for each type of psychometric test to acquaint themselves with the procedure before embarking on the main experiment. Upon concluding these tasks, participants were instructed to focus their gaze on the white reference background presented by the VR headset for a five-minute period, allowing them to acclimate to the conditions. The primary experiment commenced five minutes after participants had acclimatized to the experimental conditions.

RESULT AND DISCUSSION

Utilizing a Multivariate Analysis of Variance (MANOVA) in SPSS, the study sought to discern the impact of distinct chroma levels on participants' cognitive performance. The findings indicated significant variations in response times when participants were engaged in tasks necessitating logical reasoning. Specifically, a statistically significant difference was observed between the chroma levels of 75% and 0%, $p = .006$. For tasks emphasizing lateral thinking capabilities, the data revealed marked disparities in response times, especially between chroma levels of 75% and 30%, $p = .001$, and between 75% and 15%, $p = .031$. Furthermore, error rates in these lateral thinking exercises displayed significant variations across several chroma contrasts: 75% versus 60%, $p = .043$; 75% versus 15%, $p = .013$; 45% versus 15%, $p = .025$; and 30% versus 15%, $p = .043$. In tasks demanding meticulous attention to detail, participants' response times exhibited significant differences at specific chroma contrasts: 75% compared to 60%, $p = .036$; 75% compared to 30%, $p = .022$; 75% compared to 15%, $p = .01$; and 75% compared to 0%, $p = .004$.

These results emphasize the profound impact of chroma variations on cognitive metrics, spanning logical and lateral reasoning, as well as tasks that demand precision. The insights derived from the MANOVA analysis shed light on the intricate interplay between chroma levels and cognitive function, hinting at the potential to design VR experiences that optimize cognitive capabilities and attention to detail.

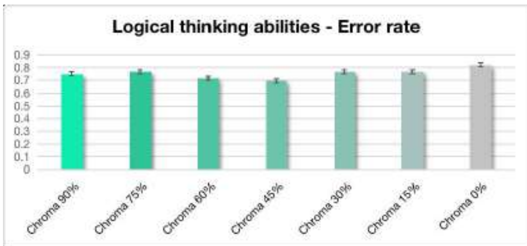

A

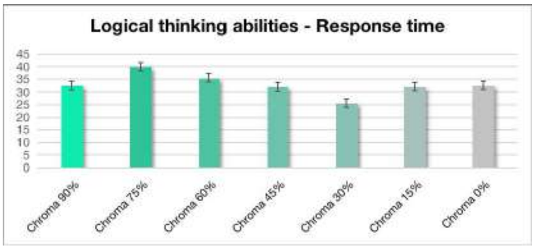

B

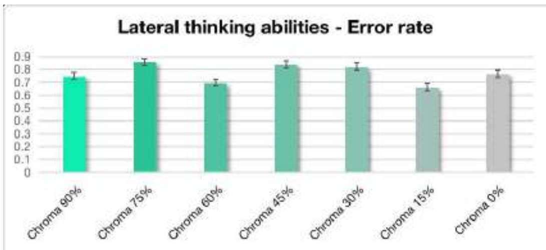

C

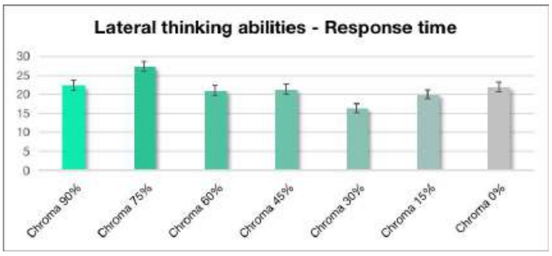

D

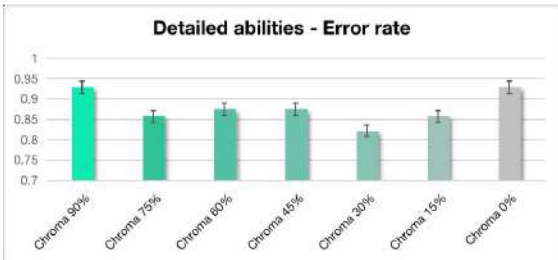

E

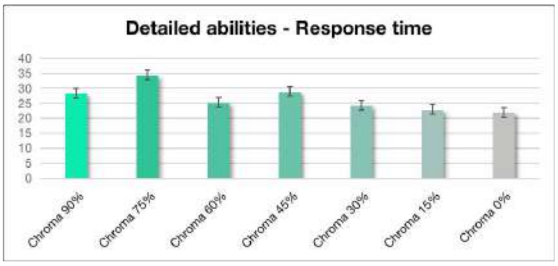

F

Figure 1. (A) Error rate of participants' performance in logical thinking abilities by background colours in VR; (B) Response time of participants' performance in logical thinking abilities by background colours in VR; (C) Error rate of participants' performance in lateral thinking abilities by background colours in VR; (D) Response time of participants' performance in lateral thinking abilities by background colours in VR; (E) Error rate of participants' attention to details by background colours in VR; (F) Response time of participants' attention to details by background colours in VR.

CONCLUSION

Our research illuminates the intricate relationship between colour chroma and cognitive performance within the realm of immersive virtual reality (VR). As immersive VR technology continues to permeate creative sectors like fashion and design, it offers unprecedented opportunities for nurturing creativity, bolstering engagement, and catalysing imagination. Yet, the quest to design VR environments that optimize emotional and cognitive responses has been hampered by a paucity of in-depth research. Our study sought to bridge this knowledge gap, with a keen focus on how colour chroma can influence the cognitive prowess of designers.

Building upon the foundational research by Xia et al., which highlighted the profound influence of colour on cognitive dynamics, our study ventured into the uncharted territories of VR. We delved into the nuanced effects of chroma variations on cognitive faculties such as logical and lateral thinking, as well as precision. Utilizing the HTC Vive VR system, our rigorous psychrometric experiments have unveiled ground-breaking insights, suggesting that strategic colour application could revolutionize immersive VR design. This exploration is further contextualized by studies such as those by Elor et al. (2021), which delve into the potential of VR beyond the novelty, especially in physical rehabilitation. Similarly, Fröhlich et al. (2018) and Škola et al. (2020) have emphasized the immersive potential of VR in fostering creativity, playfulness, and cultural heritage engagement. Tao et al. (2021) have also underscored the transformative potential of VR in health games, emphasizing the importance of game design in enhancing cognitive and physical outcomes. The marked disparities in response times across chroma levels, especially in tasks demanding logical reasoning, beckon a deeper exploration into the underlying cognitive mechanics. The linkage between specific chroma intensities and heightened cognitive arousal or impulsivity enriches our comprehension of colour's multifaceted impact. The variations observed in lateral thinking and error rates across chroma gradients further underscore the intricate dance between colour and cognition.

Our research stands as a beacon in the academic landscape, providing empirical validation of chroma's sway over cognitive performance in immersive VR settings. The correlations we've unearthed between chroma shifts and distinct cognitive metrics, such as response times and error rates, champion the idea of colour as a potent catalyst for cognitive immersion. This resonates with the broader understanding that colour's magic extends beyond mere visual appeal, influencing cognitive reactions and intellectual prowess. The ramifications of our findings are manifold, spanning both academia and real-world applications. The knowledge gleaned can pave the way for crafting VR experiences that resonate with specific cognitive goals. By adeptly tweaking colour chroma, designers hold the key to fine-tuning cognitive immersion, arousal, and meticulousness, thereby elevating the user journey. This knowledge transcends the boundaries of creativity, beckoning interdisciplinary synergies and innovations across diverse arenas. Yet, it's paramount to recognize our study's boundaries. Our research lens was primarily trained on a niche demographic of design aficionados, and the emphasis on green hues might not encapsulate the vast chromatic spectrum. Future endeavors should cast a wider net, encompassing diverse demographics and a richer palette of colours. While our insights are invaluable, the intricate interplay between chroma and cognition beckons deeper exploration. To encapsulate, our research stands as a trailblazer, demystifying the role of colour chroma in shaping cognitive trajectories within VR landscapes. Our revelations underscore the promise of judicious colour application in amplifying cognitive immersion and refining VR design. As the VR frontier expands, our insights beckon further scholarly pursuits and inventive applications, fostering cross-disciplinary alliances to harness colour's transformative potential in virtual realms.

ACKNOWLEDGEMENT

I would like to acknowledge Heriot-Watt University for providing the financial support that made this conference paper possible.

REFERENCES

Elor, A., Powell, M., Mahmoodi, E., Teodorescu, M. & Kurniawan, S. 2021. Gaming beyond the novelty effect of immersive virtual reality for physical rehabilitation. *IEEE Transactions on Games,* 14**,** 107-115.

Fröhlich, T., Alexandrovsky, D., Stabbert, T., Döring, T. & Malaka, R. VRBox: A virtual reality augmented sandbox for immersive playfulness, creativity and exploration. Proceedings of the 2018 Annual Symposium on Computer-Human Interaction in Play, 2018. 153-162.

Škola, F., Rizvić, S., Cozza, M., Barbieri, L., Bruno, F., Skarlatos, D. & Liarokapis, F. 2020. Virtual reality with 360-video storytelling in cultural heritage: Study of presence, engagement, and immersion. *Sensors,* 20**,** 5851.

Tao, G., Garrett, B., Taverner, T., Cordingley, E. & Sun, C. 2021. Immersive virtual reality health games: a narrative review of game design. *Journal of NeuroEngineering and Rehabilitation,* 18**,** 1-21.

Xia, G., Henry, P., Chen, Y., Queiroz, F., Westland, S. & Cheng, Q. 2023. The effects of colour attributes on cognitive performance and intellectual abilities in immersive virtual environments. *Computers in Human Behavior,* 148**,** 107853.

Xia, G., Henry, P., Li, M., Queiroz, F., Westland, S. & Yu, L. 2021a. A Comparative Study of Colour Effects on Cognitive Performance in Real-World and VR Environments. *Brain Sciences,* 12**,** 31.

Xia, G., Henry, P., Queiroz, F. & Westland, S. 2021b. Effects of coloured lighting in the real world environment and virtual reality. *Journal of the International Colour Association,* 27**,** 9-25.

Xia, G., Henry, P., Queiroz, F., Westland, S. & Yu, L. 2022. Colour–cognitive performance interaction in virtual reality (VR): a study of gender differences. *Journal of the International Colour Association,* 28**,** 1-6.

COLOUR PALETTE GENERATION FROM VIRTUAL FASHION IMAGES

Peihua Lai*, Qianqian Pan, Caroline Hemingray and Stephen Westland

[1]*Leeds Institute of Textiles and Colour, University of Leeds, U.K.*

*Corresponding author: Peihua Lai, Email: ss17pl@leeds.ac.uk

ABSTRACT

There is growing interest in virtual worlds (the metaverse) and one area that is already active in these virtual worlds is digital fashion. Some luxury fashion brands are using digital fashion as a way to promote their physical products; other companies seek to sell digital fashion *per se* in virtual worlds. In the gaming industry there is already an economy around buying digital fashion. Although colour forecasting and analysis is established in the real world, methods to explore colour trends in virtual worlds are in their infancy. One approach that could be useful would be to automatically extract colours of clothes from digital images and this work evaluates methods to do this. A total of 16 participants were each asked to select three colours from each of 5 images of avatars. Each image contained a single avatar and the participants were instructed to select colours that were representative of the clothes being worn by the avatar. Several computational methods were used to extract colours from the images. Specifically, various clustering approaches (such as k-means) were used and a generative AI model (pix2pix) was also evaluated. The pix2pix approach used a network that was trained on pairs of images (the input images were streetstyle fashion images; the output images were semantically segmented corresponding images). In semantic segmentation each pixel is assigned to one of several defined classes (such as clothes, skin or background); successful segmentation allows the background and skin pixels, for example, in the original image to be ignored. Palettes selected by human participants were used as ground-truth data and palettes generated by various machine models (e.g., k-means, pix2pix) were compared to these. Palettes were compared using a previously published palette-difference metric (ΔEp). The results showed that when averaged over all participants and all images the palettes generated by the pix2pix method were more similar (ΔEp = 7.7) to the ground-truth data than the palettes generated by k-means (ΔEp = 9.5) were. The experimental data show that automatic methods can generate colour palettes from clothes. Although this task is quite easy for humans, automated methods are required to enable thousands or hundreds of thousands of images to be processed in one day; that volume of analysis may be required if accurate colour trends or nowcasts are to be obtained. The methods described in this work could be used to build tools that would enable designers to process many images efficiently.

Keywords: colour palette generation, virtual fashion, image analysis

INTRODUCTION

Recently the realm of virtual fashion has been steadily capturing the interest of consumers, drawing the attention of the Generation Z group in particular. Distinguished from traditional fashion, virtual fashion breaks physical boundaries on real garments, and mainly focuses on virtual/digital products [1]. Originally conceived as representations (skins) for game characters within gaming platforms, virtual clothes have progressively expanded into non-gaming domains [2]. The context of this transformation includes social media filters and avatars in social platforms (e.g. Meta). Also, an increasing number of platforms are being established to facilitate the sale of virtual fashion apparels, such as The Fabricant and R-shape. The spending power and consumption habits of the young generation have entered a new era [2]. In the near future customers will work, play and socialise in immersive virtual worlds to meet their social satisfaction. Virtual representations of people, in the form of avatars, require virtual clothes.

Therefore, there is a huge market opportunity in the virtual fashion industry [3]. A big challenge in the development of virtual fashion clothes is the lack of fashion forecasting data and agencies.

Colour forecasting is well-established in the physical fashion industry [4]. Ideas of colour forecasting are linked to the design process, the marketing of on-trend products and products themselves. Similar to the real-world fashion market, the virtual fashion market also encompasses both design and retail. WGSN, one of the leading forecasting agencies, has explored the concept of virtual fashion and its connections to the metaverse in their trend reports, yet, do not specifically address pertinent platforms [5]. Limited researchers and companies are investigating the possible colour forecasting mechanism for the virtual fashion wardrobes industry. One of the challenges of using traditional colour forecasting methods to analyse virtual fashion images, is the irregular and diverse shape and colours of the virtual clothes. Digital clothes in virtual fashion allow more diverse colour usage and material designs. Specifically, in virtual fashion designs, the physical production is eliminated in a process of design-sell-make [2]. The shorter design chain for virtual fashion also puts pressure on designers and on the colour forecasting process itself. In other words, there is a demand for colour forecasting techniques that cater to the unique demands of the virtual fashion industry

Fashion image analysis is one of the methods to approach colour forecasting in the real fashion industry [6]. The question is whether we can use advanced techniques to emulate the colour forecasting process in the real world to the virtual fashion world. This paper explores the practicality of employing machine learning techniques to extract colour information from virtual fashion images. The avatar is one important context for virtual fashion [7]. An avatar can be customised into different characters including different face, hair, skin tone etc. Five avatars' images released from Meta were selected for a fine-grained analysis as the starting point for this project [7]. Two machine-learning methods were applied to extract colour palettes from the virtual fashion images. Human-generated colour palettes from the psychophysical experiment were used as the ground-truth data to compare the performance of these two machine learning models. Results show the possibility of using automatic methods to generate colour palettes from clothes in the virtual fashion industry. Despite being a pilot study in an explorative purpose, this research has the capacity to significantly enhance awareness within the virtual fashion field and unlock substantial market potentials.

METHODOLOGY

The rationale for this work is based on a prior study that used real fashion runway images [8]. In this study, two machine learning models were used to explore the possibility of extracting colour insights (useful colour palettes) from virtual fashion images. In machine learning research, a type of data known as 'ground truth' is routinely utilized to assess the effectiveness of an algorithm. A set of human-generated colour palettes was created for this purpose using a psychophysical experiment. The visual difference between model-generated colour palettes and human-generated colour palettes was quantified using the Palette Difference Metric (ΔEp) [9]. A statistical analysis of the difference within human-generated colour palettes, and for two different model-generated colour palettes was carried out.

Psychophysical Experiment

Sixteen fashion students with normal colour vision participated in the study. Participants were invited to the laboratory, where they each chose colours on the same computer and calibrated display. Participants were prompted to select three colours to represent the outfits (clothes) in each image. The RGB values of the three chosen colours were automatically recorded using MATLAB software. Each participant needed five minutes to complete the experiment. Figure 1 shows the five Avatar images used in this study.

Figure 1: The five Avatar images used in the study

Human-generated colour palettes for each image were stored as the 'ground truth' data. The colour difference among the palettes from each participant for each image was calculated and is called the 'inter-observer variation'. Note that the ΔEp for a model palette is calculated from each individual participant and averaged over all participants (and over all 5 images). Since there is variability between the colour palettes generated by each participant, it is not possible for a model palette to simultaneously match the palette for all of the participants. If the colour palette difference ΔEp between the palettes from a model and the human-generated palettes is similar in magnitude to the inter-observer variation, this means that the difference between the model palettes and the human palettes is similar to the difference between the palettes selected by different human participants.●

Model 1 – k-means clustering

The core of colour palette extraction in colour forecasting is the identification of pixels that are relevant to fashion. Even in a digital format, it is not challenging to identity pixels in traditional fashion images that are associated with clothing by human or advanced algorithms [10]. Nevertheless, in the realm of virtual fashion outfits, design patterns and colours can be more creative and diverse, as there is no need for physical manufacturing or even to be constrained by physics. The diverse feature of virtual fashion clothes increases the difficulty of colour extraction from images. In real colour forecasting, researchers have applied k-means clustering to generate colour palettes (containing the most frequent colours in the images) [8][11]. The standard k-means clustering has also been used for image segmentation in some other studies [12]. In this study, Model 1 is a standard application of the k-means clustering on the fashion images. The k-means clustering is implemented by using standard MATLAB function *kmeans* [13]. The input to the k-means algorithm is the image data (in this case an Nx3 matrix of RGB values where N is the number of pixels) and the number of clusters required (which refers to the number of required colours in the colour palette). For consistency, the number of the clusters was set to three in the whole study.

Model 2 – pix2pix network

In previous research, the effort to extract colours from real-world garments in the digital images has involved the integration of Generative Adversarial Networks (GANs) [14]. The pix2pix network used in Model 2 was pre-trained using 1600 fashion streetstyle images from the real world [6]. The network was trained using the MATLAB implementation called pix2pix image-to-image translation [15]. These advanced neural networks have proven to be instrumental in performing image-to-image transformations. The findings supported that using the pix2pix network into colour palettes extraction outperforms standard k-means clustering and some other machine learning algorithms [8]. Nevertheless, the previous study primarily focused on streetstyle and fashion runway images featuring real garments. The objective of Model 2 is to employ the pre-trained pix2pix network to test the effectiveness of this machine-learning pipeline when using virtual fashion images.

Model 2 contains two steps: (1) Input an original image to the pre-trained pix2pix network and generate as output a corresponding annotated image; (2) The k-means clustering is employed to extract colours directly from the original image, based on the information from the corresponding annotated image. In this case, only pixels were annotated as clothes pixels (yellow pixels from the output image) were used for k-means clustering in the step 2. Figure 2 illustrates the input image (left) and the output image (right) using the first step from Model 2.

Figure 2: Example performance for the trained pix2pix network showing the input virtual fashion image (left) and the output annotated image (right).

RESULT AND DISCUSSION

In total, 240 colour patches (5 images x 3 colours x 16 participants) were selected from the virtual fashion images. Figure 3 shows the colours chosen by all participants for one of the sample images respectively. Each row of colours corresponds to a set of three colours chosen by an individual. The task assigned to participants was made selections based on garment within the virtual fashion images. Figure 3 provides visual support for the observation that the colour selections mainly relate to the garments.

Figure 3: Colour selections for one of the sample images(left)and each row of colours on the right presents colours selected by one participant.

The inter-observer variation on the whole image-set was calculated using the palette difference metric ΔEp. The average difference between colour palettes generated each participant on each image was 7.2 CIEDE2000.

Figure 4 contains two virtual fashion images used in this study and the colour palettes generated by Model 1 and Model 2 for each image. For Model 1, k-means clustering, the palettes including both the background (white) and the skin tone. For the colour palettes generated by Model 2, as can be seen in Figure 4, visually most of the background colours and the skin tone are excluded. For the purpose of generating colour palettes for fashion images, colours of the garments are priority. It is crucial to find a strategy to separate the character and exclude skin tones in the fashion colour extraction. In addition to visual comparisons, quantitative comparison is also used to compare the colour palette difference among model-generated colour palettes.

Figure 4: Colour selections for one of the sample images(left)and each row of colours on the right presents colours selected by one participant.

Performance of different models can be compared quantitatively by using colour difference ΔEp value between the ground truth data and the model-generated data. In comparison to the Model 1 (ΔEp=9.5 CIEDE2000), colour palettes created using pix2pix network (Model 2) were more similar to human-generated colour palettes ((ΔEp=7.7 CIEDE2000). The ΔEp values were averaged across all colour palettes selected by each participant and all images.

A statistical analysis has been conducted to assess the mean difference among three groups of colour palettes: Model 1, Model 2 and humans are significantly different or not. The result shows that $F(2, 12) = 0.88$, $p=0.439 > .01$, which indicates that the colour palette difference among these groups are not significantly different. Hence, with this dataset, the performance of Model 2, visually, better than Model 1. Visually, the colour palettes generated by Model 2 are more similar to human-generated colour palettes and contains more fashion-related colour information. There are two potential factors. Firstly, insufficient sample size, as this constitutes a pilot study. The data size may lack the requisite support for further statistical analysis. Secondly, the pre-trained pix2pix network was trained on real-world fashion images; potential differences between virtual and real-world images may exist.

CONCLUSION

This study explores the generation of colour palettes for virtual fashion images using machine learning approaches. Model 2 contains a pre-trained pix2pix network to remove the background and skin tone colours for palette development, whereas Model 1 was a straightforward k-means clustering technique. In visual comparison, Model 2 performs better at creating colour palettes for virtual fashion, according to a fine-grain study of a smaller sample of virtual fashion images. Future work can be explore using more image data and advanced techniques in virtual fashion forecasting.

REFERENCES

1. Särmäkari, N. (2023). Digital 3D fashion designers: Cases of atacac and the fabricant. *Fashion Theory*, *27*(1), 85-114.
2. Belk, R., Humayun, M., & Brouard, M. (2022). Money, possessions, and ownership in the Metaverse: NFTs, cryptocurrencies, Web3 and Wild Markets. *Journal of Business Research*, *153*, 198-205.
3. Morgan Stanley. (2021) https://www.linkedin.com/pulse/redefining-value-fashion-retail-metaverse-martin-petkov (last access 25 August 2023)
4. DuBreuil, M., & Lu, S. (2020). Traditional vs. big-data fashion trend forecasting: an examination using WGSN and EDITED. *International Journal of Fashion Design, Technology and Education*, *13* (1), 68-77.
5. WGSN (2022*)*. https://www.wgsn.com/en/podcasts/exploring-cryptocurrencies-nfts-and-web3 (last accessed 25 August 2023).
6. Lai, P, Westland, S. and Booth, S. (2023). Pixel-based Object Recognition in Fashion Images to Generate Colour Palettes. International *Journal of Fashion Design, Technology and Education*, DOI: 10.1080/17543266.2023.2250820
7. Meta. (2022). https://about.fb.com/news/2022/06/introducing-the-meta-avatars-store/ (last accessed 25 August 2023).
8. Lai, P., & Westland, S. (2020). Machine learning for colour palette extraction from fashion runway images. *International Journal of Fashion Design, Technology and Education*, *13* (3), 334-340.
9. Yang, J., Chen, Y., Westland, S., & Xiao, K. (2020). Predicting visual similarity between colour palettes. *Color Research & Application*, *45* (3), 401-408.
10. Ma, Y., Yang, X., Liao, L., Cao, Y. & Chua, T.S. (2019). Who, where, and what to wear? extracting fashion knowledge from social media. In *Proceedings of the 27th ACM International Conference on Multimedia*, 257-265.
11. Huang, S. C. (2021). An efficient palette generation method for color image quantization. *Applied Sciences, 11* (3), 1043.
12. Pavan Kumar, I., Hara Gopal, V.P., Ramasubbareddy, S., Nalluri, S. & Govinda, K., (2020). Dominant color palette extraction by K-means clustering algorithm and reconstruction of image. *In Data Engineering and Communication Technology* (pp. 921-929). Springer, Singapore.
13. MATLAB. (2023). https://uk.mathworks.com/help/stats/kmeans.html?s_tid=doc_ta (last accessed 25 August 2023).
14. Lai, P. & Westland, S. (2022). Pixel-based colour image object detection in fashion, *Proceedings of the Mid-Term Meeting of the International Color Association,* Virtual Conference.
15. Pinkney, J. (2022). pix2pix. https://github.com/matlab-deep-learning/pix2pix (last accessed 25 August 2023).

PRODUCTION OF FUNCTIONAL INKS FROM NATURAL COLORANT ANTHOCYANIN FOR MEAT SPOILAGE INDICATION

Rattachai Siangyai, Pichayada Katemake, Intatch Hongrattanavichit*

Department of Imaging and Printing Technology, Faculty of Science, Chulalongkorn University, Pathumwan, Bangkok 10330 Thailand

*Corresponding author: Corresponding authors name, e-mail: intatch.h@chula.ac.th

Keywords: Anthocyanin, Nanocellulose, Functional Ink, Intelligent Packaging, pH-Indicator

Nowadays, the amount of waste caused by food spoilage in the world has increased considerably and tends to increase every single year. This is because the conventional packaging is unable to detect and indicate the qualities of the packaged goods. This issue affects the perception of consumers in terms of freshness, safety, and nutritional value. To developing of product qualities monitoring and assessment using intelligent packaging is one of the solutions that help to solve this problem by color identification on the packaging. In this research, the combination of food grade water-based binder, cellulose nanofibers which extracted from agricultural waste, and anthocyanin in various ratio for functional flexographic printing inks was prepared using mixture design method as a tool for appropriated content determination. The properties of functional ink and printed materials such as morphology, lightfastness, and mechanical properties in term of rub resistance were studied. The results found that when increased the cellulose nanofibers component, the homogeneous ink presented the smooth surface area of printed layer and higher UV resistance, resulting in the reducing of the color difference (ΔE^*_{ab}) by 38.21% when compared with no cellulose nanofibers ink. The combination of nanocellulose and binder (ratio 0.35:0.45) showed greater rub resistance value about 96.6 times when compared with the ink that has lower nanocellulose component. In addition, an increment of anthocyanin content in ink exhibited the greater apparent color transformation from red to purple in acidic to basic condition (pH 3-12) when observed with the human eyes. The obtained functional ink in this work was also tested with chicken meat to ensure that the printed material could be worked for use in commercial. Finally, the functional flexographic printing ink could be printed on paper and plastic substrates and further applied as an intelligent packaging for the varieties of fresh product packaging.

Keywords: Functional ink, Anthocyanin, Nanocellulose, Indicator, Intelligent packaging

STABILITY OF PIGMENTS AND BINDERS TO NARROW-BAND WAVELENGTH LEDS

Duantemdoung Dethsuphar[1], Pichayada Katemake[1]* and Stephen Westland[2]

[1]*Faculty of Science, Department of Imaging and Printing Technology, Chulalongkorn University, Thailand.*
[2] *School of Design, University of Leeds, United Kingdom.*

*Corresponding author: Pichayada Katemake, pichayada.k@chula.ac.th

ABSTRACT

Artworks can be vulnerable to various environmental factors, including air quality, temperature, humidity, and light. While the former three factors can be controlled to meet museum standards, the impact of light on artworks is inevitable. LED technology is widely preferred across industries due to its numerous advantages, such as energy efficiency, adjustable colour and intensity, and the absence of ultraviolet emissions. Consequently, it has become a preferred choice for illuminating museum artefacts. However, previous research has raised concerns about the safety of LED lamps for all types of pigments, as they can react differently to various wavelengths of light. This study aims to explore the LED spectrum while considering the specific requirements of museums to minimize pigment damage. To achieve this, we accelerated the process of blending historical pigments with two artist binders: acacia gum and linseed oil. Under controlled laboratory conditions, these mixtures were exposed to sixteen narrow-band LEDs within the 360–745 nm wavelength range. The primary objective was to assess the stability and lightfastness of the pigments over time. After 1000 hours of exposure, our empirical findings revealed that the choice of binder significantly influenced pigment degradation, particularly with regard to colour changes. When linseed oil was used as the binder, it resulted in more pronounced colour changes in the paint compared to acacia gum, except in the case of yellow pigments. Among the organic pigments, turmeric exhibited the most significant colour changes in both binders. On the other hand, certain inorganic pigments, like ultramarine blue, displayed considerable colour differentiation, especially when combined with linseed oil, although it remained lower than that observed in organic pigments. Interestingly, for most pigments, the highest level of discolouration occurred within the blue wavelength range (360–485 nm), attributable to its elevated energy levels. However, pigments immersed in linseed oil exhibited greater colour differentiation within the red wavelength range (610–745 nm). This research offers valuable insights into the impact of LED lighting on historical pigments in artworks, identifying the most sensitive pigments and the wavelength ranges that produce the highest degree of colour differentiation. Furthermore, the findings of this study lay the groundwork for future research on the effects of LED lighting on various materials and applications beyond the realm of museums.

Keywords: LED lighting, Museum lighting, Lighting design, Colour degradation, Ageing process

INTRODUCTION

The degradation process experienced by artworks is inevitable, and its impact becomes more pronounced over time. The possession of a comprehensive understanding regarding the materials used in artworks, including pigments, binders, and substrates, is imperative for conservators and museum technicians because the phenomenon of deterioration in artworks is not solely attributed to a single material but also encompasses the interactions between various constituent elements in an artefact. For this reason, acquiring knowledge is essential to ensure the appropriate conservation procedures.

The Indoor Environmental Quality (IEQ) indicates about the museum's environment that the potential damage to artworks is predominantly attributed to four factors: temperature, humidity, UV level, and lighting level [1]. Although the former three can be regulated within acceptable limits for museum settings, exposure to light is inevitable and can gradually deteriorate exhibited artworks. Nevertheless, various pigments exhibit sensitivity to distinct wavelength ranges of light, as exemplified by research conducted by Jo et al. [2] In their study, it was observed that LED lamps could also lead to the fading of Realgar. Similarly, other investigations, such as those undertaken by Monico et al. [3], delved into the degradation process of Lead Chromate in Van Gogh's artworks caused by UV-visible light. This study unveiled that exposure to blue light in the 335–525 nm range significantly degraded the chrome yellow pigment.

The radiative damage process displays varying severity across different colourants, binders, and light conditions. Consequently, this study aims to emphasise the investigation of historical pigments, encompassing both inorganic and organic variants, which were exposed to 16 different narrow-band wavelength ranges. The primary objectives include examining the pigment's response after exposure to light for specific durations and assessing the influence of different binders, namely acacia gum and linseed oil, on the overall degradation process.

METHODOLOGY

Colour samples

Initially, 18 organic and 59 inorganic pigments were mixed thoroughly with acacia gum and linseed oil, maintaining a 1:1 ratio for pigment-to-acacia gum and pigment-to-linseed oil. Mixing involved milling with a glass muller to achieve a homogeneous blend. Subsequently, the resulting sample solutions were uniformly applied to the substrate.

Acid-free paper was the substrate material to counteract undesirable yellowing during extended exposure. Ensuring a consistent thickness of the colour samples, the application was performed using TQC Sheen Cube Applicators and K control coater, maintaining a coating speed of 2 m/min and a thickness of 75 microns. Once thoroughly dried, the samples were cut into 1.5 x 1.5 cm dimensions and securely affixed onto acid-free paper. Each set of samples was then arranged within separate lightboxes to facilitate the subsequent exposure process.

Simulated deterioration process

The experiment used sixteen narrow-band LED light sources, each with distinct peak wavelengths in the visible spectrum range. These peak wavelengths were as follows: 367.6 nm, 385.8 nm, 394 nm, 404.6 nm, 454 nm, 469 nm, 471.8 nm, 478.2 nm, 523.3 nm, 523.3 nm, 598.8 nm, 599.1 nm, 628.1 nm, 637.6 nm, 662.8 nm, and 740.2 nm. Each LED light source was securely affixed to individual boxes measuring 50 x 50 x 60 cm. A set of LEDs comprised two 20W circuit boards. Figure 1 presents the summation of radiance and V(λ) regarding each light source.

To ensure controlled conditions, the experiment occurred in a room with a constant relative humidity of 50% and a temperature of 24 ± 1 degree Celsius. The samples were exposed to the LED lights throughout the study for 1000 hours.

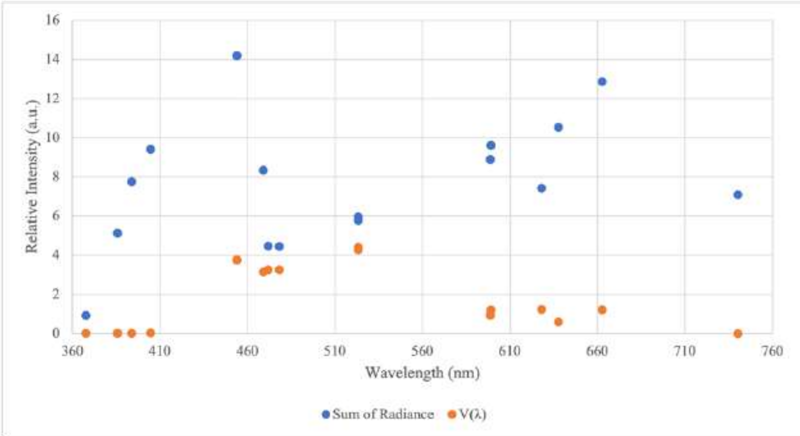

Figure 1. The summation of radiance and V(λ) of 16 narrow-band wavelengths

Colour difference analysis

The CIE 1976 colour differences (ΔE*) between 0 and 1000 hours of exposure using the were calculated. Additionally, individual values for lightness (ΔL*), colour in the green-red axis (Δa*), and colour in the blue-yellow axis (Δb*) were observed for all pigments.

The selection of colour samples for degradation assessment was based on the midrange value calculated for all samples at each peak wavelength. The outcome of this process resulted in the categorisation of colour samples into five distinct groups, white (chalk from Champagne and zinc white), blue (HAN-Blue fine, blue bice, ultramarine blue dark, ultramarine blue light, cobalt blue medium, and copper blue), purple (ultramarine violet medium, Ultramarine red 19 C, ultramarine violet 13 C, and cobalt violet deep), yellow (turmeric), and red (lac dye and natural cinnabar Monte Amiata). It is essential to emphasise that the midrange values for organic and inorganic samples exhibit variability, indicating differential characteristics between the two groups.

RESULT AND DISCUSSION

White pigments

In Chalk from Champagne, when subjected to a combination with linseed oil, discernible disparities in colour were observed, surpassing those resulting from a combination with acacia gum. The specimens treated with linseed oil exhibited the most pronounced colour variations within the spectral range of 598.8–740.2 nm, exceeding a magnitude of 10 in colour difference. Analysing the alterations of the CIEL*a*b* values, it is apparent that the specimens exhibited a tendency towards diminished lightness, accompanied by an increase in yellow and red tonalities. Zinc white's colour difference gradually decreases with the increasing wavelength, with the maximum colour difference at 7. The ΔL* and Δa* remained constant while Δb* changes corresponding to colour difference, as indicated in Figure 2.

The alteration in both white pigments dispersed in linseed oil was significant due to the degradation of the linseed oil. In contrast, the white pigment combined with acacia gum exhibited no notable changes compared to the controlled sample, except for the instance exposed to 394 nm.

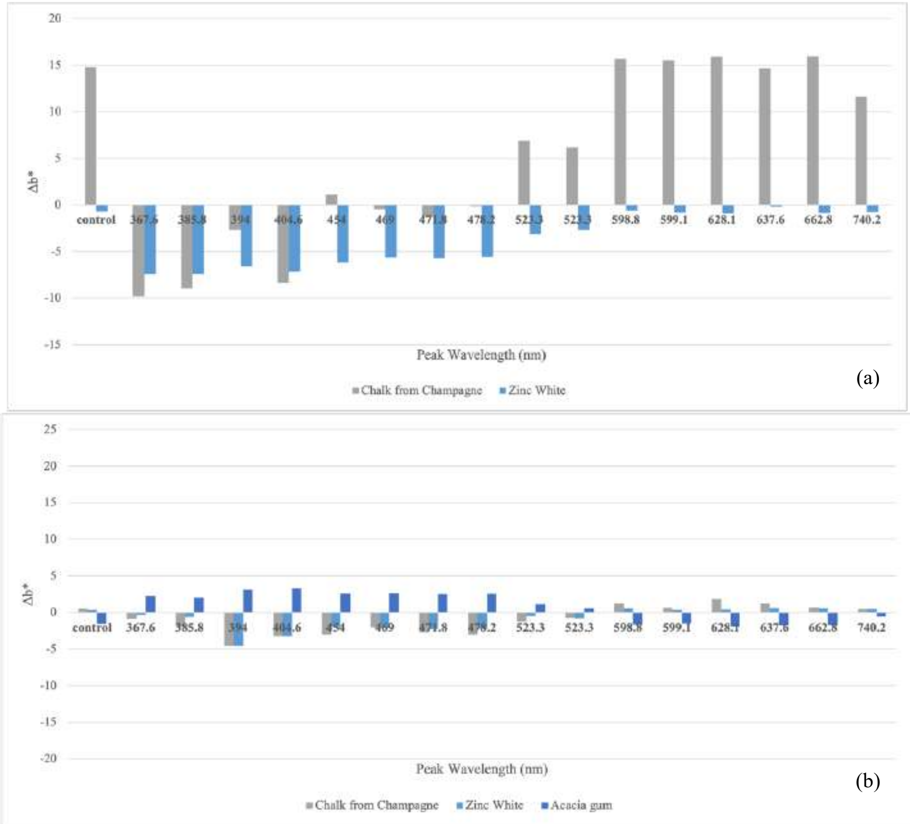

Figure 2. Δb* of (a) white pigments in linseed oil (b) white pigments in acacia gum under control condition and after 1000 hours of exposure to 16 narrow-band LED wavelengths.

Blue pigments

As depicted in Figure 3, the variation in colour for the blue samples dispersed in linseed oil exhibited its greatest extent within the wavelength range corresponding to yellow and red light. The colour differences were observed in blue and green wavelengths, respectively. Interestingly, upon comparison with the controlled sample stored in a dark room, the colour difference was notably significant only in the case of the linseed oil applied directly to the substrate. This observation closely resembled the samples exposed to the blue light, suggesting that the transpired alterations are likely attributed to changes originating from the binder, in conjunction with the pigment. Supported by the study conducted by Lazzari and Chiantore [4], it can be affirmed that the photo-oxidative degradation of linseed oil could be considered as the continuation of the hardening process. The degradation gradually progresses towards a yellow tint in the film. The potential structural indications for this yellowing involve diketones and the metal salts derived from their enol form, quinoid arrangements, or the conjugated double bonds within the chromophoric groups. The overall colour difference trends were aligned with the cumulative radiance incident upon the samples.

On the other hand, blue pigments combined with acacia gum exhibit minor changes in colour after being exposed for 1000 hours, except for blue bice, which displays a significant colour shift within the blue wavelength range. A closer examination of the CIEL*a*b* values revealed that the predominant changes come from the shifts in Δa* and Δb* components. Within the 367.6–404.6 nm range, negative Δa* and positive Δb* values were observed, indicating a transition towards increased green and yellow tones in the samples.

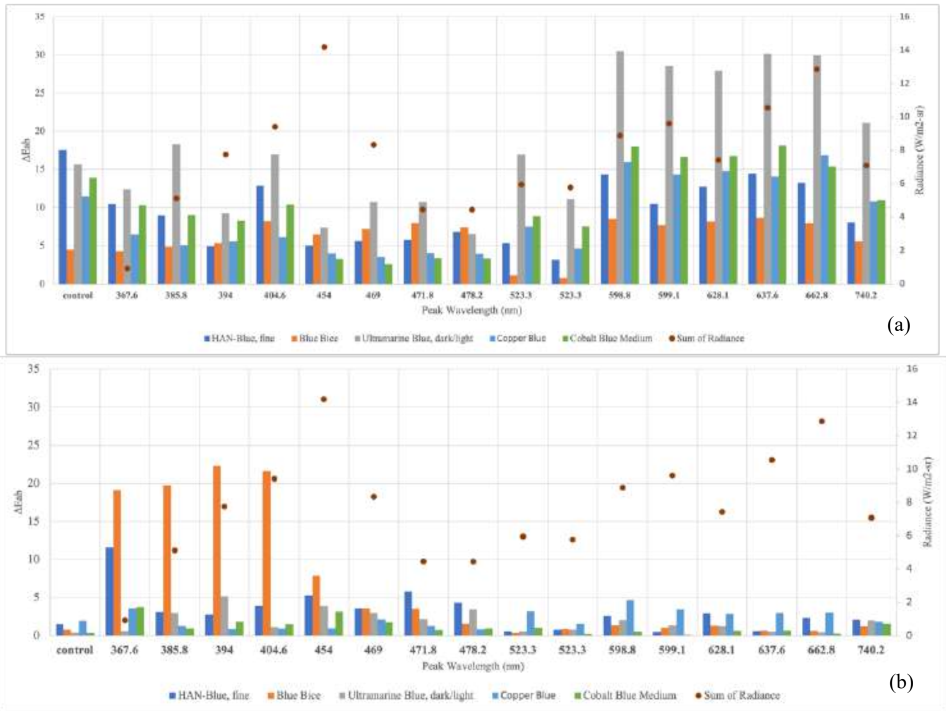

Figure 3. Colour difference of (a) blue pigments in linseed oil (b) blue pigments in acacia gum under control condition and after 1000 hours of exposure to 16 narrow-band LED wavelengths with total radiance.

Purple pigments

The alterations in purple pigments parallel the trends observed in blue pigments, primarily due to the comparable hue shared between the two, as depicted in Figure 4. Nevertheless, the purple pigments exhibit a more pronounced reddish hue. This particular hue characteristic reduces energy absorption within the red wavelength range, leading to less colour changes observed in blue pigments.

Yellow pigment

Turmeric, scientifically known as Curcuma longa L., contains the polyphenol curcumin (1,7-bis(4-hydroxy-3-methoxyphenyl)-1,6-heptadiene-3,5-dione) as its primary active compound and serves as an organic pigment. It demonstrates a lower stability compared to inorganic pigments. The results presented in Figure 5 highlight a clear reverse relationship between colour variance and wavelength when turmeric is placed in linseed oil. In contrast, when immersed in acacia gum and exposed to blue wavelengths, the colour variance gradually increases until peaking at 454 nm. Subsequently, it decreases as the wavelength extends further.

The greater colour variance in the blue wavelength range in linseed oil may arise from the alkaline nature of linseed oil (pH = 7.5), in contrast to acacia gum (pH ranging from 4.81 to 6.41 [5]), leading to reduced stability of curcumin [6]. Curcumin has been observed to undergo significant degradation in the presence of light. The primary structural changes that curcumin undergoes due to light exposure including demethoxylation and isomerisation of the keto-enol to the diketo form, and the generation of minor byproducts such as methanol or acetate [7].

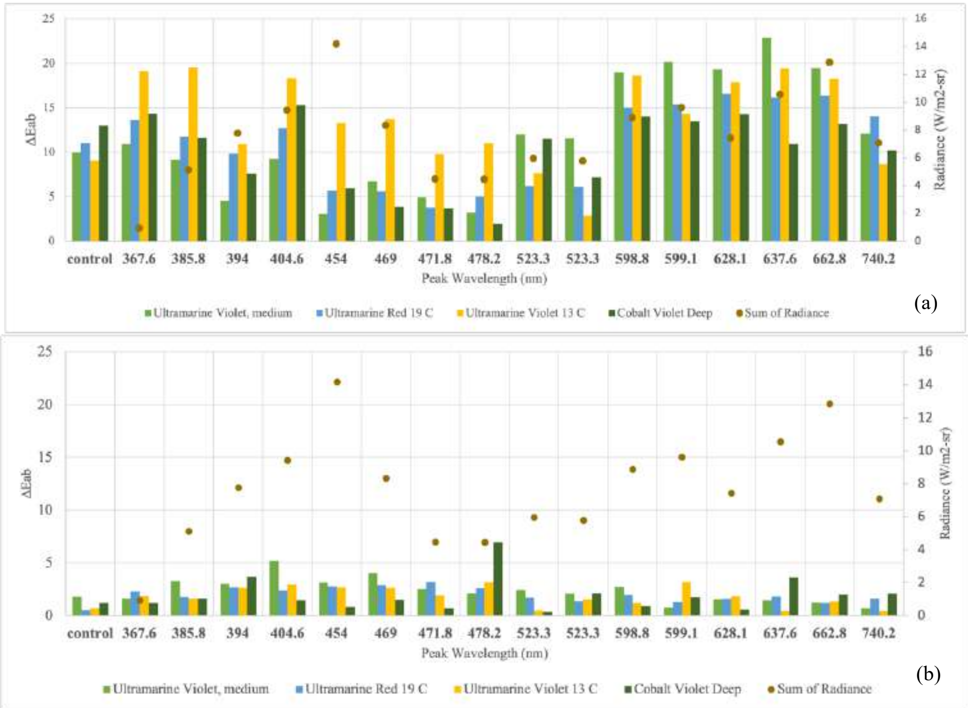

Figure 4. Colour difference of (a) purple pigments in linseed oil (b) purple pigments in acacia gum under control conditions and after 1000 hours of exposure to 16 narrow-band LED wavelengths with total radiance.

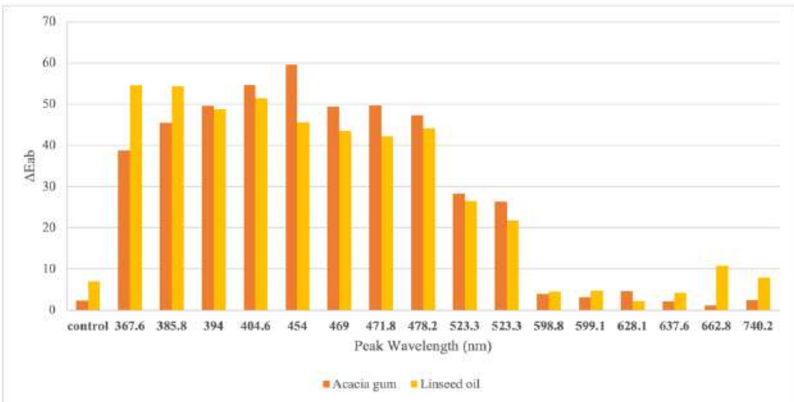

Figure 5. Colour difference of Turmeric in acacia gum and linseed oil under control conditions and after 1000 hours of exposure to 16 narrow-band LED wavelengths.

Red pigments

Lac dye, acknowledged as laccaic acid, represents an organic lake pigment obtained through the extraction process involving Coccus Lacta. The alteration in pigment appearance upon immersion with acacia gum is deemed insignificant. In contrast, the combination of lac dye with linseed oil showcases a substantial shift in colour across all wavelengths, distinguishing it markedly from the controlled sample. Notably, only at the wavelengths of 469 and 471.8 nm were the colour differences observed to be less than 10, as depicted in Figure 6. Considering all factors, there is an overall trend in progressive darkening, accompanied by a reduction in both redness and yellowness.

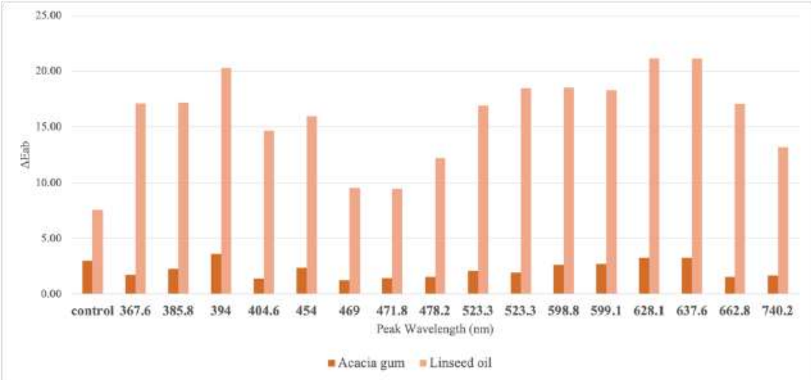

Figure 6. Colour difference of lac dye pigment in acacia gum and linseed oil under control conditions and after 1000 hours of exposure to 16 narrow-band LED wavelengths.

Cinnabar (HgS) is a prominent red mineral pigment that has been extensively used since the Roman Empire. Instances of artwork incorporating cinnabar have been documented to experience an irreversible darkening of their surfaces when exposed to sunlight and air [5]. Research findings indicate that this darkening process is directly proportional to the wavelength, meaning that light energy within the blue spectrum inflicts the most significant harm on cinnabar. Following this, green and red light also contribute to colour alteration, as indicated in Figure 7, when the pigment is immersed in both acacia gum and linseed oil mediums.

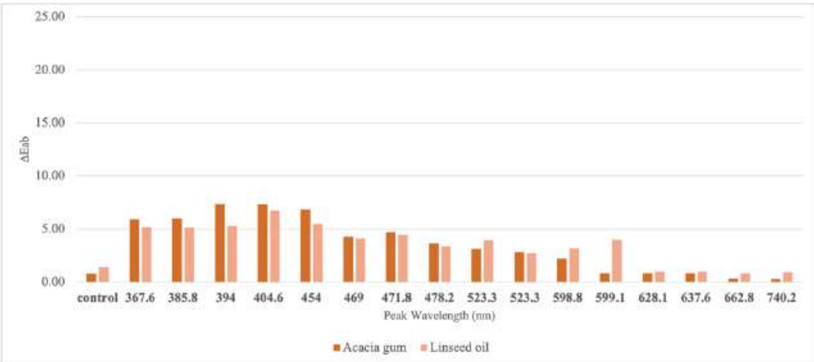

Figure 7. Colour difference of Natural Cinnabar Monte Amiata after 1000 hours of exposure to 16 narrow-band LED wavelengths.

Binders

As shown in Figure 8, focusing on the binder's outcomes, notable distinctions arise between linseed oil and acacia gum. In the analysis, linseed oil demonstrates substantial alterations, particularly evident when contrasted with acacia gum. The visual representation illustrates a noteworthy decrease in lightness for the control sample of linseed oil, aligning closely with samples exposed to wavelengths ranging from yellow to red. In addition to lightness, the db* values for linseed oil reveal a shift towards a yellow tone when exposed to yellow to red light. This change is attributed to photo-oxidative degradation, which elicits a distinct reaction compared to other wavelengths.

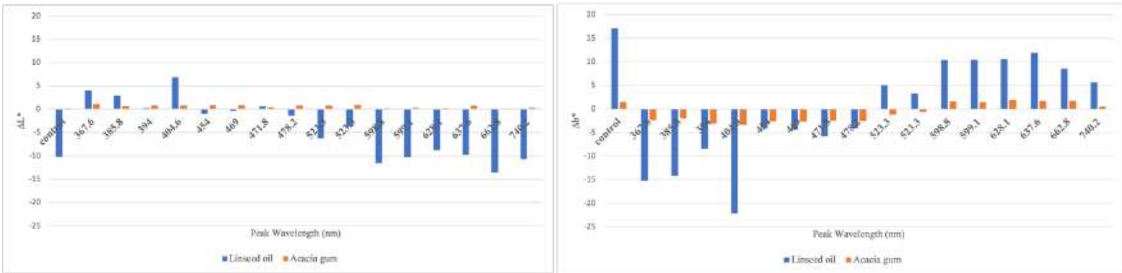

Figure 8. ΔL* (left) Δb* (right) of linseed oil and acacia gum

CONCLUSION

This study investigated the stability of pigments and binders when subjected to 16 specific narrow-band wavelengths. The research findings illuminate that the overarching degradation originates from a combination of factors, encompassing the individual behaviour of the pigment and binder and their interplay. Notably, the binder significantly drives colour alterations within the paint medium.

Significantly, pigments dispersed in linseed oil exhibited a more pronounced degree of colour alteration than those combined with acacia gum. This divergence can be attributed to the progressive degradation of linseed oil, resulting in the gradual emergence of a yellowish tint within the painted surface.

The investigation identified that the primary catalyst for the most substantial degradation is the energy inherent in the wavelengths. Consequently, the extent of pigment degradation hinges upon each colour's distinctive absorption and reflection characteristics, in conjunction with the level of radiance exposure experienced by the samples. Consequently, the sequence of degradation severity aligns as follows: the blue wavelength induces the most prominent deterioration, followed successively by the red and green wavelengths.

ACKNOWLEDGEMENT

This research project is supported by the Second Century Fund (C2F), Chulalongkorn University. The Imaging and Nuclear Techniques for Restoration of Cultural Heritages group, the Special Task Force for Activating Research (STAR) Chulalongkorn University Centenary Academic Development Project is acknowledged.

REFERENCES

1. Sharif-Askari, H. and B. Abu-Hijleh, *Review of museums' indoor environment conditions studies and guidelines and their impact on the museums' artifacts and energy consumption.* Building and Environment, 2018. **143**: p. 186-195.
2. Jo, S., et al., *LED illumination-induced fading of traditional Korean pigments.* Journal of Cultural Heritage, 2019. **37**: p. 129-136.
3. Monico, L., et al., *Degradation process of lead chromate in paintings by Vincent van Gogh studied by means of spectromicroscopic methods. 4. Artificial aging of model samples of co-precipitates of lead chromate and lead sulfate.* Analytical chemistry, 2013. **85**(2): p. 860-867.
4. Lazzari, M. and O. Chiantore, *Drying and oxidative degradation of linseed oil.* Polymer degradation and stability, 1999. **65**(2): p. 303-313.
5. Yaumi, A.L., et al., *Determination of physiochemical properties of Gum Arabic as a suitable binder in emulsion house paint.* International journal of Environment, 2016. **5**(1): p. 67-78.
6. Kharat, M., et al., *Physical and chemical stability of curcumin in aqueous solutions and emulsions: Impact of pH, temperature, and molecular environment.* Journal of agricultural and food chemistry, 2017. **65**(8): p. 1525-1532.
7. del Castillo, M.L.R., et al., *Stabilization of curcumin against photodegradation by encapsulation in gamma-cyclodextrin: A study based on chromatographic and spectroscopic (Raman and UV–visible) data.* Vibrational Spectroscopy, 2015. **81**: p. 106-111.

CORAL REEFS IN UNCERTAIN SEAS

J. E. Ingoldsby, ASLA
American Society of Landscape Architects
Natural and Cultural Landscapes
Westport, Massachusetts, U.S.A.

ABSTRACT

If we were to apply the concepts of inflow, outflow and feedback to natural systems, we would see the old adage, "For every action, there is a reaction" illustrated with clarity. A system in equilibrium that displays the full range of trophic biodiversity within a coral reef for example, thrives within a narrow set of conditions and relies on light, temperature, sedimentation, salinity, and pH. Within Nature, all species perform their function within their niches of this trophic cascade. When the cascade is broken, you have a reaction or adaptation, which we call feedback. So, if one or a series of requirements for the health of the system are impacted in a coral reef, for example the feedback loop can lead to coral bleaching and what is called regime shift, where the biodiverse reef slowly dies and is replaced with an algae/urchin stage to sea grass. These extremes represent a warmer, acidic sea.

INTRODUCTION

My work is an extension of a *Synergy-Ocean Stories* collaboration of artists chosen to translate marine research with scientists from the Woods Hole Oceanographic Institution and Oceans at MIT Joint Program, with curatorial assistance from Brown University. In my case, I had the good fortune to work with Dr. Katie Shamberger and Hannah Barkley, Alice Albert, Emily Moberg, and Whitney Bernstein of the WHOI and MIT, who provided insights, visual files, and published papers for review and assimilation on the resilience of the Rock Reef off of the Republic of Palau and global coral reefs. My role as a United Nations Artist for the Oceans and an advocate for the preservation and protection of marine ecosystems and biodiversity is to make the science accessible to the general public in public forums, through publication, and through site specific art installations. My photographically collaged digital panels and soundscapes were exhibited within *Ocean Stories* at the Rotch Library MIT, the Museum of Science-Boston, the New Bedford Art Museum, and were donated to the Sea Lab to inspire future generations of scientists.

Figure 1. *Biodiverse coral reef in equilibrium* Landscape Mosaics

The concept of Equilibrium is illustrated by the healthy Kingman coral reef within the Indo-Pacific Line Islands. Kingman reef depicts a kaleidoscopic, biodiverse reef with schools of fish, sharks, and sea turtles. The water is crystal clear. A healthy reef can eventually recover from natural stressors as typhoons and El Nino events.

The reefs degrade when natural events are coupled with anthropogenic impacts and climate change effects. Degradation of Fanning Island Reef, Kiritimati and Palmyra Islands from anthropogenic impacts is depicted as a compromised reef in early stages of disease, and bleaching.

Figure 2. *Tropical Coral Reef Degradation* Landscape Mosaics

Transformation at Kiritimati, Christmas Island occurs with the expulsion of temperature sensitive symbiotic coral Zooxanthellae and coral bleaching. Regime shift transforms the reef to an altered state of algae with sea urchins and bare stone. The biodiverse reef is dying. The water is murky, warm, and acidic. The sea floor is littered with trash and waste. There are no fish.

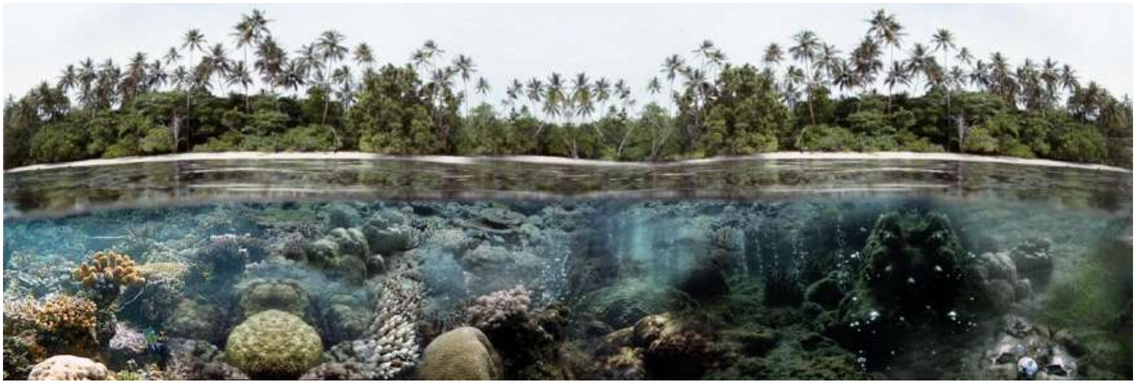

Figure 3. *Tropical Coral Reef Acidification* Landscape Mosaics

Coral reefs are resilient. Centuries of adaptation to acidic water and warm temperatures can be seen at Papua, New Guinea's volcanic vents, where a monoculture of coral exists with algae, until conditions worsen and the coral corrodes. Then the reef is replaced with temperature tolerant sea grass. This may be a glimpse into the future of our oceans.

Figure 4. *Tropical Coral Reef Resilience* Landscape Mosaics

Coral reefs are adaptive. Within a centuries old reef unique in all of the world's oceans, there is a reef displaying remarkable biodiversity within acidic and warm water at Rock Reef, Palau, Micronesia. This Rosetta Stone of genetic biodiversity is threatened with pollution and overuse and needs immediate international protection.

METHODOLOGY

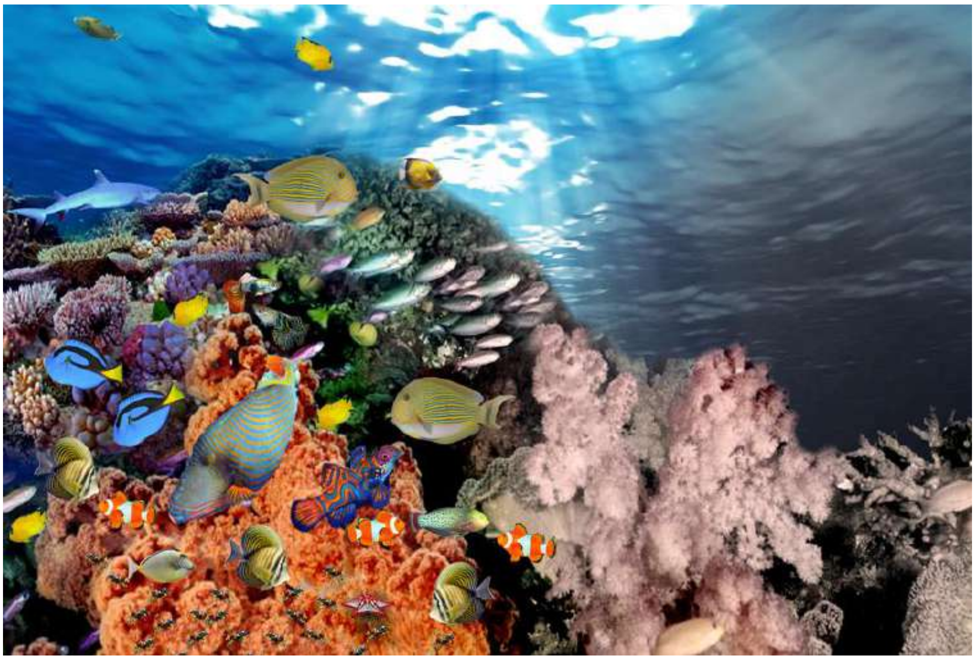

Figure 5. *Tropical Coral Reef Regime Shift* Landscape Mosaics

Regime Shift

If this radical shift in the life cycle of the coral reef is outlined, it might read as follows:

Tropical Coral Reef: Parameters for Equilibrium

Location: Kingman Coral Reef, Line Islands, Indo-Pacific, Great Barrier Reef, Australia
Soundscape: Rose Atoll, American Samoa

Light:
Light levels are critical for coral to maintain their symbiotic relationship with the photosynthetic zooxanthellae algae, which give coral their colour. With light penetration corals can survive to a depth of 150 feet (48 m).

Sedimentation:
Coral reefs require water clarity to promote photosynthesis of their symbiotic algae and an unsilted coral surface to feed and respire.

Seawater Temperature:
Optimal coral growth occurs between 73-77°F (23-25°C) Coral species can tolerate temperatures between 61-95°F (16-35°C).

Salinity:
Corals can tolerate a narrow range of salinities from 30 to 40 parts per thousand (ppt).

pH:
Coral reefs and the other ecosystems which depend on them require that atmospheric carbon dioxide remain below 350 parts per million (ppm). Pristine seawater has a pH reading of 8 to 8.3 of hydrogen ions present. The coral reefs as we know them are dependent upon a stable pH level within the oceans. Calcification or the ability of an animal to build a calcium carbonate structure or a shell depends on the saturation state of the surrounding waters.

Biodiversity:
Coral reefs are one of the most biodiverse ecosystems on Earth. All species play a part in regulating the health of the reef, from predatory sharks to herbivore fish, to scavenging crabs, and filtering shellfish.

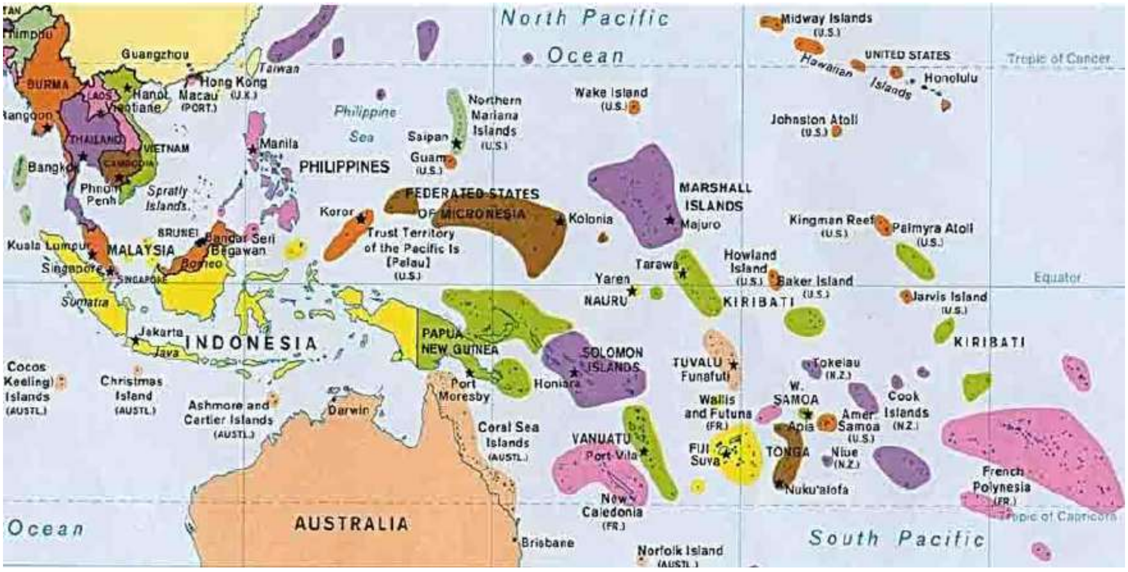

Figure 6. *Biodiversity in the Indo-Pacific Region* Indo-Pacific Conservation Alliance

Tropical Coral Reef: Parameters for Degradation

The reefs degrade when natural events are coupled with anthropogenic impacts and climate change effects. Degradation of Fanning Island Reef, Kiritimati and Palmyra Islands from anthropogenic impacts is depicted as a compromised reef in early stages of disease, and bleaching.

Location: Fanning Island Reef, Kiritimati Island, and Palmyra Island
Soundscape: Alega Bay, American Samoa Islands

Tropical Coral Reef: Parameters for Transformation

Transformation at Kiritimati, Christmas Island occurs with the expulsion of temperature sensitive symbiotic coral Zooxanthellae and coral bleaching. Regime change transforms the reef to an altered state of algae with sea urchins and bare stone. The biodiverse reef is dying. The water is murky, warm, and acidic. The sea floor is littered with trash and waste. There are no fish.

Location: Kiritimati, Christmas Island
Soundscape: Pokai Bay, O'ahu, Hawaii

Inputs:

Light:
Sedimentation- the quality of light can be affected by turbidity
CO2- acidification of the water promotes algae growth, which shades the coral.

Sedimentation:
Input: Population growth and urban development cause erosion, pollution, sewerage runoff into the sea.
Feedback Loop: The input of sedimentation and pollution creates turbidity and explosive algae growth, which inhibits coral growth.

Seawater Temperature:
Input: Greenhouse gas emission increase
Feedback Loop: Global warming, rising seawater temperatures cause coral bleaching, death and to regime change to more tolerant species as algae and sea grass.

Salinity:
Input: Greenhouse gas increase
Feedback loop: Glacier melting, increased storm events, change of salinity in oceans shall affect coral reefs and related marine species.

PH:
Input: Atmospheric CO2 and greenhouse gas emissions
Feedback Loop: Tropical coral growth rate or calcification decreases as acidity increases, causing a lower pH reading. For every 0.1 decrease in pH there is an approximate 8% decrease in calcification. (Fernand and Brewer (2007) Significance of Changing CO2 Levels)
Dr. Ken Caldeira states, "A 20% increase above current carbon dioxide levels, which could occur within the next two decades, could significantly reduce the ability of corals to build their skeletons and some could become functionally extinct within this timeframe."
Ocean acidification will have a profound impact on humans including economic loss, coastal protection, tourism impacts and fisheries.

Biodiversity:
Input: Over-fishing, tourism, aquarium trade
Feedback Loop: Over fishing has altered the ecological dynamics of marine communities allowing some species to dominate the reefs. For example, shark fining causes an explosion in herbivore and coral eating fish, which damage the reef and upset the balance of nature. Netting the herbivores allows for an algae explosion on the reef, smothering the coral. Fishing practices as dynamite and cyanide used to collect aquarium and souvenir coral and shells also kill the reef and attendant species. Ecotourism with scuba divers touching the corals and dragging anchors damage and kill the living reef.

Tropical Coral Reefs: Parameters for Resilience
Coral reefs are resilient. Centuries of adaptation to acidic water and warm temperatures can be seen at Papua, New Guinea's volcanic vents, where a monoculture of coral exists with algae, until conditions worsen and the coral corrodes. Then the reef is replaced with temperature tolerant sea grass. This may be a glimpse into the future of our oceans.
Location: Normandy and Dobu Islands volcanic seeps, D'Entrecasteau Island group, Milne Bay Province, Papua New Guinea

Tropical Coral Reefs: Parameters for Adaptation
Coral reefs are adaptive. Within a reef unique in all of the world's oceans, there is a reef displaying remarkable biodiversity within acidic and warm water at Rock Reef, Palau, Micronesia. This Rosetta Stone of genetic biodiversity is threatened with pollution and overuse and needs immediate international protection.
Location: Rock Reef, Palau, Micronesia

Tropical Coral Reefs: Policy Recommendations
Oceana, Protecting the World's Oceans has summarized the recommendations of scientists, the United Nations, and NGOs as follows to mitigate the effects of climate change on our oceans:

Adopt a policy of stabilizing atmospheric carbon dioxide at 350 ppm.
Pursue Zero net carbon emissions within decades

Promote energy efficient and low carbon fuels.
Practice energy conservation, develop efficient cleaner fuels, and promote efficient mass transit

Shift to alternative energy sources.
Eliminate subsidies to fossil fuel industries; prohibit burning coal in favor of renewable energy, stop extractions of oil, gas and coal from sensitive locations as the Arctic.

Regulate carbon releases.
Internalize emissions costs. Regulate shipping and aircraft.

Preserve natural resilience.
Protect reefs, which have shown millennial adaptation to volcanic vent warmth
and acidity, as bio-reserves to preserve the genetics for the future.

Regulate overfishing and pollution. Address climate change.

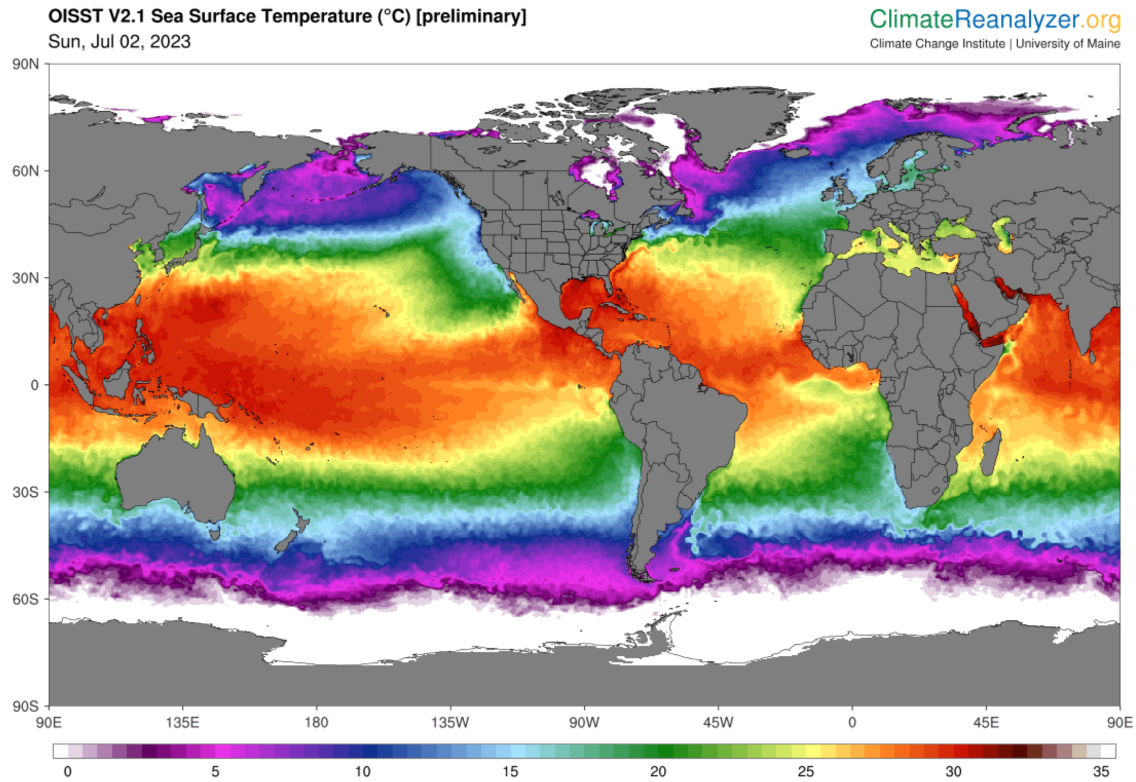

Widespread marine heatwaves (MHW) are currently found in the eastern equatorial Pacific, the Northeast Pacific, the Northwest Pacific and the Sea of Japan, the tropical North Atlantic, the Caribbean Sea, the Gulf of Mexico, the Northeast Atlantic from northern Africa to Norway, the Southwest Pacific near New Zealand, and the Southern Indian Ocean, and all sectors (Indian, Pacific, Atlantic) of the Southern Ocean. Marine Heatwaves / NOAA Physical Sciences Laboratory, July 2023

CONCLUSION

Changes in ocean water temperature have widespread implications for marine ecosystems functioning in the face of rapid global change. Many of the coral reefs cited within this paper have developed resilience to temperature, acidification, and sedimentation over thousands of years within favorable locations. The ability of tropical coral reefs within the world's oceans to develop resilience through adaptation and mutation in human time is questionable. Colonization of the world's coral reefs by adapting coral species and their endosymbiotic Zooxanthellae within human time seems improbable. The world's tropical coral reefs may become a monoculture of the most tolerant species in the near term without major policy and management shifts. The pristine coral reefs of the past may be lost to an alternate state of algal dominated reefs because of development pressures, overfishing, pollution, climate change, and lack of international consensus on a plan of action.

ACKNOWLEDGEMENTS

In my collaboration, with marine scientists at Woods Hole Oceanographic and MIT, I have vicariously traveled to the most remote islands in the Indo-Pacific to retell a Malthusian story of the coral life cycle in equilibrium, degradation, transformation, acidification, and adaptive resilience over millennial time. Special thanks to Dr. Katie Shamberger and Hannah Barkley, Thanks to Kathrina Fabricius and Laetitia Plaisance of the Australian Institute of Marine Science and to Kevin D. E. Stokesbury, Ph.D. at SMAST, UMASS-Dartmouth for his mentoring to shape the manuscript from a narrative to a research paper.

Session 3

Doi Wawee
28 November 2023

WEB USERS' ATTITUDE TOWARDS THE SIZE AND POSITION OF SIDEBAR ADS ON WEBSITES

Natchaphak Meeusah[1] Uravis Tangkijviwat[2] and Kamonthip Torsabsinchai[3]*

[1,3]*Multimedia Technology, Faculty of Mass Communication Technology,*
[2]*Color Research Center, Faculty of Mass Communication Technology,*
Rajamangala University of Technology Thanyaburi, Thailand

*Corresponding author: Kamonthip Torsabsinchai, kamonthip_t@rmutt.ac.th

ABSTRACT

In today's world, advertising has transformed the way goods and services are sold in the global markets. Advertising encourages us to purchase products and gives customers an information. There are a variety of pop-up advertising for instance lightbox, floating bar, full screen, and so on. Sidebar pop-up advertising is familiar to users, but designers should carefully consider a positioning and timing of advertising. This study, hence, aims to investigate an influence of the size of the sidebar pop-up advertising on website and to study how the position of a website's sidebar pop-up advertising influences a consumers' perspective. In the experiment, a combination of three different sizes and five positions of sidebar pop-up advertising were investigated as stimuli. Fifteen subjects with aging between 18 to 30 who have an e-commerce experience were asked for evaluating their perspective on different sidebar pop-up advertisings. The stimulus was presented on a EIZO monitor were observed under 500 lx. illumination. Subjects were asked to rate their opinions on 15 random sidebar pop-up advertisings and then answered the questionnaire with the topics of distracting, disturbing, forcing, interfering, intrusive, invasive, obtrusive, positivity, desirability and good feeling. A result showed that a pop-up advertising that was small size and located at top right position gave a high score of subject attitude. A small size or top right position of pop-up advertising was preferable. This result was a practical tool for supporting web designer to create website advertisement.

Keywords: sidebar pop-up, web advertising, website design, web users' attitude

INTRODUCTION

An advertising is an important tool for a marketing strategy that helps consumers acquire a deeper understanding of products and services, which will inevitably increase revenue. Therefore, marketers concentrate on creating online advertisements that entice users to access information and provide a positive experience. However, advertising is also intrusive and disturbing to users (1). Pop-up advertising is a potential marketing communication tool for online platforms that display information on a computer screen or an electronic device screen. Most of pervious study (2-4) stated that pop-up advertising might interrupted users when their concentrated at an information on website. Even though there are a variety of pop-up advertisings, lightbox, floating bar, full screen, and sidebar advertisings are familiar to users as a pop-up window (5). A lightbox advertising is a common format of pop-up advertising, but many previous study showed that many negative perspectives occurred. Sidebar pop-up advertising, hence, appear the most natural due to their appropriate positioning and cadence. They are displayed when users already have a good grasp of the content and are not as annoying as input pop-ups (6). There is still a lack of research on various digital advertising formats displayed on websites. Especially sidebar pop-up advertisings have been adjusted to be more natural. This study investigates attitudes regarding a display of sidebar pop-up advertising across a difference of pop-up advertising sizes and positions.

METHODOLOGY

1. PARTICIPANTS

Fifteen Japanese students from Chiba University selected as purposive sampling participated in the experiment. Participant age is between 18 to 30. All of participants have an experience to e-commerce websites and understand how pop-up advertising function.

2. EXPERIMENTAL DESIGN

This research is pre-experiment design in one-shot case study. Three sizes of pop-up advertising, consisting of 340 x 200, 375 x 250, and 400 x 300 pixels and five positions of pop-up advertising, consisting of top right, middle right, bottom right, bottom left, and middle right were assigned as stimuli. All of stimuli were presented on a same background images simulated a website design as shown in figure 1.

Each participant was asked to rate his/her attitude in terms of distracting, disturbing, forced, interfering, intrusive, invasive, obtrusive, positivity, desirability, good feeling on giving stimuli. The attitude scale was a seven-point Likert scale ranging from "strongly disagree" to "strongly agree" (7). No time limitation of the assignment.

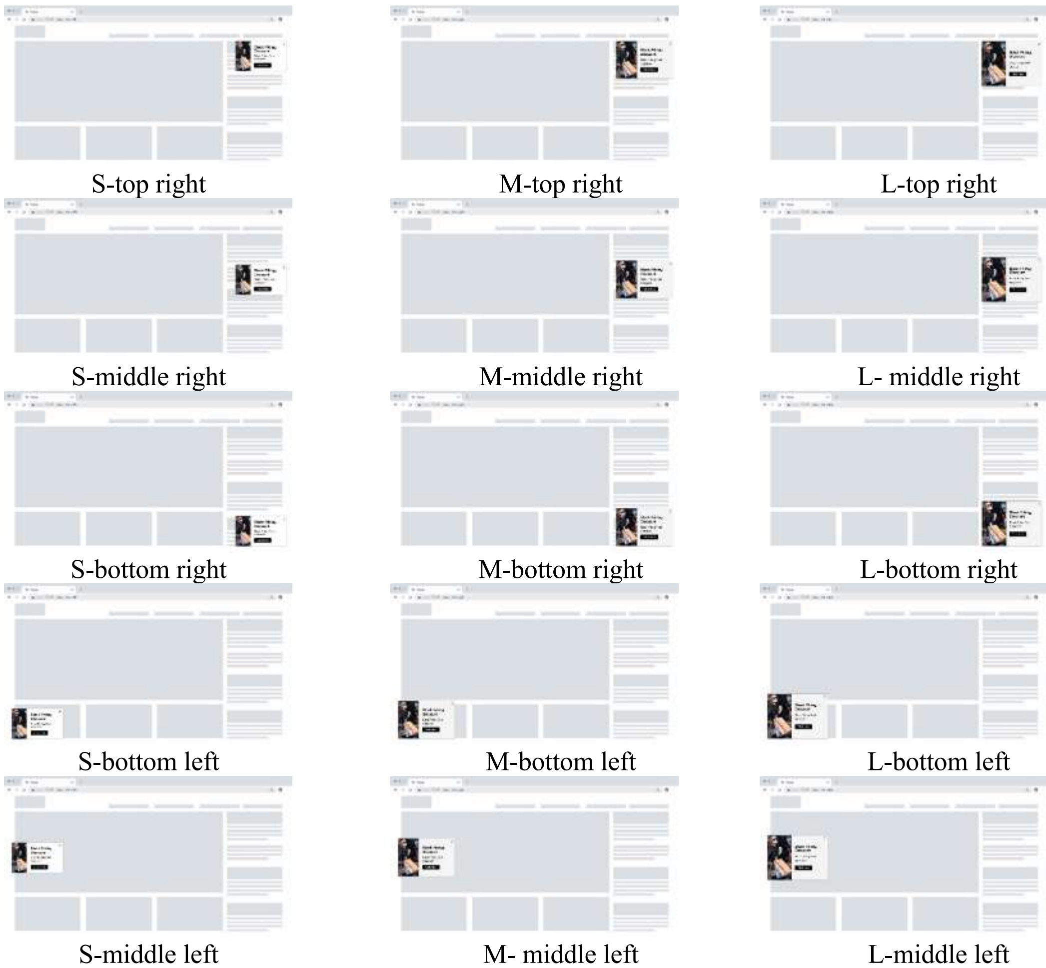

Figure 1. 15 stimuli of pop-up advertising in 3 different sizes and 5 positions

3. PROCEDULE

Before the experiment starts, each participant was asked to explore their previous experience in e-commerce websites and their understanding of pop-up advertising and then he/she was described in the research objectives, evaluation scale, and ranking criteria. The experimental procedure involves bringing one subject at a time to a laboratory with a room illumination of 500lx to view a 27 inch EIZO display. Fifteen pop-up advertising stimuli were randomly displayed. Each participant evaluated his/her attitude by using an attitude scale via a Google form.

RESULT AND DISCUSSION

Experimental results of this study can be divided into two parts: 1) a comparison of positive and negative attitudes among fifteen pop-up advertising. 2) an effect of size and position of pop-up advertising as following:

Comparison of positive and negative attitudes on pop-up advertising

Result of comparison of average positive and negative attitudes among fifteen pop-up advertising as shown in figure. 2. A ordinate axis represented an attitude score, while an abscissa was fifteen pop-up advertising. It was found that the size and position with the highest positive attitude score was a pop-up advertising that was small size and located at top right position with an attitude mean of 5.13 (S.D. of 0.165). A second rang is a pop-up advertising that was medium size with top right position, with an attitude mean of 4.42 (S.D. of 0.130). A third rang is a pop-up advertising that was small size and located at middle left position with an attitude mean of 3.50 (S.D. of 0.165). On the other hand, the size and position of pop-up advertising that had the most negative attitude was a pop-up advertising with large size and located at bottom left right a position with an attitude mean of 5.84 (S.D. of 0.233).

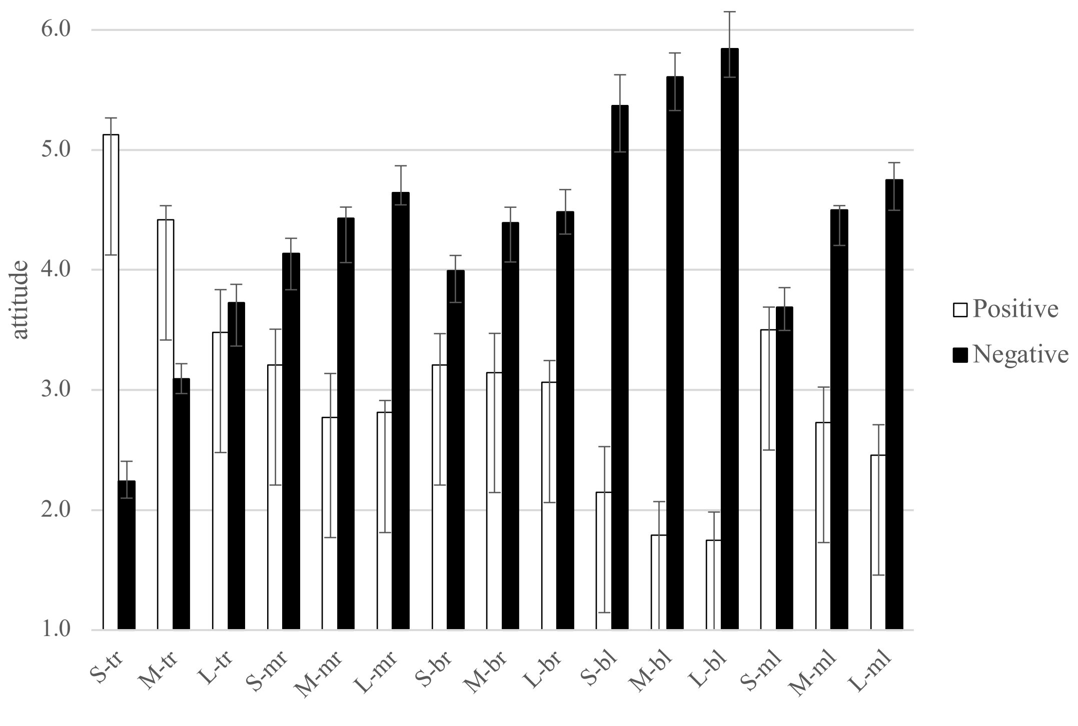

Figure 2. Attitude average comparisons for each Pop-Up ads

The positive and negative attitudes that have the greatest difference are L, M, and S sizes. A pop-up advertising with bottom left position has a difference with 4.09, 3.82, and 3.22, respectively. As attitudes that have the small difference, that is, they have similar likes and dislikes, that were a pop-up advertising with small size and located at middle left position, with large size and located at top right position, and with small size and located at bottom right position, with differences score of 0.19, 0.24, and 0.78, respectively.

Effect of size and position of pop-up advertising

The results of an analysis of the attitude study and the display size of three sizes of pop-up advertisements. As shown in Figure 3, the position where pop-up results received the most favorable reception was top right. A bottom left right position received the most negative feedback when all measurements were considered.

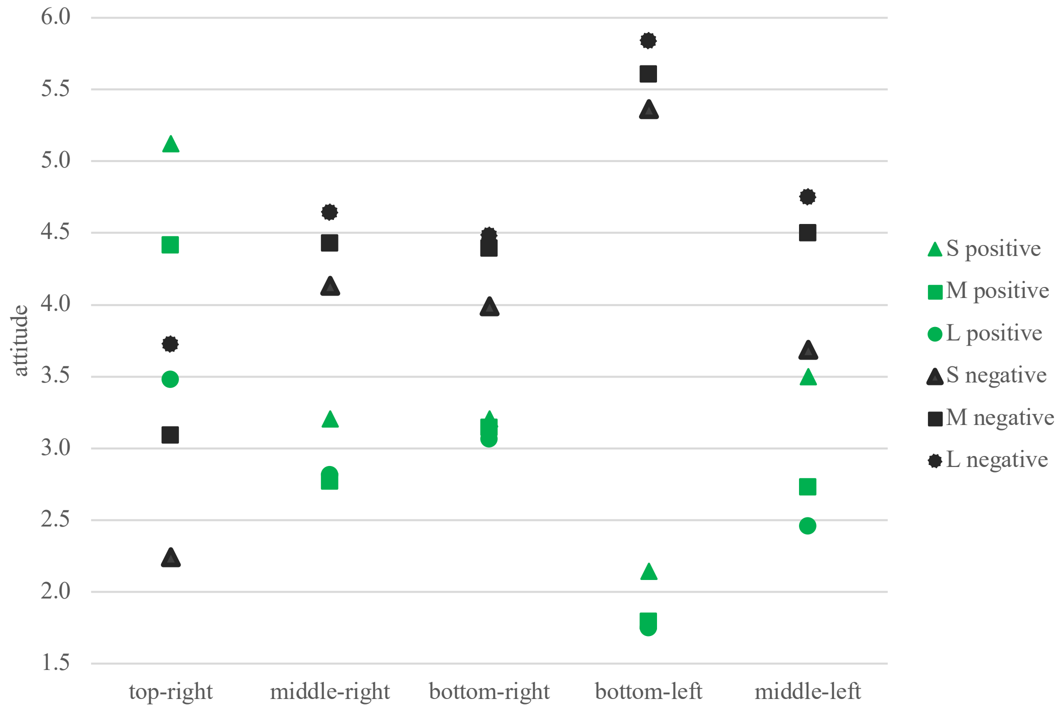

Figure 3. Negative and positive attitude comparisons for each Pop-Up ads

Effect of size for pop-up advertising

Figure 4 expressed a result of comparison among three size of pop-up advertisings –small, medium, and large size of the advertisings. It was found that the smaller size of pop-up advertising was, the higher positive attitude score was. A positive attitude score of small, medium, and large size of pop-up advertising were 3.88, 2.97, and 2.71, respectively. On the contrary, the larger size of pop-up advertising was, the higher negative attitude score was. A negative attitude score of small, medium, and large size of pop-up advertising were 3.88, 4.40, and 4.69, respectively. This implied that a small size pop-up advertising was preferable.

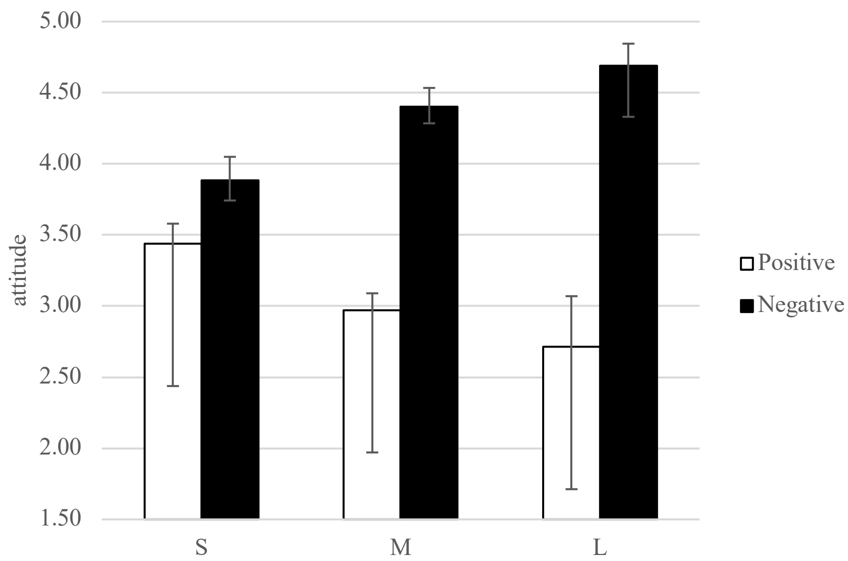

Figure 4. A comparison of negative and positive attitude score among different size of pop-up advertising

CONCLUSION

This study explored the effect of web users' attitudes toward the design of pop-up sidebar advertising. In conclusion, a small size of pop-up sidebar (340x200 pixels) should be selected as a candidate for e-commerce advertising. According to Patrali Chatterjee (8), this magnitude corresponds to a high level of user attitude on the website. On the other hand, web designers and marketers should avoid a large pop-up sidebar advertising. Furthermore, a position of pop-up sidebar advertising should be considered. A pop-up sidebar advertising with top right and bottom right corner of a screen were preferable.

ACKNOWLEDGEMENT

This study was supported by JSPS Core-to-Core Program, (grant number: JPJSCCB20220006.)

REFERENCES

1. Diao, F., & Sundar, S. S. (2004). Orienting response and memory for web advertisements: Exploring effects of pop-up window and animation. *Communication research*, *31*(5), 537-567.
2. Edwards, S. M., Li, H., & Lee, J. H. (2002). Forced exposure and psychological reactance: Antecedents and consequences of the perceived intrusiveness of pop-up ads. *Journal of advertising*, *31*(3), 83-95.
3. Bittner, J. V., & Zondervan, R. (2015). Motivating and achievement-eliciting pop-ups in online environments: A user experience perspective. *Computers in Human Behavior*, *50*, 449-455.
4. Bagozzi, R. P., & Dholakia, U. (1999). Goal setting and goal striving in consumer behavior. *Journal of marketing*, 63(4_suppl1), 19-32.
5. Poptin Website. (2023). *Create Poptins in Minutes Using a Drag & Drop Editor*. https://www.poptin.com/
6. Andrew Chornyy. (2023). *15 Types of Pop-ups to Use on Your Website*. https://shorturl.at/hqTW3

7. McCoy, S., Everard, A., Galletta, D., & Polak, P. (2004). A study of the effects of online advertising: A focus on pop-up and in-line ads. *Proceedings of the Third Annual Workshop on HCI Research in MIS*, Washington, 2(11), 50-54.
8. Chatterjee, P. (2008). Are Unclicked Ads Wasted? Enduring Effects of Banner and Pop-Up Ad Exposures on Brand Memory and Attitudes. *Journal of electronic commerce Research*, 9(1).

A STUDY OF THE USER'S EYE MOVEMENT BEHAVIOR ON DIFFERENT COLORED BANNERS OF THE COMMERCE WEBSITE USING EYE TRACKING TECHNOLOGY

Kamonthip Torsabsinchai[1] and Natchaphak Meeusah[2]*

Faculty of Mass Communication Technology, Multimedia Technology Department ,
Rajamangala University of Technology Thanyaburi, Thailand.

*Corresponding author: Natchaphak Meeusah, natchaphak_m@rmutt.ac.th

ABSTRACT

The objectives of this study were to 1) study user eye movements on the first page of the current commerce website 2) study and design banners and color schemes for commerce websites using contrast ratios 3) evaluate and analyze the eye movement behavior of customers of each age group toward product banners with different color schemes using eye movement detection technology. The participants in the research were individuals who use the website aged 25-44 years, a total of 40 people, divided into four age groups using a random sampling : 1) 10 people between the ages of 25 and 29 2) 10 people between the ages of 30 and 34 3) 10 people between the ages of 35 and 39, and 4) 10 people between the ages of 40 and 44. The Gazerecorder program is used in the test to identify the participants' eye movements showed as a heat map that displays the color value based on the user's eye fixation.

The results indicated that on today's commerce sites, most users are focused on the banner. Contrast is an essential element in the usage of color. Banners with high contrast colors that stand out from the background tend to attract the user's attention more than low contrast banners. Then, using contrast ratios, create banners and color palettes for commerce websites. We created eight sets of banners with various contrast ratios. Using colors with a higher color contrast ratio in text to the background will draw the user's gaze to the word's the details more closely. Younger users have a habit of looking around or at a wide area. As people grow older, they can fix their eyes on different areas for longer periods of time. People aged 40–44 are unlikely to look at all areas but will look at particular area.

Keywords: Eye Movement, Color, Website, Banner, Eye Tracking

INTRODUCTION

The evolution of consumer purchasing decision-making in recent years has been reflected in the growth of online retail as a highly effective marketing channel. In 2020, NRF's Winter 2020 Consumer View in United States reported that 83% of buyer say convenience while shopping is more important compared to five years ago. That was before the COVID-19 pandemic, so that percentage has likely increased [1]. During the COVID-19 pandemic, 95% of Thais believe that online shopping has improved their lives. The percentage of online purchases has experienced significant growth, increasing by 35% from 2020 to reach 65% in 2021 and will continue to be at a high level [2].

User interface design include the conception and design of visually pleasing and effective screens, web pages, as well as various visual components such buttons and icons. The field of user interface design means the design and creation of interfaces which simplify the interaction between users and a product or service.

A banner is an image which is prominently displayed, either at the top of a website or in an important location of the page, making it an excellent sales tool. It is typically used to communicate or display the most significant content on the page. Banners are a part of the design of the user interface design [3].

The effective use of eye tracking has significance in terms of the design of user interfaces with a focus on usability. Effective design will direct the visual attention of the user or consumer in accordance with the relative significance of the content. The objective is to determine the elements that the designer intends to highlight for the user or consumer's attention. Eye tracking testing is a crucial component in the field of user interface design and user experience. Studies of user interface search using eye tracking have to be extremely restricted to specific stimuli. [4].The testing will involve users who are either real users or people with scenarios that closely parallel real users.

Due to all of the above, the researcher was inspired to conduct research on user interface design and user experience on e-commerce platforms among users aged 25-44. The usage of eye tracking technology will be employed to identify the impact of user interface element placement on the visual experience of users.

METHODOLOGY

1. Procedures for data planning and analysis

1) Study and conduct research on relevant sources, such as user interface design, user experience design, and eye tracking.

2) Study the design of various sections of the current commerce website and select websites to be analyzed for design standards and guidelines. including the positioning of component.

3) Examines the color schemes used in website design and selects a different color scheme for use on the website. Additionally, its design is guided by a study conducted on color contrast ratios.

4) Design a wireframe and a prototype. Create prototypes based on all design layouts using the Figma design program. This research focuses on banners of product image, text color, and background color. The design of the layout includes the positioning of images in the center, with lettering positioned on the left and right sides. Furthermore, changes have been made to the font color and background color of the product image on the banner, taking into concern the color contrast ratios. The researchers designed a total of eight banner images using color schemes. Background-font color and button-font color were different colors. Creating and implementing color schemes with an effective contrast ratio. A high contrast ratio is any number that is greater than 4.5 or 4.5:1.They are shown in Table 1

Table 1: Banner design and color scheme

<table>
<tr><th>No.</th><th>Banner and Color</th><th>No.</th><th>Banner and Color</th></tr>
<tr><td>1</td><td>


Background-Font Color Button-Font Color

#E2AA25 #000000
Contrast Ratio : 10.01:1
AAA

#21407F #FFFFFF
Contrast Ratio : 9.98:1
AAA
</td><td>5</td><td>


Background-Font Color Button-Font Color

#EEEEEE #000000
Contrast Ratio : 18.1:1
AAA

#000000 #FFFFFF
Contrast Ratio : 21:1
AAA
</td></tr>
</table>

No.	Banner and Color	No.	Banner and Color
2	 **Background-Font Color**: #000000 #FFFFFF Contrast Ratio : 21:1 AAA **Button-Font Color**: #BE0212 #FFFFFF Contrast Ratio : 6.55:1 AAA	6	 **Background-Font Color**: #0A4219 #FFFFFF Contrast Ratio : 11.63:1 AAA **Button-Font Color**: #94004D #FFFFFF Contrast Ratio : 8.87:1 AAA
3	 **Background-Font Color**: #E2AA25 #FFFFFF Contrast Ratio : 10.01:1 AAA **Button-Font Color**: #FF9E00 #000000 Contrast Ratio : 10.14:1 AAA	7	 **Background-Font Color**: #F674B5 #000000 Contrast Ratio : 8.08:1 AAA **Button-Font Color**: #6D0194 #FFFFFF Contrast Ratio : 10.09:1 AAA
4	 **Background-Font Color**: #2F4F4F #FAEBD7 Contrast Ratio : 7.62:1 AAA **Button-Font Color**: #DAA520 #000000 Contrast Ratio : 9.38:1 AAA	8	 **Background-Font Color**: #CBC7B8 #00000 Contrast Ratio : 12.43:1 AAA **Button-Font Color**: #80634F #FFFFFF Contrast Ratio : 5.5:1 AAA

5) Using the Gazerecorder program, collect data and record the tracking of the user's eye movement towards the banner. Forty participants, divided into four age groups, offered their data. 1) 10 people between the ages of 25 and 29 2) 10 people between the ages of 30 and 34 3) 10 people between the ages of 35 and 39, and 4) 10 people between the ages of 40 and 44.

6) Showed the prototype banner images to the participant for 7 seconds per image.

7) Examine the findings of the research. The data are displayed on the map in the form of a heatmap, which is determined by the color of the image. Red indicates how many users interact with that area, while green indicates fewer users.

Figure 1. Heatmap Color and Meaning [5]

8) Summarize and analyze the results of the research.

RESULT AND DISCUSSION

The findings of the study can be summarized by dividing them into age groups of the participants in the study as follows :

1) Age range of 25 to 29

The visual movements of the 25-29 age group are going to look at the banner image from different points of view. The appearance is disjointed. Users will look at the words on the sides of a banner image with a high contrast ratio between the background color and the text before moving to the image in the middle of the banner.

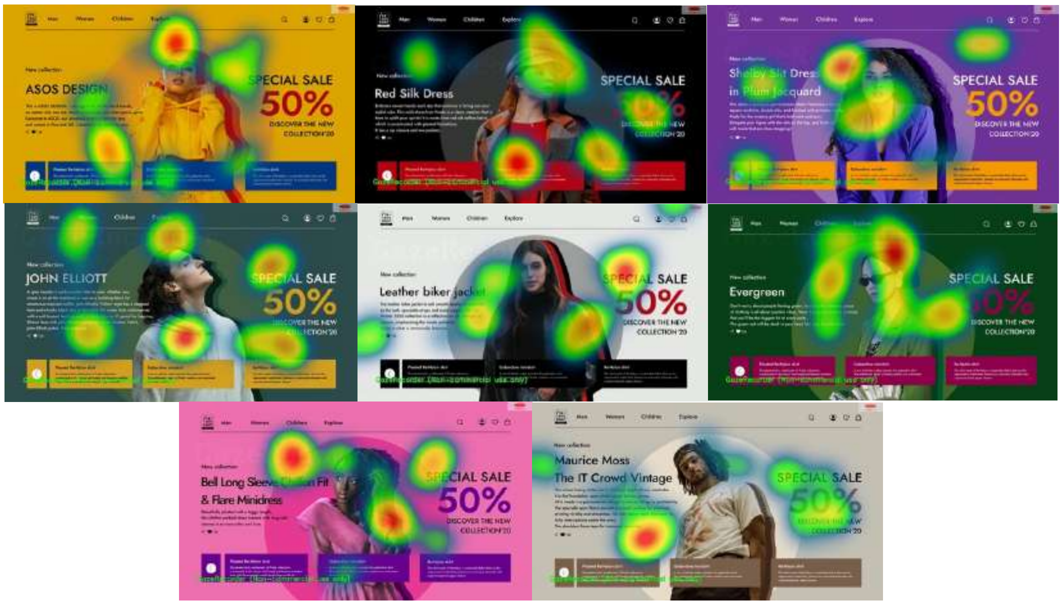

Figure 2. The 25-29-year-old sample's banner heat map

2) Age range of 30 to 34

The visual movement of those aged 30 to 34 will be more concentrated as they scan their gaze. People will focus more on significant details than users aged 25 to 29. The majority of users will keep their eyes on the center of the banner and scan the area surrounding the center of the image.

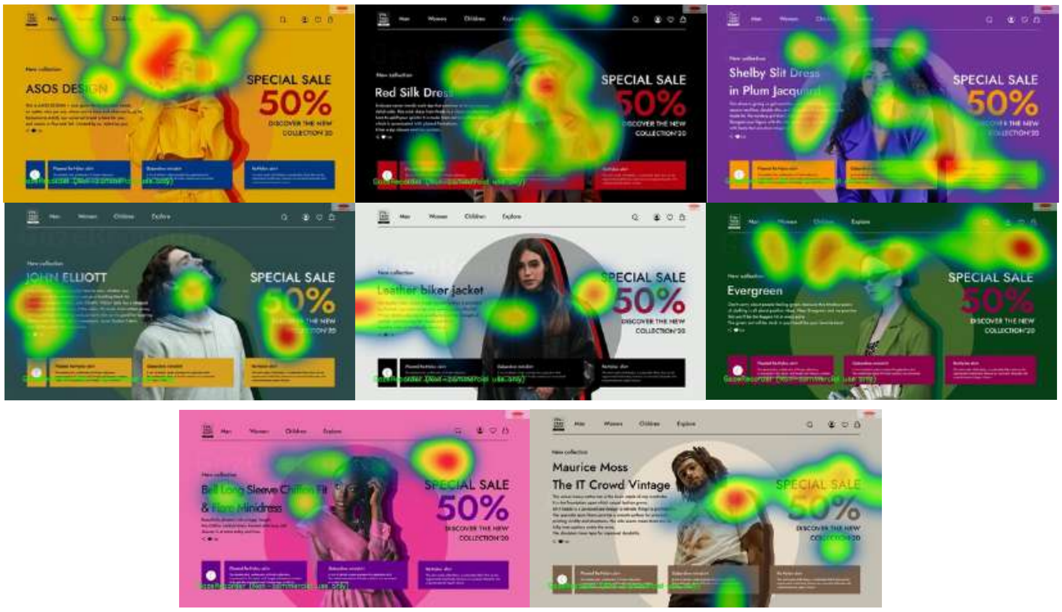

Figure 3. The 30-34-year-old sample's banner heat map

3) Age range of 35 to 39

The visual movement of the 35-to-39-year-old age will concentrate on the key elements and view the focal point as a larger point, focusing on the image or the primary character in the banner without focusing on all the components.

Figure 4. The 35-39-year-old sample's banner heat map

4) Age range of 40 to 44

The visual movement of the 40-44 age group will be focused on the banner's center image. The gaze focuses on one area in the image and stays there for a long period. Users do not look around at other points.

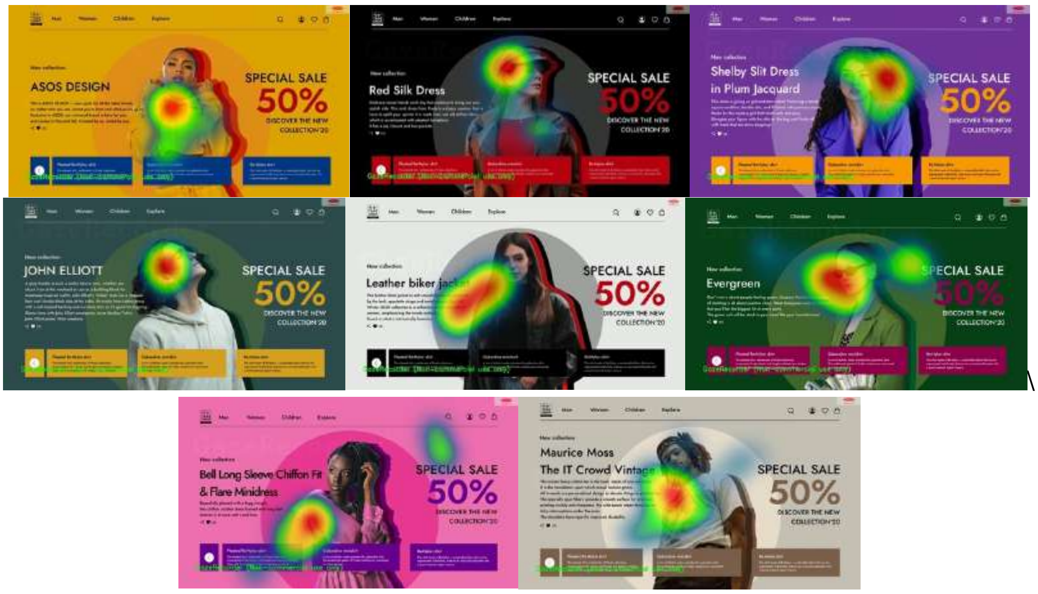

Figure 5. The 40-44-year-old sample's banner heat map

CONCLUSION

The results indicated that on today's commerce sites, most users are focused on the banner. Contrast is an essential element in the usage of color. Banners with high contrast colors that stand out from the background tend to attract the user's attention more than low contrast banners. Banner users will initially look at the words on the sides in a high contrast ratio between the background color and the text color before moving to the center image.

Users of different ages have various gaze and fixation behaviors on images. Younger people have an attraction for eye movement. Users attention not much about details. As users get older, their eyes start to focus narrowly. Additionally, concentrate more on the smaller details in specific areas of the image. The result correlates to the research results found by Djamasbi (2014) [6].When comparing the heatmaps of Baby Boomer and the Generation Y users, it was discovered that Baby Boomer users are more interested in the composition's details. Baby Boomer users are more visually focused on the red heat map than the Generation Y users, while the generation Y users consider less detail on each element. Users are going to focus on their own elements of interest while moving by. The banner's central image is frequently viewed by users. and when Banner images with a higher background-text contrast ratio, there is a chance of catching letters on the side. Users will be more likely to scan the characters on both sides of the image. The contrast ratio between the colors and fonts of the bottom three buttons has no effect on attracting users' attention.

ACKNOWLEDGEMENT

This work was supported by JSPS Core-to-Core Program, (grant number: JPJSCCB20220006.)

REFERENCES

1. Bretous,M. (2022). Consumer Behavior Statistics You Should Know in 2022. https://blog.hubspot.com/marketing/buyer-behavior-statistics
2. Kanokwan (2022). Thais are world champions who use social media to purchase products. https://bit.ly/46eaOjL
3. Imagineer (2022). The importance of banners on websites. https://bit.ly/44PxZ2K
4. Kotval, X.P., and Goldberg, J.H. (1998), Eye Movements and Interface Components Grouping: An Evaluation Method, Proceedings of the 42 nd Annual Meeting of the Human Factors and Ergonomics Society, Santa Monica: HFES, 42(5),486-490.
5. Farnsworth, B. (2021),___How to Analyze and Interpret Heat Maps. https://imotions.com/blog/learning/analyze-heat-maps/
6. Djamsbi, S.(2014). Eye Tracking and Web Experience. AIS Transactions on Human-Computer Interaction, 6(2), 37-54. doi:10.17705/1thci.00060

HUE POLARITY SELECTIVITY IN A COLOR CONTRAST-CONTRAST PHENOMENON

Shohei Kamegawa[1]*, Hiromi Y. Sato[2], Isamu Motoyoshi[3] and Yoko Mizokami [2]

[1]Graduate School of Science and Engineering, Chiba University, Japan.
[2]Graduate School of Engineering, Chiba University, Japan.
[3]Graduate School of Arts and Sciences, Tokyo University, Japan.

*Corresponding author: Shohei Kamegawa, s.kame1091@chiba-u.jp

ABSTRACT

It is known that the apparent color contrast of a texture reduces when another texture with a higher color contrast surrounds it. In the previous study, we presented results suggesting that the color contrast-contrast phenomenon is selective to the polarity of each axis in the color opponent mechanism. However, we recognized the potential influence of differences in perceived contrast for each hue among individual observers. To address this, we conducted a more rigorously controlled investigation to determine whether the color contrast-contrast effect exhibits selectivity to each axis's polarity in the color opponent mechanism. Our study used the DKL color space, defined by two cone-opposite color channels (L-M and S-(L+M)). Our stimuli consisted of textured patterns comprising colored and elongated blobs, with the background hue consistently positioned 180 degrees opposite the blob hue in the DKL color space. The hue angle of the central blob texture in the DKL space was set at 0, 45, 90, 135, 180, 225, 270, or 315 degrees. We varied the hue angle of the surrounding blob texture in 10 levels. We determined the perceived contrast balance for each hue angle in the DKL color space in a preliminary experiment for each observer. Employing the individual perceived contrast balance scaling, we measured the point at which the central texture's perceived color contrast (chroma) reached subjective equality between with and without the surrounding blob texture. Our findings revealed that the apparent color contrast of the central texture was significantly reduced when surrounded by textures of a similar hue in the DKL color space. This reduction was not consistent when it was surrounded by textures that were 180 degrees apart in hue from the central texture in certain conditions. Overall, our results suggest that the polarity of the color opponent mechanism in cardinal axes does not selectively influence the color contrast-contrast phenomenon, and multiple chromatic channels are also involved.

Keywords: Polarity selectivity, Perceived color contrast, DKL color space

INTRODUCTION

The apparent color contrast of a texture diminishes when it is surrounded by another texture with higher color contrast, a phenomenon referred to as the color contrast-contrast phenomenon. This phenomenon is similar to the achromatic contrast-contrast phenomenon, where the central texture's contrast decreases when a higher-contrast texture surrounds it. Previous research has indicated the involvement of luminance polarity selection units in the contrast-contrast phenomenon [1]. In our prior study [2], we presented results suggesting that color contrast-contrast also exhibits selectivity for the polarity of each axis in the color opponent mechanism. However, we acknowledged the potential influence of individual differences in perceived hue contrast among observers on these results. To address this, the present study examines whether hue contrast is selective for each axis's polarity in the color opponent mechanism under carefully controlled conditions.

METHODOLOGY

Stimuli

The experiment was in a darkened room, utilizing an LCD monitor (EIZO Color Edge CX271) to present the experimental stimuli. A chin rest was employed to ensure a stable observer position, and the viewing distance was set at 60 cm. The LCD monitor had specific settings: a resolution of 560 × 1440 pixels, a monitor size of 599 × 338 mm, a pixel resolution of 0.018 degrees per pixel, and an output frequency of 60 Hz. The monitor's color gamut and gamma characteristics were assessed using a Konica Minolta CS-2000A spectroradiometer. Subsequently, we applied the inverse function of the gamma function to achieve linear gamma correction based on these characteristics. The CIE chromaticity coordinates of the monitor's white point were x = 0.323 and y = 0.327. The monitor's maximum luminance was 115.3 cd/m2, while the background luminance was 53.76 cd/m2. The definition of the DKL color space used for generating the stimuli was based on the formula proposed by Brainard [3].

We conducted a preliminary experiment for each observer to assess the perceptual contrast balance across the 16 hue angles utilized in this study. In this preliminary experiment, we prepared test stimuli (Fig. 1, left) and reference stimuli (Fig. 1, right), consisting of a region featuring a circle with a diameter of 5.6 degrees. The texture was defined by Eq. (1), which is a variant of the following Gaussian function.

$$f(x,y) = C \cdot p \cdot \left\{1 - \left(1 - g(x,y)\right)^2\right\} \tag{1}$$

The function $g(x,y)$ is a Gaussian function defined by Eq. (2).

$$g(x,y) = \exp\left\{\frac{-(x\cos\theta + y\sin\theta)^2}{2{\sigma_x}^2}\right\} \cdot \exp\left\{\frac{-(x\sin\theta + y\cos\theta)^2}{2{\sigma_y}^2}\right\} \tag{2}$$

The contrast C in the stimulus is determined by Equation (3), where p represents the polarity of the contrast with values of +1 or -1. I_{ij} is the saturation of the i-th and -th pixel in a 2D image with dimensions $M \times N$. Saturation is normalized by setting the maximum value on the monitor to 1.—

$$C = \sqrt{\frac{1}{MN}\sum_{i=0}^{N-1}\sum_{j=0}^{M-1}\left(I_{ij} - \bar{I}\right)^2} \tag{3}$$

Each element of the texture had dimensions of 0.26 degrees in length and 0.09 degrees in width and was randomly placed. The average luminance within each region was consistently adjusted to match the luminance of the gray background, while the average saturation was corrected to zero. We measured the color contrast that appeared equivalent to the fixed 90-degree hue angle test stimuli by adjusting the contrast of the reference stimuli across the 16 hue angles. The contrast level was 0.2 for the test stimulus. The initial contrast value for the reference stimulus was also set at 0.2.

Figure 1. An example of stimuli in a preliminary experiment: Left, the test stimulus (hue angle: 90 deg.); Right, the reference stimulus (0 deg.).

Table 1 presents the ratios of equal contrasts for the 16 conditions, where each observer's hue angle is adjusted to achieve a 0.2 contrast at 90 degrees. The largest value of the 16 contrasts in this table is normalized to 1 for reference.

Table 1: the perceptual contrast balance of the 16 hue angles for each observer when the maximum value is calculated as 1.

Hue angle (deg.)	0	22.5	45	67.5	90	112.5	130	157.5	180	202.5	225	247.5	270	292.5	315	337.5
S1	0.45	0.5	0.6	0.81	1	0.76	0.51	0.5	0.44	0.53	0.56	0.65	0.7	0.56	0.45	0.45
S2	0.34	0.37	0.48	0.75	1	0.65	0.42	0.4	0.39	0.4	0.4	0.52	0.58	0.5	0.4	0.38
S3	0.66	0.69	0.7	0.93	1	0.66	0.59	0.52	0.55	0.61	0.65	0.7	0.68	0.64	0.6	0.58
S4	0.68	0.75	0.83	1	0.95	0.78	0.69	0.61	0.59	0.62	0.73	0.81	0.88	0.78	0.69	0.69

In the main experiment, we utilized a test stimulus consisting of a circular central and peripheral region, as depicted in Figure 2. The left image shows the same polarity in the center and periphery (0° hue angle in the periphery). In contrast, the right image illustrates the opposite polarity in the center and periphery (180° hue angle in the periphery). The central region featured a circle with a diameter of 5.6 degrees, while the peripheral region had a circle with a diameter of 12 degrees. To maintain a contrast level that allowed for the preservation of tonal gradations, the contrast was initially set at 0.2 in the central region and 0.28 in the peripheral regions before accounting for individual differences. To ensure that the apparent contrast of each hue was equal for each observer, we adjusted the contrast of the hue angles based on observer-specific ratios derived from a preliminary experiment. Given that distinguishing the center from the periphery without a boundary was challenging, we introduced a black line at the boundary between the central and peripheral regions. The hue angle of the central region consisted of 8 patterns (0, 45, 90, 135, 180, 225, 270, and 315 degrees). In comparison, the peripheral region encompassed ten patterns (0, 45, 90, 135, 180, 225, 270, 315 degrees) and two patterns (±22.5 degrees from the hue angle corresponding to the central region). In total, we employed 80 patterns of test stimuli.

In the main experiment, the reference stimuli consisted solely of the central region, as depicted in Figure 1. The characteristics of the texture elements, the distance between their centers, the mean luminance, mean saturation, and contrast remained consistent with those of the test stimuli. The hue angle for each trial matched the hue angle used in the corresponding test stimulus. The initial contrast value for the reference stimulus was set at 0.2.

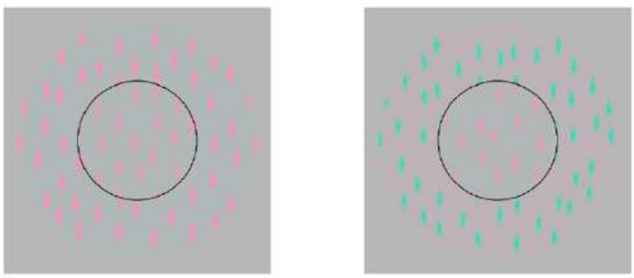

Figure 2. Test stimuli of color contrast-contrast image. Left, the same polarity condition (0 deg in both the center and periphery region); Right, the opposite polarity stimulus (0 deg in the center region and 180 deg in the periphery region). –

Procedure

The apparent saturation of the central region was assessed using the forced-choice method. During each session, the hue angle of the central region in both the test stimulus and the reference stimulus was set to a fixed value and randomly interleaved across the ten conditions with varying peripheral regions. The contrast of the peripheral region in the test stimuli remained constant, while the contrast of the reference stimulus was adjusted using a single series of the staircase method with a step size of 0.1 log contrast units. Each session of the staircase procedure terminated after conducting a minimum of 20 trials for each condition. Two sessions were conducted, ensuring a minimum of 40 trials for each condition.

The observers' response rates regarding the color contrast of each reference stimulus in each peripheral condition were fitted to a logistic function using the bootstrap method. The color contrast of the reference stimulus corresponding to a 50% response rate was subsequently determined and utilized to measure the apparent color contrast of the test stimulus.

Four observers participated in the experiment, one being the author and the others unaware of its purpose. All participants were males in their twenties, with normal or corrected visual acuity and normal color vision as determined by the Ishihara color vision test chart.

RESULT AND DISCUSSION

Figure 3 illustrates the relative values of the apparent contrast of the central region for eight conditions (0, 45, 90, 135, 180, 225, 270, and 315 degrees) with varying hue angles of the peripheral region. On the horizontal axis, positive values at 0 degrees represent the hue angle of the peripheral region. Each symbol on the graph represents a relative value of the apparent contrast. A value of 1 indicates that the apparent contrast matches the physical contrast, while values less than one suggest that the contrast is suppressed in appearance. Simulations superimposed on the results. The simulations predict a polarity-selective scenario in the case of opposite-color channels. This prediction is derived by calculating the magnitudes of the L-M and S-(L+M) axis components at each hue angle, considering suppression for the same polarity, and then computing the respective suppression. The expected value of apparent contrast in a fully polarity-selective scenario, denoted as $\alpha_{selective}$, is defined by Equation (4).

$$\alpha_{selective} = 1 - (1 - \alpha_{same})(\max(\sin\theta_c \sin\theta_s, 0) + \max(\cos\theta_c \cos\theta_s, 0)) \quad (4)$$

In the case of full polarity non-selectivity, the expected value of the apparent contrast, denoted as $\alpha_{non\text{-}selective}$, was determined using Equation (5).

$$\alpha_{non-selective} = 1 - (1 - \alpha_{same})(|\cos\theta \cos\Phi| + |\sin\theta \sin\Phi|) \quad (5)$$

In Equation (4), α_{same} represents the average of all observers' apparent contrast when the polarity is the same for each condition, θ_c is the hue angle in the central region, and θ_s is the hue angle in the peripheral region. Figure 3 shows that the central region's hue angle exhibited polarity selectivity in six conditions (0, 45, 90, 180, 225, and 315 degrees) and non-polarity selectivity in two conditions (135 and 270 degrees). When the hue angle of the central region aligns with the cardinal axis (L-M and S-(L+M)), polarity selectivity seems absent, and the response follows that of an opposite-color channel. However, in situations where the range of hue angles exhibiting contrast effects is restricted, as seen in the cases of contrast effects at 135 and 315 degrees, the explanation based solely on the opposite color channel principle falls short.

For each observer, the eight conditions with different hue angles in the central region were averaged to determine the difference in hue angle between the central and peripheral regions, as illustrated in Figure 4. The horizontal axis represents the difference in hue angle between the central and peripheral regions, while the vertical axis represents contrast. A horizontal axis value of 0 corresponds to the same polarity condition where the hue angles of the central and peripheral regions are equal. In contrast, a value of 180 corresponds to the opposite polarity condition where the hue angles are in opposition. Subsequently, a one-sample t-test was conducted to examine whether there was a significant difference from 1. Analyzing the 0-degree and 180-degree conditions, which are particularly relevant for discussing polarity selectivity, the contrast effect was significant for both conditions (p = .0025; p = .0001). These analyses collectively suggest that there is little polarity selectivity.

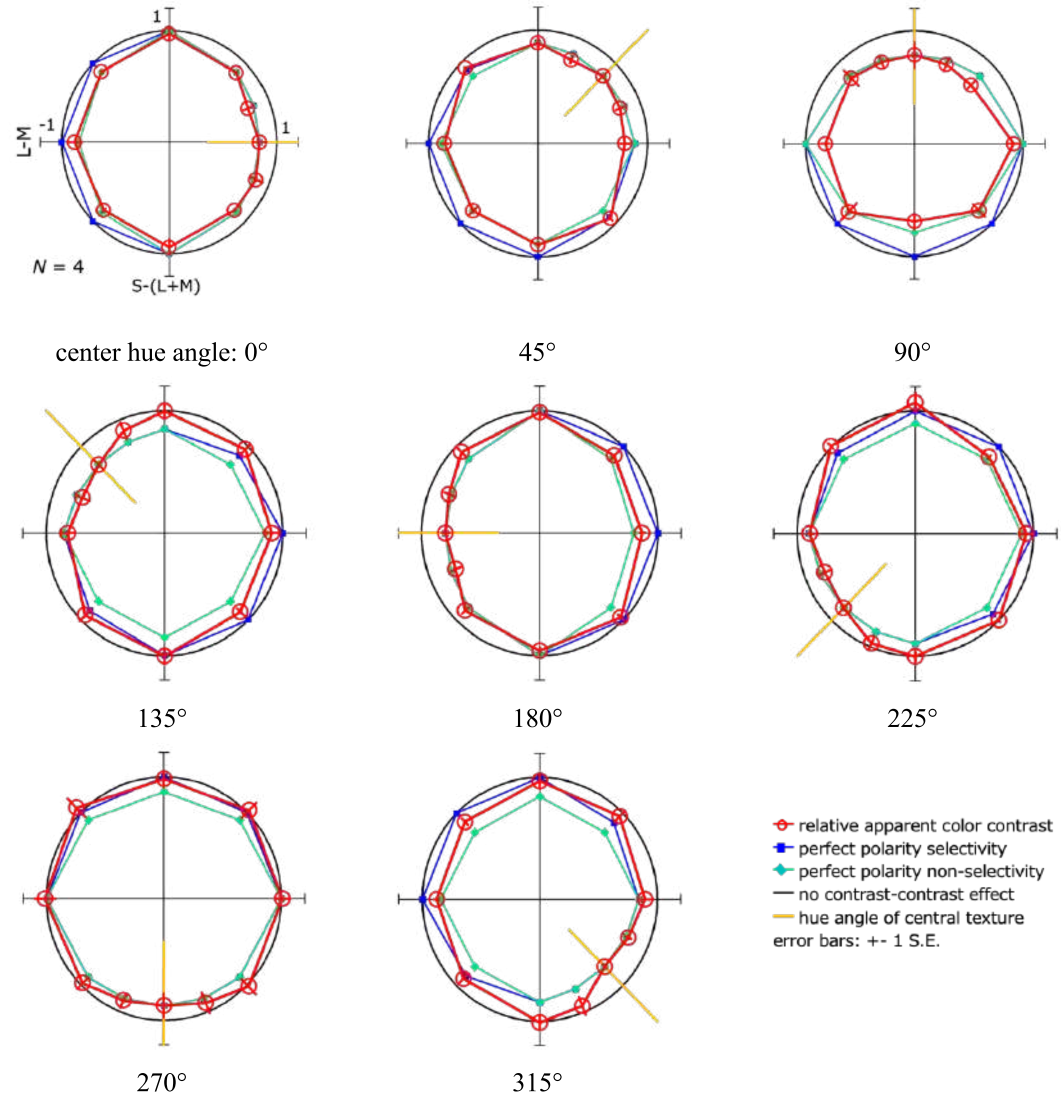

Figure 3. The perceived color contrast (chroma) of the center texture, along with simulations, overlaid on the relative values of the apparent contrast of the central region for eight conditions (0, 45, 90, 135, 180, 225, 270, and 315 degrees) as the peripheral region's hue angle varies.

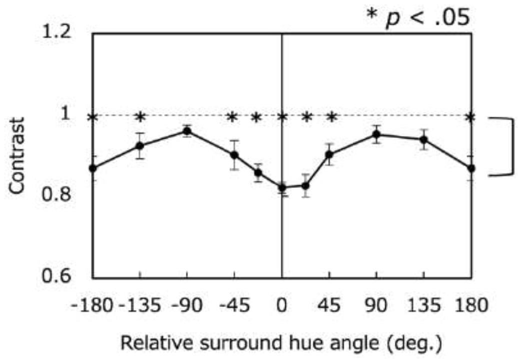

Figure 4. Average results of all conditions and one-sample t-test. The horizontal axis represents the difference in hue angle between the center and periphery, and the vertical axis represents contrast.

Our results suggest that the polarity of the color opponent mechanism does not selectively influence the color contrast-contrast phenomenon. Moreover, the opposite-color channel model [4] does not comprehensively explain the contrast-contrast effects observed at 135° and 315°. This may be primarily due to the narrowly tuned chromatic channels. Kuriki [5] demonstrated the need for two narrowly tuned channels in the blue and yellow directions and two or more broadly tuned channels at the posterior level of the opposite-color channel using contrast adaptation to color-notched noise stimuli. Chen et al. [6] also explored higher-order color mechanisms by measuring neural activity with EEG in human observers, providing evidence of higher-order color mechanisms along intermediate axes.

CONCLUSION

In this study, we conducted experiments to explore whether the color contrast-contrast effect shows selectivity towards the polarity of each axis within the color opponent mechanism. Our results suggest that hue contrast did not exhibit polarity selectivity in most conditions. Moreover, we observed that the contrast-contrast effect was narrower at particular central region hue angles, implying the possible involvement of a multichannel mechanism.

ACKNOWLEDGEMENT

This work was supported by JSPS Core-to-Core Program (JPJSCCB20220006) and JSPS KAKENHI (JP18H04183, JP21H05805, and 23H04332).

REFERENCES

1. Sato, H., Motoyoshi, I., & Sato, T. (2012). Polarity selectivity of spatial interactions in perceived contrast. Journal of Vision, 12(2), 3-3.
2. Sato, H., Kamegawa, S., Motoyoshi, I., Mizokami, Y. (2022). Effect of the hue polarity on spatial suppression of the perceived color contrast. Journal of Vision, Vol.22, 4399.
3. Brainard, DH. (1996). Cone contrast and opponent modulation colorspaces, Optical Society of America, 563-579.
4. Stockman, Andrew, and Brainard, DH., (2010). Color vision mechanisms. The Optical Society of America handbook of optics 3, 11-1.
5. Kuriki. I., (2007), Aftereffect of contrast adaptation to a chromatic notched-noise stimulus. J. Opt. Soc. Am. A, 24, 7, 1858-1872.
6. Chen, J., K, Gegenfurtner., (2021). Electrophysiological evidence for higher-level chromatic mechanisms in humans, Journal of Vision, 21(8):12, 1-14.

EFFECT OF DISPLAY TECHNIQUE ON SIMULTANEOUS COLOR CONTRAST

Janejira Mepean[1], Chanprapha Phuangsuwan[2]*, and Mitsuo Ikeda[2]

[1]Mass Communication Technology, Department of Color Technology and Design, Rajamangala University of Technology Thanyaburi, Thailand.
[2]Color Research Center, Rajamangala University of Technology Thanyaburi, Thailand.

*Corresponding author: Chanprapha Phuangsuwan, Phuangsuwan@rmutt.ac.th

ABSTRACT

This study aimed to investigate the impact of different display techniques on simultaneous color contrast (SCC), including the adaptation to illumination with adding objects and without objects in the subject room, to help observers understand illumination in the space. Three display techniques were employed: colored paper, electronic display, and the two-rooms techniques. Four color stimuli were carefully controlled, almost the same in color value, luminance, chroma, and size of stimulus among display techniques. The elementary color naming method was used to judge the color appearance of SCC at the surround and gray patch. The repetition was three times. The result found that the SCC shows the strongest in two-rooms technique compared to paper and display techniques. The current experiment with or without objects seems to have no effect on SCC. The apparent hue of SCC was not showed significant difference among display techniques.

Keywords: Adaptation, Electronic display, Elementary color naming, Simultaneous color contrast, Two-rooms technique

INTRODUCTION

The recognized visual space of illumination RVSI theory suggests chromatic adaptation, saying that the effect will be stronger if the observer adapts to the color of the illumination in the space, not to the color of the object [1]. To confirm this theory, researchers have conducted studies using various techniques, and the results agree with RVSI theory. One interesting finding was the report of a comparison of the SCC effects of different devices. This was done by comparing the adaptation to the color of illumination (two-rooms technique), the adaptation to the color of the object's surroundings (using colored paper), and the adaptation to the color of the self-luminous or electronic display. The results show differences depending on the devices; the strongest effect was shown in the two-rooms technique and the weakest effect in the object [2, 3]. However, there were some limitations to controlling stimuli, such as stimulus size, color, luminance, and appearance mode among devices. These may influence the results. In the present study, we aimed to investigate the effect of display techniques on the SCC effect using three types of display techniques: colored paper, electronic display, and the two-rooms technique under carefully controlled conditions.

METHODOLOGY

Stimuli

The SCC classical pattern was used in this experiment as shown in Figure 1(a). We simulated SCC pattern by printing on uncoated paper, on display, and mixing LED light in two-rooms (display techniques). Five surrounding colors were: red, yellow, green, blue, and gray (gray surround was the control condition). The xy coordinates were shown in Figure 1(b). All surrounding colors showed almost the same among display techniques. The gray patch (x=0.332, y=0.351) with size of 4 × 4 cm was placed at the center of each surround. The chroma of colors were quantified by CIEC*$_{ab}$; 3-43 and luminance; 18-37 cd/m^2 depending on each color as shown in Table 1. Observers sit in the subject room and observe stimulus through the window with size of 21 × 31 cm. The distance between stimulus and observer was 70 cm, the visual angle of stimulus was 17° × 25° for surround and 3.3° × 3.3° for gray patch.

(a)

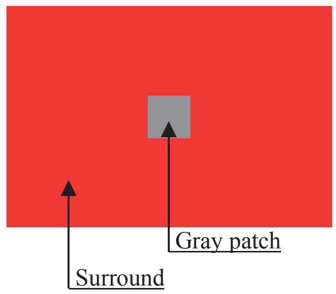

(b)

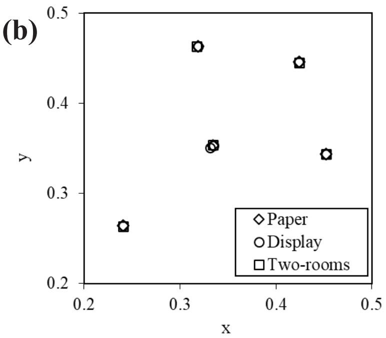

Figure 1. (a) scheme of SCC stimulus, (b) xy coordinates of stimuli under three ways of display technique.

Table 1: The luminance values, the xy coordinates, and chroma C*$_{ab}$ of colors in the paper and display stimuli.

Color	Condition	Y (cd/m^2)	x	y	C*$_{ab}$
Red	Paper	23	0.453	0.342	42
	Display	23	0.453	0.343	41
Yellow	Paper	37	0.424	0.442	42
	Display	37	0.424	0.449	43
Green	Paper	28	0.315	0.465	38
	Display	26	0.321	0.464	36
Blue	Paper	18	0.239	0.262	32
	Display	18	0.242	0.263	32
Gray	Paper	27	0.335	0.353	3
	Display	27	0.335	0.350	5
Gray patch	Paper	24	0.332	0.351	5
	Display	24	0.335	0.351	5

Table 2: The luminance values, the xy coordinates, and chroma C*$_{ab}$ of colors used in the two-rooms technique.

Color	Y (cd/m^2)	x	y	C*$_{ab}$
Red	23	0.452	0.344	4
Yellow	37	0.424	0.446	4
Green	27	0.318	0.464	3
Blue	18	0.240	0.264	3
Gray (achromatic light)	27	0.335	0.353	3
Test room	24	0.333	0.352	1

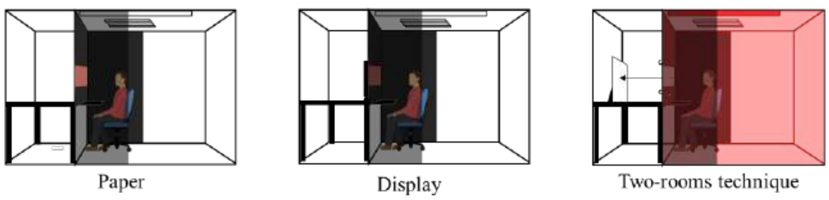

Figure 2. Three ways of display technique.

Apparatus

Figure 2 shows the experiment took place within a room with specific dimensions of 120 cm in width, 300 cm in length, and 200 cm in height, with a wall separating the rooms into two rooms called "test room" and "subject room". To delete the recognition of devices, the devices were placed in a test room, and stimuli were displayed through a window on the wall, which was designed to slope inward to minimize shadows and effectively present stimuli near the window. The test room was illuminated by two fluorescent lamps mounted parallel to the top and bottom of the window. Five fluorescent lamps (to illuminate the paper and display stimuli) and LED lamps (to simulate the stimuli colors in the two-rooms technique) illuminated the subject room. In paper and display techniques, the illuminance was approximately 1000 lx measured at a horizontal plane at the observer's eye position with a correlated color temperature (CCT) of 5500K (x, y = 0.332, 0.366) and a color rendering index (CRI) of 80. The front and side walls were covered with black cardboard (Y = 5.6, x = 0.322, y = 0.347) to force the observer to perceive the stimulus only in a specified area (through the window). In the two-rooms technique, the color was mixed by LED light combined with fluorescent light covered by color filters to simulate surrounding colors being the same as paper stimuli. The luminance of each color stimulus is shown in Table 2. Note that under the two-rooms technique, the front wall (black wall) was changed depending on the subject room illumination color simulated in the surrounding area: red (Y = 2.0, x = 0.494, y = 0.332), yellow (Y = 5.7, x = 0.429, y = 0.446), green (Y = 4.5, x = 0.314, y = 0.459), blue (Y = 2.6, x = 0.225, y = 0.239), and gray (Y = 4.5, x = 0.327, y = 0.343). The observer saw the gray patch in the test room through an aperture size of 4 × 4 cm on the front wall.

(a)

(b)

Figure 3. The front view of displayed stimulus in subject room for (a) without objects condition and (b) with objects condition

To investigate the effect of adaptation according to the RVSI theory, which says that objects in the space could help our perception to understand the illumination in that space and then adapt to the illumination, we asked the observer to judge the color of the stimulus under conditions of without objects and with objects (books, dolls, artificial flowers into the shelf installed at the front wall of the subject room) as shown in Figure 3.

Procedure

At first, the observer was instructed to look around the stimulus for two minutes for adaptation before judging the color appearance. Subsequently, he or she was asked to report the mode of appearance of the stimulus at the surrounding and at the gray patch using three color appearance modes: "object mode," in which the color appeared as the color object; "self-luminous mode," in which the color appeared as the emitted light from itself or as a light source color; and "unnatural mode," in which the color looked brighter than the object (shiny) but not the same as a light source color.

Next, the observer assessed the color appearance of the surrounding area and gray patches using the elementary color naming method, which estimated the percentages of chromaticness, whiteness, and blackness for a total of 100 percent. The apparent hues were assessed based on four hues from the opponent color theory: red, yellow, green, and blue, for a total of 100 percent. It was noted that the observers can evaluate the apparent hue in one color or in a maximum of two colors; the opponent color was not allowed to be a combination such as red vs. green and yellow vs. blue. After the assessments, the observer was asked to close their eyes for one minute while the experimenter randomly changed the stimulus color. The judgment was repeated three times in each condition. Three observers with normal color vision participated in the experiment. Two observers (CP and JM) had experience in a psychophysical experiment using the elementary color naming method for many years. Another observer (TM) was recently trained to use the elementary color naming method for assessing the color appearance.

RESULT AND DISCUSSION

We are interested in the effect of the display technique on the SCC effect. The ratio between the chromaticness of the gray patch and the chromaticness of the surrounding area was calculated using Equation (1).

$$Chromaticness\ ratio = \frac{chromaticness\ of\ gray\ patch}{chromaticness\ of\ surround} \qquad (1)$$

The average results from 3 observers compared among the three techniques are shown in Figure 4. If the ratio is equal to 1, it means that the observer perceives chromaticness of the SCC effect on gray patch as equal to chromaticness of surrounding. If it is more than 1, it indicates a strong SCC effect by chromaticness of gray patch was higher than chromaticness of surrounding. And 0 means no effect of SCC. The highest ratio showed that the strongest SCC effects occurred by two-rooms technique. There was significant difference between two-rooms and paper techniques for with objects ($p > 0.005$) and without objects conditions ($p > 0.01$). It was similarly occurred with two-rooms and display techniques for with objects ($p > 0.008$) and without objects conditions ($p > 0.007$). This is similar to the results reported in previous studies [2, 3]. Meanwhile, lower SCC effects were shown similar in both paper and display techniques. There are no significant differences between paper and display techniques in both with objects ($p < 0.08$) and without objects conditions ($p < 0.26$).

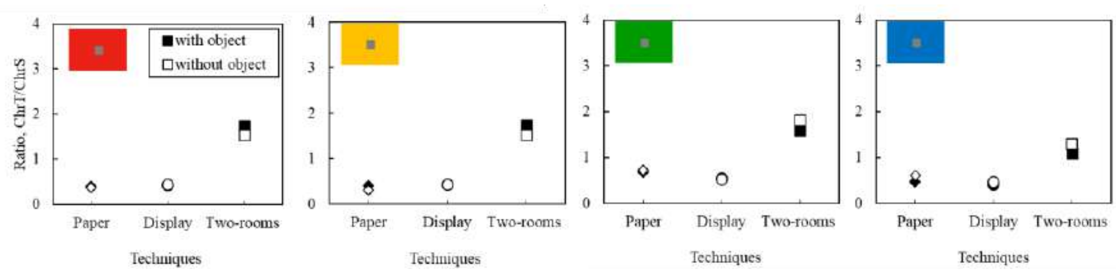

Figure 4. The chromaticness ratio of four surrounding colors shows the effect of three devices that used to display stimulus in the same condition with objects (●) and without objects (○).

The average result with objects and without objects conditions is shown in Figure 5. There was no significantly different in two-rooms technique comparing with and without objects conditions ($p < 0.23$). At the moment we cannot conclude based on the current results whether the SCC effect is affected by objects in the room or not, that might be because of the small number of observers.

The SCC determined by chromaticness appears on a gray patch surrounded by color. While there was gray surrounding it, the gray patch appeared gray. We found that increasing chromaticness correlated with decreasing the same amount of whiteness and blackness.

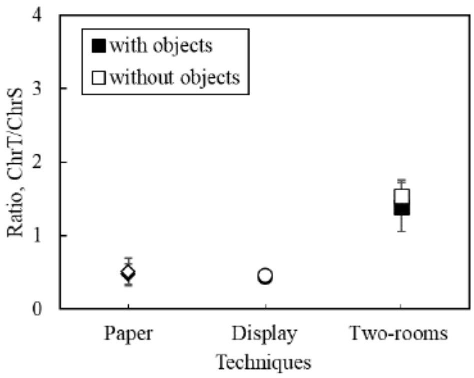

Figure 5. Averaged results from four surrounding colors compared between three devices under condition of with objects (●) and without objects (○). The error bar shows SD value.

The color appearance mode, in our suspect, is one of the factors that may contribute to the current results. A considerable influence of SCC with unnatural mode and object mode were detected in the two-rooms technique [5]. Based on the current result, there was no effect of object helping to adaptation to illumination in the space. In addition, the object mode was found in paper and display techniques. There was not found the effect of appearance mode on the SCC. This could be a result of controlling the color value, luminance, stimulus size, and even the recognition of display technique that might have an impact on how the observer perceives the scene.

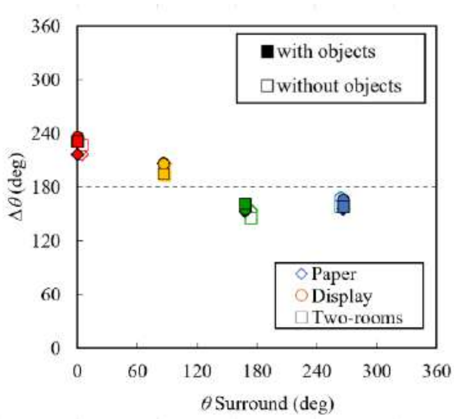

Figure 5. The hue difference ($\Delta\theta$) between three techniques under with and without objects condition plotted for the hue angle of the surrounding, dotted line was drawn at 180°.

The result of hue angle of SCC is calculated to determine hues difference by $\Delta\theta = \theta_{\text{gray patch}} - \theta_{\text{surround}}$. If $\Delta\theta$ is equal 180°, it means the apparent hue of SCC was opponent. Figure 5 is shown the result of $\Delta\theta$ between three display technique, the abscissa represents the hue angle of the surrounding color (θ_{surround}), and ordinate represents the apparent hue difference ($\Delta\theta$). The result showed that the SCC in red (4°) surround shows significant to complementary color relation ($p > 0.01$), $\Delta\theta = 218°$. In the case of yellow (88°), green (171°), and blue (265°) surrounding seem to show apparent hue of SCC in opponent relation [6] by $p < 0.12$, $p < 0.06$, and $p < 0.09$, respectively. The apparent hue of SCC in yellow $\Delta\theta$ = 192°, green $\Delta\theta$ = 169°, and blue $\Delta\theta = 177°$. The apparent hues difference of present experiment was compared with the previous experiment [2]. The result showed that there were similar in apparent hue even though the previous experiment did not control the physical values and light environment of the subject room.

CONCLUSION

1. The results implied that the display techniques influenced the SCC, which was strongest at the two-rooms technique.
2. The display techniques showed a small effect on the color appearance mode between the two-rooms and the paper and display.
3. The color appearance mode did not affect the degree of chromaticness, which implied SCC.
4. The apparent hue seems not to show any effect from the display technique.

ACKNOWLEDGEMENT

Janejira Mepean is grateful to Dr. Fusako Ikeda for the Fusako scholarship. For graduate studies in the department of Color Technology and Design, Faculty of Mass Communication Technology, Rajamangala University of Technology Thanyaburi. Additionally, this work was supported by JSPS Core-to-Core Program, (grant number: JPJSCCB20220006).

REFERENCES

1. Ikeda, M. (2004). Color Appearance Explained, Predicted and Confirmed by the Concept of Recognized Visual Space of Illumination. *Optical Review,* 11(4), 217–225.
2. Phuangsuwan, C. & Ikeda, M. (2018). Simultaneous Color Contrast Demonstrated on Different Devices. *Supplement in Journal of the Color Science Association of Japan (CSAJ*), 42-3, 54-56.
3. Phuangsuwan, C. & Ikeda, M. (2019). Device dependent simultaneous color contrast. *Supplement in Journal of the Color Science Association of Japan (CSAJ*), 43-3, 121-124
4. Phuangsuwan, C. & Ikeda, M. (2017). Chromatic adaptation to illumination investigated with adapting and adapted color. *Color Research and application*, 42, 571–579.
5. Chitapanya, P., Ikeda, M., & Phuangsuwan, C. (2018). Comparison of the simultaneous color contrast determined by colored paper and colored illumination. *Supplement in Journal of the Color Science Association of Japan (CSAJ*), 42(3+), 57-60.
6. Jameson, D. & Hurvich, L. M. (1961). Opponent chromatic induction: experimental evaluation and theoretical account. *Journal of the Optical Society of America*, 51(1), 46–53.

COLOR ANALYSIS AND CONSUMER PREFERENCES OF *SINOM* AND *KUNYITASAM* DRINKS, TRADITIONAL DRINKS FROM INDONESIA

Yunita Siti Mardhiyyah*[a], Lisa Risfana Sari[b], Rizky Noviasri[c], Irvan Adhin Cholilie[a], Anni Rahmat[d], Hadi Cahyono[b], Yuni Kurniati[d], Roostikasari Nugraheni[c]

[a] *Agro-Industrial Department, Universitas Internasional Semen Indonesia, Indonesia*
[b] *Management Department, Universitas Internasional Semen Indonesia, Indonesia*
[c] *Visual Communication and Design Department, Universitas Internasional Semen Indonesia, Indonesia*
[d] *Chemical Engineering Department, Universitas Internasional Semen Indonesia, Indonesia*
*Corresponding author: yunita.mardhiyyah@uisi.ac.id

ABSTRACT

Sinom and *Kunyit Asam* drinks are herbal drinks made from turmeric, tamarind, and several other herbal combinations. The use of tamarind leaf extract is the main characteristic of *Sinom* drink. There have been many studies related to the benefits of this herbal drink, but unfortunately due to the similarity of color, some consumers are still difficult to distinguish products and are disappointed when consuming because the expected taste is different. Therefore, this study analyzed the differences between turmeric and *Sinom* drinks specifically on the color factor while obtaining information on consumer views regarding the preferences of the two drinks. The research was conducted in two stages, namely first: color analysis of photography-based drinks by utilizing color detection website tools, second: distributing online questionnaires to consumers regarding preferences for *Sinom* and *Kunyit Asam* drinks. Data was collected from 120 respondents and being analyzed. The research was able to show the difference in the color of *Sinom* and *Kunyit Asam*, namely the yellow to red color obtained in *Sinom* drinks. As for the sour turmeric drink, the colors obtained are bright orange, bright brown, and also bright brownish red. The color tone of *Sinom* drinks desired by consumers is bright yellow to bright orange while in the *Kunyit Asam* drink is bright orange. Another finding of this study is that both drinks are favorite types of herbal drinks with consumption intensity once a week. Both drinks are quite attractive to the teenage and adult female age groups because of their various benefits. Presentation in several community activities (fasting and Eid dishes), the tradition of making your own at home and as a daily snack is a positioning for *Sinom* and *Kunyit Asam* beverage products. In the future, there is potential to develop *Sinom* and *Kunyit Asam* beverage products that have health benefits, preferred flavor, and color.

Keywords: *Kunyit Asem, Sinom, color, herbal drink, consumer preference*

INTRODUCTION

Consumers' perception of food products is influenced by various factors. Food products are requested not only to meet nutritional needs and treat health, but also from a sensory perspective [1], [2]. Sensory food items appeal primarily to the senses of sight as well as taste, smell, hearing, and touch. The sensory evaluation conducted by the eyes is the primary factor before a food product is consumed. The significance of color in food items, particularly in beverage products, should be emphasized [3]–[5]. The flavor or taste of the drink is frequently also represented by the color[3], [4], this includes traditional herbal drinks in Indonesia.

The Indonesian people have long held the belief that the herbal beverage jamu is beneficial for preserving immunity and enhancing health[6]. The existence of Covid-19 several years ago even showed an increase in the consumption of herbal medicine or herbal drinks in Indonesia [7]. The top three most consumed types of drinks are the group of drinks that use ginger, tamarind and turmeric[8]. Turmeric is a group of spices used in various traditional Indonesian drink formulas [6], [9]–[12]. Examples of types of drinks that use turmeric are *Jamu Kunyit Asem*, and *Sinom*. These two types of drinks use similar ingredients, namely turmeric (Curcuma longa L.), tamarind fruits (Tamarindus indica L.), palm sugar and water. The basic difference is that in *Kunyit Asem* drinks, several other herbal plant extracts such as kedawung seeds are usually used [13], galangal and lime [10], [14]. *Sinom* drink is a drink made from tamarind leaf extract. In some formulas, the ingredients used are only turmeric and *Sinom* leaves [14], However, there are also those who use turmeric, *Sinom* leaves and also the tamarind fruit [15], [16].

In general, people tend to associate certain colors with specific flavors or qualities, and this can influence their perception of taste and overall enjoyment of the product. Perception of taste from the color of jamu drinks has been studied in several papers. One study found that the color of jamu can influence taste perception, with colors such as white, red, blue, and yellow being preferred by the majority of participants[17]. Some assessments discuss product and color characteristics, such as differences in the size of the brewed coffee particles and the density of the black color.[18]. The RATA (Rate all that applies) sensory test method has also been used to identify the color of *Kunyit Asem and Sinom* drinks. [19]. Additionally, it has been observed that visual cues, including color, play a role in multisensory flavor perception and can influence beverage choices and consumption behaviors [3], [20], [21]. However, before this study was written, specific information about the degree of color difference between these two drinks and how consumers perceive them was not yet available. In addition, due to the similarity of color, some consumers are still difficult to distinguish products and are disappointed when consuming because the expected taste is different. Therefore, the purpose of this study is to find out how different the colors of *Sinom* and *Kunyit Asem* are, as well as what Indonesian customers perceive about both.

METHODOLOGY

The author conducted two stages of work, examining the distribution of colors in the market's sour turmeric and *Sinom* drinks along with searching for responder data. The Color Harmony app from the Play Store was used to analyze the colors of *Sinom* and *Kunyit Asem* drinks. A total of 195 photographs of *Sinom* and 135 images of the *Kunyit Asem* drink were discovered through Google search engine queries. After sorting the image data, the https://coolors.co/ website is used to evaluate them with the objective to determine the product color code (Figure 1). The https://www.colorhexa.com/ website then processes the data for obtaining a color plate with higher detail. The panelists were then given the following data to validate again the color of *Sinom* and *Kunyit Asem* drinks.

Figure 1. Color code generating procees form *Sinom* (left) and Kunyit Asem drinks.

The author asked respondents to fill out an online survey about their degree of beverage intake, preferred color, criteria for choosing beverage items, and preferred flavor (spices). People who have consumed *KunyitAsam* and *Sinom* drinks qualified as respondents, a total of 120 respondents were gathered.

RESULT AND DISCUSSION

Colors of Kunyit Asam and Sinom drinks

In simple terms, the color of these two drinks is yellow. Further investigation of the drink profiles also found that apart from yellow, the colors orange and brown were also found in these two drinks according to consumers[19]. Based on table 1, the color of *Sinom* drinks is bright yellow to bright orange. While the color distribution of *Kunyit Asam* drink is bright orange, bright red and bright brown. The processing color information from the https://www.colorhexa.com website was obtained to get the similar color palates (Figure 3). The panelists will then be shown this color scheme and asked to choose the preferred color for *Sinom* and KunyitAsem drinks.

Table 1. The result of color identification from Kunyit Asem and *Sinom* drink.

No	*Sinom* Drink			Kunyit Asem Drink		
	Color	Hex	Description	Color	Hex	Description
1		DCB818	Bright orange		C17B02	Bright orange
2		F9D301	Vibrant yellow		F79501	Vibrant orange
3		CAA900	Bright yellow		C17512	Bright orange
4		E8A829	Vibrant orange		FF621D	Vibrant red
5		BA6F17	Bright orange		F6AD00	Vibrant orange
6		D29D01	Bright orange		EFB901	Vibrant orange
7		C09B29	Bright orange		DF8000	Bright orange
8		F89C15	Vibrant orange		D36A00	Bright orange
9		E2B50D	Bright orange		B26401	Bright orange
10		DD9910	Bright orange		B16F00	Bright brown
11		DC9102	Bright orange		D76C01	Bright orange
12		D68609	Bright orange		A5711D	Bright brown
13		F9D301	Vibrant yellow		A83400	Bright red

Consumer perceptions of Sinom and Kunyit Asem drinks in Indonesia

To have a better understanding of the diverse customers of turmeric and *Sinom* drinks, an online survey was developed and disseminated via various social media. In this study, 120 respondents are gathered. Women made up 68.3% of the respondents, and their ages ranged from 17 to 30. Students in this age group have the most recent bachelor's (S1) level education. The majority ethnic group, with 81.7% of the population, is Javanese. Among the two types of drinks, *Sinom* was chosen as the drink most consumed daily, namely 55%. There are even those who choose these two types of drinks as their daily drinks (5.8%). Unfortunately, the frequency of drinking *Sinom* is still predominantly around once a week (82.5%). The serving of this traditional drink appears to be strongly tied to daily life; in addition to being a dish served at the time of breaking the fast or on the holiday of Eid al-Fitr, *Sinom* and Kunyit Asem drink is also considered a nutritious beverage and is made at home by 33% of respondents. (34%). Even more consumers (26%) believe that this beverage is like a group of appetizers that may be purchased from stores, food carts, or traveling herbalists.

Consumer ranked the health benefit as the priority in selecting herbal drink (rank 2.4 from 7-scale), followed by flavor (2.6), color (2.8), odor (2.9), price (3.0), labels (3.1) and advertisement as the last (3.4). *Sinom* (26.7%) and Kunyit Asem (30.8%) beverages are among the top choices for traditional herbal drinks. While Wedang Ronde (15%), Beras Kencur (15.8%),Wedang Uwuh (6.7%) and others are lower favorite. This was explained by the benefit of drinks. Turmeric, which is known to contain the bioactive component curcumin and has numerous health advantages [6], is an ingredient in both of these beverages. Since curcumin has a strong antioxidant capacity and inhibits the alpha glucosidase enzyme, it has been shown to increase the body's immunity, prevent cancer, and aid treat diabetes.[3], [22]. The benefit of turmeric might be obtained in the drinks too. This is thought to help with menstrual discomforts, particularly pain and odor associated with menstruation as well as dysmenorrhea. It promotes a feeling of health and freshness and assists in controlling menstruation[13]. It is thought to keep body weight stable and lessen odor. *Sinom* drink has several benefits. It contains antioxidant compounds [14], [15], which can help in improving the immune system and regulating blood pressure, blood sugar, and blood lipid levels[22]. While *Sinom* might also promote the same potential benefit of *Kunyit Asem* drink, the value is lower. It was shown that the antioxidant capacity of *Sinom* and the anti-glucosidase activities were lower than Kunyit Asem drink[14].

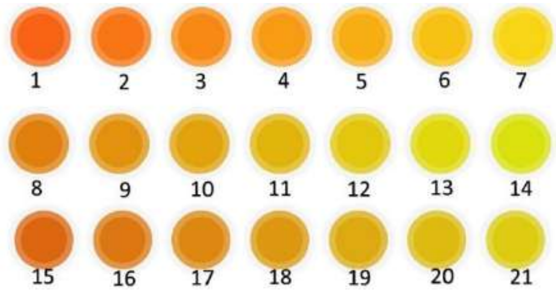

Figures 1. Color choices for *Sinom* and Kunyit Asem drinks

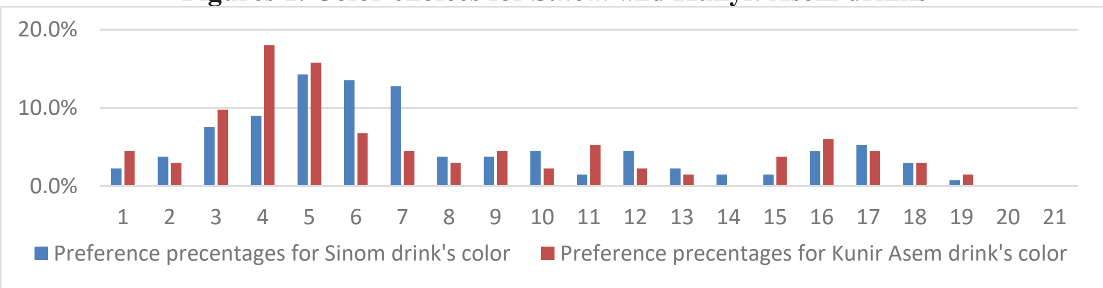

Figure 2. Preference color of Sinom and Kunyit Asem drinks

Figure 1 and 2 shows that the three colors chosen by consumers for *Sinom* products are anomer colors 5, 6 and 7 with percentages of 14%, 14% and 13%. The color choices for tamarind turmeric drink are anomer colors 3, 4 and 5 with selection percentage values of 10%, 18% and 16%. The basic color difference lies in the composition of green and magenta (table 2). Compared to colors chosen by consumers for Kunyit Asem items, colors for Sinom beverage products have a higher percentage of green. This is consistent with the green tamarind fruit leaf extract used in the synthesis of the ingredients for Sinom. The chlorophyll component in the leaves, which generates green, indicates this more intense green

Table 2. The result of consumer color preference from Kunyit Asem and *Sinom* drink.

Color Code		3	4	5	6	7
Description		vivid orange	vivid orange	vivid orange	vivid yellow	vivid yellow
HEX number		F88915	F89C15	F8AF15	F8C215	F8D515
RGB color space	Red	97.30%	97.30%	97.30%	97.30%	97.30%
	Green	53.70%	61.20%	68.60%	76.10%	83.50%
	Blue	8.20%	8.20%	8.20%	8.20%	8.20%
CMYK color space	Cyan	0%	0%	0%	0%	0%
	Magenta	44.80%	37.10%	29.40%	21.80%	14.10%
	Yellow	91.50%	91.50%	91.50%	91.50%	91.50%
	Black	2.70%	2.70%	2.70%	2.70%	2.70%
Hue angle		30.70%	35.70%	40.70%	45.70%	50.70%
Saturation		94.20%	94.20%	94.20%	94.20%	94.20%
Lightness		53.70%	53.70%	53.70%	53.70%	53.70%
Color Plate						
Product Prefrence		*Kunyit Asem*	*Kunyit Asem*	*Kunyit Asem, Sinom*	*Sinom*	*Sinom*

As for the color picked for the Kunyit Asem beverage, it contains more magenta than the color picked for the Sinom beverage. Although there is no proof that curcumin produces magenta hue, the greater percentage of magenta color in Kunyit Asem beverages is an indication of the higher turmeric concentration. Curcumin is a bright yellow pigment found in turmeric that is widely used as a coloring agent[22], [23]. However, there are studies that show curcumin can be used to produce different colors when mixed with other natural dyes. For example, mixing butterfly pea and turmeric dyes in a 1:4 ratio can produce a green color, mixing butterfly pea and sappan dyes in a 1:8 ratio can produce a purple color, and mixing turmeric and sappan dyes in a 1:2 ratio can produce an orange color[24]. Another theory is that the magenta hue of sour turmeric drinks results from their higher tamarind content than that of *Sinom* beverages. The tamarind reading displays the color reddish brown, or the hexadecimal value 5d0c04. It has 0% cyan, 87.1% magenta, 95.7% yellow, and 63.5% black in a CMYK color space.

As a case in point, there is just one type of color, which is the 5th color, and which uses the hexadecimal code F8AF15 for the two types of drinks. This suggests that it is still possible to understand the similarity warning at the center of the second beverages. Variations and differences in consent will make it very likely that the same warning signal will appear on *Sinom* and *Kunyit Asam* mines. To be sure, this study's findings indicate that flavor and health benefits rank as the two main justifications for purchasing herbal products before danger factors. As a result, the formulation of drinks (whether it is the *Kunyit Asam* or the *Sinom*) is required to have ingredients that are healthy for the body, palatable flavors, and the expected colors.

CONCLUSION

The study was able to show the difference of *Sinom* and Kunyit Asam color. It was yellow to red color obtained in *Sinom* drinks. As for Kunyit Asem, the colors obtained are bright orange, bright brown, and bright brownish red. The color tone of *Sinom* drinks desired by consumers is bright yellow to bright yellow while in the Sour Turmeric drink is bright orange. Both drinks are quite attractive to the teenage and adult female age groups because of their various benefits. Presentation in several community activities (fasting and Eid dishes), the tradition of making your own at home and as a daily snack is a positioning for *Sinom* and *Kunyit Asam* beverage products. In the future, there is potential to develop *Sinom* and *Kunyit Asam* beverage products that have health benefits, preferred flavor, and color.

ACKNOWLEDGEMENT

This work was supported by JSPS Core-to-Core Program, (grant number: JPJSCCB20220006.) and University Research and Community Service, Universitas Internasional Semen Indonesia, through the applied research grants (HRT) year 2023.

REFERENCES

[1] Lin, L., & Mao, P. C. (2015). Food for memories and culture - A content analysis study of food specialties and souvenirs. Journal of Hospitality and Tourism Management, 22, 19–29. https://doi.org/10.1016/j.jhtm.2014.12.001

[2] Meilgaard, M., Civille, G. V., & Carr, B. T. (1999). Sensory evaluation techniques. CRC Press. https://doi.org/10.1201/978100304072

[3] Spence, C. (2023). On the manipulation, and meaning(s), of color in food: A historical perspective. Journal of Food Science, 88(July 2022), 5–20. https://doi.org/10.1111/1750-3841.16439

[4] Oram, N., Laing, D. G., Hutchinson, I., Owen, J., Rose, G., Freeman, M., & Newell, G. (1995). The influence of flavor and color on drink identification by children and adults. Developmental Psychobiology, 28(4), 239–246. https://doi.org/10.1002/dev.420280405

[5] Kunz, S., Haasova, S., & Florack, A. (2020). Fifty shades of food: The influence of package color saturation on health and taste in consumer judgments. Psychology and Marketing, 37(7), 900–912. https://doi.org/10.1002/mar.21317

[6] Widyowati, R., & Agil, M. (2018). Chemical constituents and bioactivities of several Indonesian plants typically used in jamu. Chemical and Pharmaceutical Bulletin, 66(5), 506–518. https://doi.org/10.1248/cpb.c17-00983

[7] Febrianto, P. T., Budiastuti, A., Megasari, L. A., & Prastiwi, M. I. (2023). Healthy behavior and herbal drink consumption among educated youth during COVID-19 pandemic. Jurnal Sosiologi Dialektika, 18(1), 12–20. https://doi.org/10.20473/jsd.v18i1.2023.12-20

[8] Batubara, I., & Prastya, M. E. (2020b). Potential Use of Indonesian Medicinal Plants for Cosmetic and Oral Health: A Review. Jurnal Kimia Valensi, 6(1), 118–132. https://doi.org/10.15408/jkv.v6i1.16252
[9] Wijaya, I. (2012). Socio-cultural Knowledge and Perceptions of Jamu Consumption Risk: Local Wisdom of Urban Javanese Community and Its Relation to the Integration of Traditional Jamu Medicine into Formal Health System in Indonesia. Jkm, 11(2), 129–139.
[10] Dameria, L., Dewi, N. P. K., & Cudivia, V. G. (2022). The Potential Benefits of Jamu Kunyit Asam for COVID-19 . Proceedings of the 3rd Tarumanagara International Conference on the Applications of Social Sciences and Humanities (TICASH 2021), 655(Ticash 2021), 1996–2001. https://doi.org/10.2991/assehr.k.220404.328
[11] Husain, F., Yuniati, E., Arsi, A. A., Wicaksono, H., & Wahidah, B. F. (2021). Ethnobotanical knowledge on jamu herbal drink among consumer in Semarang. IOP Conference Series: Earth and Environmental Science, 743(1). https://doi.org/10.1088/1755-1315/743/1/012019
[12] Ummah, H., & Hayati, M. (2022). Preferensi Konsumen Jamu Kunyit Asam di Madura. Agriscience, 2(3), 729–742. https://doi.org/10.21107/agriscience.v2i3.13815
[13] Harmayani, E., Anal, A. K., Wichienchot, S., Bhat, R., Gardjito, M., Santoso, U., Siripongvutikorn, S., Puripaatanavong, J., & Payyappallimana, U. (2019). Healthy food traditions of Asia: Exploratory case studies from Indonesia, Thailand, Malaysia, and Nepal. Journal of Ethnic Foods, 6(1), 1–18. https://doi.org/10.1186/s42779-019-0002-x
[14] Widari, I. A. A., Mulyani, S., & Admadi, B. (2014). Kunyit Asam and Sinom Beverages Inhibition with a-Glucosidase Enzyme Activity. Jurnal Rekayasa Dan Manajemen Agroindustri, 2(2), 26–35.
[15] Windasari, W., Hariyati, N., Haq, M. syahidul, & Mudjito, M. (2021). Sinom Fresh Herbal Drink Minuman Sehat Bagi Masyarakat Terdampak Pandemic Covid 19. Transformasi Dan Inovasi : Jurnal Pengabdian Masyarakat, 1(1), 45–50. https://doi.org/10.26740/jpm.v1n1.p45-50
[16] Wulandari, R., & Azrianingsih, R. (2014). Etnobotani Jamu Gendong Berdasarkan Persepsi Produsen Jamu Gendong di Desa Karangrejo, Kecamatan Kromengan, Kabupaten Malang. Biotropika, 2(4), 198–202. https://doi.org/10.3956/2009-30.1
[17] Kurniawan, A., Piliang, Y. A., & Budiwaspada, A. E. (2023). Taste Perception from Jamu Drinks Color for Younger Generation by using Photo Products. International Journal of Management, Entrepreneurship, Social Science and Humanities, 6(1), 1–13. https://doi.org/10.31098/ijmesh.v6i1.1338
[18] Nurhayati. (2018). Aplikasi Color Analysis untuk Memprediksi Kepekatan Minuman Kopi Tubruk. Jurnal Pendidikan Fisika Dan Fisika Terapan, 2018(1), 22–26.
[19] Febrianto, P. T., Budiastuti, A., Megasari, L. A., & Prastiwi, M. I. (2023). Healthy behavior and herbal drink consumption among educated youth during COVID-19 pandemic. Jurnal Sosiologi Dialektika, 18(1), 12–20. https://doi.org/10.20473/jsd.v18i1.2023.12-20
[20] Spence, C. (2016). The Crucial Role of Color in the Perception of Beverages. https://api.semanticscholar.org/CorpusID:148418320
[21] Spence, C. (2019). On the relationship (s) between color and taste/flavor. Experimental Psychology.
[22] Wiradnyani, N. K., & Wartini, N. M. (2014). Komposisi Senyawa Penyusun Minuman Sinom (curcuma domestica val.- tamarindus indica l.). Media Ilmiah Teknologi Pangan, 1(1), 10–23.
[23] Eltoum, M. S. A., & Elfaki, Al. A. M. (2020). Extraction, Characterization, and Usage of Turmeric Curcumin for Color Coating of Metronidazole Tablets. https://api.semanticscholar.org/CorpusID:225783758
[24] Musdalifa, Chairany, M., Haliza, N., & Bastian, F. (2021). Microencapsulation of three natural dyes from butterfly pea, Sappan wood, and turmeric extracts and their mixture base oncyan, magenta, yellow (CMY) color concept. Canrea Journal: Food Technology, Nutritions, and Culinary Journal. https://api.semanticscholar.org/CorpusID:244111927

CUSTOMER PERSPECTIVES AND PREFERENCES FOR THE COLOR IN SORGHUM COOKIES CAUSED BY DIFFERENT TYPES OF SUGAR

Azzahra, Laily Rahmadina[1]; Mardhiyyah, Yunita Siti.[2]

[a] Agro-Industrial Department, Universitas Internasional Semen Indonesia, Indonesia

*Corresponding author: laily.azzahra20@uisi.ac.id

ABSTRACT

Consumer preferences for different types of cookies have been extensively studied by researchers in the food industry. These studies have revealed that consumer behavior is influenced by a variety of factors, including taste, texture, appearance, and nutritional value. Color plays a critical role in our perception of food. In this essay, will explore the relationship between color and consumer preferences for sorghum cookies in varying shades of brown. To investigate consumer preference for brown vs. dark brown sorghum cookies based on sugar content, a study was conducted using a sample at least 100 participants. The data collected from the survey will analyze with multiple linear regression method using SPSS application. The result show that the appearance variable has an important influence on consumer perspectives and preferences for color in sorghum cookies due to differences in sugar. Then it is influenced by the aroma variable and also its usefulness.

Keywords: *Cookies, sorghum, sugar, healthy food, color food*

INTRODUCTION

Sorghum is a cereal grain that has been used for centuries in various food products, including cookies. Sorghum cookies are becoming increasingly popular due to their unique taste, texture, and nutritional value. Sugar is a common ingredient in cookies and other baked goods. Sugar adds sweetness, texture, and color to baked goods. There are different types of sugar, including white sugar and brown sugar. The type of sugar used in a recipe can affect the color, texture, and taste of baked goods.

This research journal aims to investigate consumer perspectives and preferences for color in sorghum cookies due to differences in sugar. The study will explore the impact of sugar type on the appearance, taste, scent, process of the production, ingredient and the benefits that exist in ingredients of sorghum cookies and how these factors influence consumer acceptance. By understanding consumer preferences for color in sorghum cookies, this study can help food manufacturers and bakers create products that meet consumer demand and promote healthy eating habits.

The study will then proceed with a consumer survey to collect data on consumer. The survey will be conducted online and will target a diverse group of participants from different age groups, genders, and cultural backgrounds. The survey will include questions on consumer demographics, cookie consumption habits, and preferences for color in sorghum cookies. Finally The data collected from the survey will analyze with multiple linear regression method using SPSS application.

METHODOLOGY

Sampling and Data Collecting

This research is quantitative in nature using respondents. The population in this study are consumers who have tried to consume Healthy snacks. While the samples used in this study were different sorghum cookies which were influenced by the use of sugar. The number of respondents is calculated based on the Lemeshow formula as follows (Sari, Mardhiyyah, & Satiti, 208). The number of samples in this study were 101 respondents. At least it exceeds the minimum limit of the number of samples that must be used.

Operational Variable Stage

The variables used in this study are divided into 6 X variables, namely:
X1 = Appearance indicators (typical appearance of cookies, texture and interest in consuming)
X2 = Taste indicator (sweet)
X3 = Scent indicator (typical cookie scent)
X4 = Indicators of the production process (hygiene, good ingredients and length of cookie baking)
X5 = Indicators of content in ingredients (use of sugar, eggs and also sorghum flour used)
X6 = Indicator of benefits (has high health benefits)

Meanwhile, variable Y is consumer preference for the effect of color resulting from differences in the use of sugar in sorghum cookie products.

Data Analysis

Validity and Reliability Tests

A total of 15 questions made in the questionnaire were tested with validity and reliability tests. The validity test used is the Pearson bivariate correlation if r count> r table, then the instrument is significantly correlated or valid. In this study, the number N = 101, so the df value = 99 in table R. Meanwhile, the reliability test uses the Cronbach alha parameter, if (α) is more than 0.6 to be declared reliable.

Classical Assumption Test

The classical assumption test used in this study consists of normality test, and multicollinearity test. All tested with SPSS.

Multiple Linear Regression Test and Coefficient of Determination (R Square Value)

Multiple regression analysis was used to determine whether there was an influence related to variables (X1, X2, X3, X4, X5, X6) with (Y) consumer preferences on the effect of color resulting from differences in the use of sugar in sorghum cookies products. Data was analyzed using SPSS. The Multiple Linear Regression Model that will be used is:

$$Y = \alpha - \beta 1X1 + \beta 2X2 + \beta 3X3 + \beta 4X4 + \beta 5X5 + \beta 6X6$$

Description:

Y	= Preference
α	= Constant of regression decision
β1, β2, β3, β4, β5, β6	= Multiple regression coefficients
X1	= Appearance
X2	= Taste
X3	= Scent
X4	= Process
X5	= Raw Material
X6	= Benefits

Test the coefficient of determination (R Square value) based on the model obtained. The greater the R value, the better the model obtained.

Hypothesis Test

Hypothesis testing is used to determine how significant the relationship between the variables used in the test is:

a. H1: There is an influence of appearance variables (X1), taste (X2), scent (X3) process (X4), ingredients (X5), benefits (X6) on consumer perspectives and preferences for color in sorghum cookies (cream color) caused by differences in sugar.
b. H2: There is an influence of appearance variables (X1), taste (X2), scent (X3) process (X4), ingredients (X5), benefits (X6) on consumer perspectives and preferences for color in sorghum cookies (light brown color) caused by differences in sugar.
c. H3: There is an influence of appearance variables (X1), taste (X2), scent (X3) process (X4), ingredients (X5), benefits (X6) on consumer perspectives and preferences for color in sorghum cookies (dark brown color) caused by different sugars.

Table 1 Research Instrument Grids

Variable	Indicator	Item
Appearance	Typical appearance of cookies, texture and attractiveness to consume	3
Taste	Sweet	1
Scent	The distinctive aroma of cookies	1
Process	Hygiene, good ingredients and cookie baking time	3
Ingredients	The use of sugar, eggs and also sorghum flour used	3
Benefit	Has high health benefits	1
Preference	Consumer preferences in choosing cookies	3

RESULT AND DISCUSSION

Profile and Respondent Description

The 101 respondents were dominated by women with 71 people (71%) while 29 people were male (29%). The majority are aged 15-25 years with 74 respondents (74%). The occupation owned as a student / student with a total of 64%. The respondents' monthly income can also be the reason why they do not often consume healthy snacks.

Instrument Test

Validity and Reliability Tests

Table 2. Reliability Test Results

Color of sorgum cookies	*Cronbach's Alpha*	N of Items
Sorghum cookies with cream color	0,932	15
Sorghum cookies with light brown color	0,938	15
Sorghum cookies with dark brown color	0,955	15

From the data it can be concluded that the validity and reliability tests are valid.This part is generally composed of the result and the discussion. The research finding should be

Classical Assumption Test
Normality Test, Multicollinearity Test

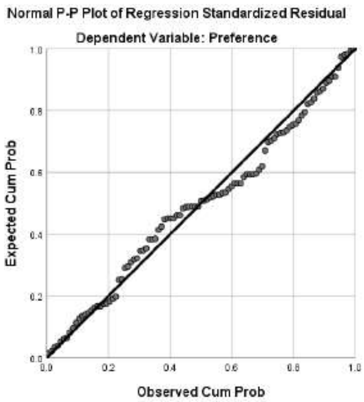

Figure 1 Sorghum Cookies with Cream Color

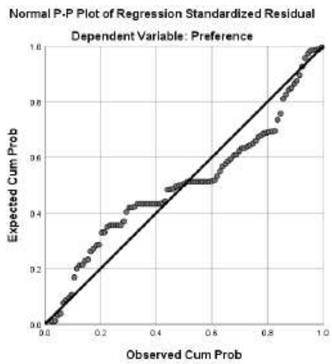

Figure 2 Sorghum cookies with light brown color

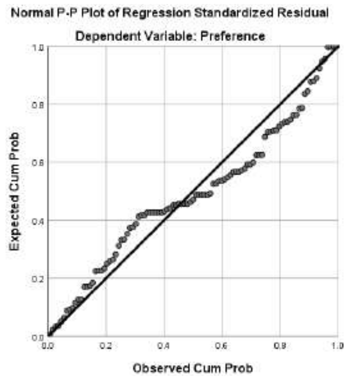

Figure 3 Sorghum cookies with dark brown color

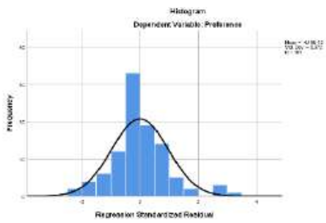

Figure 4 Sorghum Cookies with Cream Color

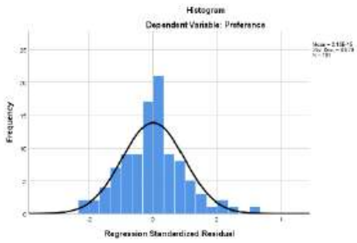

Figure 5 Sorghum cookies with light brown color

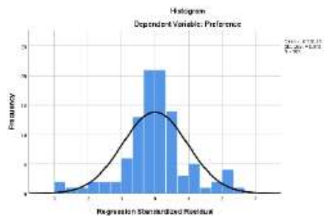

Figure 6 Sorghum cookies with dark brown color

In the results of the P-P Plot Curve and also the hydtogram curve of sorghum cookies with cream color has a more symmetrical shape and there is no tendency to the left side or right side when compared to the results of sorghum cookies with light brown color and dark brown color. Thus, the data obtained for sorghum cookies with cream color has a normal distribution value and fulfills the assumption of normality.

	Collinearity Statistics											
	Appearance		Taste		Scent		Process		Ingredients		Benefits	
	Tolerance	VIF	Tolerance	VIF	Tolerance	VIF	Tolerance	VIF	Tolerance	VIF	Tolerance	VIF
Sorghum cookies with cream color	0,354	2,823	0,462	2,166	3,232	3,232	0,363	2,755	0,608	1,644	0,510	1,960
Sorghum cookies with light brown color	0,378	2,644	0,528	1,893	0,312	3,200	0,260	3,848	0,611	1,638	0,579	1,728
Sorghum cookies with dark brown color	0,502	1,991	0,330	3,027	0,311	3,217	0,206	4,845	0,454	2,203	0,468	2,136

a. Dependent Variable Preference

If the VIF value is < 5, there is no multicollinearity, but if the VIF value is > then there is multicollinearity (Sugiyono, 2014). it can be concluded that all the variables in this study do not occur multicollinearity. From the data it can be concluded that the multicoloniearity test is valid

Hypothesis Test

The F_{table} value used in this study is 2.70 (3; 97). The Fcount value of the F test is 30.013, 39.155, 29.191> 2.70 so it can be concluded that H1, H2, H3 and H4 are accepted or the influence of appearance variables (X1), taste (X2), scent (X3) process (X4), ingredients (X5), benefits (X6) on consumer perspectives and preferences for color in sorghum cookies caused by differences in sugar. The Sig. value obtained is <0.000 <0.05 so it can be concluded that H1, H2, H3 and H4 are accepted or the influence of appearance variables (X1), taste (X2), scent (X3) process (X4), ingredients (X5), benefits (X6) on perspectives and consumer preferences for color in sorghum cookies caused by differences in sugar.

Multiple Linear Regression Test and Coefficient of Determination (R Square Value)

Based on the results shows that the R Square value is 0.811, 0.845 and 0.807 respectively. This shows that the variables of appearance, taste, scent, process, ingredients, benefits to perspective and consumer preferences for color in sorghum cookies caused by differences in sugar are 81.1%, 84.5% and 80.7% and the remaining 18.9%, 15.5% and 19.3% are explained by other factors outside the independent variables of the study. Based on testing on the sample, the regression line equation can be drawn as follows:

1. Sorghum Cookies With Cream Color

$$Y = \alpha - \beta 1X1 + \beta 2X2 + \beta 3X3 + \beta 4X4 + \beta 5X5 + \beta 6X6 \qquad (2)$$

$$= 0{,}198 + 0{,}510X1 + 0{,}092X2 + 0.069X3 - 0.303X4 + 0{,}142X5 + 0{,}430X6$$

2. Sorghum cookies with light brown color

$$Y = \alpha - \beta 1X1 + \beta 2X2 + \beta 3X3 + \beta 4X4 + \beta 5X5 + \beta 6X6 \qquad (3)$$

$$= 0{,}445 + 0{,}601X1 - 0{,}019X2 + 0.161X3 - 0.187X4 - 0{,}047X5 + 0{,}025X6$$

3. Sorghum cookies with dark brown color

$$Y = \alpha - \beta 1X1 + \beta 2X2 + \beta 3X3 + \beta 4X4 + \beta 5X5 + \beta 6X6 \qquad (4)$$

$$= -0{,}122 + 0{,}329X1 - 0{,}022X2 + 0.312X3 - 0.0{,}64X4 - 0{,}016X5 + 0{,}304X6$$

CONCLUSION

This study found that overall appearance, taste, scent, process, ingredients, benefits will have a significant influence on Consumer Perspectives and Preferences for Color in Sorghum Cookies caused by Sugar Differences. Mahony (2011) highlights that colour can significantly impact a consumer's perception of quality. In particular, a consumer's initial impression of a product often stems from its appearance, which encompasses factors like size, shape, texture, and colour. Inadequate attention to colour selection could have adverse effects on the consumer's perception of the product's quality. If a consumer deems the colour of a certain food product to be unsatisfactory, they may be deterred from tasting it, thereby making it difficult to evaluate its flavour and texture - two other crucial factors in determining quality. Moreover, for some food products, colour can be directly indicative of quality.

The results of this study are in accordance with several sources above. Respondents in this study were dominated by women, with a ratio of 71%: 29% when compared to the number of male respondents. Their age is also in the age range of 15-25 years old with status as students and students. With a monthly income of only IDR 1,000,000. This gives the fact from the respondents that they mostly do not consume healthy snacks more than once a month. Respondents who consume healthy snacks more than 2 times a month are dominated by those over 30 years old with a monthly income above RP 1,000,000.

In brief, it can be seen that the appearance variable has an important influence on consumer perspectives and preferences for color in sorghum cookies due to differences in sugar. Then it is influenced by the aroma variable and also its usefulness. Brown sugar and white sugar are both types of natural sugars that are produced from sugarcane or sugar beet plants. The main difference between them is the presence of molasses, which gives brown sugar its distinctive flavor, color, and texture (Yuwana *et all*, 2022). Brown sugar contains slightly more minerals like calcium, iron, and potassium than white sugar, but the quantities are so minuscule that they won't provide any significant health benefits (Darma, 2019). Selain itu juga sorgum sendiri memili banyak manfaat diantaranya ialah kaya akan serta, kaya akan zat besi, mengontrol diabetes dan masih banyak lagi (Sukarminah, 2017).

ACKNOWLEDGEMENT

This work was supported by JSPS Core-to-Core Program, (grant number: JPJSCCB20220006) and University Research and Community Service, Universitas Internasional Semen Indonesia, through the applied research grants (HRT) year 2023.

REFERENCES

Darma, D. P. (2019). *Karakterisasi Profil Sensori Gula Merah Tebu (Brown Sugar) dan Pengaruhnya Terhadap Kualitas Sensoris Kopi Robusta Tirtoyudo Menggunakan Metode JAR (Just-About-Right).* Malang: Universitas Brawijaya.

Mahony, A. (2011). *EFFECT OF COLOR ON THE ODOR, FLAVOR, AND ACCEPTANCE PROPERTIES OF FOODS AND BEVERAGES.* Manhattan, Kansas: Kansas State University.

Sari, N. L., Mardhiyyah, Y. S., & Satiti, D. (n.d.). Faktor Produk, Harga, dan Kualitas Pelayanan pada Keputusan Pembelian Konsumen Hisana Fried Chicken Wringinanom. *Maritime Business Management Conference*.

Sukarminah. (2017). Tepung sorgum sebagai pangan fungsional produk sinbiotik. *Jurnal Pengabdian Kepada Masyarakat*.

Yuwana, A. M., Putri , D. N., & Harini, N. (2022). Hubungan Antara Atribut Sensori dan Kualitas Gula Merah dan Tebu : Pengaruh pH dan Kondisi Karamelisasi. *Jurnal Teknologi Pangan*.

COLOUR DESIGN AND CONSERVATION OF GUMMER AND FORD LIBRARIES IN AUCKLAND, NEW ZEALAND: GUIDELINES AND COMPARISON WITH NOTABLE BUILDINGS (1923-33)

Alessandro Premier[1]* and Julian Rennie[2]

[1]*Faculty of Creative Arts and Industries, School of Architecture and Planning, Future Cities Research Hub, The University of Auckland, New Zealand.*
[2]*School of Architecture, Unitec Institute of Technology, Auckland, New Zealand.*

*Corresponding author: Alessandro Premier, alessandro.premier@auckland.ac.nz

ABSTRACT

Architect William Gummer (1884-1966) was born in Auckland, New Zealand. He left for the United Kingdom in 1908, studying at the Royal Academy of Arts in London, and qualified as an associate of the Royal Institute of British Architects. He notably worked for Sir Edwin Lutyens (and Daniel Burnham of Chicago). Upon his return home he set up the architectural practice "Gummer Ford" in 1923, (with Englishman C.R. Ford, who had travelled as the youngest member of Scott's Antarctica 1901-04 expedition). The practice produced notable buildings in Auckland, firstly in the Beaux Arts tradition and later in the Modernist idiom. One small treasure is the Remuera Library (opened in 1926), which is clad in red brick cavity construction and some solid plaster rendering to the porticos, along with high steel framed windows that activate the reading spaces. The interiors still retain their timber ceiling beams and panelling, giving a gracious and noble atmosphere well suited to the up-market, though conservative, suburb within which it sits. The goal of this research is to reveal the significance of this small architectural gem within the 'minor' heritage of New Zealand and to outline a proposal for the conservation of its colours in the near future. This study presents an analysis of the current building colours and a comparison with relevant buildings designed by the same Architectural firm within a similar period, notably: the Grey Lynn Library, (painted brick clad); the Auckland Wintergardens; the Jubilee Institute for the Blind Foundation Building; and Auckland Railway Station. The research methodology includes literature review, archival research, as well as on-site analyses. The latter includes the identification of the aforementioned buildings' colour palettes of the external façades, by using the NCS Colourpin SE tool. The colour palettes – generated according to the NCS 1950 chart – have been compared with archival material (photos and drawings) to better understand the most appropriate strategy for colour conservation. A comparison with the colour palette of the above latter three (natural brick clad) buildings provides further insights for conservation strategies. The final colour palettes will be useful to practitioners for future conservation projects of these gems from this period of early New Zealand's 20th Century architecture. Our results also provide a brief guideline for the colour conservation of the Remuera Library.

Keywords: New Zealand Heritage; Colour conservation; Cultural heritage

Figure 1a. (left) – Remuera Public Library – Main Façade facing Remuera Road, 28.08.2022. Figure 1b. (right) Former Lecture Hall with West entry, 06.08.2023. Photos by Authors.

INTRODUCTION

An important milestone for establishing public libraries in Auckland city was set in motion by local bookbinder - William Ley, with his idea of encouraging literary pursuits within the inner city and the subsequent opening of The Ley's Institute Library in St Mary's Bay, (Ponsonby), Auckland, New Zealand in March 1905. Then, as each city suburb merged with Auckland City, the council reciprocated by extending its library service into that district. The residents of Remuera, (many of whom were opposed to an amalgamation with Auckland), were appeased when they were given a wooden building as a library in October 1915. Then, in 1926 that timber building was replaced by a new brick building designed by Gummer Ford Architects (Shanahan, 1983, p.239). The new building still sits with its long (north) facing elevation onto Remuera Road, and its shorter (west) facing elevation onto the side street - St. Vincent Avenue.

The main entry into the Remuera Library is via a rather grand portico from Remuera Road, (comprising of solid plaster finished circular and square columns). Entering the main space, one surprisingly steps immediately into library space itself, (compared to the Grey Lynn Library with its tight entry vestibule). The Children's section is to the East, and the reading room to the West. The height of these spaces is 5.1m, (with down-stand beams at 4.875m AFFL), the light entering both flanking spaces is via pairs of arched steel joinery windows (like those of Grey Lynn Library). The Office space was originally in the middle, (it is now tucked behind the Children's area to the East), beyond this main entry space. This middle space also has ceiling height of 5.1m, and like Grey Lynn Library it has high set laylights bringing natural light down into this central area. Originally to the South, (and now behind this mid-space), was a separate 400 seat lecture hall (Shanahan, 1983, p.241), with its own entry from the West off St. Vincent Avenue. This external entry remains, complete with its portico. The wall between this hall space and the library has since been removed (as has the seating). The current ceiling height (and we assume of the original hall) is 5.47m (with down-stand beams at 5.20m AFFL). Originally this "hall" was softly lit (via South facing rectilinear windows), rather than the grand arched windows of the North and West Main reading spaces). Today, the opening up of this mid-space to the North and South Reading spaces enlarges the whole floor plan area allowing more book and magazine shelves (Figure 1b). This building won Gummer Ford Architects the N.Z.I.A Gold Medal award in 1928, "described as finest small library in the nation" (Shanahan, 1983, p.242).

METHODOLOGY

The research was carried out in two directions following a methodology based on literature review and a field study using the NCS Colourpin SE tool. The literature review, based on various texts and online resources, helped to galvanize the research in its two-pronged approach: namely to establish what the colour palette of the Remuera Library is, and to compare it with three other buildings designed by Gummer Ford in the 1923-33 period. Relevant colour theories and schemes of that time were also considered in the comparison. It is important to specify that we based our research on the current surface colours of each building, as it is not possible to capture some of the original colours due to the intervening modifications that have occurred over the years. It should also be noted that the buildings we considered in this study all have brick facades which are still the original brick cladding material from the 1920's. To establish the colour palette of each building a field study was carried out using the "Natural Colour System (NCS)" which is the colour model most used by professionals in this field. Surface colours were detected by pressing the NCS Colourpin SE tool directly against each surface and reading the possible matches on the Colourpin software on an adjacent smartphone. The colours have been tabulated via the NCS 1950 chart and the relative RGB values provided by the Colourpin software, (refer below). The Remuera Public Library colour palette has been compared with the colour palettes of three other facades of notable buildings of the same period designed by the same architects. That is, we compared the Remuera Library façade with the painted brickwork of the Grey Lynn Library (1924) and then with other public buildings that have natural brick facades: the Jubilee Institute for the Blind Foundation Building (1926), Auckland Railway Station (1927), and the Auckland Domain Wintergardens (1928).

RESULT AND DISCUSSION: THE REMUERA PUBLIC LIBRARY

The Remuera Public Library's façades are essentially tripartite. They are characterised by a painted plastered base (white) (1), a main body clad with unpainted bricks (2) with white painted steel window frames and an upper fascia with balustraded parapet, plastered and painted in the same colour as the building base (3). The main façade is characterised by its portico (unpainted plaster) with white entry doors. The entire building's envelope presents the same colour scheme. The indoor spaces are painted white with the exposed timber structure of the ceiling and of the internal doors. The colour scheme is relatively simple and less decorated than other public buildings of the period. The current conservation status of the building materials used are generally very good, and the bricks are also of good quality, indicating the relatively high economic budget of the construction. Several colour samples have been taken of the bricks and all of them were very similar, thus indicating the homogeneity of the brick façade and a particular care in the selection of the bricks.

REMUERA PUBLIC LIBRARY (1926)

OUTDOOR

	NCS 1950		RGB	ELEMENTS
FACADES	S 1505-G80Y		212,210,193	PAINTED PLASTER: BASE
	S 2005-Y20R		204,194,178	UNPAINTED PLASTER: PORTICO
	S 5030-Y50R		144,90,62	BRICK: NORTH SIDE
	S 5030-Y50R		144,90,62	BRICK: EAST SIDE
	S 2005-G80Y		201,199,180	WINDOW SILL: PAINTED PLASTER
	S 0803-G40Y		235,236,226	WINDOW FRAME
	S 5030-Y80R		136,78,67	DOWNPIPE
	S 0502-G		233,236,232	METAL BALUSTRADE (WHITE)
	S 8005-R80B		51,55,63	METAL BALUSTRADE (BLACK)

	NCS 1950		RGB	ELEMENTS
DOORS	S 0300-N		246,243,239	ENTRY DOOR: NORTH SIDE
	S 0500-N		240,237,233	ENTRY DOOR: WEST SIDE (OUTER)
	S 8005-Y80R		69,53,49	ENTRY DOOR: WEST SIDE (INNER)
	S 0300-N		246,243,239	DOOR: WEST SIDE

INDOOR

	NCS 1950		RGB	ELEMENTS
MAIN ROOMS	S 1000-N		225,223,221	WALLS
	S 0500-N		240,237,233	WINDOW FRAME
	S 6030-Y70R		111,54,35	TIMBER STRUCTURE
	S 6502-G		97,103,101	CARPET

Figure 2. Colour palette of the Remuera Public Library

RESULT AND DISCUSSION: COMPARISON WITH OTHER NOTABLE BUILDINGS OF THE SAME AUTHORS

The other buildings considered in this study were designed and built within just a few years, (between 1926 and 1933). The Grey Lynn Library was built two years earlier (1923-24). Although there are some noteworthy similarities between the two libraries (similar spatial planning and of the interior layout), there are also some substantial differences. The Grey Lynn's brickwork cladding was over painted, whereas the Remuera Library has remained exposed bricks (Rennie and Premier, 2022). The roof is also quite different, and the Remuera Library is less decorated, with a less articulated colour palette.

As can be seen from the following tables which collate the colour palettes from three other buildings from the similar period by Gummer Ford, the external colours are in a similar value band range, with just some minor shade variances. This is due primarily to the choice of bricks which may indicated a different budget, for example, for the Domain Wintergardens, where the external bricks are darker than the other ones (Figure 3). Downpipes are always in the same colour of the bricks. The Wintergardens were designed by William Gummer in the early 1900s in the style of the famous English partnership of Edwin Lutyens and Gertrude Jekyll and was opened in 1913. The Tropical House, designed by the expanded practice of Gummer & Ford, was added in 1928, along with the central courtyard areas (NZIA, 2023).

DOMAIN WINTERGARDENS (1928)

OUTDOOR

	NCS 1950		RGB	ELEMENTS
FACADES	S 1005-Y40R		232,219,202	PLASTER FASCIA
	S 6020-Y80R		119,75,68	BRICK: WEST PAVILION
	S 6010-Y30R		126,105,85	BRICK: EAST PAVILION
	S 2020-Y30R		217,180,139	BRICK: EAST PAVILION (INDOOR)
	S 6010-Y50R		121,96,81	BRICK: PERGOLA
	S 7010-Y70R		95,69,61	DOWNPIPE
	S 7010-Y70R		95,69,61	TIMBER SHUTTER
	S 2010-Y10R		202,188,159	ENTRY DOOR

Figure 3a. (left) Domain Wintergarden – East Pavilion, 06.08.2023. Figure 3b. (right) Colour palette of the Domain Wintergardens. Photos by Authors.

The Jubilee Institute for the Blind Foundation Building introduces "forest green" coloured external doors which is a typical paint of that period (Premier and Rennie, 2022). This building was part of a series of additions that Gummer and Ford designed for the original building. The headquarters of the Jubilee Institute for the Blind were in fact designed by Edward Bartley in 1909 - this L-shaped block was built in 1926 (Barrie and Gatley, 2007). This same building presents a colour scheme that is very similar to the Remuera Library. Besides the main body of the façade being clad with unpainted clay bricks, porticos are of unpainted plaster and window frames (timber in this case) are also painted white. The building has no base and presents a white cornice.

The Auckland Railway Station is one of the most ornate railway stations in the country. It was modelled on American prototypes. The structure of the building is made of reinforced concrete with a double-brick façade. Although the building has now been attributed a different function, the main entrance and lobby space are still accessible to the public. It received the NZIA Gold Medal in 1931 (Barrie and Gatley, 2007). The main facade presents a more articulated colour palette compared to the other buildings of this study, essentially due to the higher budget for such civic building serving a wider city public (compared to a suburban library). The base is clad with granite and fascia are clad with terracotta mouldings in yellow and pink. Doors are made of brass, instead of timber.

JUBILEE INSTITUTE - FOUNDATION BUILDING (1926)

OUTDOOR

	NCS 1950	RGB		ELEMENTS
FACADES	S 4502-Y		146,141,132	PLASTER: PORTICO
	S 4040-Y70R		161,88,68	BRICK: SOUTH SIDE
	S 5030-Y60R		142,83,58	BRICK: NORTH SIDE
	S 0804-Y10R		239,231,214	WINDOW SILL
	S 0804-Y10R		239,231,214	WINDOW FRAME
	S 5030-R		126,67,71	DOWNPIPE
	S 6020-G10Y		64,97,75	SIDE DOOR (GREEN)

Figure 4a. (left) Foundation Building of the Jubilee Institute for the Blind – Façade facing George Street, 06.08.2023. Figure 4b. (right) Colour palette of the Foundation Building. Photos by Authors.

RAILWAY STATION (1927)

OUTDOOR

	NCS 1950	RGB		ELEMENTS
MAIN FACADE	S 4005-G80Y		152,150,133	GRANITE BASE
	S 4040-Y70R		161,88,68	BRICK (1)
	S 5030-Y70R		142,83,65	BRICK (2)
	S 6020-Y60R		123,81,64	BRICK (3)
	S 2020-Y80R		209,163,152	TERRACOTTA MOUDLING (PINK)
	S 2020-Y50R		212,166,138	TERRACOTTA MOULDING (YELLOW)
	S 1515-Y50R		225,188,160	WINDOW FRAME
	S 6000-N		115,114,113	LEAD WINDOW FRAME
	S 8005-Y20R		71,62,52	BRASS DOOR
	S 2010-Y40R		210,182,157	METAL STRUCTURE (CANOPY)

Figure 5a. (left) Main Façade of the Auckland Railway Station, 11.08.2023. Figure 5b. (right) Colour palette of the Railway Station. Photos by Authors.

BRIEF GUIDELINE FOR CONSERVATION

Besides maintaining the current colour palette for the interiors and for the facades, as indicated for the Grey Lynn Library (Rennie and Premier, 2022), we would like to suggest a potential review of the colours of the main entry doors of the Remuera Library. All historical photos, as well as those available on Remuera Heritage website indicate that the original doors were in natural or stained timber (preservative) with a similar colour to the interior face of these doors – S 8005-Y80R. Further reflection on the use of carpet flooring could be assessed in regards to its embodied carbon at the next maintenance review. We assume the original timber flooring is largely intact (under the carpet), but that any parts that are found to be rotten should be replaced with matching timber flooring.

CONCLUSION

The Remuera Library's colour palette set out within this paper captures the current colours of the building, which seem to be aligned with the palettes (with subtle variations) of the Gummer Ford's three other buildings within the short time period of 1923-33. Conservation interventions should tend towards the preservation of existing colours, with a critical reflection that could be applied to the colour of external doors and potentially, to the flooring materials. This type of extensive colour mapping of New Zealand heritage buildings, in conjunction with literature review and investigation of historical material, demonstrates the potential of a more extended research on the local built heritage. A more extended colour mapping can constitute the database for a more complete archive of various architect's buildings and their associated periods, providing a comprehensive guideline, not only related to the preservation of colours, but suggesting any possible changes and upgrades for re-aligning the buildings with their original aspect if altered in the future.

Our onsite research and Colourpin analysis of final colour palettes are useful to practitioners in regard to any future conservation, without resorting to damage via 'paint scrapings'. This paper attempts to contextualise one small gem within the Gummer Ford Architect's oeuvre within New Zealand's early 20th Century architecture.

REFERENCES

1. Barrie, A., and Gatley, J. (2007). *Itinerary No. 7. Gummer & Ford 1 – Public Buildings*. Block Architecture Guides from the Broadsheet of the Auckland Branch of the NZIA, Auckland, New Zealand.
2. NCS (2007). *NCS DIGITAL ATLAS 1950*. Natural Color System: Stockholm, Sweden.
3. NZIA (2015). *Gummer & Ford - Public Buildings*. Auckland: New Zealand Institute of Architects, New Zealand.
4. NZIA (2023). *2023 Auckland Architecture Awards Winner. Domain Wintergardens (1928)* https://www.nzia.co.nz/awards/local/award-detail/11179
5. Petry, B. (1992). *The public architecture of Gummer and Ford*. M.Arch thesis, The University of Auckland, New Zealand.
6. Premier, A. and Rennie, J. (2022). Colin McCahon's House and its Colours: A Glimpse of New Zealand Beyond its Colonial Past. *Sensing Colour. Proceedings of the International Colour Association (AIC) Conference 2022*. 280-287. International Colour Association (AIC), Toronto, Canada.
7. Rennie, J. and Premier, A. (2022). A piece of New Zealand Heritage: Colour Design and Conservation of Grey Lynn Library. *XVII COLOR CONFERENCE Colour and Colorimetry Multidisciplinary Contributions* Vol. XVII A:121-128. Gruppo del Colore - Associazione Italiana Colore, Italy.
8. Shanahan, K. (1983). *The work of William H. Gummer, architect*. B.Arch thesis, The University of Auckland, New Zealand.

THE IMAGE OF PARIS: DEVELOPMENT OF COLOUR HARMONY ON THE BANKS OF THE SEINE.

Noury Larissa[1*]

[1]*PhD in History of Art and Architecture, Professor of ColourITECOM Art&Design Paris President founder "Couleur-Espace-Culture"Paris France*

*Corresponding author: larinoury@gmail.com

ABSTRACT

The colour harmony is an essential component of the environment of city of Paris. The conceptualization and manipulation of colour harmonies concerns all areas of creation, be it in urban planning, architecture or art. The mystery and brilliance of colour, its many nuances and complex harmonies, touches all historical periods and styles. Art, design and architecture, history and culture - all areas are affected.

The city of Paris with its colour harmonies, rhythm and perspective is a self-portrait of French society. In the process of social development and the perfecting of urban art, a variety of different types of colour harmonies and architectural styles were created. The introduction of colour combinations in correspondence with different styles of urban art creates a visual composition of the city, which is a synthesis of the superposition of its historical layers. The image of the city of Paris (colours, cultures, architectures) is enriched by the perception of all visual elements of our built environment (architecture, urban and landscape design, infrastructure). In order to understand urban spaces and the improvement of the city's environmental quality it is indispensable to have the knowledge about both national and local tradition, historical and modern colour preferences and cultural particularity.

Our work raises a historic panorama of the colour in the city of Paris during the II-XXIth century, highlighting certain symbolic movements such as the Middle ages, Gothic, Renaissance, Baroque, the Classicism, the Empire, the Rococo, the Eclectic style, the Art nouveau, the modernism, urban op art & pop art or the street art. Through the prism of historical and intercultural approach, our study shows the evolution of colour palettes and invites you to an imaginary journey into the infinite universe of colour harmony throughout different historical periods and styles: it shows us how the phenomenon of colour and its symbolic language have evolved alongside the centuries.

It desks the system of colours harmonies and describes the palettes which allow to understand their evolution. The harmony of colour as a separate material and colour-light reinvests the image of the city.

Keywords: *colour harmony, evolution, art, architectural styles, cultural identity*

INTRODUCTION

The city of Paris has a long history of local traditions connected to the water. Paris was born and grew up with water of the Seine that a 777-kilometre-long river and an important commercial waterway within the Paris basin in the north of France. The name "Seine" comes from the Latin ***Sequana*** the Gallo-Roman goodness of the river. Since the beginning of our times, when Paris was still called Lutetia, the city has experienced four different periods of production and distribution of water: The Roman Age, the Middle Ages, the Modern era and the nineteenth century Industrial Revolution.

Even the coat of arms of the city of Paris (French: *Blason de Paris*), in its current form, dates back to 1358 and is connected to the water. The first mention of the coat of arms of Paris appears as early as 1190 when King Philippe Augustus designed the city.
On the coat of arms, the represented vessel is the symbol of the powerful corporate body of "water merchants", dating back to the Middle Ages. The city motto is ***Fluctuat nec mergitur*** ("She is tossed by the waves, but does not sink")
The water is a part of image of Paris and its history from Roman aqueducts to nowadays.

The Gallo-Roman city was developed mainly on the hill on the south bank of the river (the Montagne Sainte-Geneviève) where, starting in the 2nd century AD, public works and monuments were constructed. Under Roman rule, Lutetia was thoroughly romanized and its architecture had the same features as roman: aqueducts, open theater, public baths were decorated with intact architectural elements such as Gallo-Roman vaults, ribs and consoles, and fragments of original decorative wall painting and mosaics.

Water of the Seine in the Middle Ages was an essential part of image of the city of Paris with its bridges and especially symbolic Notre Dame de Paris, built at the middle of island Cité. At the time of renaissance City hall was constructed by the river, place de Grève, ("Strand Square"), a place where Parisians often gathered, particularly for public celebrations and executions. Ever since 1357, the City of Paris's administration has been located on the same location where the Hôtel de Ville stands today. Moreover, the oldest monumental fountain in Paris is The Fontaine des Innocents, a monumental public sculptural construction in the new style of the French Renaissance.

Modern time, barroco, rococo, neoclassicism embellished the image of Paris by the polychromy of royal parks and its famous fountains, they were located on the site of the Vaux de Vicomte, Saint-Cloud, Versailles and other residence of royal and imperial families from the 16th century. The Bassin de la Villette, symbol of a pro-industrial culture, used to be a harbour during the era of industrialization of rivers and waterways for transport trade in Paris. Highly known for its commercial and industrial purpose, it is nowadays an animated "full of life" venue hosting many cultural events. Bassin de la Villette was inaugurated in 1808 by Napoleon Bonaparte the 1ST and was popular for leisure activities: La Rotonde de la Villette is the only vestige of an asymmetrical ensemble, which included two barriers: Saint Martin barrier and Pantin barrier.

Industrial era change the image of Paris. Haussmann's renovation of Paris was a vast public works program commissioned by Emperor Napoleon III. It included the demolition of medieval neighborhoods and the building of wide avenues, new parks, squares, the annexation of the suburbs surrounding Paris, the construction of new sewers, fountains and aqueducts. The street plan and distinctive appearance of the center of Paris today is largely the result of Haussmann's renovation.

Paris has 37 Bridges mostly constructed in industrial era. Haussmann also built the parks surrounded by water. The Bois de Vincennes (1860–1865) remains the largest park in Paris, designed to give green space to the working-class population of east Paris.

Haussmann built the park Buttes Chaumont on the site of a former limestone quarry at the northern edge of the city.

Parc Monceau, formerly the property of the family of King Louis-Philippe, was redesigned and replanted by Haussmann. Parc Montsouris (1865–1869) was built at the southern edge of the city, where some of the old catacombs of Paris had been.
The Square des Batignoles is also one of the new squares that Haussmann built in the neighborhoods annexed to Paris in 1860.

Artists and especially the impressionists were very inspired by the Seine River and by the bridges crossing the river Paul Signac & Henri Edmond Cross, Gustave Caillebotte, Camille Pissarro &Claude Monet.

New modernism and art deco by Le Corbusier in the twenties and the Museum of modern art and palace of Tokyo, Trocadero square in the thirties were the source of inspiration for Museum Pompidou: Rogers and Piano, for Square Kandinsky by pop artists Tangely and Niki de Saint Faille, the Parvis de la Defence with Agam fountain with Venice glaces, the Park de la Villette by Bernard Tshumi, the Museum Quai Branly by Jean Nouvel & Kersale and Museum – fondation Louis Vuitton. O' Genri & Daniel Burren color installation.

METHODOLOGY

The harmony of colour is a universal, transcultural phenomenon. Whether it is the creation of images, the invention of drawings for the design industry or the construction of urban spaces, it represents a system of coded messages of the visual world that helps us to apprehend, evaluate and act in different contexts.
Through the prism of historical and intercultural approach, our study and 3 published books show the evolution of colour harmony and invite you to an imaginary journey into the infinite universe of colour harmony in different cities of the world. Throughout space and time, it shows us how the phenomenon of colour and its symbolic language have evolved alongside the civilizations and societies.
Beginning from the time of primitive civilizations, they are not self-generating but are in constant dialogue with environment. They could be abstract or figurative, monochromatic or polychromatic, composed of earth materials or designed with modern tools and technologies.
The choice of colour harmonies tells us about historical-ethnographic, ethnic origin and the palette of local material shows us the relationships between different cultural and geographical contexts.

ECOLOGICAL APPROACH OF COLOUR HARMONY: XXI° century

Nowadays, the layered image of the modern town society consists of multiple *chromoplastic* levels that give dimension and refer to organizing the distribution of values.

The colour image of the city is rooted in its geographical space, but changes over time: its modifications have always been due to the evolution of architectural and urban planning of the city and is still constantly changing. If all the visual elements of urban space and land territory compose the integral image of the city, the color remains an essential part of the architectural, cultural and social heritage.
The social role of colour and light in city architecture and environment:

- Creation of a visually comfortable coloured climate, and aesthetic interest;
- Stabilization and maintenance of perception and visual activity (architectural polychromy must be applied according to different levels of perception of the building, starting from its silhouette through to the surface texture);

- visual and psychological interaction of architectural polychromy with the landscape (conjunction, camouflage or contrast with the natural landscape);
- Finding connections with the artistic traditions and culture of the colour of the area.

Today, the city of Paris aspire to offer their inhabitants a high quality of living environment while respecting its geographical properties, landscape and architectural culture of their own. This is why the debate on the sustainable town must include a chromatic environmental strategy. Currently, designing color in the towns & cities is part of new planning ideas and urban innovations. The intelligence in the choice of color codes and chromatic harmonies can revitalize urban space by promoting a sense of security and serenity among citizens.
This approach is also social because it takes into account the preferences of the population of the city. The harmonization of city centers with their peripheral and industrial areas and their landscape, the development of their dominants or visual accents can break the feeling of isolation and of disproportion. This environmental strategy allows the continuity in the perception of the town or city: to analyze the overall image of the city and of each of its neighborhoods, and of its districts and their buildings, and even the design of street furniture, landscape qualities and setting of artificial lighting.
It results to the ecology of color as a major constituent of the environmental project to be included in the global project of sustainable development of the town & city. It identifies the "genetic heritage" and create visual pallets respecting the "spirit of the place".
It will create an environment of good chromatic quality for new neighborhoods by integrating new national and international cultural contributions, and therefore leaving the door open to creation. Urban color, rich and complex, lively and full of meaning will participate in the image of the town/city of the XXI century, thus becoming more sensitive and human.

THE FUNDAMENTAL GROUPS OF COLOUR ASSOCIATIONS IN URBAN ENVIRONMENT

Our study is at the crossroads of artistic, architectural, and urban environmental design studies, based on historical and scientific reasoning. We apply the method of environmental colour study with the Natural Colour Systems as a visual analysis tool.
We propose the system of 24 colour harmonies classification which help us to explore the infinite universe of colour relationships in Art, Urban design and Architecture.
Some examples of colour harmonies.
Between two extremes - what is the future of urban environment?
The "vernacular" colour, chaotic and spontaneous or the totalitarian order of the strictly organized “pixels idealization“ & “ecocolour”?
The results of these investigations are the part of educational programs for students that we developed for different grades of academic studies according our own practice of many years teaching in Art & Design School and Universities:

- The goal is to help students think creatively and express their own personal perception, taking into consideration the diversity of world cultures, the different styles, art schools & movements of the XX th century. Art as a crossroad between visual and applied fields of art. Classification of Colour harmonies associations.
- Art & Visual harmony with environmental design and architecture. Fine art, visual communication, symbolic and cultural traditions in art and design: web design, motion design, and visual communication, digital and Immersive art, video installation.
- Image of the city and cultural identity, design & architecture of modern cities from antic civilization until XXI century.
- Artistic movements & architectural styles trough the history of society and different cultures.
- Sustainable solutions in design and architecture. Ecology, design and public space. Visual identity and urban environment, colour harmony on city’s design.

RESULTS AND DISCUSSION

The harmonies of colors in the visual environment of urban spaces compose and draw the attractiveness and polychromy of life and of the riverside part of the city, highlighting its invisible axes.

Color is definitely the most popular of aesthetic feelings and one that brings over 90% of information through visual perception. For a long time the chromatic identity of the environment is an important visual message. Colors and materials are essential components of spaces and enrich the atmosphere of the underground part of the city by giving it meaning and simplifying the orientation.

Psychological and visual adaptation is unavoidable in urban spaces. This adaptation is possible thanks to chromatic creations of public water transport, “Bateaux mouche” “Vedettes de Paris” stations, bridges or walkways.

Art and modern design (public transport stations, walkways, shelters) by their chromatic harmonies and luminosity produce a specific effect, even more differentiating, organized and amplified by the shapes and chosen colors. They are an essential part of the ecological color strategy. Their color codes vary according to their disposition, according to different points of view and different situations.

The aesthetics of the visual environment of water front spaces of the city of Paris is an essential component of its identity; the combination of colors and lights creates the image of the modern city that is responsible for promoting the security and serenity of its citizens.

COLOR FOR HOSPITALS: COLOR DESIGN VS ARTWORKS

VM Schindler[1,2]*

[1]Art & Architectural Historian, Zollikon, Switzerland
[2]Chair of AIC Study Group on Environmental Colour Design

*Corresponding author: VM Schindler, ecd.studygroup@yahoo.com

ABSTRACT

With the rise of the new profession of the color consultant/color designer in the first half of the 20th century, conscious color application evolved not only for safety and protection reasons to reduce accidents in industrial environments, but also for comfort and wellbeing. In this context, people became aware of the positive, and healing, power of color. Color research expanded to the field of hospitals. In 1942, for example, the French color consultant Jacques Fillacier (1913-1986) realized a color design for a medical-educational center. Additionally, he organized meetings with psychiatrists to discuss the role of color in society and the importance of color in health care facilities that he thought very constructive. Hospitals, clinics, and other types of care facilities stand out for a considerable diversity of functions and spaces grouped within one single architectural complex. Worth mentioning, for example, are reception halls, corridors, waiting rooms, patient rooms, examination rooms, and a large variety of further specialized rooms. One of the first to publish about this topic was Heinrich Frieling (1910-1996) in his 1954 publication about color dynamics and psychological color design, and included a color card with samples to specify colors. It is also interesting to note that psychology is a relatively recent field of research, which began to establish itself in the second half of the 19th century. Later on, Frank H. Mahnke (1947-2015) dedicated a whole chapter in his 1996 book *Color, Environment, and Human Response* on color in health care facilities. On the background of this current short historical survey, some recent projects of the last few years will be discussed. One such example is a project by Axel Buether for an intensive care unit (2018-2019; 2022). Another interesting line of research is how artists deal with color in hospital environments. One such prominent example is Bridget Riley's artistic design for a hospital in London (2014). Another example is a blue-red light installation by Swiss light artist Christian Herdeg for a large-scale interior space of a hospital in Chur (2019-2023). This paper enquires into the ways artists deal with color in hospitals and how color concepts by color designers greatly defer from the intentions of art installations and artworks. This research concludes that the color treatment by these different professional groups is not better or worse; they are not competing, but are complementary.

Keywords: color design, hospital, art in architecture, chromatic atmosphere, color

TOWARDS A FUTURE HOLISTIC INTERIOR DESIGN CONSIDERING COLOR AND LIGHTING TOGETHER.

Maurizio Rossi

School of Design, Design Department, Politecnico di Milano, Italy.

Corresponding author: Maurizio Rossi, maurizio.rossi@polimi.it

ABSTRACT

Color and lighting are intrinsic to interior design, influencing a space's aesthetics and the well-being of occupants. Despite the increasing focus on healthy interiors, research and guidelines often overlook the synergistic relationship between these elements. This desk research explores the physiological and psychological impacts of indoor color and lighting, emphasizing the need for a holistic design approach. It also identifies existing research and standards gaps, particularly in integrating color and lighting. The paper begins with examining the effects of color and light on humans, then addresses the challenges of designing for both elements. Existing standards are reviewed, revealing their limitations in addressing integrated design. Findings underscore the absence of comprehensive guidelines considering the interplay of light and color. In conclusion, this paper advocates for a unified approach to color and lighting design, highlighting the necessity for further research and guidelines. Such an approach can enable designers to create visually appealing spaces and promote occupant well-being and productivity, bridging the current research and design gap in the interior realm.

Keywords: Color, Lighting, Interior design, Holistic design

INTRODUCTION

The concept of Holism evolved in the 20th century within philosophy and biology based on the idea that the universe and its systems should be understood as an integrated whole rather than a collection of isolated parts [1] and in Gestalt psychology, which investigated how we perceive visual information into meaningful wholes [2]. In interior design, the holistic design developed also in the Bauhaus Movement. Although the term holistic design was not used in the Bauhaus, some principles of holistic philosophy were already present in this Movement, such as interdisciplinarity, user-centered design to put the person at the center of the design process and the total vision of the design intervention, in architecture as in interiors, aimed at considering all the design elements as a whole [3]. In the context of interiors, holistic design is an approach to design that takes the entire space into account rather than focusing on specific elements or features. In order to generate a harmonious and integrated human experience, it takes into account the interconnection and interdependencies of diverse parts. Considering the functionality and aesthetics of indoor settings as well as the impact on the user's emotions, physical well-being, and environmental impact, holistic design aims to improve the total user experience. The idea that everything is connected is one of the cornerstones of holistic design. This implies that adjustments made to one component of a project may affect other aspects of the space. The word Holistic refers to viewing the many project components as a totality rather than as separate parts. For example, changing the lighting in indoor environments affects the image perceived by humans and, consequently, the effects we get [4], and the same could be obviously said of surface colors [5].

In this review we consider two main elements of holistic interior design: light and color. The reason why it is so important to focus on light and color indoor for our well-being is because, as a consequence of the Industrial Revolution, the activities of human beings have been transformed, with a migration from the countryside to urban centers and the development of industrialized societies. In just a few generations, we have gone from a life spent working in the open air in the countryside to one mainly indoors. In interiors, the light, the colors, and the perceived image of the surrounding environment completely differ from the open air in which we have evolved for millions of years. This radical change in living environments occurred throughout a few generations. The dimension of change in modern society's lifestyles is often not understood in design practices. Consider that in Europe, in 1800, only 2% of the population lived and worked in cities. It has been estimated that people in today's industrialized countries spend between 80 and 90% of their time indoors [6–10]. Based on this significant change in lifestyles, we observe that 200 years are nothing compared to the evolution of human beings and, from this point of view, the change in the environments in which we live and our exposure to artificial lighting are a very recently introduced factor whose effects have not yet been thoroughly studied [11]. This paper endeavors to accomplish a dual-fold objective. First and foremost, it strives to cultivate an understanding of the paramount importance of embracing a comprehensive approach to lighting and color design in interior settings, underscoring the potential dividends for the well-being and productivity of occupants. Secondly, it embarks on an expedition to identify fissures within current research paradigms and established standards, with a particular focus on their inability to adequately encompass the synergy of color and lighting, while simultaneously proposing promising avenues for future developments in this domain.

METHODOLOGY

In the context of design, desk research is a method based on collecting information from books, peer-reviewed articles and other authoritative data sources. It is also called secondary research to distinguish it from primary research which is based on direct experimentation to test hypotheses or collect data from the real world. In this paper, desk research was used together with references to primary research conducted by the author in the last decade [4].

Color indoors. Color is a visual perception studied in various human disciplines in many different ways. Some early research conducted in the 20th century on color samples highlighted a general preference for blue-green shades over green-yellow and yellow ones [12,13]. However, saturation would interact with lightness, with blue preferred at low lightness, red and green at medium lightness, and yellow at high lightness, while dark shades of orange and green would be very unpleasant compared to bright ones [13]. Even more recently, a preference for cold shades over warm ones would have been highlighted, while more saturated colors would be preferable to less saturated ones [14]. Some research has shown differences in color preferences due to gender [15–17], although this difference may depend on cultural context [18,19] or other factors [20]. Some studies have compared industrialized societies with non-industrialized ones, showing differences in color preferences [21,22]. These results, however, are poorly applicable in Interior design, where colors are always perceived and evaluated in a more complex visual context than color samples. In two studies, the evaluations of the color samples were analyzed with those of the same colors applied to furniture objects, shown on the screen or in photographs, finding a good correspondence between the colors of the samples and those of the objects. The color preference for specific objects was motivated by the fact that some objects would have a color based on visual experience [23]; however, in the second experiment, people preferred more saturated colors on the samples than the objects. They also preferred darker colors for objects, except for walls, where lighter colors were preferred [24]. A key point of this area of research lies in the possible explanation of the mechanism of color preferences, for which three theories have been proposed. The first theory supposes this mechanism resides in the cone-opponent contrast neural mechanisms of the visual system. The blue-yellow channel would be the basis of the differences in humanity, with a preference for blue over yellow, while the red-green channel would be the basis of gender differences in color preferences [19]. A second theory states that color preferences are based on the emotions associated with colors, but this does not explain why the blue of sadness is generally preferred to yellow, which recalls joy [18]. A third theory, the ecological valence theory (EVT), states people prefer colors associated with objects they like, such as blue, which is associated with water, and do not like colors associated with objects they dislike, such as yellow-green associated with spoiled food [25]. This theory could explain the similarities [26] and the differences in color preferences between cultures [21]. Less research has evaluated the physiological effects of color. A study has shown that red has a physiological activation by acting on the galvanic skin response [27]. However, red has psychophysiological arousal effects, too, that can decrease cognitive test performance because it can be associated with the danger of failure [28]. Instead, red would improve sports performance [29] and proofreading tasks, while blue would improve creative performance [30].

Artificial lighting indoors. Over the last 40 years, much scientific research has shown that light can suppress the production of melatonin [31], control the circadian rhythm [32], affect body temperature [33], heart rate [34] and alertness [35]. Based on this and much other research, it is now accepted by the scientific community that light has non-image-forming (NIF) effects on human beings: on the circadian rhythm, on the neuroendocrine system (hormone production), and the neurobehavioral response [36]. It has been highlighted that there are four independent lighting variables to consider for NIF effects: quantity, spatial distribution, temporal pattern of exposure, and spectrum [37]. The CIE S 026/E:2018 standard defined the units of measurement to evaluate the biological potential of light. This introduces the equivalent melanopic daytime illumination (melanopic EDI in Lux), defining the units of measurement of the stimulus, adopted in the SI of measurement, but does not say anything about the effect of this stimulus, nor does it propose design guidelines. The WELL Building Standard and the UL Design Guideline 24480 are now based on units of measurement that can be derived from this CIE standard.

DISCUSSION

Regarding the meaning of color or the psychological effects on human beings, it is believed that these are mainly a function of individuals' learning and social development. However, it has been observed, through cross-cultural studies, that the psychological effects of color could also have biological bases, such as for the color red. So, the environmental and biological reasons for the effects of color are not mutually exclusive but would interact with each other [38].

Unfortunately, much of the research on color has been conducted without considering the multidimensionality of color (hue, saturation, lightness) [39] and without considering boundary conditions such as its appearance as a function of lighting [40]. Much research has only been done on young university students, while it would be appropriate to extend the research to larger and representative samples of all ages and different social backgrounds [41]. Furthermore, most research on the psychological effects of color has been conducted in the laboratory, using samples taken from color atlases, colors reproduced on PC screens, or colors on imagined objects [42], i.e., different conditions than everyday life perception of colors useful for Interior design, and this reminds us of the importance of color vision in the context [38,43]. Elliot highlighted the limited applicability of research carried out on a PC screen or with color samples and for a limited time [44]; furthermore, he defined five fundamental points for reliable experiments on the relationships between color and emotions: participant naiveté and confidentiality, verification of color vision deficiency, adequate size of the sample of participants, color specification and control, background color, and illumination. Unfortunately, even today, most color research partially or entirely ignores the management and accurate description of these factors [45]. The importance of lighting is evident in a study exploring how people react emotionally to the same color as an object or colored light in different lighting levels. Results showed that object colors were more positively associated with comfort and stability for red, green, and blue than luminous colors, but this difference was slight for yellow. Lighting levels influenced emotional responses to object colors but not luminous ones [46].

For Interior Design applications, colors should be experimented with real indoor environments in everyday life, as very few researchers have done [47–50]. Although this research has some boundary limitations, they have confirmed some key factors: color in interiors can affect people on a psychological and physiological level (positively or negatively), affect performance and well-being, and there are differences due to gender. The colors of the walls, from most preferred to least preferred, are blue, green, violet, orange, yellow, and red, while the ceiling is preferably white. The mood also depends on the lighting level, which must not be too low or too high. A moderate increase in the amount of color promotes a positive mood.

CONCLUSION

The results of the 2nd International Workshop on Circadian and Neurophysiological Photometry, in which 18 international experts in lighting, neurophysiology, sleep, and circadian rhythms participated, were published in 2022 to give recommendations for light exposure during the day, evening, and night to best support physiology, sleep, and wakefulness [51]. The design proposals are based on the EDI melanopic, on the vertical plane of the eyes, considered at 1.2m in height. Unfortunately, they do not indicate the preferable colors in Interior design. As we know, indoors, most of the light our eyes receive comes from multiple reflections of light emitted by light sources with interior surfaces because humans instinctively avoid looking directly at light sources [52]. The missing link in the Holistic Design of light and color lies in the difficulty of combining the spatial distribution of light to the eyes with its spectrum, considering the spectral reflectance contributions of surfaces such as walls and furniture [53]. This criticality is fundamental in internal environments where natural light contributes poorly; therefore, the lighting mainly depends on artificial light. The evaluation of melanopic EDI must not take place on the surface object of the visual tasks, as in traditional design, but must be evaluated on the vertical surfaces that identify the eyes of the occupants. This also involves carefully analyzing people's activity profiles, reiterated by the ISO/CIE TR21783. Determining the spectrum of the light that reaches the eyes is still a complex design action because the spectral reflectances of the internal surfaces are not generally known because modern Interior design colors can be highly variable. We know new trends try to avoid uniformity in the visual field indoors, with stimulating patterns, up to the more advanced assumptions of Biophilic Design [54]. A possible future research development could pass through the integrated design process (IDP), with the development of the software tools available to designers for building information modeling (BIM) that could integrate spectral calculation methods and databases of light sources and materials not as RGB values but as radiometric properties.

REFERENCES

1. Smuts, J. C. (1927). *Holism and Evolution* (2nd ed.). Mac Millan and Co.
2. Koffka, K. (1935). *Principles of Gestalt psychology*. Harcourt, Brace.
3. Wingler, H. M. (1969). *Bauhaus: Weimar, Dessau, Berlin, Chicago*. The MIT Press.
4. Rossi, M. (2019). *Circadian Lighting Design in the LED Era*. Springer International Publishing.
5. Elliot, A. J. (2015). Color and psychological functioning: A review of theoretical and empirical work. *Frontiers in Psychology*, *6*. doi:10.3389/fpsyg.2015.00368
6. Leech, J. A., Nelson, W. C., Burnett, R. T., Aaron, S., & Raizenne, M. E. (2002). It's about time: A comparison of Canadian and American time–activity patterns. *Journal of Exposure Science & Environmental Epidemiology*, *12*(6). doi:10.1038/sj.jea.7500244
7. Mccurdy, T., & Graham, S. E. (2003). Using human activity data in exposure models: Analysis of discriminating factors. *Journal of Exposure Science and Environmental Epidemiology*, *13*(4), 294–317. doi:10.1038/sj.jea.7500281
8. Evans, G. W. (2003). The built environment and mental health. *Journal of Urban Health: Bulletin of the New York Academy of Medicine*, *80*(4), 536–555. doi:10.1093/jurban/jtg063
9. Schweizer, C., Edwards, R. D., Bayer-Oglesby, L., Gauderman, W. J., Ilacqua, V., Jantunen, M. J., Lai, H. K., Nieuwenhuijsen, M., & Künzli, N. (2007). Indoor time–microenvironment–activity patterns in seven regions of Europe. *Journal of Exposure Science & Environmental Epidemiology*, *17*(2). doi:10.1038/sj.jes.7500490
10. Boubekri, M. (2008). *Daylighting, architecture and health: Building design strategies*. Elsevier.
11. Stevens, R. G. (1987). Electric power use and breast cancer: A hypothesis. *American Journal of Epidemiology*, *125*(4), 556–561.

12. Granger, G. W. (1952). Objectivity of Colour Preferences. *Nature*, *170*(4332), Articolo 4332. doi:10.1038/170778a0
13. Guilford, J. P., & Smith, P. C. (1959). A System of Color-Preferences. *The American Journal of Psychology*, *72*(4), 487–502. doi:10.2307/1419491
14. Palmer, S. E., Schloss, K. B., & Sammartino, J. (2013). Visual Aesthetics and Human Preference. *Annual Review of Psychology*, *64*(1), 77–107. doi:10.1146/annurev-psych-120710-100504
15. Al-Rasheed, A. S. (2015). An experimental study of gender and cultural differences in hue preference. *Frontiers in Psychology*, *6*.
16. Choungourian, A. (1968). Color Preferences and Cultural Variation. *Perceptual and Motor Skills*, *26*(3), 1203–1206. doi:10.2466/pms.1968.26.3c.1203
17. Bonnardel, V., Beniwal, S., Dubey, N., Pande, M., & Bimler, D. (2018). Gender difference in color preference across cultures: An archetypal pattern modulated by a female cultural stereotype. *Color Research & Application*, *43*(2), 209–223. doi:10.1002/col.22188
18. Ou, L.-C., Luo, M. R., Woodcock, A., & Wright, A. (2004). A study of colour emotion and colour preference. Part I: Colour emotions for single colours. *Color Research & Application*, *29*(3), 232–240. doi:10.1002/col.20010
19. Hurlbert, A. C., & Ling, Y. (2007). Biological components of sex differences in color preference. *Current Biology*, *17*(16), R623–R625. doi:10.1016/j.cub.2007.06.022
20. Beall, A. T., & Tracy, J. L. (2013). Women Are More Likely to Wear Red or Pink at Peak Fertility. *Psychological Science*, *24*(9), 1837–1841. doi:10.1177/0956797613476045
21. Taylor, C., Clifford, A., & Franklin, A. (2013). Color preferences are not universal. *Journal of Experimental Psychology: General*, *142*(4), 1015–1027. doi:10.1037/a0030273
22. Sorokowski, P., Sorokowska, A., & Witzel, C. (2014). Sex differences in color preferences transcend extreme differences in culture and ecology. *Psychonomic Bulletin & Review*, *21*(5), 1195–1201. doi:10.3758/s13423-014-0591-8
23. Taft, C. (1997). Color meaning and context: Comparisons of semantic ratings of colors on samples and objects. *Color Research & Application*, *22*(1), 40–50.
24. Schloss, K. B., Strauss, E. D., & Palmer, S. E. (2013). Object color preferences. *Color Research & Application*, *38*(6), 393–411. doi:10.1002/col.21756
25. Palmer, S. E., & Schloss, K. B. (2010). An ecological valence theory of human color preference. *Proceedings of the National Academy of Sciences*, *107*(19), 8877–8882. doi:10.1073/pnas.0906172107
26. Gao, X.-P., Xin, J. H., Sato, T., Hansuebsai, A., Scalzo, M., Kajiwara, K., Guan, S.-S., Valldeperas, J., Lis, M. J., & Billger, M. (2007). Analysis of cross-cultural color emotion. *Color Research & Application*, *32*(3), 223–229. doi:10.1002/col.20321
27. Jacobs, K. W., & Frank E. Hustmyer, J. (1974). Effects of Four Psychological Primary Colors on GSR, Heart Rate and Respiration Rate: *Perceptual and Motor Skills*. doi:10.2466/pms.1974.38.3.763
28. Elliot, A. J., Maier, M. A., Moller, A. C., Friedman, R., & Meinhardt, J. (2007). Color and psychological functioning: The effect of red on performance attainment. *Journal of Experimental Psychology. General*, *136*(1), 154–168. doi:10.1037/0096-3445.136.1.154
29. Hill, R. A., & Barton, R. A. (2005). Red enhances human performance in contests. *Nature*, *435*(7040). doi:10.1038/435293a
30. Mehta, R., & Zhu, R. (Juliet). (2009). Blue or Red? Exploring the Effect of Color on Cognitive Task Performances. *Science*, *323*(5918), 1226–1229. doi:10.1126/science.1169144
31. Lewy, A. J., Wehr, T. A., Goodwin, F. K., Newsome, D. A., & Markey, S. P. (1980). Light suppresses melatonin secretion in humans. *Science*, *210*(4475), 1267–1269. doi:10.1126/science.7434030
32. Czeisler, C. A., Kronauer, R. E., Allan, J. S., Duffy, J. F., Jewett, M. E., Brown, E. N., & Ronda, J. M. (1989). Bright Light Induction of Strong (Type 0) Resetting of the Human Circadian Pacemaker. *Science*, *244*(4910), 1328–1333. doi:10.1126/science.2734611
33. Badia, P., Myers, B., Boecker, M., Culpepper, J., & Harsh, J. R. (1991). Bright light effects on body temperature, alertness, EEG and behavior. *Physiology & Behavior*, *50*(3), 583–588.
34. Cajochen, C., Münch, M., Kobialka, S., Kräuchi, K., Steiner, R., Oelhafen, P., Orgül, S., & Wirz-Justice, A. (2005). High sensitivity of human melatonin, alertness, thermoregulation, and heart

rate to short wavelength light. *The Journal of Clinical Endocrinology and Metabolism*, *90*(3), 1311–1316. doi:10.1210/jc.2004-0957

35. Cajochen, C., Zeitzer, J. M., Czeisler, C. A., & Dijk, D.-J. (2000). Dose-response relationship for light intensity and ocular and electroencephalographic correlates of human alertness. *Behavioural Brain Research*, *115*(1), 75–83. doi:10.1016/S0166-4328(00)00236-9
36. IES. (2018). *IES TM-18-18 Light and Human Health: An Overview of the Impact of Optical Radiation on Visual, Circadian, Neuroendocrine, and Neurobehavioral Responses*.
37. Houser, K., Boyce, P., Zeitzer, J., & Herf, M. (2021). Human-centric lighting: Myth, magic or metaphor? *Lighting Research & Technology*, *53*(2), 97–118. doi:10.1177/1477153520958448
38. Elliot, A. J., & Maier, M. A. (2012). Chapter two—Color-in-Context Theory. In P. Devine & A. Plant, *Advances in Experimental Social Psychology* (Vol. 45, pp. 61–125). Academic Press.
39. Wilms, L., & Oberfeld, D. (2018). Color and emotion: Effects of hue, saturation, and brightness. *Psychological Research*, *82*(5), 896–914. doi:10.1007/s00426-017-0880-8
40. Tangkijviwat, U., Rattanakasamsuk, K., & Shinoda, H. (2010). Color preference affected by mode of color appearance. *Color Research & Application*, *35*(1), 50–61. doi:10.1002/col.20536
41. Jonauskaite, D., Althaus, B., Dael, N., Dan-Glauser, E., & Mohr, C. (2019). What color do you feel? Color choices are driven by mood. *Color Research & Application*, *44*(2), 272–284. doi:10.1002/col.22327
42. Jonauskaite, D., Mohr, C., Antonietti, J.-P., Spiers, P. M., Althaus, B., Anil, S., & Dael, N. (2016). Most and Least Preferred Colours Differ According to Object Context: New Insights from an Unrestricted Colour Range. *PLOS ONE*, *11*(3). doi:10.1371/journal.pone.0152194
43. Land, B. (1977). The Retinex Theory of Color Vision. *Scientific American*, *12*. doi:10.1038/scientificamerican1277-108
44. Elliot, A. J., & Maier, M. A. (2014). Color Psychology: Effects of Perceiving Color on Psychological Functioning in Humans. *Annual Review of Psychology*, *65*(1), 95–120. doi:10.1146/annurev-psych-010213-115035
45. Elliot, A. J. (2019). A Historically Based Review of Empirical Work on Color and Psychological Functioning: Content, Methods, and Recommendations for Future Research. *Review of General Psychology*, *23*(2), 177–200. doi:10.1037/gpr0000170
46. Lee, H., Park, J., & Lee, J. (2020). Comparison between psychological responses to 'object colour produced by paint colour' and 'object colour produced by light source': *Indoor and Built Environment*. doi:10.1177/1420326X19897109
47. Küller, R., Mikellides, B., & Janssens, J. (2009). Color, arousal, and performance—A comparison of three experiments. *Color Research & Application*, *34*(2), 141–152. doi:10.1002/col.20476
48. Kwallek, N., Lewis, C. M., Lin-Hsiao, J. W. D., & Woodson, H. (1996). Effects of nine monochromatic office interior colors on clerical tasks and worker mood. *Color Research & Application*, *21*(6), 448–458.
49. Costa, M., Frumento, S., Nese, M., & Predieri, I. (2018). Interior Color and Psychological Functioning in a University Residence Hall. *Frontiers in Psychology*, *9*. doi:10.3389/fpsyg.2018.01580
50. Küller, R., Ballal, S., Laike, T., Mikellides, B., & Tonello, G. (2006). The impact of light and colour on psychological mood: A cross-cultural study of indoor work environments. *Ergonomics*, *49*(14), 1496–1507. doi:10.1080/00140130600858142
51. Brown, T. M., Brainard, G. C., Cajochen, C., Czeisler, C. A., Hanifin, J. P., Lockley, S. W., Lucas, R. J., Münch, M., O'Hagan, J. B., Peirson, S. N., Price, L. L. A., Roenneberg, T., Schlangen, L. J. M., Skene, D. J., Spitschan, M., Vetter, C., Zee, P. C., & Jr, K. P. W. (2022). Recommendations for daytime, evening, and nighttime indoor light exposure to best support physiology, sleep, and wakefulness in healthy adults. *PLOS Biology*, *20*(3). doi:10.1371/journal.pbio.3001571
52. CIE. (1995). *CIE 117:1995 Discomfort glare in interior lighting*.
53. Webler, F. S., Spitschan, M., Foster, R. G., Andersen, M., & Peirson, S. N. (2019). What is the 'spectral diet' of humans? *Current Opinion in Behavioral Sciences*, *30*, 80–86. doi:10.1016/j.cobeha.2019.06.006
54. Wilson, E. O. (1984). *Biophilia*. Harvard University Press.

COLOR SPATIAL LAYERING IN ARCHITECTURAL INTERIORS AFTER JOSEF ALBERS' HOMAGES TO THE SQUARE AT RIT

Juan Serra[1]* and Michael Murdoch[2]

[1]*Color Research Group, School of Architecture, Universitat Politècnica de València, Spain.*
[2]*Munsell Color Science Laboratory, College of Science, Rochester Institute of Technology, USA.*

*Corresponding author: Juan Serra, juanserra@ega.upv.es

ABSTRACT

The implications of color in the perception of distances have been a matter of interest for flat representations but have received fewer attention for 3D objects and spaces. The objective of this article is to reflect about color spatial layering and its implications in the perception of the amplitude of an architectural interior. We focus on the study of one of the scarce Josef Albers's big scale Homages to the Square commissioned for an interior and painted in the lobby of the George Eastman Administration Building at Rochester Institute of Technology (RIT). This unique artwork titled Growth consists of two Homages with four shades of orange colors in reverse order that face each other on opposite walls. We have studied the original information gathered at the Josef & Anni Albers Foundation and the RIT archives to understand the circumstances of this commission, with particular interest in the debate between architectural and artistic standpoints. We have experienced and recorded our personal impressions of the colors on site, providing some possible interpretations of the spatial layering of the murals. We interpret when a color can be understood to be a square or a frame, with opaque or transparent finishing, and its corresponding spatial position. Results demonstrate that the geometric composition of the murals and their accurate disposition in the interior of the lobby let them act as modern mock perspectives with multiple interpretations of the position of the colors with respect to each other and provide a clear dynamism to the interior architecture. These color dispositions are interpreted in light with JA concepts such as "vibrating and vanishing boundaries," "color transparency," and simultaneous contrast. We conclude that JA painted a masterpiece at RIT, following his principle of do more with less, and demonstrate that the spatial depth of a color with respect to the canvas or architectural surface cannot be interpreted as an independent fact but a matter of interaction of colors within a context.

Keywords: color, distance, architecture, Albers, Homage to the Square

INTRODUCTION

The perception of color kinetics, advancing and receding colors, is a matter of interest and has been widely investigated for flat representations in two dimensions [1], but there are fewer experimentations in involving three dimensional spaces, as happens in architectural interiors. In this sense, the series of Homages to the Square painted by the artist Joseph Albers (JA), can be studied as belonging to the first group of bidimensional experimentations of color layering. JA worked on his series of Homages when he was sixty-two, over the next twenty-six years (1950-76), and made over two thousands of them [2]. He was absolutely engaged in working with these series of nested squares in different colors, experimenting the relationships, interactions, and subjective perception of color. Among the different visual effects occurring, the squares seem to shift in relation with one another, getting different spatial positions that depend on the observer's subjectivity and color illusions.

In general terms, the Homages are small scale, hand-crafted, two-dimensional experimentations of color layering, and there is still a gap to know how these interactions can be transferred into three dimensional architectural interiors, and how can these effects alter the perception of spatiality. Fortunately, among the twenty public art commissions in his life, JA made two big scale Homages for interior spaces. One commission is Let There Be Light, (Mt Bethel Church, New Haven, Connecticut, 1973), and the other and most interesting for its architectural implications are the murals Growth, painted in the lobby of the George Eastman administration building at Rochester Institute of Technology (RIT) in 1966-69. The objective of this article is to reflect about color spatial layering and its implications in the perception of amplitude of architectural interiors, after the analysis of JA's big scale Homages to the Square at RIT Campus.

THE MURALS GROWTH AT RIT

For the analysis of the murals, we have studied the original information gathered at the Josef & Anni Albers Foundation and the RIT archives to understand the circumstances of this commission, with particular interest in the debate between architectural and artistic standpoints. We have also experienced and recorded our personal impressions of the colors on site, providing some possible spatial layering interpretations of the murals.

Figure 1. Panoramic photograph of the murals Growth, taken from the main entrance to the lobby of the administration building at RIT (7/20/23).

The circumstances of the commission

The architectural project of the campus at RIT originally belonged to Eero Saarinen, but after his death in 1961 the project for the Administration Building passed to his successor firm Kevin Roche John Dinkeloo Associates, who opted for the use of the same rust-colored bricks of the rest of the campus. The lobby provided an appropriate space for large artworks located on two opposing walls and illuminated laterally by floor-to-ceiling windows, with the only limitation being the low, canopy-like segment of the ceiling which slopes, on axis, toward a corridor and impinges upon both murals, obstructing cross-lobby views of the uppermost sections of each [3, p.165] (figure 1).

After the agreement for the commission, JA presented a first sketch of the murals to the architecture firm, that initially did not meet the architects' expectations of *"giving an expansive, airy quality to the space, of adding a dimension and character which will greatly enhance it"* [4]. From the very first moment, the architecture firm was looking for an interaction with the spatial properties of the lobby: *"I am sure you will understand that we would not wish to have paintings at all if they do not enhance the space -there is a spatial, architectural need here. The space was designed specifically for these two walls to have compositions, but compositions with certain character."*[4] Probably the architecture firm went too far recommending JA to reconsider the colors of his initial proposal, and suggesting that *"because of the architectural materials, the colors should be cool, towards green and, because of the space effect, they should be light and airy, somewhat vague and not intense. We believe strongly that the colors should be quite pale and foggy, definitively green and the composition subdued feeling."* [4]

Despite these initial discrepancies in the choice of the colors that make JA *"wonder whether a further collaboration between them was possible and desired,"* [5] he agreed to develop a different version of Growth in gray or off-white colors. Robert Bryde, the disciple of Albers who executed the murals, explained that *"the first white on white (…) was to produce a transparency effect, like layers of tissue paper in a 4-3-2-1 pattern."* [6]

The development of a monochrome proposal was not incoherent in Albers initial experimentations with the Homages, in this case at a large scale, and should not be considered surprising [3, p. 169], but Albers was not satisfied with the results of this gray version of the mural. During the restoration process in 2004, there was evidence that just the North mural had this initial version in grayish colors over a dark surface [7]. It stood for a few months before Roche withdrew from participation with Albers on the project [8], and finally JA went his way and painted the two Homages with the existing four colors that range from orange to yellow.

In our opinion, the polemic between the artistic discrepancies is not very relevant, as the final version of Growth perfectly fulfills the initial expectations of enhancing the architectural space. Years later, Roche recognized that, "on the whole, the painting and the architectural spaces work very well together." [9] Even more, the project was awarded the 1972 Collaborative Achievement in Architecture Medal of the American Institute of Architects, as an example of "outstanding collaboration between practitioners of the building arts." [10]

Figure 2. a) Scheme with the dimensions and labels for each of the nested squares; b) Photograph of the North mural; c) Photograph of the South mural (7/20/23).

The opposition as a compositional concept

To have the two murals paired in opposite locations, facing each other in the same lobby, is an essential feature to understand this artwork. Albers stated that "studies in pairs demonstrate clearly the desired effects." [11, p. 10-11] and in this architectural arrangement, JA found the perfect condition to work with opponent or complementary pairs. Among the 20 public artwork commissions by JA, there are other architectural projects working with pairs, being Two Structural Constellations and Two Portals the most obvious examples to date [3, p. 171]. In Growth, both murals share the same colors but in reverse order, enhancing their differences and highlighting the multiple effects that are possible with limited means (figure 2). As a former member of the Bauhaus, Albers was committed with Mies' statement "Less is more," and wanted to achieve the maximum effect with the minimum means.

In some recordings, the titles of these two murals are "Growth" and "Youth," conceptual antonyms that emphasize the complementarity between the two compositions. In this terminological opposition, some authors see an artist's plea for a balance between science and technology with art, an idea that Albers defended in his series of lectures at trinity College (1965) and that fits with the destiny of RIT, a university for science and technology [3, p. 172]. Despite being coherent with JA thinking, the use of these two terms, growth and youth, to title this artwork is unclear, and JA indicates in some of his own personal notes, that the title of both Homages at RIT is "Growth." [12]

The geometry and colors of the murals

The multiple effects of colors in the Homages series relied on a compositional framework of four nested squares. This seemingly simple framework was carefully designed to yield a vast array of illusory spaces [13]. The proportions of the squares from the one in the center are 4, 6, 8, and 10, with a thin frame of 0.1 units in white. The squares are equidistant horizontally and closer to the bottom vertically (figure 2).

When these geometries of nested squares have color, we can identify 3 variables implicit in the compositional framework that may be useful for our analysis: "(1) Each square may be seen as lying on a different layer in illusory space, thus an Homage painting can display up to four *layers of depth*. (2) Each square may be interpreted as *opaque or translucent*— an opaque square obscures shapes that lie behind it, and a translucent square reveals the shapes that lie behind it. (3) Each square may be seen as the edge of either *a plane or a frame*—a plane is a continuous square surface; a frame is a square plane with a central square hole; thus, a frame requires two squares from the 4-square compositional framework [13].

The perceptual characteristics of the colors of Growth, identified with a colorimeter NCS Color Pin, are approximately NCS S0570-Y30R, S0560-Y30R, S0570-Y10R, S0570-Y (≈Munsell 5YR 7/12; 7.5 YR 7/10; 1.25Y 8/12; 5Y 8.5/12). Therefore, we observe an harmony of colors with the same very low blackness (high Munsell value), almost identical high chromaticness (Munsell chroma) and adjacent hues that range from a fundamental yellow to a yellowish orange.

RESULT AND DISCUSSION

According to Mai's classification, the murals Growth correspond to Homages type I, and the total amount of color layering possibilities is 120 [13]. Nevertheless, in our personal impressions of the colors on site, we identified three main spatial interpretations for each mural. We have used the following code to label them: (1) letters N and S refer to the mural placed North or South respectively; (2) the spatial order of the colors is described in order and separated with commas, where the leftmost position is nearest in illusory space and the rightmost the furthest; (3) numbers 1 to 4 identify each square in order from the center to the exterior (figure 2), the use of two numbers indicates a frame instead of a square; i.e. 1-3 is a frame with the exterior size of square 3 and a hole with the size of square 1; (4) finally letters "o" and "t" indicate if the color is opaque or transparent. All and that, our perceived interpretations for Growth are: N1= original painting; N2= 1o, 2o, 3o, 4o; N3= 1-3t, 2o, 4o; N4= 1o, 2-4t, 3o; S2= original painting, S2= 3-4o, 2-3o, 1-2o, 1o; S3= 1-3t, 2-4o, 2o; S4= 2-4t, 1-3o, 1o (figure 3).

The spatial layering suggested by the superimposition of opaque colors

At first sight, the interpretation of the colors belonging to the northern mural gives the impression of a succession of opaque nested squares put in order one onto the other, with the central yellow being the nearest, and the darkest orange the furthest and on the surface of the wall (N1). Similarly on the southern mural, the perception is of a succession of nested frames in order from an exterior in yellow that seems to be the closest and on the surface of the wall, to the central square that seems the furthest and somehow behind the wall (S1). Certainly, the slightly darkest and least chromatic orange seems the furthest, while the most vivid and pure yellow seems the closest, what is coherent with usual literature results indicating that for surfaces to appear coplanar, their lightness have to be proportional to the natural (intrinsic) lightness of the hues [14]. This effect of an opaque overlapping of squares/frames is enhanced by the effect of simultaneous contrast in the boundaries of the nested squares and therefore a kind of brighter/darker halo that appears in the contour. The closest lighter color seems to have a slight cast shadow onto the next square/frame enhancing the impression of spatial layering. This effect is slightly more evident in the upper part of the murals with wider bands and when the observer gets closer to the mural than in the lower part with thinner bands and with the distance. The effect recalls JA's exercises about "Vibrating Boundaries," that asked students to choose two colors that would produce a vibration along their boundary producing a kind of bright fizz along the border. The effect required the combination of intense, contrasting colors that were close in light/value [15]. It also recalls what JA named the "flute effect," in exercises of color gradations in bands that stressed their boundaries.

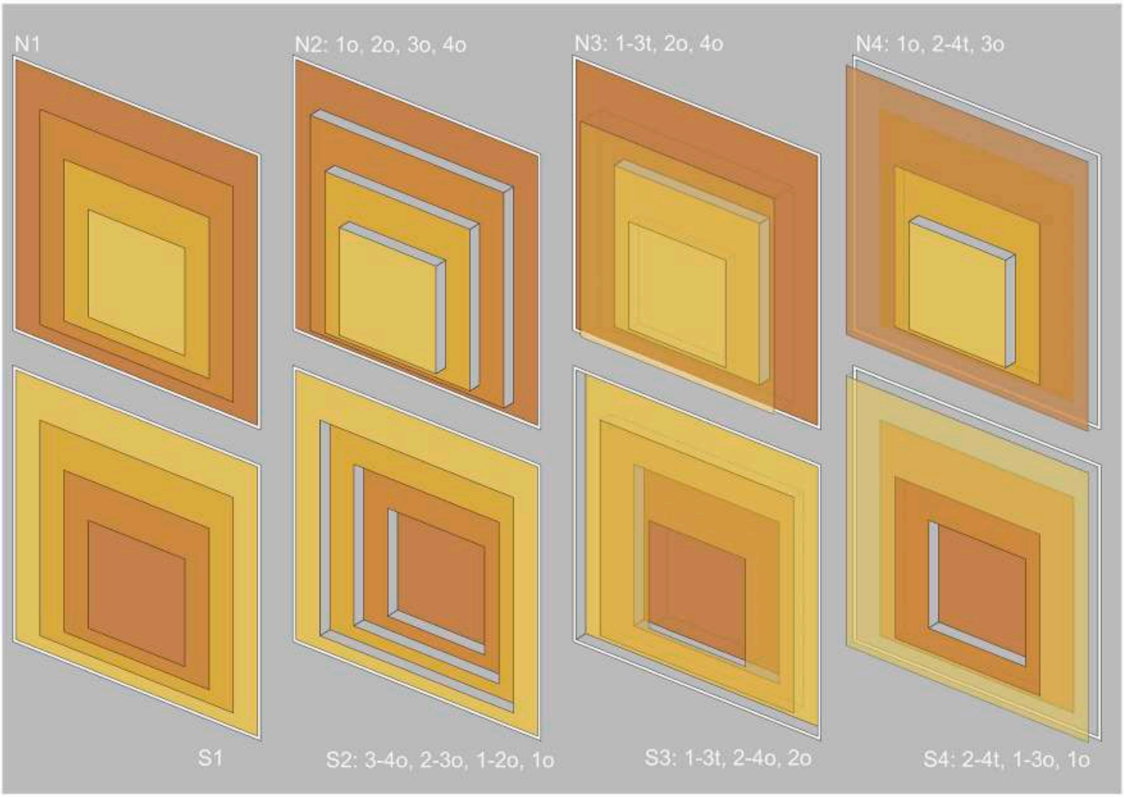

Figure 3. Personal interpretations of the color spatial layering in north (N1) and south (S1) murals. The coding indicates the squares/frames from nearest to furthest in illusory space, and if colors are opaque (o) or transparent (t).

The spatial layering suggested by the superimposition of transparent colors

The interpretation of the spatial layering in Growth is not limited to opaque colors and there are other possibilities of superimpositions of transparent over opaque colors. In this sense, the northern Homage can be interpreted to have a former transparent frame 1-3 (see N3 in figure 1), or a former transparent frame 2-4 (see N4). Similarly in southern Homage, former transparent frames 1-3 and 2-4 can be interpreted in S3 and S4 respectively. Logically, these transparent colors are always perceived to be overlapped onto the opaques and, interestingly, to be closer in distance or at the same depth as the purest yellow (see N3 and S3). Therefore, it is demonstrated JA's principle that the colors act in different ways depending on the context, and the purest yellow is not always interpreted to be the closest. In a similar way, despite the advantage due to wavelength and color stereopsis, the reddest color is not always interpreted as near, as demonstrated in other experiments [1].

In the exercises about color transparency, JA challenged the students to find the right opaque color that, placed between other two, seemed to be the perfect mixing. This exercise is interesting because it has spatial implications. I.e., if a yellowish orange is placed between a yellow and a red, the effect would be of a transparent yellow layer overlapped onto the red, and the reverse would happen with a reddish orange, a transparent red layer would be seen overlapped onto the yellow. An intermediate color can make the colors beside move back and forth.

In the interpretation of Growth, we can also see an effect of “vanishing boundaries,” that JA indicated to be “confined to adjacent, neighbouring colors and depends most decisively on equal ‘light intensity’” [11, p.63]. In the opinion of some authors, the distinction of the boundaries between adjoining colors is greater at the bottom of either mural, and more elusive at either side, and particularly at the top. “While the lower ranges suggest a four-color Homage, the upper bands of Growth lead us to perceive only three colors” [3, p.170].

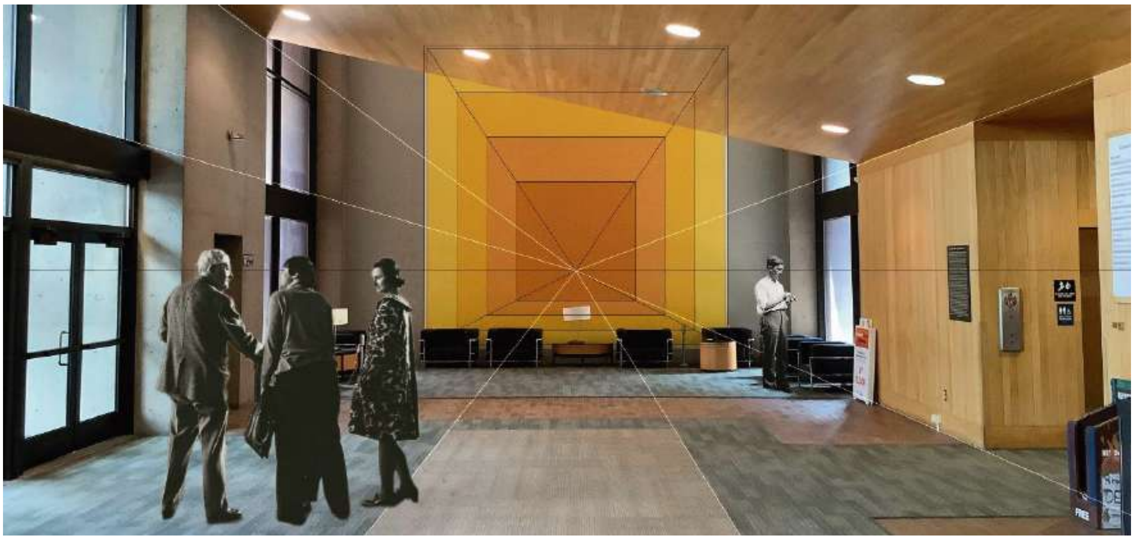

Figure 4. The perspective of the existing architecture (white lines) is coincident with that of the nested squares (black lines), obtaining a modern mock perspective. Photomontage with images of Josef and Anni Albers from [16] and [17].

The space suggested by the geometric patterns

There is an interesting finding regarding the position and size of the geometry of the Groutth murals. The four nested squares might be interpreted as an abstract representation of squares with identical size in conical perspective, so it is possible to find the corresponding position of the horizon and central vanishing point of this 2D representation (see black lines in figure 4). Interestingly, when an observer is placed in the center of the lobby facing to any of the murals, the position of the horizon and the vanishing point of existing architecture are coincident with those of the mural (see white lines in figure 4), obtaining a modern mock perspective, an artistic resource that has its roots in the history of architectural paintings, particularly during the Renaissance. Albers accurately increased the size of his Homages to the Square and painted them in a position that is not vertically equidistant to the ceiling but closer to the floor, following the same proportions of the nested squares. This decision enhances the coherence between the existing spatiality of the lobby and that suggested by the nested squares. Both spaces, real and suggested, geometrically match.

CONCLUSION

The analysis of the big scale Homages to the Square that Josef Albers painted in the lobby of the administration building at Rochester Institute of Technology, demonstrate that JA painted a masterpiece at RIT, following his principle of do more with less. The geometric composition of the murals and their accurate disposition in the interior of the lobby let them act as modern mock perspectives with multiple interpretations of the position of the colors with respect to each other and provide a clear dynamism to the interior architecture. Albers artwork demonstrates that the spatial depth of a color with respect to the canvas or architectural surface cannot be interpreted as an independent fact but a matter of interaction of colors within a context.

ACKNOWLEDGEMENT

Our gratitude to Brenda Danilowitz, Chief Curator, and Amy Jean Porter, assistant curator and digital manager of the Josef & Anni Albers Foundation for providing original material about Albers' architectural commissions. To Amelia Hugill-Fontanel, associate curator at RIT Cary Graphic arts collection, for providing material available at RIT archives.

REFERENCES

1. Guibal, C. R. C., & Dresp, B. (2004). Interaction of color and geometric cues in depth perception: when does "red" mean "near"? *Psychological Research*, 69(1–2), 30–40. https://doi.org/10.1007/s00426-003-0167-0
2. Albers, A. (2018). *Josef Albers: Interaction* (H. Liesbrock & U. Growe, Eds.). Yale University Press.
3. Benezra, N. D. (1983). *The murals and sculpture of Josef Albers* (PhD). Stanford University.
4. Platner, W. (December 19, 1966). Correspondence from W. Platner, K. Roche, J. Dinkeloo & Associates to J. Albers; archives of the Josef & Anni Albers Foundation, Bethany.
5. Albers, J. (December 28, 1966). Correspondence from J. Albers to W. Platner, K. Roche, J. Dinkeloo & Associates; archives of the Josef & Anni Albers Foundation, Bethany.
6. Bryde, R. (August 22, 1982). Correspondence from R. Bryde to N.D. Benezra; in [3, p. 167], consulted at the Josef & Anni Albers Foundation, Bethany.
7. Hamm, J. (2004). Josef Albers's monumental Homage to the Square. *Studies in Conservation*, 49 (sup2), 179–184. https://doi.org/10.1179/sic.2004.49.s2.039
8. Roche, K. (June 7, 1968). Correspondence from K. Roche to J. Albers; archives of the Josef & Anni Albers Foundation, Bethany.
9. Roche, K. (October 1, 1981). Correspondence from K. Roche to N.D. Benezra; in [3, p. 167], consulted at the Josef & Anni Albers Foundation, Bethany.
10. Roche, K. (December 13, 1971). Correspondence from K. Roche to J. Albers informing about the award; archives of the Josef & Anni Albers Foundation, Bethany.
11. Albers, J. (1963). *Interaction of color* (4th ed.). Yale University Press.
12. Albers, J. (n.d.). Lists and Notes of Architectural Commissions, archives of the Josef & Anni Albers Foundation, Bethany.
13. Mai, J. (2016). Planes and Frames: Spatial Layering in Josef Albers' Homage to the Square Paintings. *Bridges Finland Conference Proceedings*, 233–240.
14. Da Pos, O., Vishwanath, D., & Albertazzi, L. (2021). Color determinants of surface stratification. *Color Research and Application*, 46(1), 88–102. https://doi.org/10.1002/col.22585
15. Danilowitz, B., & Horowitz, F. A. (2009). *Josef Albers: To Open Eyes* (1st ed.). Phaidon.
16. Josef Albers Murals. (1969, June). *Alumni News & Views*. Rochester Institute of Technology.
17. Boissel, J. (2015). *Josef Albers and Wassily Kandinsky: Friends in Exile: A Decade of Correspondence, 1929–1940.* Yale University Press.

COLOR, THE SOUL OF SKETCHING

Ana Moreira da Silva*

CIAUD, Research Centre for Architecture, Urbanism and Design, Lisbon School of Architecture, Universidade de Lisboa, Portugal.

*Ana Moreira da Silva, anamoreiradasilva@gmail.com

ABSTRACT

Architecture and Design are, undoubtedly, based on a creative process. To solve several design problems and achieve a final solution, architects and designers need to manipulate tools with specific qualities. The relationship between freehand drawing and designers is very old, as they use this medium as a way of giving space to creative thinking. Sketching is often a tool during idea generation in the early stages of design process. It is in this initial phase of project conception in Architecture and in Design where sketches are more frequently used. Architects and Designers also use sketches throughout the different phases of the process of project development as a medium for dialogue. The production of a sketch constitutes an action and reaction which provides designers with the necessary interaction to think through the complex process of anticipating a project. A colorful sketch can more easily study and communicate the concerning materials, dimensions, and structure. The materials chosen for a project might be recognized without the use of words, since the use of color in sketches provides important visual definitions. Using colors, an architect can effortless differentiate floors and walls to make the image appear three-dimensional, showing both interior and exterior space. For designers, the use of color can be advantageous for representing and differentiate several materials and be useful, comparing several possibilities, for the final colors choice for a specific product, a graphic communication or a web design. The use of colored paper or other colored basis for sketches can immediately change the drawing perception and clarify or emphasize the design intention or communication. Under a qualitative research, based on literature review methodology, through the study and interpretation of several authors' statements, and based on the analysis of sketches using color produced by architects and designers, this paper investigates the importance of color use, aiming to stimulate reflection and bringing new perspectives on color relevance in sketches, being the "soul of sketching". We intend to rise questions and search for answers and, also, open a debate about several related issues with color and sketches.

Keywords: Color, Sketches, Architecture, Design.

INTRODUCTION

This paper stems from a current post-doc research project motivated by the need to produce more knowledge and reflection on Drawing. In this project we consider the close relation between freehand drawings and the architects and designers' activity. This post-doc main objective is to investigate the importance of freehand drawings/sketches during designing processes.

We pretend to disseminate some of the study results from one of the research phases concerning the color use relevance on the sketches for an Architecture or Design project.

Supported by a bibliographical review methodology, we aim to investigate about color concepts and the color importance in Architecture and Design practice. From this theoretical approach, we intend to analyze colored design and architecture sketches and verify or underline the relevance of color use on sketches during the conceiving process and in the project development.

DESIGN SKETCHES

According to the Cambridge English Dictionary, the word sketch describes a simple, quickly-made drawing that does not have many details. Sketches are expeditiously freehand drawings, representing general overview of an object or idea, often made as a project preliminary study. Sketching is fast and easy, giving freedom to explore ideas as quickly as they arise.

Even when done quickly, a sketch can be a powerful tool for the designer. The sketch as operational support to the practice of design has earned the interest of several authors. In these approaches is revealed recurrent concern to check the extent to which sketching will be present throughout the various stages of the process.

Some authors state that it is a necessary step of a design: its first spark. Others argue that it is the best way to capture a concept. For others is a vehicle for communication between designers working groups. For Tversky, sketching is an integral part of early design [1] both for a person working alone and for designers working in groups. Sketches can establish a visual dialogue. According to Goldschmidt, sketches provide a sort of 'backtalk' [2] that the designer uses to generate more ideas. In a team work situation, Bekker claim that the discussion and process is as valuable as the artefact, because as the design project is being created and developed, the team builds up a shared understanding of the process [3]. There is a close relationship between all design areas and the graphical representation by means of drawings.

Through sketching, embryonic ideas are quickly drawn for primary analysis before they disappear, for reflection and detailed observation, validating or discarding them, generating a constant flow of more ideas [4].

Reasoning through sketches can support the expression of an idea, exteriorizing a stream of thoughts about something occurring in our brain and external stimulus. When designers find design solutions, still in their minds, as sketching is fast and easy it gives freedom to explore ideas as quickly as they arise.

Most of the times, sketches often trigger memories and imagination and give birth to creative ideas. Rough scribbles on a piece of paper can be the start of the next design project. That is why most designers start their creative process by sketches.

Throughout the complex process which goes from one imagined object to its implementation, designer can rely on this essential medium to help him on developing the idea. The complexity, inherent in the transition from idea to its realization, is related to the specific context of the design where a wide range of factors come into play, such as the ability to understand the context and imagine the solutions, the ability to know and take advantage of the processes and of the materials as means or vehicles through which the solution materializes, the ability to transform ideas into appropriate forms, taking into account the limits and the material possibilities.

Therefore, sketches accomplish a large rang of purposes: as way of communicating, as means of discovery, as graphical method of study, as process of observation and registration, as research tool, as privileged means of formulation, representation and communication of ideas, as link in the mental and creative process.

The relevance of sketches assumes a broad sense, conferring to the act of sketching the ability to become means of multiple resources to practice in various areas of design, from architecture to interior design, from graphic design to fashion design, from product design to web design, among others.

COLOR INFLUENCES IN OBJECTS AND SPACES

Color has been studied for centuries and yet there is still much to learn about its properties and influences.

Color vision is closely associated with visual processing and human perception, being the brain the organ responsible for decoding electrical signals into experiences that make sense for humans to perceive the world. Although at first glance it seems like a relatively simple human capacity, color processing is a complex phenomenon, involving different variables [5].

Color is part of the surrounding environment and is always present in our experience, consciously or unconsciously. An object appears colored because of the way it interacts with light. Color is defined by the different wavelengths of light reaching the retina of the eye. It is an emerging perception. The human brain primarily perceives color and visual relationships then resolves other details [6].

The physiology of color analyses this interaction and the factors that determine it, involving the eye and the brain's responses to light and the sensory information they can produce. On the other hand the psychology of color studies the ways the human mind processes visual data, compares it with information stored in memory, and interprets it as color sensations. Mahnke [7] summarizes by stating that color is a sensation that the eye recognizes and the brain interprets.

To understand color phenomenon the manner in which the brain responds to visual stimuli must be considered. Even under identical conditions, the same object may appear red to one observer and more orange to another. Clearly, the perception of color depends on vision, light, and individual interpretations, and an understanding of color involves physics, physiology, and psychology.

Colors have the ability to arouse emotions in human beings, even managing to influence our state of mind and mood [5].

The most important aspect of color in daily life is probably the one that is least defined and most variable. It involves aesthetic and psychological responses to color and influences art, architecture and all design areas. One example of the bridge between color and emotional sensations is the common perception that red, orange, yellow, and brown hues are considered ´warm', while the blues, greens, and grays are considered 'cold'. The red, orange, and yellow hues induce excitement, cheerfulness, stimulation; the blues and greens induce the feelings of security, calm, and peace; and the dark browns, grays, and blacks generate sadness and melancholic feelings.

However, as the psychological perception of color is subjective, this kind of relations between colors and human feelings, despite being generally considered, depend on each individual and on his cultural background. Color symbolism, color terminology, color harmony, color preferences, and other psychological aspects of color are culturally conditioned, and they vary considerably with both place and historical period.

Colors can affect the way human beings feel, think, choose and behave. According to Broeder [8], their effects seem to be reflected in the influences between cultures enforced by the process of globalization, causing traditions and beliefs to be transferred from one society to another.

COLOR RELEVANCE IN DESIGN SKETCHES

Color is one of the design basic elements, among shape, space, line, and texture. Besides being one of basic elements, color is one of the most influential one because colors can change our perception of other elements. Shapes, spaces, lines and even textures can seem different depending on their colors.

Color is a very powerful design element and it is very effective in highlighting every element (like in graphic or communication or product design) or on creating spaces and ambiances (as in architecture, urban spaces or interior design),

As the use of sketches assumes an important role in the various areas of design, the adding of colors when sketching can be relevant for the designer during project developing phases and, also, can make the difference when communicating with the working team, with the developers or the clients or, even, with the consumers. Color can act as the soul of sketches, generating a profound change in its expression, its message and in its meaning.

Colors work like distinctive elements on all kind of objects and spaces. In our daily life, colors can communicate or create a mental and sensitive predisposition to beauty, joy, inspiration, enchantment, serenity, silence, sadness, amazement, and many others depending on the person, on the moment and on the place. At every moment of seeing, color has different effects on our emotions and our subconscious. This influences our behavior and affects our perception of objects and spaces, therefore we must consider its relevance in the different areas of design.

Color has the capacity of awake the senses that allow human beings to perceive reality with different values and meanings [9].

Pinheiro [10] states that in landscapes and urban spaces, color influences us by physically and psychologically changing balance and body functioning; it causes sensations and emotions, changes the way we see and the forms we see, influences behaviors and choices and models the landscape that surrounds us transforming the spaces we move in.

The complex phenomenon of color perception involves aesthetic and psychological responses to color and influences art, architecture and all design areas: product design, interior design, fashion design, graphic design, etc.

The common perception that red, orange, yellow, and brown hues are ´warm', while the blues, greens, and grays are considered 'cold' is a good example of the link between color and people emotional sensations. If red, orange, and yellow hues induce excitement, cheerfulness and stimulation, if the blues and greens induce the feelings of calm, and peace, if more dark colors like grey and black hues generate sadness and melancholic feelings, this assumptions are relevant when designing interior spaces and ambiances and the use of colored sketches can be helpful for the designer and for the client.

Even in recent design areas like web design, colors represent an important issue and a relevant role. According to Song and Chen [11], one of the most important elements of web design is color, where the selection and matching of colors has a significant impact on the message of a web page. As human mind is affected by colors greatly, color matching is a relevant part of web designing. Firstly, different colors will cause different sensations and perceptions, and secondly, they will play an important role in conveying information, and also affect the psychological and emotional changes of users. In web design, choosing the right color scheme is a guarantee of the effectiveness of information communication, a necessary condition for design aesthetics, and also an effective way to convey emotions.

The design effects of colors make it easier to recognize, to create contrasts, to attract attention, to make associations, and to lead to unconscious reactions. For this reason, the designer places great importance on color selection. The place where the color is used while creating the design artifact or the ambiance, the target audience and the product characteristics are the factors that influence the color selection [12].

Figure 2. Graphic designer Massimo Vignelli's sketches for a stamp. Through the colored sketches we can observe the designer's process of the final colors choice [13]

Color can be an expression tool for the designer, revealing the message you want to give because the right choice of a color can evokes psychological affinities and thereby creates an emotional state of mind. As a result of this assumptions, we can consider that color adds a kind of soul to the designer sketches.

The use of color as a design element entails both a physiological response from the viewer as well as a response based in a cultural context. Color symbolism varies from culture to culture. However, there are still certain physiological sensations that are products of the human visual system combined with experience common to all humans, this shared visual color impacts can help designers when selecting the right colors for the final results they pretend [14].

In graphic design, product design, packaging design and all areas of communication design, the color phenomenon is used to make the design appeal to the target audience. Colors are one of the distinguishing factors. When examined in visual terms, the expression that color adds to the design should be able to attract and emotionally connect with the consumer.

However, there is also other issues that the designer should pay attention to: the main brand colors and, also, the region where the design will be used because the sense of color created by the society plays a big role in the promotion of the created artifact. The designer needs to know the meanings of colors well and apply them correctly. The use of correct and striking color together with other supporting elements in its formation, can lead to a successful design. Therefore, during the creation process through sketches, the choice of color is also a part of the product or the communication, strengthening its effect [12].

The color introduction in architectural sketches can give us a more clarified vision of the future design project, as we can observe in figure 2. The same ambiance seems completely different because the adding of colors can give us more information and create a distinguished atmosphere. We can even notice the reflections in the water that were not perceived in the black and white sketch. Using watercolors gives life to sketches.

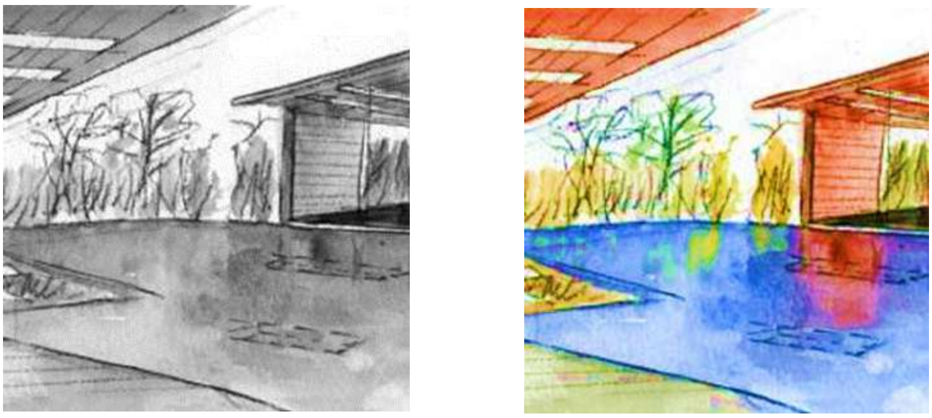

Figure 2. Color introduction on sketches can be relevant for the design process [15]

The use of colors on sketches can evidence most interesting and important aspects such as the distinctive materials and the different hues to be used in the future project, the human scale and even the lighting nuances.

CONCLUSION

Color is an intrinsic element of the environment and one of the visual attributes of the shape of objects. Colors characterize and define both objects and places.

Studies about color have explored the complex phenomenon of color perception and how it has fascinated artists, architects, designers, scientists and even poets and philosophers. Scientists agree that color can involve physical and emotional sensations.

Color psychology studies the brain's capacity to identify a color and transform it into a sensation or feeling. Colors have the ability to define our mood, our emotions and even our desires. Depending on the color, the human being perceive the dimension of an object or environment differently, since colors have the power to stimulate our brain in various ways.

Color has always interested those who express themselves through it and use it in objects, spaces or as communication material because color awakens the senses that allow human beings to perceive reality with different values and meanings. Therefore, color for the designer is one of the most important factors in design and must be examined according to the categories, and this information should be used during the designing phases.

When architects and designers operate sketches, they primarily perform as personal dialogue, breeding new options and promoting decision-making. According to our study, in the first phases of the design process, colored sketches can be essential for envisaging the possible color choices and for taking the right decisions about the use of certain colors instead of others to achieve the best final result. So, it is possible to establish a close relationship between sketch production and the use of color to enhance its communication with ourselves and with the other.

ACKNOWLEDGEMENT

The author would like to acknowledge the support given by CIAUD – Research Centre in Architecture, Urbanism and Design, Lisbon School of Architecture, Universidade de Lisboa, and by FCT – Foundation for the Science and Technology, Portugal. This work is financed by national funds through FCT - Fundação para a Ciência e a Tecnologia, I.P., under the Strategic Project with the references UIDB/04008/2020 and UIDP/04008/2020.

REFERENCES

1. Tversky, B. (2002). What does drawing reveal about thinking. Visual and spatial reasoning in design, Cambridge, Mass. MIT Press
2. Goldschmidt, G. (1992). Serial sketching: Visual problem solving in design - The backtalk of self-generated sketches. Cybernetics and Systems 23: 191-219.
3. Bekker, M. (1993). Representational issues related to communication in design teams. CHI 93, ACM. 151-152.
4. Barreira da Costa, R. (2019) Sketch Thinking - As Ideias Não-Verbais No Território Do Design De Produto. Dissertação de Mestrado, Instituto Politécnico do Cávado e do Ave.
5. Moreira da Silva, F. (2023). Color Processing and Human Perception. In: Ahram T., Karwowski W., Di Bucchianico P., Taiar R., Casarotto L., Costa P., (Eds) Intelligent Human Systems Integration (IHSI 2023): Integrating People and Intelligent Systems, Vol. 69, 223–230.
6. Wheeler, A. (2003) Designing Brand Identitiy. New Jersey: John Wiley and Sons.
7. Mahnke, F. (1996) Color, Environment & Human Response. New York: John Wiley & Sons.
8. Broeder, P. (2022). Colours of Emotion, Trust, and Exclusivity: A Cross-Cultural Study. Cultura E Scienza Del Colore - Color Culture and Science, 14(02), 14–21.
9. Santos, Z. & Simões, Z. (2021). Bairro Alto, Chromatic Proposal. In: Colour, Urban Space, Architecture and Design, Durão, M. J. (Ed.), Lisboa: Húmus.
10. Pinheiro, C. (2021). Colour in Social Housing, Routes of Discovery. In: Colour, Urban Space, Architecture and Design, Durão, M. J. (Ed.), Lisboa: Húmus.
11. Song, Y. & Chen, Y. (2023) The Possibility of Generating Color Scheme Based on Art Works for Web Design In: Ahram T., Karwowski W., Di Bucchianico P., Taiar R., Casarotto L., Costa P., (Eds) Intelligent Human Systems Integration (IHSI 2023): Integrating People and Intelligent Systems, Vol. 69, 734–741
12. Akengin, G. Arslan, A. Özen, Y. (2017) 2017, Idil Journal of Art and Language, Volume 6, Issue 31, 1077-1088.
13. https://vignellicenter.tumblr.com/post/627456921851592704/
14. Wegman, E. & Said, Y. (2011) Color Theory and Design, Hoboken, New Jersey: John Wiley & Sons, Inc.
15. https://archiscapes.wordpress.com/2015/03/23/the-art-of-sketches/

Session 4

Doi Tung
29 November 2023

COLOUR MATCHING FUNCTIONS MEASURED IN 30 YOUNG COLOUR-NORMAL OBSERVERS

Keyu Shi[1], Ming Ronnier Luo[1]*, Andrew Rider[2], Andrew Stockman[1, 2]

[1]State Key Laboratory of Modern Optical Instrumentation, Zhejiang University, Hangzhou, China.
[2]University College London Institute of Ophthalmology, EC1V 9EL London, UK.

*Corresponding author: Ming Ronnier Luo, m.r.luo@zju.edu.cn

ABSTRACT

In this study, 30 young Chinese observers (mean at 26) with normal colour vision performed colour matches on a new LED-based trichromator. The matches were compared with other colour matching standards and used to derive individual colour matching functions (CMFs). Maxwell's method was employed for colour matching, wherein triplets of lights with different wavelengths were matched against a white standard. A multi-primary visual trichromator produced 11 sets of primary triplets. These primary sets illuminated a semi-circular matching field adjacent to a second semi-circular field illuminated by a reference white. Observers adjusted the intensities of each primary set until they achieved a match with the white standard. Each match was recorded as a spectral power distribution (SPD). Thirty Chinese observers with normal colour vision participated in the experiment. Each observer completed 30 colour matches at visual field angles of both 2° and 10° in a dark environment (11 matches + 4 repeats for both 2° and 10°, totaling 30 matches). The experiment lasted approximately 1.5 hours. The SPDs for each colour match were multiplied with the CIE 2006 and 2015 standard CMFs for 2° and 10°, respectively, and integrated to calculate the chromaticity coordinates of the match. These coordinates were used to fit a 95% confidence ellipse, estimating the variability of the matches for different sets of primaries. The results indicated that different combinations of primaries could result in varying colour matching errors between observers, leading to changes in the shape, size, and orientation of the 95% confidence ellipse. Comparing CIE 1931 2°, CIE 1964 10°, CIE 2006 2°, and CIE 2006 10° CMFs, the prediction errors were 0.0070, 0.0119, 0.0067, and 0.0120 $\Delta u'v'$ units, respectively, for the 2° matches, and 0.0093, 0.0035, 0.0068, and 0.0040 $\Delta u'v'$ units, respectively, for the 10° matches. The observers' colour matching data were analyzed using a model developed by Stockman and Rider based on the CIEPO06 model. This analysis allowed estimation of the spectral position of the cone fundamentals, their photopigment optical densities, macular pigment densities, and lens densities. From the experimental results, it could be concluded that observer's individual CMFs can fit their experimental data better than the CIE standard CMFs.

Keywords: Colour matching experiment, Maxwell's method, Individual colour matching functions

INTRODUCTION

Human colour vision varies between observers because of individual differences in macular and lens optical densities, photopigment optical densities and spectral shifts in the underlying cone photopigment spectra [1]. These differences are manifested in individual differences in the shapes of the long-, middle- and short-wavelength (L-, M- and S-) cone spectral sensitivities (measured with respect to light entering the eye), which are also known as the cone fundamental LMS colour matching functions (CMFs). Before the CIE 2006 standards, the standard 2° and 10° colorimetric observers defined by the CIE to represent the average observer were defined in terms of XYZ (or RGB) CMFs. The CIE 1931 2° standard colorimetric observer was based upon the data accumulated by Guild (1931) [2] and Wright (1929) [3, 4] and constructed using the *V(λ)* function and is seriously flawed [1]. The CIE 10° 1964 standard colorimetric observer was based on colour matching measurements made by Stiles and Burch (1959) [5], and Speranskaya (1959) [6]. The rapid development of technology, including the use of spectrally narrow-band lights, makes these two standard colorimetric observers unable to meet new application requirements, because neither can be easily modified to account for individual differences. Moreover, the flaws in the 1931 observer can lead to large errors in colour reproduction even before individual differences are considered [7, 8]. Recent research has shown that using the inappropriate 2° and 10° standard colour matching functions may result in more pronounced observer metamerism on display [9, 10].

In 1991, CIE established a technical committee TC1-36 to "establish a fundamental chromaticity diagram of which the coordinates correspond to physiological significant axes". Many years later, in 2006, the CIE adopted the committee's proposal for a new physiological observer model (CIEPO06), which includes a standard LMS and RGB observer for 2° and 10° that can be adjusted for individual differences [11,12]. The CIEPO06 model is almost entirely based on the work of Stockman and Sharpe [13]. Starting from 10° RGB CMFs of 47 Stiles-Burch observers [5], the model defines 2° and 10° fundamental observers and provides a convenient framework for calculating average cone fundamentals for any field size between 1°and 10° and for any age between 20 and 80 and incorporates individual differences. In 2015, the CIE adopted a transformation from CIEPO06 LMS to XYZ.

Some researchers characterized this individual variability in the population by proposing standard deviate observers. In 2010, Sarkar *et al.* [14] proposed a cluster analysis method for observer classification, which can help effectively address the issue of observer metamerism in industrial applications, and can also be a vital tool in fundamental colour research. In 2020, Asano et al. [15] investigated the number of required categorical observers to represent colour-normal populations for personalized colour imaging. Based on the work of Sarkar and Asano, in 2020, Huang et al. [16] categorized four CMFs for young and aged observers, respectively.

The main goals of this study were first is to build an apparatus with which to measure colour matches, then measure them in a large group of observers; and last to develop a reliable method of deriving the individual colour matching functions from those matches first as LMS cone fundamentals and then as XYZ CMFs. Standard deviate CMFs will also be proposed.

METHODOLOGY

In this study, a multi-primary visual trichromator named LEDMax was developed for the colour matching. The trichromator is made up of three parts: a control panel, two identical left and right LED Cube illuminators and a viewing compartment. Figure 1 is the schematic diagram of letter two parts of the system. Each illuminator contains 18 LEDs with different centre wavelengths ranging from 400 to 700 nm. The light emitted by the left and right LED Cube units illuminate a white reflective surface in the viewing compartment, and then uniformly fill the two side-by-side semi-circular apertures.

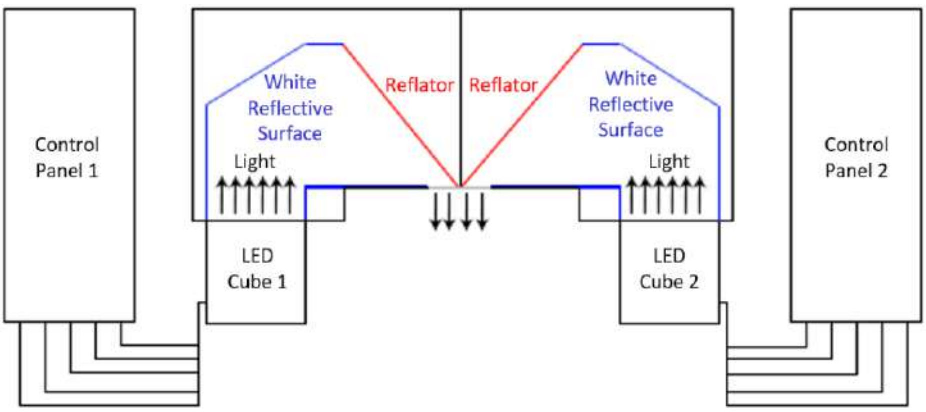

Figure 1. The Internal structure of the visual trichromator

The two LED Cube illuminators could be controlled via a colour adjustment panel. Observers were able to adjust the colour appearance of the stimuli in either of the two semicircular fields, although one field was typically fixed at the standard white.

The Maxwell's matching method [5] was chosen as the experimental method. Maxwell did the first careful, quantitative measurements of colour matching and developed the trichromacy colorimetry (1860). The method is illustrated in Figure 2.

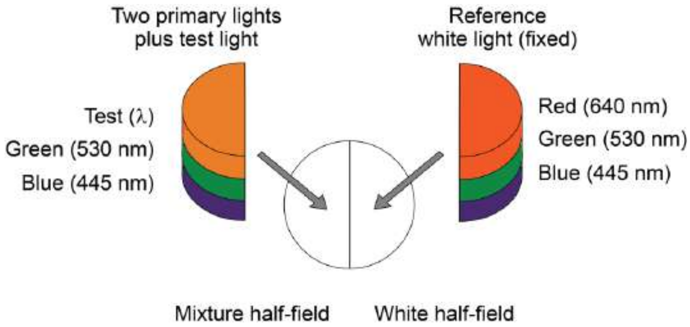

Figure 2. Maxwell's colour matching method.

As it is shown, the matched fields always appear white, so that at the match point the eye is always in the same state of adaptation whatever the combination of primary wavelengths.

Table 1 shows different primary sets were used to match the reference stimulus, which was always in the White half-field with 3 fixed LEDs at 640 nm, 530nm and 445 nm, corresponding to CCT of 7500K at luminance of 100 cd/m^2.

Table 1: The 11 different primary sets for Mixture half-field.

Primary	R (nm)	G (nm)	B (nm)
1	640	530	430
2	640	530	445
3	640	530	460
4	640	530	475
5	640	505	445
6	640	545	445
7	640	560	445
8	595	530	445
9	605	530	445
10	660	530	445
11	675	530	445

In this study, 30 young Chinese observers (mean age 26, ranging from 20 to 30) with normal colour vision performed experiment. All observers had to pass the Ishihara Colour Vision Test first. In the dark room, observers were also trained to adapt to the operation method and this process lasted for about 15-30 minutes. In the main experiment, after adapting to the testing environment for two minutes, observers began to make colour matches with FOV of 10°, until 15 matches were completed (11 matches and 4 repeats). After a brief rest and re-adaptation, the observer completed 15 further sets of colour matches for a 2° FOV. The four repeats were primary sets 2, 3, 6, 10. In total, each observer had to perform 30 colour matches, which took on average time of about 90 minutes.

RESULT AND DISCUSSION

The SPDs of all the matched stimuli that were matched by the observers were measured after completion of the experiment using the TSR from the observer's eye position. Then photometric and colorimetric values could be derived from the SPDs. Thus, Intra- and Inter-observer variation, and matching error (the colour difference between reference and observer's matching colour) could be represented by the *Δu'v'*. Before the individual colour matching functions be fitted, the calculation process of the results of 2° and 10° experiments used CIE 2006 2° CMFs and CIE 2006 10° CMFs, respectively. Figure 3 shows the 95% confidence ellipses of the matching results in 2° and 10° experiment.

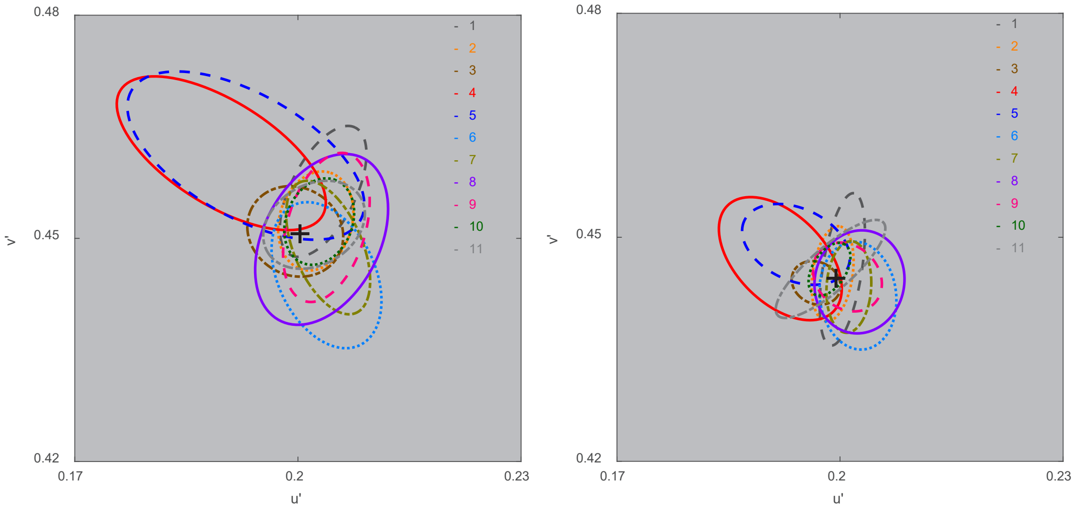

Figure 3. The 95% confidence ellipses for each primary set (left: 2°experiment, right: 10°experiment, '+': reference).

The SPDs for each colour match were then cross-multiplied with the CIE 2006 and 2015 standard colour matching functions (CMFs), for 2° and 10°, respectively, and integrated to calculate the chromaticity coordinates of the match. These were then used to fit a 95% confidence ellipse to estimate the variability of the matches for different sets of primaries. The results showed that different primary combinations could lead to different colour matching errors between observers and changes in the shape, size, and orientation of the 95% confidence ellipse. Comparisons across CIE 1931 2°, CIE 1964 10°, CIE 2006 2°, CIE 2006 10° CMFs gave prediction errors of 0.0070, 0.0119, 0.0067, 0.0120 *Δu'v'* units, respectively, for the 2° matches, and errors of 0.0093, 0.0035, 0.0068, 0.0040 *Δu'v'* units, respectively, for the 10° matches.

The experimental data will also be used to fit the individual colour matching functions. The computational method of this study is mainly based on the method developed by Stockman and Rider [17], based on CIEPO06 [13]. The strategy was first to derive mathematical functions for the logarithmic L-, M- and S- cone absorbance spectra and for the standard lens and macular optical density spectra, as Figure 4 shows.

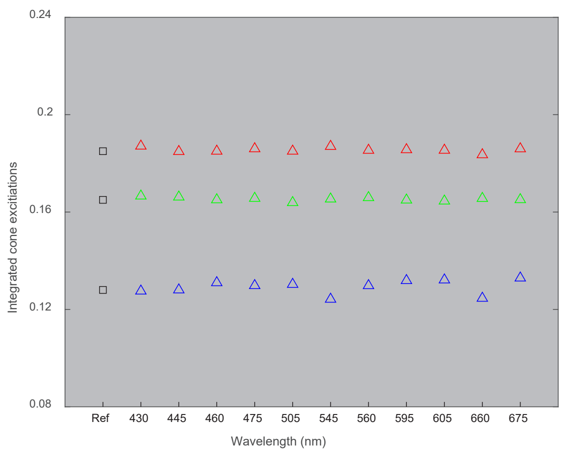

Figure 4. The process of fitting Stockman's model to each individual's matches.

With this physiological model, the cone fundamental CMFs can be derived for each individual by varying up to 7 parameters: the optical densities of the L-, M- and S-cones, i.e. l_{OD}, m_{OD} and s_{OD}; the lens and macular densities, k_{lens} and k_{mac}; and the spectral shifts of the L and M cones L_{shift} and M_{shift}. By fitting this model to each individual's matches, minimising the squared difference in the estimated L, M and S-cone excitations between the reference white spectrum and the 11 matched spectra (fitting error for seven parameters), the CMFs could be derived,

The fitted cone fundamentals of 30 observers are showed in Figure 5, while the black curves are CIE 2006 standard cone fundamentals to be compared with.

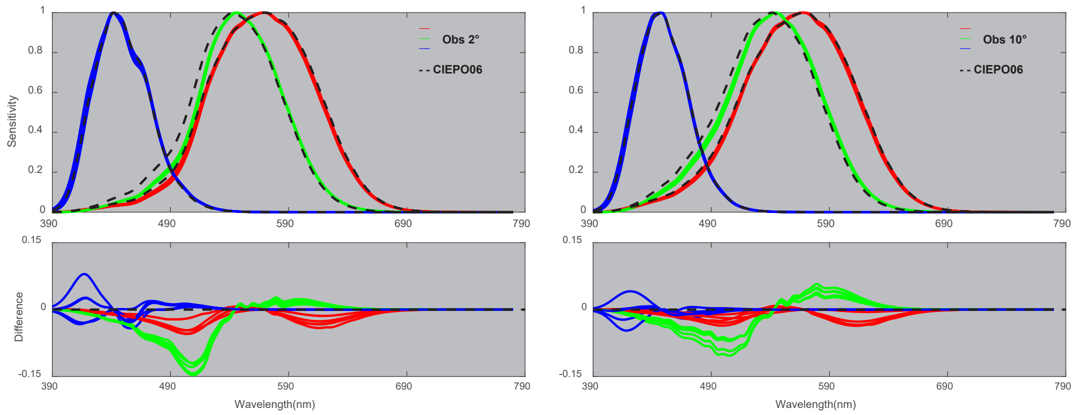

Figure 5. The fitted cone fundamentals of 30 observers (left: 2°, right: 10°, black lines: CIE 2006 2° cone fundamentals and CIE 2006 10° cone fundamentals).

After the individual colour functions are fitted, an important step is to verify that it can accurately represent the observer's visual characteristics. The most direct method is to use observer's own colour matching functions to replace the CIE standard colour matching functions when calculating the matching error. In theory, when the observer considers a pair of stimuli to be a perfect match, the colour difference calculated using the observer's own colour matching functions will be zero. However, in actual experiments, no observer can perfectly repeat the previous experiment every time and always achieve the best match. Therefore, it cannot be used as a standard for judging whether the individual colour matching function is accurate by whether the calculated matching error is zero. Thus, in this study, the judgment criterion is whether using the observer's own colour matching functions instead of the CIE standard colour matching functions can reduce the calculated colour matching error.

As mentioned before. Comparisons across CIE 1931 2°, CIE 1964 10°, CIE 2006 2°, CIE 2006 10° CMFs gave prediction errors of 0.0070, 0.0119, 0.0067, 0.0120 *Δu'v'* units, respectively, for the 2° matches, and errors of 0.0093, 0.0035, 0.0068, 0.0040 *Δu'v'* units, respectively, for the 10° matches. When the fitted individual CMFs were applied to calculation, the prediction errors became 0.0052 and 0.0023 *Δu'v'* units for the 2° and 10° matches. From the above result, it could be concluded that observer's individual CMFs can fit their experimental data better than the CIE standard CMFs.

CONCLUSION

In this study, a multi-primary visual trichromator named LEDMax was developed for the colour matching. The Maxwell colour matching experiment was performed by five observers with normal colour vision. The fixed mixture half-field was white, while the white half-field was illuminated by three standard primaries one of which was replaced by a spectrally offset primary. Observers adjusted the three primaries to match the white standard. Each observer performed 30 colour matches in the experiment, which took on average time of about 90 minutes.

The colour matching data were used to fit confidence ellipses and individual color matching functions. The results were reported in terms of inter- and intra- observer variations together with a plot of their perceptibility ellipses to represent observer metamerism.

The Stockman and Rider's method was described and used to develop CMF for each individual observer. From the prediction result, it could be concluded that observer's individual CMFs can fit their experimental data better than the CIE standard CMFs.

ACKNOWLEDGEMENT

This work was supported by the National Natural Science Foundation of China (61775190).

REFERENCES

1. Stockman, A., and Sharpe, L. T. (1999) Cone spectral sensitivities and color matching. Color vision: From genes to perception 53–88.
2. Guild, J. (1931). The colorimetric properties of the spectrum. Philosophical Transactions of the Royal Society of London. Series A, Containing Papers of a Mathematical or Physical Character 230, 149–187.
3. Wright, W. D. (1929). A re-determination of the trichromatic coefficients of the spectral colours. Transactions of the Optical Society 30, 141.
4. Wright, W. D. (1930). A re-determination of the mixture curves of the spectrum. Transactions of the Optical Society 31, 201.
5. Stiles, W. S., and Burch, J. M. (1959). NPL colour-matching investigation: final report. Optica Acta: International Journal of Optics 6, 1–26.
6. Speranskaya, N. I. (1959). Determination of spectral colour co-ordinates for twenty-seven normal observers. Optics, Spectrosc 7, 424–428.
7. Wu, J., Wei, M., Fu, Y., and Cui, C. (2021). Color mismatch and observer metamerism between conventional liquid crystal displays and organic light emitting diode displays. Optics Express 29, 12292–12306.
8. Huang, M., Li, Y., and Wang, Y. (2021). Effect of Primary Peak Wavelength on Colour Matching and Colour Matching Function Performance. Optics Express 29, 40447–40461.
9. Shi, K., and Luo, M. R. (2022). Factors affecting colour matching between displays. Optics Express 30, 26841–26855.
10. Hu, Y., Wei, M., and Luo, M. R. (2020). Observer metamerism to display white point using different primary sets. Optics Express 28, 20305–20323.
11. CIE. (2006). Fundamental chromaticity diagram with physiological axes – part 1.
12. CIE. (2015). Fundamental chromaticity diagram with physiological axes – part 2: spectral luminous efficiency functions and chromaticity diagrams.
13. Stockman, A., and Sharpe, L. T. (2000). The spectral sensitivities of the middle- and long-wavelength-sensitive cones derived from measurements in observers of known genotype. Vision research (Oxford) 40, 1711–1737.
14. Sarkar, A., Autrusseau, F., Viénot, F., Le Callet, P., and Blondé, L. (2011). From CIE 2006 physiological model to improved age-dependent and average colorimetric observers. JOSA a 28, 2033–2048.
15. Asano, Y. and Fairchild, M. D. (2020). Categorical observers for metamerism,Color Research & Application 45, 576–585.
16. Huang, M., Xi, Y., Pan, J., He, R., and Li, X. (2020). Colorimetric observer categories for young and aged using paired-comparison experiments. IEEE Access 8, 219473–219482.
17. Stockman, A., & Rider, A. T. (2023). Formulae for generating standard and individual human cone spectral sensitivities. Color Research and Application, 2023.

EFFECT OF SPATIAL DISTRIBUTION OF CHROMATICITY AND LUMINANCE ON CHROMATIC ADAPTATION

Siqi Li [1], Shining Ma [1]*, Yue Liu[1], Yongtian Wang[1] and Weitao Song[1]

[1]*Beijing Engineering Research Center of Mixed Reality and Advanced Display, School of Optics and Photonics, Beijing Institute of Technology, Beijing, China.*

*Corresponding author: Shining Ma, shining.ma@bit.edu.cn

ABSTRACT

In recent years, the studies on chromatic adaptation have been extended to dichromatic illuminations, based on the traditional CAT models derived from single illumination conditions. However, as these studies mainly focused on the impact of chromaticity distribution and collected data under dichromatic illuminations spatially invariant in luminance, it is still unknown how to estimate the adaptation state under dichromatic illuminations with non-uniform luminance distribution. The goal of this study is to investigate how spatial luminance distribution influences chromatic adaptation. Achromatic matching experiments were adopted to collect corresponding colour data for various dichromatic illuminations varying in luminance distribution. In the experiment, the Blue-Red color pair was selected. There were two transition types between the two illuminants including sharp transition and gradient transition. Additionally, in terms of the luminance distribution, a total of six non-uniform luminance combinations of two illuminations were selected (left-right): 40-120 cd/m^2, 40-240 cd/m^2, 120-240 cd/m^2, 120-40 cd/m^2, 240-40 cd/m^2, 240-120 cd/m^2. Eighteen observers with normal colour vision, as tested by the Ishihara 24-plate test, participated in the experiments. It has been found that the equivalent illuminant chromaticity was biased by the illuminant with a higher luminance level even though two illuminants occupy the same proportion. And the equivalent illuminant chromaticity always shifts to the side with increasing luminance. The significant impact of luminance distribution on the equivalent illuminant chromaticity (in terms of ratio) has been confirmed by a GLMM statistical test. Consistent with the findings in previous studies, the ratio is significantly influenced by the transition type. In addition, there is a significant interaction between the transition type and illumination distribution: the luminance change has a more pronounced impact on the adaptation state of sharp-transitioned dichromatic illuminations than that of gradient-transitioned conditions. In the future, a more comprehensive CAT model for dichromatic illuminations will be derived from the collected visual data by considering the spatial distribution of luminance and chromaticity.

Keywords: Chromatic adaptation, Dichromatic illuminations, Luminance, Transition position

INTRODUCTION

The human visual system has the ability to adjust the spectral sensitivity of three cones according to the illumination color, referred to as chromatic adaptation [1]. That means the color appearance of a physical object keeps approximately constant under various illuminations. Over the years, various chromatic adaptation transforms (CATs) have been proposed to estimate the corresponding color under test illumination including CMCCAT97 [2], CAT02 [3], CAT16 [4], etc., and they were derived from uniform illumination conditions. However, as well acknowledged, the real scene always contains more than one illuminant, such as the office setting illuminated by both daylight and artificial light, and the stage lighting as the mixture of spotlight and ambient lighting. Therefore, it is very necessary to study the chromatic adaptation in multi-chromatic illuminations. Khang and Zaidi found that when the illumination environment was composed of two illuminants, the influence of the illumination chromaticity on the object was reduced [5]. Ma et al. conducted a series of achromatic matching experiments to investigate the adaptation state under dichromatic illuminations varying in transition type, color pair, and chromaticity distribution. It has been found that for sharp transition, the adaptation state is more biased by the illuminant with a higher degree of adaptation [6]. In addition, the contribution of illumination color to the adaptation state diminishes with the viewing angle [7].

As these studies mainly focused on the impact of chromaticity distribution, the visual data was collected under dichromatic illuminations spatially invariant in luminance. Therefore, it is still unknown how to estimate the adaptation state under dichromatic illuminations with non-uniform luminance distribution. In order to further study chromatic adaptation under complex dichromatic illuminations and establish a more comprehensive CAT model, an achromatic matching experiment was adopted to collect corresponding color data for various dichromatic illuminations varying in luminance distribution in this study.

METHODOLOGY

Experiment Apparatus. To enhance the realism of the scene, a deep platform covered with non-fluorescent white paper was used as the background in this experiment, similar to that of Smet et al. [8]. From the perspective of the observer, the overall field of view (FOV) of the background was 80° (horizontal) × 70° (vertical). The stimulus was a small gray cube located in the center of the background, occupying about 6° FOV. An Epson-CB-2265U data projector mounted above the observer provided the illumination of both the stimulus and background, as illustrated in Figure 1. After optimizing the RGB driving values of the projector in the background area, the $u'_{10}v'_{10}$ chromaticity difference between the measured chromaticity and the target value was less than 0.001. Besides, since the gray cube has a field of view larger than 4°, all the colorimetric calculations in the further analysis were performed using the CIE 1964 10° color matching functions.

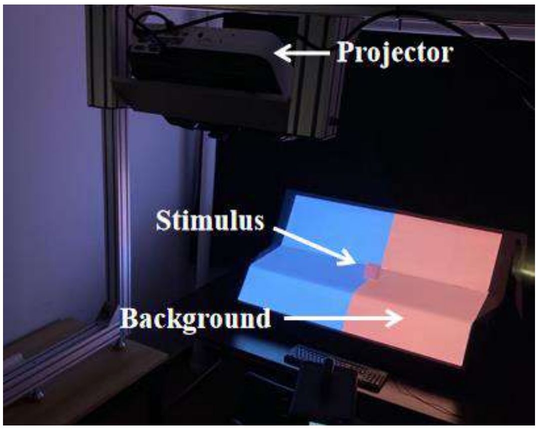

Figure 1. Experimental scene.

Experiment conditions. In the experiment, the dichromatic illumination was composed of two illuminants varying in color: the Planckian illuminant with a CCT of infinity (Binf), and the reddish illuminant (Red). The Binf illuminant, denoted as I1, illuminates the left side of the adapting field while the Red illuminant, denoted as I2, illuminates the right side of the adapting field. The spectra and u'_{10} v'_{10} chromaticities of the two illuminants were plotted in Figure 2(a) and 2(b), respectively. The transition between two illuminants was located in the center, and each illuminant occupied 50% of the adapting field. The average chromaticity of the whole scene is the same as the mean chromaticity of the two illuminants. There were two transition types between the two illuminants including sharp and gradient, as shown in Figure 3. Additionally, in terms of the luminance distribution, a total of six non-uniform luminance combinations of two illuminants were selected (left-right): 40-120 cd/m^2, 40-240 cd/m^2, 120-240 cd/m^2, 120-40 cd/m^2, 240-40 cd/m^2, 240-120 cd/m^2. In order to further quantify the adaptation state of the dichromatic illumination, for each luminance combination, achromatic matching experiments were also performed under three uniform illuminations. The chromaticities of the uniform backgrounds were selected as the chromaticity of both illuminants and the midpoint of the line (see Figure 2), and the corresponding luminance levels were selected as the luminance of the two illuminants and their average value.

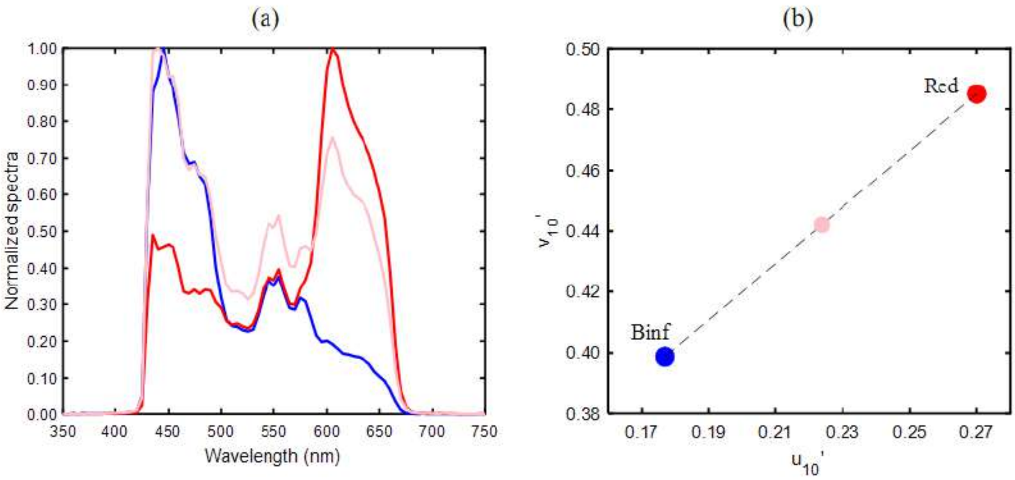

Figure 2. (a). The spectra of the two illuminants. (b). The chromaticity distribution of I1 and I2 in the u'_{10} v'_{10} chromaticity diagram.

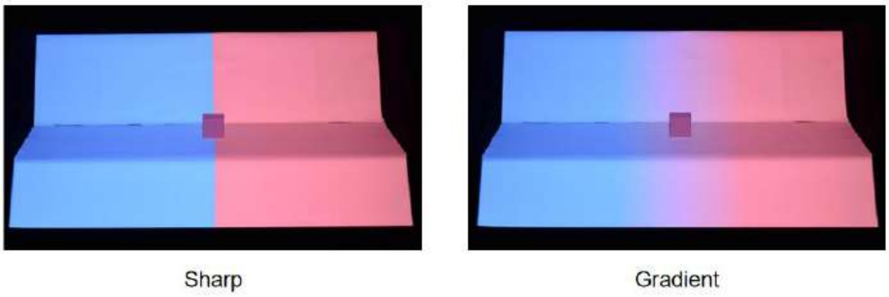

Figure 3. Non-uniform background scenes (adapting fields) under the dichromatic illuminations.

Experiment procedures. The achromatic matching method was adopted in this experiment, where the observer was required to adjust the stimulus color until it appeared neutral gray. By this means, the corresponding colors with neutral appearance were collected under various illumination conditions. Before the formal experiment, the observer was asked to sit in a fixed position, 1 *m* away from the adapting field. During the adaptation period of each round, the observer was required to stare at a black moving spot with symmetrical motion paths for 45 *s* to ensure an unbiased adaptation state. When the black spot vanished, the observer could adjust the illumination color projected on the gray cube using the arrow keys in the keyboard until the color appearance of the cube matched the neutral gray in memory. The initial color of the gray cube was randomly selected within the color gamut of the projector. The adjustment was implemented in the $u'_{10}v'_{10}$ space while keeping the luminance of the gray cube constant. Once the observer achieved a satisfactory match, the illumination would change to a new combination of dichromatic illumination and starting point. After the completion of all matching experiments in each group, the spectra of matching results were measured using a JETI specbos 1211-UV-2 spectrometer.

Observers. Eighteen observers (9 males and 9 females) aged 22 to 23 were recruited for the experiment. They are all graduate or undergraduate students with normal color vision as confirmed by the Ishihara 24-plate test, recruited from Beijing Institute of Technology.

RESULT AND DISCUSSION

Observer variability. The inter-observer variability was assessed using the mean color difference from the mean (MCDM) in the $u'_{10}v'_{10}$ space [9]. The average inter-observer variability *MCDM* values for six luminance combinations are equal to 0.014, 0.015, 0.015, 0.015, 0.014, 0.015, corresponding to 40-120 cd/m^2, 40-240 cd/m^2, 120-240 cd/m^2, 120-40 cd/m^2, 240-40 cd/m^2, 240-120 cd/m^2, respectively. The achromatic matching tasks under four dichromatic illuminations and two uniform ones were repeated twice to examine the repeatability of each observer. The intra-observer variability for each observer was estimated by the mean color difference between two repetitions over six illuminations. The intra-observer variability averaged over eighteen observers is equal to 0.0080, suggesting the reliability of collected visual data.

Luminance and chromaticity of equivalent illumination. Equivalent illumination, as previously defined by Ma in their paper [10], refers to a single illumination that can produce an identical chromatic adaptation state to that of a dichromatic illumination. For one dichromatic illumination, the equivalent illumination chromaticity can be calculated using the method explained in the previous article: the visual data collected under three uniform backgrounds provides a reference for estimating the equivalent illumination chromaticity. The ratio obtained from the chromaticity interpolation of achromatic matches was used as the luminance ratio of the two illuminants to calculate the equivalent illumination luminance. Similar to previous studies, the equivalent illumination can be simply quantified by a ratio, denoted as '$\Delta_{meq,r1}$', which illustrates the contributions of two illuminants to the adaptation state. The '$\Delta_{meq,r1}$' refers to the chromaticity/luminance difference between the equivalent illumination and I1 divided by that between I1 and I2. When $\Delta_{meq,r1}$ is less than 0.5, the equivalent illumination chromaticity is closer to I1; on the contrary, if $\Delta_{meq,r1}$ ranges from 0.5 to 1, then I2 contributes more and the equivalent illumination chromaticity is closer to I2.

The impact of transition type. For dichromatic illuminations of six luminance combinations, the $\Delta_{meq,r1}$ values were summarized in Figure 4 with two subfigures corresponding to the sharp and gradient transition, respectively. Besides, the $\Delta_{meq,r1}$ values predicted by the two models were also presented as the reference in Figure 4. One model proposed by Ma et al. [6] considers the impact of transition type and the predicted $\Delta_{meq,r1}$ values, denoted as $\Delta_{meq,r1\text{-}Ma}$, are equal to 0.50 and 0.17 (average of six luminance combinations) for gradient and sharp transition, respectively. The other model follows the gray world assumption, taking the equal illumination as the average of the whole scene, and the predicted $\Delta_{meq,r1}$ value, denoted as $\Delta_{meq,r1\text{-}GW}$, varies with luminance combination. There is a substantial influence of the transition type on $\Delta_{meq,r1}$. It can be observed that compared to the sharp transition, the variation of $\Delta_{meq,r1}$ caused by different luminance combinations is much smaller for the gradient transition. However, this trend cannot be well predicted by either $\Delta_{meq,r1\text{-}GW}$ or $\Delta_{meq,r1\text{-}Ma}$.

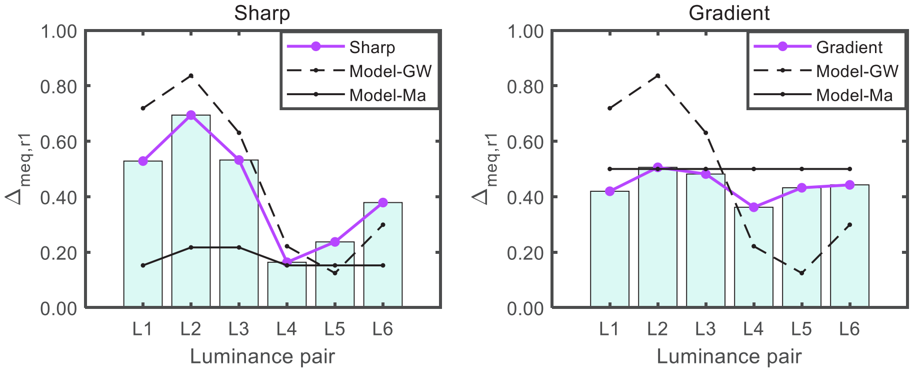

Figure 4. The $\Delta_{meq,r1}$ values under six different luminance combinations. The symbol 'L1'-'L6' represent the luminance combination: 40-120 cd/m2, 40-240 cd/m2, 120-240 cd/m2, 120-40 cd/m2, 240-40 cd/m2, 240-120 cd/m2, respectively.

The impact of spatial luminance distribution. As can be seen in Figure 4, the $\Delta_{meq,r1}$ value decreases as the luminance combination is changed from 'L1'-'L3' to 'L4'-'L6'. For combination 'L1'-'L3', the luminance of I1 is smaller than that of I2, while for combination 'L4'-'L6', the luminance of I1 is larger than that of I2. The decrease in $\Delta_{meq,r1}$ indicates that the equivalent illumination is moving toward I1, that is, toward the side where the luminance increases. The result indicates that the luminance combination substantially affects the adaptation state, and the equivalent illumination is biased to the side with larger or increased luminance. In order to further study the influence of luminance combination on $\Delta_{meq,r1}$ value, a luminance ratio $ratio_L$ was defined as given below:

$$ratio_L = \frac{L_{w,I2}}{L_{w,I1} + L_{w,I2}} \tag{1}$$

where $L_{w,I1}$ and $L_{w,I2}$ are the luminance of I1 and I2, respectively. The relationship between $\Delta_{meq,r1}$ and $ratio_L$ was plotted in Figure 5. It could be found that the $\Delta_{meq,r1}$ value monotonously increases with the luminance ratio for both the sharp and gradient transition. In addition, the six data points were fitted by a linear function for each transition type. The slopes of the linear fitting functions are equal to 0.64 and 0.11 corresponding to the sharp and gradient transition, respectively. The higher slope of the sharp transition indicates that for sharp-transitioned dichromatic illuminations, the sensitivity of $\Delta_{meq,r1}$ to the variation of $ratio_L$ is greater than that of the gradient transition. The coefficient of determination (r^2) of the fitted lines for the sharp and gradient transition are 0.90 and 0.40, respectively. It can be found that for the sharp transition, the $\Delta_{meq,r1}$ value is always highly correlated with $ratio_L$, but the correlation is less pronounced for the gradient transition.

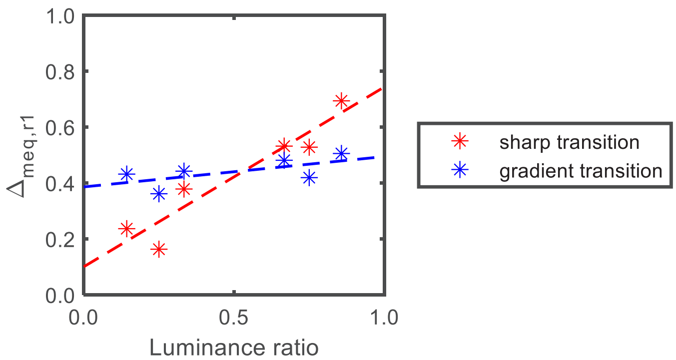

Figure 5. The relationship between the $\Delta_{meq,r1}$ value and the $ratio_L$.

CONCLUSION

The luminance distribution of dichromatic illuminations will affect the chromatic adaptation state. The equivalent illuminant chromaticity was biased by the illuminant with a higher luminance level and always shifts to the side with increasing luminance even though two illuminants occupy the same proportion. Not only that, there is a significant interaction between the transition type and illumination distribution. The adaptation state of sharp-transitioned conditions is more sensitive to the luminance change than that of gradient-transitioned conditions. In the following work, we will further establish a more comprehensive CAT model for dichromatic illuminations with complex luminance and chromaticity distribution.

REFERENCES

1. Commission Internationale de l'Eclairage. (2004). CIE 160:2004 A Review of Chromatic Adaptation Transforms.
2. Luo, M. R., Hunt, R. W. G., Hashimoto, K., Sobagaki, H., Takahama, K., Yano, T., Berns, R. S., & Fairchild, M. D. (1998). The Structure of the CIE 1997 Colour Appearance Model (CIECAM97s). Color Research and Application, 23(3), 138–146.
3. Moroney, N., Changjun, li, Ronnier Luo, M., Fairchild, M. D., Hunt, R. W., Li, C., Ronnier Luo, M., & Newman, T. (2002). The CIECAM02 color appearance model. IS&T/SID Tenth Color Imaging Conf, 23–27.
4. Li, C., Xu, Y., Wang, Z., Luo, M. R., Cui, G., Melgosa, M., Brill, M. H., & Pointer, M. (2018). Comparing two-step and one-step chromatic adaptation transforms using the CAT16 model. Color Research and Application, 43(5), 633–642.
5. Khang, B. G., & Zaidi, Q. (2004). Illuminant color perception of spectrally filtered spotlights. Journal of Vision, 4(9), 680–692.
6. Ma, S., Li, S., Sun, R., Liu, Y., Wang, Y., & Song, W. (2022). Transition type influences the adaptation state under dichromatic illuminations. Optics Express, 30(26), 47134.
7. Ma, S., Teunissen, K., Smet, K.A.G. (2023). Adaptation under dichromatic illumination. Optics Express, 10.1364/OE.494090.
8. Smet, K. A. G., Zhai, Q., Luo, M. R., & Hanselaer, P. (2017). Study of chromatic adaptation using memory color matches, Part II: colored illuminants. Optics Express, 25(7), 8350–8365.
9. F. W. Billmeyer, & P. J. Alessi. (1981). Assessment of Color-Measuring Instruments. Color Research and Application, 6(4), 195–202.
10. Ma, S., Hanselaer, P., Teunissen, K., & Smet, K. A. G. (2020). The impact of transition type on chromatic adaptation under dual lighting conditions. Color and Imaging Conference, 28(1), 36–41.

COLOR CONSTANCY AND VISUAL PERCEPTION

Fernando Moreira da Silva[1]*

(CIAUD, Research Centre for Architecture, Urbanism and Design, Rua Sá Nogueira, Pólo Universitário, Alto da Ajuda, 1349-063 Lisboa, Portugal)
[1]CIAUD, Lisbon School of Architecture, Universidade de Lisboa, Portugal.

*Corresponding author: Fernando Moreira da Silva, fms.fautl@gmail.com

ABSTRACT

The brain is the organ responsible for decoding electrical signals into experiences that make sense for humans to perceive the world. Color vision is closely associated with visual processing and human perception. The functional properties of neurons in the visual cortex are highly dynamic and can be altered by visual experience, given that visual processing in the cortex is subject to the influence of cognitive functions. Perceptions of shapes, contours, and depth are calculated from the relative positions of objects on the retina. Color constancy refers to the human ability to recognize objects with a stable color under various lighting conditions. This is only possible due to chromatic adaptation, which can be defined by the ability to adjust to the ambient lighting and see objects as they really are. This implies that we perceive that colors are "always" the same (in natural conditions), that is, for example, red for us will always be red. However, this constancy is partial, as visual perception changes when lighting also changes. We have been developing a research project based on a quasi-experiment with human beings, in order to help the understanding of brain reactions to different dimensions of color, namely color constancy, that is, the human tendency to perceive a given object as having the same color regardless of changes in lighting, angle or distance, just like human perception and cognition. This paper presents not only the thematic theoretical framing, but also the results of the practical work carried out in which 52 individuals, of different ages and genders, participated. Although at first glance it seems like a relatively simple human ability, color constancy is a phenomenon that involves different variables. With this investigation it is expected to be able to contribute to the deepening of knowledge, especially in terms of color constancy and visual perception, given that color constancy plays a fundamental role in the human perception of color.

Keywords: Color Constancy, Visual perception, Color Cognition, Human processing.

INTRODUCTION

Already for some years, we have been dealing with visual processing and human perception with regard to color vision. Since the brain is the organ responsible for decoding the electrical signals it receives from the human eye, we have been investigating the visual cortex and each of its different areas (mainly V1, V2, V3, V4 and V5), its structure and function, in which each of them plays a specific role at the level of the human visual processing.

However, knowing that areas V1 and V2 are considered to have the greatest responsibility in terms of initial visual processing, recent studies have come to the conclusion that area V4 is more active in what concerns the execution of tasks inherent in the processing of colors.

These findings led us to want to delve deeper into brain reactions to different dimensions of color, color processing, as well as human perception and cognition and the importance of color constancy. To this end, and within the scope of an ongoing research project, we have developed a quasi-experience with human beings, so that we can compare their results with the color State of the Art. This paper presents and interprets the obtained results of the quasi-experience.

VISUAL PROCESSING AND VISUAL CORTEX

Visual Processing is the brain's ability to perceive, interpret and process information received through the eyes. The capabilities of visual processing are the mechanisms that the human brain uses to decode the visualized reality, which in turn is directly related to visual perception and the visual cortex, an area in the cerebral cortex which is located in the occipital lobe, where the processing of information and visual perception take place.

One of the main tasks of the visual cortex is to integrate information from different parts of a visual image into global perceptions. Traditionally, and for a long time, the process of visuospatial integration has been attributed to higher order cortical areas. However, today we know that the V1 area of the primary visual cortex can play an important role in this whole process. According to Kapadia, Westheimer and Gilbert [1], although the receptive fields of V1 neurons, measured by a single stimulus, are quite small, stimuli outside this region can have important modulatory influences allowing neurons to integrate information from large parts of the visual field and may allow neurons at this early stage of visual processing to participate in perceptive tasks of great complexity, such as contour integration, or surface segmentation, or even the visualization of three-dimensional shapes.

The ability to make sense of complex sensory input requires the integration of information across space and time, as well as cognitive mechanisms to shape that integration. In visual perception, the very appearance of regions in the local image is determined not by the regions themselves, but by their relationship to the surrounding visual scene [2].

Changes in perception depend directly on the lived experience, thus requiring the visual cortex to be able to encode new information throughout life. Forms of visual cortical plasticity range from declarative memory, encoding information about places, faces, and events, to a form of implicit memory known as perceptual learning, which refers to the improvement in the ability to detect or discriminate visual stimuli that actually results from a repeated practice. The underlying mechanisms of cortical plasticity apply to specific cortical areas, functional properties and neural connections such as ocular dominance and thalamocortical connections in the primary visual cortex [3].

This ocular dominance is not only closely associated with visual processing but also with color vision. Rods and cones are the two types of visual receptors, located in the retina of the human eye. While rods are responsible for capturing and processing stimuli, cones capture and reflect electromagnetic waves, transforming them into electrical stimuli, allowing color vision when they reach the visual cortex itself. That is, signals are transmitted synoptically to bipolar cells, which connect to ganglion cells in the innermost layer of the retina, forming the optic nerve. However, the retinal circuit includes many other connections through the outer synaptic layer and the inner synaptic layer [4].

Visual processing involves an interaction between the retina, thalamic nuclei and various areas of the visual cortex. The visual cortex is part of the cerebral cortex, which in turn corresponds to the outer layer of the cerebral hemispheres, about 2 to 4 mm thick, containing numerous neuronal bodies. The cerebral cortex performs different functions. The occipital lobe, which is found at the back of the head and is at the sensory level related to the primary visual cortex, forms the caudal aspect of the cerebral hemisphere. The visual cortex, responsible for the integration and perception of visual information, is divided into at least five areas, present in the occipital lobe and designated according to their structure and function, commonly known as V1, V2, V3, V4 and V5. Each of these areas plays a specific role when it comes to visual processing. For example, we are aware that areas V1 and V2 are primarily responsible for initial visual processing, and V3 responds primarily to moving shapes [5].

Many of the developed studies point to the importance of the V4 area, referring not only that it is directly associated with color processing, but also that lesions in this region cause achromatopsia, a condition that affects the ability to identify or even perceive colors.

During the investigation we carried out, using functional magnetic resonance studies, it was possible to verify that the V4 area becomes more active when performing tasks that involve color processing. However, more recent studies, as mentioned by Nogueira [6], show that, in addition to V4, other areas of the brain are also involved in color vision, such as the dorsolateral prefrontal cortex, which seems to be related with color categorization.

COLOR CONSTANCY AND HUMAN PROCESSING

Perceptual constancy or perceptual constancy is the ability to recognize objects as being the same under different viewing conditions and is one of the most functionally important requirements of the visual experience. Signals of the identity and meaning of objects are the invariant attributes of that object, like features of images. Visual experience can be stored as memory and visual memory influences the processing of incoming visual information. Object recognition is based on the observer's previous experiences with those objects.

The boundaries of perception are marked by the presence of perceptual constancies, that is, objectifying capacities, given that the notion of objectivity provides the most specific constraint on the type of sensory transactions that count as perceptual [7].

Color constancy is a process whereby perceived object colors remain invariant under changing/varying illumination. According to Will Davies [8], there is a paradox regarding color constancy: on the one hand, there is a scientific consensus that achromatopsychians have at least rudimentary color constancy; on the other hand, color constancy involves invariance with respect to the perceived colors of surfaces under changes or variations in lighting, and achromatopsychians cannot perceive colors. This paradox leads us to believe that there is still a lot to discover in what concerns color constancy and the human processing.

METHODOLOGY

The methodology used in the present investigation included a Literature Review of a set of pertinent areas directly related to the problem under study, such as human perception, color processing, visual perception, the visual cortex or color constancy. In a previous stage of the study, a survey by inquiry and by interview was used. The data obtained mainly allowed us to verify information already presented by other researchers.

Thus, at this stage of the research, we developed a quasi-experiment in order to understand how color was processed, but also the brain's reactions to color, allowing a better understanding of the brain areas activated during the experiment. Regardless of changes in lighting, angle or distance, it was also important for us to check the color constancy.

After the participants gave their informed consent before starting their participation in the experiment, the quasi-experience of those ones who were selected began, with fifty-two individuals participating, 26 women and 26 men, aged between 26 and the 42 years. All of them had normal or corrected-to-normal vision. In a first step, using a color vision test, the test created by Dr. Shinobu Ishihara in 1917, which continues to be the most well-known test for the identification of color blindness, in which the perception of colors is verified, that is, the function of the retinal receptors (cones), which are sensitive to blue, green or red [9]. It was found that none of the participants had any impairment in color perception.

The experiment itself began by asking participants to visualize sequences of colored squares that varied in terms of color (green, blue, red, yellow) and perceptual distance (1 or 2 hue steps).

The colors were presented on a screen, in the form of monochromatic squares, isolated or in color pairs. They tried to identify the colors that were displayed on the screens, always obeying the same sequence.

The research focused on the effects of the categorization decision, main effects of hue distance and interaction between categorization and hue distance, predicting that areas involved in visual processing would be sensitive to hue distance, with greater adaptation to identical stimuli than not identical, as well as that the frontal lateral regions would be sensitive to color category. Researchers such as Liu, Lu & Seger [10] have also carried out research with the same objective.

As a complement, we also resorted to electroencephalography (EEG) in order to acquire electrical signals and the graphic recording of the spontaneous electrical activity of the brain during a certain period of time, through the scalp. For this purpose, caps made of elastic elastane fabric with pure tin electrodes embedded in the fabric were used. For positioning and placing the electrodes on the caps, and since all skulls are different, we opted for the International 10-20 System (figure 1).

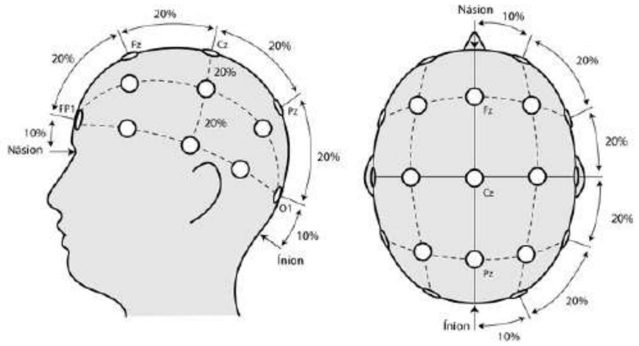

Figure 1. Representation of the 10/20 International System [11]

This system, created by Dr. Herbert Jasper in 1958, is based on the placement of 21 electrodes along the skull, taking into account the size of each person's skull and also the distances between the capture points. The system was named 10-20 precisely because it uses distance values that correspond to 10 or 20% of the skull section, measured from reference points. The electrodes were named according to the region of the brain they cover: Fronto-polar (Fp), Frontal (F), C (Central), P (Parietal), T (Temporal) and O (Occipital). Another reason for this numbering has to do with the possibility of being able to distinguish between the right and left sides, given that even numbers are used on the right and odd numbers on the left. On the other hand, those positioned exactly on the midline received a Z (Zero): Fz, Cz, Pz. The electrodes located on the ears (i.e., the earphones) were named A1 and A2, following the same numbering rule [12].

RESULTS AND DISCUSSION

We started the process with training process. In order to achieve the desired objectives, the average number of trials required was 7. During the color visualization task, participants judged whether the colored pair belonged to one-color or two-color categories. An overall accuracy rate of 94% was achieved.

It was found that when more than one key was presented, the occipital, caudate and anterior regions of the insula were active, indicating a role in perceptual processing and attention monitoring. Whenever two colors were present, rather than in the case of a single color, the dorsolateral prefrontal cortex showed greater activity, indicating a role in encoding color categories.

The cognitive control regions of the intraparietal sulcus and the pre-supplementary motor area were sensitive to the interaction of decision and distance in perceptual space, indicating a role in the combination of these functions during decision making. These results support theories that colors are categorically represented at high levels of the cognitive hierarchy and that the visual cortex is sensitive to hue rather than color category.

It was also possible to perceive that the dorsolateral frontal regions were sensitive to color categories and not to perceptual distance, showing greater activity whenever two color categories were present.

Participants also had to judge whether a given sequence of color stimuli had been extracted from one-color or two-color categories, allowing us to identify neural regions underlying perceptual and decision-making processes in color categorization.

The systematicity of the results seems to prove that, in the cognitive processes of conceptual construction and categorization, humans are more synaesthetes than traditionally thought. In fact, it seems that the mind seeks, as far as possible, equivalences between perceptions from the most diverse areas, trying to associate colors not only with objects, but also with feelings, ideas and emotions.

CONCLUSION

Color processing is a complex phenomenon, although at first glance it appears to be a relatively simple human capability. This processing involves several variables and multiple combinations of them, many of which are still a mystery to researchers. In addition, new discoveries are constantly achieved, recontextualizing previous knowledge and giving rise to new questions that need answers.

The results achieved so far, especially with the quasi-experience developed, encourage us to continue this work, given that it is an area that has enormous potential and whose possibilities for study are far from being exhausted. Thus, we intend to discover more about the relationships between the visual processing and the color constancy, as well as new areas and activities of the human brain that are connected to color recognition.

ACKNOWLEDGEMENT

The author would like to acknowledge the support given by CIAUD – Research Centre for Architecture, Urbanism and Design, Lisbon School of Architecture, Universidade de Lisboa, and by FCT – Foundation for the Science and Technology, Portugal. This work is financed by national funds through FCT - Fundação para a Ciência e a Tecnologia, I.P., under the Strategic Project with the references UIDB/04008/2020 and UIDP/04008/2020.

REFERENCES

1. Kapadia, M. K., Westheimer, G. & Gilbert, C. D. (2000). Spatial distribution of contextual interactions in primary visual cortex and in visual perception. *J. Neurophysiology, 84,* 2048–2062.
2. McManus, J. N., Li, W. & Gilbert, C. D. (2011). *Adaptive shape processing in primary visual cortex*. Proc. Natl Acad. Sci. USA 108, 9739–9746.
3. Gilbert, C. D. & Li, W. (2012). Adult visual cortical plasticity. *Neuron, 75,* 250–264.
4. Moreira da Silva, F. (2013). Colour and inclusivity: a visual communication design project with older people. Lisboa: Caleidoscópio.
5. Nolte, J. (2009). The human brain: an introduction to its functional anatomy. Philadelphia: Mosby/Elsevier.
6. Nogueira, A. C., (2021). *Neurociência das cores.* https://www.ufjf.br/lanc/2021/03/04/neurociencia-das-cores/

7. Burge, T. (2010). *Origins of Objectivity*. New York: Oxford University Press.
8. Davies, W. (2022). The paradox of colour constancy: Plotting the lower borders of perception. *Noûs*, *56*, 787-813.
9. Ishihara, S. (2021). *Ishihara's Tests for Colour Deficiency*, Concise edition. Kanehara Trading Inc, Japan: Tokyo
10. Liu, Z., Lu, W., & Seger, C. A. (2019). Perceptual and categorical processing and representation in color categorization. *Brain and Cognition, 136*.
11. Rodrigues, P. G. (2018). *Extração de Características em Interfaces Cérebromáquina utilizando Métricas de Redes Complexas*. Thesis for Master in Biomedical Engineering, Universidade ABC, São Bernardo do Campo. doi: 10.13140/RG.2.2.34910.13122
12. Bezerra, J. P. (2022). Website: https://www.brainlatam.com/blog/afinal-como-e-possivel-ler-o-eeg-em-diferentes-lugares-no-mundo-1115

RELATIONSHIP BETWEEN SOFTNESS/HARDNESS EVALUATION AND MOVEMENT CHARACTERISTICS OF BLACK FABRIC USING FABRIC'S ROTATING VIDEO –COMPARISON OF ENGINEERING AND CLOTHING STUDENTS –

Takumi Kawamata[1], Tomoharu Ishikawa[1]*, Takashi Maehara[1], Yoshiko Yanagida[2] and Miyoshi Ayama[1]

[1]*Graduate School of Engineering, Utsunomiya University, Yoto 7-1-2, Utsunomiya, Japan*
[2]*Faculty of Fashion Science, Bunka Gakuen University, Yoyogi 3-22-1, Shibuya, Japan*

*Corresponding author: Tomoharu Ishikawa, ishikawa@is.utsunomiya-u.ac.jp

ABSTRACT

This study aimed to clarify the effects of differences in clothing knowledge on the evaluation of the softness/hardness of black fabrics in online shopping. Furthermore, we investigated the influence of visual factors used as cues to evaluate the softness/hardness of the fabric. In our previous study, we conducted two experiments on the softness/hardness of black fabrics in a group of engineering students with engineering expertise to clarify visual factors. In the first experiment, subjects were asked to evaluate the natural slack and folds (fabric drape) of the fabric by placing the fabric on a cylinder and rotating the cylinder to visualize its appearance (visual experiment). In the second experiment, participants were asked to evaluate the true texture of black fabrics by visualizing/touching the fabrics (visual/touch experiment). The results of these experiments clarified the presence of an optimal rotation condition for expressing the softness/hardness of a fabric and that the angular change in the fabric drape due to rotation is a visual factor that provides evidences for evaluating the softness/hardness of a fabric. In this study, two evaluation experiments were conducted on a group of subjects with expertise in clothing, similar to that in a previous study. The differences and similarities between the groups were compared under the aforementioned optimal rotation conditions and angular changes in the fabric drape. These results suggest that students with clothing expertise relied more on the mechanical properties of the fabric than engineering subjects in the visual/touch evaluation. In the visual evaluation, the optimal rotation conditions for expressing the softness/hardness of the fabric differed between the subject groups, and the angular change in the fabric drape, which was used as a cue for evaluation, was greater for clothing subjects than that for engineering subjects. The findings of the study indicate that variations in individuals' knowledge with clothes have an impact on their evaluations of fabric texture in the context of online buying, particularly when assessing black materials.

Keywords: fabric texture, softness/hardness evaluation, movement characteristics, subject attributes

INTRODUCTION

Online purchases of clothing have increased in recent years, which have been further accelerated due to the COVID-19 pandemic.[1]. However, the issue with online shopping is the difficulty in conveying the texture of the fabric and the feel of the garment when worn since the wearer cannot touch the actual garment prior to purchase. This problem is believed to be caused by the incomplete realization of the image presentation that conveys the texture of the fabric and the lack of clarification of visual factors, such as the information in the fabric image that is used as cues by the consumers when determining the texture. Previous studies have revealed the relationship between the beauty of fabric drape (referring to the natural sagging and folds of the fabric) swaying and its evaluation based on visual information and dynamic measurement [2][3].

Moreover, the swaying of the skirt while walking was examined to clarify the relation of its physical characteristics with visual evaluation [4]. These studies suggest that fabric drape influences visual evaluation. Our previous study also showed that images taken with a draped fabric are more likely to capture the texture of a fabric than images taken with a flat fabric [5] and that a method of presenting images in which the fabric drape is rotated at an appropriate speed or acceleration is beneficial for accurately conveying the "softness/hardness" of the fabric texture. Consequently, we determined the optimal rotation conditions that could appropriately express the softness and hardness of the fabric. Subsequently, we analyzed the video images obtained when the fabric was rotated under optimal rotation conditions and found that the magnitude of the change from the maximum to the minimum angle (decreasing angle) of the fabric drape could be one of the visual cues for determining the softness/hardness of the fabric [6]. The participants in the experiment were students who did not have expertise in clothing but had expertise in engineering. Conversely, we showed in our previous study that the expertise of the subjects and other factors affect their judgment of fabric textures [7]. In particular, we showed that differences in knowledge and experience in garment production affect the judgment of fabric textures.

EXPERIMENT

Presentation fabric (for visual/touch experiments) and presentation image (for visual experiments)

In this study, 11 types of fabrics commonly used in women's clothing were used as presentation stimuli. Table 1 shows the fabrics and their bending stiffness B ($N*m^2/m$), which is one of the basic mechanical properties of the Kawabata evaluation system texture measurement technique. The bending stiffness is a measure of the ease of bending of the fabric. Each piece of fabric was cut into a circle with a diameter of 40 cm and was uniformly colored black.

Table 1: Presentation fabric

Fabric		Bending rigidity ($N*m^2/m$)
No.1	Satin back shantung	0.078
No.2	Oxford	0.444
No.3	*Yoryu*	0.053
No.4	Crepe jacquard	0.048
No.5	Stretched satin	0.124
No.6	Organdie	0.212
No.7	Silky satin	0.031
No.8	Silky lace	0.112
No.9	Velvet	0.018
No.10	Velour	0.005
No.11	*in-den*	0.276

Each fabric was draped (red frame) over the presentation table, which was rotated (Figure 1). The rotation method was a combination of four rotation speed patterns (0.50, 0.75, 1.00, and 1.25 rps; rotation per second) and four angular acceleration patterns (0.25, 0.50, 0.75, and 1.00 rps^2; rotation per square second), for a total of 16 patterns. Thus, the total number of stimuli presented in the visual experiment was 176, while 11 fabrics were presented in the visual/touch experiment. In order to suppress the influence of memory for the texture of the fabrics, the visual experiment was conducted first, followed by the visual/touch experiment. The order of presentation of each stimulus was random for each subject.

Figure 1. Examples of presented images (satin back shantung)

Experimental environment

Figure 2 shows the experimental environment for the two types of experiments: visual and visual/touch. The illuminance of the experimental room was 1000 lx and 460 lx in the horizontal and vertical directions, respectively.

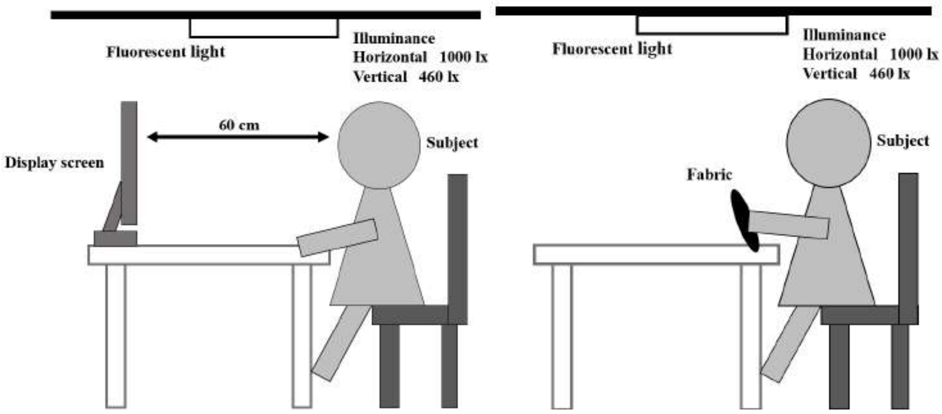

Figure 2. Experimental environment for the visual (left) and visual/touch (right) experiments

In the visual experiment, the softness/hardness of the fabric was evaluated by presenting images of the fabric rotating at different speeds and angular accelerations on a display at a viewing distance of 60 cm. In the visual/touch evaluation experiment, the participants were asked to evaluate the softness/hardness of the black fabric by viewing and touching it until they were satisfied with it to obtain the true texture (softness/hardness) of the fabric. The softness/hardness of the fabric was evaluated using a 7-point scale ranging from -3 to 3. The subjects of the experiment were 20 Japanese engineering students from Utsunomiya University who had did not have expertise in clothing and 20 Japanese clothing students from Bunka Gakuen University who had expertise in clothing. Hereafter, we refer to Japanese engineering students as Engineering Japanese (EJ) and Japanese clothing students as Clothing Japanese (CJ).

Physical factors of fabrics (method of calculating the angle of decrease of fabric drape)

The angle at which the drape of the fabric placed on the presentation table spread to the maximum by rotation was defined as the maximum angle (Figure 3, left panel), and the angle at which the drape of the fabric wrapped around the presentation table to the maximum was defined as the minimum angle (Figure 3, center panel); the difference between these angles was analyzed as the decrease angle (Figure 3, solid green line in the right panel).

Figure 3. Maximum angle (left), minimum angle (center), and decreasing angle (right)

RESULT AND DISCUSSION

Visual/touch evaluation results and optimal rotation conditions

Figure 4 shows a comparison of the relationship between the visual/touch evaluation values (average) and the bending rigidity for each fabric for each subject group. In both subject groups, the large and small values of bending rigidity were evaluated as "hard" and "soft," respectively. The correlation coefficient between the EJ, CJ, and tactile evaluation values was 0.987, which is considerably high. Figure 4 shows that the visual/touch evaluation values of most fabrics are similar; however, a significant difference is observed only for *Yoryu*. The correlation coefficients between the visual/touch evaluation values and the bending rigidity for each subject group were similar (0.856 for EJ and 0.885 for CJ); however, CJ was slightly more dependent on the bending rigidity of the fabric. It became clear that CJ tended to evaluate fabrics with low or high bending rigidity softer or harder than EJ, respectively. This suggests that differences in garment knowledge may have affected the evaluation.

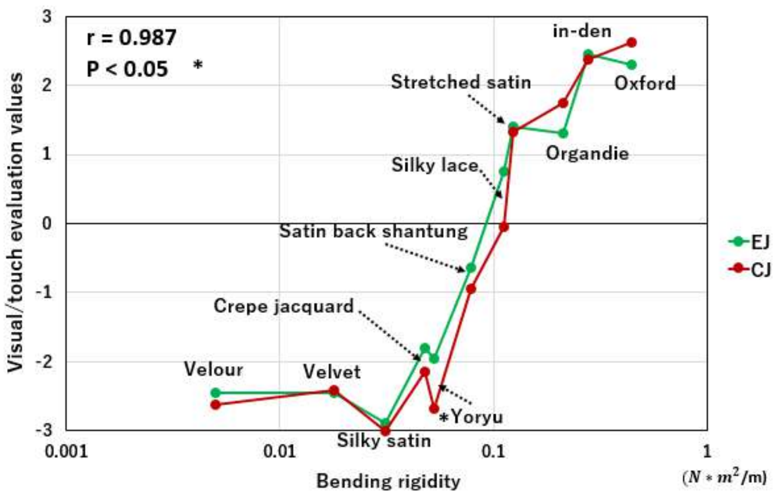

Figure 4. Visual/touch evaluation values (EJ and CJ)

The difference between the visual and visual/touch evaluations of each fabric was determined, and the rotation condition that minimized this difference was calculated as the optimal condition for conveying the softness and hardness of the fabric. The results showed that CJ tended to select a high rotation speed (1.25 and 1.00 rps) for fabrics with low bending rigidity such as velour and a low rotation speed (0.75 and 0.50 rps) for fabrics with high bending rigidity such as oxford. Conversely, the EJ tended to select a high rotation speed regardless of the bending rigidity value. No condition was reported under which both the rotational speed and angular acceleration were the same for the optimal conditions for each fabric among the groups of subjects. Although four conditions were availbale under which the rotational speed was the same, no condition existed under which the angular acceleration was the same. In particular, the optimal rotation conditions for each fabric differed between the subject groups.

Table 2: Optimum rotation conditions

Fabric	CJ		EJ	
	Rotation speed (rps)	Angular acceleration (rps^2)	Rotation speed (rps)	Angular acceleration (rps^2)
Velour	1.25	0.75	1.25	1.00
Velvet	1.25	0.75	1.25	1.00
Silky satin	1.00	0.75	1.25	0.50
Crepe jacquard	1.25	1.00	1.00	0.75
Yoryu	1.25	1.00	1.00	0.75
Satin back	1.25	0.50	1.25	1.00
Silky lace	1.25	0.25	1.00	0.50
Stretched satin	1.00	0.50	1.25	0.25
Organdie	0.50	0.50	1.25	0.75
in-den	0.50	0.25	0.50	0.50
Oxford	0.75	0.50	1.25	0.75

Analysis of the relationship between the decrease angle and visual evaluation

The relationship between the decrease angle and visual evaluation of each subject group under the optimal rotation conditions for each fabric was approximated by the least-squares error method using the following sigmoid function (Eq. 1). Figure 5 shows the characteristics of the evaluation values with respect to decreasing angle. For the approximation, a was set to 6 for the width of the evaluated value, and C was set to 3 to set the median of the evaluated value to zero. The values of the coefficients for each subject group were b = 19.66 and k = 0.238 for CJ and b = 16.24 and k = 0.231 for EJ.

$$y = \frac{a}{1 + e^{k(x-b)}} - C \tag{1}$$

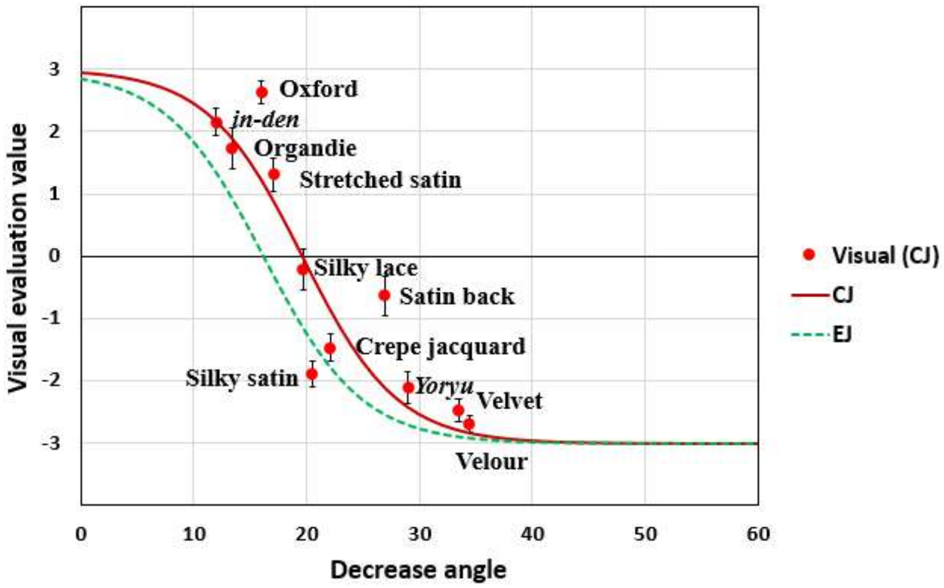

Figure 5. Relationship between the visual evaluation value and decrease angle

Figure 5 shows that the visual evaluation values for both subject groups decreased as the decrease angle increased. In addition, the evaluation values for CJ were higher than those for EJ for all decreasing angles. The coefficient k, which represents the slope of the curve, is almost the same for CJ and EJ; however, at the intersection b of the approximate curve with a visual evaluation value of 0, the value for CJ is larger than that for EJ. This can be interpreted as the evaluation value curve for the decrease angle of the clothing system shifting to the right of the engineering system curve. In particular, CJ tended to rate the softness/hardness of the fabric more highly than EJ in response to changes in the angle of the fabric drape.

CONCLUSION

In this study, to clarify the influence of differences in clothing knowledge on the judgment of the softness/hardness of fabrics, two experiments similar to those in our previous study were conducted on students with clothing expertise, and the results were compared. The results showed that the clothing students relied on bending rigidity to determine the softness/hardness of the fabrics, based on the relationship between visual and tactile evaluations and bending rigidity. The optimal rotation conditions for expressing the softness/hardness of the fabrics tended to differ among the subject groups. In addition, the clothing subjects evaluated the fabric as more hard by comparing the characteristics of the evaluation of the drape rotation images with a decrease angle of the drape.

ACKNOWLEDGMENT

This study was supported by JSPS KAKENHI Grant Number JP18H03317.

REFERENCES

1. Ministry of Internal Affairs and Communications (2022) https://www.soumu.go.jp/johotsusintokei/whitepaper/ja/r04/html/nf306000.html#d0306070
2. Yang, M., & Matsudaira, M. (2001). Relationship between visual judgement and dynamic drape behavior of fabrics. *Journal of the Textile Machinery Society of Japan*, *54*(11), 174-179. doi:10.24517/00049964.
3. Kobayashi, S., & Noshi, H. (1980). Sensory test on skirts in wear relation between the aesthetic visual image and physical properties of cloths. *Journal of the Textile Machinery Society of Japan*, *33*(5), P304-P408
4. Chiba, K., & Higuchi, Y. (1991). The swinging properties of flared skirts in walk. *The Japan Society of Home Economics*, *42*(7), 643-653. https://doi.org/10.1177/004051750407401112
5. Ishikawa, T., Tsuji, R., Sasaki, K., Miyatake, K., & Ayama, M. (2015). Investigation of fabric texture expression through dynamic alterations of drapes - Image presentation method in online shopping environments -. *International Journal of Affective Engineering: Special Issue on ISASE2015*, 2015.12. https://doi.org/10.5057/ijae.IJAE-D-15-00026.
6. Jinba, N., Ishikawa, T., Yanagida, Y., Mori, H., Sasaki, K., & Ayama, M. (2019). Visual ratings of "softness/hardness" of rotating fabrics. *IJCST*, *32*(1), 48-62. doi:10.1108/ijcst-07-2018-0088.
7. Ishikawa, T., Nakajima, T., Yanagida, Y., Mitsui, M., Sasaki, K., & Ayama, M. (2021). Effect of sensation modalities on texture evaluation of beige fabrics by Japanese and Chinese. *14th Congress AIC2021*, 2021.9.

IDENTIFICATION OF NATURAL INDIGO DYED FABRICS BY COLOR IMAGE ANALYSIS

Kannikar Kamolrat[1] and Sukanya Phongsuphap[2]*

[1]Department of Computer, Faculty of Science and Technology, Sakon Nakhon Rajabhat University, Thailand.
[2]Faculty of Information and Communication Technology, Mahidol University, Thailand.

*Corresponding author: Sukanya Phongsuphap, sukanya.pho@mahidol.ac.th

ABSTRACT

The natural-indigo-dyed fabric is a kind of eco-friendly products as every step of its production process is environmentally friendly. At present, natural-indigo-dyed fabrics become more popular, and expensive. Consequently, there are a number of counterfeit or fake natural-indigo-dyed fabrics selling in markets. To alleviate this problem, in this paper, we propose a method for differentiating the natural-indigo-dyed fabrics from the non-natural-indigo-dyed fabrics by using color image processing and rule-based classification techniques. We have performed experiments on 195 images of plain blue fabrics. Colors of fabric images are analyzed in the RGB and HSV color spaces. The images are quantized and labelled with color codes/color tones from varieties of color-naming conventions such as Natural Colour System (NCS), Inter-Society Color Council – National Bureau of Standard System of Color designation (ISCC-NBS), etc. We found that the color features such as the number of color tones and the value of hue of the dominant color tone extracted from the quantized image can be used to identify type of dyes of a fabric image as natural-indigo-dyed fabric or non-natural-indigo-dyed fabric. We can achieve the average correct classification rate of 93.3%.

Keywords: Natural Indigo color, Eco-friendly textile, Sustainability, Color image processing, Machine vision

INTRODUCTION

Nowadays, the environmental pollution becomes a serious problem worldwide. Colors of clothing from synthetic dyes are causing serious environmental pollution problems [1]. In this regard, the natural-indigo dyes extracted from indigo plants, for example, Indigofera tinctoria, I. suffruticosa Mill [2], are getting more attention. The natural-indigo dyes are one of the oldest dyestuffs used in the East since antiquity [3]. They are green or organic dyes that help to reduce harm to the environment since they are biodegradable [4]. The natural-indigo-dyes are considered as quality blue dyestuffs [5]. In addition, the color of indigo is commonly used as a symbol of independence and individualism, and also known as the king of colors and the color of kings [6]. In recent years, consumers worldwide have paid more attention to environmental issues, so consumer interest in natural-indigo-dyed fabrics becomes increasing [7-8]. On the other hand, fake natural-indigo-dyed fabrics selling in markets also become increase. To alleviate this problem, we aim to find a method based on digital technology to identify the natural-indigo-dyed fabric. In this paper, we propose a method for differentiating the natural-indigo-dyed fabrics from the non-natural-indigo-dyed fabrics by using digital color image processing and rule-based classification techniques. The details are elaborated in the next sections. The interest in finding a method for the identification of the natural-indigo-dyed fabric has been studies for many decades, for example, the studies in [9-11]. However, we still need more innovative tools.

METHODOLOGY

Our proposed method for differentiating between the natural-indigo-dyed fabrics and the non-natural-indigo-dyed fabrics consists of 3 steps: 1) Fabric image data preparation, 2) Color analysis, and 3) Dye-type determination. Details of each step are explained below.

Fabric image data preparation

Five types of fabrics are used in our experiments. There are i) *Natural Indigo-dyed Cotton* (CottonHN), ii) *Natural Indigo-dyed Rayon* (RayonHN), iii) *Synthetic Blue Nylon* (NylonMS), iv) *Synthetic Blue Polyester* (PolyesterMS), and v) *Synthetic Blue Blended-Cotton* (CottonMS). Totally, there are 195 images and all are plain blue tone fabrics. Examples of fabric images are shown in Figure 1. Characteristics of these fabrics are summarized in Table 1.

Figure 1. Examples of fabric images used in our experiments

Table 1: Characteristics of fabrics used in our experiments

No	Code	Type of fabric	Fabric-weaving	Colorant / Dye
1	CottonHN	Cotton	Handmade	Natural Indigo
2	RayonHN	Rayon	Handmade	Natural Indigo
3	NylonMS	Nylon	Machine-made	Synthetic Blue Color
4	PolyesterMS	Polyester	Machine-made	Synthetic Blue Color
5	CottonMS	Blended Cotton	Machine-made	Synthetic Blue Color

Color analysis

Colors of all fabric images are analyzed in the RGB and HSV color spaces by using digital image processing techniques [12] as follows:

1) Each fabric image is quantized in the RGB color space. The Euclidean distance between color of each pixel in the image and each color tone of the seven color-naming conventions (Basic color names, Natural Colour System (NCS), Inter-

Society Color Council – National Bureau of Standard System of Color designation (ISCC-NBS), W3C color names, Ultimate Color Vocabulary, Pantone Color System, and Spoonflower Color Guide) is computed, then color of that pixel is labelled with the closest color tone based on the minimum distance principle.

2) Histogram of the quantized image obtained from 1) is constructed by counting frequencies of the color tones appearing on the quantized image.
3) The following color features from the quantized image are extracted: the number of color tones appearing on the quantized image, the proportions of the color tones, and the dominant color tone (having the highest frequency).
4) The value of hue of the dominant color tone is calculated from the analysis in the HSV color space.

The distribution of color tones of each fabric image is analyzed from the histogram of the corresponding quantized image. Then, the color features such as the number of color tones, the value of hue of the dominant color tone, and the proportions of color tones appearing on the image are used for dye-type determination in the next step.

Dye-type determination

A rule-based classification technique [13] is used to determine dye-type of a fabric image as natural-indigo-dyed fabric (type of "natural-indigo" dye) or non-natural-indigo-dyed fabric (type of "non-natural-indigo" dye). A set of rules is constructed from the color features as explained in the color analysis section, which consist of the number of color tones, the value of hue of the dominant color tone, and the proportion of color tones appearing on the quantized image.

RESULT AND DISCUSSION

Based on the experiments performed on a set of 195 fabric images by using the proposed method, we found that there are 1,579 relevant color tones that can be used for blue tone fabric image analysis. They are derived from the seven color-naming conventions as summarized in Table 2.

Table 2: Color-naming conventions used for color quantization

No	Color-naming convention	Number of the relevant color tones
1	Basic Color	11
2	NCS	295
3	ISCC-NBS	260
4	W3C color name	344
5	Ultimate Color Vocabulary	234
6	Pantone	197
7	Spoonflower	238
Total		**1,579**

By considering the histograms, we can notice that the color distributions of the natural-indigo-dyed fabrics have more variations of color tones than that of the non-natural-indigo-dyed fabrics. Examples are shown in Figure 2. Some interesting characteristics of the five types of fabrics are summarized in Table 3. Based on the analysis of the distributions of the color tones, the color features that are suitable for use in constructing rules to differentiate the natural-indigo-dyed fabrics from the the non-natural-indigo-dyed fabrics are the number of color tones (it is greater than 14 colors for the natural-indigo-dyed fabrics), and the value of hue of the dominant color (it is in the range of [0.52, 0.7) for the natural-indigo-dyed fabrics). The rule-based dye-type classification results are shown in Tables 4 and 5. We can achieve the high average correct classification rate of 93.3%. The results indicate that the number of color tones derived from the histogram of the quantized image, and the range of the value of hue of the dominant color tone are the effective color features for identifying the natural-indigo-dyed fabrics or differentiating them from the non-natural-indigo-dyed fabrics.

Table 3: Characteristics related to color tone distribution of the five types of fabrics

No	Code	Colorant / Dye	Average number of color tones	Maximum number of color tones	Average Proportion of the dominant color tone (%)
1	CottonHN-11	Natural Indigo	82	120	14.04
	CottonHN-21	Natural Indigo	78	95	15.27
2	RayonHN-31	Natural Indigo	35	94	31.42
	RayonHN-43	Natural Indigo	32	43	24.95
	RayonHN-57	Natural Indigo	33	47	26.84
	RayonHN-58	Natural Indigo	25	40	37.57
	RayonHN-59	Natural Indigo	25	39	34.51
3	NylonMS-81	Synthetic Blue Color	5	7	55.78
4	PolyesterMS-91	Synthetic Blue Color	9	14	25.25
5	CottonMS-712	Synthetic Blue Color	8	14	60.94

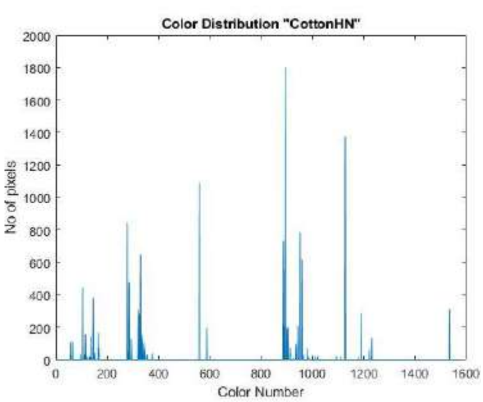

(a)

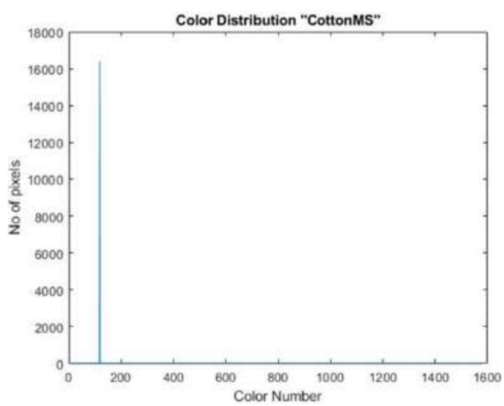

(b)

Figure 2. Examples of histogram-based color distributions of (a) Natural-indigo dyed Cotton (CottonHN), (b) Synthetic blue Blended Cotton (CottonMS)

Table 4: Dye-type classification result for five types of fabrics

No	Code	Actual Dye-type	Classified Dye-type		Total (image)
			Natural-indigo (image)	Non-natural-indigo (image)	
1	CottonHN-11	Natural Indigo	20	0	20
	CottonHN-21	Natural Indigo	20	0	20
2	RayonHN-31	Natural Indigo	20	0	20
	RayonHN-43	Natural Indigo	18	0	18
	RayonHN-57	Natural Indigo	14	4	18
	RayonHN-58	Natural Indigo	14	4	18
	RayonHN-59	Natural Indigo	13	5	18
3	NylonMS-81	Synthetic Blue	0	21	21
4	PolyesterMS-91	Synthetic Blue	0	21	21
5	CottonMS-712	Synthetic Blue	0	21	21

Table 5: Summary of Dye-type classification result by the proposed method

Actual Dye-type	Classified Dye-type		Total (image)
	Natural-indigo (image)	Non-natural-indigo (image)	
Natural Indigo	**119**	13	132
Synthetic Blue Color	0	**63**	63
Total			**195**
Accuracy			**93.33%**

CONCLUSION

This paper proposed a method of identification of the natural-indigo-dyed fabrics by using digital color image processing and rule-based classification techniques. The effective color features for differentiating the natural-indigo-dyed fabrics from the non-natural-indigo-dyed fabrics are the distribution of the color tones in the fabric image which is described by the number of color tones appearing on the quantized fabric image, and the value of hue of the dominant color tone extracted from the quantized fabric image. The images are quantized by using the 1,579 relevant colors from the seven color-naming conventions consisting of Basic color names, Natural Colour System (NCS), Inter-Society Color Council – National Bureau of Standard System of Color designation (ISCC-NBS), W3C color names, Ultimate Color Vocabulary, Pantone Color System, and Spoonflower Color Guide based on the Euclidean minimum distance principle in the RGB color space, and hue is analyzed in the HSV color space.

We still need more investigations to improve reliability of the proposed method. Our ongoing research is focused on increasing training data with varieties types of dyes and fabrics, and considering more effective classification approaches.

ACKNOWLEDGEMENT

We would like to thank Miss Navaporn Klaiudom for her help in data preparation and programming.

REFERENCES

1. Lellis, B., Favaro-Polonio, C. Z., Pamphile, J. A., Polonio, J. C., (2019). Effects of textile dyes on health and the environment and bioremediation potential of living organisms. *Biotechnology Research and Innovation*, 3, 275-290.
2. Xu, W., Zhang, L., Cunningham, A. B., Li, S., Zhuang, H., Wang, Y, Liu, A. (2020). Blue genome: chromosome-scale genome reveals the evolutionary and molecular basis of indigo biosynthesis in Strobilanthes cusia. *Plant J*. 104, 864–879.
3. Balfour-Paul, J. (1999). Indigo in South and South-East Asia. *Textile History*, 30(1), 98-112.
4. Dutta, S., Roychoudhary, S., Sarangi, B. K. (2017). Effect of different physico-chemical parameters for natural indigo production during fermentation of Indigofera plant biomass. *3 Biotech*, 7(5), 322.
5. Shi, Y., Zhang, L., Wang, L., Li, S., Qiu, Z., Ding, X., Wang, Y. (2021). Quality blues: traditional knowledge used for natural indigo identification in southern China. *J. Ethnobiology and Ethnomedicine*, 1-14.
6. Błyskal, B. (2016). Indigo dyeing and microorganism–polymer interaction. *J. Cultural Heritage*, 22, 974–983.
7. Lai, C., Chang, C. (2021). A study on sustainable design for indigo dyeing color in the visual aspect of clothing. *Sustainability*, 1-11.
8. Kabish, A. K., Abate, M. T., Alemar, Z. A., Girmay, S. (2023). The Importance of natural indigo dye and its revitalization and Ethiopian potential for indigo growing. *Advances in Materials Science and Engineering*, 1-13.
9. Schweppe, H. (1979). Identification of dyes on old textiles. *J. American Institute for Conservation*, 19(1), 14-23.
10. Kawahito, M., Yasukawa R. (2009). Characteristics of color produced by Awa natural indigo and synthetic indigo. *Materials*, 2, 661-673.
11. Degani, L., Riedo, C., Chiantore, O. (2015). Identification of natural indigo in historical textiles by GC–MS. *Anal Bioanal Chem*.
12. Gonzalez, R. C., Woods, R. E. (2002). *Digital Image Processing*. Prentice Hall.
13. Liu, H., Gegov, A., Stahl, F.T. (2014). Categorization and construction of rule based systems, *Proc. 15th International Conference on Engineering Applications of Neural Networks*, Sofia, Bulgaria; Mladenov, V. et al. (Eds.) (2014): EANN 2014, CCIS 459, pp. 183–194, Springer International Publishing, Switzerland.

CONTRAST IMPRESSION BETWEEN UPPER AND LOWER GARMENTS IN TERMS OF LIGHTNESS, INFLUENCE ON SENSIBILITY EVALUATION, AND APPLICATION TO IMAGE ANALYSIS

Shiho Murakami[1]*, Tomoharu Ishikawa[1], Shino Okuda[2], Miyoshi Ayama[3]

[1]*School of Engineering, Utsunomiya University, Japan.*
[2]*Faculty of Human Life Science, Doshisha Women's College of Liberal Arts, Japan.*
[3]*Center for Optical Research and Education, Utsunomiya University, Japan.*

*Corresponding author: Tomoharu Ishikawa, ishikawa@is.utsunomiya-u.ac.jp

ABSTRACT

The use of e-commerce sites has increased with the purchase of clothes. Modern people often coordinate upper and lower garments (hereafter referred to as two-piece garments) with some contrast. Therefore, we tried to quantify the contrast impression in two-piece garments in terms of lightness to clarify its influence on the sensibility evaluation of coordination, with a view to creating a fashion database and applying it to fashion recommendations. We conducted two experiments. The first was a contrast impression comparison experiment in which a test stimulus and a reference stimulus were presented simultaneously, and participants were asked to judge which gave a stronger contrast impression. The second was a sensibility evaluation experiment in which a single test stimulus was presented and the participants were asked to do subjective evaluations using six words: "subdued," "pretty," "neat," "bright," "plain," and "showy." For the test stimuli, 60 two-piece garments were prepared; the upper and lower garments were a floral pattern blouse and a single-color skirt, respectively. For the reference stimuli, 12 two-piece garments consisting of a blouse and skirt of different monochromatic colors were prepared. Participants were eight female students from the School of Engineering. From the results of the first experiment, the "contrast impact," which denotes the strength of the contrast impression between the upper and lower garments, was derived as a function of the lightness of the reference stimuli. Additionally, we attempted to estimate the contrast impact from the colorimetric values of the test stimuli to apply the results to other images. The results of the sensibility evaluation experiment revealed that the scores of "neat" and "subdued" were high in the upper garment with black floral patterns, while the scores of "showy," "bright," and "pretty" were high in the upper garments with colored floral patterns. To confirm whether these results were applicable to other two-piece garments, we analyzed images on a website. Using the newly derived formula for contrast impact, we calculated the contrast impact from the average lightness obtained through web image analysis. We confirmed that the contrast impact values generally aligned with the contrast impressions obtained through the subjective evaluation.

Keywords: fashion, color, contrast impact, lightness contrast, image analysis

INTRODUCTION

Recently, the use of e-commerce websites has increased worldwide, and is predicted to escalate in the field of fashion [1]. Many e-commerce websites in the fashion industry allow users to input clothing categories and trend keywords to purchase their preferred clothing items [2]. However, relatively few sites use indicators based on human sensibility and impressions in their search terms. Considering that many contemporary individuals coordinate their outfits by combining tops like blouses or shirts with bottoms like skirts or pants, it is believed that people may select tops and bottoms based on some form of "contrast." In our previous research, we defined the strength of contrast impression between tops and bottoms as "Contrast Impact (CI)" and investigated the scaling based on luminance contrast of reference stimuli and the relationship between CI and sensibility evaluations [3, 4]. It was revealed that evaluations in multiple sensibility rating terms can be well explained by the average luminance of the tops and bottoms, Cab* of the tops, and CI. However, to implement e-commerce websites that reflect these results, a new CI formula must be derived directly from the inherent characteristics of fashion images on websites, such as lightness and chroma, irrespective of the luminance contrast of the reference stimuli. Therefore, this study aimed to derive a new CI using lightness as a measure of the contrast impression between tops and bottoms and investigate its applicability to web images and its relationship with sensibility evaluations. We conducted experiments comparing the contrast impression between tops and bottoms and sensibility evaluations, and analyzed the relationship between the results obtained from each experiment. Moreover, we measured the lightness of the test stimuli and calculated a new CI formula that approximates the contrast impression between the tops and bottoms as a function of lightness. As an outset for applying the new CI formula, we used lightness and chroma information from fashion images on the web to derive a new CI from the new lightness CI formula, and investigated its applicability.

EXPERIMENT

Two experiments were conducted: a contrast impression comparison experiment and sensibility evaluation experiment. The contrast impression comparison experiment employed a method to determine the stronger impression between the test and reference stimulus The test stimulus consisted of a floral-patterned top combined with a plain monochromatic bottom, whereas the reference stimulus consisted of plain monochromatic top and bottom garments. The floral patterns were available in five colors—black, red, yellow, green, and blue—with three pattern sizes (large, medium, and small), totaling 15 variations. Plain, monochromatic bottoms were available in four colors: white, gray 1, gray 2, and black (with lightness levels of approximately 9.5, 7, 4, and 1.5, respectively). Consequently, there were 60 test stimuli conditions (15 × 4) and 12 reference stimuli conditions (combinations of the four monochromatic colors). These stimuli were produced and presented by dressing small mannequins. Sensibility evaluations were conducted on the 60 test stimuli used in the contrast impression comparison experiment. Six evaluation terms were used: "subdued," "pretty," "neat," "bright," "plain," and "showy." Participants evaluated each term using a unipolar 7-point scale (0–6). The experimental setup is illustrated in Figure 1. Eight female engineering students were recruited as participants.

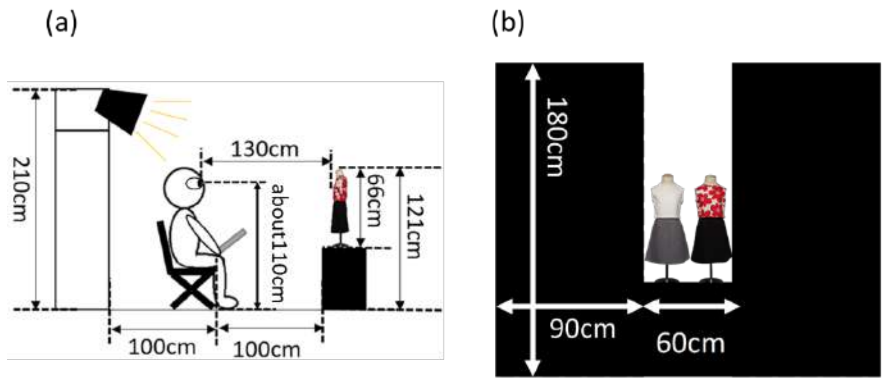

Figure 1. (a) Experimental set-up

(b) Stimuli presentations during pair comparison for the contrast impact

RESULT AND DISCUSSION

Derivation of New Contrast Impact (CI): For each combination of test and reference stimuli, the number of times that all participants collectively judged "the test stimulus has a stronger contrast impression" was tallied. The horizontal axis in Figure 2 represents the modified lightness contrast derived from the lightness of the reference stimulus, whereas the vertical axis plots the number of times the test stimulus was chosen. Lightness was calculated from the measured values of the test stimulus and a standard whiteboard using a 2D colour analyser (Konica-Minolta, CA-2500). Among the top and bottom garments, the one with the highest lightness was denoted as L^*_{high}, and that with the lowest lightness was denoted as L^*_{low}. Eq. (1) represents the modified Michelson contrast of lightness. The weight coefficients k_i and k_j in Eq. (1) were calculated for combinations of reference stimuli with white, gray 1, gray 2, and black stimuli for the top and bottom garments. The top garments were as follows—white: 2.91, gray 1: 1.04, gray 2: 0.50, black: 0.40. The bottom garments were as follows—white: 2.81, gray 1: 1.19, gray 2: 0.48, black: 0.49.

$$x = \frac{k_i \cdot L^*{}_{high} - k_j \cdot L^*{}_{low}}{k_i \cdot L^*{}_{high} + k_j \cdot L^*{}_{low}} \tag{1}$$

For each test stimulus, a sigmoid function was used to perform curve fitting, and the value of x when y was at the midpoint (y = 16 [50%]) of the number of times the test stimulus was chosen was defined as the "new Contrast Impact (CI)."

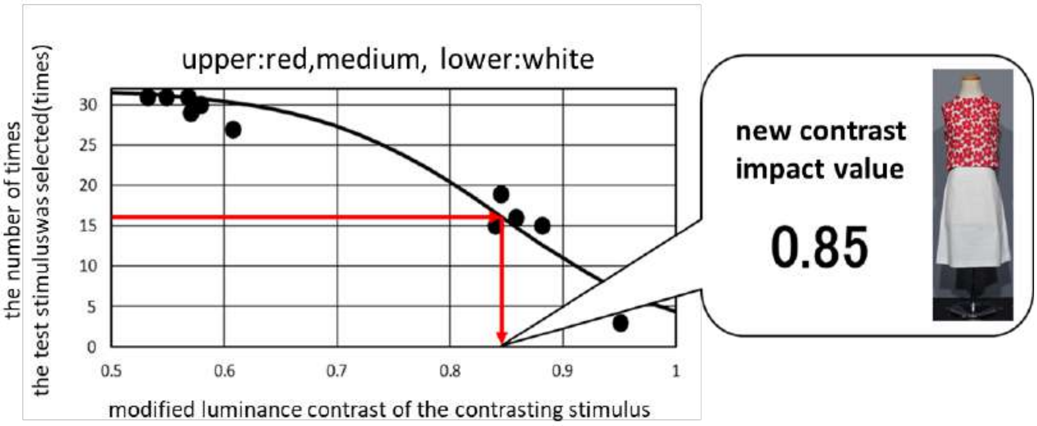

Figure 2. How to derive the new contrast impact of the test stimuli

Derivation of CI from L and C* of Test Stimulus:* In the previous section, we derived the CI value based on the lightness of the reference stimulus with a contrast impression similar to that of the test stimulus. To apply the CI value to clothing other than the test stimulus, it is necessary to calculate the CI value from the lightness and chromaticity of the test stimulus. Based on the results obtained in the previous section, we assumed that the participants judged the contrast effect based on the luminance contrast between the upper and lower garments and the color of the floral pattern. When the lightness of the skirt increased, the CI tended to increase when the upper garment was black floral pattern; whereas the CI tended to decrease when the upper garment was chromatic floral pattern. Therefore, we hypothesized that the function used to calculate the contrast between the upper and lower garments would be reversed when the upper garment is black compared to when it is chromatic. Therefore, we decided to use different equations for cases where the upper garment was achromatic or chromatic, utilizing the average lightness values of the upper and lower garments. We incorporated weight coefficients for the size and color of the floral patterns. Eq. (2) and Eq. (3) represent the cases in which the upper garment is achromatic and chromatic, respectively. The weight coefficients for the different floral pattern sizes and colors are listed in Table 1. The C^*_{ab} values for the petals were black = 14.7, red = 59.2, yellow = 83.6, green = 70.1, and blue = 35.9. Yellow, a bright and vivid color, had the highest C^*_{ab} value among the five colors. However, the contrast impact evaluation results were lower for red, green, and blue; therefore, the value of b_j was smaller than the others.

In the case of the top being achromatic,

$$X = W_i \frac{L^*skirt,av}{L^*blouse,av} + b_j C^*flower \tag{2}$$

In the case of the top being chromatic,

$$X = W_i \frac{L^*blouse,av}{L^*skirt,av} + b_j C^*flower \tag{3}$$

Table 1: Weighting coefficients for the lightness contrast between the upper and lower garments, and the color pattern of the floral design

	Weight average by size: $\boldsymbol{W_i}$
L	1.08
M	1.04
S	0.87

	Weights by color: $\boldsymbol{b_j}$
Black	0.0000
Red	0.0494
Yellow	0.0009
Green	0.0331
Blue	0.0538

Relationship between the values (X) from Eq. (2) and Eq. (3) and the CI values (Y) are shown in Figure 3. The curves represent the relationship between the two values obtained using the least-squares method in Eq. (4).

$$Y = 0.15 \cdot X^{0.40} + 0.61 \tag{4}$$

Correlation coefficient between the estimated values based on Eq. (4) and the CI values (Y) for each stimulus was r = 0.86, indicating a relatively good approximation. However, in the lower range of the x-axis values, the x-values were almost the same in some cases while the y-values increased. Future studies should consider factors other than luminance contrast and the color of the floral pattern in the derivation of Eq. (2) and Eq. (3).

Trial to Derive CI values for Online Fashion Images: We examined whether the relationship between the luminance contrast between the upper and lower garments, the color of the floral pattern (X), and the CI values (Y) obtained in this study could be applied to fashion images on e-commerce websites. We selected and processed two fashion images from an actual e-commerce website (Figure 4) to calculate the $L^*a^*b^*$ values. Image (a) was used to calculate X using Eq. (2) and image (b) was used to calculate X using Eq. (3). The CI values were calculated for each image using Eq. (4), resulting in $CI_a = 0.76$ for image (a) and $CI_b = 0.91$ for image (b). Additionally, seven participants were shown fashion images in Figure 4 and asked to determine the image that had a stronger contrast impression between the upper and lower garments. All seven participants chose image (b). These results establish that the CI values obtained in this study are applicable to the contrasting impressions perceived by humans, confirming their adaptability.

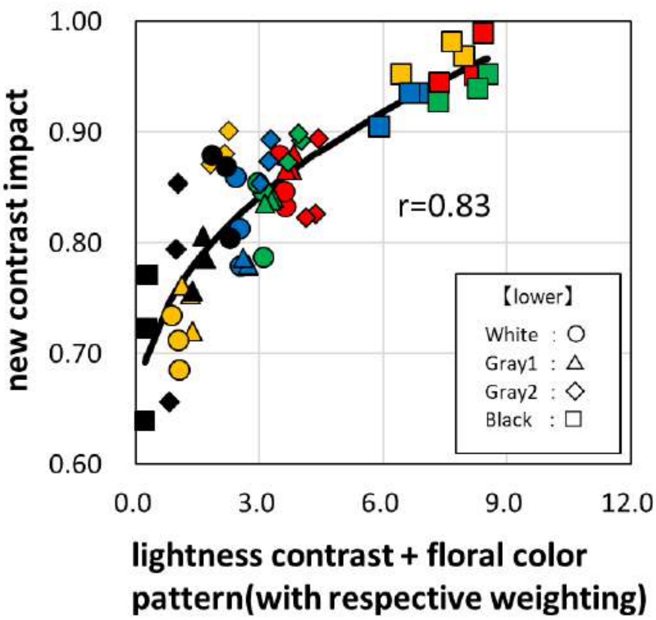

Figure 3. Relation between the weighted lightness contrast

and metric chroma of flower patterns of the test stimuli and the new contrast impact

Figure 4. Samples of fashion image and their contrast impact values

Results of the affective evaluation experiment revealed that when examining the evaluation of upper garments based on different descriptive words, chromatic colors received higher ratings for “showy” and “bright,” while achromatic colors received higher ratings for “subdued” and “plain.” The term “pretty” had no significant difference in ratings between chromatic and achromatic colors. However, for the term “neat,” upper garments in achromatic colors and blue received higher ratings, while those in red, yellow, and green received lower ratings. The fact that different descriptive words received higher ratings depending on whether the upper-garment was chromatic or achromatic in color suggests that the color of the upper-garment influences affective evaluation.

CONCLUSION

This study aimed to derive a new CI using lightness as a measure of the impression of contrast between upper and lower garments. Our goal was to investigate their applicability to web images and their relationship to sensibility evaluation. We conducted a contrast impression comparison experiment and sensibility evaluation experiment. From the results of the contrast impression comparison experiment, it was possible to estimate the CI value of online fashion images by considering factors such as the brightness contrast between upper and lower garments and the color of floral patterns. Results of the affective evaluation experiment established that the color of the upper-garment influenced affective evaluation, as different descriptive words received higher ratings when the upper-garment was in vibrant colors than when it was in muted colors.

ACKNOWLEDGEMENT

This research was supported by a grant from the Japan Society for the Promotion of Science (grant number 19K12179).

REFERENCES

1. Ministry of Internal Affairs and Communications, Information and Communications White Paper for the 2022 Edition
2. Deldjoo, Y., Nazary, F., Ramisa, A., MCauley, J., Pellegrini, G., Bellogin, A., Di Noia, T. (2021). A Review of Modern Fashion Recommender Systems. *ACM Computing Surveys, 37*(4), Article 111. doi:10.48550/arXiv.2202.02757
3. Takaishi, K., Imazu, K., Fujimoto, J., Ishikawa, T., Okuda, S., Ayama, M. (2019), Relation between contrast impact of two-piece garments and KANSEI evaluation. *Proceedings of the ACA2019 Nagoya.*
4. Ayama, M., Ishikawa, T., Sugimoto, T., Murakami, S., & Okuda, S. (2022). Measurement of the contrast impact of patterned blouse and single-color skirt combination. *Proceedings of the AIC2022 Taipei*.

Natural Hair Color Appearance and Classification Analysis

Mekides Assefa Abebe[1,2]*, Jon Yngve Hardeberg[1], Bente Hafslund[2], and Sahar Asghari[3]

[1]*Colourlab, Faculty of Information Technology and Electrical Engineering, NTNU, Norway.*
[2] *By Bente AS, Norway*
[3]*MCSL, College of Science, Rochester Institute of Technology, USA.*
*Corresponding author: mekides.abebe@ntnu.no

ABSTRACT

Understanding the natural hair composition, determined by eumelanin and phaeomelanin ratios, guides chemical reactions with hair dyes. This underscores the importance of color order systems like the DIN system in helping hair styling professionals achieve accurate hair color results. The reliance on manual assessment by experts for identifying natural hair colors and choosing dyes has limited the industry, particularly in digital platforms like e-commerce and telemedicine. In this study, we explore the feasibility of automating hair color identification using smartphone-based color imaging. We evaluate various color spaces and machine learning techniques to represent hair color and natural hair color levels. Our dataset, labeled based on universal natural hair color levels, employs multiple color appearance features for identification. We also address color fidelity concerns related to smartphone imaging through white balancing techniques. Our findings show a direct correlation between hair color appearance and melanin concentration, favoring linear regression for accurate automatic hair color identification over classification methods.

Keywords: Hair color appearance, Hair color constancy, Hair color classification and identification

INTRODUCTION

Ghosh et al. [1] note the rising popularity of hair coloring since the introduction of the synthetic colorant "Aureole" in 1909. Hair stylists must understand the hair compositions for accurate dyeing. Prior to procedures, stylists assess the customer's current hair color, type, density, and length to tailor a plan that safeguards hair health. Recognizing the natural color is crucial for successful bleaching and achieving the desired color. Hair stylists and hair color manufacturers typically adopt a visual hair color scale, known as the natural level system (Fig. 1.a), to identify customers' natural hair color. This universal system features 10 lightness levels from 1 (black) to 10 (platinum blonde), often with accompanying letters or decimals indicating tone. A simplified color wheel system (Fig. 1.b), like Ostwald's, aids stylists in determining enhancing or neutralizing colors for processes like lightening, bleaching, and coloring. Opponent colors based on the color wheel are chosen to neutralize, lighten, or darken hair [2]. Color order systems like Munsell and Ostwald are employed to represent and design these hair color wheel systems [3], as a bi-dimensional star with six vertices (Fig. 1.b), commonly used for hair coloring.

Traditionally, natural hair color identification is conducted by expert hair stylists through visual assessment using such hair color charts and the natural color level system, sometimes supplemented by hair sampling and consultation. This manual approach, while effective within hair professionals' capacity, becomes less practical for high-consumer applications like e-commerce and telemedicine. To automate this process, digital representation and quantification of universal hair color systems are necessary. However, standardization is lacking, leading to color discrepancies among salons and manufacturers. Moreover, automated identification tools for natural hair color levels are currently limited in availability.

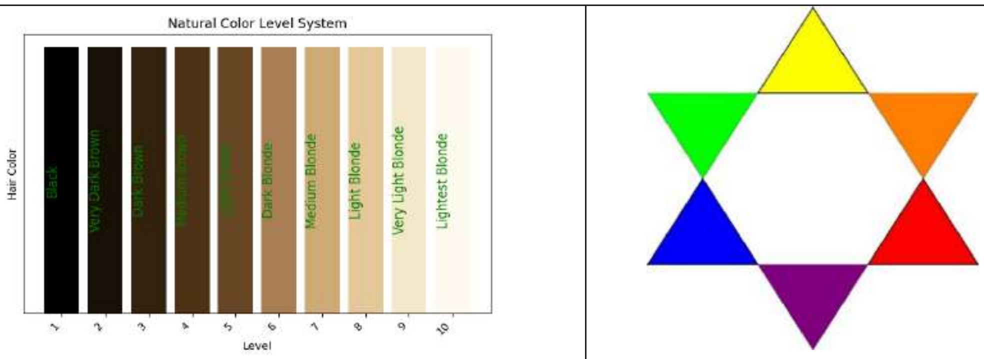

a. Natural color level system used universally.

b. The simplified color wheel generated from Ostwald color order system.

Figure 1. The two common color order systems utilized in the hair styling industry. The color level system identifies customers' natural hair color lightness levels. The color wheel guides the neutralization and colorization process by determining the underlying color pigment.

Existing state of the art shows that determining hair color is challenging due to natural variability, color changes over time, and anisotropic scattering effects [4]. Numerous attempts have been made to measure hair color, involving spectrophotometers [4], spectroradiometers [5], and image-based approaches [6] with segmented hair samples. However, these methods often require meticulous preparation, making them impractical for the cosmetics industry. The ideal solution would be a non-invasive, rapid, and automated method, but current image-based approaches face difficulties in accurately segmenting hair due to diverse textures and hairstyles. Some computer vision researches have used neural networks and machine learning techniques for automatic segmentation and hair color identification [7] [8] [9] [10] [11], but there remain limitations in targeting the hair roots and utilizing the natural color level system essential for hair styling applications.

Moreover, accurately determining a customer's natural hair color involves hair color identification and correction. In this regard, RGB pixel data is used, but method consistency lacks among color correction techniques. Some maintain RGB values, while others convert to different color spaces, with limited detail in some studies [6] [11]. Given color's sensitivity to lighting and camera differences, correction is vital, though camera and lighting data might be missing. To address this, neural networks are trained on diverse databases [12] [10] [13]. Also, current hair color studies broadly categorize hair into groups like blonde, black, brown, grey/white, and red, but determining hair tone more precisely is pivotal for cosmetic purposes. Bokaris et al. [11] used scalp images and neural networking for hair tone assessment, albeit with computational complexity and equipment challenges.

In this study, we present an analysis of efficient and automated smartphone imaging approach for hair color level identification. Our method employs smartphone images to select hair regions and determine natural hair color levels. To mitigate illumination effects and smartphone color fidelity issues, various white balancing techniques are examined. We explore classification and regression machine learning methods, with a newly generated data set, for hair color level identification. Linear regression emerges as the optimal choice due to the linear relationship between extracted hair color features and the natural hair color level system. Further details on our approach and evaluation are provided in the subsequent sections.

METHODOLOGY

The proposed smartphone-based imaging and machine learning solutions for natural hair color level identification contains 3 main stages. As shown in Fig. 2., the main stages consist of data set generation and white balancing, color feature extraction, as well as hair color level modeling and identification stages.

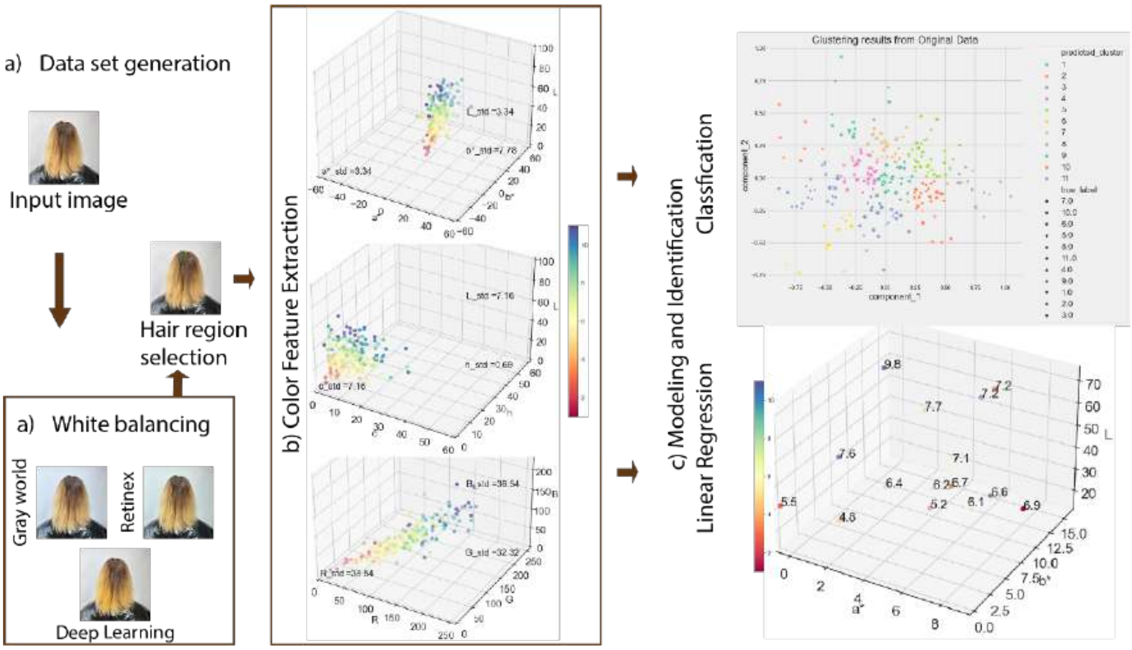

Figure 2. Components of the hair color identification approach include: sample image, hair region selection, white balancing results, the eight color features, and visualizations of K-means clustering and regression results on the original data set images. The color bars indicate the corresponding natural hair color levels of the data samples.

a) Data set generation and white balancing

In this study we gathered 252 head-shot images, with natural hair color levels expertly labeled by a hair stylist from By Bente AS, Norway. Selection masks, outlining hair regions crucial for determining color levels, were also generated with the stylist's assistance. The dataset comprises randomly gathered images from acquaintances, family, and clients, captured with various smartphone cameras in uncontrolled environments. This diversity leads to potential color discrepancies in reproducing hair color due to low color constancy. Different images with the same natural hair color level could exhibit varying sRGB values due to different illumination during capture.

To address this color inconsistency, white balancing is utilized, adjusting images to a standard illumination like CIE D65. Successful application depends on accurate scene illuminant estimation. In our assessment (as depicted in Fig. 2.a), three white balancing techniques were evaluated: Gray world, White patch retinex, and deep white balancing. Gray World [14] averages reflected light at the sensor for illuminant estimation, offering robustness for single illumination scenes. White Patch Retinex [15] employs a bright patch's color as illuminant. These traditional methods are known to struggle with complex lighting situations. To overcome this, data-driven deep learning methods like the Deep White Balancing model by Afifi et al. [16] have emerged. Their model utilizes a multi-headed encoder-decoder architecture for white balancing. Our evaluation includes their model in white balancing mode with a correlated color temperature (CCT) of 6500K, aligned with the CIELab color space used for the subsequent feature extraction stage.

b) Color feature extraction

For automated hair color identification, color is a key image feature. We represent the color of selected hair regions (highlighted in green, Fig. 2.a) by calculating eight color features from sRGB, CIELab, and LCh representations. The dominant color is computed using mean, median, and histogram-based averaging. However, no significant differences among the three resulting averages were observed. Therefore, mean pixel values of selected regions are used for the rest of our analysis. The mean color feature values for the 252 data set images are shown in Fig. 2.b.

c) Hair color level modeling and identification

As shown in Fig. 2.c, the task to model and identify natural hair color levels is handled through classification and regression approaches. During the data set generation, hair color samples are grouped into 10 labels, determined by the expert. We additionally employ the K-means clustering technique, an unsupervised method [17], to autonomously discover new color clusters. The number of clusters must be decided before clustering, using the elbow method that minimizes the distance of data points from cluster centroids. However, this method doesn't align with the 10 distinct natural hair color groups as visually evaluated. The sum of squared distances between cluster centroids keeps decreasing, making cluster number determination challenging. Thus, K-means clustering is applied with manually set number of clusters, k=10, on original and white-balanced data sets.

Given the lack of clear cohesion and separation among hair color feature clusters, as evident in Fig. 2.b, 2.c and results presented in the next section, it's more suitable to address the hair color identification problem as a regression problem. Despite the standard system having 10 distinct color levels, hair color labeling can be seen as a continuous scale. The strong correlation between color features and the expert's labels, depicted in Fig. 2.b., also suggests regression is a viable approach. Accordingly, both Support Vector Regression [18] and Linear Regression [19] were employed to assess the impact of the color features and white balancing on identification accuracy. Given the linear correlation between features and labels, Linear Regression [19] was preferred and results are presented in the next section.

The linear regression problem is represented as $Y = X\beta + \varepsilon$, where Y and ε are [252x1] column vectors containing the hair color labels and error residuals. X is a [252x8] matrix where each row represents a data point/sample, and each column represents color feature. The modeling is the linear regression to find the optimal values for the coefficients vector β that minimizes the sum of squared errors between the predicted values $X\beta$ and the actual target values Y.

RESULT AND DISCUSSION

From Figure 2.b., it is clear that our data set's mean hair color values exhibit substantial variation in the red-yellow and luminance dimensions. To understand the hair color distributions better, we explored alternative 2D perceptual spaces (CIEa vs. CIEb, Chroma vs. Hue, Lightness vs. Chroma) and principal component visualizations. The primary change of our prepared data set hair colors is seen in Chroma and Luminance, not hue. This analysis covers both original and white-balanced image color features. Our visual examination of images and hair color feature distributions did not reveal significant visible differences before and after white balancing. Hence, for deeper insights into white balancing accuracy, we assessed the three approaches using independent hair data measurements. Six volunteers' hair was captured under varied lighting (as specified in Tab. 1) using both smartphone and DSLR camera setups. Hair colors were also measured using a spectroradiometer. The captured images were then white balanced, similarly as previous section, to match D65 illumination. The color difference between the corrected images and real D65 captures was calculated, and results are detailed in Tab. 1.

The average ΔE results highlight improvements made by white balancing for stronger color-casted light sources like incandescent and fluorescent. However, the improvements, particularly with deep white balancing, were limited. It is known that these methods can falter without accurate illumination estimation. Note that our ΔE evaluation mimicked real-time hair color level identification applications by employing automatic illumination estimation, despite the data is gathered under a controlled condition. It is also observed that misleading white patch estimations can occur due to over- and under-exposures. Hence, it is reasonable that the main dataset's color features show minimal change post white balancing, given the results.

Table 1: White balancing and hair color level identification accuracy evaluation results.

	White balancing methods evaluation (ΔE2000)					K-means evaluation			Regression
Camera	**Lighting**	**Gray world**	**Retinex**	**Deep WB**	**None**	**Data sets**	**Silhouette score**	**ARI**	**r^2**
Samsung	***D65***	10.81	10.72	14.10	11.27	**Original**	0.332	0.077	0.8
	Florescent	10.33	10.57	12.63	10.29	**Deep WB**	0.362	0.094	0.77
	Incandescent	12.02	13.05	17.38	15.77	**Gray world**	0.351	0.076	0.78
Sony	***D65***	15.16	18.62	14.82	19.16	**Retinex**	0.360	0.080	0.79
	Florescent	14.94	17.03	15.35	19.19				
	Incandescent	12.71	15.48	14.79	16.55				

The clustering and regression results are also analyzed objectively and visually. K-means clustering outcome for the original image dataset features is shown in Fig. 2c. Objective assessment employed silhouette coefficient and adjusted rand index (ARI), as presented in Tab.1. Silhouette coefficient measures cluster cohesion and separation, ranging from 0 (significant cluster overlap) to 1 (well-separated clusters). ARI quantifies similarity between actual and predicted labels, with 0 indicating random assignments and 1 signifying identical cluster. Fig. 2.c. shows that k-means clustering, and expert hair color labels often disagree, supported by Tab. 1's ARI values nearing zero for original and white-balanced images. Silhouette scores on the other hand suggest coherent k-means clustering. Yet, k-means' suitability for automatic hair color identification is not strongly supported by the results.

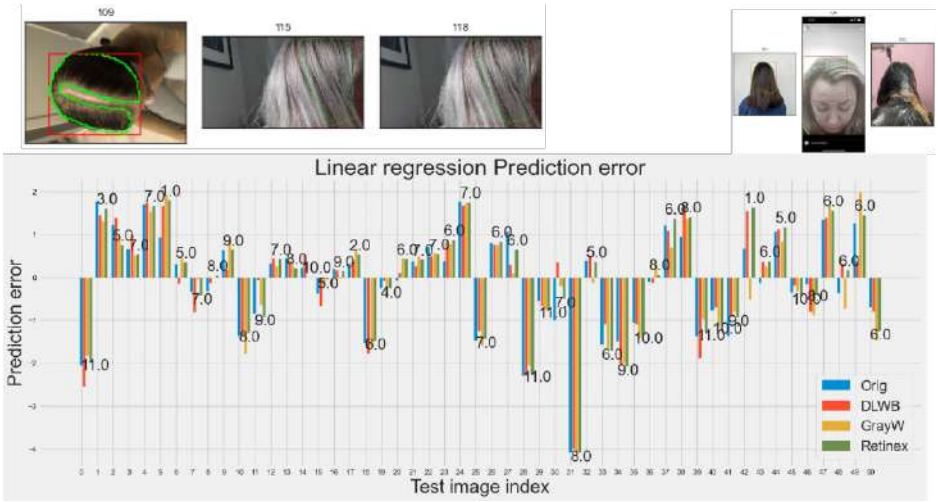

Figure 3: Linear regression model's prediction errors. Bars display errors, with accompanying numbers corresponding to ground truth expert labels. Images with notable negative (top left) and positive (top right) errors, along with their respective index numbers in the original dataset are included for visual assessment.

Finally, for the assessment of the linear regression model, we split the data set into training and 10% test sets due to the limited number of images. Fig. 3 illustrates prediction errors on the test images, together with sample images with notable deviations from the ground truth. Average r^2 values for original and white-balanced test images are also given in Tab. 1. The model showed mixed performance: while most predictions slightly differed, some significantly deviated from the expert levels (Fig. 3). Notably, darker hair was often predicted lighter and vice versa. Predictions were visually aligned with selected regions' color features, but disparities from the expert's labeling could stem from hair color region and labeling inaccuracies. On the other hand, higher r^2 means less divergence between observed and fitted data. Hence, Tab. 1's last column results imply good and comparable linear regression accuracy for original and white-balanced datasets, affirming the earlier ΔE results of the white balancing evaluation.

CONCLUSION & FUTURE WORK

This study explored automating hair color identification tasks using smartphone-based imaging and machine learning techniques. Emphasizing the need for accurate hair color representation, the methodology encompassed data set creation, color feature extraction, and hair color level modeling and identification. Conventional and deep learning white balancing methods were evaluated alongside clustering and regression techniques. While challenges in color correction and k-means clustering discrepancies were observed, linear regression exhibited potential for accurate hair color level predictions. The proposed work's limitations included a small data set, non-uniform representation of natural hair colors, absence of spatial hair features (like hair types and density), and imperfect white balancing corrections. With expanded data sets, improved color correction techniques, and comprehensive hair color features, the potential of both linear regression and deep learning solutions becomes more pronounced in the context of automating hair color identification within cosmetic and digital services domains.

REFERENCES

[1] P. Ghosh and A. K. Sinha, "Hair Colors: Classification, Chemistry and a Review of Chromatographic and Electrophoretic Methods for Analysis," *Analytical Letters,* vol. 41, pp. 2291-2321, 2008.

[2] L. Collins, *Understanding The Level System In Hair Color,* LKC studios, 2022.

[3] S. Liberini and A. Rizzi, "Munsell and Ostwald colour spaces: A comparison in the field of hair colouring," *Color Research & Application,* vol. n/a, 2022.

[4] S. Liberini, A. Avolio, S. T. Yankowski and A. Rizzi, "Consistency issues in hair spectral reflectance and colour measurements," *Coloration Technology,* vol. 136, pp. 244-254, 2020.

[5] I. Lozano, J. B. Saunier, S. Panhard and G. Loussouarn, "The diversity of the human hair colour assessed by visual scales and instrumental measurements. A worldwide survey," *International Journal of Cosmetic Science,* vol. 39, pp. 101-107, 2017.

[6] A. Zinke, M. Rump, T. Lay, A. Weber, A. Andriyenko and R. Klein, "A Practical Approach for Photometric Acquisition of Hair Color," *ACM Trans. Graph.,* vol. 28, p. 1–9, 12 2009.

[7] D. Borza, T. Ileni, e.-T. J. Darabant, D. Helbert, W. Philips, D. Popescu and P. Scheunders, "A Deep Learning Approach to Hair Segmentation and Color Extraction from Facial Images," in *Advanced Concepts for Intelligent Vision Systems*, Cham, 2018.

[8] S. Sarraf, "Hair Color Classification in Face Recognition using Machine Learning Algorithms," *American Academic Scientific Research Journal for Engineering, Technology, and Sciences,* vol. 26,, 12 2016.

[9] Y. Yacoob and L. Davis, "Detection, analysis and matching of hair," in *Tenth IEEE International Conference on Computer Vision (ICCV'05) Volume 1*, 2005.

[10] D. S. Rosen and C. Carter, "Automated hair color determination," in *Proceedings of the 2014 International Conference on Image Processing*, 2014.

[11] P.-A. Bokaris, E. Malherbe, T. Wasserman, M. Haddad and M. Perrot, "Hair Tone Estimation at Roots via Imaging Device with Embedded Deep Learning," *Electronic Imaging,* vol. 31, pp. 483-1--483-1, 2019.

[12] T. A. Ileni, D. L. Borza and A. S. Darabant, "Fast In-the-Wild Hair Segmentation and Color Classification," in *VISIGRAPP*, 2019.

[13] D. Borza, T. Ileni and A. Darabant, "A Deep Learning Approach to Hair Segmentation and Color Extraction from Facial Images," in *Advanced Concepts for Intelligent Vision Systems*, Cham, 2018.

[14] M. Ebner, "Algorithms for Color Constancy under Nonuniform Illumination," in *Color Constancy*, John Wiley & Sons Ltd, 2006, pp. 143-191.

[15] M. Ebner, "Algorithms for Color Constancy under Uniform Illumination," in *Color Constancy*, John Wiley & Sons, Ltd, 2006, pp. 103-141.

[16] M. Afifi and M. S. Brown, "Deep White-Balance Editing," in *Proceedings of the IEEE Conference on Computer Vision and Pattern Recognition*, 2020.

[17] J. A. Hartigan and M. A. Wong, "Algorithm AS 136: A k-means clustering algorithm," *Journal of the royal statistical society. series c (applied statistics),* vol. 28, pp. 100-108, 1979.

[18] H. Drucker, C. J. C. Burges, L. Kaufman, A. Smola and V. Vapnik, "Support Vector Regression Machines," in *Proceedings of the 9th International Conference on Neural Information Processing Systems*, Cambridge, 1996.

[19] G. James, D. Witten, T. Hastie and R. Tibshirani, "Linear Regression," in *An Introduction to Statistical Learning: with Applications in R*, New, York: Springer US, 2021, pp. 59-128.

[20] A. Tkachenka, G. Karpiak, A. Vakunov, Y. Kartynnik, A. Ablavatski, V. Bazarevsky and S. Pisarchyk, *Real-time Hair Segmentation and Recoloring on Mobile GPUs,* arXiv, 2019.

[21] Z. Liu, P. Luo, X. Wang and X. Tang, "Deep Learning Face Attributes in the Wild," in *Proceedings of International Conference on Computer Vision (ICCV)*, 2015.

[22] S. França, M. Dario, V. Esteves, A. Baby and M. Velasco, "Types of Hair Dye and Their Mechanisms of Action," *Cosmetics,* vol. 2, p. 110–126, 4 2015.

[23] M. D. Fairchild, Color Appearance Models, Wiley, 2013.

PERFORMANCE ANALYSIS OF THE ISHIHARA TEST BASED ON INDIVIDUAL COLORIMETRIC OBSERVER MODEL

Lijia Sun[1], Shining Ma [1]*, Yue Liu[1], Yongtian Wang[1] and Weitao Song[1]

[1]Beijing Engineering Research Center of Mixed Reality and Advanced Display, School of Optics and Photonics, Beijing Institute of Technology, Beijing, China

*Corresponding author: Shining Ma, shining.ma@bit.edu.cn

ABSTRACT

Pseudoisochromatic plate tests are commonly used in clinical color vision tests such as the Ishihara test which can rapidly screen the red-green color defects. However, many studies have demonstrated that the sensitivity and specificity of the Ishihara test cannot reach 100%, indicating that this test sometimes fails to identify subjects with normal color vision (CVN) or color vision deficiencies (CVD). And the protan/deutan classification plates could misjudge the type of color deficiency. For the subjects with the same color vision status (CVN or CVD) determined by the anomalscope, one possible explanation of the misjudgement is the variation in the perceived color difference between the foreground and background among these subjects. As a result of observer metamerism, the color difference fluctuation could be caused by the variations in individual color matching functions (CMFs). This study investigated the impact of observer metamerism on the performance of the Ishihara test by implementing theoretical simulations of individual CMFs for CVN and CVD. Yaguchi's computerized simulation algorithm and Asano's individual colorimetric observer model have been adopted to simulate the CMFs by taking the age, the field of view, and eight additional physiological parameters as input variables. A large set of CMFs for CVN and CVD (protanomaly, deuteranomaly) were populated using Monte Carlo simulation. Then the numeral-background color difference for each Ishihara plate was estimated using each simulated CMF set. The results reveal a substantial impact of observer metamerism on the numeral-background color difference for each plate, theoretically illustrating the limitations of the Ishihara test on accurate color vision examination.

Keywords: color deficiency, Ishihara test, observer metamerism, Monte Carlo simulation

INTRODUCTION

Color vision deficiency (CVD) can be classified as inherited or acquired. The former is associated with the alternations in the genes, with 8% of males and 0.5% of females affected. Various methods have been employed for the clinical diagnosis of color blindness, classified as three major types: 1. pseudo-isochromatic plates, such as the Ishihara test; 2. color arrangement inspection like Farnsworth-Munsell 100-Hue test; 3. Rayleigh-match-based anomaloscope, such as the OCULUS HMC Anomaloscope. Among these methods, pseudo-isochromatic plate tests are commonly used in clinical color vision tests which can rapidly screen the red-green color defects. However, studies have discovered that it tends to underestimate milder cases of color vision deficiency, and the protan/deutan classification plates could misjudge the type of color deficiency [1-5]. The Ishihara test sometimes fails to identify subjects with normal color vision (CVN). The discrepancies in both color reproduction and test reliability across different editions have also been noted [4,6]. As suggested by previous studies, the illumination spectrum is another influential factor in the accuracy of the Ishihara test [7-9].

For the subjects with the same color vision status (CVN or CVD) as determined by the anomalscope - the golden standard of color deficiency diagnosis, one possible explanation of the misjudgement is the variation in the perceived color difference between the foreground and background among these subjects. As a result of observer metamerism, the color difference fluctuation could be caused by the variations in individual color matching functions (CMFs). Over the years, numerous ways have been proposed to simulate the CMFs of individual observers. In 1989, the CIE TC 1-07 put forward the CIE Standard Deviate Observer to assess the extent of color mismatches between metameric color pairs caused by observer variations [10-13]. However, plenty of studies have reported that the CIE Standard Deviate Observer significantly underestimates the actual variability observed in human observers [14-16]. To address this issue, CIE further extended the standard observer to the CIE 2006 Physiological Observers (CIEPO06) on the basis of Stockman's work[17]. The CMFs for various fields of view (ranging from 2° to 10°) and observers of different ages could be derived from the model of CIEPO06. Later on, a more comprehensive individual colorimetric observer model has been proposed by Asano et al. based on the physiological model of CIEPO06. Besides the field of view and observer age, the Asano model includes eight additional physiological parameters as input variables, including the deviation of lens pigment density, macular pigment density, optical densities of the three photopigments (L, M, S), and their peak wavelength shifts[18].

The purpose of this study is to investigate the impact of observer metamerism on the performance of the Ishihara test by implementing theoretical simulations of individual CMFs. Using the Monte Carlo simulation, the individual CMFs were generated by the Asano colorimetric observer model for CVN and CVD (of different types and severity). The performance of each plate in the Ishihara test was specified by the color difference between the average chromaticity of foreground numeral and background.

METHODOLOGY

*Spectra measurement***.** For the Ishihara test, the No.13 plate (a vanishing plate) was selected as the sample plate for this study, as shown in Fig. 1(a). There are seven unique colors composing this plate, with the numeral and background occupying three and four of them, respectively. The plate was placed on the bottom of the Datacolor Tru-Vue lighting booth, illuminated by the D65 illuminant. The spectra of unique colors were measured by the Konica Minolta CS-2000 spectroradiometer with a viewing geometry of 0/45. Figure 2(b) summarizes the chromaticities of seven unique colors in the *u'v'* uniform color space calculated from the CIE 1931 2° CMFs. Note that each color was measured twice at different positions, subsequently taking the mean for further analysis.

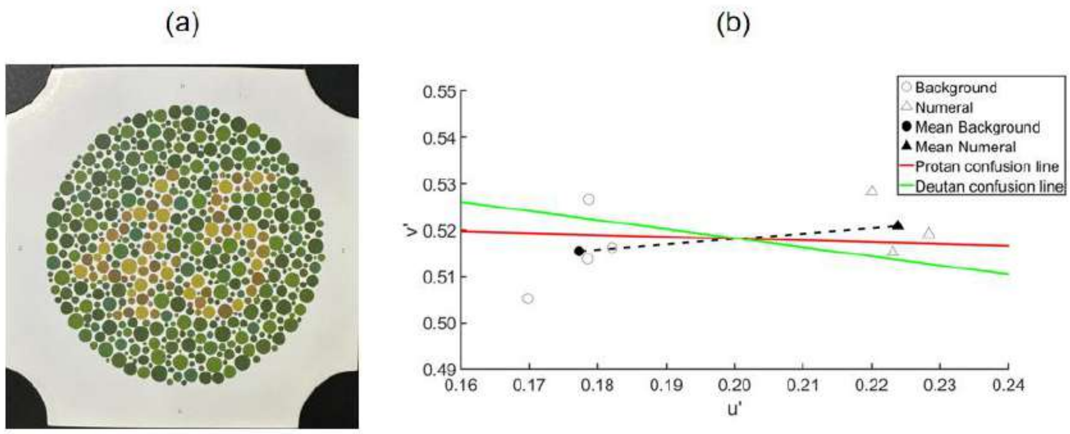

Figure 1. (a) The sample plate (No. 13) for the Ishihara test. (b) Chromaticity distribution of unique colors in the sample plate in the u'v' diagram.

Individual observer simulation. The LMS cone fundamentals of individual CVN could be generated by the Asano model, as given below:

$$lms - CMFs = f(a, v, d_{lens}, d_{macular}, d_L, d_M, d_S, s_L, s_M, s_S) \quad (1)$$

where a represents the age of the observer; v represents the field of view; d_{lens} and $d_{macular}$ represent the deviation (in percentage) from the averages lens pigment density and peak optical density of macular pigment, respectively; d_L, d_M, and d_S indicate the deviations in percentage from the averages peak optical densities of the L-, M-, and S-cone photopigments; s_L, s_M, and s_S represent the shifts in *nm* from the averages peak wavelength λ_{max} for the L-, M-, and S-cone photopigments, respectively. When the eight additional parameters are set to zero, the model remains identical to CIEPO06. The standard deviations (SDs) of the eight additional parameters used in Asano's study were equal to [18.7, 36.5, 9.0, 9.0, 7.4, 2.0, 1.5, 1.3].

For individual CVD observers with a larger λ_{max} shift from CVN, the cone fundamentals could be simulated by the combination of the Asano model and Yaguchi model [19]. It is worthwhile to note that the Yaguchi model, used to predict the color appearance of CVD, was proposed based on the physiological model of CIEPO06. As the spectral absorption shape of the L-photopigment is similar to that of the M-photopigment in the wavenumber domain, the Yaguchi model simulates the cone fundamentals of CVD with different types and severities by shifting the spectral absorption curves in the wavenumber domain. On the contrary, the Asano model implements the shift of λ_{max} by moving the absorption curve in the wavelength domain as the shift length is relatively small for CVN (< 3 *nm*). In this study, the absorption curves of L- and M- photopigments with a Δv wavenumber shift can be obtained in Eqs. (2) and (3), corresponding to protanomaly and deuteranomaly, respectively.

$$log\, A'_L(v) = log\, A_L(v - \Delta v) \quad (2)$$

$$log\, A'_M(v) = log\, A_M(v + \Delta v) \quad (3)$$

The amount of wavenumber shift Δv indicates the degree of anomaly. Except for the estimation of spectral absorption curves, the other calculation steps in simulating CVD are identical to those in the Asano model. Afterward, to ensure consistent cone responses of equal-energy-white (EEW) across all observers, the obtained cone fundamentals need to be normalized by taking the CIE 2006 2° CMFs as the reference. Then the cone fundamentals could be converted to the XYZ CMFs using the transformation matrix defined for the 2006 2° standard observer.

RESULT AND DISCUSSION

Influence of physiological parameters. For each observer, the XYZ tristimulus of each color in the sample plate was derived from the simulated XYZ CMFs and radiance spectrum. Then the XYZ tristimulus was converted to the CIE 1976 *u'v'* chromaticity. For the numeral or background, its average chromaticity was estimated as the mean *u'v'* coordinate of the corresponding unique colors. Then the numeral-background color difference was estimated for each simulated CMF set in terms of *DEu'v'*, in representative of the performance of the Ishihara test. A larger numeral-background color difference corresponds to a higher visibility of the target numeral.

To investigate the impact of each physiological parameter on the performance of the Ishihara test, the color difference between numeral and background was plotted against the deviation (in percentage) from the average value in Figure 2 and Figure 3, corresponding to protanomaly and deuteranomaly, respectively. In each subfigure, multiple curves varying in color represent different shifts of λ_{max} (in the photopigment absorption curve) equally spaced between 0 *nm* and 20 *nm*. When examining the effect of a single parameter for CVD of different types and severities, the deviations of other physiological parameters were set to zero with the observer age of 32 years. In Figures 2(a) and 3(a), the age variation ranges from 20 to 80, consistent with that defined in CIEPO06. For the other five physiological parameters, the range of abscissa is approximately three times their standard deviations (± 3SD), covering more than 99% of individuals.

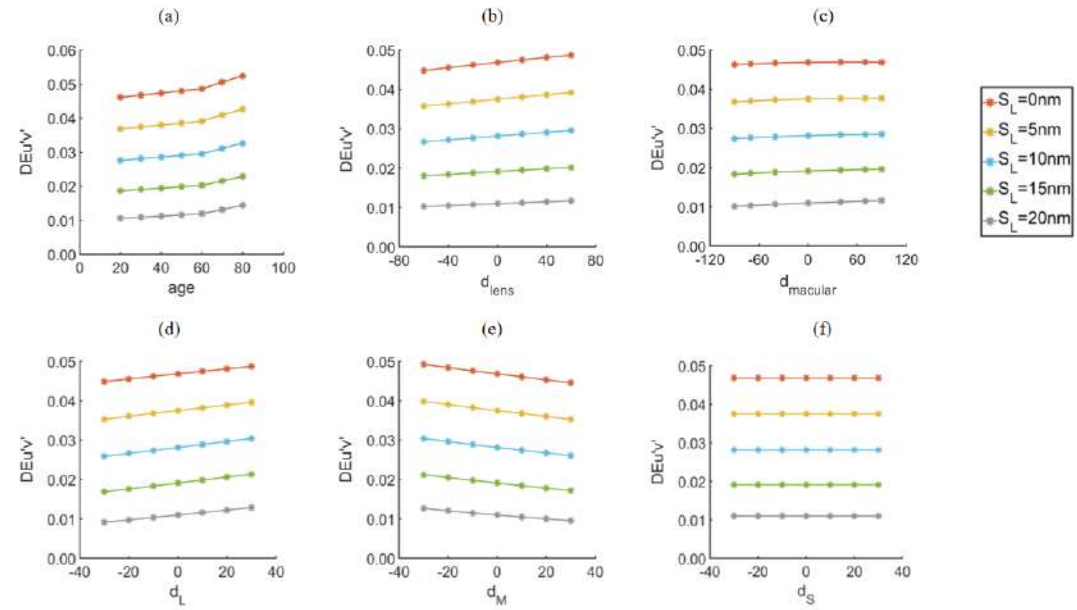

Figure 2. The influence of physiological parameters on the color difference between the numeral and background for protanomaly. In each subfigure, lines in different colors represent different s_L values equally spaced between 0 nm and 20 nm. The six parameters include (a). age, (b). d_{lens}, (c). $d_{macular}$, (d). d_L, (e). d_M, (f). d_S

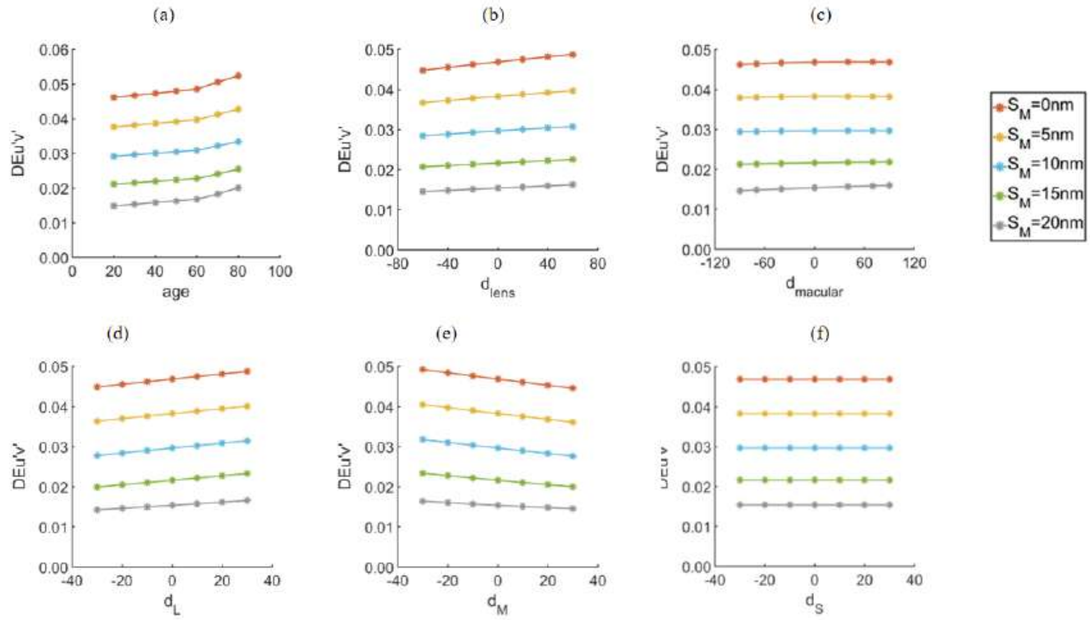

Figure 3. The influence of six physiological parameters on the color difference between numeral and background for deuteranomaly. Six subfigures correspond to six parameters as summarized in the caption of Figure 2. Lines in different colors represent different s_M values equally spaced between 0 *nm* and 20 *nm*.

It could be found that no matter the protanomaly and deuteranomaly, *DEu'v'* between the numeral and background is significantly changed with the observer's age, d_{lens}, d_L, and d_M. The observer's age has the most pronounced influence on *DEu'v'* for the test plate, with the largest variation close to 0.010. The numeral-background color difference increases with the observer's age, indicating a higher possibility to recognize the numeral for the elder observer with CVD. As for d_{lens}, d_L, and d_M, it is worthwhile to note that their effects on *DEu'v'* are more substantial for CVN than CVD. While for the other two parameters $d_{macular}$ and d_S, the numeral-background color difference remains approximately invariant as the parameter ranges from -3SD to +3SD, regardless of the peak wavelength shift of L- or M-cone. In addition, the relationship between the numeral-background color difference *DEu'v'* and each parameter for the protanomaly is similar to that for the deuteranomaly.

Performance of the Ishihara plate. To better characterize the influence of the variations in CMFs on the performance of the Ishihara plate, a Monte Carlo simulation of individual CMF has been performed for each type of color vision by adopting the SD values of five physiological parameters (d_{lens}, d_{macula}, d_L, d_M, d_s) defined in Asano's paper. For an example of CVN, there is no shift in peak wavelength for either cone. For an example of protanomaly, the peak wavelength shift of the L-cone is set at 20 *nm*, while there is no shift for the other two cones. Similarly, for an example of deuteranomaly**,** the peak wavelength shift is set at 20 *nm* for the M-cone, but equal to zero for other cones. For each type of color vision, 1000 sets of individual CMFs were generated, considered as 1000 individual observers. The histogram of the numeral-background *DEu'v'* is presented in Figure 4 and three subfigures correspond to three types of observers. It can be observed that for CVN, the *DEu'v'* values of 1000 simulated observers vary from 0.037 to 0.055. For protanomaly and deuteranomaly, color difference values range between 0.004 and 0.021, 0.007 and 0.022, respectively. For two types of CVD, if the color discrimination threshold for the sample plate ranges between 0.010 and 0.020, the observer whose perceived color difference exceeds the threshold would be misclassified as CVN, impairing the accuracy of the Ishihara test. In the future, more experiments will be implemented to obtain the color discrimination threshold of the pseudo-isochromatic plate for further analysis of its theoretical efficiency and accuracy.

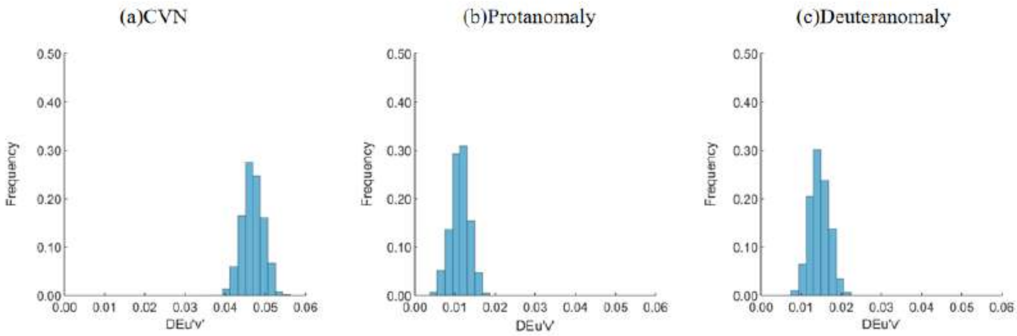

Figure 4. Histogram of the numeral-background color difference for CVN, protanomaly, and deuteranomaly.

CONCLUSION

The purpose of this study is to investigate the effect of physiological parameters on the performance of the Ishihara plate by simulating the CMFs of individual observers. It is found that most physiological parameters do have a significant impact on the color difference between numeral and background, such as age, d_{lens}, d_L, d_M, possibly resulting in the diagnosis error of the Ishihara test.

REFERENCES

1. L. H. Hardy, G. Rand, and M. C. Rittler, "Tests for the detection and analysis of color-blindness. I. The Ishihara Test: an evaluation," J.Opt. Soc. Am. 35, 268–275 (1945).

2. S. J. Belcher, K. W. Greenshields, and W. D. Wright, “Colour vision survey using the Ishihara, Dvorine, Boström and Kugelberg, Boström, and American-Optical Hardy-Rand-Rittler tests,” Br. J. Ophthalmol. 42, 355–359 (1958).
3. M. K. Haskett and J. K. Hovis, “Comparison of the standard pseudoisochromatic plates to the Ishihara color vision test,” Optom. Vis.Sci. 64, 211–216 (1987).
4. J. Birch and L. M. McKeever, “Survey of the accuracy of new pseudoisochromatic plates,” Ophthal. Physiol. Opt. 13, 35–340 (1993).
5. J. Birch, “Efficiency of the Ishihara test for identifying red-green colour deficiency,” Ophthal. Physiol. Opt. 17, 403–408 (1997).
6. D. Y. Lee and M. Honson, “Chromatic variation of Ishihara diagnostic plates,” Color Res Appl. 28, 267–276 (2003).
7. L. H. Hardy, G. Rand, and M. C. Rittler, “Effect of quality of illumination on the results of the Ishihara test,” Arch. Ophthalmol. 36,685–699 (1946).
8. I. Schmidt, “Effect of illumination in testing color vision with pseudo-isochromatic plates,” J. Opt. Soc. Am. 42, 951–955 (1952).
9. S. Tamura, Y. Okamoto, S. Nakagawa, T. Sakamoto, M. Ando, and Y.Shigeri, “Light wavelengths of LEDs to improve the color discrimination in Ishihara test and Farnsworth Panel D-15 test for deutans,”Color Res. Appl. 42, 424–430 (2017).
10. CIE. SPECIAL METAMERISM INDEX: CHANGE IN OBSERVER. CIE Publication No80. 1989;.
11. Allen E. An Index of Metamerism for Observer Differences. In: Proceedings of the 1st AIC Congress Color 69; 1970. p. 771–783.
12. Nayatani Y, Takahama K, Sobagaki H. A proposal of new standard deviate observers. Color Research & Application. 1983; 8(1):47–56. doi: 10.1002/col.5080080110
13. Ohta N. Formulation of a standard deviate observer by a nonlinear optimization technique. Color Research & Application. 1985; 10(3):156–164. doi: 10.1002/col.5080100304
14. North AD, Fairchild MD. Measuring color-matching functions. Part II. New data for assessing observer metamerism. Color Research & Application. 1993; 18(3):163–170. doi: 10.1002/col.5080180306
15. Rich DC, Jalijali J. Effects of observer metamerism in the determination of human color-matching functions. Color Research & Application. 1995; 20(1):29–35. doi: 10.1002/col.5080200106
16. Alfvin RL, Fairchild MD. Observer variability in metameric color matches using color reproduction media. Color Research & Application. 1997; 22(3):174–188. doi: 10.1002/(SICI)1520-6378(199706)22:3%3C174::AID-COL6%3E3.0.CO;2-O
17. CIE. Fundamental Chromaticity Diagram with Physiological Axes—Part 1. CIE Publication No170.2006.
18. Asano Y, Fairchild M D, Blondé L. Individual colorimetric observer model[J]. PloS one, 2016, 11(2): e0145671.
19. Yaguchi H, Luo J, Kato M, et al. Computerized simulation of color appearance for anomalous trichromats using the multispectral image[J]. JOSA A, 2018, 35(4): B278-B286.

COLOR RENDERING INDEXES FOR COLOR BLIND OBSERVERS

Rafael Huertas[1]*, Pedro Machado[1], Lucia Zapata[1], Eva M. Valero[1], Miguel A. Martínez-Domingo[1], Luis Gómez-Robledo[1], Jose L. Galindo[1] and Javier Hernández-Andrés[1]

[1]*Department of Optics, Faculty of Science, University of Granada, Spain.*

*Corresponding author: Rafael Huertas, rhuertas@ugr.es

ABSTRACT

Color rendering index (CRI) measures the ability of a light source to accurately reproduce the colors of the objects it illuminates, in comparison with a natural or standard light source. Light sources with a high CRI are desirable in color-critical applications such as neonatal care, photography, etc. The International Commission of Illumination (CIE) recommends the use of the CIE *Ra* index, which traditionally has been the international standard color rendering index. Lighting industry has experimented a revolution during last years, with the development of LED lamps, and in this case CIE *Ra*'s ability to predict color appearance has been criticized in favor of other measures. Thus, different proposals have been published in the last years, such as Color Quality Scale (CQS) index Q_a, which will be used in this work. It must be noted that the mentioned indexes are only valid for normal color vision people. However, color vision deficiencies (CVD) are quite widespread, since around 8% of the male and 0.5% of the female Caucasian population is affected by this condition. In fact, CVD has gained relevance in the last decade, with a surge of proposals for aid systems that aim to improve the color discrimination capabilities of CVD subjects. Thus, it would be desirable to have a measure of the color reproduction of a lamp valid for CVD people, which will depend on the type and severity of the deficiency. These figures could be included in the commercial lamps' specifications for the most typical CVD types. The goal of the work is adapting the CRI and CQS for CVD observes, through simulation by algorithms of CVD of different types and severities. The results show that CVD does increase the value of R_a and Q_a, as could be expected.

Keywords: Color Rendering Index, color vision deficiencies (CVD), CVD simulation algorithms.

INTRODUCTION

The main parameters to characterize light sources are the electric power, the luminous efficiency, the correlated color temperature, and the Color Rendering Index (CRI). The CRI is a crucial metric in the world of lighting and design. There are many proposals, but most of the indexes are calculated based on the average color difference between a set of samples as illuminated by the test light source and the samples as illuminated by a reference light source, such as sunlight. In essence, any type of color rendering index is a quantitative measure of the ability of a light source to reveal the colors of objects faithfully in comparison with a natural or standard light source. Thus, CRI helps us evaluate how well a light source makes colors appear real, vibrant, and true to life. Usually, the CRI value is included in the commercial lamp's specifications. Whether in residential, commercial, or industrial settings, the CRI is essential for achieving optimal lighting solutions that enhance visual comfort and overall quality of life. Light sources with a low CRI can make objects appear to have unnatural or dull colors. For example, a light source with a low CRI might make a red apple appear brown or a green leaf appear yellow. The CRI is an important consideration when choosing a light source for any application where accurate color reproduction is important, such as photography, videography, retail and commercial spaces, food presentation, museums and art galleries exhibitions, art restoration, industrial settings for quality control and inspection tasks, healthcare facilities (i.e., neonatal care) and many other activities, also daylight ones.

The International Commission of Illumination (CIE) recommends the use of the CIE R_a index [1]. Numerically, the highest possible R_a value is 100 and would only be given to a source whose spectrum is identical to the spectrum of daylight. A R_a of 90 or higher is considered to be good, while a R_a of 80 or higher is considered to be acceptable. For instance, low-pressure sodium lighting has a negative value; fluorescent lights range from about 50 for the basic types, up to about 98 for the best multi-phosphor type. On the other side, lighting industry has experimented a revolution during last years, with the development of LED lamps. This technology offers, besides of excellent efficiency, great versatility in the design of the spectral power distribution (SPD) of the lamps, with applications in different fields. Typical white-color LEDs have a R_a of 80 or more.

CIE R_a's ability to predict color appearance has been criticized in favor of measures based on color appearance models, such as CIECAM02, more recent chromatic adaptation transforms, a set of test samples with more saturated colors, etc. Several proposals have appeared in the last years. Among others, at the National Institute of Standards and Technology (NIST), Davis and Ohno proposed in 2010 the Color Quality Scale (CQS) index Q_a [2]. The Q_a scale ranges from 0 to 100, with higher numbers indicating better color rendering, in a similar way to R_a. However, CQS is a more comprehensive measure of color quality than the CRI. R_a is based on a smaller set of color samples, and it does not consider the effects of saturation and chroma on color perception. The CQS also addresses some of the other limitations of the CRI, such as its tendency to over-rate light sources that produce saturated colors.

These indexes, and others, are based on the average color difference between a set of samples as illuminated by the test light source and the samples as illuminated by a reference light source over the assumption of normal color vision. However, prevalence of CVD is not negligible but quite important. The most common type of CVD is red-green CVD, corresponding to protan type (misfunction or lack of cone L) and deutan type (misfunction or lack of cone M). Another type is blue-yellow CVD, which is much less common, and corresponds to tritan type (misfunction or lack of cone S), that will not be considered in this work. CVD can have a significant impact on a person's life. It could make it difficult to perform tasks such as reading color maps, choosing ripe fruit, distinguish the color of certain indicative lights (LEDs), etc. There is no cure for CVD in humans, although gene therapy has been tested on primates [3].

Obviously, for CVD people, the reproduction of colors capacity of the lamps would be different, depending on the type and severity of the deficiency. The goal of this work is to propose a method to compute the CRI and CQS of the lamps for CVD people.

METHODOLOGY

All computations were performed using spectral data from 380 – 780 nm in 2 nm increments. If the data (SPD or spectral reflectance) was not originally in that format, we employed derivative-constrained-spline interpolation. Extrapolation was never done.

Lamps.

For this study different SPDs have been considered from the dataset provided for use as example of computation of the TM-30-20 index [4]. It includes a set of 318 SPDs which is a subset of SPDs used in [5]. From this dataset we are going to extract some groups including only either commercial lamps or traditional illuminants. The groups are the following: the equal energy illuminant; the CIE daylight illuminants D50, D55, D60, D65, D70, D75 and D80; the 12 CIE fluorescent illuminants (F1 to F12); 17 commercial fluorescent broadband (Fig. 1a); 22 commercial fluorescent narrowband (Fig.1b); 20 commercial high intensity discharge (Fig. 1c); 6 commercial halogen (Fig. 1d); 4 commercial incandescent (Fig. 1e); 6 commercial LED hybrid (Fig. 1f); 1 commercial LED mixed (Fig. 1g) and 129 commercial LED phosphor (Fig. 1h).

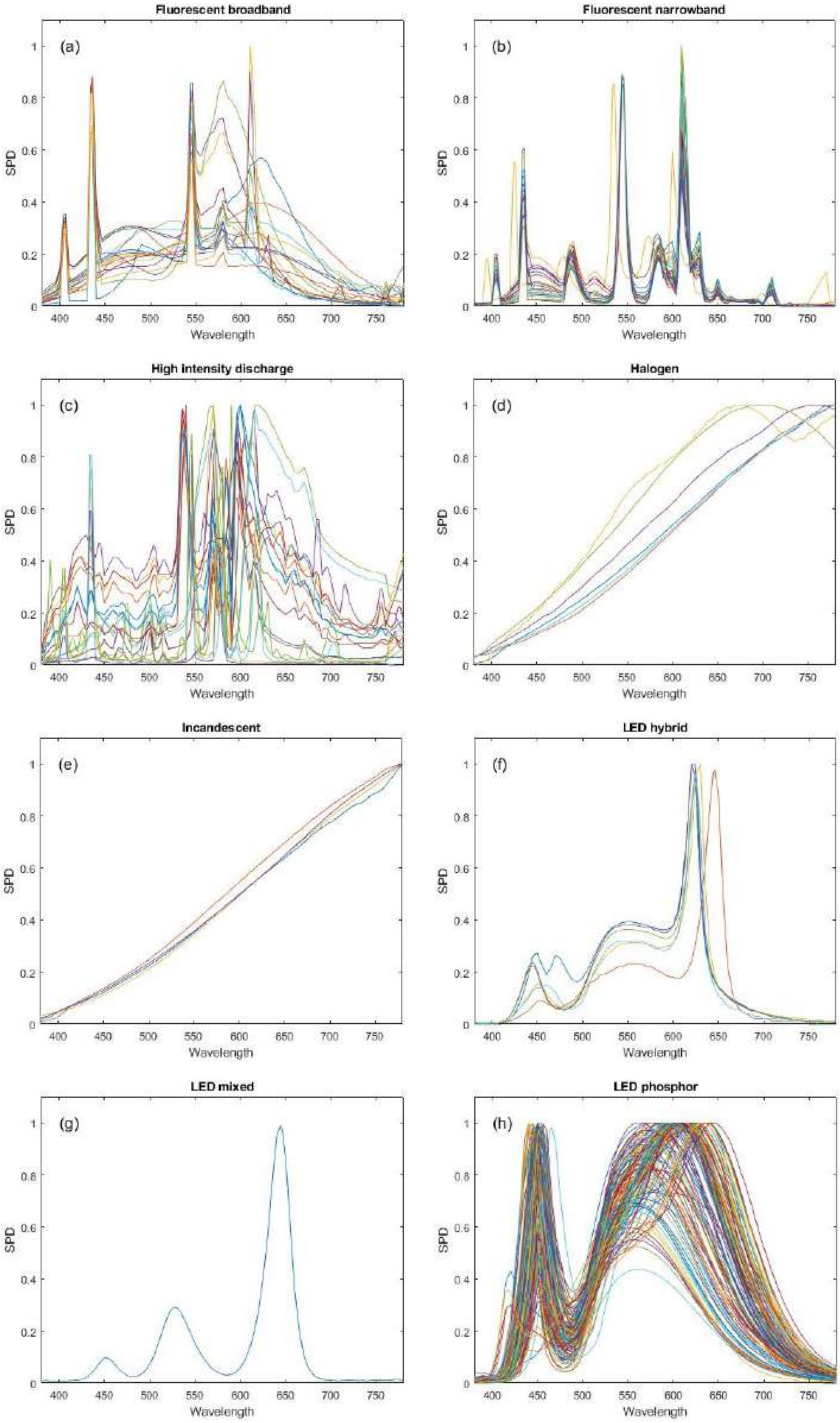

Figure 1. SPDs of the considered lamps.

CIE R_a.

The CRI currently recommended by the CIE, Ra index, has been computed according to [1], as the average color difference between a set of 8 samples as illuminated by the test light source and by the reference light source. In this work CIE D65 illuminant has been considered as the reference light for all the lamps independently of their correlated color temperature (CCT). The color differences are computed in CIE 1964 U*W*V* uniform color space after a Von Kries chromatic adaptation. A scaling is applied to compute the individual indexes, Ri, for each sample:

$$R_i = 100 - 4.6\Delta E_i \quad (1)$$

Finally, the R_a is computed as the average of the R_i for the 8 samples. Because the normalization of Eq. (1) is possible to obtain negative values of R_a.

CQS Q_a.

CQS is based on a psychophysical experiment in which observers rate the color quality of a light source using a set of 15 colored samples. The samples are designed to represent a wide range of colors, including both saturated and unsaturated colors. It has been computed following the Davis and Olmo paper method [2]. It is similar to CRI, but in this case CMCCAT2000 chromatic adaptation is applied and the color differences are computed in CIELAB color space (ΔE_{ab}). Afterwards, the root mean square (ΔE_{rms}), and a scaling factor ($Q_{i,rms}$) are calculated. To avoid negative values, a 0-100 scale conversion is applied in the following way:

$$Q_{i,0-100} = 10\ln\left[e^{Q_{i,rms}/10} + 1\right] \quad (2)$$

The index computed in Eq. (2) has been considered as Q_a in this work. Please, note that CIE D65 illuminant has been considered as the reference light for all the lamps independently of theirs correlated color temperature (CCT). Besides, the CCT factor, which correct the index for the rare case of lamps with extremely low CCTs, has not been applied.

Simulation of anomalous color vision.

The CRI and CQS have been computed for normal color vision and CVD observers using Lucassen et al. model [6]. This model introduces varying amounts of weighting of L and M cone responses in the anomalous observers, modulated by a parameter called *d*. For instance, a mild deuteranomalous condition modifies the L and M cone responses introducing a 0.3 contribution of the cone L into the M cone response. A deuteranope would be simulated using a *d* parameter value of 1. For each type, protan and deutan, 6 conditions have been modeled with *d* varying from 0 to 1 in 0.2 steps. Note that *d* is not a lineal measurement of the severity. Value *d*=0 corresponds to normal color vision, *d*=1 to protanope or deuteranope and the intermediate values of *d* to protanomalous or deuteranomalous with different severities. The cases of *d*=0.3 and 0.6 have been considered as mild and medium severity respectively for protan and deutan types.

RESULT AND DISCUSSION

Considering CVD through Lucassen algorithm, R_a and Q_a indexes change, as can be seen in Tables 1 and 2 respectively. Table 1 shows R_a values for the considered group of light sources, for normal color vision observer, protanomalous (with severity mild and medium), protanope, deuteranomalous (with severity mild and medium) and deuteranope. As could be expected, the value of both, R_a and Q_a, increases with the severity for any lamp. CVD people have a reduced color gamut; hence, some particular colors don't need to be accurately reproduced by the lamp. Moreover, the set of lamps in each group reproduce the color more similarly for CVD people, as standard deviations decrease for CVD cases.

The highest values of R_a in Table 1 correspond to CIE daylight illuminants, while the lowest to LED mixed (Fig. 1c), even with a negative value for normal color vision case. For any group of lamps, normal color vision achieves the lowest values of R_a, (in bold) while CVD protanope does the highest (in bold). However, for mild severity protanomalous the values are similar or lower than mild severity deuteranomalous.

These arguments are partially valid considering the more recent Q_a index, as shows Table 2. The best reproduction of colors (in bold) is obtained by CVD, but not always protanope type, but also deuteranope in some cases. The worst reproduction of colors (in bold) is not always for normal color vision, but medium severity deuteranomalous in some cases.

Table 1: R_a values for the group of lamps and different CVD conditions.

Color vision	Normal	Protanomalous		Protanope	Deuteranomalous		Deuteranope
Severity		Mild	Medium		Mild	Medium	
Equal energy	**88.51**	90.87	93.19	**94.82**	91.98	93.06	92.12
CIE daylight illuminants	**94.37** (4.09)	94.74 (3.76)	95.11 (3.44)	**95.34** (3.20)	95.00 (3.56)	94.89 (3.60)	94.17 (4.08)
CIE fluoresc. Illuminants	**71.22** (11.56)	75.69 (10.54)	79.31 (10.04)	**81.97** (9.90)	75.08 (10.59)	77.46 (10.74)	78.55 (11.60)
Fluorescent broadband	**75.45** (12.80)	79.43 (10.82)	82.82 (9.48)	**85.18** (8.90)	79.53 (11.15)	81.47 (10.54)	81.66 (10.66)
Fluorescent narrowband	**67.75** (12.15)	72.03 (10.84)	76.23 (9.19)	**80.12** (7.25)	73.63 (9.02)	75.79 (8.86)	76.51 (10.18)
High intens. Discharge	**50.32** (19.42)	57.11 (16.01)	62.97 (14.06)	**67.23** (14.31)	58.12 (16.92)	61.15 (15.04)	61.34 (14.40)
Halogen	**50.59** (4.38)	55.94 (3.51)	61.72 (2.58)	**66.94** (1.68)	60.33 (2.55)	60.58 (2.28)	56.80 (2.56)
Incandescent	**48.04** (1.49)	53.90 (1.34)	60.20 (1.15)	**65.96** (0.97)	58.81 (1.13)	59.20 (1.14)	55.21 (1.19)
LED hybrid	**48.30** (10.72)	55.04 (8.42)	62.36 (5.92)	**69.72** (3.12)	60.19 (6.69)	62.61 (5.14)	60.21 (5.25)
LED mixed	**-25.21**	3.35	32.61	**65.84**	24.39	46.37	45.85
LED phosphor	**64.90** (9.73)	68.44 (9.19)	71.84 (8.37)	**74.88** (7.43)	69.33 (7.50)	70.50 (8.08)	70.01 (10.05)

Table 2: Q_a values for the group of lamps and different CVD conditions.

Color Vision	Normal	Protanomalous		Protanope	Deuteranomalous		Deuteranope
Severity		Mild	Medium		Mild	Medium	
Equal energy	96.23	96.36	96.79	**98.38**	95.61	**95.54**	96.73
CIE daylight illuminants	97.52 (1.80)	97.51 (1.79)	97.68 (1.71)	**98.25** (1.52)	97.30 (2.03)	**97.15** (2.12)	97.53 (1.72)
CIE fluoresc. illuminants	**74.99** (12.95)	81.30 (9.28)	86.08 (6.75)	**90.76** (5.52)	79.83 (10.06)	85.27 (6.66)	90.62 (4.40)
Fluorescent broadband	**80.69** (13.20)	85.12 (9.61)	88.77 (6.90)	**93.08** (5.21)	83.91 (9.94)	87.38 (6.95)	90.71 (5.38)
Fluorescent narrowband	**80.22** (3.83)	85.10 (2.80)	88.34 (2.55)	91.40 (1.95)	83.31 (3.91)	87.39 (3.70)	**92.81** (3.03)
High intens. discharge	**63.29** (25.71)	71.15 (19.48)	77.11 (14.59)	**83.21** (12.25)	67.28 (19.96)	73.40 (15.15)	80.59 (14.05)
Halogen	76.45 (1.14)	77.06 (1.11)	77.92 (1.03)	**81.04** (0.85)	72.70 (1.50)	**72.15** (1.59)	77.17 (1.26)
Incandescent	75.82 (0.94)	76.38 (0.87)	77.30 (0.85)	**80.75** (0.80)	71.77 (1.05)	**71.11** (1.02)	76.34 (0.92)
LED hybrid	79.76 (4.22)	81.02 (4.73)	82.47 (4.60)	**86.26** (3.89)	77.81 (4.25)	**77.55** (5.03)	81.29 (5.80)
LED mixed	**52.64**	53.33	57.46	**68.17**	61.53	63.95	63.50
LED phosphor	**75.39** (3.94)	80.85 (3.22)	84.58 (3.40)	88.24 (3.70)	77.39 (4.01)	81.74 (4.97)	**88.74** (4.77)

Only for the commercial lamps, Fig. 2 and 3 shows the R_a and Q_a from normal color vision (black color bar) to complete (pink color bar), protanope and deuteranope respectively, in 5 steps of severity with intermediate *d* values of 0.2, 0.4, 0.6 and 0.8. Overall, Q_a is higher than R_a, especially for LED, incandescent and halogen groups. For these groups, the increase with the severity of the deficiency in Q_a is lower than R_a. Besides, the standard deviation between the lamps of the group is smaller for Q_a than R_a. No changes worth mentioning are observed between types protan and deutan for R_a or Q_a.

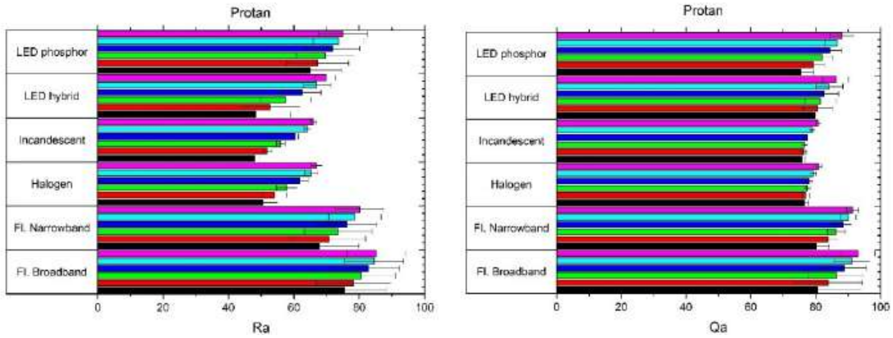

Figure 2. R_a (left) and CQS (right) values (error bars are standard deviation) for commercial lamps from normal observers (black) to protanope (pink).

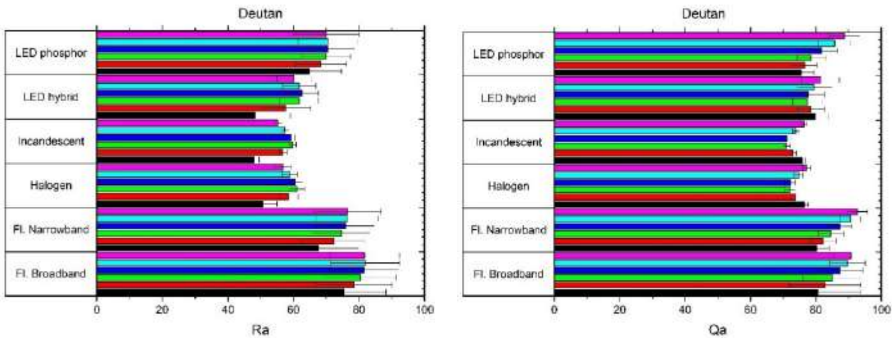

Figure 3. R_a (left) and CQS (right) values (error bars are standard deviation) for commercial lamps from normal observers (black) to deuteranope (pink).

CONCLUSION

Reproduction of colors depends on the type and severity of CVD. In general, CVD increases the values of CRI and CQS, more for R_a than for Q_a. Almost for any type of lamp, the best results are obtained for protanope, which means that a protanope observer would see the colors under a lamp with medium R_a or Q_a (computed for normal color vision observer) quite similar to the colors illuminated by the CIE Daylight D65 illuminant. The more recent index CQS Q_a obtain better values than the CRI R_a, especially for LED lamps.

ACKNOWLEDGEMENT

This work was supported by the research project FIS2017-89258-P with European Union FEDER support and PID2022-139056NB-I00 funded by the Spanish Ministry of Science and Innovation.

REFERENCES

1. Commission Internationale de l'Eclairage, "Method of Measuring and Specifying Color Rendering Properties of Light Sources: Technical Report: CIE 13.3-1995," (CIE, 1995).
2. W. Davis and Y. Ohno, "Color quality scale," Optical engineering 49, 033602-16 (2010).
3. M. Neitz and J. Neitz, "Curing color blindness--mice and nonhuman primates," Cold Spring Harb Perspect. Med. 4, a017418 (2014).
4. ANSI/IES TM-30-20, "Technical Memorandum: IES Method For Evaluating Light Source Color Rendition," 74 (2019).
5. K. W. Houser, M. Wei, A. David, M. R. Krames, and X. S. Shen, "Review of measures for light-source color rendition and considerations for a two-measure system for characterizing color rendition," Optics Express 21, 10393-10411 (2013).
6. M. P. Lucassen and J. W. Alferdinck, "Dynamic simulation of color blindness for studying color vision requirements in practice," (2006).

COLOUR DISCRIMINATION FOR VISUALLY IMPAIRED PEOPLE UNDER MIXED LIGHT LEDS AND WHITE LEDS

Ektawat Plerksophon[1], Pichayada Katemake*[1], Alain Trémeau[2,3], and Éric Dinet[2]

[1]*Dept. Imaging and Printing Technology, Faculty of Science, Chulalongkorn University, Bangkok, Thailand.*
[2]*Laboratoire Hubert Curien UMR 5516, Saint-Étienne, France*
[3]*Affiliated Researcher at Faculty of Science, Chulalongkorn University*

*Corresponding author: Pichayada Katemake, pichayada.k@chula.ac.th

ABSTRACT

Visual impairment, a spectrum ranging from moderate visual acuity to blindness, poses significant challenges to daily living, social interactions, and employment opportunities. People with visual impairments often require specialised support and accommodations to engage fully in society. One critical aspect of vision, especially for those with mild to moderate visual impairment, is colour discrimination, which plays a pivotal role in object recognition and classification based on chromatic properties. This study investigates the effectiveness of a mixed light LED (RGB+YW) with a colour temperature of 5000K compared to two controlled Light Emitting Diode (LED) lamps with warm white (4000K) and cool white (6500K) illumination in enhancing colour discrimination for individuals with mild and moderate visual impairment. Three different illuminance levels (20 lux, 200 lux, and 2000 lux) were considered, and the study involved thirty simulated participants representing mild and moderate visual impairment. Simulated mild visual impairment was achieved using cloudy lenses with a visual acuity of 6/12, while simulated moderate visual impairment involved clear lenses with a visual acuity of 6/18. The Farnworth-Munsell 100 hue test served as the stimulus for colour discrimination evaluation. The results demonstrated a significant reduction in the Total Error Score (TES) of colour discrimination as illuminance levels increased. At higher illuminance levels (200 lux and 2000 lux), the differences in performance among the light sources diminished. However, at the lower illuminance level of 20 lux, the mixed light LED outperformed both controlled white LED lamps. Interestingly, participants with similar simulated visual impairments did not exhibit consistent patterns on the polar scale of the Farnworth-Munsell 100 hue test. Additionally, it was observed that despite having lower visual acuity, individuals with simulated mild visual impairment (cloudy lenses) had higher average TES scores compared to those with simulated moderate impairment (clear lenses) at certain illumination levels. These findings underscore the significant impact of illumination levels on colour discrimination for individuals with low vision. With its specific wavelength selection, the mixed light LED shows promise in enhancing colour discrimination for individuals with mild and moderate visual impairment, particularly in low-light conditions, outperforming controlled white LED lamps. This study contributes valuable insights into improving the visual experiences of individuals with visual impairments, facilitating better participation in daily activities and professional settings.

Keywords: low vision, visual impairment, colour vision, illuminance, colour discrimination, mixed light LEDs

INTRODUCTION

Vision serves as our primary sense, permeating every facet of our existence. It plays a pivotal role in interpersonal and social communication, facilitating the conveyance of non-verbal cues like gestures and facial expressions during face-to-face interactions. [1, 2]. Proficient vision empowers individuals to sustain social connections, foster independence, and manage concurrent health conditions [3]. Visual impairment encompasses a spectrum of conditions that precipitate a diminishment in visual functionality, which can manifest as partial or complete vision loss.

This impairment may be caused by various sources, including age-related changes, ocular disorders, injuries, or neurological issues. Importantly, such impairments resist correction through conventional means like glasses or contact lenses. Globally, it is estimated that at least 2.2 billion individuals were affected by some form of vision impairment in 2019 [4]. Those grappling with visual impairment often encounter challenges in their daily routines, social interactions, and professional pursuits, necessitating specialised support and accommodations to enable their full participation in society [5]. Blurry and cloudy vision, caused by uncorrected refractive errors, cataracts that cloud the crystalline lens of the eye, and vascular occlusions [4], are among the most common symptoms of visual impairment.

Enhancing visual performance for individuals with visual impairment and the elderly hinges on several critical factors, including illumination level, luminance, and chromaticity contrast. Multiple research studies have highlighted that modifying the lighting conditions within a given environment can significantly improve the perceptual abilities of individuals, consequently enhancing their performance and emotional perception in certain tasks [6]. Leveraging high-contrast colours and illumination levels is a potent strategy to augment the visual performance of those with visual impairments. For instance, strategically using vibrant, well-defined colours can enable individuals to precisely locate and discern the depth of light switches [7]. Numerous researchers have recognised the profound impact of colour on object recognition among individuals with visual impairment [8, 9]. In addition, Bustamante et al. [2] have proposed a correlation between colour discrimination and correlated colour temperature (CCT) of light sources, noting that cooler light sources enhance hue differentiation, thereby improving overall colour distinction.

This research centres on a comparative analysis of various LED light sources to improve colour discrimination for individuals with mild and moderate visual impairments. The primary goal of this study is to assess the efficacy of mixed LEDs in contrast to commercial LEDs, with a specific focus on determining the optimal illuminance levels for individuals with mild and moderate visual impairments.

METHODOLOGY

2.1 Mixed Light LEDs

Mixed light LED technology refers to advanced LED lighting systems intentionally designed to produce a blend of various colours of light by incorporating multiple LED chips of different hues within the same lighting fixture. This innovative approach allows for generating an extensive spectrum of colour temperatures and nuanced colour combinations. An illustrative example of this approach can be found in the work of Katemake et al. [10], who employed a combination of three narrow-band LEDs, red, green, and blue, to enhance colour discrimination among the elderly population. Furthermore, yellow and white LEDs have been integrated into the system to enhance visual comfort and elevate the colour rendering index (CRI). The specific wavelengths associated with each LED channel in mixed light LEDs are presented in Table 1 as part of this experiment.

Table 1: Wavelength of each channel of Mixed-light LEDS (BV-L)

	Blue (B)	Green (G)	Red (R)
Wavelength(nm)	420-450	520-540	650-670

2.2 Experimental setup

To conduct a comprehensive comparison between mixed light LED (referred to as BV-L, 5000K) and two white LED lamps in terms of their ability to distinguish colour differences, the experiment was designed to encompass three distinct lighting conditions: BV-L (5000K), Cool White (CW) (6500K), and Warm White (WW) (4000K) LED lamps. The spectral power distribution of each of these lights was recorded. The performance evaluation of these three light sources will be carried out using the Farnworth-Munsell 100 hue test [10]. Illuminance levels on the experimental table were precisely measured utilising the Konica Minolta CL-200 Chroma meter, with three distinct illumination levels employed for each light source: 20 lux, 200 lux, and 2000 lux. The distance between the lamps and the Farnworth-Munsell 100 hue test was consistently maintained at 40 cm throughout the experiment.

2.3 Participant

Thirty participants, aged 18 to 30 years old, all possessed normal vision or had vision corrected to normalcy. All participants were tested for visual acuity. Participants were subsequently divided into two groups, each simulating the visual impairment associated with specific types of simulated low-vision glasses: blurry vision, with visual acuity of 6/18, which represented moderate visual impairment and cloudy vision, with visual acuity of 6/12, which represented mild visual impairment.

2.4 Procedure

At the start of the experiment, participants received a comprehensive briefing detailing the study's objectives and the procedural steps involved. Preliminary trial presentations were conducted to promote clarity and mitigate any potential experiential bias, allowing participants to become familiar with the testing process. Each participant was assigned specific visual impairment simulation glasses. A duration of 5 minutes was allocated for every participant to adjust to each test lighting condition before the experiment began.

2.5 Data Analysis

The one-way ANOVA was applied to individual sessions as a condition that the light source and the illuminance are combined to predict TES. Subsequently, Tukey's Honestly Significant Difference (Tukey's HSD) was applied.

RESULT AND DISCUSSION

3.1 Data Collection and Preprocessing

In each simulated condition, we gathered 135 sets of Test Error Scores (TES) based on a combination of 15 subjects across nine sessions. The collected data were systematically organised according to the specific light source, illuminance level, and the type of simulated glasses employed. A concise summary of the data structure is presented in Figure 1: effect of illuminance on the TES of blurry and cloudy visions of different light sources.

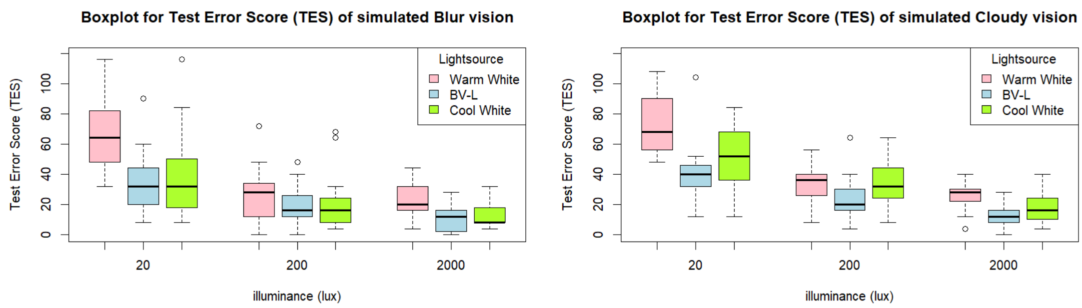

Figure 1: Effect of illuminance on the TES of blurry vision (left) and cloudy vision (right) under three light sources.

3.2 Illuminance

In our study, which investigates the impact of nine distinct lighting conditions on Test Error Score (TES), we employed the Tukey's HSD test to scrutinise disparities among the mean TES values associated with each condition, as depicted in Figure 1. It's essential to note that lower TES values are indicative of superior colour discrimination capabilities. The Tukey's HSD analysis unveiled statistically significant differences in performance across the various conditions, as outlined in Table 2 (only the significant pairs are shown). Notably, the condition of warm white 20 lux exhibited a statistically higher mean score (blurry: 68.0±26.1, cloudy: 75.5±26.3) compared to the remaining conditions (Figure 1), suggesting poorer colour discrimination capabilities in this particular condition relative to the others.

The analysis of mean differences reveals that, for the three light sources and two types of simulated low-vision glasses, there is no statistically significant disparity between illuminances of 200 lux and 2000 lux. The insignificant pairs are not included in the table.

Notably, we observed substantial mean differences between the 20 and 200 lux illuminance levels for warm white LED in simulated cloudy and blurry visions. This observation highlights that increasing the illuminance to 200 lux for warm white LED significantly enhances colour discrimination from the baseline of 20 lux, which is comparatively low when contrasted with cool white and BV-L.

Conversely, the mean differences at these two illuminance levels under BV-L and cool white LED are relatively smaller, with TES scores at 20 lux remaining relatively low. This doesn't imply a minor improvement in TES with increased illuminance but rather suggests that BV-L and cool white LED can facilitate relatively good colour discrimination even under low-light conditions as low as 20 lux.

Table 2: Tukey's HSD results for significant pairs on illuminance effect

Simulated blurry vision	Diff	SE	Simulated cloudy vision	Diff	SE
$B_{WW,200}$- $B_{WW,20}$***	-40.8	5.6	$F_{WW,200}$- $F_{WW,20}$***	-42.7	6.0
$B_{WW,2000}$- $B_{WW,20}$***	-44.3	6.7	$F_{WW,2000}$- $F_{WW,20}$***	-50.1	6.9
$B_{BVL,200}$- $B_{BVL,20}$*	-15.9	6.0	$F_{BVL,200}$- $F_{BVL,20}$**	-17.9	4.4
$B_{BVL,2000}$- $B_{BVL,20}$***	-23.6	5.8	$F_{BVL,2000}$- $F_{BVL,20}$***	-28.3	4.0
$B_{CW,2000}$- $B_{CW,20}$**	-25.6	6.0	$F_{CW,200}$- $F_{CW,20}$*	-19.5	4.7
			$F_{CW,2000}$- $F_{CW,20}$***	-34.7	5.8

* for $p < 0.05$, ** for $p < 0.01$, and *** for $p < 0.001$.

3.3 Light source

We analysed the impact of different light sources on the Test Error Score (TES).

In the simulated blurry vision, both BV-L and cool white LED exhibited lower TES values than warm white LED. Importantly, no significant difference was observed between BV-L and cool white conditions. At an illuminance level of 200 lux, no significant distinctions were detected among the various light sources. However, at the higher illuminance of 2000 lux, both BV-L and cool white LED demonstrated significantly lower TES values compared to the warm white conditions. These findings mirrored those observed for cloudy vision.

To further examine the influence of light sources, we employed Tukey's HSD analysis to elucidate the mean differences between each individual condition. The significant negative values of mean differences presented in Table 3 suggest that, for simulated blurry vision, BV-L and cool white LED offer greater colour discrimination enhancements than warm white LED, particularly at illuminance levels of 20 lux and 2000 lux. In the case of simulated cloudy vision, BV-L significantly enhances colour discrimination compared to warm white LED under both 20 lux and 2000 lux conditions.

Table 3: Tukey's HSD results for significant pairs on light source effect

Simulated blurry vision	Diff	SE	Simulated cloudy vision	Diff	SE
$B_{BVL,20}$ - $B_{WW,20}$**	-33.73	8.6	$F_{BVL,20}$ - $F_{WW,20}$**	-34.40	6.9
$B_{CW,20}$- $B_{WW,20}$*	-29.07	6.5	$F_{BVL,2000}$ - $F_{WW,2000}$**	-12.53	2.2
$B_{BVL,2000}$ - $B_{WW,2000}$**	-13.07	3.0	$F_{BVL,2000}$ - $F_{CW,200}$*	-21.6	2.9
$B_{CW,2000}$- $B_{WW,2000}$*	-10.40	3.3			

* for $p < 0.05$, ** for $p < 0.01$, and *** for $p < 0.001$.

3.4 Discussion

In this research, the impact of illuminance and light source on the colour discrimination of visual impairment have been explored. The results illustrated several interesting findings.

Firstly, the study's results emphasise the impact of illuminance on colour discrimination among individuals with visual impairments, including both those with blurry and cloudy conditions. This trend remains consistent across all lighting sources, with higher illuminance levels (specifically, 200 and 2000 lux) consistently yielding superior colour discrimination results compared to the lower 20 lux condition. These outcomes align harmoniously with prior research [10], indicating that visually impaired individuals tend to perform tasks more effectively in well-illuminated settings. However, our research suggests that an illuminance level of 200 lux is sufficient for effective colour discrimination and does not significantly differ from the performance observed under the 2000 lux condition. This valuable insight could have practical implications for the design of lighting systems. It suggests that, in settings where balancing energy efficiency and meeting the visual needs of visually impaired individuals is important, for individuals who have similar viewing conditions as in this research, a 200 lux illuminance level may be a suitable compromise.

Secondly, the study delved into comparing different light sources at varying illuminance levels. At lower illuminance levels, BV-L and cool white light sources performed better than warm white, with significantly lower TES. Notably, there was no significant difference in TES between BV-L and cool white light sources. These findings align with a study by Bustamante et al. [2], which highlighted the significant impact of Correlated Colour Temperature (CCT) on colour discrimination among visually impaired individuals. Our results demonstrated a similar trend, where higher CCT light sources tended to outperform lower CCT ones. However, an interesting observation was that BV-L showed less variability in colour discrimination across individuals when compared to the other two light sources. Furthermore, the study revealed that under more extreme conditions, namely 20 lux and 2000 lux, the choice of light source had a substantial impact on the ability of visually impaired individuals to discriminate colours. In both conditions, BV-L and cool white light sources performed better than warm white, leading to significant differences in TES. This finding suggests potential applications for specific tasks, such as guiding lights in dark environments or activities that require visual focus, which could enhance the safety of visually impaired individuals. However, there's a noteworthy conflict regarding the use of higher CCT light sources, which often contain more blue light, for tasks like guiding lights at night. While blue light can stimulate alertness, it may not be ideal for nighttime use. This suggests the need for further research to explore the relationship between exposure time, CCT, and their effects on visually impaired individuals, particularly in scenarios where nighttime alertness may not be desirable.

Thirdly, the research findings revealed an intriguing observation: individuals with simulated mild visual impairment simulating with cloudy lenses sometimes exhibited more challenges in colour discrimination compared to those with simulated moderate visual impairment simulating with clear lenses, particularly in specific lighting conditions. This finding emphasises the necessity of considering various factors beyond just visual acuity, which is traditionally used as a clinical standard to assess visual impairment when designing support and accommodations for visually impaired individuals. However, it is essential to note that this conclusion should be approached with some caution. The study employed simulated participants rather than actual individuals with visual impairments. The use of simulated participants may introduce certain biases or limitations related to their familiarity with the simulation conditions. Therefore, further research and clarification are warranted to fully understand the effect of how different types of visual impairment interact with varying lighting conditions and their impact on colour discrimination, ideally involving real visually impaired individuals to validate the findings.

CONCLUSION

In summary, this study has revealed significant insights into the interplay of illuminance, light sources, and colour discrimination in individuals with visual impairments. Higher illuminance levels, particularly 200 lux, have been found to support effective colour discrimination, offering an energy-efficient alternative. BV-L and cool white have demonstrated superior performance among light sources, although the relationship between high CCT light sources and alertness requires further examination.

Furthermore, the research has highlighted the complexity of colour discrimination in visually impaired individuals, emphasising the need to consider factors beyond traditional visual acuity measurements when devising accommodations and support. However, it is crucial to acknowledge the limitations of using simulated participants, necessitating further research involving real individuals with visual impairments.

ACKNOWLEDGEMENT

We would like to express our sincere gratitude to the 100th Anniversary Chulalongkorn University Fund for Doctoral Scholarship for their invaluable support in funding this research.

REFERENCES

1. Desrosiers, J., Wanet-Defalque, M. C., Temisjian, K., Gresset, J., Dubois, M. F., Renaud, J., Vincent, C., Rousseau, J., Carignan, M., & Overbury, O. (2009). Participation in daily activities and social roles of older adults with visual impairment. *Disabil Rehabil*, *31*(15), 1227-1234. https://doi.org/10.1080/09638280802532456
2. Bustamante, P., Acosta, I., León, J., & Campano, M. A. (2021). Assessment of color discrimination of different light sources. *Buildings*, *11*(11), 527.
3. Wang, J. J., Mitchell, P., & Smith, W. (2000). Vision and low self-rated health: the Blue Mountains Eye Study. *Investigative ophthalmology & visual science*, *41*(1), 49-54.
4. Organization, W. H. (2019). World report on vision.
5. La Grow, S. J., & Daye, P. (2005). Barriers to employment identified by blind and vision-impaired persons in New Zealand. Social Policy Journal of New Zealand, 26, 173.
6. Evans, B., Sawyerr, H., Jessa, Z., Brodrick, S., & Slater, A. (2010). A pilot study of lighting and low vision in older people. *Lighting Research & Technology*, *42*(1), 103-119.
7. Markowitz, M. (2006). Occupational therapy interventions in low vision rehabilitation. *Canadian Journal of Ophthalmology*, *41*(3), 340-347.
8. Wurm, L. H., Legge, G. E., Isenberg, L. M., & Luebker, A. (1993). Color improves object recognition in normal and low vision. *Journal of Experimental Psychology: Human perception and performance*, *19*(4), 899.
9. Wang, Y.-Z. (2001). Effects of aging on shape discrimination. *Optometry and Vision Science*, *78*(6), 447-454.
10. Katemake, P. et al. (2022). Development of visual assistive tools for the elderly and the low vision. *NRCT Report.*
11. Cheng, W., Ju, J., Sun, Y., & Lin, Y. (2016). The effect of LED lighting on color discrimination and preference of elderly people. *Human Factors and Ergonomics in Manufacturing & Service Industries*, *26*(4), 483-490.

THE EFFECT OF CHANGES IN MELANOPSIN STIMULATION OF THE SURROUNDING LIGHT ON BRIGHTNESS AND COLOR PERCEPTION

W. Shibata[1], R. Tokunaga[2]* and S. Tsujimura[3]

[1]*Graduate Degree Program of Global and Transdisciplinary Studies, Chiba University, Japan.*
[2]*Graduate School of Global and Transdisciplinary Studies, Chiba University, Japan.*
[3]*Graduate School of Design and Architecture, Nagoya City University, Japan.*

*Corresponding author: R. Tokunaga, tokunaga@chiba-u.jp

ABSTRACT

Intrinsically photosensitive retinal ganglion cells (ipRGCs) have a visual substance called melanopsin that contributes to brightness perception. Recently, its contribution to color perception has been considered. Since melanopsin contributions were investigated in peripheral vision and across the visual field, the effects of melanopsin stimulation in peripheral vision on foveal brightness and color perception remain unclear. In this study, we examined whether modulating melanopsin stimulation in peripheral vision affects brightness and color perception in foveal vision. In the experiment, two LED light sources were independently modulated: the test and surrounding lights. We calculated cone stimulations as constants and three different melanopsin stimulation levels (− 40 %, 0 %, + 40 %) for each light. Two modes of color appearance, the light source color mode (LCM) and object color mode (OCM), were set for the test stimulus to investigate the relationship between melanopsin stimulation and mode of color appearance. The observers evaluated the apparent whiteness and chromaticness of the test stimulus in the foveal vision condition (FV) and the peripheral vision condition (PV) by the method of elementary color naming. The results of both visual conditions showed that the whiteness and chromaticness of LCM were significantly different from OCM. Particularly, the whiteness of OCM in FV decreased as melanopsin stimulation of the surrounding light increased, and there was no such tendency in PV. Interestingly, the chromaticness of OCM in FV increased as melanopsin stimulation of the surrounding light increased. The results suggest that melanopsin might affect brightness and color perception, and the influence differs depending on the mode of color appearance, especially in the condition of OCM in FV. Our data represent that changes in the melanopsin stimulation levels in peripheral vision affect the foveal brightness and color perception.

Keywords: melanopsin, adaptation, brightness perception, color perception, the mode of color appearance

INTRODUCTION

Human color vision was considered to process light through cones and rods. Intrinsically photosensitive retinal ganglion cells (ipRGCs) were discovered around 2000 as a new photoreceptor and had a visual substance called melanopsin. Previous studies have shown that melanopsin is involved in visual functions, especially brightness perception [1-3]. Zele *et al.* [1] and Yamakawa *et al.* [2] employed brightness estimation, and Brown *et al.* [3] employed brightness discrimination to examine brightness perception for the visual stimuli of cone metamer with different melanopsin stimulation levels. They found visual stimuli were perceived brighter at higher melanopsin stimulation levels than at lower levels. Color perception also has been considered in some studies. Cao *et al.* [4] and DeLawyer *et al.* [5] investigated the color appearance of the visual stimuli with modulating melanopsin stimulation. They reported that observers tend to perceive more greenish under high melanopsin stimulation levels. In these studies, the visual stimuli were presented in peripheral vision or the entire visual field since the distribution density of ipRGCs is relatively high in the peripheral retina [6]. There are few studies focused on the presentation conditions such as the size and position of visual stimuli. Barrionuevo *et al.* [7] performed color matching using visual stimuli with three different field sizes and different levels of melanopsin stimulation. They reported that melanopsin might be involved in S-cones sensitivity functions in large fields. Higashi *et al.* [8] compared the color appearance in foveal and peripheral vision. It was revealed that different eccentricity of the stimulus affects color perception.

Most of the previous studies have examined the contribution of melanopsin to brightness and color perception either in peripheral or foveal vision, and have presented visual stimuli in the limited visual field. In our daily lives, we rarely spend our time with a limited visual field and see things in foveal vision with lighting across the visual field. No previous study has investigated the effects of melanopsin stimulation in peripheral vision on foveal brightness and color perception. To achieve such a daily visual environment, we attempted to introduce two light sources so that different melanopsin stimulation levels are performed in each visual field. In this research, we investigated whether modulating melanopsin stimulation in peripheral vision affects foveal brightness and color perception.

METHODOLOGY

Apparatus The experiment was conducted in a dark room. Figure 1 shows the schematic diagram of the experimental setup. It was divided into an observation room and a stimulation room. The observers looked at a square hole with a visual angle of 2° as a test stimulus through an intervening wall. A surrounding light source (Hand-made LED light source) was in the observation room, and a test light source (LEDCube, THOUSLITE) was in the stimulation room. Sixteen LEDs were in the surrounding light source (peak wavelength: 417, 442, 443, 449, 475, 504, 521, 540, 592, 609, 610, 634 and 660 nm) and 15 LEDs were in the test light source (peak wavelength: 368, 385, 405, 422, 441, 447, 476, 505, 525, 542, 594, 610, 635, 658 and 672 nm). Both light sources were controlled independently to modulate the melanopsin stimulation levels. A diffuser (frosted glass diffuser, Edmund optics) was placed between the test stimulus and the test light source to diffuse the light from the test light source.

Two visual conditions were set: the foveal vision condition (FV) and the peripheral vision condition (PV). In PV, the fixation point was placed at a distance of 7° from the test stimulus to present the test stimulus to the nasal retina [2,6] as shown in Fig. 1(b). The fixation point was a black cross with a visual angle of 2°.

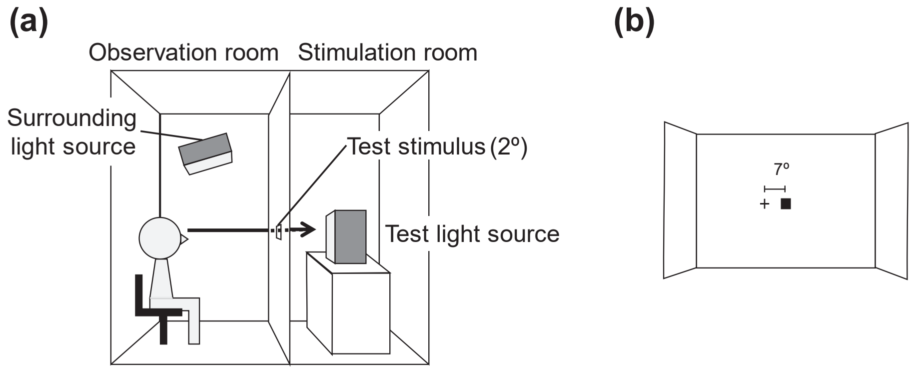

Figure 1. Schematic diagram of apparatus (a) The side view of the experimental apparatus, and (b) The front view from the observers. A central square in (b) is a hole as a test stimulus where the observers judge the color appearance. A cross is a fixation point displayed only in PV, and the observers judge the color appearance of a test stimulus while looking at a fixation point.

Visual stimuli To examine the effects of melanopsin stimulation on our foveal brightness and color perception, we set the three levels of melanopsin stimulation. Table 1 shows the details of the surrounding lights and the test lights. The chromaticities were calculated using CIE 2006 10° LMS cone fundamentals [9]. The three surrounding lights that have the same chromaticity coordinates with constant cone stimulations but different melanopsin stimulation levels were achieved using the silent-substitution method [10]. The melanopsin stimulation levels were based on Mel-Standard (Mel_S), + 40 % for Mel-High (Mel_H), and − 40 % for Mel-Low (Mel_L). Three different test lights were set the same way as the surrounding lights. The cone stimulations were calculated based on Stockman *et al.* [11,12], and melanopsin stimulation was based on Tsujimura *et al.* [10] and Yang *et al.* [13]. Figure 2 shows the spectral distributions, which were measured with a spectral irradiance meter (CL-500A, KONICA MINOLTA). We assumed rods were saturated above 5 cd/m² [14].

In the experiment, we also examined the influence of two modes of color appearance of the test stimulus: light source color mode (LCM) and object color mode (OCM). The luminance of object color mode was achieved by setting an ND filter (ND1.0, FUJIFILM) between the diffuser and the test light source. Although the test stimulus was the hole in which the observers saw the light, the observers perceived it as if there was a surface in OCM.

Table 1. Values of Stimuli Used in Experiment

	Surrounding lights				Test lights of LCM				Test lights of OCM			
	Lum (cd/m²)	CIE 2006 10° x	CIE 2006 10° y	Mel*	Lum (cd/m²)	CIE 2006 10° x	CIE 2006 10° y	Mel	Lum (cd/m²)	CIE 2006 10° x	CIE 2006 10° y	Mel
Mel_H	170.3	0.329	0.331	268.1	310.8	0.331	0.329	486.1	60.2	0.330	0.331	95.0
Mel_S	170.4	0.330	0.331	191.1	311.2	0.331	0.330	349.5	60.1	0.331	0.331	67.4
Mel_L	169.7	0.330	0.330	114.2	311.3	0.330	0.330	207.8	59.9	0.330	0.331	40.4

*Mel : the melanopsin stimulation levels

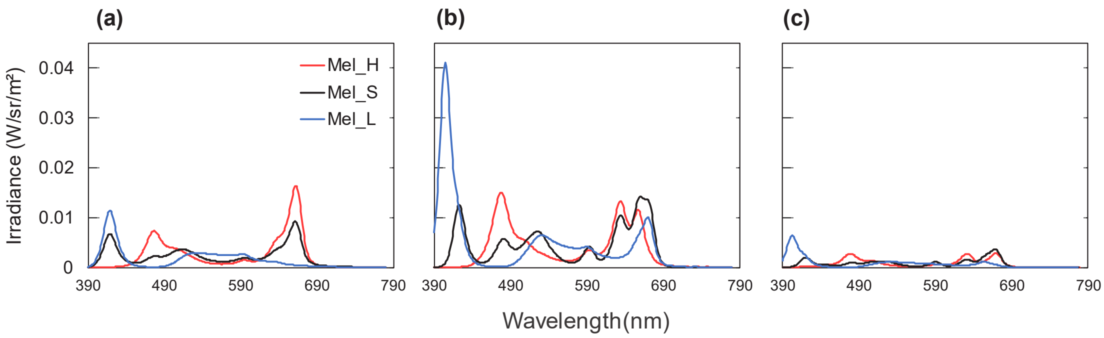

Figure 2. Spectral power distributions of (a) Surrounding lights, (b) Test lights of LCM, and (c) Test lights of OCM. The line color showed the different levels of melanopsin stimulation.

Procedure and Observers The observers sat at 80 cm from the test stimulus with the left eye masked. They evaluated the appearance of the test stimulus with their right eye, looking at the test stimulus in the foveal vision condition (FV) and the fixation point in the peripheral vision condition (PV). The color appearance of the test stimulus was evaluated using the elementary color naming method based on Boynton *et al.* [15]. The observers had a practice session in which they judged the mode of color appearance as Task 1 and elementary color naming as Task 2. In Task 1, observers were instructed to answer the mode of color appearance of the test stimulus: light source color mode, object color mode, or in between [16]. In Task 2, they were instructed to evaluate the appearance of the test stimulus: whiteness, blackness, and chromaticness in percentage.

In the experiment, the observers entered a dark room and adapted to the surrounding light for 5 minutes. No test stimulus was presented during the adaptation period. In one run, the observers performed Task 1 and Task 2 every minute up to 10 times. One session was composed of 6 runs with 3 different test lights and 2 modes of color appearance per surrounding light, and performed for 3 different surrounding lights. Such 18 sessions were repeated 5 times for 2 visual conditions. The observers made the evaluations 1800 times in total. They were instructed to close their eyes between each run. The sessions were conducted a maximum of twice a day, with an interval of 4 hours.

Four observers (aged 21-23 years) participated in the experiment. All observers were confirmed to have normal color vision using the Ishihara Pseudo-Isochromatic Plate Test.

RESULT AND DISCUSSION

The whiteness We analyzed data of four observers using MATLAB R2022b (The MathWorks, Inc.). We report only the 10th judgment here, i.e., after 10 minutes of adaptation to the surrounding light. Figure 3 shows the results of the apparent whiteness for LCM and OCM for all four observers. The horizontal axis indicates three levels of melanopsin stimulation of the surrounding light, and the vertical axis indicates the whiteness in percentage. In the foveal vision condition (FV) in Fig.3(a), the whiteness of LCM (*Mean* = 92.90, *SD* = 8.67) was significantly different from OCM (*Mean* = 35.99, *SD* = 21.78); the mean of LCM was higher than OCM from a paired *t*-test (t (59) = 19.77, $p < .001$). The peripheral vision condition (PV) in Fig.3(b) also shows that the whiteness of LCM (*Mean* = 95.35, *SD* = 6.37) was significantly different from OCM (*Mean* = 40.83, *SD* = 22.78); the mean of LCM was higher than OCM (t (59) = 17.16, $p < .001$). These results can be interpreted as the observers perceiving the test stimulus as a surface in OCM. More blackness is needed to perceive the surface in OCM, object color mode. Therefore, the whiteness decreased in OCM because the blackness might have increased.

In Fig. 3(a), LCM in FV showed no decrease in whiteness even though the melanopsin stimulation of the surrounding light increased. OCM in FV, however, although the absolute values of whiteness varied among four observers, the whiteness decreased with increasing the melanopsin stimulation of the surrounding light for all observers except for observer 2. The whiteness decreased as the surrounding light varied from Mel_L to Mel_H ($p < .001$) or Mel_S to Mel_H ($p < .001$) from a two-way analysis of variance (ANOVA). The result of OCM in FV is expected to be due to the brightness contrast between the surrounding light and the test stimulus. The brightness contrast makes the test stimuli look darker as the periphery is bright and vice versa. In this experimental condition, the luminance and chromaticity coordinates of the three surrounding lights are the same so that no brightness contrast should occur. The brightness contrast occurs despite such experimental settings, implying that the brightness contrast could be attributed to the difference in melanopsin stimulation of the surrounding light. Yamakawa *et al.* [3] examined the contribution of melanopsin to brightness perception by presenting visual stimuli in peripheral vision that modulated melanopsin stimulation. They reported that the higher the melanopsin stimulation, the brighter the perception. Therefore, the result of OCM in FV suggests that melanopsin influenced brightness perception, causing a brightness contrast between the test stimulus and the surrounding light. On the other hand, the whiteness of LCM in FV, as the test stimulus appeared as the light source color mode, the whiteness might have been judged with no relation to melanopsin stimulation of the surrounding light.

In Fig. 3(b), both LCM and OCM in PV showed no tendency of the whiteness shift with varying the surrounding light. This result was the same as FV for LCM but different for OCM. If melanopsin contributes to brightness perception, brightness contrast occurs between the test stimulus and surrounding light in OCM in PV, the same as in FV. In other words, the whiteness should decrease with increasing melanopsin stimulation of the surrounding light. The result of OCM in PV might be explained based on Mullen *et al.* [17-19]. We set up two hypotheses on the basis of their finding that the luminance mechanism in the visual field has an even distribution but gradually declines toward the periphery. One is that although melanopsin contributes to brightness perception, the effect of brightness contrast would have declined toward the periphery. Another one is that the influence of melanopsin on brightness perception in peripheral vision is not apparent in object color mode. Previous studies examining the contribution of melanopsin to brightness perception have yet to consider the mode of color appearance of visual stimuli. Further studies are needed to know the relationship between the mode of color appearance of visual stimuli and the melanopsin stimulation levels.

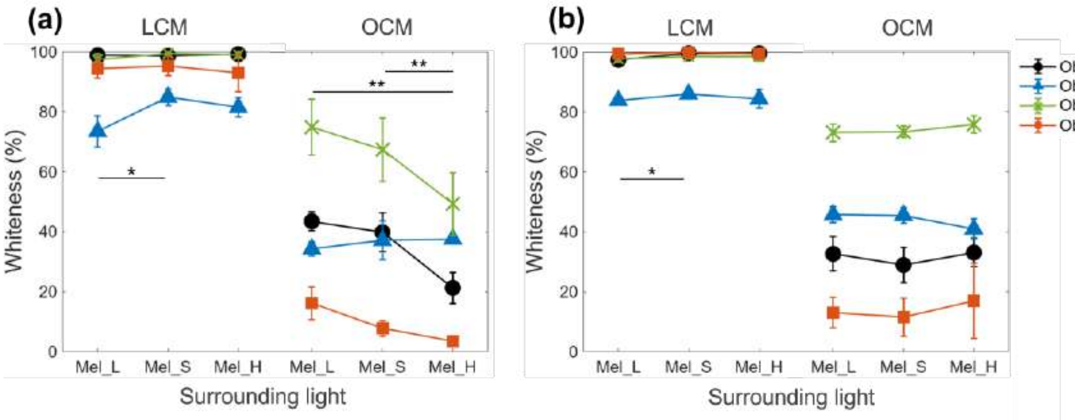

Figure 3. Difference in whiteness from the elementary color naming method. (a) The foveal vision condition (FV) and (b) the peripheral vision condition (PV). Symbols correspond for four observers (n = 4 observers; *Mean* ± *SD*). **$p < .001$, *$p < .01$

The chromaticness The chromaticness was analyzed in the same way as the whiteness. In both visual conditions, the chromaticness of LCM was significantly different from OCM according to a paired t-test. In FV, the chromaticness of LCM (*Mean* = 2.15, *SD* = 3.01) was lower than OCM (*Mean* = 24.37, *SD* = 22.36) (t (59) = − 7.82, $p < .001$). In PV, it also showed that the chromaticness of LCM (*Mean* = 0.75, *SD* = 1.16) was lower than OCM (*Mean* = 11.82, *SD* = 11.97) (t (59) = − 7.20, $p < .001$). In the case of OCM in FV, the chromaticness varied associated with changes in the melanopsin stimulation levels of the surrounding light. It increased significantly when the surrounding light varied from Mel_L to Mel_S ($p < .001$) or from Mel_S to Mel_H ($p < .001$) except for observer 2. Even though the chromaticity of the surrounding lights was kept constant, as shown in Table 1, the evaluated chromaticness was different. In addition, more chromaticness was perceived as melanopsin stimulation of the surrounding light increased. This result suggests that melanopsin stimulation of the surrounding light might affect color perception.

CONCLUSION

In this study, we examined whether modulating melanopsin stimulation in peripheral vision affects brightness and color perception in foveal vision. The evaluated whiteness of LCM was significantly different from OCM for both in FV and PV, and it was also seen in chromaticness. This indicates that the observers judged the whiteness and chromaticness depending on the mode of color appearance regardless of the visual conditions. Furthermore, the whiteness and chromaticness differed as the melanopsin stimulation levels of the surrounding light varied, especially OCM in FV. The result suggests that melanopsin contributes to brightness and color perception in our experimental conditions. Additional research is needed to clarify the relationship between the mode of color appearance and the melanopsin stimulation levels.

ACKNOWLEDGEMENT

This work was supported by JSPS KAKENHI Grant Number JP23K11281.

REFERENCES

1. Zele, A.J., Adhikari, P., Feigl, B. & Cao, D. (2018). Cone and melanopsin contributions to human brightness estimation. *J. Opt. Soc. Am. A, Opt. Image Sci. Vis.,* 35, B19-B25.
2. Yamakawa, M., Tsujimura, S. & Okajima, K. (2019). A quantitative analysis of the contribution of melanopsin to brightness perception. *Sci. Rep.,* 9, 1-8.
3. Brown, T.M., Tsujimura, S., Allen, A.E., Wynne, J., Bedford, R., Vickery, G., Vugler, A. & Lucas, R.J. (2012). Melanopsin-based brightness discrimination in mice and humans. *Curr. Biol.,* 22, 1134-1141.
4. Cao, D., Chang, A. & Gai, S. (2018). Evidence for an impact of melanopsin activation on unique white perception. *J. Opt. Soc. Am. A, Opt. Image Sci. Vis.,* 35, B287-B291.
5. DeLawyer, T. & Shinomori, K. (2023). Melanopsin-driven surround induction on the red/green balance of yellow. *J. Opt. Soc. Am. A. Opt. Image Sci. Vis.,* 40(3), A40-A47.
6. Melanie, R., Marijke, C.M.G., Domien, G.M.B., Bonnie, V. & Serge, D. (2005). Nasal versus temporal illumination of the human retina: effects on core body temperature, melatonin, and circadian phase. *J. Biol. Rhythms.,* 20, 60-70.
7. Barrionuevo, P.A., Filgueira, C.P. & Cao, D. (2022). Is melanopsin activation affecting large field color-matching functions? *J. Opt. Soc. Am. A. Opt. Image Sci. Vis.,* 39(6), 1104-1110.
8. Higashi, H. & Okajima, K. (2023). Daylights with high melanopsin stimulation appear reddish in fovea and greenish in periphery. *PLoS ONE,* 18(4): e0285053.
9. CIE (2006). Fundamental chromaticity diagram with physiological axes. Parts 1 and 2. Technical Report 170-1. Vienna: Central Bureau of the Commission Internationale de l' Éclairage.
10. Tsujimura, S., Ukai, K., Ohama, D., Nuruki, A. & Yunokuchi, K. (2010). Contribution of human melanopsin retinal ganglion cells to steady- state pupil responses. *Proc. Biol. Sci.,* 277(1693), 2485-2492.
11. Stockman, A. & Sharpe, L.T. (2000). The spectral sensitivities of the middle- and long-wavelength-sensitive cone derived from measurements in observers of known genotype. *Vis. Res.,* 40(13), 1711-1737.
12. Stockman, A., Jägle, H., Pirzer, M. & Sharpe, L.T. (2008). The dependence of luminous efficiency on chromatic adaptation. *J. Vis.,* 8(16), 1-26.
13. Yang, P.L., Tsujimura, S., Matsumoto, A., Yamashita, W. & Yeh, S.L. (2018). Observerive time expansion with increased stimulation of intrinsically photosensitive retinal ganglion cells. *Sci. Rep*., 8(1), 11693.
14. CIE. (2010). Recommended system for mesopic photometry based on visual performance. CIE 191:2010. International Commission on Illumination.
15. Boynton, R.M. & Gordon, J. (1965). Bexold-Brucke hue shift measured by color-naming technique. *J. Opt. Soc. Am*, 55, 78-86.
16. Thiangthangtum, Y., Ikeda, M. & Shinoda, H. (2004). Room Illuminance rather than Immediate Surrounding Luminance Determines Natural to Unnatural Color of an Object Border. *Opt. Rev.,* 11, 235-239.
17. Mullen, K.T., Sakurai, M. & Chu, W. (2005). Does L/M cone opponency disappear in human periphery? *Perception*, 34(8), 951–959.
18. Mullen, K.T. & Kingdom, F.A. (2002). Differential distributions of red-green and blue-yellow cone opponency across the visual field. *Vis. Neurosci*, 19(1): 109-118.
19. Hansen, T., Pracejus, L. & Gegenfurtner, K.R. (2009). Color perception in the intermediate periphery of the visual field. *J. Vis.*, 9(4):26, 1–12.

Session 5

Doi Tong
29 November 2023

IS COLOR PREFERENCE AFFECTED BY PERSONALITY?

W. Cheng[1]* and L. Ou[1]

[1] *National Taiwan University of Science and Technology, Taipei, Taiwan*

*Corresponding author: Wen-Hsin Cheng, d11022504@mail.ntust.edu.tw

ABSTRACT

Factors affecting individual differences in color preference have been a subject of interest but are still not fully understood. In psychology, personality traits have been found to make an important contribution to variation among individuals. It is fair to wonder whether there is any relationship between color preference and personality. Do personality traits of an individual have any impact on his/her personal color preference? What about other potential factors such as gender and age – do they also affect color preference? To answer these questions, we conducted an online questionnaire including a color preference ranking task, a short version of Chinese Big Five Inventory (BFI-15), and questions about personal information such as gender, age range, professional background, and month of birth. We received a total of 997 responses from color-normal individuals currently living in Taiwan, with age ranged from teenage to just under 70 years. In the questionnaire, the color preference ranking task focused on mobile phone case colors, with 4 sets of ranking tasks, each consisting of 6 colors. Participants were asked to rank them according to color preference for mobile phone cases. The color samples used in the ranking task were selected from the Practical Color Coordinate System. Set 1 colors comprised 6 hues, all with the vivid tone: red, orange, yellow, green, blue, and purple. Set 2 included three tones of reds: vivid red, light red, and dark red, in addition to vivid blue, light yellow, and dark green. Set 3 included three tones of greens: vivid green, light green, and dark green, in addition to vivid purple, light blue, and dark red. Set 4 included three tones of blues: vivid blue, light blue, and dark blue, in addition to black, gray, and white. K-means clustering techniques were used to divide the 997 participants into 5 groups based on their color ranking results. Each group shows similar distributions of personality scores from the BFI-15 test. We also used K-means clustering to divide all participants into 5 groups based on their BFI-15 scores, and found that each group shows similar color preference ranking results. These findings indicate that the participant's personality traits had little impact on color preference. Data analysis was also performed regarding the other potential factors affecting color preference including gender, age, and professional background. The results indicate that, among these variables, age shows the strongest impact on color preference rankings. It was found that light colors were ranked highest across all age groups, and that vivid colors ranked lowest, especially in younger age groups. The rankings for vivid colors tend to get higher and higher as age increases, indicating a strong impact of age on color preference ranking. Personality traits were also found affected by age. The older the age group, the lower scores for "neuroticism", and the higher scores for "extraversion" and "conscientiousness". These findings are useful to develop guidelines of color designs for various age groups.

Keywords: Color Preference, Personality Traits, Ageing Research.

INTRODUCTION

The application of color ranges from individual clothing and personal items to residential environments, making individual preferences for specific colors a popular topic. Identifying the underlying factors and patterns behind these preferences is an important issue across various fields.

Personality traits have been found to play a significant role in the variation between individuals. Thus, it is interesting to examine whether personality has a direct impact on color preferences. It should be noted, however, that the composition of the human mind is highly intricate, and individual's personal background may also influence preferences. Numerous theories have demonstrated potential relationship between personal backgrounds and color preferences. Nevertheless, when it comes to personality, there is no clear evidence indicating a correlation between the two. This study aims to examine both personality and personal background to identify underlying factors affecting color preference.

METHODS

To achieve the aims described above, we conducted an online questionnaire survey, with 997 responses from participants who did not have color vision deficiencies.

The questionnaire was divided into three sections. The first section gathered basic information about the participants, including age, gender, occupation, zodiac sign, and nationality. The second section consisted of a personality assessment, utilizing the Chinese Shortened Version of the Big Five Inventory, a test that measures the five major personality traits.

The third section was a color preference ranking task for mobile phone cases. The ranking task consisted of a total of 16 color samples, selected from the Practical Color Coordinate System (PCCS). These 16 colors were organized into four color sets, each containing six colors. There are overlapping colors among the four sets, allowing for comparisons and connections between these colors. To reduce influence of variations in display devices used by individual participants, all colors were selected to present significant color differences between them.

The first set consisted of vivid colors: red, green, blue, yellow, orange, and purple. The second set included three tones of red: vivid red, light red, and dark red. Apart from these red colors, the other three colors had distinct hues and tones: vivid blue, light yellow, and deep green. The third set consisted of three tones of green: vivid green, light green, and deep green, along with vivid purple, light blue, and deep red. The fourth set included three tones of blue: vivid blue, light blue, and deep blue, along with black, white, and gray. The four sets of color samples are shown in Figure 1.

Figure 1
The four sets of color samples used in this study.

The participants consisted of 997 individuals, including 282 males and 715 females. In terms of age distribution, there were 166 participants aged 16 to 20, 574 participants aged 21 to 30, 161 participants aged 31 to 40, 47 participants aged 41 to 50, and 49 participants aged 51 to 58.

RESULT AND DISCUSSION

Color preference in general

In the Big Five Inventory, each of the five personality traits was measured by three questions, making a total of 15 questions. Each question described a specific personality trait, for example, being helpful and selfless. Participants rated themselves on a scale from 1 (least like me) to 5 (most like me) based on how well the description matched their personality. The scores from the three questions related to each trait were then averaged to obtain a score for each individual trait.

In the color ranking method, each of the six colors in a set is assigned a score based on preference. The most favored color receives a score of 6, the second-favored color receives a score of 5, and so on in descending order. The average score is then calculated for each individual color, and the color with the highest average score is considered the most preferred within that set.

Figure 2 shows the average color preferences of all 997 participants. Using Set 1's vivid tone colors as the main axis and the second, third, and fourth sets' vivid red, vivid green, and vivid blue as the joints, the colors can be arranged from top to bottom, and from left to right, based on their ratings. The higher a color is positioned on this graph or the further to the left it is, the more it was liked by the participants. Such an arrangement of color samples can help us analyze the trends of color preference ratings.

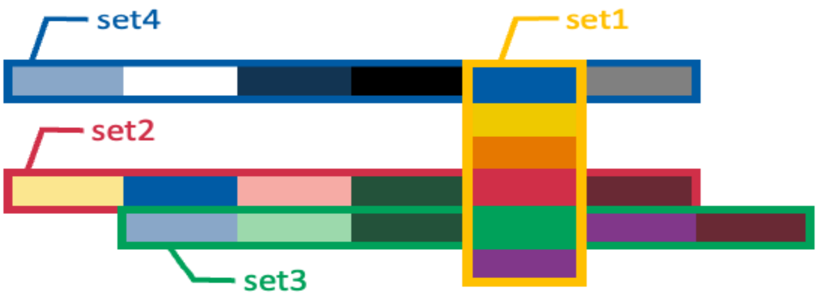

Figure 2
The average color preference rankings of the 997 participants

Color preference and personality trait

All participants were divided into 5 clusters using K-means techniques based on the Big Five Inventory results; the 5 clusters were called P1 to P5, as shown in Figure 3. After conducting one-way analysis of variance (ANOVA), the F-value for the five clusters were found to be as follows: 291.2, 124.8, 82.8, 382.6, and 146.6. All the p-values were lower than 0.05, indicating that there are significant differences in personality among these five clusters. Note that the five clusters P1 to P5 were arranged based on the neuroticism trait scores, i.e. P1 participants tended to have the lowest score on neuroticism, while P5 participants tended to have the highest score on neuroticism.

The color preference results for each cluster (P1 to P5) are shown in Figure 4, and the trend of color preference for each cluster seems to agree well with the overall mean values (Figure 2), suggesting that there are little difference in color preference among participants with different personality traits. Figure 5 shows the personal backgrounds of participants in each cluster, where a noticeable increase in the proportion of females and a decrease in average age across clusters can be observed. This seems to suggest a connection between personality trait and gender, as well as a connection between personality trait and age.

K-means was used again to divide the questionnaire results into three clusters and into four clusters. It was found that, similar to the five-cluster results, as the neuroticism score increases, there seems to be a trend of a higher proportion of females and a decreasing average age. In terms of color preferences, the trends for both the three-cluster and the four-cluster results were found to agree well with the overall mean results (Figure 2), suggesting little difference in color preference among different personality groups.

Figure 3 Clusters P1-P5 based on the results of the Big-Five personality questionnaire

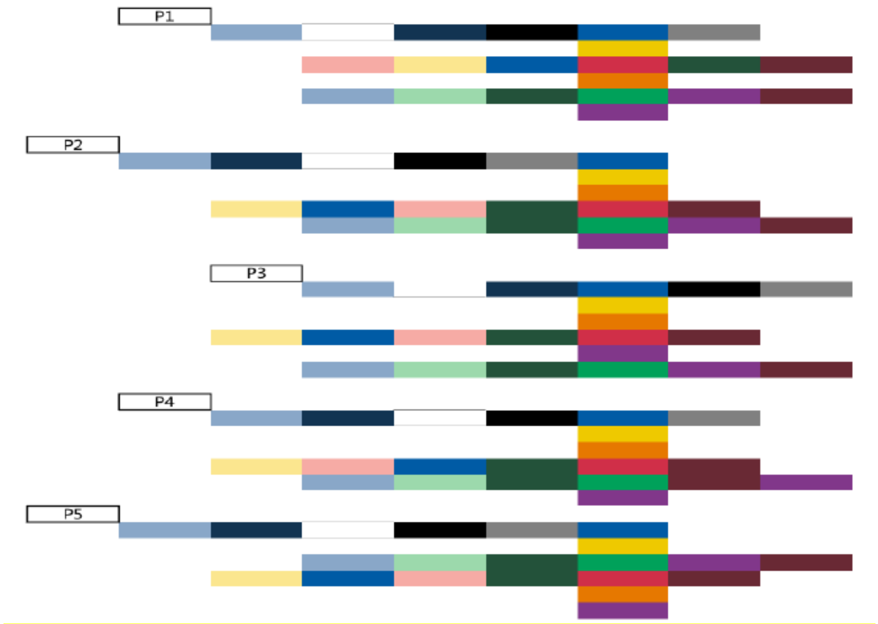

Figure 4 The color preference results for clusters P1-P5

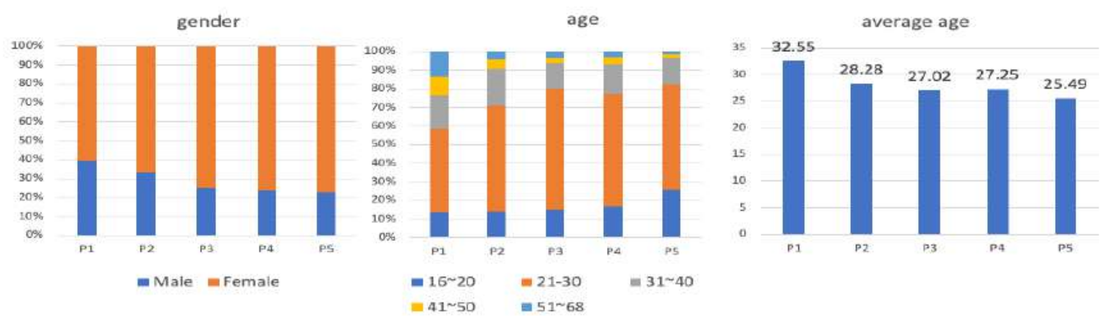

Figure 5 Personal backgrounds for clusters P1-P5

Color preference and age

When grouping participants by age and arranging them in ascending order of average age, as shown in Table 1 with the cluster labels A1 to A5, it is evident that as age increases, there is a tendency for vivid colors to be rated higher, as shown in Figure 6. Additionally, as the Neuroticism trait score decreases, the Conscientiousness and Extraversion trait scores both tend to increase, as shown in Figure 7. The neuroticism trait scores had an F-statistic of 15.412 after one-way analysis of variance (ANOVA), with a p-value lower than 0.05. This indicates that there are significant differences in personality among the five age clusters. In post hoc testing, there were insignificant differences (p-values > 0.05) observed between adjacent clusters, such as clusters A1 vs A2, A3 vs A4, and A4 vs A5. However, significant differences were found among non-adjacent clusters, indicating that as the age gap increases, there are strong variations at the significance level of 0.05 in the neuroticism trait scores.

Table 1 Clusters A1-A5 based on the age of participants

Cluster	A1	A2	A3	A4	A5
Number	166	574	161	47	49
age	16-20	21-30	31-40	41-50	51-68

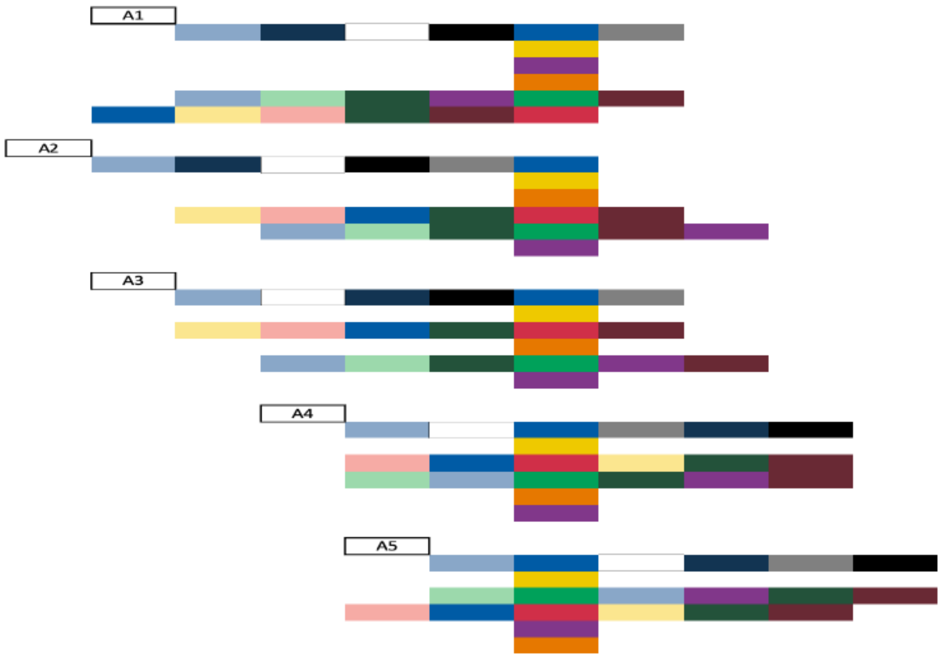

Figure 6 The color preference results for clusters A1-A5

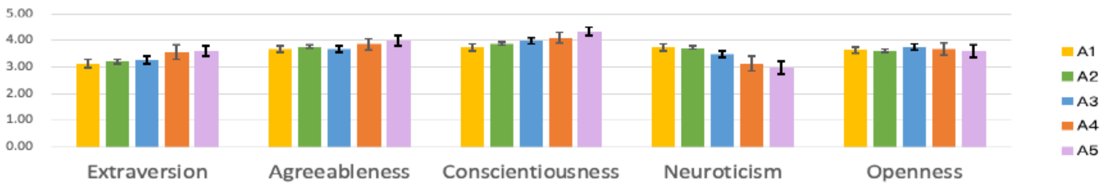

Figure 7 The Big-Five personality mean scores for clusters A1-A5

CONCLUSION

According to the questionnaire results, color preference does not seem to be directly linked with personality. When participants were divided based on personality traits, there was little significant difference in color preference among individuals with different personality types. Instead, personality seems to be related to age. When participants were grouped by age, as age increases, the Neuroticism trait score tends to decrease, and there seems to be a trend of increasing Conscientiousness and Extraversion trait scores. It was also discovered that age seemed to be related to preference for vivid colors. When participants were grouped by age, there seems to be a trend of increased preference for vivid colors as age increases. Older participants tended to rate vivid colors higher than young participants. These findings may be useful to the development of color design guidelines tailored for different age groups.

ACKNOWLEDGEMENT

This research was supported by the National Science and Technology Council, Taiwan (NSTC 112-2410-H-011-025).

REFERENCES

Ren-Hau Li, Hsin-Yu Chung, The development of a Chinese shortened version of the Big Five Inventory (BFI), *Psychological Testing,* 2020, 67.4: 271-299.

EXAMINATION OF THE COLOR IMAGE SCALE FOR CONTEMPORARY WESTERN CULTURE: PHASE ONE OF A MULTIPHASE APPROACH

Julie Lamarra[1]*
* Corresponding author: Julie.Lamarra@usu.edu

(Utah State University, 6000 Old Main Hill Logan, Utah 84322)
[1]Faculty, Technology, Design and Technical Education, Outdoor Product Design and Development, Utah State University, United States.

ABSTRACT

Color perception is a complex process influenced by various factors such as context, culture, and demographics. Designers spend significant time selecting color palettes that resonate with their target audience. The Color Image Scale, developed by Shigenobu Kobayashi in 1989, is a sematic-focused color palette framework widely used in design. It outlines techniques to establish psychological contextualization of colors and color palettes based on perceptions of objects within different design disciplines and lifestyle categories. The study seeks to contextualize Western perceptions of color palettes by exploring and optimizing the matrix associations proposed in Kobayashi's seminal work, the Color Image Scale (CIS). This paper proposes a phased research model to contextualize Western perceptions of color palettes. The framework categorizes color palettes on a matrix based on the overall palette on the vertical axis, described as soft (lighter value), hard (darker value), the temperature ranging from hues of red to blue (hot to cool) on the horizontal axis and additionally on a third dimension described as clear, grayish denoting to shifts in chroma. To achieve this goal, the researchers developed an online survey that targeted North American designers trained in apparel design, industrial design, interior design, and graphic design-associated industries, as well as non-designers. The survey collected participants' word association responses to various combinations of color palettes (single-hue sample n=214; three-hue sample n=180). This exploration challenges the findings utilized in the original study, which included a Japanese-only demographic (n = 40), 120 chromatic and ten achromatic color profiles, and a 180-word database. Overall, this study contributes to a better understanding of the influence of context, culture, and demographics on color perception and word associations while also serving as a foundation for further research that focuses on semantic associations of color palettes for Westernized target audiences.

Keywords: Color-Palette Perception, Color Image Scale, Design, Culture

INTRODUCTION

Background Information. Color is a fundamental aspect of human perception and communication, playing a significant role in our daily lives, aesthetics, and cultural expressions [1]. Across different cultures, colors hold distinct meanings and are used to convey various emotions, symbolize traditions, and represent social and spiritual concepts [2][3][4]. Understanding the diverse interpretations of color palettes across cultures is essential for effective cross-cultural communication and design.

The Color Image Scale. The Color Image Scale (CIS) is a comprehensive framework that categorizes colors based on their emotional and psychological associations [2]. It helps us understand how colors are perceived universally and across various cultures [6][7][8][9][10]. The CIS is a widely recognized framework that has been extensively employed in empirical research to investigate the emotional and psychological aspects of color perception [5][6][11]. This scale categorizes colors based on their emotional and psychological associations, providing researchers with a structured tool to explore how colors are perceived universally and across different cultures.

Empirical studies utilizing the CIS have contributed to a deeper understanding of color preferences, emotional responses, and cultural variations in color meanings [5][6]. Researchers have employed this scale to examine how colors evoke specific emotions [9][10] and to uncover cultural differences in color symbolism [12]. Moreover, the CIS is applied in various fields, including marketing and design, as a valuable tool for designers, marketers, and psychologists to navigate the intricate interplay between color, culture, and human perception to inform color choices in branding [13] and cross-cultural communication [8].

Research Rationale. Color perception is a multifaceted process influenced by various factors, including context, culture, and demographics of the audience; these factors significantly influence color perception and emotional connotations [10][14][15]. Additionally, colors are dynamic and can change in meaning over time, often influenced by historical, cultural, and societal factors [4][7][14][16][17]. Adding to the complexities, language and cultural context also influence how colors are described and associated with specific wavelengths [18]. This language-based variation underscores the need for culturally sensitive color palette creation, as color categories and distinctions vary across cultural demographics [18][19]. This diverse language interpretation impacts memory, learning, and color contrast perception [17][20]. Designers working with color should account for these complexities when selecting palettes for diverse audiences, necessitating a deeper understanding of color perception within different cultures [10].

Project Objectives. This research project aims to test and subsequently adapt the CIS framework to the context of Western design culture in a multiphase approach. This paper covers phase one of the objectives. The overarching objectives of this study are as follows: (a.) *Phase One: Data Collection and Analysis of the CIS*. In the first phase, the research team surveyed Western designers from various design-related fields and non-designers. The survey collected word associations and emotional connotations related to color palettes based on the original CIS. This data compared the level of agreement to the initial CIS findings. (b.) *Phase Two: Machine Learning Modeling*. Subsequent phases will involve the development of machine learning models. These models will predict emotional responses to color palettes, bridging the gap between subjective color experiences and objective computational analysis. (c.) *CIS Refinement*: Throughout the research, the CIS will undergo continuous refinement to align with Westernized semantic color associations. This research aims to enhance our understanding of color perception within Western design contexts by pursuing these objectives. Additionally, it seeks to facilitate the development of tools that enable designers to create culturally resonant and emotionally impactful design solutions.

METHODOLOGY

The CIS framework is based on the Munsell framework of hue, tone, and chroma [2]. As demonstrated in Figure 1, the colors within the scale are divided into four chroma sets—vivid, bright, subdued, and dark. Each chroma category is filtered further between tone values ranging from vivid to dark grayish across the spectrum of hues, between Red (R) and Red Purple (RP). The CIS categorizes hue between extremes of soft and hard, clear and grayish, and warm and cool. These categories represent the tone of a particular hue.

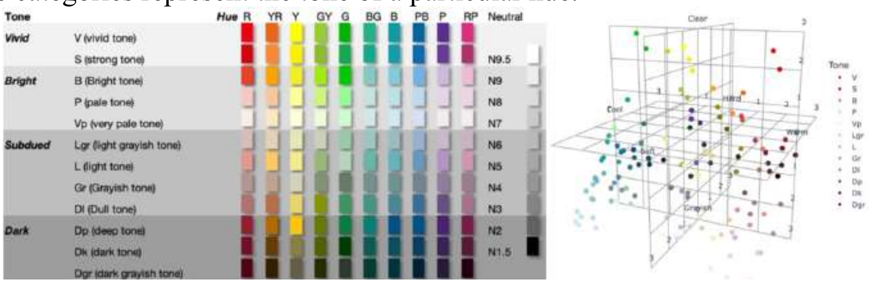

Figure 1 Hue and Tone matrix & The CIS in three dimensions

Note. The combined color distribution equates to 120 chromatic and ten achromatic hues. Each dot represents a color from the hue and tone matrix with the signifying label associated with the tone.

Data Collection and Survey Design. Initiation of phase one included an online survey, which was designed and administered through the online platform Qualtrics. The survey was designed to collect comprehensive data from North American participants, including designers from various design-related industries and non-designers (one-hue sample, n = 214; three-hue sample, n = 180). This diverse sample aims to capture multiple perspectives on color perception and emotional connotations in Western contexts.

The survey posed word association prompts related to various combinations of color palettes. Specifically, it explored 1,035 palette combinations within 16 categories, closely adhering to the structure outlined in the CIS [2]. Participants were encouraged to provide intuitive responses, revealing the emotional resonances and word associations evoked by these palettes. The online survey cycled through all 180 adjectives and 1,035 palette combinations systematically. This approach ensured a robust dataset for analysis. Importantly, participants were drawn from diverse demographics, including variations in age, gender, ethnicity, geographical location, income, and education level.

Analysis Techniques. The analysis of the collected data involved a range of statistical and computational techniques. Several statistical methods, including ANOVA, regional and sectoral analysis, regression analysis, and odds ratio, were employed to cross-reference and validate the original CIS in the context of Western design culture. Descriptive statistics were analyzed to verify the applicability of the CIS to Western design culture, exploring the relationships between color palettes and emotional associations. The comprehensive dataset enabled in-depth examination, providing insights into how CIS color palettes are perceived within the Western context.

Participant Selection and Data Collection. The survey intentionally targeted a broad range of participants to collect diverse data. Participation in the survey posed no adverse risks or benefits to the participants. It strictly focused on collecting data related to color perception and emotional connotations, with no data collection pertaining to identifiable personal information. The data collected through this survey forms the foundation for subsequent phases of the research, including the development of machine learning models to predict emotional responses to color palettes and further refinement of the CIS for Western culture.

RESULT AND DISCUSSION

The result and discussion section is divided into two main parts: one focusing on the outcomes of the research and the other delving into the implications and interpretations of these findings.

General Statistics. The analysis of the provided statistics offers insights into the extent of alignment between participants' color categorizations and the categorizations presented in the CIS. Notably, for single-hue categorizations, an average agreement of 54.6% was observed across all survey participants. This finding implies that, on average, participants' categorizations concurred with those enumerated in the CIS reference book 54.6% of the time. Conversely, the moderate agreement slightly diminished to 52.4% for three-hue categorizations. Participants' categorizations of three-hue combinations corresponded with the CIS book's categorizations at an average rate of 52.4%. These statistics collectively offer a panoramic view of the alignment degree between participants' color categorizations and those posited within the CIS reference book, encompassing both single-hue and three-hue categorizations. The closely aligned percentages indicate a consistent agreement pattern across both categorization types.

ANOVA (Likelihood-Ratio Tests). Supplementary to the statistical models, three distinct likelihood ratio tests were conducted to discern the potential significance of adjective category and tone as predictors of agreement. For the single-hue model, the comparison between the full model and the model excluding the adjective category yielded an ANOVA table demonstrating that the adjective category does not exhibit statistical significance (p-value >0.12) as a predictor of agreement with the CIS. This finding substantiates that participants' alignment with the CIS research remains independent of adjective usage. Concurrently, the agreement figures for single-hue categorizations reinforce that alignment, regardless of adjective use, does not manifest strongly, implying a nuanced relationship between participants' perceptions and original CIS categorizations.

Moreover, the ANOVA comparison between the full single-hue model and the model devoid of tone unveils tone as a statistically significant predictor (p-value < 0.001) of agreement with CIS for single-hue colors. This finding implies that participants displayed varying degrees of concordance with original CIS categorizations contingent upon specific tonal attributes. However, the level of agreement with tone hovered only slightly above 50%, indicating a marginal alignment beyond random chance. Similarly, the ANOVA analysis demonstrated analogous results in the context of three-hue categorizations. Specifically, the adjective category failed to emerge as a significant predictor of agreement (p-value 0.14), substantiating its limited role in determining participant alignment with CIS categorizations. Conversely, the exclusion of tone from the model significantly reduced agreement (p-value <0.001), underscoring tone's role in shaping participant perceptions of three-hue combinations. Once again, the degree of agreement remained modest, with participants exhibiting a marginal tendency to align with the original CIS tonal categorizations.

Regional and Sectorial Analyses. The study also explored regional and sector-specific variations in participants' categorizations and associations with color palettes. Spatial analyses indicated slight variations in alignment with the CIS across different regions in North America. For example, participants from the Midwest exhibited a slightly higher alignment percentage (57.2%) compared to the West (53.8%). These regional disparities suggest that cultural and environmental factors might influence color perception and associations within the Western context that are not entirely in line with the CIS demographic. However, further research is needed to delineate these differences more precisely.

Additionally, sectorial analyses revealed insights into the perceptions of color palettes among participants from various design-related industries. Participants associated specific color palettes differently based on their respective sectors. For instance, industrial designers exhibited a slightly higher alignment percentage (56.5%) with original CIS categorizations than graphic designers (53.7%). This discrepancy highlights the potential impact of professional backgrounds on color perception and associations. Designers from different sectors may prioritize specific attributes or emotional connotations in their work, thus shaping their color perceptions accordingly. However, the tested Westernized semantic association should correspond to the color palettes.

Discussion. This study's findings align with existing empirical research within the field of color perception [3][4], culture [8][16], and design [15][20], contributing to our understanding of the intricacies of color associations and their implications [10][14][16][17][18][19]. The findings in this study abstemiously align with assertions of color palette and semantic association based on the original CIS. Firstly, the study's observation of moderate alignment between participants' categorizations and the CIS resonates with prior research that has delved into the multifaceted nature of color perception and meanings [21][22][24]. Moderate agreement means that the findings have some alignment, establishing semantic and color differentiation that needs further exploration within this specific demographic. These findings underscore the notion that color interpretations can vary based on cultural, psychological, and contextual factors, thus emphasizing the necessity for a more nuanced approach to color categorization tailored to Western design culture. Furthermore, identifying tone as a predictor of alignment with CIS findings aligns with previous research highlighting the critical role of various color dimensions, such as hue, saturation, and brightness [17]. This correspondence underscores the understanding that distinct tonal attributes can evoke diverse emotional responses and possibly influence color perceptions.

The exploration of regional and sector-specific variations in color perception and associations also corresponds with the broader literature on cultural and contextual environmental factors can impact color associations, rendering them contingent on specific contexts influences on color meanings [10][14][16][17][18][19][22][23][24]. Additionally, the identification of sector-specific differences in color perception aligns with research that has recognized the significance of professional backgrounds in shaping color preferences and interpretations [10][17][15][21].

Lastly, the emphasis on bridging the gap between the CIS's Japanese origins and its applicability in contemporary Western design contexts corresponds with the broader goal of cross-cultural research in color psychology. Previous studies have underscored the significance of considering cultural and regional nuances in color perception to create culturally sensitive design solutions [19]. This first phase of research findings aligns with and contributes to the existing body of empirical research by highlighting the need for customization and refinement of color categorization frameworks within Western design contexts. The emphasis on tone, regional variations, sector-specific differences, and a holistic approach corresponds with existing research trends in color perception, culture, and design [22][24][26].

The plan for future investigations, including the integration of machine learning models and a focus on individual demographic factors for the analysis and prediction of color preferences and emotional responses, reflects a holistic approach to understanding color perception and aligns with the current trajectory of color psychology research [26]. This approach resonates with existing research trends that underscore the importance of considering individual differences, such as age, gender, ethnicity, and education, in color perception [7][10].

CONCLUSION

This research shed light on the intricate interplay between color perception, culture, and design within the Western context. The analysis revealed that myriad factors, including regional disparities, professional backgrounds, and the nuanced dimensions of color, such as tone and adjective categories, could influence color meanings and associations. The alignment between participants' categorizations and the original CIS is moderate, suggesting that customization, optimization, and refinement of the CIS for Western design culture are necessary. Adjective categories were identified as having limited significance in predicting alignment, whereas tone emerged as a more influential factor in shaping color perceptions.

Regional analyses indicated that environmental and cultural factors may play a role in color associations, with slight variations in alignment observed across different regions in North America. Similarly, sector-specific analyses revealed that professional backgrounds, such as industrial design versus graphic design, may impact color perception and associations. These findings underscore the complexity of color associations within Western culture and emphasize the importance of tailored approaches to color palette optimization in different design domains.
The implications of this research extend to design practice, offering designers a valuable tool to optimize color palettes for Westernized target audiences. By considering regional and sector-specific variations in color associations, designers can create culturally resonant and emotionally engaging design solutions.

In summary, this research represents a crucial step in bridging the gap between the CIS's Japanese origins and its applicability in contemporary Western design contexts. It underscores the significance of considering cultural and regional nuances in color perception and offers a pathway to more effective and culturally sensitive color palette optimization in design practice. The integrative approach that combines AI technology and focus group methodologies in future phases aims to create color palettes that resonate deeply with Western cultural perceptions and preferences, advancing the field of color design in a culturally sensitive manner.

REFERENCES

1. Cooksey, C. (2013). Tyrian Purple: The First Four Thousand Years. Science Progress, 96(2), 171–186. https://doi.org/10.3184/003685013x13680345111425
2. Kobayashi, S. (1989). Color image scale. Kodansha International.
3. Grieve, K. W. (1991). Traditional beliefs and colour perception. Perceptual and Motor

4. Gage, J. (2012). *Colour and culture: Practice and meaning from antiquity to abstraction*. Thames and Hudson.
5. Ou, L.-C., Luo, M. R., Woodcock, A., & Wright, A. (2004a). A study of colour emotion and colour preference. part I: Colour emotions for single colours. *Color Research & Application*, *29*(3), 232–240. https://doi.org/10.1002/col.20010
6. Ou, L.-C., Luo, M. R., Woodcock, A., & Wright, A. (2004b). A study of colour emotion and colour preference. part II: Colour emotions for two-colour combinations. *Color Research & Application*, *29*(4), 292–298. https://doi.org/10.1002/col.20024
7. Ou, L.-C., Luo, M. R., Woodcock, A., & Wright, A. (2004c). A study of colour emotion and colour preference. part III: Colour preference modeling. *Color Research & Application*, *29*(5), 381–389. https://doi.org/10.1002/col.20047
8. Kiyoki, Y., Sasaki, S., Trang, N. N., & Diep, N. T. N. (2012). Cross-cultural multimedia computing with impression-based semantic spaces. *Conceptual Modelling and Its Theoretical Foundations: Essays Dedicated to Bernhard Thalheim on the Occasion of His 60th Birthday*, 316-328.
9. Kang, D., Shim, H., & Yoon, K. (2018). A method for extracting emotion using colors comprise the painting image. *Multimedia tools and applications*, *77*, 4985-5002.
10. Valdez, P., & Mehrabian, A. (1994). Effects of color on emotions. Journal of Experimental Psychology: General, 123(4), 394-409.
11. Itten, J. (1973). The Art of Color: The Subjective Experience and Objective Rationale of Color. Wiley.
12. Yu, Hui-Chih. "A cross-cultural analysis of symbolic meanings of color." *Chang Gung Journal of Humanities and Social Sciences* 7.1 (2014): 49-74.
13. Horiguchi, S., & Iwamatsu, K. (2018). From Munsell color system to a new color psychology system. *Color Research & Application*, *43*(6), 827-839.
14. Hemphill, M. (1996). A note on adults' color–emotion associations. *The Journal of Genetic Psychology*, *157*(3), 275–280. https://doi.org/10.1080/00221325.1996.9914865
15. Labrecque, L. I., Patrick, V. M., & Milne, G. R. (2013). The marketers' prismatic palette: A review of color research and future directions. *Psychology & Marketing*, *30*(2), 187–202. https://doi.org/10.1002/mar.20597
16. Madden, T. J., Hewett, K., & Roth, M. S. (2000). Managing images in different cultures: A cross-national study of color meanings and preferences. *Journal of International Marketing*, *8*(4), 90–107. https://doi.org/10.1509/jimk.8.4.90.19795
17. Palmer, S. E., & Schloss, K. B. (2010). An ecological valence theory of human color preference. Proceedings of the National Academy of Sciences, 107(19), 8877-8882.
18. Kay, P., & Regier, T. (2006). Language, thought and color: recent developments. *Trends in cognitive sciences*, *10*(2), 51-54.
19. Bennett, M. J. (1998). Intercultural communication: A current perspective. *Basic concepts of intercultural communication: Selected readings*, *1*(1), 1-34.
20. Brainard, D. H., & Hurlbert, A. C. (2015). Colour vision: Understanding #thedress. Current Biology, 25(13), R551-R554.
21. Singh, N., & Srivastava, S. K. (2011). Impact of Colors on the Psychology of Marketing — A Comprehensive over View. *Management and Labour Studies*, *36*(2), 199–209. https://doi.org/10.1177/0258042X1103600206
22. Manav, B. (2007). Color-emotion associations and color preferences: A case study for residences. *Color Research & Application*, *32*(2), 144–150. https://doi.org/10.1002/col.20294
23. Plutchik, R. (2001). The Nature of Emotions: Human emotions have deep evolutionary roots, a fact that may explain their complexity and provide tools for clinical practice. *American Scientist*, *89*(4), 344–350. https://doi.org/https://www.jstor.org/stable/27857503
24. Tham, D. S., Sowden, P. T., Grandison, A., Franklin, A., Lee, A. K., Ng, M., Park, J., Pang, W., & Zhao, J. (2020). A systematic investigation of conceptual color associations. *Journal of Experimental Psychology: General*, *149*(7), 1311–1332. https://doi.org/10.1037/xge0000703
25. Tuan, Y.-F. (1995). *Passing strange and wonderful: Aesthetics, nature, and culture*. Kodansha International.
26. Jonauskaite, D., Wicker, J., Mohr, C., Dael, N., Havelka, J., Papadatou-Pastou, M., Zhang, M., & Oberfeld, D. (2019). A machine learning approach to quantify the specificity of colour–emotion associations and their cultural differences. *Royal Society Open Science*, *6*(9), 190741. https://doi.org/10.1098/rsos.190741

THE EFFECTS OF COLOUR IN HUMAN FABRIC PERCEPTIONS

Xu Han [1]*, Luwen Yu[2], Liting Li[1], Kaida Xiao[3], Ningtao Mao[3] and Guobin Xia[4]

[1] *Academy of Arts & Design, Tsinghua University, China.*
[2] *Computational Media and Arts, Hong Kong University of Science and Technology (GZ), China.*
[3]*School of Design, University of Leeds, Leeds, United Kingdom.*
[4] *School of Textiles and Design, Heriot-Watt University, United Kingdom.*

*Corresponding author: Xu Han, xu-han18@mails.tsinghua.edu.cn

ABSTRACT

The impact of colour on human perceptions of different fabrics is a topic of great interest to researchers, designers, manufacturers, and customers alike. To shed light on this important issue, this study investigated the relationship between coloured-fabric and human perceptions of different fabrics. A total of sixty coloured-fabric samples were carefully selected from twenty distinct colours and three materials, namely cotton, linen, and silk. An experiment was conducted using the psychophysical method, with eighty participants (forty males and forty females) evaluating sixty fabric samples in random order under simulated D65 illumination. Participants rated eight perceptions, including Temperature, Thickness, Gender, Activity, Pleasure, Arousal, Interest, and Preferences, using the 7-point-Likert scale method.

The coloured-fabric samples were plotted in the CIELAB space, and the results revealed that the human fabric perceptions were significantly affected by fabric colour across all three materials, albeit at varying levels. The degree of L* was found to have a significant impact on all eight human fabric perceptions, particularly Silk-Arousal, which had a correlation coefficient of 0.89. Both degrees of a* and b* also influenced some of the fabric perceptions, but the effect varied depending on the material type. For instance, the a* value exhibited a more pronounced effect in femininity of linen (0.50) as opposed to cotton (0.46), and in the realm of fabric pleasure, the b* value exhibited a more pronounced in cotton (0.55) compared to silk (0.47). Overall, this study highlights the complex interplay between fabric colour and human perception and underscores the importance of considering fabric colour in the design and manufacturing of textiles. The findings may have practical implications for designers, manufacturers, and retailers in terms of developing products that meet consumers' needs and preferences. This study may also serve as a foundation for future research on fabric perception, which could help to expand our understanding of the ways in which fabric colour affects human perception.

Keywords: Coloured Fabric, Visual Perception, Tactile Perception, Fashion Design.

INTRODUCTION

Fashion design entails a multifaceted process that seamlessly integrates various elements, including fabric material, texture, and colour, to craft garments that are both visually appealing and functionally effective. Designers carefully select materials that align with their artistic vision and intended message for the garment (Kawamura, 2005). This selection process considers attributes such as durability, drapability, texture, and suitability for the desired design. Fabric material significantly impacts the sensory experience of wearing a garment. Designers take into account factors like comfort, tactile sensations, and thermoregulation when making material choices. For example, cotton is favoured for its breathability and softness, while silk is known for its luxurious texture and visual sheen (Veblen, 2003). Linen offers a distinct tactile experience and relaxed aesthetic (Ryan, 2012). The chosen material can greatly enhance or inhibit the overall sensory and functional aspects of the garment. On the other hands, colour serves a pivotal role in fabric design, evoking emotions, conveying cultural symbolism, and influencing visual perceptions. Colour psychology contributes to the perception of clothing, as different colours evoke various emotional responses and messages. Warm colours like red may evoke excitement and passion, while cooler tones like blue might suggest calmness and professionalism (Ou & Luo, 2014). Designers skilfully leverage these psychological effects to elicit specific emotional reactions and elevate the visual impact of their designs. Moreover, sustainability considerations have spurred a shift in material selection. Designers now explore eco-friendly alternatives like organic cotton and recycled fabrics (Fletcher, 2012). These choices not only align with sensory preferences but also contribute to broader environmental and ethical concerns.

Currently, research investigating the combined effects of fabric material and colour on human sensory perception in clothing design is in its nascent stages. The fabric material chosen significantly influences the sensory encounter of wearing a garment, encompassing aspects of comfort, texture, and aesthetics. Additionally, the colour integrated into the fabric contributes to visual stimuli, potentially shaping human perception in diverse ways. Further exploration is required to comprehensively grasp the intricate interplay between fabric material, colour, and sensory perception in the realm of clothing design.

For this study, human perception scales have been used to investigate the effect of colour for fabric appearance. The research aims have been classified as 1) to explore whether colour will influence human perceptions in the same material; and 2) to explore how the relation between colour values influence the perceptions.

EXPERIMENTAL DESIGN AND METHOD

The main purpose is to explore the effect of colour in human fabric perception in fashion design. Thus, twenty target colours were selected from popular colours for spring/summer clothing in 2022 (colour name and information please see TABLE I); and three different martials were selected to determine human fabric proception.

Table 1: Colour information.

Colour	L*	a*	b*	C*	h	ΔE
Dark red	25.84	32.57	17.82	37.30	28.28	5.02
Red	36.61	55.75	22.74	60.21	22.20	2.72
Light red	68.15	17.62	3.78	18.03	12.26	2.87
White	80.85	0.32	0.34	0.55	46.49	2.60
Beige	77.00	1.24	7.39	7.50	80.35	3.19
Black	10.90	0.04	-0.92	1.39	277.69	2.68
Light gray	71.63	0.22	-0.44	0.58	248.29	3.50
Light blue	70.16	-3.86	-7.76	8.70	244.67	3.52
Blue	39.91	-4.38	-16.61	17.32	255.21	3.23
Dark blue	19.56	1.09	-10.49	10.54	275.92	1.27
Green	68.87	-12.00	30.99	33.24	111.12	3.75
Dark green	39.12	-40.87	21.91	46.38	151.81	3.69
Cyan	76.92	-7.15	-0.16	7.17	181.19	1.63
Light purple	70.32	6.42	-6.44	9.11	314.92	3.13
Purple	59.86	13.99	-12.56	18.85	318.52	3.91
Brown	47.21	9.66	16.85	19.44	60.31	2.67
Light brown	68.20	6.00	14.30	15.53	67.51	2.25
Light yellow	75.90	-5.60	33.49	33.96	99.60	7.97
Yellow	68.58	8.42	55.91	56.60	81.62	4.98
Orange	64.93	21.71	32.00	38.68	55.94	4.88

In this study, 60 coloured fabric samples were selected. Each of the samples was defined as CIE L*a*b* and CIE L*C*h values which were measured using a VeriVide DigiEye System in the D65 lighting condition (Li and Zhu, 2012). TABLE III reports the actual measured colours from all samples, and also show the average *⊿*E between same colour with different materials.

Furthermore, variability in colour appearance in likely to be significantly smaller than variability in colorimetric measurements. This visual-matching process introduced a small amount of error; however, observers would recognise the fabric samples as being categorically either red, yellow, or green etc. (Yu et al., 2023).

In this study, one psychophysical experiment was conducted to investigate the human perceptions for single coloured-fabric. Eight bipolar perception scales were used in this experiment: warm-cool, thick-thin, masculine-feminine, calm-active, displeasure-pleasure, tense-relax, boring-funny and dislike-like (Ou et al., 2004). The experiment was situated in the dark psychology experiment room. Each participant assessed sixty 20*20 cm coloured-fabric samples one by one with a random order in a uniform grey with L*of 50 was used as the background inside the cabinet, with a 60 cm distance from participants' eyes to the samples. In the experiment, participants were asked to see and touch the coloured fabric samples for 30 seconds, then evaluated the eight perception scales (in a random order) in 7-point Likert scale as a question "Which word is more closely associated with the coloured fabric presented—warm or cool?"

In this study, a total of 80 participants were recruited to take part (comprising of 40 males and females, between the age 18-35 years old), all participants were students or staff at the University. All observers had colour science training before the experiment was conducted.

RESULTS

The comparative data is converted to interval-data *z* scores (Yu et al., 2023). The findings elucidate a uniform perceptual inclination among the participants towards the assorted materials under investigation. Noteworthy is the robust resonance elicited by silk materials across all eight dimensions of perception. In stark contrast, linen materials exhibit a marked attenuation in perceptual responsiveness, particularly evident within the realms of thickness-thinness, warmth-coolness, and masculinity-femininity scales. Please see FIGURE 1.

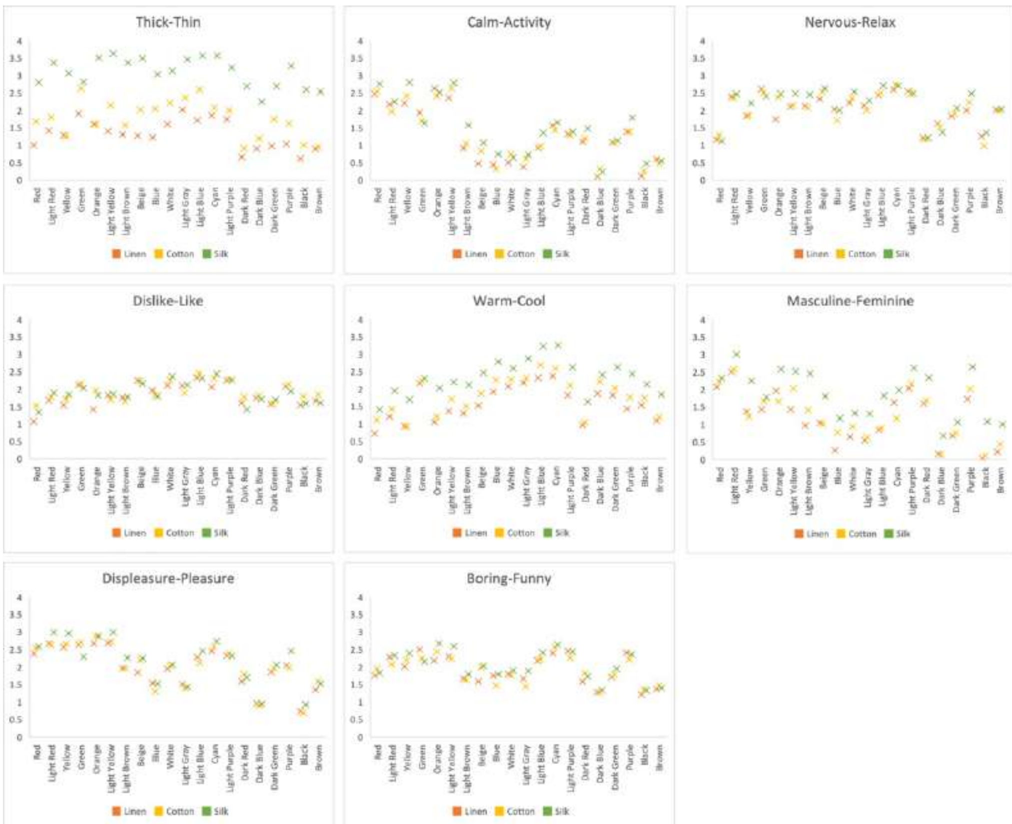

Figure 1. Example of figure

On the other hand, the outcomes of human perception regarding diverse fabric colours and materials are depicted in FIGURE 1. Notably, Orange, Green, and Light-Yellow exhibit heightened engagement, for example in calm-activity and boring-funny scales, while Light Red evokes a pronounced sense of femininity across all materials. In terms of fabric preference, Light Blue garners prominence in cotton and linen. Cyan manifests multifaceted attributes, for instance, it assumes a cooling disposition in linen and silk, and a demeanour of relaxation and levity in cotton applications.

Paired t-tests were executed to assess perceptual disparities across colours within cotton, linen, and silk. Among 24 tests, all materials exhibited notable variations in eight dimensions. Notably, thickness-thinness, warmth-coolness, and masculinity-femininity displayed substantial distinctions. Over 70% of comparisons indicated significant fabric perception differences across materials ($p < 0.05$). Noteworthy occurrences include 50% significant divergence between linen-cotton, 87.5% between linen-silk, and 87.5% between cotton-silk. Silk materials notably exhibited a comparable perception to both cotton and linen. The results also underscore the intriguing observation that silk materials displayed perceptual tendencies that were largely analogous to those of both cotton and linen. This brings attention to the complexity of fabric perception and its interplay with material attributes.

Table 2: Paired T-Test for eight motion scales in three materials for the same colour.

Motion Scales	Paired Samples Test	Sig. (2-tailed)
Thick-Thin	Linen - Cotton	**0.000***
	Linen - Silk	**0.000***
	Cotton - Silk	**0.000***
Calm-Activity	Linen - Cotton	0.263
	Linen - Silk	**0.000***
	Cotton - Silk	**0.000***
Nervous-Relax	Linen - Cotton	0.571
	Linen - Silk	**0.006***
	Cotton - Silk	**0.002***
Dislike-Like	Linen - Cotton	**0.026***
	Linen - Silk	0.122
	Cotton - Silk	0.359
Warm-Cool	Linen - Cotton	**0.000***
	Linen - Silk	**0.000***
	Cotton - Silk	**0.000***
Masculine-Feminine	Linen - Cotton	**0.048***
	Linen - Silk	**0.000***
	Cotton - Silk	**0.000***
Unpleasure-Pleasure	Linen - Cotton	0.154
	Linen - Silk	**0.001***
	Cotton - Silk	**0.024***
Boring-Funny	Linen - Cotton	0.686
	Linen - Silk	**0.003***
	Cotton - Silk	**0.002***

The fabric samples, differentiated by colour, were mapped within the CIELAB colour space. The resultant findings underscore the considerable influence of fabric colour on human perceptions across the spectrum of three distinct materials, albeit to varying extents. Notably, the L* component exerted a statistically significant impact on all eight facets of human fabric perception. Particularly noteworthy is the robust correlation coefficient of 0.89 observed between the L* value and Silk-Arousal perception. Both the a* and b* components also yielded discernible effects on select fabric perceptions, with the magnitude of influence contingent upon the specific material under scrutiny. For instance, the a* value exhibited a more pronounced effect in femininity of linen (correlation coefficient of 0.50) as opposed to cotton (correlation coefficient of 0.46). Likewise, in the realm of fabric pleasure, the b* value exhibited a more pronounced in cotton (correlation coefficient of 0.55) compared to silk (correlation coefficient of 0.47). This multifaceted relationship between fabric attributes and human perception highlights the intricate interplay of colour, material, and perceptual responses.

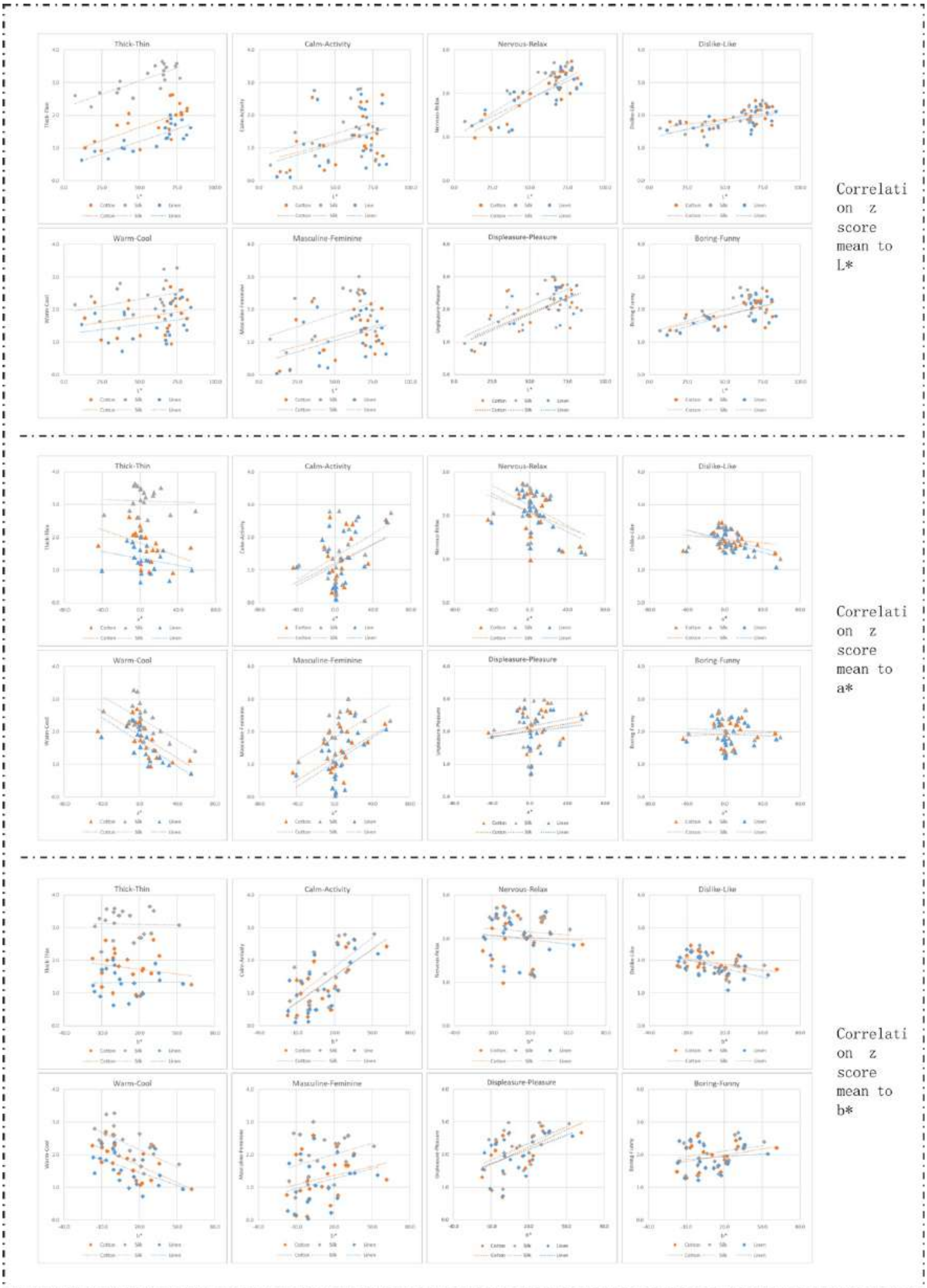

Figure 2. The correlation between motion scales in CIELAB space.

CONCLUSION

Overall, this study highlights the complex interplay between fabric colour and human perception and underscores the importance of considering fabric colour in the design and manufacturing of textiles. The findings may have practical implications for designers, manufacturers, and retailers in terms of developing products that meet consumers' needs and preferences. In the future work, this study may also serve as a foundation for future research on fabric perception, which could help to expand our understanding of the ways in which fabric colour affects human perception.

REFERENCES

1. Eiseman, L. (2000). *The Pantone guide to communicating with color*. Grafix Press.
2. Fletcher, K. (2012). *Sustainable fashion and textiles: Design journeys*. Routledge.
3. Kawakubo, R. (2016). Rei Kawakubo/Comme des Garçons: Art of the In-Between. *The Metropolitan Museum of Art*.
4. Kawamura, Y. (2005). *Fashion-ology: An introduction to fashion studies*. Berg.
5. Li, Q. Z., & Zhu, C. Y. (2012). Comparison of color measuring methods for yarn dyed woven fabrics. *Advanced Materials Research*, *441*, 651-655.
6. McQuiston, L., & Rissanen, T. (2018). *Zero waste fashion design.* Bloomsbury Publishing.
7. Montgomery, F. (2010). *Introduction to fashion design*. John Wiley & Sons.
8. Ou, L. C., & Luo, M. R. (2014). A practical approach to color emotion prediction: A study on how emotions are evoked by individual colors and color pairs. *Color Research & Application*, 39(3), 283-291.
9. Ou, L. C., Luo, M. R., Woodcock, A., & Wright, A. (2004). A study of colour emotion and colour preference. Part I: Colour emotions for single colours. *Color Research & Application*, *29*(3), 232-240.
10. Ryan, J. M. (2012). *Linen: From flax seed to woven cloth*. University of Virginia Press.
11. Veblen, T. (2003). *The theory of the leisure class*. Dover Publications.
12. Yu, L., Yun, C., Xia, G., Westland, S., Li, Z., & Cheung, V. (2023). Analysis of research strategies to determine individual color preference: N-alternative forced choice, rank-order, rating and paired comparison. *Color Research & Application*, *48*(2), 222-229.

Rosé de Provence colour choice in young adults

Valérie Bonnardel[1,4]* N. Pouzalgues[1,2], A. Chevallier[2], T. Lorey[1,3] and G. Masson[1,2]

[1]*Chair Vin Rosé Provence, CIVP&KEDGE BS, France.*
[2]*Centre de Recherche et d'Expérimentation sur le vin Rosé, France.*
[3]*School of Business, Kedge Business School, France*
[4]*Department of Psychology, University of Winchester, United Kingdom*

*Corresponding author: Valérie Bonnardel, colorlabvinrose@gmail.com

ABSTRACT

Rosé wines offer a large colour gamut in comparison to White and Red wines and their subtle colour plays a central role in wine quality and typicality assessments in consumers and experts. Using colour samples from the NCS colour ordered system, Rosé Wine colour representations were investigated in young adults relatively inexperienced regarding wine-testing. In a colour choice task, participants were requested to select the best exemplar and then their ideal colour for a Rosé Wine and for a Rosé de Provence. Individual differences related to Wine -knowledge, -appreciation and -consumption are the main factors to produces significant differences in colour choice between "knowledgeable" and "less knowledgeable" novices. "Knowledgeable" novices choose redder with less chroma while "less knowledgeable" novices prefer yellower with greater chroma for their Ideal colours. Pairwise comparisons further refine the origin of these differences in function of Gender and the Type of wine. Taken together, results suggest that cognitive factors including learnt multi-sensory associations appear to be a driver in novices' wine colour representations and preference.

Keywords: Rosé wine, Colour Cognition, Natural Colour System, CIE L* a* b*.

INTRODUCTION

Rosé wine distinctive colour diversity results from complex interactions between man-made factors, namely wine-making processes (e.g., maceration) and natural factors such as grape variety, grape maturity, and terroir [1]. It is well established that colour is critical in sensory expectations that originates from prior associations between colour, flavour and taste for the experienced taster. Artificially modifying the colour of a white Wine to resemble a Rosé Wine influences chemosensory properties in both experts and to a lesser extent in novices [2]. In Provence area, it has been further documented among wine professionals, that colour plays an important role in confirming typicality judgment previously assessed from non-visual cues of aromas and flavors [3]. Considering the central role of colour in Rosé Wine making and assessment, the question then arises on its influence in novices who have a less extended experience of learnt multi-sensory associations. Since colour has immediate cognitive and emotional meanings, it should nevertheless prompt expectations based on memory novices may have acquired on wine. In the present study we address the role of colour in wine category specificity by asking young novices to indicate the colour representing the best exemplar of a Rosé Wine in general and that of a Rosé de Provence. Participants were further asked to indicate their Ideal colour for the two wines categories.

Endorsing recommendations of the use of standardized colour chart and observation conditions, we used samples from the Natural Colour System (NCS) presented under standard observation conditions [4]. The NCS samples specified in term of Hue, blackness and chromaticness were converted into CIEL*a*b*, 1976, (CIELAB). CIELAB colour space was adopted by the International Organisation of Vine and Wine (IOV, OIV-MA-AS2-11), as an analytical method to specify wine's lightness (L*), redness-greenness (a*) and yellowness-blueness (b*). Besides facilitating the desirable experimental replicability, the use of a standard colour ordered system, will allows us to specify colour's choice in terms of its perceptual attributes of hue and chroma.

METHODOLOGY

Participants : Sixty-four students (33 F, 31M, Mean = 20.6 years, SD=1.2) studying at Kedge Business School participated to the experiment. The majority were bachelor students in Wine and Tourism programme living in Bordeaux area in France. Their mean self-assessed knowledge in wine from 1 (very bad) to 5 (very good) is Mean = 2.55, SD =.87. The mean Wine appraisal from 1 (not at all) to 5 (very much) is Mean = 3.63, SD = .125 for Red, Mean = 3.97, SD = 1.54 for White and Mean=3.36, 1.03 for Rosé wine. Differences between wine types are not significant. The mean Wine consumption frequency on a scale from 0 (never) to 5 (everyday) is Mean = 2.83, SD = .94 and that of Rosé Wine from 0 (never) to 6 (at least once a week) is Mean = 3.11, SD = 1.4.

Material : Eighty-eight NCS samples were carefully selected by a panel of Rosé Wine experts from the Rosé Wine Experimentation and Research Centre. The selected samples included colours that were considered outside the realistic Rosé Wine colour gamut. The 88 samples were organised in an array across Hue (horizontal axis) versus chromaticness (c) / blackness (s) (vertical axis) displayed in VeriVide light booth CAC-120 under a D65 illuminant with an average intensity of 1500 lux.

Procedure : After filling the online demographic questionnaire, and prior to the colour choice task, participants were asked if they made a distinction between Rosé Wine in general and Rosé de Provence. Thirty-three participants reported that they did ('Yes-group') while 31 did not ('No-group'). Participants were then invited to select the best exemplar (or Prototypical) colour and then their Ideal colour for each wine category even if they did not discriminate between them. There was no time constraint and Participants could change their choice until entirely satisfied. The study was approved by the Kedge BS ethic board.

RESULT AND DISCUSSION

1- NCS colour sample selection

Out of the 88 NCS colour samples, 62 were chosen across the four categories, 24 were chosen only once and the most frequent sample (S 0530-Y90R) was selected 16 times. Using the NCS Explore application, the CIEL*a*b* d/8 (D65/10º) coordinates and the sRGB values were determined.

NCS chromaticities plotted in CIELAB are distributed within an ellipsoidal shape. The ellipsoidal spreading is more elongated for Rosé de Provence compared to Rosé Wine with a linear regression R^2 of .42 vs. .17 respectively, suggesting a typical colour direction (along Y60R/Y70R) in case of Rosé de Provence (Figure 1).

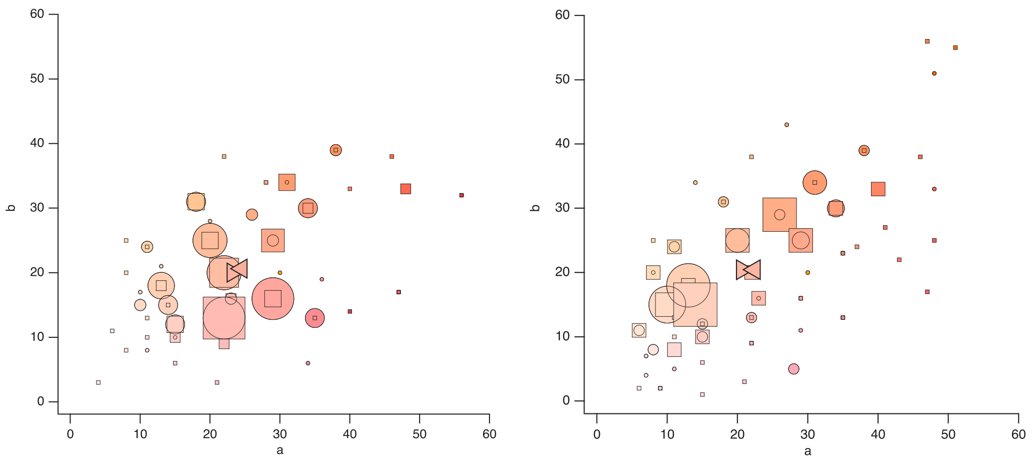

Figure 1: CIELab chromaticities of NCS selected samples

Prototypical (circles) and Ideal (squares) colours for Rosé (left) and Rosé de Provence (right) wines. Symbols' size are proportional to Ps number (N) who selected a given sample (N = 1 to 7). Triangles correspond to mean chromaticities for the Prototypical (right oriented apex) and Ideal (left oriented apex) colours.

Chroma value (Eq. 1) and hue angle (Eq. 2) for each sample were computed as follow:

$$C_{ab} = (a^2+b^2)^{1/2} \quad (1)$$

$$h_{ab} = tan^{-1}(b/a) \quad (2)$$

A hue angle of about 90º is yellow and that of about 25º is red.

Mean Rosé Wine chroma of Prototypical ($Mean_p$ = 31.48, SD = 9.98) and Ideal ($Mean_I$ = 32.82, SD = 12.58) colours are slightly higher compared to those of Rosé de Provence ($Mean_p$ = 29.77, SD = 13.47) and ($Mean_I$ = 31.12, SD =14.71). For the two wines categories, Prototypical colours chroma is slightly greater compared to that of Ideal colours, but differences are not significant. Mean Rosé Wine's hue of Prototypical colour ($Mean_p$ = 41º.51, SD = 12.47) is significantly redder compared to that of Rosé de Provence ($Mean_p$ = 44º.68, SD = 13.82), $t(63) = -1.88$, p =.032. Although, compared to Prototypical colour, Ideal Rosé de Provence colour is redder ($Mean_I$ = 42º.45, SD = 14.62) it fails to reach significance (p =.065). Overall, for both wine categories, Ideal colours are redder with a slightly lower chroma compared to their Prototypical colours.

2 – Difference in Chroma (ΔC) (Eq. 3) and hue (Δh) (Eq. 4) between Prototypical and Ideal colours

$$\Delta C = C_{ab,Ideal} - C_{ab,\,prototypical} = (a_{Ideal}^2+b_{Ideal}^2)^{1/2} - (a_{Prototypical}^2+b_{Prototypical}^2)^{1/2} \quad (3)$$

$$\Delta h = h_{ab,Ideal} - h_{ab,\,prototypical} = tan^{-1}(b_{Ideal}/a_{Ideal}) - tan^{-1}(b_{Prototypical}/a_{Prototypical}) \quad (4)$$

Potential differences within each group factors of 'Gender' and 'Wine Category Distinction' for the six demographic variables were checked. For factor 'Gender', there are significant differences in Red Wine -appraisal, with a higher score in Males ($Mean_M$ = 4, SD= 1.10) compared to Females ($Mean_F$ = 3,27, SD =1.3, $t(62) = 2.41$, $p_{2\text{-sided}}$= .019, Cohen's d = 1.21 and in Rosé-Wine consumption which is higher in Males ($Mean_M$ = 3.52, SD = 1.26) compared to Females ($Mean_F$ = 2.73, SD = 1.44), $t(62) = 2.32$, $p_{2\text{-sided}}$ =.023, Cohen's d = 1.36.

For factor 'Wine Category Distinction', as expected there is a significant difference in Participant's Wine-Knowledge self-evaluation, with a higher evaluation in Yes-group ($Mean_{Yes}$ = 2.88, SD = .69) compared to No-group ($Mean_{No}$= 2.19, SD=.91), $t(62) = 3.39$, $p<.001$, Cohen's $d = .82$. A greater evaluation in Yes-group is also observed for Red-Wine appraisal ($Mean_{Yes}$ = 3.97, SD =1.3 vs. $Mean_{No}$ = 3.26, SD=1.29), $t(62) = 2.35$, $p_{2\text{-}sided}$, =.022, Cohen $d = 1.21$ and for Wine Consumption ($Mean_{Yes}$ = 3.06, SD =.89 vs. $Mean_{No}$ = 2.58, SD =.92), $t(62) = 2.11$, $p_{2\text{-}sided}$ =.039, Cohen $d = .92$. These variables will be included as covariates to adjust for the mean of the independent variables of 'Gender' and 'Wine Category Distinction'.

A 2x2x2 mixed design ANCOVA with 'Wine Category' (Rosé, Rosé de Provence) as repeated measure and 'Gender' (Males, Females) and 'Wine Category Distinction' (Yes, No) as independent measures and 'Wine-Knowledge', 'Rosé Wine-consumption' and 'Red Wine-Appraisal' and 'Wine-Consumption' as extraneous variables were conducted to explore differences between Prototypical and Ideal colours in Chroma (ΔC) and hue (Δh). A positive ΔC indicates a higher Chroma for the Ideal colour while a positive Δh indicates a yellower and a negative value a redder hue of Ideal compared to Prototypical colour.

Chroma

There is a significant effect of 'Wine Category Distinction' factor. With a ΔC decrease in the Yes-group ($Mean_{Yes}$ = -1.65, SE = 1.7) vs. and increase in the No-group ($Mean_{No}$ = 4.44, SE = 1.75), $F_{1\text{-}60} = 5.72$, $p = .02$, $\eta_p^2 = .093$, suggesting that Participants who do not make distinction between Rosé and Rosé de Provence choose colours with higher chroma for their Ideal colour, while those who do, prefer colours with lower chroma.

To clarify the origin of significance, pairwise comparisons, with Bonferroni adjustment for multiple comparisons, were performed for the three 2-ways interactions and the one 3-ways interaction. 'Wine Category Distinction' difference is significant for Rosé Wine ($Mean_{Yes}$ = -2.07, SE = 2 vs. $Mean_{No}$ = 4.86, SE = 2.07), $F_{1\text{-}60} = 5.3$, $p = .025$, $\eta_p^2 = .086$, and further significant in Males ($Mean_{Yes}$ = -4.8, SE = 2.9 vs. $Mean_{No}$ = 4.47, SE =3.04), $F_{1\text{-}60} = 4.74$, $p = .034$, $\eta_p^2 = .078$, but not in Females. Hence significant difference between Yes- and No- groups is still reported within Rosé Wine, in Males, and those who distinguish Rosé de Provence from Rosé Wine tend to select colours with significantly less chroma for their Ideal Rosé Wine colour compared to Males who do not make this distinction. No other differences are significant. (Figure 2)

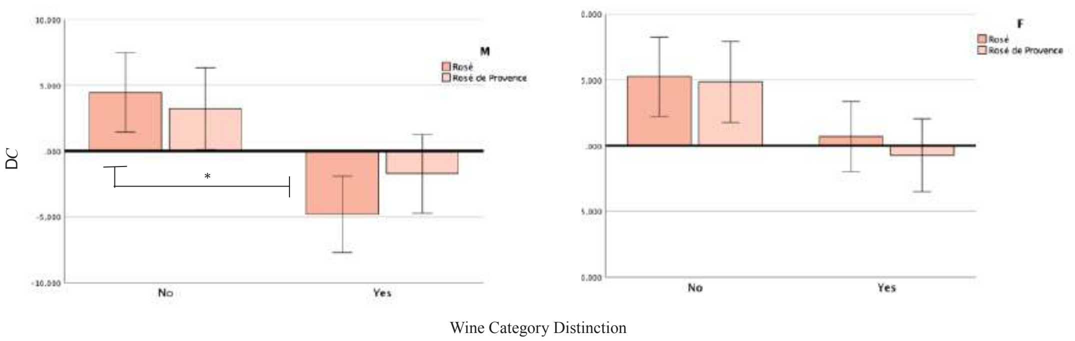

Figure 2: ΔC for Rosé and Rosé de Provence in function of 'Gender' and 'Wine Category Distinction'. Error bars correspond to 1 Standard Error.

*: significant pairwise comparison at $p < .05$. See text for other significant differences.

Hue

No main factor effect is significant but a 'Wine Category' * 'Wine Category Distinction' interaction is significant. In case of Rosé Wine, hue shift is positive/unchanged in Yes-group

(Mean$_{Yes}$ = .48, SE = 1.86) and negative in No-group (Mean$_{No}$ = -2.73, SE = 1.92), with the opposite for Rosé de Provence; hue shift is negative in Yes-group (Mean$_{Yes}$ = -4.21, SE =2.12) and positive/unchanged in No-group (Mean$_{No}$ = .02, SE =2.19), $F_{1\text{-}56} = 4.53$, $p = .038$, $\eta_p^2 = .075$. Participants in Yes- group choose redder colour for the Rosé de Provence Ideal colour, while a redder colour is selected by Participants in the No-group for Rosé Wine ideal colour.

The 'Wine Category' difference is still significant in the Yes-group where hue shift for Rosé Wine is positive/unchanged (Mean$_{Rosé}$ = .48, SE = 1.86), and negative for Rosé de Provence (Mean$_{RP}$ = -4.21, SE = 2.12), $F_{1\text{-}56} = 4.06$, $p = .049$, $\eta_p^2 = .068$.

Furthermore, a gender difference is significant in No-group. Males hue shift is positive (Mean$_{M}$ = 2.54, SE = 2.46) while negative in Females (Mean$_{F}$ = -5.06, SE = 2.43), $F_{1\text{-}56} = 4.3$, $p = .043$, $\eta_p^2 = .071$. This significant difference is still observed within Rosé de Provence with a positive Males hue shift (Mean$_{M}$ = 4.86, SE =3.22) vs. a negative Females hue shift (Mean$_{F}$ = -4.82, SE = 3.18), $F_{(1\text{-}60)} = 4.3$, $p = .043$, $\eta_p^2 = .071$.

Finally in Rosé de Provence, Males hue shift is negative in Yes-group (Mean$_{Yes}$ = -4.8, SE = 3.08) and positive in No- group (Mean$_{No}$ = 4.86, SE = 3.22), $F_{(1\text{-}56)} = 4.59$, $p = .037$, $\eta_p^2 = .076$ (Fig. 3).

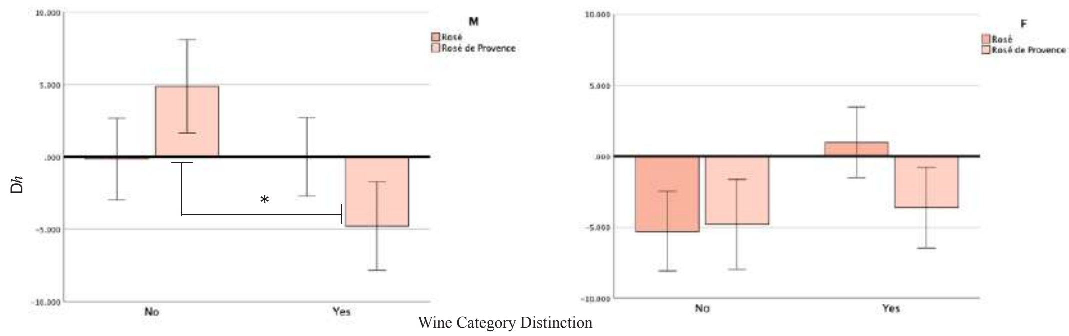

Figure 3: Δh for Rosé and Rosé de Provence in function of 'Gender' and 'Wine Category Distinction'. Error bars correspond to 1 Standard Error.

*: significant pairwise comparison at $p < .05$. See text for other significant differences.

.

CONCLUSION

Distinction between Rosé Wine and Rosé de Provence divided our participants in two groups who further differed on individual differences of self-assessed Wine Knowledge, Red Wine-appraisal and Red- and Rosé- frequency consumption. This group difference of "Knowledgeable novices" vs. "less Knowledgeable" novices happens to influence colour choice in both chroma and hue. For the two wine categories, "Knowledgeable" novices prefer colour with less chroma, while "less Knowledgeable" novices choose colours with higher chroma for their ideal colour. Divergence between the two groups regarding hue is wine category specific. Rosé Wine hue shift is minimal for "Knowledgeable" novices but both males and females select redder colour for their Ideal Rosé de Provence. For "less Knowledgeable" novices, disagreement exists between males and females for Rosé de Provence; females prefer a redder hue and males a yellower hue as their Ideal colour.

In this experiment using NCS samples under standard illuminant, it has been possible to reveal subtle but significant differences in hue and chroma in Prototypical and Ideal colour in function of wine category. Individual difference based on Wine -knowledge, -appreciation and -consumption appears to be a determinant factor in setting these mental representations and suggest that cognitive factors including knowledge and learnt multisensory associations drive Wine Prototypical and Ideal colour's representations.

ACKNOWLEDGEMENT

We wish to acknowledge La Caisse d'Epargne Côte d'Azur, La Région Sud-Provence Côte d'Azur, Le Département des Bouches du Rhône and Le Centre Interprofessionel des Vins de Provence as the *Chair Vin Rosé Provence's* sponsors.

REFERENCES

1. Masson, G. (2009). Singularité et diversité des vins Rosés. In *Le Vin Rosé*, Flanzy, C, Masson, G & Millo, F (Eds). Bordeaux, Ferret-Bordeaux. 95-97.
2. Wang, Q. J. & Spence, C. (2019). Drinking through rosé-coloured glasses: Influence of wine colour on the perception of aroma and flavour in wine experts and novices. *Food Research International*, 126 (08678), p. 1-11. doi: 10.1016/j.foodres.2019.108678.
3. Coulon-Leroy, C. Symoneaux, R & Pouzalgues, N. (2018). Is the typicality of "Provence Rosé wines" only a matter of color? *OENO One*, 52 (4), p. 1-15. doi.org/10.20870/oeno-one.2018.52.4.2125
4. Fairchild, M. D. (2021). Visual and photographic assessment of wine color. *Color Research and Application*, 48 (1), p. 21-31. doi.org/10.1002/col.22787

A STUDY ON THE RELATIONSHIP BETWEEN CLOTHING PREFERENCE AND COLOR COGNITION

Shuang He[1], Longxin Yue[2], Liting Li[1]*, Pei Sun[2]

(Academy of Arts & Design, Tsinghua University, Haidian District, Beijing P.R.C.100084)
[1] Department of Textile & Fashion Design, Academy of Arts & Design, Tsinghua University, China.
[2] Department of Psychology, School of Social Science, Tsinghua University, China.

*Corresponding author: Liting Li, liliting@mail.tsinghua.edu.cn

ABSTRACT

Color cognition and preference have always been the main fields in consumer psychology and become more prominent in the fast-moving consumer goods industry, such as clothing and apparel. This research investigated the relationship between color cognition and clothing preferences. Previous studies have largely relied on questionnaires, user interviews and other sociological methods. Participants are typically asked to observe color sample images and express their preferences for different colored clothing. However, the neural mechanism of clothing color preference has yet to be discovered. Color cognition can be explained from both neurological and social learning perspectives. Although social learning has been the major approach, neurological explanations may offer a more fundamental approach to exploring the causation and understanding the physiological basis of color psychology effects.

This study employs functional magnetic resonance imaging (fMRI) methods, a widely used technique to explore brain structure and functions. This research proposes two hypotheses: 1) there are significant differences in brain activity caused by color cognition between people majored in art and those not majored in art, and 2) differences in color cognition will correlate clothing preference behavior. An fMRI experiment was conducted on 20 college students at Tsinghua University, including 10 males and 10 females (20–30 years old, average = 27). Eight of the participants are major in art and design, while 12 have no training in art. Participants were asked to rate their preference for clothing items based on the color on a 5-level Likert scale, during which their brain activity was recorded by an MRI scanner.

The results reveal a strong relationship between color cognition and clothing preference, and a correlation between color preference and clothing color preference. Our findings suggest that there is a significant difference between experts' and novices' ratings of green color. Brain regions in the temporal lobe and visual cortex, which are associated with artistic experience and memory, are more activated in the expert group.

Keywords: Color preference, Color cognitive affect, Functional MRI, Clothing design

INTRODUCTION

From the early days of psychology, there has been extensive research on color cognition. Interpretations of the psychological effects of color include perspectives from both biological inheritance [2] and sociological learning [3-4]. Numerous color experiments have been conducted to explore differences in color cognition and preference across gender [2], age [7], ethnicity [8], and historical changes [9]. As a dominant element in fashion design [6], color, as one of the most intuitive design elements, influences both the style of clothing design and consumer preferences. The cumulative attitudes, consumption perspectives, and lifestyles manifested by individuals in the process of selecting, purchasing, and using clothing, which have evolved and diversified over the course of history, reflect the general psychology and lifestyle of a specific era [10].

Investigations of clothing color preferences have been carried out for a long time and many studies have presented different results of color preferences through questionnaires [21], color associations [5], and preference ranking [11]. With the improvement of experimental conditions and the help of modern cognitive psychology instruments, deeper color experiment analyses now become available. Researchers such as Cao [12] and Jiang [13] in their research on Event-related potentials (ERPs) found that value, saturation, and hue of color can affect consumer perceptions and preferences for clothing, explaining the cognitive differences between color blocks and clothing colors. With the increasingly wide application of functional magnetic resonance imaging (fMRI) in consumer psychology and cognitive neuroscience, analyzing BOLD signals can reveal brain activity regions during task stimulation. Previous fMRI studies have shown that different aesthetic experiences can activate the medial orbitofrontal cortex (mOFC), while stronger aesthetic experiences could lead to more intense activity in this region, which is related to purchase decisions and willingness to pay [14].

Does professional background influence aesthetic preferences? Bunzeck et al. selected musicians, music enthusiasts, and those without any musical background for an EEG experiment, asking them to listen to the same Beethoven piece. Results showed that the EEG amplitude of those having no musical understanding was the lowest, while that of professional musicians was the highest [15]. In studies on the neural correlations of beauty, Zeki et al. addressed this point and suggested that the region of medial frontal activations related to aesthetic experiences be labeled 'Field A1' [17]. Field A1 encompasses the medial orbital frontal cortex (mOFC), medial prefrontal cortex (mPFC), ventromedial prefrontal cortex (vmPFC), and anterior cingulate cortex (aCC). Neuroscience research confirms that preferences in selection and reward receipt processes are associated with vmPFC [18].

Color, as a significant visual stimulus capable of eliciting direct aesthetic responses, leads individuals to form aesthetic experiences and preferences [16]. Investigating preferences for clothing colors offers a reflection on the zeitgeist of the current era and serves as a manifestation of an individual's aesthetic experiences, cultural background, and decision-making psychology. Accordingly, this study employs functional magnetic resonance imaging (fMRI) technology, with a focus on clothing color preferences, aiming to uncover the underlying color psychology phenomena and their influential factors. The experimental design adopts an expert-novice research paradigm, wherein participants are categorized into 'expert group with an art background' and 'novice group without an art background'. The Region of Interest analysis (ROI) is positioned in Field A1 as labeled by Zeki et al. We proposed H1: There are significant differences in color cognition between individuals from art and non-art majors; H2: Differences in color cognition will correlate clothing preference behavior.

METHODOLOGY

In this study, participants first finished a color preference rating for 15 clothing colors under the MRI environment. Then, they completed ratings for 15 blocks of the same colors within a laboratory module. Ratings were given on a scale from 1-5, with 1 corresponding to 'strongly dislike' and 5 to 'strongly like'.

The MRI experiments employed the Siemens MAGNETOM Prisma 3Tesla MRI for scanning. The laboratory ran at a constant temperature of 20°C. As shown in Figure 1, participants wore experimental garments and earplugs while lying in the MRI scanner. They viewed the experimental tasks on a display screen via a mirror mounted on the coil and gave responses using a right-hand keypress. Within the MRI lab, apart from the task display, no other light sources were present.

Figure 1: Participate in the MRI experiment. Source: Sinorad

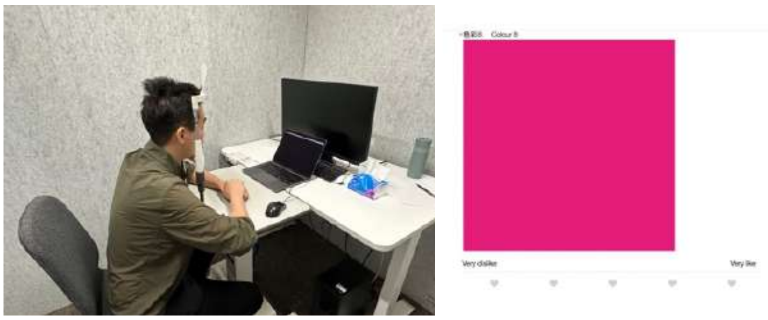

Figure 2: Participate in the questionnaire survey(left); an example of the questionnaire(right)

After completing the MRI experiment, participants were asked to fill out a 10-minute questionnaire, rating the same colors for preference. Questionnaire ratings were conducted in a laboratory module devoid of any light source. As shown in Figure 2, the questionnaire randomly presented the same color (500*500 pixel). Participants rated their color preferences using a 5-level Likert scale.

Participants

A total of 20 students from Tsinghua University participated in this experiment (ages 20-30, average age 27); comprising 10 females and 10 males. Of these, 8 (4 females, 4 males) were from the Academy of Arts & Design, constituting an expert group of art majors, while 12 (6 females, 6 males) were from non-art majors, constituting the novice group. All participants were right-handed, passed vision and color blindness checks (no color blindness or color weakness), and signed an informed consent. This study was approved by the Ethics Committee of the Department of Psychology at Tsinghua University.

Materials

Experimental stimuli included 15 clothing images of the same color values (1920x1080 px) and 15 colors (500x500 px) for questionnaire ratings. Colors were chosen based on the Adobe CIELAB system's 12-hue circle, selecting 12 chromatic colors and 3 achromatic colors (black, white, gray). Screen color temperature was measured using the Calibrite Color checker Plus, with color temperatures ranging between 5500-6500 k.

Figure 3. Experimental material

Table 1: The CIELAB value for the fifteen color samples.

Adobe CIELAB Colors	L*	a*	b*	R	G	B
Yellow	90	-13	85	236	232	24
Orange	62	42	69	229	114	0
Red	48	73	64	225	6	0
Rose red	51	74	2	227	28	121
Pink	55	80	-35	234	38	195
Violet	21	51	-67	68	0	53
Blue-violet	17	46	-77	16	6	159
Blue	52	3	-58	48	127	226
Blue-green	80	-38	-7	93	219	211
Green	76	-62	65	68	214	44
Medium green	71	-61	43	0	199	86
Yellow-green	91	-53	83	154	255	28
White	96	-1	-2	244	245	240
Grey	58	-1	-1	136	139	141
Black	8	-2	-7	16	24	32

Research Procedure

Based on the study by Samuel E. Rasche et al. [19], the procedure was programmed using the MATLAB Psychtoolbox software. Participants, while inside the MRI scanner, were allowed to see 15 images of clothing, and then were instructed to rate their preferences on a scale from 1 to 5. Two buttons were set for rating and each trial began with a neutral score of 3. The task adopted an event-related design: a cross-fixation point lasted for 1 second, stimulus presentation for 2 seconds, giving participants a 4.5-second window to respond (Figure 4). The experimental task comprised 4 rounds of randomized stimulus presentations, with each round containing 15 trials.

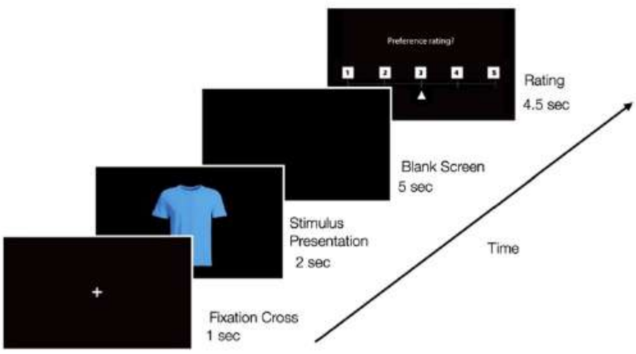

Figure 4. Experimental design

The scanning sequence for the task procedure included field mapping, T2*(run 1), T2*(run 2), T2*(run 3), T2*(run 4), as well as a T1 structural sequence. The total scanning time for each participant lasted 20 minutes. At the end of the scanning, participants would complete a 10-minute color preference questionnaire.

RESULTS AND DISCUSSION

Functional images were preprocessed using SPM12 (http://www.fil.ion.ucl.ac.uk/spm12/; RRID: SCR_007037). For each participant, the first five volumes of each functional run were discarded for signal equilibrium. The remaining images were corrected for slice timing and head motion and then spatially normalized to Montreal Neurological Institute (MNI) space via unified segmentation (resampling into 2 mm × 2 mm × 2 mm voxel size). Spatial smoothing was applied with a Gaussian kernel of 6 mm full width at half maximum (FWHM) for univariate analysis and 2 mm FWHM for RSA. Through the data analysis of T-test and Pearson correlation coefficient, the results show that there is a significant difference in color cognition and preference between experts and novices, and that color preference directly affects the choice of clothing colors.

Behavioral results: commonalities and differences coexist

In terms of behavioral outcomes, we first ranked the participants' preferences for color blocks in the questionnaire. It was observed that, both groups showed the highest preference scores for white and blue-green (as shown in Figure 5). This congruent choice makes us contemplate the effects of color association. As C.W. Valentin suggested, the reason why red and yellow often give an impression of warmth is due to their frequent association with the heat of the sun or fire [5]. The fact that this experiment was conducted during the summer months, as well as environmental factors such as the white environment and constant temperature of 20°C within the fMRI lab may have laterally influenced the participant's selection preferences, which led to a preference for the same colors by both novices and experts, and the influence of these factors was more direct than artistic experience.

Figure 5. Preference rankings for the novice and expert group

Table 2: The experimental score for the fifteen color samples.

Adobe CIELAB Colors	fMRI score	Novice group	Expert group	Sig.	questionnaire score	Novice group	Expert group
Yellow	2.92	2.88	2.97	0.859	3	2.75	3.38
Orange	3.23	2.99	3.59	0.182	2.85	2.67	3.13
Red	2.43	2.46	2.38	0.883	2.7	2.83	2.50
Rose red	2.67	2.42	3.09	0.274	3	2.92	3.13
Pink	2.32	1.99	2.81	0.076	2.6	2.42	2.88
Violet	2.39	2.43	2.31	0.805	3.05	2.83	3.38
Blue-violet	2.34	2.54	2.03	0.267	2.95	3.00	2.88
Blue	3.47	3.73	3.06	0.193	3.6	4.00	3.00
Blue-green	4.02	3.98	4.06	0.853	4	3.67	4.50

Green	2.58	2.94	2.03	0.038	3.1	3.58	2.38
Medium green	2.77	2.93	2.53	0.349	3	3.67	2.0
Yellow-green	3.17	3.01	3.41	0.451	3.35	3.08	3.75
White	4.27	4.38	4.09	0.507	4.3	4.17	4.5
Grey	3.31	3.10	3.63	0.245	3.4	3.25	3.63
Black	2.94	3.01	2.81	0.642	4.05	3.75	4.50

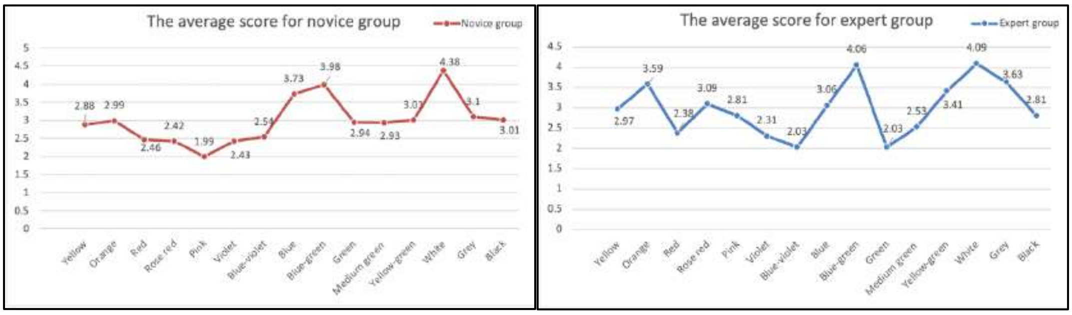

(a) **(b)**

Figure 6. The average scores for novice and expert group

Then, we employed a T-test to examine the significant differences in preference data. Table 2 displays the average preference scores for clothing colors in the fMRI behavioral task, scores from both the novice and expert groups, the significance level of their differences, and their corresponding scores for color blocks in the questionnaire.

From the color scores, it can be observed that novices favor white the most, followed by blue-green, blue, grey, yellow-green, and black, with pink receiving the lowest rating. On the other hand, experts prefer white the most, with blue-green, grey, orange, and yellow-green following accordingly and blue-violet and green having the least preference. Comparing the scores between the two groups, we noted that the difference in preference scores for the green color was the most significant (Sig.<0.05).

The verbal reports from the expert group indicated that they rated their preference for green lower because they believed that green had a higher degree of saturation and was not suitable for color matching, while the novice group was not affected by the green saturation. The difference in green preference reflects the difference in color perception between experts and novices. In the next step of fMRI data analysis, this paper will take GREEN color as an example to explore the brain activation level of novices and experts.

fMRI results: The influence of artistic experience

What drives the differential ratings between the two groups regarding green clothing? Figure 7(a) presents the images of the stimulus displayed, while 7(b) and 7(c) depict brain activity of novice and expert participants respectively at the time of clothing stimulus.

Based on the above, this study analyzes the brain activation imaging of 8 novices (after excluding data from 4 in the novice group with less prominent activation) and 8 experts. Results illustrate that brain activations in the novice group predominantly take place in the occipital lobe's visual cortex, suggesting their primary reliance on visual recognition to determine their color preferences.

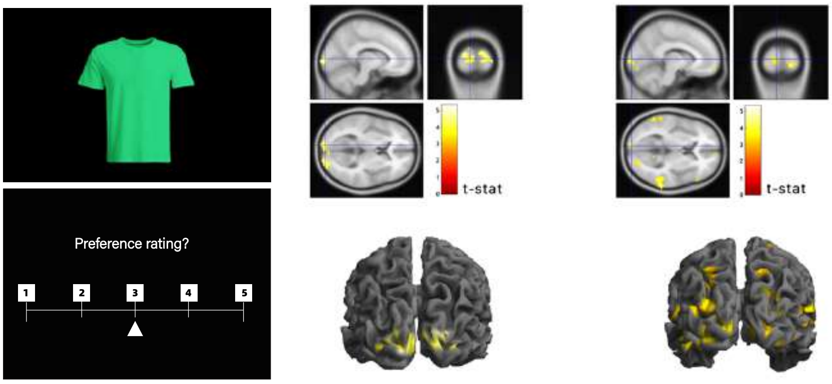

(a) (b) (c)

Figure 7. Activated areas of the brain by green clothing

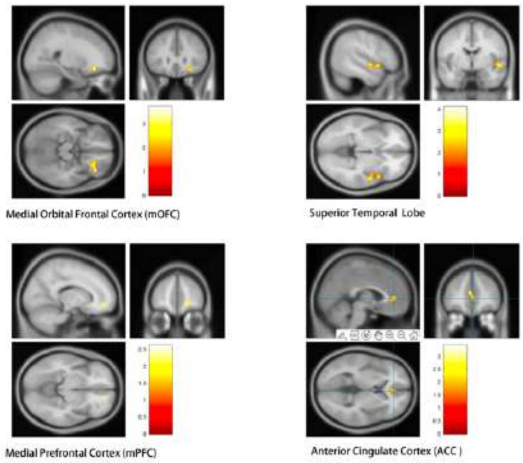

Figure 8. Significant differences in activated brain regions in expert group

As shown in Figure 8, there are significant differences in brain activation between the expert group and the novice group ($p<0.05$). The experts exhibited increased activations in the medial orbital frontal cortex (mOFC), medial prefrontal cortex (mPFC), and anterior cingulate cortex (aCC), aligning with the Field A1 as labeled by Zeki et al. [17]. Beyond the Field A1, we also observed that the expert group had additional activation in the superior temporal lobe. These results are visualized using xjView toolbox (https://www.alivelearn.net/xjview)。

Previous research has confirmed that the mOFC is associated with functions relating to emotions, motivations, learning, and behavioral decision-making. The mPFC is believed to have various social, emotional, and cognitive functionalities [18]. The superior temporal lobe relates to memory, comparison, and other higher neural activities. The ACC primarily involves emotion regulation and cognitive attention [20]. These results imply that when faced with color choices, experts tend to activate brain regions corresponding to behavioral decision-making, cognition, and memory to a greater extent.

CONCLUSION

This paper aims to explore the influence of color cognition on clothing preferences and the preferences between experts and novices. The research findings validate the hypotheses posited earlier in this paper. Drawing from behavioral experiments and fMRI results, several conclusions can be made:

We took the green color as an example and localized to the activated brain regions of the two groups of participants when they saw the green clothing stimulus. It was found that the novice group's brain regions were activated in the occipital visual cortex, suggesting that their color preferences are predominantly guided by visual recognition. The expert group activated the Field A1 as well as the superior temporal lobe, and the experts mobilized more behavioral decision-making, cognition, and memory when faced with color choices, which contributed to the difference in results between the two groups.

In terms of differences in preferences, long-term artistic experience affects the cognition of color and preferences. As a mass consumer product, preferences for clothing are similarly influenced. In terms of commonality of preferences, color preferences may be influenced by the surrounding environment, temperature, and seasonal factors at the time of the experiment, and the two groups of participants presented a portion of the same color choices (WHITE, BLUE-GREEN), which are more directly influenced by these factors than by artistic experience.

Due to the high cost of employing fMRI technology, this study did not include a large number of participants as samples. Besides, the participants are all students from Tsinghua University. This paper also did not discuss other factors that might influence color preference, such as regional differences, culture, and education levels. As a result, the findings might not apply to other specific groups, indicating a limitation of this research.

Overall, with the advancement of technology and art, using fMRI technology we can not only clearly see the results of color preference and related brain activities, but also verify that long-term art experience promotes color perception, resulting in a diversified trend of choice preference. This experiment is an attempt and exploration of color cognition and clothing color preference, relying on data indicators does not fully unveil the charm and complexity of color, the conclusions of this paper are for the data of this experiment, while color cognition and preference are dynamic and evolving, a comparative analysis of brain region activity for other colors is pending in this paper.

ACKNOWLEDGEMENT

This work was supported by Professor Liting Li and Associate Professor Pei Sun. Thanks to all the participants who helped to complete the experiments in this paper.

REFERENCES

1. Chen, L. (2018). *Research on Business Women's Clothing Color Based on Consumer Cognitive Psychology*.Master's thesis, Donghua University, Shanghai, China.
2. Tong, N., & Kuang, S.B. (2021). Sex differences in the visual system. *Advances in Biochemistry and Biophysics* (07), 779-787. doi:10.16476/j.pibb.2020.0398.
3. Stephen E. Palmer1 and Karen B. Schloss (2009), An ecological valence theory of human color preference, *PNAS*, 107(19): 8877–8882
4. Davis Jac T. M., Robertson Ellen, LewLevy Sheina, Neldner K., Kapitany Rohan, Nielsen Mark & Hines Melissa. (2021).Cultural Components of Sex Differences in Color Preference. *Child Development, 92*(4), 1574–1589. doi:10.1111/CDEV.13528.
5. C.W. Valentine. (1991). The experimental psychology of beauty. Beijing: Peking University Press.
6. Li, Liting & Julie, K. (2004). Design Starts with Color - Analysing and Comparing the Significance of Color in Clothing Design. *Proceedings of the First Asian Color Forum*.2004:157-162+256.
7. Gong, Shi-Min &Lee Wen-Yuan. (2017). Color preference model for elder and younger groups. *Journal of the International Color Association*. (2017): 18, 33-42.
8. Zhang, Zenghui & Lin, Zhongxian. (1993). A study of color preferences in 3-6 year old Zhuang and Mongolian children. *Psychological Development and Education*(03),23-26.

9. Wang, Yirong. (1997). An experimental study of color preferences among Chinese university students. *Psychological Science (06),* 559-560. doi:10.16719/j.cnki.1671-6981.1997.06.019.
10. Liu, Yuanfeng. (2009). Changes in the Consumer Culture of Beijing Clothing. *Textile Journal*,2009,30(03):94-98.
11. Tami L. Bergstrom. (1989) Clothing Color and Person Perception. (Master thesis). University of Wyoming, the United States.
12. Cao, Xiaoqing, Liu, Zunli & Lu, Cheng. (2019). A study on the effect of yellow brightness saturation on the sense of superiority of clothing. *Silk* (09),50-55.
13. Jiang, Hsiao-feng. (2011). The mechanism of clothing color brightness on human emotion (Doctoral dissertation), Soochow University, China.
14. Zeki, S., & Kawabata, H. (2004). Neural correlates of beauty. *Journal of Neurophysiology,* 91(4), 1699-1705.
15. Bunzeck, N., Wuestenberg, T., Lutz, K., Heinze, H. J., & Jancke, L. (2005). Scanning silence: mental imagery of complex sounds. Neuroimage, 26(4), 1119-1127.
16. Leder, H., Belke, B., Oeberst, A., & Augustin, D. (2004). A model of aesthetic appreciation and aesthetic judgments. *British Journal of Psychology*, 95(4), 489-508.
17. Ishizu, T., and Zeki, S. (2011). Toward a brain-based theory of beauty. PLoS One 6, e21852.
18. Matthew D. L., Mark A. Straccia, Meghan L. Meyer, Meng Du, & Kevin M. Tan. (2019). Social, self, (situational), and affective processes in medial prefrontal cortex (MPFC): Causal, multivariate, and reverse inference evidence. *Neuroscience and Biobehavioral Reviews,* (2019) 311–328. doi:10.1016/j.neubiorev.2018.12.021
19. Samuel E. Rasche, Ahmad Beyh, Marco Paolini & Semir Zeki. (2022). The neural determinants of abstract beauty. *bioRxiv*. doi: 10.1101/2022.07.13.499869. 2022.07.13.
20. Zhang, M., Wang, Y., Liu, H., Zhang, S. C. & Fish, B. W... (2006). Functional magnetic resonance imaging study of the anterior cingulate gyrus involved in nociceptive modulation. Chinese Medical Journal (30), 2127-2130.
21. Li, Liting (2007). Color in China - An analysis of the results of a survey on the color preferences of Chinese urban residents. China Fashion Color Association. (eds.) Contemporary Color Applications in Asia: Proceedings of the Fourth Asian Color Forum (pp. 66-70). China Textile Press.

EFFECTS OF THE COLORS OF SANITARY MASKS ON FACIAL ATTRACTIVENESS AND IMPRESSION

Masato Sakurai[1]* and Ena Takeda[1]

[1]*Department of Computer Science, Faculty of Informatics, Shizuoka Institute of Science and Technology, Japan.*

*Corresponding author: Masato Sakurai, sakurai.masato@sist.ac.jp

ABSTRACT

People usually use white sanitary masks before the outbreak of the novel coronavirus infection (COVID-19), but after the epidemic, sanitary masks in a variety of colors, including black, are now available. It has been reported that wearing a sanitary mask uniquely affected facial attractiveness because of occlusion and unhealthiness priming [1] and negative manifestations of black mask attitudes decreased after the COVID-19 epidemic [2]. Thus, it is important to investigate the effects of the color of sanitary masks on the attractiveness and impression in the present when people wear sanitary masks daily, from the viewpoints of impression formation and application to the design of masks. Therefore, to clarify the effects of the color of sanitary masks on facial attractiveness and its impression in this study, it is carried out a subjective evaluation experiment using images with different colors of sanitary masks. In the experiment, based on the colorimetry results of commercially available color masks, a total of 19 colors (9 highly saturated colors, 7 lower saturated and highly lighter colors, and 3 achromatic colors) were created as the stimulus. The face image without a mask was covered with the image of a white mask taken separately and filled in for each of those 19 colors. Six types of face images (three females and three males) were selected as the face images without masks. Therefore, a total of 120 stimuli were used, including 114 face images with masks and 6 without masks. Those stimuli were randomly presented by the display placed in front of the participants and they rated the attractiveness and impression of the presented stimuli. The attractiveness was rated on a scale of 1 to 10, with 1 being "not at all attractive" and 10 being "very attractive". Those impressions were evaluated using the bipolar 7-level SD method with 20 adjective pairs. Ten students (five females and five males) participated in this experiment. In the results, the attractiveness of the stimuli with color masks tended to be between 4 and 7, with slightly high ratings for the high-lightness colors compared to those without the mask. According to the results of one-way ANOVA, it is suggested that the colors of the masking affect facial attractiveness in this experiment. From the factor analysis based on the results of the SD method, it is obtained the three factors were affinity, uniqueness, and maturity. It is suggested that the impression of wearing a mask can be explained by these three factors.

Keywords: Colors, Sanitary mask, Facial attractiveness, Impression, SD method

INTRODUCTION

In Japan, people usually used white masks when they were sick, such as when they caught a cold. And, the white masks were very common before the outbreak of the novel coronavirus infection (COVID-19), but after the epidemic, sanitary masks in a variety of colors, including black, are now available. Wearing a mask is not only hygienic, but it is also considered to change the impression of the face because it hides part of the face. It has been reported that wearing a sanitary mask uniquely affected facial attractiveness because of occlusion and unhealthiness priming [1] and negative manifestations of black mask attitudes decreased after the COVID-19 epidemic [2]. Thus, it is important to investigate the effects of the color of sanitary masks on the attractiveness and impression in the present when people wear sanitary masks daily, from the viewpoints of impression formation and application to the design of masks. Therefore, the purpose of this study is to clarify the effects of the color of sanitary masks on facial attractiveness and its impression in this study. It is carried out a subjective evaluation experiment using images with different colors of sanitary masks.

METHODOLOGY

Stimuli

Based on the measurement results of commercially available color masks, nine highly saturated colors (No. 1: red, 2: blue, 3: pink, 4: yellowish green, 5: yellow, 6: purple, 7: orange, 8: emerald, 9: turquoise), seven highly light colors (No. 10: pale (p-) pink, 11: p-red, 12: p-green, 13: p-orange, 14: p-blue, 15: p-yellow, 16: p-pearl), and three achromatic colors (No. 17: gray, 18: black, 19: white) were used. Figure 1 shows the chromaticity of these colors. A face image without a mask (ATR Facial Expression Image Database DB99, ATR) was covered with a white mask image taken separately and image processed in each of 19 colors. Six types of face images (three female (F03, F10, F13) and three males (M01, M06, M09)) were selected as the face images without masks. Therefore, a total of 120 stimuli were used, consisting of 114 masked face images (19 colors and 6 face images) and 6 unmasked face images. Figure 2 shows examples of the stimuli in this experiment. The background was gray.

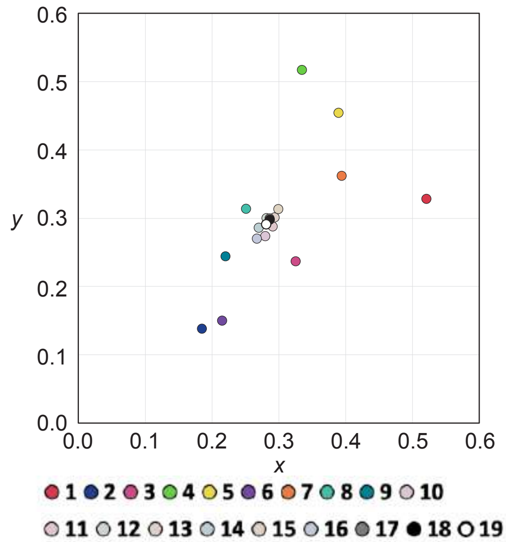

Figure 1. Chromaticity of Color Masks Used in This Experiment

Figure 2. Examples of the Stimuli of F10 (without mask, No.1, 11, 18, 19)

Procedure

After three minutes light adaption by the D_{65} fluorescent lamps in the experimental booth, the participants were asked to evaluate the attractiveness and impression in stimuli presented with the evaluation sheet. The attractiveness was rated on a scale of 1 to 10, with 1 being "not at all attractive" and 10 being "very attractive". Those impressions were evaluated using the bipolar 7-level SD method with 20 adjective pairs. Table 1 shows these adjective pairs of SD method in this experiment. For example, in this SD method, 7-level was follows; -3: extremely unfriendly, -2: very unfriendly, -1: unfriendly somewhat, 0: neither unfriendly nor friendly, 1: friendly somewhat, 2: very friendly, 3: extremely friendly. The stimuli were presented randomly. The participants performed the evaluation of one time for each stimulus with a break every 40 trails, and the total was 120 times evaluations. Prior to the experiment, the participants had an enough time to practice for the evaluation.

Table 1: Twenty Adjective Pairs in SD Method

20 adjective pairs (-) - (+)	
unfriendly - friendly	vulgar - elegant
strict - gentle	unhealthy - healthy
childish - adultlike	looks small - looks big
unattracitve - attractive	sober - flashy
unsexy - sexy	older - younger
unintelligent - intelligent	blurred - clear
dark - bright	static - dynamic
cold - warm	feminine - masculine
common - unique	unimpressive - impressive
unpreferable - preferable	heavy - light

Apparatus

The experimental booth was covered with a black curtain. It was illuminated by the D_{65} fluorescent lamps of the light booth and the illumination of screen in the display was around 200 lx. The display (Color Edge CS230, EIZO) was placed in front of the participant and the viewing distance was 600 mm. The participants were asked to press with the numerical keypad to present next stimulus when they finished evaluating each stimulus.

Participants

Ten students participated in this experiment. They were five females and five males. And they had the normal color vision.

RESULT AND DISCUSSION

Attractiveness

Figure 3 shows the average results of attractiveness evaluation for F10 in all the participants responses. In this figure, the horizontal axis indicates the stimulus number, the vertical axis is the subjective evaluation value of attractiveness evaluation, respectively. Each bar is painted with the color of each stimulus except for the unmasked (w/o mask) stimulus. Each error bar indicates the standard deviation between participants.

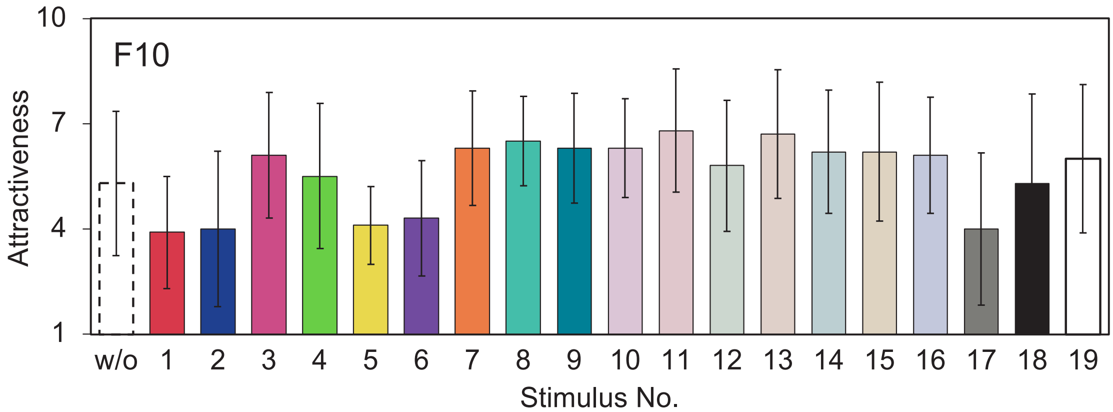

Figure 3. Average Results of Attractiveness Evaluation for F10

In this figure, the value of attractiveness of the stimuli with color masks tended to be between 4 and 7, with slightly high ratings for the high-lightness color masks compared to those without the mask. The high-lightness pale red (No.11) is most evaluated and high-saturated red (No.1) is worst one in image F10. The same trend is observed in other face images. The results of one-way analysis of variance, it is suggested that there is an effect of mask color with facial attractiveness in those results.

Impression with SD Method

Figure 4 shows the SD profile of typical results for F10 in all the participants responses. In this figure, the horizontal axis indicates the levels of SD method in each adjective pairs, the vertical axis is 20 adjective pairs with side by side, respectively. Each symbol corresponds with the stimulus number with the bottom of the figure.

The high-saturated red of No.1 is rated for unique, flashy, and dynamic impression, while the high-lightness pale red of No.11 is rated for friendly, brightness, and healthy impression. The black of No. 18 leaves a somewhat unhealthy impression, while the white of No.19 and without mask are obtained the same tendency in the impression. The same trend is observed in other female face images, but black is the same tendency with white and without mask in male face images. It is suggested that it corresponds with the previous study [2].

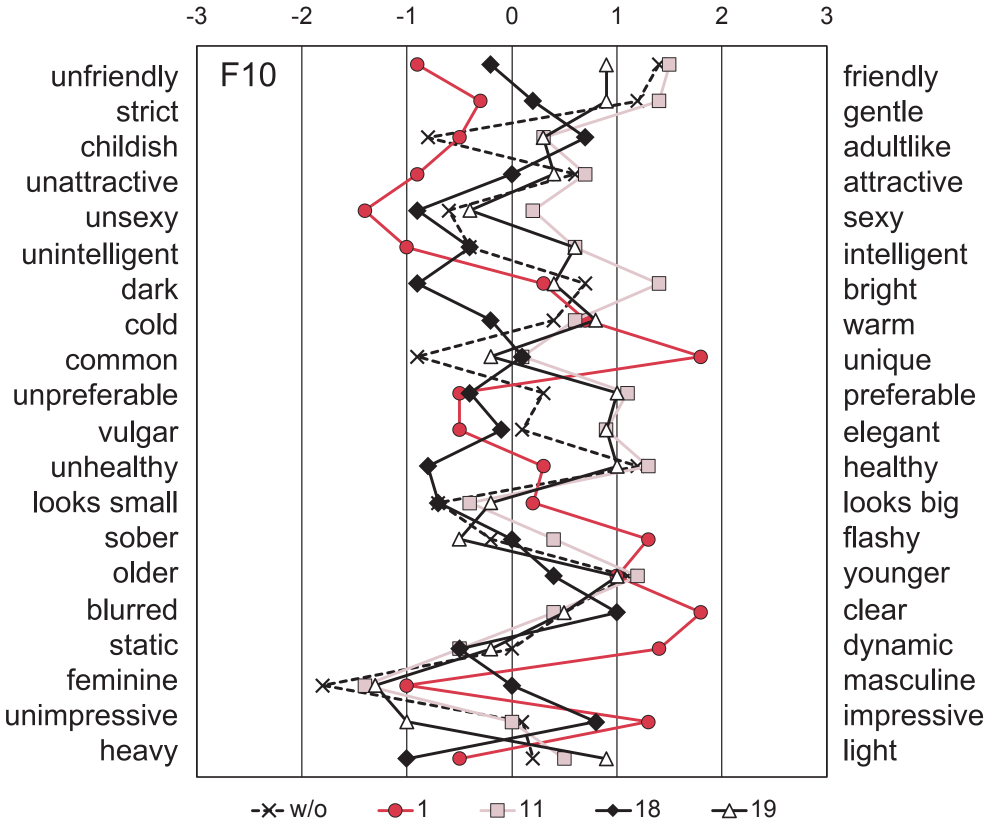

Figure 4. SD profile of typical results for F10

A factor analysis was performed using the results of all stimuli in the impression evaluation of the SD method. Table 2 shows the results of the factor loadings in the factor analysis. The row and column indicate 20 adjective pairs and values of each factor loadings. The cumulative contribution of the three factors was about 59%. As shown in table, under the first factor loadings, the values of "dark – bright", "cold - warm", "strict – gentle" are highly positive values. In the second factor loadings, the values of "common - unique", "unimpressive - impressive", "sober - flashy" are highly positive values. In the third factor loadings, the value of "childish - adultlike" "unintelligent - intelligent", "unsexy - sexy" is highly positive values. In this paper, the first, second, and third factors are called "affinity", "uniqueness", and "maturity", respectively. It is suggested that the impression of color masks in this experiment can explain by the degrees of affinity, uniqueness, and maturity.

Results of Factor Loadings Based on the Results of All the Stimuli in SD Method

20 adjective pairs	1st factor **affinity**	2nd factor **uniqueness**	3rd factor **maturity**
dark - bright	**.808**	.138	-.087
cold - warm	**.741**	.046	-.105
strict - gentle	**.700**	-.077	.031
unfriendly - friendly	**.677**	-.198	.262
unhealthy - healthy	**.670**	.122	.049
heavy - light	**.658**	-.099	-.110
unpreferable - preferable	**.535**	-.110	.439
older - younger	**.491**	.376	-.031
feminine - masculine	**-.322**	.033	.065
common - unique	-.145	**.874**	.146
unimpressive - impressive	-.163	**.866**	.065
sober - flashy	.078	**.848**	.020
blurred - clear	.044	**.721**	.061
static - dynamic	.376	**.424**	-.294
childish - adultlike	-.344	.090	**.873**
unintelligent - intelligent	-.142	-.042	**.790**
unsexy - sexy	.126	.186	**.670**
unattracitve - attractive	.392	.081	**.599**
vulgar - elegant	.199	-.164	**.581**
looks small - looks big	.036	-.108	**-.182**
proportion of var. (%)	30.2	20.7	7.9
cumulative proportion of var. (%)	30.2	50.9	58.8

CONCLUSION

To clarify the effects of the color of sanitary masks on facial attractiveness and its impression, it is carried out a subjective evaluation experiment using images with different colors of sanitary masks. In the results, the attractiveness of the stimuli with color masks tended to be between 4 and 7, with slightly high ratings for the high-lightness colors compared to those without the mask in this experiment. According to the results of one-way ANOVA, it is suggested that the colors of the masking affect facial attractiveness in this experiment. From the factor analysis based on the results of the SD method, it is obtained the three factors were affinity, uniqueness, and maturity. It is suggested that the impression of wearing a mask can be explained by these three factors.

REFERENCES

1. Miyazaki, Y., Kawahara, J. I. (2016). The sanitary-mask effect on perceived facial attractiveness. *Japanese Psychological Research*, 58, 261–272.
2. Kamatani, M., Ito, M., Miyazaki, Y. & Kawahara J. I. (2021). Effects of Masks Worn to Protect Against COVID-19 on the Perception of Facial Attractiveness. *i-Perception*, 12(3).

PREROGATIVES FOR TEACHING COLOR

Pedro Souza[1]*

(Unicamp – Brazil)
[1]Arts Institute, Unicamp, Brazil.

*Corresponding author: Pedro Souza, pedropinho88@gmail.com

ABSTRACT

Trying to propose new ways of teaching color, this text seeks to discuss important topics about the teaching method about color, focusing on practices and the use of usual references, exercises with new technologies and seeking to debate color with students, seeing it through the lens of current society. The importance of leaving the content (what is taught) in the background, to the detriment of how it is taught, to whom and where. Using references such as John Dewey, Yuk Hui and Paulo Freire, who corroborate with the ideas of a liberating, humanizing and fragmenting teaching, which places the student as the main part of the educational process, but in particular, of the world's experimentation processes, the text will ultimately seek to demonstrate the practices and exercises with color that emerged from this debate. The idea is to bring the individualities of each student into the teaching spotlight, the particularities of each one. The aim of this text is to remove the concepts of color from a pedestal of universal knowledge and start to observe the local, social, cultural and historical needs of each student and their relationship with color. We want to show exercises and experiences with color capable of instilling in students the desire to deal with and understand color. Classroom exercises, apparently normal, but which have a greater purpose than simply transmitting knowledge, the objective is to led to the creation and emergence of personal and private color systems and theories.

Keywords: Color, Education, Teaching, Location.

INTRODUCTION

Seeking to develop guidelines for teaching color, this text will address the author's main concerns regarding the constant focus on color content to the detriment of students' practices, experiments and experiences. The text is divided into four parts, focusing on showing the importance of establishing "*how*" to teach color, for "*whom*" and "*where*", and debating teaching alongside current practices, using new technologies and contemporary debates about color and teaching.

WHAT IS TAUGHT ABOUT COLOR?

In this text we will deal with education, specifically the teaching of color. And to achieve this, we will seek practices that are consistent with a plural, altruistic, secular and inclusive society. Firstly, however, it is necessary to point out that not all "education" is liberating, humanized and inclusive. There are rigid and conservative educational practices, which we reject as they do not provide the values listed above.

When thinking about teaching color, most teachers immediately experience certain difficulties regarding the depth of the topic. Low training in elementary education[1] regarding the use of colors causes a chain reaction culminating in low understanding and use of colors in

[1] Data extracted from Milena Quatter's thesis shows that only 35% of elementary school teachers had any contact with color theory in their respective degrees in arts or communication. [4]

academic teaching; In addition, the curricula of arts and communication courses do not seem to focus on this topic, its use and the perception of colors.

The subject of color is complex and can include areas such as physics, chemistry and biology, among others, often not present in the training of many teachers. Even so, there are guidelines regarding the main issues to be addressed on the topic. Milena Quatter (2019), in her doctoral thesis, provides rich material on what should be taught in an arts curriculum when it comes to teaching color. The Basic Parameters for Teaching Color (PBEC in portuguese) brought by the author are clear and follow an understandable logic of the main themes and sciences involved when dealing with the topic of color, enabling interdisciplinarity and transdisciplinarity for those who follow the booklet regarding what to teach.

Some concepts brought up by her are common to several other authors throughout history: (i) color, (ii) light, (iii) electromagnetic spectrum, (iv) visible spectrum, (v) photoreceptors, (vi) additive synthesis, (vii) primary colors, (viii) secondary colors, (ix) subtractive mixing, (x) color wheel, (xi) tertiary colors, (xii) hue, (xiii) luminosity, (xiv) clarity, (xv) monochromatic values, (xvi) achromatic values, (xvii) saturation, (xviii) analogous hues, (xix) complementary hues, (xx) simultaneous contrast, (xxi) color harmony, (xxii) warm colors and cold colors. [4]

Many may argue that this content is universal, and therefore fundamental in teaching color. For sure, all this content can be important in the development of students, but it is essential to understand that it is not the content about color that interests us, but rather how to use it, who uses it and where.

HOW DO WE TEACH ABOUT COLOR?

The main guidelines and concepts have already been postulated, and throughout history several discoveries regarding color have been listed, we already have some interesting bibliography about what should be taught as has been demonstrated. In order to seek some inclusive and altruistic way to teach color will use some authors who corroborate the ideas of a liberating, human and fragmented teaching, enabling and expanding students' creativity, and placing them as the main part of the learning process. But in particular, the processes of experiencing the world.

"It is not denied that any experienced object can become an object of reflection and cognitive inspection. But the emphasis is on "becoming"; the cognitive is never fully inclusive: that is, when the material of a previously non-cognitive experience is the object of knowledge, it and the act of knowing are included within a new and broader non-cognitive experience – and this situation can never be transcended. Only when the temporal character of things experienced is forgotten is the idea of the total "transcendence" of knowledge affirmed. [1]"

There will only be reflection if color becomes the object of investigation. But it is impossible to transcend the experience with it, that is, when we experience color within a certain context, we will immediately be giving way to other infinite possibilities of experimentation. Therefore, it is necessary to leave it in the hands of the students and trust them with knowledge through experience. In this way, we want the experience to lead the student to knowledge, for their personal and unique development. The "*how*", regarding teaching color, therefore, concerns experience, it is through experience that we want to teach color.

TO WHOM AND WHERE IS COLOR TAUGHT TO?

It's not just what to teach, nor how, but being aware of who and where we teach. Thinking about experience and nature as united, inseparable, brings perspectives on the teaching of color not as separate processes - the subject who learns and the object apprehended; student/observer x light/color/pigment - but rather, understanding the student, the organism that absorbs the color, both belonging to a place, loaded with its meanings, particularities and pluralities. Hence the need to act on the topic with students in a comprehensive manner, respecting the individualities and locations of each one. Each place will bring its demands, its culture, its limitations, its social issues and each individual will bring their ancestry, symbols, deficiencies and values. Color teaching must embrace all this subjects.

The teaching of color that we will seek to bring into our practices is liberating, therefore. This is characterized as Freirian in the sense of enabling educational practices that enable self-knowledge and liberation from social standards imposed by the capitalization of people, things and science. Therefore, we believe in the importance of questioning profitable color systems and the color industry with only ways to capitalize. This industry creates rigid requirements for the use of color, such as the standardization of colors in products, symbolic gender associations (pink for girls, blue for boys), the sale of color systems ready for quick consumption, among other practices that aim to profit as the sale of color. For Freire, “the ability to learn, not only to adapt, but, above all, to transform reality, to intervene in it, recreating it [2]” is eminent.

Among the possible practices to combat the capitalization of color, the teaching of individual practices and reflections on one's own reality can instill in the student self-knowledge and perception of their reality.

“Why not establish a necessary “intimacy” between the curricular knowledge that is fundamental to students and the social experience they have as individuals? Why not discuss the political and ideological implications of such neglect on the part of those in power for the poor areas of the city? [2]”

We do not intend, in this work, to belittle the teaching of color focused on practical content and the usual experiences with color, nor even to propose a unique and particular way of creating and teaching color. Yuk Hui has a concept that interests us, the “locality”. The author seeks the essence of the individual, who, loaded with his cultural and social baggage, produces art. Experiencing the work is experiencing who creates it, the inseparability of experience and nature is also present here. The experience with the work is inseparable from the experience with whoever produces it. In this way, gender, class, ancestry, culture and other aspects also make up this location of the artist that the Chinese author talks about. “The essence of art is its locality”[3]

For us, teachers, too, the essence of teaching needs to be the location of each student, the knowledge they are building needs to be linked to the knowledge that exists, there, in each one's location. There is no content more important than those necessary to the current experiences and practices of the students themselves. Their self-knowledge should be the focus of teaching color. Each student's contact with color is unique, and should not be measured by content considered universal, as the aim is to observe localities, particularities, personalities. There is no room for the universal in the locality.

PROPOSALS FOR ANOTHER TEACHING OF COLOR

Taking this premise into account with the question of how, where and to whom we teach color, we are developing a course initially called “Color Theory: current practices and technology”. Still in the development stage, this discipline will contain different practices and exercises already carried out at other times throughout the educational practices of the author of this text. Without denying the contents, we will seek to propose a modern teaching of color, which covers the contents but discusses them together with current issues and contemporary debates.

We therefore have some proposals that must at least be taken into consideration if we seek to teach color dissociated from the issues of capitalizing and generalizing color and its use. (i) Debate the commercialization of color in classroom and draw comparisons with other historical moments. This debate can be used to present different color systems and encourage students to produce their own systems, leading to other concepts. (ii) Address the exaggerated consumption of very saturated audiovisual products, or their effects on childhood, for example. It can help present concepts such as saturation, contrast, primary colors, and can help understand students' localities. (iii) Analyze color in contemporary works from different media, such as cinema, video games, manga, TV series, etc. In addition to contributing to the development and interest of students, this proposal can be the gateway to different concepts, depending on the work chosen and the approach. (iv) Free painting under different lighting. In addition to instigating and providing debate about perception; simultaneous contrast, photoreceptors can also be addressed. (v) 3D glasses workshop, conceiving and providing new technologies for teaching, this workshop seeks to address topics such as simultaneous contrast, visible spectrum, light, additive synthesis, among others.

Figure 1. Painting exercises in different lighting and the 3D glasses workshop

These are some interesting exercises that can be approached and used and that can form the prerogatives we are looking for here. We are initially looking for prerogatives to later compose a color theory course. At first, we will only establish these first considerations regarding the topic.

The exercises were carried out in the State University of Campinas - Unicamp, in the Arts Institute. The author of this text was guest professor in a visual arts course, and managed to offer the students the experiences described. Some exercises can be seen in figures 1 and 2. This are classroom exercises, apparently normal, but which have a greater purpose than simply transmitting knowledge, the objective is to led to the creation and emergence of personal and private color systems and theories based on students preferences, lifestyle, ancestry, social class, etc.

Figure 2. Work written by students analyzing color in films and video games

CONCLUSION

The aim of this text was to bring initial premises for the teaching of color that are not based only on concepts, but on pedagogical practices that can guide teachers towards plural, inclusive and liberating teaching.

The development of the course is still ongoing and other exercises and practices will be developed for this. After the first completion of the course, we expect creative and current approaches from students towards color, applying them to their lives and contributing to each person's self-knowledge.

ACKNOWLEDGEMENT

State University of Campinas - Unicamp, and the Arts Institute for the opportunity offered to show my work.

REFERENCES

1. Dewey, John. (1980) *Experiência e natureza*. (Col. Os pensadores). São Paulo, SP: Abril Cultural.
2. Freire, Paulo. (2000). *Pedagogia da autonomia: saberes necessários à prática educativa.* São Paulo: Paz e Terra.
3. Hui, Yuk. (2020). *Tecnodiversidade.* São Paulo, SP: Ubu Editora.
4. Quatter, Milena. (2019). *A cor no livro didático de arte.* Campinas, SP: Unicamp-Tese de doutorado - Orientadora: Anna Paula Silva Gouveia.

TEACHING MATERIAL DESIGN AND EDUCATION RACTICES OF COLOR EDUCATION FOR CHILDREN IN CHINA

Cathy Wong[1]* Annie Lee[2]

[1]*School of Architecture and Planning, Hunan University, China.*
[2]*Children's color aesthetic education service center, Hunan University, China.*

*Corresponding author: Cathy Wong, 1040519488@qq.com

ABSTRACT

Children's color education is a systematic education aiming at cultivating children's color vision. This paper intends to discuss the current situation and future development of children's color education in China. By comparing the color-related content in China's existing art textbooks, the paper analyzes the shortcomings of China's color education. Based on the law of children's psychological development and the law of disciplinary development, the study puts forward the design and practices of children's color education textbooks from the perspectives of knowledge system construction, the matching of the time stage and teaching method implementation, with a view to providing universal teaching materials for the development of Chinese children's color education.

Keywords: Chinese children, color education, textbook design

INTRODUCTION

Color education for children is a systematic education for cultivating children's sensation of color. It aims to promote children’s comprehensive development in terms of aesthetic, creativity, expression and cognition. Compulsory education stage in the Chinese education system refers to the education for children aged 6-12 years old. Since this stage is critical for children's cognitive and emotional development, cultivating children's sensitivity, understanding and application of color will help to introduce visual perception and color sensation and also establish the system of color sensation application.

At present, aiming to improve children's aesthetic level, application, and cultural understanding, based on practical experience from various countries that include color education, color training has been adopted in China with painting as the main way. Recently. China has issued a number of guidelines such as the "Double Reduction Policy" (2021) and the " Art Curriculum Standards for Compulsory Education" (2022), which, from the perspective of art education as a whole, propose the construction of a systematic teaching system in which each stage of aesthetic education are connected with its former and later one, in-class and after-class activities are integrated, and the various elements of art education are interconnected [1].

However, neither measurement system nor children's color theory are complete at the present stage. Therefore, the gap between different social classes on the awareness of color introduction remains relatively huge, and the development of color aesthetics education in China is relatively fragmented and slow, thus leaving a lot of progress to be made [2]. In this way, we choose the compulsory education stage as a breakthrough to promote the comprehensive development of education on color and aesthetic for children.

STATUS QUO OF COLOR EDUCATION IN CHINA

In order to investigate the current situation of Chinese children's color education in compulsory education, we drew on the research methods of previous researchers. Among the 13 sets of elementary school art textbooks under the curriculum standards guidance of the Ministry of Education, we selected four sets that were applied more. We compared their knowledge points related to color education. The results are as follows.

Domestic teaching materials have relatively great limitations in terms of the color science education. Most of them only involve the simple introduction of color properties, which only aims at serving for the subsequent learning of painting skills. The physical properties of color and its deeper value of life are not thoroughly discussed, and color is only regarded as a painting tool.

In terms of the psychological feeling of color and painting skills, domestic textbooks turn out to be relatively good. However, the application of color is limited to painting while practices of real-life scenarios are ignored. The lack of such practices hinders students from applying color knowledge to a wide range of fields, and thus their color-related abilities and knowledge are not fully trained.

In terms of color culture, there is a large gap in domestic teaching materials. Although efforts have been made to integrate art learning with traditional culture in the textbooks, the textbooks pay insufficient attention to the rich cultural connotations carried by colors. Colors in different cultures have different symbolic meanings and emotional connotations, and understanding these cultural backgrounds is crucial to the in-depth understanding and application of colors. Domestic teaching materials have paid attention to integrating art learning with traditional culture, but the interpretation and inheritance of color culture need to be further strengthened.

It can be seen that the domestic art textbooks has limiataions in terms of color education, which mainly lies in insufficient introduction of the physical and physiological nature of color, the lack of color practice in real-life scenarios, and the inadequte discussion of color culture. In order to enhance students' comprehensive color-related abilities and knowledge, the design of teaching materials should consider the diversity and complexity of color in a more comprehensive way, and combine color knowledge with practical application [3].

DESIGN OF COLOR EDUCATION TEXTBOOKS

Dewey elaborated the science of education in Experience and Education: "True education requires an organic combination of systematic knowledge, appropriate corresponding stages, and optimal educational methods, so that students can gain a deep understanding in practical experience, and thus be able to better apply it to life and society [4]." Based on this theory, we have divided color education as the following according to the principles and logic of textbook design to ensure that education is more scientific and effective in promoting the gradual accumulation and practical application of students' color knowledge.

The design of color teaching materials shall be able to produce a universal and standardized version that accommodates flexible education circumstances due to various regional color cultures [5-6]. Such color teaching materials, featuring "seeking universality while preserving differences", are designed to be both standardized and flexible enough to consider into local characteristics. They can not only contribute to the overall improvement aesthetic education in China, but also promote children's understanding of and interaction with color in different places.

3.1 Systematic Knowledge

The knowledge of children's color aesthetic education teaching materials are divided into three sections, namely color cognition, color application, color culture. According to the appropriate age stage and cross-disciplinary subjects, the knowledge and teaching system is designed.

The Color Cognition section mainly includes color-related scientific knowledge, aiming at cultivating students' color-related ability and knowledge. The color science system covers the physical and physiological aspects of color. Grasping color knowledge as a whole can broaden children's horizons, enhance artistic literacy and creativity.

The application of color aims to cultivate children's ability to use color in practice and to apply color to specific creations. In teaching practice, through visual practice, cultural exploration and other teaching means, children can deeply feel the artistic expression and cultural value of color.

The section on color culture deals with the unique symbols and emotional connotations carried by colors in different cultures, emphasizing the diversity and inclusiveness of cultures. Guiding children to understand the perception and application of color in different cultures can cultivate children's ability to appreciate and respect various cultural forms.

3.2 Stages of Children's Color Aesthetic Education

Based on the laws of children's color perception development, this textbook focuses on:

In grades 1-2, children begin to recognize colors and their relationship to objects, relate their own experiences to colors. In this period, teaching should focus on developing children's color cognitive ability and emotional expression. We could guide children to understand the formation of color and its basic nature, encourage them to use color to express their emotions and feelings, so as to cultivate their ability to express their emotions, lay the foundation of color cognition.

In grades 3-4, children show more individuality in the application of color and are able to freely express emotions and stimuli through color. During this period, teaching should focus on developing children's creative and aesthetic abilities in color, and further guiding them to gain a deeper understanding of how color is expressed. We could encourage students to leverage their individuality and imagination in color expression, and are guided to observe the correspondence between colors and objects in nature, to fully express their emotions and thoughts through colors freely in their creations.

Entering grades 5-6, children are able to perceive the sensory effects of color and are gradually introduced to the concept of color culture. At this stage, teaching should focus on cultivating children's ability of color perception and cultural understanding. We could guide children to perceive the effect of color through actual sensory experience, and gain a deeper understanding of the sensory effect of color. Introduction of color culture and artistic exploration can also be carried out so that children are guided to explore the symbolic significance and emotional connotation of color in different culture. [7-8]

3.3 Optimal Education

The children's color aesthetics textbook should pay attention to how to construct a system of color perception appropriately with the child as the main subject. In order to achieve this goal, the constructivist teaching theory is decided as the main basis of the teaching principle of this textbook. According to the constructivist teaching theory, color education is viewed as a process that stimulates students' active participation and exploration. Children should actively construct their own system of color perception through hands-on experience, creativity and cooperation [9].

The constructivist teaching theory opposes dogmatism and focuses on learning guided by students' interests and strengths. In color courses, teachers should no longer be a single knowledge imparter, but should be transformed into a listener and a guider who encourage students to explore their unique personal strengths and try out innovative methods. For example, when explaining the channels of color perception, students should be encouraged to actively participate in classroom experiments, observe color phenomena firsthand in class, grasp the constancy of color, complementary colors and their effects, the residual image, assimilation and other knowledge, and use the law to try out different color combinations to create unique effects. Through observation and experience, children can gradually discover their own preferences and strengths, which lay the foundation for the development of color vision and personal integrity.

In addition to individualized guidance, the constructivist teaching theory emphasizes the integration of education with real-life situations. Children should participate in authentic, meaningful activities to acquire knowledge, develop skills and abilities. In color curriculum, teachers can guide children to choose scenarios that are closely related to their daily lives. For example, the relationship between color and warning signs is explained in the light of the safety problems in daily life. Children are asked to design signs for tackling real problems that exist in daily lives based on the color knowledge they have acquired, and to design composite traffic signs where different colors schemes tell different messages like languages. Through participation in real, meaningful activities, children can consolidate their understanding of color knowledge and applying it to real life.

Under the guidance of the constructivist view of education, targeted teaching strategies are crucial. In color classes, teachers can guide children to explore the deeper meaning of local traditional colors, based on the local culture. For example, for children growing up in Beijing, they can explore the cultural heritage of the "Ancient Capital of the Six Dynasties". Starting from the Tang Dynasty, which is the most prosperous period in Chinese history, they can use specific cultural elements as an specific example to guide students to deeply understand the meaning and value of local traditional colors. This teaching method not only helps to enhance children's perception and understanding of colors, but also evoke their emotional resonance and respect for local culture, thus an effective implementation of the constructivist theory.

- In term of practice in teaching, we can refer to the methods of elementary art education in Japan and Korea. Art education in Japanese elementary school emphasizes practical operation and guides students to experience a sense of beauty. Their textbooks encourage hands-on practice, combines art with life science, focuses on the learning the design of systems and conventional color names, and emphasizes that students experience a sense of beauty through practical operation [10]. Korea, on the other hand, uses a variety of teaching aids, including drawing colors, color cards, colored shirts, and simulators, to practically facilitate students' learning process [11].

Table 1 Color Textbook Unit Curriculum Design Chart

Module Topic: Color Science		
order of lessons	teaching goal	Teaching methods
1 natural color	Observation of the correspondence of colors and objects in nature, scientific causes	Make plant collage observations and creations
2 color sequence	Recognize the laws of hue, and be able to arrange sequences with a single element of lightness, purity, and hue	Make colorful hats and decorate them with paint or collage
3 light and color	Recognize the three primary colors and color light, and compare the effects of mixing the three primary colors of the pigment with the three primary colors of the color light	Make a stained glass window using light-transmitting cellophane
4 Vision & Color	Recognizing why the human eye sees color	Perform color visual perception exercises
5 Color psychology	Recognizing the correspondence between color and psychological feelings	Painting with colorful bricks and enjoying the fun of working with them
Unit Theme: Traditional Chinese Colors		
1 The color code of the Forbidden City	Recognizing the five-color view and appreciating the colors of the Forbidden City's architecture	Design of traditional works based on the five-color concept
2 Hierarchy of color	Understand the general knowledge of social color grades and the characteristics of colors corresponding to different grades in different dynasties.	Design a color poster for a dynasty
3 Tang dynasty colors	Using the Tang Dynasty as an example, understand the color characteristics of the era	Making a Tang Dynasty Lady Bookmark
4 Traditional Name of Colors	Understanding traditional Chinese colors and their representative color names	Drawing on the theme of one of the twenty-four solar terms
5 The Journey of a Legendary Landscape Painting	Exploring the cultural reasons for the use of color and elegance in the Song Dynasty	Drawing a three-dimensional map of a thousand miles of rivers and mountains

Unit Topic: Color Application		
1 Color & Taste	Understand the correspondence between color and taste and use color to express taste	Designing food packaging with the relationship between color and taste
2 Color and Mood	Understand the correspondence between different emotions and colors, and use color combinations to express emotions	Make thank you cards in specific colors to give to teachers or parents
3 Fashion & Color	Understand the relationship between color and fashion aesthetics, and try to incorporate popular colors into the creation of apparel.	Mixing up favorite colors and hand-painting canvas bags
4 Safety and Color	Recognizing the relationship between color and traffic safety symbols	Creating signage work that compounds the color language of traffic signage
5 Colors of the World	Recognizing the relationship between regional cultures and ethnic differences	Design a poster using the color characteristics of the region

CONCLUSION

This study analyzes in depth the context of children's color aesthetic education in China. The study discusses the design and implementation of color aesthetic education teaching materials, based on the logical system of children's color vision development and the logical system of color discipline development.. In the design of teaching materials, we establish a systematic knowledge framework, and arrange the teaching assignment according to the characteristics of children's color vision development stage. Based on constructivism, designing the education method is the keys to achieving good teaching results. We expect that this study will provide useful references for the optimization and development of color education in China.

REFERENCES

1. Zhang Ting. (2013). The development history of art curriculum in primary and secondary schools in new China and its revelation [D]. Jiangxi Normal University.
2. Niu Cuiping. (2020). Natural color education for young children: values, goals and countermeasures. Journal of Shaanxi Preschool Normal College, 36, 1-6.
3. LIU Jianlin,RONG Tingting. (2015). Research on the content of appreciation teaching in junior high school art textbooks[J]. China Teacher,S2, 127.
4. John Dewey. Art as Experience.1931.
5. Guan Huiyong. (2007). Research on the design teaching content of art textbooks for primary and secondary schools in China. East China Normal University.
6. Chen Xiaoyan. (2015). A comparative study of art teaching materials in junior high school between Renjiao and Renmei editions . Henan Normal University.
7. Vitor Lowenfeld. (1957). Creative and Mental Growth.
8. 김경아, 김정근. (2011). 아동 인지 발달에 따른 색채 교육 내용 실태. 한국실내디자인학회 논문집,20(4),136-144.

9. YANG Weidong,JIAN Nan. (2011). A review of constructivist learning theory[J]. Theory Guide,05,77-80.

10. Chen W. (2007). An overview of constructivist learning theory. Academic Exchange,03,175-177.

11. 이경희. (2002). Verde채디자인교육의 효율화를 위한 컬러 시스템의 연구.Archives of Design Research, 39-52.

12. Allred, S., & Brainard, D. (2007). Scene complexity affects lightness constancy with respect to changes in object slant and surround reflectance [Abstract]. Journal of Vision, 7(15), 51.

EXPLORING THE EFFECTS OF COLOURS OF DIGITAL MATERIALS ON LEARNERS' COMPREHENSION IN HIGHER EDUCATION

Zhe Gong[1]*, Philip Henry[1], Francisco Queiroz[1], Soojin Lee[1] and Guobin Xia[2]

[1]*School of Design, University of Leeds, UK.*
[2]*School of Textiles and Design, Heriot-Watt University, UK.*

*Corresponding author: Zhe Gong, sdzg@leeds.ac.uk

ABSTRACT

Recent studies demonstrate that colours could attract attention, improve concentration and readability, as well as enhance information recall. Although colour design is essential in education, more scientific research is needed to examine the optical colours for instructional materials. This project encompasses a focus group, pre-experiments, and main experiments to understand the effects of colours on human comprehension in digital learning environments. Forty participants completed a comprehension ability test with 16 questions displayed on eight different background colours: red, orange, yellow, green, blue, purple, grey, and black. Note that to ensure consistent contrast between foreground and background colour, grey fonts were used for the black background and black fonts for the other seven colours. It also assessed the different colour materials' preferences, readability, and legibility. The study found that native English speakers performed better in the tests with grey and red background colours, with higher correction rates and shorter response times for the two colour conditions. There were significant differences in the evaluation scores between grey and black backgrounds, which have black and grey foreground colours, respectively. On the other hand, the colours did not significantly affect non-native English speakers' comprehension ability. However, the two groups had no significant differences in the subjective preference assessment, legibility, and readability. This study suggests that people's cognitive performance may improve under light background and dark foreground colour combinations. Also, learners' preferred colours may not lead to a better understanding of text-based information. Educators, instructional designers, and developers of digital educational materials can benefit from these insights to enhance digital learning experiences by optimising the integration of colour and addressing the impact of language proficiency.

Keywords: Colour design, digital learning material, comprehension assessment, higher education.

INTRODUCTION

Studies have acknowledged the importance of using colours in designing learning materials in higher education; however, more empirical knowledge is needed. For example, Roberts stressed that *"Even though the use of colour in the production of instructional materials is widespread, its relative effectiveness as an aid in improving student achievement remains inconclusive and at best contradictory"* [1, p. 26]. Also, Diachenko et al. highlighted the potential of using colour in designing learning material in higher education that can enhance students' perceptions and memorisation [2]. Some studies have shown that colour or colour combinations can help people recall information and form colour coding [2, 3]. Therefore, the present study aims to explore the effects of colours of learning materials on students' comprehension ability in higher education settings. It addresses three questions: First, how do modern learners feel about the readability and legibility of different colour materials and their preferred colour choice for digital materials? Second, which colour setting enables learners to comprehend text-based information most effectively? Last, whether students' preferred colour of learning material leads to their better understanding of the textual information.

METHODOLOGY

Fonts

When it comes to fonts for the test learning materials, 'Verdana' and 'Microsoft's Times New Roman' were selected based on screen information design principles set by Pettersson [4]. The font size was set at the optimal size range with a body size of 24 points (typically 32px) for text and a body size of 30 points (typically 40px) for the headings in the Verdana typeface. In the footnote section below the learning material, in the serif font Time New Rome, with a body size of 18pt (typically 24px) [5].

Background Colours

This study carefully selected eight colours for the background of digital learning materials to ensure text-based information's effectiveness and maximise the digital materials' legibility and readability. The eight background colours include six chromatic colours (such as red, orange, yellow, green, blue, and purple) and two achromatic colours (such as black and grey). Especially the six chromatic background colours were systematically selected from the Adobe HSB colour system [6]. For example, hue is measured in degrees of the colour circle ranging from 0 to 360 (red = 0°,orange= 30°; yellow= 60°; green = 120°; blue = 240° and purple= 270°). From each degree, choose a colour and ensure that the contrast between these colours and black remains at the same level.

Foreground (Font) Colours

Grey was used as the foreground colour for the black background, and black was used as the foreground colour (font colour) for the other colours. The font colour of the learning materials is black, and the contrast with the background colour is guaranteed to reach a higher level to ensure the readability of the learning materials to the greatest extent [7]. Against different colour backgrounds, the black text will be more readable compared to other colours [8]. So, in the coloured background condition, all text colours are black, with an RGB value of C=0,0,0, while in the black background, reference grey will be used as the foreground colour.

Luminance Contrast between Background and Foreground (Font) Colours

The luminance contrast between the background and critical visual cues is essential to ensuring the readability of learning materials, and some researchers suggest that this contrast should be fixed in 3:1 OR 7:1 threshold set by the W3C specifications [9, 10, 11].

Using linear colour components C= [R, G, B], one may get the relative luminance by:

$$L = 0.2126R + 0.7152G + 0.0722B \tag{1}$$

Knowing the relative luminance, calculate the contrast ratio of a coloured text and background by the formula:

$$(L1 + 0.05) / (L2 + 0.05) \tag{2}$$

- L1 is the relative luminance of the lighter of the foreground or background colours, and
- L2 is the relative luminance of the darker of the foreground or background colours.

Relative luminance of text and background colour (L1>L2). The ANSI/HFS 100-1988 standard requires that the contribution from ambient light be considered when calculating L1 and L2. The value is based on the (IEC-4WD) Typical Viewing Flare [11]. After the calculation, please see Table 1 for the colour samples and values.

Table 1: The sRGB colour coordinates of the eight background colours (H_ Hue, S_ Saturation, B_ Brightness, R_ Red, G_ Green, B_ Black).

Colour name	Colour sample	H	S	B	R	G	B	Contrast ratio
Reference Grey		0	0%	60%	153	153	153	7.37
Red		0	60%	100%	255	102	102	7.34
Orange		30	100%	94%	240	120	0	7.39
Yellow		60	100%	62%	158	158	0	7.34
Green		120	100%	70%	0	178	0	7.37
Blue		240	45%	100%	140	140	255	7.31
Purple		270	52%	100%	189	122	255	7.39
Black		0	0%	0%	0	0	0	

Note: The colour names indicate the hue value of the colours and ensure that all combinations of foreground and background colours have their contrast controlled around 7.3. The saturation and brightness will need some tweaking, so some of these colours may not represent the name.

Participants and Demogrphic Distribution

In this experiment, participants were selected based on the following three criteria: (1) having normal vision, (2) currently having a higher education, and (3) having experience in online education learning education. Based on the above screening conditions, 44 participants were recruited for this experiment, half males and half females. After the first round of data counting and screening, valid data from 40 participants were adopted for the final data analysis, with an average age of 28.32 (19-42 years old). The specific experimental setting and cultural background, etc., are shown in the table below. After the first round of data counting and screening, valid data from 40 participants were adopted for the final data analysis, with an average age of 28.32 (19-42 years old). The 40 participants were carefully distributed based on the condition of the physical learning environment and gender. Table 2 shows the participant distribution.

Table 2: The distribution of the 40 participants (offline and online).

	Offline Condition			Online Condition			
Gender	Chinese	Mixed Culture	Native Speaker	Chinese	Mixed Culture	Native Speaker	Total
Female	5	2	3	5	2	3	20
Male	5	3	2	5	3	2	20
Total	10	5	5	10	5	5	40

Online Questionnaires

An online questionnaire evaluated participants' online learning experiences, colour preferences, and readability and legibility of digital learning materials. The questionnaire contains 29 questions (and takes about 7 minutes to complete.)

Comprehension Test Materials

Comprehension tests are designed to test verbal skills and understanding of written text with word change questions. These questions avoid the limitations of single- or multiple-choice questions, allowing participants to guess without understanding the text. Participants can make sentences comprehensible by changing the position of words, as shown in Figure 1.

Example:

Change the position of FOUR WORDS only in the sentence below in order for it to make complete sense.

The discovery of today's plastics materials begins with the semi-synthetic history of a series of thermoplastic in the mid-nineteenth century.

Answer:

The **history** of today's plastics begins with the **discovery** of a series of **semi-synthetic** thermoplastic **materials** in the mid-nineteenth century.

Notes:
1. Synthetic: produced by combining different artificial substances, rather than being naturally produced.
2. Thermoplastic: a plastic that is soft and bendable when heated but hard when cold.

Figure 1. An example of the comprehension test, the word-changing questions used in the main experiment.

Each participant was required to answer 16 questions throughout the experiment. Under each background colour, participants will answer two different questions. To ensure that the difficulty of the various questions does not affect the final experimental results, the combination of material content and colour needs to appear randomly, not in a fixed order.

Procedures

First, the experiment divided the 40 participants into two distinct environments. For half of them, a real-time connection was established through Microsoft Teams software, allowing them to engage with the researcher remotely. They undertook the experiments online, where the physical surroundings were beyond their control. In contrast, the remaining participants participated in the experiment in an offline lab environment equipped with a D65 standardised light source and a standard sRGB display setting. Upon entering the lab, these participants had 1-2 minutes to acclimate to the surrounding ambient light.

Second, prior to commencing the experiment, all participants needed to complete the online Ishihara Colour Blindness Test), ensuring their possession of normal Colour vision.

Third, following the colour blindness test, participants were directed to complete an online questionnaire, which typically required around 8-9 minutes.

Lastly, sixteen experimental questions were presented to the participants randomly. Once they felt prepared, they answered the questions while the researcher meticulously recorded the time to complete each inquiry.

RESULT AND DISCUSSION

Figure 2 shows the group comparison results of correction rates and response time from the comprehension test between the native and non-native English groups. Three outstanding findings were captured:

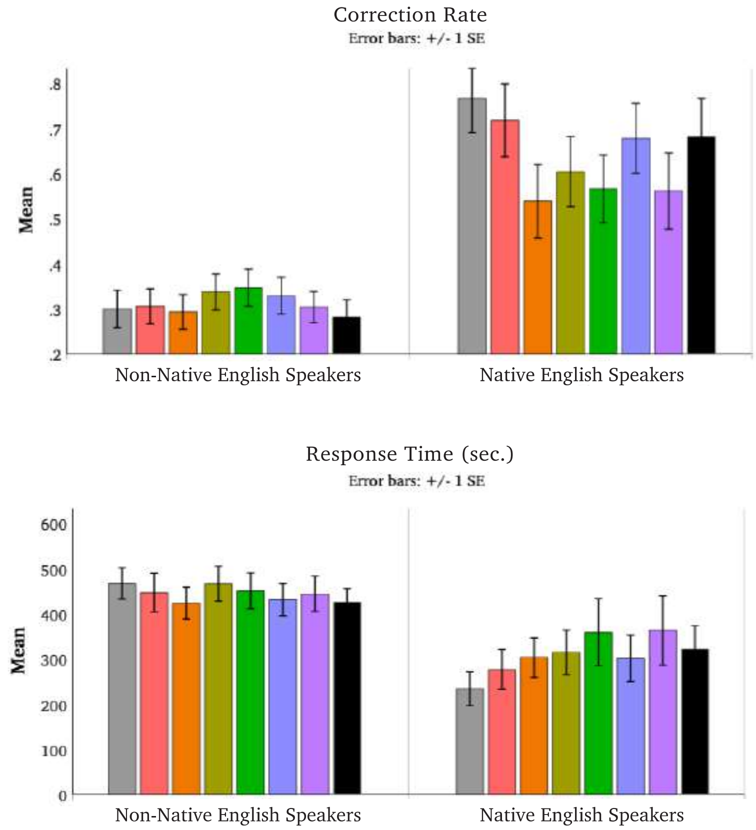

Figure 2. Correction Rate and Response Time Mean Comparison in the group of Native and Non-Native English Speakers

First, the average correction rates of the comprehension test for the native English group were slightly over twice as high as for the non-native English group across all eight colour conditions; for example, on average, the correctness mean for the group of non-native English speakers was 0.0315, while the overall correctness mean for native English speakers was 0.638.

Second, the average response time of the non-native English group was significantly higher than that of the non-native English speakers group. These results are not surprising since their natural English is different.

Third, most interestingly, the differences in either correction rate or response time across the eight different colour materials were significantly more prominent in the native English group than in the non-Native English group. For example, the native English speakers performed best on average in the grey condition (M: 0.77; SD: 0.34), which is followed by red (M: 0.72; SD: 0.36), blue (M: 0.68; SD: 0.35), and black (M: 0.68; SD: 0.37). They showed lower correction rates in the other four colours, which ranged between 0.50 and 0.60. Regarding response time, the data for the native English speakers' group demonstrated a wider range, with a difference of approximately 130 seconds between the maximum and minimum values. Analysing the data of the native English speakers' group, two colours, namely Grey (M: 232.98; SD: 168.72) and Red (M: 276.01, SD: 197.20), stood out as superior, with average completion times below 300 seconds. This indicates that participants took less time to complete the test under these two Colour conditions.

The different pattern between the two groups may be explained by more significant individual differences regarding English comprehension tests in the non-native English group. Although we assume their proficiency in English reasonably is similar, it should be disregarded that the English ability is complex and encompasses multiple dimensions of language or literacy ability. For example, non-native English speakers did not show a more significant data variation in the correction rates or response time among colours. The influence of colour on their comprehension of textual information was minimal.

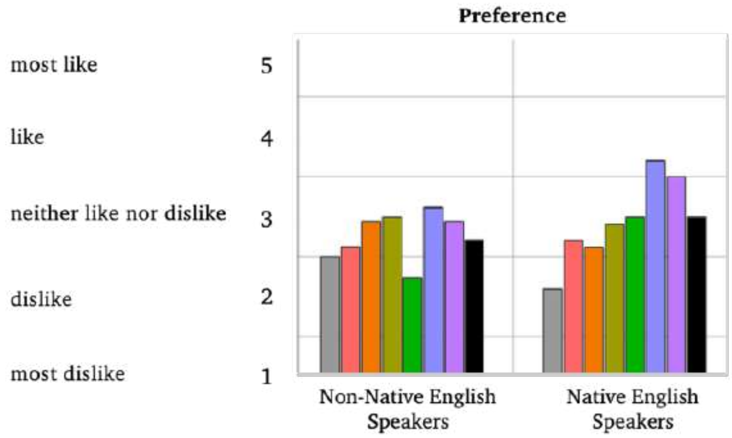

Figure 3. Preference results from the online questionnaire.

Figure 3 showed that regardless of the group, blue emerged as the participants' favourite colour, followed by purple. Similar trends regarding readability and legibility were observed when combining different colour backgrounds with text. This finding is consistent with Hall and Hannah's findings: "Variations in text-background readability findings emphasise the interconnected of readability vis- à-vis colour preference [12]." Even at different age stages, 8-9-year-old children's colour preferences show surprising similarities to those of adults [13]. In addition to colour preferences, Brooker and Franklin's study highlights a significant difference in cognitive performance based on colours. Performance is notably worse in the presence of red compared to grey [13]. The effect of colour remains consistent across different tasks. These findings prove that colour can influence children's cognitive performance, with red specifically having a detrimental effect.

In summary, although there was no significant difference in the comprehension test performance for non-native English speakers in the different colour conditions, there was a significant variation in the survey data, i.e., in the colour preference.

CONCLUSION

Individual colour preferences may affect digital materials' readability but do not significantly affect text-based comprehension tests. Whether or not a participant's native language was aligned with the language in which the test material was written considerably impacted the final results. After removing the barriers created by language, the conclusions of this study showed that participants performed best in the grey colour condition and far better than the other colour conditions.

Although the black background material had the same colour combination as the grey background material, regarding participant performance, combining the more delicate background condition (grey and red) and the darker foreground condition (black) is better than the black background, with the light foreground colour not even as good as the blue colour condition.

ACKNOWLEDGEMENT

I want to thank Dr Philip Henry, Dr. Francisco Oliveira de Queiroz, and Dr. Soojin Lee for their unwavering support, guidance, and valuable insights while crafting this conference paper. Their expertise and encouragement have been instrumental in shaping the outcome. Additionally, I sincerely appreciate all the participants who willingly participated in the experiments, contributing their time and valuable perspectives.

REFERENCES

1. Roberts, W. E. (2009). *The Use of Cues in Multimedia Instructions in technology as a way to reduce Cognitive load.* North Carolina State University. Retrieved from http://repository.lib.ncsu.edu/ir/bitstream/1840.16/4434/1/etd.pdf.
2. Diachenko, I., Kalishchuk, S., Zhylin, M., Kyyko, A., & Volkova, Y. (2022). Color education: A study on methods of influence on memory. *Heliyon, 8*(11), e11607-e11607.
3. Zufic, J., & Kalpic, D. (2009). More efficient e-learning through design: color of text and background. I*n E-Learn: World Conference on E-Learning in Corporate, Government, Healthcare, and Higher Education*, 3314-3319.
4. Pettersson, R. (2010). Information design–principles and guidelines. *Journal of Visual Literacy*, *29*(2), 167-182.
5. Rambally, G. K. (1986). The influence of color on program readability and comprehensibility. In *Proceedings of the seventeenth SIGCSE technical symposium on Computer science education*, 173-181.
6. Camgöz, N., Yener, C., & Güvenç, D. (2002). Effects of hue, saturation, and brightness on preference. *Color Research & Application: Endorsed by Inter-Society Color Council, The Colour Group (Great Britain), Canadian Society for Color, Color Science Association of Japan, Dutch Society for the Study of Color, The Swedish Colour Centre Foundation, Colour Society of Australia, Centre Français de la Couleur, 27*(3), 199-207.
7. Williams, R. (2015). *The non-designer's design book: Design and typographic principles for the visual novice*. Pearson Education.
8. Richardson, R. T., Drexler, T. L., & Delparte, D. M. (2014). Color and contrast in E-Learning design: A review of the literature and recommendations for instructional designers and web developers. *MERLOT Journal of Online Learning and Teaching*, *10*(4), 657-670.
9. Lin, C. C. (2003). Effects of contrast ratio and text color on visual performance with TFT-LCD. *International journal of industrial ergonomics*, *31*(2), 65-72.
10. Roberts, W. (2017). The use of cues in multimedia instructions in technology as a way to reduce cognitive load. *Journal of Educational Multimedia and Hypermedia*, *26*(4), 373-412.
11. *Web Content Accessibility Guidelines (WCAG) 2.1*. (2018, 05 June 2018). Retrieved 19 Jan. from https://www.w3.org/TR/WCAG21/
12. Hall, R. H., & Hanna, P. (2004). The impact of web page text-background colour combinations on readability, retention, aesthetics and behavioural intention. *Behaviour & information technology*, *23*(3), 183-195.
13. Brooker, A., & Franklin, A. (2016). The effect of colour on children's cognitive performance. *British Journal of Educational Psychology*, *86*(2), 241-255.

EFFECTS OF CLASSROOM WALL COLOR ON UNIVERSITY STUDENTS' PERFORMANCE AND ATTENTION

Mahshid Baniani[1]*

[1]*Department of English Language Studies, Faculty of Foreign Language Studies, Mejiro University, Japan.*

*Corresponding author: Mahshid Baniani, mahshid@geijutsu.tsukuba.ac.jp

ABSTRACT

Wall color is one of the largest physical components in a classroom and it stimulates students' cognitive responses and affects their behavior as well (Duyan et al, 2016). There are several studies regarding the effects of color on human behavior, however research studies focused on learning environments are scarce. The aim of this study is to examine the impact of color on attention and performance of university students. To reach the purpose of this study, an experiment consisting of three tasks (questionnaire, performance test, and attention test) was conducted. The participants were 40 Japanese university students between the ages of 20 and 24. The participant was seated at a desk where a colored paper was hung in front of the desk, and they had to perform the tasks. The colored papers consisted of red (5R 7-10), pale red (5R 8-4), orange (10R 7-10), pale orange (10R 8-4), yellow (5Y 8.5-10), pale yellow (5Y 9-4), green (7.5GY 8-10), pale green (7.5GY 9-4), blue (10B 7-8), pale blue (10B 8-4), purple (2.5P 7-8), and pale purple (2.5P 8-4). They were also required to do the experiment in front of the plain wall which was white. First, the participants were asked to select their most favorite and least favorite color among the colors. They were also asked about their mood. In the questionnaire section, while looking at the colored paper, they had to say whether they like the color or not, if the color makes them feel calm, helps them focus, or if it motivates them to study. They also needed to associate the color with the first word that came to their mind. Then, they needed to do the Bourdon Attention Test developed by Benjamin Bourdon (1955), and finally a performance test which consisted of writing the *yomikata* (or way of reading, pronunciation) of Kanji characters suitable for their level. All the questions were done randomly among the participants. It was observed that purple was the least favorite color among the participants ($P<0.05$). They said that it makes them feel bad and nervous. Participants performed poorly in front of reds, purples, and white in both attention and performance tasks ($P<0.05$). On the contrary, they performed well in front of green and pale green in both tasks ($P<0.05$). They also said that these colors motivate them to study and help them focus. Participants performed better in front of high value and lower saturated colors in the attention task, while they performed better in front of higher saturated colors in the performance task. Additionally, liking or disliking a color didn't have a statistical correlation with the students' performance and attention. Moreover, white may not be the most suitable color for learning environments as most believe it to be.

Keywords: Wall Color, Task performance, Attention, Classroom, Kanji

INTRODUCTION

Wall color is one of the largest physical components in a classroom and it stimulates students' cognitive response and affects their behavior as well [1]. There are several studies regarding the effects of color on human behavior, however research studies focused on learning environments are scarce.

The aim of this study is to examine the impact of color on attention and performance of university students.

METHODOLOGY

PARTICIPANTS

40 Japanese university students (20 female and 20 male) between the ages of 20 and 24 (M=21.7) participated in this study.

PROCEDURE

To reach the aim of this study, an experiment consisting of three tasks (questionnaire, performance, attention) was conducted. The participant was seated at a desk where a colored paper was hung in front of it and had to perform the tasks. Munsell notation of the selected colors can be seen in Table 1. As can be seen, colors with high value (brightness) were chosen. They were also required to perform the tasks in front of the plain wall which was white.

Table 1. Munsell notation of the colors used for the panels

Color name	Hue	Value	Chroma	Color name	Hue	Value	Chroma
Red	5R	7	10	Red (Pale)	5R	8	4
Orange	10R	7	10	Orange (Pale)	10R	8	4
Yellow	5Y	8.5	10	Yellow (Pale)	5Y	9	4
Green	7.5GY	8	10	Green (Pale)	7.5GY	9	4
Blue	10B	7	8	Blue (Pale)	10B	8	4
Purple	2.5P	7	8	Purple (Pale)	2.5P	8	4

First, the participants were asked to choose their favorite and least favorite color among the colors. They were also asked about their mood. Then the three tasks were conducted in random order as follows:

Questionnaire: In this section, while looking at the colored panel (and the wall), the participants had to say whether they like the color or not, if the color makes them feel calm, helps them focus, or motivates them to study. They also needed to look at the color and write the first word that comes to their mind.

Attention Test: They needed to do the Bourdon Attention test developed by Benjamin Bourdon (1955). The test was composed of 20 lines with 22 letters in each line, and in total there were 440 letters. The participants were asked to find the letters “a, b, q” and mark them in less than two minutes.

Performance Test: In this task, the participants had to write the *yomikata* (or reading, pronunciation) of Kanji characters suitable for university level.

All the participants performed all the three tasks. However, the order of colors, tasks, and questions were done randomly among them.

RESULTS

COLOR PREFERENCE

In this section, the participants were asked to select their most and least favorite colors among the 12 colors of the colored panels.

As can be observed from Figure 1, reds and blues were among the favorite colors of the participants. Participants mainly associated red with happiness and love. Pale red was associated with cherry blossoms. Blue was mainly associated with being cool and refreshing. Pale blue was associated with water and sky.

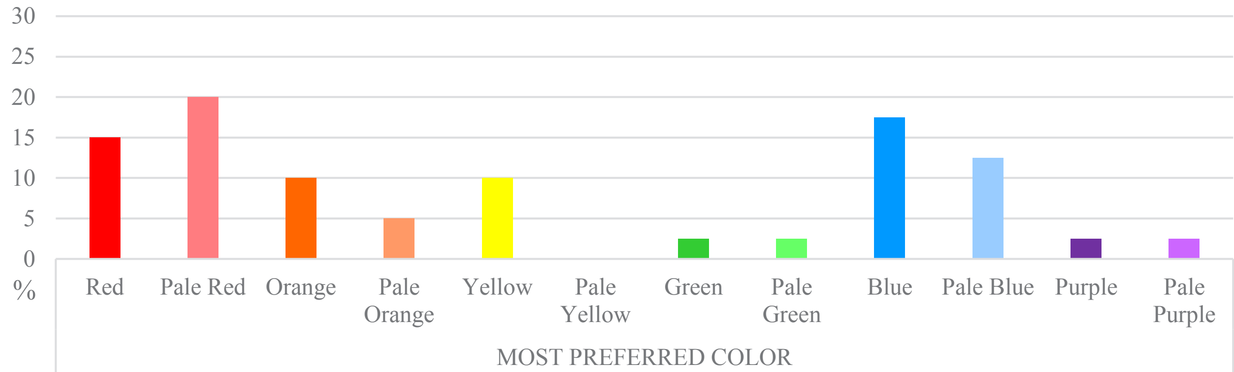

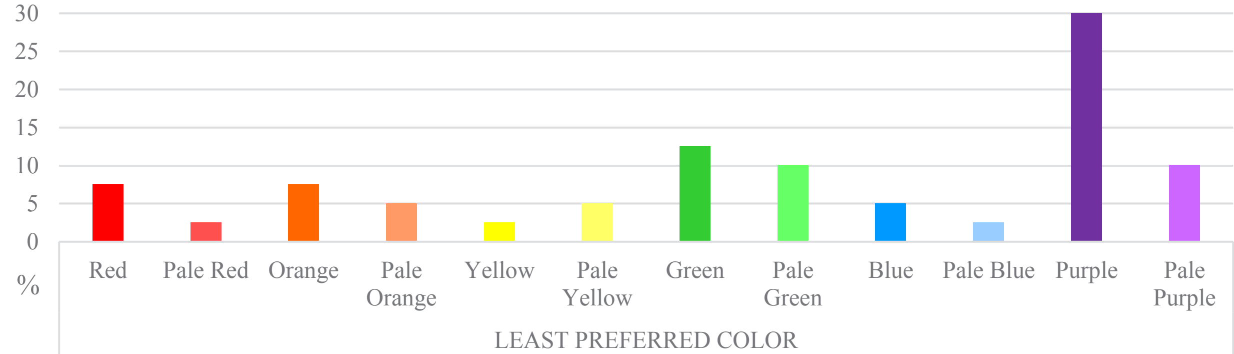

Figure 1. Most and least preferred colors of the participants

Purple was the least favorite color of the participants ($P<0.05$). Participants who selected purple as their least favorite color said that purple makes them feel bad and nervous.

ATTENTION TEST

Participants needed to do the Bourdon Attention Test in front of the colored panels and the white wall. The test was composed of 20 lines with 22 letters in each line. Participants were asked to find the letters a, b, and q in the text in 2 minutes. The test was evaluated using the hundred system. First it was checked if the participants marked any letter aside from a, b, and q, which no one did. Then the correct letters were calculated in ratio to the total number of correct letters. The results can be seen in Figure 2.

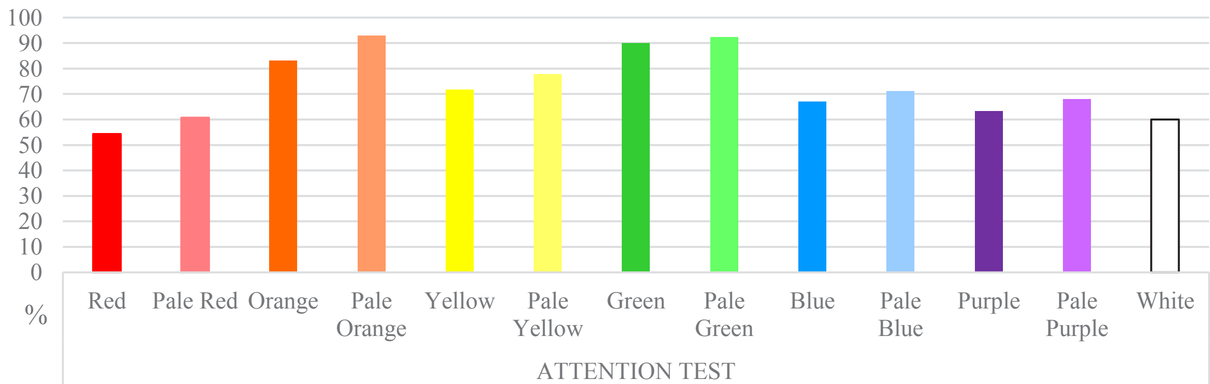

Figure 2. Results of the Attention Test

As can be observed from Figure 2, participants had the highest test score in front of pale orange, pale green, and green. On the contrary, attention scores were lowest for colors red, white, and pale red. Interestingly when asked, although participants did say that red doesn't help them focus or motivate them to study, but they did say that pale red does make them focus or motivate them to study. In case of white, only 30% said that it helps them focus or motivates them to study. Moreover, in total, participants performed better in front of higher value and lower saturated colors (pale colors) rather than higher saturated ones.

PERFORMANCE TEST

In this section, participants had to write the *yomikata* (reading or pronunciation) of 6 Kanji characters in 1 minute. The number of correct *yomikata* was calculated. The results can be seen in Figure 3.

As can be observed, participants had highest scores in front of green, pale green, and yellow. They had the lowest scores in front of red, pale red, purple, pale purple, and white. Contrary to results observed in the attention test, performance scores were higher for higher saturated colors.

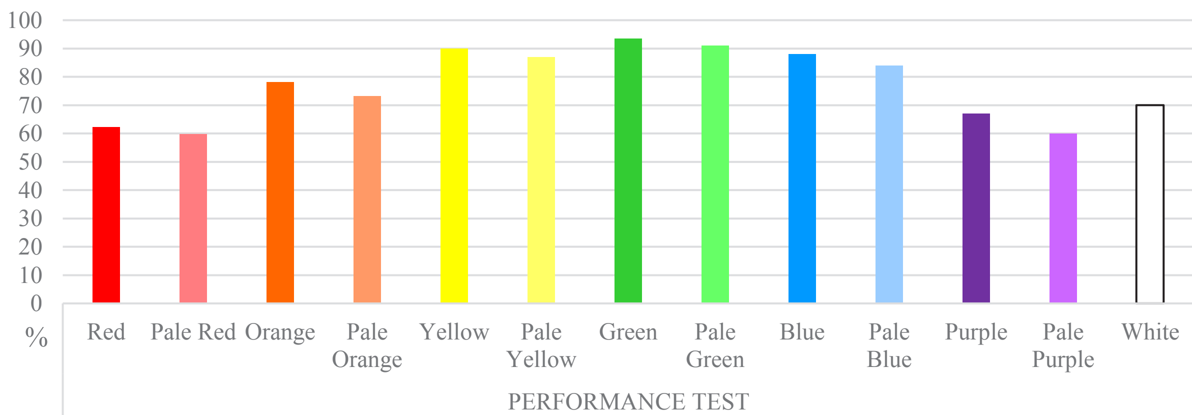

Figure 3. Results of the Performance Test

DISCUSSION

The purpose of this study was to examine the impact of color on the attention and performance of university students. For this reason, an experiment consisted of 3 tasks was conducted in front of 12 colored panels and the white wall.

Blues and reds were the most favorite colors of the participants which has been seen in other studies (for example: Grieve, 1991) as well [2]. Purple was the least favorite color among the participants. Ulusoy et al. argued that purple can be interpreted to convey negative meanings more than other colors [3]. Similarly, in this study participants associated purple with feeling bad and nervous.

Participants performed well in front of green and pale green in both attention and performance tasks ($P<0.05$). Moreover, they performed poorly in front of reds, purples, and white in both tasks. Duyan et al. concluded that students had the lowest performance in the red (5R 7/8) wall color conditions [1]. Additionally, in a study conducted by Kwallek et al. on the effects of nine different hues on short-term worker productivity, the findings supported the notion that participants performed worse in the white office interior than in any of the other eight interior colors [4].

In the attention task, participants performed better in front of high value and lower saturated colors, while they performed better in front of higher saturated colors in performance task. This could be because the higher saturated colors are more arousing and therefore, they may have stimulated individuals and enhanced their performance, but at the same time, the colors were too arousing and more distracting for them to be able to focus completely on the attention test as this task needed more attention and focus than the performance test.

CONCLUSION

In sum, it was observed that liking or disliking a color didn't have a statistical correlation with the students' performance and attention (except for purple). Participants performed well in front of green and pale green in both tasks ($P<0.05$). They also said that these colors motivate them to study and help them focus. On the contrary, they didn't perform well in front of reds, purples, and white. Therefore, white may not be the most suitable color for learning environments as everyone believes it to be.

REFERENCES

1. Duyan, F., & Unver, R. (2016). A research on the effect of classroom wall colours on students' attention. *ITU Journal of Faculty of Architecture,* 17(2), 73-78.
2. Grieve, K. W. (1991). Traditional beliefs and color perception. *Perceptual Motor Skills,* 72, 1319-1323
3. Ulusoy, B., Olgunturk, N., & Aslanoglu, R. (2020). Colour semantics in residential interior architecture on different interior types. *Color Research and Application*. 45, 941-952
4. Kwallek, N., Lewis, C. M., Lin-Hsiao, J. W. D., & Woodson, H. (1996). Effects of nine monochromatic office interior colors on clerical tasks and worker mood. *Color research and Application,* 21, 448-458

PIGMENTS APPLIED IN PHRA DHEVABHINIMMIT (CHAI THIAMSILPAJAI)'S PAINTING ANALYZED BY PORTABLE MICRO X-RAY FLUORESCENCE

Nawarat Kaew-on* and Tanaporn Kaewkong

Restaurateurs Sans Frontières Laboratory, Studio for art conservation and restoration, 6 Soi Kasemsan 2, Rama I Road, Wangmai, Phayathai, Bangkok 10330 Thailand

*Corresponding author: Nawarat Kaew-on, rsfasie_nawarat@hotmail.com

ABSTRACT

This paper presents the scientific investigations of the painting by Phra Dhevabhinimmit or Chai Thiamsilpajai (1888 – 1947), a well-known Thai artist of the Rattanakosin era who performed many of famous and important artworks in Thailand. One of his historical performances was being the leader for the restoration of Wat Pra Sri Rastanasasdaram, Grand Palace, Bangkok in 1931 where he painted the panel number 1 of the Ramayana story mural on the balcony. The scientific analysis for works of art has not been sufficient in Thailand recently. During the restoration treatment in 2021, the oval paper painting painted by this artist in 1934, named "Narai Banthomsin", was therefore taken to scientifically examine. Studying of his color pallet was done using combination of two methods; the UV examination and X-Ray fluorescence (XRF) to evaluate pigments applied. UV light at the wavelength 365 nm was used to identify if the painting was retouched, while the XRF as a non-destructive technique was used for characterization of the inorganic pigments. The XRF mapping (MA-XRF) and point inspecting were carried out in this analysis. The main colours present in the painting were white, blue, red, yellow, green, and brown. The results highlighted the presence of lead white ($2PbCO_3.Pb(OH)_2$) for the ground layer, lead and lithopone white ($BaSO_4.ZnS$) for the white areas, cinnabar (HgS) for the red, orpiment (As_2S_3) for the yellow, and probably brown ochre (Fe_2O_3) for brown. Presenting of copper and arsenic suggests that green is the emerald green. Blue is likely an organic blue that is unable to identify by XRF method.

Keywords: Phra Dhevabhinimmit, X-Ray fluorescence, pigment identification, Thai painting

INTRODUCTION

Phra Dhevabhinimmit or Chai Thiamsilpajai (1888 – 1947), is one of the most important Thai artists of the Rattanakosin era in the 19th to 20th century, during the reigns of King Rama V to VII [1]. He performed many of historical artworks in Thailand. In 1931, he was the master of the major restoration on Ramayana story murals around the balcony of the Wat Pra Sri Rastanasasdaram, Grand Palace, Bangkok. In this restoration, Phra Dhevabhinimmit also painted the mural painting panel No.1 (Figure 1), which is "the hermit Janaka finding Sida in a glass bowl" [1-3]. Not only that, he was also a key leader in the preparations for King Rama VII coronation [1]. He also designed the royal seal of King Rama VII and VIII. Phra Dhevabhinimmit with collaboration with professor Silp Bhirasri designed the monument of Thao Suranaree [1]. In 2021, the author received the painting named "Narai Bantomsin" (Figure 1), which was painted by Phra Dhevabhinimmit, for restoration. The content of the painting consists of Vishnu sleeping with Brahma rising up in the middle of Nabhi and beside him with his wife Lakshmi, all sitting on the Ananda Naga, in the midst of the ocean (sea of milk). The painting is dated back in 1934 [2].

Scientific studying the color palettes of important Thai artists has never been so widely performed before. This research is therefore performed by using the nondestructive technique, X-ray fluorescence spectroscopic for pigment identification. XRF is a nondestructive technique, it is helpful to evaluate the cultural assets, neither touching it nor damaging it at all. Inorganic pigments on the painting or mural paintings can be analyzed without even any micro sample taken. With the portable equipment, the investigations can be run in situ, without moving the objects from its original place. It is one of the harmless ways to obtain information about the materials and techniques applied by archeologists, scientists, and conservators, although it can only detect limited elements (from magnesium to uranium) [4-6]. To ensure that the original materials is determined, this research employed UV examination to verify whether the art work was restored or intervened previously.

This article aimed to scientifically discuss the studied pigments in the palette of Phra Dhevabhinimmit by studying the painting named "Narai Banthomsin, 1934".

Figure 1. (a) The "Ramayana, the hermit Janaka finding Sida in a glass bowl", 1931, Tempera Mural painting Panel No.1 Wat Pra Sri Rastanasasdaram, Grand Palace, Bangkok [3], and (b) the painting "Narai Banthomsin, 1934" [2].

METHODOLOGY

Figure 2a presents the oval shape painting "Narai Banthomsin, 1934", tempera on paper that was sent for restoration treatment. The painting's condition appeared to have been exposed to smoke resulting in a black-brown color at the sky area. In this study, to ensure that the investigation proceeded with the original pigments painted on the the painting, UV examination was carried out to study if there were any restored areas or intervention before the painting was taken to analyze by a nondestructive XRF method [7-8].

UV Examination: One pair of the UV lamp were exposed on each side of the painting to obtain the most homogeneous illumination of the surface. The bulbs are UV LED radiation power: 14250 mW, UV max spectral emission: 365 nm.

X-Ray Fluorescence: Base on the UV examination results (Figure 2b), locations of different colors over the painting surface were selected to analyze by X-Ray fluorescence technique, as shown in Figure 2c. The ground layer and main colors, which included white, blue, red, yellow, green, and brown were investigated and discussed. The equipment was the portable

Elio instrument (ELIO, XGLab Bruker). The measurements were performed in the point mode, using 50 kV and 80 mA for 60 seconds acquisition time. Tube target material was Rh, and sample to detector material was Air. The diameter of the radiated spot is 1 mm. The mapping mode was also performed in conjunction with the point mode measurements. Mapping acquisitions were made using 50 KeV and 80 mA for 60 mins, the area is 20 x 20 mm^2. This article displayed the mapping of the certain areas only. The pigments were recognized on the basis of the characteristic chemical composition from the XRF spectra of the analyzed locations.

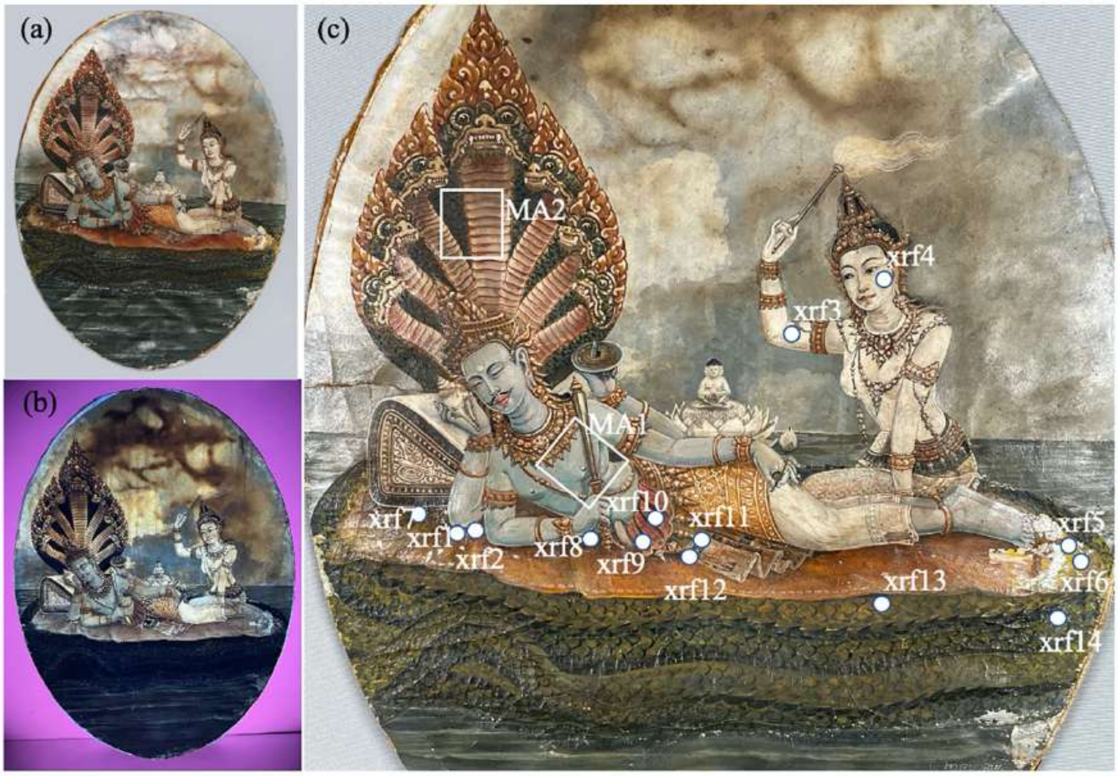

Figure 2. (a) the painting under visible (b), UV light illumination (b), and (c) XRF inspected locations.

RESULT AND DISCUSSION

Visual exam and UV Light

Following usual practice, the painting was first observed under UV light. Figure 2a and 2b compare the images under the examination with UV light and visible light. Results clearly present the sky areas that were likely exposed to smoke.

X-ray Fluorescence

The XRF results are presented in the Table 1, arranged by color. The characteristic elements for different pigments are given in bracelets where they are mentioned. Figure 3 shows the characteristic XRF spectra of the ground layer, white, yellow, and red color, while the XRF spectra of dark blue, dark brown, and green are presented in the Figure 4.

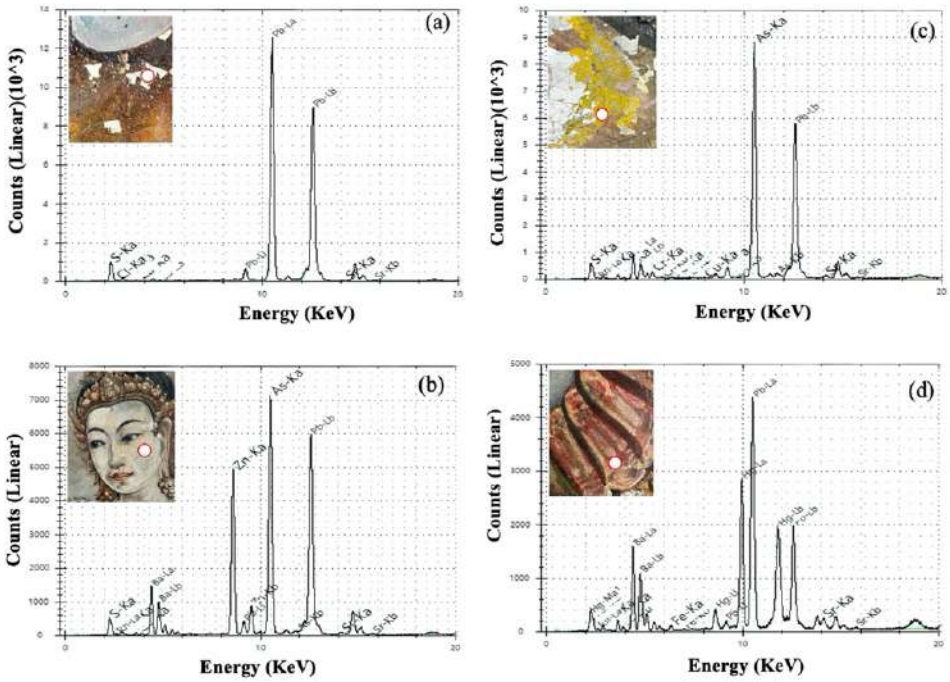

Figure 3. Details of visible images and spectra features of paints denoted as (a) ground, (b) white, (c) yellow, and (d) red.

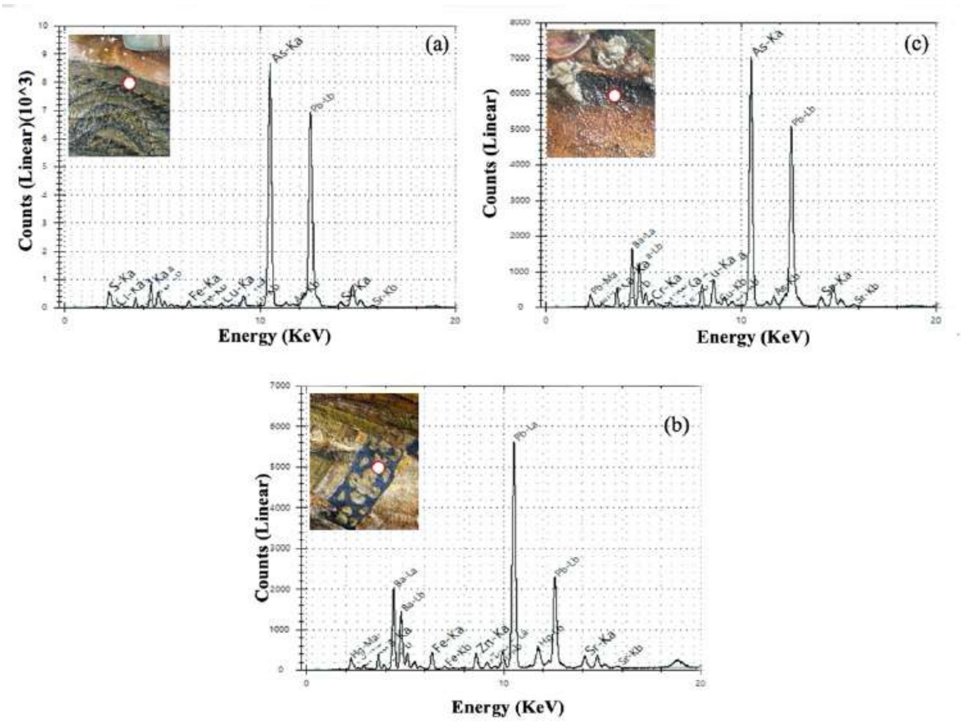

Figure 4. Details of visible images and spectra features of paints denoted as (a) green, (b) dark blue, and (c) dark brown.

Ground layer: For the ground layer measurement, the point mode was carried on the cracked areas of the paints (xrf1 and xrf2 of the Figure 2c). Figure 3a presents the visible image denoted as ground and strong signals of Pb. Thus, the lead white ($2PbCO_3.Pb(OH)_2$) is highly considered as the preparatory layer in this painting. The use of lead white as white pigment and preparatory layer is common for that time period [9]. Lead white was locally available in Thailand, Malaya and the Philippines through Chinese intra-Asian trade as evidenced by export records in early nineteenth-century texts in the Hong Kong Daily Press [9]. Literature and interviews also support the supply of Chinese lead white for traditional Thai mural painting. Furthermore, lead white was identified in the panel painting study which revealed that local church records indicated it was imported, most likely from China [9].

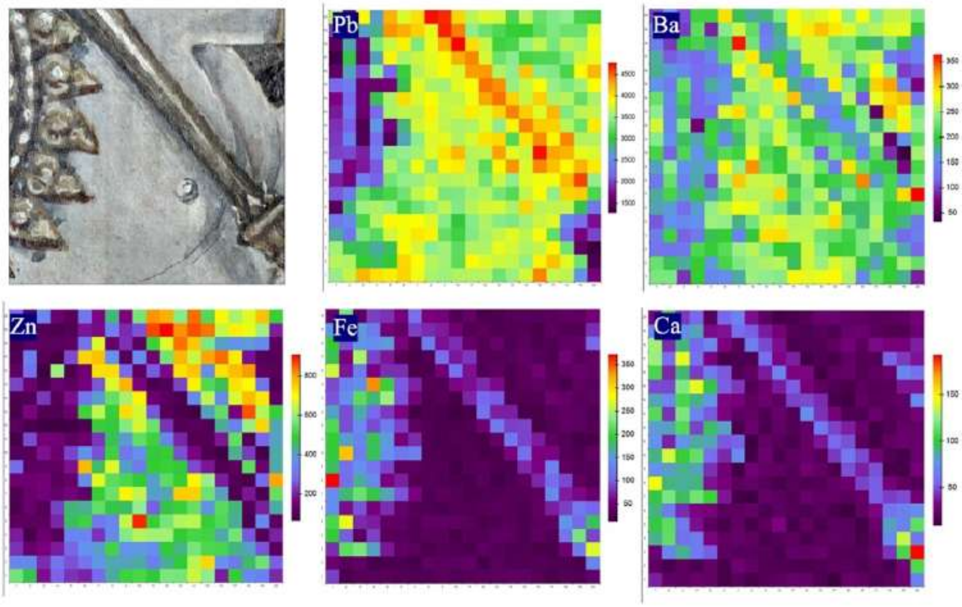

Figure 5. The mapping analysis results of the MA1 location.

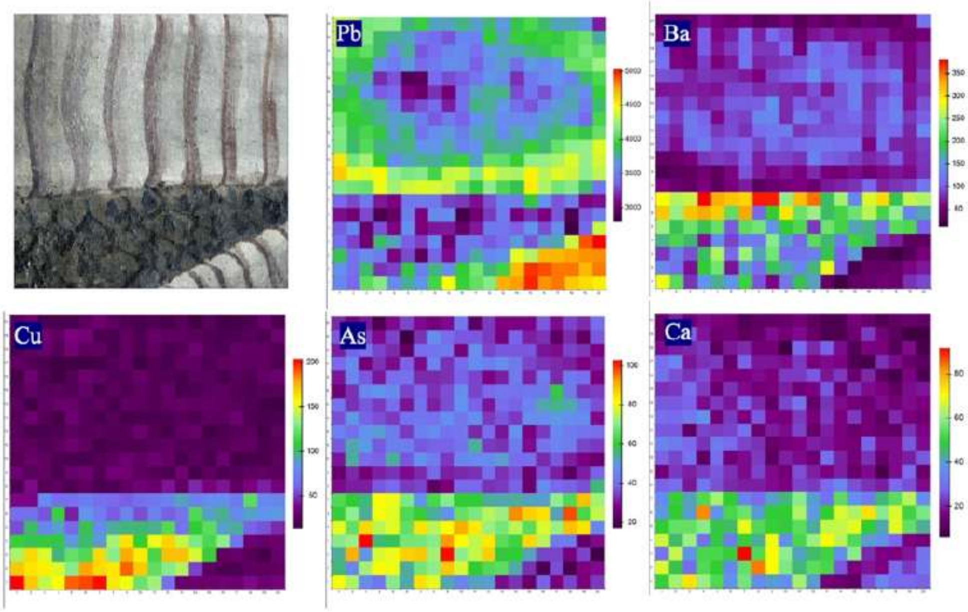

Figure 6. The mapping analysis results of the MA2 location.

Table 1: The table presents the detected elements found in different colors, related to possible pigments applied (with its chemical composition).

color		Location no.	detected elements *major; **minor; (tr) trace	Possible pigment applied	Chemical composition
ground		xrf1	*Pb, S; tr(Fe, Cl, Ca, Ba, Fe, Sr, Zn)	Lead white (Pb)	$2PbCO_3.Pb(OH)_2$)
		xrf2	*Pb, S; tr(Cl, Ba, Ca, Sr)	Lead white (Pb)	$2PbCO_3.Pb(OH)_2$)
white		xrf3	*Pb, Zn; **Ba; tr(As, S, Fe, Ca, Cl)	Lead white (Pb), zinc white (Zn)?, Lithopone white (Zn, Ba)	$2PbCO_3.Pb(OH)_2$), ZnO?, BaSO4·ZnS
		xrf4	*Pb, Zn; **Ba; tr(Ca, Sr, As)	Lead white (Pb), zinc white (Zn)?, Lithopone white (Zn, Ba)	$2PbCO_3.Pb(OH)_2$), ZnO?, BaSO4·ZnS
Yellow		xrf5	*Pb, As; tr(S, Ba, Cl, Ca, Cr, Fe)	Realgar (As), or Orpiment (As)	(AsS, As_2S2 or As_4S_4), As_2S_3.
		xrf6	*Pb, As; tr(S, Ba, Cl, Ca, Cr, Fe)	Realgar (As), or Orpiment (As)	(AsS, As_2S_2 or As_4S_4) ,As_2S_3.
Dark brown		xrf7	*Pb; **Ba, Fe; tr(Zn, Hg, Ca, Sr)	Brown ochre (Fe)	Fe_2O_3
		xrf8	*Pb, **Ba, Fe; tr(As, Ca, Fe, Sr, Zn)	Brown ochre (Fe)	Fe_2O_3
red		xrf9	*Hg, Pb; **Ba; tr(Fe, Ca, Sr)	Vermillion (Hg)	HgS
		xrf10	*Hg, Pb; **Ba; tr(Fe, Ca, Sr)	Vermillion (Hg)	HgS
Dark blue		xrf11	*Pb; **Ba; tr(Hg, S, Ba, Ca, Cr, Cu, Cl)	Unable to identify by XRF	-
		xrf12	*Pb; **Ba; tr(Hg, S, Ba, Ca, Cr, Cu, Cl)	Unable to identify by XRF	-
green		xrf13	*As, Pb; tr(Ba, Cu, Zn, Cr, Ca, Sr, Cl)	Copper based blue-Emeral green?	$3Cu(AsO_2)_2.Cu(CH_3COO)_2$.
		xrf14	*As, Pb; **Ba, Cu, Zn; tr(Fe, Ca, Cl)	Copper base green-Emeral green (Cu, As)? Confirmed by mapping, Emeral green	$3Cu(AsO_2)_2.Cu(CH_3COO)_2$.

Pigments

White; white color was inspected on the areas of face and arm (xrf3, xrf4) of the angel lady (Laksami), the results showed the presence of strong signals of lead and zinc (Figure 3b). Barium was also significantly found. Lead white ($2PbCO_3.Pb(OH)_2$), zinc white (ZnO), and lithopone white ($BaSO_4.ZnS$) could considerably be in the white areas [10]. Presenting of arsenic could be considered as interference of arsenic-base pigments used in this painting. Thanks to mapping mode analysis for further clarification about doubted white pigments. Mapping results showed that Pb, Zn, and Ba clearly present in the same areas (Figure 5). Thus, white pigments on this painting are lead white and lithopone white. In addition, mapping results (Figure 6) suggest that lead white and lithopone white were not applied in all same areas.

Yellow; The point of xrf5 and xrf6 represented the yellow color. Presenting of strong Pb, As, and trace of S, Ba, Cl, Ca, Cr, and Fe is shown in Figure 3c and Table 1. As and S could considerably be coming from of orpiment (AsS, As_2S_2 or As_4S_4) or realgar (As_2S_3) [11]. Pb is highly possible as the lead white of the preparatory layer. However, considering the color hue that appears as yellow other than orange, orpiment is believed to be in the pallet. Orpiment or yellow sulphide of arsenic is used for bright yellow or gold, while realgar or red sulphide of arsenic is for bright reds. These both pigments were used since the 16th century BC and continued in use until the 19th century [12].

Red; the analysis of the red color shows the presence of Hg, Pb, Ba, and trace of Fe, Ca, Sr ((Table 1 and Figure 3d). Considering the strong peaks of Hg and hue of red color, vermillion (HgS) is highly believed to be applied for the red areas, while Pb is considerably coming from the lead white of the preparatory layer. Vermillion or cinnabar is called "chard" in Thai, is the brilliant red color. Chard color is not only popular in Thai art but also art throughout Southeast [13].

Green; the characteristic chemical elements obtained from green areas, at the Naka's skin (xrf13, xrf14) present clear As, Pb, Ba, Cu, and trace of Zn, Cr, Ca, Sr, Cl, as shown in the Figure 4a. Presenting of clear Cu identified the pigment as copper-based ones. Finding arsenic and copper in the green could be identified as either the emerald green (copper (II)-acetoarsenite: $3Cu(AsO_2)_2.Cu(CH_3COO)_2$ [10]) or copper based-green pigments mixed with orpiment. Thanks to the mapping mode analysis that confirm these results that As and Cu presented in the same area (Figure.6). Thus, it is highly possible that the green is the emerald green. The green pigment was probably first commercially produced in Austria in 1914, and was used until the 1960s [12].

Dark blue; spectra of point selected in dark blue color show strong peaks of Pb and As, and the trace of S, Ba, Ca, Cr, Cu, Cl (Figure 4b and Table 1). Elements presented in this blue are not considered as blue pigments. Pb, As, and Cu were likely contamination of white and green. Thus, the dark blue is potentially identified as an organic pigment which is unable identify by XRF technique.

Dark brown; spectra of points selected in the dark brown color (xrf7, xrf8) presented strong signal of Pb, Ba, Fe and trace of Zn, Hg, Ca, and Sr (Figure. 4c). Clear peak of Fe identified the pigment applied as brown ochre (Fe_2O_3), this investigation is supported by mapping analysis results (Figure.5) that Fe clearly presented in brown areas. Ca is probably coming from black that was mixed with brown to make it darker.

CONCLUSION

The painting "Narai Bantomsin, 1934" of Phra Dhevabhinimmit was analyzed by portable micro-XRF. XRF provided substantial information about the materials present in the paintings. Six colors; white, yellow, red, green, dark blue, dark brown, and preparatory layer in the paintings; were focused and presented in this paper. The results reported the use of lead white as the ground layer and white pigment, lithopone white, orpiment, brown ochre, vermillion red, emeral green, and another organic dark blue.

ACKNOWLEDGEMENT

The authors gratefully acknowledge the private art collectors, Piriya Vachajitpan, the founder and committee of Thai Art Collector Association (TACA), the CEO of The Art Auction Center who gave permission for the analyses of the painting. The authors would also like to thank the Robert Bougrain, director of Restaurateurs Sans Frontières Laboratory, Studio for art conservation and restoration and the restorers for all support.

REFERENCES

1. Tuanan, (17 March 2022) Dheva Shine Narai Bantomsin. Anurak Magazine. https://www.anurakmag.com/art-and-culture/03/17/2022/เทวา-ฉาย-นารายณ์บรรทมสินธุ์

2. Golden Jubilee Art Celebration Committee and Rama IX Aat Museum Foundation. Art in the reign of Rama IX, on the occasion of the 50th Anniversary of HM King Bhumibol Adulyadej's Accession to The Throne. (1996). volume 1 plate 1-258 page 43 Phra Thewaphinimmit Navachaya, 1934. ISBN 974-89782-5-7.

3. Mukdamanee, V., Thaothong, P., Tantisuk, P., Boonma, M., Isaradej, M., Piromrak, A., Krue-on, S., Chumwong, T., & Srisukprasert, T., (1998). Rattanakosin Art: The reign of King Rama 1-VIII. Amarin Printing and Publishing Public Company Limited. Page 234. ISBN .974-600-575-8.

4. Molari, R., & Roberto, A. (2021). Pigment analysis in four paintings by Vincent van Gogh by portable X-ray fluorescence (XRF). *Radiation Physics and Chemistry*, 181 109336.
5. Kriznar, A., Muñoz, M.V., F, de la Paz., Respaldiza, M. A., & Vega, M. (2008). Non-Destructive XRF Analysis of Pigments in a 15th Century Panel Painting. 9th Int. *Conference on NDT of Art 2008.* Jerusalem, Israel, May 2008. https://www.ndt.net/?id=6125 p25.
6. Vornicu, N., Geba, M., & Bibire, C. (2009). Non-destructive analysis in a study of the religious art objects. *Journal of Physics: Conference Series, 182, PROCESSES IN ISOTOPES AND MOLEKULS 24-26 September, 2009, Cluj-Napoca, Romania.* doi: 10.1088/1742-6596/182/1/012044.
7. Serafima, S., Duliu, O.G., Manea, M.M., Niculescu, G. (2016). FTIR, XRF and optical microscopy analysis of the painting layer of an early 19th century icon. *Romanian Reports in Physics, 68 (1), 191–202, 2016.*
8. Kriznar, A., Maria del Valme Muñoz**,** Respaldiza, M.A., and Vega, M. (2012) Materials applied in Bernardo Martorell's painting analysed by portable XRF**.** *ArcheoSciences.36.*37-46.
9. Tse, N., & Sloggett, R. (2008). Southeast Asian Oil Paintings: Supports and Preparatory layers. Preparation for painting: the artist's choice and its consequence, *Archetype Publications*.pp.161-170.
10. Molari, R., & Roberto, A. (2021). Pigment analysis in four paintings by Vincent van Gogh by portable X-ray fluorescence (XRF). *Radiation Physics and Chemistry*, 181 109336.
11. Brocchieri, J., Viguerie, L.D., Sabbarese, C., & Boyer, M. (2020). Combination of noninvasive imaging techniques to characterize pigments in Buddhist thangka paintings. *X-Ray Spectrom.* 1–12. DOI: 10.1002/xrs.3189.
12. Barnett, J.R., Miller, S., & Pearce, M. (2006). Colour and art: A brief history of pigments. *Optics & Laser Technology.* 38, 445–453
13. (October 29, 2019) What is Thai Painting, Royal Thai Art International Co., Ltd https://doi.org/10.4000/archeosciences.3712.

CHROMATIC BIO-INDICATORS OF BIOFILM COMMUNITY STRUCTURE ON STONE HERITAGE

Beatrice Sarti[1]*, Federica Villa[2], Francesca Cappitelli[2], Alessandro Rizzi[1]

[1] *Department of Computer Science, University of Milan, Italy.*
[2] *Department of Food, Environmental and Nutritional Sciences, University of Milan, Italy.*

*Corresponding author: Beatrice Sarti beatrice.sarti@unimi.it

ABSTRACT

Colorful microorganisms in form of subaerial biofilms (SABs) colonize the surfaces of outdoor stone monuments worldwide. These colored patinas, beyond being an esthetic issue, could indeed have a deteriorative, neutral, or even bio-protective role for the stone. Since color is the hallmark of all SABs, we argue that the SAB spectral reflectance can be a way to obtain information on the effect of a SAB on the underlying stone. To this end, the funded project "CHROMA(Bio)" wants to develop a simple decision-making tool based on SABs' spectral profiles (the color) to guide heritage professionals in making the appropriate choice to remove or keep the SABs on lithic surfaces. Thus, the color fingerprints of SABs can be used as a (bio)indicator of SH susceptibility, being associated with the deteriorative, neutral, and bioprotective roles of the biofilms.
Knowing the composition of a SAB is the first step in understanding the effects it can have on the lithic substrate. The correlation between color and SABs has been widely studied to analyze early biological colonization, substrate bio-receptivity, and to evaluate the effectiveness of stone-cleaning treatments. However, the main studies from the literature are all performed through the CIELAB color space coordinate system, and classical colorimetry may be insufficient to obtain precise compositional information. As far as we know, nobody has used spectral reflectance data to obtain information on the composition of the SAB community. The present work describes this approach, presenting studies about the correlation between the structure of the active bacterial community and the reflectance spectra of SABs. Preliminary results from a measurement campaign on tombstones are here presented. For each SAB sampled on different graves, we acquired the reflectance spectra and collected biomass for the analysis of the metabolically active bacterial community. Even though more in-depth studies need to be performed, the preliminary statistical analysis suggests a correlation. The proof of concept about the correlation between spectral reflectance and SAB community composition can be the starting point for a more in-depth evaluation of the role of the SAB on the lithic substrate, which will serve as a bioindicator for heritage professionals to determine the SABs' impacts on the stone.

Keywords: Sub-aerial biofilm (SAB), Biodeterioration, Bioprotection, Bacterial community, Reflectance Spectra.

INTRODUCTION

Outdoor historic stone buildings and sculptures often exhibit colorful patinas on their surface [1]. These biological patinas, known as subaerial biofilms (SABs), are complex microbial communities embedded in an extracellular polymeric matrix and located at the stone-air interface. Beyond being an esthetic issue, these biological colonies also have interactions with the lithic substrates of the cultural heritage. However, this interaction could be not only biodeteriorative as is frequently thought, but also neutral or even protective for the stone heritage [2–7].

The assessment of the SABs' role on the stone is complex, expensive and time-consuming. It requires multidisciplinary and costly analyses that combine molecular investigations of SABs with accurate evaluations of the state of conservation of the lithic substrates [8]. Traditional conservation strategies are currently based on the removal of SABs from artistic surfaces without any evaluation of the SAB's actual impacts on the substrate [9]. However, the surface damage brought on by cleaning procedures is irreversible, and the common cleaning chemicals are dangerous to both people and the environment and could promote recolonization by more resistant microorganisms [10]. The funded project "CHROMA(Bio)" wants to develop a simple decision-making tool based on SABs' spectral profiles (the color) to guide heritage professionals in making the appropriate choice to remove or keep the SABs on lithic surfaces. Thus, the color fingerprints of SABs can be used as a (bio)indicator of SH susceptibility, being associated with the deteriorative, neutral, and bioprotective roles of the biofilms.

The first step in understanding the SAB's role on the lithic substrate is studying the structure and composition of the microbial community. Our research is placed in this context. In particular, in this study, we wanted to lay the basis to correlate the SAB's spectral profile with the structure and composition of its bacterial community. This idea derives from the fact that color is an indicator of the physiology and activity of the microbial community [11–13]. To determine the correlation between color and SAB composition, we analyzed the reflectance spectra of some SABs along with their metabolically active bacterial community inhabiting different tombstones.

The correlation between color and SABs has been widely studied to analyze early biological colonization [14–16], substrate bio-receptivity [17, 18], and to evaluate the effectiveness of stone cleaning treatments [19, 20]. However, the main studies from the literature are all performed through the CIELAB color space coordinate system, and classical colorimetry may be insufficient to obtain precise compositional information. As far as we know, nobody has used spectral reflectance data to obtain information on the composition of the SAB community.

The proof of concept about the correlation between spectral reflectance and SAB community composition can be the starting point for a more in-depth evaluation of the role of the SAB on the lithic substrate, which will serve as a bioindicator for heritage professionals to determine the SABs' impacts on the stone.

METHODOLOGY

Six tombstones were sampled in November 2021 for a total of seven subaerial biofilms (Table 1). Sampling points were chosen on each tombstone in areas where the visible patinas appeared relatively uniform. For each point, both spectral and biological information was acquired. For control and future work purposes, reflectance spectra were also collected from areas of the stone surfaces that displayed no visual colonization.

Table 1. Summary of the samples acquired

ID	SAB color and description	Tombstone color
92Gr	Olive green with a hint of gray, uneven texture	Light pinkish-gray texture with small black inclusions of small size, the overall color sensation is light gray
133Br	Dark brown/black with a hint of reddish-violet, uniform and not crusty texture	Light gray texture with small black inclusions of small, the overall color sensation is gray
133Gr	Dark grayish-green, uneven texture	Light gray texture with small black inclusions of small, the overall color sensation is gray
395Gr	Light green, uneven texture with a dusty appearance in some areas.	Black texture with big white inclusions, the overall color sensation is gray
407Gr	Green, uneven texture	Black texture with big white inclusions, the overall color sensation is gray
412Bl	Dark black/gray, uneven texture	Light gray texture
413Gr	Light green, uneven crusty texture	Dark pinkish-claret texture

Color sampling

Reflectance spectra were acquired in situ with the CM-2600d portable spectrophotometer by Konica Minolta. The instrument was configured to measure a 3 mm diameter area, including the UV component and in the spectrum calculation, and performing the acquisitions in SCE (Specular Component Excluded) mode, which accounts for the subtraction of the specular reflection component of the illuminant from the sample's reflected light. Each spectrum was obtained by averaging three consecutive measurements.

SAB sampling, RNA extraction and sequencing analysis

SAB samples were collected using sterile swabs and were immediately processed for RNA extraction. RNA was extracted using the RNeasy PowerBiofilm Kit (Qiagen), following the manufacturer's instructions. After reverse transcription (Reverse Transcription Kit, Qiagen), high-throughput sequencing analysis of the bacterial 16S rRNA gene's V3-V4 region was performed using the MiSeq platform (Illumina) with v3 chemistry, generating 2 x 300 paired-end reads. The primers CS1_341F and CS2_806R were used for the amplification [21]. Raw sequencing data were processed and analyzed using QIIME2 and DADA2 to pre-process, quality filter, trim, de-noise, pair, and model the reads. Chimeric sequences were detected using the consensus method [22], and the remaining sequences were clustered into operational taxonomic units (OTUs). Taxonomic assignments were performed using a Naïve-Bayes classifier trained on the SILVA database [23].

Diversity and statistical analyses

All the analyses were performed in Python using *colour* (https://www.colour-science.org/) and *scikit-bio* (http://scikit-bio.org/) packages. The Principal Coordinate Analysis (PCoA) were performed on both spectral and biological data, calculating the dissimilarity matrix with the Euclidean and Bray-Curtis distances respectively. K-mean method was then used to cauterize the data.

RESULT AND DISCUSSION

The reflectance spectra of green biofilms (Figure 1a) exhibit variations in both the shape and intensity of their respective peaks, with discrepancies not exceeding 10%. Among the green SABs, sample 395V exhibits the most pronounced spectrum divergence. Similarly, the spectral profiles of brown and black samples (Figure 1b) have similar intensities (with a maximum difference of 6%), yet they differ in in the presence of a peak centered around 565 nm, which is absent in brown sample 133M.

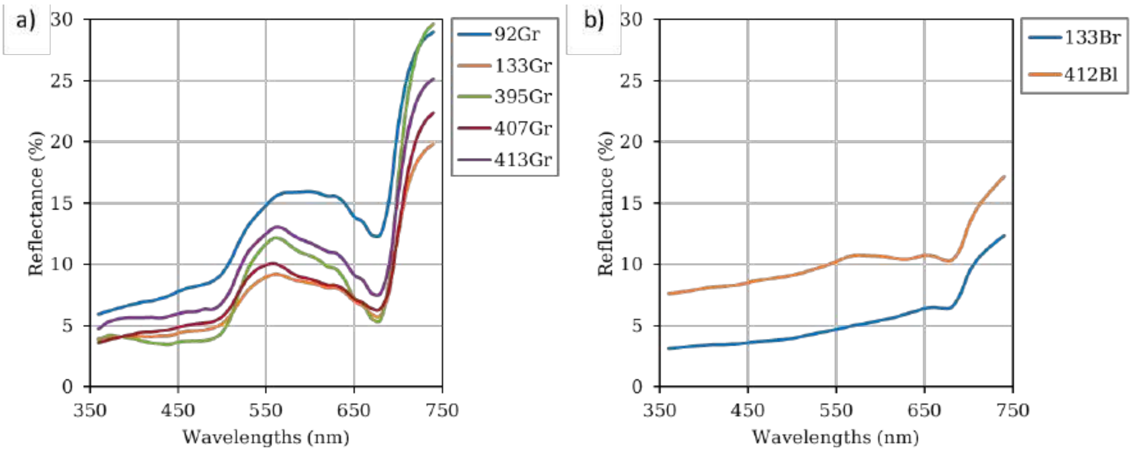

Figure 1. Reflectance stectra of (a) green SABs and (b) black/brown SABs

Figure 2 shows the composition of the bacterial community at the Phylum level. The bacterial communities associated with the stone surfaces are predominantly composed of microorganisms belonging to the phyla Cyanobacteria, Proteobacteria, Deinococcus-Thermus, and Planctomycetes. These phyla play fundamental ecological roles in the community's survival on the stones: Cyanobacteria supply carbon through photosynthesis, Proteobacteria aid in biofilm formation for community cohesion and water retention, Deinococcus-Thermus confer high UV radiation tolerance [24], while Planctomycetes ensure adaptation to a wide range of habitats, including extreme environments [25]. At lower taxonomic levels, the microbial composition exhibits notable variation among different samples: despite sharing similar colors, the majority of SABs possess distinct compositions (results not shown).

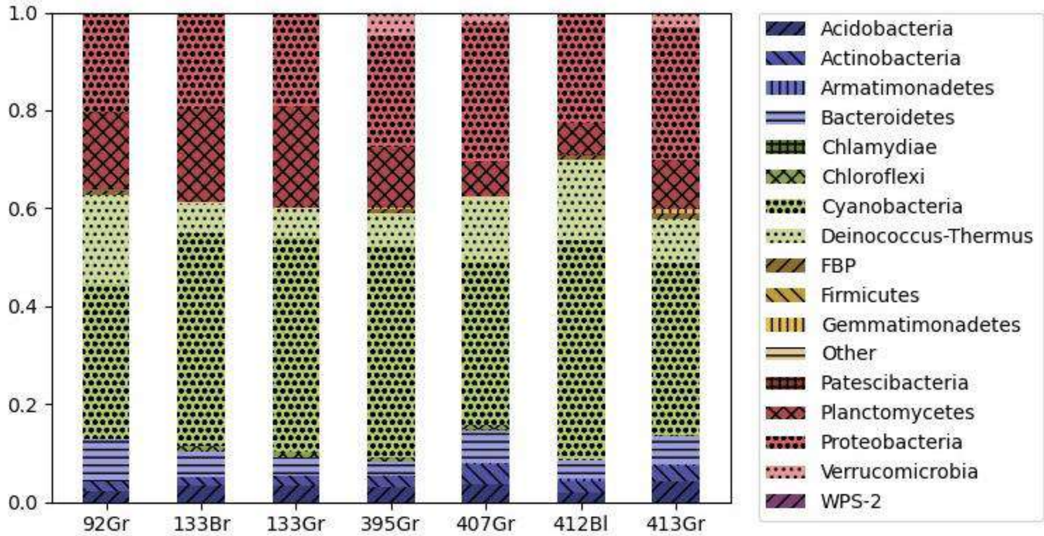

Figure 2. Relative abundance of the major phyla identified in bacterial communities from the biofilms grown on the tombstones.

Figure 3 shows the results of the PCoA analysis for both the spectral information and the composition of the bacterial community at the genus level. The samples exhibit the same categorization of clusters in both datasets, suggesting that a correlation between spectral and biological information exists.

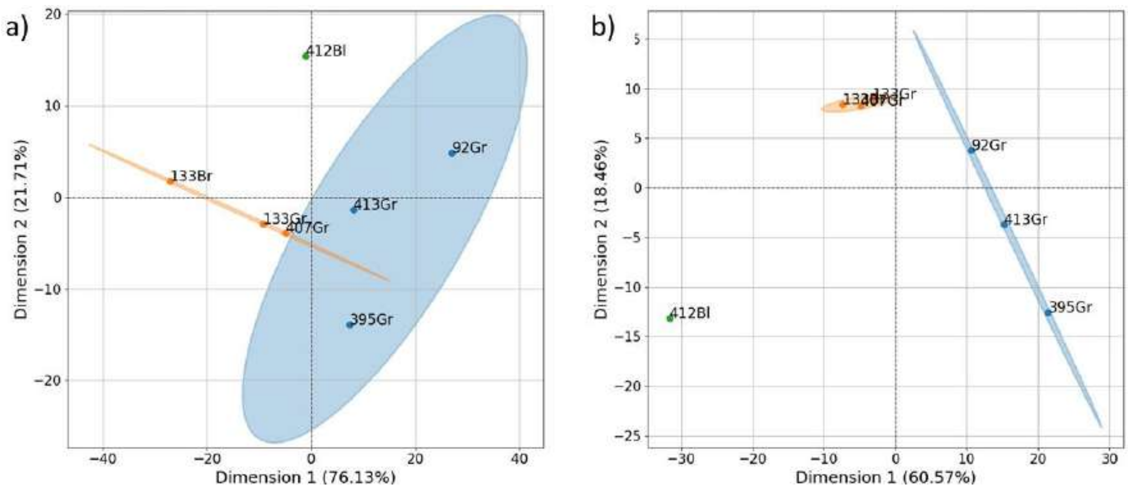

Figure 3. PCoA results for (a) the reflectance spectra and (b) the metabolically active bacterial community at genus level.

It is important to emphasize that these findings represent preliminary results, and further comprehensive investigations are necessary. Future research should investigate the influence of tombstones on spectral acquisition, aiming to refine our understanding of this interplay. Additionally, efforts should be directed towards developing a robust correlation model, enabling the prediction of microbial composition starting from the reflectance acquisition in the visible region of the SABs color. Such endeavors promise to advance our comprehension of these complex relationships and their potential applications in heritage conservation practices.

CONCLUSION

In this paper, we investigated whether the biofilm spectral reflectance can be linked to the SAB's community structure and composition. The proof of concept about the correlation between spectral reflectance and SAB community composition can be the starting point for a more in-depth evaluation of the role of the SAB on the lithic substrate, which can support heritage specialists in deciding whether to remove or leave the microbial colonies from the stone surfaces. These preliminary results seem to be promising for this correlation, but more in-depth studies need to be performed.

ACKNOWLEDGEMENT

This work is part of the project "CHROMA(Bio)" - Spectral reflectance profiles of colored subaerial biofilms as indicators of stone heritage susceptibility to biodeterioration - MUR PRIN 2022 - LS9

REFERENCES

1. Villa, F., Wu, Y.-L., Zerboni, A., & Cappitelli, F. (2022). In Living Color: Pigment-Based Microbial Ecology At the Mineral–Air Interface. *BioScience*, *72*(12), 1156–1175. https://doi.org/10.1093/biosci/biac091
2. Gulotta, D., Villa, F., Cappitelli, F., & Toniolo, L. (2018). Biofilm colonization of metamorphic lithotypes of a renaissance cathedral exposed to urban atmosphere. *Science of The Total Environment*, *639*, 1480–1490. https://doi.org/10.1016/j.scitotenv.2018.05.277
3. Coombes, M. A., Viles, H. A., & Zhang, H. (2018). Thermal blanketing by ivy (Hedera helix L.) can protect building stone from damaging frosts. *Scientific Reports*, *8*(1), 9834. https://doi.org/10.1038/s41598-018-28276-2
4. Sanmartín, P., Villa, F., Cappitelli, F., Balboa, S., & Carballeira, R. (2020). Characterization of a biofilm and the pattern outlined by its growth on a granite-built cloister in the Monastery of San Martiño Pinario (Santiago de Compostela, NW Spain). *International Biodeterioration & Biodegradation*, *147*, 104871. https://doi.org/10.1016/j.ibiod.2019.104871
5. Gadd, G. M., & Dyer, T. D. (2017). Bioprotection of the built environment and cultural heritage. *Microbial Biotechnology*, *10*(5), 1152–1156. https://doi.org/10.1111/1751-7915.12750
6. Liu, X., Koestler, R. J., Warscheid, T., Katayama, Y., & Gu, J.-D. (2020). Microbial deterioration and sustainable conservation of stone monuments and buildings. *Nature Sustainability*, *3*(12), 991–1004. https://doi.org/10.1038/s41893-020-00602-5
7. Villa, F., Ludwig, N., Mazzini, S., Scaglioni, L., Fuchs, A. L., Tripet, B., … Cappitelli, F. (2023). A desiccated dual-species subaerial biofilm reprograms its metabolism and affects water dynamics in limestone. *Science of The Total Environment*, *868*, 161666. https://doi.org/10.1016/j.scitotenv.2023.161666
8. Favero-Longo, S. E., & Viles, H. A. (2020). A review of the nature, role and control of lithobionts on stone cultural heritage: weighing-up and managing biodeterioration and bioprotection. *World Journal of Microbiology and Biotechnology*, *36*(7), 100. https://doi.org/10.1007/s11274-020-02878-3
9. Pinna, D. (2017). *Coping with Biological Growth on Stone Heritage Objects: Methods, Products, Applications, and Perspectives*. CRC Press.

10. Villa, F., Gulotta, D., Toniolo, L., Borruso, L., Cattò, C., & Cappitelli, F. (2020). Aesthetic Alteration of Marble Surfaces Caused by Biofilm Formation: Effects of Chemical Cleaning. *Coatings*, *10*(2), 122. https://doi.org/10.3390/coatings10020122
11. Wada, N., Sakamoto, T., & Matsugo, S. (2013). Multiple Roles of Photosynthetic and Sunscreen Pigments in Cyanobacteria Focusing on the Oxidative Stress. *Metabolites*, *3*(2), 463–483. https://doi.org/10.3390/metabo3020463
12. Martin-Cerezo, M. L., Garcia-Lopez, E., & Cid, C. (2015). Isolation and Identification of a Red Pigment from the Antarctic Bacterium Shewanella; frigidimarina. *Protein and Peptide Letters*, *22*(12), 1076–1082. https://doi.org/10.2174/0929866522666150915122247
13. Suresh, M., Renugadevi, B., Brammavidhya, S., Iyapparaj, P., & Anantharaman, P. (2015). Antibacterial Activity of Red Pigment Produced by Halolactibacillus alkaliphilus MSRD1—an Isolate from Seaweed. *Applied Biochemistry and Biotechnology*, *176*(1), 185–195. https://doi.org/10.1007/s12010-015-1566-6
14. Prieto, B., Rivas, T., & Silva, B. (2002). Rapid Quantification of Phototrophic Microorganisms and their Physiological State through their Colour. *Biofouling*, *18*(3), 237–245. https://doi.org/10.1080/08927010290014917
15. Sanmartín, P., Vázquez-Nion, D., Silva, B., & Prieto, B. (2012). Spectrophotometric color measurement for early detection and monitoring of greening on granite buildings. *Biofouling*, *28*(3), 329–338. https://doi.org/10.1080/08927014.2012.673220
16. Vázquez-Nion, D., Silva, B., Troiano, F., & Prieto, B. (2017). Laboratory grown subaerial biofilms on granite: application to the study of bioreceptivity. *Biofouling*, *33*(1), 24–35. https://doi.org/10.1080/08927014.2016.1261120
17. Vázquez-Nion, D., Silva, B., & Prieto, B. (2018). Influence of the properties of granitic rocks on their bioreceptivity to subaerial phototrophic biofilms. *Science of The Total Environment*, *610–611*, 44–54. https://doi.org/10.1016/j.scitotenv.2017.08.015
18. Vázquez-Nion, D., Silva, B., & Prieto, B. (2018). Bioreceptivity index for granitic rocks used as construction material. *Science of The Total Environment*, *633*, 112–121. https://doi.org/10.1016/j.scitotenv.2018.03.171
19. Sanmartín, P., Villa, F., Silva, B., Cappitelli, F., & Prieto, B. (2011). Color measurements as a reliable method for estimating chlorophyll degradation to phaeopigments. *Biodegradation*, *22*(4), 763–771. https://doi.org/10.1007/s10532-010-9402-8
20. Pozo-Antonio, J. S., Montojo, C., López de Silanes, M. E., de Rosario, I., & Rivas, T. (2017). In situ evaluation by colour spectrophotometry of cleaning and protective treatments in granitic Cultural Heritage. *International Biodeterioration & Biodegradation*, *123*, 251–261. https://doi.org/10.1016/j.ibiod.2017.07.004
21. Rapin, A., Pattaroni, C., Marsland, B. J., & Harris, N. L. (2017). Microbiota Analysis Using an Illumina MiSeq Platform to Sequence 16S rRNA Genes. *Current Protocols in Mouse Biology*, *7*(2), 100–129. https://doi.org/10.1002/cpmo.29
22. Callahan, B. J., McMurdie, P. J., Rosen, M. J., Han, A. W., Johnson, A. J. A., & Holmes, S. P. (2016). DADA2: High-resolution sample inference from Illumina amplicon data. *Nature Methods*, *13*(7), 581–583. https://doi.org/10.1038/nmeth.3869
23. Quast, C., Pruesse, E., Yilmaz, P., Gerken, J., Schweer, T., Yarza, P., … Glöckner, F. O. (2013). The SILVA ribosomal RNA gene database project: improved data processing and web-based tools. *Nucleic Acids Research*, *41*(D1), D590–D596. https://doi.org/10.1093/nar/gks1219
24. Kiel, G., & Gaylarde, C. C. (2006). Bacterial diversity in biofilms on external surfaces of historic buildings in Porto Alegre. *World Journal of Microbiology and Biotechnology*, *22*(3), 293–297. https://doi.org/10.1007/s11274-005-9035-y
25. Lage, O. M., & Bondoso, J. (2014). Planctomycetes and macroalgae, a striking association. *Frontiers in Microbiology*, *5*. https://doi.org/10.3389/fmicb.2014.00267

BEAUTY OF COLOUR IN THE LIGHT AND THE SHADE OF JAPANESE TRADITIONAL NOH COSTUME

Masayuki Osumi[1]*

[1]*Office Color Science Co., LTD., Japan.*

*Corresponding author: Masayuki Osumi, masayuki-osumi@nifty.com

ABSTRACT

NOH costume measurement was performed on two representative sites, and was performed at three different angles with respect to the sample plane vertical direction. The lighting direction is assumed to be illuminated from the side with respect to the trunk axis, considering the actual NOH stage. CIELAB values were obtained from the spectral imaging measurement results, and the distribution on the color space was shown. The entire field of view is woven with silk thread, and gold cut foil is partially used, and directional lighting is applied to the woven part, which, combined with the luminous reflection associated with the woven structure, gives a glittering impression. The chrysanthemum pattern is orange, and the unique lustrous reflection of silk is observed. The background is composed of shallow onion-colored weaves. Plotting the distribution in the CIELAB color space against the entire screen, the relationship between the four parties is clearly visible under 15° illumination. When the illumination angle is shifted from 45° to 75°, the silk threads shift in the direction of low brightness and low saturation. Moreover, in the gold cut foil, the reflection component in the specular direction decreases, and especially at 45°, the distribution amount is greatly attenuated compared to 15°, and disappeared at 75°. Furthermore, to supplement the knowledge, scraps of NOH costume were obtained and contact measurement was performed. The detail image by changing of illumination direction and 3D shape observation by focus stacking was performed by digital optical microscope (KEYENCE VHX-7000), and 3D shape measurement was also performed by KEYENCE VR-5000, and specular reflection intensity was measured by a 0/0 optical system (Spectra-2-Profiler, BYK Gardner). As a result, the specular reflection intensity of the gold cut foil part is quite high. However, the luster of silk also maintains a certain height. When a person wears a NOH costume, there are quite a few flat parts such as sleeves. In the act of rotating around the trunk, the movement of specular reflection from the fixed lighting is twice as fast as the angular velocity of the axis. That is, when the axis of the body is rotated by an angle θ, the specular reflection changes by 2θ. In this respect, there is a splendor of transition, but at the same time, to express it more beautifully, it is also necessary for the trunk to realize a solid movement. I believe that this is an important relationship between NOH dance and costumes.

Keywords: Costume, Lighting, Spectral Imaging, 3-Dimensional Measurement, Digital Microscopy

INTRODUCTION

The textures of ancient Japanese crafts, with their complex surface structures brought about by elaborate techniques and ingenuity, have been repeatedly tried and tested by many artisans, and have been elevated to a higher level of perfection. The classical performing arts, such as NOH costumes, are the essence of Japanese art. I had the opportunity to measure the specially restored costumes used in the Japan classical performing arts of NOH. In this study, we analyzed and discussed characteristics of NOH costumes based on the measurement results using gonio-photometric spectral imaging and various optical instruments. The NOH costume was restored by WATABUN Co., Ltd., a long-established manufacturer of KYOTO NISHIJIN weaving. A part of the restored costume shows the atmosphere of autumn with chrysanthemums on fence, snow flake with plums. And realized by silk vermilion, shallow onion-colored weaving, and gold cut foil used for this costume.

METHODOLOGY

The system used for the measurement consisted of a liquid crystal tunable filter (LCTF) with a bandpass transmission wavelength that can be varied as desired within the wavelength range of visible light and one frame of an image is captured at each scan wavelength. To reduce noise as much as possible, a monochrome CCD camera with Peltier cooling and anti-blooming with 16-bit output was used as the imaging sensor. The exposure time for each wavelength was optimized during calibration to adjust for differences in the spectral distribution of the light source, the spectral transmission characteristics of the LCTF, the spectral response characteristics of the CCD sensor at each wavelength to ensure efficient measurements. To enable multi-angle illumination, a light guide with a linear output end was used and the measurement wavelength was measured every 10 nm from 420 to 700 nm with a half-width of 10 nm transmission bandwidth. The monochrome CCD sensor has 772 × 580 pixels and a Peltier cooling system that can cool the photosensitive area down to below zero degree, and an anti-blooming mechanism is also provided. The light source was a white LED (CCS, Japan) with high color rendering, combining R, G, and B phosphors with ultraviolet LED excitation. Measurements were taken at two representative locations at three angles (15°, 45°, and 75°) relative to the vertical direction of the sample. The measurement field of view was approximately 32 mm × 24 mm. The direction of illumination was assumed to be from the side of the trunk axis, as in an actual NOH stage.

Figure 1. a. Restored NOH costume b. Spectral imaging system c. Measurement scene

RESULT AND DISCUSSION

Chrysanthemum pattern and hedge on a shallow green ground

Spectral imaging measurements were made on a hedge with a chrysanthemum pattern on a shallow green ground, and representative areas were picked up as rectangles in the measurement field of view to obtain the average L^* values within the range. The three areas are the chrysanthemum pattern, the shallow green ground, and the interweaving of the gold foil on the hedge. All of the L^* values decreased as the illumination angle increased. However, the degree of decrease was different for each part. The ground part did not change significantly, but the chrysanthemum pattern and the part with interwoven foil leaf on the hedge showed a significant decrease. This is a phenomenon that depends on the reflective properties of the materials, such as silk yarns and foil, and the weave structure. The CIELAB value were obtained for the entire measurement field, and their distribution in the color space is shown Figure 2. The entire field of view is woven with silk threads, giving it the unique beauty of NISHIJIN weavings. When directional illumination is applied to the woven area, it gives a shimmering impression in combination with the reflection of gold luster associated with the weave structure. The chrysanthemum pattern is orange in color, with a shiny reflection inherent to silk. In the right lower part of the field of view, a leaf pattern is decorated with green threads. When the distribution in the CIELAB color space is plotted for the entire image, the relationship among the four elements of the foil of the hedge, the chrysanthemum pattern, the leaves, and the shallow

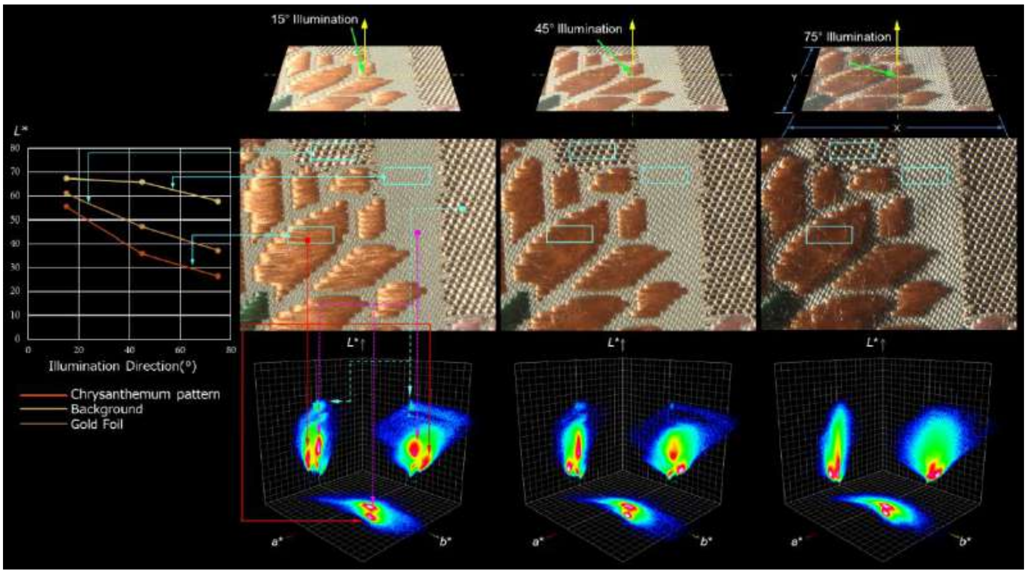

Figure 2. Spectral Imaging Measurement Results of Chrysanthemum and Fence Sites on Shallow Onion - Change in *L and CIELAB colour distribution by Illumination Angle**

green background can be clearly seen under the 15° illumination. As the illumination angle shifts from near vertical to horizontal from 45° to 75°, the design of the colored silk threads shifts toward lower brightness and lower saturation. In addition, the reflection component in the direction of normal reflection is reduced in the foil, especially at 45°, where it is significantly attenuated compared to 15°, and it is somewhat eliminated at 75°. *L** was plotted for each pixel within the rectangular area and its distribution was calculated (Figure 3). In the chrysanthemum pattern area, the rectangular area was set to include an obvious ortho reflective area, and it was confirmed that *L** was widely distributed at an illumination angle of 15°. In the chrysanthemum pattern, the silk threads are arranged in the lateral direction of the field of view, indicating direction-dependent reflection behavior. On the other hand, in the ground center of the distribution does not shift to a very low value. It can be inferred that the weave structure is such

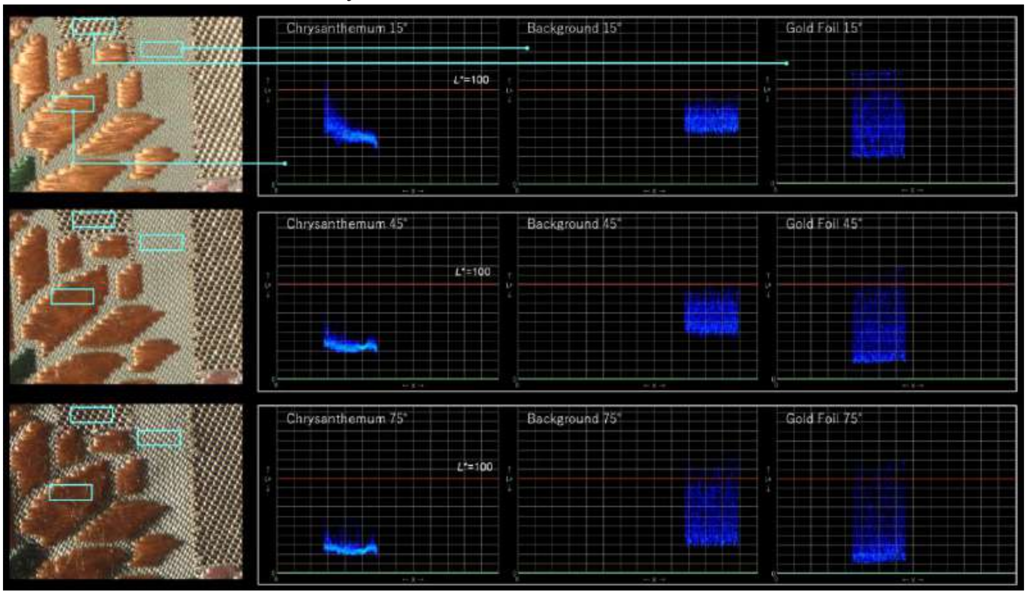

Figure 3. Spectral Imaging Measurement Results of Chrysanthemum and Fence Sites on Shallow Onion - Change in *L distribution by Illumination Angle**

that the angular change between the normal reflective area and the shaded area is balanced. In the area of the foil, the width of the distribution does not change much, or the center of the distribution shifts to a lower value, and the distribution that appears to be positive reflection in particular attenuates and disappears as the angle increases. The upper distribution at 15°

illumination is probably the result of reflections above the range of the instrument staying near the upper limit and being plotted.

Dew grass on red ground

Next, the results of the measurement of the red-ground area are described (Figure.4). The entire field of view is woven with silk threads, and when we focus on the grass and ground areas, the grass area shows a shiny reflection inherent to silk, similar to the chrysanthemum pattern described earlier. Figure 8 shows a graph of the average L^* values within the rectangular area. The L^* values of the turf pattern and the two red areas decreased as the illumination angle increased. However, the degree of decrease was different for each area, with the ground area showing no significant change, while the grass area showed a large attenuation. The overall brightness tended to decrease, but the lightness was reversed at 15° and 45°.

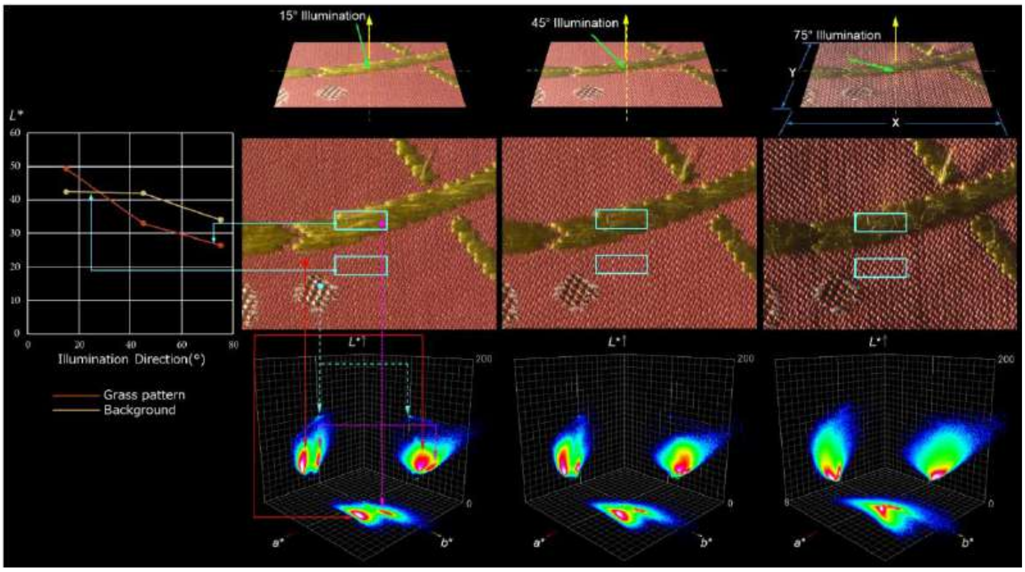

Figure 4. Spectral Imaging Measurement Results of Dew grass on red ground - Change in L^* and CIELAB colour distribution by Illumination Angle

When the distribution in CIELAB color space is plotted against the entire image, the relationship between the two is clearly visible under 15° illumination: the design of the colored silk threads

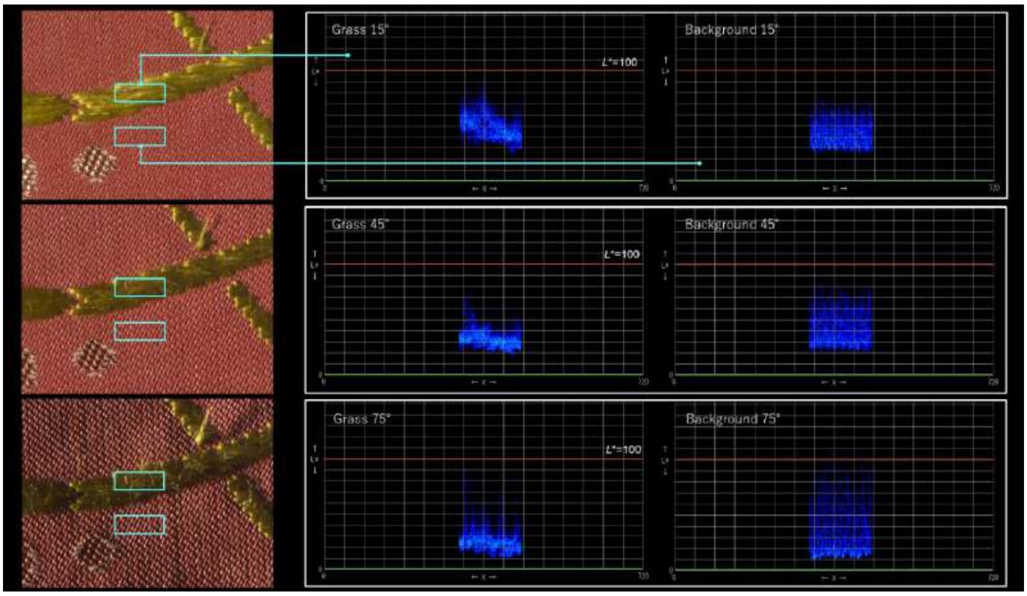

Figure 5. Spectral Imaging Measurement Results of Dew grass on red ground - Change in L^* distribution by Illumination Angle

shifts toward lower lightness and lower chroma as the illumination angle shifts from near-vertical to horizontal from 45° to 75°. The reflection component of the dewy area, a small area of the field of view, decreases in the direction of normal reflection, especially at 45°, where it is significantly attenuated compared to 15°, and at 75°, where it disappears somewhat, the same as in the dewy area of the hedge on the shallow green ground. The L^* distribution in the rectangular area shows that the L^* distribution in the grass area is widely distributed at an illumination angle of 15°, and as the illumination angle increases, the distribution range becomes narrower and the center of the distribution changes to a lower value. The silk yarns are distributed in the transverse direction of the field of view, resulting in a direction-dependent reflection behavior. On the other hand, the red area has a very different weave structure, and the width of the distribution is wider. The center of the distribution gradually shifted to lower values.

Surface profiling using an optical microscope

On the other hand, the restored object was so valuable that only non-contact, short-time, low-light measurement was allowed to minimize damage during measurement, which was quite restrictive. To supplement our knowledge, we obtained scraps of NOH costumes and performed contact measurements. The composition of the NOH costume includes a weft-weave silk painting, a weft-weave silk thread weaving, and a weft-weave foil, which is similar to the chrysanthemum design. However, the shape of the foil differs significantly from that of the restored NOH costume. Specifically, the shape and the intensity of the direct reflection were measured, and changes in the shape were observed by digital optical microscopy in accordance with the direction of illumination, 3D shape observation by DFD (Depth from Defocus), and 3D shape measurement using KEYENCE VR-5000. The results of these observations are shown in Figure 6. When the lighting conditions were changed and the observation was conducted under the side-illumination and single-illumination conditions, the changes in the area of the foil were particularly pronounced.

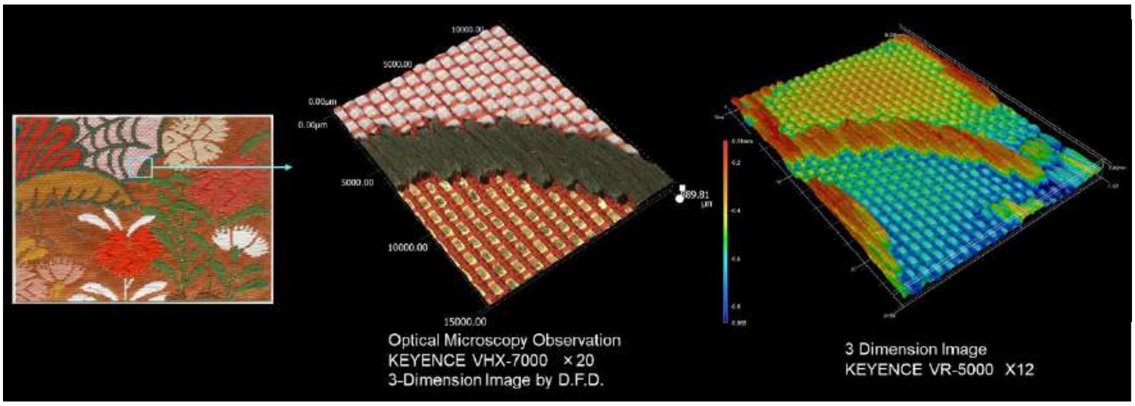

Figure 6. Fragment of NOH Costume Microscopy Observation

Measurement of reflection intensity

The 3D shape was observed using the Spectra 2 Profiler (BYK Gardner, Germany) as a contact measurement device, and the 0/0 optical system was used to measure the intensity of the direct reflections (Figure 7). The results show that the intensity of the specular reflection is considerably high in the area of the foil, and is more extreme in the case of the pattern with metallic reflections than in other areas. Therefore, when the costumes are viewed in the position of the specular reflection, the reflection of the foil is dominant. This pattern, which is often used on hedges and snow rings, is clearly visible. However, the luster of the silk also maintains a certain degree of height. This makes the outlines of the costume stand out and appeal to the viewer's eyes with a certain degree of brightness. When a person wears a NOH costume, the sleeves and other flat parts of the costume are quite flat in appearance. In a performance in which the trunk rotates on its axis, the movement of the positive reflection from the fixed illumination is twice as fast as the angular velocity of the axis. In other words, if the body axis is rotated by an angle θ, the positive reflection changes by 2θ. This is where the glimmer of fading light comes in. At the same time, however, it is necessary to achieve a firm movement of the trunk in order to express beauty. Herein lies the important relationship between NOH dance and costumes.

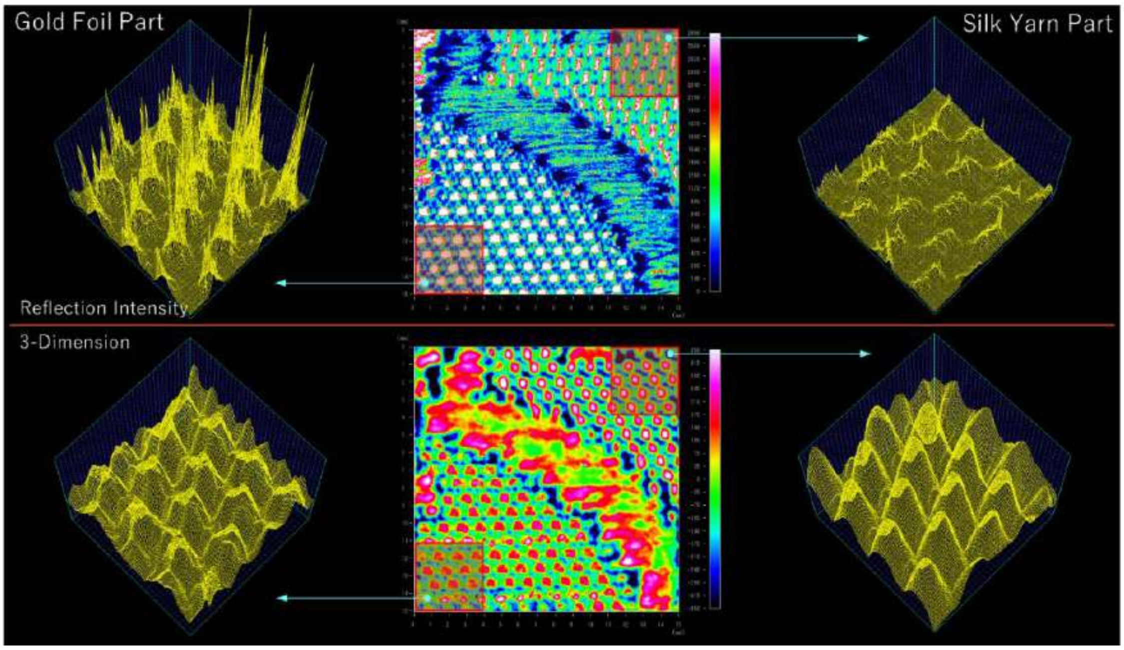

Figure 7. Measurement results of 3D shape observation and specular reflection intensity

CONCLUSION

This study was provided a unique opportunity to measure the spectral radiance of a restored NOH costume using gonio-spectral imaging. Spectral imaging measures the spectral radiance factor, which is independent of the spectral characteristics of the illumination and the sensitivity of the light-receiving sensor, and leads to the acquisition of accurate color information. Therefore, it is valuable in terms of use as a digital archive for cultural properties. On the other hand, accurate information also enables various analyses. With the angular measurement information obtained this time, it was possible to consider the characteristics of NOH costumes under various types of lighting from the viewpoint of texture. I think that in the long history of NOH, there have been many ways to make the movements of NOH costumes beautiful in light and shade, as in the case of the torchlight performance of NOH dance plays.

ACKNOWLEDGEMENT

The NOH costume to be measured was restored by WATABUN Co., Ltd. from the NISHIJIN textile and was exhibited at the 8th exhibition of the Collab Gallery at the Tokyo Polytechnic University in 2022, Colour Beauty in Shades - Japanese Tradition. We had a rare opportunity to make measurements.

REFERENCES

1. Masayuki Osumi, Recent technology of measurement in metallic pearl color. Journal of the Color Science Association of Japan. vol 33, No.1. 2009.
2. Isao Fujimoto, Study for the disperse imaging by high resolution multi spectral camera, Bulletin of Hiroshima Institute of technology, vol 44, 2010.

Session 6

Doi Wawee
29 November 2023

AUGMENTING COLOUR COMMUNICATION IN ENGLISH, GREEK AND THAI

D. Mylonas[1]*, A. Koliousis[1], J. Stutters[2], P. Katemake[3], A. Stockman[4] and R.T. Eskew Jr.[5]

[1]*Faculty of Computing, Mathematical, Engineering and Natural Sciences, Northeastern University London, UK.*
[2]*Faculty of Brain Sciences, University College London, UK*
[3]*Faculty of Science, Chulalongkorn University, Thailand.*
[4]*Institute of Ophthalmology, University College London, UK.*
[5]*College of Science, Psychology, Northeastern University Boston, US.*

*Corresponding author: Dimitris Mylonas, dimitris.mylonas@nulondon.ac.uk

ABSTRACT

The number of colour names varies across languages. To augment colour communication between speakers of different languages, we need a multilingual method to map how we perceive colours to the words we use to describe them. We evaluate the performance of a supervised colour naming model, Rotated Split Trees (RST), trained by responses from a crowdsourced colour naming experiment in English, Greek and Thai. We assess the generalizability of the model across several colour spaces where it performed best in the CIELUV. A comparison of RST with previous computational colour naming methods using independent psychophysical data in English showed that RST achieves state-of-the-art performance for basic colour categories and identifies five additional categories (n = 16) on the surface of the Munsell system. A demonstration of the performance of RST in segmenting a synthetic image across the colour gamut into colour names in English (n = 30), Greek (n = 28) and Thai (n = 46) further supports earlier findings that speakers can identify 30-50 colour names in their native language.

Keywords: colour, naming, computational, multilingual, communication

INTRODUCTION

Colour naming describes our cognitive capacity to organise millions of discriminable colours into a smaller set of colour categories named, for example, as yellow, turquoise and navy blue. Colour names vary across languages, lexically, in number and in range of reference. To augment colour communication within and across different languages, it is necessary to have a multilingual method for mapping perceptual to cognitive aspects of colour. Computational colour naming methods aim to automate the process of classifying colours to colour names that are meaningful to speakers of various languages across the colour gamut. For example, given the numerical coordinates of a sample in some colour space, what is the best name to describe it in different languages?

Previous efforts [1-7] have predominantly focused on a limited set of 11 basic colour terms (BCTs)[8]. But we [9, 10], and others [11, 12], have shown that BCTs can neither capture the full range of visible colours, nor represent the extensive colour lexicons used by native speakers. In this study, we evaluate a recent supervised machine learning method, namely Random Split Trees (RST) [13], in various colour spaces that not only identifies the basic colours but also captures subtleties of colour nomenclature in wide cultural use in English, Greek and Thai. Our goal is to augment colour communication between speakers of different languages.

METHODOLOGY

In the collection of our behavioural data, we extend previous cross-cultural studies which used only the most saturated colour samples by also sampling the interior of the colour solid. A further methodological improvement includes the departure from usual methods which would use a small number of observers and/or the use of only a restricted set of basic colour terms. Instead, thousands of volunteers from linguistically and demographically diverse populations freely named a large number of colours online (available at: https://colournaming.org). Test stimuli were 2 degree uniformly coloured discs with a black outline of 1 pixel, presented against a neutral grey background. The stimuli consisted of 589 simulated samples approximately uniformly distributed in the Munsell Renotation Data and restricted in the sRGB gamut, plus 11 achromatic samples [14].

We trained RST by 10,000 responses in the crowdsourcing colour naming experiment from 500 participants in English, 10,000 responses from 500 participants in Greek and 5,000 from 250 participants in Thai. RST ensembles a set of random binary decision trees where each tree grows using the full training dataset and splits nodes at random. Tree-based ensembles are essentially a set of hyper-rectangles that can be sensitive to rotations when partitioning the decision space; therefore, prior to any splitting, we randomly rotate the representation space to further induce diversity within the constructed forest and to improve accuracy at determining the form of colour categories in a three-dimensional space.

RESULT AND DISCUSSION

EVALUATION OF COLOUR SPACES

To investigate whether the choice of colour space influences the results of RST, we compared the performance of the model using Leave-One-Out and Leave-Planes-Out cross-validations in RGB-linear, CIE XYZ 1931, CIELAB, CIELUV and CIECAM02-UCS, assuming the sRGB viewing conditions. In the Leave-One-Out mode, we exclude a test chip from the training data and predict its histogram of colour names from the trained model. In the Leave-Planes-Out mode, we exclude the test chip and all the chips with the same, chroma, or lightness or hue dimensions. Each colour space was scored by RMS of Bhattacharyya distances between observed and predicted histograms of colour naming responses shown in Table 1.

Table 1: Comparison of colour spaces for classification in colour names using RST.

Colour Spaces	Leave-One-Out	Leave-Planes-Out
RGB (linear)	0.99	1.03
sRGB	0.99	1.03
$CIEXYZ_{1931}$	0.97	1.14
$CAM02UCS_{sRGB}$	0.95	1.02
$CIELAB_{D65}$	0.92	0.97
$CIELUV_{D65}$	0.91	0.96

Overall, the predictions of the RST algorithm were better in the approximately perceptually uniform colour spaces (CIELAB, CIELUV, CAM02-UCS) than in the non-uniform (RGB, sRGB, CIE XYZ 1931) spaces. The best colour space in terms of accuracy of predictions in both cross-validation modes was CIELUV in agreement with the reports of a recent study on colour clustering [15], although CIELUV's advantage was slight.

COMPARISON TO EARLIER COMPUTATIONAL COLOUR NAMING MODELS

To compare the performance of RST against previous colour naming models based on the monolexemic psychophysical data of Sturges and Whitfield [16] in British English, we first followed the approach described by Guest & Laar [17] and restricted the responses to their last word resulting in 320 distinct colour terms instead of just the eleven terms of previous colour naming models. We trained the RST with these monolexemic responses and inferred their histograms for the 330 patches of the Munsell array [8] in CIELUV.

In Figure 1, we show the segmentation of the simulated Munsell array by RST against Sturges & Whitfield's distributions of BCTs drawn with black boxes (*n* = 111 chips). The RST model assigned the 330 chips to 16 colour terms: the 11 BCTs with perfect accuracy, as well as additional terms like turquoise, lilac, maroon, peach, mauve, and teal.

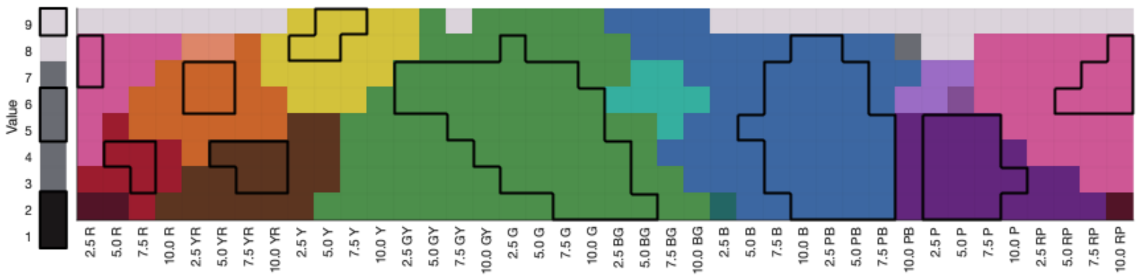

Figure 1. Segmentation of simulated Munsell array into 16 monolexemic colour terms by RST model. Coordinates of their centroids were used to colour each name category. Sturges & Whitfield's mapping of BCTs in British English are drawn with black boxes.

In Table 2., we show the comparison of the performance of the RST model against previous colour naming models of Lammens's Gaussian model (LGM) [3]; MacLaury's English Speaker (MES)[4]; Benavente and Vanrell's Triple Sigmoid model (TSM)[1]; Seaborn's fuzzy k-means model (SFKM) [6]; Benavente et al's Triple Sigmoid- Eliptic Sigmoid model (TSMES) [2]; van de Weijer et al's Probabilistic Latent Semantic Analysis (PLSA)[7]; Parraga & Akbarinia's Neural Isoresponsive Colour Ellipsoids model (NICE) [5]; and Mylonas & MacDonald's Maximum a Posteriori (MAP)[9]. RST achieved the same performance as other state-of-the-art colour naming models (SFKM, TSMES, and NICE), with 100% accuracy for 111 coincidences based on Sturges & Whitfield's results for the 11 basic colour categories. Additionally, RST identified five terms on the Munsell array.

Table 2. Comparison of colour naming models on the Munsell array (n=330 chips) against Sturges & Whitfield (1995) results. The data for LGM, MES, TSM, SFKM, TSEM, PLSA and NICE was obtained from Table 4 in Parrage & Akbarinia (2016).

Models	Coincidences	Errors	%
LGM	92	19	17
MES	107	4	4
TSM	108	3	3
SFKM	111	0	0
TSEM	111	0	0
PLSA	109	2	2
NICE	111	0	0
MAP	110	1	1
RST	111	0	0

COMPUTATIONAL COLOUR NAMING IN ENGLISH, GREEK AND THAI

To automate the colour naming task across different languages, we trained the RST model on unconstrained multilingual datasets in English, Greek, and Thai. Figure 2, shows the performance of the model on segmenting a synthetic image, which includes not only the surface but also the interior of the colour gamut [10], into lexical colour categories.

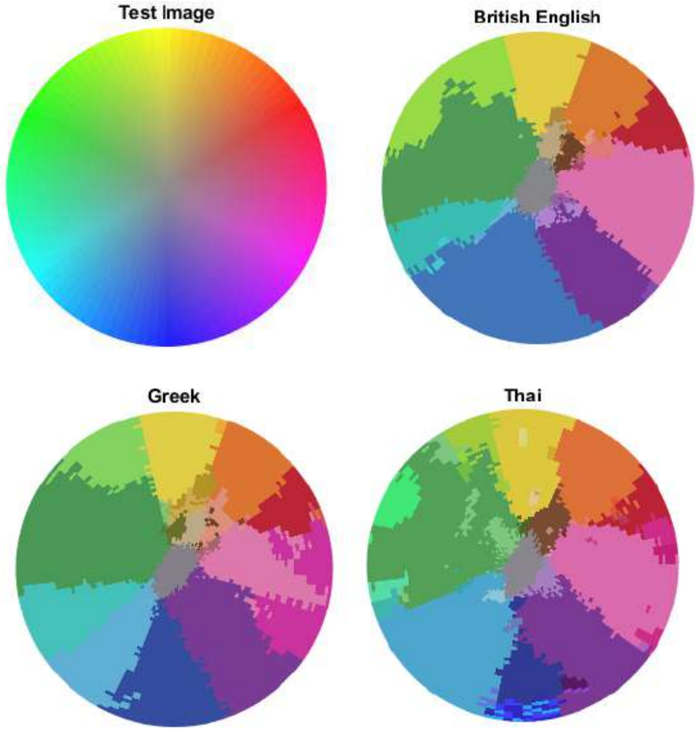

Figure 2. Segmentation of synthetic test image. Test image (1st row – left). Segmentation of test image in British English (1st row – right), Greek (2nd row – left) and Thai (2nd row – right) colour names. Coordinates of their centroids were used to colour each name category.

Learning from British English speakers, the RST algorithm assigned the colour coordinates of the synthetic image into 30 colour names. The seven largest categories were BCTs: *green, blue, grey, pink, purple, yellow* and *orange*. *Red* and *brown* were the 10th and 13th largest categories. *Turquoise* (8th) and *lime green* (9th) were the non-basics with the largest coverage in the test image with *lilac* (11th) and *beige* (12th) found also to cover regions larger than *brown*. *Red* was restricted to the most saturated colours with *salmon*, *peach*, *pink* and *orange* covering the pale region of the same hue angles. *Turquoise* was assigned to pixels all the way from the neutral axis to the limit of the gamut while *lilac* was restricted to the pale regions of *purple*.

With data sourced from Greek speakers, RST identified 28 lexical colour categories in the test image. The five largest categories were the BCTs *green* (*prasino*), *purple* (*mov*), *grey* (*gri*), *blue* (*ble*) and *pink* (*roz*). *Yellow* (*kitrino*) was the 8th, *orange* (*portokali*) was the 10th, *red* (*kokkino*) was the 12th and *brown* (*kafe*) was the 19th largest categories. *Sky blue* (*galazio*), the proposed second blue basic category in Greek, was the 6th largest category covering regions from the neutral axis to the limits of the gamut. Similarly, turquoise (*tirkuaz*) was the 7th most common category. *Lime green* (*lahani*) and *fuchsia* (*fouxia*) were also very popular categories followed by *beige* (*bez*), *salmon* (*somon*) and *olive* (*ladi*). *Lilac* (*lila*) was assigned to >1% of pixels.

Learning colour names from Thai speakers, the RST algorithm identified 46 colour names in the synthetic image. Again, the seven largest categories were the BCTs *green* (*khiaw*), *grey* (*thaw*), *sky blue* (*fa*), *pink* (*chompu*), *purple* (*muang*), *yellow* (*leaung*) and *orange* (*som*). *Brown* (*namtan*) and *red* (*dang*) were the 10th and 12th largest categories. The proposed second basic blue (*namngen*) was the 9th most common category. The largest non-basics were *light green* (*khiawon*) and *light purple* (*muangon*). Compared to all other languages, the *turquoise* category in Thai (*faomkhiaw*) was assigned to a much smaller number of pixels (<1%).

Overall, our results reinforce previous findings that the colour space can be segmented into 30-50 colour categories [10-12]. The large discrepancy in the number of identified colour categories between Thai (n = 46) and both English (n = 30) and Greek (n = 28) is likely due to the more frequent use of modifiers reported in Thai [18]. A more recent study [19] also found that Thai speakers use 20 highly frequent monolexemic colour terms to describe the surface of the Munsell system, compared to the 16 terms reported for English in this study.

CONCLUSION

In conclusion, we present a supervised computational colour naming model, namely Random Split Trees, to automate colour naming in English, Greek and Thai. Our tools and data allowed the analysis of colour names both on the surface and within the colour gamut. Our model performs best in CIELUV and achieves the same level of state-of-the-art performance as earlier models, but goes a step further by identifying 5 additional lexical colour categories in English on the surface of the Munsell system. The performance of the model across the colour gamut in English, Greek and Thai aligns with empirical findings of earlier studies showing that native speakers can identify 30-50 colour names without training.

ACKNOWLEDGEMENT

We thank all anonymous participants of the colour naming experiments. DM, AK, JS and RE were funded by the FY22 TIER 1 Seed Grant from Northeastern University, USA. DM was also supported by the University College London (UCL) Computer Science—Engineering and Physical Sciences Research Council, UK, Doctoral Training Grant: EP/M506448/1–1573073.

REFERENCES

1. Benavente R, Vanrell M. (2004) Fuzzy colour naming based on sigmoid membership functions. In *CGIV 2004: 2nd European Conference on Color in Graphics, Imaging, and Vision,* 135–9. Aachen, Germany: IS&T.
2. Benavente, R., Vanrell, M., & Baldrich, R. (2008). Parametric fuzzy sets for automatic color naming. *Journal of the Optical Society of America A*, *25*(10), 2582–2593.
3. Lammens, J. (1994). *A computational model of color perception and color naming*. PhD Thesis. State University of New York at Buffalo.
4. MacLaury, R. E. (1992). From brightness to hue: An explanatory model of color-category evolution. *Current Anthropology*, *33*(2), 137–186.
5. Parraga, C. A., & Akbarinia, A. (2016). NICE: A Computational Solution to Close the Gap from Colour Perception to Colour Categorization. *PLoS ONE*, *11*(3).
6. Seaborn, M., Hepplewhite, L., & Stonham, J. (2005). Fuzzy colour category map for the measurement of colour similarity and dissimilarity. *Pattern Recognition*, *38*(2), 165–177.
7. Weijer, J.V., Schmid, C., & Verbeek, J. (2007). Learning Color Names from Real-World Images. In *CVPR 2007: IEEE Conference on Computer Vision and Pattern Recognition,* 1–8. Minneapolis, MN, USA.
8. Berlin, B., & Kay, P. (1969/1991). *Basic color terms : their universality and evolution*. Stanford, Calif.: Center for the Study of Language and Information.
9. Mylonas, D., & MacDonald, L. (2016). Augmenting basic colour terms in English. *Color Res. Appl.*, *41*(1), 32–42.
10. Griffin, L. D., & Mylonas, D. (2019). Categorical colour geometry. *PLOS ONE*, *14*(5), e0216296.
11. Chapanis, A. (1965). Color names for color space. *American Scientist*, *53*, 327–346.
12. Derefeldt, G., & Swartling, T. (1995). Colour concept retrieval by free colour naming. Identification of up to 30 colours without training. Displays, 16(2), 69–77.

13. Mylonas, D., Caparos, S., & Davidoff, J. (2022). Augmenting a colour lexicon. *Humanities and Social Sciences Communications,* 9(1), 1–12.
14. Mylonas, D., & MacDonald, L. (2010). Online Colour Naming Experiment Using Munsell Samples. In *CGIV 2010: 5th European Conference on Colour in Graphics, Imaging, and Vision and 12th International Symposium on Multispectral Colour Science*, 27-32. Joensuu, Finland: IS&T.
15. Douven, I. (2017). Clustering colors. *Cognitive Systems Research*, *45*, 70–81.
16. Sturges, J., & Whitfield, A. (1995). Locating basic colours in the Munsell Space. *Color Research and Application*, *20*(6), 364–376.
17. Guest, S., & Laar, D. V. (2000). The structure of colour naming space. *Vision Research*, *40*(7), 723–734.
18. Katemake, P., Mylonas, D., MacDonald, L. W., & Prasithrathsint, A. (2015). Comparison Among Three Methods for Thai Colour Naming. *AIC 2015 Midterm Meeting*. Tokyo, Japan.
19. Panitanang, N., Phuangsuwan, C., & Ikeda, M. (2022). Basic color terms in Thai. *Color Research & Application*, 47(6), 1402–1425.

"GEOMETRY" OF COLOR HARMONY IN THE CIELAB COLOR SPACE: EVIDENCE FROM AN ONLINE EXPERIMENT ACROSS COUNTRIES

Yulia A. Griber[1]*, Tatiana Samoilova[1], Abdulrahman S. Al-Rasheed[2], Victoria Bogushevskaya[3], Elisa Cordero Jahr[4], Yacine Gouaich[5], James Manteith[6], Philip Mefoh[7], Jimena Vanina Odetti[8], Gloria Politi[3], Tatiana Sivova[9]

[1]*Smolensk State University, Russia.*
[2]*King Saud University, Saudi Arabia.*
[3]*University of Salento, Italy.*
[4]*Universidad Austral de Chile, Chile.*
[5]*University of Mostaganem, Algeria.*
[6]*Apraksin Blues magazine, USA.*
[7]*University of Nigeria, Nigeria.*
[8]*Instituto Tecnológico Superior de Puerto Vallarta, Mexico.*
[9]*Yanka Kupala State University of Grodno, Belarus.*

*Corresponding author: Yulia A. Griber, e-mail: y.griber@gmail.com

ABSTRACT

In physical environments and cultural landscapes, we most often deal not with separate colors, but with color combinations. When choosing a color, we usually try to "fit" it into a preexisting color context, making the new color combination harmonious. Yet are the "laws" of color harmony fundamental to our shared cognitive architecture, or are they cultural products that vary from country to country? To answer these questions we conducted an experiment with 599 participants aged 18 to 76 from eight different countries, including Algeria (MA = 26.2 years; SD = 8.8; 49 men, 26 women), Belarus (MA = 19.8 years; SD = 9.1; 19 men, 63 women), Italy (MA = 29.0 years; SD = 12.8; 23 men, 67 women), Mexico (MA = 20.0 years; SD = 7.0; 34 men, 23 women), Nigeria (MA = 34.7 years; SD = 10.5; 29 men, 32 women), Russia (MA = 24.6 years; SD = 6.3; 17 men, 72 women), Saudi Arabia (MA = 24.5 years; SD = 8.6; 28 men, 38 women), and Chile (MA = 34.3 years; SD = 15.1; 35 men, 43 women). To create experimental stimuli, we used 10 color combinations composed by the Russian avant-garde artist Mikhail Matyushin and his disciples for the *Reference Book of Color* (1932) based on shades that were typical in architectural design – yellow ochre, light umber, light ochre, and burnt umber. We removed the "intermediary" linking color from each of the selected color triads and asked participants to adjust the color of this band according to their liking. Mapping 2,995 color choices into CIELAB and CIELCh color space to identify their chromatic characteristics (hue, lightness, and chroma), we demonstrate graphically that color triads in different cultures have a different "geometry" in CIELAB color space and on the color circle. We conclude that the revealed patterns of these relationships reflect cross-cultural "shifts" of human perception of color harmony. The analysis presented in this paper will facilitate opportunities for architects, designers, and other color professionals to create culturally specific harmonic color combinations in urban environments.

Keywords: color combination; color triads; color harmony; online experiment; CIELAB

INTRODUCTION

In physical environments and cultural landscapes, we most often deal not with separate colors, but with color combinations [5; 10]. When choosing a color, we usually try to "fit" it into a preexisting color context, making the new color combination harmonious [2]. Yet are the “laws” of color harmony fundamental to our shared cognitive architecture, or are they cultural products that vary from country to country? We conducted an online experiment to survey whether the strategies for building harmonious color combinations have cross-cultural specifics, and to establish the "geometric" parameters of the identified differences in the CIELAB color space.

METHODOLOGY

Participants: The experiment involved 599 participants aged 18 to 76 from eight different countries, including Algeria (MA = 26.2 years; SD = 8.8; 49 men, 26 women), Belarus (MA = 19.8 years; SD = 9.1; 19 men, 63 women), Italy (MA = 29.0 years; SD = 12.8; 23 men, 67 women), Mexico (MA = 20.0 years; SD = 7.0; 34 men, 23 women), Nigeria (MA = 34.7 years; SD = 10.5; 29 men, 32 women), Russia (MA = 24.6 years; SD = 6.3; 17 men, 72 women), Saudi Arabia (MA = 24.5 years; SD = 8.6; 28 men, 38 women), and Chile (MA = 34.3 years; SD = 15.1; 35 men, 43 women).

Experimental stimuli: To create experimental stimuli, we used 10 color combinations composed by the Russian avant-garde artist Mikhail Matyushin and his disciples for the *Reference Book of Color*. This book, first published in Leningrad in 1932 and republished in 2007 [7], addressed the practical use of color in interior and exterior architectural design, textile, porcelain, wallpaper, printing, and other industries. It included a large article entitled “The Law of the Variability of Color Combinations”, and four sections with color charts. The charts were hand-painted with gouache by a group of Matyushin's students, young artists Irina Walter, Olga Vaulina, Sofia Vlasyuk, Valida Delacroix, Tatiana Sysoeva, and Elena Khmelevskaya.

Like Matyushin's color science in general, the charts were based on observations and experiments studying the psychophysiological factors of color perception and human color vision processes under different conditions (for more details see [3]). The authors considered the *Reference Book of Color* “a first step in determining the regularity of color relations” [7, p. 15]. They saw the book as primarily aiming to establish the “connection between the conceptual color in science and the material color in practice” [7, p. 28].

All charts that we selected for creating experimental stimuli were published in the last (IV) Section of the book [7, pp. 25-30]. Their bottom stripe colors were typical in architectural design – yellow ochre (chart 1), light umber (charts 2 and 3), light ochre (chart 4), and burnt umbre (chart 5). The top stripe colors were predominantly light (mean L=69.52) with low chroma (mean C=10.05). Two of these colors (charts 3 and 5) were located on the color circle between green and yellow (h°=112.56 and 175.45, respectively), while the other three fall within the 20° arc in the range between blue and green (215.71 ≤ h° ≤ 239.97) (Table 1).

Table 1: Bottom and top stripe colors of experimental stimuli

Chart	Bottom	L*	a*	b*	Top	L*	a*	b*
1		60.79	2.96	36.80		59.23	-3.96	-4.36
2		72.09	1.89	8.72		68.15	-3.12	-2.24
3		76.34	1.00	10.01		80.42	-10.72	25.81
4		86.78	3.41	35.53		71.78	-1.67	-2.89
5		34.47	17.09	16.92		65.77	-15.90	1.26

We saved the selected charts in JPEG format with the maximum resolution (Figure 1, left), and then removed the "intermediary" linking color (replaced it with white) from each of the color triads. The top and bottom colors remained unchanged (Figure 1, right).

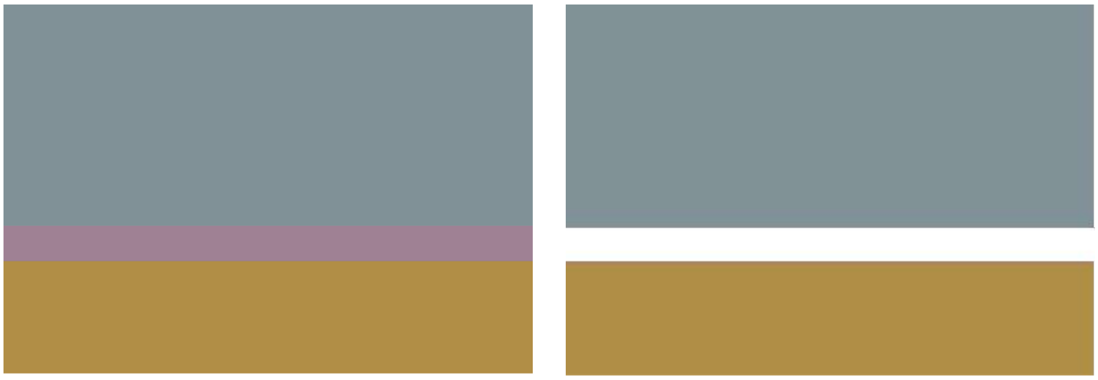

Figure 1. A chart from the *Reference Book of Color* (left) and an experimental stimulus (right)

Procedure: The idea of the experiment was to ask modern respondents from around the world to choose a color for the uncolored middle band of the color chart by Mikhail Matyushin, and then compare the resulting color combination with the corresponding color chart from his *Reference Book of Color* (in a similar way D. I. Braun & K. Doerschner investigated the perception of color and spatial balance in abstract art in "art- naïve" German and Chinese participants [1]).

In *Experiment 1*, participants had the task of finding the color they would like best for a middle (target) stripe in a chart presented on the computer screen. We showed each participant 5 color charts in a random order, one at a time, and instructed them as follows: *In this experiment, we would like to ask which color combinations you personally like. We will show you 5 color charts. Each chart consists of three horizontal stripes of different widths. The colors of the top and bottom stripes are fixed and you cannot change them. You will be asked to select a color for the white (uncolored) stripe in the middle. Choose the color you feel makes the whole combination as harmonious as possible.*

In *Experiment 2*, we asked participants to compare each of the color charts they created with the corresponding original – the chart from Matyushin's *Reference Book of Color* – and indicate which one they liked better. The time for both tasks was not limited.

At the final stage of the study, the participants were asked to fill out a small questionnaire, reporting their age, gender, place of birth, country of permanent residence, native language, art education and known color vision disorders.

Data analysis: To analyze the "geometric" properties of color triads, we visually projected them into the CIELCh color circle and CIELAB color space.

The data processing was performed with Python and included the conversion of colors collected in the database from the HEX format to CIELAB and CIELCh, and then their visualization with polar scatter plots.

To calculate the distance between two colors in three-dimensional color space, we used the color difference metric CIEDE2000 (ΔE^*00) (see e.g., [6; 8]).

For computing the triangles' angles in CIELAB color space we used the cosine formulas (Eq. 1), (Eq. 2), and (Eq. 3):

$$\alpha = \arccos (b^2 + c^2 - a^2) / 2bc \quad (1)$$
$$\beta = \arccos (a^2 + c^2 - b^2) / 2ac \quad (2)$$
$$\gamma = \arccos (a^2 + b^2 - c^2) / 2ab, \quad (3)$$

where a, b, and c are color distances ΔE^*00 between the top, bottom, and middle colors.

Cluster analysis of the data was carried out using the k-Means method [4] and Ward's hierarchical algorithm [9].

RESULT AND DISCUSSION

Mapping 2,995 color choices into CIELAB and CIELCh color space to identify their chromatic characteristics (hue, lightness, and chroma), we demonstrate graphically that color triads in different cultures have a different “geometry” on the color circle (Figure 2).

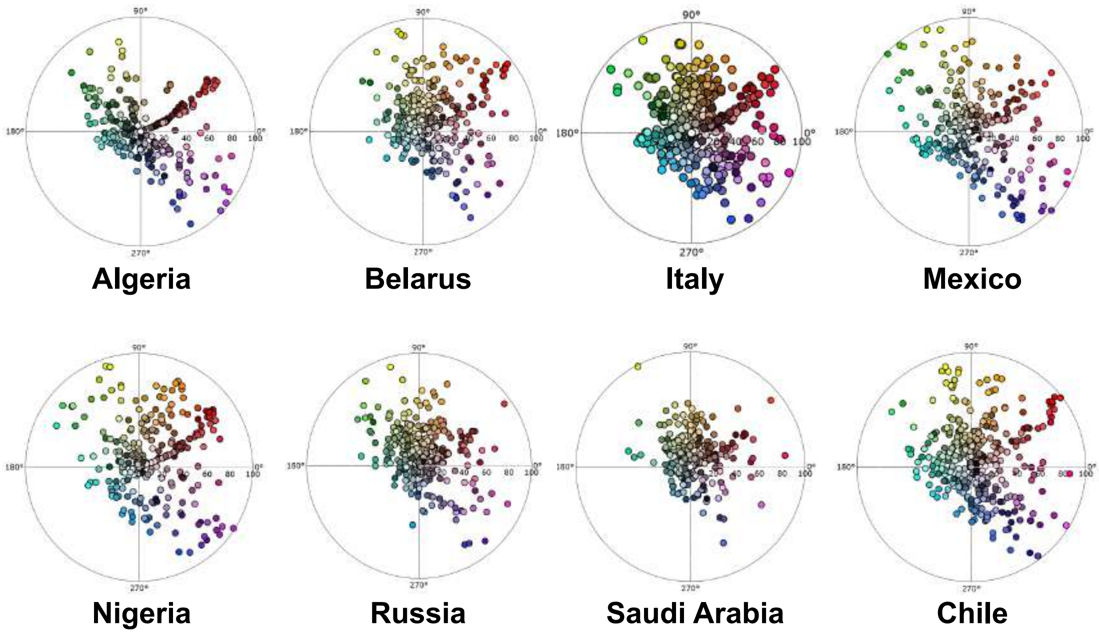

Figure 2. Hue (h°) and chroma (C) of colors, selected in different countries; projection into the CIELCh color circle

Representatives of different cultures use fundamentally different strategies for building harmonious color combinations. Residents of Algeria, Nigeria, Mexico and Chile are more likely to choose saturated shades. On the contrary, participants from Russia, Belarus and Saudi Arabia prefer moderate colors. The color selections also differed in hue: Saudis were less likely than representatives of other cultures to use purple; participants from Russia and Belarus were less likely to use blue-green, and respondents from Algeria and Nigeria less likely to use red-yellow.

To further analyze “geometric” properties of the color triads plotted in CIELAB color space, we computed the color differences between the vertices of each triangle according to the CIEDE2000 formula [6; 8] and used them as a measurement of length for each side of the triangles. Using the cosine formulas (Eq. 1), (Eq. 2), and (Eq. 3), we also computed internal angle values in each triangle and calculated their areas.

Cluster analysis of the data using the k-Means method showed that participants from Saudi Arabia, Nigeria, Russia, Belarus, and Italy were more likely than residents of other countries to choose an intermediary hue relatively close to the two given others in the CIELAB color space. As a result, the triangles formed by the two given and one selected colors more often had a very small area (yellow cluster in Figure 3). Respondents from Algeria used this strategy rarely and chose a color at a rather large distance from the given ones (blue and green clusters in Figure 3). Residents of Chile and Mexico mostly focused on the length of the segment between the given colors and most often chose a color in such a way that the adjacent angle was sharp (blue and red clusters in Figure 3).

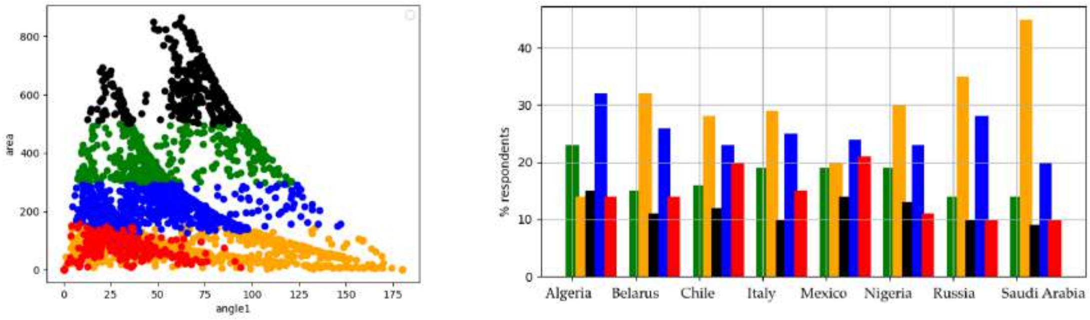

Figure 3. Results of cluster analysis of color choices of experiment participants in the CIELAB color space: boundaries of clusters (left) and prevalence of clusters in different countries (right)

Application of Ward's hierarchical algorithm in the data analysis allowed us to cluster countries by the degree of similarity of the "geometry" of harmonious color combinations in the CIELAB color space. We revealed the closest strategies of building color harmony between the residents of Russia and Belarus, Mexico and Chile, as well as between Nigeria, Italy, and Saudi Arabia (Figure 4).

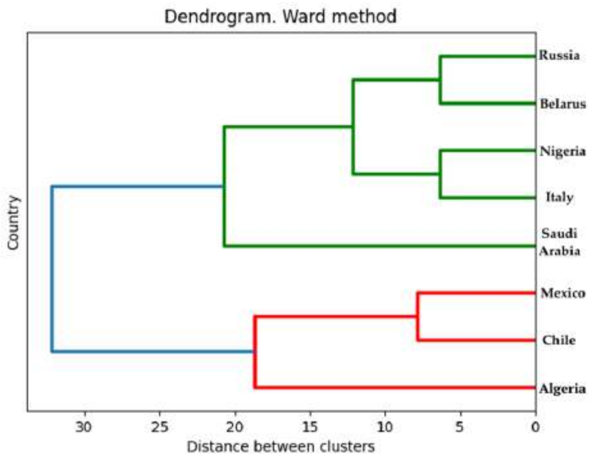

Figure 4. Dendrogram representing outcomes of the cluster analysis of countries by the degree of similarity of the "geometry" of harmonious color combinations in the CIELAB color space

Analysis of 5,990 valid comparisons proposed by the participants in the experiment showed that in most cases they liked their own color choice more than the choice of Mikhail Matyushin, despite the fact that the choice of the participants in many cases resulted in combinations fundamentally different from those in the artist's color charts.

CONCLUSION

We conclude that the revealed patterns reflect cross-cultural "shifts" of human perception of color harmony. The analysis presented in this paper will facilitate opportunities for architects, designers, and other color professionals to create culturally specific harmonic color combinations in urban environments. Research should be continued to describe gender and age influence on the strategies for building harmonious color combinations in different cultures, as well as to expand the number of participating countries.

ACKNOWLEDGEMENT

The project was supported by the Russian Science Foundation (grant No. 22-18-00407; https://rscf.ru/en/project/22-18-00407/).

REFERENCES

1. Braun, D. I., & Doerschner, K. (2019). Kandinsky or me? How free is the eye of the beholder in abstract art? *i-Perception 10*(5), 1-29. https://doi.org/10.1177/204166951986797
2. Burchett, K. E. (2002). Color harmony. *Color Research and Application, 27*(1), 28-31. https://doi.org/10.1002/col.10004
3. Griber, Y. A. (2022). The "geometry" of Matyushin's color triads: Mapping color combinations from the *Reference Book of Color* in CIELAB. *Arts, 11*(6), 125. https://doi.org/10.3390/arts110601
4. Hartigan, J. A., & Wong, M. A. (1979). Algorithm as 136: A k-means clustering algorithm. *Journal of the Royal Statistical Society. Series C (Applied Statistics), 28*(1), 100-108. http://dx.doi.org/10.2307/2346830
5. Li, K. R., Yang, Y. Q., & Zheng, Z. Q. (2020). Research on color harmony of building façades. *Color Research and Application 45*(1), 105-119. https://doi.org/10.1002/col.22448
6. Luo, M. R. (2015). CIEDE2000, history, use, and performance. In: Luo, R. (Ed.). *Encyclopedia of Color Science and Technology*. Berlin, Heidelberg: Springer. https://doi.org/10.1007/978-3-642-27851-8_7-1
7. Matyushin, M. (1932/2007). *Spravochnik po tsvetu: Zakonomernost' izmenyayemosti tsvetovykh sochetany [A Reference Book of Color: The Laws Governing Variability of Color Combinations]*. Moscow: D. Aronov (in Russian).
8. Sharma, G., Wu, W., & Dalal, E. N. (2005). The CIEDE2000 color-difference formula: Implementation notes, supplementary test data, and mathematical observations. *Color Research and Application 30*(1), 21-30. https://doi.org/10.1002/col.20070
9. Ward, Jr. J. H. (1963). Hierarchical grouping to optimize an objective function. *Journal of the American Statistical Association, 58*(301), 236-244. https://doi.org/10.1080/01621459.1963.10500845
10. Westland, S. et al. (2007). Colour harmony. *Colour: Design & Creativity, 1*(1), 1-15.

COLOUR SPECIFICATION FOR AN ENGLISH-CHINESE COLOUR NAMES DICTIONARY

Qinyuan Li[1,2*], John Hutchings[2], Kaiping Chang[3], Yuxin Ye[4], Ming Ronnier Luo[1,2*]
[1]State Key Laboratory of Modern Optical Instrumentation, Zhejiang University, CHINA
[2]University of Leeds, United Kingdom
[3]Techmoi International Limited, Taiwan, China
[4]Thousand Lights Lighting (Changzhou) Limited; Changzhou, China
*Corresponding author: Qinyuan Li, cm18ql@leeds.ac.uk

ABSTRACT

The present work is a concise booklet summarising 136 commonly used English colour names taken from the Hutchings Colour Compendium [1]. All colours are divided into 10 colour categories (red, yellow, green, blue, etc). It is aimed to be used as an education tool to understand English and Chinese Mandarin colour names associated with different objects, and for colour naming of products. In this study, 136 images corresponding to each colour name were found from the internet or real objects captured by camera. A psychophysical experiment was conducted to obtain colour specifications for these colour names using three colour order systems, Munsell, NCS, and Pantone. The results showed that using NCS achieved better association with the colour names and corresponding images. In the book, each colour name includes an image, a colour patch, and colour specifications in terms of Munsell, NCS and Pantone, together with instrumental CIELAB values.

Keywords: colour specification, colour names, colour order systems, colour communication

INTRODUCTION

Colour communication is vital for education, design, industry, and in everyday life [2]. People may give names to describe the colour, or specify by selection of a match from a colour atlas. Physically available colour atlases, such as Pantone, Munsell, and NCS, are popular in both the design and manufacturing processes. Pantone is probably the most widely used due to the relatively low cost and ease of use. The colour patches in Pantone, together with its unique code, make the selection and communication of colour between individuals and industries quick and convenient. Similarly, colour patches in Munsell and NCS are well specified being based on specific colour attributes rather a simple code [3,4]. However, Pantone is not based on perceptual attributes corresponding to human colour perception. The different perceptual colour attributes used in Munsell (Hue, Value, Chroma) and NCS (Hue, Blackness, Chromaticness) are not directly correlated, therefor in this work we have used all three colour order systems [4,5].

Human beings learn to use colour names when categorising objects and communicating with parents from an early age. Previous categorising studies used unconstrained methods (observers were free to record the name of physically available colour patches), as well as constrained methods (observers selected the colour patches corresponding to the given colour names) to better investigate the understanding of colour names [6, 7]. For the constrained method, as a hue name (e.g., red) is often associated with an object we have included both in this study. Each colour category contains different objects in the same hue.

The objective of this study is to develop an educational tool to use in the colour naming of products. Colour names are listed together with corresponding images, colour patches, and colour specifications in terms of Munsell, NCS, and Pantone, together with measured CIE LAB values. In this way, we shall be able to understand English and Chinese Mandarin colour names associated with different objects.

METHODOLOGY

Image samples

136 colour names are included in the Dictionary. The image corresponding to each colour name was found from the internet or real objects captured by a camera. All images were divided into 10 hue categories (red, yellow, green, blue, etc.), and each image contained a region of interest (ROI) displaying a commonly used colour name. The image subjects varied widely and included all perceptual colour hues. To aid the understanding of the colour names and images, Chinese Mandarin colour names were found based on the image subject and displayed as well. Table 1 shows examples of colour names and the corresponding images with each ROI..

Table 1: Example of English and Chinese Mandarin colour names and the corresponding images and ROI

				
Black: a raven (乌鸦黑) The colour name is raven black.	Blue: blue lapis lazuli（青金石，天蓝色) The colour names are lapis blue, or blue lazuli, or lazuli.	Brown: mahogany wood（桃花心木的棕色) The colou name is mahogany.	Green: grass green (草绿色) The colour name is grass green.	Grey: a silica stone (硅石灰) The colour name is silica.

				
Purple: Tyrian purple royal robe (泰尔红紫皇家礼袍) The colour name is Tyrian purple or royal purple.	Orange: oranges. L. Grace Juan photo (橙色，橘色) The colour name is orange.	Red: fresh human blood (输液袋，血红色，猩红色) The colour name is blood red.	White: snow (雪白色) The colour name is snow white.	Yellow: canary bird (金丝雀黄，淡黄色) The colour name is canary, or canary yellow.

Experiment

A psychophysical experiment was performed to obtain the colour specifications in terms of Munsell, NCS, and Pantone by matching the colour patches to the ROI of each image. Firstly, a calibrated Apple MacBook Air laptop was used to display the 136 images which contain the ROI, and the English and Chinese Mandarin colour names. The laptop displaying the image and the physical colour atlas were placed side by side in a spectrum tunable LED lighting system, Thouslite LEDView® Cabinet, using a D65 simulator at an illuminance of 1400 lux with a CIE colour rendering index of 99, in a darkened room, as shown in Figure 1.

To reduce observer fatigue, the 136 images were divided into two groups randomly, each containing 68. Each image was specified using Munsell, NCS, and Pantone colour atlases, respectively, and each time 5 observers matched the colour patches with ROI of the image. In total 30 observers (22 females, 8 males) aging from 20 to 33 participated in the experiment.

When using NCS and Munsell atlases the respective hue wheel was first used to select a hue match. One colour patch matching the ROI best in the relevant hue page was then selected. Observers were also asked to choose three other colour patches around the target colour patch that closely match. Then, the neighbouring two hue pages were shown to the observer, one being selected as the closest hue. That is, the maximum number of colour patches for one ROI could be 8. When using Pantone, observers viewed all colour patches to select up to 8 colour patches that match the ROI. CIELAB values under D65/10° of all the colour patches were measured using a Konica Minolta CM700-D spectrophotometer under the conditions of small aperture, UV inclusion and specular exclusion. For each observer, the average LAB values (D65/10°) of the selected up to eight patches was determined.

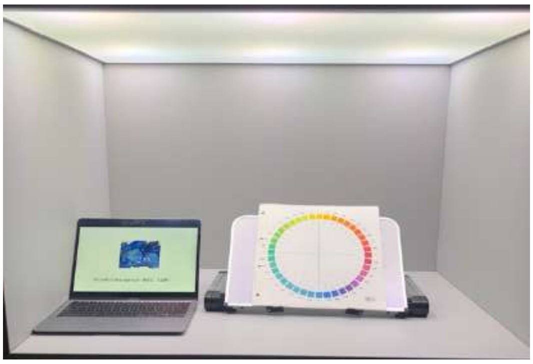

Figure 1. The experiment schematic diagram

RESULT AND DISCUSSION

Inter-observer variation

For each colour order system, the Mean Colour-Difference from the Mean ΔE_{00} unit (MCDM) was calculated and averaged across all images, indicating the inter-observer variation of each colour order system. The smaller the values of the MCDM, the more consistent the subject's performance in the colour matching and specification. Table 2 lists the mean inter-observer variation of the three colour order systems. It was found an MCDM of 5.87, representing typical matching an image ROI using physical colour tools, with 5.96, 5.19, and 6.46 for Munsell, NCS, and Pantone, respectively. Both NCS and Munsell outperformed Pantone. This is highly likely the former two have colour perception attributes, i.e., Blackness (s), Chromaticness (c), Hue (Φ) in NCS, and Hue, Value, Chroma in Munsell. Pantone only has a single numerical specification.

Table 2: Inter-observer variation of three colour order systems and the mean

	Munsell	NCS	Pantone	Mean
MCDM	5.96	5.19	6.46	5.87

Comparison of accuracy of colour order systems in specification

To better compare the accuracy of each colour order system in colour matching and specification, two CIELAB values were determined: i) the average LAB values of the five observers' answers for each colour order system, and ii) the average LAB values from three colour order systems (i.e., the 30 observers' answers), which is also defined as the true answer. The colour difference ΔE_{00} between each of the colour order systems and true answer were calculated and shown in Table 3. The smaller colour difference, the more accurate the colour order system. It shows that using NCS achieved the highest accuracy in colour specification with the ΔE_{00} of 2.73, followed by Munsell 3.83, and Pantone 4.53.

Using NCS achieved the highest consistency and accuracy in colour specification, followed by Munsell, while using Pantone achieved the lowest consistency and accuracy. As noted in methodology, when using NCS and Munsell observers needed to select a hue first, then match the colour patches in the particular hue page. When using Pantone matched colours are directly selected from thousands of colour patches. That is, the method of using NCS and Munsell is more organised, and observers can match the colour step-by-step without the confusion of facing many colour patches all together. An organised method is therefore suggested for colour matching and colour specification.

Table 3: The ΔE_{00} between each colour order system and the true answer

	Munsell	NCS	Pantone	Mean
ΔE_{00}	3.83	2.73	4.53	3.70

Decision of colour patches for colour specification

For each image, up to 40 answers (5 observers selected up to 8 colour patches individually) were obtained for Munsell, NCS, and Pantone, respectively. The 8 colour patches selected by one subject may overlap with those selected by others. To finally decide the colour patch in each of the colour order system to be used as the colour specification, the ΔE_{00} between true answers and observers' answers were determined. The colour patch in a particular atlas having the smallest colour difference from the true answer was decided as the colour specification and published in the book, together with the LAB values.

The ΔE_{00} between true answers and colour specification of each colour order system were calculated and shown in Table 4. Compared to the colour difference of each colour order system, Table 3, the colour differences of the final decision of colour specification are lower, indicating a good accuracy of the colour specification decided in this study.

Table 4: The ΔE_{00} between true answers and the final decision of colour specification

	Munsell	NCS	Pantone	Mean
ΔE_{00}	3.35	2.64	3.32	3.11

CONCLUSION

The present study provides comprehensive colour specifications of Munsell, NCS, and Pantone for 136 commonly used colour names of objects in 10 colour categories. Image corresponding to each colour name was found from the internet or real objects captured by a camera. Compared to Munsell and Pantone, NCS showed higher consistency between observations and higher accuracy in specifying colours. The colour specifications for each image were defined and published in the Dictionary, together with the CIELAB values.

REFERENCES

1. Hutchings J. B., Gavitt, R.F., Pointer M.R., The English Language, a Colour Word Compendium, 2nd edition, The Colour Group (GB). https://www.colour.org.uk/wp-content/uploads/2019/12/ColourCompendium.pdf
2. Zaslavsky, N., Kemp, C., Tishby, N., & Regier, T. (2020). Communicative need in colour naming. *Cognitive neuropsychology*, *37*(5-6), 312-324.

3. Luo, M. R. (2006). Applying colour science in colour design. *Optics & laser technology*, *38*(4-6), 392-398.
4. Luo, M.R., Rhodes, P., Xin, J., & Scrivener, S. (1992). Effective colour communication for industry. *Journal of the Society of Dyers and Colourists*, *108*(12), 516-520.
5. Wright, W. (1984). The basic concepts and attributes of colour order systems. *Color Research & Application*, *9*(4), 229-233.
6. Lin, H., Luo, M. R., MacDonald, L. W., & Tarrant, A. W. (2001). A cross-cultural colour-naming study. Part I: Using an unconstrained method. *Color Research & Application, 26*(1), 40-60.
7. Lin, H., Luo, M.R., MacDonald, L.W., & Tarrant, A. (2001). A cross-cultural colour-naming study: Part II—Using a constrained method. *Color Research & Application, 26*(3), 193-208.

The origin and development of colour names and categories, and the biological basis for colour categories.

Don Dedrick[1]*

[1]Department of Philosophy, University of Guelph, Canada.

*Corresponding author: ddedrick@uoguelph.ca

ABSTRACT

The idea that colour categories have perceptual salience goes back to the work of Mark Bornstein in the 1970's and 1980's [4], [5], [6]. Bornstein's idea was that equivalence classes of perceptually discernible stimuli, such as the stimuli English speakers name red, are perceptually salient *qua* categories. It is the grouping and its boundaries that have salience, and it is a perceptual as opposed to linguistically driven salience because it is present in non-linguistic infants. There were issues with Bornstein's studies, addressed later by Anna Franklin and colleagues. [13] But even this more careful research led to this unsatisfying characterization, from Franklin herself: "The finding that perceptual colour categorization is shown before the acquisition of colour terms, in some ways, raises more questions than it answers. For example, if there is an innate set of perceptual colour categories, why do different languages segment the colour space differently from each other?" [12] Franklin has summarized a more nuanced account of the relationship between what is prior to language for infants and what is categorically evident in languages [11], but the main point remains and persists, even in recent research that aims to show a relationship between infant colour categories and categorical response in retinogeniculate pathways. As Skelton, Catchpole, Abbot and Franklin write in 2017: "One important question for further research is how we transition from a prelinguistic color categorization based largely on biological mechanisms to a lexical color categorization that may make additional or fewer distinctions." [17]. An interesting question in relation to this puzzle is: where do the biological mechanisms impact lexical categorization? It is tempting to see them as a foundation on which linguistic categorization builds. But we argue here, this metaphor might be misleading, and not just because the super-structures seem mismatched to the foundation, as Skelton et al [17] note. Anthropological research suggests that colour names often originate in the names of objects. Colour words originate with object specific reference [3], [18]. This tendency appears to be reflected in the individual developmental process, in the sense that acquiring a colour name, for a child, involves its fast mastery for an exemplar object colour and a consequent "slow mapping" of its category [19]. These two dimensions relating to colour term origination and acquisition suggest that biological mechanisms which make categories salient are most influential after groups, and individuals, possess proto-colour terms and attempt to establish and map categorical boundaries in a labelled colour space—a space whose structure is brought into existence by the mapping process and constrained, perhaps, by categorical saliencies as well as other cognitive and social demands [21].

Keywords: basic colour terms, basic colour categories, colour categories, colour naming.

INTRODUCTION

The idea that colour categories have perceptual salience goes back to the work of Mark Bornstein in the 1970's and 1980's [4], [5], [6]. Bornstein's idea was that equivalence classes of perceptually discernible stimuli, such as the stimuli English speakers name red, are perceptually salient *qua* categories. It is the grouping and its boundaries that have salience, and it is a perceptual as opposed to linguistically driven salience because it is present in non-linguistic infants. There were issues with Bornstein's studies, addressed later by Anna Franklin and colleagues. [13] But even this more careful research led to this unsatisfying characterization, from Franklin herself: "The finding that perceptual colour categorization is shown before the acquisition of colour terms, in some ways, raises more questions than it answers. For example, if there is an innate set of perceptual colour categories, why do different languages segment the colour space differently from each other?" [12] Franklin has summarized a more nuanced account of the relationship between what is prior to language for infants and what is categorically evident in languages [11], but the main point remains and persists, even in recent research that aims to show a relationship between infant colour categories and categorical response in retinogeniculate pathways. As Skelton, Catchpole, Abbot and Franklin write in 2017: "One important question for further research is how we transition from a prelinguistic color categorization based largely on biological mechanisms to a lexical color categorization that may make additional or fewer distinctions." [17]

The constraints on colour naming and categorization

The elephant in the room for any discussion of colour naming and colour classification—colour categories—is the Berlin and Kay [1], [15] theory of basic colour terms (BCT) and basic colour categories (BCC). According to this theory, which has wide if not universal acceptance, there is a very limited number of BCTs—terms that satisfy a range of criteria for significance and use. The original work by Berlin and Kay [1] posited 11 BCTs (red, yellow, green, blue, orange, brown, purple, pink, grey, black, and white), while much current literature focuses mainly on a smaller number of BCTs for the so-called Hering primaries (red, yellow, green, blue, black, white). One reason for focusing on these BCTs has got to do with another major claim, in the early work by Berlin and Kay [1] comparison of languages not only shows a striking similarity of term distribution, but a possible ordering of languages into stages. Each stage in this proposed order could be specified by way of a conditional rule such as this example for a three BCT language: *if three BCTs, then red, white and black*. There are 5 stages in the current "evolutionary" ordering [15], with most of the world's languages at one of these stages. The BCTs so ordered in these 5 stages are BCTs for the Hering primaries. A third constraint concerns category focality: BCCs have best examples, sometimes called focal colours or prototypes [20]. These examples tend to be similar, cross culturally (as with the cross-cultural similarity of BCTs)

These then are the constraints for any theory that aims to explain, as Charles Witzel says "where colour categories come from." [20]. Such a theory must, to put things as generally as possible, tell us (1) why there is non-random variation in BCTs cross culturally and, (2), why colour categorical schemes (partitions of a colour space into BCCs) appear to develop in the order that they do, (3) why some colours are universally focal. Cultural relativism, the view that colour terms are determined strictly by cultural values [9], has a hard time with these constraints [20]. Relativism can explain variation, but how can it deal with the striking similarities revealed by the universalist findings initiated by the work of Berlin and Kay and continuing in a robust research program, to this day? [20] We shall have more to say about this shortly. First let us consider the issue which we started with—the long-standing puzzle over the relationship between infant colour categorical salience and adult categorical competence.

Colour category salience

Perceptual salience—of some colours more than others—has long been featured in explanations for the regularities discussed above. Shades of colour focal to a category as well as categories themselves have received significant discussion, and these bear on (3) above. Maybe focal colours are innately salient and play a role in the development of colour categories? Alternatively, maybe colour categories themselves are salient? This question pertains specifically to (1) and (2) and thus we will deal mainly with constraints (1) and (2).

The literature on colour categorical perception is complex and also problematical [20]. Roughly speaking, categorical perception occurs when subjects take inter-category distinctions to be more salient than intra-category distinctions. When infants are the subjects in experiments designed to show categorical perception (as they often are in the colour literature), saliency is measured in terms of habituation and dishabituation: how long does an infant look at a colour sample? How quickly does it look away? A central problem with colour categorical perception involves the location of the effect (if there is one). Is it an effect driven at low levels of the visual system, or at higher, cognitive levels? There is a sense in which this dispute is not important to our concerns. That is because whether the effect is low or high, the results of all of these experiments lead to the problem we summarized in the introduction. There is a mismatch between what the categorical perception experiments show and what we might expect, given the constraints. Here is how Bornstein summarized his own work in 1985: "An otherwise reasonable surmise from the fact that hue categorization precedes color naming developmentally would be that, in this one realm at least, linguistic identification simply overlays perceptual cognitive organization and thereby enormously facilitates semantic development. Paradoxically, it does not" [5]. Here is how the state of the art was summarized in Skelton et al 2017: "One important question for further research is how we transition from a prelinguistic color categorization based largely on biological mechanisms to a lexical color categorization that may make additional or fewer distinctions" [17].

Because this latter research explores colour categorical effects in retinogeniculate pathways, the authors are confident they have uncovered a low level "biological" mechanism as opposed to a higher level cognitive one. Yet the puzzle so straightforwardly described by Bornstein remains. How do you get from the biological mechanisms (or any mechanisms showing pre-linguistic categorical salience) to the linguistic colour categorical schemes—which differ cross culturally, however predictably—that we find in human languages (constraint (2), above) We point out here that the question isn't really about whether the pre-linguistic scheme matches up with the linguistic BCT models. The question is, why is there more than one linguistic model in the first place? Why is there any development at all, as opposed to just an "overlay" on the biological categories?

In this section we have quoted Bornstein from 1985 [5], and then from Skelton et al from 2017 [17], and we treated them as enmeshed in a similar problematic: why don't the colour categories in language track the prelinguistic categories? Bornstein, and this is evident elsewhere in his article and in other publications, is *surprised* lexical categories, as they develop, don't track the pre-linguist categories. It is, as he says a "paradox." This view at heart is a normative one. The paradox put most crudely has these two sides: A. colour categories x, y, z are prelinguistic. B. lexical colour categories may or may not correspond to x, y, z. This is a paradox (in a paradox, both sides cannot be true) only if one assumes there is reason to believe there should be an invariance between A and B. Indeed, Bornstein [4] goes on to talk about how some languages exhibit a natural form of "developmental continuity", while others, exhibit developmental discontinuity, perhaps as a consequence of special linguistic or cultural experience [4] (see also [10] for a detailed discussion of Bornstein's views on continuity). The idea of developmental invariance—that some biologically grounded traits resist developmental inputs has a long and problematical history in biology. It is problematical even for traits that do seem to show developmental invariance because, as the philosopher of biology Paul Griffiths says, "the fact that a trait is invariant across normal environments leaves it entirely open whether this is because the trait is insensitive to environmental factors or because the causally relevant factors are invariant across normal environments" [14]. The upshot of this ambiguity is twofold. On the one hand, a trait present at (or before) birth, may be susceptible to causes in the environment that disrupt the initial phenotype. But this is only a "disruption" if one believes there should be developmental continuity, which one should not assume. Secondly, even if there is universality, it does not follow that it is a consequence of a fixed and immutable developmental program. That is because similar environments (i.e., similarity in developmental inputs, across organisms) may bring about similar outcomes. We propose that both sides of this biological maxim are at work in colour naming/categorization. In particular, we hold that the categorical regularities are not accessed in early development. This is a function of two things: the way colour names and categories are initially formed, and the way in which, and what it is, speakers (children) learn when they learn "their colours" for their (socially embedded) colour categories.

Where do colour categories come from? (1)

The psychologist Jules Davidoff gives an answer to a related question, which bears on the issues we've been discussing: "The distinction, in Berinmo [a language spoken in Papua New Guinea] between leaves that are edible (green) and those that are inedible (yellow) makes up two of their terms. Their red term is the name of a berry which, like most berries, is a dark, saturated red when at its best to eat. The red term in other cultures is the word for blood (Rivers, 1905), which is a similar hue to the color of ripe berries. So a physiological explanation for the origin of color terms is not needed for any language, nor is it needed for the similarity of its terms to those in other languages for which there would be similar natural constraints." [9]

If we want an answer to where some specific colour term comes from, we shall get it from the sort of local cultural account described here. Interestingly, Davidoff generalizes this form of account to "other languages" as well. If you need an answer to where BCTs come from, for any BCT in any language (taking Davidoff literally here) you can get this answer in terms of the sorts of local facts that cultural anthropologists (and cultural relativists) trade in. You don't need to explain its similarity to that of words in other languages; you don't need to appeal to physiological facts (such as the biological salience of colour categories). You've got everything you need, explanation wise, in the context of a specific language. You don't need to satisfy the constraints we've discussed.

Davidoff's claims do not fully address Witzel's question since they apply to colour names not color categories. It is easy to run these two together and, indeed, the Berinmo have both BCTs and BCCs. While this is true, there is reason to believe that Davidoff's origin story for Berinmo red, etc., conceals a rich developmental history. Here is a just-so story designed to capture that history.

Imagine there are the following stages in the "coming from" story: First, there is a colour term with object reference which is restricted in its application. Nonetheless, colour is the property the term is referring to (or, at least, that's part of its reference)—we think that's true because the object related term is marked linguistically in some way. At this point there is no category, nor is there a BCT which has the capacity to function as a superordinate term. Such terms are proto-BCTs. When the reference-class for such terms is expanded, possibly by speakers/cognizers making judgements of similarity to the original object reference colour (the berry, in Davidoff's case, for Berinmo red), then the word for Berinmo red will function as a quasi-abstract category name. Next, by social consensus (because we are talking about words in a language, this must be the case) speakers agree as to the limits of the quasi-abstract category. Things just stop being correctly named Berinmo-red at some arbitrary point. Speakers have a conception of the colour Berinmo-red, but they don't have a conception of colour as an abstract domain. (They have abstracted a colour category, Berinmo-red, but they have not abstracted a domain of chromatic internally related colours: colours that are defined relative to one another rather than in relation to an exemplar). But the cognitive process of extracting the colour from the object (to put it bluntly) is not specific to the berry and its colour. It can be (this is Davidoff's point) applied in other cases as well: edible leaf-colour (Berinmo green) and inedible leaf-colour (yellow) are abstracted by the same process, so that you now have three object related, abstractions. While this state of affairs might remain like this, some groups of speakers/cognizers can and do make the further step of abstraction to colour as a domain of comparison, according to which one doesn't just use similarity to assign membership in a category (quasi-category). This involves comparisons of relative similarity: A (red) is more like B (yellow) than it is like C (green). These comparisons begin as individual judgements, for indexicalized object related colour, but they also open up the abstract world of internally related colours, and the possibility of thinking about colour, not just some version of colour-of. When this happens, BCTs have emerged as true superordinate terms, with referents that are true abstract colours.

Our main point in offering up this "just-so story" is to point out that colour categorical schemes (the distribution of terms in a language; their similarity to other such distributions) is at the endpoint of one sort of process. It is not until the domain of colour has been abstracted as a domain of internally related properties (of objects) that questions of boundaries between colours, can arise. At this point, and not before, speakers/cognizers can exploit a variety of perceptual and cognitive aspects of their experience to construct, in a socially/linguistically embedded way, a colour categorical scheme. It as it this point that the colour language for a group becomes organized, and it is a social, cognitive achievement rather than a mapping from prelinguistic experience. Part of the nature of colour categories—the fact that they form equivalence classes of non-identical stimuli—is that they are not perceivable, at least not until one has explicitly abstract orders such as the Munsell system (which is often used as the stimulus set for BCT/BCC research). Categorical perception, relative similarity, focality, saturation...these (and other) cognitive skills and markers can be exploited by speakers/cognizers only after colour experience has been cognitively scaffold in preparation. Biologically based perceptual categories do not express themselves directly into language because it's too hard for speakers/cognizers to do so. That's the message of our just-so story, but it's also the message we get from anthropology and from developmental psychology.

Where do colour categories come from? (2)

Local explanations of the sort Davidoff describes have one foot in the local and the other in the abstract. Nowhere is this clearer than in reduplicative languages such as Samoan [16] where, for example, *mū* means 'red hot; to burn' and *mūmū* means 'red'. The duplication of the root says: *talking about colour now*, and the historical linguistic relationship to the non-colour base word is clear. Not all languages exploit duplication for colour (or any) words, but the case need not be conceptually different for non-duplicative languages, just less clear to us. Abstract colour words do not come to us in abstract form—unless by loan, or cultural transmission across languages—they are something that needs to be accomplished conceptually and socially, and with that social accomplishment comes a distinct set of desiderata: once one can understand one's colour related words in terms of abstract, internal relations among BCT reference classes one can begin to think about them in a variety of ways. Questions like *is it more red than yellow*? start to make sense—and this sort of question, evaluating relative similarity (is A more like B than it is like C?) can function as a conceptual base for an abstract classificatory system.

Reduplicative languages form colour words by duplication, indicating explicitly the dual nature of colour words. It is true that duplicated colour terms were not counted in the original basic colour term theory [1]. They fail to satisfy certain of the conditions for being a BCT (notably, the conditions that states BCTs are (i) not the name of objects; and (ii) mono lexical. But these criteria need to be treated with some flexibility, not so that anything can count as a BCT but so that words which function as abstract colour classifiers are treated as such. That a word is *used* as an abstract colour classifier is, as several writers (e.g., [2], [3]) have pointed out, more important than its retained objectual referent. In any case, for the argument here, reduplicated colour terms show plainly something that may be harder to see in other cases: BCTs have a grounding in objectual reference, but the thing that is grounded is independent of that referent in the sense that BCTs come to name a colour, not a coloured thing. So, for example, discussion as to whether a word is abstract *enough* is common throughout Berlin and Kay's original analysis of the ethnographic literature [1] and central to the (early Berlin and Kay) idea of the BCT. BCTs in a language have etymological ties to objects, even though those ties may not be obvious or even known to speakers. Etymology and historical colour semantics uncovers relations of colour words to things that are discoveries of objectual grounding. The linguist Carole Biggam walks the reader through some examples and discusses the difficulties involved in actually making such origin-cases [2]. That is the origin story, for BCTs, and that is the story Davidoff is tapping into.

From a developmental perspective, children take a significant amount of time to master abstract colour terminology (BCTs). Children may learn BCT names in one-shot learning, and then take years to get the adult reference class correct enough to be competent colour language users [19]. The difficulty of learning colour words has a name in German: *farbendummheit* --"colour stupidity." Dedrick discusses this [10]; Wagner et al contextualize it in terms of developmental psychology [13]. What is difficult for speakers is not seeing the colour of an object as an abstract property (so Wagner et al argue) but reaching accordance as to what counts as a member of the emerging abstract category. Over time, children bring their understanding of the category into line with adult naming competence.

In her work on the origin of concepts the cognitive scientist Susan Carey [7], [8], argues explicitly against the continuity hypothesis—the idea that there is or should be an unproblematical transition from prelinguistic ("innate" in her terminology) concepts to adult versions of those concepts. In the case of numerical cognition, she makes the case that what children know about number, as infants, and what they come to know as a consequence of the development of adult numerical cognition are related, but not continuous. There is a principle children need to master to make that transition, one which, for example, non-human animals do not make. It is not a certain thing that, in some domain, there will be discontinuity, that is an empirical question. But Carey does state three criteria which she defends [7], [8], and which aim to predict discontinuous cognitive domains: (1) The CS2 (second, developed, cognitive system) should be very difficult to learn, (2) learners of CS2 should make systematic, far reaching errors, (3) CS2 should not be a feature of all cultures in the historical record, whereas CS1 (the base, undeveloped cognitive system) should be.

Interpreting the domain of colour cognition in terms of Carey's ideas about discontinuity is not a trivial task, but there is good evidence (some of which has been discussed here) that colour cognition does satisfy her three criteria. (1) and (2) are revealed in the developmental literature, while (3) is, for CS2, the upshot of cross-cultural investigations and, for CS1 would be, say, just the perceptual salience of categories we have been discussing. That salience, grounded in the retinogeniculate pathways, is taken to be a fact about human physiology and not culturally specific (though that is an empirical question).

CONCLUSION

If a domain is cognitively discontinuous, what follows? The details will be specific to the domain. In the case of numerical cognition, children need to master a "successor principle" and will not be competent counters until they do. In the case of colour cognition, we have sketched a hypothetical model for the transition (the just so story of BCC origins) and what it involves. Crucial is the inductive step from abstracted object colour to the abstraction of colour as a domain in which one can think.

The just-so story of where colour categories come from can be articulated at the level of individual speakers and individual language groups, and it doesn't need to make any reference to the BCT/BCC constraints. It need make no claims to satisfy them or not. How then, does one deal with the constraints? We want to say that the scaffolding that makes BCTs/BCCs possible, such that they can be compared cross-culturally as a language of colour doesn't require any particular saliences, and one of the virtues of both the Davidoff origin story and Wagner's developmental ideas, is that they should give us pause as to the value of any sort of perceptual salience that is effective prior to the actual practices whereby proto-BCTs are formed. They originate as the names of things, and only through a cognitive, developmental process is their reference expanded to a domain of colour independent, functionally, of the origins. The linguist Carole Biggam [2] offers a just so story similar to ours (this is but a portion of her account): "The majority of colour concepts will remain tied to particular entitles, as in the case of BEAR-COLOURED, and they are likely to have been labelled by words which, at least initially, have transparent meanings related to the entity. However, a few colour concepts may be found to be so important, and used so frequently, that they eventually free themselves from their object prototypes, and become applicable to any appropriately coloured entity" [2].

The idea of "importance" is connected for Biggam to practical value, as it is for Davidoff, but the key conceptual development in her account (if not Davidoff's) is that this importance transforms itself—from an important thing that has a certain colour, to a colour that is important, *qua* colour category.

If mastering colour words to an adult level of competence is difficult for children, it is much harder for those constructing their colour categories in the first place, on the ground, bootstrapping an abstract conception of colour out of their object specific interests. It's like the difference between supervised and unsupervised learning in neural networks. Children have a teacher that corrects their usage and guides them, slowly towards adult competence in a classificatory task—even this process is difficult! Without a teacher, what resources do nascent colour categorizers have access to? One answer would be this: they have access to, say, categorical perception, grounded in biology, and perhaps other perceptual aspects of colour (an irregularly shaped colour space; focality, perhaps). That's the Bornstein project which, we have seen leads to the conundrum with which we started: the perceptual and the linguistic don't match up in the way we should expect. But maybe we should have different expectations. Categorical perception is about category boundaries and their salience. We are arguing that BCC emergence require significant cognitive scaffolding that has to be in place to make questions about boundaries in an abstract colour space viable questions for language users. The capacity to detect categorical salience isn't anything like the ability to name basic colour categories to an adult level of confidence. We know this because of the difficulty children have in learning the colour categories of adult speakers in a language. Colour categories must be invented, bootstrapped off of the names for things, and then refined in a socially embedded way. It is in this context that, we propose, aspects of our perceptual experience such as categorical salience may be exploited, though not, as we have seen, in a developmentally continuous way. On this view, the constraints on BCT/BCC don't shape colour language from its origins.

REFERENCES

1. Berlin, B. & Kay, P. (1969). *Basic Color Terms: Their Universality and Evolution*. Berkeley, Ca: University of California Press.
2. Biggam, C. P. (2012). *The Semantics of Colour*. Cambridge, UK: Cambridge University Press.
3. Blust, R. (2001). Reduplicated colour terms in Oceanic languages, In Pawley, A., Ross, M. and Tryon, D. editors, *The boy from Bundaberg: Studies in Melanesian linguistics in honour of Tom Dutton*. PL514:23-50. Pacific Linguistics, The Australian National University, 2001. doi.org/10.15144/PL514.23
4. Bornstein, M.H. (1987). Perceptual Categories in vision and audition. In Stevan Harnad (Ed.). *Categorical Perception: The groundwork of cognition*. Cambridge: Cambridge University Press.
5. Bornstein, M.H. (1985). On the Development of Color Naming in Young Children: Data and Theory. Brain and Language 26: 72-93. doi: 10.1016/0093-934x(85)90029-x
6. Bornstein, M., Kessen, W., and Weiskopf, S. (1976). Color vision and hue categorisation in young human infants. *Journal of Experimental Psychology: Human Perception and Performance*, 2, 115–29.
7. Carey S. (2011). *The Origin of Concepts*. Oxford University Press.
8. Carey S. (2009) Where Our Number Concepts Come From. *The Journal of Philosophy*. 106: 220-254. doi: 10.5840/Jphil2009106418
9. Davidoff, J. (2015). Color Categorization across Cultures. In *Handbook of Color Psychology*, Andrew J. Elliot, Mark D. Fairchild, and Anna Franklin (Eds.). Cambridge UK: Cambridge University Press, 259–78.
10. Dedrick, D. (2002). The roots/routes of color term reference. *Theories, Technologies, Instrumentalities of Color: Anthropological and Historiographic Perspectives*. Barbara Saunders and Jaap van Brakel (Eds.) University Press of America, 53-68.
11. Franklin, A. (2015). Development of Color Categorization. In *Handbook of Color Psychology*, Andrew J. Elliot, Mark D. Fairchild, and Anna Franklin (Eds.). Cambridge, UK: Cambridge University Press, 279–94.

12. Franklin, A and Davies., IRL. (2005). Converging Evidence for Pre-Linguistic Colour Categorizations. In *Progress in Colour Studies Volume II: Psychological Aspects*, N. J. Pitchford and C.P. Biggam (Eds.) Amsterdam: John Benjamins, 101-20.
13. Griffiths, P. E. (2001). What is innateness? *The Monist* 85 (1):70-85.
14. Franklin, A., Pilling, M., & Davies, I. R.L. (2005). The nature of infant color categorization: Evidence from eye movements on a target detection task. *Journal of Experimental Child Psychology, 91*(3), 227–248. doi.org/10.1016/j.jecp.2005.03.003
15. Kay, P. (2015). Universality of color categorization. In *Handbook of Color Psychology*, A.J. Elliot, A. Franklin, and M.D. Fairchild (Eds.), Cambridge: Cambridge University Press, 243–244.
16. Snow, D. L. (1971). Samoan color terminology: a note on the universality and evolutionary ordering of color terms. *Anthropological Linguistics*, 13:8: 385-90.
17. Skelton A. E., Catchpole G., Abbott J.T., Bosten J.M., Franklin A. (2017). Biological origins of color categorization. *Proc Natl Acad Sci* U S A. May 23;114(21): 5545-5550, https://www.pnas.org/doi/full/10.1073/pnas.1612881114
18. Groh, A. (2016). Culture, Language and Thought: Field Studies on Colour Concepts. *Journal of Cognition & Culture*, 16(1/2), 83–106. doi.org/10.1163/15685373-12342169
19. Wagner, K., K. Dobkins, & D. Barner. (2013). Slow mapping: Color word learning as a gradual inductive process. Cognition, 127(3), 307–317. doi.org/10.1016/j.cognition.2013.01.010
20. Witzel, C. (2019). Misconceptions About Colour Categories. *Review of Philosophy and Psychology* 10: 499–540. https://doi.org/10.1007/s13164-018-0404-5
21. Zaslavsky, N., Kemp, C., Tishby, N. & Regier, T. (2020) Communicative need in colour naming. *Cognitive Neuropsychology*, 37:5-6, 312-324, doi: 10.1080/02643294.2019.1604502

Session 7

Doi Tung
1 December 2023

COLOR AFTERIMAGE APPEARANCE MEASURED WITH NATURAL COLOR SYSTEM

Vincent C. Sun[1]*, Ching Wei Peng[2], and Ming Chuan Fu[3]

[1] *Department of Mass Communication, College of Journalism and Mass Communications, Chinese Culture University, Taiwan.*
[2 3]*Department of Visual Communication Design, The College of Design, NTUA, Taiwan.*

*Corresponding author: Vincent C. Sun, csun@faculty.pccu.edu.tw

ABSTRACT

A color afterimage is the perceived hue that appears in the visual field when viewing a blank background after an inducing or adapting chromatic stimulus has been presented in that area for a certain duration. Color afterimage experiences are triggered by physical stimuli but persist even in the absence of such stimuli. It is a private perceptual experience, yet it remains a significant focus of scientific investigations. Researches of color afterimages usually focus on the appearance of these afterimages, and various methods for measuring their appearance had been developed. Some researchers tried to uncover links between color afterimages and other color-related phenomena, such as simultaneous color contrast, complementary colors, color constancy, chromatic adaptation, color memories, and even the misbinding of color and form. The neural basis of color afterimages has also been a focal point in several studies, exploring whether the chromatic adaptation mechanism occurs in the retina, the brain, or both. The authors presented a preliminary literature review paper on the procedures for measuring afterimage appearance at the ACA 2022 conference. In this current study, the authors adopted the Natural Color System (NCS) as the reference system for measuring and representing the color appearance of afterimages. The inducing (adapting) stimuli consisted of selected color patches with various hues and nuances (blackness and chromaticness) according to the NCS notations, while the induced (adapted) afterimage hues were determined by matching the perceived afterimages to a color circle comprised of 40 patches. These 40 patches were chosen from the standard 40 NCS hues, all with the same nuance value in the initial phase. After establishing the hue for a given induced patch, a second-stage matching task utilized a set of patches with reduced chromaticness to achieve a nuance match. All stimuli were presented on a calibrated digital LCD panel based on the official NCS RGB values within the sRGB color space. The hue contrast between the inducing stimuli and induced afterimages, as well as the spatial and temporal parameters of the inducing stimulus presentation, were fine-tuned through a pilot study to enhance the perception of afterimages. The resulting data were used to construct a color afterimage map in the NCS color space and provide practical guidelines for designing applications involving induced color afterimages.

Keywords: Color Afterimage, Color Appearance, Natural Color System

INTRODUCTION

The perceptual phenomenon of seeing a faintly colored, blurry blob on a blank surface after gazing at a vivid color stimulus for an extended period typically exhibits characteristics that distinguish it from the initial induced color stimulus. The color of this afterimage is notably less saturated and often features hues that are opposite to those of the inducing stimulus. Some experts in color theory have Some experts in color theory defined the hues of afterimages as the complementary hues of the induced colors [1], a concept that diverges from the standard definition of complementary colors established by the CIE [2]. Afterimages represent a kind of perception perceived without concurrent external physical stimuli, yet they are apparently induced by prior physical stimuli.

The stimuli that induce a color afterimage do not necessarily have to be presented within the same visual field area where the afterimage is subsequently perceived. Anstis et al. [3] demonstrated that perceived colors resulting from simultaneous contrast could generate afterimages even in the absence of a preceding physical color stimulus on the area, and conversely, color afterimages could also give rise to simultaneous contrast colors. Additionally, studies utilizing the "two-room technique" [4; 5] showed that the perception of chromatic colors induced by exposure to chromatic illuminations could generate color afterimages. These afterimages exhibited appearances corresponding to the perceived colors which did not align with how the spectrum would appear when viewed in isolation [6; 7].

Color constancy phenomena have also been observed in the context of color afterimages. For instance, when a Mondrian pattern comprises various color patches illuminated by light of a specific spectral composition, these patches may exhibit particular colors that diverge significantly from the colors indicated by their reflected spectra. In cases where individuals observed afterimages following their viewing of these Mondrian patterns, the afterimage colors tended to follow with the perceived colors of the patches rather than the colors dictated by their reflected spectra [8]. Specifically, a patch that appeared neutral when viewed in isolation but took on a distinct color due to the workings of the color constancy mechanism would produce an afterimage color that mirrored its appearance within the Mondrian pattern context [8].

The investigation of the neural representation and mechanisms underlying color afterimages represents another critical aspect of research into afterimage phenomena. The traditional perspective posited that afterimages stemmed from neural adaptation occurring in retinal cells [9]. Based on the previously mentioned study about afterimages of Mondrian patterns, Zeki et al. [8], drawing on the previously mentioned study of Mondrian pattern afterimages, proposed that colored afterimages possessed a cortical representation, as color constancy could only be adequately explained through cortical mechanisms. However, it's important to note that in their study, afterimage colors were determined by observing the perceived afterimage across the entire Mondrian pattern, and color constancy could potentially apply to the comprehensive adapted retinal representation. Therefore, it remains a possibility that a retinal mechanism alone could still play a role in determining afterimage colors in this specific scenario. In vivo direct neural measurements revealed that primate retinal ganglion cells generated rebound responses following the termination of prolonged adapting stimuli. These responses could potentially serve as the afterimage signals for subsequent visual information processing [10]. Nevertheless, misbindings of color to form in afterimages observed during dichoptic viewing conditions implies the presence of a neural representation for binocular combination and suggests the essential involvement of cortical mechanisms in the generation of color afterimages [11].

While afterimages can be induced by indirect percepts, as previously mentioned, those resulting from viewing physical stimuli remain the most common phenomena. Studies that have delved into the chromatic aspects of afterimages typically aimed to address related issues, such as complementary colors [12], the sensitivities of L-M cones [9], and even their relevance to neurodevelopmental disorders [13]. In the present study, our focus was specifically on the color appearance of afterimages following the observation of a colored patch. Our goal was to establish a practical relationship between the colors that induce (adapt) afterimages and the corresponding colors of the induced afterimages in standard viewing conditions. We deliberately selected color samples from the Natural Color System (NCS) color space, which provided a representative array of chromatic samples that properly depict color appearance [14; 15], as opposed to adapting samples selected from the CIE diagram [16], which lacks meaningful information about color appearance [17]. The afterimage colors were also obtained through direct matching with NCS samples and presented within the NCS color space. This enabled us to illustrate the relationships between the inducing samples and the induced afterimages within the context of the NCS color space, offering valuable insights for applying afterimage effects in design applications.

METHODOLOGY

The experimental environment was set up in a room with reduced illumination. A calibrated LCD screen (Eizo) was used for stimulus presentation. A Cedrus RB-530 response pad is employed as the response device. The distance between the participant and the screen when looking straight ahead is 1 meter. The participants were reminded to maintain an upright sitting posture during the test. There were a total of 21 participants, with 3 of them participating in the experiment twice to check the procedure's reliability. The age range of the participants was 22-30 years old, with 5 students having a non-visual arts background, and the remaining 16 participants were graduate and undergraduate students majored in visual arts or visual design. Among the participants, there were 3 males and 18 females. All participants were screened for normal color vision.

Drawing from the insights gained during the pilot study, we chose the inducing hues from the standard NCS hue wheel, comprising 40 hues, with an interleaved separation of one. This selection method yielded a total of 20 hues that were utilized as inducing colors. Each of these 20 inducing stimuli was carefully picked to correspond to the NCS nuance featuring the highest chromaticness (c) value associated with that particular hue (as shown in Figure 1). To ensure accuracy and consistency, all RGB values employed for displaying the NCS samples on the LCD monitor in this study were derived from the NCS-CIELAB-RGB Translation Table.

Given the fluctuating nature of afterimages, we employed a modified two-phase task inspired by the work of Zeki et al. [8] to ascertain the afterimage colors for each participant. In the initial phase, participants were presented with a color wheel comprising 40 standard NCS hues, all possessing the nuance 1040 (as depicted in Figure 2). This phase served to select the afterimage hue. Subsequently, based on the afterimage hue chosen in the first stage, a second-stage matching task was conducted. This task involved annulus patches featuring varying NCS chromaticness values, facilitating an additional afterimage-inducing procedure with the same inducing hue, thus determining the saturation of the afterimage color. A detailed depiction of the experimental procedures is illustrated in Figure 3.

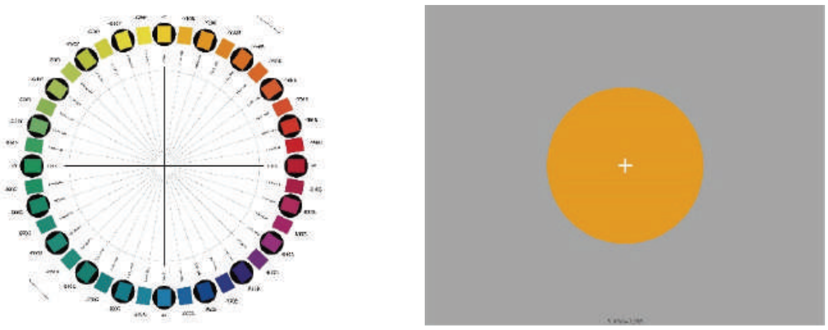

Figure 1. The stimuli used to induce afterimages.

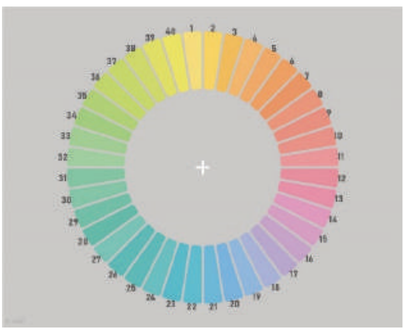

Figure 2. The color wheel displayed for the selection of afterimage hues.

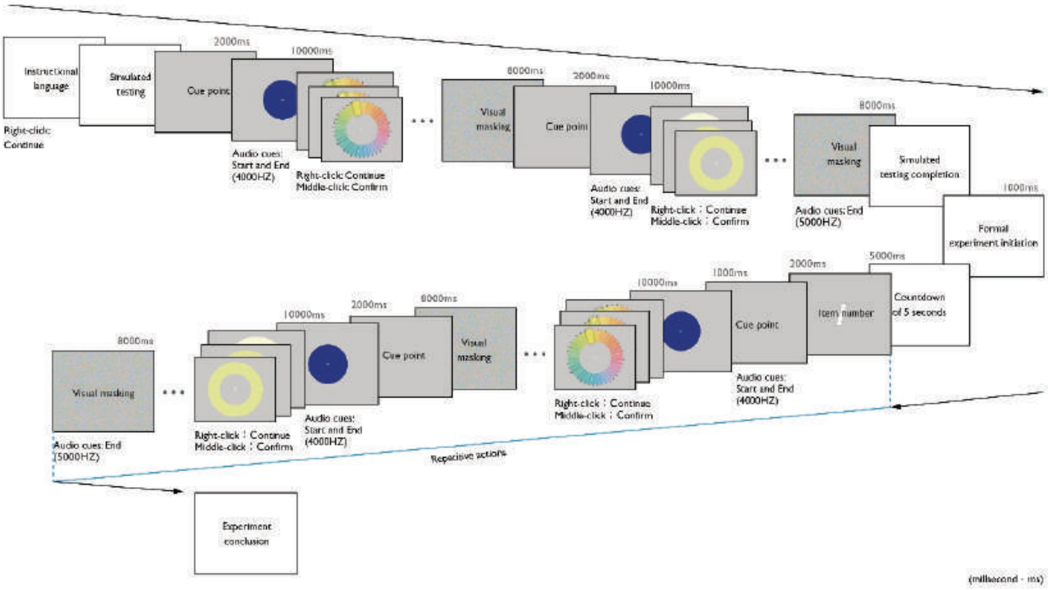

Figure 3. The procedures for obtaining an afterimage color in the present study.

RESULT AND DISCUSSIONW

We adopted the plot style recommended by Koenderink et al. [16] to visually represent the resultant afterimage colors for each participant and each inducing color, as depicted in Figure 4.

Figure 4. The afterimage colors for each participant (Sj) and each inducing color

The chromaticness (c) values of the afterimages resulting from each inducing stimulus play a pivotal role in comprehending the attributes of afterimage colors. To illustrate the nuances of all perceived afterimage colors across the 21 participants, we utilized NCS triangles. Figure 5 showcases individual triangles designated for specific inducing colors, with the perceived afterimage colors represented as circles positioned accordingly. Variations among participants in afterimage hues are indicated by tints and accompanying text labels. In total, there are twenty individual triangles corresponding to all the hues employed in this study. However, Figure 5 displays only four of them, specifically the triangles associated with the hues Y, R, B, and G.

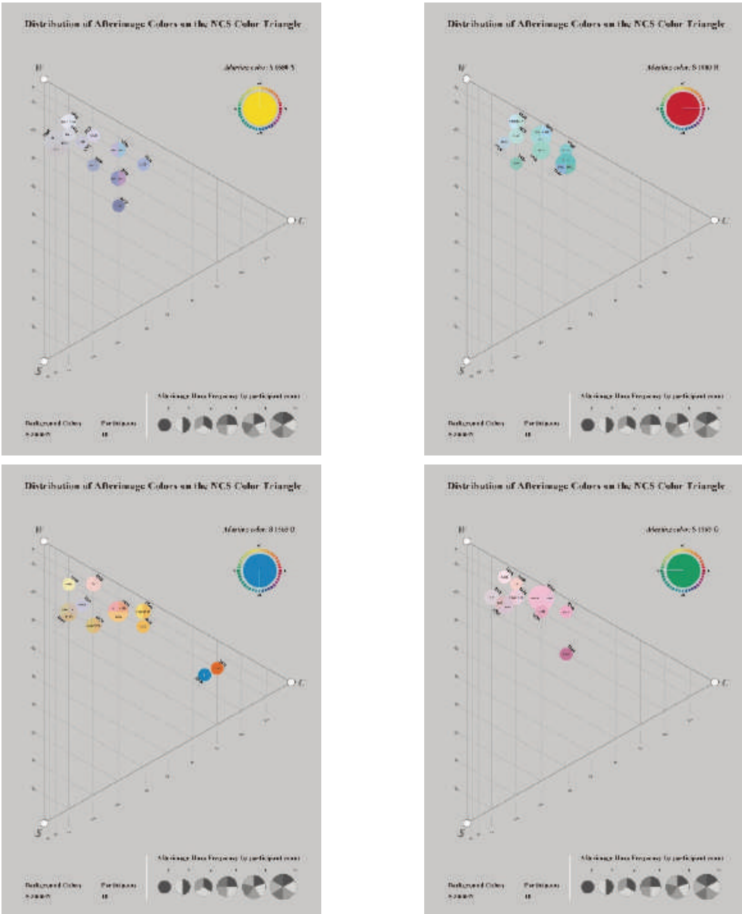

Figure 5. Nuances of perceived afterimage colors for NCS Y, R, B, G hues.

CONCLUSION

The current study involved a direct assessment of human participants with normal color vision, measuring their perception after viewing a colored patch. Both the adapting stimuli and the resulting afterimages perceived against a neutral background were all represented within the NCS color space using standard digital samples. The outcomes reveal a coherent mapping of afterimage colors, notwithstanding a few outliers that could potentially be attributed to operational errors. In common scenarios, afterimage colors consistently exhibit lower saturation and increased whiteness (w) in comparison to their inducing colors. These findings can offer valuable guidance to artists and designers when dealing with afterimages.

ACKNOWLEDGEMENT

The authors would like to extend our heartfelt gratitude to Ching-Yu Wu for his exceptional dedication and expertise in coding the computer program that played a pivotal role in the success of this research project. His invaluable contribution has significantly enhanced the efficiency and accuracy of our work.

REFERENCES

1. Green-Armytage, P. (1996). Complementary Colours-Description or Evaluation? In L. Sivik (Ed.), *Colour and psychology* (pp. 205-209). Stockholm: Scandinavian Colour Institute
2. Wyszecki, G., & Stiles, W. S. (1982). *Color Science - Concepts and Methods, Quantitative Data and Formulae. 2nd Edition*. New York: John Wiley & Sons.
3. Anstis, S., Rogers, B., & Henry, J. (1978). Interactions between simultaneous contrast and coloured afterimages. *Vision Research, 18*, 899-911.
4. Ikeda, M. (2004). Color appearance explained, predicted and confirmed by the concept of recognized visual space of illumination. *Optical review, 11*, 217-225.
5. Mihara, Y., Hamada, K., Phuangsuwan, C., Mitsuo, I., & Mizokami, Y. (2017). Change of color appearance of invariant psychophysical color by the chromatic adaptation to illumination. *Journal of the Color Science Association of Japan, 41*(3+), 58-59.
6. Phuangsuwan, C., & Ikeda, M. (2017). Chromatic adaptation to illumination investigated with adapting and adapted color. *Color Research & Application, 42*(5), 571-579.
7. Phuangsuwan, C., Ikeda, M., & Mepean, J. (2018). Color appearance of afterimages compared to the chromatic adaptation to illumination. *Color Research & Application, 43*(3), 349-357.
8. Zeki, S., Cheadle, S., Pepper, J., & Mylonas, D. (2017). The constancy of colored after-images. *Frontiers in human neuroscience, 11*, 229.
9. Williams, D. R., & MacLeod, D. I. (1979). Interchangeable backgrounds for cone afterimages. *Vision Research, 19*(8), 867-877.
10. Zaidi, Q., Ennis, R., Cao, D., & Lee, B. (2012). Neural locus of color afterimages. *Current Biology, 22*(3), 220-224.
11. Shevell, S. K., CLAIR, R. S., & Hong, S. W. (2008). Misbinding of color to form in afterimages. *Vis Neurosci, 25*(3), 355-360.
12. Cuasante, J. M. G., Muñoz, F. A., & Riaño, M. C. (2020). A Methodology for the Prediction of Complementary Colours in Chromatic Afterimages. *Colour Turn*(2).
13. Maule, J., Stanworth, K., Pellicano, E., & Franklin, A. (2018). Color afterimages in autistic adults. *Journal of Autism and Developmental Disorders, 48*(4), 1409-1421.
14. Hård, A., Sivik, L., & Tonnquist, G. (1996). NCS, natural color system - From concept to research and applications. Part I. *Color Research and Application, 21*(3), 180-205.
15. Hård, A., Sivik, L., & Tonnquist, G. (1996). NCS, natural color system - From concept to research and applications. Part II. *Color Research and Application, 21*(3), 206-220.
16. Koenderink, J., van Doorn, A., Witzel, C., & Gegenfurtner, K. (2020). Hues of color afterimages. *i-Perception, 11*(1), 2041669520903553.
17. 孫慶文, & 李天任. (2009). 色彩系統之介紹與應用. *光學工程季刊, 108*, 42-51.

DEVELOPING CCT AND LUMINANCE CORRCTION FUNCTIONS FOR HIGH DYNAMIC RANGE BASED ON REAL-WORLD SCENE

Yuechen Zhu[1]* and Ming Ronnier Luo[2]

[1] *State Key Laboratory of Modern Optical Instrumentation, Zhejiang University, CHINA.*

*Corresponding author: Ming Ronnier Luo, m.r.luo@zju.edu.cn

ABSTRACT

A real-world scene in a LED lighting room with high dynamic range was established in this study. Highlight area of the scene was set to 50,000 lux with an additional LED spotlight to simulate the sunrise. A simultaneous colour matching experiment was conducted, 1680 matches were accumulated. It can be found that CCT and luminance are relatively independent of each other in HDR lighting conditions. The CCT values matched on the display were higher than the real scene especially under the low CCT lighting conditions, and the CCT difference decrease with the CCT of the real scene increase. The luminance compression of human visual system could be largely affected by the average luminance of the scene. Finally, the visual results were used to fit CCT and luminance correction functions with a high coefficient of determination.

Keywords: High Dynamic Range Imaging, Real-World Scene, Luminance Correction, CCT Correction

INTRODUCTION

The dynamic range of real-world scenes can be quite high, ratio of 100,000:1 is common in the natural world. So current devices cannot capture or display. A new technology called high dynamic range imaging (HDRI/HDR) emerges to reduce the luminance gap between the captured images and the real scenes. It is a process in which a greater dynamic range of light is captured throughout the lightest and darkest areas of an image.

Tone Mapping Operators (TMOs) were used to reproduce the visual perception of a scene with a high dynamic range (HDR) on low dynamic range (LDR) media [1]. There have been existing models. Reinhard et al. proposed a new global tone reproduction operator to help solve the tone reproduction problem based on a sigmoidal curve [2]. Lischinski et al. presented an interactive tool for making local adjustments of tonal values and used Human Visual System (HVS)-inspired methods [3]. Luo and Mehmood et al. developed a perceptual tone mapping and colour correction models based on CIECAM16 for HDR Imaging [4].

But the above models were developed based on experimental results using no-reference assessment method. Luo and Shi et al. also conducted a colour matching experiment to get the corresponding colours in HDR conditions and modified the CIECAM16 using the visual data [5]. The limitation of the study is that only coloured patches were used and the experimental setting was different from the real HDR scene.

In this paper, a real-world scene in a LED lighting room with high dynamic range was established. And an additional LED spotlight was used to light up the area of sun and simulated the sunrise scene. A simultaneous colour matching experiment was conducted and the visual results were used to fit CCT and luminance correction functions using linear and nonlinear regression of least-squares procedure. It can be found that CCT and luminance are relatively independent of each other in HDR lighting conditions and the luminance compression of human visual system could be largely affected by the average luminance of the scene.

METHODOLOGY

A photo of sunrise printed by Giclee printing in A0 size was used as a test sample in the experiment, which was completely matte with good colour quality. The whole scene was set to 12 lighting conditions using 4 uniform surface LED light sources, including 3 illuminance levels (500, 1000, 3000 lux) and 4 CCTs (3000, 4500, 6500, 8000K). And an additional LED spotlight was used to light up the area of sun and simulated the sunrise scene. Thus, highlight area (sunrise) of the sample was set to 50,000 lux constantly among all the lighting conditions. A Macbeth Colour Checker Chart (MCCC) was placed in the scene to realize a quick adaptation and was also used as the test colours for the colour matching. Figure 1 shows the position of the test sample, the MCCC and lighting equipment. The viewing environment was specially arranged for observers to view only the print in the viewing field through an observation window on the wall, and lighting equipment would not be seen. The print in view looked like a real sunrise. Figure 2 is the illustration of the experimental setup showing detailed setting.

(a)

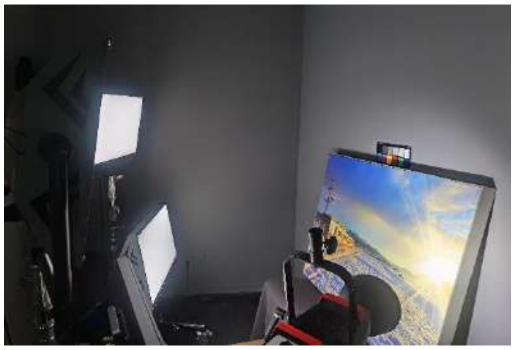

(b)

Figure 1. Test sample and lighting environment.

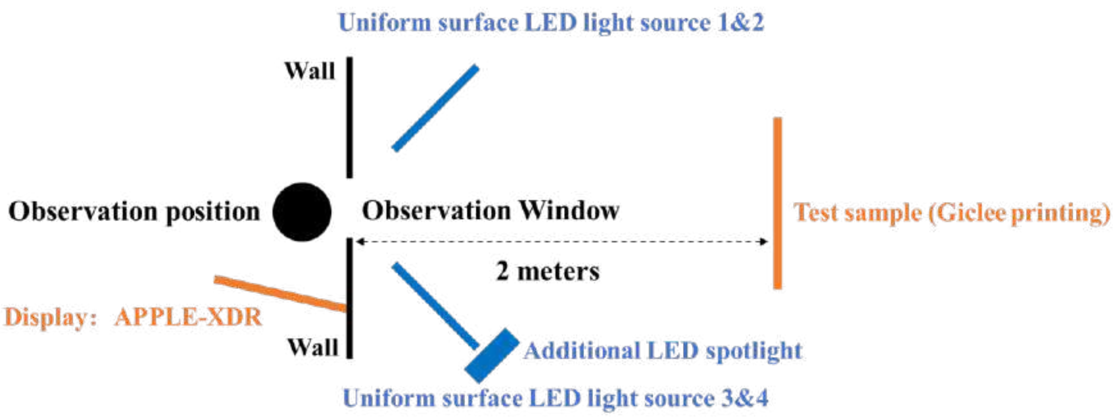

Figure 2. Experimental setup.

After adapting to the lighting conditions, observers were asked to adjust each of 6 patches in terms of a grey scale on an Apple Pro Display XDR (luminance level: 525 cd/m^2), and match the bottom row of MCCC in the real scene. Figure 3 shows the experimental interface, note that there was a reference patch (RGB = [255 255 255]) displayed in the upper right corner of the screen to simulate the highlight in the real scene. The task was to match the CCT and luminance of the patches until they matched the real scene simultaneously. In total, 20 normal colour vision observers took part in the experiment, and 1,680 matches were accumulated, i.e., 6 patches × (12 lightings + 2 repeats) × 20 observers = 1,680 matches.

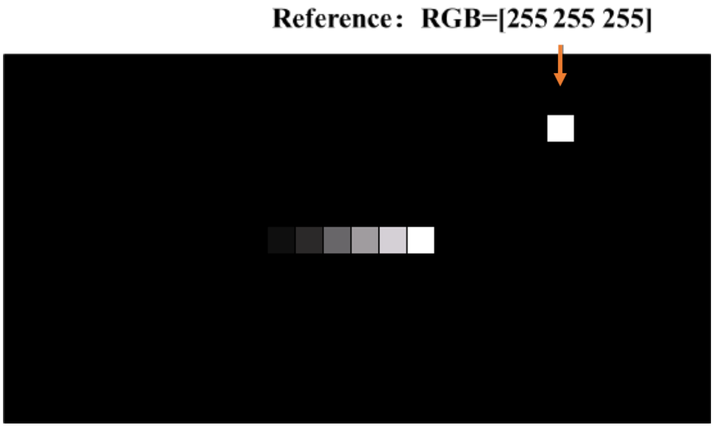

Figure 3. Experimental interface.

RESULT AND DISCUSSION

Mean Colour Difference from the Mean (MCDM) were calculated to represent the observer variation of the results. The inter- and intra- observer variation were 3.5 and 2.3 units of CIEDE2000, showed in Table 1, which was comparable to previous studies using colour matching method.

Table 1: observer variation

	Inter	Intra
CIEDE2000	3.51	2.28
CIEDE2000c	1.11	1.34

Because of the high consistency of the results from different observers, average results were used in the following analysis. Twelve sets of corresponding data were accumulated under 12 lighting conditions. Figure 4 shows the average result in terms of CCT (K). As for the luminance of No.1 patch (black) was extremely low among all the lighting conditions, the CCT was difficult to distinguish, the results of CCT were obtained by averaging the results from No.2 to No.6 grey patch.

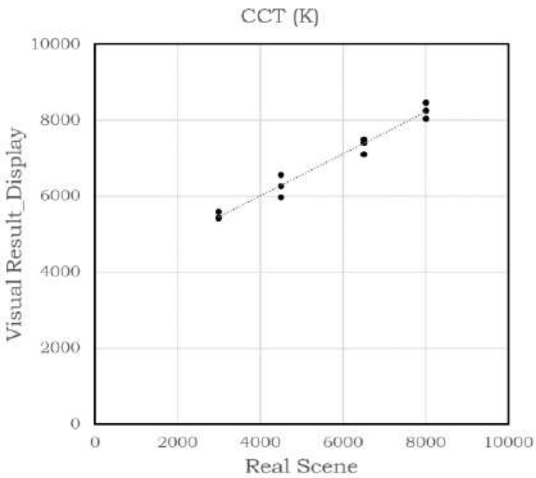

Figure 4. The average visual result in terms of CCT (K).

It can be found that the CCT values matched on the display were higher than the real scene especially under the low CCT lighting conditions. The CCT difference decrease with the CCT of the real scene increase. Until the CCT increased to 8000K, the visual results were very close to the real scene. And the luminance had little effect on CCT in HDR lighting conditions. Linear equation was used to fit the results with a high coefficient of determination (R^2=0.97), see Eq. (1).

$$CCT_P = 0.5517 * CCT_S + 3796 \tag{1}$$

Where CCT_S is the CCT of the real scene, CCT_P is the predicted CCT on the display.

Figure 5 shows the average result in terms of luminance (cd/m²). It can be proved again that CCT and luminance are relatively independent, which means the CCT had little effect on luminance in HDR lighting conditions. And the luminance compression of human visual system could be largely affected by the average luminance of the scene.

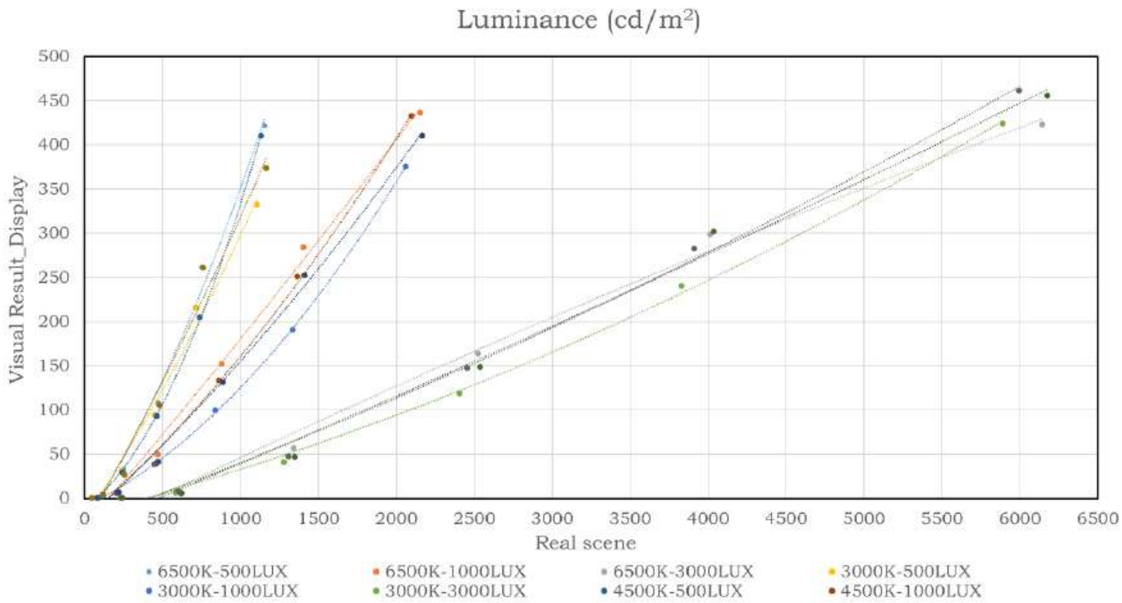

Figure 5. The average visual result in terms of luminance (cd/m²).

The visual results were used to fit a luminance correction function using nonlinear regression of least-squares procedure, and gave a good prediction performance (R^2=0.98), see Eq. (2).

$$\begin{aligned} f1 &= 13.0935 \times L_M - 8946.7 \\ f2 &= 0.8358 \times {L_M}^{-0.1373} \\ L_P &= L_D \Big/ \left(1 + f1 \times e^{-{L_S}^{f2}}\right) \end{aligned} \tag{2}$$

Where L_M is the average luminance of the whole scene, L_D is the maximum luminance of the display, L_S is the luminance of the real scene (pixel by pixel), L_P is the predicted luminance on the display.

Then, 3 real scenes were measured by a hyperspectral camera to test the performance of the functions. Figure 6 shows the prediction results, it can be found that the contrast of the image was be enhanced, and the CCT looks closer to the real scene.

	3000K	4500K	8000K
Scene 1			
Scene 2			
Scene 3			

Figure 6. The prediction performance of the functions.

CONCLUSION

A real-world scene in a LED lighting room with high dynamic range was established in this study. The whole scene was set to 12 lighting conditions using 4 uniform surface LED light sources, including 3 illuminance levels (500, 1000, 3000 lux) and 4 CCTs (3000, 4500, 6500, 8000K). Highlight area of the scene was set to 50,000 lux with an additional LED spotlight to simulate the sunrise. A simultaneous colour matching experiment was conducted, 6 grey patches of Macbeth Colour Checker Chart (MCCC) were selected for the colour matching. Totally, 20 observers took part in, and 1680 matches were accumulated.

This study mainly drew 4 conclusions:

1. CCT and luminance are relatively independent of each other in HDR lighting conditions, which means luminance had little effect on CCT and CCT also had little effect on luminance.
2. The CCT values matched on the display were higher than the real scene especially under the low CCT lighting conditions, and the CCT difference decrease with the CCT of the real scene increase. Until the CCT increased to 8000K, the visual results were very close to the real scene.
3. The luminance compression of human visual system could be largely affected by the average luminance of the scene. Thus, the average luminance of the scene should be considered as a parameter in the correction functions.
4. The visual results were used to fit CCT and luminance correction functions with a high coefficient of determination.

REFERENCES

1. Narwaria, M., Da Silva, M. P., Le Callet, P., Pepion, R. (2014). Signal Processing: Image Communication. *Tone mapping based HDR compression: Does it affect visual experience?,* 29(2), 257-273. doi: 10.1016/j.image.2013.09.005.
2. Reinhard, E., Devlin, K. (2005). IEEE Transactions on Visualization and Computer Graphics. *Dynamic range reduction inspired by photoreceptor physiology*, 11(1), 13-24. doi: 10.1109/TVCG.2005.9.

3. Lischinski, D., Farbman, Z., Uyttendaele, M., Szeliski, R. (2006). ACM SIGGRAPH 2006 Papers: Association for Computing Machinery. *Interactive local adjustment of tonal values*, 646–653. doi: org/10.1145/1179352.1141936.
4. Imran, M., Xiaoxuan, L., Usman, M., Ming, R. L. (2022). Journal of the Optical Society of America A. *Method for developing and using high quality reference images to evaluate tone mapping operators*, 39(6), 11-20. doi: 10.1364/JOSAA.450581.
5. Xinye, S., Yuechen, Z., Ming, R. L. (2021). Color and Imaging Conference. *A new corresponding color dataset covering a wide luminance range under high dynamic range viewing condition*, 184-187. doi: 10.2352/issn.2169-2629.2021.29.184.

New Vividness and Depth Equation developed by CAM16 Q, M

Molin Li[1] and Ming Ronnier Luo[1]*

[1]*State Key Laboratory of Modern Optical Instrumentation, Zhejiang University 310027, China.*
*m.r.luo@zju.edu.cn

ABSTRACT

Color appearance model serves as a framework for describing the stimulus of human vision by colors in real-world scenarios, consisting of three fundamental dimensions: Lightness, Chroma, and Hue. Berns introduced scales for Vividness and Depth based on a combination of lightness and chroma, formulating their metrics (V*, D*) using the CIELAB model. However, the applicability of these scales is limited in high dynamic range environments due to the constrained contrast of Lightness based on a reference white. This study designs a psychophysical experiment based on Magnitude Estimation, utilizing a Thouslite LEDView cabinet capable of adjustable luminance levels ranging from 10 cd/m^2 to 10,000 cd/m^2. We collected two-dimensional scale data for four metrics: Vividness, Depth, Whiteness, and Blackness, totaling 6,400 estimations. Utilizing this data, experimental models were developed based on the CIECAM16 Q and M scales, yielding STRESS value of 12 for Vividness and 14 for Depth.

Keywords: Vividness, Depth, Color Appearance Model, 2-D Color Appearance Scales

INTRODUCTION

The Color Appearance Model (CAM) is extensively employed in the textile, printing, and imaging sectors for color reproduction and color management across various media. The fundamental structure of CAM primarily encompasses three core color scales: Lightness, Colorfulness, and Hue Angle, both in absolute and relative measures. However, color variations in real-life scenarios often extend beyond these foundational scales. For instance, as the concentration of color pigments on white paper increases, Lightness decreases, while colorfulness concurrently rises. Addressing these intricacies, Berns (2014) proposed the concept of the two-dimensional color appearance scales [1]. Drawing from the CIELAB model's Lightness (L*) and Chroma (C*), he derived metrics for Vividness (V*), Depth (D*), and Clarity (T*). Herein, V* signifies the distance of a color from neutral black, representing the direction in which color increases alongside Lightness and Chroma from the backlight surface to the photometric plane. D* characterizes the transition from white light to pure color, where the color's Lightness diminishes while Chroma escalates. T*, on the other hand, denotes the distance between the color and the background color. While Berns did not conduct psychophysical experiments specifically for the 2-D color appearance scales, Cho et al. (2017) did undertake such experiments [2]. Cho's research engaged participants from both British and Korean ethnicities, utilizing 6-point interval scales to evaluate Vividness, Depth, Whiteness, and Blackness. The definitions for Blackness and Whiteness were adopted from the Natural Color System (NCS). Drawing upon the experimental data, Cho proposed distinct two-dimensional scale models using two methods: the Hue-based equation and the Ellipsoid-based equation. However, Cho et al. did not provide a clear definition for "origin", and the samples they selected did not encompass both high and low luminance, as well as low chroma samples. There's also a need to investigate, within the context of the 2-D scales, whether Lightness or Chroma holds a greater weight. Importantly, most previous studies were conducted under standard luminance (~ 500 cd/m^2) using light boxes, leaving research on scales under high luminance scenarios notably scarce. The primary direction of this research comprises two main objectives. First, we aim to design a 2-D color appearance scale experiment under high dynamic range conditions, based on a defined "origin" and ratio scale. The goal is to produce reliable experimental data. Subsequently, utilizing this data and drawing on the CIECAM16 Q and M metrics, we intend to introduce an absolute scale 2-D color appearance model.

EXPERIMENT

Materials and Equipment

In the study, we employed the NCS ATLAS II as the experimental sample, which features chromaticness ranging from 03 to 80 and blackness from 06 to 70 [3]. This sample consisted of a 5x5 inch material with an L* value of 65.5, harmonizing with the background. Central to this setup is a 3x3 inch section of the NCS ATLAS II, which exhibits a distinct gloss. Measurements of spectral reflectance were captured using a Konica Minolta CM700D spectrophotometer. The backdrop for the experiment was a neutral gray background with a CIELAB value of [65.5, -1.6, 3.4]. Observations were made in a Thouslite LEDView cabinet, a specialized lightbox with luminance adjustability ranging from 0.1 cd/m^2 to 100000 cd/m^2. Additionally, spectral power distributions (SPD) were recorded using a Konica Minolta CS2000 spectrophotometer. The SPD was calibrated for the lightbox at four reference white luminance levels: 10 cd/m^2, 100 cd/m^2, 1000 cd/m^2, and 10000 cd/m^2. Notably, the lowest luminance for the color patch achieved was 0.3 cd/m^2, resulting in an overall color stimulus dynamic range of 75.57 dB. The schematic diagram of the actual experimental setup is shown in Figure 1.

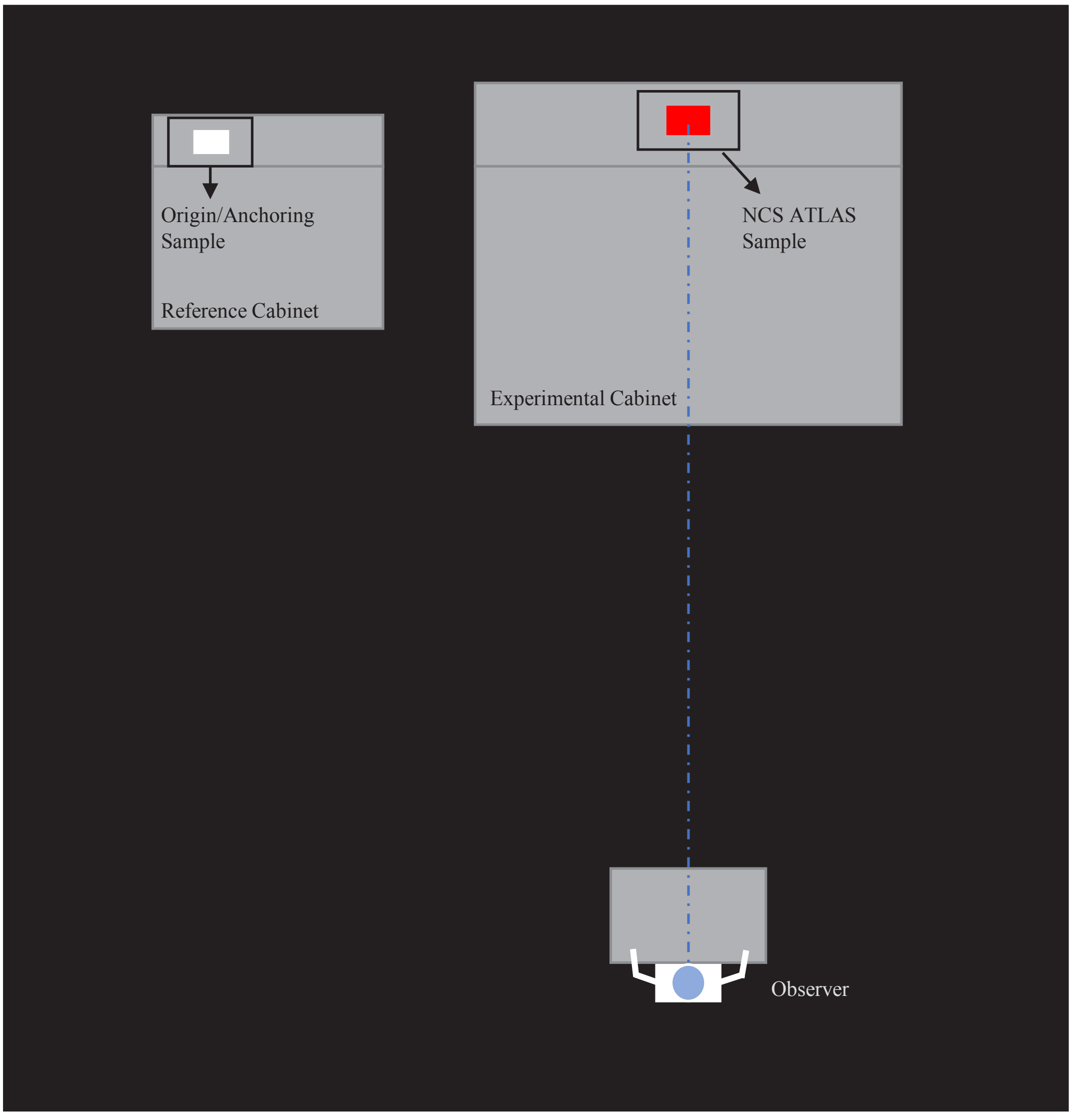

Figure 1. The demonstration of the experiment environment. The reference was to set the anchoring/origin sample and to do the training session. The experimental cabinet is to do the formal experiment which can adjust the illuminance from 0.1 cd/m^2 to 100000 cd/m^2.

Procedures

The experiment was structured into three main phases: an introductory phase, a training phase, and a formal experimental phase. In the introductory phase, participants were first required to undergo a color-blindness test to ensure normal vision before being presented with a guidance page in Chinese. The guidance detailed the definition, characteristics, and graphical representation of the scale to be used, using 'Vividness' as an example scale. Vividness was defined as "the distance a color stimulus is from neutral black," and it was stated that vividness increases with chroma or brightness, with neutral black having a vividness of zero.

During the training phase, once participants acknowledged their understanding of the scale, they were provided with 7-9 NCS color chips of varying hues but smaller sizes than the main experimental sample. They were instructed to arrange these chips on a Munsell color page in accordance with Value (vertical axis) and Chroma (horizontal axis) to facilitate their understanding of the Lightness and Chroma scales. After confirming their arrangement, participants were asked to identify the direction of the vividness scale as described in the guidance. The sequence of chips was then randomized, and participants were required to rearrange them in ascending order of vividness and to perform magnitude estimation on the reordered chips.

In the formal experimental phase, the experimenter defined 'origin' and 'anchoring color' within a reference lightbox. The lightbox was closed after participants memorized these colors, although they could request a pause for re-memorization if necessary. The formal experiment consisted of four luminance stages, with each stage preceded by a color adaptation period varying between 15 seconds and 2 minutes based on the luminance level. These stages were presented in random order. After adaptation, participants had 15 seconds to place the randomized color patch within the experimental lightbox and were then required to score them. 40 patches were selected for the formal set, and four patches were randomly selected for repetition.

Overall, the experiment was composed of four different scales, each tested in a session that consisted of a 20-minute training phase and a 70-minute formal experimental phase.

RESULT AND DISCUSSION

Results

The results of this experiment encompass four scales: Vividness, Depth, Whiteness, and Blackness. In total, there were 10 participants (5 males and 5 females) involved in the study, with an average age of 23.7 years. All participants had normal vision. In a single experimental session, participants were required to make estimations 44 times for each of the four illumination levels, resulting in a total of 7,040 estimations.

Result Analysis

The Standardized Residual Sum of Squares (STRSS) is a statistical measure used to quantify the difference between observed and predicted values in regression models [4]. In this study, STRESS is used as a metric to measure the agreement between experimental data and measured data. Its formula is shown in Equation x.

$$STRESS = \sqrt{\frac{\Sigma(\mathrm{FE_i - V_i})^2}{\Sigma V_i^2}} \tag{1}$$

The calculation of F is $F = \frac{\Sigma E_i V_i}{\Sigma E_i^2}$.The E_i represents the predicted data from the model, while V_i represents the visual data obtained from the experiment.

Comparison among the existing scales

The experimental visual data was analyzed by calculating the STRESS values in comparison with the predicted values from CIECAM16 J, Q, C, M, and the Berns V* D* scales [5]. This analysis aimed to determine the tendencies in the visual data from this experiment and evaluate the effectiveness of the Berns scales.

Table 1: Comparison of STRESS values between the existing scales and visual data. CIECAM16 J, Q, C, M, and Berns V*, D* were selected for the analysis.

Models	CIECAM16 J				CIECAM16 Q				Berns V^*			
Levels (cd/m^2)	V	D	W	K	V	D	W	K	V	D	W	K
10	20	69	37	74	20	56	48	63	14	60	51	69
100	22	67	37	77	19	55	46	67	13	58	50	73
1000	21	66	36	79	17	54	44	69	12	57	49	75
10,000	21	70	39	81	20	59	47	71	13	62	52	77
TOTAL	29	68	38	78	32	69	58	80	24	59	51	74
Models	CIECAM16 C				CIECAM16 M				Berns D^*			
Levels (cd/m^2)	V	D	W	K	V	D	W	K	V	D	W	K
10	43	54	80	70	43	54	80	70	51	24	82	42
100	41	49	80	75	41	49	80	75	48	20	81	49
1000	40	48	79	77	40	48	79	77	47	18	79	52
10,000	41	51	81	78	41	51	81	78	49	22	81	53
TOTAL	45	51	80	75	41	54	81	78	52	21	81	50

From Table 1, it can be observed that with respect to the Vividness scale, Berns V^* consistently outperforms in terms of STRESS across all luminance levels. However, when all the data is consolidated, its performance deteriorates. Furthermore, its performance surpasses that of CIECAM16 J and Q when compared to CIECAM16 C and M. This could potentially be attributed to the overall experimental samples having a greater luminance dynamic range than chromaticity. As for the Depth scale, Berns D^* also demonstrates superior STRESS values. Concurrently, neither CIECAM16 J, Q nor CIECAM16 C, M manage to deliver a relatively commendable STRESS performance. Additionally, the STRESS performance of CIECAM16 J across each illuminance level is inferior to that of CIECAM16 Q.

Based on the aforementioned analysis, we can glean the following insights: the combination of Lightness and Chroma is beneficial for describing scales such as Vividness and Depth. The experimental data suggests that Vividness has a greater inclination towards luminance as compared to chromaticity. Berns' proposed model is effective in predicting two-dimensional sensory scales under standard conditions; however, its predictive accuracy diminishes in scenarios with high dynamic range.

New 2-D color appearance model based on Hellwig Q_{hk} and CAM16-UCS M'

To address the issues identified in the previous analysis, Equation x has been proposed. The structure of Equation x is realized through a weighted distance formula. Here, Q_{hk} is a scale optimized for the HK effect by Hellwig's on the CIECAM16 Q formula [6]. On the other hand, M' represents the colorfulness scale in CAM16-UCS. In this framework, k_o denotes the luminance proportion, employed to adjust the overall scale ratio. Concurrently, k_r is used to adjust the ratio between brightness and colorfulness. Q_{hko} signifies the reference luminance in the scene. It's formulated as a quadratic function of La, serving to correct inconsistencies in reference white across varying scenes.

$$Vividness = k_o\sqrt{Q_{hk}^2 + k_r M'^2} \tag{2}$$

$$Depth = \frac{k_o}{Q_{hko}}\sqrt{(Q_{hk} - Q_{hko})^2 + k_r M'^2} \tag{3}$$

$$Q_{hko} = k_1 L_a^2 + k_2 L_a^2 + k_3 \tag{4}$$

Table 2. All coefficients of Equation (2), Equation (3) and Equation (4). The r represents the correlation coefficient between the experimental data and the predicted data.

	k_o	k_r	k_1	k_2	k_3	*STRESS*	*r*
V	0.86	5.82				12	0.94
D	120.31	0.82	0.71	6.74	55	14	0.94

Through the aforementioned framework, the visual data was fitted using the least squares method by applying the above equation, resulting in Table 2 and Figure 2. It can be observed that for Vividness, the value of k_r is significantly greater than 1, indicating a higher weight on brightness compared to chroma. On the other hand, for Depth, k_r is close to 1, suggesting a balanced proportion between brightness and chroma. Furthermore, based on the STRESS values, it can be inferred that the new equation provides a better description of the experimental data compared to Berns' equation. This is supported by the high correlation coefficient, indicating a strong fit between the model and the experimental data.

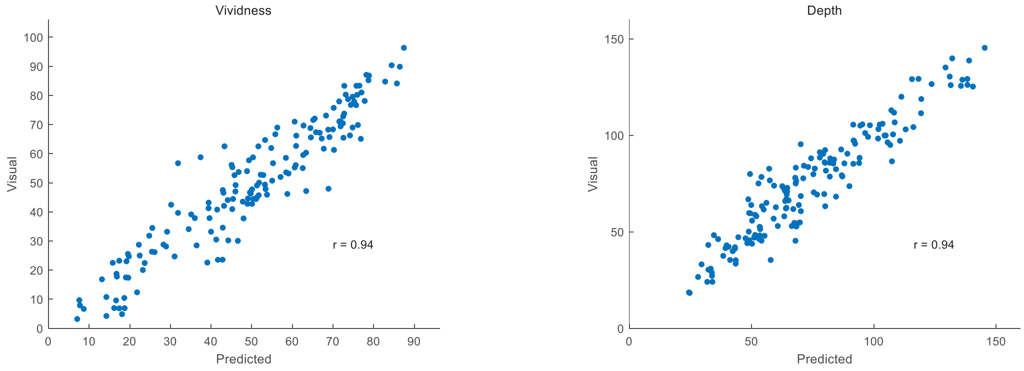

a) Vividness   b) Depth

Figure 2. The plot of visual data versus the predictions from the new Vividness (V), Depth (D) using Equation (2), Equation (3) and Equation (4).

CONCLUSION

The main contribution of this study was the design of a two-dimensional color appearance experiment based on magnitude estimation. The experiment included four scales, namely Vividness, Depth, Whiteness, and Blackness, with over 7040 estimations collected from high dynamic visual datasets. These datasets were utilized to evaluate the performance of both the one-dimensional color appearance scale in CIECAM16 and the two-dimensional color appearance scale proposed by Berns. Among them, Berns' two-dimensional color appearance model exhibited the best performance but still fell short in covering high dynamic range scenes. Based on this conclusion, this research introduced a new framework for a two-dimensional color appearance model using Hellwig Q_{hk} and CAM16-UCS M' as absolute scales. Future work will focus on applying the 2-D color appearance scales to real-world image scenarios and further developing distance-based formulas for the two-dimensional color appearance model.

ACKNOWLEDGEMENT

This work was supported by the National Natural Science Foundation of China (61775190).

REFERENCES

1. Berns, R. S. (2014). Extending CIELAB: Vividness, depth, and clarity. *Color Research & Application*, 39(4), 322-330.

2. Cho, Yoon Ji, Li-Chen Ou, and Ronnier Luo. "A cross-cultural comparison of saturation, vividness, blackness and whiteness scales." *Color Research & Application* 42.2 (2017): 203-215.
3. Hård, A., & Sivik, L. (1981). NCS—Natural color system: A Swedish standard for color notation. *Color Research & Application*, 6(3), 129-138.
4. *CIE 217:2016*, "Recommended Method for Evaluating the Performance of Colour-Difference Formulae," (2016).
5. Li, C., Li, Z., Wang, Z., Xu, Y., Luo, M. R., Cui, G., ... & Pointer, M. (2017). Comprehensive color solutions: CAM16, CAT16, and CAM16-UCS. *Color Research & Application*, 42(6), 703-718.
6. Hellwig, L., Stolitzka, D., & Fairchild, M. D. (2022). Extending CIECAM02 and CAM16 for the Helmholtz–Kohlrausch effect. *Color Research & Application*, 47(5), 1096-1104.

COLOUR, FORM AND PRODUCT - FORM GHOSTS IN DESIGN EDUCATION

Eva-Lena Bäckström

Umeå institute of Design, Umeå University, Sweden

ABSTRACT

In the design process, selecting colours and creating a palette is usually done digitally or with two-dimensional samples. However, when it comes to product design, the colour of the product is made and manufactured in the physical three-dimensional space, and will be perceived differently than in a digital presentation or on a physical surface. This study aims to investigate the significance of colour choices and highlight the difference between the perception of subtractive and additive colour on three-dimensional objects. It also emphasizes the importance of artistic training in design education.

The study involves creating an interactive object that embodies a function, has a recipient in mind, and a context chosen by the user, which is clarified through the specific colour selection. These objects are known as "form ghosts" because they are low-fi and resemble products but with minimal detail and design features. The task requires working systematically to provide reasoning for one's results and presenting a well-developed colour proposal that aligns with the product.

The goal of "form ghosts" is to shift the focus from form creation to the process of developing a colour proposal. It is worth considering if the lack of refinement in the form ghosts leads to simplified colour choices. Nonetheless, utilizing form ghosts as a tool in the colour process can be a first step in comprehending and reflecting on the appearance of a hue on a three-dimensional object in a physical context.

Keywords: Colour, product design, design education

INTRODUCTION

In design making colour proposals and choosing hues for a palette is usually done by using painted or printed samples from commercial color-order collections, true color systems and color collections described by Holtzschue L. [1] This could be a limitation because it mainly offers a two-dimensional representation of a hue. It is comparable to evaluating a 2-dimensional sample with a flat surface like a book page or a painted wall since the exposure of light is even without shadows on a complex form. When it comes to three-dimensional objects, flat samples can be misleading since we perceive colour differently on a 3-dimensional form. Though the objects local colour is the same, different shades of a hue are an inherent property of a three-dimensional object because of light, viewing angle and shadows. The same limitations as 2D sampling occur when creating a colour palette in a digital space. In rendered pictures, it can be difficult to state the products' inherent colour because of the shadow and light created to simulate space and form. Problems in making accurate translations from digital to physical media can also occur when transferring a digital hue to a physical sample since we perceive additive colour differently than subtractive colour. Only using digital tools limits the process of evaluating a colour proposal for a three-dimensional object.

When working as a professional designer you must be able to provide colour proposals for different kinds of production methods, you need to understand the colouring process, and how colour perception works in physical versus digital environments. My artistic development work resulted, among other things, in formulating the task "Colour on form" for BFA students

(Bachelor of Fine Art) in industrial design at Umeå Institute of Design (UID). This assignment is part of a two-week course in artistic training in the first year of the BFA program at UID. This course also includes artistic techniques like painting and an introduction to colour theory that covers basic concepts such as perception, colour harmony and colour systems. Students also train in how to communicate their results, create briefs for production and use the professional NCS system for colour communication.

To work with colour in a physical, non-digital space is one of the main objectives of the student assignment. The task is to build a small object that represents a product that invites interaction. The shape of the object should have a secondary function serving as a 3-D canvas for looking at the effect of colour and light in a physical space. The surface of the object should be smooth, and the focus is on the choice of hue. Structure and gloss should not be added since it would influence the hue and increase the complexity. One reason not to work on the structure of the surface is that it's more time-consuming and not feasible during the time frame provided for the assignment. Also, the different proposals can equally be compared to each other with a focus on the hue.

METHODOLOGY

For students today the computer is an important tool and a comfort zone where the results can be presented with accuracy and a professional look. However, in product design, the colour of the product is created and manufactured in the physical space and will be perceived differently than in a digital presentation. I introduced the concept of "form ghost" at AIC2018 [2] as an object to interact with, similar to a product that can serve as a template for colour proposals. I call these objects "form ghosts" because they are objects that resemble products but with few details and design features. The purpose of this task is to draw students' attention to the difference between perceiving subtractive and additive colour. It means that they should understand that humans perceive colour differently in these contexts and the different conditions of light and shadow in a physical space versus a digital space. Also, they should work out strategies for how to specify a colour proposal using colour systems for the production of physical objects.

The students' assignment is to build a form ghost that should represent a function and have an intended recipient and a context. Keywords should clarify the characteristics expressed through the choice of hue. To clarify the purpose of the products, students tend to three guiding perspectives that build the product concept:

- Property
- Function
- Context

When stating the Property, it should be from a technical aspect and what the object can perform. The Function should reflect what makes the user react in terms of interaction. For example, to grab, push or look. The Context of the product should also be clear as if it's used outside in natural light, day, or night, or inside.

The form ghost shall be presented with a mood board that conveys the design concept with images and keywords. The mood board can be created digitally and show inspiring images, with context, colour palette and to implement the story around the imagined product features. In this way, students can build a strategy for the design process.

The students are provided with scrap wood material from a company producing semi-finished products for therapeutic purposes. I have chosen this material since the pieces have a good finish and are easy to join and combine into objects that characterize a small object you can interact with. With low effort, it's possible to create a sketch of an object resembling a product. For example, it's possible to build a wood block with raised spherical details, repeated sticks mounted on a surface or cones combined with spheres, that represent different objects that invite to interact with.

The colour palette should be created with paint in a creative process by blending paint and testing different mixes of hues. For the painting, we use acrylic paint in warm and cold primary colours. I have chosen the following hues, cadmium yellow (as warm yellow) lemon yellow (as cold yellow) crimson (as cold red) vermilion (as warm red) ultramarine (as warm blue), preussian blue (as cold blue) lately changed to cobalt blue since preussian blue tend to darken the shades too much. Different shades of the primary hues are when cold tending towards blue/green and when warmer the hue tends to have more red/yellow pigment. also, titanium white and mars black can be used to create pastel and darker shades.

The use of patterns and graphics are not allowed. One of the points of this assignment is to focus on colour to invite the user to interact. Symbols have a semantic function to communicate and guide the user and this would draw attention from the response to the selected hue.

This is a singular assignment and not part of a project and because of the allotted time, the students should focus on the process of colour and not on designing an object in detail. These pre-formulated building blocks will limit the work to make decisions regarding form exploration thus directing the focus on the choices of hues, contrast, and placement. The task is individual, and each student makes their own physical object, samples and a printed mood board created digitally. Presentations are made in a studio where students show the result, describe the process, and argue for the proposal. In this way, the object is possible to look at from different angles because it is tangible and can be moved around. It's also possible to go outside to see how the object looks in natural light and understand the effects on hues in different light sources.

I let the students create the form ghosts since I believe that perceiving three-dimensional forms in a physical space will deepen the understanding and support the evaluation when choosing hues. Seeing how the students carry out this study gives an idea of the possibilities of using form ghosts as a first step in the process of choosing colours for a product.

Figure 1. Student work, "Colour on Form" BFA1, UID 2018.

RESULT AND DISCUSSION

By looking at the students' results between 2016-2022 I have drawn the following conclusions. The task of building a product that you can interact with is a well-suited task for a design student as the semiotics values could be discussed as well as the aesthetics of the colour choice. The seminars would boost discussions on how well-conceived the proposals were, and if the intended interaction was conveyed by the choice of colour.

I could also experience several issues like students deviating from the assignment indicated that the brief needed clarification. First years I handed out this assignment and stated that the wooden object should be painted with white ground to give a neutral and even surface to paint on. This resulted in some students choosing to keep white in their palette since they regarded it as a given factor. When I removed this criterion, the “form ghosts” were made with a greater variety of hues. Some students also deviated from the objectives and chose to present decorative passive objects. The result of this was that the function “to be a decor” didn’t invite interaction thus missing the point of the assignment. This is followed by a weak argumentation mainly on the aesthetics and not the semiotic values of the colour choice. It was not stated in the objectives whether the object/product should be active or passive which would have been obvious by the three keywords.

In some cases, students made objects in scale meant to be outside or scaled down looking like miniatures. It didn’t say in the written brief that the object should be scale 1:1 and the consequence was that the colour choice by its size couldn’t be evaluated. This was an opportunity to emphasize and discuss the effect of how we perceive colour in different scales.

The mood boards were created digitally, and this showed how different we perceive colour on a computer screen or printed matter. Students became aware of the challenge to make the digital and physical work match and became obvious when comparing the printed outcome of a digital mood board. They experienced differences between the intended outcome of the radiant digital picture and what they could convey with ink or laser toner print. The printout would often come out “wrong” and not as bright as on the screen or the other way around the saturated physical samples were difficult to create on screen.

In the oral presentation of the assignment, it was said that each hue must be monochrome and possible to identify in the NCS system. However, some students like to overlook this and create graded and shaded transitions between hues. In product design, this can be achieved in various ways, but generally, injection moulded and painted pieces are monochrome. If you do colour grading, the result doesn't have to be accurate because the colour is on a sliding scale in terms of hue, blackness, and saturation. The designer's task is to make decisions and propose a colour or palette that can be specified in a colour system to be put into production. Students often hesitate before the final decision and the reason is that it must be a precise colour code or sample to be able to be transferred to production. In the NCS system, you must look for the relationship between hues and you also indicate the blackness and chromaticness which gives you several options to choose from. To be secure in the final choice you must select and evaluate several samples in a time-consuming and demanding process.

In this assignment the structure of the surface was not considered which would have had an impact as showed in the research by Jongerius H. [3] The simplicity of the form and the even surface may have contributed to the outcomes appearing unsophisticated with low refinement. To introduce structure and gloss would mean taking the study one step further.

Guided by the principles of the keywords referring to property, function and context, the student can work methodically and argue for their process and result. One purpose of this task is also to train the ability to argue for and discuss the result. A reaction to a colour proposal is based on factors like individual, cultural, and general preferences as pointed out by Bergström, B [4]. Taking into account the individual and sociocultural preferences a designer must be skilled to be able to clarify that the proposal is well thought out and viable for the specific context. During the seminar students get feedback from their peers and discussion arises about semiotic interpretation and aesthetics. They gain an understanding of what colour expresses from a collective to a personal level related to the "Color experience pyramid" by Mahnke F.H. [5]

Figure 2. Student work, "FORM GHOSTS" BFA1, UID 2018.

CONCLUSION

The objective of this work was to find new strategies for working with colour in my teaching in industrial design resulting in the introduction of colour studies on three-dimensional physical shapes. The meaning of the lo-fi "form ghosts" was to direct the effort on the colour choice and reduce the focus on designing the form in detail. This resulted in simplified objects, but also a predominant choice of palettes with primary colours, colour blocking and high contrast.

My pedagogic ambition is to raise awareness of the fact that digital and physical colour appear different and that should be taken into account when we choose and specify hues for physical objects. One intention with this assignment was also to provide design students with a basic experience of making colour choices in a physical space and not only in 2D and digital environments. Mixing real paint, painting objects, and evaluating them with different light give them an experience of the difference in perceiving colour with digital and physical samples. They should also gain know-how of how to communicate their result, create briefs for production and use professional systems like NCS for colour communication.

As a method in the colouring process, it can serve as a first step in understanding and reflecting on the appearance of a hue on a physical three-dimensional object. This gives attention to the difference between using digital tools and physical samples to convey a colour proposal. It will show how insufficient digital colour representations are when creating colour palettes for products. If considered as a pre-study, further explorations can be done to develop the design of the object in tune with the colour. The result can probably be that if the form develops the choice of hues may be more sophisticated. Nevertheless, this assignment can serve as a basic step to explore the relationship between form and colour in a physical space and its ability to initiate interaction. Transformation experiments by Swirnoff, L. show that colour is a significant factor when perceiving form. [6] The results of my study show not only how colour affects how we perceive form but also if the choice of hue can initiate interaction.

This project raises the importance of artistic training in higher design education in Sweden. Creating colour proposals is still often considered an intuitive and artistic task not given as much time as form-giving and presentation techniques. Both in student and professional projects colour sometimes gets less attention and can be efficiently solved by using prefabricated palettes from trend forecasters and suppliers. When downgrading the process of the colour choice we risk ruling it out as an important strategic design feature of a product. In this study, the focus is reversed, and time is given to work methodically to find argumentation for one's result and to deliver well worked-through colour proposal in tune with the product.

ACKNOWLEDGEMENT

I would like to thank Maria Göransdotter, associate professor in design history and design theory at Umeå Institute of Design, and Director of PhD studies in industrial design for the support in writing this paper.

REFERENCES

1. Holtzschue, L. (2011). *Understanding color [Elektronisk resurs]: an introduction for designers*. (4th ed.) Hoboken, N.J.: Wiley.

2. Bäckström, E-L. *The unexpected meeting: How to create unique colour choices for products*, Proceedings of the International Colour Association (AIC) Conference 2018: Colour & Human Comfort, 2018, s. 283-287, https://urn.kb.se/resolve?urn=urn:nbn:se:umu:diva-153864

3. Jongerius, H. & Manse, S. (2016). *I don't have a favourite colour: creating the Vitra colour & material library*. Berlin: Gestalten.

4. Bergström, B. (2022). *Colour choices: a practitioner's guide to designing colour schemes*. (1st edition). Lund: Studentlitteratur.

5. Mahnke, F.H. (2002[1996]). *Color, environment, and human response: an interdisciplinary understanding of color and its use as a beneficial element in the design of the architectural environment*. New York: Wiley.

6. Swirnoff, L. & Swirnoff, L. (2003). *Dimensional color*. (2. ed.) New York: W.W. Norton & Company

COLOUR DESIGN FOR FAÇADE INTEGRATED PHOTOVOLTAICS ON CAMPUS-A CASE STUDY IN HONG KONG

Wanting Wang[1], Kaiyan Xu[1] and Changying Xiang[1]*

[1]Division of Integrative Systems and Design, the Hong Kong University of Science and Technology, China.

*Corresponding author: Changying Xiang, changyingx@ust.hk

ABSTRACT

Climate change is one of the grand challenges we are tackling nowadays. To mitigate carbon emissions and promote a sustainable urban transition, renewable energy systems such as building integrated photovoltaics (BIPV) can strongly support the goal of a carbon-neutral society. To fully explore the solar energy harvesting potentials of building envelopes, large façade areas also need to be utilized for PV integration. Differing from roof applications, façade integrated photovoltaics (FIPV) usually demand a high level of aesthetic performance, in which the colour design plays an essential role and demands carefully thought strategies through the cooperation of architects, urban designers, PV engineers and even users. In this study, we take a façades renovation campaign at the Hong Kong University of Science and Technology as a case study to explore a feasible workflow process of colour design for FIPV in campus environments. Applying FIPV systems to educational buildings can provide not only clean electricity but also a positive educational impact of sustainability for students. The key challenges lie in balancing the aesthetic performance, energy productivity, respect and updates for the existing campus identity, and providing noticeable educational effects.

This FIPV renovation campaign starts with a series of design workshops, in which a group of interdisciplinary experts is involved to define the expected design outcomes. Then the solar potentials of campus facades are simulated with the Rhino-based plugin ClimateStudio to identify to most suitable areas for FIPV applications. Meanwhile, a survey is conducted to get the opinions of users (students and staff) on existing colour environments of the campus, the results will be used as a reference for architects and PV experts when co-generating colour design proposals for the FIPV. The NCS- Nature Colour System, is employed in this project to link the work of architects and engineers. The principle of structure colour will be applied for the coloured FIPV to achieve high energy efficiencies, where only a tiny fraction of solar irradiation is reflected to achieve the desired colours through interference effects. Finally, various coloured FIPV proposals designed by the expert team will be presented in public, and the most voted one will be selected for implementation.

Based on a real campus renovation campaign scenario, this project tests a novel user-participated design process for generating aesthetically pleasing, energy-efficient FIPV. The design outcomes and reflections can serve as good references for research and development in related fields, and also can provide valuable impact for sustainability from the educational perspective.

Keywords: Colour harmony, Façade integrated photovoltaics, Campus design, Zero-carbon, Architecture

INTRODUCTION

Buildings, as a significant contributor to climate change, account for approximately one-third of global energy consumption[1]. Faced with this challenge, the application of Building Integrated Photovoltaics (BIPV) has become increasingly important. BIPV technology integrates building envelopes with photovoltaics materials, transforming buildings into energy producers. Compared to traditional rooftop photovoltaic systems, Facade Integrated Photovoltaics (FIPV) offer greater electricity generation capacity, higher aesthetic appeal, and enhanced design flexibility. The traditional BIPV systems, which utilize dark blue or black with low-lightness photovoltaic panels, present limitations in terms of aesthetic appeal. Consequently, there is a growing interest among scholars in exploring the colour design of BIPV components, as it plays a crucial role in determing the overall aesthetics of buildings. Aesthetics at both building and district levels. At community or district level, the usage of FIPV systems also needs to consider the identity of local built environment, apart from the need to balance aesthetic performance, energy productivity. To address these challenges, this study presents a case study of a façade renovation campaign at the campus of Hong Kong University of Science and Technology (HKUST), exploring a feasible workflow process for optimizing the colour design of FIPV systems in campus environments. The design outcomes and reflections of this study can serve as valuable references for research and development in related fields, while also promoting sustainability education from an educational perspective.

RELATED WORK

2.1 Coloured BIPV Module

Pilot projects of coloured BIPV products have been implemented in several countries, demonstrating the maturity and feasibility of these solutions[2, 3]. Coloured BIPV modules possess the ability of adapting various materials and shapes, injecting more diversity into urban contexts (e.g. the use of BIPV facades combined with LED lights further enhances the diversity and creative expression of building exteriors at night)[4]. Currently, various customization technologies are employed in the market to achieve coloured or textured BIPV components, including: (i) solar cells with anti-reflective coatings; (ii) semi-transparent and/or coloured photovoltaic active layers; (iii) layers or intermediate films with solar filters, coloured or patterned coatings; (iv) coloured polymer encapsulation films; and (v) printing, coating, or alternative finished glass[5]. Moreover, holistic design optimization and architectural integration strategies are crucial in maximizing the benefits of coloured PV modules, ensuring their seamless integration into diverse building designs and urban environments. Typically, the power conversion efficiency of coloured BIPV modules experience a reduction in comparison with black PV modules due to the incorporation of supplementary materials and process steps necessary to achieve diverse colours and designs. It has been approved that the colour lightness of PV materials has a strong association with the energy production efficiencies[6]. When comparing colours with the same brightness, the hue of the colour becomes the most influential parameter. A theoretical study[7]proposed a design methodology of integrating opaque photovoltaics in various colours in order on building facades. Through computational analysis and an online survey, the results demonstrated promising energy production efficiency of pixelated coloured FIPV facades and were widely perceived by the majority of participants as being consistent with the urban environment.

2.2 Colour Preference

To describe, represent, and organize colours scientifically, various colour systems are developed, such as NCS, CIE and others. The NCS-Natural Colour System is based purely on human perception of colour, which classifies colours into six basic colours, and describes colours through defining hue, saturation, blackness, and whiteness to provide a standardized way of describing and communicating colours. The CIE colour system is based on scientific observation and measurement, which uses three standardized colour matching functions to obtain the tristimulus values of colours, and provides multiple colour spaces (such as CIE XYZ, CIELAB, and CIELUV) for accurately representing and comparing colours.

Colour preference arise from individuals’ average affective responses to colour-associated objects, representing a crucial aspect of visual experience[8]. The study of colour preference in architectural and urban colour has garnered significant attention and has been extensively explored. Cubukcu et al. evaluated different images using a 7-point semantic differential scales to measure the colour preferences of architects and non-architects for building exterior colours[9]. In another study, a series of building facades were studied by obtaining 308 simulated photos using a dual-colour combination mode to explore the harmony of building colours from a visual evaluation perspective, the results revealed that the harmony of building colours is higher when the brightness of the base colour is high and the brightness difference between the dual-colour combinations is greater [10]. Xiang et al. utilized the local urban NCS colour chart and colour harmony strategy to design the colour scheme for the selected photovoltaic integrated exterior wall, and employed a five-point semantic differential scale to evaluate the aesthetics of the design by the participants[11]. In addition to the semantic differential evaluation method, some researchers also employ eye-tracking experiments as an evaluation tool. Eye-tracking experiments can be used to analyze participants' visual attention and perception processes. By tracking the trajectory of eye movements and fixation points, researchers can understand the distribution of attention and visual areas of interest when participants view specific designs or images. Wang et al. conducted an eye-tracking experiment to examine the objects that captured higher attention when observing the historical urban area of Macau. Their aim was to analyze the relationship between individuals' attention, visual preferences, and architectural colours in the environment[12]. Zhang et al. obtained the colour range for visual comfort of subway spaces through a combination of questionnaire surveys and eye-tracking experiments. The results indicated that when the saturation was between 60% and 52%, brightness was between 68% and 20%, or the hue was in the range of orange, yellow, and green, human visual perception was more comfortable[13]. J. Y. Cho et al. investigated the impact of different applications of colour combinations in a space on emotional responses, perceived luxury, and intention to stay. The authors first simulated an indoor environment using rendering software and then collected relevant data through surveys and eye-tracking technology. The results indicated that the same colour combination evoked different emotional responses when applied in different physical environments[14].

HKUST campus location and the pilot project

The selected location for this study is within the campus of the HKUST (22.33°N, 114.26°E, elevation=120m appx.). The university's architecture primarily follows a modernist style, with most buildings incorporating mosaic decorative ceramic tiles, creating a clean and distinctive architectural appearance. Additionally, the majority of buildings feature a predominantly white colour palette, providing ample opportunities for colour design in our experiment.

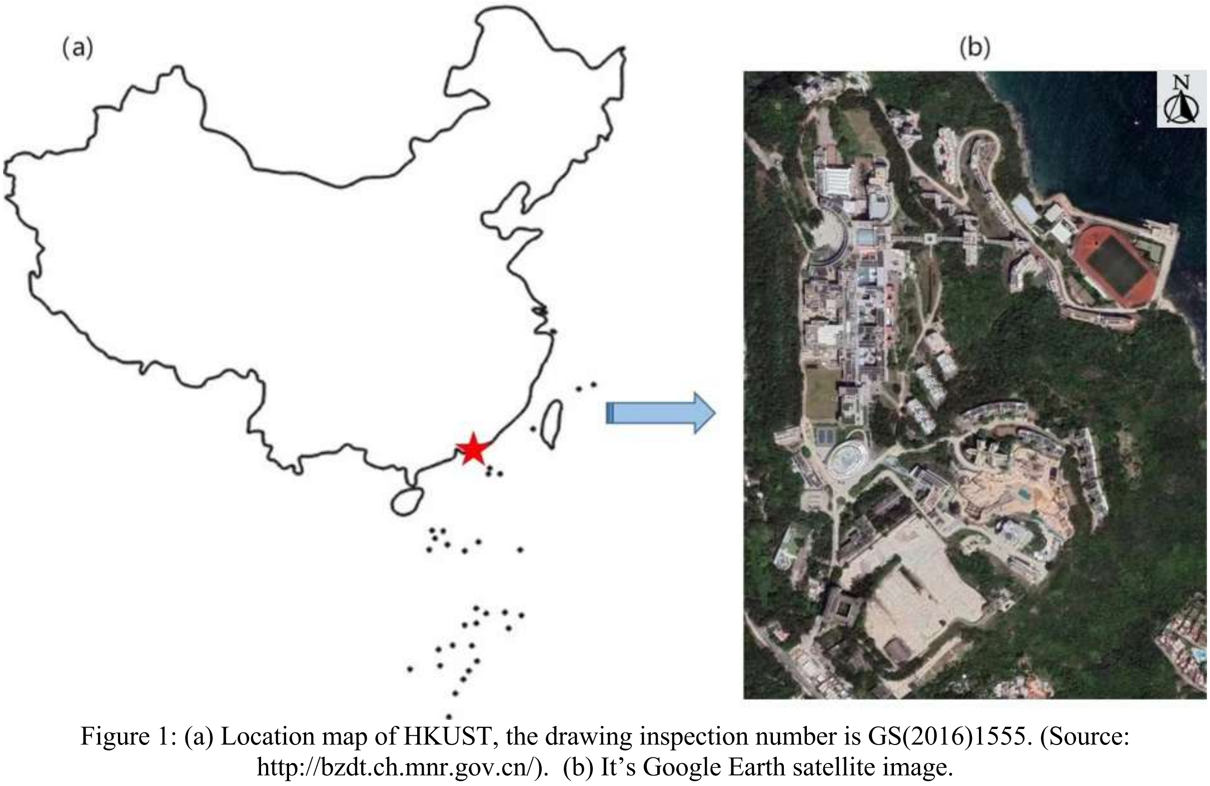

Figure 1: (a) Location map of HKUST, the drawing inspection number is GS(2016)1555. (Source: http://bzdt.ch.mnr.gov.cn/). (b) It's Google Earth satellite image.

A staff apartment Tower 19 was selected as the pilot project for FIPV renovation (Figure 2). Due to the budget limitation, only its southern façade will be designed and renovated, since the southern façade is neat and receives the highest annual solar irradiance (around 1300 kWh/m^2year) besides the roof, followed by the eastern, western and northern facades.

Figure 2: Exterior facade of Tower 19

METHODOLOGY

The research methodology for this study consists of three steps. The first step was a satisfaction questionnaire on the existing colours of HKUST campus, and a colour preference survey to collect ideas for the FIPV applications on campus. Based on the first step's result, a series of FIPV colour design were developed for the pilot project, and another survey was conducted to select the most preferred design. The third step included simulating the solar potential of campus building facades and designing FIPV colour schemes for selected pilot building.

4.1 Questionnaire Design

The first questionnaire consists of three parts with a total of 13 questions. The participants were students and faculty members of the university who have normal colour perception and recognition abilities and all respondents were voluntary. It started with collecting non-sensitive personal information of the participants, followed by a survey on their satisfaction with the colours of the buildings on the HKUST campus -the participants were asked to use adjectives to evaluate their satisfaction with the existing colours of the campus buildings. Then, they were asked to select their most preferred NCS colours for the campus FIPV renovations: choosing preferred a main NCS hue range (Y-R, R-B, B-G, G-Y) and a secondary NSC hue range (if applicable) from the NCS hue circle

Based on the first questionnaire survey results, we developed a number of FIPV colour design proposals, and subsequently conducted the second questionnaire survey to ascertain the final colour scheme. The content of this questionnaire comprised 14 carefully curated questions, encompassing preferences and opinions on a diverse array of design aspects. Central to our design philosophy was the incorporation of yellow, green, and blue as the primary hues, supplemented with complementary secondary shades. In total, 34 distinct design variants were crafted, each representing a unique amalgamation of these colour elements. This approach not only facilitated a comprehensive exploration of the aesthetic building but also ensured that the final selected design would be both representative and well-received by the target audience.

4.2 Solar Potential Analysis

To analyse the façade solar potential of pilot building Tower 19, its building geometry and the surround environment was modelled in Rhinoceros 3D environment, then a professional plugin ClimateStudio, which is an accurate and efficient tool to simulate the solar irradiance, was applied to conduct simulation.

The solar irradiance analysis was conducted on an annual basis. To accurately determine the solar energy potential of the external wall to guide subsequent design, we carried out a solar irradiation simulation on Tower 19 (modifying the sensor spacing to 1 meter, with "rtrance" consistent with Table 1 and material parameters consistent with Table 2. The model data was sourced from the Hong Kong Geo Data Store, which aided in effectively reproducing the campus environment in the analysis[15]. To account for climatic influences on solar potential, weather data (.epw) specific to Hong Kong was integrated into the analysis. Both direct and diffuse solar irradiation, as well as solar mutual reflections from the surrounding environments (grounds, facades) were simulated, the 'rtrace' parameters used for Radiance-based simulation were shown in Table 1, while the materials set for buildings and landscape were displayed in Table 2.

Ambient bounces	**Ambient division**	**Ambient super samples**	**Max number of passes**	**Ambient resolution**	**Ambient accuracy**	**Sensor offset from surface**
3	1000	64	50	300	0.01	0.1

Table 1: Set of "rtrace" parameters used for the Radiance-based simulations

3D Model components	**Materials**	**Type**	**Surface**	**Roughness**	**Rvis (tot)**	**Rvis (diff)**
Facades	Bright Concrete Wall	Glossy	Exterior Building	0.2	36.9%	36.8%
Ground	Grass 5	Glossy	Plant	0.2	15.7%	15.6%

Table 2: Materials setting for solar radiation mapping in ClimateStudio

The results of the annual solar radiation simulation fell within a range of 0 to 1500 kWh/$m^2 year$. In order to discern the solar potential of various facades and to identify the most viable ones for FIPV implementation, the simulated values were classified into five categories. The categories were delineated as follows: very high (1200-1500 kWh/$m^2 year$), high (900-1200 kWh/$m^2 year$, medium (600-900 kWh/$m^2 year$), low (300-600 kWh/$m^2 year$), and very low (0-300 kWh/$m^2 year$).

4.3 Energy Performance Calculation

Step 1: Efficiency of selected coloured PV systems

The initial phase of this task involves the transformation of NCS colour codes, essential to the FIPV design, into the designated CIE LAB and CIE XYZ colour spaces[16]. Following this, these CIE XYZ values are converted into an energy loss metric in accordance with a specific formula. This multi-step process ultimately culminates in the final computation of relative efficiency[6].

Step 2: The energy calculation

Energy Production=$\sum_{i=1}^{n}(ASI_i * A_i) \times ARE_i \times E_b \times PR$ (1)

Where ASI_i is the average solar irradiation on an effective building envelope area, A_i is the effective area, ARE_i is the average relative efficiency of coloured FIPV for each envelope area, E_b is the efficiency of a typical black silicon PV (set as 24%), RP is the performance ratio (set as 80%)[17].

RESULT AND DISCUSSION

5.1 Colour Design for Selected Building

In Hong Kong, the southern facades receive the most solar radiation during the winter and the least during the summer. This is attributed to Hong Kong's location on the Tropic of Cancer, where the sun is positioned to the north of the buildings during the summer months. Consequently, during the summer, sunlight is obstructed by the walls facing south, resulting in the least annual solar radiation received. Conversely, during the winter solstice, the sun has the lowest angle in the sky, making its rays more perpendicular to the southern walls of the buildings, leading to an increase in the absorption of direct solar radiation. Additionally, influenced by monsoonal patterns, Hong Kong possesses a subtropical climate characterized by a mild winter and relatively fewer clouds, further contributing to the heightened solar radiation absorbed by southern facades during this period. Overall, when compared to other orientations, the southern facade consistently registers a higher solar energy potential intake throughout the year (**Error! Reference source not found.**).

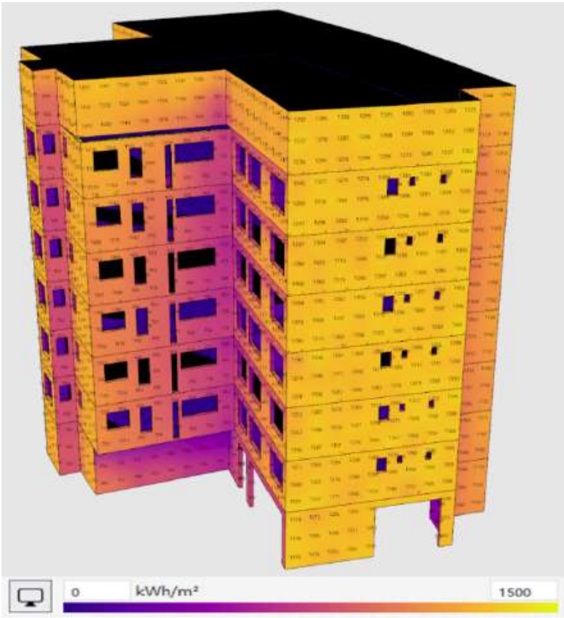

Figure 3: Detailed solar radiation mapping of Tower 19

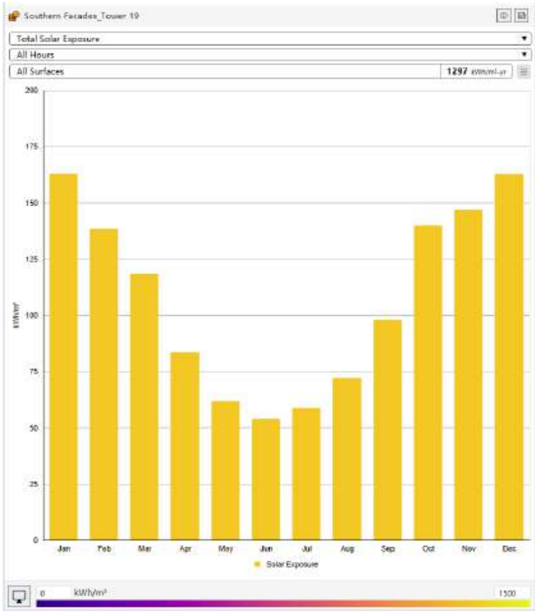

Figure 4: Total solar exposure on the southern facade of Tower 19

5.2 Survey Results

The survey was conducted in two stages. The first stage was centered around colour range preferences, wherein the colours for the coloured FIPV panels were selected from the detailed NCS colour palette (**Error! Reference source not found.**). A total of 103 questionnaires were collected. After eliminating the invalid ones, the results revealed that, for the primary colour tones of residential area buildings, 54.73% of respondents leaned towards the Y-R hue series and G-B. In the selection of secondary colour tones for residential buildings, approximately 54.05% of individuals predominantly opted for Y-R and G-B. These survey outcomes offered valuable insights into the aesthetic preferences of the respondents, contributing to our understanding of design preferences within the campus. The second stage of the survey pertained to the design proposals for tower 19 coloured FIPV. Based on the outcomes of the initial questionnaire, different combinations of coloured FIPV were designed (Figure 6 shows a portion of the questionnaire survey questions). A total of 120 valid questionnaires were collected, and the results indicated a higher satisfaction level among participants for three specific design proposals (Figure 7).

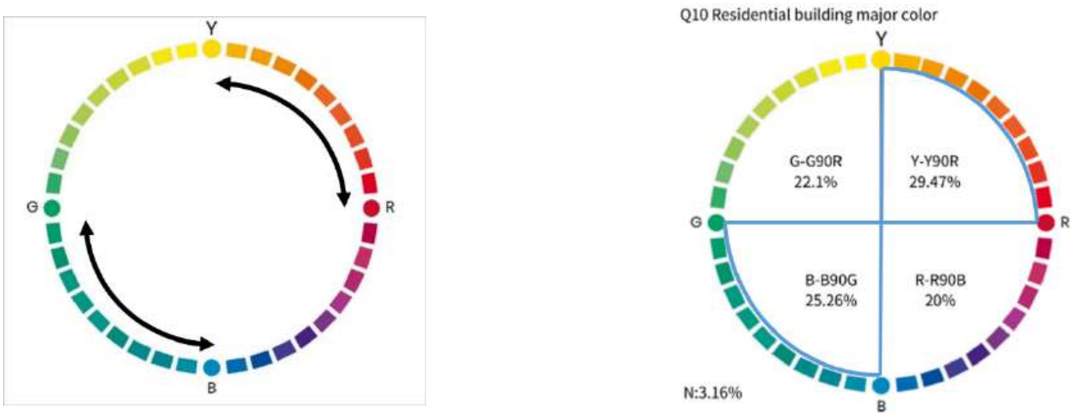

Figure 5: Two most selected NCS hue ranges for coloured FIPV design

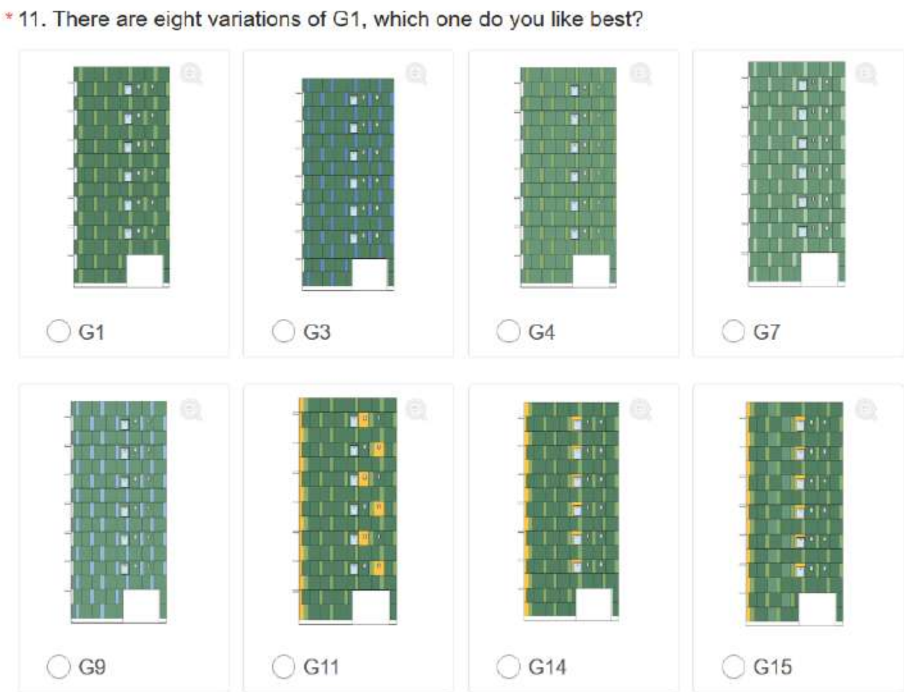

Figure 6: A portion of the questionnaire survey questions

5.3 Coloured FIPV Design for Tower 19

Adding colours on PV panels will reduce its original electricity productivity efficiency. Methods of using interference layers could achieve low efficiency loss (high relative efficiency in comparison with black PV). Based on the interference colour PV model[6], the efficiencies of the coloured FIPV, across three different schemes of the colour palette, are listed in Table 1, ranging from 21.4% to 22.3% (using the efficiency of commercialized black N-type Top-Con PV, set at 24%, as a reference, and the performance ratio (PR) set at 80%). Subsequently, the annual energy production was estimated using Equation 1, and the associated reduction in carbon emissions was also calculated based on the carbon emission factors published by the Hong Kong government (The amount of carbon emissions per unit is 0.68 kg CO2-e for the year 2022)[17]. According to the results of a questionnaire survey, a higher number of respondents preferred the primary colours of facade colour schemes to be blue and red rather than green. However, from a power generation perspective, green photovoltaic panels have a higher efficiency, resulting in a larger amount of electricity generated (Table 3). By considering both the architectural aesthetics and the electricity generation capacity comprehensively, we ultimately opted for a blue-dominated coloured FIPV design scheme for Tower 19.

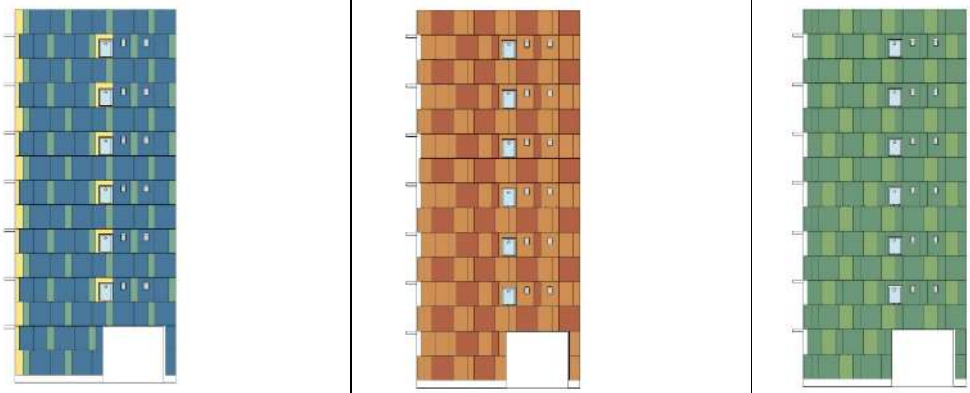

(S3040-G & S3040-B)	(S3040-Y10R & S3040-Y80R)	(S3040-G & S3040-B30G)

Figure 7: Higher satisfaction level among participants for three specific design proposals

NCS colours of FIPV	Relative efficiency loss compared with a black PV with 24% efficiency	Estimated relative efficiency	Estimate efficiency	Annual electricity production (kWh)-total facade	Annual carbon dioxide emission reduction (kg CO_2e)
S3040-G	7%	93%	22.3%	34900	23732
S3040-B	7%	93%	22.3%		
S3040-Y10R	11%	89%	21.4%	33100	22508
S3040-Y80R	9%	91%	21.8%		
S3040-G	7%	93%	22.3%	35800	24344
S3040-B30G	8%	92%	22.1%		

Table 3: Estimated energy efficiency and energy productivity of coloured FIPV with selected NCS colours

CONCLUSION

The results from the energy modeling indicate that, by adopting a comprehensive approach to architectural design, incorporating photovoltaic panels into the building facade can be an effective method for capturing solar energy in the built environment and minimizing greenhouse gas emissions in the analyzed community, all while maintaining the local urban aesthetic and architectural character. However, a limitation of this study is that during the energy productivity calculation and survey stages, the brightness levels of the coloured PV panels were not considered. Future research can focus on the energy flexibility of coloured photovoltaic panels. As different colours and brightness levels affect the efficiency of PV panels, it is crucial to explore how to optimize the combination of coloured PV panels to maximize aesthetics, efficiency, and even distribution of electricity. This involves not only a thorough investigation into the impact of different colours and brightness levels on PV panel efficiency but also integrating architectural design and urban planning to ensure that while maintaining the aesthetics of the buildings and the city, energy utilization is also maximized.

REFERENCES

[1] M. González-Torres, L. Pérez-Lombard, J. F. Coronel, I. R. Maestre, and D. Yan, "A review on buildings energy information: Trends, end-uses, fuels and drivers," *Energy Reports,* vol. 8, pp. 626-637, 2022/11/01/ 2022.

[2] *Solaris*. Available: https://solarchitecture.ch/solaris-416/

[3] *The school with the largest solar facade in the world*. Available: https://actu.epfl.ch/news/the-school-with-the-largest-solar-facade-in-the--9/

[4] *GreenPix LED and PV glass curtain wall*. Available: https://www.archdaily.com/245/greenpix-zero-energy-media-wall

[5] M. Pelle, E. Lucchi, L. Maturi, A. Astigarraga, and F. Causone, "Coloured BIPV technologies: Methodological and experimental assessment for architecturally sensitive areas," *Energies,* vol. 13, no. 17, p. 4506, 2020.

[6] A. Røyset, T. Kolås, and B. P. Jelle, "Coloured building integrated photovoltaics: Influence on energy efficiency," *Energy and Buildings,* vol. 208, p. 109623, 2020/02/01/ 2020.

[7] C. Xiang, B. S. Matusiak, A. Røyset, and T. Kolås, "Pixelization approach for façade integrated coloured photovoltaics-with architectural proposals in city context of Trondheim, Norway," *Solar Energy,* vol. 224, pp. 1222-1246, 2021/08/01/ 2021.

[8] S. E. Palmer and K. B. Schloss, "An ecological valence theory of human color preference," *Proceedings of the National Academy of Sciences,* vol. 107, no. 19, pp. 8877-8882, 2010.

[9] E. Cubukcu and I. Kahraman, "Hue, saturation, lightness, and building exterior preference: An empirical study in Turkey comparing architects' and nonarchitects' evaluative and cognitive judgments," *Color Research & Application: Endorsed by Inter-Society Color Council, The Colour Group (Great Britain), Canadian Society for Color, Color Science Association of Japan, Dutch Society for the Study of Color, The Swedish Colour Centre Foundation, Colour Society of Australia, Centre Français de la Couleur,* vol. 33, no. 5, pp. 395-405, 2008.

[10] K. R. Li, Y. Q. Yang, and Z. Q. Zheng, "Research on color harmony of building façades," *Color Research & Application,* vol. 45, no. 1, pp. 105-119, 2020.

[11] C. Xiang and B. S. Matusiak, "Aesthetic evaluation of facade integrated coloured photovoltaics designs–an international online survey," *Journal of the International Colour Association,* vol. 28, pp. 24-30, 2022.

[12] P. Wang, W. Song, J. Zhou, Y. Tan, and H. Wang, "AI-Based Environmental Color System in Achieving Sustainable Urban Development," *Systems,* vol. 11, no. 3, p. 135, 2023.

[13] L. Zhang, X. Li, C. Li, and T. Zhang, "Research on visual comfort of color environment based on the eye-tracking method in subway space," *Journal of Building Engineering,* vol. 59, p. 105138, 2022/11/01/ 2022.

[14] J. Y. Cho and J. Suh, "Spatial color efficacy in perceived luxury and preference to stay: An eye-tracking study of retail interior environment," *Frontiers in psychology,* vol. 11, p. 296, 2020.

[15] *Hong Kong Geo Data Store*. Available: https://geodata.gov.hk/gs/csdi_redirect?l=en&redirect_page=%2Fgs%2Fview-dataset%3Fuuid%3D92bc152a-28f0-4aa2-8a93-031eec932a48%26sidx%3D0

[16] *NCS Colour AB*. Available: https://ncscolour.com/design-old/work-digitally-with-ncs/colouring-to-a-new-level/

[17] C. Xiang and B. S. Matusiak, "Façade Integrated Photovoltaics design for high-rise buildings with balconies, balancing daylight, aesthetic and energy productivity performance," *Journal of Building Engineering,* vol. 57, p. 104950, 2022/10/01/ 2022.

A COLOR VALUE FRAMEWORK FOR COLOR DESIGN OF LIFESTYLE PRODUCTS.

Sudhakar Damodaraswamy[1] and Nijoo Dubey[2]*

[1]*User Experience Design, Professor of Practice, School of Design and Innovation, RV University, India.*

[2]*Universal Design, Associate Professor, National Institute of Design, India.*

Nijoo Dubey, nijoodubey@nid.edu.in

ABSTRACT

This study probes the association between the design of Colour, Material, and Finish (CMF) for lifestyle products and the perception of a product's value proposition. This paper details a survey conducted on the reasons for the use of colour on products and the analysis of the results for discernible patterns. Observed patterns are categorised, labelled, defined, inherent hierarchies identified, and revalidated through examples. The outcome of the analyses is the Colour Value Framework (CVF), presented as a hierarchically organised set of vocabularies representing the dominant patterns in the use of colour for coding value propositions into products. The applicability of the CVF in the CMF design process is discussed.

Keywords: AIC2023, Chiang Rai, Thailand (CMF design process, lifestyle products, value proposition design)

INTRODUCTION

Colour design for mass-produced products is a complex coming together of manufacturing processes, trends, marketing strategies, consumer preferences, and aesthetics [1]. The designer's challenge is to manage the above constraints together so as to achieve an appropriate colour offering. In the aesthetic of the product, the designer hopes to achieve an appearance that externalises the values a product carries within itself [2]. This in turn is expected to influence the perceived value of the product by the consumer [3] [4].

The Colour Value Framework (CVF) is an outcome of a study done on the sidelines of a larger research on the CMF design process. The typical CMF Design Process is a multi-stage process involving research, deriving of narratives, defining of a CMF strategy, ideation, and design development [5]. The defining of the CMF strategy in itself is an objectives-driven activity that factors in a variety of requirements that flow in from multiple directions including, colour trends, consumer preferences, market positioning, brand identity, archetypal references and the expression of a product's attributes [6]. Developing and communicating value is an important prerequisite of a design activity [7]. Given the variety and choice of product alternatives available to a consumer, the CMF design is required to align, compliment, differentiate, express, communicate, and in effect offer a calibrated value proposition to its intended audience [8].

A study of the current colour research landscape reveals that while there is plenty of discussion on colour preferences, and colour and value perception, there has been little attempt at a categorical study relating specifics of colour application to product value propositions. This study aims to answer two significant questions, 1) What are the kinds of value propositions that a designer attempts to attribute to a product through the use of colour? 2) Can these value propositions be categorised into a structured framework to be used as a reference during the CMF design process?

METHODOLOGY

The study began with a one-question survey in a social media forum for designers asking them to list: 1) up to three products for which they designed the CMF in the recent past, 2) the colours used in the CMF design, 3) the reasons for the choice of colours used in the CMF design. The reasons provided by the design practitioners were considered to represent in essence, the value propositions coded into the products through the use of colours in the CMF design. Responses were received from 34 designers with a total of 75 CMF design cases. Interpretative Qualitative Case Study Analysis method [9] was used for the analysis of survey data. A final validation of the results was done through a simple sorting test involving a set of participants.

RESULT AND DISCUSSION

Survey and Analysis

The analysis of the survey data from the 75 design cases was done in two parts. First, the identification of dominant patterns in the data through the use of Interpretative Qualitative Descriptors. Second, the consolidation of the descriptors into a list of concise vocabulary labelled Value Categories. Table 1 shows a short sample of the analysis done on the 75 design cases.

The final set of eight Value Categories derived from the analysis represents the categorical reasons for the use of colour to code specific value propositions in the CMF design of products (see Table 1).

Table 1. Samples of the design cases with derived Descriptors and Value Categories

Product	Stated reasons for colour use	Interpretative Qualitative Descriptors	Value Categories
Fridge Stabilizer	Matching with the CMF of economy variant fridges in the market	Expresses an archetypal quality	Archetypal
Ground Control Station	Colours to match different materials such as MS, Aluminium, ACP, FRP	Aligns to a functional necessity	Pragmatic
Pedestal Fan	Matching with the elegant luxurious marble finish interiors	References an aesthetic category	Categorical
Frontloading Washing Machine	To cater to premium segment consumers	Directs a relative value perception	Relational
Kitchen Appliance	Giving highlight to food in the kitchen rather than appliances	Performs a performative function	Performative
Sport shoes	To give it a rugged forest feel	Invokes a metaphorical association	Associative
Walking stick	To evoke joy and playfulness	Evokes an emotional response	Emotive
Pooja Unit (Shrine)	As most customers would prefer that colour	References a symbolic association	Symbolic

The Colour Value Framework

Lifestyle products tend to be positioned at varying levels of the market depending on the product's value proposition [10]. For the CMF designer, this implies varying levels of ambitions in a CMF design objective, ranging from something basic at one end of the scale, to something novel and imaginative at the other end. This range can be likened to scales used to typify the level of innovation in the design of products or services [11]. Borrowing from such references a hierarchical scale was developed with four levels as: 1) evolutionary, 2) progressive, 3) radical, and 4) experimental. This scale which we will call Value Frames, essentially expresses the level of conceptual 'stretch' applied in the creation of CMF designs in order to meet the design ambitions. It is found that the ordering of the Value Categories in relation to the Value Frames produces a convincing hierarchical alignment between the Value Categories and the Value Frames, shown in Table 2 below.

Table 2. The Colour Value Framework - Value Categories mapped to Value Frames

Value Frames	**Evolutionary**	**Progressive**	**Radical**	**Experimental**
Value Categories	1. Archetypal	3. Categorical	6. Associative	8. Symbolic
	2. Pragmatic	4. Relational	7. Emotive	
		5. Performative		

With reference to the initial questions triggering this study, Table 2 offers the final consolidation, mapping the eight Value Categories against the four Value Frames to create the Colour Value Framework (CVF). As established, the eight Value Categories represent the different value propositions attempted in the course of a CMF design process. The four Value Frames offer a hierarchical basis to the conceptual stretch required, to generate different value propositions.

Applicability of the Colour Value Framework

The CVF has the potential to perform two important functions in the CMF design context, 1) serve as a vocabulary for precise articulation, and 2) serve as a referenceable framework for precise positioning. In the first instance, the vocabulary derived as part of the CVF, namely the Value Frames, and the Value Categories, can help in the precise articulation of the target value proposition to be achieved through the CMF design. In the second case, the CVF can help provide a referenceable structure to deliberate on the precise positioning of a product's value proposition.

Validation study

The performance of the Value Categories as effective labels was validated in two parts. In the first part, Refrigerator images were used as samples to validate and create definitions for the Value Categories (see Table 3). Following this, a Sorting Test [12] using preselected Coffee Makers was conducted with seven invited participants to test for percentage conformity in the understanding and relatability of the Value Category labels with their intended meaning (see Table 4). The success rate in both the validations strongly attests to the reproducibility and effectiveness of the Value Categories as representative labels for value propositions attempted in the CMF designs.

Table 3. Value Categories with examples drawn from current refrigerator models*

			
1. Archetypal value Use of colour to conform to prevalent palettes existing in the marketplace to suggest standardisation as a value proposition	**2. Pragmatic value** Use of colour to suggest that practical considerations have been applied (e.g., dual colours) as a value proposition	**3. Categorical value** Use of colour to conform to existing aesthetic categories with stylistic orientation (e.g., Art Deco) as a value proposition	**4. Relational value** Use of colour borrowed from stereotypical references used to suggest a market value (e.g., premium value) as a value proposition
			
5. Performative value Use of colour to perform a specific aesthetic role relevant to their contexts of use (e.g., décor) as a value proposition	**6. Associative value** Use of colour to suggest expressive metaphorical associations as a value proposition	**7. Emotive value** Use of colour to evoke emotional references as a value proposition (e.g., the colour tone above is used to indicate a relaxing, informal atmosphere)	**8. Symbolic value** Use of colour with symbolic associations (e.g., SMEG UAE uses the colours of the flag) as a value proposition

Table 4. Results from validation of Value Categories using Coffee Makers

	Archetypal	Pragmatic	Categorical	Relational	Performative	Associative	Emotive	Symbolic
Design sample used								
% Conformity	86	86	71	100	57	71	71	86

CONCLUSION

This study probes the fundamental association between colours and the value propositions coded into products through CMF design with a view to understanding if there are dominant categorizable patterns in the use of colour. The study was able to identify eight dominant categories that represent the dominant reasons for the use of colour to code value propositions in products. The clarity and unambiguity of the labels used to represent the categories were ascertained. The hierarchical progression of these categories in four levels representing the conceptual stretch required in the CMF design was arrived at.

The final consolidation of this study in the form of a CVF provides both a vocabulary and a structured basis to deliberate on the coding of value propositions during the CMF design process. We believe that the CVF can benefit the CMF design process in a number of ways: help recognize the value of colour use in coding value propositions into products; reduce ambiguity in the articulation of design objective statements; serve as a matrix for relative positioning of product value propositions; provide a referenceable vocabulary for discursive situations. It is felt that a stronger validation of the framework in application scenarios will help refine it further.

ACKNOWLEDGEMENT

We would like to acknowledge the use of product images from, Samsung, SMEG S.p.A., Koninklijke Philips N.V., BOSCARE Limited, KAFF Appliances, BRG Appliances, Cuisinart, illycaffe S.p.A., Bella Housewares, Bialetti Industrie S.p.A., for the purpose of this study.

We heartily thank the students of RV University School of Design and Innovation, Aishwarya MG, Janhavi Chetan Jadhav, Aanya Bakshi, Sreeshanth S, and the faculty, for helping us operationalise portions of this study. We acknowledge our respective institutions, RV University, and the National Institute of Design, India, for their intellectual support during this research.

REFERENCES

1. Xi'an Academy of Fine Arts, China, & Liu, Y. (2020, September 10). *Research on the value of CMF design in industrial products*. Design Research Society Conference 2020.
2. Batra, N. (2022, March 9). *CMF in Industrial Design*. Lesmor Design.
3. Sánchez-Fernández, R., & Iniesta-Bonillo, M. Á. (2007). *The concept of perceived value: A systematic review of the research.* Marketing Theory, 7(4), 427–451.
4. Suryadi, N., Suryana, Y., Komaladewi, R., & Namuri, D. (2018). *Consumer, customer and perceived value: Past and present.* Academy of Strategic Management Journal, 17.
5. Becerra, L. (2016). *CMF Design: The Fundamental Principles of Colour, Material and Finish Design*. Frame Publishers BV, *36-63.*
6. Iannitto, E. (2019). *The Customer Value: A Bibliographical Review.* International Journal of Marketing Studies, 11(3), 106.
7. Westcott, M., Sato, S., Mrazek, D., Wallace, R., Vanka, S., Bilson, C., & Hardin, D. (2013). *The DMI Design Value Scorecard: A New Design Measurement and Management Model.* Design Management Review, 24(4), 10–16.
8. *Consumer Tech insights: Three tips for successful CMF design* | WGSN. (n.d.). Retrieved July 14, 2023.
9. Sinha, D. S. K. (2017). *Case Study Approach in Qualitative Research*. International Journal of Research Culture Society, Volume - 1, Issue - 7, 99-103.
10. Kaul, A., & Rao, V. R. (1995). *Research for product positioning and design decisions: An integrative review.* International Journal of Research in Marketing, 12(4), 293–320.
11. Mr. Kris Miner, M. B. A. (2010). *The Four Levels of Innovation.* 2010 Volume 13 Issue 4, 4.
12. Sherwin, K. (2018). *Card Sorting: Uncover Users' Mental Models for Better Information Architecture*. Nielsen Norman Group. Retrieved September 14, 2023, from https://www.nngroup.com/articles/card-sorting-definition/

A COLOUR RENDERING CHART FOR PREFERRED COLOUR

Ming Ronnier Luo*

1. State Key Laboratory of Modern Optical Instrumentation, Zhejiang University, CHINA

*Corresponding author: m.r.luo@zju.edu.cn

ABSTRACT

A colour rendition chart, Preferred Memory Colour Chart (PMCC), has been produced. It includes 30 colours including memory colours, reference gamut colours and a grey sale. The theory behind these colours will be introduced。 Finally, a number of applications will also be covered.

Keywords: colour specification, colour names, colour order systems, colour communication

INTRODUCTION

Reference charts that include colour patches and images have been developed and are frequently used in evaluating the colour fidelity and variability of imaging devices in the colour reproduction chain. The typical example is the Xrite ColorChecker chart (XCCC) [1]. It includes 24 colours to cover a wide colour gamut and include typical scenes and colours that are likely to cause errors when reproduced, such as skin tones, neutral colours, memory colours, highlight and shadow scenes, etc. It is, therefore, suitable as test samples for the evaluation of colour differences in complex digital images. Following the same idea, a new colour rendition chart, named Preferred Memory Colour Chart (PMCC), has been developed and is described in this article. It is very much focused on the memory colour.

Figure 1 shows the PMCC chart. It has the same size as XCCC, 23.5 cm by 29.0 cm, and has 6 more colours than that of XCCC. The 30 colours are arranged as 6 by 5 arrays and are divided into three categories: 1) preferred memory colour (top 3 rows), 2) colour reproduction primaries (the 4th row) and 3) a neutral scales (the 5th row). Each colour, specified by a number and colour name, is given below,

- The 1st row: 1) Caucasian, 2) Oriental, 3) South Asian, 4) African, 5) Pork, 6] Carrot;
- The 2nd row: 7) Orange, 8) YR, 9) Banana, 10) YG, 11) Green apple, 12) Grass;
- The 3rd row: 13) BG, 14) Smurf, 15) Blue sky, 16) Lavender, 17) PR, 18) Purple Garbage;
- The 4th row: 19) Unitary red, 20) Unitary yellow, 21) Unitary green, 22) Unitary blue, 23) Cyan, 24) Magenta; and
- The 5th row: 25) White, 26) Grey-80, 27) Grey-70, 28) Grey-50, 29) Grey-35, 30) Black.

Each colour, plotted in a*b* plane in Figure 2, is specified in terms of spectral reflectance function (R%), and CIELAB values under D65/10° condition.

Figure 1 The PMCC chart.

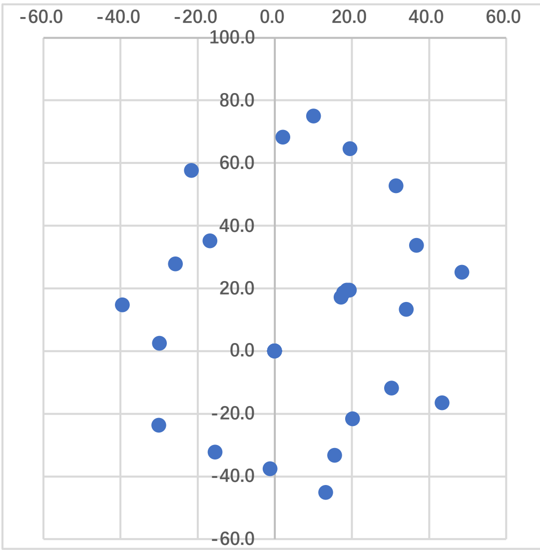

Figure 2 The PMCC colours plotted in a*b* plane

For the memory colour category, the colours were obtained by two psychophysical experiments [2,3] on mobile displays. In the first experiment, the images of 8 models from 4 ethnic groups (Caucasian, Oriental, South Asian and African) were captured by a . In the second experiment, 28 familiar objects (such as fruits, vegetables, flowers, etc) were selected and their original images were either captured by a camera illuminated by a D65 simulator at 1000 lx level or by searching from website. Each was then rendered to 50 images in different colour directions. These images were then scaled by 106 observers from 4 ethnic groups in terms of preference and naturalness. The results of each object were used to established the preferred memory colour centre. For the primary colour category, these together with the black and white can form a three-dimensional reference colour gamut. The former 4 colours , Colour 19-22, are the unitary colours corresponding to R_9, R_{10}, R_{11}, R_{12} of CIE colour rendering index, R_a [4] For the neutral colour category, they have the CIE L* values from 96 (white), 82, 68, 52, 38 to 22 (black). The primary sets include saturated red, green blue, yellow, cyan and magenta.

COLOUR REPRODUCTION

Each colour in PMCC was produced via a strict quality control process. The physical objects for each 'preferred memory colour' were first collected and measured using a d/8 sphere-based spectrophotometer. The average value from 40 measurements was taken as standard. The average colour in L*, a*, b* values and spectral reflectance function were used to represent the colour in question.

From the experimental results, it was found that most of the preferred memory colours are usually brighter and more colourful than the real measured colours. Computer formulation was performed using the high-grade pigments with lightfastness in the range of 7 to 8. The reproduction goal is to not only accurately reproduce the colour in L*a*b* values but also to keep the shape of the measured spectra as close as possible. Note few colours were not able to reproduce due to out of the colour gamut of the coating system. This is to keep the constant hue angle and to compress its lightness and chroma values.

Strict colour tolerance is applied between different charts. All charts to agree with the production standard to have less than one CIEDE2000 colour difference [5].

APPLICATIONS

Hunt introduced [5] various types of digital imaging reproduction, the most important ones including namely spectral, colorimetric, appearance, preferred respectively. The PMCC can be used to achieve the above types of colour reproduction. Various applications are listed in Table 1, together with the PMCC proposed for the application for three industries, camera, display and illumination.

Table 1 summarises the application areas in 3 industries: camera, display and lighting.

Appli-cations	Neutra-lity	Unitary hue shift	White balance	Natural-ness index	Skin index	Colour gamut	Calibrti on model	ICC	ISP	Colour rendering
PMCC Colours	25-30	19-22	25	1-18 except 8, 12, 13, 17	1-4	19-24	1-30	1-30	1-30	1-18
Camera	√	√	√	√	√	√	√	√	√	
Display	√	√	√	√	√	√	√	√	√	
Lighting		√	√	√	√	√				√

The followings describe each application

- For the colour quality metrics, PMCC colours can be used to evaluate degree of neutrality using the 6 neutral colours, of unitary hue shift using Colours 19-22, and of white point using Colour 25 in terms of CIEDE2000 units, i.e. the larger colour difference, the more deviation from the desired colour perception. The skin index and overall naturalness index have been established to compute the image quality score using the acceptance elliptical models [2,3].

- The PMCC Colours in 19-24 form a reference gamut, which can be used to calculate a ratio of the gamut of an imaging device [6] or of a lighting [7], and that of the reference, i.e. the larger the ratio, the wider the colour gamut.
- The top 3 rows of PMCC colours can also be used as reference colours to evaluate colour rendering quality of light sources via colour rendering indices such as R_a [8], R_f [7].
- For the colour calibration of imaging devices, same as XCCC, all PMCC colours can be used to derive characterization models between device signals and CIE XYZ values, such as GOG, Polynomial, 1D-LUT models.. Also, technology can be used to perform curve fitting to achieve a 3D-LUT [10] and produce ICC profile [11].
- The PMCC colours are effective to derive algorithms for image signal processing (ISP), such as automatic white balance (AWB) [12], preferred colour reproduction [13], etc.
- Finally, the PMCC colours provide visual aid to compare the performance of colour reproduction between the target in a viewing cabinet and the reproduction on a display or to evaluate the PMCC colours illuminated under test light sources against observers' memory colours.

CONCLUSIONS

A new colour target, Preferred Memory Colour Chart (PMCC), has been invented and produced. Its design, manufacturing, and theory have been introduced. It has three major applications, a physical target to characterise imaging devices, to evaluate the objective and subjective quality of devices or images. Quality, and to provide a visual aid to check the cross-media colour reproduction, or lighting quality.

In conclusion, PMCC can be a valuable aid to perform all types of digital image colour reproduction, especially preferred reproduction.

REFERENCES

1. C. S. McCamy, H. Marcus, J. G. Davidson, A color-rendition chart, Journal of applied photographic Engineering, 2:3 (1976) 95-99.
2. R. Peng, M. R. Luo, Y. Zhu, X. Liu and M. R. Pointer, Preferred skin reproduction of different skin groups, Vision Res. 207 pp108210, 2023.
3. M. Cao, and M. R. Luo, A study of preferred and natural memory colours across different ethnic groups, , Color Research and Application 48 (2023)178-200.
4. CIE 013. 3-1995 Method of measuring and specifying colour rendering properties of light sources.
5. M. R. Luo, G. Cui and B. Rigg, The development of the CIE 2000 colour difference formula, *Color Res. Appl.* **26** (2001) 340-350.
6. R. W. G. Hunt, The reproduction of colour, 2004, Willey, New York.

7. L. Xu, C. Xu, M. R. Luo, Accurate gamut boundary descriptor for displays, Optics Express, 30(2)(2022), pp1615-26.
8. ANSI/IES TM-30-18, IES Method for Evaluating Light Source Color Rendition, 2018.
9. H. Z. Zeng and M. R. Luo, Colour and tolerance of preferred skin colours on digital photographic images, *Color Res. Appl.* 38(2013), pp30-45.
10. H. R. Kang, Computational Color Technology, SPIE Press, Bellingham, WD USA.
11. ICC.2:2019 (Profile Version 5.0.0-iccMAX) Image Technology colour management – extensions to architecture, profile format and data structure, @ICC 2019 International Color Consortium.
12. L. Wang and M. R. Luo, To perform white balance using skin memory color, International Colour Association (AIC) 2023.
13. H. Z. Zeng and M. R. Luo, A Preferred Skin Color Enhancement Method for Photographic Color Reproduction, *Proc. SPIE: Color Imaging: Device-Independent Color, Color Hardcopy, and Graphic Arts* , (2011).

TM-30-20 AND CIE-CRI-R_a: INVESTIGATION OF COLOUR RENDERING OF WHITE PC LEDS

Karin Bieske* and Christoph Schierz

Lighting Engineering Group, Department of Mechanical Engineering, Technische Universität Ilmenau, Germany.

*Corresponding author: karin.bieske@tu-ilmenau.de

ABSTRACT

Nowadays, phosphor converted LEDs (pc LED) are used in indoor lighting applications. Colour rendering properties play an important role in the development of powerful LED light sources. The current standard method of calculating these properties is the CIE colour rendering index CIE-CRI R_a. Studies have revealed inconsistencies between this method and its rating by subjects, especially in LED lighting. In the meantime, new methods have been developed, but have not yet found their way into application. The colour fidelity index R_f and the colour gamut index R_g from IES TM-30-20 are new metrics published by the Illuminating Engineering Society of North America. The colour rendering properties of 21 pc LED light sources with different R_f values between 69 and 97 and R_g values between 92 and 114 as in the fidelity index and gamut index of the TM-30-20 have been investigated. Scenarios illuminated by pc LEDs and a tungsten halogen lamp (TL) with the same luminous colour (CCT = 3800 K) and the same illuminance on the test surface were presented to 34 subjects. An assortment of coloured objects was arranged identically in two adjoining booths and participants rated the test scenarios in comparison with the reference illuminant (TL) according to different criteria of colour difference, saturation, likeability and naturalness. In addition, the subjects were asked which of the object colours matched their expectation for the objects and how they rated the overall colour quality of the objects independently of the reference.

The results show that the assessment of colour quality is determined by both the fidelity index and the gamut index. While the fidelity index correlates strongly with the colour difference and the observed colour shift compared to the reference, as expected, the gamut index maps saturation well. The liking of a lighting situation correlates more strongly with the R_g value than with the R_f value. Both indices are equally important for assessing the naturalness of colours. This also applies to the assessment of the colour quality of a light source. Basically, there is a high correlation between the CIE-CRI R_a and the R_f value.

Keywords: colour rendering, pc LED, TM-30-20, colour fidelity, subjective assessment

INTRODUCTION

Nowadays, LEDs are predominantly used for interior lighting. Typically, phosphor converted LEDs (pc LEDs) are used to produce different white luminous colours. The emission of blue LEDs is down-converted to light with longer wavelengths using phosphors and mixed with a radiation component of the blue LEDs to produce white light. The phosphors are typically a mixture of different types of phosphor. This makes it possible to adjust the spectral power distribution (SPD) of the LEDs and optimise their colour rendering properties. Accurately describing the colour rendering properties of light sources is essential for setting the right development targets when designing the spectral power distribution of LEDs.

The current standard method of calculating the colour rendering index CIE-CRI R_a (R_a) is that recommended in 1995 as CIE 13.3 [1]. Studies have revealed inconsistencies between this method and its rating by subjects, especially in LED lighting [2]. For years, possibilities for improvement have been sought. On the one hand, the calculation method is improved based on new findings in colourimetry. On the other hand, the spectral power distribution of light sources has been optimised, for example by using different types of phosphor materials, as these largely define colour quality. In 2020, the Illuminating Engineering Society (IES) published the Technical Memorandum TM-30-20, a new calculation method for colour rendering of white light sources [3]. It combines colour fidelity, rated with the R_f index, and the colour gamut, rated with R_g index: this describes the area enclosed by the average chromaticity coordinates in each of 16 hue bins.

Thornton has suggested that the larger the colour gamut, the better is the colour discrimination because the chromaticity coordinates are further apart in the colour space [4]. There is also an assumption that light sources with larger gamut enable colours to be perceived as more saturated, more brilliant and more natural [5]. Xu assumes that the size of the area enclosed is proportional to the maximum possible number of colours that can be represented [6]. RGB-LEDs serve as an example of LEDs with narrow SPD. They may have a large gamut index but the rendering of certain colours may be inexact. It therefore makes sense to combine the two indices [7].

The colour fidelity index R_f, like the CIE-CRI R_a, is a reference-based method in which a test illuminant is compared to a reference illuminant with the same correlated colour temperature (CCT). The colour fidelity index R_f of a lighting describes the average colour shift across 99 test colours (CES) compared to a reference illuminant. Its value ranges from 0 to 100. Additionally, the gamut index R_g compares the areas between test and reference illumination spanned by the colour coordinates of 16 hue bins derived from the 99 test colours in CIECAM02 colour space and describes the average saturation of the test colours. A neutral rating has a value of 100, values > 100 indicate an increase in saturation, while values < 100 indicate a decrease. The range of values of the gamut index R_g increases as the colour fidelity index R_f decreases [3].

Royer has carried out a study of LED illumination in a test room with coloured objects. The illumination produces white light from seven types of tunable, coloured LEDs with varying R_f and R_g values. The study concluded that observers generally prefer LED light sources with a fidelity index (R_f) greater than 75 and a gamut index (R_g) of 100 or higher [8]. This result was examined in respect of pc LEDs [9], [10]. This showed that colours with the same R_f value were perceived as more saturated under lighting with high R_g values and were more pleasing than with lower R_g values. Building a database is important to evaluate the performance of different metrics. This paper contrasts the TM-30-20 metrics with the CIE-CRI R_a and investigates the correlation between subjective judgements and these indices.

METHODOLOGY

Two adjoining booths with two sections, one for the illumination unit with a diffuser and another for test objects, were used (Figure 1a). In one booth (size: 46 cm x 96 cm x 48 cm), the light sources installed were a tungsten halogen lamp (TL: Eiko: SoLux GX 5.3) together with three types of blue LEDs and seven different LEDs incorporating a variety of green and red phosphors. Combining a variety of LEDs enabled various SPDs to be produced, which were identical to those of white pc LEDs. 21 combinations of LEDs with R_f values between 66 and 94 and R_g values between 92 and 114 were investigated in comparison with a reference (Figure 2). The reference illuminant in the second booth was provided by a TL (Ref.: $R_a = 99$, $R_f = 97$, $R_g = 99$). All lighting conditions had an identical luminous colour ($CCT = 3800$ K) and the same illuminance of 600 lx in the centre of the floor of the booth.

The colour rendering values of the examined LED spectra, CIE-CRI R_a, are almost identical to the R_f values and differ on average by 2 in a range from 0 to a maximum of 6 evaluation units. The coefficient of determination for the correlation of the R_f values to the CIE-CRI R_a is $R^2 = 0{,}97$.

An assortment of identical coloured objects was arranged equally in the two booths. The choice of objects ensured that a wide range of hue, saturation and lightness was covered. They were objects from daily life: they included plants, food, consumer goods, office and printed materials, and colour rendition charts (Color Checker). The chromaticity coordinates of the objects in the CIE CAM02-UCS colour space are shown in Figure 1c.

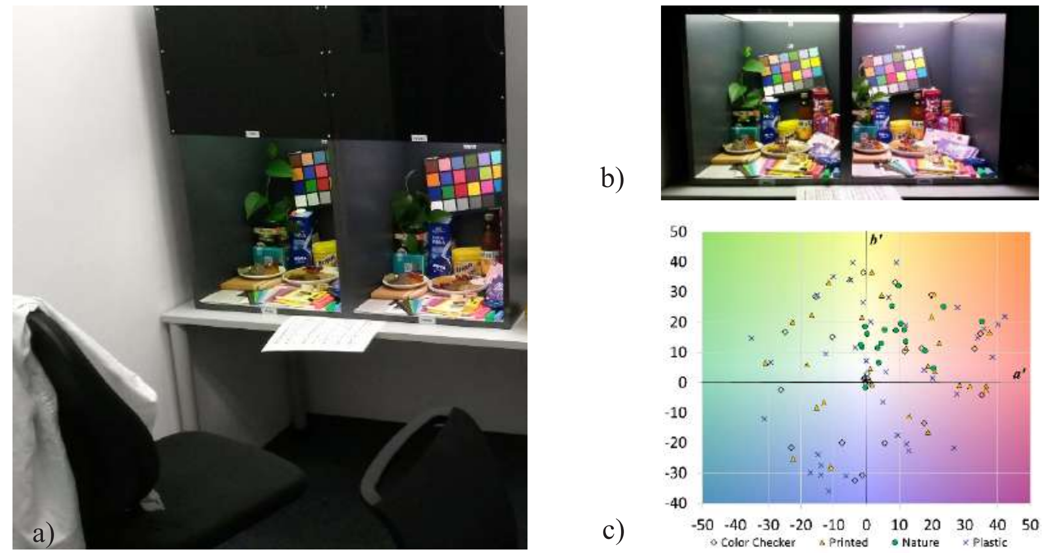

Figure 1. a/b) Experimental setup with test objects, c) Chromaticity coordinates of the test objects in the CIE CAM02-UCS colour space when illuminated with a Planckian radiator at *CCT* = 3800 K

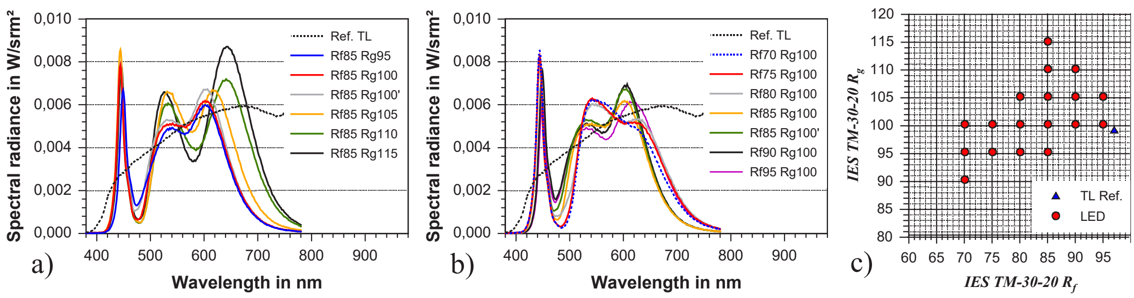

Figure 2. a/b) SPD of selected test scenarios, c) R_f-R_g-pairs of test scenarios investigated

Do you perceive a colour difference between the objects in the left booth and those in the right booth?					
Colour difference (CD)	1 = none	2 = small	3 = moderate	4 = great	5 = very great
How do you find the colours of the objects in the left booth in comparison to those on the right hand side?					
Saturation (S)	1 = very saturated	2 = somewhat saturated	3 = no difference	4 = somewhat unsaturated	5 = very unsaturated
Brightness (PB)	1 = very bright	2 = somewhat brighter	3 = no difference	4 = somewhat darker	5 = very dark
Temperature (T)	1 = very warm	2 = somewhat warmer	3 = no difference	4 = somewhat cooler	5 = very cool
Colour shift (CS)	1 = none	2 = small	3 = moderate	4 = large	5 = very large
Likeability (LA)	1 = very nice	2 = somewhat nicer	3 = no difference	4 = somewhat less nicer	5 = much less nice
Naturalness (NL)	1 = very natural	2 = somewhat more natural	3 = no difference	4 = somewhat less natural	5 = very unnatural
In which booth do the colours of the objects better match your expectation?					
Expectation (EP)	1 = left	2 = right	3 = both	4 = neither	
Ignoring the right hand side, how do you rate the colour quality of the objects in the left hand booth?					
Colour quality (CQ)	1 = very good	2 = good	3 = moderate	4 = poor	5 = very poor

Figure 3. Items of the questionnaire

34 participants between 23 and 48 years old (Ø 35 ± 7 years), 10 of them women, took part in the investigation. All of them with normal colour vision. They evaluated the colour rendering

properties simultaneously in both booths using a questionnaire. This evaluation included the comparison between object colours seen under the test illuminant and those under the reference illuminant according to the criteria: colour difference (CD), saturation (S), brightness (PB), colour cast temperature (T), liking (LA) and naturalness (NN). In addition, the subjects were asked which of the object colours matched their expectation for such objects and how they rated the general colour quality (CQ) of the objects independently of the reference. The items of the questionnaire are shown in Figure 3.

The presentation of the different lit scenarios was in random order. There was a repeat of the test for four scenarios. Additionally, a scenario with identical spectra (TL vs. TL) was presented. Mean values (MV) and confidence intervals (CI 95%) were calculated for the test subjects' responses and evaluated for the test parameters R_a, R_f and R_g. Coefficients of determination R^2 were determined for the linear regression and a 2nd degree polynomial regression over the subject judgements. For a comparison between the metrics, an analysis of variance and post hoc tests were carried out.

RESULT AND DISCUSSION

Results of the questionnaire are presented in Figure 4. Mean values (MV) ± confidence intervals (CI95%) are shown for all subjects ($N = 34$). Table 1 summarises the coefficients of determination R^2 of the linear regression over the mean values for individual items and different metrics R_a, R_f, and R_g. In addition, information about the correlations of the individual items for the evaluation of colour quality is given.

Table 1: Coefficient of determination R^2 of the linear regression (*,,*** denote the significance level for R^2)**

Item	R^2 for R_a	R^2 for R_f	R^2 for R_g	R^2 for CQ
Colour quality CQ	0,62 ***	0,65 ***	0,70 ***	1,00 ***
Colour difference CD	0,80 ***	0,78 ***	0,10	0,59 ***
Saturation S	0,25 **	0,31 **	0,95 ***	0,77 ***
Colour shift CS	0,77 ***	0,77 ***	0,29 **	0,80 ***
Perceived brightness PB	0,01	0,01	0,42 ***	0,18 *
Temperature T	0,55 ***	0,63 ***	0,05	0,26 **
Likeability LA	0,32 **	0,37 ***	0,90 ***	0,86 ***
Naturalness NN	0,61 ***	0,62 ***	0,67 ***	0,93 ***

It can be seen in the diagrams in Figure 4 and from the coefficients of determination R^2 from Table 1 that the evaluation of the subjective colour quality of an illuminant is a multi-dimensional problem, and both indices R_f and R_g are important measures in this context. While the R_f value gives a good description of colour difference, colour shift and the perception of a warmer or colder luminous colour effect compared to the reference light source, the R_g value explicitly reflects the assessment of saturation. Whether a scenario is perceived to be likeable depends very much on how saturated the colours appear. The gamut index can be used to describe the preference for a lit situation.

Both indices are important in the rating of naturalness. At constant R_f value, pc LEDs have a more likeable and saturated effect the higher the R_g value, up to a certain point. For the item naturalness as a function of the R_g value, a 2nd degree polynomial regression was also carried out (Figure 5). This resulted in a coefficient of determination of 0,78. The fit function shows a maximum at $R_g = 110$. According to this, the objects appear most natural at this gamut index value. LED light sources investigated with higher R_g values are therefore perceived as less natural. It also leads to the perception of greater colour shifts and more distinct colour differences. There are thus limits to the increase of saturation in the LED spectrum. As the R_f value rises, so does the subjective colour rendering rating, and the perceived differences to the reference illuminant decrease.

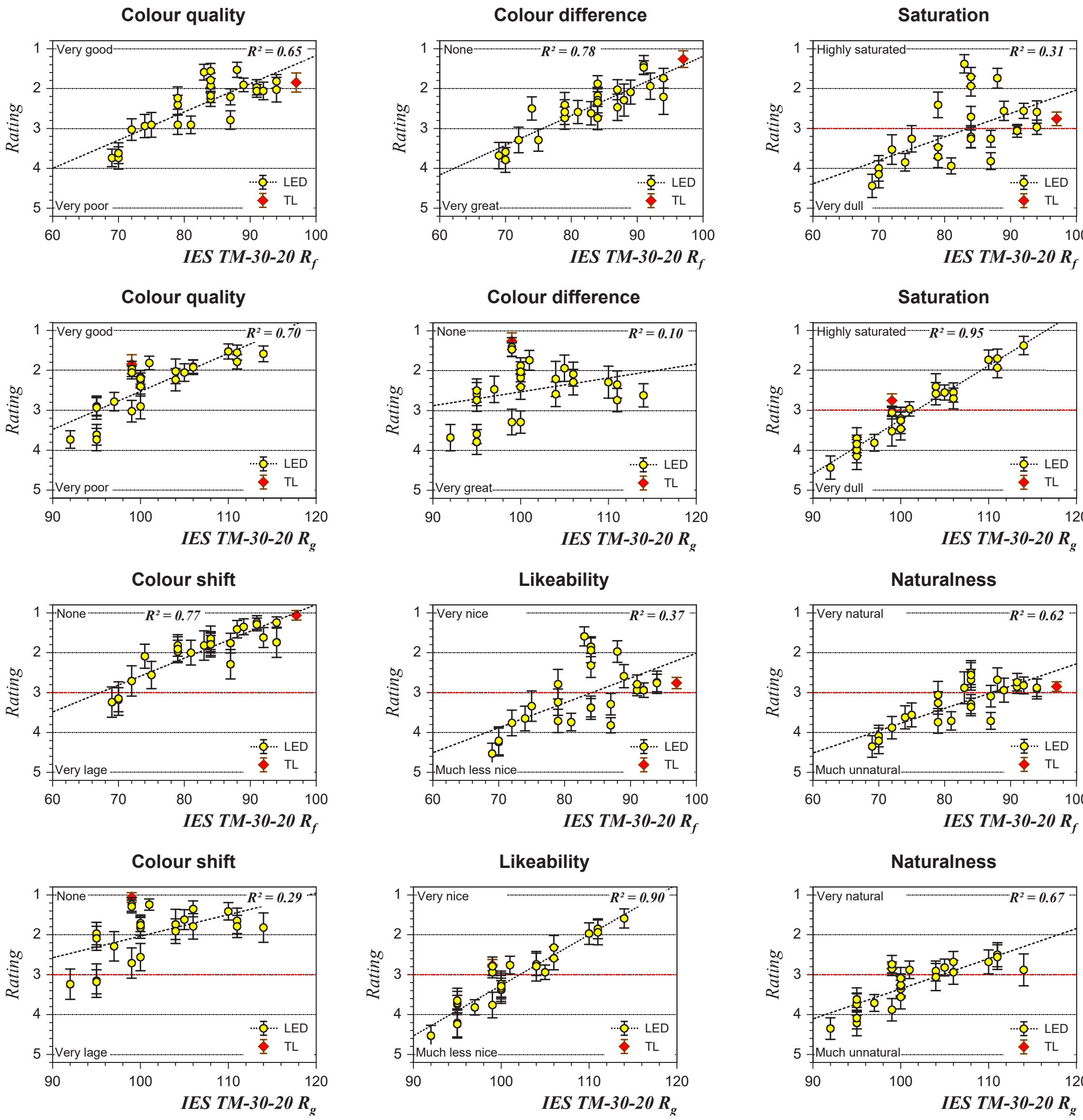

Figure 4. Subjective judgements of the test persons (mean value and confidence interval) for R_f and R_g. The coefficient of determination R^2 of the linear regression, which was determined for the mean judgements for each scenario ($N = 25$), is given in each case.

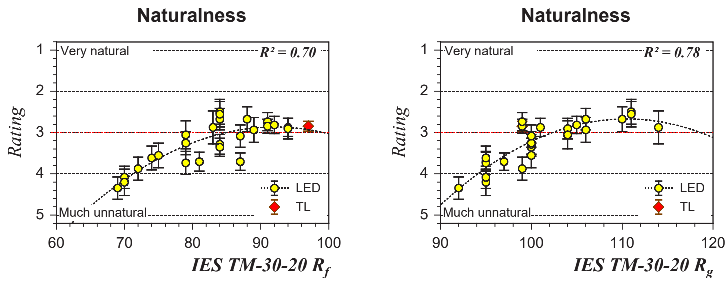

Figure 5. Subjective judgements of the test persons regarding the naturalness of the object colours (mean value and confidence interval) for R_f and R_g. The coefficient of determination R^2 of the 2nd degree polynomial regression ($N = 25$), is indicated in each case.

Spectral power distributions with the following parameters were rated best: 1) $R_f \geq 90$ for $R_g = 100$, 2) $R_f \geq 85$ for $R_g = 105$, and 3) $R_f \geq 85$ for $R_g = 110$.

CONCLUSION

The likeability of an object colour (compared to the reference) cannot be predicted solely based on the fidelity index R_f. Since the fidelity index, like the CIE-CRI R_a, only describes the difference in colour appearance compared to the colour appearance under a reference illuminant, it does not measure likeability. Consequently, to consider subjective colour likeability when designing the spectral power distributions of LEDs, it is important to also use criteria like the gamut index R_g. The gamut index captures the subjective likeability dimension of colour perception.

The presented investigation indicates that $R_f \geq 80$ and $100 \leq R_g \leq 110$ are useful prescriptive values for designing the SPD of LEDs. The subjects found that scenes illuminated with an R_f value of 85 or higher and an R_g value of 100 or higher appeared as natural as, or even more natural than, the reference illuminant when it comes to the colour of objects.

The strong correlation between the CIE-CRI R_a and R_f values ($R^2 = 0{,}97$) suggests that they can be used interchangeably, allowing the study's R_f results to be applied to CIE-CRI R_a values.

ACKNOWLEDGEMENT

The investigation was carried out in cooperation with OSRAM Opto Semiconductors GmbH in Regensburg, Germany. Without this support, the experimental setup would not have been possible. The conception and implementation of the test person study was handled as part of Hartwig's master's thesis [9].

REFERENCES

[1] CIE (1995). Method of Measuring and Specifying Colour Rendering Properties of Light Sources, *CIE 13.3*.

[2] Narendran, N. & Deng, L. (2002). Color Rendering Properties of LED Light Sources, *Proceedings of SPIE*, *4776*, p. 61-67.

[3] Illuminating Engineering Society of North Amerika (2020). IES Method for Evaluating Light Source Color Rendition, IES TM-30-20.

[4] Thornton, W. A. (1972). Color-discrimination index. *J Opt Soc Am.*, *62* (2). p. 191-194.

[5] Rea, M. S., Deng, L. & Wolsey, R. (2004). Light Sources and Color. *NLPIP Lighting Answers (Rensselaer Polytechnic Institute, Troy, NY). 8*(1/Oct).

[6] Xu, H. (1983). Color-rendering capacity of illumination. *J Opt Soc Am. 73*(12/ Dec),1709-13.

[7] Bodrogi, P. & Jungnitsch, K. (Eds.). (2015). Farbqualität: Definition und Anwendungen. *Publ. 31*. Deutsche Lichttechnische Gesellschaft (LiTG), Berlin

[8] Royer, M. P., Wilkerson, A., Wei, M., Houser, K. & Davis, R. (2016) Human perceptions of colour rendition vary with average fidelity, average gamut, and gamut shape. *Lighting Res. Technol. 49*(8), 966-91. DOI: 10.1177/1477153516663615.

[9] Hartwig, U. (2017) TM-30-15, Analyse und Probandenstudie, Masterthesis TU Ilmenau.

[10] Bieske, K., Hartwig, U., Schierz, Ch., Wilm, A., Horst, C. (2018) TM-30-15 and CIE-CRI-Ra: Investigation of colour rendering of white pc LEDs. *Light & Engineering. 26*(2), p. 81-87.

[11] CIE (2004). A color appearance model for colour management systems: CIECAM02. *CIE 159*.

A set of optimal reflectance curves to detect and reduce inter-instrument differences between spectrophotometers

Anders Nilsson[1]* and John Seymour[2]

[1]*NCS Colour AB, Sweden.*
[2]*Clemson University, USA.*

*Corresponding author: Anders Nilsson, anders.nilsson@ncscolour.com

ABSTRACT

To improve Inter-Model Agreement (IMA) between spectrophotometers to allow for digital colour communication the spectral reflectance of a large set of NCS Colour Samples was measured in different instruments. A large set of mathematical models to improve the IMA were tested. Different calculation methods were then used to select an optimal model and a set of optimal reflectance curves to improve the IMA.

Keywords: Digital color standards, Spectrophotometers, Inter Instrument Agreement, Spectral curves

INTRODUCTION

Background

In industry, communicating colour standards by measurement data digitally instead of physical standards is desirable. Providing accurate physical standards to all production sites and suppliers over time is costly and time consuming for a company. Accurate physical standards must be produced, checked, transported, and maintained over a long period of time[1].
Digital colour standards in the form of spectral measurements, can be stored in a database, accessed globally, are unique and do not change over time or by wear.

Common industrial tolerances are < 0.5 $\Delta E_{ab}/\Delta E_{00}$, to fulfil this need, measurement accuracy must then be < 0.17 $\Delta E_{ab}/\Delta E_{00}$or better (normally 1/10 of the tolerance is needed but for colour measurement, 1/3 is often accepted <source>). Manufacturers of spectrophotometers normally specify repeatability and Inter-Instrument Agreement (IIA) as a measure of the accuracy. Repeatability is the uncertainty in 30 measurements on the white calibration standard under a short period, without removing the standard from the measurement port. This uncertainty is normally very low, 0.05 ΔE_{00} or less, for most high-end instruments. The IIA is normally defined as the colour difference of a set of the 12 BCRA series II tiles. The average ΔE difference between the individual instrument and the instrument producers reference instrument of the same model is stated and sometimes also the maximal deviation as the IIA. Thes values are often around 0.1 $\Delta E_{ab}/\Delta E_{00}$ for stationary instruments and 0.15 $\Delta E_{ab}/\Delta E_{00}$for portable. From this specification, in worst case, two individual instruments may differ by twice these figures.

Motivation

To use digital colour standards, a company and its suppliers need to use high-end instruments of the same model from the same manufacturer. There is today no accepted way to compare the closeness of agreement between the result of instruments of different models or from different manufacturer (having the same measurement geometry), Inter-Model Agreement, IMA[2]. Moreover, if disagreement between instruments is found, no standardized method exists to correct for these differences.

Goal

This study investigates a broad set of reflectance spectra to find an optimal set of physical samples for quantifying and improving Inter-Model Agreement by "Correcting" the measurements from a "Test" instrument to the measurements of a "Reference" instrument. This set of spectral curves can then be proposed as an international standard for quantifying and "Correcting" differences between spectrophotometers.

METHODOLOGY

A selection of NCS standardized colour samples was measured in different instruments under controlled conditions. Different mathematical models were tested with different selections of samples to "Correcting" a test instrument to a reference instrument for the complete set of samples. A set of models, giving good agreement without introducing unnecessary complexity was selected. Based on these results, a general set of spectral reflectance's is suggested.

Samples

A set of 710 colour samples was selected from the 2050 standardized NCS colour samples [5], see Table 1. The selection was based on the purest and deepest colours to give the most variable spectral reflectance curves. The basic selection was all samples on the lines; 05 in blackness and 05 in whiteness for all 40 hues, se Figure 1. In addition, the nuance 3030 was included for all hues to represent a medium chromatic spectral curve. The grey scale having chromaticness = 0, was also included. In total 711 samples were selected.

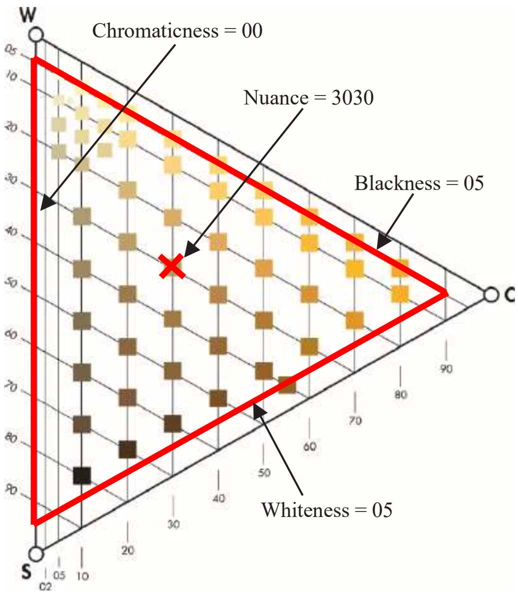

Figure 1. Main areas in NCS colour triangle for sample selection.

Table 1: 711 selected NCS standard samples.

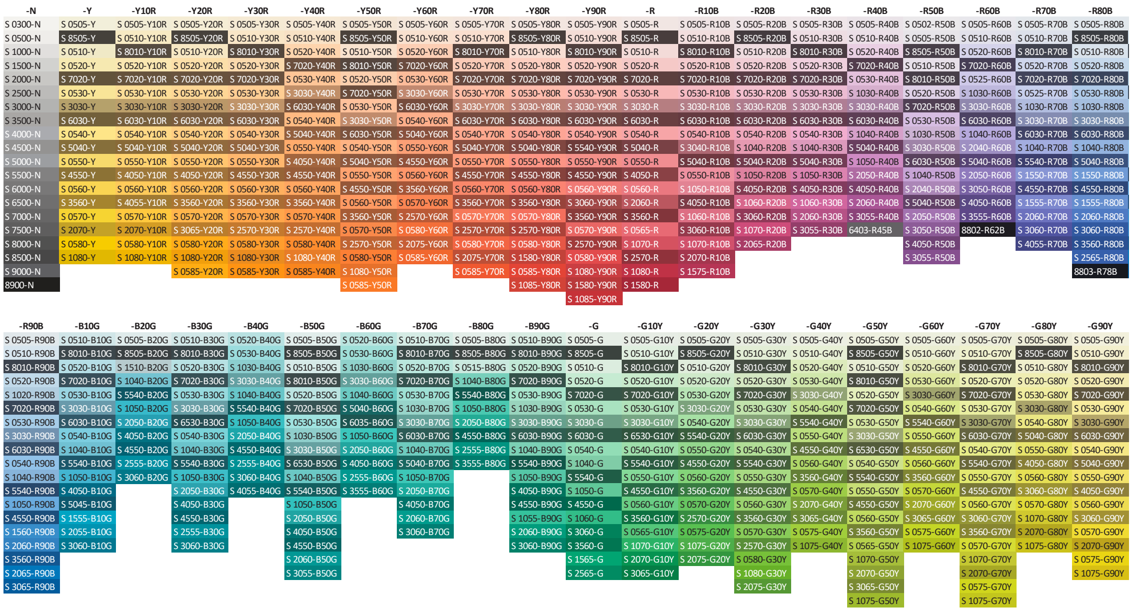

Instruments

Six different spectrophotometers of different models were included in this investigation, see Table 2. Three instruments with measurement geometry di:8° and three with 45°:0° geometrywere included. All are high-end spectrophotometers of different models from three different manufacturers, both stationary and portable types. The selected measurement geometries are the most used in industry. Table 3 show the six Reference-Test instrument combinations that can be selected, without mixing geometries.

Table 2: tested instruments.

No	Geometry	Manufacturer	Model	Type	Pitch
1	di:8°	Konica-Minolta	CM-3700A	Stationary	10nm
2	di:8°	X-Rite	Color i7	Stationary	10nm
3	di:8°	Konica-Minolta	CM-700d	Portable	10nm
4	45°:0°	Konica-Minolta	CM-25cG	Portable	10nm
5	45°:0°	Konica-Minolta	CM-2500c	Portable	10nm
6	45°:0°	Datacolor	DC45G	Portable	10nm

Table 3: instrument combinations tested.

Combination	Geometry	Reference	Test
1	di:8°	CM-3700A	Color i7
2	di:8°	CM-3700A	CM-700d
3	di:8°	Color i7	CM-700d
4	45°:0°	CM-25cG	DC45G
5	45°:0°	CM-25cG	CM-2500c
6	45°:0°	CM-2500c	DC45G

Measurement environment

All measurements were done in a temperature-controlled environment with 23° ± 0,5°. Samples were conditioned in this environment for at least 5 hours before measurements. Stationary instruments were warmed up at least 1 hour before measurements. Portable instruments were connected to power source during measurements.

Measurement procedure

The samples were measured at least two times with 90 degrees rotation between the measurements in each instrument. The instruments where calibrated 8 times during each measurement series. The backing for all samples was black. All measurements were saved as spectral data from 400nm to 700nm in step of 10nm.

Reproducibility

The specification of spectrophotometers normally contains data on repeatability and Inter-Instrument Agreement (IIA). Repeatability is recorded as the uncertainty from 30 measurement of the white calibration tail under a short period, without removing the tail from the measurement port. This uncertainty is normally very low, 0.05% or less, for all instruments. The IIA is normally a measurement of the 12 BCRA series II tiles compared to the same tiles measured on a reference instrument of the same model by the manufacturer. Both these measures are of little interest for comparing instruments of different models and from different manufacturers.

One interesting measure is reproducibility, here defined as the difference between two measurements on the same sample, using the same procedure in one instrument, but with calibration in between. The time between the two measurements should not be too long, the stability of the samples must not be a factor. For this study, all measurements for one geometry were completed within two weeks. Table 4 show the average colour difference, ΔE_{00} and the standard deviation of ΔE_{00} between measurement 1 and 2 for all 711 samples in the six instruments. The di:8° geometry performs better than 45°:0° as was expected as the 45°:0° geometry is more sensitive to small surface and gloss variations compared to the di:8° geometry, and the apertures are smaller

Table 4: reproducibility for each instrument, average for ΔE_{00} and standard deviation.

No	Brand	Model	Av.	Sdev
1	Konica-Minolta	CM-3700A	0.014	0.010
2	X-Rite	Color i7	0.029	0.015
3	Konica-Minolta	CM-700d	0.021	0.014
4	Konica-Minolta	CM-25cG	0.056	0.030
5	Konica-Minolta	CM-2500c	0.064	0.045
6	Datacolor	45G	0.066	0.035

Models

Different mathematical regression models were tested. The models build on polynomials of the reflectance and the first and second derivate of the reflectance for each wavelength. The model uses the notation R'_λ for the corrected reflectance on the left side and R_λ for the reflectance from the instrument to be corrected on the right side for each wavelength λ. The notation R_λ^n are the reflectance per wavelength raised to n. The notation $dR_\lambda{}^n$ is the first derivative and $d^2R_\lambda{}^n$ as the second derivative for the reflectance per wavelength raised to *n*. The right side of all tested models numbers 1-35 are listed in Table 5. The calculated coefficients a_i are omitted for clarity. Equation (1) below show an example of regression model No. 16 in Table 5, including left side and coefficients. The least-squares method is used to find the coefficients $a_0 \ldots a_m$ that minimizes the difference between R and R' [4]. This is repeated for each wavelength, λ, between 410nm and 690nm. The wavelengths 400nm and 700nm are given the same correction as 410nm and 690nm respective, to keep the original spectral curves continuity.

$$R'_\lambda = a_0 + a_1 R_\lambda + a_2 R_\lambda^2 + a_3 R_\lambda^3 + a_4 dR_\lambda + a_5 d^2 R_\lambda \tag{1}$$

Deterning of the optimal training set

In the following experiments, a small subset of the spectra were chosen as the training set, with testing of the corrections being done on all 711 original samples. The subset was chosen so as to optimize the figure of merit.

Different figures of merit can be selected. The most obvious one is to minimize the average ΔE between the reference and test instrument for all samples. ΔE_{00} (CIEDE2000) is the primary figures of merit in this investigation. Different ΔE formulas or sums of absolute reflectance differences may be used as figures of merit and give different results. Test was performed with ΔE_{ab} and $\sum_{\lambda,n}|R - R'|\,\bar{y}$. The $\bar{y}$ is the CIE 1931 standard colorimetric observer, used as a weighting function to reflect the sensitivity of the eye. Both these figures of merit performed worse than ΔE_{00}.

Given the astronomically large number of possible subsets of 711 spectra, two algorithms were chosen to find the optimal subsets. In the culling method, we started with all the spectra and gradually pruned them back. In the inverse culling method, we started with a small set and gradually added to the set.

Calculations – "culling"

To select a subset of all the measured samples we define a figure of merit and then use a method called "culling" [3]. This method uses a figure of merit that is always calculated on the complete set of N number of samples. The culling starts by creating N subsets by removing the N:th colour sample, S_N, from the complete set. Then the figure of merit is calculated for all subsets and the subset with the best result is selected. This subset with S_N removed is then used to repeat the process. When the subset is smaller than a decided number of samples, here 50, and the removal of more samples do not improve the merit function, the goal has been met. The smallest number of samples was decided to be 20 but are in any case limited by the model chosen.

"Inverse culling"

A related method is to start the process with a small subset and then use the figure of merit to decide which sample is to be added or subtracted from the subset in each process step. The natural subset to start with is the grey scale. Another starting point is to select the spectral curves having maximum positive or negative derivate for each wavelength.

RESULT AND DISCUSSION

Selection of regression model

Table 5 show all tested regression models and the best result for all the 710 samples using ΔE_{00} as merit function. The di:8° and the 45°:0° instruments must be compared separately. The maximum number of samples after culling was 50. The result is for two instruments with di:8° geometry (1 and 2) and two width 45°:0° geometry (4 and 6). Instruments from different brands were chosen to capture most differences due to construction details.

This result clearly indicates that the model must include both the first and the second derivate. This suggests that the selected instruments differed somewhat both in wavelength alignment and in bandpass. The model also needs to capture the nonlinearity with a third degree or higher polynomial function. This may be due to nonlinearity in the electronics. In the case of the spherical instruments this may be due to re-illumination, where the light reflected from the sample illuminates the inside of the sphere, which in turn re-illuminates the sample.

Based on this result, two regression models were selected for in depth analysis. This also reduces the calculation time that is a large obstacle in testing the different models.

Table 5: tested regression models with average ΔE_{00} result for instrument combinations 1 and 4, two di:8° and two 45°:0° instruments from different manufacturers.

No	Model	di:8	45:0
1	R_λ	0.207	0.259
2	$R_\lambda + R_\lambda^2$	0.220	0.188
3	$R_\lambda + dR_\lambda$	0.152	0.180
4	$R_\lambda + R_\lambda^2 + R_\lambda^3$	0.213	0.183
5	$R_\lambda + R_\lambda^2 + dR_\lambda$	0.151	0.096
6	$R_\lambda + dR_\lambda + dR_\lambda^2$	0.161	0.166
7	$R_\lambda + dR_\lambda + d^2R_\lambda$	0.070	0.154
8	$R_\lambda + R_\lambda^2 + R_\lambda^3 + R_\lambda^4$	0.221	0.182
9	$R_\lambda + R_\lambda^2 + R_\lambda^3 + dR_\lambda$	0.153	0.079
10	$R_\lambda + R_\lambda^2 + dR_\lambda + dR_\lambda^2$	0.150	0.093
11	$R_\lambda + R_\lambda^2 + dR_\lambda + d^2R_\lambda$	0.069	0.089
12	$R_\lambda + dR_\lambda + dR_\lambda^2 + d^2R_\lambda$	0.070	0.145
13	$R_\lambda + R_\lambda^2 + R_\lambda^3 + R_\lambda^4 + R_\lambda^5$	0.215	0.182
14	$R_\lambda + R_\lambda^2 + R_\lambda^3 + R_\lambda^4 + dR_\lambda$	0.376	0.074
15	$R_\lambda + R_\lambda^2 + R_\lambda^3 + dR_\lambda + dR_\lambda^2$	0.155	0.080
16	$R_\lambda + R_\lambda^2 + R_\lambda^3 + dR_\lambda + d^2R_\lambda$	0.069	0.070
17	$R_\lambda + R_\lambda^2 + dR_\lambda + dR_\lambda^2 + d^2R_\lambda$	0.071	0.087
18	$R_\lambda + dR_\lambda + dR_\lambda^2 + d^2R_\lambda + d^2R_\lambda^2$	0.072	0.144
19	$R_\lambda + R_\lambda^2 + R_\lambda^3 + R_\lambda^4 + R_\lambda^5 + dR_\lambda$	0.157	0.076
20	$R_\lambda + R_\lambda^2 + R_\lambda^3 + R_\lambda^4 + dR_\lambda + dR_\lambda^2$	0.156	0.077
21	$R_\lambda + R_\lambda^2 + R_\lambda^3 + R_\lambda^4 + dR_\lambda + d^2R_\lambda$	0.069	0.067
22	$R_\lambda + R_\lambda^2 + R_\lambda^3 + dR_\lambda + dR_\lambda^2 + d^2R_\lambda$	0.070	0.068
23	$R_\lambda + R_\lambda^2 + dR_\lambda + dR_\lambda^2 + d^2R_\lambda + d^2R_\lambda^2$	0.072	0.086
24	$R_\lambda + R_\lambda^2 + R_\lambda^3 + +R_\lambda^4 + R_\lambda^5 + dR_\lambda + dR_\lambda^2$	0.156	0.078
25	$R_\lambda + R_\lambda^2 + R_\lambda^3 + R_\lambda^4 + R_\lambda^5 + dR_\lambda + d^2R_\lambda$	0.069	0.068
26	$R_\lambda + R_\lambda^2 + R_\lambda^3 + R_\lambda^4 + dR_\lambda + dR_\lambda^2 + d^2R_\lambda$	0.069	0.065
27	$R_\lambda + R_\lambda^2 + R_\lambda^3 + dR_\lambda + dR_\lambda^2 + d^2R_\lambda + d^2R_\lambda^2$	0.069	0.066
28	$R_\lambda + R_\lambda^2 + R_\lambda^3 + R_\lambda^4 + R_\lambda^5 + dR_\lambda + dR_\lambda^2 + d^2R_\lambda$	0.070	0.063
29	$R_\lambda + R_\lambda^2 + R_\lambda^3 + R_\lambda^4 + dR_\lambda + dR_\lambda^2 + d^2R_\lambda + d^2R_\lambda^2$	0.070	0.066
30	$R_\lambda + R_\lambda^2 + R_\lambda^3 + R_\lambda^4 + R_\lambda^5 + dR_\lambda + dR_\lambda^2 + d^2R_\lambda + d^2R_\lambda^2$	0.070	0.063
31	$R_\lambda + R_\lambda^2 + R_\lambda^3 + dR_\lambda + dR_\lambda^2 + dR_\lambda^3 + d^2R_\lambda + d^2R_\lambda^2 + d^2R_\lambda^3$	0.069	0.067
32	$R_\lambda + R_\lambda^2 + R_\lambda^3 + R_\lambda^4 + R_\lambda^5 + dR_\lambda + dR_\lambda^2 + dR_\lambda^3 + d^2R_\lambda + d^2R_\lambda^2$	0.072	0.062
33	$R_\lambda + R_\lambda^2 + R_\lambda^3 + R_\lambda^4 + R_\lambda^5 + dR_\lambda + dR_\lambda^2 + d^2R_\lambda + d^2R_\lambda^2 + d^2R_\lambda^3$	0.069	0.063
34	$R_\lambda + R_\lambda^2 + R_\lambda^3 + R_\lambda^4 + dR_\lambda + dR_\lambda^2 + dR_\lambda^3 + d^2R_\lambda + d^2R_\lambda^2 + d^2R_\lambda^3$	0.069	0.063
35	$R_\lambda + R_\lambda^2 + R_\lambda^3 + R_\lambda^4 + R_\lambda^5 + dR_\lambda + dR_\lambda^2 + dR_\lambda^3 + d^2R_\lambda + d^2R_\lambda^2 + d^2R_\lambda^3$	0.069	0.063

Selected regression models

From Table 5, model numbers 21 and 26 was selected, see equation (2) and (3). These are the simplest models giving results close to the more complicated models. Model 21 uses a 4th degree polynomial and linear first and second derivate. Model 26 adds a non-linear component for the first derivate, the physical interpretation for this component is hard to see. Maybe the interaction between wavelength shift and nonlinearity to some extent can be modeled by this parameter. Alternately, this could be due to imprecise bandpass correction on one or both of the instruments. (Ideally, spectra from all instruments should be bandpass corrected to best emulate a 1 nm instrument, but this is an imprecise operation.)

Model 21 $$R'_\lambda = a_0 + a_1R_\lambda + a_2R_\lambda^2 + a_3R_\lambda^3 + a_4R_\lambda^4 + a_5dR_\lambda + a_6d^2R_\lambda \quad (2)$$

Model 26 $$R'_\lambda = a_0 + a_1R_\lambda + a_2R_\lambda^2 + a_3R_\lambda^3 + a_4R_\lambda^4 + a_5dR_\lambda + a_6dR_\lambda^2 + a_7 \quad (3)$$

"culling" results

Table 6 and Table 7 show the "culling" result for model 21, equation (2) and model 26, equation (3) respectively. The **Ref** and **Test** columns lists the two instruments compared before and after correction. The **Raw** column is the average ΔE_{00} between the uncorrected (or raw) measurements from the two instruments. The columns **Prof.** and **Sdev** is the average and standard deviation for the ΔE_{00} between the measurements form the Ref instrument and the corrected measurements

from the Test instrument. The column **Samp.** Is the number of samples in the subset result from the “culling” calculations, followed by an illustration of the colours of these samples.
Model 26 gives marginally better result than 21. To note is also that the result for the instruments with 45°:0° geometry gives similar results as di:8° instruments even though the reproducibility for the 45°:0° instruments often is in the same order as the result. This may indicate that the reproducibility is a random component, that evens out in the correction. Combination No. 2 gives the best correction, here we have two di:8° instrument from the same manufacturer that probably were designed to have similar measurement properties. But surprisingly in this case, the average raw difference was large. Combination No. 5 shows smaller raw difference, this is also expected since the reference instruments is the successor of the test instrument from this manufacturer.

Table 6: culling result for model 21.

No	Ref	Test	Raw	Prof.	Sdev.	Samp.
1	CM-3700A	Color i7	0.282	0.068	0.045	43
2	CM-3700A	CM-700d	0.369	0.040	0.027	44
3	Color i7	CM-700d	0.376	0.076	0.058	39
4	CM-25cG	DC45G	0.305	0.067	0.041	43
5	CM-25cG	CM-2500	0.125	0.058	0.043	42
6	CM-2500	DC45G	0.313	0.075	0.052	37
		Average:	0.295	0.064	0.044	

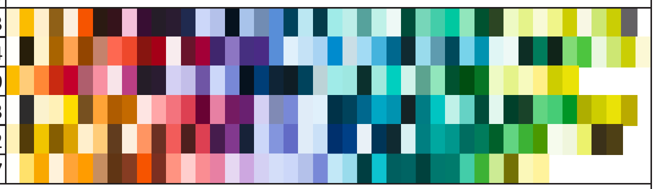

Table 7: culling result for model 26.

No	Ref	Test	Raw	Prof.	Sdev.	Samp.
1	CM-3700A	Color i7	0.282	0.071	0.048	46
2	CM-3700A	CM-700d	0.369	0.039	0.026	41
3	Color i7	CM-700d	0.376	0.072	0.049	41
4	CM-25cG	DC45G	0.305	0.067	0.041	33
5	CM-25cG	CM-2500	0.125	0.058	0.043	45
6	CM-2500	DC45G	0.313	0.071	0.050	42
		Average:	0.295	0.063	0.043	

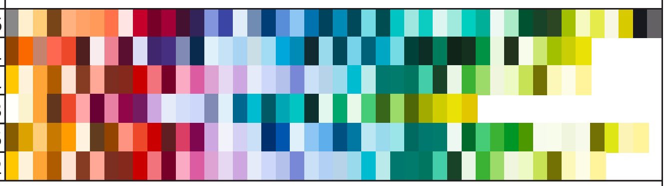

“Inverse-culling” result

Table 8 and

Table 9 show the “Inverse-culling” result for model 21and model 26 using the grey-scale as the starting point to find a subset.

Table 10 show the “inverse-culling” result for model 21 when a subset of spectral curves having maximal negative or positive derivate was selected as the starting point. All these calculations shows similar good correction result, but the selected subset of samples is very different.

Table 8: inverse culling for model 21, using grey scale as start selection.

No	Ref	Test	Raw	Prof.	Sdev.	Samp.
1	CM-3700A	Color i7	0.282	0.071	0.046	36
2	CM-3700A	CM-700d	0.369	0.040	0.027	27
3	Color i7	CM-700d	0.376	0.077	0.058	37
4	CM-25cG	DC45G	0.305	0.069	0.041	39
5	CM-25cG	CM-2500	0.125	0.059	0.050	35
6	CM-2500	DC45G	0.313	0.072	0.056	50
		Average:	0.295	0.065	0.046	

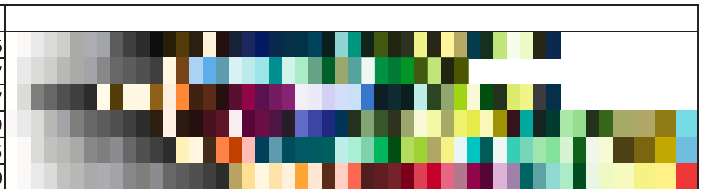

Table 9: inverse culling for model 26, using grey scale as start selection.

No	Ref	Test	Raw	Prof.	Sdev.	Samp.	
1	CM-3700A	Color i7	0.282	0.072	0.049	42	
2	CM-3700A	CM-700d	0.369	0.043	0.028	35	
3	Color i7	CM-700d	0.376	0.076	0.06	42	
4	CM-25cG	DC45G	0.305	0.069	0.042	50	
5	CM-25cG	CM-2500	0.125	0.059	0.048	50	
6	CM-2500	DC45G	0.313	0.071	0.055	50	
		Average:	0.295	0.065	0.047		

Table 10: Inverse culling for model 21, using max derivate as start selection.

No	Ref	Test	Raw	Prof.	Sdev.	Samp.	
1	CM-3700A	Color i7	0.282	0.077	0.047	43	
2	CM-3700A	CM-700d	0.369	0.044	0.027	50	
3	Color i7	CM-700d	0.376	0.080	0.060	50	
4	CM-25cG	DC45G	0.305	0.069	0.041	50	
5	CM-25cG	CM-2500	0.125	0.059	0.046	50	
6	CM-2500	DC45G	0.313	0.072	0.055	50	
		Average:	0.295	0.067	0.046		

Nonlinearity

The result shows that a higher order polynomial is needed to correct the spectral curves between the tested instruments. To investigate this further, Table 11 show plots of the grey-scale differences between all six instrument combinations. For each combination the wavelengths 410nm, 460nm, 510nm, 560nm, 610nm and 660nm was plotted. A 4th order polynomial trendline with the R^2 value (coefficient of determination) is inserted in each plot. As expected, combination 2 and 5 show more linearity as these instruments are from the same manufacturer. When mixing instruments from different manufacturers, a clear u-shape curve is visible showing the nonlinearity. The u-shape is sometimes turned upside down depending on the selected order of the reference and test instrument.

Table 11: reflectance difference between instruments at selected wavelengths shows nonlinearities.

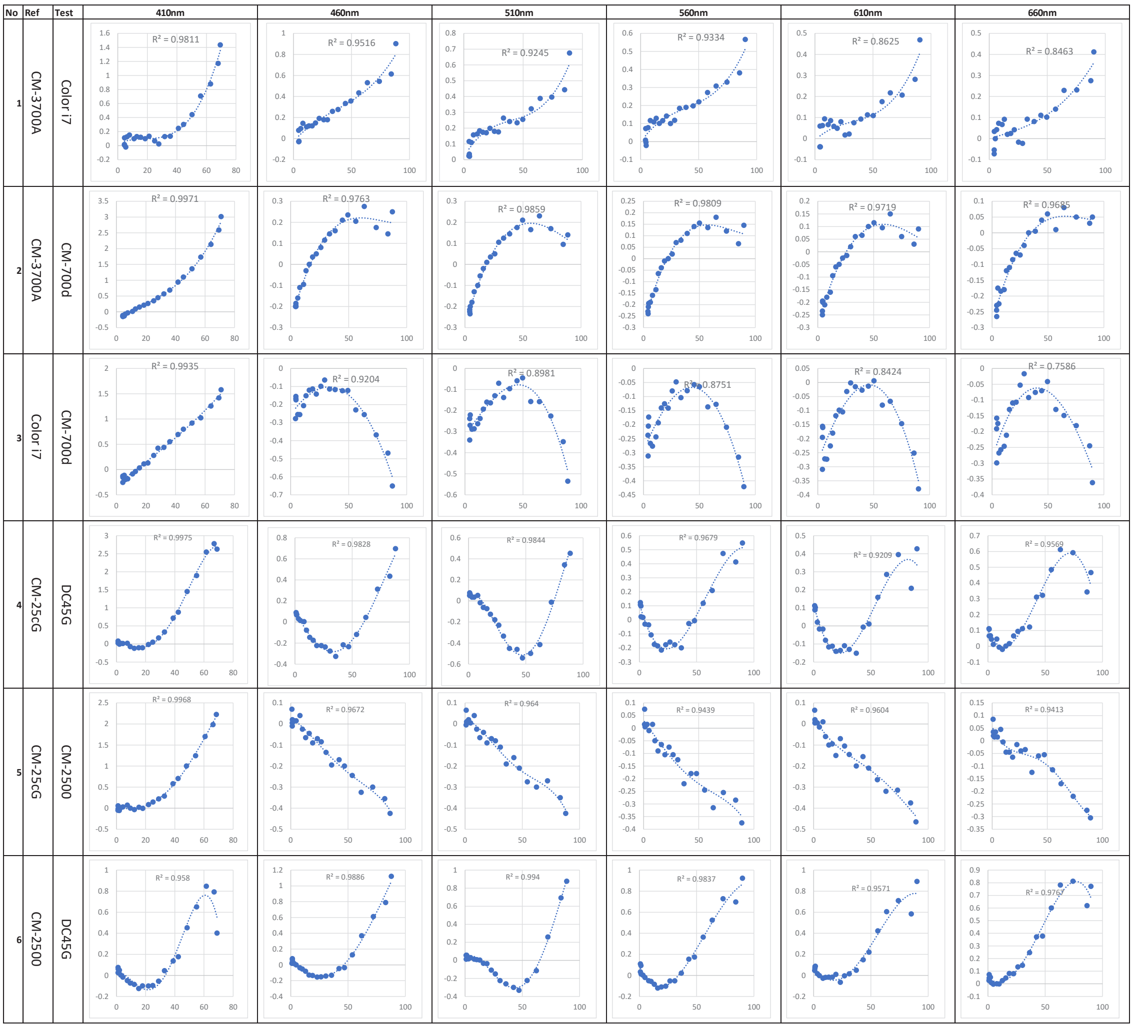

Conclusions

Using the investigated methods, the IMA of all tested instruments can be improved significantly. Before correction most instruments had an average difference around 0.3 ΔE_{00}, this is two times the limit set out for effective digital colour communication. After correction, the average difference is around 0.07 ΔE_{00}, this is two times better than the needed accuracy.

Optimal set of reflectance curves

One goal for this investigation is to find an optimal set of samples (spectral curves) to compare two instruments to each other then correct one instrument to the other. The mix of colour samples that the different calculation methods give for each instrument combination as shown in Table 6 to Table 10 make this hard, since one clear optimal was not found. No conclusion could yet be reach on this point in this investigation.

On the other hand, this paper does provide a useful extension of previous work[4], which found that the BCRA II set of tiles does not provide a rich enough set of spectral transitions, but suggested other small sets of paints samples that would perform better for correcting one instrument to another. This paper provided a systematic way to select optimum sets of samples, and demonstrated that many sets have near optimum performance.

REFERENCES

1. ASTM D5531. (2023). *Standard Guide for Preparation, Maintenance, and Distribution of Physical Product Standards for Color and Geometric Appearance of Coatings.* ASTM International.
2. ASTM E2214. (2020). *Standard Practice for Specifying and Verifying the Performance of Color Measuring Instruments*. ASTM International.
3. Ingleson, & Brill. (2005). Methods of Selecting a Small Reflectance Set as a Transfer Standard for Correcting Spectrophotometers. *Color Research & Application*, 13-17.
4. Seymour, J. (2019). Technical Arts Graphics Association Conference. *Update to Evaluation of Reference Materials for Standardization of.*
5. SS 19102. (2022). *NCS Colour Atlas*. SiS, Swedish Institute for Standards.

SPECTRAL REFLECTANCE AND DETERIORATION SIMULATION OF TOYOHARA KUNICHIKA'S JAPANESE WOODBLOCK PRINT

Satoko Taguchi[1]*, Shino Okuda[2], and Katsunori Okajima[3]

[1]*Tokyo University of the Arts, Japan.*
[2]*Doshisha Women's College of Liberal Arts, Japan.*
[3]*Yokohama National University, Japan.*

*Corresponding author: Satoko Taguchi, taguchi.satoko@fa.geidai.ac.jp

ABSTRACT

Deterioration simulation models of cultural properties are useful for predicting their deteriorated appearance and for planning conservation and restoration for cultural properties. To elaborate deterioration simulation models, data obtained from material analysis and deterioration tests are important as well. In the previous study, we analyzed colour materials using an X-ray fluorescence spectrometry and a 2D spectroradiometer for the Japanese woodblock print (Ukiyo-e) "Mitate hashi zukushi Nihonbashi," Parody of Collection of Bridges / Nihon-bashi Bridge (private collection) produced by Toyohara Kunichika (1835-1900) who was a Japanese artist active from the late Edo period to the Meiji period. Based on the analysis results, we made colour patches for the colour materials used in the Ukiyo-e. The deterioration test of the Ukiyo-e and colour patches were conducted for 168 hours using a sunlight irradiation device, and the spectral reflectance properties of them were acquired after 0, 8, 16, 24, 48, 72, 96, 120, 144, and 168 hours by 2D spectroradiometer. Using the measurement values of a representative point in the colour patch, we produced the deterioration simulation images. The simulated images showed a fading tendency similar to that of the Ukiyo-e, but the simulated image did not reproduce non-uniformity of the colour in the Ukiyo-e. In this study, we investigated the change of spectral reflectance of Ukiyo-e and colour patches as a function of the degradation time. Spectral reflectance measurements of the red, purple, and black colours of the Ukiyo-e and the colour patches before degradation showed similar spectral shapes in the dark and light areas of each colour. Areas with lighter blue colour material have a different spectral function from areas with darker colour material. This may be due to the effect of the colour of the paper used as the base material for the ukiyo-e. The spectral reflectance of Ukiyo-e after degradation testing showed a tendency of increasing or decreasing values over time with almost no change in spectral shape, but different changes were observed for the purple colour material. From these spectral reflectance measurements, we proposed a new degradation simulation program considering the non-uniformity of colour materials of the Ukiyo-e, suggesting that the new simulation can reproduce the colour of the Ukiyo-e more realistic.

Keywords: Ukiyo-e, deterioration, X-ray fluorescence analysis, 2D spectroradiometer, simulation.

INTRODUCTION

To inherit valuable cultural properties to the future, it is essential to control deterioration by maintaining the preservation environment, and to use various techniques for conservation and restoration. In particular, simulation technology for cultural properties is useful when considering conservation and restoration plans for cultural properties because it can restore the original appearance of the objects and predict their future deterioration. However, some cultural properties restored by simulation do not accurately reflect the tendency of deterioration of the colour materials used in the paintings. Therefore, we created colour patches of each colour material used in them, and obtained data from degradation tests using the colour patches.

In previous studies, we have conducted colour material analysis using X-ray fluorescence analysis and 2D spectral measurement on Toyohara Kunichika's Ukiyo-e painting "Mitate hashi zukushi Nihonbashi," Parody of Collection of Bridges / Nihon-bashi Bridge (private collection). In addition, we have prepared colour patches of each colour material and conducted degradation tests using a sunlight irradiation system to construct a simple degradation simulation [1]. As a result, both of Ukiyo-e and simulated images as to change over time showed almost similar fading tendencies. However, those simulated images were generated using the data of a single representative point in the colour patch, so we could not reproduce the colour non-uniformity observed in actual Ukiyo-e.

In this study, we measured the spectral reflectance values of an Ukiyo-e and colour patches, then analyzed the colour non-uniformity. Based on the results, we proposed a new deterioration simulation method which consider the non-uniformity of colour materials used in Ukiyo-e.

METHODOLOGY

We selected an Ukiyo-e as a cultural property material. The Ukiyo-e "Mitate hashi zukushi Nihonbashi," Parody of Collection of Bridges / Nihon-bashi Bridge (private collection, 335mm×235mm) by Toyohara Kunichika (1835-1900) is a famous Ukiyo-e woodblock print artist active from the late Edo period to the Meiji period. Colour patches we measured were made by applying vermillion, cochineal, methyl violet, prussian blue, and carbon black colour materials to Japanese paper. Colour patches were prepared based on information from analysis of Ukiyo-e colour materials by an X-ray fluorescence analyzer (XRF, XL3t-900S-M, Thermo-Niton) and a 2D spectroradiometer (SR-5000, TOPCON). In ukiyo-e produced from the Edo to Meiji periods, the main colour materials used were safflower, madder, vermillion, and cochineal for red, indigo, dayflower and Prussian blue for blue, a mixture of safflower and dayflower or methyl violet for purple, and carbon black for black. From the end of the Edo period, colourful synthetic dyes and pigments were used for it as colour materials [2]. For the base material, Japanese paper, mainly made from *kozo*, was used. The Ukiyo-e and colour patches were tested for degradation for 168 hours using a sunlight irradiation system (SXL-500V2, SERIC). The vertical irradiance of the sunlight irradiation system is approximately 1kW/m^2. In CIE 157:2014 [3], materials used for Ukiyo-e are classified as medium responsivity in the classification of the response of materials to visible light, the exposure time was set based on its annual exposure limit of 150,000 lx h/y. The spectral data of the colour patches after 0, 8, 16, 24, 48, 72, 96, 120, 144, and 168 hours were obtained by a 2D spectroradiometer. Degradation simulation images were created based on the colour information of the colour patches obtained in the degradation test.

RESULTS AND DISCUSSION

Figure 1 shows the Ukiyo-e and an image of a simulation generated based on the colour patch before the degradation test (after 0 hours).

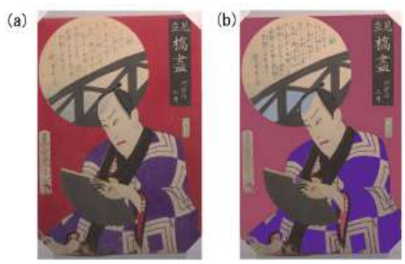

Figure 1. (a) Ukiyo-e and (b) simulated image based on colour patch data before degradation

Our previous degradation simulations showed a fading which was similar to that of Ukiyo-e [1]. However, the simulated images appeared monotonous because the images were created using information from a single representative point in the colour patches. The red, blue, purple, and black areas in the Ukiyo-e appeared to be covered with a single colour material, while close observation revealed unevenness of coloring in each area. In general, Ukiyo-e was produced using the woodblock print technique, and these uniformities were thought to have been caused by the printing process. For each colour used in the Ukiyo-e, the spectral reflectance was measured at selected points of different shades. Figures 2 and 3 show the spectral reflectance data of the red and blue areas of the Ukiyo-e, respectively.

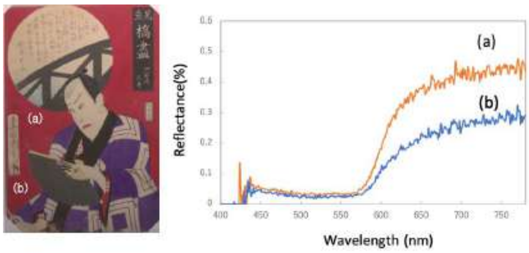

Figure 2. Spectral reflectance of Ukiyo-e. (a) bright red, (b) dark red.

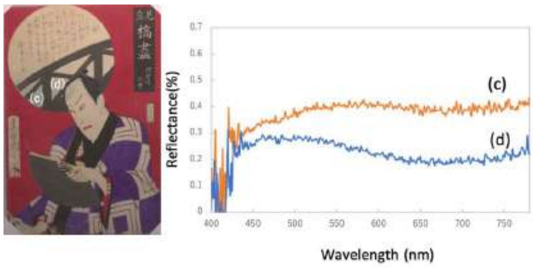

Figure 3. Spectral reflectance of Ukiyo-e. (a) bright blue, (b) dark blue.

While the spectral reflectance shapes of Figure 2 (a) light red and (b) dark red look similar, the value of the reflectance of (b) was lower than that of (a). On the other hand, in the areas where blue colour material was used, different spectral shapes were observed for Figure 3 (a) dark blue and (b) light blue. The colour material was thinly applied in the area (b), which was affected by the colour of the Japanese paper. The colour patches used in this study were prepared based on the traditional Ukiyo-e print technique [2], but it was difficult to apply the colour material evenly, and unevenness of colour was observed. The measured spectral reflectance values of the light and dark areas of each colour patch showed a similar tendency to that of the Ukiyo-e.

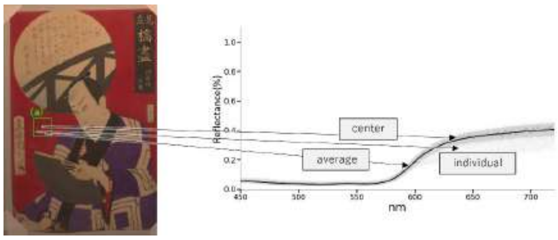

Figure 4. Spectral reflectance distribution of the red area in Ukiyo-e. (before degradation.)

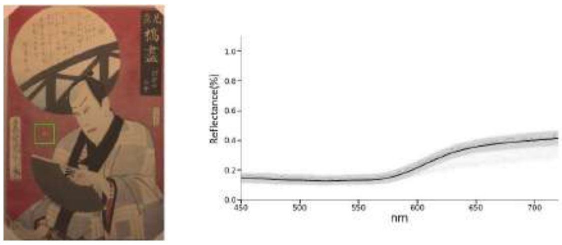

Figure 5. Spectral reflectance distribution of the red area in Ukiyo-e. (after 168 hours.)

To produce accurate simulated images, we conducted a detailed analysis of the spectral reflectance distribution. The spectral reflectance of the red area (a) in the Ukiyo-e is shown in

Fig. 4; the black line shows the average value within the area, the dark gray line shows a single point in the center, and the light gray line shows the individual spectral reflectance. Figure 5 shows the distribution of spectral reflectance of the Ukiyo-e after 168 hours in deterioration test. The measurement results showed that spectral reflectance values after 168 hours of deterioration test increased around 450~600 nm compared to that of the Ukiyo-e before degradation while no significant change in spectral shape was observed.

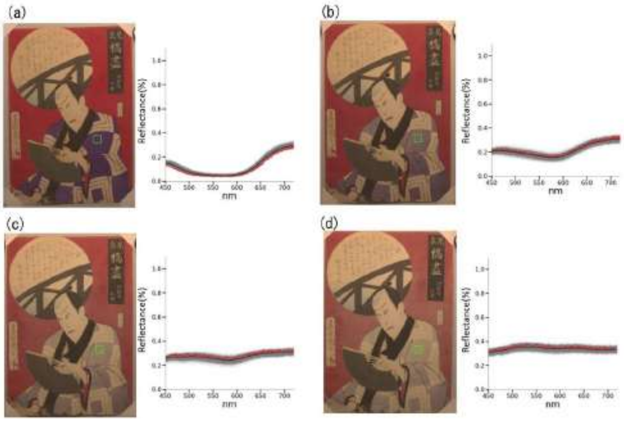

Figure 6. Spectral reflectance distributions of the purple area in Ukiyo-e. (a) before degradation, (b) after 24 hours, (c) after 96 hours, and (d) after 168 hours.

On the other hand, the change of the spectral reflectance of the purple areas of the Ukiyo-e was different from that of the red areas. Figure 6 shows the changes over time of the spectral reflectance distribution of the purple areas; the reflectance around 500-650 nm increased with time and became flat after 168 hours. It was thought that the purple colour faded due to the degradation test, which was caused by the effect of the colour of the paper over time. By considering the distribution of spectral reflections due to these colour materials, we can create a degradation simulation that more accurately reproduces the colours of Ukiyo-e.

CONCLUSIONS

In this study, we measured the spectral reflectance values of Ukiyo-e materials and colour patches and analyzed the non-uniformity of colours for more accurate deterioration simulation of cultural properties. We confirmed the differences in the distribution of spectral reflectance before and after the degradation test of Ukiyo-e and determined the characteristics of each colour material. Spectral reflectance measurements after degradation tests revealed that the differences were not uniform for each colour material. In the future, we will conduct a deterioration simulation by examining not only the spectral reflectance data as revealed in this study but also the change in luminance over time for each colour material and the effect of the base material, Japanese paper.

ACKNOWLEDGEMENTS

This study was supported by JSPS KAKENHI (Grant Number: 18KK0282). We would like to thank Masato Nagata for generating the digital images of the Ukiyo-e.

REFERENCES

1. Taguchi, S., Okuda, S., Okajima, K. (2022). Colour Materials Used in Toyohara Kunichika's Japanese Woodblock Print Painting (Ukiyo-e) and its Deterioration. *Proceedings of the Asia Colour Association (ACA)2022*, 314-317.
2. Cesaratto, A. et al. (2018). A timeline for the introduction of synthetic dyestuffs in Japan during the late Edo and Meiji periods. *Heritage Science. 6(22)*, 1-12.
3. CIE. (2004). Control of damage to museum objects by optical radiation, CIE 157: 2004.

Session 8

Doi Tong
1 December 2023

GAUDI'S CHROMATOLOGY IN PARK GÜELL AS CASE STUDY

Maria João Durão*

CIAUD, Lisbon School of Architecture, Universidade de Lisboa, Portugal.

*Corresponding author: Maria João Durão, mariajoaodurao@gmail.com

ABSTRACT

This paper describes the results of an on-going research project concerning colour materials used in one of Antoni Gaudí's major works, the Park Güell. The full body of research on 'Gaudi's Chromatology' includes other UNESCO's declared World Heritage Sites, namely Casa Milá, Casa Battló, Sagrada Familia, all built in Barcelona by Gaudí. Gaudí was born in 1852 in Reus, Tarragona having moved to Barcelona in order to study architecture, where he became the chief architect of major works in the city. Eusebi Güell acquired an estate situated on the southern face of Monte Carmelo, 17-hectares overlooking Barcelona and the sea. Güell intended to build a housing development in the style of the British garden city, and entrusted Gaudi with such an ambitious project. The work began in 1900 and with the death of Güell, the City Council made this site a public park in 1926. Across the turn of the century, new ideas pushed science and technology further, aligning with Gaudí's constant need to experiment and innovate in all architectural and design realms where colour materials are a fundamental factor. Catalan Modernism was the expression of aesthetic renewal allied to the idea of expansion of Catalonia to the future where tradition and modernity were intertwined. Barcelona was the maximum expression of such a desire, Gaudí was its top architect and Park Güell, an exemplar of Catalan Modernism. The methodology adopted explored the many colour materialities and functions used in Park Güell, resulting in 5 clusters: 1) Main entrance to the Park, the caretaker's lodge and the administrative lodge; 2) Dragon Staircase; 3) Hypostyle Room or covered Marketplace; 4) Nature Square and undulating bench; 5) communication networks made of routes and viaducts. The cluster organization of colour themes made it possible to identify typologies of materials used in each cluster and also to add a layer of significance drawn from references to Gaudí's Christian religious beliefs, his convictions in the rebirth of the Catalan nation, i.e. the Renaixença, and his cultural influences of Greece and Rome. The conclusion of the study contributes to a better understanding of the complexity of colour materialities and processes used by Gaudí that make up his chromatology.

Keywords: colour, materialities, Design, Gaudi, Park Güell

A COLOUR STORY: HOW DESIGNERS USE COLOUR AS A VISUAL STORYTELLING TOOL IN SNEAKER DESIGN

Kel Jackson[1]* and Youngmi Christina Choi[2]

[1]*Student, School of Design Research, PGR, Royal College of Art, United Kingdom.*
[2]*Faculty, School of Design, Design Products, Royal College of Art, United Kingdom.*

*Corresponding author: Kel Jackson kelsey.jackson@network.rca.ac.uk

ABSTRACT

This study aims to unpack foundational colour design practices to discuss how colour designers leverage colour as a visual storytelling device. Analysing how colour designers use colour might open up more significant opportunities for cross-disciplinary research between designers and the disciplines of colour psychology, chemistry, and art while enabling more experimentation surrounding studying colour preference in context. This study focuses on the practices of Colour Designers in the athletic footwear industry, specifically the processes of visual storytelling on sneakers using colour. Knowledge of what a colour designer in the athletic footwear industry does and how designers use colour as a visual storytelling device is primarily learned and held by those practising colour design, creating a gap in aspects of the design process in academia. While there is a lack of academic research, there is a wealth of qualitative data shared within the sneaker culture surrounding the significance of colour in sneaker design and the impact of colour on sneaker culture, potentially making sneakers a fitting artefact to discuss how colour designers leverage colour in visual storytelling. This study aims to conduct a material culture study and narrative inquiry to create a "history of things" examination of the Air Jordan 1 High Top (AJ1) launch colourways released in 1985. This study utilises the lead author's ten years of experience as a practising colour designer working with brands such as Nike to expose the potential colour design practices used in creating the AJ1 through autoethnographic writing and design artefact creation. These writings and design artefacts aim to shine a light on foundational colour design practices to inspire more research into the field of colour design. The results of this study suggest an intentional relationship between the design stakeholders of the Air Jordan 1, and colour leveraging colour as a visual communication tool. Through creating design artefacts inspired by the Air Jordan 1 1985 colourways, including blocking exercises and an extracted colour palette, the lead author illustrates the influences on the colour design process that help define aesthetically pleasing blocks and how designers use blocking and colour to create cohesive visual storytelling.

Keywords: Colour Design, Sneaker Design, Colour Storytelling, Colour Design Process, Applied Colour Science

INTRODUCTION

This study seeks to unpack the significance of visual storytelling in colour design for sneakers and how a material culture study, autoethnographic writing and design artefact creation might contribute to educating colour researchers outside of design on how colour designers (CD) utilise colour. While there is a lack of academic research on CD in sneaker culture (SC), there is a wealth of documentation by the members of the culture, most notably the history of colour used on sneakers [1,2]. The wealth of qualitative data through storytelling might make sneakers a fitting artefact to examine how colour designers in the athletic footwear industry (AFI) might use colour to create visual storytelling. This study analyses the Air Jordan 1 (AJ1) because of its impact on the industry through colour. Through this study, the authors aim to shed light on AJ1's significance in sneaker colour design and culture and educate on foundational colour design practices like colour blocking and applying colour combinations.

The lead author of this study brings over ten years of experience as a colour designer in the AFI. This study selected a Nike sneaker because of the lead author's familiarity with the Nike design process and product as the lead author gained the majority of their knowledge and experience of colour design and design storytelling through working at Nike as CD starting in 2012 as a freelancer or an independently contracted designer and then as a salaried designer from 2013 to 2019. During this time, the lead author worked on a wide range of projects, including applying colour and creating visual storytelling for footwear and apparel. The strategies or approach to colour palette creation or application, colour trends, material applications, or colour preferences are subject to the lead author's experience with Nike. However, sharing this experience might help raise relevant questions surrounding studying colour preferences in context by engaging designers who leverage and manipulate colour meanings and preferences.

Colour is an influential tool designers use to create carefully crafted visual messages involving the principles of aesthetics (balance, colour, movement, pattern, scale, shape and visual weight) [3]. Aesthetic principles combined with colour theory and meanings create a product personality[4,5], known colloquially in the AFI as visual storytelling. In the sneaker industry and culture, colour is synonymous with the sneaker models, creating buzz and driving revenue [6]. Sneakerheads, a moniker used inside sneaker culture for sneaker enthusiasts [7], engage with colour visual storytelling by memorising colourways or different colour combinations or placements on footwear models and release dates [6]. You can find the sneakerhead fandom debating the accuracy of re-releases through colour matching and placement and lining up for small releases of colour, materials, and graphic stories to wear, resell or collect [7].

While for many design teams inside and outside the AFI, colour is just an aspect of a designer's work. However, sneaker companies like Nike, Adidas and New Balance leverage colour's storytelling power to drive user interest and demand by employing designers who specialise in colour for product design, which includes apparel, sneakers and accessories [8]. The colour designer collaborates with other design stakeholders like footwear designers, graphic designers, textile designers, developers, marketers, product line managers and merchandisers to create visual storytelling intended to utilise colour to evoke a feeling from the user [8]. Users engage in colour preference with products based on colour meanings [9] defined through historical and cultural references, including meanings crafted by SC and influenced by the user's personal experiences at times defined through the user's engagement in SC [7,10].

METHODOLOGY

This study was conducted through a material culture study with narrative inquiry surrounding the artefact (AJ1) and its cultural relevance supported by autoethnographic writings and design artefact creation based on the lead author's personal experiences as a colour designer. Building from a long tradition of material culture study, author Giorgio Riello introduced a method that weaves in narrative to create deeper personal understandings of artefacts, which Riello calls "history of things" [11]. While an artefact analysis or material culture study without narratives or ethnography may interest those studying the manufacturer of sneakers or sneaker dyes and pigments, this article aims to add research on the cultural impact of colour in both sneaker design and SC.

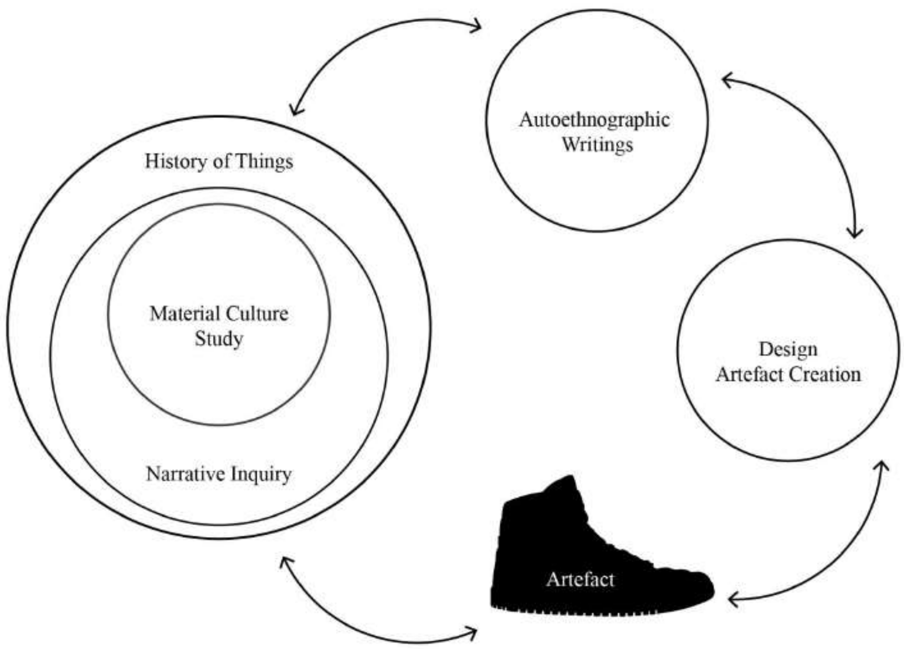

Figure 1. Outline of Methods History of things supported by material culture study and narrative inquiry to analyse the artefact [11,12], which inspired autoethnographic writings [13] and design artefact creation [14].

This study builds its inquiry from Charles F. Montgomery's "steps or exercises" for a material culture study as outlined by authors Blandy and Bolin, which examines overall appearance, form, ornament, colour, analysis of materials, techniques employed by craftspeople, trade practices, function, style, date, attribution, history of an object, the artefact's history of ownership, condition and appraisal [12]. Montgomery's fourteen "steps or exercises" were employed as they may enable the extraction of data to support this study's approach to the "history of things" by investigating both the aesthetic qualities of the artefact (colour, material, make, and alterations) along with seeking to examine the motivations of the craftsperson/designer and significance of the artefact within the design culture and the consumer culture. Unpacking the physical information paired with the historical and cultural background may have enabled the lead author to unpack their practical experience as a CD. To uncover CD practices utilised in the artefact studied, the lead author created design artefacts supported by autoethnographic writing [13] aiming to build an understanding of the role of colour designers in creating sneakers and their (visual) stories [14].

Data Collection

The material culture study, narrative and image research were conducted by reading AJ1 histories in sneaker magazines and listening to podcasts hosted by sneakerheads unpacking the history of the AJ1 along with their personal experiences within the culture and with the artefact supported by books on sneakers/SC. Sources were selected for their focus solely on the AJ1 model, discussion specifically of colour design of the AJ1 and through the narratives of sneaker design and sneakerhead culture through the lens of the AFI.

Study Design

This study focused on the known first-year releases of the AJ1. This list may not comprise this shoe's official or unofficial releases in 1985, as Nike or SC have not kept rigorous records. Available release information for early AJ1 colourways is only available through the culture's collective memory. This list was compiled by cross-referencing the data with what is publicly available via the Jordan Brand and the Department of Nike Archives (DNA), a website and physical archive run by Nike. This study collected images of each of the known 1985 releases via digital archives like Nike DNA and sneakerhead fan sites like Flight Archives. Each image was labelled with the following information, if available: release date, nickname and colour palette names. Nicknames for the colourways are relevant as they are shorthand in the culture to refer to specific colourways and can give insight into the origins of the visual storytelling for each colourway.

Through analysing images of the known releases and reacting to the history of colour in the design of the artefact, the lead author unpacked their knowledge of colour design for sneakers through autoethnographic writing, discussing their own experiences during the colour design process detailing how and why the lead author might approach the colour palette, colour placement, and proportions. To help illustrate the concepts shared, a CAD (Computer Aided Design) was rendered on Adobe Illustrator using an image of the original Air Jordan 1" Black Toe" (figure 4, left). The Jordan "Wing" logo was omitted from these renderings to help separate the CAD created for this study with CADs from Nike or Jordan brands.

Limitations

This study had no access to the physical artefacts to enable using more traditional methods of artefact analysis or material culture studies, which conduct physical tests to determine the artefact's materials, make or colour first-hand. While contemporary versions of the AJ1 are widely available, considerable advancements in manufacturing, materials, design and colour make them unsuitable for this study. As with many historical artefacts, the exact colours are lost to time as the originals are discoloured and cracking with age, limiting capturing the precise hues of the original releases [6]. This study captured approximate colour palettes utilising the eyedropper function in Adobe Illustrator to create the design artefacts to illustrate the colour design process.

As with many artefacts, the stakeholders in this culture, design stakeholders, sneaker companies and sneakerheads, share history through storytelling, which can hold contradictions. Contradictions, along with alignments, are acknowledged throughout this study. While accurately placing the artefact into historical context and understanding the exact chain of events which enabled this artefact to hold influence in this culture may be helpful, this study also sought to understand the mythology around the artefact, which may uncover the greater context of colour as a storytelling device. By employing autoethnography, this study is limited to a singular perspective on a complex industry whose practices are often protected from outside observation and tailored to each company's processes and cultures.

RESULT AND DISCUSSION

Air Jordan 1

Figure 2. Michael Jordan with the “Bred” colourway or “banned” black/red CW of the launch of Air Jordan 1. Photographed by Jacobus Rentmeester for LIFE magazine, 1984.

Context

When Nike signed Michael Jordan straight out of college on his way to his rookie year in Chicago, footwear colours in the (American) National Basketball Association (NBA) followed a strict NBA rule called "uniformity of uniform", where player's footwear had to be at least 51% white and matched both their team's uniform and their teammate's footwear [2]. For much of the 1984-85 season, Jordan wore Nike "AirShips" in a white/red colourway that adhered to the rules and looked much like the sneakers his teammates and opposing teams wore. To create Jordan's first custom sneaker, the Air Jordan 1 (AJ1), Jordan worked directly with Nike Sneaker Designer Peter Moore to give feedback on Nike's existing designs and insights into his specific needs.

From materials to silhouette, most shoes worn by basketball players in the 1980s followed a formula: "leather upper and a pretty hard outsole midsole combination" [6]. Under Jordan's direction, Moore took inspiration from competitor brands like Adidas and Converse that Jordan had played in while in college, along with existing Nike Basketball sneaker models. Jordan's feedback led to a design that didn't stray too far from existing sneaker designs aside from minor alterations. Jordan gave feedback he wanted something "eye-catching" and "low to the ground" and that Nike's existing basketball sneaker midsoles were too high, so Moore reduced the height of the midsole, or the area between the shoe upper and the outsole, or shoe bottom, (see figure 3, below). A thinner midsole may have made it more aesthetically pleasing and aided in what is now considered an iconic silhouette. When it came to footwear construction innovation, Moore only added an "air" cushioning to the heel that was invisible to the viewer, creating a design that couldn't rely on "design innovation" like materials, technologies or new design techniques as a way to disrupt the market [1].

“The idea was to break the colour barrier in footwear…Prior to that, 99 percent of shoes were white or black, so I decided to design a shoe that would really take colour well. And the colours were red, black and white” AJ1 Sneaker Designer, an excerpt from his Book *Peter Moore: A Portfolio* [1].

Figure 3. Anatomy of the Air Jordan 1 [15,16].

Nike had taken a considerable risk signing Jordan and wanted to take "something eye-catching" to industry disruption. By harnessing the storytelling power of colour, Nike had created an icon out of the player, the shoe and launched the second wave of sneaker culture [7]. Moore created the "Black Toe" colourway to match Jordan's NBA team, the Chicago Bulls team colours (red/black/white) but pushed the 51% white rule. Jordan disliked the colourway and requested "Carolina Blue" to pay homage to his college team, but Nike decided that although they sought to push the boundaries, the shoe still needed to stick to team colours [1]. Some sources say that he called them "the devil's colours", maybe because of a rival of his college team, but this moniker added to the brand's aura [2].

To solidify this myth, Nike created a black/red colourway that pushed the NBA's rules and came to be known as the NBA's "banned shoe" [1]. While reports of the exact sequence of events vary, most sneaker historians agree that despite Nike's advertising campaign, which touted the AJ1 as a "banned shoe", the ban wasn't on the model. It was the (black/red) colourway nicknamed in the sneakerhead community as "Bred" (Figure 1) [6]. The "Bred" colourway (Figure 2, see above) was introduced at the All-Star Weekend's Slam Dunk Contest in February 1985, which is not an official NBA event [2]. However, the appearance of the colourway led the NBA commissioner's office to write a now infamous warning to Nike to remind them that Jordan couldn't wear the black/red colourway during an official NBA game. Still, from this, the myth of the "banned shoe" gave Nike the storytelling lore and added to Jordan's myth as someone who was pushing boundaries [6]. The colour and the storytelling around the colour made the Air Jordan 1 an icon of the sneaker industry and launched the second wave of SC [7].

While the Air Jordan 1 isn't the first shoe or even sneaker to leverage colour as a way to stand out in the industry or to drive a narrative, it is an example of how colour can influence the sneaker industry and capture the SC's love of colour and storytelling [6]. Moore understood colour's cultural power. Designers often describe colour as the emotional or "volatile" part of the design [4,17]. Colour designers understand that colour will be the first thing the user sees. The goal is to pique the user's interest and draw them in.

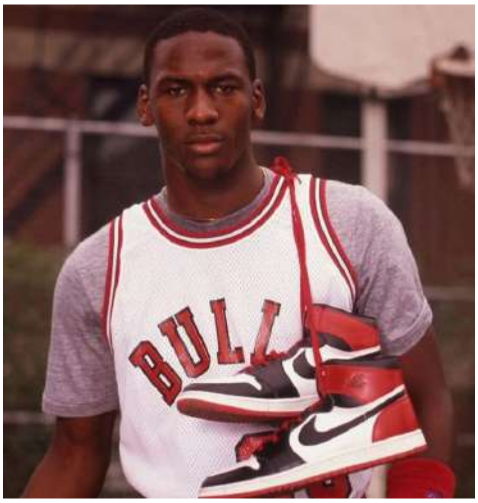

Figure 4 (Left). “Black Toe" or “home” colourway of the launch of Air Jordan 1. Photographed by Jacobus Rentmeester for LIFE magazine, 1984 Image via Highsnobiety.com[2].
Figure 5 (Right). (1985) Jordan playing in “Chicago '' colourway developed to minimise NBA fines Image via Highsnobiety.com, Getty Images [2].

As sneaker historians from the podcast "Sneaker History" outlined in their episode overviewing the history of AJ1, the two colourways that Jordan wore for the NBA were the "Black Toe" colourway (figure 4), initially designed for home games and "Chicago" (figure 5), created to minimise the fines from the NBA for uniform violations, were not new colours. Black or red and white were already worn by his teammates [6]. The colours were not groundbreaking tones or dye formulas of red, black or white tones, nor were the material applications innovative. Still, the blocking or leveraging of the sneaker's design by applying colour(s) to the panels, stitching, and materials to manipulate the visual read of the sneaker within the context of basketball sneakers was. The sneaker designer Moore created large, bold panels and design lines, allowing for multiple variations on the red/black/white palette. As the "Sneaker History" podcast host pointed out, what Jordan accomplished off the court disrupted the sneaker industry [6], where the panels created by the designer easily take on any colour, a wide variety of materials and finishes. This approach led to the storytelling-driven, highly anticipated limited releases that laid the foundation for much of the sneaker industry's athletic and fashion-driven parts [6].

Colour Design

Figure 6. “Row 1” Side by side comparison of the “Black Toe” and “Chicago” colourways, blocking. Details [18]; Images via Nike DNA[24]

Using the first two black/red/white commercial releases of the AJ1 High Top (Figure 6, Row 1), we can examine how simple design lines with a variety of panels and overlays, which are pieces of the shoe that are either stitched or fused to the upper, [16] give the CD many configurations for colour placement. This example illustrates how the same colour palette can look and feel different by changing the colour block and proportions. When CDs apply colour to sneakers, analysing the colour proportions is critical to the CD design process of either establishing a new colourway in the marketplace or driving a successful colour narrative. In this case, Nike reduced the amount of black from the "Black Toe" CW and increased the red for the "Chicago" CW to avoid NBA fines but in colour stories that are born from more conceptual visual storytelling that may be pulling from sources based in fashion, culture, nature, etc., the "colour read" or colour proportions will help make a visual connection to the inspiration.

Figure 7. "Blocking Exercise" diagram shows how applying (black/red/white) using different "blocks" can create distinctive looking sneakers.

To illustrate how many colour blocking options a designer might have, even with just the original three colour (black/red/white) colour palette, the lead author created a "Blocking Exercise" (Figure 7 "Blocking Exercise") or an exploratory design exercise that iterates a variety of colour placement options and colour proportions. A CD or sneaker designer might conduct this exercise during the initial design phases of sneaker design to ensure the applied design lines, overlays or panels created enough pleasing blocking options. A CD might also use a blocking exercise on an established sneaker design to help them familiarise themselves with it or find unexplored blockings. These exercises are usually done through a design program like Adobe Illustrator or a growing number of 3D programs, using a CAD (Computer Aided Design), generally a 2D or 3D rendering of the shoe's design. In the example above, a CAD was created for this study on Adobe Illustrator drawing from an image of the original Air Jordan 1 "Black Toe" (Figure 4, left).

Figure 8. "Blocking Exercise" isolated to show examples of what might be considered symmetrical, asymmetrical or a "bad" block.

When exploring colour blocking, a CD will use aesthetic principles and feedback from other design stakeholders and consumers to help determine what blocks are "aesthetically pleasing". A CD aims to choose the blocks that feel "balanced", either implementing symmetry or asymmetry. The goal of a successful block is to avoid highlighting areas of the shoe that the CD doesn't want to bring attention to or blocking areas or pieces together that create unpleasant shapes. The CD might prioritise highlighting brand details. For the case of Jordan/Nike, the "swoosh", Jordan "Wings", and tongue top logo might be the highest priority. Additional areas a CD might want to draw the user's eye to are new technologies or unique materials. Creating consistent blocking will help the colour design feel intentional and pleasing to the eye. Blocking can also tie a design story together, mainly when storytelling includes other sneaker models.

Figure 9. "Row 2", shows the Air Jordan with the same colour block but a variety of colours can create variety by playing with contrast. Details: [18,19], images via Nike DNA[24].

Row 2 (Figure 9, "Row 2") illustrates how using the same block but changing the colours and contrast might also create distinctive options. While consistent blocking draws the narrative together, applying a variety of colour combinations that vary in hue and tone creates diversity to appeal to a broader audience. By leveraging a variety of hues, shades and tones, the CD can tell various (visual) stories which might help establish seasonality or evoke a feeling in the user. For example, a dark outsole to make the sneaker look visually more durable, applying light or bright colours to make the sneaker look visually lighter, or neon/bright colours to areas of the shoe that are new to highlight the "innovation" possibly making the shoe feel more futuristic. Depending on the material make-up of the shoe, the CD also implements technical knowledge. For example, a white collar, or the edge around the opening where you put your foot, might be avoided because sweat, dirt and wear can discolour the material. Understanding how specific colours or applications might interact with each other and the wearer's environment is also essential. For example, placing light or white materials next to dark, bright blue or red materials could result in colour migration or bleeding/staining from the darker colour onto the light colour.

Figure 10. "Row 2 Colour Palette", shows the Air Jordan with the same colour block but a variety of colours can create variety by playing with contrast. Details: [18,19]; Images via Nike DNA[24].

This study created a potential original palette using the Illustrator eyedropper tool to isolate the likely original hues of each sneaker from row 2 (Figure 10 "Row 2 Colour Palettes"). This exercise might help us imagine what colour palettes the original footwear designer applied. To support the more colourful CWs, the designer used various neutrals colours and several blues to support the release of the "Bred" black/red with white midsole (see Figure 3 Anatomy of a Shoe). What is immediately striking in this palette is the amount of multiple and potentially competing hues of blue, which a CD today would most likely avoid. However, if we look at the nicknames of each of these shoes, we might get some insight into the design storytelling that may have driven how the designer applied the colours. The "UNC" colourway is an excellent example of using the athlete to move the storytelling. Using the team's colours, this CW connects its audience with Michael Jordan's life and his college basketball career at the University of North Carolina [20]. Using an earlier request from the athlete for this colourway leverages the myth behind the AJ1, creating buzz for the sneaker.

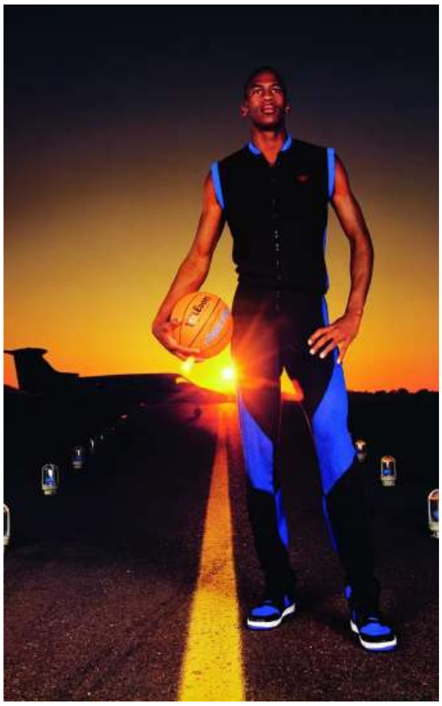

Figure 11. "Be True to Your School" Nike Dunks Ad (left), 1985. Photo via: Complex.com [21].

Figure 12. Michael Jordan "Flight Guy" (right) poster, 1985. Photographed by Chuck Kuhn. Photo via Footwearnews.com [22].

The remaining two blue colourways, "Kentucky/Storm Blue" and "Royal", have less definitive origins. However, unpacking what we know about these CWs could help discuss other visual storytelling inspiration areas. The "Kentucky/Storm Blue" CW can link to the Nike Dunk, a sneaker with a similar silhouette and design lines introduced in August 1985 (See figure 11 "Be True to Your School") [23]. Often, CDs will link models or visual storytelling from across a line together. By leveraging colour palettes and as discussed earlier, blocking a CD can link models together or reference a past sneaker CW, which is a vital part of SC. The duplicate blues could have been an intentional move by Nike and Jordan to create a more style-influenced CW. While never worn on the basketball court or worn by the athlete during a basketball game, the Royal colourway was hand-chosen by Jordan to be featured in a now infamous photoshoot (see above Figure 12, "Flight Guy") [22]. The royal blue is attributed to be one of Jordan's all-time favourite colourways and may have influenced how the athlete portrayed his brand off-court [22]

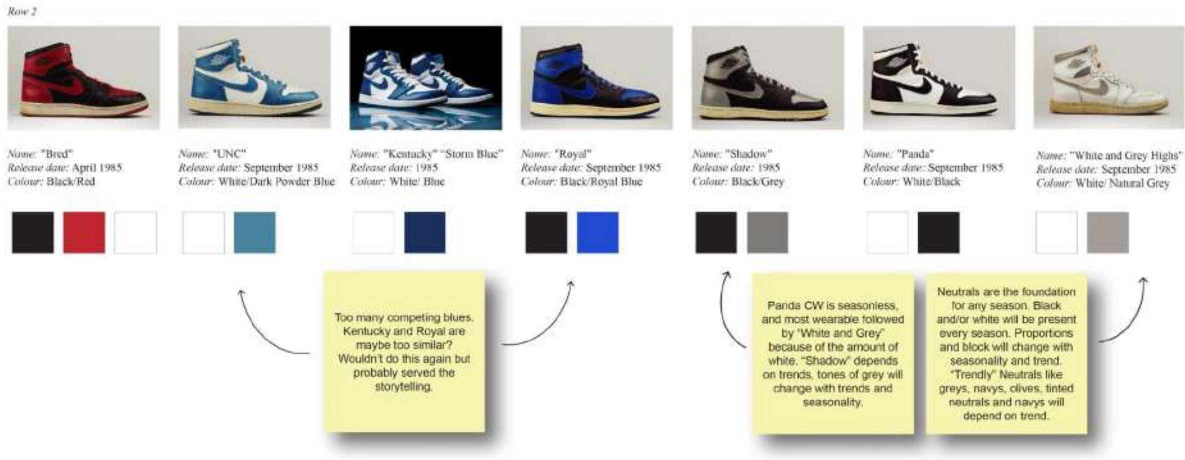

Figure 13. "Row 2 Colour Palette Breakdown", discusses from the perspective of a Colour Designer the influences on the palette and application. Details: [18,19]; Images via Nike DNA[24].

Finally, the foundation of any season is neutral colours. As seen through the "shadow", "panda" and "white and grey" colourways, these CWs are the most wearable and purchased in any collection. Breaking of the "block" for the "white and grey" CW may have been intentional to create a more classic look by making white the primary read. The greys used in CWs like "shadow" are subject to change, as the exact hues and tints depend on trends, along with other trend-driven neutrals like navy, khaki, olives and browns. CDs looking to create a more "classic" neutral CW like "White and Grey" might avoid greys with more "nuance" or too visibly tinted with yellow, red, blue or greens. Black, white or Black/white colour ways like "panda" are enduring. Blocks for these colourways may evolve and have some seasonality or depend on the season, like primarily white or all over white for summer months and mostly black or triple black for winter months.

CONCLUSION

This study was conducted through a material culture study with narrative inquiry surrounding the artefact (AJ1) and its cultural relevance supported by autoethnographic writings and design artefact creation based on the lead author's personal experiences as a colour designer in the sneaker industry. While there is a lack of academic research on colour design for sneakers, the authors believe that the wealth of qualitative data through storytelling might make sneakers a fitting artefact to examine how colour designers in the athletic footwear industry (AFI) might use colour to create visual storytelling. By shedding light on foundational colour design practices like colour blocking and applying colour combinations, this study hopes to inspire colour researchers outside of design to engage with designers to leverage more questions about colour preference in the context of design.

By engaging material culture study and narrative inquiry through Riello's "History of Things," this study could unpack the history and mythology around how the sneaker designer created the AJ1 to intentionally leverage colour as an industry disruption and a storytelling device. Through autoethnographic writing and design artefact creation, this study uncovered how designers leverage aesthetic principles during blocking exercises, the voices inside and outside of the design process who might help define a good block vs. a bad block and how consistent colour blocking might help translate a design narrative on to other sneaker models.

By analysing the colourways and palettes used in the 1985 AF1 Hi Top releases, this study discussed creating distinctive colour options by leveraging hue, tint and saturation to create CWs that appeal to various users. Finally, this study unpacked the importance of neutrals within the industry and outlined how seasonality and trends might dictate how CDs select and apply neutrals.

Recommendations/Further Research

This study gave a window into the colour design processes and their influences. While this paper aimed to initiate a conversation between colour designers and researchers about how CD leverages colour in visual storytelling, it also fails to cover the entire colour design process or all the aspects of visual storytelling with colour. Other areas that would benefit from further research are:

1. How do designers leverage consumer information through design briefs to create colour visual storytelling?
2. How do colour designers use image research and inspiration image boards to define visual storytelling for colour palettes?
3. How do language and storytelling from colour trend forecasting influence the sneaker industry?
4. How do materials and finishes influence colour design and visual storytelling creation?

REFERENCES

1. Davis, J. (2023, April 5). The Surprising History of the Air Jordan. *Esquire*. https://www.esquire.com/uk/style/g43495247/air-jordans/
2. Hammell, D. (2018, October 15). The Complete History of the Nike Air Jordan 1. *Highsnobiety*. https://www.highsnobiety.com/p/air-jordan-1-guide/
3. Brunel, F. F., & Kumar, R. (2007). Design and the Big Five: Linking Product Aesthetics to Product Personality. *ACR North American Advances*, *NA-34*. https://www.acrwebsite.org/volumes/12858/volumes/v34/NA-34
4. Adams, S. (2017). *Designer's Dictionary of Colour* (1st edition). Abrams.
5. Mugge, R., Govers, P. C. M., & Schoormans, J. P. L. (2009). The development and testing of a product personality scale. *Design Studies*, *30*(3), 287–302. https://doi.org/10.1016/j.destud.2008.10.002
6. Falchi, R., Engvall, N., Guillory, M., & Malhotra, R. (Directors). (2019, August 27). *Air Jordan 1: The Good, The Bad & The Ugly* (78). https://sneakerhistory.com/2019/08/27/air-jordan-1-the-good-the-bad-the-ugly/
7. Kawamura, Y. (2018). *Sneakers: Fashion, Gender, and Subculture (Dress, Body, Culture): Amazon.co.uk: Kawamura, Yuniya: 9781350105683: Books*. Bloomsbury Visual Arts. https://www.amazon.co.uk/Sneakers-Fashion-Gender-Subculture-Culture/dp/1350105686
8. O'Flaherty, M. C. (2021, May 24). The Secret Psychology of Sneaker Colors. *The New York Times*. https://www.nytimes.com/2021/05/24/style/sneaker-color-psychology.html
9. Schloss, K. B., & Palmer, S. E. (2015). Ecological aspects of color preference. In A. J. Elliot (Ed.), *Handbook of Color Psychology*. https://doi.org/10.1017/CBO9781107337930.022
10. Madden, T. J., Hewett, K., & Roth, M. S. (2000). Managing Images in Different Cultures: A Cross-National Study of Color Meanings and Preferences. *Journal of International Marketing*, *8*(4), 90–107. https://doi.org/10.1509/jimk.8.4.90.19795

11. Riello, G. (2017). Things that shape history: Material culture and historical narratives. In *History and Material Culture* (2nd ed.). Routledge.
12. Blandy, D., & Bolin, P. E. (2012). Looking At, Engaging More: Approaches for Investigating Material Culture. *Art Education*, *65*(4), 40–46.
13. Méndez, M. (2013). Autoethnography as a research method: Advantages, limitations and criticisms. *Colombian Applied Linguistics Journal*, *15*(2), 279–287.
14. Cross, N. (2001). Designerly Ways of Knowing: Design Discipline versus Design Science. *Design Issues*, *17*(3), 49–55.
15. Styles, U. (2005). *Sneakers: The Complete Collectors' Guide: Unorthodox Styles*. https://www.amazon.com/Sneakers-Complete-Collectors-Unorthodox-Styles/dp/0500512159?source=ps-sl-shoppingads-lpcontext&ref_=fplfs&psc=1&smid=A1KY5HRJRH6YF1
16. Vuong, M. (2019, September 9). Sneaker Anatomy 101 [Fashion Blog]. *Sneaker Freaker*. https://www.sneakerfreaker.com/features/sneaker-anatomy-101
17. Batchelor, D. (2000). *Chromophobia*. Reaktion Books.
18. Verheijke, G. (2022, January 19). Ox Street | All the OG Air Jordan 1 Colorways Explained. *Oxstreet Magazine*, Buying Guides.
19. Flight Archives. (2021). Air Jordan 1—Original Colorways and History [Fashion Blog]. *Flight Archives*. https://www.flightarchives.com/aj1-og-original-colorways
20. Karve, A. (2023, January 17). It's a Blue World without UNC—The Story Behind the Iconic Colorway | SNKRDUNK Magazine. *SNKRDUNK Magazine | Sneaker News and Release Information Find Your Favorite Jordan, Nike Adidas and More.* https://snkrdunk.com/en/magazine/2023/01/18/unc-blue-air-jordan-michael-jordan-history/
21. Sanchez, L. (2014, March 21). A Brief History of The "Be True To Your School" Nike Dunk Series [Fashion News]. *Complex*. https://www.complex.com/sneakers/a/sole-collector/a-brief-history-of-the-be-true-to-your-school-nike-dunk-series
22. Jones, R. (2017, March 30). How an Iconic Michael Jordan Photo Immortalized the 'Royal' Air Jordan 1. *Footwear News*. https://footwearnews.com/shoes/outdoor-footwear/air-jordan-1-royal-flight-guy-portrait-michael-jordan-sneaker-release-331785/
23. Cheung, A. (2022, March 4). Nike Dunk Versus Air Jordan 1: What Are The Key Differences? *The Sole Supplier*. https://thesolesupplier.co.uk/news/nike-dunk-vs-air-jordan-1-key-differences/
24. Nike. (2023). Air Jordan 1 retro & OG archive collection. *Department Nike Archives*. https://www.nike.com/jordan/air-jordan-1

THE UNIQUE COLOR WORLDS OF PAINTERS WITH COLOR VISION DEFICIENCY

Tsukasa Muraya[1]*, Yunoka Taniguchi[2], Yasuyo Ichihara[3] and Shoji Sunaga[4]

[1]*Chikushijogakuen University, Japan*
[2] *School of Design, Kyushu University, Japan*
[3]*Kogakuin University, Japan*
[4]*Faculty of Design, Kyushu University, Japan*

*Corresponding author: Tsukasa Muraya, t-muraya@chikushi-u.ac.jp

ABSTRACT

Background: In previous research about color vision deficiency in artists, color-deficient painters were judged in terms of their painting ability through comparison with the color usage of painters with normal color vision. Researchers have focused on the color usage skills of color-deficient painters in a similar manner to "normal" painters, but have not explored whether color-deficient painters choose colors according to the "normal" color world or a desire to create works in line with their own color worlds. **Objectives:** The purpose of the current study was to obtain insight into how modern artists with color vision deficiency use colors. **Methods:** We conducted in-depth interviews with three award-winning (national or international) professional Japanese painters. We asked them questions related to their attitude toward their color vision and color choice strategies, and qualitatively analyzed the interview responses. The three participants were T. Harada (born in 1954), who mainly uses watercolors and is an internationally renowned creator of picture books; J. Goto (born in 1968), a Japanese-style artist internationally renowned for paintings of ethnic Asians and a creator of picture books; and Y. Kurosaka (born in 1991), who is entering the contemporary art field, mainly uses oil paints, and won one of the biggest national art competitions in 2019. **Findings:** Japanese society has perceived people with color vision deficiencies as unsuitable to be artists because of their lack of color sense. The artists in this study nevertheless made their color vision deficiencies public when they were aspiring to become artists, because they wanted to improve society's understanding of color vision deficiency and encourage children with such deficiencies who may want to be artists in the future. We found that all three painters felt that the use of colors was important to express their feelings and aesthetic sense, and they disliked choosing colors using a personal computer or a color-measuring device merely to comply with normal color vision. At the same time, they were also keen to ensure that their color usage was not strange to people with normal color vision and used harmonious color combinations in their works for people with all types of color vision. **Conclusion:** Each painter in this study has their own color use strategy. The strategies are not only based on the "normal" color world but also on the painters' color worlds. The painters are aiming to create original works as professional artists on the basis of their unique color vision.

Keywords: Color vision diversity, Color vision deficiency, Art, Inclusion, Art education

INTRODUCTION

In previous research, color vision deficiency in artists was explored in two ways. The first approach aimed to identify historically famous artists with color deficiency on the basis of their unusual color usage. Their paintings were often nearly monochromatic, relying mainly on variations in lightness. Some artists predominantly used two colors, typically blue and yellow, in their works, and others intentionally created polychromatic paintings with high-contrast color combinations. It was also suggested that color-deficient artists show little interest in coloring their creations [1]. However, there is evidence that artists with color vision can use colors normally through the application of several strategies, such that color blindness does not preclude the possibility of achieving fame [2] [3]. These strategies included checking the color name on the labels of color tubes, developing a regular order for arranging color pigments on the palette, and seeking assistance from individuals with normal color vision with whom they were in close proximity during the creative process [1]. Both approaches evaluate color-deficient artists' ability through comparison with artists with normal color vision. There is evidence that color-deficient painters obtain insight from their unique color worlds that promote originality [4]. However, the nature of this insight has not yet been explored in depth.

Few peer-reviewed papers on this topic have been published in Japan. In Japanese society, color-deficient people have been viewed as inferior. For example, color-deficient children may quickly lose interest in art because of using the "wrong" colors, according to friends or teachers, when making sketches or reproducing a famous picture in art class. Moreover, many art and design departments of universities and design companies ask candidates to complete a color perception test, and ophthalmologists published a poster in 2015 warning color-deficient children that obtaining a job in fields requiring precise color distinguishment would be difficult [5].

To change this situation, the term "color vision variation" was introduced by the Genetics Society of Japan in 2017 [6]. According to this term, color vision exists on a continuum rather than being divisible into binary normal/abnormal categories. However, this notion has not been fully assimilated by Japanese society; most people still believe that color deficiency prevents people from being an artist or a designer. Nevertheless, there are several color-deficient professional artists in Japan, although it is not clear if they use colors in the same manner as artists with normal color vision by employing certain strategies or intend to create works according to their own color worlds. It is also unclear if they obtain insight for their creations via their unique color vison. This study aimed to determine whether modern artists with color vision deficiency are affected by their limited color vision and how they apply strategies to deal with this. The goal was to provide a basis for evaluating the works of these artists form the perspective of color vision diversity.

METHODOLOGY

We conducted in-depth interviews with three award-winning (national or international) Japanese professional painters (Table 1). Takehide Harada (born 1954) is a painter who combined watercolors and pastels in his works. This internationally renowned creator of picture books has won several major international picture book awards. Jin Goto (born 1968) is a Japanese-style painter who uses natural mineral pigments and is known for his paintings of ethnic Asians. He has also created picture books. Finally, Yu Kurosaka (born 1991) is entering the contemporary art field and mainly uses oil paints. He won one of the biggest national art competitions in 2019. We conducted semi-structured online interviews with Takehide Harada and Jin Goto; Yu Kurosaka was interviewed in person. The main questions concerned how they selected and applied colors, how they deal with their color vision deficiencies, the essence of their works, and how they want those works to be evaluated. The research was conducted from December 3, 2022 to February 7, 2023. We analyzed the interview data using a qualitative method.

Table 1 Basic details of the color-deficient artists participating in this study

Name (year of birth)	Color vision type	Main painting materials	Awards
Takehide Harada (1954)	Deuteranopia	Watercolors, pastels, pencils, etc.	Grand prize, UNICEF the Ezra Jack Keats international picture book Award, 1994
Jin Goto (1968)	Deuteranomaly	Natural mineral pigments (Japanese-style painting)	The White Ravens2014, Internationale Jugendbibliothek München
Yu Kurosaka (1991)	Deuteranopia	Oil paints	Grand prize, Shell Art Award 2019

RESULTS AND DISCUSSION

Overview of the artists' works

Takehide Harada is known for sensitive use of pastel colors (Figure 1). He has published many picture books and has abundant experience in the production of cover illustrations for books authored by famous Japanese writers. He prefers to use watercolors even though pale colors are difficult to distinguish for color-deficient people.

Goto's works use vivid colors and a Japanese painting style (Figure 2), and the main motif is Asian beauty. He has been to several Asian countries, meeting people and looking at scenery directly before trying to reproduce them. Red is a special color for Goto; indeed, red is loved in many Asian countries, and there are many different types of red.

Kurosaka's works are abstract, and some are representational paintings (Figure 3). The character of this young painter's work is changing. He won the grand prize of the Shell Art Award in 2019, which is one of the biggest competitions for young artists in Japan. During the interview, he

Figure 1. Letters de Pacheral, by Takehide Harada (watercolors and pencils, 7 × 5 cm (cover for a picture book published by Asahi Shimbun in 1999).

Figure 2. Deo Maiju ―Chiisana megami (in Japanese)/Kumari ― The living goddess (Nepal), by Jin Goto (natural mineral pigments, 60.6 × 50 cm. (from the website of Jin Goto; published in 2010).

described his use of trustworthy colors [7], i.e., colors perceived similarly between those with color vision deficiencies and trichromats, such as blue and yellow. However, his color choices have changed as his color world has developed.

Color choices

All three painters said that color was one of the most important elements of their works, such that they paid considerable attention to it. However, they do not use color measurement devices or rely heavily on color names when choosing colors, and dislike using colors merely because they are considered "correct" by trichromats (e.g., red sun or green trees) if they feel those colors are not in accordance with their feelings.

None of the painters aimed to use colors in the same way as trichromat painters, owing to a desire for originality as professional artists. This does not accord with previous research on the color usage tendencies of color-deficient artists. The artists in this study fought against feelings of inferiority regarding their lack of color sense, but subsequently established their own strategies to express their color worlds. Harada could not distinguish among some pale colors used in his works. He concentrates when using colors and eschews the use of "correct" colors that are unfamiliar to him for fear of losing the richness of his works. He also uses colors mixed inadvertently on his pallet. Kurosaka uses the same strategy of applying inadvertently mixed colors, but he masks the color names printed on tubes of paint and moved his atelier from Tokyo to a village rich in nature to escape from the color world of trichromats and trying to systematize his own color world. Goto used the "okikae" skill in his works, i.e., he used colors to express motifs in an idealized way, where this technique arose from the limited color variation of natural minerals. In Japanese-style painting, adherence to real-world appearances is not required; painters can choose their own colors. Therefore, Goto could express his own color world according to his firsthand impressions of Asian countries. He also doubted that there was a marked difference in color sense between himself and those with normal color vision viewing his paintings, but he did not focus on this issue and sought to create original works as a professional painter.

Figure 3. Between night and morning, by Yu Kurosaka (145.5 × 97 cm; published on the idemitsu website in 2019).

Insights arising from color vison

Despite his love of drawing, Harada despaired about pursuing a career in art when he noticed social oppression of the color blind in his youth. He had been afraid of using color, even after being awarded several notable prizes, given his bad experiences in relation to his color usage. He could not distinguish some colors in his works and could not be sure about how people perceived his color usage. Therefore, he sometimes asked his family to appraise his color usage, especially when using a new color, and the answers from his family were always to the effect of "not strange." This indicated that his color usage was harmonious and not discomforting for trichromats. Harada believed that the actual color world must be more beautiful than his own color world, but he knew he would never be able to perceive the former. This instilled a sense of loss and fueled his desire to use idealized colors; his sense of loss and this desire in fact arose from his particular type of color vision.

Goto stated that he did not have many bad experiences regarding his color use because his color vision deficiency was not severe. However, his teacher in art school said that he used red excessively when drawing leaves. Although not traumatic, this experience prompted him to pay more attention to others' perceptions of colors and to adjust color usage such that trichromats viewing his work would not perceive it as strange. Goto remains unsure about how different his color world is from those of others, and he also believes that originality is the most important trait of the professional artist. Goto exploits his particular color vision as a means of achieving originality, believing that color vision deficiency is actually a strength in this respect. He also expressed the hope that his use of color would help children who love to express themselves through painting to achieve the confidence needed to pursue a professional art career.

Kurosaka used to have an inferiority complex regarding his use of colors, but his complex gradually dissipated after winning a major art competition in 2019. He revealed his color vision deficiency to the public for the first time during interviews with mass media following his victory. His interest in color use and color deficiency increased in line with his suspicion that his color usage was strongly affected by the trichromat color system. Thus, he challenged himself to create art works free from the influence of his school education. Kurosaka was unhappy that society was based only on the trichromat color world, so he resolved to systematize his own color world through his creations. He also wanted his audience to question whether they truly see the world according to their own senses or merely as prescribed by society. To that end, some of his color choices ware deigned to evoke a degree of discomfort in those viewing his works.

General discussion

All three artists interviewed in this study exploited their particular color vision when creating works of art. Harada experienced a sense of loss in relation to his inability to sense the actual color world, which he believes is likely more beautiful than his own color world, and thus purposed to express beauty through idealized motifs. Goto, meanwhile, aimed to convey his impressions of Asian countries according to his unique color sense and skills. He believes his color vision enhances the originality of his works and therefore focuses on using colors according to his own preferences. Finally, Kurosaka's works encourages the viewer to consider society's influence on color perceptions by evoking a degree of discomfort.

Against this background, all three artists used strategies different from those of earlier color-deficient artists, who tried to adjust their color usage for compatibility with the color worlds of trichromats. As such, they do not rely on color names or color-measuring devices. Harada and Kurosaka even utilize colors inadvertently mixed on their pallets. All three artists aim to exploit their own unique color worlds in their works, rather than conforming to "normal" color use. Their harmonious use of colors can be both appealing and interesting for trichromats. After a period characterized by feelings of inferiority or doubt about their own color vision, all three artists embraced their color worlds as a means of achieving originality as artists. Moreover, they encourage children hoping to pursue careers as artists to have confidence in their own color worlds and continue to express their imagination and skills accordingly, rather than conforming to trichromatic-based painting. Society may now be ready to embrace color vision diversity because of the efforts of color-deficient artists.

CONCLUSION

The purpose of the current study was to gain insight into how modern color-deficient artists deal with their limitations and deploy colors. All three artists interviewed use specific strategies to apply colors in their works, different from those documented in previous studies. They reported being conscious of the color worlds of trichromats but did not aim to use colors in conformity therewith. All of them stated that color is an important element of their works and only use colors compatible with their feelings. Thus, they aim to use colors that, while not fully adherent to the color world of trichromats, are nonetheless still attractive to them. Recently, the idea of color vision diversity has entered into the consciousness of Japanese society but the concept remains difficult to understand; people tend to believe that everyone shares the same color world. Color-deficient artists have shown us that each color world has its own sense of harmony, and the works of such artists can convey beauty in a unique manner.

ACKNOWLEDGEMENTS

This work was supported by JSPS KAKENHI Grant Number JP 21H04342. We thank Michael Irvine, PhD, from Edanz (https://jp.edanz.com/ac) for editing a draft of this manuscript.

REFERENCES

1. Lanthony, P. (2001). Daltonism in painting. *Color Research & Application*, *Supplementary Volume 26*, s12-s16.
2. Marmor, M. F., & Lanthony, P. (2001). The dilemma of color deficiency and art. *Survey of Ophthalmology*, *45(5)*, 407-415.
3. Barry, L. C., Ross, W. H. (2009). Colour blindness does not preclude fame as an artist: celebrated Australian artist Clifton Pugh was a protanope. *Clinical and Experimental Optometry*, *92(5)*, 421-428.
4. Marmor, M. F. (2016). Vision, eye disease, and art: 2015 Keeler Lecture. *Eye*, *30*, 287-303.
5. Japan Ophthalmologists Association. Shikikaku kensa no susume (in Japanese). https://www.gankaikai.or.jp/colorvision/20151005_poster.pdf (accessed 19 February 2023).
6. The Genetics Society of Japan. Idrngaku yougo kaitei nitsuite (in Japanese). https://gsj3.org/wordpress_v2/wp-content/themes/gsj3/assets/docs/pdf/revisionterm_20170911.pdf (accessed February 19, 2023).
7. The Asahi Shimbun Digital. Shikikakushougai aru gaka ga kataru “Shinrai suru enogu” sono iro towa (in Japanese). https://www.asahi.com/articles/ASMDK3GK3MDKUCVL002.html (accessed September 10, 2023).
8. Harada, T. (1999). Letters de Pacheral (watercolors, pencils, 7 × 5 cm; picture book cover published by Asahi Shimbun).
9. Goto, J. (2010). Deo Maiju – Chiisana megami (in Japanese)/Kumari – The Living Goddess (Nepal) (natural mineral pigments, 60.6 × 50 cm; published on the website of Jin Goto [https://gotojin.wixsite.com/website/works]) (accessed September 10, 2023).
10. Kurosaka, Y. (2019). Between night and morning (145.5 × 97 cm; published on the idemitsu website [https://www.idemitsu.com/jp/enjoy/culture_art/art/2019/winner_interview.html]) (accessed 10 September 2023).

ACHIEVING COLOR RICHNESS IN PAINTING – CONCEPTS & TECHNIQUES OF CONVENTIONAL & DIGITAL PAINTINGS

[1]Woon Lam Ng, [2]Carey Ngai and [3]David Kian Wei Chan

[1,3]School of Art, Design & Media, HASS, Nanyang Technological University, Singapore.
[2]Fine Art Department, College of Arts, Xiamen University, China.

Corresponding author: Woon Lam Ng, ngwoonlam@ntu.edu.sg

ABSTRACT

Color richness may include using a wider hue range or creating subtle variations with complex transitions. Painting techniques from the Renaissance to Post-Impressionism are compared and discussed together with digital painting techniques. The investigation also covered the interactive behaviors of painted pigments with underpainting. The Munsell Color Space (MCS) was used to illustrate the color theory and pigment technology advancement which was connected to the breakthrough of painting practice especially from the period before and after Impressionism. The evolvement of painting techniques. The optical behaviors behind the approaches are elaborated based on the underpainting, pigment availability and color optical behaviors. Some misconceptions about color application concepts, like the concept of color harmony are also discussed. Digital painting techniques are compared based on their process and working logic. Case studies cover how the fundamental concepts of optical color behaviors are shared among conventional and digital painting. The Munsell Color System is also brought into discussion related to how it helps artists or art students explore colors or bridge clashing colors. Therefore, multiple hues can be applied while the image unity is maintained. Discussions of digital painting approaches cover its initial palettes, underpainting and pre-painted drafts with conventional painting media and its rationales. The design of digital brush characters is also discussed and compared with the conventional painting concept. It shows both the conceptual similarity and technical differences between the conventional and digital painting processes. The investigation provides opportunities and suggestions for improving digital and conventional painting to achieve color richness.

Keywords: Painting, Glazing, Scumble, Drybrush, Digital.

INTRODUCTION

In 2009, I had an interesting encounter with a student during my class, '2D & Color Workshop'. While the student was demonstrating how he had used many colors, his image did not present any color richness. In essence, the concept of how colors used are seen as 'rich' has to be better understood. Color richness in paintings can be categorized into two simple forms. The first type of color richness is the subtle variations across a narrow range of hues. This approach was common in classical paintings before the invention of many prismatic colors [1]. The second type is the archetypal understanding of using many different hues. The crux of the matter is the lack of understanding of why when multiple hues are used, the hues often clash instead of making the image look rich and unified. Incidentally, this issue also causes beginners to use formulated color sets suggested by the two-dimensional symmetrical color system [2], known as color harmony. However, the color harmony concept based on the Greek living philosophy [3] has been proven with ambiguity [4],[5],[6]. Researchers have further concluded that the usage is contextually dependent [7] and not quantifiable [8]. Compared to the two-dimensional color system, the uniform color space framework like the Munsell Color Space (MCS) [9] or the three-dimensional color navigation process by the Gamblin paint company [10] could better indicate practical differences of colors. This research will illustrate how different art techniques achieve color richness, and how the MCS assists users in maintaining image unity even when using a wider range of distinctive hues.

METHODOLOGY

This research covers two aspects. First, to define what is color richness as mentioned in the *Introduction*. Thereafter, to discuss the differences and similarities between the two definitions in relation to traditional and digital painting processes. The visual foundations behind the color richness are comprehensively supported through analysis of old masterpieces, contemporary watercolors, oil paintings and digital paintings. The areas of work are summarized through the research questions (RQ) listed below:
RQ1: What are the fundamental ways of presenting color richness in painting?
RQ2: What are the types of fundamental optical approaches to create color variations?
RQ3: How does an artist work with more hues while the visual unity is still maintained?

To answer these research questions, it is important to define the various forms of color richness in relation to their approach, as color richness has to include perceptual richness as well as the visual unity of an image.

RESULT AND DISCUSSION

Types of Color Richness - Color Variations in Paintings:
Color richness is the result of certain types of variations in color application. Regardless of traditional paintings during the Renaissance to Post-impressionism period or contemporary digital paintings, there are two main types of color variations observed. The first is the subtle variation within a narrow hue shift. Old masterpieces are painted with mostly earth colors to create subtle changes of hues across the surfaces of forms or generate transitions between two distinctive patterns to represent two objects.

Figure 1(a) Christ and the Woman taken in Adultery by Pieter Bruegel the Elder, 1565, Oil on panel (a grisaille), 24.1 cm × 34.4 cm & (b) Details [11], [12]

The grisaille painting (Fig. 1(a)) was painted mostly in neutral grayish brown. However, in a close-up view (Fig. 1(b)), the minor variations of brown, black and gray can be clearly observed. Before the industrial revolution made prismatic pigments easily available, high chroma pigments were rare and costly. Painters would use an indirect underpainting process known as Grisaille before applying prismatic pigments. That minimizes wastage [5].

Old masters push the limits of subtle differences with grays and browns to create contrast and suggest the richness of colors. In effect, it is common for Western art to use earthly colors to depict common subjects, skin tones and figures, etc. In Chan's demonstration (Fig. 2), the hue and values of browns and grays were adjusted while keeping the chroma low to paint the still life. It demonstrates how various browns of different skin tones could be achieved similarly.

Figure 2. Details of Hubris 92 x 92cm Oil on linen 2018, by David Chan Kian Wei.

In contrast, Impressionists use dabbed strokes with vibrant hues to create color variations [13]. When viewed afar viewers experience an optical blending of colors. Since the availability of prismatic pigments during that period, painters could take advantage and apply more hue variations. In the late 19th century, at the height of Impressionism, John Singer Sargent who was trained at a classical French academy, also combined his classical low chroma palette with the Impressionistic hue variations and painted with a hybrid process of both [14]. This hybrid process has therefore expanded the scope of achieving color richness and is still commonly used today.

There is a slight difference in digital painting. It combines digital layers with which opacity can be adjusted to arrive at color variations [15]. The range of colors could stretch from more neutral browns and grays to vibrant chromatic hues. Figure 3 demonstrates that subtle variations of browns and grays and chromatic colors can coexist in the painting. Since digital painting is presented through a direct light source from the device, it can present higher chroma through its larger color gamut than traditional pigments reflecting light. In Figures 3(a) & (b), the earthly colors are rich with subtle variations, while the reddish-orange tents and yellowish highlights on the figures' shoulders are presented in high chroma. In essence, it demonstrates Sargent's hybrid color method. Yu overlays textural and broken brush patterns to enhance the color variations [16]. A few chromatic colors are kept while image unity is maintained. Image unity and color clashing of distant hues are discussed in the later section.

Figure 3(a) & (b). Details of In the Alley by Yu, Donglu, digital painting [17], [18]**.**

Techniques to Achieve Color Richness

Beginning artists may mistakenly mix many colors to imitate masterpieces. In reality, masters achieve color richness through optical results of interactive layers. These layers are created based on two approaches, namely scumble (drybrush) and glazing (layering). The techniques can be further broken down into direct (*alla prima*) and indirect painting. In short, using an optical-blending effect, brush techniques such as grisaille, scumble, glazing, *sfumato* [19] and *velatura* [20] all contribute to color richness. This effect is pronounced in both digital and traditional methods.

Grisaille is the underpainting (Fig. 1(a)), used by the Renaissance masters to construct forms and space with black, white or brown before painting or layering with more chromatic colors which is known as the indirect painting process. Figure 1(b), Bruegel paints thinly and allows the brown-coated canvas to be partially visible [21]. That is created through the scumble technique, which is a form of dry-brushing process so that pigments could not fully cover the painted surface [22]. The randomized textures create optical interaction between the top and partially visible underlayers. A wider range of subtle color variations can be produced than physically mixing colors. Similarly, scumble techniques can be applied to the top layers. Details of Constable's oil painting and Turner's watercolor (Fig. 4(a) & (b)) demonstrate the color variations based on the same technique.

Figure 4(a). Details of the Hay Wain by John Constable, 1821, Oil on canvas [23]**;**
(b) Details of the Lake of Zug by J.M.W. Turner, 1843, Watercolor over graphite [24]

Quoting what Constable explains, *"I intend what I paint always to be viewed from a certain distance, you will then get rid of my white spots"* [25], the textural white spots would combine with other colors under them and produce color variations without having to mix each color through a tedious process. Constable is therefore able to work with a very limited palette while still achieving color richness [25]. Turner's painting (Fig. 4(b)) also shows layers of brushwork of different hues and values that overlay and create color variations.

A similar approach is demonstrated in a painterly digital painting (Fig. 5(a)). The richness of greens is achieved through multiple textural layers of greens. Some digital painters may also use gouache paint for underpainting to create initial textures or explore color palettes. It is quick and efficient in generating rich optical color mixtures. Figure 5(a), values, hue and chroma of greens are varied and painted in a textural manner to create optical interactions. Viewers experience a whole range of differences from strong contrast to subtle variations. Similarly, Ngai demonstrates it through traditional oil painting (Fig. 5 (b)) with layers of scumble-like paint. The hues of green are also varied to further enrich the color range. Ngai further demonstrates the co-existence of browns, grays and chromatic hues with transitions through the interplay of light and shadows (Fig. 6). This further validates Sargent's hybrid color approach again while the image unity is to be discussed in the next section.

Figure 5(a). Details of a digital painting by John J. Park [26]; **(b) Details of a painting of trees by Ji-Chuang Wei.**

Figure 6. Details of a painting of an interior space by Ji-Chuan Wei, Oil on canvas

In *Texture Synthesis of Digital Painting,* the author also elaborates on the importance of textural layers in the digital painting process by saying that the absence of textures will create a stalk and digital look. Therefore, experienced digital painters will customize brushes that could create noise-like busy patterns to generate textural effects [27]. Some keep a library of photographs with various textures to be overlaid on the surfaces to create variations and hence color richness [16]. It is also mathematically proven to be quite impossible to digitally create the same level of color variation through pixel painting. Based on a medium resolution of 250K pixels, a traditional painted image may have more than 100,000 different colors [28] when it is converted to digital.

Glazing or layering is another contrasting technique against scumble which works by putting semi-translucent layers on top of dried painted layers. Based on the level of translucency and pigment characters, it can be further derived. *Sfumato* [19] and *velatura* [20] belong to this group. Instead of painting opaque layers on top of dried layers, this translucent layering is able to shift the hue of the underlayer towards a certain direction without having to mix the targeted color [29]. It is commonly used as the transparent watercolor technique so that watercolorists can make good use of the brightness of watercolor paper, letting light reflect through the translucently painted layers. This creates higher luminosity that could not be easily achieved through opaque mixtures. It is also used to darken the value of colors and improve the color range. Webb demonstrates this in his watercolors [30]**.** Figure 7, the purplish shadows are painted on top of the yellowish brown underlayer and create rich variations of grays and browns that cannot be easily achieved through mixing colors physically.

Figure 7. Details of a watercolor by Woon Lam Ng, Watercolor on paper, 56 x 38cm.

During the Renaissance, glazing might be applied very thinly [29]. Da Vinci uses this technique to create very soft and slow transitional edges, known as *sfumato* [19]. The slow transition creates small value change, and the brushwork and contour are almost invisible. Some glazed layers are only 50um in thickness in Da Vinci's paintings [19]. This process allows Renaissance painters to create rich color variations with limited choices of pigments.

Glazing can also be applied with semi-opaque pigments. It is commonly applied to shift the value lighter with lighter pigments. When a milky layer of white pigment is applied on top of a dried layer, creating a silk-like layer, the underlayer will shift to a lighter value, forming a pastel-like and milky finish, known as *velatura* [20]. While all these techniques create color richness, image unity must also be maintained. Hence, enriching color could not be done by simply creating more colors while the overall color composition is ignored. The color richness and color design have to be planned simultaneously. The tension of colors has to be carefully considered and designed to achieve image unity. The MCS serves as a robust framework for this purpose as discussed below.

Maintaining Visual Unity with Rich Colors

The practical contrast of any 2 colors can be mapped by a uniform color space, like the asymmetrical MCS [9]. The practical advantage is that MCS does not forcefully compress color range using mathematical transformations like many symmetrical 3D color models - HSV HSL or NCS. Hence, the color difference mapped between any 2 or more colors can be used to obtain intermediate colors that fall between these colors. All these colors can be seen as vectors within the MCS color space [31]. Transitional colors can be obtained and used as bridging colors between any contrasting colors. Practically, all the color-enriching techniques above will sweep through these bridging colors because they are optical mixtures of the initial colors. Hence, they naturally form the transitions and buffer the visual tension of over-contrasting colors seated at extreme vector ends in the MCS. The rest of the colors are unlikely to cause color clashing issues if they are not from extreme ends. For example, earthly colors even with huge value differences, can easily work together, since all fall within a narrow color space around the central core of the MCS. The overall hue and chroma differences are manageable. Tinted colors like Impressionistic colors, though they are different in hue, are located within a smaller and skew cone color space at the top of the MCS. The actual color differences are smaller. Hence, color clashing also will not happen too [6]. In summary, the MCS maps all practical differences. When color clashing arises, transitional colors can be located between the clashing colors within the MCS while all the techniques above are able to help practitioners obtain these transitions and solve the issue.

CONCLUSION

Color richness comes from either the subtle variations between earthly colors or larger differences between distant hues in a uniform color space like the MCS. The techniques used in traditional painting are fully applicable to digital painting since both rely on the same logic – optical interactions of various layers of colors through glazing or scumble. The issue that may arise with the use of distant hues is image unity. That can be resolved by creating bridging colors referring to the MCS for the practical differences between hues. A wide range of intermediate transitional colors can be obtained and solve this issue.

ACKNOWLEDGEMENT

We would like to thank Nanyang Technological University for its support of this research.

REFERENCES

1. Lyon, C. (1991). Unveiling Monet. *MoMa*, *7*, pp14-23.
2. Itten, J. (1970). *The Elements of Color* (1st ed.). John Wiley & Sons, INC.
3. Burchett, K. E. (2005). *A Bibliographical History of The Study and Use of Color From Aristotle to Kandinsky*. The Edwin Mellen Press, Ltd.

4. Arnkil, H., & Schwarz, A. (2023). Colour harmony in the context of teaching. *Journal of the International Colour Association*, *33*, 119–135.
5. Ng, W. L. (2021b). The teaching of the concept of color harmony and its ambiguity. *Asia-Pacific Journal of Humanities and Social Sciences*, *1*(2), 20–27.
6. Ng, W. L. (2021a). *A study of the teaching of color theory for visual art students at tertiary institutions in Singapore*. 217.
7. Collins, J. (2004). Turner, Whistler, Monet. Toronto, Paris and London. *The Burlington Magazine*, *146*(1219), 709–710. http://www.jstor.org/stable/20073738
8. Mahyar, F., Cheung, V., Westland, S., & Henry, P. (2007). *Investigation of complementary colour harmony in CIELAB colour space*. Proc. AIC midterm meeting, China.
9. Unknown. (2017). *Munsell Color System*. https://www.munsell.com
10. Gamblin. (2011). *Navigating Color Space*.
11. Bruegel the Elder, P. (1565). *Christ and the Woman Taken in Adultery* [Oil on panel]. https://sites.courtauld.ac.uk/aah/pieter-bruegel-the-elder-christ-and-the-woman-taken-into-adultery-1565/
12. Unknown. (2016). *Bruegel in black and white: Three Grisailles reunited*.
13. Watson, C. W. (1963). *The use of broken color in scenic design*.
14. Hoopes, D. F. (1965). John S. Sargent: The Worcestershire Interlude, 1885-89. *The Brooklyn Museum Annual*, *7*, 74–89.
15. Tan, J., Lien, J.-M., & Gingold, Y. (2015). Decomposing Digital Paintings into Layers via RGB-space Geometry. *ArXiv Preprint ArXiv:1509.03335*.
16. Lardner, J. (2012). *Digital Art Techniques for Illustrators & Artists: The Essential Guide to Creating Digital Illustration and Artworks Using Photoshop, Illustrator and*. A & C Black Publishers.
17. Hellard, P. (2013). *EXPOSÉ 11: The Finest Digital Art in the Known Universe* (Vol. 11). Ballistic Publishing.
18. Yu, D. (2013). *In the Alley* [Digital (Photoshop)].
19. De Viguerie, L., Walter, P., Laval, E., Mottin, B., & Solé, V. A. (2010). Revealing the sfumato technique of Leonardo da Vinci by X-Ray Fluorescence spectroscopy. *Angewandte Chemie International Edition*, *49*(35), 6125–6128.
20. Hills, P. (2006). Titian's veils. *Art History*, *29*(5), 771–795.
21. Allart, D., Currie, C., & Bubb, R. (2016). *Pieter Bruegel the Elder, The Death of the Virgin*.
22. Lockhart, R. M. (2010). *Scene Painting: Research and the Importance of a Scenic Morgue*.
23. Constable, J. (1821). *The Hay Wain* [Oil on canvas]. https://www.nationalgalleryimages.co.uk/asset/901/
24. Turner, J. M. W. (1843). *The Lake of Zug* [Watercolour on paper]. https://www.metmuseum.org/art/collection/search/337499
25. Brighton, C. (1994). John Constable's anomaly. *The British Journal of Aesthetics*, *34*(1), 81–92.
26. Park, J. J. (2019). *Untitled* [Digital]. https://www.instagram.com/p/B3c8d48h2zm
27. Tonge, G. (2011). *Digital Painting Tricks & Techniques: 100 Ways to Improve Your CG Art*. Penguin.
28. Lewis, J.-P. (1984). *Texture synthesis for digital painting*. 245–252.
29. Reiche, I., Müller, K., Eveno, M., Itié, E., & Menu, M. (2012). Depth profiling reveals multiple paint layers of Louvre Renaissance paintings using non-invasive compact confocal micro-X-ray fluorescence. *Journal of Analytical Atomic Spectrometry*, *27*(10), 1715–1724.
30. Webb, F. (1997). *Webb on Watercolor* (5th ed.). North Light Books.
31. Ng, W. L. (2018). Practical application of browns and grays based on a vector concept—The practical strength of the asymmetrical Munsell color space. *Color Research & Application*.

Color Standards in City Planning and Shop Facade Design Changes: Field Survey of Two Urban Landscape Formation Districts in Nagoya City, Japan and Analysis of Corporate Identity Elements

T. Mukaiguchi[1]*, M. Harada[1], T. Terashima[1], T. Ono[1]
[1]*Graduate school of Design and Architecture, Nagoya City University, Nagoya, Japan.*

*Corresponding author: T. Mukaiguchi, muka@sda.nagoya-cu.ac.jp

ABSTRACT

The enactment of the Landscape Law in 2004 marked a major change in Japan's landscape policy. Previously, landscape policy had focused on the voluntary preservation of traditional landscapes by some local governments through ordinances. However, now many cities are promoting comprehensive landscape formation under the Landscape Law. Landscape formation districts are special regulation districts in each city that target important areas for landscape formation. Store designs in landscape formation districts must comply with landscape regulations, but the designs are frequently incompatible with the standard design that expresses the store's easily recognizable corporate identity (CI). Color is a crucial component of CI, but it is also one of the most important targets of landscape regulations. Many landscape codes require buildings and advertising to have low color saturation, and many franchise chains that have been characterized by vibrant store designs must now comply with these color codes. This research aims to develop a method that can balance landscape and store identity in a landscaped district. In reality, the redesign of franchise chain stores involves changing from bright colors to more subdued ones and a variety of other methods. Therefore, we will systematically organize and analyze the design change methods by surveying the actual situation. In Nagoya City's landscape formation districts, the survey covered "Hirokoji and Otsu Streets" and "Yotsuya and Yamate Streets." Along the 7.1-km stretch of streets in these districts, there are a variety of shops. Through a field survey, we analyzed the design changes made to the facades of each shop in comparison with the general facade design in areas without landscape regulations. The analysis examined the characteristics of design changes in each of the six store business categories: a) banks, b) convenience stores, c) various agents, d) coffee shops, e) fast-food restaurants, and f) small general stores. "Sign Background," "Symbol Mark," "Logotype," "Advertising Information," and "Other" such as standing signs and awnings were given special consideration. As a result, the following specific methods were identified: (1) inverting the sign's image and background, (2) using cut-out letters in the logotype, (3) making the logotype or sign background monotone, (4) reducing the size of the sign, (5) omitting the logotype or symbol, and (6) moving the sign inside the store. However, there was no method to reduce saturation or brightness. Which method is more important appears to be determined by the nature of the business.

Keywords: AIC2023, Chiang Rai, Thailand, landscape regulations, facade design, corporate identity (CI), field survey

INTRODUCTION

The passage of the Landscape Law in 2004 marked a significant shift in Japanese landscape policy. Until then, landscape policies had been voluntary measures implemented by individual local governments and had long been limited in scope, with target areas limited to historic districts and other areas. Following the enactment of the Landscape Law, comprehensive landscape master plans based on the law were developed in 646 local governments throughout Japan (as of the end of March 2022). Moreover, several regulated districts were established in many cities under each master plan. Among them, the landscape formation districts discussed in this paper are the most important regulated districts in each city, and the color regulation is a crucial indicator to guide the landscape formation of the districts.

Balancing landscape compliance and maintaining corporate identity (CI) is challenging for franchise store operators. Color codes are frequently violated by the standardized facade design and corporate colors that chain stores establish on their own. This requires store operators to consider new store designs that maintain their identity while adapting to the public good of landscape harmony.

The study's ultimate goal is to establish a method that balances landscape harmony and CI in areas where landscape regulations are imposed. Changing store designs to comply with landscape regulations is more than just switching from bright to more subdued colors. Different methods and various innovations have been developed in response to landscape regulations. This study aims to capture the actual conditions of facade design through on-site surveys and then analyze the results to provide useful suggestions for facade design.

Inoue et al. (2014) attempted to reveal the reality of traditional Japanese streetscapes, and Tsukamoto et al. (2020) investigated changes in the color selection of advertising materials in regional cities in Japan. However, there have been few related studies, and none have investigated store design through landscape planning comprehensively and systematically.

METHODOLOGY

This study aims to verify, through a field survey, the actual situation of store design in a landscape formation district that imposes color restrictions. In the field survey, the district's store designs were examined to determine the actual conditions of the methods used to maintain CI on the facades of each chain store. In addition to photography, visual colorimetry was performed using color charts to record Munsell codes and PCCS tones (Color Co-ordinate System by Japan Color Research Institute).

The study will be conducted in several cities in the future, but as a first step, survey areas were selected in two of the landscape formation districts outlined in the Nagoya City Landscape Plan. Since March 2007, Nagoya City, a regional core city with a population of approximately 2.3 million, has had a landscape plan in accordance with the Landscape Law. Table 1 provides an overview of the field survey, and Figure 1 shows the locations of the surveyed wards. The two target areas are "Hirokoji and Otsu Streets" in the business district and "Yotsuya and Yamate Streets" in the neighborhood business district near residential areas. The field survey was carried out on sunny days in August 2022. The target of the survey were franchise chain stores.

Figure 1. Layout of Landscape Formation Districts in "Nagoya City Landscape Plan"

Additions to the illustrations for "Nagoya City Landscape Plan,"

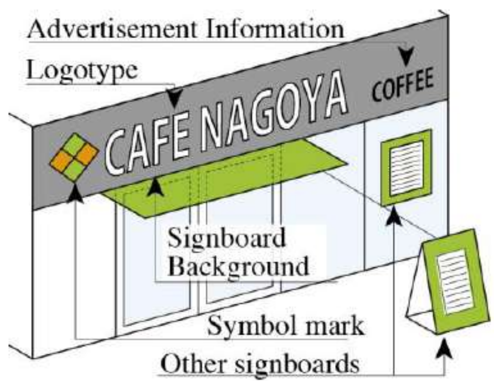

Figure 2. Corporate identity elements in store facade design

Table 1. Overview of the two landscape formation districts to be surveyed (2022)

District	Hirokoji and Otsu Streets	Yotsuya and Yamate Streets
Outline	This zone traverses the central area of Nagoya City. It extends for about 2.5 km along Hirokoji Street and about 0.8 km along Otsu Street, each extending from the street to a depth of 30 m.	A district with many residences, universities, temples and shrines, etc., a short distance from the city center. The regulation area is about 3.8 km, each extending from the street to a depth of 30 m.
Date of survey	August 12, 19 and 21, 2022	August 22, 26 and 27, 2022
Survey method	1. Photography 2. Visual colorimetry using the Japan Paint Manufacturers Association (2021) L standard colors for paints (pocket version)	
Target stores	All chain stores, number of stores surveyed: 164	All chain stores, number of stores surveyed: 89

Table 2. Color-related regurations in Nagoya City Landscape Plan

Subject		Hirokoji and Otsu streets	Yotsuya and Yamate streets
Building	Basic matter	The form, design, color, size, and location of buildings should align with the streetscape.	
	Color		The exterior colors should harmonize with the surrounding landscape, including buildings and trees, and be subdued. However, the use of colors as accents in a restrained area is accepted.
Structures	Basic matter	The form, design, color, size, and location of structures should align with the streetscape.	The form, design, color, size, and location of structures should align with the streetscape.
Outdoor advertisements	Basic matter	The form, design, color, size, and location of the advertising materials align with the streetscape	The form, design, color, size, and location of the advertising materials align with the streetscape
	Color	(a)Highly saturated and fluorescent colors should be used sparingly, such as by limiting their usage to smaller areas and utilizing them as accents. (b)When the top of the display surface is 10 meters or more above ground or the display area exceeds 15 square meters, the following rules apply: (Articles in the middle are omitted.) -Colors with a saturation exceeding 14 are not permitted. -Colors with a saturation of 10 or less should be used for at least half of the display area, and colors with a saturation of 12 or less should be used for at least two-thirds of the display area. (c) When using a color scheme with a strong stimulus, such as complementary colors, caution should be exercised by reducing the saturation. (d) Letters and designs should be arranged in a well-balanced manner. Pay attention to the number of colors and text used to avoid a cluttered appearance.	(a)Highly saturated colors should be used cautiously, for instance by restricting their use to a limited area and utilizing them efficiently as accents. The use of fluorescent colors is prohibited. (b) Additionally, if the height of the display surface is 10 meters or more above the ground, specific regulations apply (Articles in the middle are omitted.) -Colors with a saturation exceeding 14 are not permitted. -Colors with a saturation of 10 or less should be used for at least half of the display area, and colors with a saturation of 12 or less should be used for at least two-thirds of the display area. (c) When using a color scheme with a strong stimulus, such as complementary colors, caution should be exercised by reducing the saturation. (d) Letters and designs should be arranged in a well-balanced manner. Pay attention to the number of colors and text used to avoid a cluttered appearance.

Before the analysis, we organized the landscape regulations related to color restrictions in the districts that were the subject of the field survey. Table 2 shows the extracted color regulations from the Nagoya City. The landscape regulations regarding the color of business designs apply to buildings, structures, and outdoor advertising. The basic rule for commercial areas on "Hirokoji and Otsu streets" is "to be in harmony with the streetscape," whereas residential areas on "Yotsuya and Yamate streets" are "to be calm and in harmony with the surrounding landscape, including buildings and trees." Furthermore, detailed regulations for outdoor advertising have been introduced. There are specific limitations on the use of highly saturated and fluorescent colors, as well as restrictions on the size and area of the display area and color restrictions based on Munsell values.

The store design analysis focused on the five elements of CI shown in Figure 2: "Sign Background," "Symbol Mark," "Logotype," "Advertising Information," and "Others," including Standing Signs and Awnings. The standard design of each chain store was determined from several new store facades located in areas not subject to landscape regulations. We then determined how store designs responded to landscape regulations in the landscaped districts under study.

RESULT AND DISCUSSION

The following table lists 87 stores in six industries with a relatively large number of stores: a) banks, b) convenience stores, c) various agents, d) coffee shops, e) fast-food restaurants, and f) small general stores. In the right column, blue letters indicate a positive landscape rating (suitable for landscape regulation), whereas red letters indicate a negative rating (avoids regulation or does not comply with regulation). The following is a summary of the industry characteristics.

a) Banks: There are 20 branches of 10 companies in the district and many have adapted to landscape regulations. Specific methods included reducing the size of the sign, eliminating the sign background and using cut-out letters, using monochrome logotypes, and inverting the figure and ground on the sign to reduce the area of corporate colors used. Meanwhile, the regulations have been circumvented in some cases by displaying conventional signs and advertising information on the interior side of the building through glass and on the premises, which is not subject to landscape regulations (See Figure 3 i).

b) Convenience stores: There are 15 stores from 4 companies, and only 4 were landscape-compliant stores. Reduced sign size and the use of clipped letters were used in the examples of landscape compliance, all of which maintained highly saturated corporate colors. Even among landscape-compliant stores, new stores in glass curtain wall buildings were notable for installing traditional signage indoors through the glass. (See Figure 3 ii)

c) Various agents: There were 12 stores from 8 companies in 3 major industries (mobile phones, real estate leasing, and real estate sales), but only 3 stores deviated from the standard design. In many cases, the standard design was established within the landscape regulations and did not differ from that of general stores. However, real estate leasing tended to use corporate colors with more saturated sign backgrounds, whereas no response to landscape regulations could be confirmed, and a passive response was noticeable.

d) Coffee shops: There were 12 stores from 5 companies, many of which comply with landscape regulations. Coffee shop chains typically use less saturated corporate colors, and many coffee shops can meet landscape regulations without changing their standard store design. Their attempts to harmonize with buildings showed more aggressive efforts to comply with landscape regulations. For example, it can be inferred that the two stores that reversed the colors of the figure and the background changed the background of their sign to match the exterior wall color of the building they occupy.

e) Fast-food restaurants: There were 12 stores from 10 companies, and except for one store, no landscape compliance was observed. Many of the standard stores in this industry are decorated with bright signs, and many of the stores in the study area were no exception. Additional advertising, such as climbing banners on the street, was visible.

f) Small general stores: There were 11 stores run by 3 different companies. Many of them were in violation of landscape regulations. The standard storefront in this industry, like fast-food restaurants, is predominantly eye-catching in design, and many of the stores in this district were no exception. However, only two stores that complied with the landscape code showed a proactive response to the landscape code, such as the use of cut-out letters. (See Figure 3 iii) The others tended to add a variety of additional advertising materials to their storefronts, even when their signage showed compliance with the landscape rules. (See Figure 3 iv)

i) Bank No.[H023] ii) Convenience store No.[H060] iii) Fast-Food Restaurants No.[H029] iv) Small General Stores No.[H085]

Figure 3. Example of the actual store facade design

Table 3. Field Survey Results by Store Sector

Store Sector	Name of chain store *1	Corp. Color	Corporate identity elements *2 *3: Back-ground	Symbol Mark	Logotype	Ads. Info.	Other	Store-by-Store Changes, Item brackets indicate store number. *4 Blue letters indicate a positive landscape rating, whereas red letters indicate a negative rating.
a) Banks	Mizuho Bank		DBL, BL		WH, RD			[H056] [H143] Signage size reduction
a) Banks	Aichi Bank	RD			Mtl			[H102] Omission of symbol, [Y012] Cut-out logotype and symbol
a) Banks	Sumitomo Mitsui Banking	GN	GN, WH	BGN	WH, DGN			[H032] Figure–ground color inversion, [H139] Cut-out logotype and symbol, [H141] Metal cut-out logotype, [Y048] ent. signage uses only logotype with cutout, standard design signage added to retaining wall and site
a) Banks	Sumitomo Mitsui Trust Bank	BBL	BBL, WH	BGN, DGN, or BBL	WH			[H023] Monochrome cutout logotype, standard design signage added to site and a column.
a) Banks	Mitsubishi UFJ Bank	RD	WH, RD	RD	BK, WH			[H111] [Y021] No response to landscape rules, [H153] Figure–ground color inversion, No signboards, [Y004] Signage size reduction, [Y040] Figure–ground color inversion, signage size reduction, no signboards.
a) Banks	Mitsubishi UFJ Trust and Banking		RD	WH	WHd			[H161] Cut-out of metal logotype on glass, no sleeve sign, place additional signage in the store.
a) Banks	The Shoko Chukin		WH, GN	GN to BL, YL	WH			[H122] Figure–ground color inversion
a) Banks	Shinsei Bank	BL		BL/WH	GY			[H050] no response to landscape rules, placing additional signage in the store.
a) Banks	Ogaki Kyoritsu	GN			MTL			[H017] Color change to GN and BK with cut out letters, no sleeve signage, [H057] no response to landscape rules
a) Banks	The Chukyo Bank	RD	RD, BL	WH	WH			[H077] Background color of sign change to BL.
b) Convenience Stores	Seven Eleven	OR GN, RD	WH, OR GN, RD		OR GN, RD			[H001] [H013] [Y061] No response to landscape rules, [H043] Signage size reduction, placing additional signage in the store.
b) Convenience Stores	Daily Yamazaki	OR YL	YL, OR WH		YL, BK	RD, BL		[H115] No response to landscape rules
b) Convenience Stores	Family Mart	GN, BL	GN, BL, WH	GN, BL, WH	BL			[H015] [H076] [Y037] No response to landscape rules, [H060] Cut-out lettering signboard, logotype color change BL to GN, placing additional signage in the store, [H126] Background size reduction, cut out lettering, logotype color change BL to GN, flag ads [H146] Signage size reduction
b) Convenience Stores	Lawson	BL	BL, PK, WH	BL, WH	BL			[H004] [H158] [Y059] No response to landscape rules, [Y064] Additional advertising information.
c) Various Agents – Mobile Phone	au	OR	OR		WH			[H107] No response to landscape rules, [H119] Figure–ground color inversion, walls and eaves color change to OR
c) Various Agents – Mobile Phone	Softbank		WH	GY	DGY			[H108] [Y054] [Y081] No response to landscape rules
c) Various Agents – Mobile Phone	Y mobile	RD	RD		WH			[H051] [Y055] No response to landscape rules
c) Various Agents – Mobile Phone								[Y081] Figure–ground color inversion
c) Various Agents – Estate Leasing	ABLE	GR	GR		WH			[H094] Entrance wall color change to GR, [H136] [Y087] No response to landscape rules
c) Various Agents – Estate Leasing	NISSHO	BL	WH, BL	BL, RD	BK	WH		[H048] [Y035] No response to landscape rules
c) Various Agents – Estate Leasing	Minimini	RD	WH, RD	RD	RD			[Y034] No response to landscape rules
c) Various Agents – Estate Leasing	Unilife	OR	OR WH	WH, OR, RD, GY	WH	WH	OR	[Y57] No response to landscape rules
c) Various Agents – Real Estate Sales	Daikyo Anabuki	DBL	DBL, OR BL		WH,OR,BL			[Y042] No response to landscape rules
c) Various Agents – Real Estate Sales	Sumitomo Real	DBL	DBL	YL	WH			[Y003] Cut-out Logotype
c) Various Agents – Real Estate Sales	Sumitomo Forestry Home Service	GN	WD	GN	BK			[Y053] Logotype color change to DGY
c) Various Agents – Real Estate Sales	Mitsui Rehouse	RD	DRD, OR, RD, WH		WH, BK			[Y009] [Y046] No response to landscape rules
d) Coffee Shops	DEAN, DELUCA				WH			[H133] No response to landscape rules
d) Coffee Shops	Café de crié	DBR		DBR/MTL	WH		DBR	[H039] Logotype is cut-out, [H144] No response to landscape rules
d) Coffee Shops	Cafe veloce	DRD			WH& DRD		DRD	[H005] No response to landscape rules
d) Coffee Shops	Starbucks Coffee	DGN		DGN/WH	WH		DGN	[H091] [H121] [H147] No response to landscape rules, [H140] Omission of store name
d) Coffee Shops	Doutor	YL	BK		WH, YL		YL	[H036] [H101] Figure–ground color inversion, [Y005] No response to landscape rules
e) Fast Food Restaurants (Continue to next page)	Tenkaippin	RD	WD	WH/RD	BK		WH, RD, BK	[H013] No response to landscape rules, flag ads.
e) Fast Food Restaurants	Maruokashoten	RD	RD	RD/WH	WH, RD	RD/WH	WH, RD	[H156] No response to landscape rules, flag ads, light bulbs decoration around ads.
e) Fast Food Restaurants	Nakau	RD,GN	RD		WH & BK	WH/GR		[H012] [H032] [H052] No response to landscape rules
e) Fast Food Restaurants	Yayoiken	RD,DBL,YL	WH, WD		BK	WH/BK		[H067] No response to landscape rules
e) Fast Food Restaurants	Yoshinoya	OR,DGN	BK	OR	BK, WH			[H092] No response to landscape rules
e) Fast Food Restaurants	Matsuya	OR,BL, YL	YL, BL	OR, BL, YL	BL		OR, BL, YL	[H035] No response to landscape rules
e) Fast Food Restaurants	Sukiya	RD, YL	YL, RD		WH	YL	YL, RD, WH	[Y075] No response to landscape rules
e) Fast Food Restaurants	MOS BURGER's	RD,GN	GR, RD	WH	WH		GR, RD, WH	[Y058] No response to landscape rules

	Hinoya Curry	RD,GN	GR		WH, RD	YL		[H061] No response to landscape rules
	Curry House CoCo Ichibanya	YL	YL	WH, YL, BK	BK		WH, YL, BK	[H046] No response to landscape rules
f) Small General Stores	Cocokara fine	PK,BL	WH	PK	BL	WH, PK, BL	WH, PK, BL	[H024] [H098] No response to landscape rules, [Y067] No response to landscape rules, flag ads.
	Sugi Pharmacy	RD,GN	WH	RD, WH	RD	RD, YL, GR	RD, YL, GR	[H008] [H065] Figure–ground color inversion: background color changed from WH to RD, [H022] [H138] [H159] No response to landscape rules, [H085] Cutout logotype and symbol, placing additional signage in the store
	Matsumotokiyoshi	RD,BL, YL	DBL	RD, YL	DBL & YL	DBL, RD, YL	DBL, RD, YL	[H003] Cut-out logotype and symbol, change logotype and symbol color to monotone, [H074] No response to landscape rules

1. Those whose standard store design is unclear and those that are unique were excluded.
2. The color combinations are as follows: figure–ground of a color (figure color/ground color), multiple colors in order of area (color, color), with border (color & border color)].
3. Colors are abbreviated as follows: White (WH), Black (BK), Gray (GY), Dark Gray (DGY), Red (RD), Dark Red (DRD), Yellow (YL), Green (GN), Bright Green (BGN), Dark Green (DGN), Blue (BL), Bright Blue (BBL), Deep Blue (DBL), Dark Brown (DBR), Orange (OR), PINK(PK), Wood (WD), Metal (MTL)
4. [H] is the store number on "Hirokoji and Otsu Streets" and [Y] is on "Yotsuya and Yamate Streets."

CONCLUSION

This paper clarifies the actual conditions of store design through field research in two landscape development districts in Nagoya, Japan. Although the awareness of the landscape regulation differs depending on the industry, the common methods of store design to comply with the landscape regulation were as follows: (1) reverse the figure and background of signage and reduce the area of bright colors, (2) use cut-out letters in the logotype or cut-out symbols, (3) monotonous logotype or monotonous background of signage, (4) reduce the size of signage, (5) omit any logotype or symbol, and (6) move the signage inside the store. Method 1 through 5 are for the landscape plan, whereas item 6 is a means of circumventing the regulations by displaying a standard design sign through the glass.

Although the landscape plan contains color regulations, the field survey found no instances of corporate colors being used with reduced saturation or brightness. According to the survey, stores with vibrant corporate colors complied with the landscape plan without changing their corporate colors, such as by reducing the area of their corporate colors.

Even within the same chain, there were differences in responses from store to store. It is possible that the store owners' and tenant owners' intentions had an impact. However, note that the landscape regulations are applied at the time of renewal, and some of the stores that have not changed include properties not previously included in the landscape plan.

ACKNOWLEDGEMENT

This work was supported by JSPS KAKENHI Grant Number JP23H03682 (Masayuki Harada). The authors would like to thank T. Yamauchi for his cooperation in the field survey.

REFERENCES

1. 1. This paper is a revised version of the following paper not peer-reviewed: Terashima.T., Harada.M., Ono.T., Yamauchi.T., Mukaiguchi.T. (2023). Color Standards in Landscape Planning and the Actual Situation of Design Changes on Store Facades: Part 1 Field Survey on Store Facades in Two Landscape Districts in Nagoya and Analysis of CI Elements (in Japanese), *AIJ Journal Architectural Institute of Japan Tokai Branch Research Report,* Volume 61 Pages 573-576
2. Inoue.R., Nakano.S. (2014). A Study on Landscape of Historical Street: Case study of Matsue City Traditional Preservation Area, Townscape Formation Area and Neighborhood Area (in Japanese) , *AIJ Journal of Technology and Design*. Volume 20 44 Pages 311-316
3. 3. Tsukamoto.S., Sugaya.J., Hidaka.K. (2020). The Effect of Design Guideline on Color Choices for Outdoor Advertisement in Ashiya City (in Japanese), *Journal of the Color Science Association of Japan*, Volume 44 3 Pages 97-98
4. City of Nagoya, Urban Landscape Office. (2018). *Nagoya City Landscape Plan (in Japanese)*.

THE IMPACT OF CHROMATIC PALETTES IN SOCIAL NEIGHBOURHOODS' ENVIRONMENTS: CAUSE AND CONSEQUENCE OF HUMAN INTERACTIONS.

Cristina Caramelo Gomes [1, 2]*

[1]CITAD, Lusíada University of Lisbon, Rua da Junqueira, 188-198, 1349-001 Lisboa, Portugal
[2]CIAUD, Research Centre for Architecture, Urbanism and Design, Lisbon School of Architecture, Universidade de Lisboa

* Corresponding author: Cris_caramelo@netcabo.pt

ABSTRACT

This article aims to focus on the visual perception of social neighbourhood environments and initiate a discussion on actions that can facilitate their seamless integration into the urban fabric. To achieve this goal, we analyse two case studies located in the Lisbon Metropolitan Area. These case studies involve coloured social neighbourhood environments, each with distinct colour schemes: one inspired by the work of Bruno Taut and the colour palettes of Le Corbusier, and the other employing public art on the blank walls of buildings. Ultimately, our objective is to comprehend how colour influences the perception of social housing environments, shapes the identity of places and communities, fosters individuals' sense of belonging, and influences interactions among users, as well as between users and the physical environment.

Keywords: Colour, Design for Social Sustainability, Social Neighbourhoods, Human Interactions, Urban Art

INTRODUCTION

The interactions between users and the built environment depend on how the spatial layout features respond to users' needs and expectations. In simpler terms, the availability of functionalities, the presence of public spaces, commercial areas, educational and healthcare services, as well as accessibility, coexist with the geographical location, orientation, form, and textures of buildings, with aesthetics emerging as a critical factor. The way the built environment supports users' identities and daily routines, while also fostering interactions between individuals and spaces, buildings, and infrastructure, plays a significant role in shaping the sense of identity within a place and its community, as well as cultivating a sense of belonging. Users perceive the built environment through the lens of their culture and personal experiences, finding meaning and symbolism in its use. The features of spatial layout and user experiences together contribute to the concept of place, reinforcing the sense of belonging, often referred to as the "sense of place." Social dwelling neighbourhoods are characterized as communities with distinct social and cultural patterns, as well as varying approaches to spatial use and daily routines. Buildings often fail to meet these needs due to compliance with municipal regulations and the challenge of accommodating diversity, which makes it difficult to establish standard behaviours. Consequently, when the formal and functional aspects of buildings do not align with community requirements, the neighbourhood's image, shaped by the morphology and colours of its facades, can become a source of segregation. In contrast to common or luxury neighbourhoods, which tend to use colour sparingly, social neighbourhoods often display a vibrant and colourful image. This colourful appearance contributes to the neighbourhood's identity but can also foster a sense of exclusion among residents, hindering the development of a sense of belonging. Without a sense of belonging, positive interactions with the physical environment and among individuals become challenging. This can lead to a decline in the sense of community and an increase in neighbourhood violence. Despite the widespread knowledge and information collected through close observation of reality, this model persists.

It is widely acknowledged that the use of colour can alter one's perception of building geometry and contribute to creating liveable and dynamic environments that stand out from their surroundings while defining their identity. However, in settlements where chromatic palettes and compositions lack diversity and interest, or where various hues and tones compete for attention without proper planning or harmony, as is often the case in the majority of social neighbourhoods in the Portuguese context, the result is a dull or chaotic cacophony that further segregates the place and its inhabitants, impacting human behaviours and interactions.

SOCIAL HOUSING NEIGHBOURHOODS

Social housing neighbourhoods have emerged as a response to the need for housing units among those who cannot afford properties in the regular marketplace. These urban communities originated in Europe after the First World War and, after more than a century, they continue to be a necessity. This is especially true in times when real estate prices have reached levels that are unaffordable for a significant portion of the population, pushing the limits even for those who meet financial and social requirements. In Europe, interpretations and models of social neighbourhoods may vary, but they share some common characteristics: they are typically located on the outskirts of major metropolitan areas, consist of housing units with minimal space and basic finishes, exhibit high population density, and are home to diverse and multicultural residents (OECD, 2020). These residential areas exhibit a blend of a sense of community and segregation due to the factors mentioned above, often accompanied by elevated levels of violence. The multicultural nature of these communities' results in different patterns of everyday experiences and varying approaches to the use of indoor and outdoor spaces. The possibilities offered by the architectural morphology and building typology, as well as the available services in the area, can either encourage or hinder interactions among individuals. Typically, interactions among residents are confined to those within the neighbourhood. Limited cultural or functional local activities, a lack of information about the behaviour of neighbourhood residents, and the overall image of the residential area may not be particularly attractive to outsiders. The image of these places is consistently characterized by the uniformity of building shapes and the colours applied to the built complexes. However, due to the lack and/or deficiency of maintenance and careless use, these areas often present an unpleasant and segregating appearance, both for their inhabitants and for those who use the surrounding areas. The colours used in these settlements vary, ranging from less saturated to more vibrant hues. These colour choices are often made with the intention of either blending in with or standing out from the surrounding urban fabric.

From conceptual authors to residents, there are differing interpretations of the chosen colour schemes. Some view the chromatic choices as a reflection of the community's identity, while others perceive them as indicators of segregation, as colours often act as distinguishing markers of location. Regardless of the specific chromatic palette chosen, over time, the lack of maintenance and experiences with graffiti contribute significantly to the unfavourable image of these important and necessary types of settlements.

SOCIAL HOUSING NEIGHBOURHOODS AND COLOUR

Colour emerges as a quality of the natural and built environment, but it is individuals who imbue it with a blend of meanings and associations drawn from cultural, social, and other experiences in their daily lives. As human beings, we recognize, interpret, and are accustomed to encountering polychrome in various aspects of daily life, where colour serves as a communicative element conveying character, information, function, symbolism, and aesthetics. However, translating the concept of colour into the built environment presents challenges, as colour in this context does not relinquish its principles or diminish its significance (Caramelo Gomes, 2023). In the realm of colour research, the topic of colour in social housing neighbourhoods is not frequently addressed, as indicated by the literature review. To delve into the subject of colour in social housing environments, it is important to reference the work of Bruno Taut, who was influenced by the Garden City movement, rooted in Utopian Socialism and the Expressionist movement. The amalgamation of these movements' ideas allowed Taut to be recognized as the chromatic architect of Modernism. In his work, Bruno Taut introduced innovative approaches to planning, style, and garden design, setting standards for modernist social housing. He saw colour as an affordable means to introduce interest and delight into otherwise drab and economically disadvantaged areas. From his work, we can draw parallels to the importance of the Horseshoe complex, which exhibits a chromatic palette similar to one of our case studies. The Horseshoe serves as an example where Taut proposed solutions to some of the issues identified in contemporary social housing environments.

The Horseshoe complex is located in a southern suburb of Berlin and was constructed between the First and Second World Wars. This architectural complex, inspired by the principles of functionalism and the Garden City movement, is dedicated to social housing, and is widely regarded as the pioneering model for humanizing high-density urban environments (Pruden, 2018). Within this complex, the chromatic palette aimed to transcend mere functionality, infusing maximum dynamism and vibrancy into all the facades. Its purpose was to establish an intimate sense of identity between the residents and the place. Furthermore, Taut successfully realized his utopian vision by striking a harmonious balance between the natural and built environment, as well as between beauty and purpose (Fedko-Blake, 2017).

Figure 1 and 2. Horseshoe social housing environment. Author Architectureinberlin, 2008

The UNESCO classification of the Horseshoe complex (UNESCO, 2006) played a crucial role in preserving its original features and ensuring ongoing maintenance to maintain its aesthetic and historical significance. However, this is not the prevailing reality in most social housing environments. Typically, a drab image is presented, with facades bearing the marks of time and neglect. Depending on the neighbourhood's location and the population that inhabits it, graffiti often appears on the facades alongside signs of the area's violence levels. These graffiti representations typically aim to convey a message from the inhabitants or those who identify with the neighbourhood. However, they do not contribute to the social and economic rehabilitation of the area or to the encouragement of external interventions for a more inclusive and interactive environment.

Recently, these social neighbourhoods, along with some degraded areas, have become canvases for artistic expressions in the form of street art. Street art serves as a means to communicate social messages through painting, sculptural elements, and installations, impacting the beautification of the place, the identity of the community, and residents' engagement. The impact of street art in urban areas depends on the artistic representation and the viewers' interpretation, whether they are inhabitants, external visitors, or those seeking the work of a particular artist. However, the primary goal is always to promote interaction among individuals and between them and the physical environment. Street art emerges as a statement because artists have the freedom to create and define subjects that draw the community's attention and engage people in important discussions (Boscaino, 2021). By enhancing the sense of identity and belonging and attracting people from different backgrounds, street art promotes inclusivity and diminishes the sense of segregation, thereby fostering interaction among individuals, regardless of their social, economic, cultural, or local origins.

CASE STUDIES

Outurela

The Outurela social housing context was constructed in the 1990s and is primarily inhabited by people of African origin (Município de Oeiras, ?). It is a well-established complex with housing units, basic services, schools, and sports facilities. Information available on the municipal website and in local newspapers indicates that there is a strong sense of community and interactions among the inhabitants. This sense of community is fostered through various educational and leisure programs for youth, contributing to a peaceful atmosphere (Jornal da Região, 2010). While there are efforts to promote interaction and positive behaviours through social programs, the limited availability of public spaces hinders spontaneous human interactions among the residents and between them and individuals from outside the neighbourhood. However, the presence of social activities programs, public transportation, essential services, and a commercial centre on the outskirts of the area (serving as a link between the social neighbourhood and a residential area catering to middle/high-income residents) mitigates the feeling of isolation among inhabitants.


Figures 3 and 4. Buildings facades' chromatic palette. Author, 2023

Nonetheless, a sense of segregation persists, as residing in a social housing neighbourhood is often indicative of a particular social and economic situation (RTP, 2008). This feeling is exacerbated by the perceived monotony of the buildings and the vibrant chromatic palette used in Outurela, which contrasts with the more subdued colours in nearby settlements resulting from the municipal area's development, catering to a different social and economic demographic. A visit to the neighbourhood and interactions with residents confirm the information obtained from various, albeit dated and sporadic, sources.

In addition to solar considerations, the utilization of the space, and the application of various shades and tints deviating from the original facade colour, the chromatic palette used in the Outurela neighbourhood bears a resemblance to those employed by Bruno Taut in Horseshoes and the one created by Le Corbusier in 1959 (Le Corbusier's Colour System - the Architectural Colour Palettes, n.d.). While architects and designers may appreciate this chromatic choice as a homage to recognized professionals, it is perceived negatively by the inhabitants as a source of differentiation.

When viewed from an elevated perspective or in an aerial view, the stark chromatic contrast between this social housing complex and those targeting the regular real estate market becomes apparent. Some of the buildings feature graffiti representations that lack quality and reinforce the common stereotype of violence and drug-related issues associated with social neighbourhoods. The lack of understanding regarding the reasons behind this chromatic choice could be mitigated through participatory design sessions. These sessions would serve to comprehend the changes necessary for the social housing complex to meet current housing functions and user requirements. In doing so, the neighbourhood's functionality and image would emerge as a reflection of the inhabitants' input, ultimately contributing to the sense of place, community identity, and belonging.

Quinta do Mocho

Quinta do Mocho is a social neighbourhood situated in the eastern outskirts of Lisbon. Its initial purpose was to address the housing needs of people, primarily from Africa, who faced social and economic challenges. This area had long been associated with violence and drug-related issues, which led to its isolation. The lack of interaction with outsiders left residents feeling embarrassed and stigmatized by their own community. The local environment was shaped by community behaviours, and municipal intervention was minimal. Quinta do Mocho lacked urban amenities and public transportation connections to other areas of the Lisbon metropolitan region. Due to safety concerns related to violence, private transportation was reluctant to enter the area. The uniformity of building shapes and colours added to the neighbourhood's challenges, impacting users' orientation as well as the ability of firefighters and ambulances to navigate effectively. In 2014, the "O bairro i o Mundo" project, part of the C4i (Communication for Integration) initiative by the European Council, was launched. This project aimed to demystify the negative perceptions associated with stigmatized areas like social housing neighbourhoods. It resulted from a partnership between the Municipality of Loures and the Theatre Association IBISCO, promoting three days of cultural activities and a street art exhibition. The festival featured both nationally and internationally renowned artists, along with lesser-known talents, whose collaboration extended beyond the festival itself (Silva, 2015). This initiative played a pivotal role in changing the identity and perception of the Quinta do Mocho area.

Figure 5, 6, 7, 8. Examples of Street Art in Quinta do Mocho. Author, 2023

The paintings adorning the facades of the buildings in Quinta do Mocho introduced a diverse range of chromatic palettes, all with the shared purpose of engaging with the community's unique characteristics (getLISBON, 2022). As the number of these artworks increased, so did the popularity of free guided tours led by community residents. These tours were designed to help visitors appreciate and understand the paintings, their social and cultural symbolism, and the community itself (Streetartmovementblog, 2017). The existence of the street art festival and the ongoing collaboration with street art artists had a profound impact on both the neighbourhood and the sense of belonging within the community. It encouraged interactions between local residents and individuals from different economic, social, and cultural backgrounds. The paintings, with their diverse chromatic palettes and meaningful messages, added aesthetic value to the area's layout, personalised building facades, and provided reference points for those who experienced the place for various reasons. In essence, street art gave a voice to the local community and transformed Quinta do Mocho into a vibrant and more inclusive environment.

A self-guided visit to this location reveals that nearly 10 years after the Festival, the neighbourhood is in need of maintenance and a rejuvenation of the Festival's principles. Despite the presence of public transportation, accessing the area, even by private car, is not straightforward. The paintings adorning the facades of buildings along the streets and public spaces promise an engaging and vibrant cultural and social experience. However, personal exploration of the area also shows that some public spaces are occupied by old furniture used by residents for communal meals and social interactions, while others serve as repositories for discarded and abandoned items that no one wants anymore. The condition of the buildings reflects the passage of time, careless use, a lack of maintenance, and human behaviour that does not necessarily invite or welcome visitors.

ISSUES TO DISCUSS

The role of colour in social housing neighbourhoods warrants closer attention from researchers. Colour is an inherent quality of the built environment, but its significance lies in the individual's capacity to imbue it with meaning and symbolic associations. However, in the context of the built environment, the application of colour often reflects a neglect of its dimensions and its subsequent impact on human experiences. Social housing settlements frequently exhibit distinctive chromatic palettes, regardless of whether they are dull or vibrant, setting them apart from neighbouring areas intended for the regular real estate market. Colour, along with other architectural features, can inadvertently contribute to the segregation of these neighbourhoods within the urban fabric, as it can identify their location and existence from various perspectives. The neglect of colour's dimensions in urban planning is a recurring issue, regardless of the social, economic, and cultural context of the area and its inhabitants. This oversight becomes particularly critical in social housing environments, given the diverse backgrounds of the individuals who reside in them. Establishing a meaningful connection between the place and its residents is vital to minimize violent behaviours, encourage the presence of visitors, and counteract perceptions of segregation. Street art emerges as a potential positive response to this challenge. Regardless of their chromatic palettes, the images created through street art convey important messages to the community and significantly impact the community's sense of identity and belonging. Furthermore, they invite visitors to the area, promoting diverse human interactions. Street art has the unique capacity to customize buildings, public spaces, and communities, offering intriguing perspectives. However, to achieve a sustainable outcome, planned actions for introducing street art in these neighbourhoods must be well-thought-out and cyclical, including maintenance of the artworks, to ensure lasting benefits.

Art will always serve as a communication channel that facilitates interaction between individuals and between individuals and the physical environment. However, the effectiveness of this premise hinges on whether the conveyed messages truly embody the voice of the community in a given place. Without this authentic representation, art may fail to foster interactions with outsiders, nurture the sense of identity within the community and the place, and cultivate a feeling of belonging. Colour, as a vital aspect of artistic representation and symbolism, plays a significant role, whether applied to a façade or incorporated into street art. Colour should be employed with a thorough understanding of its various dimensions, aiming to enhance the humanisation of the built environment and individual well-being. This necessitates its consideration from the outset of the planning and design process, rather than relegating it to a mere decoration of the building or urban environment and overlooking its profound effects on the quality of the user experience.

ACKNOWLEDGEMENT

This work is financed by national funds through FCT - Fundação para a Ciência e a Tecnologia, I.P., under the Strategic Project with the reference UIDB/04026/2020 and the Strategic Project with the references UIDB704008/2020 and UIDP/04008/2020.

REFERENCES

1. OECD (2020), "Social housing: A key part of past and future housing policy", Employment, Labour and Social Affairs Policy Briefs, OECD, Paris,
2. Caramelo Gomes, C. (2023). Colour? What Colour? A difficult understanding between urban environment' professionals and users. AHFE (2023) International Conference. AHFE Open Access, vol 112. AHFE International, USA.
3. Pruden, S. (2018) "Absolutely Palpable Utopias" The Expressionist Ideas Behind Bruno Taut's GEHAG Housing Estates. *Mount Royal Undergraduate Humanities Review* (MRUHR). 5.
4. Fedko-Blake, V. (2017, April 26). Profiling Germany's utopian modernist architect Bruno Taut. Culture Trip. https://theculturetrip.com/europe/germany/articles/profiling-bruno-taut-germany-s-utopian-modernist-architect
5. UNESCO (2006) Housing Estates in The Berlin Modern Style – Nominations for inscription on the UNESCO world heritage list. https://whc.unesco.org/uploads/nominations/1239.pdf
6. Architectureinberlin. (2008, November 12). The Britz 'Horseshoe' Estate, Bruno Taut, Martin Wagner. Architecture in Berlin. https://architectureinberlin.wordpress.com/2008/10/11/the-britz-horseshoe-estate-bruno-taut-martin-wagner/
7. Boscaino, M. (2021) Developing a Qualitative Approach to the Study of the Street Art World. *Street Art and Creativity. The future: Urban Creativity Studies*, vol.7, nº2
8. Jornal da Região (2010) OUTURELA/PORTELA Projecto Bairro agarra juventude. Jornal da Região: OUTURELA/PORTELA Projecto Bairro agarra juventude (jornaldaregiao.blogspot.com)
9. Câncio, F. and Leitão, A. (2008) Outurela. *A Vida Normalmente.* Outurela – RTP Arquivos
10. Le Corbusier´s Colour system - The Architectural Colour Palettes. (n.d.). https://www.lescouleurs.ch/en/the-colours/colour-system/
11. Silva, C. C. (2015, December 6). Como um bairro problemático se transformou numa galeria de arte pública. PÚBLICO. https://www.publico.pt/2015/12/06/local/noticia/quinta-do-mocho-como-um-bairro-problematico-se-transformou-numa-galeria-de-arte-publica-1716490
12. getLISBON. (2022, July 14). A Galeria de Arte Urbana da Quinta do Mocho • getLISBON. getLisbon. https://getlisbon.com/pt/descobrindo-pt/arte-urbana-quinta-do-mocho/
13. Streetartmovementblog. (2017, December 30). Quinta do mocho: visitas guiadas à maior galeria a céu aberto. The SAM. https://streetartmovementblog.wordpress.com/2017/12/10/quinta-do-mocho-visitas-guiadas-a-maior-galeria-a-ceu-aberto/

A STUDY ON THE IMPRESSION DIFFERENCE BETWEEN FACECHART AND ACTUAL MAKEUP LOOKS

Chi-Ying Hsu[1and 2]* and Wen-Yuan Lee[3]

[1] The Graduate Institute of Design Science, Tatung University, Taiwan.
[2] Lecturer, Asia Colors, Taiwan.
[3] Department of Media Design, Tatung University, Taiwan.

* Chi-Ying Hsu, aa0925300036@gmail1.com

Keywords: makeup color, impression, facechart

ABSTRACT

Facechart is commonly used to represent makeup designs and is an educational training tool for makeup artists. This study intended to understand the difference between the impressions given by makeup looks on facechart and those on actual faces. This study conducted an experiment in which 71 observers were invited to make impression judgments on ten makeup looks on actual images and facecharts on 19 impression scales. The impression scales included adjectives: "elegant," "friendly," "professional," "authoritative," "dependable," "competent," "solemn," "genuine," "warm-hearted," "modest," "gentle," "sociable," "healthy," "serious," "responsible," "natural," "self-confident," "energetic," and "thoughtful." These ten makeup looks are drawn on a facechart and applied on the actual face of a female model. The facechart is a 70-pound A4 photocopy paper printed with face outline, facial features, and hair, mapping out where to place makeup products, i.e., lips, blush, eye shadow, eyeliner, and false eyelashes.

The experimental data obtained from the experiment were analyzed using a profile chart, RMS values, and T-test. The results revealed that the impressions given by the makeup looks on the facechart and those on the actual face are significantly different in most impression scales.

INTRODUCTION

Makeup artists have used the facechart in the industry for decades. Essentially, it's a piece of paper with a printed outline drawing of a face. Makeup artists used this outline to map out where to place different makeup products, including face powders, eyeshadows, lipstick, etc. Makeup artists use facechart to evaluate the makeup look before applying it to the face. In other words, the makeup look on the facechart is the makeup artist's color plan and the primary material for beginners to practice makeup. What makeup artist pursues is that the makeup look on the facechart is consistent with those on the actual face.

In Taiwan, fashion-related courses in vocational high schools utilize facecharts as training material. Students use facecharts to practice color combination, various makeup techniques, blending methods, and conceptualizing comprehensive makeup styles (Chen, 2012; Hsu et al., 2021; Lien, 2019). In addition, the exam outline of The National Vocational Skills Competition for Home Economics Students, organized by the Ministry of Education, Taiwan, aiming to encourage students specializing in home economics to demonstrate their skill levels (K-12 Education Administration, 2023), also uses the facechart to evaluate the skill level.

Facecharts are a significant practice modality in the beauty industry, allowing makeup artists to communicate the desired makeup look effectively with their clients. (Anchieta et al., 2021; Blunder, 2019; Kondrevich, 2020; O'Sullivan & Pinto, 2022) Hence, examining certification for Level B Technician for beauty in Taiwan employs facecharts to evaluate makeup techniques and the overall makeup aesthetic. (Hsu et al., 2021; Lin & Yang, 2021).

But the facechart is a two-dimensional flat plane, and the human face is three-dimensional. Even if the makeup is ultimately transferred from the facechart to the human face, we are still curious whether the impression given by the same makeup look can be consistent on the facechart and the human face. This study intended to understand the difference between the impressions of makeup look on facechart and those on actual faces.

EXPERIMENTAL PLAN

To achieve the aim, this study conducted an experiment in which 71 observers were invited to make impression judgments on ten makeup looks on actual images and on facecharts on 19 scales. Each observer provided 380 impression judgments, i.e., (10*19)*2=380; in total, 26980 judgments were collected. These 71 observers include 28 males and 43 females. The average age is 23.06 (SD=14.49), including 50 teenagers and 21 adults.

The impression scales included adjectives: “elegant,” “friendly,” “professional,” “authoritative,” “dependable,” “competent,” “solemn,” “genuine,” “warm-hearted,” “modest,” “gentle,” “sociable,” “healthy,” “serious,” “responsible,” “natural,” “self-confident,” “energetic,” and “thoughtful.” The data collected used a 7-step categorical judgment, indicating the strength of how well the impression scale describes the makeup looks, from “irrelevant” to “strongly related to.” For the experimental samples, ten makeup looks were used. The techniques used for each look are summarized in Figure 2.

These ten makeup looks are drawn on a facechart and applied on actual face of a female model. The facechart is a 70-pound A4 photocopy paper printed with face outline, facial features, and hair, mapping out where to place makeup products, i.e., lips, blush, eye shadow, eyeliner, and false eyelashes. According to the makeup plan on the facechart, it is applied to a female model's face to create ten makeup looks. The facecharts are given in Figure 1. These makeup looks were created by the first author, who held a teaching position for seven years in the Department of Fashion Styling at Yuda Vocational High School, Taiwan.

The digital camera was used to take each makeup look on the female face under average exposure at a standard color temperature. The photos taken were displayed on the iPad for the observer to make impression judgments, as shown in Figure 2.

Table 1: Makeup Techniques for 10 Looks.

No.	Makeup technique
M1	The eye shadow is a reddish-brown gradient, and the blush and lipstick adopt similar colors. It is commonly known as the dry rose in the cosmetics market.
M2	The eye shadow is a brown gradient, the blush is reddish brown, and the lipstick is red. The representative character is Marilyn Monroe.
M3	The upper eyeshadow is a pink gradient; the lower eyeshadow uses glitter. The blush and lipstick adopt a pink color.
M4	The eye shadow is a wine-red gradient, and the blush and lipstick adopt similar colors.
M5	The eye shadow is black gradient, and the blush and lipstick adopt pink color—emphasis on thick black eye makeup (including eyeshadow, eyeliner, and thick false eyelashes). The representative figure is the Canadian female singer Avril.
M6	Clear and natural nude makeup. The eyeshadow is a light brown gradient, and the blush and lipstick adopt light pink.
M7	The eye shadow adopts a purple two-stage style, and the blush and lipstick are similar colors.
M8	The eyeshadow is blue highlights, and the blush and lipstick adopt fuchsia.
M9	The eye shadow is a brown gradient, and the blush and lipstick adopt reddish brown.
M10	The eye shadow and blush are a light orange gradient, and the lipstick adopts a pumpkin orange color. The blush is large and horizontal, spanning the bridge of the nose.

Figure 1: Ten makeup looks used in the experiment as facechart.

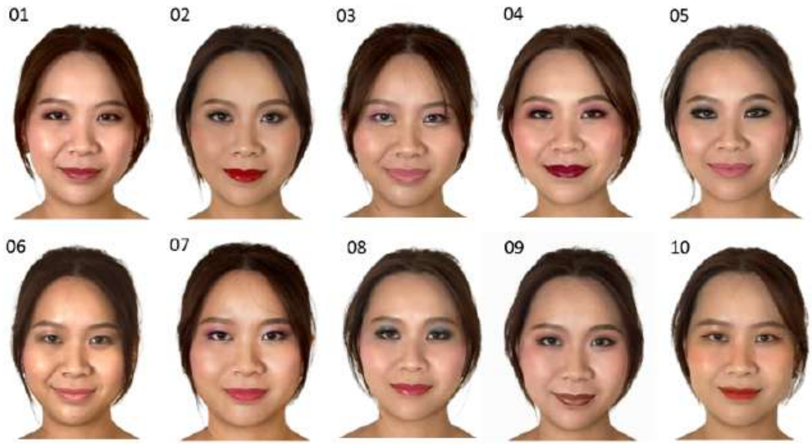

Figure 2: Ten actual looks used in the experiment as image makeup.

INTRA- AND INTER-OBSERVER VARIATIONS

The data collected from seven-step categorical judgement on each scale were converted into numbers. The higher the number, the more it fits the adjective description. In prior to analysis, the intra- and inter-observer variations were examined by RMS (root mean square). The former is to see whether the observers can repeat their judgment or not. The latter examines how well the individual observer agrees with the mean results. The RMS equation is given below.

$$\text{RMS} = \sqrt{\frac{\sum (X_i - Y_i)^2}{n}}$$

For intra-observer variation, X_i and Y_i are the initial and replicated judgement, respectively. For inter-observer variation, X_i and Y_i are individual data and all observers average, respectively. n is the number of data. For RMS of 0, it represents a perfect agreement between two data array. It can be seen that the intra-observer variations was ranged between RMS of 0.51 and 2.90. And the inter-observer variations was ranged between RMS of 0.93 and 2.63, as shown in Figure 3. Whether intra- or inter-observer variations, the RMS values are less than 3.0, indicating that the observers can provide consistent judgments, and the impression judgments obtained from individual observers agree with those obtained from all observers.

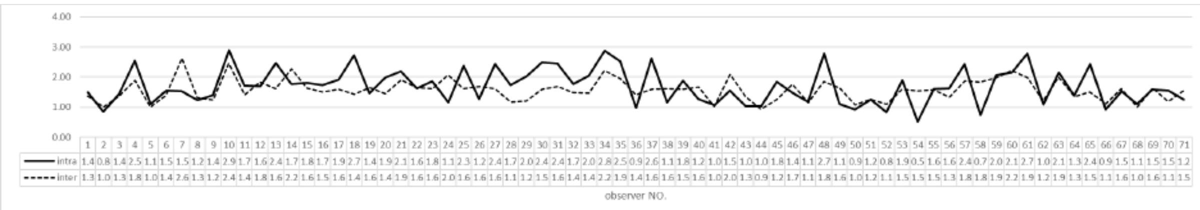

Figure 3: RMS for inter- and intra-observer variation

THE IMPRESSION DIFFERENCE BETWEEN ACTUAL MAKEUP LOOKS AND FACECHART

To understand the difference between the impressions given by makeup looks on the facechart and those on the actual face, the experimental data were illustrated in the profile chart, as shown in Figure 4. The RMS was used to calculate the actual difference, which can be used to observe the difference between two data arrays intuitively. The results are given in Table 2. Then, a T-test was used to see the statistical difference between the two data sets. The results are given in Table 3.

In Figure 4, the solid line represents the mean values of impression obtained from actual makeup looks, and the dotted line represents those obtained from the facechart. In Figure 4, it can be seen that the two-line trend appears in five patterns.

1. The first pattern is that the two lines overlap, meaning that all impressions of makeup looks on the facechart are consistent with those on the actual face. The makeup of M2 was found to belong to this pattern.

2. The second pattern is that the two lines are close and only some data points overlap, which means that the makeup impression on the facechart is close to those on real face, and some makeup impressions are consistent. M1 and M9 were found to belong to this pattern.
3. The third pattern is that the two lines appear parallel and close, which means that all the makeup impressions on the facechart are different from those on the real face, but all the difference is not large. It was found that the makeup of M4, M5, M7, and M8 all belong to this mode.
4. The fourth pattern is that the two lines are far apart, but there are still some data points that are close, which means that the impressions of makeup on the facechart are different from those on the real face and only on a few impression scales are close, including M6 and M10.
5. The fifth pattern is that the two lines are parallel and far apart, which means that the makeup looks on the facechart are inconsistent with those on the real face in all impression scales. The makeup of M3 was found to appear as this pattern.

Further, RMS was used to observe how distinct the impressions given by makeup looks on the facechart were from those on the actual face, and T-test was used to examine the statistical differences. The results obtained from RMS and T-test are given in Table 2 and Table 3, respectively.

In Table 2 and Table 3, it can be seen that the impression given by the makeup on the facechart and those on the actual face are significantly different in most impression scales. Only a few makeup impressions on the facechart are consistent with the real face. The overall difference in terms of RMS value is 1.96 on average. Regarding ten makeup looks, the RMS ranges between 1.44 and 2.40. Regarding the 19 impression scale, the RMS ranges between 1.81 and 2.28.

In terms of 10 makeup looks, M3 was found to have the most significant difference in impression between makeup looks on the facechart and the real face, M2 the minimum difference. In other words, the impression given by the makeup look consisting of a pink gradient on the upper eyeshadow, glitter on the lower eyeshadow, and pink blush and lipstick cannot be conveyed using a facechart. The impression given by the makeup look consisting of a brown gradient on the eyeshadow, a reddish brown blush, and red lipstick can be conveyed by a facechart.

Regarding the 19 impression scales, 'self-confident' was found to be the least discrepant scale. In other words, the impression scale of "self-confident" given by makeup on a facechart is the closest to the impression of the same makeup on the actual face.

RESULT AND DISCUSSION

This study intended to understand the difference between the impressions given by makeup look on facechart and those on actual faces. This study conducted an experiment in which 71 observers were invited to make impression judgments on ten makeup looks on facechart and actual makeup looks on 19 scales.

The results revealed the impression given by the makeup looks on the facechart and those on the actual face are significantly different in most impression scales. So, is the point of applying makeup on the facechart only to practice using cosmetics? However, it is worth noting whether the outline of the face on the facechart is similar to the actual face and whether the coloring strength of the cosmetics on paper and the skin makes the coloring results different. Future studies are recommended to explore the influence of face shape on the facechart.

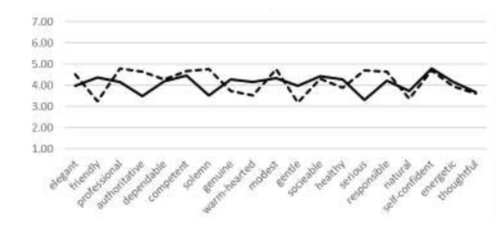

(a) Makeup 1

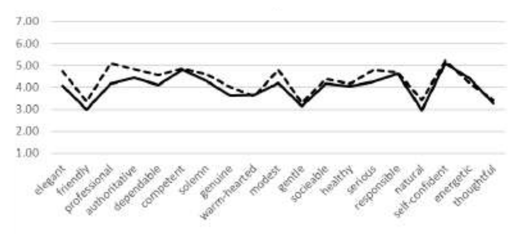

(b) Makeup 2

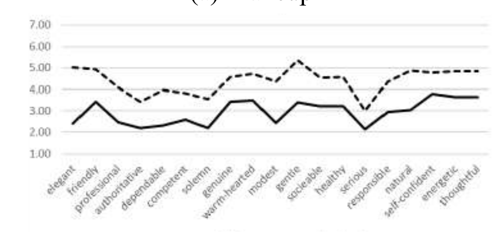

(c) Makeup 3

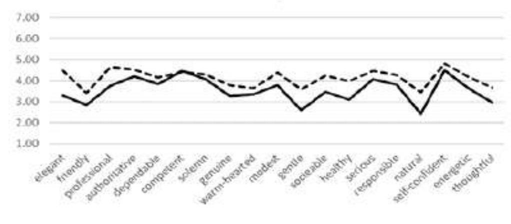

(d) Makeup 4

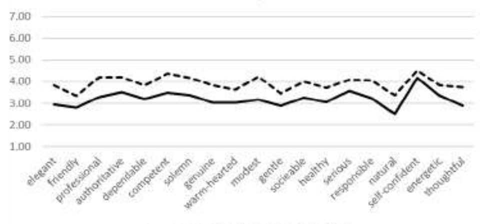

(e) Makeup 5

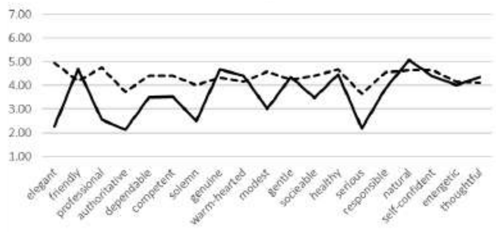

(f) Makeup 6

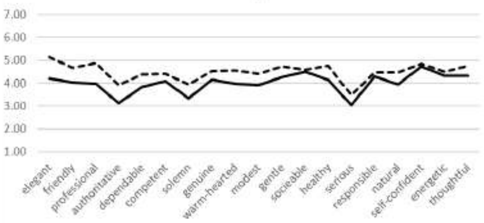

(g) Makeup 7

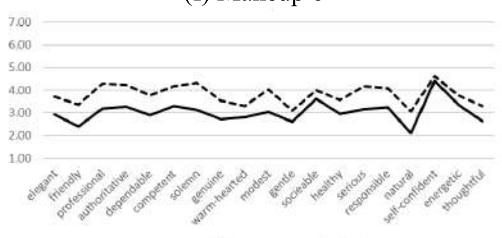

(h) Makeup 8

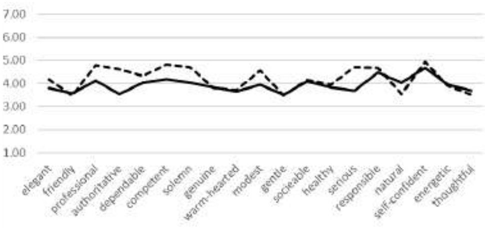

(i) Makeup 9

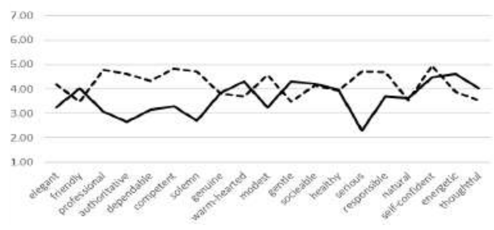

(j) Makeup 10

Figure 4 Profile chart of makeup looks on each impression scale. The solid line represents the actual makeup looks, and the dotted line represents the facechart.

Table 2: RMS between facechart and actual makeup looks

impression scales	makeup looks										
	M1	M2	M3	M4	M5	M6	M7	M8	M9	M10	Mean
elegant	2.22	1.49	3.26	2.58	2.23	3.29	1.89	1.76	1.84	2.23	2.28
friendly	2.12	1.45	2.59	1.86	1.82	2.42	1.99	1.67	1.68	2.05	1.97
professional	2.14	1.46	2.31	2.15	2.19	2.97	1.76	2.09	1.82	1.87	2.08
authoritative	2.49	1.58	1.87	2.06	2.24	2.49	2.01	2.42	1.97	1.58	2.07
dependable	1.92	1.38	2.19	1.85	2.00	2.03	1.78	1.94	1.72	1.75	1.86
competent	1.9	1.38	2.13	1.84	2.10	2.29	1.79	2.15	1.73	1.81	1.91
solemn	2.64	1.62	2.11	2.25	2.46	2.37	1.64	2.33	2.07	1.41	2.09
genuine	1.94	1.39	2.15	1.84	2.00	1.84	1.77	1.87	1.78	1.86	**1.84**
warm-hearted	2.16	1.47	2.15	1.93	1.76	2.09	1.85	1.52	1.78	1.98	1.87
modest	1.70	1.31	2.55	2.02	2.22	2.45	1.55	2.14	1.89	1.75	1.96
gentle	2.14	1.46	2.81	2.22	1.89	2.19	1.94	1.63	1.99	1.99	2.03
sociable	2.16	1.47	2.55	2.10	2.27	2.07	1.53	1.82	1.94	1.85	1.98
healthy	1.82	1.35	2.53	2.26	1.95	1.87	1.65	1.85	1.85	1.91	1.90
serious	2.60	1.61	1.82	1.94	2.19	2.15	1.92	2.36	2.17	2.03	2.08
responsible	2.07	1.44	2.31	1.78	1.91	1.97	1.65	2.33	1.71	1.75	1.89
natural	1.94	1.39	2.91	2.17	1.8	2.19	1.76	1.85	1.94	2.27	2.02
self-confident	1.78	1.33	2.49	1.99	1.95	1.79	1.59	1.87	1.60	1.70	**1.81**
energetic	1.82	1.35	2.24	2.18	1.76	1.92	1.54	1.86	1.91	1.85	**1.84**
thoughtful	1.85	1.36	2.57	2.04	1.84	1.89	1.73	1.82	1.72	1.81	1.86
Mean	2.07	**1.44**	2.40	2.06	2.03	2.23	1.75	1.96	1.85	1.87	1.96

Table 3: The significant differences between facechart and actual makeup looks by T-test. (95% significant level)

impression scale	M1	M2	M3	M4	M5	M6	M7	M8	M9	M10	Number of significant differences
elegant	*	**	***	***	**	***	***	***		**	9
friendly	***		***	*	*		**	***		*	7
professional	*	***	***	***	***	***	***	***	**	***	10
authoritative	***		***		*	***	***	***	***	***	8
dependable		*	***		**	***	**	***		***	7
competent			***		***	***		***	**	***	6
solemn	***		***		**	***	**	***	**	***	8
genuine	*		***	*	**			***			5
warm-hearted	*		***		**		*	*		**	6
modest	*	*	***	*	***	***	**	***	**	***	10
gentle	**		***	***	*			*		**	6
sociable			***	**	**	***					4
healthy			***	***	**		**	*			5
serious	***	*	***		*	***		***	***	***	8
responsible			***	*	***	**		**		***	6
natural			***	***	***		*	***	*		6
self-confident			***							*	2
energetic			***	*	*					**	4
thoughtful			***	**	***		*	**		*	6
Number of significant differences	10	5	19	12	18	10	11	16	7	15	

REFERENCES

Anchieta, N. M., Mafra, A. L., Hokama, R. T., Varella, M. A. C., Melo, J. d. A., da Silva, L. O., da Silva, C. S. A., & Valentova, J. V. (2021). Makeup and its application simulation affect women's self-perceptions. *Archives of Sexual Behavior*, *50*(8), 3777-3784.

Blunder, S. (2019). *Makeup Artist Face Charts: Facechart Makeup Book - Blank Paper Practice Face Chart Accessory for Professional Makeup and Student*. Independently Published. https://books.google.com.tw/books?id=zOZnzQEACAAJ

Chen, H. M. (2012). *Fashion Makeup Design*. Chuan Hwa.

Hsu, H.-H., Wu, C.-F., Cho, W.-J., & Wang, S.-B. (2021). Applying computer graphic design software in a computer-assisted instruction teaching model of makeup design. *Symmetry*, *13*(4), 654.

K-12 Education Administration, M. o. E. (2023). National High School Skill Competition of Information. In. Taiwan: Ministry of Education.

Kondrevich, L. (2020). *Facechart Drawing with Makeup*. WOO Publishing. https://books.google.com.tw/books?id=L2UEzgEACAAJ

Lien, H. (2019). *fashion illustration-styling & makeup*. Chuan Hwa.

Lin, S. C., & Yang, H. P. (2021). *Facechart of National Beauty Level B Examination*. CHUN,YING.

O'Sullivan, K., & Pinto, J. (2022). *Fashion Runway Makeup Looks, Makeup Inspiration Look Book: 25 Makeup Looks Inspired by the Runways of Top Fashion Designers*. Independently published.

INFLUENCE OF LIGHTING SPECTRA ON FACIAL APPEARANCE IN STATIC IMAGES, MOVIES, AND REAL ENVIRONMENT

Takuma Iwasaki[1]*, Hiromi Y. Sato[2] and Yoko Mizokami[2]

[1] *Graduate School of Science and Engineering, Chiba University, Japan.*
[2] *Graduate School of Engineering, Chiba University, Japan*

*Corresponding author: Takuma Iwasaki, taku_iwasaki2000@chiba-u.jp

ABSTRACT

Due to the COVID-19 pandemic, there has been a significant increase in the frequency of online meetings. Prior research has examined the impact of lighting on facial appearance in traditional face-to-face settings. In our study, we have demonstrated that lighting conditions also play a substantial role in shaping facial appearance within the context of online meetings. However, our investigation was limited to static images, and we did not explore the influence of dynamic facial movements. This study investigates the varying impact of lighting spectra on facial appearance across different contexts: static images, movies, and face-to-face interactions. We captured facial photographs of a model under the illumination of both desk lights and a base light, each with distinct correlated color temperatures (CCT) and spectral power distributions. During the evaluation phase, observers assessed multiple attributes, including brightness (dark-bright), preference (undesirable-desirable), naturalness (unnatural-natural), skin color (greenish-reddish and bluish-yellowish), texture (rough-smooth), shading intensity (weak-strong), clarity (unclear-clear), and visibility (hard to see - easy to see). During the evaluation phase in the online condition, images or movies featuring the model's face under different lighting conditions were displayed on an LCD monitor in a dark room. Conversely, an observer directly evaluated the model's face in the face-to-face condition. Initially, we compared static images captured in online and face-to-face settings. We deployed seven desk lights and ten cameras to photograph the model for this experiment. The evaluation results obtained in the face-to-face environment surpassed those in the online environment. This observation implies that the quality of facial impressions in images may deteriorate due to factors related to camera characteristics or the inherent limitations of static 2D representations. Next, we proceeded with a comparison between static images and movies. Our experimental setup involved five desk lamps and four cameras. The model's head displayed basic movements in the video recordings, including nodding. The evaluation results indicated a slightly superior performance for static images compared to movies. In both experiments, we consistently found that lighting conditions with a higher color rendering index were rated more favorably, even when the CCT remained the same. These results suggest that people tend to look better in real-life situations. However, they also highlight that the influence of lighting spectra remains notably similar in both static images and movies.

Keywords: Lighting, Lighting spectra, facial appearance, online meeting, real environment

INTRODUCTION

Lighting plays a crucial role in shaping facial appearance [1]. Furthermore, online meetings have become increasingly prevalent with the advent of the COVID-19 pandemic. Many studies have examined how lighting affects facial appearance in traditional face-to-face settings. For instance, it has been observed that lower correlated color temperature (CCT) lighting, such as that from a desk light, tends to result in lower evaluations of brightness [2]. Additionally, the spectral power distribution (SPD) of lighting is of significance, as it can influence the perceived facial color even when CCT remains constant [3]. While a few experiments have explored the impact of lighting in online environments [4], there is still a need to compare face-to-face and online contexts and examine the differences between static images and movies.

This research addresses these gaps by investigating disparities between online and real-world environments and comparing static images to movies regarding their response to varying lighting conditions.

METHODOLOGY

Experimental equipment

To create stimuli for our experiments, we captured photographs and movies of the model's face illuminated by a desk light under various conditions. The side view of the booth is shown in Figure 1. The model was seated at a desk in a booth lit by a white base light providing an illuminance of 250 lx at the desk. A camera, positioned at the same height as the model's face and 50 cm away from it, was used for image and video capture. The desk light was situated at a height of 45 cm and 40 cm in depth from the model's face. In online conditions, the images or movies of the model's face were presented on an LCD monitor in a dark room, as shown in Figure 2. In face-to-face conditions, the observers directly evaluated the model's face in the booth.

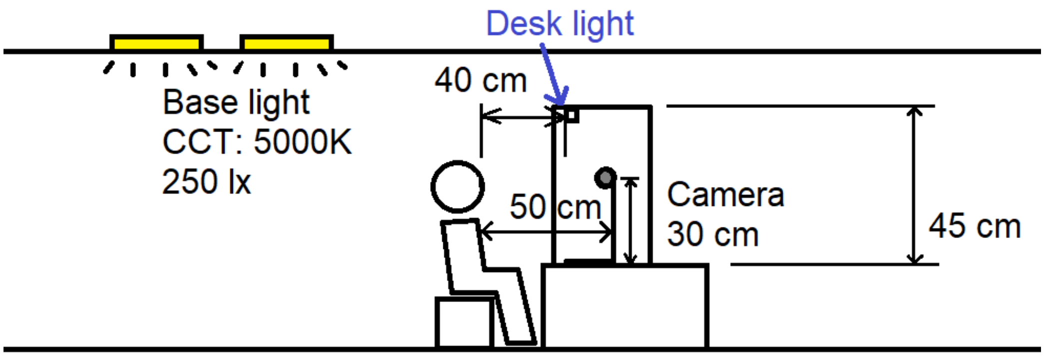

Figure 1. A schematic side view of the room where we captured images and videos of the model's face

Figure 2. Example of the display in the evaluation phase

Experiment 1: The Comparison between Face-to-Face and Online Environments

Our first experiment examined the difference between face-to-face and online environments. We employed seven desk lights, each characterized by distinct spectral power distributions (SPDs) – a combination of narrowband and broadband spectra – and CCTs approximately set at 5000 K or 3000 K, as illustrated in Figure 3. The relative spectral power is on the figure's vertical axis, while the horizontal axis represents the wavelength. These desk lights were named as follows: Red-enhanced (CCT: 5000 K, the color rendering index: $R_a = 52$), High color rendering (CCT: 5000 K, $R_a = 95$), Vivid color (CCT: 5000 K, $R_a = 94$), Normal type (CCT: 5000 K, $R_a = 82$), Low blue-light (CCT: 5000 K, $R_a = 90$), Fresh food (CCT: 5000 K, $R_a = 95$), and Incandescent color (CCT: 3000 K, $R_a = 97$). We used ten cameras to capture photographs of the model's face.

During the evaluation phase, facial images captured under seven different lighting conditions using a single camera were sequentially displayed on a screen within a darkened room. Each image occupied a visual angle of approximately 10 degrees by 10 degrees. Observers assessed each image individually, and the subsequent image taken by another camera was displayed. There was no time limit for the observation process. Ten observers evaluated these facial images before evaluating the model's face in a face-to-face setting. In the face-to-face environment, an observer sat in front of the model at a distance of 110 cm and assessed the model's face under each desk light. The model tried to remain as still as possible. The base light condition in this environment remained consistent with that used in the online setting.

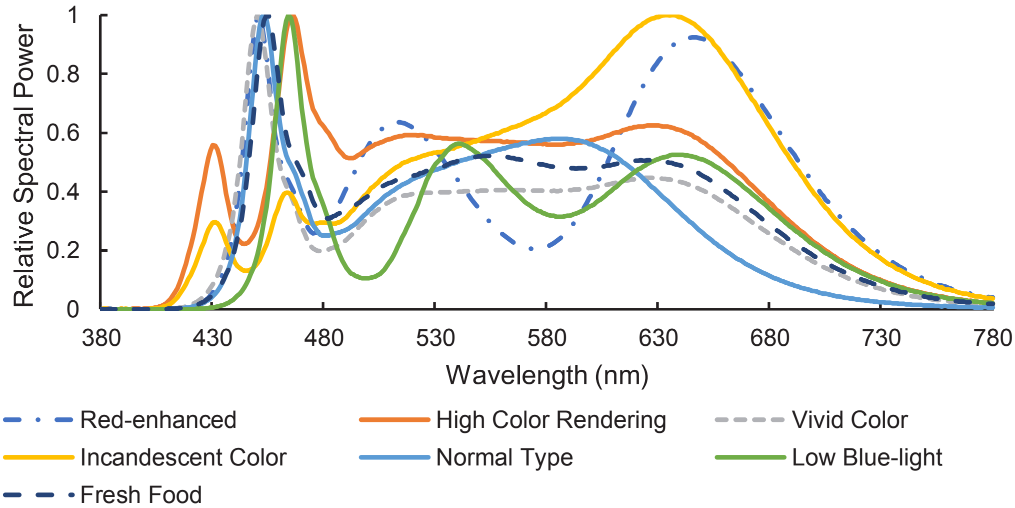

Figure 3. The relative radiant intensity of the desk lights used in the experiments

Experiment 2: The Comparison between Static Images and Movies

Our second experiment aimed to investigate the distinctions between static images and movies. We selected five desk lights from Experiment 1: Redness-enhanced, High color rendering, Normal type, Blue-light weakened, and Incandescent color, as shown in Figure 3. We also employed four cameras to capture photographs of the model's face.

During the evaluation phase, facial images captured under five lighting conditions using a single camera were presented sequentially on a screen. Each image had a visual angle of approximately 10 degrees by 10 degrees. There was no time limit for the observation process. However, they were instructed to observe at least one full rotation during the auto-play of the movies. The evaluation procedure began with the assessment of static images, followed by the evaluation of the movies. The ten observers participated in each condition.

RESULT AND DISCUSSION

The result of Experiment 1

The results for preference and naturalness in Experiment 1 are depicted in Figure 4. The vertical axis represents the evaluation criteria, while the horizontal axis corresponds to the evaluation scores. Each data point reflects the average assessment from all cameras and observers, with error bars indicating the standard deviation. Generally, evaluations in the face-to-face environment scored higher compared to those in the online environment. The results of the three-way ANOVA indicate a significant difference between the online and face-to-face conditions ($p < .05$).

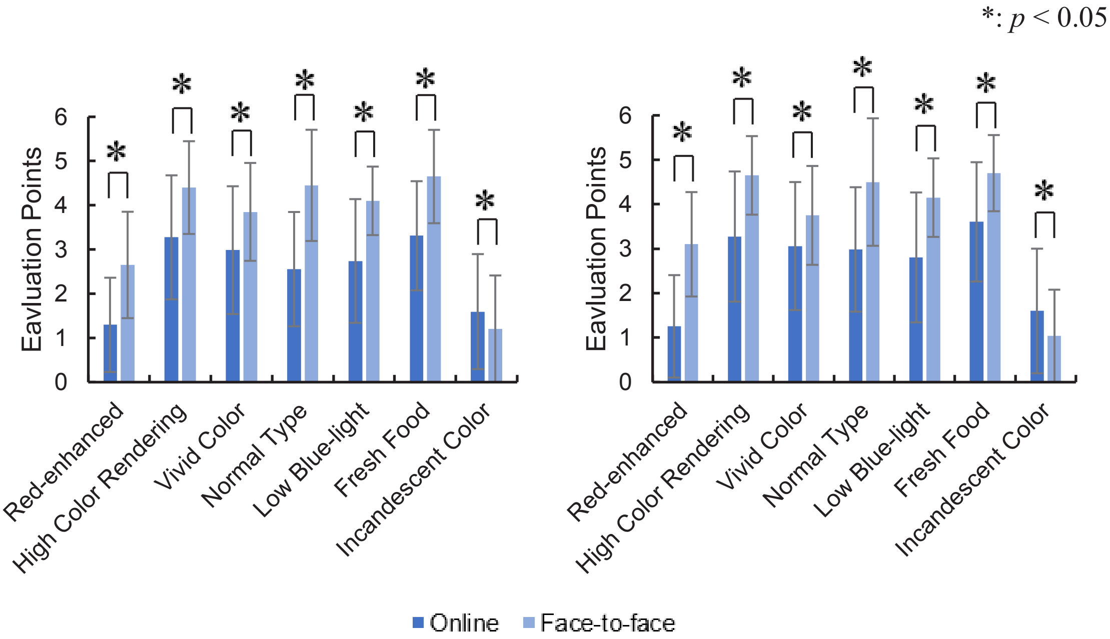

(a) Preference (b) Naturalness

Figure 4. The results for Preference and Naturalness in Experiment 1

The result of Experiment 2

The results for preference and naturalness in Experiment 2 are presented in Figure 5. The vertical axis represents the evaluation scores, while the horizontal axis corresponds to the evaluation scores. Each data point represents the average assessment from all cameras and observers, with error bars indicating the standard deviation. Overall, it is apparent that movie evaluations tended to be slightly higher than those based on static images. However, we did not find a statistically significant difference in the current results.

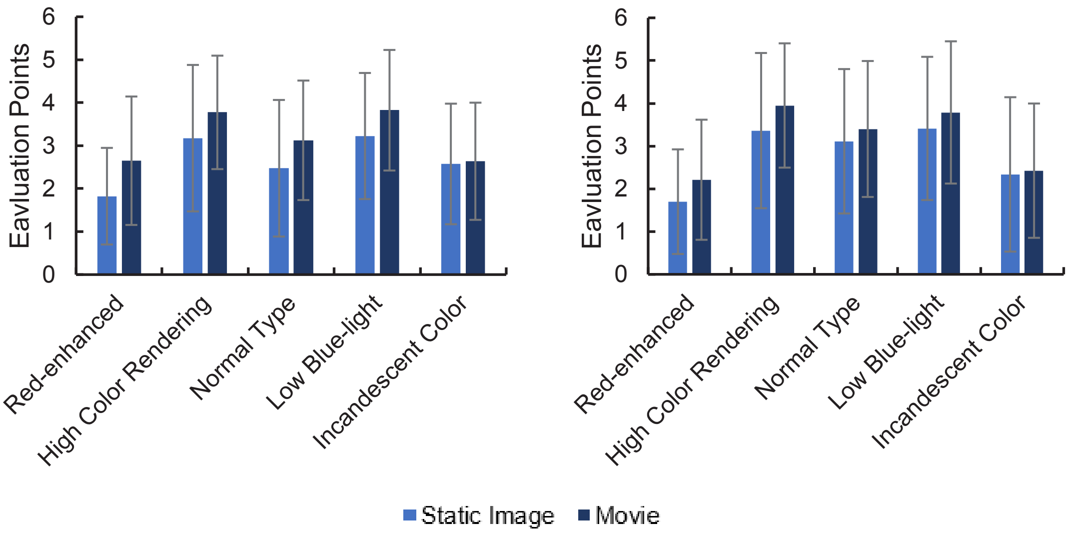

(a) Preference (b) Naturalness

Figure 5. The results for Preference and Naturalness in Experiment 2

Discussion

We analyzed the relationship between the evaluation results and the color rendering index R_a. Figure 6 illustrates the correlation between the color rendering index and preference or naturalness based on the findings from Experiment 1. The vertical axis represents the evaluation scores, the horizontal axis displays the average color rendering index (R_a), and the straight line represents the approximate trendline, excluding the incandescent color condition. Both preference and naturalness are higher for desk lights with a higher color rendering index. This suggests that lighting conditions resembling natural light tend to create a more favorable facial impression.

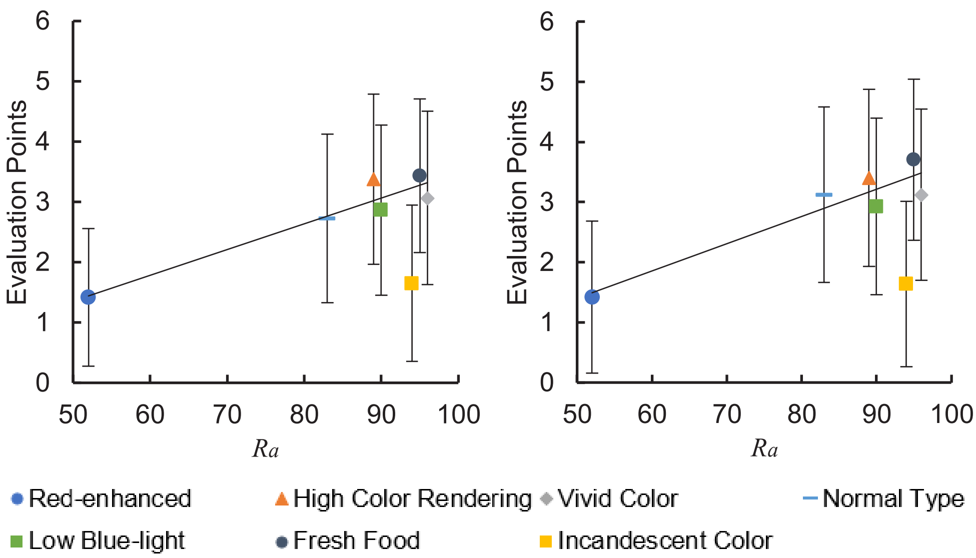

(a) Preference (b) Naturalness

Figure 6. The relationship between the color rendering index and the evaluation scores for preference and naturalness, as observed in Experiment 1

CONCLUSION

n this study, we conducted experiments to investigate disparities between online and real-world environments and between static images and movies. Regarding the experimental environment, we observed higher evaluation scores in the real-world setting compared to the online environment. Concerning the experimental stimuli, we noted slightly higher evaluation results for movies than for static images. Notably, even when the correlated color temperature (CCT) was the same, lighting with a high color rendering index consistently received higher evaluations, suggesting that lighting conditions resembling natural light tend to create a more favorable facial impression.

ACKNOWLEDGEMENT

This study was supported by JSPS Core-to-Core Program (JPJSCCB20220006) and JSPS KAKENHI (JP19H04196, JP21K 05805, and 23H04332).

REFERENCES

1. Lim, D. Y., Lee, A. L., & Or, C. C. F. (2022). Incongruence in lighting impairs face identification. *Frontiers in Psychology, 13*, 834806
2. He, J., Lin, Y., Yano, T., Noguchi, H., Yamaguchi, S., & Matsubayashi, Y. (2017). Preference for appearance of Chinese complexion under different lighting. *Lighting Research Technology*, *49*, 228-242.
3. Sato, C., Fuchida, T., Kobori, T., Komatsubara, H., & Suzuki, T. (1993). Subjective evaluation of natural skin and make-up skin color under incandescent lamps and fluorescent lamps. *Journal of Illumination Engineering Institution Japan*, *77*(10), 627-635 (in Japanese)
4. Iwasaki, T., Sato, H. & Mizokami, Y. (2022). How does the lighting condition affect facial appearance at an online meeting? *Proceedings of the 13th Asia Lighting Conference*, 84-91

EXPLORING RELATIONSHIPS BETWEEN SKIN TONE AND PERSONAL COLOUR

Suchitra Sueeprasan*, Nattapat Sakulpuchapong and Napatsorn Srichinarat

Department of Imaging and Printing Technology, Faculty of Science, Chulalongkorn University, Thailand.

*Corresponding author: Suchitra Sueeprasan, suchitra.s@chula.ac.th

ABSTRACT

Personal colour analysis is a process of identifying an individual's best colours based on their skin tone and skin undertone. It is typically performed by a trained analyst and generally involves a method to determine skin undertones and a fabric draping method. This analysis is costly and highly subjective. Since personal colour depends on skin tone and skin undertone, it is possible that there is a relationship between colorimetric values of skin tone and personal colour types. This study investigated the relationships between skin tone colorimetric values and personal colour types. Forty subjects participated in the experiments. Their skin tones in cheek areas were measured in terms of CIELAB colour values with a spectrophotometer (D65/2, specular included). The vein test, in which the veins on the inside of the individual's wrist were examined, was performed to determine a subject's skin undertone (warm, cool, or neutral undertone). Each subject was then classified into one of the seasonal personal colour types (spring, autumn, winter, or summer) by means of the fabric-draping method. According to the principles of personal colour analysis, warm undertones (spring and autumn colour types) go well with warm hues (such as yellow, orange and red). In contrast, cool undertones (winter and summer colour types) look best with cool hues (such as green, blue and purple). Seasonal colour types differ in brightness and saturation. For example, spring colours are in a range of warm hues that are bright and saturated, while autumn colours are deep and rich warm hues. The results showed the potential of skin colorimetric data for personal colour analysis. For higher precision, more data are needed. The colorimetric distributions of the four seasonal colour types were clearly separate. The summer and winter types had reddish skin, but they were separated by chroma and lightness. The skin tones for the summer type had low chroma but high lightness, while for the winter type had high chroma. The similar trends were found for the spring and autumn types (yellowish skin tones). The skin tones for the spring type had lower chroma than those for the autumn type.

Keywords: Personal colour analysis, skin tone, skin undertone, seasonal personal colour

INTRODUCTION

Personal colour refers to the colours that best complement an individual's natural complexion, hair, and eye colours. Wearing colours that suit a person best can enhance their overall appearance and make them look healthier, more vibrant, and more attractive. It can benefit work or personal relationships by boosting confidence and self-esteem and leaving a good impression. Personal colour analysis is a process of identifying an individual's best colours based on their skin tone and skin undertone [1]. It can help people determine which colours of clothing, makeup, and accessories will flatter them the most and make them look their best. Personal colour analysis is typically performed by a trained analyst and generally involves a method to determine skin undertones and a fabric draping method [2,3]. This analysis is costly and highly subjective. It is also strictly performed under natural daylight. Hence, it is advantageous to have an easily-performed, objective method. Since personal colour depends on skin tone and skin undertone, it is possible that there is a relationship between colorimetric values of skin tone and personal colour types.

The Four Season Framework

Seasonal colour analysis categorizes individuals into four broad color types based on their skin tone, undertone, and other personal characteristics. Each type is associated with a specific season (spring, summer, autumn, and winter), and individuals within each type are advised to wear colors that harmonize with their natural coloring [4].

Spring: Individuals with warm, golden undertones find their colours in the spring palette, featuring vibrant hues like coral, periwinkle, and soft greens.

Summer: Cool undertones, such as rosy or olive complexions, define the summer palette, which includes serene pastels, soft blues, and lavender shades.

Autumn: Warm undertones with earthy and rich complexions are categorized under the autumn palette, boasting warm, deep shades like cinnamon, moss green, and burnt orange.

Winter: Cool undertones with striking contrast are characteristic of the winter palette, featuring bold, jewel-toned colours like royal blue, emerald green, and true red.

Skin Tone and Undertone in Personal Colour Analysis

To determine one's seasonal palette accurately, understanding one's skin tone and undertone is paramount. Skin tone refers to the overall coloration of the skin, while undertone refers to the subtle hints of colour beneath the surface [2]. Traditionally, subjective methods relied on visual assessment, which often led to misclassification and suboptimal colour choices.

Replacing subjective methods with objective skin colour measurement empowers individuals to make informed decisions about clothing, makeup, and personal styling. Scientifically validated personal colour analysis ensures that the chosen colours harmonize with an individual's natural complexion, enhancing their appearance and bolstering self-confidence [3]. This study thus explored the complex interplay between personal colour and skin colour measurement.

METHODOLOGY

Forty subjects, 14 males and 26 females, 19–24 years old, participated in the experiments. Their skin tones in cheek areas were measured in terms of CIELAB colour values with a Konica Minolta CR-700 spectrophotometer (D65/2, specular included, MAV aperture size). To determine their skin undertone (warm, cool, or neutral), the vein test [2] was performed, whereby the inside of the individual's wrist were examined under natural light. If the veins appeared blue, the subjects were classified as having cool undertones. If they appeared green, the subjects had warm undertones. If their veins appeared both blue and green, they had neutral undertones.

Spring **Summer** **Autumn** **Winter**

Figure 1. Draping test

The fabric-draping method [3] was performed to classify the subjects into one of the seasonal personal colour types (spring, autumn, winter, or summer). This method involves draping different coloured fabrics around an individual's shoulders. The analyst will observe how the colours interact with the individual's natural complexion, hair color, and eye color to determine which colors make them look most vibrant and healthy. As shown in Figure 1, a set of fabric swatches in a range of colours, including warm and cool tones varying in lightness and chroma, was placed on a subject's shoulders. There were four sets according to the four seasons of personal colour types. Each set was placed one after the others to determine which set looked best on the subjects. In this study, the personal colour analyses were carried out by two experimenters who were trained by a professional.

RESULT AND DISCUSSION

From 40 subjects, 8 subjects had cool undertones, 13 warm undertones, and 19 neutral undertones. Figure 2 illustrates the colorimetric distributions in CIELAB for the three undertones. The 60-degree hue-angle line is included in the a^*, b^* plot. This line separates the yellow and red categories of Pantone SkinTone Guide samples [5]. The samples above the 60-degree line are labelled as yellow skin tones, corresponding to warm undertone. On the contrary, the samples below the 60-degree line are red skin tones, corresponding to cool undertones. The distributions of skin undertones found in this study did not agree well with the Pantone categories. Both warm and cool undertones spread across the 60-degree line. However, the warm undertones covered a wider range from yellowish to reddish. In contrast, the cool undertones covered a wider range of chroma. In the case of neutral undertones, the distributions spread widest, covering from yellowish to reddish, and from low to medium chroma. The clear trends to determine skin undertones using colorimetric values were not observed. One possible reason was that the number of samples was too few. Given the Pantone categories divided by the 60-degree line, there are 7 yellow skin sample located below the line. Since there are 110 samples in Pantone SkinTone Guide, the exceptions of 7 show the clear separation between the two categories. However, only 8 warm undertones were found in this study, 4 of which lied below the separate line, and 3 above. If there had been more samples, the trend regarding the hue-angle could have been observed. Nevertheless, it can be observed that cool undertones tended to have lower b* values (yellowness) than warm undertones.

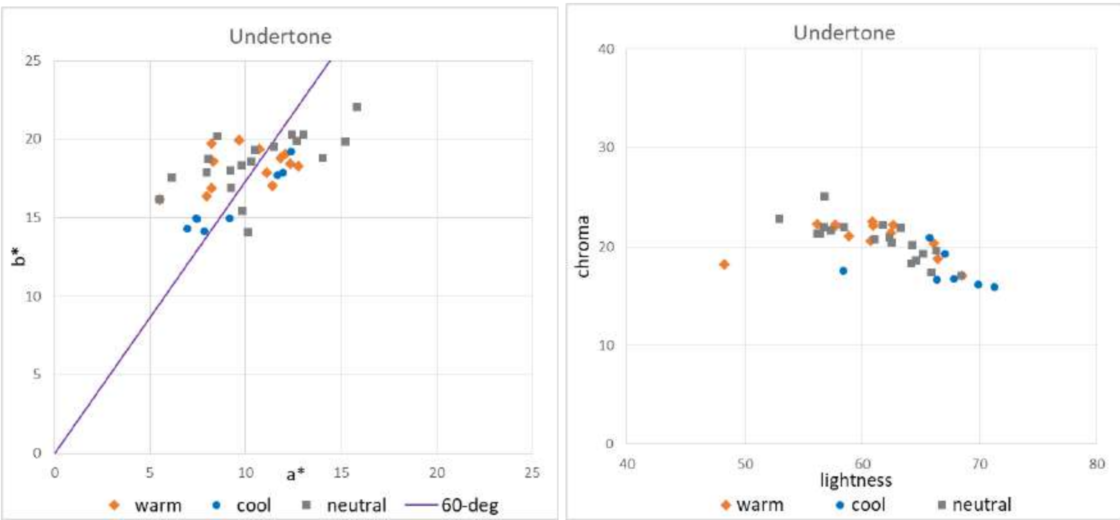

Figure 2. Distributions of skin undertones in CIELAB colour space.

It is important to note that the vein test and any other subjective methods of personal colour analysis are not definitive. Thus, another possible reason for unclear colorimetric trends was that the classifications of skin undertones were not precise. Some subjects' undertones may be less apparent using the vein test and were classified into the wrong undertones. Besides the vein test, there are several methods to determine skin undertones such as the jewelry test [2]. This suggests that future studies should include more methods of personal colour analysis for precise results.

Considering the spread of lightness, it was found that the three undertones covered the range from low to high. This finding agrees well with the principles of personal colour analysis, in which skin undertones can vary in the shade of skin tones (light, medium, and dark). When combining skin undertones and skin tones, personal colour can be categorized into four seasonal types (spring, summer, autumn, and winter).

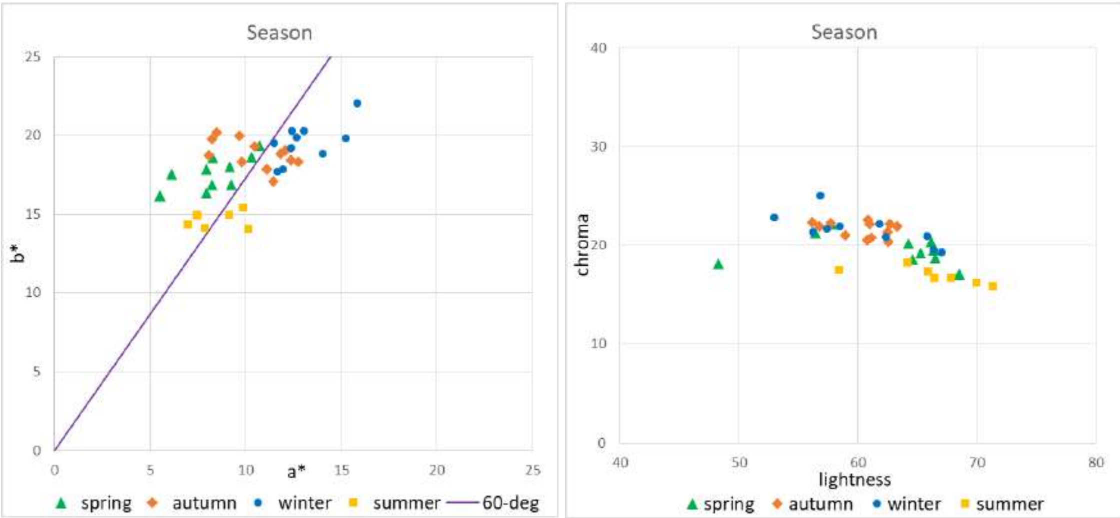

Figure 3. Distributions of seasonal personal colours in CIELAB colour space.

Figure 3 shows the distributions of four seasonal personal colours in CIELAB. Spring and autumn types are categorized by warm undertones, while summer and winter by cool undertones. It was found that subjects with a personal colour of winter (cool undertones) had reddish skin tones with high chroma and lightness ranging from low to high. On the other hand, subjects having warm undertones and classified as spring or autumn personal colour types had yellowish skin tones. In the case of summer, the skin tones varied from yellowish to reddish with low chroma and high lightness. The distributions of seasonal personal colour showed noticeable trends. The summer and winter types having the same undertones (cool) were clearly separated by chroma and lightness. The winter type had higher chroma, while the summer type had higher lightness. The similar trends were also found for the seasonal types having warm undertones (spring and autumn). The autumn type had higher chroma, while the spring type had higher lightness.

CONCLUSION

The results showed the feasibility of personal colour analysis based on skin colour measurements. The distributions of colorimetric values agreed well with the four seasonal personal colour types. However, clear trends were not found in the distributions of skin undertones. The methods to determining skin undertones may not be precise. All existing methods of personal colour analysis are subjective. Individual variations exist. Some may be more apparent in one method than the others. While there are general guidelines for each seasonal colour type, not everyone fits neatly into these categories. Consequently, the future work should include more methods to confirm the results. More skin samples are also needed for higher precision.

ACKNOWLEDGEMENT

The authors wish to acknowledge the financial support from the Faculty of Science, Chulalongkorn University. Thanks also go to all subjects who took part in the experiments.

REFERENCES

1. Cassidy, T. D. (2007). Personal colour analysis, consumer colour preferences and colour forecasting for the fashion and textile industries. Colour: Design & Creativity, 1(1), 6.
2. Nasr, M. M. (2018) Identifying the role of skin tone in choosing the suitable colors for outfits & fashion accessories, International Journal of Textile and Fashion Technology, 8(3), 1-14.
3. Mathis, C. M., & Connor, H. V. (1994). The triumph of individual style: a guide to dressing your body, your beauty, yourself. Colombia: Timeless Editions.
4. Jackson, C. (2011). Color me beautiful: Discover your natural beauty through the colors that make you look great and feel fabulous. Ballantine Books.
5. Iranmanesh, B., Gholamianpour, A., Kandi, S. G., Ansari, K., & Asl, M. A. (2017, December). Brief overview of PANTONE SkinTone Guide chart in CIEL* a* b color space. *The 7th International Color & Coating Congress*, Tehran, Iran, Amirkabir University of Technology.

CONTINUOUS SKIN COLOR CLASSIFICATION OF WARM-NETURAL-COOL

YungKyung Park[1]*

[1]*Art & Design Department, Associate Professor, Ewha Womans University, Republic of Korea.*

*Corresponding author: YungKyung Park, yungkyung.park@ewha.ac.kr

ABSTRACT

Make-up customized by the individual is preferred, based on the diagnosis of individual skin color. Because of this tendency, it is necessary to diagnose skin color accurately. There are no difficulties when distinguishing between different races, but there is a problem in dividing similar skin colors like Koreans' skin colors. Cosmetic liquid foundation colors were measured and labeled in three color tones Warm, Cool, and Neutral. Each tone had six levels of shading which had different lightness and chroma. In the CIELAB space, only hue could distinguish Neutral-Warm-Cool tone, and in the Lightness-Chroma plane, it was not possible to distinguish due to severe overlap. In addition, since it is not continuous between natural, cool, and warm, it is not possible to know a continuous tone with only the hue value. The CIELAB color space may be suitable for specifying skin color, but the tone is limited. The interval between RGB will be able to inform the classification of tone and it will be able to continuously represent changes in tone. The ratio between the interval of RGB values is considered a variable for predicting the tone. This new index has the advantage of obtaining tone as a continuous value of Warm-Neutral-Cool while using RGB color space. Through this new index, not only the classification of tone but also the degree of tone can be known.

Keywords: Skin color, Warm, Neutral, Cool, RGB color space

INTRODUCTION

In the beauty industry, there has been a tendency of globalized preference for whiteness and/or light skin color. Nowadays interest in personal color is gradually growing for skin color. Make-up customized by the individual is preferred, based on a diagnosis of individual skin color. In accordance with this tendency, it is necessary to diagnose skin color accurately. Human skin color is controlled by both genetic and environmental factors and is affected by several factors such as multi-layers, veins, spots, pigmentations, etc. They can determine skin color bringing about skin color changes, so skin color varies across different body locations and is therefore inaccurate. For these reasons, human skin color is hard to measure as a single-color value. Since it is not single-color, there are also studies to analyze skin color on images [1]. However, there is a disadvantage that verification is difficult because it consists of RGB color space, not a measuring instrument. Despite the lack of strict classification rules, each cosmetic brand set up a standard of skin color dividing skin tone broadly into two; cool tone or warm tone with several stages depending on brightness. However different criteria aren't standardized, and it is difficult to apply one criterion to all races. Therefore, this study investigated how to classify the tone and brightness of human skin by hue. Hue is easier for non-professionals to answer and has a wider choice than warm and cool skin color. Companies cannot match cosmetics to all skin colors. Especially for women in Korea, the difference in skin color will not be much different from other races but still can be classified by different hues [2]. However, even within them, cosmetics are divided into warm, cool, and neutral and each brightness stage exists. In the CIELAB space, it can be said that measuring skin color is the most common method. Borza et. al [3] study used RGB, HSV, and Lab to classify facial images as skin tone, but Lab is said to be the most suitable color space with the lowest errors. There are no major lumps when distinguishing between different races, but there is a problem in dividing similar skin colors like Koreans' skin colors.

METHODOLOGY

Due to the difficulty of measuring skin color, the tendency was analyzed by analyzing the foundation color that reproduced skin color. The foundation's color is uniform and opaque when present in a liquid state, making it easy to measure. Cosmetic liquid foundation colors were measured using a spectrophotometer CM-5. The products were poured into a quartz chalet and measured under D65 SCI and 10-degree conditions. The products were labeled in three color tones Warm (W), Cool (C), and Neutral (N). Each tone had six levels of shading which had different lightness and chroma. The measurement procedure is shown in Figure 1 and the measured values are shown in Table 1. RGB values are converted using CIELAB values in 8-bit (0~255) sRGB space. The color chips used RGB values for visualization.

Figure 1. Measurement procedure for liquid foundation

Table 1: Measured values and RGB values of each tone and shade of liquid foundation

Tone No.	L	a	b	C	h	R	G	B	color
W10	87.9	9.6	24.0	25.9	68.1	255	213	174	
W20	85.0	11.0	26.0	28.2	67.1	250	204	163	
W30	79.0	12.0	29.0	31.4	67.5	235	186	141	
W40	72.0	14.3	28.0	31.5	63.0	218	166	125	
W50	62.0	14.0	26.0	29.5	61.7	188	140	104	
W60	56.0	13.0	24.0	27.3	61.6	169	125	92	

Tone No.	L	a	b	C	h	R	G	B	color
N10	90.0	10.0	12.5	16.0	51.4	255	219	201	
N20	87.7	11.6	19.5	22.6	59.3	255	211	182	
N30	82.0	16.0	26.0	30.5	58.4	249	192	155	
N40	74.0	18.0	30.0	35.0	59.0	230	169	127	
N50	63.0	16.0	26.0	30.5	58.4	194	141	106	
N60	52.0	13.0	20.0	23.9	57.0	156	115	90	

Tone No.	L	a	b	C	h	R	G	B	color
C10	84.0	16.0	22.0	27.2	54.0	253	198	168	
C20	80.0	17.0	24.0	29.4	54.7	244	186	153	
C30	76.0	19.0	26.0	32.2	53.8	236	174	139	
C40	67.8	20.3	27.7	34.4	53.7	215	151	115	
C50	57.0	18.0	22.0	28.4	50.7	178	124	99	
C60	52.0	16.0	22.0	27.2	54.0	161	113	86	

The first analysis was through the CIELAB space. Through the analysis of the Lab space, we looked at how the distribution of each tone (N, W, C) appeared in color. Next, we looked at how each tone can be distributed in RGB space and explained separately.

RESULT AND DISCUSSION

The measurement of all 18 colors is shown in Figure 2. The graph on the left shows L* (Lightness)-C* (chroma), and all three shapes have the highest chroma value at medium brightness. However, there are different chroma and lightness distributions for each shade. The maximum chroma value of Neutral and Cool is also like the Lightness of the maximum chroma value. The shade with the lowest chroma was Neutral, and the lower the chroma, the higher or lower the lightness.

In CIELAB space, only hue could distinguish Neutral-Warm-Cool tone, and in the Lightness-Chroma phase, it was not possible to distinguish due to severe overlap. The skin color may not have three tones clearly but maybe Neutral close to Warm, or Neutral, which is not biased toward either Warm or Cool. In the a*-b* plane, you can see that the three tones are divided by regions, but the problem is that they are not continuous. As expected, Neutral is in the first quadrant of the a*-b* plane, with warm and cool on both sides. In the case of Neutral, as the shade darkens, it moves away from the origin and returns, and Cool and Warm do not move as much as Neutral, and the shade changes in a small circle. In addition, since it is not continuous between Neutral, Cool, and Warm, it is not possible to know a continuous tone with only the hue value. The CIELAB color space may be suitable for specifying skin color, but the tone is limited. Another limitation is that although the tones are relative to each other, the absolute value may vary depending on the product or race. Therefore, it needs to be analyzed in another color space.

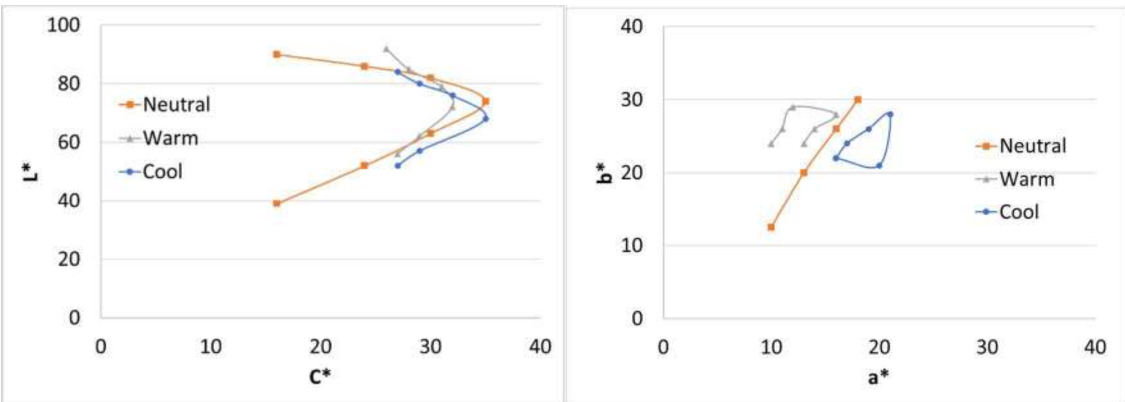

Figure 2. Measured values of each tone and shade of liquid foundation plotted on CIELAB L*-C* and a*-b*

Next, the tone was analyzed in RGB space, not CIELAB. The sRGB values listed in Table 1 are graphed in Figure 3 for each tone.

As you can see from the graph, R is the largest in all tones, followed by G and B. Warm shows that RGB values decrease as the shade darkens, but the intervals between the three values change similarly and the intervals are constant. On the other hand, in the case of Neutral and Cool, G and B are relatively close compared to R. You can see that Cool has a narrower gap between G and B. It can be predicted that the interval between RGB will be able to inform the classification of tone and that it will be able to continuously represent changes in tone.

The ratio between the interval of RGB values is considered as a variable for the equation of predicting the tone. Eq (1) is the equation for the tone classification index.

$$\text{Tone classification index} = \frac{(G-B)(R-B)}{(R-G)^2} \tag{1}$$

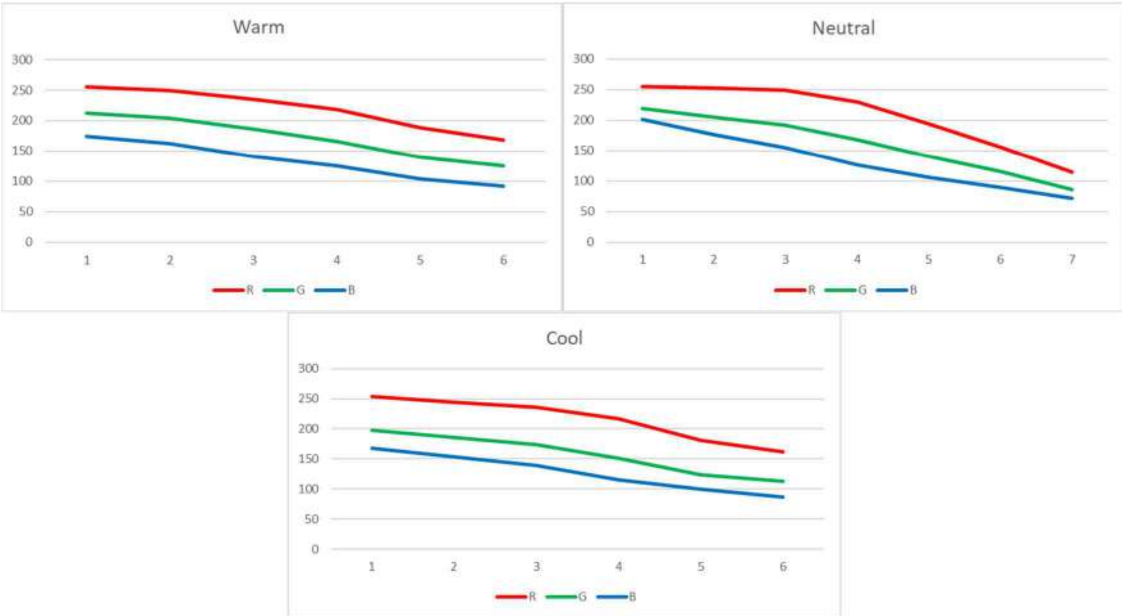

Figure 3. RGB values of each tone and shade of liquid foundation

Regardless of the shade, the larger the difference between R and G, the more it goes from Warm to Neutral to Cool can be seen on the graph. In Equation 1, the tone classification index decreases as the denominator increases, and the value of Warm has a low index. The lower index is the Warmest, and the higher the value, the Cooler it can be seen in Neutral. By this, the degree of Warm is calculated by continuous values, and which tone is closest among the three tones. This new index has the advantage of obtaining tone as a continuous value of Warm-Neutral-Cool while using conventional RGB color space. The tone classification could be W-N-C or WW-WN-NN-NC-CC or values between them.

CONCLUSION

Clusters with similar measurements, such as Korean skin color, were divided into tones. CIELAB color space is used the most to classify tone, but it is difficult to divide skin color tone into continuous values by hue or tone in classifying tone. To overcome this, a new 'tone classification index' was proposed using the relationship between R, G, and B values by measuring by the existing method but converting it into RGB values. Through this new index, not only the classification of tone but also the degree of tone can be known.

REFERENCES

1. D. A. Molina, L. Causa, & J. Tapia. (2020). Reduction of bias for gender and ethnicity from face images using automated skin tone classification. Paper presented at the - *2020 International Conference of the Biometrics Special Interest Group (BIOSIG),* 1-5.
2. D. Park, H. Hong, & Y. Park. (2019). Fine Classification of Korean Skin Color by Tone and Hue. *Journal of Korea Society of Color Studies, 33*(3), 36-44.
3. Borza, D., Nistor, S. C., & Darabant, A. S. (2017). Towards automatic skin tone classification in facial images. In *Image Analysis and Processing-ICIAP 2017: 19th International Conference, Catania, Italy, September 11-15, 2017, Proceedings, Part II 19* (pp. 299-309). Springer International Publishing.

APPARATUS TO STUDY TOTAL APPEARANCE

Jinyi Lin[1] , Tingwei Huang[2], Keith Hoover[3], Ming Ronnier Luo[1]*

1. *State Key Laboratory of Modern Optical Instrumentation, Zhejiang University, CHINA*
2. *Thousand Light Lighting (Changzhou) Ltd, Changzhou, China*
3. *Black Swan Textiles, LLC, USA*

*Corresponding author: Corresponding authors name, e-mail m.r.luo@zju.edu.cn

ABSTRACT

An appearance communication system for total appearance study and supply chain management, named LEDSimulator, was introduced in the previous AIC conferences[1,2,3]. A total appearance study was conducted based on the system, and two refines were added to improve the accuracy and generality of the system.

Keywords: Total appearance, spectral tunable LED lighting, LEDSimulator, Look-up table

INTRODUCTION

Total appearance is attracting growing attention. Devices have been developed to scale total appearance including 4 attributes: colour, texture, gloss and translucency. One of them is called LEDSimulator (LS), a colour communication system for supply chain management. The LS has been introduced in the previous AIC conferences. The system was also designee to be used in supply chain, i.e. to invent colours by designers, to specify colours by brands, and to reproduce coolers by dyers. The colour information was transformed in terms of CIELAB and spectral reflectance and truthfully reproduced by projecting colour on various textured substrates for appearance communication. Hence, we can investigate the impact of the projected colour on different textures, or interaction between colour and texture attributes. It has been tested at different sites in the textile industry. The unique feature of LS is to greatly reduce the lead time from design to production, designers can foresee the colours in the final texture.

Figure 1. System appearance

System hardware

The LEDSimulator consists of a viewing cabinet (LEDView) in the front and a dark room for projection in the rear (Fig.1). The front light box provides A multi-channel adjustable LED light source for creating a standard light environment, including D65, D50,A,TL84 and other light sources, as in most standard colour laboratories. In addition, the system is supplied with fluorescent tubes. The rear structure consists of a fixed darkroom with LED panels on both sides. The darkroom provides a stable light environment and is used to fix other structures, including the illuminated substrate. The LED Panels evenly project light from the three channels onto the base, which forms a colour display with a large gamut of the base texture. This colour display can be observed by an observer looking through the viewing window at the back of the light box.

System software and colour management

The viewing cabinet and LED Panels mentioned above are controlled by user-operated software for light source customization and colour display(Fig.2). Colour management is necessary for LED Panels. The colour management process mainly includes colour input, colour preprocessing, colour display and feedback. Colour input support R%/ illuminant, CIELab, etc., this usually has two methods, the user input standard colour file (.QTX), or choose the colour on the software interface, software including Lab or Lch data input and colour palette to meet different needs. The pre-processing mainly includes CIECAT16 to achieve the conversion of different light source environments. Colour display using the classical LUT(Look-up table) method, through interpolation and matching to determine the RGB channel value closest to the target colour, and finally displayed on the observation window. Users can then adjust depending on the colour displayed until they get the colour they want. The displayed colour can also be measured by a spectrophotometer (such as JETI) and compared to the input colour for error monitoring. The result of this comparison is called the sub-system accuracy. A 55-colour test set was used to test accuracy and a typical set of accuracy results is usually in the range of 0.25-0.40 CIEDE2000[4].

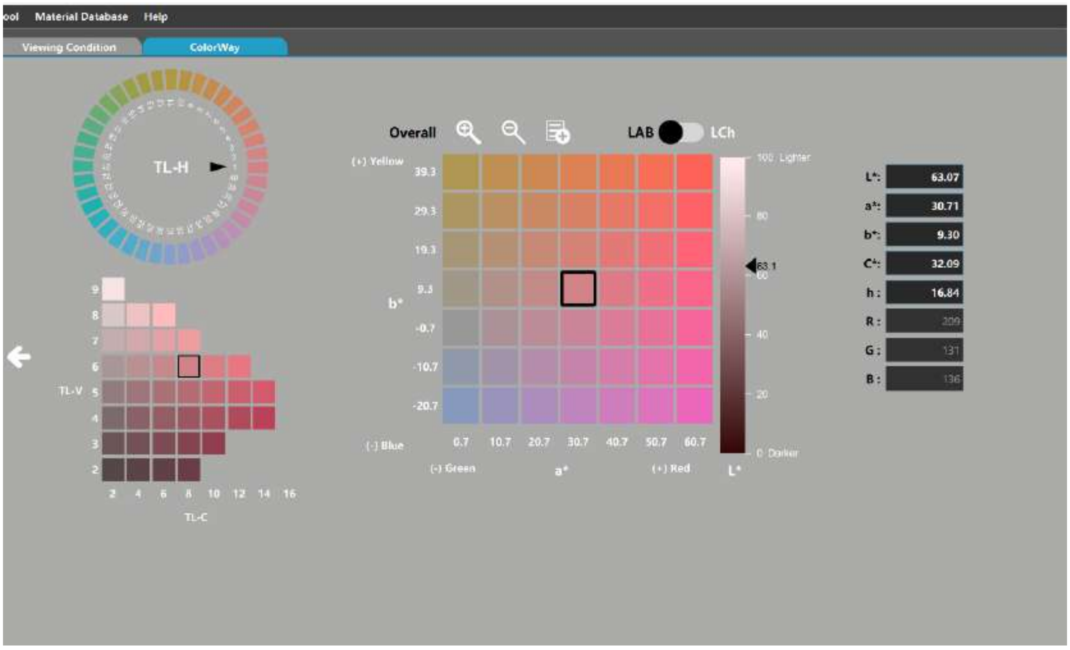

Figure 2. "ColorWay" interface for colour manipulation of a virtual

REFINES TO THE SYSTEM

Two refines to the system were applied this year, addressing two issues or requirements in the use process.

Polynomial calibration attempt for the metamerism

During the use of LEDSimulator, such situations may occur: This is a common use when an observer simultaneously looks at the display colour in the window and the real sample illuminated by the cabinet on the side of the window, their colour perception is different, even though the results measured by the spectrophotometer show that the CIEXYZ of the two colours are extremely close. In fact, for such a cross-device display device, the same colour visually has a different spectrum, which is a phenomenon of metamerism.

Such metamerism may be caused by the following factors: 1) different colour realization methods, in the cabinet, continuous analog spectrum irradiates samples with specific reflectance to form colours, while in the dark room, relatively narrow band LED spectrum irradiates on the substrate (they usually have a reflectance curve close to 1 and flat); 2) observer chromaticity spectrum, all colour XYZ is obtained by the CIE recommended standard observer, but in reality, the observer CMF (colour matching function) is different from the CIE standard observer, for the display of the same way, this difference will not appear. But in the case of cross-device replication, this difference is critical; 3) The difference between the simulated light source and the CIE standard light source, due to the high fit of the simulated light source, in fact, this difference has little impact on the system, and the estimated colour difference is about 0.2 CIEDE2000, compared with the total colour difference of 2.13.

So we ran a colour-matching experiment, The experimental settings were as follows: 10 experienced subjects (six males and four females, aged 21 – 27, with normal colour vision, and majoring in colour science), performed colour matching by adjusting the projected light in the system to match 60 physical colour samples viewed in a D65-500 lx light source. The colour system used for matching is “ColourWay”. Subjects adjusted CIELCh first, and, when close in neutral colours, the CIELAB colour system was applied to improve matching accuracy.

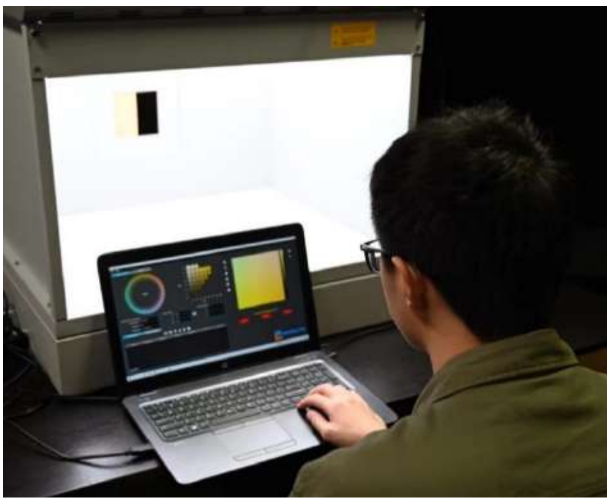

Figure 3. A subject is performing a colour matching experiment

Since the problem of metamerism is rooted in spectral differences, more research on metamerism is needed to fully solve it. In this case, a polynomial based calibration method is temporarily adopted to reduce this difference to a lower level[5]. The specific method is to transfer the input data of order 3 to the Lab space and expand it to dimension 9 (items 1-3 are the original input data, and items 4-9 are the combination of quadratic terms), and then get its value with the target value (the result of colour matching) through least square fitting.

In this method, the input colour is transformed by a polynomial matrix, and the result is more close to the human eye. In theory, this will reduce the colour difference observed by the observers from 2.13 to 0.65.

A new LUT approaches for projector characterization——AutoLUT

Now let's put our eyes back to the beginning of the system development, why the system uses LUT rather than a more efficient model (such as GOG model[6]), the answer is the crosstalk between LEDPanel, that is, the colour rendering between RGB channels does not follow the principle of superposition, but will interfere with each other. Therefore LEDSimulator adopts LUT method for colour management.

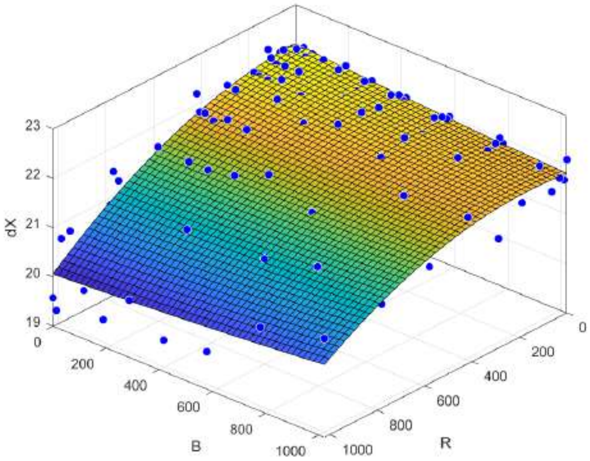

Figure 4. The delta X for different R and B as the G channel increases from 0 to 1023, In the absence of crosstalk, the image would have been a plane

This choice resulted in great colour accuracy, but it also created a problem. In actual use, users need to use their own samples as a substrate, which have different reflectance and textures, sometimes not even white or gray. Because of the LUT-based colour management system, this change of substrate means that a new LUT needs to be built, which usually means more than 40 minutes of time, and more importantly, most users do not have a spectroradiometerr like JETI, which makes it impossible to change the base while maintaining colour accuracy.

On the other hand, users can usually obtain reflectance data for custom samples. A method was developed to quickly build LUTs with only the input of reflectance, which is called AutoLUT. It is implemented as follows:

Step 1: To work out the 3 channels × 11 unequal intensity levels of the target substrate

$$SPD_T = SPD_R * \frac{R\%_T}{R\%_R} \tag{1}$$

where descriptors T and R represent target and reference respectively; SPD and R% are spectral power distribution and spectral reflectance of each sample, respectively.

Step 2: To compute SPD to XYZ

$$XYZ = CMF * SPD \tag{2}$$

where he CIE1964 10°.standard colourmetric observer (CMF) is used to establish the LUT, i.e.

Step 3: To compute the attenuation coefficient matrix

$$A_X = \frac{(X_{RGBr})}{(X_{Rr} + X_{Gr} + X_{Br})} \tag{3}$$

where $\boldsymbol{A_X}$ for attenuation coefficient of X, $\mathbf{X_{Rr}}$ for X of a particular R when G and B are equal to 0, $\boldsymbol{X_{RGBr}}$ for X of particular R, G, B that X_{Rr}, X_{Gr}, X_{Br} take, subscript, r, for reference LUT

Step 4: To calculate the simulated LUT

$$X_{RGBt} = (X_{Rt} + X_{Gt} + X_{Bt}) * A_X \tag{4}$$

where t for target LUT. For Y and Z, the calculation is the same as for X

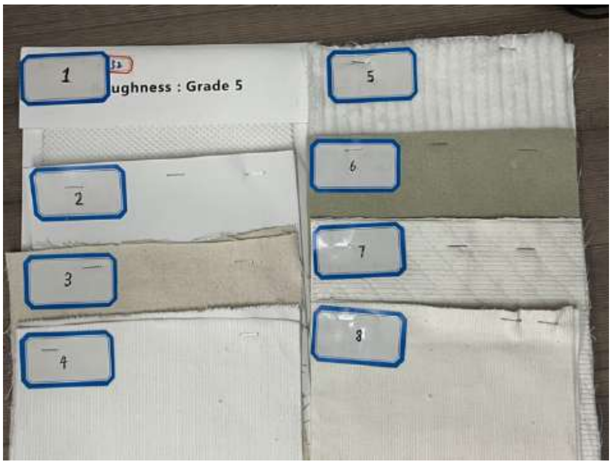

Figure 5. eight custom samples

The results are verified by the accuracy tests described above, using eight custom samples, as shown in Fig.5. Results are shown in Table 1. And the same tests are performed on the GOG model and polynomial model, as shown in Table 2. The results show that AutoLUT has the advantages of speed and accuracy on projector-like display devices with channel crosstalk.

Table 1. Accuracy result of eight custom samples, the numbers in parentheses represent test sets that are out of the gamut

Sample	DE00 with default LUT	DE00 with AutoLUT
Custom-T1	1.22	0.77
Custom-T2	1.53	0.67
Custom-T3	6.30	0.36
Custom-T4	1.45	0.35
Custom-T5	0.89	0.39 (1/55)
Custom-T6	12.21	0.47 (6/55)
Custom-T7	2.21	0.53
Custom-T8	2.20	0.32

Table 2. Performance comparison of multiple models

	Number of measurements	Time (minutes)	Accuracy (DE00)
GOG model	33 (Spectroradiometer)	1	2.67
Polynomial model (11 levels)	33 (Spectroradiometer)	1	2.37
LUT model	1331 (Spectroradiometer)	40	0.42
AutoLUT model	1 (Reflectance spectrophotometer)	1	0.48

CONCLUSION

A device for total appearance research is introduced, and its hardware composition and colour management workflow are briefly described. At the same time, two improvements to the system are introduced. One is to conduct a colour matching experiment to try to improve the effect of the phenomenon of metamerism, and to this end, a polynomial model modification is applied, and reduced the colour difference observed by the observers from 2.13 to 0.85.. The second is AutoLUT, developed for custom sample LUT, which has achieved the desired speed and accuracy. In summary, a total appearance study based on this system was carried out, and the experimental results improved the performance and generality of the system.

REFERENCES

1. C. He, J. Zhang, M. R. Luo, A Design Tool: Appearance simulator based on spectrum tunable LED lightings, AIC2020 proceedings, Avignon, France
2. J. Lin, K. Shi, M.R. Luo, Colour Performance Evaluation for LEDSimulator Technology, AIC2021, Milan, Italy
3. J. Lin, K. Shi, T. Huang, J. Zhang, X. Xiong, M.R. Luo, Colour modelling on a virtual display system – LEDSimulator, AIC2022, Toronto, Canada
4. M. R. Luo, G. Cui and B. Rigg, The development of the CIE 2000 colour difference formula, Color Res. and Appl. 26 (2001) 340-350.

5. Hong, G. W., M. R. Luo, and P. A. Rhodes. A Study of Digital Camera Colourimetric Characterisation Based on Polynomial Modelling, Colour Res. Appl. 26 (2001) 76-84. Colour Res. And Appl.
6. Berns, R. S. , Methods for characterizing CRT displays. Displays 16. 4(1996):173-182.

OPTICAL MEASUREMENTS OF SPARKLE AND GRAININESS

N. Basic[1]*, C. Aebischer[2] and P. Blattner[1]

[1]*Federal Institute of Metrology METAS, Optics, Switzerland.*
[2]*Haute ecole d'Ingénierie et Architecture Fribourg HEIA-FR, Switzerland.*

*Corresponding author: Nina Basic, nina.basic@metas.ch

ABSTRACT

Large effect pigments in coatings are widely used in industrial applications because of their eye-catching colour and visual texture effects known as sparkle and graininess. Sparkle is defined by ASTM E284-17 as 'the aspect of the appearance of a material that seems to emit or reveal tiny bright points of light that are strikingly brighter than their immediate surround and are made more apparent when a minimum of one of the contributors (observer, specimen, light source) is moved.' When the same material is observed under diffuse illumination, a granular appearance is observed, which is known as graininess. Whereas methodology for colour measurements is already well established, the methodology for visual texture effects is not. The measurement scales for both graininess and sparkle, that correlate the physical measurements with the visual assessments, are currently under discussion in the International Commission on Illumination (CIE JTC 12). This includes the methodology for sparkle and graininess measurements and evaluation. The objective of this work is to use this methodology currently under discussion in CIE JTC 12 to evaluate the sparkle and graininess on a large set of samples. For sparkle, the measurements were made at bidirectional geometries; 15°:0°, 45°:0°, and 75°:0° using a multi-angle reflectance setup (MARS). For graininess on the other hand, measurements were made at measurement geometry di:8° using mini diffuse appearance setup (MIDAS). In both cases, the spatial distribution of the sample's luminance factor needs to be characterized by capturing luminance factor images. Each pixel of a luminance factor image represents a luminance factor averaged over that pixel's field of view. The luminance factor images were taken at the selected measurement geometries using calibrated cameras. Since the contrast between bright sparkle points and the background is high, high-dynamic range imaging was used. Based on the luminance factor images, sparkle and graininess quantities were calculated, following the previously mentioned methodology. The sample set measured in the study consisted of 180 samples and can be divided into 4 subsets. First subset contains 25 achromatic samples with five pigment concentrations and five pigment sizes. This allowed us to systematically check how the concentration and the size of the effect pigments affects the sparkle and graininess quantities. Second subset contains achromatic samples that exhibit very high texture effects and was used in comparison with the first subset. Third subset contains samples where the same coating with effect pigments is applied on both black and white background. This allowed us to investigate the coating's background effect on the sparkle and graininess quantities. The fourth subset contains chromatic samples which allowed us to explore the texture effects of colour samples. Next steps will include the visual assessments of these samples to check the proposed measurement scales for both visual textures.

Keywords: sparkle, graininess, effect pigments, reflectance measurements

Session 9

Doi Wawee
1 December 2023

Auto-white Balance Algorithm of Skin Colour Based on Asymmetric Generative Adversarial Network

Sicong Zhou[1] Hesong Li[2] Wenjun Sun[2] Fanyi Zhou[2] Yang Yang[2] and Kaida Xiao[1]*

[1]*Leeds Institute of Textiles and Colour, University of Leeds, Leeds, UK.*
[2]*Shenzhen Transsion Holdings Co., Ltd., Shenzhen, China*

*Corresponding author: Kaida Xiao, k.xiao1@leeds.ac.uk

ABSTRACT

Skin colour constancy under non-uniform correlated colour temperatures(CCT) and multiple light sources has always been a hot issue in colour science. A more high-quality skin colour reproduction method has broad application prospects in camera photography, face recognition, and other fields. The processing process from the 14bit or 16bit RAW pictures taken by the camera to the final output of 8bit JPG pictures is called the image processing pipeline, in which the steps of the auto-white balance algorithm have a decisive impact on the skin colour reproduction result. The traditional automatic white balance algorithm is based on hypothetical statistics. Moreover, the estimated illuminant colour is obtained through illuminant estimation. However, the traditional grayscale world, perfect reflector, and other auto-white balance algorithms perform unsatisfactorily under non-uniform or complex light sources. The method based on sample statistics proposes a new solution to this problem from another aspect. The deep learning algorithm, especially the generative adversarial network (GAN) algorithm, is very suitable for establishing the mapping between pictures and pictures and has an excellent performance in the fields of image reconstruction, image translation, defogging and colouring. This paper proposes a new solution to this problem. Through the asymmetric UNet3+ shape generator, which integrates better global and local information to obtain a more refined correction matrix incorporating details of the whole image. The discriminator is Patch-discriminator, which focuses more on image details by changing the attention field. The dataset used in this article is the Liverpool-Leeds Skin-colour Database (LLSD) and some supplementary images, including the skin colour of more than 960 subjects under D65 and different light sources. Finally, we calculate the CIEDE2000 colour difference between the test skin colour JPEG picture corrected by the auto-white balance algorithm and the skin colour under the corresponding D65 to evaluate the effect of white balance correction. The results show that the asymmetric GAN algorithm proposed in this paper can bring higher quality skin colour reproduction results than the traditional auto-white balance algorithm. By adjusting the input parameters, the asymmetric GAN algorithm can also be applied to the color reproduction of RAW format images.

Keywords: Auto-white Balance, Skin Colour, Generative Adversarial Network, Colour Reproduction

INTRODUCTION

Skin colour, as one of the most critical features of the human face, directly or indirectly reflects the content of physiological factors such as haemoglobin and melanin and is affected by geographical area, climate, environment, etc. Therefore, it has many applications in face recognition[1], hormone measurement[2-3], and cancer detection[4]. Reproducing the proper skin colour from the perspective of colour science is the basis for evaluating skin colour, and it is also a necessary prerequisite for applying colour science to this specific problem.

The colour reproduction in this article focuses on the hot issue in colour science of unknown non-uniform correlated colour temperature (CCT) and skin colour constancy under unknown light sources. This research hopes to provide a higher-quality skin colour reproduction method that can be used in camera photography, face recognition, and other fields that have broad application prospects. The processing process from the 14bit or 16bit RAW pictures taken by the camera to the final output of 8bit JPG pictures is called the image processing pipeline, in which the steps of the auto-white balance(AWB) algorithm have a decisive impact on the skin colour reproduction result, which is also a key industry issue that mobile phone, chip and camera manufacturers are concerned.

So far, researchers have developed many AWB algorithms, which can be classified based on statistical assumptions or image samples. The AWB algorithm based on statistical assumptions does not rely on input image information. It uses existing experience or hypothesis in colour science to make a global estimate of the image to obtain the relevant parameters or matrices of the AWB algorithm for different channels. The algorithm based on image learning uses various image features to train colour reproduction models through various neural network structures. An overview of common AWB algorithms is shown in the table below.

Table 1: An overview of common AWB algorithms

Classification	AWB Algorithm	Supervised	Light Source
Statistical assumptions	GreyWorld(GWM)[5]	-	Single
	Max-RGB[6]	-	Single
	Shades of Grey (SoG)[7]	-	Single
	Grey Edge[8]	-	Single
	Perfect Reflector Method (PRM)[9]	-	Single
	Dynamic Threshold[10]	-	Single
	Retinex AWB[11]	Y	Multi
Samples	Neural Networks(NN) with colour histogram[12-16]	Y	Single, Multi
	NN with traditional algorithm[17]	Y	Single, Multi
	Deeper Neural Networks[18-21]	Y	Single, Multi

However, traditional AWB algorithms such as GWM and PRM perform poorly under uneven or complex light sources. The method based on sample statistics proposes a new solution to this problem from another aspect. Deep learning algorithms, especially the Generative Adversarial Network (GAN) algorithm, enhance the stability of the mapping between pictures by introducing a discriminator. Therefore, this article attempts to improve the AWB field's GAN network.This article's primary work and innovation are as follows.

Propose an asymmetric UNet3+ generator in GAN, used for skin colour reproduction in the unknown light environment and non-uniform colour temperature environment.

Supplement the images, organize the LLSD dataset, and generate facial images in various environments through RAW Camera Filter.

Verify and compare the differences between the proposed and traditional AWB algorithms, providing suggestions and directions for future RAW image processing.

METHODOLOGY

Network Structure

Our proposed network structure includes an asymmetric UNet3+ generator and patch discriminator. The asymmetric UNet3+ network structure used by the generator is continuously improved on the basis of previous research [22], and refers to the structures of UNet++ [23] and UNet+++ [24]. The discriminator uses the Patch GAN structure [25]. The overall structure of the network is shown in the figure below.

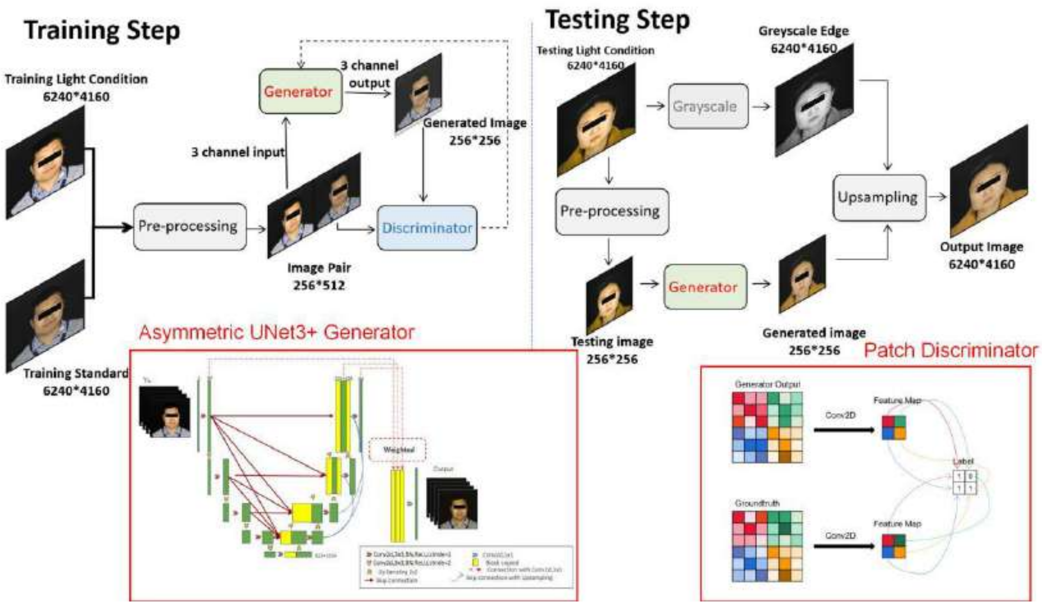

Figure 1. Whole Network Training and Testing Steps of GAN

The training process of the neural network is essentially the mapping process shown in Equation (1), and the testing process is shown in Equation (2).

$$Y_{h,w} = f_{3\times3}(r_{h,w}, g_{h,w}, b_{h,w}) \tag{1}$$

$$(r_{h,w}, g_{h,w}, b_{h,w}) = f_{3\times3}^{-1}(Y_{h,w}) \tag{2}$$

In the formula, h and w are the height and width of the image. 3x3 represents the patch size selected by the network. Y represents the pixel values of the input image.

During the training process of the network, the Training Light Condition (Y_{lc}) comes from the face pictures under different light sources simulated after software processing, and the Training Standard (Y_s) pictures are in the standard D65. The face pictures collected under the light source with 256*512 resolution are preprocessed and combined into a generator. The generator generates a three-channel output value Yo after obtaining the three-channel value from Y_{lc} and outputs it to the discriminator. The generator, the output value Y_o and the standard value Y_s are identified in the discriminator, the probability that Y_o is an actual image is judged, and the relevant parameters are returned to the generator. Repeat the above process continuously until the training is completed. The final trained generator model will be saved and can be called directly during testing.

The asymmetric UNet3+ Generator structure is shown in the figure. The input of the middle layer comes from the same layer and the shallower Encoder, and they are subjected to feature fusion operation through the concatenate function. As a fulcrum for the lateral flow of information, the middle layer replaces the long-connected structure of UNet and retains the short-linked structure of integrated local information in UNet++. Preserving upsampling between intermediate layers ensures that information can be transferred from deep to shallow layers. That is, the output of the middle layer of the first layer will obtain all the local information downsampled by the entire model and the local information under each receptive field in the Encoder. In the Decoder structure, a global jump connection similar to UNet3+ is used, which enables the global information to be obtained in the Decoder, and the information of the Decoder also comes from the middle layer, which makes it possible to complete the global information and local information in the Decoder. Each receptive field's interaction concatenates the local and global features under each receptive field. The specific operations included in downsampling and upsampling are shown in the figure, including Cov2D convolution, BN and ReLU. To ensure the uniform resolution between layers, the resolution is reduced by setting the convolution stride when downsampling and the resolution are increased by Upsampling2D operation.

The generator add a combination of binary cross-entropy and dice coefficient as the final loss function:

$$L_{all} =- 1/N \sum_{i=0}^{M} v_{0,1} \sum_{n}^{N} \sum_{b}^{B} \sum_{h,w}^{H,W} (0.5Y_{lc} logY_o + (2Y_{lc}Y_o/(Y_{lc} + Y_o))) \tag{3}$$

In the formula, Y_{lc} and Y_o represent the predicted probabilities of input light condition images and generated images. N represents the batch size, and M means layers of the network. B represents the number of channels. Finally, H and W represent the height and width of images.

RESULT AND DISCUSSION

The original image of the input image comes from the Liverpool-Leeds Skin-colour Database (LLSD)[26] and includes face data collected by some research groups. These face data were taken in the laboratory and were not disturbed by other light sources except the background light source with a set colour temperature. In order to simulate the impact of different manual white balance settings in the camera on the image colour, we use the Adobe Camera Raw function in Photoshop to simulate the image output of different WB presets in the camera. In this experiment, a raw RGB image can be rendered into 34 camera-specific sRGB images. In this experiment, a total of 4862 groups of pictures were finally generated.

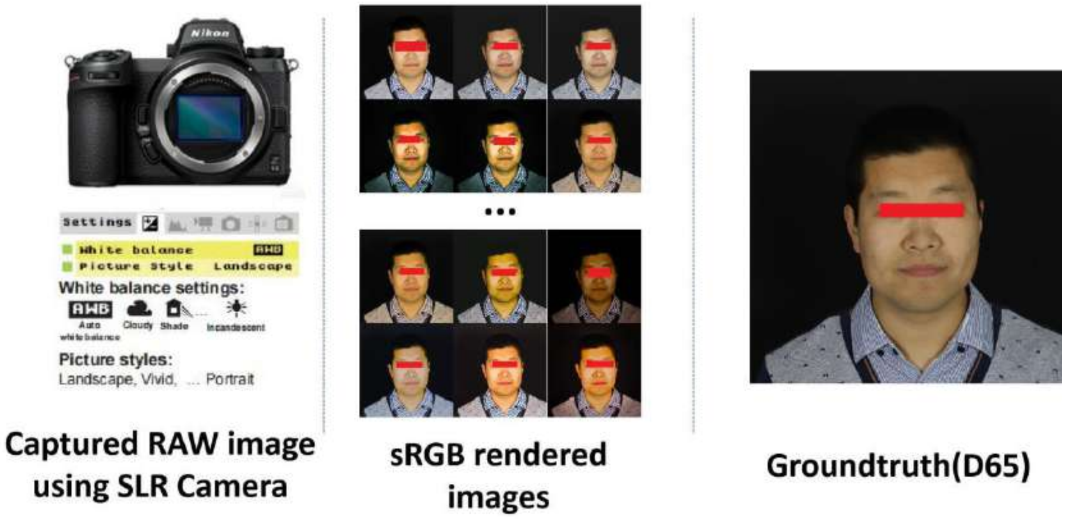

Figure 2. Example of Rendering sRGB Training Images

The experimental data used the aforementioned 4862 groups of pictures consisting of face pictures under different light environments and face pictures under the D65 standard light environment. Among them, 244 groups are used for testing, 4374 groups are used for training, and 244 groups are used for value. This unbalanced setting is because in the colour reproduction problem, the difficulty is mainly concentrated on the generator, and larger-scale image data helps the generator generate a model closer to the actual image.

This experiment's network using a PC equipped with an AMD Ryzen 7 5800H CPU and an RTX 3060 Laptop GPU. The optimizer uses Adam to prevent overfitting, the learning rate is set to 0.0002, and the batch size is set to 2. The experimental environment version is set to Python: 3.5.6, CUDA: 9.2, Keras: 2.2.2, and Tensorflow: 1.10.0.

The pictures generated by the experiment are finally compared with the face pictures under the standard D65 light source, and CIEDE2000 is used to evaluate the colour difference. It can be seen that the traditional GWM algorithm does not perform as expected in the face processing problem under this picture set. This is because the large-scale black colour blocks in the background cause the overall colour richness of the picture to be insufficient, which makes the colour of the whole picture deviate. This results in a bluish cast to the overall image. The algorithm based on deep learning can better retain the original details and outlines in the picture and obtain better results based on fine-tuning the colour.

Figure 3. Colour Difference of Experiment Results using Heating Map

A heat map analyzes the colour difference of different pixels. The colour of the bar on the right changes from green to red, representing the change of colour difference from small to large. In the entire face picture, the code proposed in this article is generally satisfactory in terms of the overall colour difference of the image. The colour difference can be generally reduced for a face with a significant overall colour difference. However, the colour difference in the surrounding area can be generally reduced for a face with a slight colour difference.

CONCLUSION

The network structure currently proposed in this paper includes a an asymmetric UNet3+ generator and a block discriminator, which help obtain a colour reproduction effect that differs from traditional algorithms. In the follow-up experiments, I will also explore the white balance algorithm of this network applied to the RAW image of the Bayer matrix data structure.

ACKNOWLEDGEMENT

The authors thank *Shenzhen Transsion Holdings Co., Ltd.* for this work.

REFERENCES

1. Bar-Haim, Y., Saidel, T., & Yovel, G. (2009). The role of skin colour in face recognition. *Perception*, 38(1), 145-148.
2. Henderson, A. J., Lasselin, J., Lekander, M., Olsson, M. J., Powis, S. J., Axelsson, J., & Perrett, D. I. (2017). Skin colour changes during experimentally-induced sickness. *Brain, behavior, and immunity*, 60, 312-318.
3. Fink, B., & Matts, P. J. (2008). The effects of skin colour distribution and topography cues on the perception of female facial age and health. J*ournal of the European Academy of Dermatology and Venereology*, 22(4), 493-498.
4. Storring, M., Andersen, H. J., & Granum, E. (2000, March). Estimation of the illuminant colour from human skin colour. *In Proceedings Fourth IEEE International Conference on Automatic Face and Gesture Recognition* (Cat. No. PR00580) (pp. 64-69). IEEE.
5. Rizzi, A., Gatta, C., & Marini, D. (2003). A new algorithm for unsupervised global and local color correction. *Pattern Recognition Letters*, 24(11), 1663-1677.
6. Funt, B., & Shi, L. (2010, November). The rehabilitation of MaxRGB. *In Proc. of the Eighteenth Color Imaging Conference*. Simon Fraser University.
7. Finlayson, G. D., & Trezzi, E. (2004, January). Shades of gray and colour constancy. *In Color and Imaging Conference* (Vol. 2004, No. 1, pp. 37-41). Society for Imaging Science and Technology.

8. Van De Weijer, J., Gevers, T., & Gijsenij, A. (2007). Edge-based color constancy. *IEEE Transactions on image processing*, 16(9), 2207-2214.
9. Barnard, K., Martin, L., Coath, A., & Funt, B. (2002). A comparison of computational color constancy algorithms. ii. experiments with image data. *IEEE transactions on Image Processing*, 11(9), 985-996.
10. Weng, C. C., Chen, H., & Fuh, C. S. (2005, May). A novel automatic white balance method for digital still cameras. *In 2005 IEEE International Symposium on Circuits and Systems (ISCAS)* (pp. 3801-3804). IEEE.
11. Banić, N., & Lončarić, S. (2013). Light random sprays Retinex: exploiting the noisy illumination estimation. *IEEE Signal Processing Letters*, 20(12), 1240-1243.
12. Cardei, V. C., Funt, B., & Barnard, K. (2002). Estimating the scene illumination chromaticity by using a neural network. *JOSA a*, 19(12), 2374-2386.
13. Finlayson, G. D., Hordley, S. D., & Hubel, P. M. (2001). Color by correlation: A simple, unifying framework for color constancy. *IEEE Transactions on Pattern Analysis and Machine Intelligence*, 23(11), 1209-1221.
14. Xiong W, Funt B. Estimating illumination chromaticity via support vector regression[J]. *Journal of Imaging Science and Technology*, 2006, 50(4): 341-348.
15. Gehler, P. V., Rother, C., Blake, A., Minka, T., & Sharp, T. (2008, June). Bayesian color constancy revisited. *In 2008 IEEE Conference on Computer Vision and Pattern Recognition* (pp. 1-8). IEEE.
16. Gao, S., Yang, K., Li, C., & Li, Y. (2013). A color constancy model with double-opponency mechanisms. *In Proceedings of the IEEE international conference on computer vision* (pp. 929-936).
17. Finlayson, G. D. (2013). Corrected-moment illuminant estimation. *In Proceedings of the IEEE International Conference on Computer Vision* (pp. 1904-1911).
18. Barron, J. T. (2015). Convolutional color constancy. *In Proceedings of the IEEE International Conference on Computer Vision* (pp. 379-387).
19. Bianco, S., Cusano, C., & Schettini, R. (2017). Single and multiple illuminant estimation using convolutional neural networks. *IEEE Transactions on Image Processing*, 26(9), 4347-4362.
20. Shi, W., Loy, C. C., & Tang, X. (2016). Deep specialized network for illuminant estimation. *In Computer Vision–ECCV 2016: 14th European Conference, Amsterdam, The Netherlands*, October 11–14, 2016, Proceedings, Part IV 14 (pp. 371-387). Springer International Publishing.
21. Ershov, E., Savchik, A., Semenkov, I., Banić, N., Koščević, K., Subašić, M., ... & Nikolaev, D. (2021). Illumination estimation challenge: The experience of the first 2 years. *Color Research & Application*, 46(4), 705-718.
22. Zhou, S., & Kamata, S. I. (2022, July). Near-Infrared Image Colorization with Weighted UNet++ and Auxiliary Color Enhancement GAN. *In 2022 7th International Conference on Image, Vision and Computing (ICIVC)* (pp. 507-512). IEEE.
23. Zhou, Z., Siddiquee, M. M. R., Tajbakhsh, N., & Liang, J. (2019). Unet++: Redesigning skip connections to exploit multiscale features in image segmentation. *IEEE transactions on medical imaging*, 39(6), 1856-1867.
24. Huang, H., Lin, L., Tong, R., Hu, H., Zhang, Q., Iwamoto, Y., ... & Wu, J. (2020, May). Unet 3+: A full-scale connected unet for medical image segmentation. *In ICASSP 2020-2020 IEEE international conference on acoustics, speech and signal processing (ICASSP)* (pp. 1055-1059). IEEE.
25. Isola, P., Zhu, J. Y., Zhou, T., & Efros, A. A. (2017). Image-to-image translation with conditional adversarial networks. *In Proceedings of the IEEE conference on computer vision and pattern recognition* (pp. 1125-1134).
26. Xiao, K., Yates, J. M., Zardawi, F., Sueeprasan, S., Liao, N., Gill, L., ... & Wuerger, S. (2017). Characterising the variations in ethnic skin colours: a new calibrated data base for human skin. *Skin Research and Technology*, 23(1), 21-29.

A study of image features and color classification in tongue diagnosis in traditional Chinese medicine

Huang Qingmei[1]*, Zhang Shen[2], Weiziyuan[3],Liang Rong[4], Wang lingyan[5],

[1,2,3]*National Laboratory of Color Science and Engineering, Beijing Institute of Technology, China.*
[4]*School of Traditional Chinese Medicine, Beijing University of Chinese Medicine, China.*
[5] *Shanghai Daosh medical technology Co. , Ltd , China.*

*Corresponding author: Huang Qingmei, huangqm@bit.edu.cn

ABSTRACT

Tongue diagnosis in traditional Chinese medicine (TCM) is a prominent diagnostic method frequently practiced by modern TCM doctors. It is defined as observing changes in tongue appearance, especially color, for disease diagnosis. This method often relies on the subjective experience of TCM doctors, However, recent advancements in Tongue Imaging Instruments enabled objective analysis of color features of the tongue. This study utilized modern digital image processing technology and color science principles to analyze standardized tongue images captured by Tongue Imaging Instruments. We firstly reviewed TCM literature to summarize color category terminologies in tongue diagnosis. Next, fuzzy c-means clustering was applied to separate tongue coating and tongue body color properties. The respective color gamut boundaries were then determined through the b* channel in the CIELAB color space due to low variance in this channel (<2.25). The majority of samples (85.15%) were collected from the tip of tongue region for tongue body images, while tongue coating images were sampled evenly in 5 equally divided areas on the tongue surface. Lastly, support vector machine (SVM) and backpropagation neural network (BPNN) methods were used for color feature classification in relation to TCM tongue diagnosis color definitions. The results showed that the classification accuracy of tongue body and tongue coating in the test set is 0.96 and 0.92 respectively for the SVM classifier, compared to 0.89 and 0.87 respectively for BPNN. When tongue body and tongue coating were combined, the classification accuracy decreased to 0.89 by using the SVM classifier. Overall, this study explores the digital color properties of traditional color definitions in TCM tongue diagnosis, and provides a research basis to further the quantifiability and objectiveness of this diagnostic method.

Keywords: tongue diagnosis, tongue color category, color space, segmentation, classification

INTRODUCTION

With the development and modernization of traditional Chinese medicine (TCM) tongue diagnosis, the color classification of tongue coating and tongue body has seen an improvement in its standardization. In the TCM Diagnostics by Li CanDong et al. [1], the color of the tongue body is divided into six categories: pale red, pale white, red, dark red, purple, and blue; the color of the tongue coating is divided into three categories: white, yellow, and gray-black. Historically, the color categories for tongue diagnosis observations are largely dependent on the personal subjective experience of individual TCM doctors, and is therefore adds uncertainty to color classifications due to a lack of objective and quantitative methods. An example to combat this is the state of tongue classification sample atlas made by Liang Rong et al. [2], where color-corrected tongue images were curated as references for clinicians.

In recent years, with the development of color science and imaging technologies, especially the emergence of the Tongue Imaging Instrument, new ways of capturing tongue images and analyzing the state of tongue categorization have become possible. Therefore, providing the quantitative color descriptions of digital tongue images, separating tongue coating and tongue body, and recognizing the state of tongue color categories have become fundamental challenges that require urgent solutions.

To address these problems, Li CongBo et al. [3] analyzed the distribution patterns of the red, pink and light-white tongue colors in the CIELAB color space. They also employed numeric fitting methods to classify tongue colors and extracted reference color characteristics. In addition, Yu XingLong et al. [4] extracted the 4 x 4 RGB values from manually collected tongue images, using which they conducted sample training and parameter adjustments to define tongue body category definition domains. In another study by Xu JiaTuo et al. [5] they utilized the ‘split-merge algorithm’ to achieve separation between the tongue body and the tongue coating, and quantified them in a color space in correlation with different medical conditions. Zhang D. et al. [6] extracted the tongue body color categories in the CIELAB color space and conducted classification and prediction analyses between normal individuals, appendicitis patients and pancreatitis patients.

The current study aims to investigate the TCM tongue diagnosis color category classification based on the CIELAB color space. It aims to propose solutions addressing issues in tongue body and tongue coating separation, as well as difficulties in identifying and classifying color characteristics in digital tongue images. Additionally, Support Vector Machine (SVM) and Back Propagation Neural Network (BPNN) methods were explored to automate the classification of tongue colors. Ultimately, it aims to provide a research foundation for the quantification of TCM diagnosis method, and improve the applicability of digital tongue images.

2 METHODOLOGY

2.1 Color measurements experiment of tongue color

State of tongue is a traditional term of tongue diagnosis in TCM, which describes the correspondence between the overall state of tongue and disease. Color is an important factor of state of tongue, which is divided into tongue body color and tongue coating color. This study categorized the tongue body color into 7 types: Pale red, Red, Dark red, Dark purple, Pale white, Pale purple and Purple blue. Additionally, the tongue coating colors were categorized into 4 types: White, Grey, Yellow, and Black coating. Tongue color measurement samples were obtained from Liang Rong et al. [2]. Example images of tongue colors are shown in figure 1.

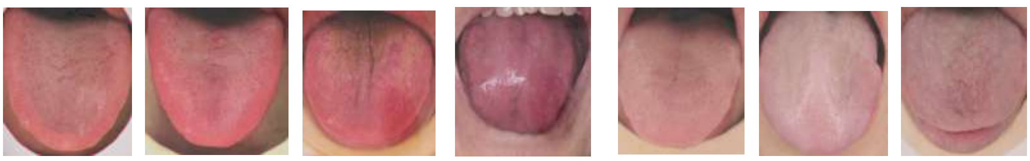

(a) Typical tongue body color categories

(b) Typical tongue coating color categories

Figure 1. State of tongue color categories in TCM

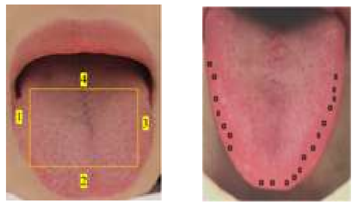

(a) (b)

Figure 2. Tongue color measurement position

To adhere to the observational methods in TCM as much as possible, this study utilized the method of manually selecting points of interest for sample color selection/measurement from typical tongue images, paired with confirmation from specialists. For the tongue body, 20 points of interest were selected for each color, the locations for which are shown in figure2(b). As the tongue coating, 20 points of interest were selected from the center of tongue and root of tongue areas, which are the area within the rectangle and the area marked as 4 in figure 2(a).

The tongue images were placed in a D65 lightbox with 0/45 Illuminating and viewing condition. By using a PR-715 spectroradiometer (Photo Research), the spectral radiance values for each of the points of interest were measured and recorded for a color category. The XYZ tristimulus values were obtained by comparing against a standardized white plate, from which the L*a*b* values were calculated. This method was repeated for each color category (7 tongue body color categories and 4 tongue coating categories).

The t-test method was utilized to analyze the distinction between datasets of different color categories to verify whether 20 sample points were sufficient to represent the required color characteristics for tongue body colors. Using SPSS, a t-test was performed using the L*a*b* values for all tongue body color categories, all of which showed significant differences ($p<0.05$). Therefore, it can be concluded that taking samples from 20 points of interest provided an adequate representation of tongue body colors.

2.2 Segmentation and sampling method on tongue image

2.2.1 K-means clustering algorithm and Fuzzy C-means (FCM) clustering algorithm

The K-means algorithm is an algorithm for putting N data points in an I-dimensional space into *K* clusters. In this case of segmented tongue body and tongue coating on tongue image, *K=2*. To start the K-means algorithm, the K means are initialized in random values. Fuzzy C-Means(FCM) Clustering is a soft version of k-means, where each data point has a fuzzy degree of belonging to each cluster. The flow of the algorithm is shown in Figure 3.

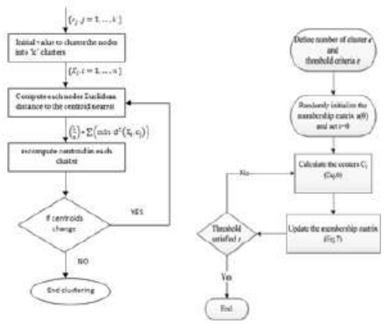

(a) K-means (b). FCM

Figure 3. Flow of the Clustering algorithm

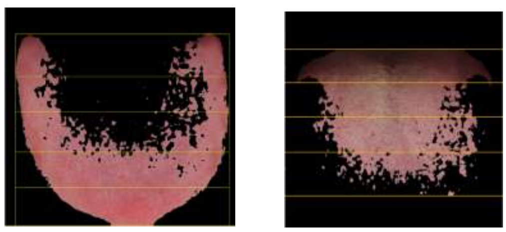

(a) tongue body (b) tongue coating

Figure 4. Sampling by 5 region

2.2.2 Sampling method for tongue color category for tongue image

The variance is used to evaluate the uniformity and plausibility of tongue color sampling on the tongue image in this study.Variance reflects the degree of variation in a dataset, and is calculated through the mathematical formula below.

$$\delta^2 = \frac{(M-x_1)^2+(M-x_2)^2+(M-x_3)^2+\cdots(M-x_n)^2}{n} \qquad (1)$$

Within this formula, M represents the average value of the dataset, n represents the sample size, x is the individual data points.

The tongue body and tongue coating images are sectioned into 5 equal areas, in line with TCM methods (shown in figure 4).

2.3 SVM and BPNN model

2.3.1 Multi-class Support Vector Machine

Support Vector Machine (SVM) by design is used for binary classification, and can be used to be trained on a large amount of data and perform classification tasks. However, in the current study, there are multiple tongue color categories. Therefore, the original SVM was extended to a classifier capable of handling multiple categories. Shown in figure 5(a)

If 2 categories are randomly selected from *n=k* number of categories to be used as the training database, then *k(k-1)/2* number of classifiers would be generated from *n=k* number of samples. Therefore, if there are 4 different categories (A,B,C,D), then 6 classifiers are required (when *k=4*). During training, each classifier is also trained on two categories, namely, category 1 and category 2. The difference between each classifier and the one-vs-all approach is that in each classifier, category 2 has only one type of sample.

Therefore, 6 classifiers were trained to distinguish between 4 categories. During training, samples were classified using all 6 classifiers, and the output category from each set got a +1 score. The category with the highest score in the end then becomes the decided category. The many-to-many approach is not affected by data imbalance and is therefore commonly used to implement multi-class classification tasks.

For the tongue body color categories (*k=6*), 15 classifiers need to be constructed. For the tongue coating color categories (*k=4*), 6 classifiers need to be constructed.

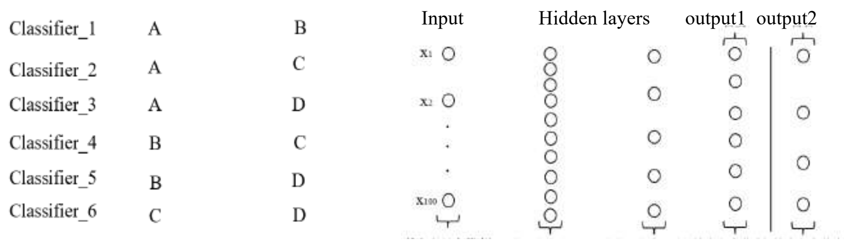

(a) SVM (b) BPNN

Figure 5. Flow of the Clustering algorithm

2.3.2 BPNN model

When using a backpropagation neural network (BPNN) for tongue image classification, the number of output nodes in the neural network is typically equal to the number of classes or categories you want to classify the tongue images into. This means that for our model (*n=6* for tongue body categories, *n=4* for tongue coating categories), there are 6 and 4 output nodes respectively.

Due to the limited number of sample points in our tongue image database, the data was amplified for the neural network training. The 1000 data nodes were divided into 100 x 10, with each of the 100 pixels representing the color characteristics of the tongue body or the tongue coating. Thus, each tongue body or tongue coating image is represented with 10 characteristics, and there are 100 nodes as input for the network. The network ultimately selected for training is shown in figure 5(b).

The neural network's structure is designed with 100 input nodes, two hidden layers (the first with 10 nodes and the second with 5 nodes), and 6 output nodes for tongue color training and 4 output nodes for tongue coating training.

When designing structure of the neural network, the activation function between the input nodes and hidden layers, as well as between hidden layers, is set as the sigmoid function. The activation function between the hidden layers and output nodes is set as softmax for multi-class classification. To optimize the model's error backpropagation during classification, the cross-entropy loss function is chosen.

3 RESULT AND DISCUSSION

3.1 Tongue color characteristics in the CIELAB color space

3.1.1 Color distributions for tongue body colors and tongue coating colors

The three-dimensional distribution of the 7 tongue body colors and 4 tongue coating colors in the CIELAB color space were generated using MATLAB, as shown in figure 6-1(a) and figure 6-2(a) respectively. To facilitate the analysis of colorimetric parameters for the color categories, the colorimetric data distributions in the a*-b* plane and C-H plane for the tongue body color categories in figure 6-1(b) and 6-1(c), as well as for the tongue coating in figure 6-2(b) and6-2(c).

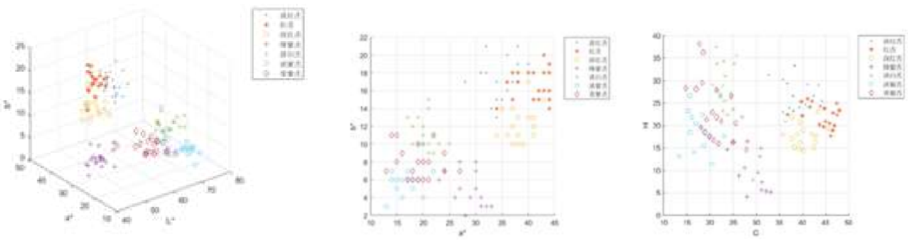

（a）$L^*a^*b^*$ （b） $a^*–b^*$ （c）C-H

Figure 6-1 colour distribution for tongue body

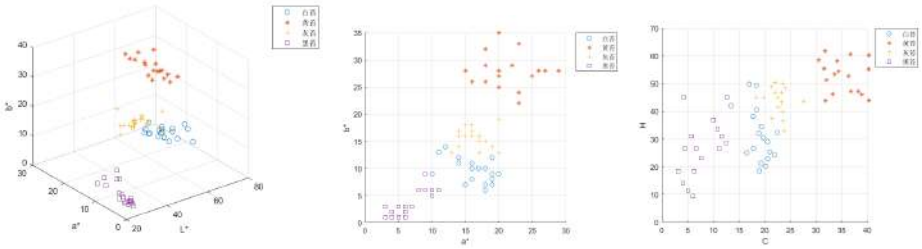

（a）$L^*a^*b^*$ （b） $a^*–b^*$ （c）C-H

Figure 6-2 Colour distribution for tongue coating

The color distributions for tongue body color categories are shown in figure 6-1. The 7 different tongue body color categories can be differentiated by their varying L*a*b* values. Among the categories, the red, dark-red and pale red categories have similar L*a*b* values but they have different distributions. It can be observed that the red tongue has a higher a* value than the pale red tongue, whereas the dark-red tongue has a smaller b* value than the red tongue. We can therefore distinguish between the three categories, and this also highlights the visual observations perceptions of the different color characteristics. By comparison, the tongue body color category differentiation is more obvious on the b* axis. As for the tongue body color distribution on the C-H plane, it can be observed that there is not much variation between different color categories in hue (H), but there is a marked variation in saturation (C). As shown in figure 7, the 4 tongue coating color categories exhibit clear boundaries on the b* axis and C axis.

3.1.2 Analysis of the boundary between tongue coating color and tongue body color

Color distributions were visualized in the CIELAB color space, four tongue body color categories – pale red, red, dark-red and dark-purple, as well as all tongue coating color categories were included (in figure 7).

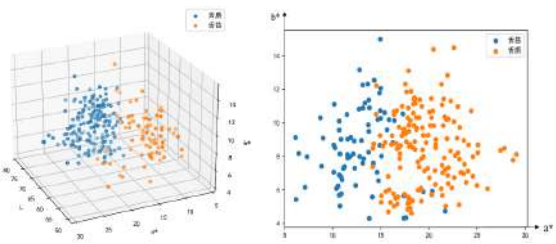

(a) CIE $L^*a^*b^*$ (b) a^*-b^*

Figure 7 Colour distribution for tongue coating and tongue body

As shown in figure 7(b) where blue dots represent the tongue coating sample points and orange dots represent tongue body sample points, we can see that the tongue body points are mostly concentrated in the red region, and show a distinctive boundary to the tongue coating points on the a* axis. Therefore, we can distinguish between tongue body and tongue coating colors based on the a* axis component.

3.2 Segmentation and sampling on digital tongue images

This study utilized digital tongue images captured with a Tongue Imaging Instrument (DS01-B, Shanghai Daosheng Medical Technology Co.Ltd.) that has undergone color correction, as shown in Figure 8(a). Image segmentation algorithms were used to remove regions outside of the tongue surface area, the final tongue surface image is shown in figure 8(b).

As established in section 3.1.2, the tongue coating and the tongue body color distributions are separated by a clear boundary in the a* channel. Therefore, we attempted to use the K-means clustering algorithm and the Fuzzy C-means (FCM) clustering algorithm to achieve segmentation of the tongue surface. This was achieved using the Python programming language using the ‘skfuzzy’ library. The segmentation results are shown in figure 9.

(a) (b)

Figure 8 Tongue imaging

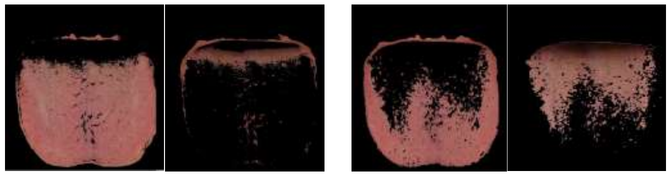

tongue body tongue coating tongue body tongue coating

(a) K-mean (b) FCM

Figure 9 Segment Result for tongue image

According to traditional Chinese medicine theory, tongue coating is generally present in the root and middle areas of the tongue surface. As shown in Figure 9(a), the K-means clustering algorithm can only separate the tongue coating in the root region of the tongue. This is because the tongue coating in the root area tends to be yellow, which is significantly different from the tongue color, making it easier to separate. However, the tongue coating in the middle area of the tongue is similar in color to the tongue body, leading to misjudgment as tongue body, resulting in the absence of tongue coating in the middle area.

Figure 9(b) shows the improved tongue surface segmentation using the FCM clustering algorithm. Because the FCM clustering algorithm is a type of fuzzy clustering algorithm, it tends to require more iterations for categories with closely related characteristics, as well as introducing membership degrees to address the oversimplification problems seen in hard clustering methods. In conclusion, FCM clustering algorithm provides a better separation between tongue body and tongue coating and is therefore adopted by the current study for tongue surface segmentation.

As previously demonstrated in section 3.1.1, the tongue body and tongue coating colors are best separated on the b* axis (yellow).

The variance in CIELAB b* was calculated for each of the 5 areas’ pixels for all 20 tongue images captured with a Tongue Imaging Instrument(shown in figure 4), for both the tongue body and tongue coating, the results are shown in Figure 10.

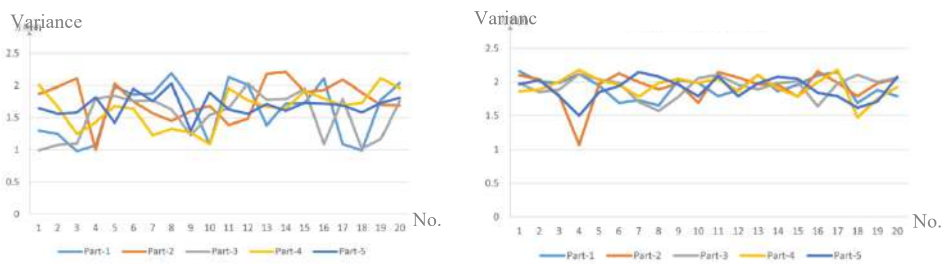

(a) tongue body (b) tongue coating

Figure 10 The b * variance of five parts in tongue image

The b* component variance for both the tongue body and tongue coating is primarily within 1-2, with the maximum variance value <2.25. The relatively small fluctuations in the b* component confirm that the samples for both tongue body and tongue coating can be collected at random within each of the 5 tongue areas.

The maximum variance value for the tip of tongue area is 2.03, which indicates a good color consistency. Therefore several sample points can be selected in this area to represent the color characteristics of the tongue tip.

The tip of tongue b* variance accounts for 85.15% of total tongue body b* variance ($\sum \sigma^{b1^8}$ / $\sum \sigma^{b^8}$). Therefore, 85.15% of the tongue body samples can be acquired from the tongue tip area. The rest 14.85% of the sample points can be acquired within the other 4 areas on the tongue surface (variance <2.25).

As for the tongue coating, the sample points (n) can be taken from each of the 5 tongue surface areas (variance < 2.25 in all 5 areas), for a total of 5n sample points representing the color characteristics.

The current study selects the b* value for 1000 pixels for inputting into a classifier to categorize the color features for the tongue body and tongue coating. For tongue body colors, 852 sample points come from the tip of tongue area, and 37 sample points in each of the 4 other areas (m=1000 in total). For the tongue coating colors, 200 sample points were taken from each of the 5 areas (m=1000 in total).

3.3 Tongue color classification for the digital tongue images

The current study utilized the 'tongue dataset' from Github as the sample database, which included 300 digital tongue images taken with a Tongue Imaging Instrument.

The 6 tongue body color categories are identified as pale-white (n=35), red (n=73), dark-red (n=51), purple (n=36), blue (n=33), pale red (n=72). The 4 tongue coating colors are yellow coating (n=63), white coating (n=140), grey coating (n=50) and black coating (n=47).

The tongue coating and tongue body color were classified using the b * channel color feature of CIELAB.

Classification accuracy is expressed as the proportion of the correct number of classifier output tongue images in the total number of input tongue images.

3.3.1 Multi-class Support Vector Machine

SVM scripts were written in the Python programming language, and the 'sklearn' library was utilized for the SVM many-to-many algorithm. The sample dataset of 300 digital tongue images were divided into a training dataset (n=210) and a testing dataset (n=90)

The SVM classification accuracy for the training dataset (n=210) shows that, for the tongue body, aside from the 6th classifier with an accuracy of 0.95, the accuracy rates for all 14 other classifiers were 1. For the tongue coating, the accuracy rates were 0.95, 1, 0.93, 1, 1, 0.92 for 6 classifiers respectively.

As for the testing dataset (n=90), the 15 trained classifiers correctly classified tongue body color in 86 images (0.96 accuracy). Tongue coating color was correctly classified by the 6 trained classifiers in 83 images (0.92 accuracy)

It needs to be considered that a state of tongue diagnosis cannot be represented if the tongue body and tongue coating color categories are not correctly identified simultaneously. Therefore, when the accuracy rates of both tongue color components are considered together, the accuracy rate for color classification of the tongue surface image is 0.89.

3.3.2 BPNN

The neural network algorithm was implemented through the PyTorch deep learning framework. In the training dataset, a total of 197 images were correctly classified for the tongue body color (0.94 accuracy), and 191 images were correctly classified for the for the tongue coating color (0.84 accuracy). In the test dataset, the classification accuracy for the tongue body color and the tongue coating color was 0.89 and 0.97 respectively. When classification accuracy when both are combined is 0.84.

Therefore, when there is limited data for training, the use of neural network to identify of tongue color categories is inadequate.

CONCLUSION

Our analysis of the tongue color distributions in the CIELAB color space showed clear boundaries between the tongue body colors and the tongue coating colors in the a* axis. As for color categories within the tongue body and tongue coating colors, boundaries could be observed in the b* axis. Therefore, the separation between tongue body and tongue coating was achieved using the FCM clustering algorithm in the a* channel of CIELAB. Whereas the color characteristics for each color category were selected from the images through the b* channel. Finally, the SVM classifier was used to achieve tongue color classifications for the digital tongue images, for which the accuracy rates were 0.96 and 0.92 for the tongue body and tongue coating respectively. The accuracy rates were 0.89 and 0.87 respectively when the BP neural network method was utilized for classification. When the tongue body and tongue coating classification accuracies were combined, the SVM classifier accuracy rate was 0.89.

The current study proposed a method for separating the tongue body and tongue coating based in the a* channel of CIELAB, as well as collecting color characteristics from the sample points in the b* channel. This provides a foundation for improving the classification accuracy rate from classifiers. The emphasis TCM tongue diagnosis places on the different tongue surface areas when observing the tongue body colors was also considered, as 85.15% of sample points for the tongue body color were collected from the tip of tongue region. Finally, we extended the SVM classifier into a multi-class structure to simultaneously classify the colors of both tongue coating and tongue body in tongue images, providing support for correlating combinations of tongue coating and tongue body colors with specific medical conditions or symptoms.

However, it needs to be considered that this study was conducted using a specific digital tongue image database. When variations in the standardization or sample size between different tongue image databases are considered, it is likely that the classification results would show variation. Therefore, future studies could compare classification results or increase the tongue image sample size to further investigate classification methods. Furthermore, improvements in the standardization of color correction systems of the Tongue Imaging Instruments could help curate consistent databases, which allows for future studies to better validate tongue color classification algorithms.

ACKNOWLEDGEMENT

We would like to thank Yige Sun for much help with paper writing and proofreading.

REFERENCES

1. Li Candong et al. (2016).TCM Diagnostics- -the 4th edition. *China Press of Traditional Chinese Medicine*, 2016
2. Liang Rong, Wang Zhaoping. (2021).Wall chart of TCM constitution identification, 2nd edition [M]. *Henan Science and Technology Press*. 2021.
3. Li Bocong, Huang Qingmei, et a1. (2007).A method of classifying tongue colors for traditional Chinese medicine diagnosis based on the CIELAB color space[C]//*Medical Biometrics, Springer Berlin Heidelberg*, 2007:153-159
4. Yu Xinglong, etc. (1994). Research on the automatic identification method of TCM tongue diagnosis [J]. *Chinese Journal of Biomedical Engineering*, 1994,13 (4): 336-344
5. Xu jiatuo, et al. (2004).Computer analysis and identification of tongue image color features [J]. *Journal of Shanghai University of Chinese Medicine,* 2004,18 (003): 43-47
6. Wang Yiran, Zhang Xinfeng. Tongue classification based on the AdaBoost cascade framework [J]. *Beijing Biomedical Engineering,* 2020

TO PERFORM WHITE BALANCE USING SKIN MEMORY COLOR

Liqing Wang[1], Yuechen Zhu[1], Xiaoxuan Liu[1], Ming Ronnier Luo[1,2,*]

[1]State Key Laboratory of Modern Optical Instrumentation,Zhejiang University,CHINA.
[2]School of Design, Leeds University, Leeds, UK; m.r.luo@zju.edu.cn

*Corresponding author: Ming Ronnier Luo, m.r.luo@zju.edu.cn

ABSTRACT

The accurate reproduction of color is highly desired for the imaging industry. To achieve this, white balance is an important component. It is a process to retrieve the white point, typically described in CCT and Duv of the lighting environment. It takes the impact of light source on objects' color into consideration, find the white point in the picture, and adjust the color in image until it's close to our visual perception. In this research, an image process algorithm was developed to perform automatic white balance(AWB) based on the known color center from a color target, such as the Preferred Memory Color Chart(PMCC).

In previous research, each preferred memory color on the chart was described as an ellipse in CIELAB color space. When a color is selected, such as certain skin color , the parameters of its color ellipse like color center and boundary are determined. CIELAB includes parameters of X/X0, Y/Y0, Z/Z0, so it can be considered as a chromatic adaptation. Under different illumination, the skin color should have the same Lab values considering the different white point, which provides a new method to predict the white point by adjusting the Lab value of the skin color in an image to match the memory skin color. In this study, a target detection algorithm YOLOv5 based on CNN was implemented to identify the face region in the image. Then the above mentioned skin color ellipsoid was used to compute the accurate skin region. The third step, the RGB image was transformed to Lab space, and the centroid of skin color pixel was calculated, so that the white point to change the Lab value of the centroid was optimised until it reaches the memory skin color. In the last step, CIE CAT16 was used to transform the image from the predicted white point to D65, allowing for the comparison of the processed image with the ground truth image taken under D65 to evaluate the algorithm. In the experiment, the images of three skin types, Caucasian, Pakistan and Chinese, were captured in the studio lighting condition. Each type includes a male and a female model. Each model was captured against a mid-grey background under color temperatures at 8000K, 6500K, 5000K, 4000K,3000K,and the same lightings against different background colors such as red,green,yellow,blue to test our method. The background of the image also had an impact on the result. Chromatic backgrounds will somewhat mix with the light source, and become the second light source, then change the actual color temperature. In conclusion, a new way to perform AWB of images by minimization of the difference between the skin color and its memory color was found. It can be useful to perform AWB when there is no neutral point in the image.

Keywords: CIELAB, AWB, memory color, skin color.

INTRODUCTION

Color constancy is a perceptual ability of the human visual system that allows us to perceive the colors of objects consistently, regardless of changes in lighting conditions. It ensures that we see objects with relatively stable colors even under different sources of illumination. White balance, on the other hand, is a process used in digital imaging devices to replicate this color constancy. It involves adjusting the colors in an image to account for the color temperature of the light source illuminating the scene. This adjustment helps to produce accurate and visually pleasing colors in photographs or videos, making them appear as close to how the human eye would perceive them in a given environment. The white balance process generally consists of two steps: estimating the illumination and then adjusting the white balance accordingly. About white balance, a lot of previous algorithms are proposed, such as gray-world, white patch, edge-based white balance[1], gamut mapping[2], machine learning based white balance, and etc[3-6]. In situations where images have a significant interference of background colors or lack a reference white, existing algorithms may not perform well. Therefore,a skin-tone-based white balance algorithm designed for processing such images containing portraits was proposed. This algorithm leverages skin-tone pixels within the image to estimate the illuminant of the scene and subsequently applies white balance adjustments. This approach effectively mitigates color deviations in the image. Furthermore, when processing images with varying background colors, it has been observed that different background hues can have a notable impact on the effectiveness of skin-tone white balancing.

METHODOLOGY

Facial skin pixel segmentation

The initial phase involves extracting the actual skin-tone pixels. This is accomplished through the integration of a neural network-based object detection algorithm along with an adaptive threshold segmentation algorithm, ensuring precise segmentation of skin-tone pixels.

The initial step involves employing a facial recognition algorithm to extract the facial region from the image, thereby minimizing interference from background colors. Subsequently, the facial region's image is converted from sRGB to XYZ color space, with D65 as the reference white point. The image is then transformed to the LAB color space. Utilizing the adaptive skin-tone ellipsoid model within the LAB space allows for the extraction of a substantial portion of skin-tone pixels from the image. In figure 1 shows an example of the facial skin pixel segmentation.

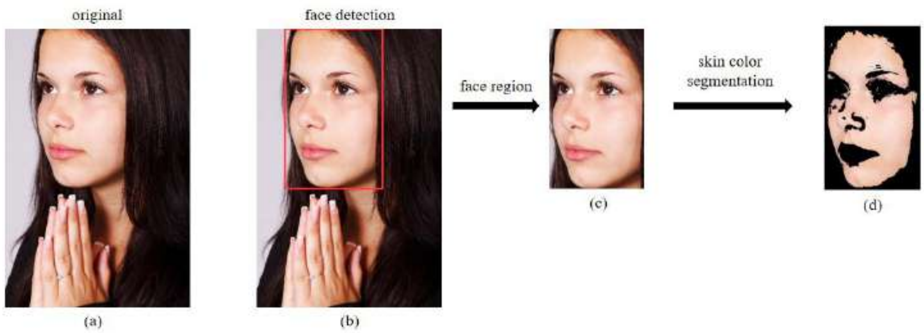

Figure 1. An example of skin color pixels segmentation process

In figure 1, (a) is the example image. (b) is the image processed after face detection, the location of face region was determined. (c) is the face region divided from the full image, eliminating interference from background pixels that may be close to skin color. After these three steps, skin color segmentation was applied to get the accurate skin mask. Based on prior research findings, it is established that skin colors conform to an ellipsoidal distribution within the CIELAB color space[7]. Furthermore, under D65 illumination conditions, the parameters defining the ellipsoid associated with a particular ethnicity in the CIELAB color space are clearly defined[8]. Skin color ellipsoid from PMCC[9-11] was used as a reference and each pixel in the image was examined to determine if it fell within the boundaries of this ellipsoid. Because the actual lighting conditions are unknown, skin tones in the image may not fall within the standard ellipsoid. Therefore, it is necessary to adjust the standard skin tone ellipsoid in order to encompass most of the skin tone pixels in the image. To achieve this, the average center of the skin tones within the standard ellipsoid is calculated in LAB space. The center position of the PMCC standard skin tone ellipsoid is then adjusted to this value, and the skin tones are re-evaluated. This process is repeated until the ellipsoid's position stabilizes, resulting in the acquisition of the actual skin tone ellipsoid in the image. This facilitates pixel-level skin tone segmentation. The skin pixels segmentation of example image is showed in (d).

Illumination estimation and white balance

It's known in previous study that regardless of the lighting conditions during the image capturing, as long as the right reference white point was chosen during the conversion from XYZ to LAB, most of the skin color pixels' Lab value should fall within the standard skin color ellipsoid. However, in the aforementioned steps, when using D65 as the reference white point, the obtained skin tone center in the image may not necessarily fall within the standard skin tone ellipsoid. This implies that D65 may not be the actual light source in the image. Therefore, based on the discrepancy between the skin tone center in the image and the center of the standard ellipsoid, it is possible to estimate the light source. By finding an appropriate light source, most of the skin tones in the image can be made to align with the standard ellipsoid.

The calculate equations are listed below:

$$XYZ_{W^1} = Lab2xyz\,(100+\Delta L, \Delta a, \Delta b, XYZ_W) \tag{1}$$

$$\Delta L = L_i - L_s \tag{2}$$

$$\Delta a = a_i - a_s \tag{3}$$

$$\Delta b = b_i - b_s \tag{4}$$

Lab2xyz() represents a function that can convert Lab to XYZ value. L_s, a_s, b_s represent the center value of standard skin color ellipsoid. L_i, a_i, b_i represent the center value of skin color ellipsoid in the image. XYZ_W is white point used before, XYZ_{W^1} is the new white point.

By employing the aforementioned equations, it is possible to identify a suitable reference white point. Using this white point to convert the image pixels' XYZ values to LAB, the majority of the skin-tone pixels will fall within the standard skin-tone ellipsoid. At this point, it can be inferred that the chosen white point serves as an estimation for the actual scene illumination. After obtaining the illumination estimation, the CAT16 model is employed to perform chromatic adaptation, thereby transforming the image to appear as it would under the target illumination. When the target illumination is set to D65, it can be considered as achieving white balance.

Figure 2 below shows an example of illumination estimation, and the corresponding data was listed on the image. The estimated CCT(correlated color temperature) is very close to the actual value.

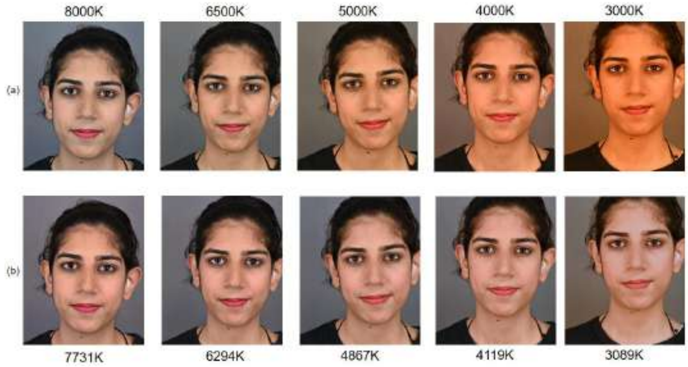

Figure 2. An example of illumination estimation and white balance

(a) is the original image taken in the studio. The images were all captured against a grey background, with the ambient light conditions ranging from left to right: 8000K, 6500K, 5000K, 4000K, 3000K. The white balance settings were consistently configured at 6500K. As a result, images with incorrect white balance were obtained. (b) represents the corrected result of the incorrectly white-balanced images in (a) after applying the skin-tone-based white balance algorithm proposed in this paper, and then converting to D65. Additionally, the algorithm predicts the correlated color temperature (CCT) value of the estimated illumination.

Dataset

In this study, a dataset was assembled comprising 150 images with incorrect white balance. The dataset encompasses a variety of factors, including two genders (male and female), three ethnicities (Caucasian, Pakistani, Chinese), five distinct background colors (gray, red, green, yellow, blue), and five different lighting source color temperatures (D80, D65, D50, D40, D30). It's worth noting that all images were captured using the WB setting at D65, establishing the images under D65 lighting as the ground truth reference group.

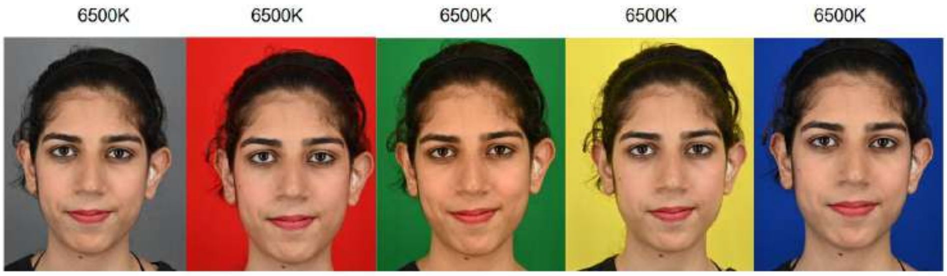

Figure 3. An example of images in database

RESULT AND DISCUSSION

After establishing the dataset with various colored backgrounds, the white balance algorithm proposed in this paper was applied to process the images. Subsequently, an analysis and estimation were conducted on how different colored backgrounds affect the results of illumination estimation.

Table 1 presents the average illumination estimation results for images with five different colored backgrounds, under five distinct color temperatures. Under each color temperature, illumination estimation was performed on images featuring various colored backgrounds, different ethnicities, and genders. The obtained results were averaged and are listed in the table.

Table 1: Illumination estimation results for images captured under five different lighting condition.

Actual CCT	8000K	6500K	5000K	4000K	3000K
Average estimation	7692K	5997K	4456K	3548K	2644K
ΔT/T	0.04	0.08	0.11	0.11	0.12

All images' illumination estimation results were gathered together and averaged. And the results in Table 1 shows that the relative errors of the CCT of estimated illumination are all lower than 0.15, and it decreases as the CCT becomes higher. This indicates that under larger color temperature, illumination estimation tends to be more accurate. However, when the color temperature are smaller, individual variations in skin tones can lead to a slightly higher level of error in the illumination estimation.
Simultaneously, when processing images with different colored backgrounds as illustrated in Figure 3, it was observed that under the same ambient light source color temperature, different background colors had a noticeable impact on the results of illumination estimation.

Table 2: Illumination estimation results for images captured under D80 lighting condition against five different color backgrounds.

color background	gray	red	green	yellow	blue
predict CCT	7164K	6841K	7161K	6638K	7369K
Duv	0.0099	0.0083	0.0110	0.0098	0.0106
ΔT/T	0.10	0.14	0.10	0.17	0.08

CONCLUSION

By integrating the PMCC, object detection algorithm, skin color segmentation, illumination estimation, and the CAT16 image rendering model, these components have been combined to create a white balance algorithm that demonstrates exceptional performance across an extensive and diverse database of colored backgrounds.

Given the significant impact of skin tone on our visual perception, the algorithm places a preference on utilizing skin color as the reference for white balance. This innovative approach ensures that the accurate and preferred rendering of skin tones takes precedence. As a result, the generated images exhibit a heightened visual appeal and a more authentic, natural appearance.

REFERENCES

[1] J. Van de Weijer, T. Gevers, and A. Gijsenij, "Edge-based color constancy," Ieee Transactions on Image Processing, vol. 16, pp. 2207-2214, Sep 2007.
[2] D. A. Forsyth, "A NOVEL ALGORITHM FOR COLOR CONSTANCY," International Journal of Computer Vision, vol. 5, pp. 5-36, Aug 1990.
[3] J. T. Barron, Y. T. Tsai, and Ieee, "Fast Fourier Color Constancy," in 30th IEEE/CVF Conference on Computer Vision and Pattern Recognition (CVPR), Honolulu, HI, 2017, pp. 6950-6958.
[4] Y. M. Hu, B. Y. Wang, S. Lin, and Ieee, "FC4: Fully Convolutional Color Constancy with Confidence-weighted Pooling," in 30th IEEE/CVF Conference on Computer Vision and Pattern Recognition (CVPR), Honolulu, HI, 2017, pp. 330-339.

[5] M. Afifi, M. S. Brown, and Ieee, "Deep White-Balance Editing," in IEEE/CVF Conference on Computer Vision and Pattern Recognition (CVPR), Electr Network, 2020, pp. 1394-1403.
[6] M. Afifi, B. Price, S. Cohen, and M. S. Brown, "When Color Constancy Goes Wrong: Correcting Improperly White-Balanced Images," in 2019 IEEE/CVF Conference on Computer Vision and Pattern Recognition (CVPR), 2020.
[7] H. Z. Zeng and R. Luo, "Preferred Skin Color Enhancement for Photographic Color Reproduction," in Conference on Color Imaging XVI - Displaying, Processing, Hardcopy, and Applications, San Francisco, CA, 2011.
[8] H. Z. Zeng, R. Luo, and Is, "Preferred Skin Colours of Africans, Caucasians, and Orientals," in 19th Color and Imaging Conference - Color Science and Engineering Systems, Technologies, and Applications, San Jose, CA, 2011, pp. 211-216.
[9] R. Peng, M. R. Luo, Y. C. Zhu, X. X. Liu, and M. Pointer, "Preferred skin reproduction of different skin groups," Vision Research, vol. 207, p. 15, Jun 2023.
[10] M. K. Cao and M. R. Luo, "Preferred skin tones on mobile displays under illuminants having different correlated colour temperatures," Vision Research, vol. 198, p. 12, Sep 2022.
[11] M. K. Cao, M. R. Luo, Y. Lu, and K. Xaio, "A study of preferred and natural memory colours across different ethnic groups," Color Research and Application, vol. 48, pp. 178-200, Mar 2023.

IMAGE STATISTICS AND THE PERCEPTION OF SUMMARY COLOR OF NATURAL MATERIALS#

Y. Zhang[1] and I. Motoyoshi[1]*

[1]*Department of Life Sciences, The University of Tokyo, Japan.*

*Corresponding author: Isamu Motoyoshi, imotoyosi.ac@gmail.com

ABSTRACT

Natural surfaces are composed of multi-dimensional and non-uniform materials. We measured the perceived summary color of 120 natural surfaces and their PS-synthesized and phase randomized versions. We found that the perceived summary colors were nearly identical between the original and synthetic images, and predictable by pixel luminance-color measurements. The results suggest that the human visual system estimates the summary color of natural surfaces based on low-level image statistics.

Keywords: summary color, material, image statistics

INTRODUCTION

Natural surfaces such as fabrics, food and skin usually involve complex and heterogeneous structures with multiple materials. Nonetheless, we easily perceive a single summary color that represents the entire surface. This summary-color perception is the ecologically-valid perceptual judgement about 'color' we do in our daily lives, but has largely been ignored in conventional color studies that defined color perception as visual estimation of the physical reflectance of a local surface and investigated its mechanism using artificial stimuli such as uniform patches and CG objects, which hardly exist in the real world. Here, we examined the perceived summary color for a large variety of natural surfaces and explored visual information that determines the perceived summary color of an object in the real world. In contrast to the prediction of classical theories of surface-color perception that requires extremely heavy computation to estimate and integrate local reflectance, we found that the human visual system utilizes simple image statistics to efficiently estimate the summary color of complex natural surfaces.

METHODOLOGY

Stimulus Visual stimuli were 120 photograph images of real-world surfaces and their Portilla-Simoncelli (PS)-synthesized images and phase-randomized images (Figure 1). Our preliminary rating experiments confirmed that the perception of material properties such as 3D shape, gloss, and softness, were substantially impaired in both types of synthetic images.

Figure 1. Examples of surface images used in the experiment: the original images (top), PS-synthesized images (middle), and phase-randomized images (bottom).

Procedure The apparent summary colors of a total of 360 images (4.6 x 4.6 deg) were measured using an asymmetric color matching method. Ten observers (~23 years old on average) adjusted the lightness and color of the uniform reference patch (1.2 x 1.2 deg) in CIE La*b* space so that its color was equal to the summary color of the target surface. Observers were asked to match the summary color in accordance with the common sense, and not to use any special knowledge about the physical and chemical properties of the surface. They were also encouraged to adjust the color using the continuous color appearance spectrum, bypassing the use of categorical color names. Each observer spent 4-5 hours to complete the matchings for all 360 images. For each image, we calculated the average matched [L, a*, b*] across ten observers.

RESULT AND DISCUSSION

Figure 2 shows the matched summary colors plotted on the a*-b* plane (left) and on the L-Chroma plane (right). We found that for all stimuli except one (239/240), the matched summary color for the synthetic images was not significantly different from that for the original images (T^2 test based on the Mahalanobis distance, corrected for multiple comparisons using Benjamini–Hochberg's FDR (0.05)). These results strongly support the idea that the perception of summary colors of natural surfaces (unlike the perception of other material properties such as gloss) is determined only by low-level image statistics.

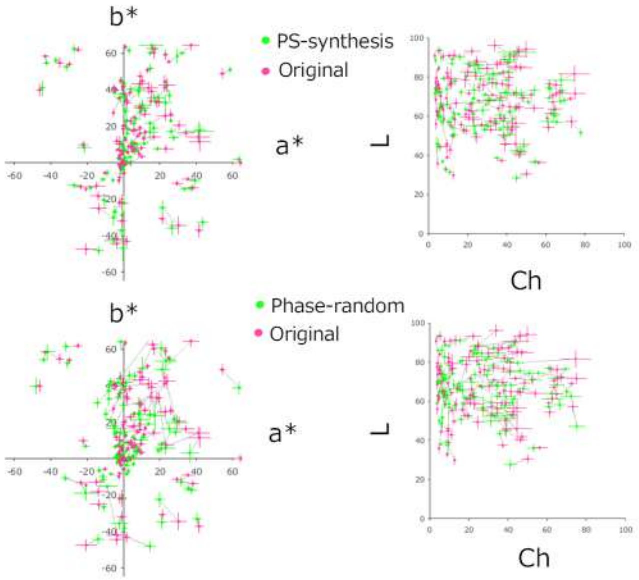

Figure 2. Comparison of the matched summary colors between the original and synthetic images. The upper panels show the results for the original vs. PS-synthesized images, and the lower panels the results for the original vs. phase-randomized images, respectively. The left panels represent the data on the (a*, b*) plane, and the right panels the data on the (chroma, L) plane, respectively. Error bars represent +-1 s.e.m. across observers.

We compared the matched summary colors with the pixel mean of the image, and found that for nearly all stimuli, the matched summary colors were lighter and more saturated than the pixel mean of the image, as illustrated in Figure 3. The previous studies have reported similar overestimations in the surface color perception of CG objects and in the average color estimation of random-dot patterns [1, 2, 3]. Several studies have also suggested more specifically that the humans tend to ignore bright highlights and dark shadows to estimate the color of a solid object [4].

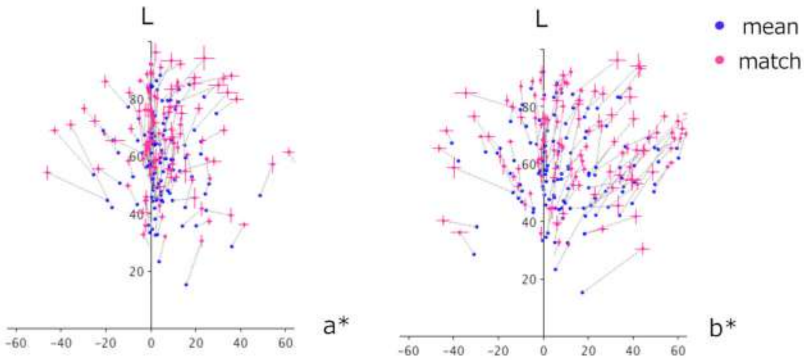

Figure 3. Comparison of the matched summary color with the pixel mean of the image. The red circles represent the matched summary color (original image) and the blue circles the pixel mean. The left panels represent the data on the (L, a*) plane, and the right panels the data on the (L, b*) plane, respectively. Error bars represent +-1 s.e.m. across observers.

On the basis of the results observed in Figure 3 and of the previous findings, we proposed a simple model for the summary color perception (Figure 4), assuming that the perceived summary color is determined by (1) the robust average of the image, and (2) the enhancement of color saturation. Specifically, the model calculates the average L_{mean}, a^*_{mean}, and b^*_{mean} of pixels in the image region in which the L contrast, $C(x,y) = L(x,y)/L_{mean}-1$, of the image $L(x,y)$ is within a range from C_{lim}- to C_{lim}+ , and multiplies a^*_{mean} and b^*_{mean} by M respectively. The resulting (L, a*, b*) value is then assumed to be matched as the summary color of that surface image.

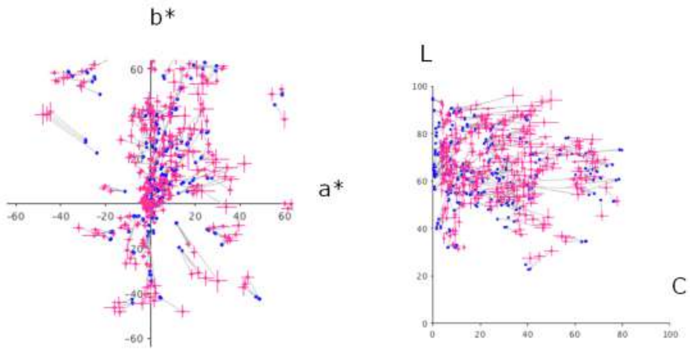

Figure 4. Model-predicted matching data and observer matching data (all 360 images). The red circles represent the matched summary color by human observers and the blue circles those predicted by the robust-average model. The left panels represent the data on the (a*, b*) plane, and the right panels the data on the (Chroma, L) plane, respectively. Error bars represent +-1 s.e.m. across observers.

We conducted a numerical simulation in which the three parameters [C_{lim}+, C_{lim}-, M] were optimized to minimize the distance between the La*b* value predicted by the model and the mean La*b* value of human observers. The results showed that, with the optimized parameters, [C_{lim}+, C_{lim}-, M] = [2.00, -0.40, 1.20], very high correlation coefficients between the human and model data: [L, a*, b*] = [0.95, 0.95, 0.97] ($p<10^{-190}$, $p<10^{-182}$, $p<10^{-218}$). Moreover, a T^2 test performed for the individual images showed that the predicted data were significantly different from the human data for only 1 out of 360 images (multiple comparisons were corrected (FDR)).

These results clearly demonstrate that the summary color perception of real-world surfaces are well predicted and accounted for by low-level image statistics which are easily computed without any high-level information such as shading or 3D shape. It should be noted that one can expect even more accurate predictions by incorporating other texture statistics as represented in the early visual cortex: V1/V2 [e.g., 5].

CONCLUSION

The present study investigated visual mechanisms for the perception of the summary color of natural surfaces, by using a much larger number of stimuli which were far more ecologically-valid than those used in the past surface-color perception studies. Our results showed that observers perceived nearly the same perceived summary colors for statistically synthesized images as for the original natural images even though they could not properly perceive material properties (e.g., gloss) nor 3D shape (e.g., bump) in the synthetic images.

According to classical computational theories of surface color perception, in order to estimate the summary color of a surface, the visual system must 'reconstruct' various types of reflectance properties for every local part of surface area with considerations of illumination and surface directions in the external 3D space (e.g., shading and constancy). If this is the case, the perceived summary color should have been largely different in the synthetic images that lacked many cues of 3D structures. In contrast to this prediction, however, our results showed no evidence for the use of such high-level information, and suggest that the human visual system utilizes simple image statistics to estimate the summary color of complex natural surfaces. This strategy is indeed efficient as those statistical information can be easily computed in the early visual cortex.

It is yet unclear how the visual system computes critical image statistics for summary-color perception. The visual system may have neural units that are able to robust average of color signals withing a large receptive field. Or the visual system may serially sample local color information at many places within a surface, then integrate them to make a decision about the summary color of the entire surface [6]. The results of our subsequent experiments shows that the perceived summary color does not change even with a short stimulus duration (100 ms), supporting the rapid one-shot computation.

The perceived material properties were severely impaired in synthetic images while the summary color perception was not. This discrepancy appears to indicate that the perception of most material properties except color requires high-level visual information beyond image statistics. However, our subsequent experiments demonstrated that the perceived material properties (gloss, 3D bumps, softness) were fairly preserved in images synthesized with high-level statistical representation in DNN. This supports the notion that the perception of surface properties is generally based on textural / statistical information in the 2D image.

ACKNOWLEDGEMENT

This study was supported by JSPS KAKENHI JP20H01782 and JP20K21803, JP23H01054 to IM, and by JST SPRING-GX JPMJSP2108 to YZ. A part of the study has been published in Scientific Reports [7] after the AIC abstract was submitted.

REFERENCES

1. Kuriki, I. (2004). Testing the possibility of average-color perception from multi-colored patterns. *Optical Review*, *11*(4), 249-257.
2. Toscani, M., Valsecchi, M., & Gegenfurtner, K. R. (2013). Optimal sampling of visual information for lightness judgments. *Proceedings of the National Academy of Sciences*, *110*(27), 11163-11168.
3. Kimura, E. (2018). Averaging colors of multicolor mosaics. *JOSA A*, *35*(4), B43-B54
4. Giesel, M., & Gegenfurtner, K. R. (2010). Color appearance of real objects varying in material, hue, and shape. *Journal of vision*, *10*(9), 10-10.
5. Portilla, J., & Simoncelli, E. P. (2000). A parametric texture model based on joint statistics of complex wavelet coefficients. *International Journal of Computer Vision*, *40*, 49-70.
6. Brenner, E., Granzier, J. J. & Smeets, J. B. (2007). Perceiving colour at a glimpse: The relevance of where one fixates. *Vision Research, 47*(19), 2557–2568.
7. Zhang, Y. & Motoyoshi, I. (2023). Perceiving the representative surface color of real-world materials. *Scientific Reports, 13*, 6300.

RELIABLE UNCERTAINTY EVALUATION OF MEASUREMENTS OF COLOR QUANTITIES

E. Ikonen[1,2]*, Y. Rezazadeh[1], and K. Maham[1]

[1]*Metrology Research Institute, Aalto University, Finland.*
[2]*VTT MIKES, VTT Technical Research Centre of Finland Ltd, Finland.*

*Corresponding author: Erkki Ikonen, erkki.ikonen@aalto.fi

ABSTRACT

Many color quantities, such as reflective tristimulus values and color coordinates, are defined in terms of ratios of spectral integrals. Reliable uncertainty evaluation of measurement results of such quantities is challenging because ratios of spectral integrals critically depend on partial correlation between measured values at different wavelengths. There are three types of uncertainty components related to spectral correlation: fully correlated like geometrical factors and amplifier gains, fully uncorrelated like detector noise, and spectrally partly correlated. The first two types of correlations do not contribute significantly to the uncertainty of ratio of spectral integrals. The third type of uncertainty components is the most important here and can be further divided to known and unknown spectral correlations. An example of an uncertainty component with known correlation properties is the distribution temperature of lamp filament that leads to deviated spectral irradiance values which can be approximately calculated by the Planck radiation law. For the unknown correlations, it has been difficult to assess quantitatively the uncertainty because the spectral shape of deviation from the true value is unknown and not necessarily linear. This work presents a novel solution to the problem of evaluating the uncertainty related to unknown partial correlations.

Keywords: Uncertainty, color coordinates, spectral integrals, partial correlation, key comparisons

1. INTRODUCTION

Colorimetry plays a pivotal role in quantifying human perception of color, bridging the gap between the subjective experience and objective measurement. By employing standardized color spaces and accurate instrumentation, colorimetry enables the quantification of color attributes. This is crucial across industries such as design, manufacturing, and digital imaging, which require consistent color reproduction with low measurement uncertainty.

Much of quantitative colorimetry is based on tristimulus values X, Y, Z and color coordinates $x = X / (X+Y+Z)$ and $y = Y / (X+Y+Z)$. Emissive tristimulus values are spectral integrals, such as

$$X = \int L_e(\lambda)\, \bar{x}(\lambda)\, d\lambda, \tag{1}$$

and corresponding equations for Y and Z. In Eq. (1), $L_e(\lambda)$ is the spectral radiance and $\bar{x}(\lambda)$ as well as related $\bar{y}(\lambda)$ and $\bar{z}(\lambda)$ are defined CIE standard observers [1]. Reflective tristimulus values are defined as ratios of spectral integrals due to normalization by spectral power distribution of the illuminant. Key measurements for colorimetry to determine the radiance of a surface are spectral irradiance or spectral reflectance measurements.

Reliable uncertainty estimates are difficult to obtain for color coordinates x and y because a constant multiplicative factor in front of $L_e(\lambda)$ cancels out in the ratio of spectral integrals, producing zero uncertainty due to such fully correlated uncertainty components which affect similarly at all wavelengths. Furthermore, fully uncorrelated uncertainty components (like noise) also produce a very small uncertainty. For a realistic uncertainty estimate, effects of measurement errors which are correlated at neighboring wavelengths but possibly uncorrelated at distant wavelengths should be considered. However, it is often unknown how much such harmful partial correlation affects the measurement result in practice. Only a probable maximum value, called severe effect of partial correlation, can be obtained [2]. To reach a meaningful numerical estimate for the uncertainty of quantities defined in terms of ratios of spectral integrals, it was then necessary to make a strong assumption of equal weights of fully correlated, fully uncorrelated and severely partially correlated components in the uncertainty evaluation [2,3].

The objective of this work was to study the validity of the above assumption of equal weights of the different correlation components and search for better justified assumptions as the basis of uncertainty evaluation of ratios of spectral integrals. For this purpose, we have studied a sample of radiometry key comparisons in the Key Comparison Database maintained by BIPM in Paris [4]. The comparisons have typically a dozen of participants and they can be considered as the most carefully performed measurements in optical radiometry. Spectral analysis of the deviations of the results from the key comparison reference value (KCRV) in seven comparisons gave a consistent outcome that the average harmonic amplitudes of the deviations are inversely proportional to the harmonic order. It can be concluded that such spectral structure is probably present in all carefully performed measurements in radiometry and colorimetry. This novel result allows to carry out a quantitative uncertainty evaluation of color quantities defined in terms of ratios of spectral integrals. The new method has a solid statistical justification to estimate the effect of most probable spectral deviations from the true value, corresponding to the earlier problematic unknown partial correlations.

METHODOLOGY

1.1. Key comparison analysis

Figure 1(a) shows an example of deviations from the KCRV in the spectral irradiance comparison CCPR-K1.a. The fitting was done over the spectral range λ_1 = 250 nm to λ_2 = 2500 nm. The fitted solid line is constructed as a sum of spectral components,

$$\delta(\lambda) = \sum_{i=0}^{N} A_i f_i(\lambda), \tag{2}$$

where A_i is the fitted amplitude of ith harmonic component and functions $f_i(\lambda)$ form an orthogonal basis when integrating the wavelength λ from λ_1 to λ_2. Specifically, $f_0(\lambda) = 1$.

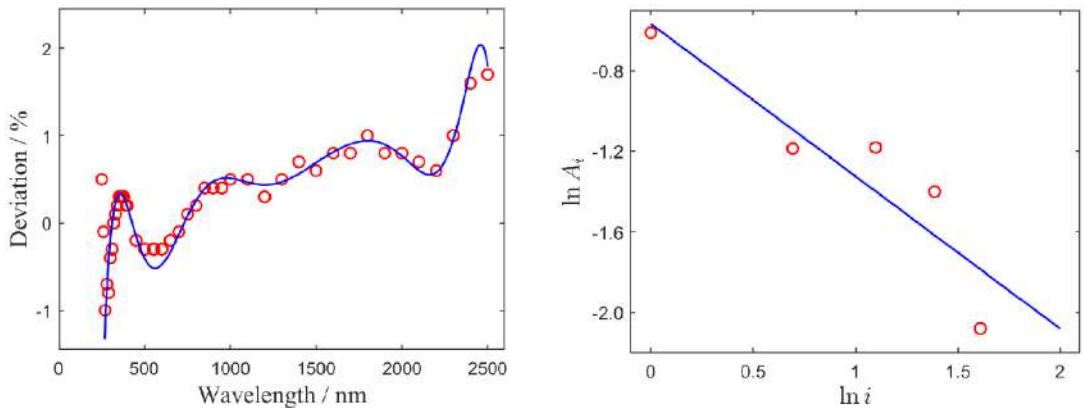

(a) (b)

Figure 1. (a) Deviations of a participant's data from KCRV in spectral irradiance comparison CCPR-K1.a (open circles). Solid line is a fit by Eqs. (2) and (3) with N = 5. (b) Logarithm of average deviation amplitudes $\bar{A}_i$ of eleven participants at different basis function orders i in CCPR-K1.a key comparison. Amplitude $\bar{A}_0$ is excluded from the data. The linear fit indicates a universal slope close to -1 observed in all studied key comparisons.

Sinusoidal basis functions with random phase φ_i have been used earlier in analyses of the effects of unknown correlations [2]. Here we fit phases φ_i and use Legendre polynomials $P_i(\lambda)$, scaled by their standard deviation σ_i according to $g_i(\lambda) = P_i(\lambda)/\sigma_i$, as the basis functions

$$f_i(\lambda) = g_{2i-1}(\lambda)\cos\varphi_i + g_{2i}(\lambda)\sin\varphi_i, \tag{3}$$

where $i = 1, 2, \ldots, N$. This is an advantageous choice because the first order Legendre polynomial $P_1(\lambda)$ forms a constant slope as a function of wavelength. Equation (3) then allows better fits to the deviations from the KCRV than use of sinusoidal basis functions. The basis functions $f_i(\lambda)$ formed with the help of Legendre polynomials correspond to sinusoidal harmonics of order i.

Eleven participants of spectral irradiance comparison K1.a had sufficient spectral coverage to use the Legendre polynomials in analysing the harmonic content of deviations from KCRV up to $N = 5$ in Eq. (2). The obtained results on average amplitudes $\bar{A}_i$ of these eleven participants are shown in Fig. 1(b) on log-log scales. Fit of the line

$$\ln \bar{A}_i = a + b \cdot \ln i, \tag{4}$$

where a is the intercept, gives the slope $b = -0.76$.

The KCDB contains data from six other CCPR key comparisons which can be used for similar analysis as carried out for K1.a. The results are shown in Table 1. For some comparisons, the number of spectral points was low, and the number of basis functions could be extended only up to $N = 4$ in Eq. (2). The report on spectral diffuse reflectance comparison K5 [4] contains two different data sets A and B, which are here treated as separate comparisons.

The slope parameters of all key comparisons of Table 1 are roughly equal. The average slope is $b = -0.96$ with a standard deviation of 0.14 in the sample of seven comparisons. According to Eq. (4) the average amplitude of basis functions is proportional to i^b or approximately $\bar{A}_i \cong e^a/i$, when $b \cong -1$. The observed power law corresponds to $1/f$ noise because the harmonic order i is proportional to frequency. It is noteworthy that various tests of synthesizing key comparison results by random numbers always yielded $b \cong 0$.

Table 1: Summary of spectral analysis of deviations from key comparison reference values. The number of basis functions used is $N + 1$ and b is the slope describing the decay of the amplitudes of basis functions (i.e., harmonics) with increasing order number.

Key comparison [4]	N	Slope b
CCPR-K1.a	5	-0.76
CCPR-K1.b	5	-1.03
CCPR-K2.a	4	-0.82
CCPR-K2.b	5	-0.86
CCPR-K2.c	4	-1.09
CCPR-K5(A)	5	-1.03
CCPR-K5(B)	5	-1.12
Average ± standard dev.		-0.96 ± 0.14

2.2. Application to uncertainty evaluation

Although the deviations from the true value in the key comparison analysis are often smaller than the measurement uncertainty, the revealed spectral structure may lead to (unknown) correlations between the values measured at close-by wavelengths. This finding has implications to uncertainty evaluation of spectral integrals, where the largest contribution comes from partial correlations [2,3]. As described below, the universal power law $\bar{A}_i \propto 1/i$ allows to improve the reliability of determined uncertainties, because the earlier rough assumption of equal probability of fully correlated, partially correlated and non-correlated uncertainty contributions can be replaced by a more quantitative approach.

The method of analyzing the effect of severe partial correlations on the ratio of spectral integrals, such as those appearing in color coordinates x and y, is based on introducing a deviated spectral radiance $L_{e,dev}(\lambda)$ according to

$$L_{e,dev}(\lambda) = [1 + \delta(\lambda)\, u_c(\lambda)]\, L_e(\lambda), \tag{4}$$

where $L_e(\lambda)$ is the nominal spectral radiance, $\delta(\lambda)$ is a deviation function to be described in more detail below, and $u_c(\lambda)$ is the relative combined standard uncertainty of spectral radiance, consisting of various uncertainty components of unknown correlation properties. For the earlier uncertainty analysis through Monte Carlo (MC) simulation, function $\delta(\lambda)$ was calculated according to [2,3]

$$\delta(\lambda) = \sum_{i=0}^{N} \gamma_i f_i(\lambda)\,, \tag{5}$$

where $N + 1$ is the number of basis functions used and γ_i are the coordinates of a random point on the surface of an (N+1)-dimensional unit sphere, i.e., they meet the normalization condition

$$\sum_{i=0}^{N} \gamma_i^2 = 1. \tag{6}$$

Each MC cycle generates new values for γ_i and the phases φ_i of the orthogonal and normalized basis functions $f_i(\lambda)$. The deviated spectral radiance of Eq. (4) is used in Eq. (1) and in the corresponding equations for Y and Z to calculate color coordinates x and y as ratios of spectral integrals X, Y, and Z. After many cycles of MC simulation, the obtained values of x and y give their joint probability distribution and estimates for their standard deviation and covariance for a fixed value of N.

The values of coordinates γ_i define the amplitudes of the basis functions. The problem of the MC simulation method described in the above paragraph is that the amplitudes γ_i are completely independent of each other which leads to a strong dependence of the standard deviation on the selected value of N. Severe partial correlations are typically obtained at values of N between 2 and 5. To obtain a reasonable numerical estimate for the uncertainty of color coordinates, it was thus necessary to make an additional strong assumption that the weights of contributions by fully correlated, fully uncorrelated and severely partially correlated uncertainty components are equal [2].

In analysing the spectral deviations from key comparison reference values, it was concluded in Sec. 2.1 that the amplitudes of the basis functions $f_i(\lambda)$ follow the power law $\bar{A}_i \propto 1/i$. When this result is substituted in Eq. (5) with $\gamma_i = \bar{A}_i \propto 1/i$ and the normalization condition of Eq. (6) is used, the equation for the deviation function gets the form

$$\delta(\lambda) = \gamma_0 + \gamma_1 \sum_{i=1}^{N} f_i(\lambda)\,/\,i, \tag{7}$$

where $\gamma_0 = \sin\varphi$,

$$\gamma_1 = \frac{\cos\varphi}{\sqrt{\sum_{i=1}^{N} 1/\,i^2}} \tag{8}$$

and φ is a random phase from a uniform distribution between 0 and 2π. The orthogonal basis functions $f_i(\lambda)$ used for the MC analysis are given by Eq. (3), where the phases φ_i also get random values from a uniform distribution between 0 and 2π.

RESULTS AND DISCUSSION

The deviation function $\delta(\lambda)$ of Eq. (7) was used with the spectral radiance of Eq. (4) in the MC simulation to calculate the probability distribution of color coordinates x and y as the ratio of spectral integrals like that presented in Eq. (1). As an example case, the nominal spectral radiance $L_e(\lambda)$ was selected in such a way that it has the same spectral shape as CIE Illuminant A [5] in the wavelength range 360 nm – 830 nm, but any other spectral range or shape of the surface radiance, obtained as a combination of reflectance and illumination spectrum, could be used. The relative standard uncertainty of spectral radiance was taken as $u_c(\lambda) = 0.01$ and the wavelength step in the measurements as 5 nm, leading to a maximum value of $N = 235$ in the MC simulations. The color coordinates get expected values $\langle x \rangle = 0.4476$ and $\langle y \rangle = 0.4074$. Figure 2 shows as red circles the expanded uncertainties at 95 % confidence level as derived from the obtained probability distributions of x and y.

In Fig. 2, the results by Eq. (7) are also compared with the results calculated according to Eq. (5). It is seen than the former results reach a stable uncertainty estimate at large values of N, while the latter uncertainties reduce with increasing N. The reason for reducing uncertainty is that the emerging higher harmonics change x and y only little in the latter case, although they contribute significantly to the standard deviation of $L_{e,dev}(\lambda)$. The solution to the problem of obtaining a unique uncertainty for x and y was solved in [2] by assigning equal weights to the contributions of different correlation types. Such procedure leads to 0.0008 and 0.0007 as the expanded uncertainty of x and y, respectively. In the case of Eq. (7), the weight of higher harmonics reduces as $1/i$, which leads to well-defined uncertainty estimates of 0.0013 and 0.0008, respectively, for large values of N. The obtained uncertainties for color coordinate y are close to each other, while the uncertainties of x deviate by a factor of 1.6. The latter values obtained from Eq. (7) are more reliable because they are based on improved information on partial correlations affecting ratios of spectral integrals.

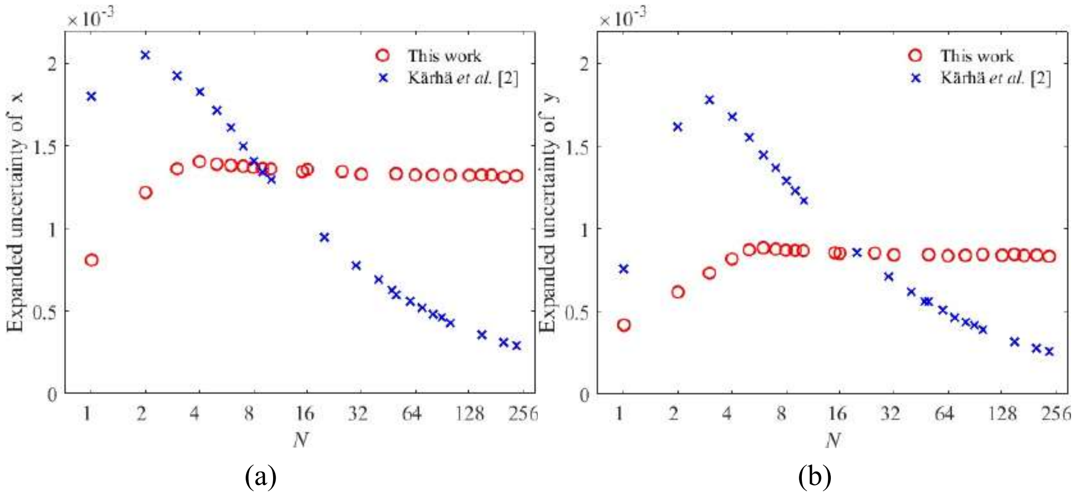

Figure 2. Expanded uncertainty of color coordinates x (a) and y (b) calculated by Monte Carlo simulation. Results indicated by blue crosses are similar as those reported in Ref. [2] and they are calculated according to Eq. (5) using sinusoidal basis functions, while red circles are calculated by Eq. (7) using Legendre polynomials as basis functions. On the horizontal scale, parameter N is related to the number of basis functions used in the equations.

The MC method described by Eq. (7) allows improved reliability in uncertainty estimates of quantities defined in terms of ratios of spectral integrals, concerning severe partial correlations whose spectral shape is unknown. In some cases, the correlation between measurement results at different wavelengths is known. A straightforward example of such case is illumination of a white surface with radiation from a black body of measured temperature. The probability distribution of measured temperature can be directly converted to the probability distribution of spectral radiance using the Planck radiation law. For a standard uncertainty of 10 K at the black body temperature of 2856 K, the uncertainty of color coordinates x and y was calculated to be an order of magnitude smaller than that presented in Fig. 2.

Another uncertainty component type of known correlation properties is provided by noise where measurements at each wavelength are fully uncorrelated. For a 1 % relative standard deviation of noise in measurement of spectral radiance, the contribution to the expanded uncertainty of color coordinates x and y is about 0.0003 in both cases. These are minor fractions of the uncertainties due to unknown partial correlations of similar magnitude as presented in Fig. 2.

When a proper uncertainty analysis for quantities, such as color coordinates, has been carried out, the results can be further used to determine values of other quantities with their uncertainties. In that step, the covariance matrix of correlated quantities needs to be taken into account, i.e., the non-diagonal element $\langle (x - \langle x \rangle)(y - \langle y \rangle) \rangle$ in the case of color coordinates. The diagonal elements of the covariance matrix are the squares of the standard uncertainties, and the non-diagonal elements can be calculated by similar MC simulation as the diagonal elements in the case of unknown partial correlations.

CONCLUSION

The results confirm that the uncertainty components due to partial correlation are much larger than those uncertainty components that have full spectral correlation or that are fully uncorrelated between different wavelengths. If the partial correlations are not properly considered, the uncertainty of ratios of spectral integrals will become severely underestimated. For the first time, a reliable uncertainty estimate can now be presented for any color quantity defined in terms of ratios of spectral integrals, such as reflective tristimulus values and color coordinates.

ACKNOWLEDGEMENT

The project 19ENV04 Metrology for Aerosol Optical Properties (MAPP) leading to this publication has received funding from the EMPIR programme co-financed by the Participating States and the European Union's Horizon 2020 research and innovation programme. This work is partly funded by the Academy of Finland Flagship Programme, Photonics Research and Innovation (PREIN), decision number: 320167.

REFERENCES

1. CIE S 014-1:2006 Colorimetry-Part 1: CIE Standard Colorimetric Observers (Vienna).
2. Kärhä P, Vaskuri A, Mäntynen H, Mikkonen N, and Ikonen E (2017). Method for estimating effects of unknown correlations in spectral irradiance data on uncertainties of spectrally integrated colorimetric quantities. *Metrologia* **54**, 524 - 534.
3. Vaskuri A, Kärhä P, Egli L, Gröbner J, and Ikonen E (2018). Uncertainty analysis of total ozone derived from direct solar irradiance spectra in the presence of unknown spectral deviations. *Atmospheric Measurement Techniques* **11**, 3595 - 3610.
4. https://www.bipm.org/kcdb/comparison/quick-search.
5. CIE S 014-2/E:2006 CIE Colorimetry-Part 2: Standard Illuminants for Colorimetry (Vienna).

Poster Paper

RELATIONSHIP BETWEEN COLOR PREFERENCE AND PERSONALITY TRAIT IN SELECTING CLOTHING

Shinji Nakamura*

School of Psychology, Faculty of Education and Psychology, Nihon Fukushi University, Japan.

*Corresponding author: Shinji Nakamura, shinji@n-fukushi.ac.jp

ABSTRACT

In this study, we investigated the effects of participants' color preferences on their behavior in choosing a color of clothing, especially considering how their personality traits mediate between the color preference and clothe-choosing behavior. In the survey, the participants were asked to select "most preferred/hated color", "most preferred/hated clothing color", "most wearing/non-wearing color)" from nine candidate colors (red, orange, yellow, yellow-green, green, blue, purple, pink, brown). After selecting the colors, the participants were also asked to report the impressions of those colors using a Semantic Differential method which employed 15 pairs of adjectives. In addition, the participant's personality trait was measured using "Ten Item Personality Inventory Japanese version (TIPI-J)". TIPI-J can simultaneously assess "Openness to experience", "Conscientiousness", "Extraversion", "Agreeableness" and "Neuroticism" based on a well-known "Big-Five theory." The results indicated that the participants whose preferred color was consistent with their preferred clothing and wearing colors exhibited significantly lower neuroticism. This result suggests that those who were more concerned about evaluation by others (those with higher neuroticism) had difficulty in selecting clothing color based on their own color preferences, but had inclination to select their clothing color to fit in an occasion and avoid becoming conspicuous. The current investigation has successfully evinced that the personality trait can mediate the relationship between color preference and clothing choosing behavior.

Keywords: Color preference, Cloth Choosing, Personality trait

INTRODUCTION

Most of the psychological research on color preferences to date has used a method of asking about the degree of preference or aversion to the color itself (abstract color preference, or general color preference) without presenting or evoking a concrete object that has been colored. However, what we actually see are colors applied to the objects. What does this abstract color preference really mean (see [1] for further discussion concerning relationship between the abstract and specific color preferences). In order to further investigate the relationship between the abstract and the specific color preferences, this study focuses on "clothing," which has a wide range of color variations and its color is highly important in purchase decisions, but also has certain scene constraints. Previous studies have shown that there is a significant correlation between the psychological image of preferred/hate colors and the participants' own personality image (e.g., [2]), suggesting the possibility that personality characteristics and image of colors (of clothes) have a mediating effect on the influence of color preference in clothing color selection. In this study, we examine the effects of participants' personality traits and color image on the relationship between abstract color preference and clothing color selection.

METHODOLOGY

Participants

A total of 103 undergraduate students (56 males and 47 females, mean age 19.2 years) participated in the survey.

Procedures

The participants answered their "most favorite color (preference color)," "favorite clothing color (clothing preference color)," "frequently worn clothing color (wearing color)," "most dislike color (hate color)," "dislike clothing color (clothing hate color)," and "least worn clothing color (non-wearing color)," by selecting one color from the following nine options: red, orange, yellow, yellow-green, green, blue, purple, pink, and brown. The colors were indicated by Japanese words (Japanese Kanji [Chinese] characters).

Furthermore, impressions of each selected color were measured by the Semantic Differential method using 15 bipolar adjective pairs, such as "bright-dark," "cheerful-gloomy," and so on (seven points scale). In addition, the Japanese version of the Ten Item Personality Inventory (TIPI-J) was used to measure the participant' personality traits. TIPI-J is a psychological scale developed in accordance with the Big Five theory, and measures the participants' personality traits using a five-factor structure: extraversion, agreeableness, conscientiousness, neuroticism, and openness (10 items, 7 points scale).

Ethical statement

After explaining the outline of the survey, we explained to the survey participants that 1) the survey would be conducted anonymously, 2) the survey results would be statistically processed and no personal data would be made public, and 3) they would not suffer any disadvantages if they did not agree to participate in the survey or withdrew from the survey.

RESULT AND DISCUSSION

Distribution of Preferred and Hated colors

Figures 1-3 show distributions of three different types of participant's preferred colors (preference color, clothing preference color and wearing color) and hated colors (hate color, clothing hate color and non-wearing color) for all participants, male, and female participants, respectively. Blue was most selected as the reference color, the clothing preference color and the wearing color. Although this tendency was shared with the male and the female participants, but it was more pronounced among the male. Whereas the percentage of participants who selected brown as their preference color was very low, both male and female selected brown as their clothing preference color and wearing color to a certain extent. As for hated colors, both male and female showed a high tendency to select pink as their hate color, as well as the clothing hate color and the non-wearing color.

In order to examine the differences in the selection ratios between male and female, a two-factor χ^2 test was conducted for each of the six preferred and hated colors. Significant differences in color selection ratios were confirmed in the wearing colors ($\chi^2(8)=22.05$, $p=.002$). Residual analysis indicated that males selected blue as their wearing color more frequently than females, and females selected brown as their wearing color more frequently than males.

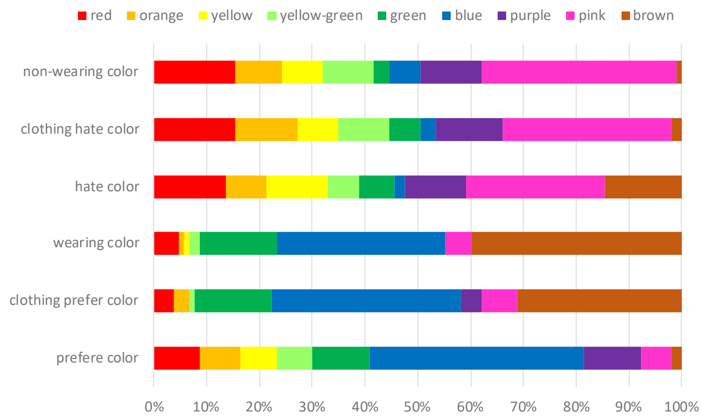

Fig.1 Distributions of prefered /hated colors(All participants)

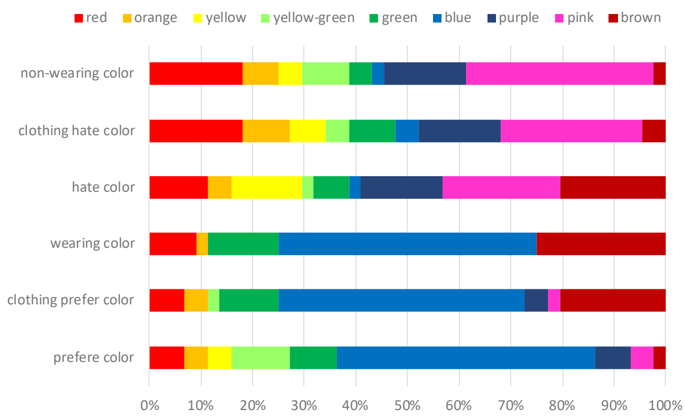

Fig.2 Distributions of prefered/hated colors (male)

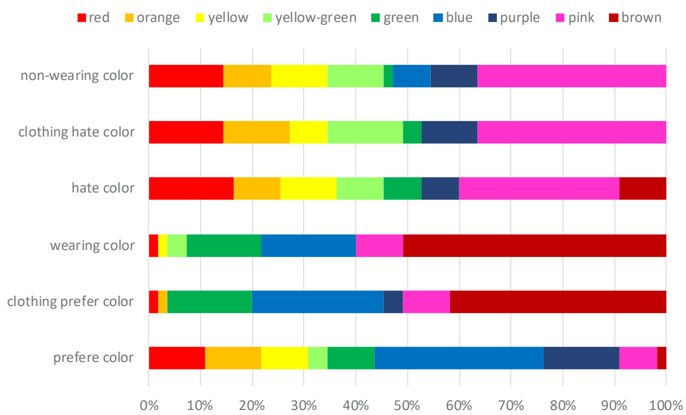

Fig.3 Distributions of prefered/hated colors (female)

Relationship between personality traits and consistency/inconsistency among preferred/hated colors

Figures 4-6 indicate averaged participants' personality scores as a function of consistency/ inconsistency between preferred colors. The group whose preferred color was inconsistent with their clothing preference color showed a significant tendency to have higher neuroticism scores than the group whose preferred color was congruent. Similarly, the participants whose preferred color was inconsistent with their clothing color showed a significant tendency to have higher neuroticism than those whose preferred color was congruent ($t(101)=1.61$, $p=.054$, $t(101)=1.78$, $p=.039$, respectively). This result indicates that participants with higher neuroticism would be highly concerned about their evaluation from others, and they cannot choose their favorite clothing nor actually select their clothing based on their own favorite color.

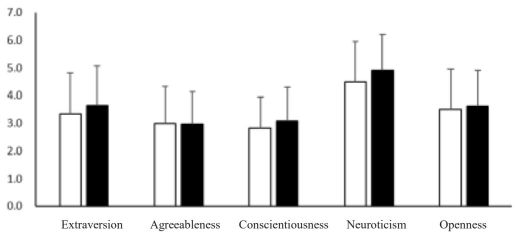

Fig. 4 Averaged personality scores for participants whose preference and clothing preferred colors were consistent/inconsistent

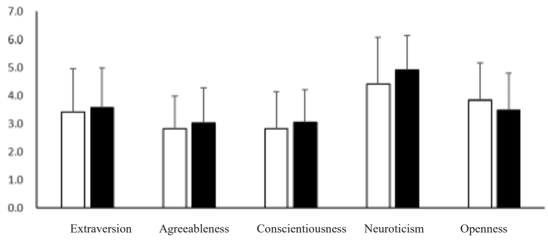

Fig.5 Averaged personality scores for participants whose preference and wearing colors were consistent/inconsistent

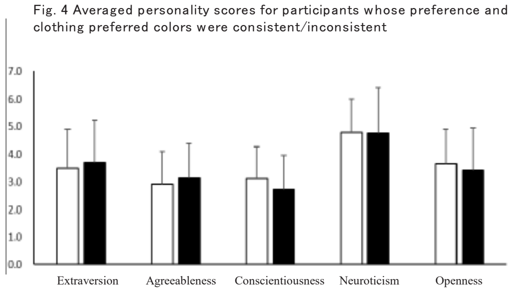

Fig. 6 Averaged personality scores for participants whose clothing preference and wearing colors were consistent/inconsistent

Color Image of Preferred/Hated Colors －

Factor analysis was applied to the results of the SD measurements, and got three factors, namely “activity” ("passionate/intelligent," "dynamic/static," etc.), “flexibility” ("soft/sharp," "feminine/ masculine," etc.), and “clarity” ("clean - dirty," "clear - muddy," etc.).

Figures 7 and 8 show the evaluation scores for the preferred colors (preference color, clothing preference color, and wearing color) and the hated colors (hate color, clothing hate color, and non-wearing color). One sample t-tests with Bonferroni correction were conducted, in order to assess whether there was a significant discrepancy from the median point of SD evaluation (minimum significance level was set to 5%). Clarity was significantly higher in the preference color ($t=12.68$) than the baseline. In the clothing preference and the wearing colors, activity was lower ($t=-5.01$, -5.08), and flexibility ($t=-2.93$, 3.89) and clarity ($t=-4.32$, 2.93) was higher. In the hated color, activity was significantly higher ($t=6.22$) as compared with the baseline. Furthermore, in the clothing hate and the non-wearing colors, activity ($t=8.61$, 7.55) and clarity

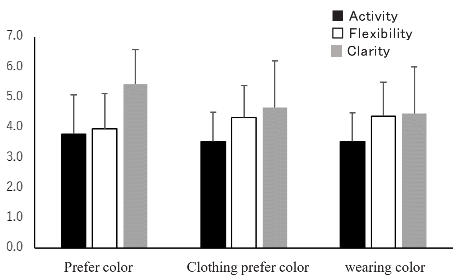

Fig. 7 Averaged evaluation scores for preferred colors

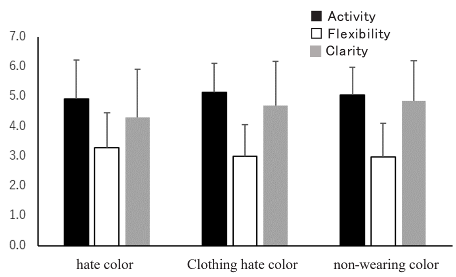

Fig. 8 Averaged evaluation scores for hated colors

(t=4.84, 6.35) were higher but flexibility (t=-7.34, -7.46) was lower. In particular, flexibilities for three different hated colors (hate color, clothing hate color, and non-wearing color) were remarkably low, and strongly suggested that colors not giving a flexible image are not preferred, both in terms of abstract color preferences and specific color preferences (regarding clothing selection). In addition, the deviation from the baseline was greater for the specific color preferences (clothing preference, wearing, clothing hate, and non-wearing colors) than for the abstract color preferences (preference and hate colors), suggesting that the effect of the psychological images of the designated color (color image) may be greater in the specific color preferences than the abstract color preference.

Relationship between Color Images of Preferred/Hated Colors and Personality Traits

In order to examine the similarities in color images among the preferred colors and among the hated colors, the three-dimensional spatial distance between any two selected colors, namely the color image distances, were calculated based on the three evaluation scores (activity, flexibility, and clarity) for each participant. Table 1 indicates Pearson's coefficients of correlation between the participants' personality scores and the color image distances. Color image distance between clothing preference color and wearing color exhibits a weak but significant negative correlation against conscientiousness scores. Thus, the participants with higher conscientiousness tend to wear clothing whose color image was similar with their favorite clothing color. It is said that those who have higher conscientiousness also have higher abilities in controlling their behavior and higher tendencies to plan their behavior in advance. It is possible to consider that they may choose/buy their clothing based on their specific color preference in their everyday livings. Similarly, color image distance between prefer color and clothing wearing color indicates a significant negative correlation against openness. Those with higher openness would open their mind toward new experiences, and might have tendency to boldly select clothing with an image similar to one's favorite color (somewhat ignoring contextual/situational constraints).

Tab.1 Coefficients of correlation between color image distance and personality score

	Prefer-Clothing prefer	Clothing prefer-Wearing	Prefer-Wearing	Hate-Clothing hate	Clothing hate-Non_wearing	Hate-Non_wearing
Extraversion	0.14	0.02	0.03	0.02	0.14	0.08
Agreeableness	0.00	0.08	0.04	-0.18	0.00	-0.10
Conscientiousness	-0.04	-0.23*	-0.05	0.07	0.14	0.15
Neuroticism	0.11	0.08	0.17	-0.02	-0.07	-0.03
Openness	0.01	-0.10	-0.21*	0.08	0.06	0.04

*p <.05

CONCLUSION

The present study examined how personality traits affects the relationship between abstract and specific color preferences, using clothing selection as a subject. The results of the questionnaire showed that neuroticism was significantly lower among those whose preferred color was consistent with their wearing color, and so on. These results suggest that participants' personality traits could play some roles in clothing selection based on their color preferences. In general, it is assumed that abstract color preferences are relatively stable within the participants as their subject-specific characteristics, and that various specific color preferences would stem form the abstract color preference with being mediated by various situational factors. This study successfully demonstrates the usefulness of assuming personality traits and color images as mediating variables, for examining the relationship between abstract and specific color preferences.

On the other hand, the correlations between the color image distance and personality traits shown in this study were all quite weak. This may be due to the weak mediating effect of personality traits, along with the method employed in this study. In this study, nine candidate color categories were presented as color names, and the participants were asked to select only one preferred/hated color from among them. The specific colors that the participants imagine against the color names were distributed quite broad (e.g., whether they imagine bright red or dull red, light red or dark red from a color name of red was not controlled in this study). Thus, the color image of the selected color should have been unfocused. In the future, it will be necessary to further examine the effects of the color image employing more direct method, such as presenting actual clothing colors or color charts.

REFERENCES

1. Palmer, S.E., & Schloss, K.B. (2010). An ecological valence theory of human color preference. *Proceedings of the National Academy of Sciences*, **107**, 8877-8882.

2. Charles, M. & Moyer, W. W. (1992). Correspondence of self-referent statements and color preference. *Perceptual and Motor Skills*, **74**, 993-994.

DIFFERENCES IN THE IMPRESSIONS OF PROFESSIONAL WOMEN'S MAKEUP LOOKS ON DIFFERENT GENDERS AND AGE LEVELS

Chi-Ying Hsu[1 and 2*] and Wen-Yuan Lee[3]

[1] *The Graduate Institute of Design Science, Tatung University, Taiwan.*
[2]*Lecturer, Asia Colors, Taiwan.*
[3] *Department of Media Design, Tatung University, Taiwan.*

* Chi-Ying Hsu, aa0925300036@gmail1.com

Keywords: makeup look, impression, career women makeup

ABSTRACT

People constantly apply makeup at the workplace to improve others' impressions. Literature shows that applying cosmetics affects impressions of attractiveness, femininity, and morality. This study aims to (1) understand the impression of professional women’s makeup looks; (2) clarify different sexes' and age levels' impressions of professional women's makeup looks. This study conducted an experiment in which 71 observers were invited to make impression judgments on ten makeup looks on 19 scales. Each observer was asked to provide scores for the faces wearing ten makeup looks against 19 positive impression scales. These ten makeup looks were applied to a female face's lips, blush, eyeshadow, eyeliner, and false eyelashes. The impression scales included adjectives: “elegant,” “friendly,” “professional,” “authoritative,” “dependable,” “competent,” “solemn,” “genuine,” “warm-hearted,” “modest,” “gentle,” “sociable,” “healthy,” “serious,” “responsible,” “natural,” “self-confident,” “energetic,” and “thoughtful.” The data collected used a 7-step categorical judgment.

The results showed that (1) Makeup with brown eyeshadow and natural or reddish lip color tended to top the list of 19 positive adjectives. But if the makeup has shimmer or glitter, it is easier to be ranked at the bottom of the 19 positive adjectives, (2) An insignificant gender difference was found in the impressions of professional women's makeup, (3) Observers of different age levels have no difference in their impression of regular makeup looks. But for makeup with strong contrast, such as glitter, brown gradient, blue, and black colors, observers of different ages have significantly different impressions of these makeup looks.

INTRODUCTION

People constantly apply makeup at the workplace to improve people's impressions. Proper makeup can deliver good impressions, including attractiveness, femininity, morality, health, self-esteem, etc. (Anchieta et al., 2021; Mittal & Silvera, 2020; Mulhern et al., 2003; Schneider & Moroń, 2022; Workman & Johnson, 1991). This study aims to (1) understand the impression of professional women’s makeup looks; (2) clarify different sexes' and age levels' impressions of professional women's makeup looks.

EXPERIMENTAL PLAN

This study planned an experiment in which 71 observers were invited to make impression judgments on ten makeup looks on 19 scales to achieve the aim. Each observer provided 190 impression judgments, i.e., 10*19=190; in total, 13490 judgments were collected. These 71 observers include 28 males and 43 females. The average age is 23.06 (SD=14.49), including 50 teenagers and 21 adults.

The impression scale includes 19 positive adjectives describing professional women, including “elegant,” “friendly,” “professional,” “authoritative,” “dependable,” “competent,” “solemn,” “genuine,” “warm-hearted,” “modest,” “gentle,” “sociable,” “healthy,” “serious,” “responsible,” “natural,” “self-confident,” “energetic,” and “thoughtful.” The data collected used a 7-step categorical judgment, indicating the strength of how well the impression scale describes the makeup looks, from “irrelevant” to “strongly related to.”

Apply makeup techniques to the lips, blush, eye shadow, eyeliner, and false eyelashes on the same female model's face to create ten makeup looks. Table 1 summarizes the makeup techniques applied to each look. The digital camera was used to take each look under average exposure at a standard color temperature. The photos taken were displayed on the iPad for the observer to make impression judgments, as shown in Figure 1.

Table 1: Makeup Techniques for 10 Looks.

No.	Makeup technique
M1	The eye shadow is a reddish-brown gradient, and the blush and lipstick adopt similar colors. It is commonly known as the dry rose in the cosmetics market.
M2	The eye shadow is a brown gradient, the blush is reddish brown, and the lipstick adopts red color. The representative character is Marilyn Monroe.
M3	The upper shadow is a pink gradient; the lower eyeshadow use glitter. The blush and lipstick adopt pink color.
M4	The eye shadow is a wine-red gradient, and the blush and lipstick adopt similar colors.
M5	The eye shadow is black gradient, and the blush and lipstick adopt pink color—emphasis on thick black eye makeup (including eyeshadow, eyeliner, and thick false eyelashes). The representative figure is the Canadian female singer Avril.
M6	Clear and natural nude makeup. The eyeshadow is a light brown gradient, and the blush and lipstick adopt light pink.
M7	The eye shadow adopts a purple two-stage style, and the blush and lipstick are similar colors.
M8	The eyeshadow is blue highlights, and the blush and lipstick adopt fuchsia.
M9	The eyeshadow is a brown gradient, and the blush and lipstick adopt reddish brown.
M10	The eye shadow and blush are a light orange gradient, and the lipstick adopts a pumpkin orange color. The blush is large and horizontal, spanning the bridge of the nose.

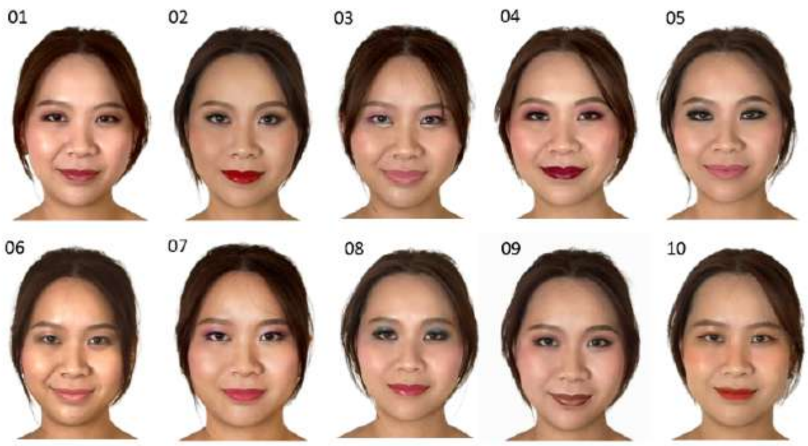

Figure 1: Ten makeup looks used in the experiment.

INTRA- AND INTER-OBSERVER VARIATIONS

The data collected from seven-step categorical judgment on each scale were converted into numbers. The higher the number, the more it fits the adjective description. Prior to analysis, the intra- and inter-observer variations were examined by RMS (root mean square). The former is to see whether the observers can repeat their judgment. The latter examines how well the individual observer agrees with the mean results. The RMS equation is given below.

$$\mathrm{RMS} = \sqrt{\frac{\sum (X_i - Y_i)^2}{n}}$$

For intra-observer variation, X_i and Y_i are the initial and replicated judgement, respectively. For inter-observer variation, X_i and Y_i are individual data and all observers average, respectively. n is the number of data. For RMS of 0, it represents a perfect agreement between two data array.

It can be seen that the intra-observer variations was ranged between RMS of 0.46 and 3.57. And the inter-observer variations was ranged between RMS of 0.93 and 2.63, as shown in Figure 2.

The results showed that six observers (No18, 25, 27, 34, 48, and 61) could not provide consistent judgments (intra-observer variations>3), excluding from the following analyses. The data obtained from sixty-five observers were used to analyze the impression induced by makeup looks. These sixty-five observers included 25 males and 40 females. The average age is 23.48 (SD=15.02), including 46 teenagers and 19 adults.

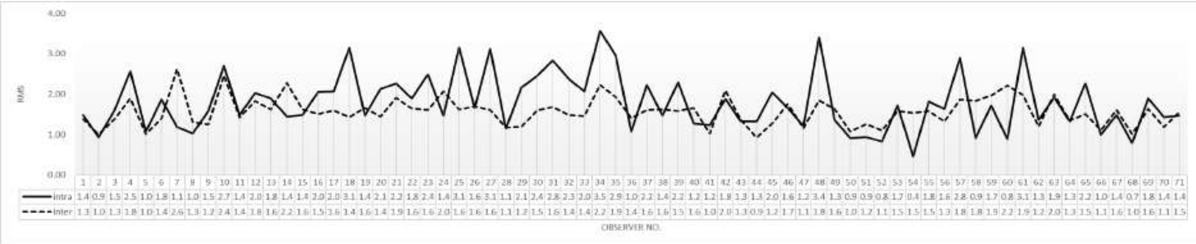

Figure 2: RMS for inter- and intra-observer variation

THE IMPRESSION OF PROFESSIONAL WOMEN'S MAKEUP LOOKS

To understand the impression of professional women's makeup looks, the mean values of each makeup look were calculated on each scale, and each makeup look was sorted along each impression scale, as shown in Figure 3. It can be seen that on these impression scales, M1, M2, and M6 often appear in the first place. The common feature among these three makeup looks is that they all featured brown eyeshadow and natural or reddish lip color. In addition, it can also be seen that the makeup looks that often appear at the bottom of the impression scales are M3 and M8. A common feature of both looks of makeup is the presence of shimmer or glitter.

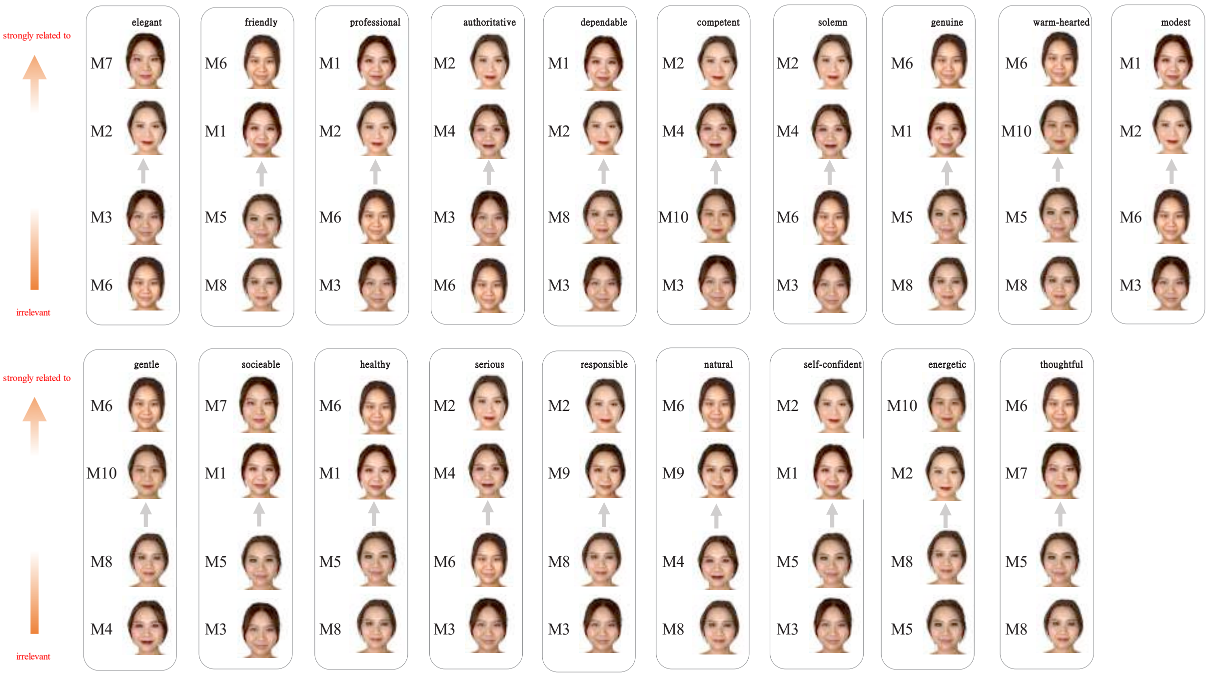

Figure 3: The order of makeup looks on each impression scale

THE IMPRESSION DIFFERENCE BETWEEN SEXS ON MAKEUP LOOKS

A profile chart was drawn to observe the difference in the makeup of different genders, as shown in Figure 4. In Figure 4, solid lines represent the male observer, and dashed lines represent the female observer. In Figure 4, it can be seen that solid lines and dashed lines almost overlap, indicating an insignificant gender difference. Only a few makeup looks differ on a specific impression scale. The more obvious difference occurs in M5 makeup, the Avril makeup. Male observers think M5 makeup is more professional, authoritative, solemn, and serious than female observers.

Figure 4: Profile chart of makeup looks on each impression scale. Solid lines represent male observer, dashed lines represent female observer.

THE IMPRESSION DIFFERENCE BETWEEN TEENAGER AND ADULT ON MAKEUP LOOK

The profile chart was illustrated to understand the impression difference between teenagers and adults on makeup looks, as shown in Figure 5. Unlike gender, the age difference can be clearly seen in Figure 5, which is indicated by the solid line and dashed line separated by the makeup look of M3, M4, M5, M8, and M9. Adult observers perceived M3, M4, M5, M8, and M9 makeup looks higher than teenagers on 19 impression scales. On the other hand, the makeup look of M1, M2, M6, M7, and M10 have no age difference.

The makeup looks of M1, M2, M6, M7, and M10 have a consistent impression on observers of different age levels. Such makeup configurations can be recognized as a regular makeup look. Using such makeup configurations in a work environment minimizes the occurrence of inaccurate impressions.

M3, M4, M5, M8, and M9 makeup looks have different makeup impressions between teenagers and adults. Adults rated these five looks higher on these 19 impression scales. These five makeup looks use flash powder, wine-red, brown, blue and black colors to show a strong contrast. This may be because adult's life experiences lead to an impression of makeup that differs from teenagers.

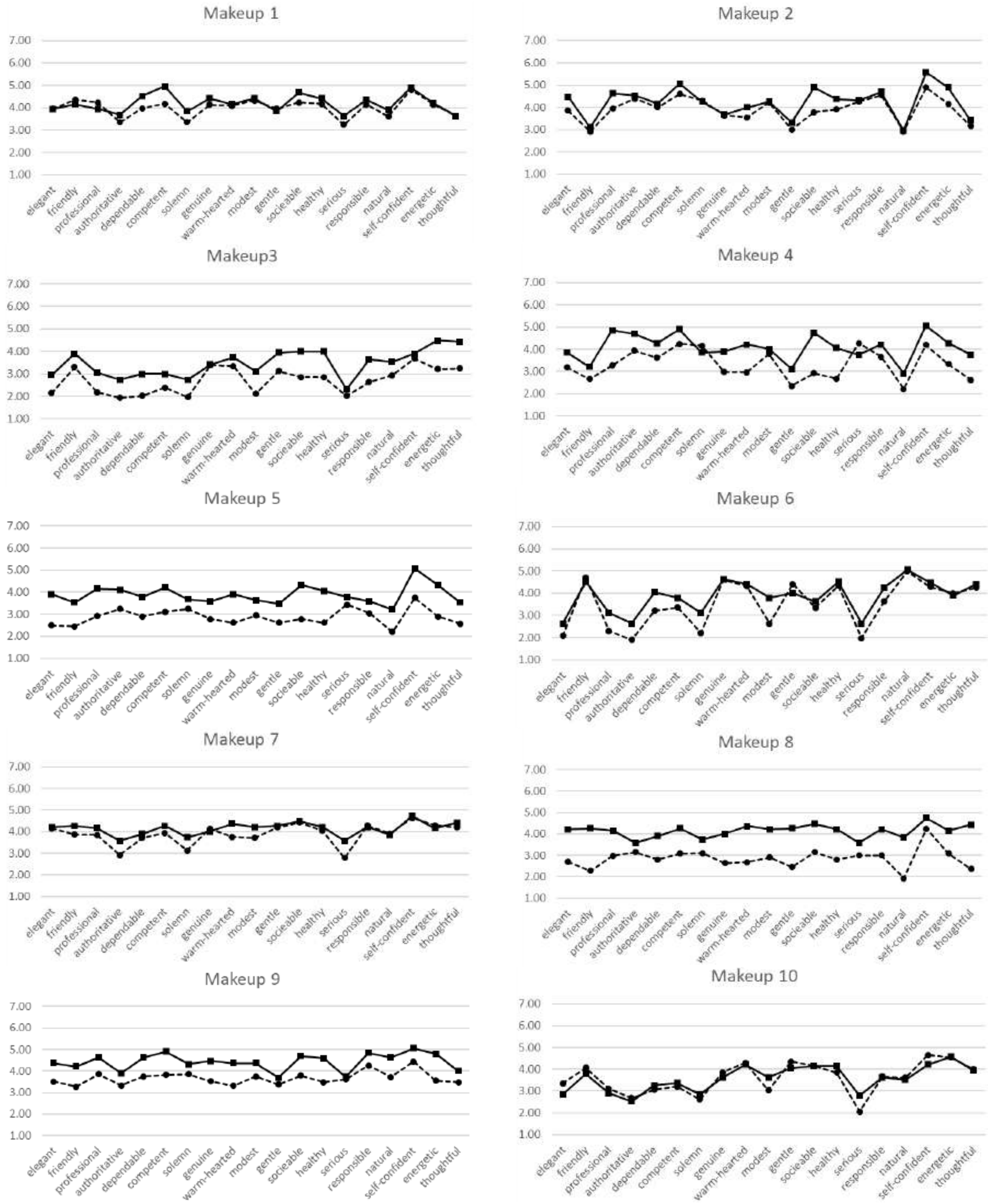

Figure 5: Profile chart of makeup looks on each impression scale. Solid lines represent adult observer, dashed lines represent teenager observer.

RESULT AND DISCUSSION

In order to (1) understand the impression of professional women’s makeup; (2) clarify different sexes' and age levels' impressions of professional women's makeup. This study conducted an experiment in which 71 observers were invited to make impression judgments on ten makeup looks on 19 scales. The results showed that (1) Makeup with brown eyeshadow and natural or reddish lip color tended to top the list of 19 positive adjectives. But if the makeup has shimmer or glitter, it is easier to be ranked at the bottom of the 19 positive adjectives, (2) An insignificant gender difference was found in the impressions of professional women's makeup, (3) Observers of different age levels have no difference in their impression of regular makeup looks. But for makeup with strong contrast, such as those used glitter, brown gradient, blue, and black colors, observers of different ages have significantly different impressions of these makeup looks.

REFERENCES

Anchieta, N. M., Mafra, A. L., Hokama, R. T., Varella, M. A. C., Melo, J. d. A., da Silva, L. O., da Silva, C. S. A., & Valentova, J. V. (2021). Makeup and its application simulation affect women’s self-perceptions. *Archives of Sexual Behavior*, *50*(8), 3777-3784.

Mittal, S., & Silvera, D. H. (2020). Makeup or mask: makeup’s effect on salesperson trustworthiness. *Journal of Consumer Marketing*, *37*(3), 271-277.

Mulhern, R., Fieldman, G., Hussey, T., Leveque, J. L., & Pineau, P. (2003). Do cosmetics enhance female Caucasian facial attractiveness? *International journal of cosmetic science*, *25*(4), 199-205.

Schneider, Z., & Moroń, M. (2022). Facial makeup and perceived likelihood of influence tactics use among women: A role of attractiveness attributed to faces with and without makeup. *Current Psychology*, 1-12.

Workman, J. E., & Johnson, K. K. (1991). The role of cosmetics in impression formation. *Clothing and Textiles Research Journal*, *10*(1), 63-67.

THE IMPACT OF GOALKEEPER UNIFORM COLOR ON PENALTY KICK PERFORMANCE IN A VIDEO GAME—USING FIFA22 FOR THE EXPERIMENT

Yi-Chan Lu , Wen-Yuan Lee

Department of Media Design, Tatung University, Taiwan

louis40407@gmail.com

Keywords: Color, Game Design

ABSTRACT

The effect of color on an athlete's performance is often discussed in sports science, especially in ball games or 1-on-1 competitions. The literature seems to point out that jersey color can affect an athlete's performance. However, this kind of research still has obvious limitations, such as the differences between individual players, the current situation of players, luck, team atmosphere...etc, reducing the credibility of such studies.

E-sports here provides a unique opportunity to examine whether the jersey's color affects the players' performance. It can be set so that the players do not have individual differences. The players' ability can be controlled to be consistent and independent of luck or influenced by external factors such as team atmosphere. That said, it's easier to examine how jersey colors perform on players in an e-sports environment than in the real world.

This study invited 32 participants to play a penalty kick scene in the "FIFA 22" game, intending to reduce the influence of other factors in the real world through the characteristics of the video game and explore whether the color of the jersey really has an impact on the performance of athletes. Participants included 18 females and 14 males, aged between 18 and 26, with an average age of 22. Each participant was asked to face goalkeepers wearing seven colors of jerseys and required to kick ten penalty kicks against the goalkeeper in each color jersey, a total of 70 balls for each participant. These seven colors include red, yellow, blue, green, black, white, and gray colors. Two data were collected, one was the expectation for each kick, and the other was the number of goals scored. The former asks the participants to verbally report the expectation for each kick (1 point means no goal, 10 points mean it will be scored), and the latter is the number of successful goals.

ANOVA (Analysis of Variance) was used to see the difference between the seven colors. The results showed that no matter of expected or actual goals, there is no significant difference between jersey colors, implying that the color of the uniform worn by goalkeepers does not appear to exert a noteworthy influence on their ability to score goals.

INTRODUCTION

The effect of color on an athlete's performance is often discussed in sports science, especially in ball games or 1-on-1 competitions. The literature suggested that athletes wearing red clothing in combat sports had a higher chance of winning than those wearing blue. (Hill & Barton, 2005). Studies on British football have found that teams wearing red shirts had more success in league rankings and win percentages than teams wearing other colors (Attrill, Gresty, Hill, & Barton, 2008). Research has also shown that athletes' physiological responses can be affected by the color of the jersey, with wearing a red jersey in combat sports increasing heart rate and perceived exertion compared to wearing a blue jersey. (Dreiskaemper, Strauss, Hagemann, & Büsch, 2013).Greenlees *et al.* conducted an experiment to see how the color of a football player's jersey affected the expectation of a successful goal. The findings revealed that players facing red-clad goalkeepers scored fewer penalty kicks compared to those facing blue or green-clad goalkeepers. However, no differences in the expectancy of success were observed. These results suggest that athletes wearing red uniforms might have an advantage over their opponents. (Greenlees et al., 2013) In addition, the color of an athlete's uniform affects how others perceive them, with red uniforms associated with higher aggression and lower fairness ratings. (Krenn, 2015).

The literature seems to point out that jersey color can affect an athlete's performance. However, this kind of research still has obvious limitations, such as the differences between individual players, the current situation of players, luck, team atmosphere...etc, reducing the credibility of such studies.

E-sports here provides a unique opportunity to examine whether the jersey's color affects the players' performance. It can be set so that the players do not have individual differences. The players' ability can be controlled to be consistent and independent of luck or influenced by external factors such as team atmosphere. That said, it's easier to examine how jersey colors perform on players in an e-sports environment than in the real world.

METHODOLOGY

The literature indicates that jersey color can affect an athlete's performance. To verify this phenomenon, this study invited 32 participants to play a penalty kick scene in the "FIFA 22" game, intending to reduce the influence of other factors in the real world through the characteristics of the video game and explore whether the color of the jersey really has an impact on the performance of athletes. Participants included 18 female and 14 male, aged between 18 and 26, with an average age of 22.

Each participant was asked to face goalkeepers wearing seven colors of jerseys and required to kick ten penalty kicks against the goalkeeper in each color jersey, a total of 70 balls for each participant. The participant can ask for a break after every 40 kicks. These seven colors include red, yellow, blue, green, black, white, and gray colors.

Prior to the experiment, a briefing session was given to explain the details of the experiment. After the briefing, the participants were instructed to adopt a comfortable sitting posture that they typically use while playing games for the experiment. Each participant was given 3-5 minutes of practice mode to familiarize themselves with this game.

This experiment used laptops with an Intel(R) Core(TM) i7-8750H CPU and Nvidia GeForce GTX 1050 graphics card. The average frame rate of the display was 37.5. The participants used PS5 DualSense Wireless Controllers for game operation. In the game, the goalkeeper and the kicker are represented by the same player. The goalkeeper is portrayed as Manuel Neuer, while the kicker is portrayed as Neymar da Silva Santos Júnior. Both players were set the same rating of 90 in FIFA 22. Figure 1 shows FIFA 22 game screen used in the experiment.

Figure 1: FIFA 22 game screen used in the experiment.

In the experiment, two data were collected, one was the expectation for each kick and the other was the number of goals scored. The former is to ask the participants verbally report the expectation for each kick (1 point means no goal, 10 points means it will be scored), and the latter is the number of successful goals.

RESULTS

This study used two sets of data for analysis, one is the expectation, and the other is the actual number of goals scored. Using ANOVA (Analysis of Variance) to see the difference between the seven colors. If the goalkeeper wearing a particular color jersey can significantly increase or decrease the number of penalties, it means that the goalkeeper's jersey color really affects penalty performance.

Figure 2 and 3 illustrate the mean value for expected and actual goals, respectively. The results obtained from ANOVA showed no matter of expected or actual goals, there is no significant difference between jersey colors (for expected goals, $F=1.001$, $p = .423$, for actual goals, $F=0.595$, $p = .735$.) These findings implied that the color of the uniform worn by goalkeepers does not appear to exert a noteworthy influence on their ability to score goals.

To further test whether there is a gender difference in the effect of jersey color on player performance, Figure 4 shows the average expected and actual goals scored by male and female participants against goalkeepers wearing different colored jerseys. T-test was used for testing. The results showed no difference between genders (for the expected goal, $F=37.981$, Sig.=0.094, for the actual goal, $F=1.008$, Sig.=0.908.)

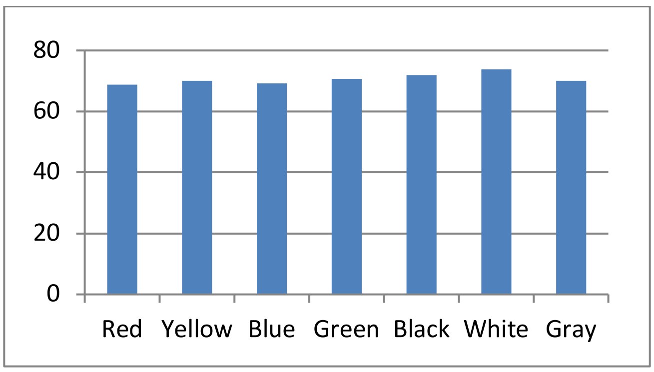

Figure 2: Average expected goals against goalkeepers wearing different colored jerseys.

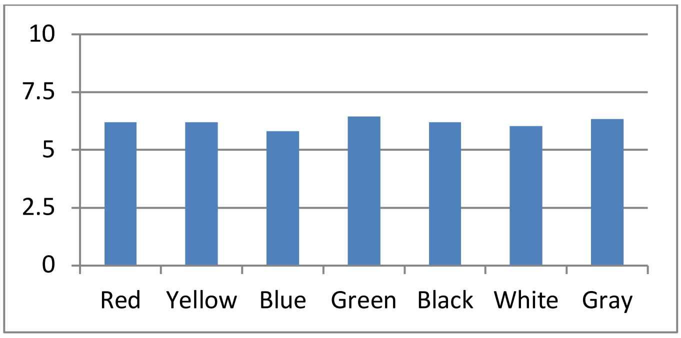

Figure 3: Average actual goals against goalkeepers wearing different colored jerseys.

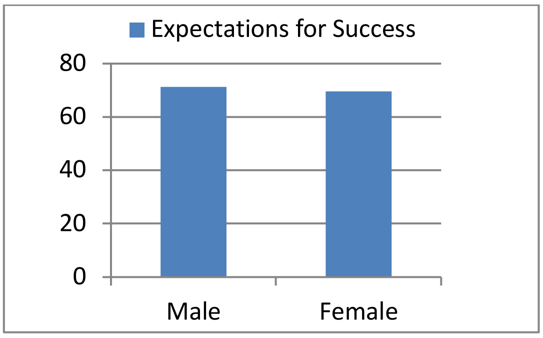

(a)

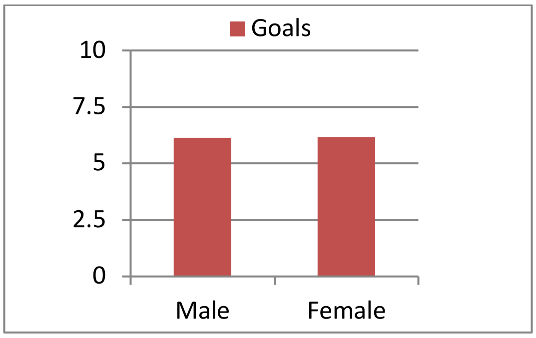

(b)

Figure 4: Average expected and actual goals scored by male and female participants against goalkeepers wearing different colored jerseys.

CONCLUSION AND DISCUSSION

The main scope of this study is to explore the impact of jersey color on the performance of athletes. However, in real sports games, many factors affect the outcome. To examine the effect of jersey color on athletes, this study moved the experiment to an electronic game platform. The results showed that the color of the goalkeeper's jersey did not make a significant difference in the expected success of penalties and goal performance.

REFERENCES

1. Attrill, M. J., Gresty, K. A., Hill, R. A., & Barton, R. A. (2008). Red shirt colour is associated with long-term team success in English football. *J Sports Sci, 26*(6), 577-582. doi:10.1080/02640410701736244
2. Dreiskaemper, D., Strauss, B., Hagemann, N., & Büsch, D. (2013). Influence of red jersey color on physical parameters in combat sports. *Journal of Sport and Exercise Psychology, 35*(1), 44-49.
3. Greenlees, I. A., Eynon, M., & Thelwell, R. C. (2013). Color of soccer goalkeepers' uniforms influences the outcome of penalty kicks. *Perceptual and motor skills, 117*(1), 1-10.
4. Hill, R. A., & Barton, R. A. (2005). Red enhances human performance in contests. *Nature, 435*(7040), 293-293.
5. Krenn, B. (2015). The effect of uniform color on judging athletes' aggressiveness, fairness, and chance of winning. *J Sport Exerc Psychol, 37*(2), 207-212. doi:10.1123/jsep.2014-0274

EXAMINE THE UNIVERSAL COLOR EMOTION MODELS AND ADDITIVE THEORY BY THE COLOR EMOTIONS EVOKED BY TWO-COLOR COMBINATIONS ON 3D COLOR CONFIGURATIONS

Shi-Min Gong [1]*and Wen-Yuan Lee[2]

[1] Department of Commercial Design, Ming Chuan University / Taiwan.
[2] Department of Media Design, Tatung University / Taiwan.

*Corresponding author: Shi-Min Gong, gong73@mail.mcu.edu.tw

ABSTRACT

The study of color emotion has always received attention. Previous studies used a single color to see the color emotions. In recent years, studies on design practices have begun to study the emotion induced by more than two colors. In addition, some previous studies also showed that the color emotion evoked by a color combination can be determined by the average value of the color emotion evoked by a single color, indicating the additive theory. However, these studies only discuss planar color configuration, which makes us curious whether such conclusions apply to three-dimensional color configuration. Therefore, this study used the authors' previous experimental data to examine the universal color emotion models and the additive theory. A total of 32 observers were invited to participate in the psychophysics experiment, and the observers assessed 141 color samples on three color-emotion scales: warm-cool, heavy-light, and active-passive. The results show that the experimental data highly correlates with the predicted value for additive theory. However, the prediction results for the main and secondary colors are not ideal. The results showed that the universal model for color emotion can also be applied to the 3D color configuration of two-color combinations. Still, the ratio of main and secondary colors is recommended to be 6:4.

Keywords: color emotion, 3D color configuration, color design, additive theory

INTRODUCTION

The study of color emotion has always received attention. Previous studies [3-5, 8-10, 15] used a single-color to see the color emotions. In recent years, studies on design practices, such as urban design[14]or product design[2], have begun to study the emotion induced by more than two colors. In addition, some previous studies[6, 16] also showed that the color emotion evoked by a color combination can be determined by the average value of the color emotion evoked by a single color, indicating the additive theory. However, these studies only discuss planar color configuration, which makes us curious whether such conclusions apply to three-dimensional color configuration. Therefore, this study used the authors' previous experimental data[7] to examine the universal color emotion models and the additive theory[16-18].

EXPERIMENTAL PLAN

This study used the authors' previous experimental data[7] to examine universal color emotion models and the additive theory [16-18] using two-color combinations within a 3D configuration. A total of 32 observers were invited for the experiment, including 13 males and 19 females, with an average age of 21. The experiment was conducted in a darkroom, each experimental sample was presented in a viewing cabinet and illuminated using a D65 simulator. The viewing distance was about 45 cm with a 45/45 illuminating/viewing geometry, each observer was instructed to evaluate each experimental sample based on the dimensions of "warm/cool," "heavy/ light," and "active/passive," as shown in Figure 1(b). The luminance levels on three surfaces of the experimental sample were measured. They were 230.5 cd/m^2, 165 cd/m^2, and 112.5 cd/m^2, respectively, as shown in Figure 1(a).

In terms of the color configuration, to meet the needs of product design, the frequently-seen cuboid shape configured with a side circle was used as the color configuration in the experiment, as shown in Figure 1 (a). The main color was applied to the cuboid shape, and the secondary color was on the side circle.

To produce two-color combinations, 11 basic color terms (red, orange, yellow, green, blue, brown, purple, pink, white, black, and gray) according to Berlin and Kay [1] (1969) were selected to be the main colors. Each main color was produced according to the foci color in the boundaries in CIELAB space proposed by Lin et al. [11-13]. In addition, five types of color scheme techniques, as proposed by Yano [19], were used to produce secondary colors, including “neighboring tone with neighboring hue,” “different tone with the same hue,” “same tone with different hue,” “chromatic-achromatic combination,” and “achromatic-achromatic combination.” 141 color combinations were applied to the cuboid configured with a side circle, as shown in Figure 1(c). Each color was measured by a GretagMacbeth® Eye-One. The CIELAB values were calculated under CIE D65 and 1964 standard colorimetric observers.

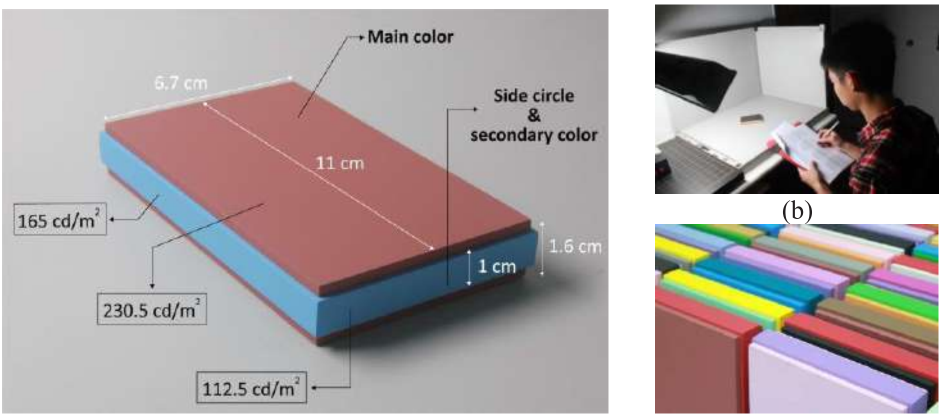

(a) (b) (c)

Figure 1: The experimental samples and situation

Prior to analysis, intra- and inter-observer variations were evaluated using the root mean square (RMS). The former examined whether the observers can repeat the same judgment or not. The latter examined how well the individual observer agreed with the mean results. RMS equation is given below. An RMS of 0 represents a perfect agreement between two data arrays.

$$\mathrm{RMS} = \sqrt{\frac{\sum(X_i - Y_i)^2}{n}}$$

The results are illustrated in Figure 2. The intra-observer variation and inter-observer variation range between RMS of 0.69 and 2.19. Observer 19 was found to have an RMS value exceeding 2.0 on intra-observer interpretation. Therefore, the data of this observer was excluded from further analysis.

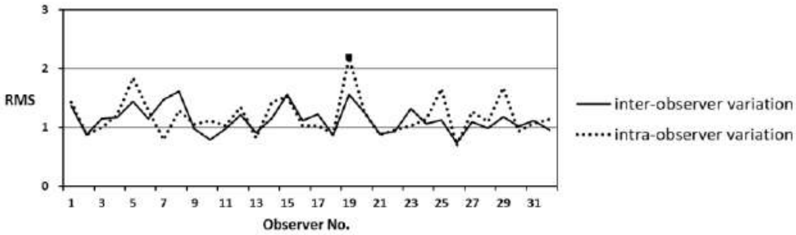

Figure 2: Intra- and Inter-observer variation

RESULT

To understand the difference in color emotion between planar and 3D configurations, this study brings the experimental data of the experiment into the model of Ou et al.[17, 18] to obtain the predicted value, the universal color emotion models are presented in Eq 1(warm-cool), Eq 2 (heavy-light), and Eq 3(active-passive). Furthermore, the three models were tested through additivity theory [16] using color-combination data. The additive theory of color emotion can be described as shown in Eq 4.

$$\text{warm-cool} = -0.89+0.052C^*_{ab}\left[\cos\left(h_{ab}-50^\circ\right)+0.16\cos\left(2h_{ab}-350^\circ\right)\right] \quad \text{Eq 1}$$

$$\text{heavy-light} = 3.8-0.07L^* \quad \text{Eq 2}$$

$$\text{active-passive} = -3.4+0.067\left\{(L^*-50)^2+1.93(a^*+1)^2+1.05(b^*-9)^2\right\}^{\frac{1}{2}} \quad \text{Eq 3}$$

$$\text{additivity theory} = (E_1+E_2)/2 \quad \text{Eq 4}$$

where L^* is the CIELAB lightness;
a^* is the CIELAB redness/greenness axis;
b^* is the CIELAB yellowness/blueness axis;
C^*_{ab} is the CIELAB chroma;
h_{ab} is the CIELAB hue angle;
E_1 is the color emotion values for colors 1;
E_2 is the color emotion values for colors 2.

The correlation coefficient was used to explore the correlation degree between the predicted values obtained from the models and the experimental data. The results are shown in Table 1. The correlation coefficients showed that all color emotion scales had highly significant correlations in planar and three-dimensional configurations for additive theory, with a correlation coefficient of 0.79 for warm/cool, -0.87 for heavy/light, and 0.83 for active/passive.

However, the correlation coefficient between the predictions of the main color and the secondary color and the experimental data is relatively low, especially the secondary color, which is only 0.4 for the active-passive model.

Therefore, this study used RMS minimization to obtain the optimal ratio between the emotion values obtained for main and secondary colors. The results showed that when the ratio of the main color to the secondary color is 6:4, the correlation coefficient between the prediction values and the experimental data is improved, with a correlation coefficient of 0.81 for warm/cool, -0.89 for heavy/light, and 0.85 for active/passive. From this result, the universal model for color emotion can also be applied to the 3D color configuration of two-color combinations. Still, the ratio of main and secondary colors is recommended to be 6:4.

Table 1:The correlation of color emotions between the predicted values and the experimental data.

	main color	secondary color	additive theory (5:5)	6 to 4 weight (6:4)
warm-cool	0.75	0.52	0.79	0.81
heavy-light	-0.76	-0.48	-0.87	-0.89
active-passive	0.69	0.40	0.83	0.85

CONCLUSION

In the current study, a psychophysical experiment was conducted to examine the universal color emotion models and additive theory [16-18] by the color emotions evoked by two-color combinations in 3D configurations. The results show that the universal color emotion models and additive theory can predict color emotions evoked by color combinations applied to the 3D color configuration. If the 5:5 of the additive theory is changed to 60% of the emotional value of the main color and 40% of the emotional value of the secondary color. In that case, the prediction will be effectively improved.

REFERENCES

1. Berlin, B., & Kay, P. (1969). *Basic Colour Terms: Their Universality and Evolution.* Basic Colour Terms: Their Universality and Evolution.
2. Ding, M., & Bai, Z. (2019). Product color emotional design adaptive to product shape feature variation. *Color Research & Application*, *44*(5), 811-823.
3. Gao, X.-P., & Xin, J. H. (2006). Investigation of Human's Emotional Responses on Colors. *Color Research & Application*, *31*(5), 411–417.
4. Gao, X.-P., Xin, J. H., Sato, T., Hansuebsai, A., Scalzo, M., Kajiwara, K., Guan, S.-S., Valldeperas, J., Lis, M. J., & Billger, M. (2007). Analysis of Cross-Cultural Color Emotion. *Color Research & Application*, *32*(3), 223-229.
5. Gong, R., Wang, Q., Hai, Y., & Shao, X. (2017). Investigation on factors to influence color emotion and color preference responses. *Optik*, *136*, 71-78.
6. Hogg, J. (1969). The Prediction of Semantic Differential Ratings of Color Combinations. *The Journal of General Psychology*, *80*(1), 141-152.
7. Lee, W.-Y., & Gong, S.-M. (2022). The relationship between colour harmony and colour emotions—using two-colour combinations applied on 3D colour configuration. *Coloration Technology*, *138*(4), 397-406.
8. Lee, W.-Y., Luo, M. R., & Ou, L.-C. (2009). Assessing the Affective Feelings of Two- and Three-Dimensional Objects. *Color Res. Appl.*, *34(1)*, 75-83.
9. Lee, W.-Y., & Pai, S.-Y. (2012). The affective feelings of colored typefaces. *Color Research & Application*, *37*(5), 367-374. https://doi.org/https://doi.org/10.1002/col.20698
10. Lee, Y.-J., & Lee, J. (2006). The development of an emotion model based on colour combinations. *International Journal of Consumer Studies*, *30*(2), 122-136.
11. Lin, H., Luo, M. R., MacDonald, L. W., & Tarrant, A. W. S. (2001). A cross-cultural colour-naming study. Part I—Using an unconstrained method. *Color Research & Application*, *26*(1), 40-60.
12. Lin, H., Luo, M. R., MacDonald, L. W., & Tarrant, A. W. S. (2001). A cross-cultural colour-naming study. Part II—Using a Constrained Method. *Color Research & Application*, *26*(3), 193-208.
13. Lin, H., Luo, M. R., MacDonald, L. W., & Tarrant, A. W. S. (2001). A cross-cultural colour-naming study. Part III—A colour-naming model. *Color Research & Application*, *26*(4), 270-277.
14. Manav, B. (2017). Color-emotion associations, designing color schemes for urban environment-architectural settings. *Color Research & Application*, *42*(5), 631-640.
15. Ou, L.-C., Luo, M. R., Woodcock, A., & Wright, A. (2004). A study of colour emotion and colour preference. Part I: Colour emotions for single colours. *Color Research & Application*, *29*(3), 232-240.
16. Ou, L.-C., Luo, M. R., Woodcock, A., & Wright, A. (2004). A study of colour emotion and colour preference. Part II: Colour emotions for two-colour combinations. *Color Research & Application*, *29*(4), 292-298.
17. Ou, L.-C., Yuan, Y., Sato, T., Lee, W.-Y., Szabó, F., Sueeprasan, S., & Huertas, R. (2018). Universal models of colour emotion and colour harmony. *Color Research & Application*, *43*(5), 736-748.
18. Ou, L.-C., Yuan, Y., Sato, T., Lee, W.-Y., Szabó, F., Sueeprasan, S., & Huertas, R. (2019). 【correction】Universal models of colour emotion and colour harmony. *Color Research & Application*, *44*(1), 153.
19. Yano, R. (2008). *The Art of Designing* (X. Liu, Trans.). Solutions Publishing.

LOCAL COLOR, CONSTANCY AND ILLUSION

Alfonso de Lucas Tron

Universidad Nacional Autónoma de México

Facultad de Estudios Superiores Acatlán, Mexico

109849@pcpuma.acatlan.unam.mx

ABSTRACT

The term **«Local Color»** serves to designate the colorant aspect of a body for its eventual representation in a drawing or a painting. It is sensorily and semantically referred and derives from the idea that two or more persons see the same chromatic quality of a body in spite the ubication of each observer with respect to the object and despite that the direction of the light gives rise to different impressions. Based on this approach, this work in turn derives from a phenomenological exercise that has for its **objective** to show that local color is a sensoriperceptual process that establishes a distance between the impression that the retinal cells register and their eventual processing in the brain, exhibiting in the end an illusory effect that does not correspond to the reality. This derives from the **thesis** that the laws of Gestalt perceptual organization order the sensory impressions, providing a stable and permanent coloration, from which it follows that the constancy of color is what determines the local color. Vision is explained by the sensoriperception that this is a process comprising two stages: the sensory impression in which the photoreceptor cells generate an intense mosaic with the stimuli of the wavelengths, and the perceptual, in which the brain organizes such stimuli under the principles of Gestalt perceptual organization. This process produces as a result a continuous and stable colorant aspect that it is related to the constancy of the color that, in the end, is appreciated as local color. Although the artistic part originates from an illusory effect, it is possible to approach the real appearance of the body by educating the sight through the techniques of chiaroscuro.

Keywords: local color, sensory perception, illusion, color constancy.

INTRODUCTION

Local color is employed in the instruction of drawing and painting for several purposes: stimulating the person practicing it to see the fair nuance or tint of a body; match the color through mixtures of paint; model this by means of chiaroscuro and, in general, develop visual dexterities in order to approximate the visual *reality* of the pictorial. It is, therefore, a semantic and sensory association in which two or more individuals are in agreement about seeing the same colorant quality as if were a Pantone palette card. The irony is that the location of each observer with respect to the object and the direction of the light provokes different chromatic impressions. This begs the question, why is it that an object has the same color if everyone has a different sensory perception?

METHODOLOGY

To answer this question, this work itself derived from a phenomenological exercise that has as its **objective** to show that local color is the result of a sensoriperceptual process that establishes a distance between the impressions that the retinal cells register and their eventual processing in the brain, finally demonstrating an illusory effect whose appearance is exhibited in local color. The latter derives from the **thesis** that the Gestalt laws of perceptual organization order the sensory perceptions, providing a stable and permanent coloration from which it is fitting to conclude that the constancy of the color determines the local color.

1. Sensoriperception

Sensoriperception explains the functioning of sight by means of a process constituted of two "stages" or "´phases": the sensory and the perceptual, though it is understood that sight itself does not make such a distinction, because it functions as a perfectly organized unit. (Coren, Ward, & Enns, 2001, págs. 1-14)

a) Sensory Phase

Once light enters the eyeball and makes contact with the ***retina***, the photoreceptor cells convert the light into signals of an electric and chemical nature that cannot be described in terms of units of light. (Mueller & Mae, 1974, págs. 75-76). The retina is a delicate membrane comprising millions of light-sensitive cells grouped into two types: cones and rods. The **cones** are similar to funnels and are responsible for the chromatic sensations. The human retina comprises approximately 7 million cones. The **rods** are similar to cylinders; in the human retina; there are approximately 125 million rods that are located and distributed in the ends of the retina. They do not perceive in a sharp manner or in detail, but are outfitted for night vision. (Forgus & Melamed, 2003, págs. 79-82) The two sets work in unison; they complement the sharpness and the amorphous quality to see an image in its plenitude in terms of tonalities and colors. The photosensitive cells remit the information to the brain by means of the optical nerve, thus initiating the **perceptual** phase.

b) Perceptual Phase

The brain is the organ charged with converting the information in the eyes on seeing. According to Kant, the sensations only constitute the "material" or "prime matter" of our knowledge, which still lacks being ordered and being conformed in a varied manner in order to form with such material the image of the external world: we do not see with the eyes, but through them. (Müeller-Freienfels, 1966, págs. 269-271). In the brain, material objects become visual objects, adorning the bodies with the attributes proper to them, such as form, dimensions, texture, clarity and, of course, color. To the sensory matter are added psychological elements that give form and content to the look. Both phases are so dependent on each other that, if one is lacking, sight simply cannot be implemented: vision or sight works as if it were of all of a piece.

3. Chromatic Map and the Laws of Gestalt Perceptual Organization

Selective absorption is the physical principle in which an opaque surface retains determined wavelengths and releases others that are perceived by the human eye as color. (Griffith, 2008, págs. 328-329) The shape of each body and the direction of the light establish that certain areas of the surface will demonstrate greater and lesser luminous intensity depending on the light's angle of incidence. In this manner, the body exhibits brilliant zones, parts that are mediumly illuminated, and others that are dark or dim reflections of the adjacent bodies. The body, in reality, exhibits a set of "zonified" tonalities that can vary from one moment to the next on the production of a minimal change in the illumination. Solely under laboratory conditions can there be a strict control of light.

Figure 1. Changes of illumination stimulate the retinal cells in a different way, causing different aspects. Thus, each of the retinal cells will receive the impression of determined wavelengths that will be different, even, from those next to them.

The ocular retina then *decomposes* the information that arrives by means of the light into millions of stimuli, giving rise to an enormous **chromatic map** that must of necessity integrate itself into an organized set. "According to Michael Shreeve (2005, pág. 14) "Modules separated in the visual cortex decompose the image into color, form, and orientation The result is sent to specialized areas that analyze the components and that interpret a greater amplitude of aspects of the image."

This monumental mosaic is sent to the brain for its processing in order for the diversity to be transformed into a unit under the Gestalt principles, in which all stimulator schemas tend to be seen in such a way that the structure results in being as simple as the given conditions allow it to be. (Arnheim, 2008, pág. 69): the totality is much more than each of the parts that make it up. In this configuration, there participate the laws of grouping concerning which we may mention, among others, those of similitude, proximity, continuity, figure, and background, etc. (Carterette & Friedman, 1982) The organization incorporates psychological material such as thoughts, desires, emotions, feelings, sensations, memories, values, etc., with which the visual images are not only representations of the external world, but also representations that acquire a personal and subjective character.

4. Constancy and Local Color

On modifying the sensory impressions, the observer could suppose that such changes refer to the perception of different objects despite their being the same ones. To counteract the instability of the ocular information, the perception stabilizes the stimuli through a perceptual effect denominated **color constancy** (Walsh & Kulikowski, 2010). This is similar to organizing the chromatic map of the photoreceptor cells; the greater part of the tonalities that the body exhibits is *suppressed*, offering a uniform and stable appearance that is not altered in the face of changes in illumination. The aspect of the object is that of a flat and uniform coloration and an accentuated hue, which is known in the artistic milieu as local color, although it is an illusory effect that is a far cry from being an exact replica of the external world.

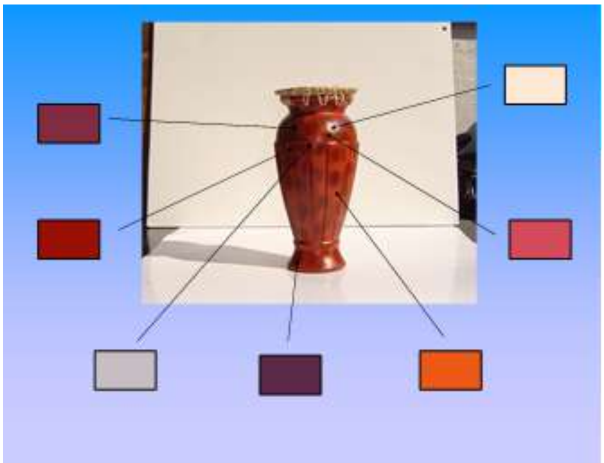

Figura 2a

Figura 2b

Figure 2. The body, due to its absorption of light, exhibits an enormous number of tonalities (Figure a) that the perception, in constancy of clarity, integrates into a stable and uniform appearance that is, in the last analysis, the local color (Figure b).

CONCLUSIONS

Color constancy, which appears at the end of the process of sensory perception, is that which is known as local color. Given that it offers an illusory appearance, it gives rise to doubts concerning whether various persons who look at the same body perceive the same colorant quality, as if it were a Pantone template. A probable way to corroborate this is through the practice of painting, in which various subject practitioners attempt to match the color by means of mixtures of paint, to later compare these. This would aid in corroborating whether the color constancy proves that two or more persons see "the same".

The drawing taken from the natural, called imitation, is concerned with whether the practitioner achieves perceiving the real aspect, in order for its eventual representation through the drawing or the painting through the practice of chiaroscuro. It is surprising the manner in which professional painters achieve the aspect of local color through employing a delicate play of lights and shadows, which permits one to see that the educated eye surpassed the illusory aspect of the constancy.

As we can see, this is a theme that has not yet been exhausted; it leads to continuing to work with it due to its undeniable importance in artistic instruction. We would not wish to end this work without mentioning citing a maxim of the Master Painter, Leonardo da Vinci, which is applicable here: *la pittura è cosa mentale*: “Painting is a mental thing”.

REFERENCES

Coren, S., Ward, L. M., & Enns, J. T. (2001). *Sensación y percepción.* México: Mc Graw-Hill Interamericana.

Mueller, C. G., & Mae, R. (1974). *Luz y visión.* Estados Unidos de Norteamérica: Time, Inc.

Forgus, R. H., & Melamed, L. E. (2003). *Percepción. Estudio del desarrollo cognoscitivo.* México: Trillas.

Müeller-Freienfels, R. (1966). *Tu alma y la ajena. Una psicología práctica para todos.* Barcelona: Labor.

Griffith, W. T. (2008). *Física conceptual.* México: McGraw-Hill/Interamericana.

Shreeve, J. (2005). En pos del vínculo entre mente y cerebro . *National Geographic*, 1-31.

Arnheim, R. (2008). *Arte y percepción visual.* Madrid: Alianza Forma.

Carterette, E. C., & Friedman, M. P. (1982). *Manual de percepción. Raíces históricas y filosóficas.* México: Trillas.

Walsh, V., & Kulikowski, J. (2010). *Perceptual Constancy.* New York: Cambridge University Press.

●

Color Characteristics of Korean Purple-based and Green-based Natural dyeing Fabric

Anshika Shukla [1] and Junghee Yang[2] and Hyewon Park[3]*

[1] *Master Course, Dept. Of Interdisciplinary Program in Senior Human Ecology of Graduate School, Changwon National University, Republic of Korea.*
[2] *Lecturer, Dept. Of Clothing & Textiles, Changwon National University, Republic of Korea.*
[3]*Professor, Dept. Of Clothing & Textiles, Interdisciplinary Program in Senior Human Ecology of Graduate School, Changwon National University, Republic of Korea.*

*Corresponding author: Hyewon Park, email: hwpark@changwon.ac.kr

Keywords: Korea natural dyeing fabric color, fabric color analysis, purple-based color, Green-based color

ABSTRACT

This study analyzed the color and tone of green and purple materials among traditional natural dyeing materials in Korea and identified their color characteristics. To this end, 107 materials were randomly collected from commercially available green and purple materials, and the H V/C value was measured with a color difference meter. The measurement results were classified using Munsell's 10-color system and 12 PCCS tones. As a result, in terms of color characteristics, the RP series appeared dominantly among the colors of purple-based natural dyeing materials, followed by the P, R, and PB series, respectively, in all material groups (silk, cotton, viscose rayon, ramie, hemp, and wool). As for the colors of green-based natural dyeing materials, the GY series was found dominantly in all material groups (silk, cotton, viscose rayon, ramie), followed by G and Y, respectively. Regarding tonal characteristics, purple-based natural dyeing materials were found in the order of d > g > ltg > sf tones, and tones of medium brightness/medium saturation and medium brightness/low saturation were found intensively. The green natural dyeing materials were found in the order of ltg > g > sf tones, and the tones of medium brightness/low saturation were dominant, and the tones of medium brightness/medium saturation were also highly distributed. The results above may contribute to product planning in various design industries that utilize Korean natural dyeing materials.

INTRODUCTION

'Eco-friendliness' is becoming a global trend in relation to solutions for current environmental problems, such as climate change and environmental pollution. In the fashion world, eco-friendly fashions using recycled, upcycled, and vegan materials are being chosen by consumers who value so-called value consumption. Natural dyeing in Korea is an environmentally friendly method in line with the eco-friendly trend that can reduce carbon emissions compared to synthetic dye dyeing methods. Natural dyes express their colors with the materials extracted from natural plants, minerals, and animal materials in that they do not cause environmental pollution, such as water contamination, unlike synthetic dye dyeing methods. Natural dyes of nature can express various colors, such as Korea's traditional five colors (yellow, red, blue, white, and black) and neutral colors (purple, green, dark blue, red, and sulfur yellow). Previous studies on natural dyeing colors in Korea mainly dealt with yellow, red, and blue, which are saturationtic colors of the five cardinal colors (Choi, Ryu & Kweon, 2005; Lee et al., 2012; Nam, Yu & Park, 2022; Shin & Choi, 2013; Yang & Park, 2023; Yi & Choi, 2009; Yi, Lee & Choi, 2022).

Purple and green natural dyeing materials among neutral colors are the color series often found in the market among natural dyeing materials of various color series distributed in Korea. Purple is an intermediate color between red and black, and it has been a symbol of high status in Korean traditional clothing along with yellow (gold) since ancient times and has been banned for the general public. Green is an intermediate color between blue and yellow and is produced by mixing indigo and yellow dyes that produce a blue tone. During the Joseon Dynasty, as blue dyeing advanced, green and blue were widely used regardless of class by mixing with yellow. The royal family and also ordinary people wore green clothes at weddings. Studies on natural dyeing in purple and green include studies on dyeing using plants and on color sensibility and preference (Jo, Cho & Choi, 2022; Kim et al., 2013; Shin, Kim & Choi, 2018; Yoo, 2007). Compared to studies on yellow, red, and blue, there were no studies that analyzed objective color data by collecting actual natural dyeing data. As such, purple and green natural dyeing materials, which have been used popularly in Korean costumes since ancient times, are valuable research topics as there are not many studies on color series that are often found in the market in Korea or natural dyeing color analysis studies by academic circles.

This study aims to analyze the color of Korean natural dyeing materials in the purple and green series, which are the intermediate colors of Korea's five cardinal colors. For this, the color and tone characteristics of commercially available purple and green natural dyeing materials were examined. The results may be used as basic data for design planning using Korean natural dyeing materials and as data for building a color database of Korean natural dyeing materials.

METHODOLOGY

The empirical data of this study are green and purple natural dyeing materials sold in the Korean market, and purple and green materials sold in the Dongdaemun market, natural dyeing research institute, traditional dyeing workshop, and internet shopping mall were randomly collected. For the collected materials, materials that were identified to be green and purple based on visual perception analysis were finally analyzed, and there were 107 materials including 85 purple fabrics (silk 40, cotton 30, viscose rayon 2, ramie 9, hemp cloth 2, wool 2) and 22 green fabrics (silk 6, cotton 7, viscose rayon 3, ramie 6). The natural dyeing materials were collected from August 2021 to January 2022.

To analyze the color and tone of the analysis target, color, brightness, and saturation were measured with a Minolta, JP/CR-400 color difference meter under a BOTECK Super Light-VI light source device. For measurement, the average value from three colorimetric measurements was used. The derived HV/C values were classified according to Munsell's 10-color system and 12 PCCS tones, and the colors and tones were analyzed.

RESULT AND DISCUSSION

1. Color Analysis

All purple-based natural dyeing materials colors were analyzed into R, PB, P, and RP series. The RP series appeared dominantly with 48 specimens (56.5%), followed by the P series with 22 (37.6%), while the R (4 specimens, 4.7%) and the PB (1 specimen, 1.2%) series had a small distribution. Silk (40 specimens, 47.1%) was the most prevalent among purple natural dyeing materials, followed by RP (20 specimens, 23.5%), P (16 specimens, 18.8%), and R (4 specimens, 4.7%), and appeared dominantly in the RP and P series. Cotton (30 specimens, 35.3%) was the second most prevalent among purple-based natural dyeing materials, and RP (20 specimens, 23.5%) and P (10 specimens, 11.8%) series were analyzed. Viscose rayon (2 specimens, 2.4%) appeared in RP and P series (1.2%), one in each series, and ramie (9 specimens, 10.6%) in P (5 specimens, 5.9%), RP (3 specimens, 3.5%), and PB (1, 1.2%) series, respectively. Hemp cloth and wool appeared twice, respectively (2.4%), only in RP. Purple-based natural dyeing materials appeared in the RP series and showed the highest distribution. P series appeared in all materials except for hemp cloth and wool. Although a small distribution, the R series appeared in silk and the PB series in ramie.

The colors of green natural dyeing materials were Y, GY, and G series, and GY series was most prevalent with 17 specimens (77.3%), followed by the G series with 3 (13.6%) and the Y series with 2 (9.1%). Silk (6 specimens, 27.3%) had 4 specimens in the GY series (18.2%) and 2 in G (9.1%), and cotton (7 specimens, 31.8%) had 5 specimens in the GYs series (22.7%) and 2 in Y (9.1%). Viscose rayon (3 specimens, 13.6%) had only GY (3 specimens, 13.6%), and ramie (6 specimens, 27.3%) had 5 specimens in GY (22.7%) and 1 in G (4.5%). All green natural dyeing materials were analyzed for GY series and showed a large distribution. The G series appeared in silk and ramie, and the Y series appeared only in cotton.

Table 1 : Color Analysis of Purple-based and Green-based Natural Dyeing Fabrics

Frequency(%)

	Material	R	YR	Y	GY	G	BG	B	PB	P	RP	Total
Purple	Silk	4(4.7)	0	0	0	0	0	0	0	16(18.8)	20(23.5)	40(47.1)
	Cotton	0	0	0	0	0	0	0	0	10(11.8)	20(23.5)	30(35.3)
	Viscose rayon	0	0	0	0	0	0	0	0	1(1.2)	1(1.2)	2(2.4)
	Ramie	0	0	0	0	0	0	0	1(1.2)	5(5.9)	3(3.5)	9(10.6)
	Hemp cloth	0	0	0	0	0	0	0	0	0	2(2.4)	2(2.4)
	Wool	0	0	0	0	0	0	0	0	0	2(2.4)	2(2.4)
	Total	4(4.7)	0	0	0	0	0	0	1(1.2)	22(37.6)	48(56.5)	85(100.0)
	Material	R	YR	Y	GY	G	BG	B	PB	P	RP	Total
Green	Silk	0	0	0	4(18.2)	2(9.1)	0	0	0	0	0	6(27.3)
	Cotton	0	0	2(9.1)	5(22.7)	0	0	0	0	0	0	7(31.8)
	Viscose rayon	0	0	0	3(13.6)	0	0	0	0	0	0	3(13.6)
	Ramie	0	0	0	5(22.7)	1(4.5)	0	0	0	0	0	6(27.3)
	Total	0	0	2(9.1)	17(77.3)	3(13.6)	0	0	0	0	0	22(100.0)

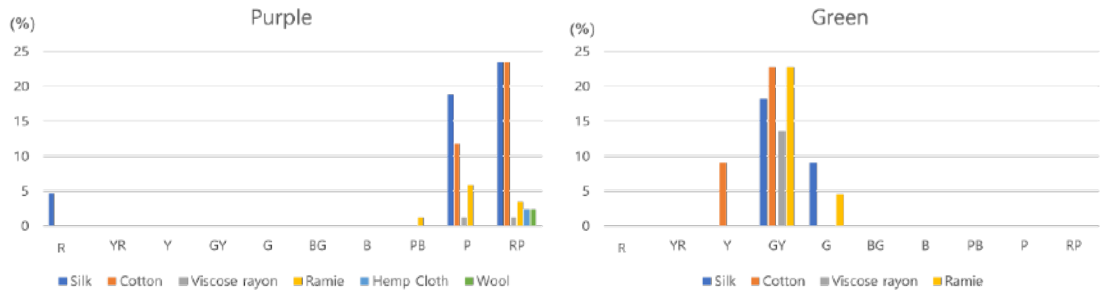

Figure 1. Color of Purple-based and Green-basesd Natural Dyeing

2. Tone Analysis

The b, v, and dk tones did not appear in purple-based natural dyed materials. d was most prevalent with 24 specimens (28.2%), and g (18, 21.2%), ltg (17, 20.0%), and sf (12, 14.1%) showed a large distribution, followed by s = dkg (5 specimens, 5.9%) > dp (2 specimens, 2.4%) > p = lt (1 specimen, 1.2%), respectively. In silk, ltg (13 specimens, 15.3%) showed the largest distribution, followed by g (8 specimens, 9.4%) > d (7 specimens, 8.2%) > sf (6 specimens, 7.1%), and medium brightness/low saturation tones appeared prevalently. Next, s (3 specimens, 3.5%), dkg (2 specimens, 2.4%), and dp (1 specimen, 1.2%) were also analyzed. For cotton, d was most prevalent with 14 specimens (16.5%), followed by g (7, 8.2%) > ltg (3, 3.5%) > sf = dkg (2, 2.4%) > s = dp (1, 1.2%), mostly distributed in medium brightness/medium saturation and medium brightness/low saturation tones. Viscose rayon appeared only in sf (2, 2.4%) tone of medium brightness/medium saturation. For ramie, sf, d, and g of medium brightness/medium saturation and medium brightness/low saturation appeared, two in each series (2.4%), and p, lt, and s also appeared once in each series (1.2%). For hemp cloth, g and dkg of medium and low brightness/low saturation appeared once each (1.2%). For wool, d and ltg of medium brightness/low saturation and medium brightness/medium saturation appeared once each (1.2%). In purple-based natural dyeing materials, many tones had medium brightness/medium saturation and medium brightness/low saturation, showing dominance, and none appeared in tones of low brightness/medium saturation and high brightness/high saturation.

The overall tones of green natural dyeing materials were ltg (8 specimens, 36.4%) > g (5 specimens, 22.7%) > sf (3 specimens, 13.6%) > p = lt (2 specimens, 9.1%) > b = s (1 specimen, 4.5%), respectively. For silk, 2 specimens appeared in each of the medium brightness/low saturation tones in sf and ltg (9.1%) and 1 each (4.5%) in high brightness/low saturation tone and high brightness/high saturation tone in p and b series. Cotton appeared in g (4, 18,2%) and ltg (3, 13.6%) tones of medium brightness/low saturation. In viscose rayon, sf, ltg, and g appeared once in each series (4.5%) in tones of medium brightness/low saturation and medium brightness/medium saturation. In ramie, lt and ltg appeared twice in each series (9.1%) in high brightness/medium saturation and medium brightness/low saturation, and p and s appeared once in each series (4.5%) in high brightness/low saturation and medium brightness/high saturation. In the green natural dyeing materials, ltg tones appeared in all materials, and many g tones also appeared many times, showing that tones of medium brightness/low saturation were strong, and tones of medium brightness/medium saturation appeared. Meanwhile, tones of low brightness did not appear in all saturation groups.

Table 2 : Tone Analysis of Purple-based and Green-based Natural Dyed Fabrics

Frequency(%)

	Material	p	lt	b	v	s	sf	d	dp	dk	ltg	g	dkg	Total
Purple	Silk	0	0	0	0	3(3.5)	6(7.1)	7(8.2)	1(1.2)	0	13(15.	8(9.4)	2(2.4)	40(47.1)
	Cotton	0	0	0	0	1(1.2)	2(2.4)	14(16.	1(1.2)	0	3(3.5)	7(8.2)	2(2.4)	30(35.3
	Viscose rayon	0	0	0	0	0	2(2.4)	0	0	0	0	0	0	2(2.4)
	Ramie	1(1.2)	1(1.2)	0	0	1(1.2)	2(2.4)	2(2.4)	0	0	0	2(2.4)	0	9(10.
	Hempcloth	0	0	0	0	0	0	0	0	0	0	1(1.2)	1(1.2)	2(2.4)
	Wool	0	0	0	0	0	0	1(1.2)	0	0	1(1.2)	0	0	2(2.4)
	Total	1(1.2)	1(1.2)	0	0	5(5.9)	12(14.1)	24(28.2)	2(2.4)	0	17(20.0)	18(21.2)	5(5.9)	85(100.0)
Green	Material	p	lt	b	v	s	sf	d	dp	dk	ltg	g	dkg	Total
	Silk	1(4.5)	0	1(4.5)	0	0	2(9.1)	0	0	0	2(9.1)	0	0	6(27.3)
	Cotton	0	0	0	0	0	0	0	0	0	3(13.6)	4(18.2)	0	7(31.8)
	Viscose rayon	0	0	0	0	0	1(4.5)	0	0	0	1(4.5)	1(4.5)	0	3(13.6)
	Ramie	1(4.5)	2(9.1)	0	0	1(4.5)	0	0	0	0	2(9.1)	0	0	6(27.3)
	Total	2(9.1)	2(9.1)	1(4.5)	0	1(4.5)	3(13.6)	0	0	0	8(36.4)	5(22.7)	0	22(100.0)

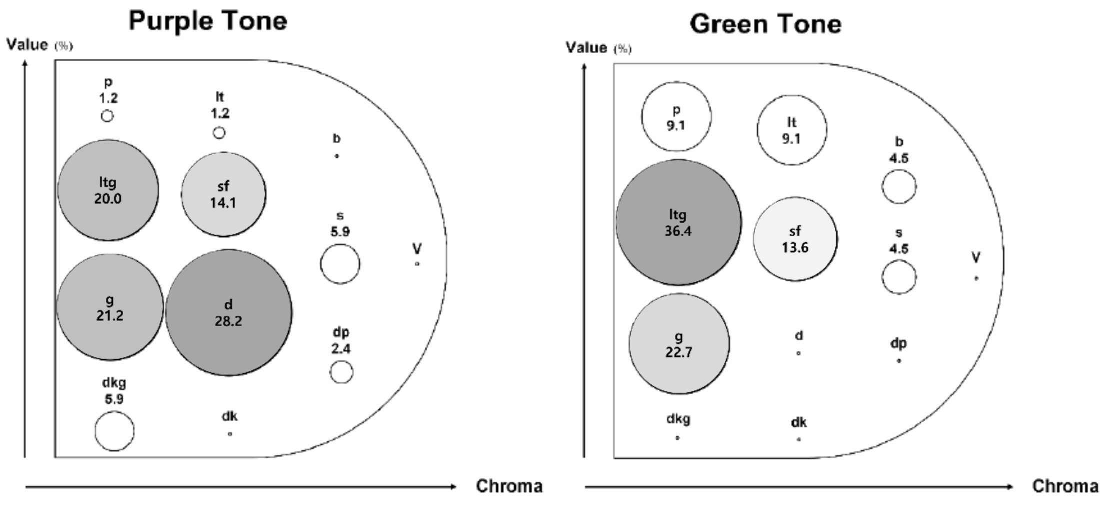

Figure 2. Tone of Purple-based and Green-based Natural Dyeing

CONCLUSION

This basic study on natural dyeing that meets the global trend of eco-friendliness analyzed the color characteristics of natural materials in Korea dyed in purple and green, which have been widely used in Korean clothing since ancient times and are often seen in Korean natural dyeing materials. Purple-based natural dyeing materials were analyzed in the order of RP, P, R, and PB series, and green-based natural dyeing materials were analyzed in the order of GY, G, and Y series. As for the colors of the purple-based natural dyeing materials, RP series showed a dominant distribution in all materials, followed by P series except for hemp cloth and wool. R series was analyzed only in silk, and PB series only in ramie. As for the color of green-based natural dyed materials, GY series was analyzed in all material groups, G series was analyzed in silk and ramie materials, and Y series was analyzed only in cotton.

Regarding tonal characteristics, d tones of medium brightness and medium saturation showed the highest distribution in purple natural dyeing materials, followed by g, ltg, and sf tones. Overall, the tones of medium brightness/medium saturation and medium brightness/low saturation were analyzed dominantly. In green natural dyeing materials, ltg tone appeared with the largest distribution, followed by g tone, and a medium brightness/low saturation tone was dominant. In addition, sf tones appeared frequently, indicating a high distribution of medium brightness/medium saturation tones. It was also found in the high brightness group of p and lt. As for purple and green natural dye tones, the middle tones were dominant in both color systems. Purple was dominant in the low-brightness series and green in the high-brightness series.

Based on the color and tone characteristics of the purple and green natural dyeing materials above, it was possible to identify the difference according to the type of material, even in the same color series. It can contribute to product and color planning in various industries that utilize Korean natural dyeing materials. In addition, it can be used as basic data for research on green and purple natural dyeing colors, which are not prevalent. As a follow-up study, it is intended to expand the analysis by establishing a color database of natural dyeing materials in Korea. As a limitation, some of the materials sold on the market should be analyzed, and caution should be taken in expanding the interpretation of the results.

ACKNOWLEDGEMENT

This work was supported by the National Research Foundation of Korea Grant funded by the Korea Government(NRF-2021R1F1A1046141).

REFERENCES

1 Choi, Y. J., Ryu, H. S., & Kweon, S. A. (2005). A study of color image on silk fabrics dyed with yellow natural materials. Journal of the Korean Society of Clothing and Textiles, 29(6), 868-876.

2 Jo, H. J., Cho, Y. J. & Choi, J. H. (2022). A study on natural dyeing using chlorophyll extract. The Journal of Next-generation Convergence Technology Association, 6(8), 1492-1501. doi.:10.33097/jncta.2022.06.08.1492

3 Kim, J. T., Son, B. Y., Lee, J. S., Baek, S. B., Kim, S. L., Kim, M. J., Jung, G. H. & Kwon, Y. U. (2013). Natural dyeing fabrics with leaf and stem of purple corn. Korean journal of crop science, 58(2), 113~118. doi.:10.7740/kjcs.2013.58.2.113

4 Lee, A. R., Sarmandakh, B., Kang, E. Y. & Yi, E. J. (2012). Effect of colorimetric characteristics and tone combination on color emotion factors of naturally dyed color combination fabrics: Focus on yellowish and reddish fabrics. Journal of the Korean Society of Clothing and Textiles, 36(10), 1028-1039. doi:10.5850/JKSCT.2012.36.10.1028

5 Nam, C. W., Yu, J. S., & Park, H. W. (2022). Color characteristics and images of Korean blue-based natural dyeing fabrics. Journal of the Korean Society of Costume, 72(4), 1-25. doi:10.7233/jksc.2022.72.4.001

6 Shin, J. D. & Choi, J. M. (2013). Colorimetric properties, color sensibility and color preferences for mulberry/cotton blended fabrics dyed with natural indigo. Korean Journal of Human Ecology, 22(2), 365-374. doi:10.5934/kjhe.2013.22.2.365

7 Shin, J. D., Kim, Y. W., & Choi, J. M. (2018). Effects of colorimetric properties and color

sensibility factors on color preferences for green yellow natural dyed silk fabrics: Focused on combination dyeing with indigo and Japanese pagoda tree. Korean Journal of the science of Emotion & sensibility, 21(1), 143-154. doi:10.14695/KJSOS.2018.21.1.143
8 Yang, J. H., & Park, H. W. (2023). Color analysis and color image characteristics of Korean natural dyed fabric: focused on yellow and red based dyes. Journal of the Korean Society of Costume, 73(2), 67-85. doi:10.7233/jksc.2023.73.2.067
9 Yi, E. J. & Choi, J. M. (2009). Color sensibility factors for yellowish and reddish natural dyed fabrics by 40s middle-aged consumers. Journal of the science of Emotion & sensibility, 12(1), 109-120.
10 Yi, E. J., Lee, S. H., & Choi, J. M. (2022). A comparative study of color emotion and preference of Koreans and Chinese for two-color combination by naturally dyed fabrics with persimmon and indigo. Journal of the Korean Society of Clothing and Textiles, 46(1), 33-48. doi:10.5850/JKSCT.2022.46.1.33
11 Yoo, H. J. (2007). Dyeing protein fiber to green color using natural mugwort and indigo. Human Ecology Research, 45(4), 53-59.

KOREAN PERSONAL COLOR EXPERTS' EMPIRICAL PERCEPTIONS OF THE PERSONAL COLOR SYSTEM

Dakyeong Ham[1], Hyewon Park[2]*

1Master Course, Major in Clothing & Textiles, Interdisciplinary Program in Senior Human Ecology, Changwon National University, South Korea
2Professor, Major in Clothing & Textiles, Interdisciplinary Program in Senior Human Ecology, Changwon National University, South. Korea

*Corresponding author: Hyewon Park, hwpark@changwon.ac.kr

ABSTRACT

In this day and age, visual values have become important, and people of all ages are highly interested in their appearance. Therefore, it can be seen that people want to start by identifying their personal color as a way to create an image of their ideal appearance. Personal color is an individual's natural body color, which refers to the color of skin, hair, and eye color, and it is the color that harmonizes with the color of one's body, i.e., the color that looks best. The purpose of this study is to identify the positive and negative aspects of personal color diagnosis that are widely used in Korea by personal color experts and suggest improvements. The research methods are focus group interviews and content analysis. Five personal color experts were questioned. The results are as follows: the participants were fashion and beauty college lecturers, makeup artists, and hairdressers. When asked about the necessity of a personal color, all respondents thought it was necessary, and positive words such as effective image expression, help to communicate, compensate for disadvantages, give confidence and value, meet customer needs, and help to choose products appeared. On the other hand, the negative opinions include the influence of lighting and environmental influences, such as lighting, differences between indoors and outdoors, difficulty in classification, the need for complementary solutions, inappropriateness for Asians, a need for system segmentation, a need for quantitative analysis, and a need for unified training. From these results, it can be concluded that the current personal color system in Korea needs more granularity and needs to be complemented by a quantitative system.

Keywords: Personal Color System, Korean Beauty Experts, Four-Season Images

INTRODUCTION

Why do people pursue good looks? From the moment we are born, we are evaluated by others for our height, weight, size, appearance, symmetry of facial features, length and style of hair, fashionable clothes, and outfits. In other words, we are judged silently, unconsciously, and almost instantly by all the qualities known as “physical attractiveness.” Social scientists in various fields have studied a phenomenon sometimes referred to as ‘lookism’ and concluded that people often define a person based on the evaluation of appearance, such as first impressions [1]. Recently, communication on social media has become a significant daily culture centering on internet media. The ideal standard of look derived from this phenomenon turns into a message through the development and rapid spread of mass media and has a great influence on individual values and body image [2]. Modern people perceive their body image in the ever-changing standard frame of appearance and make various efforts to overcome physical defects or complexes about their appearance [3]. Understanding the personal color is useful as the first step to complete the makeup, hairstyle, and fashion style, which are the methods of creating a beautiful image. As personal color diagnosis leads to expectations and confidence in the image enhancement effect, the diagnosis by personal color system is steadily increasing while interest in personal colors in

Korea is growing.

Previous studies on the personal color system in Korea include Park (2001, 2002), Shin (2002), Kim (2003, 2006), Park (2005), Moon (2005), and Kim (2007), which dealt with the classification of personal color types and the relationship between appropriate clothing colors and makeup colors according to personal colors. However, most of the domestic personal color education adopted the overseas system as it is, causing issues such as it does not fit well with the characteristics of Koreans, and the analysis results come out differently because each educational institution uses different systems and diagnostic tools. In addition, using diagnostic tools from France, the United States, Germany, and Japan causes irrationality during diagnosis because environmental color and cultural color characteristics are reflected in them [4]. This study intended to analyze the current situation of the currently implemented personal color system and find its strengths and weaknesses to develop a personal color system suitable for Koreans. This study aimed to conduct a focus group interview (FGI: Focus Group Interview) targeting personal color experts in Korea and derive positive and negative keywords from actual diagnosis experiences based on the results to suggest improvements.

METHODOLOGY

For this study, a literature study was conducted to examine previous studies related to the personal color system. Next, a focus group interview (FGI) with personal color experts was conducted, and answers to the questions were analyzed. As for the questions, eight questions were selected based on previous studies, and the interviews were recorded freely to confirm what the experts felt empirically <Table 1>. Then, conclusions were drawn by interpreting positive and negative keywords. The interview subjects were five people who worked as personal color experts in Changwon and Busan in Korea <Table 2>. As for the interview process, participants were contacted by phone, explained the purpose of the study and how to process the data, and asked whether they would participate. In addition, with the participant's consent, the interview contents were recorded and transcribed <Figure 1>. The collected data were analyzed using thematic analysis, widely used in general qualitative research. Generally, thematic analysis is used to initially analyze collected data or identify a general perspective on a specific problem [5]. Since this study aimed to suggest improvements in implementing the personal color system, thematic analysis was chosen as a qualitative data analysis method to identify the characteristics from the expert's point of view. In-depth interviews with experts were conducted between February 15-27, 2023.

Table 1: Interview Questions

1. What is your occupation and age? How many years have you worked in the fashion beauty field?
How many years have you been performing personal color testing?
2. As a fashion beauty expert, do you think personal color testing is necessary? What is the reason?
3. Is the current personal color test system effective for Koreans? Please feel free to share your experiences.
4. Do you think the intuitive predictions and diagnosis results in the personal color test for Koreans are generally consistent? (Please specify the consistency in percentage)
5. If there was a case where the intuitive prediction and diagnosis results did not match, what do you think is the reason?
6. Were there any additional requirements for the personal color test?
7. What should be improved to apply the current personal color test system to Koreans more effectively?

Figure 1. Interview with Experts

Table 2: General Characteristics of Research Participants

N	Name	Age	Occupation/Experience	Experience with Personal Color
1	Lee, H.	43	College Lecturer / 15 years	7 years
2	Kim, J.	44	College Lecturer / 20 years	10 years
3	Lee, Y.	50	Image Making Consultant / 25 years	15 years
4	Kim, S.	38	Makeup Artist / 20 years	12 years
5	Ha, Y.	41	Makeup Artist / 17 years	4 years

RESULT AND DISCUSSION

1) Preceding Studies Examination Results

The Personal Color System diagnoses the colors of the four seasons that harmonize with each person's unique body color (skin color, hair color, eye color) and produces color images for make-up, hair, clothes, and so on according to the colors that suit the person and the colors that do not. This system finds one's own personal color within the structure of seasonal colors. Robert Dorr (1905-1980), who first discovered human color, said that there are warm and cool skin colors, and Johannes Itten (1888-1967) of Germany studied the subjective color composition of humans by dividing it into four types for each season. For the first time in 1981, Carol Jackson of Canada classified human images into four types by season, provided appropriate color palettes for each, suggested appropriate clothing and color makeup methods, and published a book titled 'Color Me Beautiful.' With this book, the personal color system began actively applied in many countries, such as the United States, Europe, and Japan [6].

It is necessary to define personal color and personal color diagnosis differently. Personal color is an individual's body color, and personal color diagnosis is an application of colorology that uses the properties of color to find a color that harmonizes with an individual's personal color and image. Here, a color system is used to diagnose personal color. As for the color system, there are four types based on the four seasons proposed by Carole Jackson in 1981, nine types proposed based on the Asian race by Donna Fujii (USA, Japan) in 1992, and eight types by Petits Pratiques (France). In Korea, since 2005, the CCI Color Research Center has divided each season into two types based on the four-season color system and classified and implemented eight types. Other personal color diagnosis methods using various processes are also in use, but not many studies on standardized diagnosis processes. Most existing personal color diagnosis methods implemented in Korea use a four-type classification (Carole Jackson) or an eight-type classification (CCI Color Institute). It is difficult to suggest colors in detail to customers, and the subjectivity of the diagnostician intervenes in the diagnosis process, which are the limits [7].

2) Focus Group Interview Topic Analysis Result

Following positive and negative keywords were derived by analyzing the focus group interview (FGI).

Positive Keywords

A personal color diagnosis system is required, effective for image expression, helpful in expressing opinions, complementing weaknesses, maximizing strengths and confidence, attaching values, upgrading images, matching perfectly, satisfying customer needs, need for self-management, increasing self-esteem, helpful in choosing products, image change, satisfaction of desire, consulting matching purpose, colorimeter reliability.

Negative Keywords

Need for standardized professional education for training experts, misdiagnosis, misjudgment, the large influence of lighting, different conditions, the difference between indoor and outdoor, improvement of diagnostic cloth, unnecessary, lack of consistency, intersection, difficulty in classification, need for supplementary solution, not a fixed answer, systematization of solution, error, need for diagnosis kit exclusively for nail, lack of education, ineligibility for Asians, various standards for each individual, need to be customized for Koreans, condition mismatch, need for system segmentation,

In addition, three important topics were confirmed through the interview, as shown in <Table 3>.

Table 3: Identification of Problems Based on Interview Results and Summary of Interview

Problems	Interview Details
1. Quantification of the diagnostic system, creating an environment to eliminate prejudice	"Because the types are classified by analyzing various characteristics of individuals, we need a test device, quantified by applying systematic steps." "We need to meet the person to be diagnosed face-to-face when he or she is ready, and the tone of voice (intonation, speech) when greeting gives the examiner a stereotype." "We need a 3D color comparison system. It would be nice to have a system to measure and check by substituting color."
2. Need for a system suitable for Koreans and training for diagnosis experts	"There are differences in the techniques applied by each association. We need a standardized system." "American and German diagnostic papers are inappropriate. Japanese diagnostic papers are common in Korea, but we need a diagnostic system suitable for Koreans." "There may be errors in diagnosis depending on the skill of the examiner. Because the experience and skills of the examiner are important, it is necessary to train the examiner."
3. In addition to the diagnosis result, it is necessary to present a solution suitable for the customer's purpose	"We need a complex consulting (interior, style matching) so customers can be happy instead of ending the process with the determination of personal colors. Now, we need to be able to suggest the direction of color with the image that our customers pursue." "The direction of diagnosis can be varied depending on the purpose by distinguishing what the customer pursues is something inside the door or outside." "I hope additional solutions will be systematized so that when customers need a change, we can provide consulting plus something extra outside the formula."

CONCLUSION

This study was conducted based on focus group interviews with personal color system experts to suggest improvements in implementing the personal color system in Korea. As a result, there is a demand for improvement, indicating that there should be a personal color diagnosis system suitable for Korea. In the era of diverse communication, an individual's identity and expression of himself/herself are very important in communicating with society. Therefore, it is hoped that more systematic and diverse research on personal color diagnosis will be conducted. As a result of diagnosis through this study, it was suggested that a detailed analysis method is needed for Koreans according to the various conditions of each individual when implementing the personal color system and that the quantitative diagnosis system should be improved. However, as this study was conducted on five personal color diagnosis experts, caution should be taken in extending its interpretation, and more quantitative and qualitative studies are expected to be conducted in the future.

REFERENCES

1. Patzer, Gordon L. (2008). Looks:why they matter more than you ever imagined. New York (State): AMACOM.
2. Heinberg, L. J. Thompson, J. K. & Stormer, S. (1995). Development and validation of the sociocultural attitude towards appearance questionnaire. International Journal of Eating Disorders, 17(1), 81-89.
3. Cruickshank, W. M. (1971). Psychology of exceptional children and youth. Englewood Cliffs, New Jersey: Prentics Hall.
4. Cha, H. Y., Bang, H. J., & Kim, J. h. (2012). Comparative Analysis of Diagnostic Results of Domestic and Foreign Personal Color System- Focusing on UK, Japanese, Korean, German Personal Color System. Korean Journal of Beauty 18(1) (2012): 17-25.
5. Kelly, M. (2010). The Role of Theory in Qualitative Health Research. Family Practice. 27(3). 21-32.
6. Cha, H. Y., & Kim, J. H. (2014). The Comparative Study of Color Value in Personal Color Diagnosis Drapes of Domestic and Foreign The Comparative Study of Color Value in Personal Color Diagnosis Drapes of Domestic and Foreign. Journal of the Korean Society of Makeup Design, 10(2). 52.
7. Jung, Y. S. (2021). A Study of the Quantitative Diagnosis Model of Personal Color. Journal of Convergence for Information Technology, 11(11), 277–287. https://doi.org/10.22156/CS4SMB.2021.11.11.277

COMPARISON OF COLORS IN METAVERSE AND OFFLINE SPACE OF FASHION BRANDS

Kyuhee Ahn[1] and Gyoungsil Choi[2]*

[1] *Master Course, Art & Design, Ewha Womans University, Republic of Korea.*
[2] *Professor, Art & Design, Ewha Womans University, Republic of Korea.*

*Corresponding author: Gyougsil Choi, gschoi@ewha.ac.kr

ABSTRACT

Fashion brands aim to enhance their brand value and increase their operating profits by providing an optimal consumer experience in their physical stores. Thus, the color scheme of brand stores is a crucial marketing factor. However, with the emergence of digital media-based stores like metaverse stores, it has become necessary to compare how brand colors are applied online and offline. In metaverse spaces, where a sense of space is created through flat displays, the color scheme is different from that of physical stores even if they belong to the same brand. This study aims to determine the degree of variation in brightness, saturation, or color required to represent a sense of space in a digital environment, which is different from the physical space. In this study, three fashion brands (Gucci, Polo Ralph Lauren, and Bulgari) that have both offline stores and a presence on Zepeto, a popular metaverse platform in Korea, were selected as study subjects. The analysis showed that the metaverse brand space in Zepeto creates a sense of space through a clear contrast in brightness and saturation. As the user experience in the digital environment is achieved through flat media, it is important to emphasize the effect of entry and retreat to enhance visibility.

Keywords: metaverse, offline space, fashion brands

INTRODUCTION

Fashion brands have been using their offline store spaces, such as brand stores and flagship stores, to communicate better with their customers. Color design in these spaces is a crucial marketing factor as it implicitly expresses the brand's identity and orientation, making it easier for consumers to recognize the brand. To reach even wider audiences, fashion brands are now exploring new marketing channels, such as metaverse-oriented virtual stores. For instance, Nike and Ralph Lauren have partnered with popular U.S. metaverse Roblox to introduce virtual spaces and fashion items that reflect their brand identity. Similarly, Marc Jacobs and Valentino have used Nintendo's video game, "Animal Crossing," as a platform to showcase their brand through a runway show. As the popularity of metaverse continues to grow rapidly, the fashion industry is increasingly looking to leverage this technology. It is important to have a consistent brand image across online and offline experiences, and color plays a critical role in achieving this. However, expressing a sense of space through color in a digital environment is different from doing so in a physical space. This study aims to explore these differences and provide pioneering data on the use of color in the metaverse.

METHODOLOGY

This study focuses on three fashion brands - Polo Ralph Lauren, Gucci, and Bulgari - that have offline stores and maps in Zepeto, a popular metaverse platform in Korea. Zepeto is an AR avatar service that was launched in August 2018 and is operated by Naver Jet (Z). It has gained popularity due to its collaboration with famous brands and entertainment agencies, with 300 million subscribers and 20 million global monthly active users. Users can experience different spatial content on various topics through maps. The research approach involved Kang's (2022) classification of space into structural elements, directing, and decorative elements. The study focused on the background - floors, walls, and ceilings - which are structurally fixed and essential elements for constructing space. Objects for display, which account for a high proportion of the screen and are used repeatedly, were classified as objects. The study aimed to analyze how color, brightness, and saturation are expressed in both the background and objects that make up the space.

RESULT

Brand 1. Gucci

For this study, Gucci was chosen as one of the luxury brands with its sole flagship store in Korea and actively showcasing its brand not only offline but also in the metaverse. The survey focused on the colors used in the offline store of the Gucci flagship store located in Cheongdam, and three exhibition spaces from the nine available on the Zepeto world map "Gucci Garden Architects Seoul" were chosen to represent the brand.

Figure 1. Zepeto map of Gucci

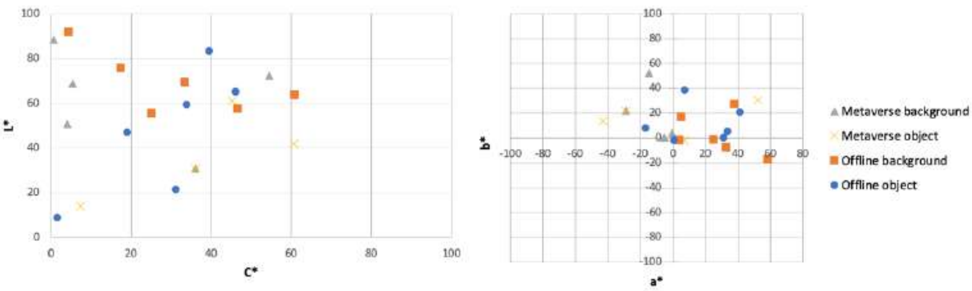

Figure 2. Color distribution of Gucci (Left: L*-C* graph, Right: a*-b* graph)

When viewing images in the metaverse, the background is typically brighter than the object, resulting in a diagram that appears to be divided in half. Both the background and object are generally distributed throughout the image. In offline images, the brightness is distributed from prominent to high, with the background having a higher distribution of medium-high brightness. Saturation is typically between 20 and 40 for both background and object, and is distributed at regular intervals. Color distribution is more difficult to determine in offline images, as the background is mostly distributed in gray and yellow, while the object is distributed in all colors except blue and green. In the offline background, yellow-red and red-blue are the most prominent colors, while the object is mainly distributed in yellow-red with some green-yellow. The overall color scheme tends to harmonize with yellow-red as the main color throughout the space, with a slight bias toward red-blue compared to the metaverse.

Brand 2. Polo Ralph Lauren

For this study, the researchers chose Ralph Lauren as the second fashion brand to analyze on Zepeto's map. They focused on the World of Ralph Lauren virtual store and took three pictures of the cafe and exhibition display areas. The team also visited the Ralph Lauren Flagship Store in Garosu-gil, Sinsa-dong to conduct a color survey of the walls, floors, ceilings, and objects using the NCS index color sampling method.

Figure 3. Zepeto map of Polo Ralph Lauren

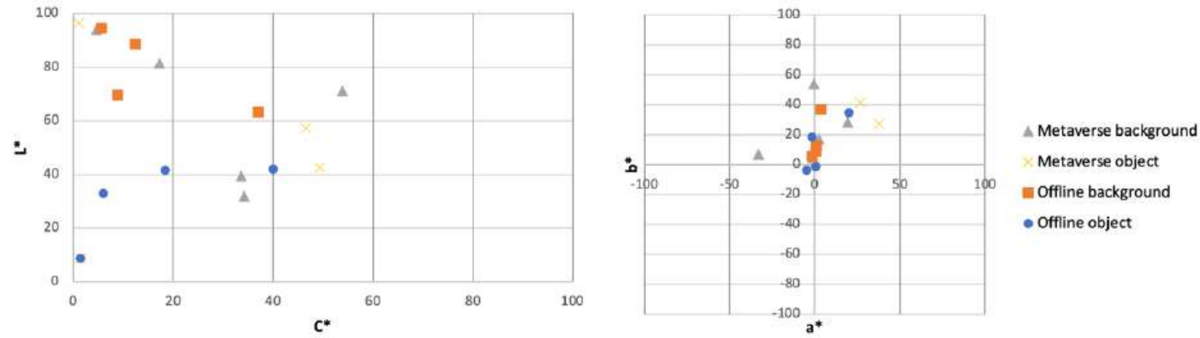

Figure 4. Color distribution of Polo Ralph Lauren (Left: L*-C* graph, Right: a*-b* graph)

It can be challenging to establish a regular pattern in the lightness and saturation of Background and Object in Metaverse. However, offline stores present a clear contrast between Background and Object's lightness. Typically, Background is distributed in high brightness, whereas Object is distributed in high brightness. The saturation distribution usually follows the same pattern. Occasionally, Metaverse's Objects may appear darker than the Background, but they are still brighter than those in offline stores. When examining the Ralph Lauren brand's metaverse store, it is apparent that a wide range of colors were utilized, including GY and YR, with both Objects distributed within YR. In contrast, offline stores typically use medium and low colors of similar hues centered on Y for both Background and Object. Nevertheless, they provide a clear contrast in brightness, resulting in a visual sense of stability, allowing the object to stand out against the bright background.

Brand 3. Bulgari

For this analysis, the Italian luxury jewelry brand Bulgari was chosen as the final subject. A survey of virtual store colors was conducted using a map of the "Sunset in Jeju" pop-up store on Zepeto in 2022, focusing on three areas: display spaces, main spaces, and rest areas. Additionally, the Bulgari store in Galleria Luxury Hall, selected as Korea's first High Jewelry Flagship Store, was chosen as the target for the offline color survey.

Figure 5. Zepeto map of Bulgari

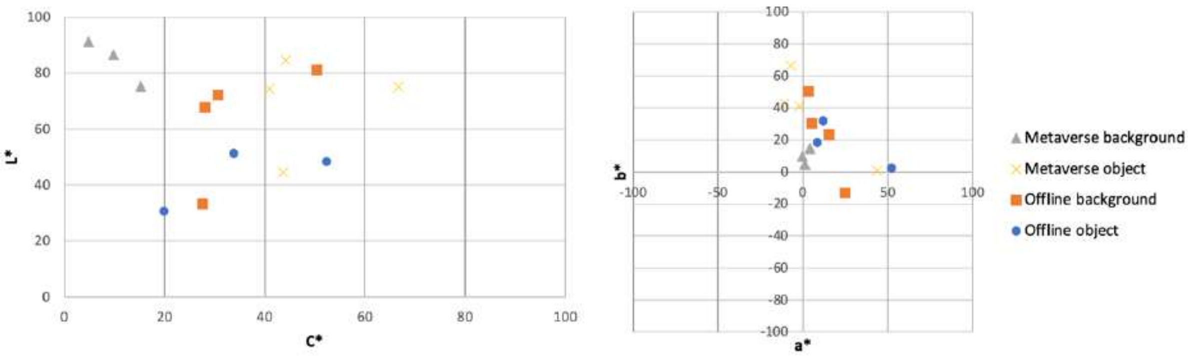

Figure 6. Color distribution of Bulgari (Left: L*-C* graph, Right: a*-b* graph)

In the metaverse, the overall image is expressed with high brightness, and the saturation difference between Background and Object stands out and tends to be clearly distinguished. In offline stores, while the brightness of Background is high, the object is relatively low in brightness, so attention is focused, and the chroma distribution is more concentrated than the metaverse, providing a stable visual experience as a whole. The chroma of the metaverse is more diverse than offline. In the metaverse, the difference is large as Background is distributed in YR and Object is distributed in GY and R. In contrast, offline, objects are concentrated in YR, and Background is widely distributed with some ranges overlapping from GY to RB around the color of the object, There isn't much of a noticeable difference in color between the two.

DISCUSSION

A study conducted by Ryu, Seo, and Lee in 2016 found that color has a greater influence on the perception of space than spatial shape. To maintain brand identity across metaverse and offline spaces, it is important to use consistent colors. However, there may be differences in brightness and saturation between the digital and physical spaces. Kim (2008) demonstrated that color perception in architectural spaces is affected by brightness and chroma, with colors closer to high brightness and low chroma being less psychologically stimulating. This study suggests that the lower background brightness of the metaverse can cause psychological stress and fatigue if high-chromatic colors are used in offline spaces. Therefore, brands should avoid using high-chromatic colors in their physical spaces. Choi (2018) also found that using similar color series for the floor and surrounding areas can help improve concentration and reduce visual irritation, impression, and fatigue. This study also observed that the color series of walls and floors should be similar, with high brightness applied to certain walls for effect. In offline stores, high brightness is commonly applied to the ceiling and floor, as it gives a sense of stability and has been proven to reduce stress by Kim (2008).

CONCLUSION

Based on the study, it was found that in the metaverse, objects use relatively high chroma colors to create a sense of space. This highlights the need to increase visibility and emphasize the effect of entry and retreat in the digital environment in order to achieve a better user experience. However, when constructing offline stores for the same brand, it is important to give visual stability to those who are in the space. This can be achieved by setting the background brightness high and configuring the objects low while ensuring a unified chroma distribution. In both metaverse and offline environments, colors are used in a wide range from high to low brightness. However, high-chromatic colors are avoided as they can exhaust the view of people staying in the space. In conclusion, color plays a crucial role in the user's spatial experience.

REFERENCES

1. Kang Jisoo. (2022). *A Study on the sense of height of interior space related to color-Focusing on the color change of floors, walls, and ceilings*.
2. Kim Byeongsoo, Choo Seungyeon, Seo Wonduck. (2008). *A Study on Visual Perception Effects of Color for Digital Color Plan*, Vol.24, No.3.
3. Ryu Seungwon, Seo Eunji, Lee Jinsook. (2016). *A Study on the Correlation Analysis Between the color and shape.* AIC 2017 Jeju 2017.
4. Choi Jinkyung., & Kim, Juyeon. (2018). *Characteristics of Gaze through Spatial Color of Indoor Space Image*.
5. Naver Z Corporation
6. Lee Imbok. (2021). *Metaverse, A Future Already Started.* Chongeurusup, pp.6-24.

RECOGNITION OF SMARTPHONE BUTTONS ACCORDING TO SIZE AND SHAPE

Jiwon Yeo[1] and Yungkyung Park[2]*

[1] *Master Course, Art & Design, Ewha Womans University, Republic of Korea.*
[2] *Professor, Art & Design, Ewha Womans University, Republic of Korea.*

*Corresponding author: Yungkyung Park, yungkyung.park@ewha.ac.kr

ABSTRACT

There are numerous instances of button design featuring different colors and styles. However, this study aims to analyze the size and shape that are commonly recognized as a button. Based on the iPhone 14 Pro, the size of the 16 steps was determined by referencing the size of the button currently offered by Apple. The increase in size was also set in direct proportion, both horizontally and vertically, to create the fundamental stimulus. After conducting the size and shape experiments, the results were categorized into positive and negative evaluations. Subsequently, additional experiments were carried out to modify the button properties (such as arrangement, shadow, color, and outline) of the stimuli that received negative evaluations. Stimuli that were not initially recognized as buttons in size and shape showed the same negative results, even when different properties of buttons were assigned. However, in the arrangement case, it was confirmed that some negative evaluation stimuli received positive evaluation depending on the number of stimuli arranged on the screen.

Keywords: Button Size, Button Form

INTRODUCTION

When designing a button on a smartphone, it is important for users to be able to quickly understand that they can act by pressing the button. Inducing the action of seeing and pressing a button is called action-inducing design. It is a device that helps guide people to use things more easily. Since each combination of button size and style has a different level of visual importance, it is helpful to display the hierarchy of actions. Showing visual cues about how things should work is something to consider when designing not just buttons.

There are various ways to make a button stand out, but in this paper, we focused on the size and shape of the button. In addition to size and shape, parameters such as arrangement, shadow, color, and outline were used to determine the factor that had the greatest influence on recognizing something as a button.2)

As a result, this study aims to determine the factors that cause individuals to perceive screen speed figures as buttons.

METHODOLOGY

The research was conducted together with theoretical and empirical studies. In the theoretical study, the theoretical foundation necessary for this study was established by referring to previous studies to find out the size 6) used as a button in smartphones, the characteristics of button design 7), and the elements recognized as buttons. The empirical study consisted of a total of two

experiments. The first experiment aims to determine the size of stimuli that individuals perceive as buttons on a smartphone screen. It utilizes a two-point scale to assess whether stimuli are perceived as buttons or not. The evaluation was carried out in the second experiment by assigning attributes such as arrangement, shadow, color, and outline to the stimuli that received negative evaluations in the first experiment.
To determine the button size, we used the iPhone 14 Pro display (2556*1179px) as a reference point and the average finger tap size (44*44px) provided at the Apple Worldwide Developers Conference (WWDC) as a standard. The range of stimuli includes the minimum size of the UI button used by Apple Inc. and spans from 40px to 1179px, with 16 steps in total. In addition, a total of 48 stimuli were produced by dividing the method of increasing the size of the button into three cases: increasing in direct proportion, lengthening horizontally, and lengthening vertically. In the experiment, to eliminate any additional influence from the shape or color of the stimulus, a square of achromatic black (Bk) color was chosen as the basic shape and used to create the stimulus.

Table 1: Experimental Stimuli

	40px	120px	200px	280px	360px		1160px	1179px
Direct proportional						…		
Horizontal								
Vertical								

In the second experiment, an additional study was conducted to investigate how the evaluation changed when the stimuli that received a negative evaluation in the first experiment were given properties such as arrangement, shadow, color, and outline.
The stimuli that received negative evaluations in the first experiment were 14 in direct proportion, 11in horizontal, and 16 in vertical.
For the recognition evaluation stimuli based on arrangement, since the number of arrangements that can be made differs depending on the size, stimuli that can fit on the screen of the iPhone 14 Pro were selected.
For the recognition evaluation stimuli based on shadows, a total of 41 stimuli were produced with a negative evaluation by applying the same shadow effect.
For the recognition evaluation stimuli based on colors, they were designed by referencing previous studies.1)3)4)5) Referring to the color ranking based on the behavioral psychology of Korean subjects, it consisted of Vivid (V) tones of Yellow (Y), Orange (O), Red (R), and Blue (B) according to the PCCS color system. Samples were randomly produced with various colors.
For the recognition evaluation stimuli based on outlines, samples were created by outlining 41 negatively evaluated stimuli with the same thickness of 10p. Since all experiments were conducted with the same background color (White, W), the stimulus color was switched to White (W) and the outline color to Black (Bk).

RESULT AND DISCUSSION

A one-way analysis of variance (ANOVA) was conducted to determine whether there was a significant difference in the recognition evaluation based on the size and shape of the button. The analysis revealed a significant difference ($p<0.05$) in the shape of the recognition evaluation based on size.

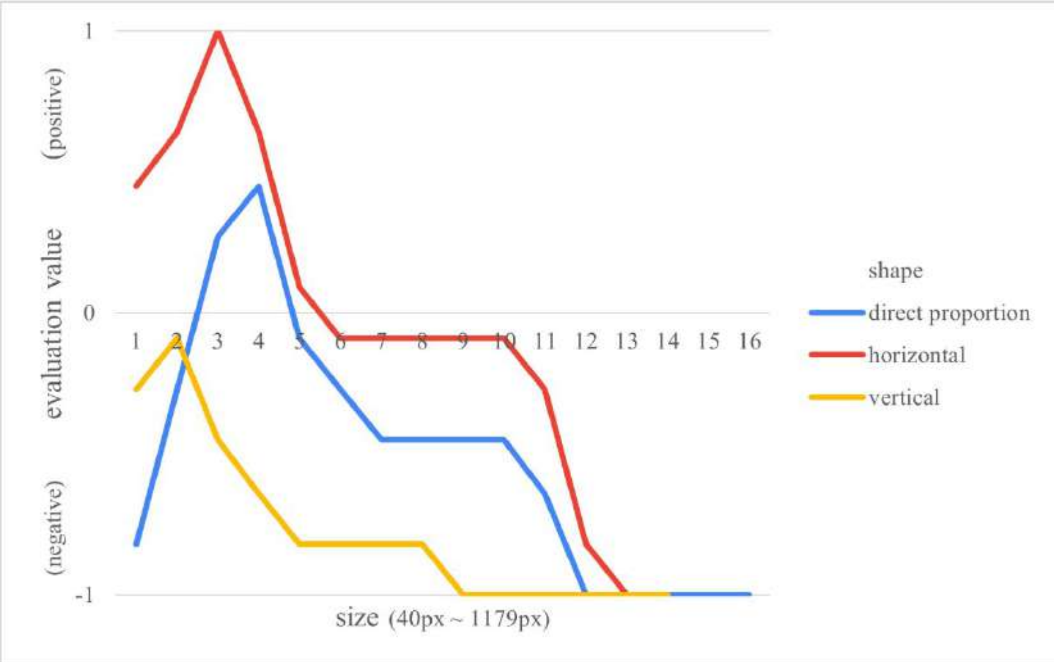

Figure 1. Evaluation average according to size and shape

Analyzing Figure 1, it was found that, on average, the horizontal growth case had a higher score than the direct proportion or vertical growth cases. Through this, it was confirmed that stimuli of smaller or larger than a certain size were not recognized as buttons, and the level of recognition varied depending on the shape.

A one-way analysis of variance (ANOVA) was performed to determine whether there was a significant difference in recognition evaluation based on the button shape arrangement. As a result of the analysis, it was confirmed that there was a significant difference ($p < .001$) in the button evaluation based on the arrangement. As a result of the analysis, the three shapes were divided into two groups. Direct proportion and vertical were grouped together, while the horizontal result differed from the others. Therefore, an analysis was conducted to evaluate the arrangement based on its shape.

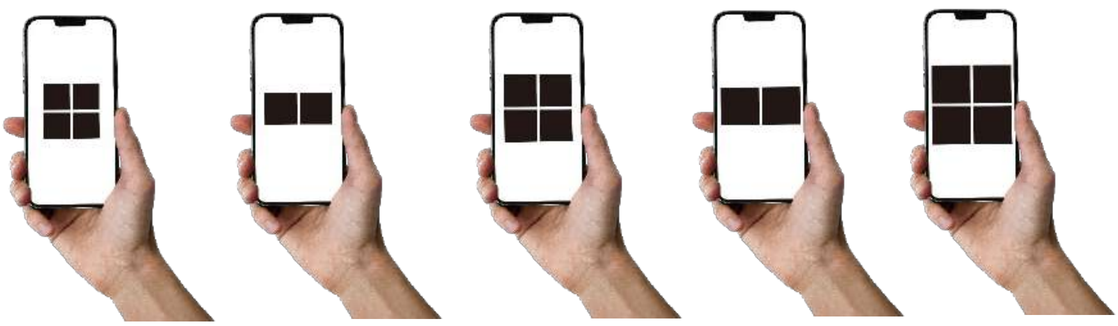

Figure 2. Positive evaluations of direct proportion according to the arrangement

According to Figure 2, the stimuli that received positive evaluations had sizes of 360px, 440px, and 520px. Additionally, the types of arrangements were 2-array and 4-array. Although one stimulus was large enough to receive a negative evaluation in the first experiment (which focused on size and shape), it was found that the subjects recognized each stimulus as a button due to its arrangement.

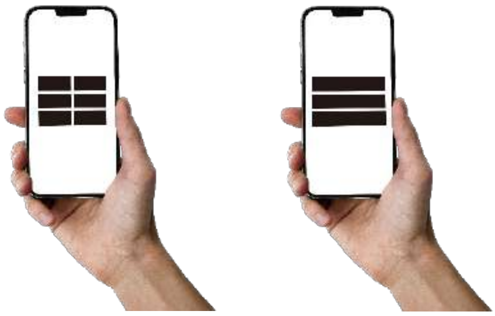

Figure 3. Positive evaluation of horizontal according to the arrangement

According to Figure 3, among the average evaluations in the horizontal axis, there are two stimuli that received negative ratings. Numbers 3 (520px/6 arrays) and 13 (840px/3 arrays) are characterized by having margins on both sides that are less than 40px when arranged. Through this result, it was confirmed that the width of the blank space also affects the evaluation of button recognition.

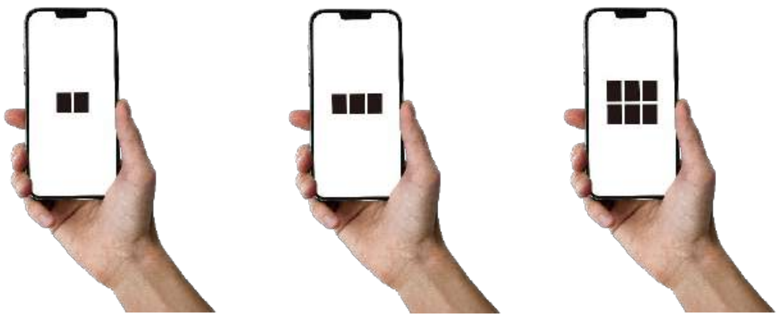

Figure 4. Negative evaluations of vertical according to the arrangement

According to Figure 4, among the vertical evaluation averages, the sizes of stimuli No. 1, No. 2, and No. 4 that received positive evaluations are all 120px, and their arrangements are two, three, and six, respectively.
According to the analysis of variance (ANOVA), it was found that there was no significant difference in the evaluation result of recognition with respect to Shadows, Colors, and Outlines.

CONCLUSION

As a result of the survey, if a button was not recognized based on its size or shape, it was not identified as a button, even if it had button properties such as shadow, color, and outline. However, in the case of arrangement, some negative stimuli could be evaluated positively depending on the number of them arranged on the screen.

REFERENCES

[1] Ku, G. (2008). Learning to de-escalate: The effects of regret in escalation of commitment. *Organizational Behavior and Human Decision Processes*, *105*(2), 221-232. doi:10.1016/j.obhdp.2007.08.002
[2] Lee Sun, & Park Young - kyung. (2017). Correlation between user characteristics and color choices: preference, explicitness, and behavioral psychology. Academic Conference of the Korean Colour Society, 34-37.
[3] Cho Sung-il, Park Sung-joon, Jung Eui-seung, Lim Young-jae, & Jaeho Choi (2010). A study on the layout of the touchscreen phone menu according to various gripping methods. Journal of the Korean Society of Industrial Engineering, 36 (1), 52-58.
[4] Mizutani, Y., Kitaguchi, S., & Sato, T. (2017). Colour Influence of Input Button on User's Pressing Motivation, Visual Attraction, and Preference-Analysis Using Paired Comparison. AIC 2017 Jeju, 67-67.
[5] Sun, X., Plocher, T., & Qu, W. (2007, July). An empirical study on the smallest comfortable button/icon size on touch screen. In International Conference on Usability and Internationalization (pp. 615-621). Springer, Berlin, Heidelberg.
[6] Hsieh, T. J. (2017). Multiple roles of color information in the perception of icon-type images. Color Research & Application, 42(6), 740-752.
[7] Komine, S., & Nakanishi, M. (2013, July). Optimization of GUI on Touchscreen Smartphones Based on Physiological Evaluation–Feasibility of Small Button Size and Spacing for Graphical Objects. In International Conference on Human Interface and the Management of Information (pp. 80-88). Springer, Berlin, Heidelberg.

PIGMENTS APPLIED IN "AUTUMN (1956)" PAINTING OF FUA HARIPITAK, THE FIRST AND MOST OUTSTANDING ARTIST OF THAI CONTEMPORARY, ANALYZED BY PORTABLE MICRO-XRF

N. Kaew-on* and T. Kaewkong

Restaurateurs Sans Frontières, Studio for art conservation and restoration, 6 Soi Kasemsan 2, Rama I Road, Wangmai, Phayathai, Bangkok 10330 Thailand

*Corresponding author: Nawarat Kaew-on, rsfasie_nawarat@hotmail.com

In Thailand, the use of scientific techniques to analyze arts is insufficient. This article aimed to scientifically discuss the studied pigments in the palette of well known Thai artist, Fua Haripitak. Fua is the first and most prominent artist of Thai Contemporary in the 20th century. More importantly, he is not only outstanding for contemporary art but also Thai art and preserving Thai art. Fua was awarded as Thai national artist in 1985, eight years before he has passed away at age 83 years old. The painting technique of this artist had never been extensively investigated and it was found that there had been counterfeit works in the art market. Analysis the pigments on the painting named "Autumn (1956)", oil on canvas, which was painted in 1956 during the period when the artist was staying in Italy, was focused and documented. The non-destructive micro-X-ray fluorescence (XRF) technique by combining the XRF mapping (MA-XRF) and point inspecting method were employed to analyze the pigments of the painting. Examination by UV light at the wavelength 365 nm was carried out to investigate and find if there were restorations before the execution process XRF acquisition. This method is commonly used to ensure that the investigation proceeded with the original pigments painted by the artist. The results showed that the pigments applied are common for the period of time: lead white (Pb) and lithopone white (Zn, Ba) in the preparation, zinc white (Zn), vermillion red (Hg), chrome-based green (Cr) which is highly possible to be the viridian green considering from its hue, cadmium yellow (Cd), and brown ochre (Fe). Blue pigments in the artist pallet were not clearly identified as well as the black pigment. Blues were probably the organic pigment, while the bone black should have been used for black color as it was indicated strong presenting of calcium and trace of phosphorous (Ca, P).

Keywords: Fua Haripitak, Pigments characterization; X-Ray fluorescence; Thai contemporary artist

INTRODUCTION

Fua Haripitak (1910-1993) is the first and most outstanding artist of Thai contemporary. He started his art education at the Poh-Chang Academy of Arts, the important art school in Thailand, before having a chance to study with professor Silpa Bhirasri (Corrado Feroci), an Italian artist who effectively contributed to the modern art of Thailand in the 20th century. Fua has been regarded as "the principal of the art for Thailand" due to his works and techniques inspired the creation of modern art by next-generation artists [1]. Not only being the artist and teacher, Fua Haripitak also contributed works in traditional Thai art as the conservator for Thai mural paintings. He inspected mural paintings in important ancient temples and copying mural patterns to keep as an evidence of the national historical heritages. He restored important paintings in 23,000 temples throughout Thailand. Fua Haripitak has been praised the Ramon Magsaysay Award in 1983, and named as National Artist of Thailand in 1985 [1-3].

In Thailand, the use of scientific techniques to analyze arts is insufficient, while forgeries have been increased in the art market. Fua Haripitak is the most famous Thai artists whose works have been often forged. In 2022, the author received the painting which has been questioned that whether it was painted by this artist. To answer the question, a group of paintings that has been painted by this artist at the corresponding time, were therefore used as references. Although the paintings painted by Fua Haripitak have been widely popular, little is known about the pigments that he used. Characterization of pigments in the palette of the artist is one of the methods that can verify the painting. Pigments of reference paintings were therefore studied. Nondestructive technique, the XRF (X-ray fluorescence) spectroscopic was carried out. This technique has been very important method to identify pigments. As it is a non-destructive technique, is, therefore, helpful to evaluate the cultural assets, neither touching it nor damaging it at all. Inorganic pigments on the painting or mural paintings can be analyzed by this technique without even any micro sample taken. With the portable equipment, the investigations can be run in situ, without moving the objects from its original place. It is one of the harmless ways to obtain information about the materials and techniques applied by archeologists, scientists, and conservators, although it can only detect limited elements (from magnesium to uranium) and provide semiquantitative results [4-6].

This article aimed to scientifically discuss the studied pigments in the palette of Fua Haripitak by meaning of the XRF. The painting named "Autumn,1956" was chosen for the analysis and discussion. This research is part of the project, dedicated to the characterization of painting by Thai artists in the 20th century.

Figure 1. The "Autumn 1956" painting, and its back panel.

METHODOLOGY

Painting Description: The "Autumn 1956" painting has been owned by a private collector; it is oil on canvas with dimension 40X50 cm. The back side presents the Italian words that are readable as "vialle d' autunno 1956", number 1, 2 and 3 were also written (Figure 1).

UV Examination: In this study, to ensure that the investigation proceeded with the original pigments painted on the the painting, the painting was observed under UV light to get more precise information about later intervention and retouches on the painting surface. For this, one pair of the UV lamp were placed on each side of the painting to obtain the most homogeneous illumination of the surface (the bulbs are UV LED radiation power: 14250 mW, UV max spectral emission: 365 nm).

X-Ray Fluorescence: According to the UV examination results the pigments and ground of the painting were further analyzed in different colors and tonalities by X-Ray fluorescence. The main colors including white, red, green, yellow, brown, ochre, dark blue, were chosen to investigate. The equipment used for this work was the portable Elio instrument (ELIO, XGLab Bruker). The measurements were made in the point mode, using 50 kV and 80 mA for 60 seconds acquisition time. Tube target material was Rh, and sample to detector material was Air. The diameter of the radiated spot is 1 mm. The mapping mode was also performed in conjunction with the point mode measurements. This article displayed the mapping of the certain area only. Mapping acquisitions were made using 50 KeV and 80 mA for 60 mins, the area is 20 x 20 mm^2. In the painting, 29 points were selected over the entire surface to analyze different colors. The pigments were recognized on the basis of the characteristic chemical composition from the XRF spectra of the analyzed locations. Figure 2 presents the UV photo and the selected spots where XRF measurements were performed on the painting. In the results section, the characteristic elements for different pigments were given in bracelets where they were mentioned (Table 1).

Figure 2. The painting under UV light illumination (left), and the selected points, analyzed by XRF fluorescence (right).

RESULT AND DISCUSSION

Visual exam and UV light

Following usual practice, the painting was first observed under UV light. The examination with UV light (Figure 2) showed none of retouched areas or later interventions. Image obtained under UV light helped at the selection of the points analyzed by X-Ray fluorescence.

XRF on the painting

As mentioned previously, the painting was analyzed in 29 points of different colors and tonalities. The most important chemical elements detected by XRF were Zn, Pb, Hg, Cr, Ba, and Fe. Table 1 shows some characters of the pigments on the painting.

Ground layer: The areas without paints observing under UV light at the sky and the lower edge of the painting were inspected (xrf1, xrf2, xrf3, and xrf4). The results showed that the strong signals of Zn and Pb were detected, minor of S, Cl and trace element of Ba, Ca, Sr were also presented. Clear presenting of zinc, lead, sulfur, led to investigate that the lead white [$2PbCO_3 \cdot Pb$

$(OH)_2]$ or zinc base pigments which could be zinc white (ZnO) or lithopone white ($BaSO_4 \cdot ZnS$), could possibly be in the ground. Calcium sulfate ($CaSO_4$), and calcium carbonate ($CaCO_3$) were also possibly in the ground layer [7]. Fortunately, the areas of the ground without paints on the back side of the painting allowed for mapping analysis. Figure 3 presents the mapping results of the ground on the back side. It revealed that Ca was not detected in the ground layer. Thus, the ground layer was highly believed to be a mixture of lead white [$2PbCO_3 \cdot Pb(OH)_2$] and lithopone white ($BaSO_4 \cdot ZnS$).

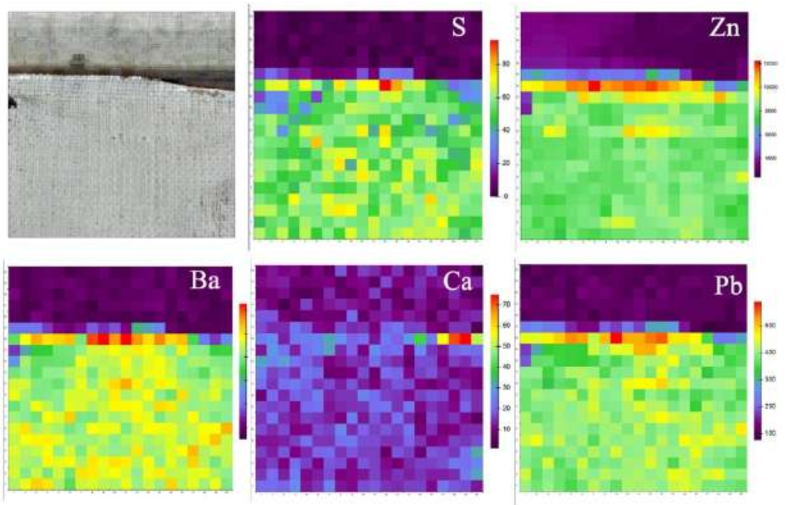

Figure 2. Visible image and corresponding MA-XRF maps of the ground on the canvas.

Pigments: None of the XRF-spectra results are presented here, the interpretations and discussion of all colors are listed in the Table 1.

White pigments: The white areas on the painting were chosen to inspect (xrf5, xrf6, xrf7). The white elemental composition indicated the presence of strong signal of Zn, and trace of S, Cl, Ba, Ca, and Fe. The pigment applied was zinc white (ZnO).

Red pigments: Two small points of the red were inspected (xrf8, xrf9). The XRF spectra showed clear peaks of Hg, Zn, and trace elements of S, Ca, Ba, Fe. These results suggested that the vermillion (HgS) was the major red pigment on the painting.

Green pigments: Three points of green were inspected (xrf10, xrf11, and xrf12). On all of the green points, XRF measured strong signal of chromium, thus indicating the possible use of veridian green and chrome green (respectively $Cr_2O_3 \cdot 2H_2O$ and Cr_2O_3) as well as Cr-base yellow in mixture with blue [8]. Veridian generally can be in a form of hydrated chromium oxide $Cr_2O_3.2H_2O$, which contained water molecules in its crystal structure and was of vivid color with a bluish tint. The pigment chromium oxide green with the formula of Cr_2O_3 was similar to hydrated chromium oxide but does not contain water molecules in its crystal structure. Its appearance was rather dull and more in the direction of olive green [9]. According to the color appearance that was bluish other than olive green, the pigment in the palette of the artist would highly be in the form of hydrated chromium oxide.

Brown pigments: In the two points of brown (xrf13, xrf14), beside strong signal of zinc, there were iron and calcium. The iron was certainly coming from the iron oxide (Fe_2O_3) of brown ochre or either burnt or raw sienna. Visual observation found that this brown color appeared darker than the hue of burnt or raw sienna. It was possible that either the artist added the black to make darker brown or unintentionally added the black on the painting. Nevertheless, calcium would be coming from the carbon black on the painting [10].

Table 1: This table presents the elements found in different colors on the painting "AUTUMN 1956" related to pigments applied (with its chemical composition).

color	spot number	detected elements *Major; **minor; and (tr) trace elements detected	possible pigments	chemical composition
ground	xrf1, xrf2, xrf3, xrf4	*Zn, Pb, S; tr(Ba, Ca, Sr)	zinc white (Zn), lead white (Pb), lithopone white (Zn, Ba, S)	ZnO $2PbCO_3{\cdot}Pb(OH)_2$, $BaSO_4.ZnS$,
white	xrf5, xrf6, xrf7	*Zn; (tr)S, Cl, Ca, Ba, Pb, Cu, Fe	Zinc white (Zn)	ZnO
red	xrf8, xrf9	*Hg, Zn; (tr)Ca, Ba, Fe	Vermillion (Hg)	HgS
green	xrf10, xrf11, xrf12	*Zn, Cr; (tr) Ba, Ca, Cl, Fe, Cd, Sr	Chromium based pigment such as viridian (Cr).	$Cr_2O_3{\cdot}2H_2O$ and several possibilities
brown	xrf13, xrf14	*Zn; **Fe, Ca**; (tr) K, Cl, Ba, Pb	Brown ochre	Fe_2O_3
yellow	xrf15, xrf16, xrf17	*Zn, Ba; (tr) S, Cl, Ca, Cd, Sr, Fe	Cadmium yellow (Cd)	CdS
Yellow ochre	xrf18, xrf19	*Zn, Fe; **Ba; (tr) Pb, Ca, Cl, Sr)	Yellow ochre (Fe)	$FeO(OH)$
dark blue	xrf20, xrf21, xrf22	*Zn; (tr) Ca, Pb, Cl, Ba, Fe	Unable to give a clear information by XRF	-
blue	xrf26, xrf27	*Zn; **Fe; (tr) Pb, Ba, Ca, Cu, Cr, Sr	Prussian blue (Fe)?	
light blue	xrf23, xrf24, xrf25	*Zn; (tr) Ba, Ca, S, Cl, Fe	unable to specify if it is inorganic pigment.	
black	xrf28, xrf29	*Zn; **Ca, P; (tr) S, Cl, Fe, Ba	Bone black (Ca, P)	

Yellow pigments: Three locations of yellow (xrf15, xrf16, xrf17) were inspected. Results have revealed elemental composition of zinc, barium, sulfur and trace of calcium, cadmium, iron, and strontium. Though zinc and barium presented strongly but however, these two elements could not be identified as zinc yellow (zinc potassium chromate with a formula of $K_2O{\cdot}4ZnCrO_4{\cdot}3H_2O$) or lemon yellow (barium chromate, $BaCrO_4$) since chromium was not presented. Therefore, cadmium yellow would highly be the key yellow pigment mixed with zinc white. Trace elements of Ca and Fe were possibly interference of calcium and iron base pigments.

Yellow ochre pigments: The location number xrf18, xrf19 were represented and inspected. Relatively clear spectra of Fe showed that the principle pigment was yellow ochre ($FeO(OH)$) mixed with white of zinc oxide.

Blue pigments: Many areas of the painting were painted in several shades of blues, therefore different tonalities of the blue were selected and measured. With regards to the Dark blue (xrf20, xrf21, xrf22) and Light blue (xrf23, xrf24, xrf25) colors, there were only clear strong peak of Zn and the trace elements of other elements. These XRF spectra data were not sufficient to characterize these dark and light blues thus suggesting the use of an organic pigment. For blue (xrf26, xrf27), there were significant spectra of Zn and Fe. Presenting of Fe may lead to investigate that Prussian blue was used in this painting, however the information was not enough to summarize.

Black pigments: Two locations (xrf28, xrf29) of black color were inspected. Results revealed clear signal of calcium and phosphorous. Almost all black pigments generally used in painting are of organic provenience and, therefore, impossible to identify by XRF due to the low Z number of their characteristic chemical elements [11]. However, in some cases a hypothetic existence of one of these pigments can be established. The presence of Ca peaks in dark or black areas can point toward the use of a pigment of animal origin (bone black). The use of bone black was possibly confirmed by the presence of P [11]. Therefore, for this painting, it would summarize that the animal (bone) black was used.

CONCLUSION

A non-destructive analysis of the "Autumn 1956" painting was carried out in order to obtain information of pigments applied. The painting was examed with UV light and by X-Ray fluorescence. Results showed that the pigments applied were typical for the period of time: zinc white (Zn), vermillion red (Hg), veridian green (Cr), yellow ochre (Fe), and iron oxide brown (Fe). Probably also organic bone black was used in the pallet. Yellow was highly possible to be cadmium yellow (Cd), while the blues were unlikely revealed by this technique. The ground layer presented the possibility of mixing of lead white and lithopone white. This research is a part of a works dedicated to the characterization of material applied in the Thai painting in the 20th century. According to the base of these elements were possible to identify the pigments or at least to hypothesize the applied painting materials. However, for more precise answer, other techniques should also be employed.

ACKNOWLEDGEMENT

The authors gratefully acknowledge the private art collectors, Kittiporn Jalichandra, the founder of Thai Art Collector Association (TACA) who gave permission for the analyses of the paintings painted by Fua Haripitak. The authors would also like to thank the Robert Bougrain, director of Restaurateurs Sans Frontières Laboratory, Studio for art conservation and restoration for his all support, and Luigi Fieni the restorer/photographer for his helpful photography of the painting presented in this article.

REFERENCES

1. R. Kateruam, (n.d.), *Fua Haripitak, the principle of Thai art.* Office of National Museums. https://www.finearts.go.th/thailandmuseum/view/14496-เฟื้อ-หริพิทักษ์---ครูใหญ่แห่งวงการศิลปะ.
2. W. Tantivittaypitak, (2017), *The rebellious spirit of Fua Haripitak.* The 101. World. https://www.the101.world/fua-haripitak/.
3. Tul, (7 December 2012), *Fua Haripitak.* ArtBangkok.com by official support from the Office of Contemporary Art and Culture Ministry of Culture. http://www.artbangkok.com/?p=10340.
4. Kriznar, A., Muñoz, M.V., F, de la Paz., Respaldiza, M. A., & Vega, M. (2008). Non-Destructive XRF Analysis of Pigments in a 15th Century Panel Painting. 9th Int. *Conference on NDT of Art 2008.* Jerusalem, Israel, May 2008. https://www.ndt.net/?id=6125 p25.
5. Vornicu, N., Geba, M., **&** Bibire, C. (2009). Non-destructive analysis in a study of the religious art objects. *Journal of Physics: Conference Series, 182, PROCESSES IN ISOTOPES AND MOLEKULS 24-26 September, 2009, Cluj-Napoca, Romania*. **doi:** 10.1088/1742-6596/182/1/012044**.**

6. Ha, J. W., & Lee, S. J. (2015). Identification of natural inorganic pigments used on 18th century Korean traditional mural paintings by using a portable X-ray fluorescence. *Journal of Industrial and Engineering Chemistry,* 28, 328–333. doi:10.1016/j.jiec.2015.03.011.
7. Molari, R., & Roberto, A. (2021). Pigment analysis in four paintings by Vincent van Gogh by portable X-ray fluorescence (XRF). *Radiation Physics and Chemistry*, 181 109336.
8. Rosi, F., Grazia, C., Fontana, F,. Gabrieli, F., Pensabene Buemi, L., Pampaloni, E., Romani, A., Stringari, C., & Miliani, C. (2016) Disclosing Jackson Pollock's palette in *Alchemy* (1947) by non-invasive spectroscopies. *Heritage Science*, 4(18), 1-13. DOI 10.1186/s40494-016-0089-y.
9. (n.d.). *Pigments Sorted by Elements.* ColorLax. https://colourlex.com/pigments/pigments-by-elements/pigments-containing-elements-ti-v-cr-mn/.
10. Castro, K., Alonso, M.P., Rodríguez-Laso, M.D., Etxebarria, N., & Madariaga, J.M. (2007). Non-invasive and non-destructive micro-XRF and micro-Raman analysis of a decorative wallpaper from the beginning of the 19th century. *Analytical and Bioanalytical Chemistry*, 387, 847-860.
11. Kriznar, A., Muñoz, M.V., Respaldiza, M.A., & Vega, M. (2012). Materials applied in Bernardo, Martorell's painting analysed by portable XRF. *ArcheoSciences*, 36, 37-45. doi.org/10.4000/archeosciences.3712.

MULTIBAND IMAGING WITH SMARTPHONE CAMERAS FOR SPECTRAL REFLECTANCE ESTIMATION

Shogo Nishi[1]*, Ryo Ohtera[2] and Shoji Tominaga[3,4]

[1]*Department of Engineering Informatics, Osaka Electro-Communication University, Japan.*
[2]*Kobe Institute of Computing, Graduate School of Information Technology, Japan.*
[3]*Department of Computer Science, Norwegian University of Science and Technology, Norway.*
[4]*Department of Business and Informatics, Nagano University, Japan.*

*Corresponding author: Shogo Nishi, e-mail s-nishi@osakac.ac.jp

ABSTRACT

In recent years, smartphones have become widespread and the performance of built-in camera modules has improved remarkably. In addition, it is possible to capture images in RAW image format even with a smartphone camera. Therefore, in principle, it is possible to estimate spectral information such as spectral power distribution and surface spectral reflectance as well as SLR (Single-Lens Reflex) cameras. We have previously verified the estimation of spectral information by combining a smartphone camera and multiple LED illuminators. However, because we focused on the construction of the theory of spectral reflectance estimation, we have not yet verified multiband imaging utilizing the portability of the smartphone camera. Therefore, we will realize multiband imaging with a passive illumination method using a smartphone camera and a gelatin filter. The proposed system requires a filter to be attached to the lens. In this type of imaging, filter replacement may cause problems with the misalignment of the camera optics. The Wiener method is a well-known method for estimating spectral reflectance, but in this study, a more generalized method, linear minimum mean-square error (LMMSE) estimation method, is employed and its effectiveness is also verified. In the experiment, two gelatin filters were used to achieve multiband imaging. The filters were chosen to have opposite spectral transmission characteristics to each other. In this multiband imaging, 6-band multiband images can be obtained. When estimating the surface spectral reflectance of an object at an arbitrary location in a scene from image data acquired with the proposed imaging system, it is necessary to correct for the inhomogeneity of the spatial distribution of illumination intensity and determine the parameters of gain and noise dispersion included in the observation model. The estimation process can be simplified by calibrating the imaging system with a standard sample of known spectral reflectance. The LMMSE estimation method incorporating these processes was employed to estimate spectral reflectance from the obtained 6-band images. The smartphone used in the experiment was Apple iPhone 7. The subject of the photographs was X-rite's Color Checker PASSPORT, and Labsphere's Spectralon was used as the standard white plate. They were remotely photographed in the same scene. An incandescent light bulb was used as the illumination light. RMSE (Root-Mean-Square Error) was obtained for quantitative evaluation of the estimation method. The average RMSE of the subject object was 0.04154 for the Wiener estimation and 0.04072 for the LMMSE method. It was found that the LMMSE method gave better results than the Wiener estimation. Future experiments will be performed outdoors to take advantage of the portability of smartphones. We also plan to verify experiments to further improve the estimation accuracy of this method.

Keywords: Smartphone camera, Multiband imaging, Spectral reflectance, LMMSE estimation.

INTRODUCTION

In recent years, smartphones have become increasingly popular, and the performance of their built-in camera modules has improved remarkably. Smartphone cameras are characterized by their portability, affordability, and convenience compared to single-lens reflex cameras.

Furthermore, it is noteworthy that smartphone cameras are integrated with advanced information processing systems comparable to those found in personal computers. Hence, it is expected that dedicated applications will be developed in fields where spectral sensing is valuable, such as medical diagnosis, healthcare, food quality inspection, and environmental monitoring [1-3]. From the perspective of image measurement, another significant advantage is the ability to capture images in the RAW format. Consequently, it is now possible to estimate spectral information, including spectral distribution and spectral reflectance, from image data in a manner analogous to conventional single-lens reflex camera measurements.

Surface spectral reflectance provides object-specific physical characteristics. Therefore, knowing the spectral reflectance of objects in a scene is important not only for colorimetry, but also for various situations such as object recognition and identification, realization of color constancy, and reproduction of object appearance. Therefore, many methods have been proposed to estimate surface spectral reflectance from image data in various fields such as colorimetry, image science and technology, and computer vision. One well-known estimation method is the Wiener estimation method [4-7]. This method is based on a statistical approach and is modeled to account for noise in the imaging system. It is the most common, reliable, and accurate method when the spectral sensitivity function of the imaging system is known. We have previously proposed a more generalized Wiener estimation method and theoretically demonstrated that it outperforms conventional methods in estimation accuracy [8]. However, since the validation experiments were conducted under extremely stable conditions, the accuracy of the image measurement using the portability of smartphone cameras was not sufficiently verified.

This paper aims to establish a multiband imaging technique using a smartphone camera and to estimate spectral information from acquired images. The imaging method will be passive (post-spectral) imaging to take advantage of the portability of smartphone cameras. In addition, we will verify the accuracy of estimating spectral reflectance using the generalized Wiener estimation method.

MEASUREMENT AND ESTIMATION METHODS

Imaging System

The smartphone used in this study is the Apple iPhone 7. The built-in camera module has approximately 12 megapixels and a bit depth of 12 bits. The camera output was recorded in the digital negative (DNG) format (lossless RAW image format) standardized by Adobe. Although the spectral sensitivity of the sensor can be estimated indirectly by using color samples with known spectral reflectance [9], in this paper the spectral response function was obtained by direct measurement using a wavelength-tunable light source OL490 manufactured by Gooch & Housego. Figure 1 shows the measured spectral sensitivity function of the iPhone7. In this study, multiband imaging was implemented by a passive method. We constructed a 6-band imaging system by adding two filters to the camera. The added filters are gelatin filters SP-6 and SP-7 manufactured by Fujifilm Corporation. The spectral transmittance distribution of these filters was measured using a spectroradiometer CS-2000 manufactured by Konica Minolta. A new spectral response function is obtained by multiplying the spectral transmittance distribution of the filters by the spectral response function of the camera. Finally, by combining these spectral sensitivity functions, a multiband camera with 6-band spectral sensitivity can be realized. The spectral sensitivity obtained by the above process we call the total spectral sensitivity. Figure 2 shows the total spectral sensitivity.

LMMSE estimation method

We propose a multiband imaging system that combines a smartphone RGB camera and two filters. In a previous study [9], linearity was demonstrated between the raw camera output of smartphone cameras and the surface-spectral reflectance. Therefore, we assume the following camera output model for multiband imaging system.

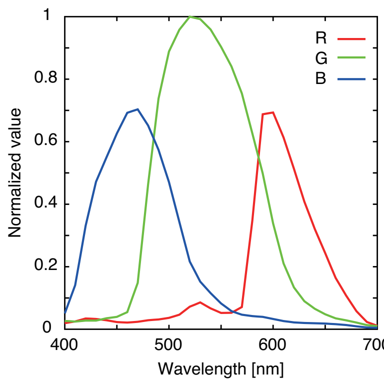

Figure 1. Spectral sensitivity funcion

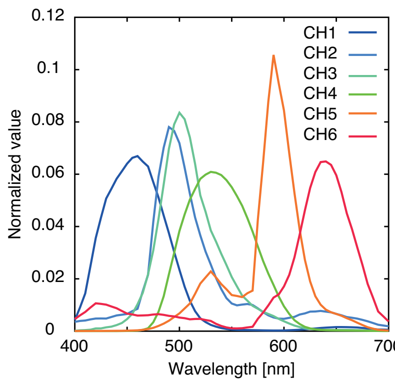

Figure 2. Total spectral sensitivity

$$y_i = g \int_{400}^{700} x(\lambda) e_m(\lambda) r_c(\lambda)\, \mathrm{d}\lambda + n_i, \tag{1}$$

where $x(\lambda)$ is the surface spectral reflectance of the object, $e_m(\lambda)$ is the spectral power distribution of the light source, and $r_c(\lambda)$ (c = 1, 2, 3) is the spectral sensitivity function of the camera, respectively, and the wavelength range is the visible range between 400 nm and 700 nm. The parameter g is unique to the imaging system, which depends on the conditions of the imaging system, such as the locations of the camera and light sources, including illumination intensities. Furthermore, n_i represents the noise of the imaging system. It is assumed that n_i is white noise with zero mean and variance a and uncorrelated with $x(\lambda)$. The discrete representation of this camera output model can be expressed as

$$\mathbf{y} = g\mathbf{A}\mathbf{x} + \mathbf{n}, \tag{2}$$

where matrix **A** represents the system matrix obtained by the product of the spectral power distribution $e_m(\lambda)$ and the spectral sensitivity function $r_c(\lambda)$ of the camera. When the matrix **A** and the noise property are known, the surface spectral reflectance **x** is estimated from the observed value **y** based on the camera output model Eq. (2). The surface spectral reflectance **x** can be estimated using the Wiener estimator expressed in the following equation.

$$\hat{\mathbf{x}} = g\mathbf{R}\mathbf{A}^t \left(g^2 \mathbf{A}\mathbf{R}\mathbf{A}^t + a\mathbf{I}\right)^{-1} \mathbf{y}, \tag{3}$$

where the matrix **R** represents the correlation matrix and is determined using various spectral reflectance data sets. We previously estimated spectral reflectance using Eq. (3), but to improve the estimation accuracy, we used a more generalized estimation method [8]. The estimated value is obtained by linear transformation of the observed value **y** by a constant vector.

$$\hat{\mathbf{x}} = x_0 + g\mathbf{P}\mathbf{A}^t \left(g^2 \mathbf{A}\mathbf{P}\mathbf{A}^t + a\mathbf{I}\right)^{-1} (\mathbf{y} - g\mathbf{A}\mathbf{x}_0), \tag{4}$$

where x_0 is the means of **x**. The covariance matrix of **x** is defined as $\mathbf{P} = \mathbf{E}[(\mathbf{x} - \mathbf{x}_0)(\mathbf{x} - \mathbf{x}_0)^t]$, where $\mathbf{E}[\mathbf{x}]$ represents the expectation operator to obtain the mean or representative value of **x**. Equation (4) is an estimation method called "linear minimum mean-square error" (LMMSE) estimator [10].

RESULT AND DISCUSSION

The proposed multiband imaging system is composed of an iPhone 7 and two filters. The measurement system is shown on the left side of Figure 3, and an example of filter attachment (SP-7) is shown on the right side of Figure 3. The smartphone camera was fixed on a tripod, and X-rite's Color Checker PASSPORT was used as the target object. Additionally, a white reference standard Spectralon manufactured by Labsphere was placed within the scene and captured simultaneously with the target object. Illumination was provided by two distinct light sources: incandescent lamp and natural daylight, with image acquisition carried out under each of these lighting conditions. The spectral reflectance was estimated from the acquired multi-band images

Figure 3. Measurement system and two attached filters

using both Wiener estimator and Linear Minimum Mean Square Error (LMMSE) estimator to evaluate the performance of the proposed system. Figure 4 illustrates the estimated results of spectral reflectance obtained through LMMSE estimator. The red line corresponds to results obtained in a controlled darkroom environment using incandescent bulbs, the green line represents outcomes in an indoor daylight environment, and the black line corresponds to measurements obtained via a spectroradiometer. While the estimation accuracy was slightly reduced under daylight conditions compared to the results obtained under incandescent lamp lighting, all spectral reflectances, except for White (index number 19), demonstrated robust estimation. In order to perform quantitative evaluation, the Root-Mean-Square Error (RMSE) was calculated. When the lighting conditions were provided by incandescent lamp, the RMSE for the Wiener estimator was 0.0415, whereas for the LMMSE estimator, the RMSE was 0.0407.

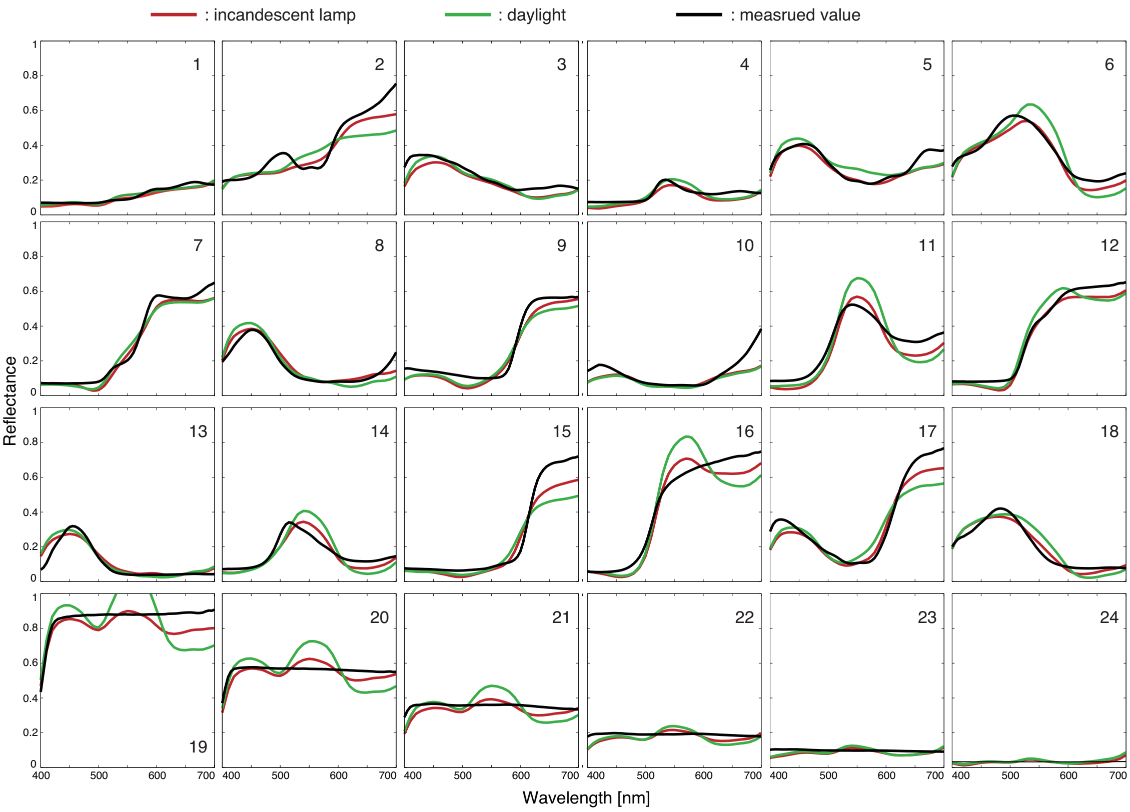

Figure 4. Estimation results applying LMMSE method under different lighting conditions

Similarly, under daylight lighting conditions, the RMSE for the Wiener estimator was 0.0636, while for the LMMSE estimator, the RMSE was 0.0594. These results clearly demonstrate that the LMMSE estimator outperforms the Wiener estimator.

CONCLUSION

In this paper, we estimated spectral reflectance from acquired images by multiband imaging with a smartphone camera. We achieved multiband imaging based on a passive approach by attaching two filters to the camera. We compared the estimation accuracy of the Wiener estimator and the LMMSE estimator using multiband images captured under two different lighting conditions, demonstrating the superiority of the LMMSE estimator. In the future, we will focus on establishing multiband imaging technology outdoors and verifying the accuracy of spectral reflectance estimation.

REFERENCES

1. Rateni, G., Dario, P. and Cavallo, F. (2017). Smartphone-based food diagnostic technologies: a review. *Sensors 17*(6), 1453. doi:10.3390/s17061453.
2. McGonigle, A. J. S., Wilkes, T. C., Pering, T. D., Willmott, J. R., Cook, J. M., Mims, F. M. and Parisi, A. V. (2018). Smartphone spectrometers. *Sensors 18*(1), 223. doi:10.3390/s18010223.
3. Burggraaff, O., Perduijn, A. B., van Hek, R. F., Schmidt, N., Keller, C. U. and Snik, F. (2020). A universal smartphone add-on for portable spectros-copy and polarimetry: iSPEX 2. *Proc. SPIE* 11389, 113892K. doi:10.1117/12.2558562.
4. Haneishi, H., Hasegawa, T., Hosoi, A., Yokoyama, Y., Tsumura, N. and Miyake, Y. (2000). System design for accurately estimating the spectral reflectance of art paintings. *Appl. Opt.* 39, p.6621-6632.
5. Shimano, N. (2006). Recovery of spectral reflectances of objects being imaged without prior knowledge. *IEEE Trans. Image Process.* 15, p.1848-1856.
6. Yoo, J. H., Kim, D. C., Ha, H. G. and Ha, Y. H. (2016). Adaptive spectral reflectance reconstruction method based on Wiener estimation using a similar training set. *J. Imaging Sci. Technol.* 60, 020503.
7. Nahavandi, A. M. (2018). Noise segmentation for improving performance of Wiener filter method in spectral reflectance estimation. *Color Res. Appl.* 43, p.341-348.
8. Tominaga, S., Nishi, S. and Ohtera, R. and Sakai, H. (2022). Improved Method for Spectral Reflectance Estimation and Application to Mobile Phone Cameras. *J. Opt. Soc. Am. A*, *39*(3), p. 494-508.
9. Tominaga, S., Nishi, S. and Ohtera, R. (2021). Measurement and estimation of spectral sensitivity functions for mobile phone cameras. *Sensors* 21, 4985. doi:10.3390/s21154985.
10. Poor, H. V. (1994). *An Introduction to Signal Detection and Estimation.* Springer.

AUTOMATIC COLOR CALIBRATION WITHOUT COLOR CHART

D. Muselet*, F. Cortes Jaramillo, P. Colantoni and A. Trémeau

Université Jean Monnet Saint-Etienne, CNRS, Institut dOptique Graduate School, Laboratoire Hubert Curien UMR 5516, France

*Corresponding author: Damien Muselet, damien.muselet@univ-st-etienne.fr

ABSTRACT

Classical color cameras are not color measurement devices and do not provide color images that characterize the surfaces in the scene, but rather depend on many external parameters such as the lighting conditions or the sensor sensitivities. The classical solution to extract calibrated colors consists in inserting a color chart in the scene before the acquisition and to transform the colors with respect to these reference surfaces. However, a color chart is not always available. In this paper, we propose a solution to calibrate the colors of an image without any color chart. Our idea consists in training a deep neural network to predict the colors of a color chart as if it had been in the scene while acquiring the image. We show that this artificial insertion helps in calibrating the colors and removing the impacts of the light and sensors.

Keywords: Color calibration, color chart, deep learning, regression, color distance.

INTRODUCTION

The colors of the pixels in images are dependent on many parameters such as the light source color and position, the sensor sensitivities of the camera or the camera internal processing pipeline. Nevertheless, for many tasks in computer vision (classification, segmentation, tracking, …) it could be very useful to make these colors invariant to these external parameters such that they only characterize the observed surfaces.

In this context, a reference color chart can be placed in the scene before acquiring the images. Since the colors of this chart are known in a calibrated color space (CIE LAB, CIE XYZ, …), we can evaluate a color transform from the current RGB components to these reference colors. The color calibration of the image consists in applying this color transform to all the pixel colors.

Unfortunately, it is not convenient to place a color chart in a scene before the acquisition and many images have already been acquired without color chart. Especially, our work is part of the European project PREMIERE [1], where we are processing color videos acquired under uncontrolled conditions. Consequently, we propose to artificially introduce a color chart in a color image, as if it had been present in the scene during the acquisition. To predict the colors of the color chart, given a color image (without color chart), we propose to use a deep neural network. To train this regression convolutional neural network (CNN), we propose to use datasets available online whose images contain a classical 24-patches color checker. These datasets are mainly provided to solve the color constancy task. In this study, to perform color calibration, we go a step further and train a network to predict the colors of the patches.

METHODOLOGY

The workflow of our proposed solution is displayed in Fig. 1. Starting from a color image with a color chart, we train a network whose input is the image without this color chart and the output is the chromaticities of the 19 patches of the chart in the image (including all color patches and only one grey-level patch). In this work we only considered the chromaticities meanwhile the color brightness was not considered. Since the bottom row of the chart is constituted by grey patches, we consider only one of these patches, since they have the same chromaticity coordinates.

To train our network, we remove the color chart from the image and feed the network with this image without color chart. The chromaticity coordinates of the 19 patches of the color chart are extracted from the cropped color chart image and save as ground truth (r_{real},g_{real}). Then, we train the network to predict 19 pairs of chromaticity values (r_{pred},g_{pred}). The network is supervised with the mean square error as loss function between the ground truth (r_{real},g_{real}) and the predictions (r_{pred},g_{pred}).

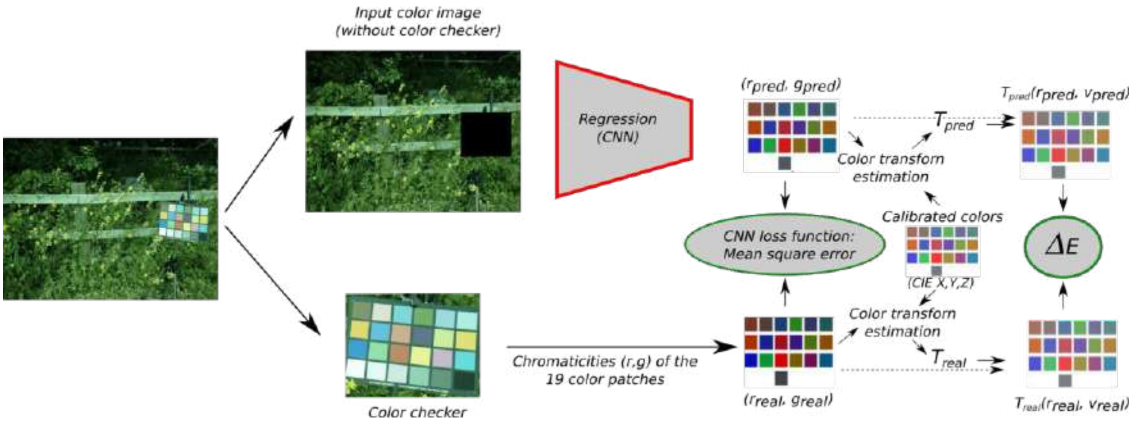

Figure 1. Workflow of the proposed solution

Since the purpose of our method is to calibrate the colors of the image, we evaluate the quality of this calibration step by comparing the results obtained by our predicted values with the ones obtained by the real ground truth values. This allows us to check the quality of our calibration step without color chart compared with the quality of the classical approaches that require a color chart in the image.

For the calibration step, we use the approach proposed by Finlayson et al. in [2]. This work evaluates and applies a color homography between two sets of colors, without requiring the brightness of each color. This is very interesting for our work where we prefer to concentrate on the chromaticities to train our deep neural network.

Thus, in order to calibrate the colors of an image (when a color chart is present in the scene), we can extract the real chromaticities (r_{real},g_{real}) of the 19 patches and evaluate the best color homography T_{real} that transforms these coordinates to calibrated color data, such as the CIE XYZ colors of these patches under a reference illuminant (D65). The results of this calibration step applied to the color chart are XYZ coordinates expressed as T_{real}(r_{real},g_{real}).

Furthermore, with this approach, we can calibrate the colors by exploiting only the predictions of the chromaticities of the color chart (r_{pred},g_{pred}). Thus, we can evaluate the best homography T_{pred} that transforms these data to the calibrated XYZ coordinates of the color chart and get the XYZ result T_{pred}(r_{pred},g_{pred}). The quality of this calibration step can be evaluated by comparing these two outputs T_{real}(r_{real},g_{real}) and T_{pred}(r_{pred},g_{pred}). Since these coordinates represent XYZ triplets, to assess the quality of the calibration we can evaluate the color distance between them. We have chosen the ΔEab color difference for this purpose.

It is worth mentioning that this color distance is used as a final calibration quality check but not in the training process.

NETWORK ARCHITECTURE AND DATA

For our experiments, we used images from the ColorChecker RECommended (CCREC) color constancy dataset [3], which contains 568 indoor and outdoor images acquired by two cameras Canon 1D and Canon 5D. For our experiments, following the classical approaches, we used 3-fold cross validation to evaluate our model.

For our tests, to predict the light color in one image, we exploited the recent and accurate network proposed in [4] that is based on deep bag-of-features. Thus, we created a deep network with 3 convolutional layers (60, 30 and 30 kernels, respectively), followed by a Bag-of-Features pooling with 150 codewords and finally 3 dense layers (128, 64 and 38 neurons, respectively). The neurons of the last layer have a sigmoid activation while the other ones have ReLU activations. The number of neurons in the last layer is equal to 38, since we predict the 2 chromaticity coordinates of the 19 reference patches.

We used classical data augmentations (small rotations, shifts, zoom and flip) and the Adam optimizer with 500 epochs. The learning rate was fixed to 1.10^{-4}.

RESULT AND DISCUSSION

It is worth mentioning that all the tested images have not been seen by the network at training time. So, we are checking here how well we can calibrate an unseen image without a color chart in it. The quality of the chromaticity prediction has been already checked in a recent study for another purpose [5]. In this section, we concentrate on the quality of the calibration step, given these predicted chromaticity values.

Since we are running a 3-fold cross validation experiment, we cumulate the results over the 568 test images. Fig. 2 represents the distribution of the ΔE_{ab} difference between the colors calibrated with a color chart and the colors calibrated with our method without color chart. We can see that most of the color differences are between 0 and 10. The median value over all these color differences is at 5.1, which is an encouraging result to study further this approach of color calibration without color chart.

In Figure 3, we provide some examples of images from the dataset with the corresponding color difference values. This helps to understand the cases where our calibration process is working, sometimes better, sometimes worse. For example, we can see that when a large diversity of colors is present in the image (top left or top right image), the results are better (low color differences). We also noticed that when we process outdoor images with a light source not far from natural D65 (top middle image), the calibration is also good. The second row shows images where our algorithm does not provide good calibration results (large color difference). This can be explained by different elements. For some images, when there are two light sources (bottom left image), the calibration does not perform well, because our chromaticity prediction assumes a single uniform light source. Some other images do not show enough color diversity, as in the bottom middle image. Finally, we can see inter-reflections in the bottom right image that disturb the chromaticity prediction, and hence the calibration step. These specificities, which are not rare in many real images, will be considered in future works to improve our approach.

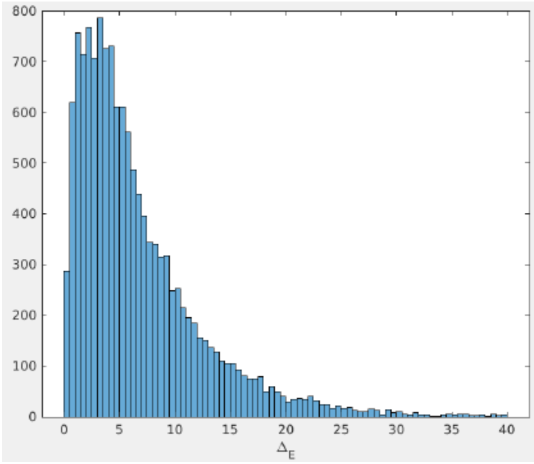

Figure 2. Color difference distribution for the 568 test images

CONCLUSION

In this paper, we proposed a solution to calibrate the colors of any image without the use of any color checker in the scene. For this purpose, we resort to a deep neural network that predicts the colors of a reference color chart, as if it had been in the scene at the acquisition time. Based on these predictions, we used a color homography to transform them to calibrated components (CIE XYZ) and hence to remove the impact of the external parameters (light source, acquisition device) on the colors. We have shown that our solution provides good results in many situations, but still needs to be improved in some specific cases. For example, to tackle the problem of non-uniform lighting, it would be better to predict light color locally (and not globally). Furthermore, optical phenomena, such as inter-reflections, can disturb the calibration step and so must be taken into account in the process to improve the approach.

$\Delta_E = 0.68$ $\Delta_E = 0.88$ $\Delta_E = 1.57$

$\Delta_E = 13.02$ $\Delta_E = 12.43$ $\Delta_E = 16.10$

Figure 3. Example of test images from the ColorChecker RECommended dataset [3]

ACKNOWLEDGEMENT

This work was supported by HORIZON-CL2-2021-HERITAGE-01-04 grant. Project: 101061303 — PREMIERE. (https://premiere-project.eu/).

Funded by the European Union

REFERENCES

1. https://premiere-project.eu/
2. Finlayson G. D., Gong H., Fisher R. B. (2019), Color homography: Theory and applications, I*EEE Trans. Pattern Anal. Mach. Intell.*, vol. 41, no. 1, pp. 20–33.
3. Hemrit G., Finlayson G. D., Gijsenij A., Gehler P. V., Bianco S., Drew M. S. (2018), Rehabilitating the color checker dataset for illuminant estimation, ArXiv, vol. Abs/1805.12262.
4. Laakom F., Passalis N., Raitoharju J., Nikkanen J., Tefas A., Iosifidis A., Gabbouj M. (2020), Bag of color features for color constancy, *IEEE Transactions on Image Processing*, vol. 29, pp. 7722–7734.
5. Dubuisson I., Muselet D., Basso-Bert Y., Tremeau A., Laganière R. (2022), Predicting the colors of reference surfaces for color constancy, *IEEE International Conference on Image Processing (ICIP)*.

PAKISTANI TRUCK ART COLORS: INSPIRING FASHION DESIGNERS BY REFLECTING LOCAL HERITAGE ON THE GLOBAL STAGE

Syeda Ume Farwa[1], Jinsang Yu[2], Hyewon Park[1*]

[1]*Master's Course, Major in Clothing & Textiles, Interdisciplinary Program in Senior Human Ecology, Changwon National University, South Korea*
[2]*Professor, Major in Architectural Design of Eco Housing, Interdisciplinary Program in Senior Human Ecology, Changwon National University, South Korea*
[1*]*Professor, Major in Clothing & Textiles, Interdisciplinary Program in Senior Human Ecology, Changwon National University, South Korea*

*Corresponding author: Hyewon Park, hwpark@changwon.ac.kr

ABSTRACT

Truck art is a popular form of folk art that originated in Pakistan and has gained international recognition. It has become an iconic and recognizable feature of Pakistani culture. Truck art is believed to have originated in the 1920s. Truck drivers began to personalize their vehicles with colorful paintings and decorations to make them stand out from other trucks. Over time, truck art evolved into a unique and complex art form that showcases Pakistani culture and identity, thus making its way to "glocalization". The use of color in both truck art and dress is often symbolic, with different colors representing different meanings and emotions. Different terms are being used to express the image of truck art that involves vibrant, playful, multicolored, kaleidoscopic, and bold artwork. This study aims to explore these various terms in relation to their place in the color wheel and how these colors of truck art influence fashion designers to incorporate this local art into their designs. This qualitative research project encompassed an examination of 122 truck art images and 50 truck art-inspired dress images. The objective was to identify the distinctive colors and tones inherent to truck art, along with evaluating how effectively fashion designers integrated these elements into their collections. To conduct a comprehensive analysis, the study employed CMC 23 - Munsell color conversion software, delving into the Hue, Value, and Chroma of 469 truck art colors and 279 colors from dress images. The resulting data was processed using a PCCS Tone map, enabling a three-dimensional color analysis and tone investigation. This comparison highlighted the dominance of R, Y, G, YR, and PB as the primary colors utilized in both the truck art and fashion designs. Additionally, the prevalent tones were characterized by their vivid, bright, and strong qualities on the PCCS tone map, aligning with a high saturation level in terms of Chroma. In summary, this research employed advanced color analysis techniques to explore the colors and tones inherent in truck art and their incorporation into fashion designs. The dress images corresponded very well to the color palette and themes of truck art. In conclusion, the incorporation of cultural heritage in the way one dresses is very effective in presenting the culture and heritage and giving way to a non-verbal mode of expression. In the future, it would be wise to create a permanent line of dress collection as a traditional symbol that can be expressed to emphasize the value of local heritage.

Keywords: Pakistani Truck Art, Local Heritage, Fashion Design Inspiration

INTRODUCTION

Art, a manifestation of human sensibilities, enhances our lives by evoking emotions and sentiments in an unexpected and delicate manner [1], which is displayed around us in a variety of styles, forms, and arrangements [2]. Whereas heritage embodies the legacy we inherit from the past, shapes our present experiences, and becomes the valuable inheritance we bestow upon future generations. Both our cultural and natural heritage hold an unparalleled significance, serving as priceless wellsprings of life and inspiration [3]. With advancements in technology, local cultures are spreading worldwide thus inspiring the world. Truck art, which refers to decorative vehicle painting characterized by its bold use of colors, intricate patterns, hand paintings, cultural symbols, calligraphy and personalization, is a well-known form of folk art originating in Pakistan that has garnered international acclaim and became an emblematic and distinguishable aspect of Pakistani culture. It has also inspired the fashion industry worldwide. This globally well-known genre is thought to have emerged in the 1920s from South Asia, particularly in Pakistan, and evolved in the most vibrant and innovative ways. Over time, truck art developed into a distinct and intricate art form that celebrates Pakistani culture and identity [4]. In the 1970s, Pakistan's truck and bus decoration tradition gained global recognition through photographs taken by European and American tourists. Later, in the late 1980s, the Pakistani government and entrepreneurs organized truck art exhibitions abroad, solidifying its reputation as a celebrated folk art genre on the global art scene by the early 2000s [5]. This decorative vehicle painting is not exclusive to Pakistan, but the way it has evolved and thrived in the country is a fascinating post-colonial, postmodern, and glocal phenomenon [6]. Within that community the fashion industry started looking up to truck art as fashion design inspiration, and it has become popular even among international brands like Dolce & Gabbana. High-end Pakistani designers such as Maheen Khan, Rizwan Beyg, and Zahra Ahmed, as well as high-street brands like Khaadi and Gul Ahmed have integrated the colorful motifs and patterns of truck art into their clothing lines [1]. But little research has been conducted on the impact of colors in the truck art for fashion inspiration, despite the fact that the colors of truck art are one of the main characteristic features of this cultural heritage.

Thus following qualitative study on the role of truck art colors in inspiring the fashion designers, aims to achieve a systematic and detailed elaboration of colors which are characteristic to truck art by identifying the hues and tones of which this art is composed. Secondly, this study will explore the hues and tones of the colors which are incorporated into the truck art-inspired fashion collections. Through the means of this study, the influence of local culture upon the global level will be better understood.

METHODOLOGY

Qualitative research was conducted by a content analysis method. The procedure was carried out in three steps. For the first step, a literature review was conducted, which was comprised of reading research papers, articles, magazine blogs, news, and books about truck art, colors, art, culture, and local heritage in order to identify other researchers' opinions about colors in truck art and advancements in research on this globally famous art. The second step involved the collection of truck art images and truck art-inspired fashion apparel images. A total of 122 truck art images were collected, of which 93 images were of originally captured photos of trucks on the highway stops and their decoration workshops using mobile phone cameras, and 29 images were collected via the internet from Google images, Pinterest images, and online news articles. 52 images among them were removed as some of the images were of similar vehicles from multiple angles, while others were removed due to poor lighting conditions during the photo capturing process and a few due to their blurry quality, leaving us with a total number of 70 truck art images. A total number of 50 images of truck art-inspired dresses were collected using Google images, online fashion magazines, and news articles. The third step involved the analysis of images finalized after the thorough selection procedure. At this stage, all images were first labeled with numbers in order to avoid the risk of repetition. After labeling, 70 images of truck art and 50 images of dresses were analyzed using CMC 23 – Munsell color conversion software. Three dimensions of colors were analyzed which were hue, tone (value and chroma) of each color extracted from the images. For truck art images there were a total of 469 analyzed colors from 70 images whereas for the truck art inspired dress' images the total number of colors analyzed were 279 from the 50 dress images. The analyzed data was then graphed using the PCCS (Practical Color Coordination System) tone map to determine the tones of colors. Lastly, dress images were analyzed by conducting a parallel comparison with truck art images.

RESULT AND DISCUSSION

Literature Review

The findings from the literature review revealed that previous researchers often employed descriptors such as bold, bright, vibrant, and kaleidoscopic when referencing the colors within truck art. Recent studies on truck art have delved into various aspects such as the themes, subjects, and motifs depicted in this distinctive form of vehicular art by Zahra & Abdullah, 2020 [7]. Additionally, anthropological investigations have explored the diffusion of truck art from its local origins to a broader audience [1], and there has been a historical and contextual inquiry into the evolution of truck art in the 21st century [8]. This observation underscored the necessity for a systematic and comprehensive investigation into the specific colors characterizing truck art. The study reviewed articles, dissertations, online sources, and conference papers from January to August 2023. Results revealed a consistent trend: many sources covered truck art's history and artistic elements, but lacked a focus on its color palette. This research aims to fill this gap by providing a comprehensive analysis of truck art colors.

A significant research gap exists in studying the influence of truck art colors on fashion trends. Despite the vibrant color palette being a defining aspect of this cultural heritage, little attention has been given to its impact on fashion. Additionally, there is a limited exploration of truck art's connections with other artistic genres. Existing research mostly relies on theoretical rather than empirical evidence, with few attempts to bridge truck art and fashion through practical findings.

Hue and Tone Analysis of Truck Art Images

Figure 1, 2, 3, and 4 are sample pictures of truck art shown to provide a glimpse of what it looks like from the perspective of daily life rather than highly advanced photo images taken by professional photographers.

Figure 1. Photograph originally sourced by author from Taxila, Pakistan (2023)

Figure 2. Photograph originally sourced by author taken on highway stop from Rawalpindi to Lahore, Pakistan (2023)

Figure 3. Original photograph of a truck in Taxila, Pakistan sourced by author (2023)

Figure 4. Photograph of a truck parked alongside road in Pakistan sourced by author (2023)

The analysis of 70 truck art images revealed that red was the dominant hue at R=19.2%, followed by yellow at ‘Y’=13.4%, green at ‘G’=12.6%, yellow-red at ‘YR’=12.4%, purple-blue at ‘PB’=12.2%, green-yellow at ‘GY’=10.9%, blue-green ‘BG’ and blue at ‘B’=6.6%, red-purple at ‘RP’=3.8%, and purple at ‘P’=2.3%. A total of 469 colors were analyzed in the images, as shown in Table 1 and Figure 5. In terms of tones, the analysis indicated that vivid colors were the most prevalent at ‘v’=25.2%, followed by strong tones at ‘s’=16%, bright tones at ‘’b’=14.7%, dull tones at ‘d’=14.1%, deep tones at ‘dp’=13.2%, soft tones at ‘sf’=6.6%, pale tones at ‘p’=3.4%, light greyish tones at ‘ltg’=2.3%, greyish tones at ‘g’=1.9%, dark tones at ‘dk’=1.3%, dark greyish tones at ‘dkg’=0.9%, and light tones at ‘lt’=0.4%. The distribution of tones is depicted in Table 2 and Figure 6 while the resultant tones are shown through the PCCS tone map in Figure 7.

Table 1: Color Analysis of Truck Art Images

Color Hue	R	YR	Y	GY	G	BG	B	PB	P	RP	Total
No	90	58	63	51	59	31	31	57	11	18	469

%	19.2	12.4	13.4	10.9	12.6	6.6	6.6	12.2	2.3	3.8	100

Figure 5. Percentage color wheel for truck art images

Table 2. Tone Analysis of Truck Art Images

Tone	p	ltg	g	dkg	lt	sf	D	dk	b	s	dp	v	Total
No	16	11	9	4	2	31	66	6	69	75	62	118	469
%	3.4	2.3	1.9	0.9	0.4	6.6	14.1	1.3	14.7	16	13.2	25.2	100

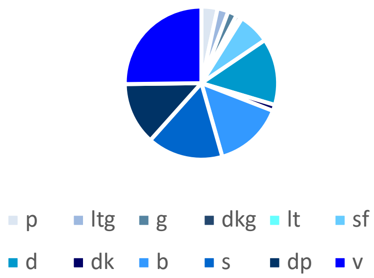

Figure 6. Percentage tone wheel for truck art images

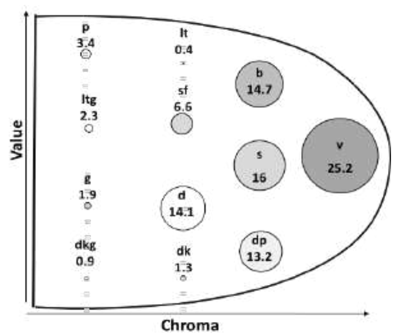

Figure 7. Tone of truck art images

Hue and Tone Analysis of Truck Art Inspired Dress' Images

Several dress designs that draw inspiration from this local heritage are showcased through Figure 8, 9, 10, and 11 as sample images.

Figure 8. Rizwan Beyg (2018) https://eco-a-porter.com

Figure 9. Dolce and Gabbana truck art inspired dress (2019) https://www.pinterest.com

Figure 10. Rizwan Beyg truck art summer collection (2013), https://pfdc.org

Figure 11. Gul ahmed truck art summer collection (2019) https://www.facebook.com

The analysis of 50 images featuring truck art-inspired dresses revealed that red was the most prominent hue at R=25.4%, followed by Y at 16.5%, YR at 14.3%, PB at 14%, GY at 8.2%, B at 6.1%, RP at 5.4%, G at 4.9%, BG at 3.2%, and P at 1.8%. A total of 279 colors were analyzed, as presented in Table 3 and Figure 12. In terms of tones, the most prevalent tone used in the dresses was vivid at 25.4%, followed by bright tones at 15.8%, with similar use of ‘s’ and ‘sf’ tones at 12.2% each. Other analyzed tones included dp=8.6%, d=5%, p=5%, ltg=4.6%, lt=3.9%, g=3.2%, dkg=2.9%, and dk=1.1%. The complete breakdown of tones is provided in Table 4, and Figure 13 illustrates the percentage values of tones on a color tone wheel. Figure 14 shows the tone values on the PCCS tone map.

Table 3: Color Analysis of Truck Art Inspired Dress Images

Color Hue	R	YR	Y	GY	G	BG	B	PB	P	RP	Total
No	71	40	46	23	14	9	17	39	5	15	279
%	25.4	14.3	16.5	8.2	5	3.2	6.1	14	1.8	5.4	99.9

Figure 12. Percentage color wheel for truck art inspired dress’ images

Table 4. Tone analysis of Truck art inspired dress’ images

Tone	p	ltg	g	dkg	lt	sf	d	dk	b	s	dp	v	Total
No	14	13	9	8	11	34	14	3	44	34	24	71	279
%	5	4.6	3.2	2.9	3.9	12.2	5	1.1	15.8	12.2	8.6	25.4	99.9

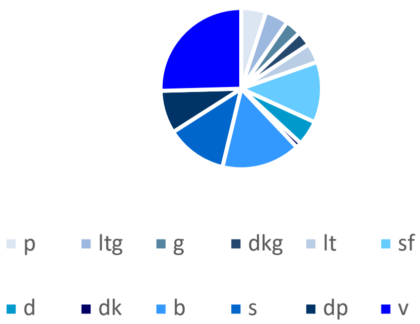

Figure 13. Percentage tone wheel for truck art inspired dress’ images

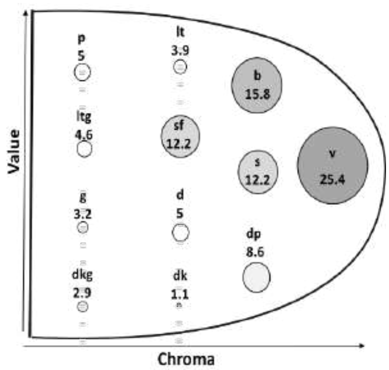

Figure 14. Tone of truck art inspired dress’ images

CONCLUSION

In conclusion, this study unequivocally demonstrates that the colors integral to truck art are vivid, bright, and strong. Consequently, the investigation establishes that when fashion attire is inspired by truck art, it not only integrates the motifs prevalent in this art form, but also adheres closely to the distinctive color palette synonymous with truck art. The prevalence of vivid, bright, and robust colors in both truck art and its corresponding fashion collections exhibits a striking similarity. The primary limitation encountered in this research pertained to time constraints and the restricted availability of truck art-inspired collections, a result of the currently limited emphasis by designers on truck art. These findings underscore the potential for incorporating such artistic elements in the realm of fashion, contributing to the reinforcement of glocalization, as fashion is a universal aspect of human life.

This study's significance extends to future research endeavors centered around truck art, providing a structured foundation for subsequent investigations. Moreover, advocating for the special recognition of the truck art color palette within the realms of fashion and culture is recommended. The academic insights offered by this research hold practical implications for industrial projects, facilitating the precise identification of the truck art color palette. Additionally, this study lays the groundwork for future scholars to delve into the emotional and cultural significance embedded in this color scheme for individuals and communities alike. Notably, this study stands as a unique contribution, offering academic exploration into the colors of Pakistani truck art—a pioneering effort in its domain thus far.

ACKNOWLEDGEMENT

This research is funded by the Financial Program of basic protection science fields at Changwon National University in 2023.

REFERENCES

1. Kazmi, S.M., Rahman, G. (2021) From folk to popular: the evolution and diffusion of truck art in Pakistan into mainstream culture through the fashion industry. Pakistan Journal of Social Research, 3(1), 66-79.
2. Sheikh, S. Z. (2018, September). Impact of truck art, as popular culture on Pakistani society. International Journal of Multidisciplinary and Current Research, 6. DOI: 10.14741/ijmcr/v.6.5.10.
3. World heritage convention. (n.d). UNESCO. [https://whc.unesco.org/en/about/ - last accessed 20th July 2023].
4. Khan, A. S. (2021, February 11). Truck Art — Made in Pakistan: An Observational Analysis into the Origins, Design Aesthetics, and Cultural Impact of Truck Art. Medium. [https://aaminasuleman.medium.com/truck-art-made-in-pakistan-b57fc9ee7099 - last accessed 18th April 2023].
5. Paracha, N. F. (2016, August 19). The elusive history and politics of Pakistan's truck art. Dawn newspaper. [https://www.dawn.com/news/1278386 - last accessed 25th June 2023].
6. Ali, F. (2021). The bold and beautiful: portraiture in Pakistani truck art. (Master's thesis, Georgia State University). DOI: https//doi.org/10.57709/25963344
7. Zahra, F., Abdullah, S. (2020). Vehicular art themes: five Indian subcontinental art forms that inspire Pakistani truck visuals. International Journal of Innovation, Creativity and Change, 14(1). www.ijicc.net.
8. Khan, S, M. (n.d). Truck art and its transformations in the 21st century from popular culture to high culture. [https://easaa.org/wp-content/uploads/2023/01/Samra-Khan-19.pdf - last accessed 31st May 2023].
9. Beyg, R. (2018, February). 'Pakistan Modern': celebrating modern truck art and traditional embroidery. Commonwealth Fashion Exchange. [https://artsandculture.google.com/story/8wUxTZZ1BqAMJg - last accessed 15th March 2023].

A REFLECTION ON THE KOREAN COLORIST AND COLOR QUALIFICATION OVER THE PAST THREE DECADES

Gyeonghwa Lee* and Vien Cheung

School of Design, University of Leeds, United Kingdom

*Corresponding author: Gyeonghwa Lee, ml13g3l@leeds.ac.uk

ABSTRACT

This research aimed to examine the usage and changes of the term colorist via a Korean online digital archive of newspapers in the 20th century based on socioeconomic and cultural developments. In addition, any changes with respect to the required knowledge to get the Engineer Color certificate were examined by looking at the two criteria for the examination, along with changes in terms of the main five subjects in written exam papers over the last two decades. Based on this, the color knowledge and performance that has been expected to be acquired while preparing for the Engineer Color certificate in terms of practicality were reflected on from the viewpoint of a color designer, color design researcher, and color design educator based on the experience of the authors of this research. The latter was based on autoethnography relying on both authors' experience. One has obtained the Korean Engineer Color certificate, working in the design industry, and color design research and the other one has various color certificates and many years of color education experience in UK Higher Education. From this research, it was expected that required essential color knowledge and any changes in this would be revealed. Moreover, the practicality and usefulness of the Engineer Color certificate for design practice were reflected upon from the position of a designer and design educator. Thus, this research provides benefits to the design community by exploring what knowledge of color needs to be considered as essential in color design education at the same time as reflecting on its practical applicability in real design practice.

Keywords: Colorist, Engineer colorist, Color certificate, Korean colorist

INTRODUCTION

The term colorist (colourist) has had a long history. According to Oxford English Dictionary [OED] (2023), the earliest known usage of the term colorist as a noun appears in the late 1600s, in the writing of William Aglionby (Figure 1). Since then the term colorist has been used widely and there are five main meanings and usages for the definition of the noun colorist based on OED (2023). These include someone who does painting (1685-), one skilled at writing (1759-) someone dyeing textiles (1772-), a hairdresser (1891-), and someone working in the film industry (1916-). As can be seen, the term colorist has gradually broadened and used in various areas.

1685 The Carraches seem to have had all the Qualities together, being Excellent Designers, Admirable Colourists.
W. Aglionby, *Painting Illustrated* iii. 124

Figure 1. Earliest evidence of the term colorist from OED

In South Korea (in the Korean online digital archive of newspapers dating back to the 20th century) the first mention of the word 'colorist' was in the 1960s. The second was in the 1970s and the third was in the early 1980s. However, in the 1990s, the word 'colorist' was mentioned frequently compared to the past (Figure 2).

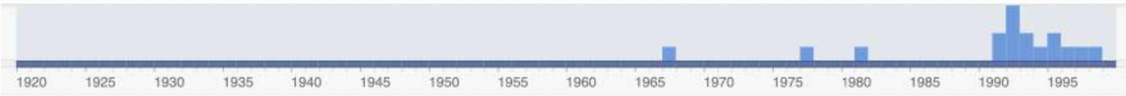

Figure 2. Emergence of the term colorist in South Korea

In response to social, economic, and cultural developments in the early 21st century (on the 27th of April in 2002), the Engineer Colorist Certificate was established by Presidential Decree in South Korea (Human Resources Development Service of Korea, 2023). In 2023, the area of color is still one of only twelve specified design areas categorized by South Korea's National Competency Standards. This indicates that color design is one of the main design areas in the South Korean design industry. In order to gain the Engineer Colorist Certificate [ECC] in South Korea, a certain number of points on both a written examination and a color performance test needs to be scored. According to the Human Resources Development Service of Korea (2023), over 20,000 people received the Engineer Colorist Certificate between 2002 and 2021. At present, there are a lot of color consulting institutes as well as companies running their own color design and research teams or institutes in South Korea.

There has been a fast development and changes in terms of areas of color design and recognition of the importance of color in design practice in South Korea. However, so far, there has been no detailed investigation of how the term 'colorist' emerged and has been used in South Korean culture over time. Also, there has been little investigation by researchers about changes in terms of color knowledge required to receive the Engineer Color Certificate or reflection on the practical use of the ECC in South Korea. Thus, these issues will be discussed.

METHODOLOGY

Data for this research were collected qualitatively using both document analysis and autoethnography. Document analysis is defined as entailing "a systematic procedure for reviewing and evaluating documents through finding, selecting, appraising (making sense of), and synthesizing data contained within them" (Kutsyuruba, 2023, p.139). There are four steps proposed by Dalglish et al. (2020) for document analysis which were applied in this research: readying the materials, extracting data, analyzing data, and distilling findings. The materials used for document analysis are of three types in this research: (1) the Korean online digital archive of newspapers (from 1920 to 1999) which includes five Korean newspaper companies, (2) previous written examination papers (from 2003 to 2022), and (3) the criteria for the examination. In addition, autoethnography is also used, as a method that "uses a researcher's personal experience to describe and critique cultural beliefs, practices, and experiences" (Adams et al., 2015 cited in Poulos, 2021, p.4). For these reasons, the experience of the authors in design practice, and education as a colorist were utilized as a research tool.

RESULTS AND DISCUSSION

Based on the analysis of the Korean online digital archive of newspapers, the term 'colorist' emerged (in the press) in the area of design in 1981. However, the main contents of the newspaper article discussed the point that various colored fabrics could be useful materials for decoration in individual houses but did not seem to refer to the term 'colorist' as a job in the design industry.

Before the 1990's, it seems that the term 'colorist' is used to describe artists who use various colors or simply those painting cartoon paper in Korean society. The word 'colorist' is mentioned more often in 1990's mostly in the area of design. This was the first period when the term 'colorist' referred to a job, but was particularly in fashion design areas (Table 1, newspaper No.5). A year after that, the job 'colorist' was discussed as one of the promising jobs in the 21st century regardless of the area of design (Table 1. newspaper No.7). In 1992 and 1993, two newspapers started to mention the job 'colorist' in the fashion design area (Table 1, newspaper No.8 and 10). However, the main focuses were different. For example, one talked about the job 'colorist' being suitable for females in the fashion design industry but another one stated that the post of 'colorist' was already a popular job in more advanced countries. It says the more developed countries become, the more subdivided jobs are.

Table 1: Evidence for use of the term colorist (context of its use) in Major Korean Newspapers

No.	Name of Newspaper	Date	Area(s)	Theme	Main Context
1	The Chosun Ilbo	15.Jan 1967	Film industry	Korea's First long-length cartoon film	Twenty-five people painted colors on papers to make Korea's first full-length cartoon film
2	The Chosun Ilbo	26.Jan. 1977	An introduction to an artist	An account of the artist's style of painting	Referring to the artist as a colorist who uses a variety of colors
3	The Kyunghyang Shinmun	19.Oct. 1981	Textile Design	Interior decoration using textiles	Advantages of using fabric decoration in houses
4	The Kyunghyang Shinmun	30.Sep. 1991	Fashion design	Trend color in fashion of the year	The use of strong color (black and white combinations and various tones of red color) due to the trend of a retro mood from the 1960s
5	The Kyunghyang Shinmun	07.Oct. 1991	Fashion and Textile	Fashion colorist	Introduction of the job title colorist as roles in the fashion and textile design industries
6	The Kyunghyang Shinmun	14.May. 1992	An art review	A personal review of an artist's style of painting	Discussing the artist as a colorist, as he uses strong colors
7	Maeil Business News	25.Jun. 1992	New Jobs	Promising jobs in 21st century	This introduces the job colorist as one of the promising jobs for the 21st century, and gives reasons based on anticipated changes in society
8	The Kyunghyang Shinmun	16.Aug. 1992	Fashion design	One of the promising jobs in the fashion design area for women	Among the many areas of fashion design, the role of colorist is particularly prominent for women
9	The Kyunghyang Shinmun	24.Sep. 1992	Art Exhibition	Introducing an artist who used a strong complementary color	Using complementary color to express a deep sense of space
10	The Dong-A Ilbo	29.May. 1993	Fashion design	Roles of the colorist	Roles of the colorist in the fashion design area. It is a new job in Korea, but it is already in the spotlight in other countries

(continued)

11	The Hankyoreh	27.Sep. 1993	A new Job	Interviewing a color institute founder about the role of colorists	Roles of colorists, in particular in consulting companies, educating people at companies, selecting colors
12	The Kyunghyang Shinmun	11.May. 1994	Economy	New businesses and new job	Here the roll of a colorist is a new job. The more advanced the country becomes, the more jobs it will have
13	The Kyunghyang Shinmun	28.Sep. 1995	Industrial Design	Colorist at car company	The role of colorist in a car company. The importance of color for cars
14	The Kyunghyang Shinmun	28.Sep. 1995	Industrial Design	Car designers: stylists and colorists	Overall process for a new car launched focusing on designers' roles in a car company
15	The Kyunghyang Shinmun	7.Feb. 1996	Digital Color	Storytelling in relation to color association	Artists and color professionals will be involved to create dramas unlike previous Korean dramas
16	The Chosun Ilbo	29.Apr. 1997	Essay	Essay on ancient Korean heritage	After discussing ancient tombs and murals, the description of various colors is expressed using the word colorist
17	Maeil Business News	11.Mar. 1998	Fashion design	Colorist as a professional job in the fashion design area	Roles of the colorist in the design area in general

It can be seen that the term ‘colorist’ was recognized in the early 1990’s. It was mentioned mostly in relation to the fashion and textile design industry. However, after 1995 the term ‘colorist’ and related roles started to be described in more detail in different areas of design such as industrial design and digital color imaging (Table 1. newspaper No.13, 14, and 15). This could be interpreted as meaning that the mid 1990s was a turning point in the Korean design industry. Since then two universities have established majors named ‘color’ in 2003 and ‘color design’ in 2007 in their postgraduate schools.

In the early 21st century, information was not easy to find in comparison with the period of the newspaper archive or the present time. One of the authors of this paper recognized the new job ‘colorist’ and such a role in a clothing company while reading a newspaper when she was a university student. In the middle of the first decade of the 21st century, the job ‘colorist’ was still quite rare and difficult to find. Very few positions were located in the fashion and car industries at this time. However, the job ‘colorist’ is not unfamiliar for people in general anymore. Now, it is difficult to find the areas where colorists are not involved. Since 1991 when the job ‘colorist’ was first mentioned, it seems that there has been a fast development and awareness of the job ‘colorist’ and the areas colorists work in during the last thirty years. We now turn to consideration of color certificates.

There are two types of Color Certificate accredited by the Human Resources Development Service of Korea: Industrial Engineering Colorist [IEC] and Engineering Colorist [EC]. The EC certificate is at a higher level than IEC, and is for people whose major at University is relevant to design or those having several years of experience in the design industry. In this paper, EC is the focus of discussion. From an investigation of the written exam paper for EC from 2003 to 2022, it can be seen that there have not been changes in terms of the main five subjects studied for the certificate in a broad manner. They are Color psychology marketing, Color design, Color management, Color perception theory, and Color systems (Table 2).

Table 2: Comparison of criteria for the examination for Engineer Color Certificate in different periods (major changes highlighted blue in bold)

Date range: 2007.01.01-2010.12.31		
Subject	Main Section	Subsection
Color Psychology Marketing	Color Psychology	Emotional Reaction to Color
		Color and Culture
		Functions of Color
	Color Marketing	Concept of Color Marketing
		Color Market Research
		Consumer Behavior
		Color Marketing
		Advertising Strategy
Color Design	Design in General	Definition of Design
		History of Design
		Principles of Design
	Color Design Practice	Color Planning
		Color Planning in Eight Design Areas
Color Management	Color and Material	Color and Material
		Material
		n/a
	Colorimetry	Colorimetry machine
		Colorimetry
	Color and Lighting	Understanding and use of a Source of Illumination
		Visual Inspection
	Digital Color	Digital Color Basics
		Digital Color System and Management
	Mixing Color	Mixing Color Basics
		Methods for Mixing Color
	Color Quality Regulations	Terminology for Color
		Color Quality Regulations
Color Perception Theory	Principle of Color Perception	Lighting and Color
		Color Perception
	Color Mixing	Secondary Color
	Color and Sense	Attributes of Perception of Color
		Color Perception and Emotional Effect
Color Systems	Color Systems	Color Standards
		Munsell Color System
		Ostwald Color System
		CIE and **ISO**
		Other Color Systems
	Color Names	Color Naming System
	Korean Traditional Color	**Korean Traditional Color System**
		Korean Traditional Color Names
	Theory of Color Harmony	Color Harmony
		Color Harmony Theories

(Contined)

Date range: 2022.01.01-2025.12.31		
Subject	Main Section	Subsection
Color Psychology Marketing	Color Psychology	Emotional Reaction to Color
		Color and Culture
		Functions of Color
	Color Marketing	Concept of Color Marketing
		Color Market Research
		Consumer Behavior
		Color Marketing Strategy
		n/a
Color Design	Design in General	Definition of Design
		History of Design
		Principles of Design
	Color Design Planning	Color Planning
		Color Planning in Nine Design Areas
Color Management	Color and Material	**Raw Material of Color**
		Understanding of Material
		Surface Finishing
	Colorimetry	Colorimetry machine
		Colorimetry
	Color and Lighting	Understanding and use of a Source of Illumination
		Visual Inspection
	Digital Color	Digital Color Basics
		Digital Color System and Management
	Mixing Color	Mixing Color Basics
		Methods for Mixing Color
	Color Quality Regulations	Terminology for Color
		Color Quality Regulations
Color Perception Theory	Principle of Color Perception	Lighting and Color
		Color Perception
	Color Mixing	Secondary Color
	Color and Sense	Attributes of Perception of Color
		Color Perception and Emotional Effect
Color Systems	Color Systems	Color Standards
		CIE System
		Munsell Color System
		NCS System
		Other Color Systems
	Color Names	Color Naming System
	Korean Traditional Color	**Korean Traditional Color**
		n/a
	Theory of Color Harmony	Color Harmony
		Color Harmony Theories

To investigate further in detail differences in the criteria for the examination over time, the periods 2007-2010 and 2022-2025 were looked into closely (Table 2). Regarding the subject of color psychology marketing, the subsection 'advertising strategy' was removed. It appears that 'color marketing' has been emphasized in recent years. As for the subject of color design, the only change we can see is in the numbers of design areas for color design practice. Multimedia design has been added. In terms of the subject of color management, it seems that color, material and finish (CMF) has been emphasized. For the subject of color perception theory, there has not been any change. Lastly, in relation to color systems, the Ostwald Color System has been replaced with the Natural Colour System (NCS). Also, the portion of the contents related to Korean traditional color has been reduced. Overall, there have not been significant changes.

One of the authors' has obtained both the IEC and EC and has experience of work with color in practice. Reflecting on this, it is difficult to relate knowledge gained for the certificates with practice in the color design industry. For instance, students doing the certificates may be taught that colors (or colored surfaces) need to be measured/described under the same condition (e.g. gray background using a 45-degree stand in a color matching light box, illuminated by a light that approximates a CIE D65 illuminant). However, a color matching light box was used subsidiarily in industry. The important issues in industry for making a decision for selection of colors were weather, time of day, humidity, experience and so on. These factors also may need to be taught to people who want to be colorists or obtain color certificates. This is one particular example from personal experience in the product color design industry. It would be useful to listen to the experience of a number of colorists from different areas of design practice to establish what ought to be taught to colorists in the future.

CONCLUSIONS

There has been a rapid development and awareness in terms of the job titled 'colorist' and the roles of colorists in South Korean design culture over the last three decades. On the other hand, little difference was found on the criteria for the examination for Engineer Color Certificate when comparing two sets of guidelines. The practicality of knowledge obtained from the certificate was reflected upon based on one of the authors' experience. This research provides improved understanding of the cultural background of the role of colorists in South Korean society. Also, this research offers insights about what knowledge of color needs to be regarded as essential in color design education through reflecting on its practical applicability in real design practice.

REFERENCES

1. Oxford English Dictionary. (n.d.). Colourist. In oed.com. Retrieved September 11, 2023, from https://www.oed.com/dictionary/colourist
2. Human Resources Development Service of Korea. (2023, September 11). *국가자격 종목별 상세정보* [Detailed explanations of national qualifications]. http://www.q-net.or.kr/crf005.do?id=crf00503&jmCd=1982&gSite=Q&gId
3. Kutsyuruba, B. (2023). Document Analysis. In: Okoko, J.M., Tunison, S., Walker, K.D. (eds) *Varieties of Qualitative Research Methods* (pp. 139-146). Springer Texts in Education. Springer, Cham. doi.org/10.1007/978-3-031-04394-9_23
4. Dalglish, S, L., Khalid, H., & McMahon, S. A. (2001). Document analysis in health policy research: the READ approach. *Health Policy Plan*, *16;35(10)*, 1424-1431. doi: 10.1093/heapol/czaa064.
5. Poulos, C, N. (2021). *Essentials of autoethnography.* American Psychological Association.

TEXT MINING ANALYSIS ON KOREAN PERCEPTION OF PERSONAL COLORS

Min Seo Kwon and Se Jin Kim [2] *

Interdisciplinary Program in Senior Human Ecology, Changwon National University, Changwon, South Korea.
[2]*Department of Clothing and Textiles, Changwon National University, South Korea.*

*Corresponding author: Se Jin Kim, e-mail: sejinkim@changwon.ac.kr

ABSTRACT

Despite extensive research on personal color, there is a lack of studies shedding light on recent perceptions in South Korea. Thus, this study aims to examine the public perceptions of personal color to provide implications for relevant industries. To this end, we analyzed big data consisting of social media texts. The data were obtained from Naver, a Korean and international web portal, Daum, and Google articles. Data were analyzed using the CONCOR algorithm with the NetDraw feature on Ucinet6. A total of 8,700 texts were extracted, and four groups were identified: “nurturing personal color experts,” “personal color-related events,” “self-image,” and “personal color education programs.” The results suggest that personal color has become an occupation and area of education, and that Korean people perceive personal color as an instrument for evaluating their identities. These results highlight the potential of personal color in various fields and shed light on the direction of fostering experts.

Keywords: AIC2023, Chiang Rai, Thailand, Personal colors, text mining, Korean perception, self image, Fashion industry

INTRODUCTION

In modern society, personal image and individuality hold great significance. The history of personal color—referring to the unique colors that one possesses—dates back quite some time, but the concept of personal color has recently garnered attention in Korean society as a crucial consideration in expressing one's personal image. Personal color extends across all means of expressing appearance, from clothing to accessories and makeup, and it plays a pivotal role in shaping one’s personal image and creating harmony (Woo & Kim, 2011). Color is an invaluable asset to one’s personal image, and it functions as a crucial means of expressing one’s unique individuality as well as communication in social relationships (Byun & Lee, 2019). Personal color has been extensively researched as an essential topic in the evolving fashion industry with a growing emphasis on individualized services in the era of the fourth Industrial Revolution. However, studies have primarily focused on its use and applications, with a lack of research shedding light on recent user views. Thus, this study aims to survey people’s perceptions of personal color to present implications for relevant industries. The findings of this study would highlight the latest perceptions and trends of using personal color in Korea as well as the areas of its application beyond apparel. Hence, the results would be useful in determining the direction of using personal color in the fashion industry.

LITERATURE REVIEW

Personal color refers to the unique palette of colors that harmonize with an individual's natural body tones and is determined by their inherent skin, hair, and eye colors. The components of such distinctive body colors are diagnosed and classified into different types, and a system for diagnosing and recommending color groups that suit each type is referred to as the personal color system (Lee & Park, 2012). Several studies have been conducted on personal color in Korea. Lee (2023) proposed styles in beauty and fashion that utilize color combinations based on the personal color system. Kim and Choi (2022) analyzed the association between images based on facial shapes and personal color types and showed that facial shape and image could be some variables in determining personal color. Shin and Kim (2023) investigated the perception of personal color among the MZ generation and its influence on makeup behavior. Additionally, Ahn and Im (2022) examined the association among perception of personal color, makeup behavior, self-esteem, and body image in female college students. Choi (2021) generated an algorithm based on the data collected from the distribution of diagnosed facial skin tones according to personal color types in the Z generation who prefer using the internet and various digital platforms. They attempted to use the data to develop an accurate and convenient personal color-type diagnosis program. Ryu and Han (2021) analyzed the impact of personal color perception on eyeshadow and lipstick color selection, as well as makeup satisfaction among women in their 20s. In other words, recent studies have tended to investigate the application of a personal color system, its relevance to other fields, its influence on individuals' behaviors and satisfaction, and personal color perceptions among college students, young adults in their 20s, and the MZ generation.

METHODOLOGY

We used big data analysis, particularly a technique known as text mining, to survey the public perception of personal color in Korea. The ideas shared by individuals online create a significant volume of data. Consequently, we sought to gain insights on how people perceive personal color by mining texts from online posts containing information or opinions. This methodology is appropriate for the purpose of this study, as online posts are valuable for understanding people's views on the subject. Online data were collected using Textom, a social big data analysis platform. Data from the past three years, from February 2020 to February 2023, were collected from web posts and news articles searched through Naver and Daum—the two most popular search engines in Korea. The search term was "personal color" (in Korean). Keywords were extracted and analyzed for frequency using Textom, and a one-mode symmetrical matrix was derived. We performed CONCOR (cluster) analysis and visualized the results using the NetDraw feature on Ucinet6 to determine the connections among the keywords based on the matrix formulated based on the frequency of the identified words. CONCOR analysis is a technique for measuring structural equivalence by repeating correlation analysis until convergence and analyzing the relationship based on the results (Jang & Hwang, 2020).

RESULT AND DISCUSSION

With "personal color" as the keyword, 8,700 texts were mined. Among them, the top ten words in terms of frequency were as follows: personal color (3779), color (1044), diagnosis (1027), process (479), program (426), brand (404), test (340), self (336), certification (303), and recruitment (297). TF-IDF results, which show the importance of the terms, were not markedly deviant from the order of term frequency. These results suggest that the focus is generally on events and programs related to personal color, such as personal color diagnosis. Based on these results, we performed CONCOR analysis, and four theme groups emerged: "nurturing personal color experts" consisting of operation, target, process, hosting, and recruitment; "personal color-related events" consisting of keywords such as lecturer, residents of the province, Gyeonggi province, and participation; "self-image" consisting of keywords such as warm tone, skin, color, beauty, image, self, personal, and "personal color education programs" consisting of keywords such as makeup, lecture, process, consulting, service, and program. These results highlight that personal color has become an occupation and area of education in Korea, and that the Korean people perceive it as a tool for determining one's personal identity

Table 1: Frequency anlysis results

rank	word	result
1	Personal color	3779
2	color	1044
3	diagnosis	1027
4	process	568
5	program	426
6	brand	404
7	test	340
8	self	336
9	certification	303
10	recruitment	297

Table 2: TF-IDF anlysis results

rank	word	result
1	Personal color	195.051
2	diagnosis	73.293
3	color	58.808
4	process	40.495
5	brand	31.303
6	certification	24.333
7	program	24.263
8	self	22.394
9	recruitment	21.636
10	test	19.101

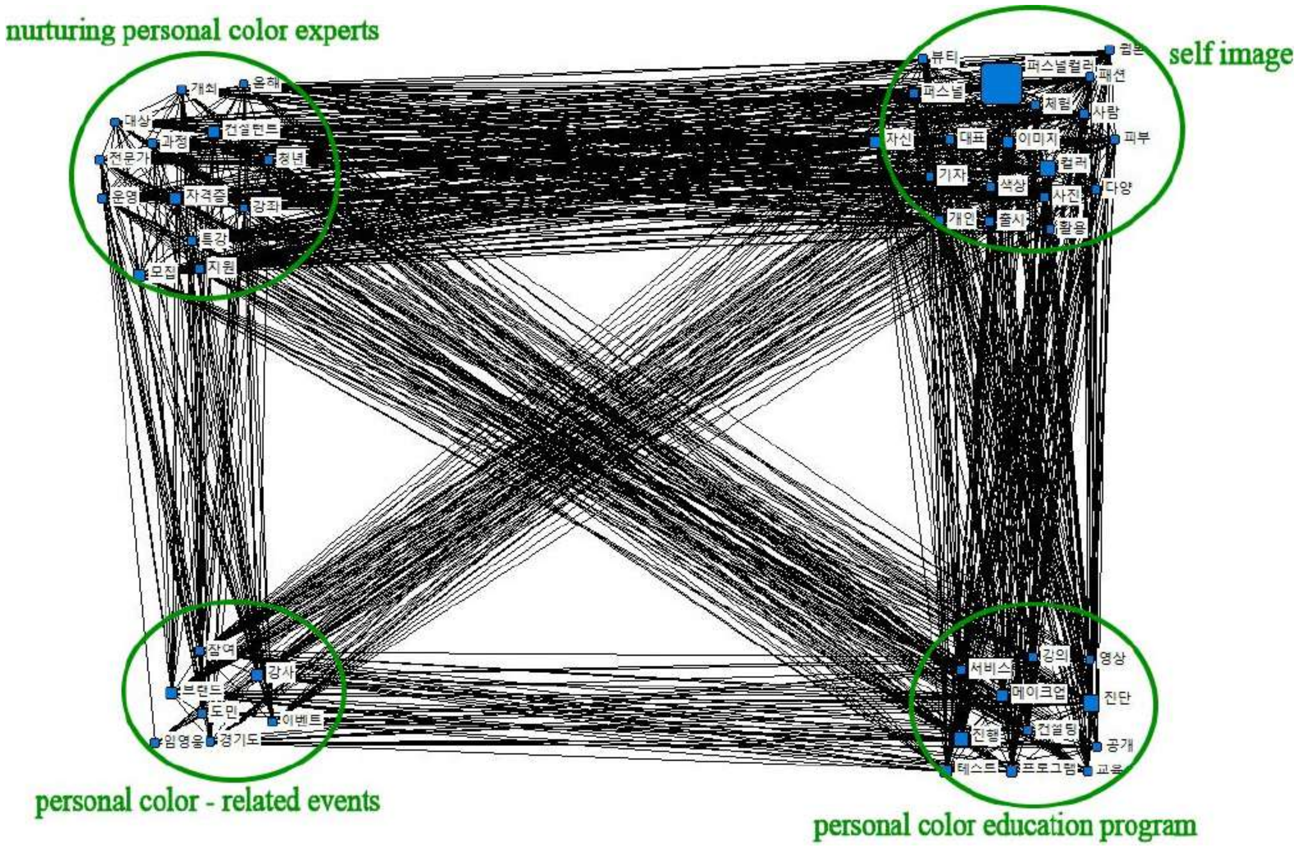

Figure 1. concor analysis visualization results

CONCLUSION

This study aimed to analyze people's perception of personal color using big data analysis, ultimately presenting implications for relevant industries. The following results were obtained through big data analysis: personal color education programs, personal color-related events, nurturing personal color experts, and self-image. These themes suggest that personal color can be utilized not only in the apparel industry but also in the beauty and hair industries. Furthermore, our results also show that personal color has become an important tool in expressing one's image, which led to the development of various industries and efforts to foster experts. Considering previous findings that a personal color system is applied in various areas, that personal color affects people's behaviors and satisfaction, and that personal color perception is an important factor in shaping self-image (Ahn & Im, 2022), our findings shed light on the applicability and useful directions of using personal color in the fashion industry, such as fostering experts, promoting education programs, and hosting relevant events. Future studies should build on our findings to additionally provide valuable data for product color planning and marketing strategy development and shed light on strategies to foster color and personal color experts—an emerging profession. Although this study only analyzed the case in Korea, future studies should conduct studies in other countries and examine the gap in perceptions across regions.

REFERENCES

1. Ahn, C. R., & Im, E. J. (2022). The relationship between female university students' personal color perception, makeup behavior, self-esteem and body Image. *Journal of Investigative Cosmetology, 18(1), 53-64.*

2. Byun, J. Y., & Lee, Y. J. (2019). A study on the change of perception after personal color diagnosis and application of job seekers. *Journal of the Korea Institute of the Spatial Design, 14(6), 51-60.*
3. Choi, M. L. (2021). Study on the face color distribution aimed at creating algorithms to determine the personal color type -focused on Z generation-. *Journal of Korean Beauty Society, 27(1), 170-181.*
4. Im, E. J., & Park, M. S., & Ha, J. H.(2017). The correlation among perception and application of personal color and beauty styling - women in their 20s and 30s -. *Journal of Investigative Cosmetology, 13(4), 369-379.*
5. Kim, Y. H., & Oh, Y. S., & Lee, J. H. (2018). Research of quantitative modeling that classify personal color skin tone. *Journal of the Korean society of clothing and textiles, 42(1), 121-132. 10.5850/JKSCT.2018.42.1.121*
6. Lee, J. Y. (2023). A study on the color arrangement of personal color & beauty and fashion. *Journal of Korean Beauty Society, 29(2), 485-498.*
7. Lee, J. A., & Kim, C. H. (2020). The effects of personal color awareness on color cosmetic purchase criteria and purchase behavior. *Journal of Korean Beauty Society, 26(3), 635-645.*
8. Lee, E. Y., & Park, K. S. (2012). Analysis of facial coloration in accordance with the type of personal color system of female university students. *The Research Journal of the Costume Culture, 20(2), 144-158.*
9. Park, Y. S., & Chun, H. K., & Yim, E. H. (2019). Qualitative research on motivations, decision-makers, and effects of personal color consulting. *Journal of The Korean Society of Fashion Design, 19(2), 37-56.*
10. Shin, S. R., & Kim, E. H. (2023). The influence of perception of personal color on makeup behavior in generation mz. *Journal of Korean Beauty Society, 29(3), 697-708.*
11. Woo, S. J., & Kim, Y. S. (2011). A study on the point makeup purchasing and using behavior according to the personal color awareness. *The Research Journal of the Costume Culture, 19(5), 889-902.*

COLOR QUALITY CONTROL OF MULTICOLORED FABRICS CONTAINING COLOR GRADIENTS BASED ON SPECTRAL IMAGING AND UNSUPERVISED SEGMENTATION METHOD

Nian Xiong[1] and Renzo Shamey[1]*

[1]Color Science and Imaging Laboratory, TECS, North Carolina State University, Raleigh, USA.

*Corresponding author: Renzo Shamey, rshamey@ncsu.edu

ABSTRACT

Efficient and accurate measurement of colors in multicolored stimuli containing color gradients using commercial instruments or computer vision techniques can be challenging due to the complexity of the patterns and the limitations of appropriate image segmentation methods. An approach using a spectral imaging system with an effective unsupervised color segmentation is presented to determine the $L^*a^*b^*$ values for each of the colors in multicolored patterns. The colorimetric attributes of the color patches in the ColorChecker chart were measured spectrophotometrically, and the spectral imaging responses of the patches were collected. The correction matrix between the measured and calculated colorimetric values was obtained by minimizing the average color differences between the two sets of data. The correction matrix was then applied to the captured multicolored pattern fabric sample images to obtain the $L^*a^*b^*$ values of each pixel in the multicolored patterns. The images represented in the $L^*a^*b^*$ color space were segmented using the nearest color neighbor clustering (NCNC) method. The average colorimetric attributes of each color cluster were calculated and reported as the predicted color attributes. To assess the performance of the method, a set of multicolored printed samples were tested and the color differences between the spectrophotometrically measured $L^*a^*b^*$ values and the predicted values were compared. The results show that, under appropriate color seeding and thresholding, NCNC clustering method generates satisfactory segmentation of the multicolored printed fabric images. The mean and maximum color differences between the measured and predicted samples were 2.65 and 4.15 $DE2000_{(1:1:1)}$ units. The chromatic difference between the spectrophotometric and imaging-based measurements was found to be larger than the lightness difference.

Keywords: color measurement, multispectral imaging, color quality control, image segmentation

INTRODUCTION

The color quality control of textile products containing multicolored patterns requires a significant amount of effort either for extended spectrophotometric measurements or for the complex subjective visual assessments. As such, the use of imaging-based color quality control methods not only could save time but also provide additional details, such as the spatial color inhomogeneity or the appearance of color transitions, e.g. streakiness, stripes, etc., compared to results obtained from measurements using colorimeters, spectrophotometers, spectroradiometers, or hyperspectral systems [1]. This information can help the operator determine the overall color appearance of the objects. This paper aims to present an imaging-based method for evaluation of multicolored textile fabrics. The steps involved include building a multispectral imaging-based color measurement system and implementing an accurate color image segmentation method to cluster the pixels that share similar color properties so that they can be evaluated separately. The evaluation result of each color cluster is used to determine an overall color quality evaluation.

METHODOLOGY

Imaging system

An LED-illumination-based imaging system was built and used for the color measurement of multicolored textile fabrics. As shown in Figure 1, the imaging system is composed of a camera, and a re-engineered DigiEye illumination chamber (VeriVide, UK), where the fluorescent lamps were replaced with specially designed LED bars on each side of the chamber. The chamber's inner space is shaped to provide quasi-diffuse illumination. A monochromatic camera (Thorlabs, USA) was placed on top of the chamber with the lens pointing to the center of the sample holder. Thus, the illumination and viewing geometry was approximately D/0.

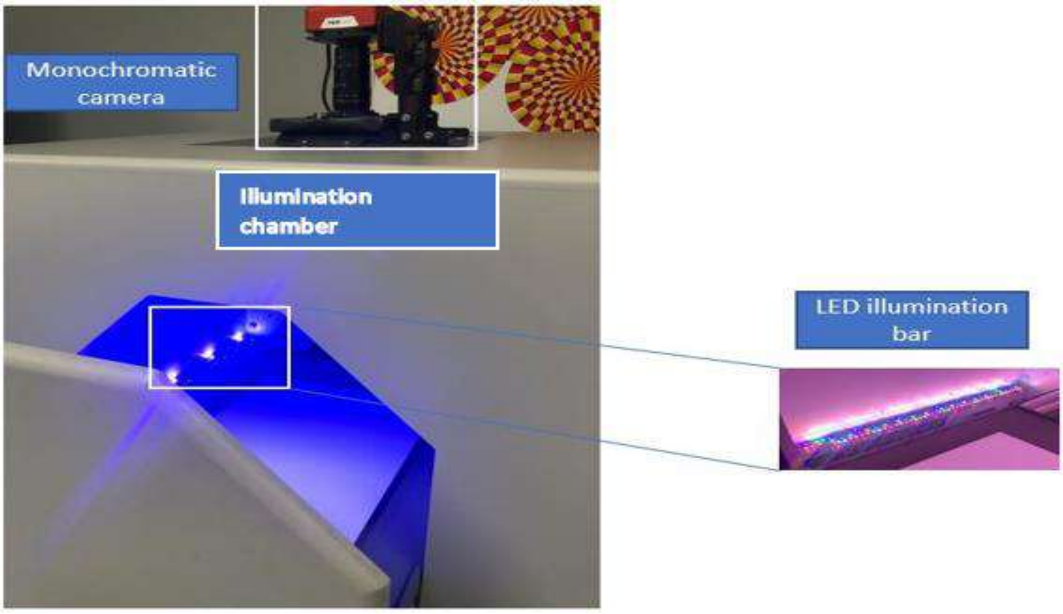

Figure 1. The LED-based imaging system composed of a monochromatic camera, illumination chamber, and LED illumination bar.

Experimental procedure

The experimental procedure is depicted in Figure 2. Once a multispectral raw image of the multicolored textile fabric was captured, the system employed the non-uniformity correction, the white point calibration, and then the pixel values of the fabric image were converted to $L^*a^*b^*$ values based on the color calibration matrix. The converted pixel values were used as the input in the segmentation algorithm. The fabric image was then clustered into different regions and the mean colors of each region were used to represent the measured values of each color cluster.

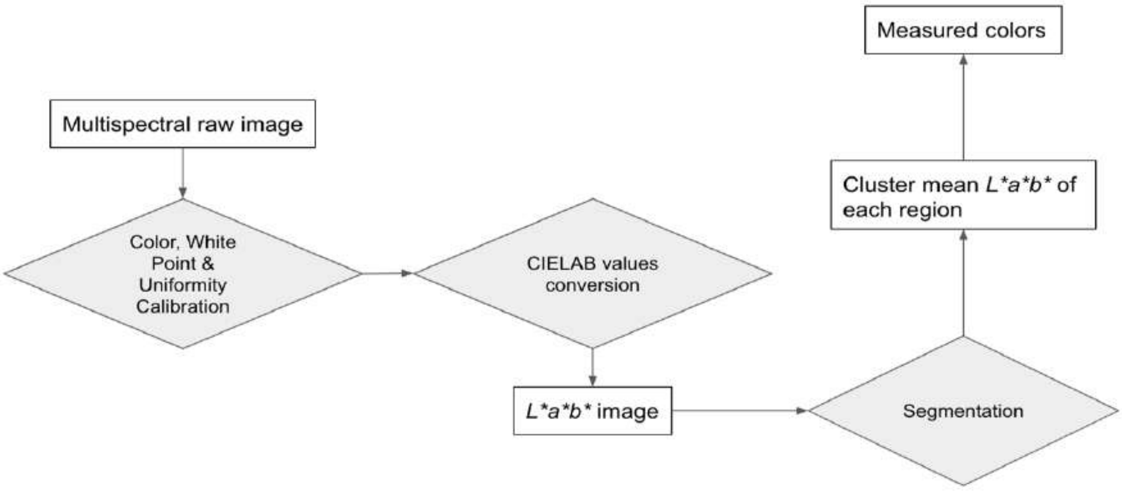

Figure 2. The experimental workflow.

Color segmentation

Color segmentation is an essential task when clustering the pixels on the pattern image that have similar color properties, thus an appropriate clustering algorithm should be employed before individual color clusters can be determined. An algorithm was developed for analysis of a multicolored fabric pattern containing both solid colors and gradient color segments, as described in the following section.

Given that the number of solid colors in the pattern is S and the number of gradient colors is G, the solid color seeds are specified for the fabric image as $\boldsymbol{x_s} = [L_s^*,\ a_s^*,\ b_s^*]$, where s $\in \{1, \dots, S\}$ prior to the segmentation. In the first algorithm, each gradient color segment is defined by the average of the two solid color seeds that form that color gradient segment. The average gradient color seeds are $\boldsymbol{x_g} = \left[L_g^*,\ a_g^*,\ b_g^*\right]$, $g \in$ {S +1, …, S +G}. This method uses a single color difference threshold for the detection of each color gradient segment. A set of color difference thresholds, generated from the solid color seed pairs, is used to test against the hypothesis that the pixel (i, j) is a gradient color pixel. For example, the threshold t_g for $\boldsymbol{x_g}$ is min $(\Delta E_{00}(\boldsymbol{x_g}, \boldsymbol{x_{gs1}}), \Delta E_{00}(\boldsymbol{x_g}, \boldsymbol{x_{gs2}}))$, where $\boldsymbol{x_{gs1}}$ and $\boldsymbol{x_{gs2}}$ are the two solid colors that form the color gradient with an average color of $\boldsymbol{x_g}$, $gs1$, $gs2 \in \{1, \dots, S\}$. ΔE_{00} represents the computed color difference based on CIE DE2000 metric. Each color gradient has a threshold t_g, $g \in \{S+1, \dots, S+G\}$. The algorithm could be briefly described in three steps and the detailed workflow of the algorithm is shown in Figure 3.

Step 1: Iterate over each pixel (i, j) in $N(i, j)$, the pixel is assigned to the color gradient map $U_g(i, j)$ if $\exists\ \Delta E_{00}(\boldsymbol{I}\,(i, j)\ ,\ \boldsymbol{x_g}) < t_g\ \ \forall\, \mathrm{g} \in \{S+1, \dots, S+G\}$. A gradient color map is defined as $U_g(i, j) = \{(i, j) |\ c(i, j) = g\}$ such that each pixel (i, j) has a cluster number $c(i, j) \in \{S+1, \dots, S+G\}$.

Step 2: For each pixel (i, j) in the remaining pixels map $R(i, j) \subseteq N(i, j)$, it is assumed the pixels are all solid colors. For each pixel (i, j) in $R(i, j)$, compute $\Delta E_{00}(\boldsymbol{x_s}, \boldsymbol{I}(i, j))\ \forall$ s $\in \{1, \dots, \mathrm{S}\}$ and assign $c(i, j) = s$ where $\Delta E_{00}(\boldsymbol{x_s}, \boldsymbol{I}(i, j))$ reaches the minimum. The solid color pixels map is defined as $D_s(i, j) = \{(i, j) |\ c(i, j) = s\}$ such that each pixel (i, j) has a cluster index s $\in \{1, \dots, S\}$.

Step 3: Remove the unwanted isolated pixels in the segmentation map of each cluster, i.e. $C_K(i, j) = \{(i, j) |\ c(i, j) = k\}\ \forall$ k $\in \{1, \dots, \mathrm{K}\}$. First, reconstruct the color image of each cluster, $\boldsymbol{O_k}(i, j) = [L_{ij}^*,\ a_{ij}^*\ , b_{ij}^*]$. The binarized cluster maps $O_k^b(i, j)$ is formed by applying adaptive binary thresholds on the first dimension of $\boldsymbol{O_k}(i, j)$ and taking its complementary set afterward.

The morphological opening filter M, which is a sphere-shaped structuring element with a radius size of r is applied in the binarized cluster maps, i.e. $O_k^b(i,j)$. The corrected binary cluster map $O'_k(i,j)\ \forall\ \mathrm{k}\ \in\{1,\ldots,\mathrm{K}\}$ is formed by $(O_k^b(i,j)\ominus M)\oplus M$. The refined segmentation map $C'_K(i,j)$ is reconstructed based on the corrected binary cluster map $O'_k(i,j)\ \forall\ k\ \in\{1,\ldots,\mathrm{K}\}$.

While this algorithm is designed for patterns that contain both color gradient and solid color regions, it can also work for patterns that contain solid color regions only by removing Step 1 in the workflow and only conducting Steps 2 and 3 and generating the segmentation map based on the clustering result of the solid colors.

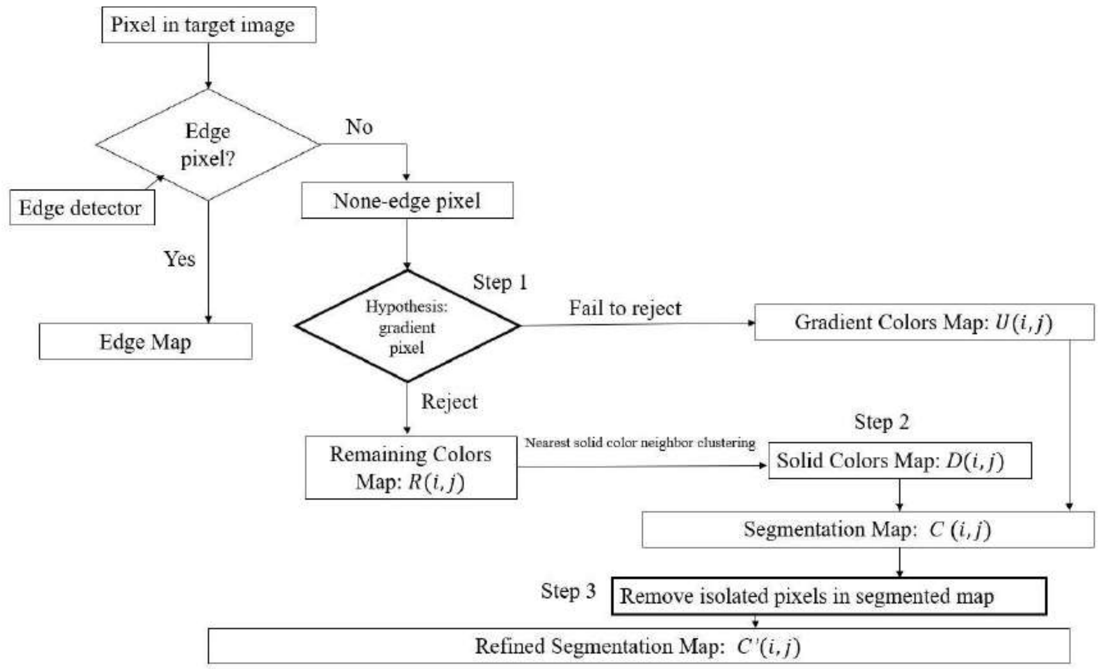

Figure 3. The segmentation algorithm scheme.

RESULTS AND DISCUSSION

Seven multicolored pattern fabrics as shown in Figure 4, were examined using the methodology described above. Two sets of colored patterns were tested, camouflage samples, (patterns 5-7 in Figure 4) and some other printed samples (patterns 1-4 in Figure 4). Camouflage patterns generally employ low chroma colors and tend to occupy a small region of the color space. Some such patterns also contain color transitions. Other patterns may incorporate more colorful and brighter colors. The average $\Delta E_{00}(1{:}1{:}1)$ color difference between the spectrophotometric versus the imaging-based measurements for all tested samples was 2.65 with a max of 4.15. Results for 26 out of 28 colors show a color difference below 4 units. The average ΔCH (chromatic difference) between the two systems was found to be larger than the average lightness difference. Thus, component differences for each set of samples were analyzed. The mean ΔE_{00} color difference for colors in the non-camouflage group was 3.02 which was slightly larger than that for the colors in the camouflage samples which had a mean ΔE_{00} color difference of 2.30.

The noticeable color difference threshold commonly adopted in industry for solid colors is approximately one ΔE_{ab} unit [2]. However, for multicolored materials, there is no widely agreed-upon threshold for determining general acceptability. Empirical findings suggest that the acceptable tolerance for multicolored material is significantly larger. Several studies propose that the average distinguishable difference is around 2.4 ΔE_{ab} units [3]. The average difference between spectrophotometric and imaging based colorimetric for the two sets of samples tested in this study show a comparable level of accuracy. In addition, the system described here is capable of handling various complex patterns that contain solid as well as transitional color regions. Table 1 lists a comparison of the colorimetric attributes for various samples shown in Figure 4. In Table 1 the L_1^*, a_1^*, b_1^* values in the gray shaded column are the spectrophotometric values.

Table 1. A comparison of spectrophotometric and imaging-based colorimetric attributes for each color in patterns 1-7 shown in Figure 4.

Pattern	Color	L_1^*	a_1^*	b_1^*	L^*	a^*	b^*	DL^*	DC^*	DH^*	$DE_{00\,(1:1:1)}$
1	1	62.05	-40.09	25.46	61.71	-37.95	28.75	-0.29	0.03	-3.92	2.00
	2	58.53	40.60	34.09	55.83	39.33	36.84	-2.47	0.26	2.90	3.10
	3	41.40	4.25	-37.48	41.47	9.67	-38.34	0.06	0.67	5.18	3.62
2	1	75.62	-23.16	7.19	76.72	-25.08	11.20	0.79	1.45	-3.07	2.62
	2	42.35	17.27	4.81	39.71	14.40	6.87	-2.35	-1.62	2.93	3.63
	3	43.31	-9.76	-29.72	44.23	-13.08	-22.40	0.85	-2.20	-6.00	4.15
3	1	75.64	-26.39	7.77	70.78	-26.92	10.55	-3.62	0.59	-2.46	4.00
	2	69.13	-18.42	-21.41	66.23	-17.14	-25.01	-2.31	0.82	3.21	3.11
	3	44.46	-9.51	-30.03	46.31	-13.14	-32.98	1.76	1.62	-2.42	3.09
	4	80.91	-3.20	52.53	83.07	0.37	52.51	1.46	-0.03	-3.57	2.80
4	1	53.22	-30.90	-5.61	56.37	-33.41	-7.56	2.99	1.16	1.41	3.35
	2	15.03	-3.40	-14.89	16.51	-4.00	-10.07	0.98	-1.39	-1.33	2.17
	3	49.98	22.21	17.13	48.35	25.44	18.76	-1.62	1.56	-0.64	2.31
	4	69.10	3.28	52.53	71.53	5.28	53.18	1.87	0.24	-1.94	2.30
5	1	62.86	3.39	12.71	61.73	2.87	13.28	0.96	-0.18	-0.64	1.26
	2	43.68	-1.33	2.73	43.22	-1.76	5.14	0.42	-1.99	0.50	2.13
	3	53.71	-0.06	4.78	52.44	-0.55	7.02	1.24	-1.80	-0.38	2.25
6	1	39.87	2.02	17.51	36.57	1.29	20.05	-2.83	1.30	0.95	3.30
	2	27.08	-4.62	6.02	25.57	-6.41	9.43	-1.12	2.83	-0.53	3.10
	3	35.01	6.14	14.28	32.67	6.20	20.05	-1.90	-1.05	-1.00	2.45
	4	15.72	-0.52	-0.92	13.84	-1.75	0.32	-1.23	1.32	-1.59	2.44
7	1	41.48	-3.55	15.06	42.25	-1.48	15.66	0.70	-0.04	-2.14	2.61
	2	26.99	4.28	3.41	29.79	4.90	4.82	2.12	1.12	0.64	2.49
	3	61.10	1.07	11.79	61.45	2.22	10.16	0.30	-0.81	-1.38	2.02
	4	57.28	4.66	15.09	57.92	5.83	13.41	0.58	-0.42	-1.68	2.08
	5	38.19	5.83	13.63	39.30	6.40	13.45	0.96	0.17	-0.59	1.18
	6	49.48	-0.98	19.93	49.74	1.13	17.94	0.26	-1.06	-2.12	2.63
	7	52.59	0.06	15.03	51.74	1.63	14.20	-0.84	-0.39	-1.62	2.23

Among all colors in various patterns only 2 colors in pattern 2 show relatively larger differences while in many cases the results are comparable between the two systems.

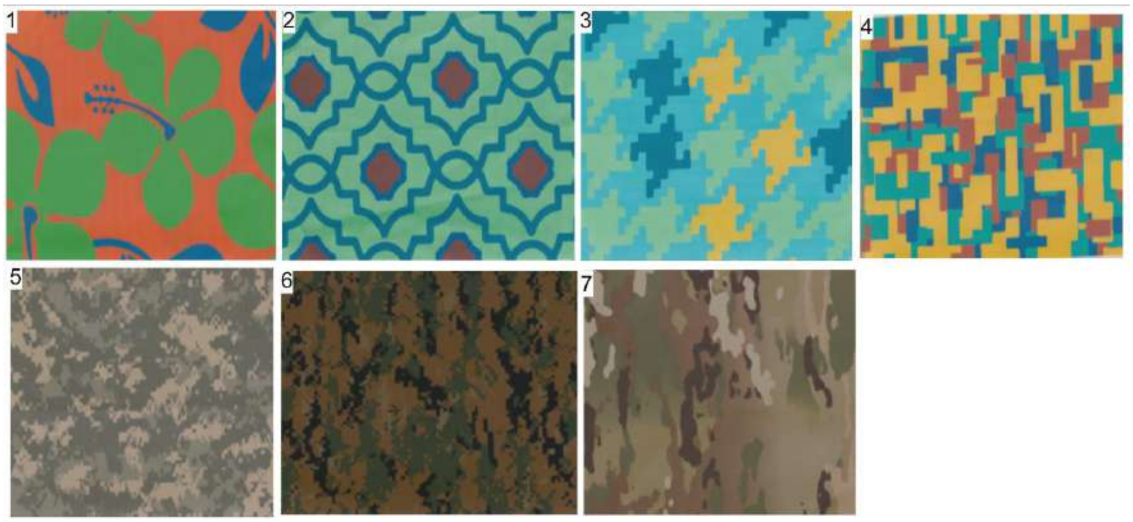

Figure 4. Printed fabric sample patterns tested in this study.

CONCLUSION

In this study the accuracy of color measurements based on a proposed imaging system including a segmentation algorithm was investigated. Several multicolored samples including camouflage and non-camouflage patterns were examined. The average DE00(1:1:1) color difference between the spectrophotometric and imaging-based measurements is 2.65 units with a max of 4.15 units. For 93% of the measured colors the color difference between the two systems was around or below 3 units. The proposed unsupervised image segmentation algorithm can be used to segment multicolored patterns that contain solid and gradient colors. The accuracy of color measurement in the imaging-based system can be further improved. Nonetheless, it offers a more efficient method for measuring complex multicolored samples, which would be beneficial for assessing the color quality of patterned materials. Furthermore, differences in results between the two systems may be insignificant in digital color quality control systems where in many cases only a pass / fail assessment based on larger acceptability thresholds may be necessary.

ACKNOWLEDGEMENT

The authors acknowledge and appreciate the funding received from the US Army which supported this research.

REFERENCES

1. https://www.datacolor.com/business-solutions/product/spectravision/
2. Shamey, R., Lin, J., Sawatwarakul, W., & Cao, R. (2014). Evaluation of performance of various color-difference formulae using an experimental black dataset. Color Research & Application, 39(6), 589-598.
3. Brainard, D. H. (2003). Color appearance and color difference specification. The science of color, 2(191-216), 5.
4. Xiong, N. (2023). Multicolored Pattern Segmentation and its Application in Color Quality Control., PhD dissertation, North Carolina State University, USA.

EFFECT OF COLOR PURITY OF LED LIGHT ON TASTE THRESHOLD

Hiroshi Takahashi*, Kento Tsuchida and Sota Asaga

Department of Electrical & Electronic Engineering, Kanagawa Institute of Technology, 1030 Shimo-ogino, Atsugi, Kanagawa 243-0292, Japan.

*Corresponding author: Hiroshi Takahashi, htakahashi@ele.kanagawa-it.ac.jp

ABSTRACT

We assess the flavor of food not only based on taste, but with all of our senses based on color, smell, texture and sound. Maga reported that the color green decreased the threshold to tasting sweetness and bitterness, and increased the threshold to sourness. The color yellow increased the threshold to sourness and sweetness, and the color red increased the threshold to bitterness. Maga also reported that color did not significantly affect the threshold to saltiness. Jin et al. reported that lighting was an important factor affecting taste sensation. However, there are few studies on the exact relationship between environmental lighting color and taste sensation. Therefore, in this study, we aim to clarify the effect of chromatic light on taste threshold. In this experiment, we used white (W) and chromatic light. Two color purity levels (100% and 60%) were established for red (R), green (G), blue (B), yellow (Y), cyan (C) and magenta (M) light. Red light of 100% purity is denoted by R100, red light of 60% purity is denoted by R60, and other light colors are similarly denoted. The illuminance was adjusted to 400 lx at a height of 109 cm from the floor. Four kinds of taste solutions (sweet, salty, sour and bitter) were prepared at nine different concentration levels. The experiment was mostly conducted once daily per subject. However, when multiple experiments were conducted on the same day, we set an interval of more than 1 hour between experiments. To assess taste threshold, subjects tasted a taste solution at a specific concentration and were asked to select how the solution tasted from one of five options: “sweet”, “salty”, “sour”, “bitter”, or “I don’t know”. The taste threshold obtained in this experiment was normalized. Normalization was performed based on the average taste threshold of all colors of lighting for each subject. In the case of the threshold to tasting sweetness and saltiness, no effect of lighting color was observed. In the case of sourness, the threshold was high under B60, B100 and low under G60. In the case of bitterness, the threshold was high under Y60, Y100 and low under R60, G60. Additionally, the threshold was low under G60 for all taste solutions. Therefore, it was suggested that the light color of G60 might enhance taste sensitivity.

Keywords: taste threshold, lighting color, color purity, taste sensitivity, colored taste solution

INTRODUCTION

We assess the flavor of food not only based on taste, but with all of our senses based on color, smell, texture and sound. Maga (1974) reported that the color green decreased the threshold to tasting sweetness and bitterness, and increased the threshold to sourness. The color yellow increased the threshold to sourness and sweetness, and the color red increased the threshold to bitterness. Maga (1974) also reported that color did not significantly affect the threshold to saltiness [1]. Jin et al. (2005) reported that lighting was an important factor affecting taste sensation [2]. Takahashi et al. (2019) suggested that similar changes in taste threshold might occur between the case of changing the light color and changing the color of the taste solution [3]. However, there are few studies on the exact relationship between environmental lighting color and taste sensation. In this study, we aim to clarify the effect of chromatic light on taste threshold.

EXPERIMENTS

In this experiment, we used white (W) and chromatic light. Two color purity levels (100% and 60%) were established for red (R), green (G), blue (B), yellow (Y), cyan (C) and magenta (M) light. For each color hue direction, 100% purity was defined as the color having the highest purity that can be represented by the LED light source. 60% of the distance to the main wavelength of the maximum purity of each hue was defined as 60% purity. Here, red light of 100% purity is denoted by R100, red light of 60% purity is denoted by R60, and other light colors are similarly denoted. The light colors used in this experiment are marked on the chromaticity diagram shown in Figure 1. The illuminance was adjusted to 400 lx at a height of 109 cm from the floor.

Four kinds of taste solutions (sweet, salty, sour and bitter) were prepared at nine different concentration levels. Table 1 shows each solution concentration. The following procedure was used in the experiment:

(1) Subjects were given 1 minute to adapt to white lighting at 400 lx.

(2) Subjects were given 10 minutes to adapt to the experimental lighting conditions.

(3) Taste threshold was measured.

The experiment was mostly conducted once daily per subject. When multiple experiments were conducted on the same day, we set an interval of more than 1 hour between experiments. To assess taste threshold, subjects tasted a taste solution at a specific concentration and were asked to select how the solution tasted from one of five options: "sweet", "salty", "sour", "bitter", or "I don't know". The presentation order of the concentration of the taste solution was as shown in Figure 2, with reference to the work of Jin et al. (2005) and Byung et al. (1997) [4]. One-factor analysis of variance (ANOVA) was performed, with the factor being lighting color, and multiple comparisons were performed using Fisher's least significant difference method.

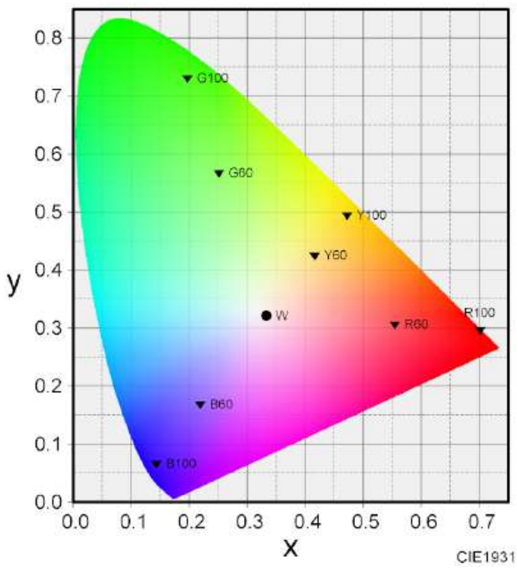

Figure 1. Experimental light colors on the CIE 1931 chromaticity diagram

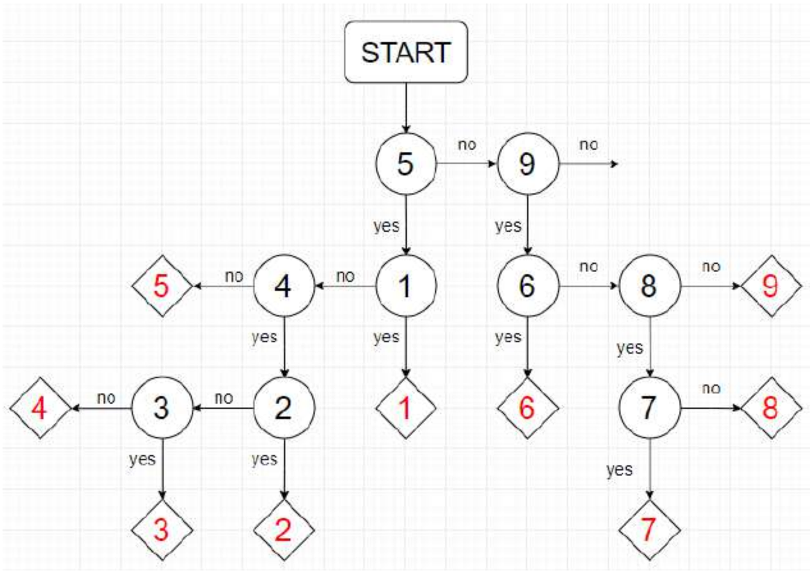

Figure 2. The presentation order of the concentration of the taste solution

Table 1: Taste solution concentration. [%]

Concentration number	1	2	3	4	5	6	7	8	9
Sweet	0.4	0.6	0.8	1.0	1.2	1.4	1.6	1.8	2.0
Salty	0.05	0.075	0.1	0.125	0.15	0.175	0.2	0.225	0.25
Sour	0.0005	0.001	0.002	0.004	0.006	0.008	0.01	0.012	0.014
Bitter	0.00005	0.0001	0.0002	0.0005	0.001	0.002	0.005	0.0075	0.01

RESULT AND DISCUSSION

Figure 3 shows the averages of the taste thresholds of all subjects. It was found that light color caused a change in taste threshold. However, since the influence of individual differences was large, the taste threshold was normalized.

Figure 4 shows the average rate of change of the normalized taste threshold. Normalization was performed based on the average taste threshold of all colors of lighting for each subject. In the case of the threshold to tasting sweetness and saltiness, no effect of lighting color was observed. In the case of sourness, the threshold was high under B60, B100 and low under G60. In the case of bitterness, the threshold was high under Y60, Y100 and low under R60, G60. Additionally, the threshold was low under G60 for all taste solutions.

ANOVA results showed a significant difference ($p<0.05$) between G60 and B60 in the case of sourness. A significant trend ($0.05<p<0.1$) was observed between G60 and W in the case of saltiness and between R60 and Y60 in the case of bitterness. No significant differences were observed under the other conditions.

Some taste solutions were found to have similar trends in taste threshold between this study and a study by Maga on different colored taste solutions, while others were found to be completely different.

For sweetness, in the case of study by Maga, the threshold was found to be high for red and yellow and low for green. However, in this study, sweetness was not found to be affected by light color. For saltiness, almost no change in the threshold was observed due to the influence of color in both this study and the study by Maga. For sourness, in the case of study by Maga, the threshold was found to be high for yellow and green. However, in this study, the threshold was not found to have changed when the green purity was 100%, and the threshold was found to be low when the green purity was 60%. For bitterness, the threshold was found to be high for red in the study by Maga. However, the threshold was found to be high for yellow in this study. It is considered that the color affecting the taste threshold may be different between the object color and the light source color.

Here, the spectral waveforms of the light colors are compared. Light colors containing both a medium wavelength (510 nm to 560 nm) component and a long wavelength (610 nm to 660 nm) component, and having the highest intensity in either, tend to coincide with a low threshold for tasting sourness. This suggests that sourness can be easily perceived when the light color of the wavelength, having the highest intensity in either, includes a medium wavelength component and a long wavelength component.

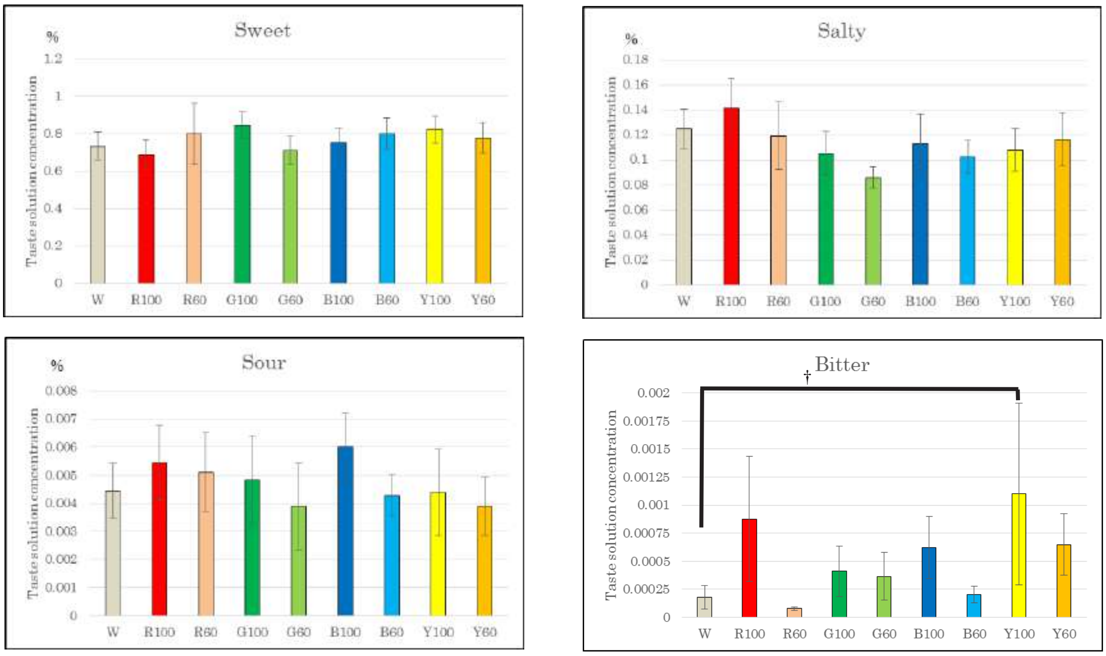

Figure 3. The averages of the taste thresholds of all subjects

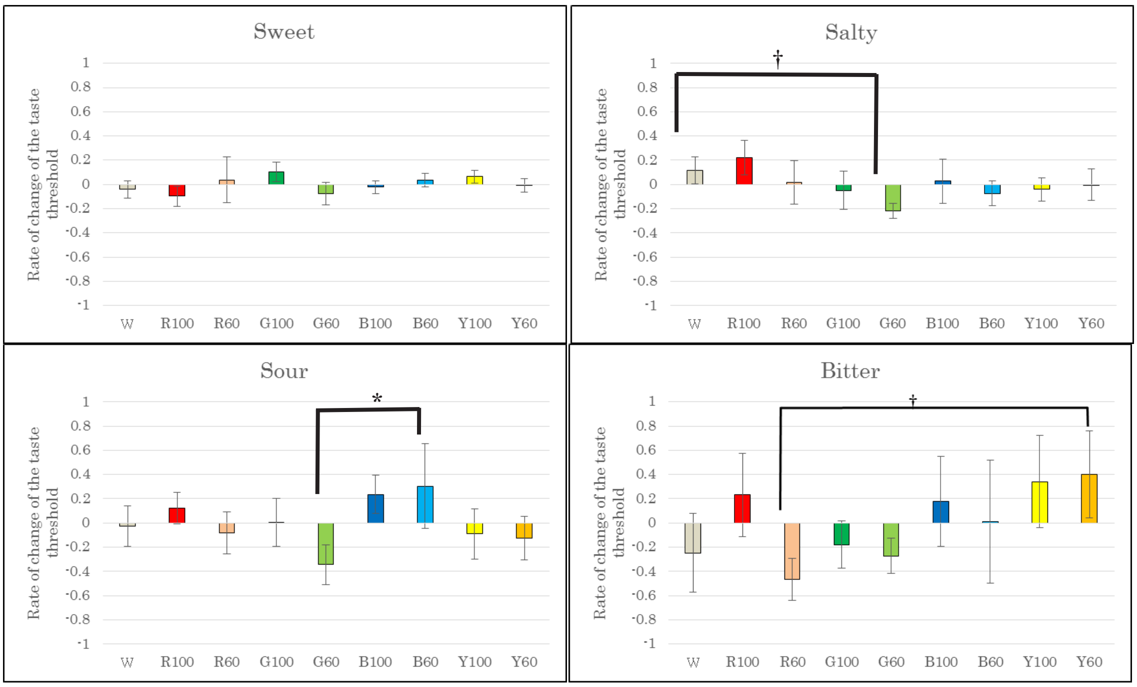

Figure 4. The average rate of change of the normalized taste threshold (* represents P<.05)

CONCLUSION

In this study, we examined the effect of lighting color on taste threshold. The results are summarized as follows:

(1) Changes in taste threshold due to the color of lighting differ depending on taste.

(2) It was suggested that the light color of G60 might enhance taste sensitivity.

(3) Light color containing both a medium wavelength component and a long wavelength component and having the highest intensity in either decreased the threshold to tasting sourness.

REFERENCES

1. Maga, J. A. 1974. Influence of color on taste thresholds. *Chemical Senses and Flavor* 1 : 115-119.
2. Jin, X., Katsuura, T., Iwanaga, K., Shimomura, Y., and Inoue, M. 2005. Effects of different lighting on the amount of saliva and taste threshold in Japanese and Chinese. *Japanese Journal of Physiological Anthropology* 10(1) : 9-16.
3. Takahashi, H., and Saito, D. 2019. Influence of the color of lighting on taste threshold. *Proceedings of the International Colour Association(AIC) Conference 2019* : 594-597.
4. Byung, C. M., and Sakamoto, K. 1997. An analysis of gustatory evoked potentials for the four taste qualities with a special reference to individual taste thresholds. *The Japanese Journal of Taste and Smell Research* 4(1) : 43-54.

MEASUREMENT OF RGB-LMS COLOR SPACE TRANSFORMATION MATRIX FOR DICHROMAT

Yuhang Zhang[1]* and Hiroyuki Shinoda[2]

[1] *Graduate School of Information Science and Engineering, Ritsumeikan University, Japan.*
[2] *Faculty of Information Science and Engineering, Ritsumeikan University, Japan.*

*Corresponding author: Yuhang Zhang, gr0424ki@ed.ritsumei.ac.jp

ABSTRACT

Color vision simulation is one of the basic technologies to achieve color-barrier-free in digital environments. Dichromat color vision is simulated by projecting colors onto the plane composed by vectors of perceptual colors for dichromats, along the direction of confusion line in LMS color space. To simulate dichromat color vision in display RGB color space, the RGB-LMS color space transformation is necessary and mostly the transformation is conducted through the colorimetric XYZ space by display calibration prior to the simulation. However, a professional colorimeter is not available to most users in their calibration process. Besides, the transformation between XYZ-LMS color space must, in somehow, to reflect each user's individual color vision characteristics. In this study, a novel method is proposed to obtain the direct transformation function between RGB-LMS color spaces, through two psychophysical experiments measured gamma value of the display nonlinear characteristics and transformation matrix between linearized RGB color space and LMS color space respectively. This paper mainly discusses the second one. In the first experiment, the gamma value of the display nonlinear characteristics is obtained through visual matchings between a solid color and a color of juxtaposed additive color mixture. The transformation matrix between linearized RGB color space and LMS color space is estimated in the second experiment named an image discrimination experiment. In the image discrimination experiment, a dichromat observer is to select images similar to the original image in color appearance, from many simulation image subsets made by various RGB-LMS color transformation matrices. Then the mean of matrices for selected images is calculated as the current best matrix. The procedure of observer's image selection and the update on the current best matrix is repeated until the variation of matrices converges into one matrix. Furthermore, in the dichromat simulation computation of the experiment, appropriate projection planes are set according to the transformation matrix so that all the simulated colors should stay inside the display RGB gamut. The verification experiment was conducted by pseudo-dichromat observers. That means all the experimental images were presented to normal trichromat observers through the predefined type of dichromat simulation. As the result, obtained display gammas were agreed with those measured by a colorimeter and the estimated transformation matrices were consistent with those calculated from the predefined type of dichromat simulation and the display calibration data.

Keywords: Color vision deficiency, color vision barrier-free, color vision simulation, individual difference

INTRODUCTION

A popular method for simulating dichromat color vision was proposed by Brettel et al. [1] (see Fig. 1). In their simulation, all colors in digital images are first transformed from the display RGB color space to the LMS color space via the XYZ color space. The colors are then projected along the direction of the color confusion line onto one of two planes composed of three perceptual color vectors of dichromats and the vector of achromatic light. This process achieves color vision simulation in the LMS color space. Finally, the projected colors are transformed back to the RGB color space from the LMS color space to create the simulated images.

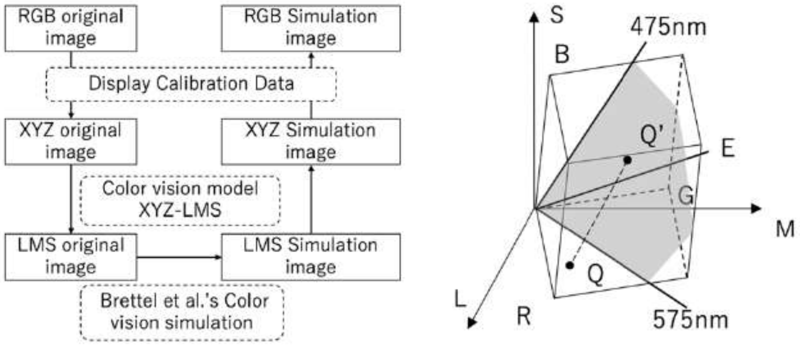

Figure 1. Brettel et al. s' Dichromat simulation. A flow chart of dichromat simulation (left) and the projection of colors for protanopia in LMS color space (right)

However, this transformation function may not always be optimal depending on the individual display and user. Not all displays necessarily follow the sRGB standard, and display calibration is needed to find the transformation function between RGB and XYZ color spaces in advance. In this study, a new method has been proposed for measuring the direct transformation function between the display RGB color space and the LMS color space with psychophysical experiments, allowing for the individual characteristics of the display and the user's color vision to be obtained.

METHODOLOGY

RGB-LMS Transformation function: The proposed method refers to the method of Vienot et al. [2] that colors are transformed directly between the RGB and LMS color spaces without passing through the XYZ color space, see Eq. (1) (2). The transformation matrix in Eq. (1), named " axLMS ," is composed of three vectors corresponding to the linearized RGB ($R^{\gamma_R}G^{\gamma_G}B^{\gamma_B}$) axes in LMS color space. The transformation matrix in Eq. (2), named "axRGB," is composed of three vectors corresponding to the LMS axes in linearized RGB color space. In this paper, we only introduce the measurement experiment of transformation matrix.

$$\begin{bmatrix} L \\ M \\ S \end{bmatrix} = \begin{bmatrix} L_R & L_G & L_B \\ M_R & M_G & M_B \\ S_R & S_G & S_B \end{bmatrix} \begin{bmatrix} R^{\gamma_R} \\ G^{\gamma_G} \\ B^{\gamma_B} \end{bmatrix} \tag{1}$$

$$\begin{bmatrix} R^{\gamma_R} \\ G^{\gamma_G} \\ B^{\gamma_B} \end{bmatrix} = \begin{bmatrix} R_L & R_M & R_S \\ G_L & G_M & G_S \\ B_L & B_M & B_S \end{bmatrix} \begin{bmatrix} L \\ M \\ S \end{bmatrix} \tag{2}$$

Measurement of RGB-LMS transformation matrix: To measure color confusion lines for an individual dichromat observer, an image discrimination experiment was developed based on the logic that a dichromat observer cannot distinguish a properly simulated image from the original. The confusion lines, which correspond to the ratios of the components in transformation matrix, are obtained by replacing Eq. (1) with Eq. (3).

$$\begin{bmatrix} L \\ M \\ S \end{bmatrix} = \begin{bmatrix} 1 & L_G & L_B \\ M_R & 1 & M_B \\ S_R & S_G & 1 \end{bmatrix} \begin{bmatrix} R^{\gamma_R} \\ G^{\gamma_G} \\ B^{\gamma_B} \end{bmatrix} \tag{3}$$

The experimental procedure for a protanope observer is illustrated in Fig. 5. A series of simulation images is generated using a dichromat vision simulator. To generate the sixteen variants of the matrix, a small perturbation D is applied to axLMS as shown in Eq. (4), in this case, for a protanope:

$$axLMS = \begin{bmatrix} 1 & L_G & L_B \\ M_R \pm D & 1 & M_B \pm D \\ S_R \pm D & S_G \pm D & 1 \end{bmatrix} \tag{4}$$

In the process of image discrimination, observers are required to select simulation images that appear identical to the original image. If the transformation matrix is capable of fully representing the relationship between RGB and LMS color spaces, then a simulated image created using that matrix should appear identical to the original to the dichromat observer.

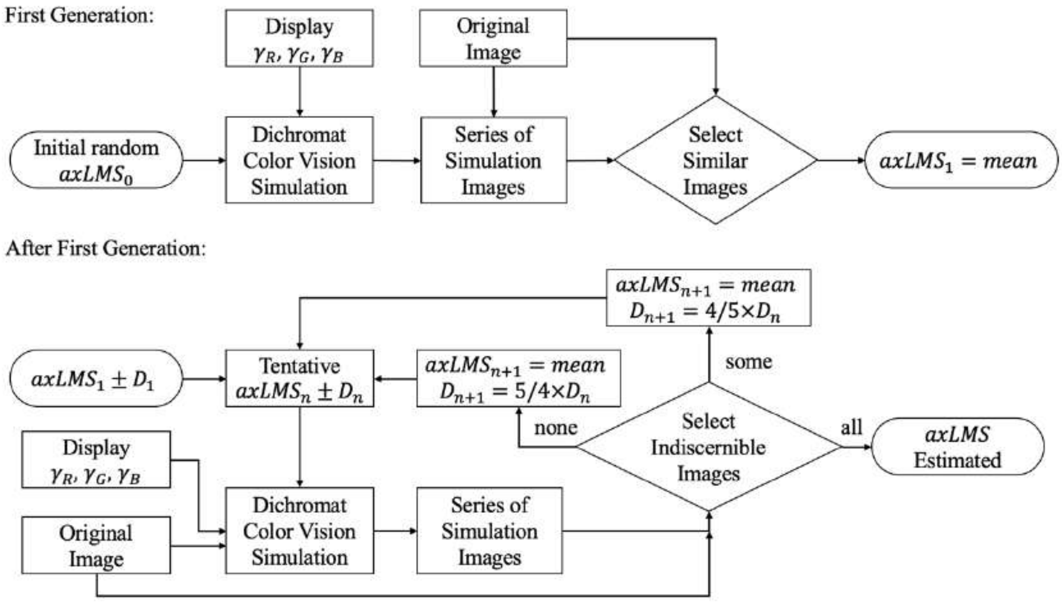

Figure 2. The flow chart of the experimental method

The experiment has two generation as shown in Fig. 2. In first generation, each parameter in $axLMS_0$ are set to a relatively large random number to quickly determine the approximate value of axLMS. Observers are required to select at least one image out of the 16 simulated ones that most similar to the original image (Referring to image in the top right of Fig. 4). After first generation, range D_1 is set smaller to accurately measure axLMS. Observers are required to select any images from the 16 simulated ones that appear to have almost no color difference from the original image. Compared to the first generation, this image selection is more stringent, demanding that the chosen images show almost no perceptible color difference from the original (Referring to the image in the bottom right of Fig. 4). If no selection is made, and it directly proceeds to the next generation. The experiment concludes when all 16 simulated images in a generation are identical to the original image.

Conditional projection planes: To fully guarantee simulation colors in the RGB display gamut, we referred the method proposed by Fukuda et al. [3], adopted four projection planes in our dichromat simulation. The conditional projection planes are defined based on the observer's color vision type and the value of specific parameters in axLMS (detailed illustrated in Fig 3).

Experimental condition: Verification experiment for transformation matrix was conducted under the same conditions as gamma measurement experiment, with two trichromatic observers, one male and one female. The experimental stimuli were generated using Matlab_R2021b and Psychtoolbox[4]-[6]. The displays used were MacBookPro 2017, IpadAir3, IpadPro 2018, and Hasee notebook ZX7-SP5D1. For each experimental condition, observers conducted 10 trials and recorded the average value of the transformation matrix.

Although all the observers were trichromatic, the Smith & Pokorny XYZ-LMS matrix [7] was utilized to simulate pseudo-dichromat vision in validation experiments. The target matrix axLMS$_t$ was calculated using the RGB-XYZ function obtained from prior colorimetric measurements, combined with the XYZ-LMS transformation matrix proposed by Smith & Pokorny [7]. Consequently, the validity of the experiment can be demonstrated by comparing the experimental results axLMS with the target matrix axLMS$_t$.

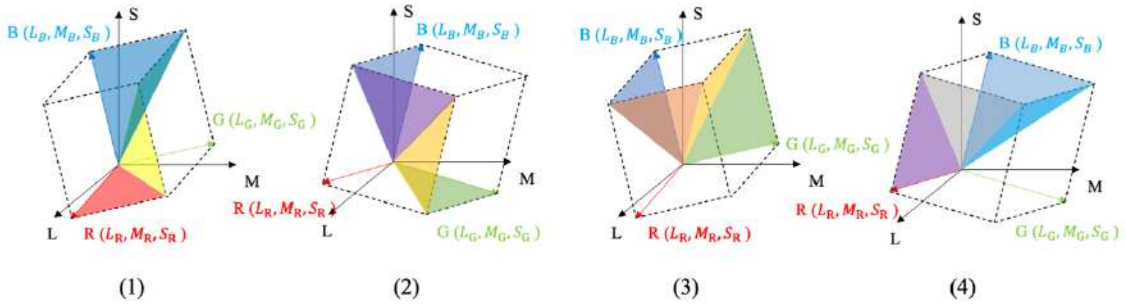

Figure 3. Temporary projection planes: (1) protanope, deuteranope $S_R \leq S_G$ (2) protanope, deuteranope $S_R > S_G$ (3) Tritanope $L_B > M_B$ (4) Tritanope $L_B \leq M_B$

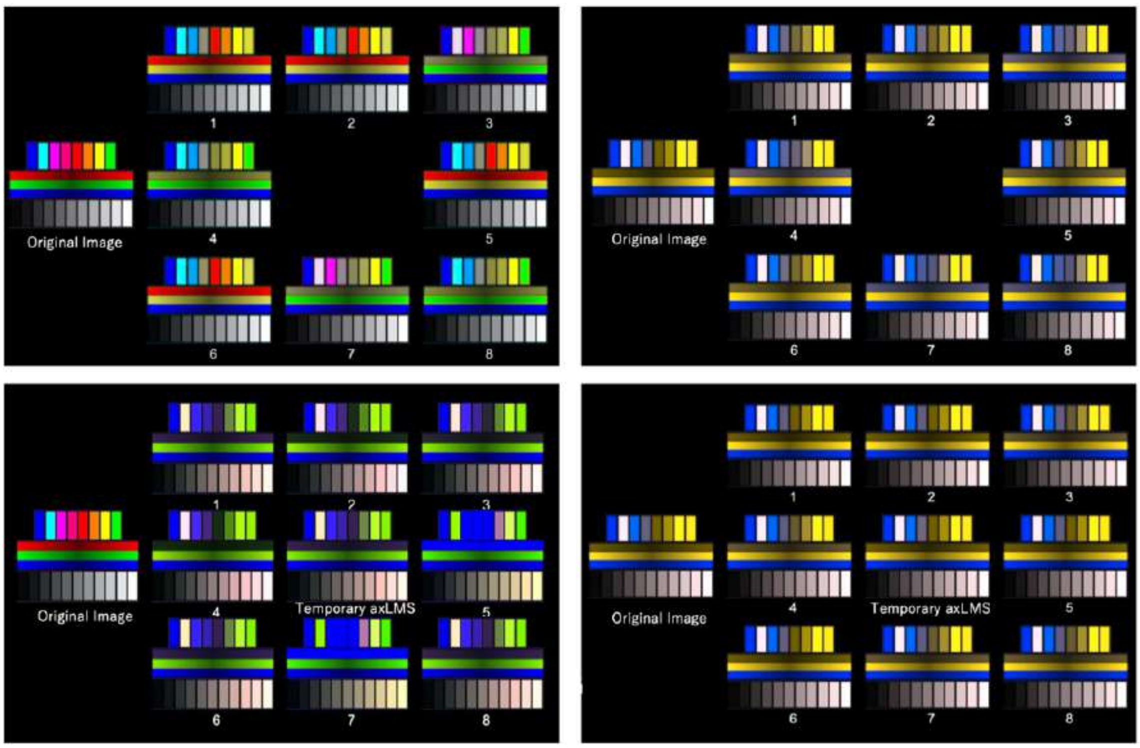

Figure 4. Stimuli for protanope dichromat (left) and for pseudo-protanope validation experiment (right) in first generation (up) and second generation(bottom)

As an example, the experimental stimuli for protanope are shown in Fig. 4. The top images represent experimental stimuli for first generation, while the bottom images represent that of second generation. On the left side are the experimental stimuli for dichromats, and on the right side are validation experimental stimuli for pseudo-dichromats. In all experimental stimuli, the single image on the left represents original image. In original image, colors of various hues were selected as much as possible to enhance the accuracy of the experiment. For first generation experimental stimuli (up of Fig. 4), the 8 images on the right are 8 out of 16 simulated images based on random axLMS_0 values. For second generation, the center image among the nine images on the right is dichromat simulation image, which simulated by temporary axLMS. The other eight images are dichromat simulation images that used 8 of the 16 tentative transformation matrices (bottom of Fig. 4).

Table 1 displays the settings of axLMS_0 and D_1 under all conditions and axLMS_t when display in MacBookPro 2017.

Table 1: Experimental conditions for MacBookPro 2017

	$axLMS_0$	D_1	$\mathrm{axLMS_t}$
P	$\begin{bmatrix} 1 & L_{Gt} & L_{Bt} \\ 0\sim0.35 & 1 & 0\sim0.35 \\ 0\sim0.35 & 0\sim0.35 & 1 \end{bmatrix}$	$\begin{bmatrix} 0 & 0 & 0 \\ \pm0.03 & 0 & \pm0.03 \\ \pm0.03 & \pm0.03 & 0 \end{bmatrix}$	
D	$\begin{bmatrix} 1 & 0\sim3.5 & 0\sim0.35 \\ M_{Rt} & 1 & M_{Bt} \\ 0\sim0.35 & 0\sim0.35 & 1 \end{bmatrix}$	$\begin{bmatrix} 0 & \pm0.3 & \pm0.03 \\ 0 & 0 & 0 \\ \pm0.03 & \pm0.03 & 0 \end{bmatrix}$	$\begin{bmatrix} 1 & 1.987 & 0.154 \\ 0.121 & 1 & 0.139 \\ 0.000 & 0.055 & 1 \end{bmatrix}$
T	$\begin{bmatrix} 1 & 0\sim3.5 & 0\sim0.35 \\ 0\sim0.35 & 1 & 0\sim0.35 \\ S_{Rt} & S_{Gt} & 1 \end{bmatrix}$	$\begin{bmatrix} 0 & \pm0.3 & \pm0.03 \\ \pm0.03 & 0 & \pm0.03 \\ 0 & 0 & 0 \end{bmatrix}$	

RESULT AND DISCUSSION

Table 2 presents the results of one of ten experiments conducted under the condition of using a MacBook Pro 2017 display. The data in table 2. shows the average value of axLMS and its standard deviation from 10 experiments. The "G" represents how many generations the axLMS measurement has gone through. By these data in Table 2, it can be observed: Although the data range of axLMS_0 is large, axLMS can still converge near $\mathrm{axLMS_t}$.

Table 2: Result of MacBookPro2017

	axLMS	$\mathrm{axLMS_t}$	G
P	$\begin{bmatrix} 1 & \mathrm{L_{Gt}} & \mathrm{L_{Bt}} \\ 0.123 \pm 0.017 & 1 & 0.141 \pm 0.035 \\ 0.006 \pm 0.010 & 0.059 \pm 0.034 & 1 \end{bmatrix}$		12
D	$\begin{bmatrix} 1 & 1.946 \pm 0.134 & 0.162 \pm 0.022 \\ \mathrm{M_{Rt}} & 1 & \mathrm{M_{Bt}} \\ 0.000 \pm 0.000 & 0.080 \pm 0.016 & 1 \end{bmatrix}$	$\begin{bmatrix} 1 & 1.987 & 0.154 \\ 0.121 & 1 & 0.139 \\ 0.000 & 0.055 & 1 \end{bmatrix}$	14
T	$\begin{bmatrix} 1 & 1.876 \pm 0.138 & 0.156 \pm 0.014 \\ 0.117 \pm 0.009 & 1 & 0.137 \pm 0.009 \\ \mathrm{S_{Rt}} & \mathrm{S_{Gt}} & 1 \end{bmatrix}$		7

To intuitively evaluate the results of verification experiment for transformation matrix measurement, we propose an evaluation method that converts the elements in axLMS into the confusion color direction in the linearized RGB color space. As mentioned earlier, two transformation matrices axLMS and axRGB are mutually inverse matrices. To illustrate this, considered as protanope observer. As shown in Eq. (5) to (7), the six parameters of the experimental result axLMS (M_R, M_G, M_B, S_R, S_G, S_B) correspond to (R_L, G_L, B_L) in axRGB, respectively. Then the direction of the L axis can be expressed as Eq. (8).

$$R_L = (M_G \times S_B - M_B \times S_G) \div |axLMS| \tag{5}$$

$$G_L = (M_B \times S_R - M_R \times S_B) \div |axLMS| \tag{6}$$

$$B_L = (M_R \times S_G - M_G \times S_R) \div |axLMS| \tag{7}$$

$$R_L : G_L : B_L = (M_G \times S_B - M_B \times S_G) : (M_B \times S_R - M_R \times S_B) : (M_R \times S_G - M_G \times S_R) \quad (8)$$

Fig. 5 shows the confusion lines for axLMS, and $\mathrm{axLMS_t}$ in the linear RGB color space, ranging from 0 to 1, passing through the center point (0.5, 0.5, 0.5). The green line represents the 10 experimental results of axLMS under the same conditions, the red line represents the average value of axLMS, and the blue line represents $\mathrm{axLMS_t}$. As observed in Fig. 5, the red line is close to the direction of the blue line. From this, the effectiveness of the proposed experimental method was demonstrated.

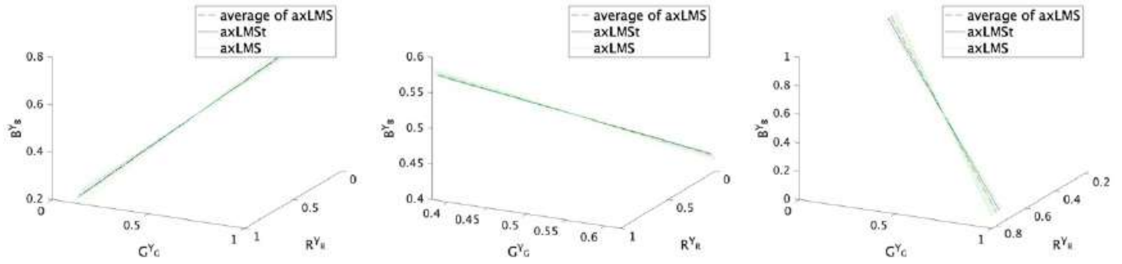

Figure 5. Result evaluation

CONCLUSION

In this paper, we proposed a method to obtained RGB-LMS transformation matrix. Through psychophysical experiment without using calibration devices. However, the transformation matrix measurement experiment still has some disadvantages: the plane of dichromat's perceptual color cannot be determined through this experiment. Because when color vision is anomalous trichromatism, the color on the same confusion line cannot be regarded as the same color.

REFERENCES

1. Brettel, H., & Vienot, F., & Mollon, J. D. (1997). Computerized simulation of color appearance for dichromats. JOSA, A, 14(10), 2647-2655.
2. Vienot, F., & Brettel, H., & Mollon, J. D. (1999). Digital video colourmaps for checking the legibility of displays by dichromats. Color Research & Application, 24(4), 243-252.
3. Fukuda, H., & Hara, S., & Askawa, K., & Ishikawa, H., & Noshiro, M., & Katuya, M. (2015). Computer Simulation of Color Confusion for Dichromats in Video Device Gamut under Proportionality Law. IPSJ Transactions on Computer Vision and Applications, 7, 41-49.
4. Brainard, D. H. (1997). The Psychophysics Toolbox. Spatial Vision, 10, 433-436.
5. Pelli, D. (1997). The VideoToolbox software for visual psychophysics: Transforming numbers into movies. Spatial Vision, 10, 437-442.
6. Kleiner, M., & Brainard, D., & Pelli, D., & IngLing, A., & Murray, R., & Broussard, C. (2007). What's new in Psychtoolbox-3?. Perception, 36, 1-16.
7. Smith, V. C., & Pokorny, J. (1975). Spectral sensitivity of the foveal cone photopigments between 400 and 500 nm. Vision Research, 15(2), 161-171.

THE INFLUENCE OF SPOT VARNISHING ON THE COLOUR APPERANCE OF PRINT TYPEFACES IN UV INKJET PRINTING

Somporn Nilmanee[1*], Supachai Pisuchpen[1], Vorachet Juntiya[2], and Meechai Luddee[3]

[1]*Packaging and Material Technology Program, Center of Excellence in Bio-Based Materials and Packaging Innovation, Faculty of Agro-Industry, Prince of Songkla University, Hatyai Campus, Songkhla, Thailand*
[2]*School of Health Science, Mae Fah Lung University, Thasud Muang, Chiang Rai, Thailand*
[3]*Faculty of Agro-Industry, King Mongkut 's University of Technology North Bangkok, Prachinburi Campus, Thailand*

*Corresponding author: Somporn.ni@psu.ac.th

ABSTRACT

Varnishing is commonly used in the packaging printing industry to protect and decorate the print, and it has an influence on colour appearance. This study describes and compares the colour difference (ΔE^*) of a print typeface between a non-varnishing finish and spot varnishing finish procedures with matte and gloss effects. For printing samples in a UV LED inkjet printer, a white duplex paper board is the substrate used in commercial packaging printing. The printed samples used solid ink colours of cyan, magenta, yellow, and black in typographic test form on positive and negative shapes. According to colour measurement, the surface layer of the black printed sample produced a lightness value (L^*) for gloss varnishing that was significantly darker, whereas the lightness values for cyan, yellow, and magenta were only slightly darker. The maximum acceptable colour difference was obtained in printed samples of non-varnishing and matte varnishing finishes. When comparing the non-varnishing finish of cyan, magenta, yellow, and black samples, the gloss vanishing layer was applied to the printed sample surface to raise the colour difference value. For visual comparison, the microscopic images generated a legible typeface of positive shapes for a surface finishing process of non-varnishing, spot varnishing, both matte and gloss effects. This demonstrated that the front elements of the positive shape version were made of dark colour on a light background, while the front elements of the negative shape version were created of white paper on a dark background. The colour appearance of positive shape version had an effect on the typeface's legibility by sharpening the line edges and enhancing the strokes. On the other hand, the negative shape version's ink colour spreading and noise edge caused the text to be blurry and unclear, reducing its visibility and legibility. As a result, the use of vanishing and colour collection in graphic design for packaging should improve depending on text size, background shape type, and printing substrate.

Keywords: colour difference ($\triangle$E), inkjet printing, vanishing, packaging design, colour appearance

INTRODUCTION

Varnishing is one of the most effective procedures for protecting and decorating the printed surface in order to get the desired print typeface and color appearance. Inkjet printing technology is widely employed in the packaging industry. The color of UV ink is caused by pigment dispersion during photochemical and monomer reactions with radicals caused by UV light irradiation. The UV curing technique deposits a firm layer of UV ink onto the substrate in an instant. The quality aspects of LED - UV digital printing generate without pollution, more resistant surface, an incredibly cost-effective method, the faster drying times, the impressive effect design, image quality improvement, special printing technique and printing on demand. The decorative technique in printing systems for packaging industries is the improvement of varnish finish on ink color surface. UV clear ink provides the superior function of varnishing effect to apply onto the produced color for gloss finish and matte finish with inkjet printing systems. According to vanishing advantages, in the packaging industry, baring or combining UV inks are frequently used to decorate and protect varnishing on printed surfaces of various substrates. Hudika *et al*. (2020) evaluated inkjet UV varnishing by estimating optical print characteristics in different surfaces with matte and gloss finish. The results showed that the black colour was reproduced in colour tolerance. This study indicated that UV varnishing causes small colour differences which are in most not visible to the human eye. Gloss measurements showed that varnishing with gloss effect significantly increase gloss values on the substrate and the printed ink film. In the research of Galić *et al*. (2015) resulted the influence of UV varnishing on diversified colorimetric properties of spot colours. The gloss of printing substrate with UV varnishing process contributes to visual appearance enhancement. It also affects values of colorimetric changes and the printed mechanical protection. In the work of El - Rahman *et al*, (2021) studied the LED-UV curing system used diodes that convert electrical current into light. The UV light causes chemical reactions in the molecules within the liquid, forming chains of polymers until the liquid becomes a solid.

For printing substrate issue, the investigation of Majnarić *et al*. (2012) measured smoothness, colour and gloss onto different surfaces of printing substrate as offset paper grade by application of the UV varnishing technique. The results shows that the absorbency decreases on gloss coated paper, while it increases on uncoated paper. It also indicated that percent of UV varnish coating of layer was not relevant for absorbency an optical property. Investigation of Li *et al*. (2020) and Valdec *et al*. (2021) concluded the influence of colour appearance that was depended on the UV-curable inkjet printing parameter and substrate surfaces. They were involved the spreading and penetration of ink that due to printing distance, number of overprints, ink colour on printing substrate. The results also indicated that colour appearance was affected the greatest lightness and colour difference (ΔE) toward the reference colour [5]. Therefore, the aim of this study is to influence of non-varnishing and spot varnishing with both matte and gloss effect on colour difference (ΔE) with UV LED curing inkjet printing.

METHODOLOGY

Preparation of printed samples

The printing process used Adobe Illustrator to create test forms of positive and negative shapes, as well as a colour background. The condition of test form determination was performed on the colours validation of Cyan (C), Magenta (M), Yellow (Y), and Black (K) in both spot - glossy and spot - matte finishes, including without vanishing effect. The print substrate used in this study was white duplex paper board 450 g/m^2, which was prepared for printing with an UV LED - inkjet printer (Mimaki, UCJV 155-160, Japan) at a resolution of 600 x 1200 dpi of all printed substrate samples. There were two types of printing clear ink UV- LED modes based on the varnishing effects of glossy finish and matte finish.

Colour and optical measurement of prints and varnished samples

CIE L* *a***b** values were measured using a spectrophotometer (X-rite eXact tm, USA) at D50 illuminant, 2 observer, 0°/45 geometry to evaluate the colorimetric characteristics of printed ink samples according to ISO 12647-6 2020 standard. Colour difference (△E) values of UV varnishing and non-varnishing samples for primary colours CMYK were measured for each sample. Digital microscope images (1000x, China) were captured and magnified using an optical system and a digital camera. These images were displayed on a computer monitor with camera software via a USB port, which allows elements to be transferred (positive, negative text and colour background). The microscopic images were visually assessed at a 25x enlargement.

RESULT AND DISCUSSION

CIE L*a*b* coordinates and colour difference

Each measurement method was performed five times with average values. The CMYK printed colors in matte varnish and non-varnish were unaffected by the evaluation of the lightness (L*) coordinate, while the L* values of the printed sample ink colours in UV clear ink varnish were slightly decreased as the imager obtained darker colors for the gloss effect (Figure 1). In the values of a* and b* coordinates, the varnishing of gloss finish and matte finish was not affected by changing the four ink colours, as shown in Figures 2 and Figure 3. Furthermore, Figure 4 shows the colour difference (△E) values of printed colour inks with and without varnish for matte and gloss effects. The △E values of CMYK ink colours referring to gloss varnish and non-vanish effect were greater than those of the reference colour relating to matte varnish and non-vanish effect. The rationale suggested that black colour with LED- UV inkjet ink and varnishing effect were obtained the greater the ink's ability to absorb light and the higher the density value (Hudika *et al*., 2020, Majnarić, *et al*., 2012).

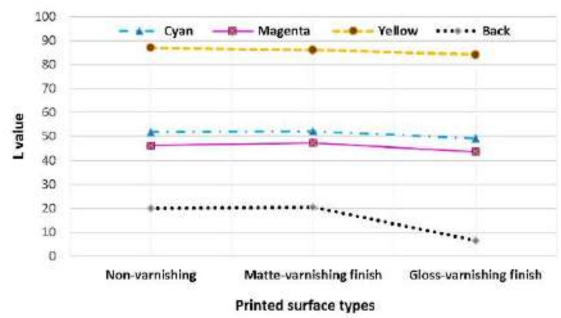

Figure 1. L coordinate of the evaluated samples with L* values

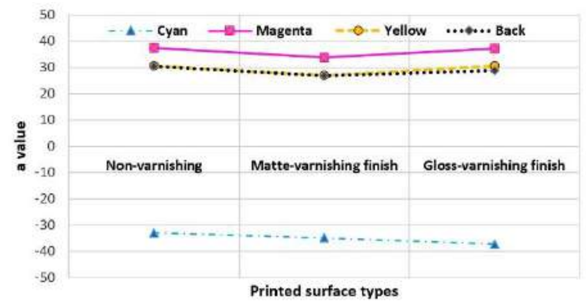

Figure 2. a* coordinate of the evaluated samples with a* values

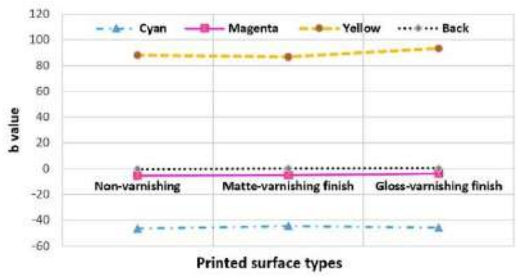

Figure 3. b* coordinate of the evaluated samples with b* values

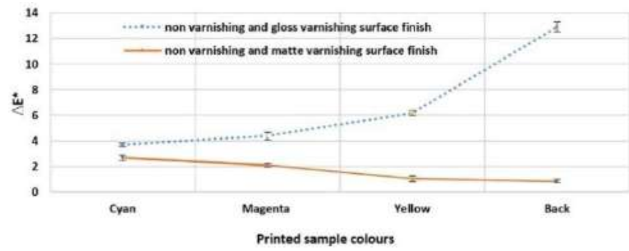

Figure 4. Colour difference of the evaluated samples between non-varnish and gloss and matte varnish of on substrate surface

Effects of microscopic images

The printed colour samples were evaluated visually using microscopic images through the use in colour appearance under the effects of non-varnish, matte varnish, and gloss varnish, as shown in Figure 5. The results show typical surfaces of white paperboard duplex smoothness for gloss varnish on all ink colours, as CMYK had a higher colorfulness than without varnish. In addition, the saturation was increased by increasing the value of C* (chroma) in CMYK ink samples when employing glass spot vanishing on the printed surface. The density values for printed colour ink represent the ink's ability to absorb light. The findings of the study by Hudika *et al*. (2020) were similar to those of this investigation. They showed the reason for the visible colour with the UV vanish coating. The gloss finish reflected the light and produced a natural shadow that appears to surround the varnish printing element due to the optical colour discrepancies. It could provide a contrast and then distinguish the surface element, but it did not involve increased edge noise (edge raggedness), spreading, or penetration of ink on the substrate's surface.

The spot vanish effect was applied to the text in sample form using a clear UV inkjet printer that displayed the text in CMYK colour with different densities. The printing density values were connected to the standard densities of their specific colours, including the ink surface thickness and varnish finish coating layer. These factors have an effect on the legibility of the text and picture enhancement acceptable for consumer access to product information on packaging.

Ink Colour	Non varnishing	Matte – varnishing	Gloss - varnishing
Cyan			
L*	52.0	51.6	50.1
C*	58.0	54.7	60.0
h*	234.3	233.8	231.3
colour density	1.21	1.20	1.32
Magenta	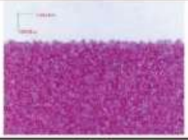		
L*	40.1	45.7	43.7
C*	71.4	71.6	74.6
h*	355.2	357.8	356.8
Colour Density	1.32	1.37	1.62
Yellow			
L*	86.9	83.8	85.9
C*	86.1	89.8	93.1
h*	95.0	93.7	94.6
Colour Density	1.28	1.28	1.48
Black			
L*	19.5	17.4	6.8
C*	0.33	0.27	2.4
h*	224.7	237.9	171.7

Figure 5. Microscopic images of the printed colour samples with different surface types

Microscopic varnish element analysis

The optical study of the UV ink printed colour under all three conditions was conducted using a digital microscope and a text pattern. The phenomenon of colour contrast is based on the brightness of a yellow background, and a black text form appears to contrast differently. The text pattern of printing the UV ink is shown in Figure 6a. Figure 6b shows a printed sample with a matte varnish coating on the text layer. Figures 6a and 6b illustrate the extraction of edge boundaries from text. On the other hand, Figure 6c exhibits the colour improving its visibility with a few edges spreading for the text colour of printing and the gloss vanish effect. In terms of negative shape, ink spreading could have a negative effect on the print quality of sample elements. A colour background in a negative shape resulted in especially tiny texts and poor text legibility (Figure 6d, 6e and 6f). According to positive shape, the text colour with gloss varnishing was definitely described as having more saturation, which influences its visibility (Figure 6i). As a result, the spot varnish character was interpolated into the ink surface to sharpen the edge of image detection (Valdec *et al*., 2021).

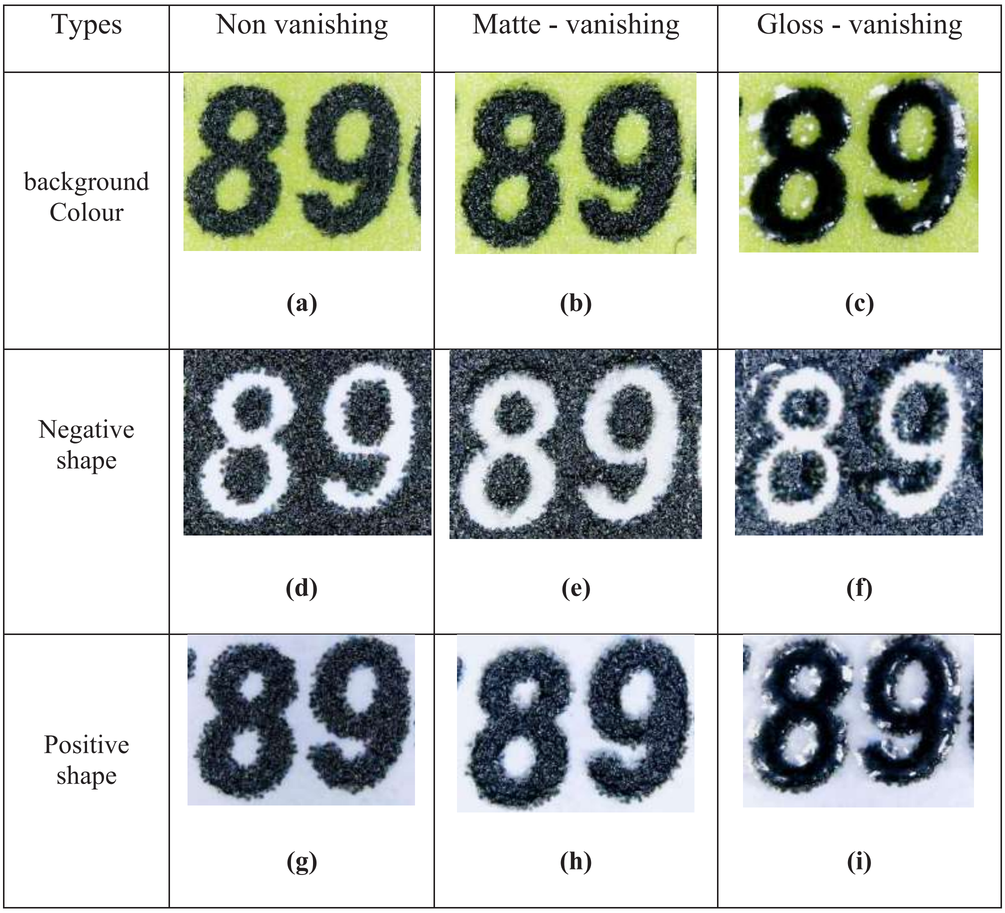

Figure 6. Microscopic images of the printed typeface samples with different conditions

CONCLUSION

The analysis of measurement results can show that the visual colour appearance of spot varnish UV ink in each circumstance is related to CIELAB coordination for inkjet digital printing. The alternative for the packaging industry or designer is to consider utilizing the spot UV vanish printing strategy for add-value graphic design that expresses benefits for branding and marketing advertisements such as brand identification, product name, picture, or priority aspect. The comparison of colour differences under the circumstances of the artwork design employing non-varnishing and varnishing both matte and gloss effects is an important factor for packaging design. The application of spot UV varnish has grown in popularity for packaging printing on a variety of substrates. Both digital printing and conventional printing processes can use spot UV to add beautiful decoration to substrate surfaces. This study concludes that spot varnish on the overtop layer influences colour appearance and colour difference, as well as visibility and legibility in packaging design.

ACKNOWLEDGEMENT

The authors would like to thank Faculty of Agro - Industry, Prince of Songkla University, Hatyai campus, Thailand to support the equipment. The authors are grateful for support the substrate from Spack & Print Public company limited, Thailand in this research.

REFERENCES

1. Hudika, T., Majnarić, I., & Cigula, T. (2020). Influence of the varnishing surface coverage on optical print characteristics. *Technical journal*. 14(4), 428-433. doi: 10.31803/tg-20191129104559
2. Galić, E., Ljevaak, I., & Zjakić, I. 2015. The influence of UV Varnish on Colorimetric Properties of Splot Colors. Procedis Engineering. 100. 1532 – 1538. DOI:10.1016/j.proeng.2015.01.525
3. El – Rahman, A. A., Saad, E., Aydemir, C., Özsoy, S. A., & Yenidoğan, S. (2021) Dry methods of the printing inks. Journal of Graphic Engineering and Design, 12(2), 29-37.
4. Majnarić, I., Mirković, I.B., & Golubović, K. (2012). Influence of UV curing varnish coating on surface properties of paper. *Tehnički vjesnik*. 19, 51-56.
5. Li, N.W., Ho, C.P., Yick, K.L., & Zhou, J. Y. (2020). Effect of UV-Curable inkjet printing parameters on physical, low-stress mechanical, and aesthetic properties of polypropylene knitted fabrics. *Fibers and Polymers*. 21, 2788-2798. DOI:10.1007/s12221-020-1295-5
6. Valdec, D., Hajdex, K., Majnarić, I., & Čerepinko, D. (2021). Influence of printing substrate on quality of line and text reproduction in flexography. *Applied Science*. *11*(17), 1-16. doi:10.3390/app11177827

INVESTIGATING THE EFFECT OF LIPSTICK COLOUR ON SKIN COLOUR PERCEPTION FOR CHINESE FEMALE

Yifei Chen[1]*, Kaida Xiao[1] and Muriel Rigout[2]

(University of Leeds, LS2 9JT, United Kingdom)

[1]*School of Design, University of Leeds, UK.*

[2]*School of Design, University of Leeds, UK.*

*Corresponding author: Yifei Chen, sd192yc@leeds.ac.uk

ABSTRACT

The behaviour of using paint to decorate human bodies has been continuously practised by humanities for a considerably long history. The use of cosmetics can be considered one of the most representative ways of self-decoration because it can define humans from an individual perspective. Among all types of cosmetics applied, lipstick is worth focusing on since it is the category that has been consumed and discussed frequently in the past 5 years. Studies show that applying makeup can increase females' attractiveness by enlarging femininity. However, current studies mainly focus on the lightness and contrast between features and skin, lacking discussion regarding colours. The correlation of lipstick colour to skin tone remains uncertain. Additionally, with current research's discovery of a special geometric pattern on the human body: a biological illusion, this research will further explore the colour assimilation of lip and skin considering skin tone as an influencing factor. The research aims to determine how skin colour influences the lip colour decision-making process. The research specifically focused on the lip colour preference of young Chinese female cosmetic users based in Leeds, UK. Ten volunteers were invited and asked to apply six lipsticks from Maybelline Super-Stay matte ink lip crayon collection. Measurements were taken by Spectroradiometer under D65 light resources. External observers were invited to rate each picture in perceptual lightness, yellowness, redness and attractiveness, to explore how lipstick affects the perceptual skin colour from these four dimensions.

Keywords: facial attractiveness, colour assimilation, lipstick colour.

INTRODUCTION

Human-beings have a long history of using paint as part of the self-decoration [1]. Previous works concluded that facial attractiveness is determined by averageness, symmetry and sexual dimorphism [1-3]. Averageness and symmetry can hardly be affected due to the natural properties of lipsticks. Sexual dimorphism is how much feminine and masculine traits can be perceived from human faces. It is statistically proven that female faces with more feminine features are considered more attractive by observers from both genders [2-3].

Face pigmentation relative to shape from shaping influences perceived sexual dimorphism classification [4-5] and female skin colour is lighter than males [6]. Among all facial features, the lip plays an important role in influencing attractiveness level. The intention behind such behaviour might be related to changing colour contrast in lightness and redness to enlarge femininity [7]. With the maturation during the adolescent period, prominent, red, supple and fuller lips are developed as one of the sexual dimorphism traits [8].

Apart from facial skin-feature contrast [1-3], face chromaticness can also be a clue in perceptual attractiveness [9]. Researchers found that lipstick colour can cause a unique pattern of simultaneous contrast in human faces, which is called the biological illusion [10]. Biological illusion explains the pattern of lightness induction that the geometric illusion on the human body turns to show assimilation instead of contraction. This has further confirmed this illusion by evaluating Japanese females 'preference for red and orange lipsticks, in which these two tones made faces look reddish and increased the level of yellowness in their skin [9-10].

So far, recent research has applied computer-generated photos to explore the pattern of changes in perceived face colour and skin colour tone. Four colours, pink, orange, red, and violet have been included in previous research [9] and colour selection in this research is based on these. To better recreate real-life situations and to include more various skin colours, real-person images will be used instead of computer-generated photos.

This research aims to evaluate the effect of lipstick colours on the perceived skin colour, in terms of the lightness, redness, yellowness, and attractiveness of facial images. To better represent the real-life situation, real facial images were captured and used in this experiment rather than computer-generated facial images.

METHODOLOGY

Ethics

This study was operated following the University of Leeds Ethical Guidance and the protocol is approved by the University of Leeds ethical review department. Consent for participation in this research was obtained from each individual participant. The information sheet written in English was given and explained before the experiment started.

Experiment

Stage 1: six lipsticks from the Maybelline Super-stay Ink Crayon Lipstick collection were selected for this research due to their colour vibrancy and matte texture. The colours selected covered a range of 1 light neutral (product No.90), 2 light pink (product No.15), 3 dark pink (product No.80), 4 dark neutral (product No.20), 5 orange-red (product No.115) and 6 dark purple (No.60) as shown in Figure 1.

Figure 1. Lipstick colour selected.

Ten Leeds-based Chinese females (age range 23-35 years; mean 26.6) participated in this stage to collect facial images with 6 lipstick colours and skin data. The participant is required to sit in the VeriVide light booth. The light booth provided a mid-grey background and an even, diffuse illumination of CIE D65 light resource. Six points from the bare face with no makeup (left cheekbone, right cheekbone, nose tip, chin, upper lip, lower lip as shown in figure 2) were measured by Konica Minolta Spectroradiometer CS-2000. Next, 6 lipsticks were applied to the participant in a certain order from light to dark. Images were captured after each stage of the lipstick application by a Canon EOS 6D Mark II digital camera with the setting of focus length 24mm, ISO 500, shutter speed 1/50, aperture f10 and manual exposure. The camera was controlled remotely by the Canon EOS Utility system which allows the position and the settings to remain unified. The distance between the face and the devices is 60 cm. Participants were required to look straight into the camera and perform a neutral facial expression during the entire experiment process. Figure 2 shows the environment of facial image capture and skin data measurement. Sixty facial images were captured in total.

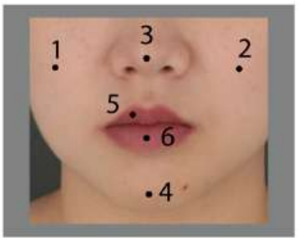

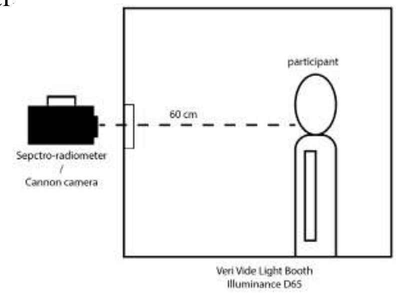

Figure 2. Example of a processed face **Figure 3. Stage1 settings**

To accurately present the facial colour and skin colour on the display, a series of characterisation processes were applied in the following procedures:

1. A camera characterisation model was built using the face and lip colour chart as the training dataset. The spectral power distribution (SPD) across 400-700 nm was measured at the interval of 1 nm for each of the colour patches using Konica Minolta Spectroradiometer CS-2000. The corresponding CIE XYZ tristimulus values were then calculated with the CIE1931 CMFs and the measured SPD of the 6500K illumination. In addition, the colour chart was captured at the same position as the human face using the digital camera with the same settings, and the average RGB values of each colour patch were derived from the captured image. Moreover, a subset of facial skin colour and lip colour data measured in this study was also used as a training dataset, including the CIE XYZ tristimulus values calculated from the measured SPD and RGB values derived from facial images. A third-order polynomial regression technique was applied as the mapping method to transform the RGB data of camera image to CIE XYZ tristimulus values [11]. Together with the training dataset, a prediction model for estimating skin and lip colours was generated. The model performance was evaluated using the training dataset as the testing dataset, and average CIELAB colour difference of all samples is 2.2. After the camera characterisation process, the RGB values of ever pixel of the facial images were transferred to CIE XYZ tristimulus values.

2. Given that the facial images need to be presented on a display, and the luminance of the display and the lighting booth was significantly different, a chromatic adaptation transform (CAT16) was applied to transform the CIE XYZ tristimulus values under the illuminant in the lighting booth to the CIE XYZ tristimulus values under the display luminance [12].

3. A gain-offset-gamma (GOG) model [13] was built for a professional BenQ display which was used in the experiment, transferring the CIE XYZ tristimulus values predicted after camera characterisation and chromatic adaptation transform to the display RGB values. The GOG model performance is good with the average CIELAB colour difference of grey scale colour patches 0.34.

All facial images captured in this experiment were processed in the order of camera characterisation, chromatic adaptation transform, and display characterisation. Last, characterised photos captured by the digital camera were cropped into 700x600 pixels. Only the lower face (from mid-nose to chin) was shown to the observer to reduce the influence of face features. Figure 4 shows ten model's skin colour in CIE L*a*b* value averaged by measure point 1 and 2.

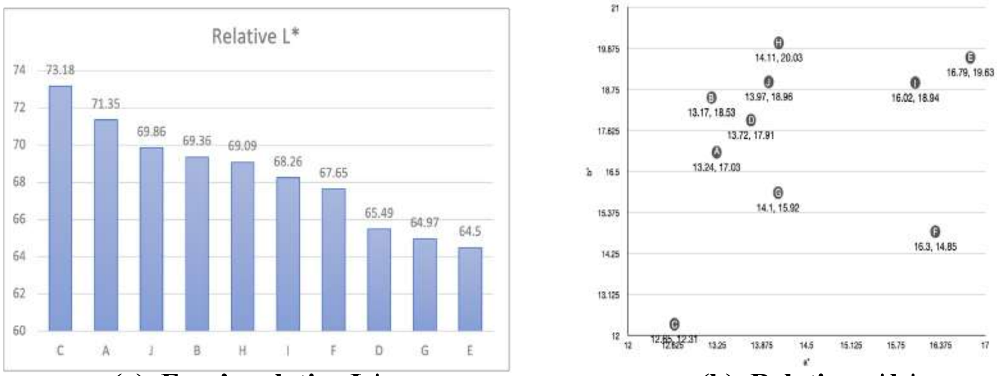

(a). Face's relative L* **(b). Relative a*b***

Figure 4. CIE L*a*b* value of faces

Stage 2: images collected from the previous stage were presented to 30 Chinese females (age range 23-36 years; mean 25.74) on a pre-characterised BenQ display. The interface of the experiment is shown in Figure 3. Images were set to a similar size as seen physically. The surrounding colour of the image was set to a mid-grey (L*=50). The Ishihara test was conducted on the same device before the experiment started. If qualified, the participant will be given an information sheet and consent form to explain the experiment. The participant was sitting in front of the BenQ monitor in a completely dark environment at a 40-centimetre distance from the screen. Sixty pictures were shown randomly to each observer to review. The 7-point Likert-type scale was used in the observer judgement to rate the perceived lightness, yellowness, redness, and attractiveness, where 1 refers to completely no influence and 7 refers to the most positive influence. Each observer conducted the experiment twice to ensure consistency.

lipstick	L*	a*	b*
1	56.81	28.93	12.28
2	56.18	36.56	5.84
3	51.21	39.93	4.06
4	52.69	34.19	16.07
5	49.60	44.75	20.07
6	42.54	41.53	1.37

Table 1. Lipstick on white paper

RESULT AND DISCUSSION

Results

30 responses were collected and filtered using Pearson's Correlation method for intra-consistency (r>0.5) The outcomes represent the perceived face colour in lightness, redness, yellowness and attractiveness.

Figure 5 shows a Pairwise comparison result referencing Lipstick 1. An ANOVA test shows that the influences of lipsticks on lightness, yellowness, and attractiveness regardless of skin are significant (p=0.000), but redness is not (p=0.164). Perceived Lightness (14 responses)： the mean of the responses is 3.485 (95% CI, ±0.186). Perceived redness (9 responses): the mean of the responses is 3.709 (95% CI, ±0.196). Perceived yellowness (20 responses): the mean of the responses is 3.709 (95% CI, ±0.196). Perceived attractiveness (20 responses): the mean of the responses is 3.118 (95% CI, ±0.148).

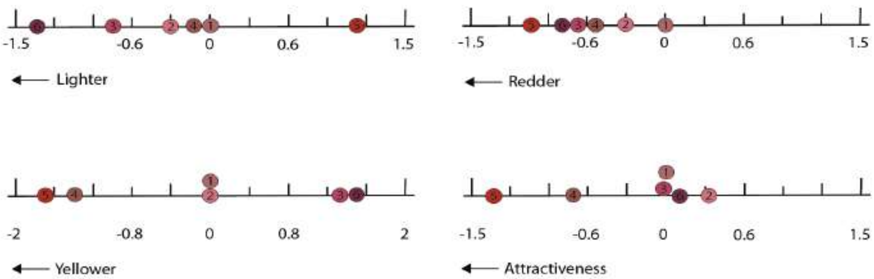

Figure 5. Pairwise comparison results, all faces

Discussion

Lightness: three colours: 2 light pink, 3 dark pink, and especially 6 dark purple have significantly made the skin brighter. The effect of pink colours brightening skin colour is consistent with previous study [10]. Dark purple has the greatest brightening effect among all colours while orange-red has the least. Neutral colours (1&4) perform similarly.

Redness: redness performance is similar to the red-green rank, apart from 2 and 4. These two lipsticks are similar in the red-green dimension but differ in b* the most. This result follows the pattern of biological illusion, an assimilation of lip colour to skin [10]. However, redness will not be included in the further discussion in this paper because the sample size of this measurement scale is relatively smaller and shows a low inter-group consistency (Cronbach's Alpha = 0.475). Future studies on how consistency can be improved will be conducted.

Yellowness: yellowness performance is similar to the yellow-blue value rank, apart from two light colours 1 and 2. This result also follows the skin colour assimilation pattern which a high yellowness colour will make skin appear warmer. However, the two light colours do not follow this skin assimilation pattern nor show a significant variance between these two colours, even though a relatively obvious difference in b* exists.

Attractiveness: with lightness: previous studies state that facial attractiveness is positively correlated to lightness and contrast in female faces as it enlarges sexual dimorphism [14]. The performance of 2, 3 and 6 might disagree with the lightness consensus. Similar to the previous study on the beauty and acceptance of lipstick colours, Chinese females find that pink and violet lip colours on the Japanese female average face are the least beautiful and acceptable [10]. Meanwhile, orange and red colours were rated the highest attractiveness score in the previous and this current study, regardless of perceptual lightness change [10]; with yellowness: it can be concluded from Figure 5 that 4 and 5 have made faces significantly yellower and are considered more attractive by observers. The preference for a yellower face is regarded as a healthier sign of higher carotenoid levels in the human body [15].

CONCLUSION

In conclusion, the lip colour biological illusion effect influences perceptual skin colour in a general pattern regardless of specific skin colour. Lipstick No. 4 and 5 perform the best on the attractiveness rating scale even though they did not make skin appear lighter. The results of high yellowness and redness assimilation are preferred to high lightness might indicate that facial attractiveness is more related to health rather than feature-face contrast. In other words, healthiness is regarded as more important compared to sexual dimorphism in Chinese female observers. Although it has not been discussed in this paper, the ten individuals' results showed various significances, especially in the yellowness and attractiveness dimensions. Future studies will further explore how each lipstick colour interacts with different types of skin colour among Eastern Asian and Caucasian females.

REFERENCES

1. Russell, R. (2010). Why Cosmetics Work. In Adams, R, B., Ambadu, N., Nakayama, K., & Shimojo, S (Eds.), *The Science of Social Vision* (pp.186-203). Oxford University Press.

2. Perrett, D, I., Lee, K, J., Penton-Voak, I., Rowland, D., Yoshikawa, S., Burt, D, M., Henzi, S, P., Castles, D, L., & Akamatsu, S. (1998). Effects of sexual dimorphism on facial attractiveness. *Nature,* 394, 884-887.

3. Rhodes, G., Yoshikawa, S., Palermo, R., Simmons, L. W., Peters, M., Lee, K, Halberstadt, J., & Crawford, J. R. (2007). Perceived health contributes to the attractiveness of facial symmetry, averageness, and sexual dimorphism. *Perception*, 36(8), 1244–1252.

4. Bruce, V., & Langton S. (1994). The use of pigmentation and shading information in recognising the sex and identities of faces. *Perception*, 23(7), 803-822.

5. Russell, R. (2003). Sex, Beauty, and the Relative Luminance of Facial Features. *Perception*, 32(9), 1093-1107.

6. Carrito, M, L., & Semin, G, R. (2019). When we don‘t know what we know. *Cognition*, 191(2019), Article 103972.

7. Danel, D., & Pawlowski, B. (2007). Eye-mouth-eye angle as a good indicator of face masculinisation, asymmetry, and attractiveness (Homo sapiens). *Journal of Comparative Psychology*, 121(2), 221-225.

8. Samal, A., Subramani, V., & Marx, D. (2007). Analysis of sexual dimorphism in human face. *Journal of Visual Communication and Image Representation*, 18(6), 453-463.

9. Kiritani, Y., Tong, X.,&Chang, I. (2021). Prior makeup experience determines whether similar colours are suitable for complexions. *Journal of Science of Design*, 5(1), 97-104.

10. Kiritani, Y., Okazaki, A., Motoyoshi, K., Takano, R., & Ookubo, N. (2017). Color illusion on complexion by lipsticks and its impression. *J-STAGE*, 36(2), 4-16.

11. He, R., Xiao, K., Pointer, M., Bressler, Y., Liu, Z., & Lu, Y. (2022). Development of an image-based measurement system for human facial skin colour. *Colour Research and Application,* Article 814158.

12. Li, C., Li, Z., Wang, Z., Xu, Y., Luo, M. R., Cui, G., Melgosa, M., Brill, M. H., & Pointer, M. (2017). Comprehensive color solutions: CAM16, CAT16, and CAM16-UCS. *Colour Research and Application*, *42*(6), 703–718.

13. R.S. Berns. (1996). Methods for characterising CRT displays. *Displays*, 16(4), 173-182.

14. Jones, A., Russell, R. & Ward, R. (2015). Cosmetics Alter Biologically-Based Factors of Beauty: Evidence from Facial Contrast. *Evolutionary Psychology*, 13(1), p.147470491501300.

15. Stephen, I. D., Coetzee, V., & Perrett, D. I. (2011). Carotenoid and melanin pigment coloration affect perceived human health. *Evolution and Human Behavior, 32*(3), 216–227.

COLOR CHANGE OF THE TEN SYMBOLS OF LONGEVITY CADETS IN THE LATE JOSEON DYNASTY

Wona Lhi[1] , Gyoungsil Choi[2]

[1] *Master Course, Color Design, Ewha Womans University, Seoul, Republic of Korea*
[2]*Professor, Color Design, Ewha Womans University, Seoul, Republic of Korea*

*Corresponding author: Gyoungsil Choi, gschoi@ewha.ac.kr

ABSTRACT

The ten symbols of longevity is an auspicious picture that expresses the rise and fall of the world, such as immortality and longevity. Although the origin form of the ten symbols of longevity has not been revealed, it can be seen through literature that it has been passed down as the custom of Sehwa(*a picture the king gives to his servants at the beginning of the year*) since the end of the Goryeo Dynasty. Most of the extant ones were painted in the late Joseon Dynasty. It in the late Joseon Dynasty were classified according to their pictorial characteristics. 'Type 1' is relatively outdated. 'Type 2' is influenced by Western Painting in the period. 'Type 3' is similar to Obongbyeong(*Sun and Moon and Five peaks*) or Bandohwa(*The Sun, the Moon, and Sacred Peachese*). This study aims to analyze the color change of paintings in connection with the phenomenon of social change in the late Joseon, focusing on the iconography of the ten symbols of longevity in the late Joseon Dynasty. Representative digital screen colors of 'Type 1', 'Type 2', and 'Type 3' were obtained from the NCS color index. The RGB and $L^*a^*b^*C^*$ values of colors were obtained from using the CIELAB. As social changes occurred in the late Joseon Dynasty and natural pigments were replaced by artificial pigments in the West, the expression of color gradually changed from relatively old to highly saturated colors. It is particularly noteworthy that the color change is blue and green. By replacing azurite with Prussian blue and malachite with emerald green, the colors became more vivid than in previous paintings. As a result of examining the color characteristics, the colors of painting expression, which were suppressed under the influence of Neo-Confucianism in the early and middle Joseon Dynasty, changed to bright colors.

Keywords: Ten Symbols of Longevity (*Sibjangsaengdo*), Color Analysis, Joseon Dynasty

INTRODUCTION

The ten symbols of longevity, known as "Sipjangsaengdo" in Korea (From then on, it is called Sipjangsaengdo), depicted the desire for longevity and were a significant theme in Korean traditional paintings. Since the mid-Joseon period, they have become popular among the public as auspicious paintings, reflecting the spread of longevity culture. The philosophical background of Sipjangsaengdo was influenced by Taoism (Doism) and folk tales related to divine beings. Although Confucianism was the dominant ideology of the Joseon Dynasty, the royal court sought stability and power through the mythical world of Taoism and Buddhism in their court rituals and daily lives. During the early Joseon period, the emphasis on Confucianism as the foundation of the nation's ideology and the social order based on the class system led to a restrained use of colors in paintings, thus resulting in a monochromatic expression. However, with the rise of Silhak(R*ealist school of Confucianism*) in the late Joseon Dynasty, the development of agriculture, commerce, and the weakening of the class system allowed the general public to emerge as creators and consumers of paintings. As a result, decorative color paintings created by Dohwaseo (Painting bureau) began to adorn not only the royal palaces but also the living spaces of commoners, leading to a revival of color expression that had been passed down since before the Joseon period. Similar to the transformation of painting styles influenced by the times, Sipjangsaengdo also underwent changes in its form and color over time, while adhering to the traditional techniques and formats of Dohwaseo. Furthermore, the increased use of artificial pigments such as Prussian blue and malachite significantly influenced the color transformation of Sipjangsaengdo.

To date, there has been a lack of detailed color analysis studies on Sipjangsaengdo. Based on previous research (Park, 2002), this study focuses on three representative types of Sipjangsaengdo from the late Joseon Dynasty known to the academic community. The aim is to analyze the composition and color variations in the paintings according to the ideological and social changes of the period, with a particular focus on the influence of pigment changes on the color transformation of Sipjangsaengdo of during the period.

METHODOLOGY

Data Collection and Analysis Targets

The analysis focuses on the types of Sipjangsaengdo classified by the research on them during the later period (Park, B. S., 2002). Korean traditional paintings can be broadly categorized into four periods: ①early period (1392-1550), ②mid-period (1550-1700), ③late period (1700-1850), and ④the last period (1850-1910) based on stylistic changes. <Table 1> divides Sipjangsaengdo of the late Joseon period into three formats based on their painting characteristics.

'Type 1' represents the early period with the influence of the classical styles and the characteristics of Hwawon(a king's painters) painting style from the mid to late period. The colors are relatively low in brightness and saturation. The composition emphasizes undulating waves, and only white cranes are depicted in this format. 'Type 2' represents the typical Sipjangsaengdo during the late and the last periods. It shows the influence of Western Painting with spatial depth and perspective. Compared to 'Type 1', it has higher brightness and saturation, with a predominant blue-green color. The cranes are depicted in white, blue, and yellow. 'Type 3' is the only one with a known year of production (1800). It has higher brightness and saturation than 'Type 1' and 'Type2', and the peaches disappear, while the use of Prussian blue intensifies the blue color and shows high chromaticity in pigmentation.

Figure 1. Sipjangsaengdo in chosun Dynasty

Table 1: Types of Sipjangsaengdo (Park, 2008)

	classification	Type1(unknown)	Type 2 (unknown)		Type 3(1880)
characteristics	possession	National Museum of Korea	Hoam Art Museum(**H**)	National Palace Museum(**N**)	Oregon Univ.Museum
	wave	Prominence	diminished	disappeared	disappeared
	peach	Week expression	emphasised	emphasised	disappeared
	white deer	white deer	disappeared	disappeared	disappeared
	crane	white crane	white crane, blue crane, yellow crane	white crane, blue crane, yellow crane	white crane, blue crane, yellow crane
	color	vert-blue	blue-green	increased use of blue	a deep blue
	tone	dark grayish,	deep	strong	vivid

	composition	Three god mountain	High mountains and deep valleys	High mountains and deep valleys	High mountains and deep valleys
	perspective		○	○	
	pigment	Malachite, azurite	Prussianblue(Prominence)	Malachite, Emerald green , Prussian blue	Malachite, Emerald green , Prussian blue

The components of Sipjangsaengdo

The 13 types of components representing Sipjangsaengdo are the sun, moon, clouds, mountains, rocks, water, turtles, cranes, deer, bamboo, pine, yeongji (ganoderma), and peaches. 'Ten' in the Ten Symbols of Longevity is just not a number, but means 'completeness,' 'fullness,' 'infiniteness,' and 'eternity. Components are emphasized or disappeared depending on the time.

Analysis Method Components of Sipjangsaengdo

① Estimating the colors of the 13 components in the four types of Sipjangsaengdo using digital data and the NCS (Natural Color System) index.

② Obtaining the RGB values of the estimated colors.

③ Obtaining the $L^*a^*b^*C^*$ values.

④ Plotting the L^*C^* and a^*b^* graphs to analyze the colors.

RESULT

Analysis of a^*b^* Graphs for Each Type of Sipjangsaengdo

For the analysis of a^*b^* graphs, it is observed the color variations within each type of Sipjangsaengdo.

Referring to <Figure 2> , The Type 1 is a standard.

①Pine Trees : Columns

In the case of Type 2 (Hoam Art Museum, **H**) pine trees, the colomns are divided into two colors: brown and orange. When compared with Type 1 pine tree as a standard, Type 2 (Hoam Art Museum) pine trees exhibit a more yellowish hue and higher saturation, showing two distinct color variations. Type 2 (National Palace Meseum, **N**) pine trees have significantly higher saturation and a more reddish hue compared with the Type 1.

Type 3 (Oregon) pine trees also have higher saturation and a reddish hue compared with Type 1 , but the saturation and lightness are slightly lower than those of Type 2 (**H**).

②Pine trees : needles

Type 2 (**H**) pine needles exhibit color variations between a yellowish and a bluish. Type 2 (**N**) pine needles have higher saturation and appear green in color than Type 2(**H**).

Type 3 pine needles have a slightly more yellowish hue compared to Type1 and Type 2.

③Green rocks :

The green rocks changed to a higher level of green saturation in type 2(**H,N**) and then lowered the saturation again in type 3.

④Blue rocks :

The blue rocks changed to a highly saturated blue in type 2(**H,N**) and blue with red added in type 3.

The analysis of the a^*b^* graphs provides insights into the color variations and characteristics of each type of Sipjangsaengdo. The graphs visually represent how the colors change within each type, highlighting differences in saturation, hue, and lightness.

Analysis of L^*C^* Graphs and Tone for Each of Types

By examining the L^*C^* graphs and analyzing the tone variations, the following observations can be made:

Referring to < Figure 3>, which shows the L^*C^*

As it moves from Type 1 to Type 2(**H,N**) to Type 3, there is a gradual increase in overall lightness (L^*) and chroma (C^*).

This indicates that the colors become brighter and more saturated as changing from Type 1 to Type 3.

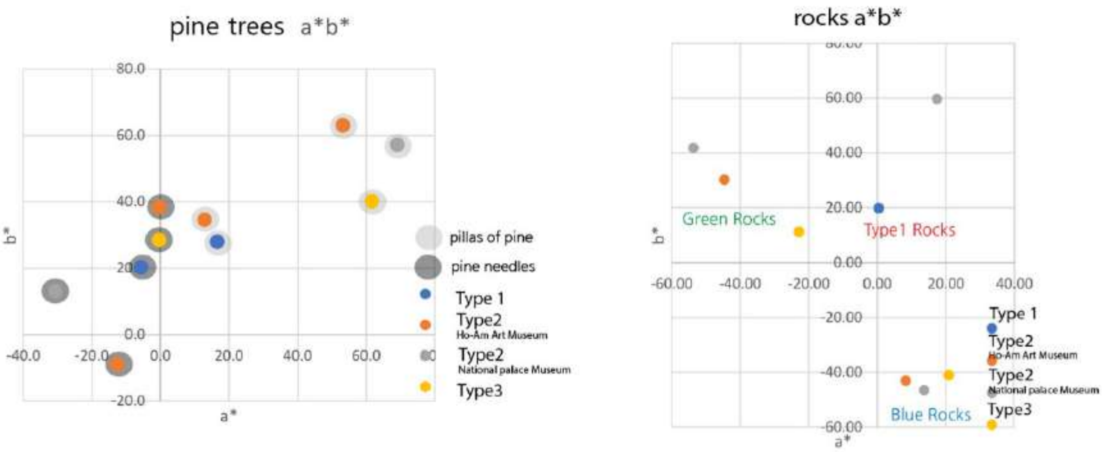

Figure 2. Sipjangsaengdo **by types- Pine Trees, Rocks a^*b^* Graph**

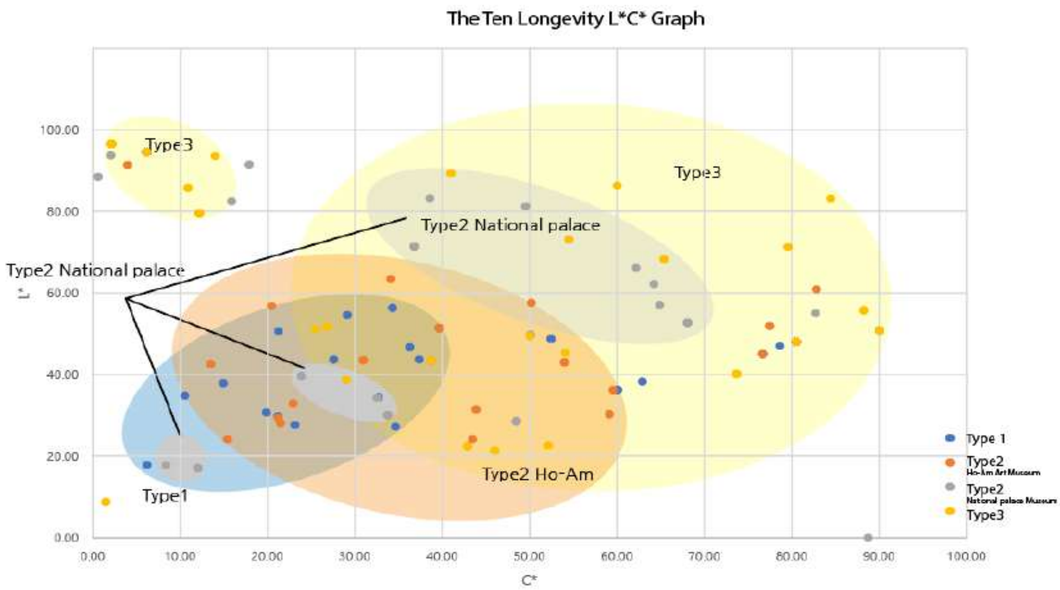

Figure 3. Sipjangsaengdo **by Types L^*C^* Graph**

Referring to < Table 2>, which describes the tone variations:

The colors transition from dark grayish to vivid as we move from Type 1 to Type 3.

It means that the overall tones of Sipjangsaengdon from Type 1 to Type 3 become more vibrant and lively.

Table 2: Tone analysis of Sipjangsaengdo

L*C* Tone		
Type 1	National Museum of Korea	dark grayish, grayish, dull, soft
Type2	Ho-Am Art Museum(**H**)	dark grayish, light grayish , soft, deep
	National Palace Museum of Korea(**N**)	dark grayish ,dull, pale, strong
Type3	The Oregon University Museum	dull, pale, deep, strong, vivid,

The analysis of the L^*C^* graphs and tone variations provides insights into the brightness, saturation, and overall tone changes within each type of Sipjangsaengdo. It demonstrates the gradual shift towards brighter and more vivid colors as we progress through the different types.

DISCUSSION

In the mid-Joseon Dynasty, the use of blue and green pigments increased as restoration projects were carried out due to wars and civil wars. However, because of the lack of natural pigments, they were mixed with imported pigments and used. In the late Joseon Dynasty, traditional natural (mineral) pigments were replaced by western artificial pigments as inexpensive western synthetic pigments were imported through neighboring countries. Documentary paintings of the 17th and 18th centuries used green with malachite, blue with azurite or organic blue pigments. Malachite and azurite are natural pigments that have been used in the East and West since ancient times.

After the 19th century, Western pigments such as emerald green and Prussian blue appeared. These pigments produced more intense and distinct color effects than conventional pigments. Malachite was used with emerald green, but azurite was not used with Prussian blue. In the 19th century there was a slight price difference between malachite and emerald green, and a large price difference between azurite and Prussian blue. Therefore, the expensive azurite was not commonly used. Synthetic organic pigments were gradually used in court paintings because of their high chroma and excellent color development and blending. After the 19th century, black, white and red pigments such as lead white, vermilion and organic red continued to be used, while green and blue pigments were replaced by Western pigments such as emerald green and Prussian blue.

In the early Joseon Dynasty, Northern school of painting led the art world that has no objection to the use of color. However, the influence of Confucianism reduced the demand for vivid colors and the use of color. In the mid-Joseon period, a style of painting that emphasized the virtues of classical scholars appeared, and paintings were drawn with ink rather than using color. During this period, Confucian aesthetics, which regarded simplicity as a virtue, reached its peak. The production of decorative paintings itself was discontinued, and court paintings emphasizing colors were renewed. In the case of Buddhism, many line paintings were produced excluding colors. However, in the late Joseon Dynasty, color expression became free and rich due to the influence of Silhak and the import of pigments. In genre paintings and folk paintings, various colors were used to express vitality and symbolic elements. This enabled the art of the late Joseon Dynasty to realize a variety of colors and freedom of expression.

The introduction of Silhak and the substitution of pigments influenced the colors of paintings in the late Joseon Dynasty. There are previous studies that show that the color of the ten symbols of longevity has changed over time. From the early Joseon Dynasty to the late Joseon Dynasty, the use of green, blue, and red tended to stand out in paintings. This can be explained by the influence of western pigments such as Prussian blue, emerald green, and carmine, which were introduced to Joseon in the late 19th century and have high chroma.

In particular, Type 3 of Sipjangsaengdo , the color of the green rocks was changed to a greenish tone with yellow added, and the color of the blue rocks was highly saturated and lively by using Prussian blue. This means that Sipjangsaengdo were painted in the splendid bluish-green color of Guyeong's(仇英1482-1559) painting style, in which the green color is subtly painted and blue color is painted on top of it, and the sharp contrast between green and blue stands out.

Based on these research results, it can be inferred that the color change of Sipjangsaengdo in the late Joseon Dynasty had an effect.

In conclusion, Sipjangsaengdo during the late Joseon Dynasty underwent changes in composition and coloration in accordance with the historical context. These changes resulted in a transformation of color from dark and low-saturated gray tones to vibrant and highly saturated hues. These changes were influenced by the societal change of the late Joseon period, including the introduction of practical learning (silhak) and the adoption of new pigments.

CONCLUSION

In the late Joseon Dynasty, as the composition of Sipjangsaengdo paintings changed according to the flow of the times, there was a change in color from low chroma and low brightness to high chroma and high brightness.

REFERENCES

1. Park, B.S. (2002). *A Study of Late Joseon Dynasty Ten Symbols of Longevity*. Master's Thesis, Graduate School of Hongik University, Seoul.
2. Park, B.S. (2008). *A Study of Ten Symbols of Longevity Screens in the Collection of the Oregon University Museum* : National palace Museum of Korea. Gogung Cultural Journal, No. 2, National Palace Museum, Seoul.

EFFECT OF COLOR QUANTIZATION ON COLOR HARMONY

Shreeniwas Sharma[1]*, Jyoti Tandukar[2] and Rabindra Bista[3]

[1]*PhD Student, Dept. of Computer Science and Engineering, Kathmandu University, Nepal.*
[2]*Associate Professor, Dept. of Electronics and Computer Engineering, Institute of Engineering, Tribhuvan University, Nepal.*
[3]*Associate Professor, Dept. of Computer Science and Engineering, Kathmandu University, Nepal.*

*Corresponding Author: Shreeniwas Sharma, shree220@gmail.com

ABSTRACT

Among the many approaches to the study of color harmony tried so far, a relatively recent method is to leverage the large number of human-created and ranked color palettes, such as those hosted at colourlovers.com. Analysis of these large datasets could provide insights into the nature of color harmony, but is usually overwhelming because of the sheer number of slightly differing colors. This paper discusses the possibility of quantizing the colors in these color palettes to a manageable set of discrete colors without significantly affecting the aesthetics of the palette. One method of quantization is to map the palettes from continuous color space to the set of 2744 perceptually uniform colors provided by the Munsell renotation data. Another method of quantization is to perform a K-means clustering of the colors of all the palettes to get a set of limited colors. For comparison purposes, this paper divides the colors into 2744 clusters in CIELAB color space and quantizes to their centroids. It was found that the quantization error was minimum for the latter method. Colors from both the original and quantized color palettes were applied to a pattern. Several such combinations were presented to the respondents in random order and asked to like or dislike the colored pattern. It was found that when respondents liked a colored pattern, they also liked the same pattern colored with the quantized color palette. Likewise, when they disliked a colored pattern, they also disliked the pattern with the quantized color palette. This means that color quantization has minimal impact on the harmony perception of the color palette. This simplification makes it possible to perform further analysis on the relationships of colors for color harmony. Considering the quantized colors as words and palettes as sentences, it is now possible to use methods such as the n-Gram approach to create new color combinations.

Keywords: color harmony, large datasets, color quantization, Munsell color space, K-means clustering

INTRODUCTION

Background

Color harmony is the aesthetically pleasing arrangement of colors within a composition. It is a fundamental concept in design, art and visual composition. Color harmony is important in different fields such as graphic design, interior design, fashion, fine arts etc. Currently, it is a multi-disciplinary study involving principles from physiology, psychology and technology for creating visually impactful and engaging compositions.

Color and color arrangement has been piquing the interest of scholars of all times since Aristotle, Sir Isaac Newton, Johann Wolfgang von Goethe, ME Chevreul, Johannes Itten to name a few [1]. The 20th century saw continued development in the study of color harmony with new theories and advancements in technology influencing the field. Albert H. Munsell, an American painter and teacher, developed the Munsell Color System, a three-dimensional model for describing colors based on hue, value and chroma. Munsell's work has had a lasting impact on the study of color harmony and has been widely used in various industries.

In the 21st century, the study of color harmony has continued to evolve, with researchers incorporating advancements in technology, cognitive science and cultural studies. In recent times, there has been a rapid increase in the number of human-created harmonious color combinations. At sites like colourlovers.com, color.adobe.com, coolors.co, users have created and ranked a large number of colors and color palettes. This study focuses on the data available at colourlovers.com which provides an API [2] that gives access to the full range of data that it has collected since 2005. Currently, there are 10 million colors, 5 million color palettes and 6 million colored patterns available for analysis of color aesthetics and color harmony.

In a study by O'Donovan et al. [3], the authors proposed an algorithm to extract harmonious color palettes from large datasets, specifically utilizing data from colourlovers.com. They analyzed over 200,000 color palettes from colourlovers.com and used an optimization-based approach to generate a compatibility model for color palettes. The study showcases the potential of using large datasets from online communities to study color harmony trends and preferences.

The Problem

The problem with using large datasets of colors to study color harmony is that there are several recurrences of colors that appear similar, but are considered different by algorithms because their numerical values vary slightly. This study aims to establish that it is possible to quantize the large dataset of colors to a limited set of colors without significantly affecting the user's preference with regard to color harmony.

As per Burchett [4], color preference may vary by different attributes such as order, similarity, association, area, interaction and configuration. The user may like or dislike a color or color palette based on these parameters, but the user's response should be the same for a slightly different color, or a palette consisting of slightly different colors.

Objective

The objective of this study is to perform quantization of color palettes using different methods. By presenting the original color palette and quantized color palette in random order, the user is asked to like or dislike the color palette. It is expected that users who like the original color palette will also like the quantized color palette. Users who dislike the original color palette will also dislike the quantized color palette. By doing this experiment, this study aims to establish that the perception of color harmony is not affected by minor changes in the individual colors such as those introduced during color quantization.

METHODOLOGY

Data Acquisition

The top ranked color palettes from colourlovers.com were acquired with a syntax such as https://www.colourlovers.com/api/palettes/top?format=json&showPaletteWidths=1&numResults=100&resultOffset=0. The resultOffset can take values such as 100, 200 and so on up to 900 resulting in the top 1000 color palettes. Adding a hueOption parameter (with values being one of red, orange, yellow, green, aqua, blue, violet, and fuchsia) to the syntax provides access to 8000 more palettes, which include the top 1000 palettes too. A majority of color palettes in colourlovers.com have 5 colors. Out of the 8000 color palettes, 7152 had 5 colors. This study makes use of these 7152 color palettes.

Color Quantization

Color quantization is the process of mapping colors in a continuous color space to the closest color in a set of discrete colors. Color quantization is usually considered in the context of images where the number of distinct colors used in the image is reduced while maintaining visual quality [5]. Here, we use color quantization in the context of color palettes. The colors in the color palettes downloaded from colourlovers.com can take on any value from continuous color space.

Several methods are available for color quantization including median cut algorithm, octree quantization, uniform quantization and K-means clustering. In this study, we use uniform quantization and K-means clustering.

Color Distance Formula

In this study, the K-means clustering algorithm uses the CIE76 color distance formula (Eq. 1) for performance reasons.

$$\Delta E_{ab} = \sqrt{(L_2^* - L_1^*)^2 + (a_2^* - a_1^*)^2 + (b_2^* - b_1^*)^2} \quad (1)$$

While quantizing the continuous color space to discrete color space, the CIEDE2000 color distance formula (Eq. 2) is used.

$$\Delta E_{00} = \sqrt{\left(\frac{\Delta L'}{k_L S_L}\right)^2 + \left(\frac{\Delta C'}{k_C S_C}\right)^2 + \left(\frac{\Delta H'}{k_H S_H}\right)^2 + R_T \frac{\Delta C'}{k_C S_C}\frac{\Delta H'}{k_H S_H}} \quad (2)$$

where $\Delta L'$, $\Delta C'$ and $\Delta H'$ are differences in lightness, chroma and hue between two colors respectively. S_L, S_C, and S_H are weighting functions for lightness, chroma, and hue, and R_T is a rotation term that compensates for the interaction between chroma and hue. k_L, k_C, and k_H are parameters that depend on the viewing conditions.

Uniform Color Space

For uniform quantization, we use the Munsell color system (Figure 1).

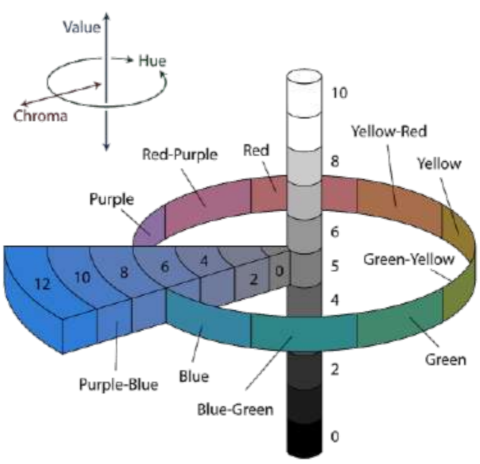

Figure 1: The Munsell color system, showing a circle of hues at value 5 chroma 6, the neutral values from 0 to 10 and the chromas of purple-blue (5PB) at value 5.[1]

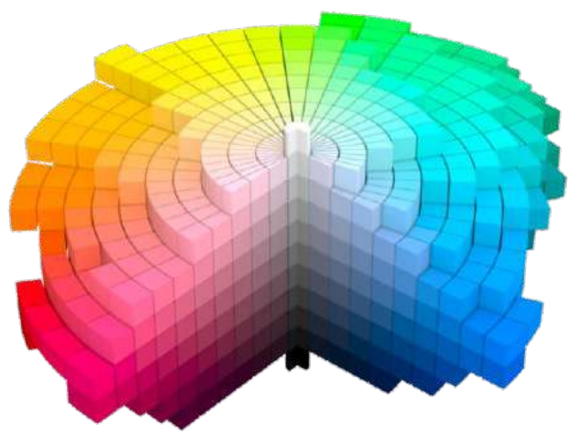

Figure 2: Three-dimensional representation of the 1943 Munsell renotation (with a portion cut away).[2]

The Munsell color space is a three-dimensional color space developed by Albert H. Munsell in the early 20th century. It is based on the concept of a perceptually uniform color space where equal distance between colors represents equal differences in perceived color. The color space

[1] From *The Munsell color system* [Diagram], by Jacob Rus, 2007, Wikimedia Commons. (https://commons.wikimedia.org/wiki/File:Munsell-system.svg). CC BY-SA 3.0.
[2] From *sRGB approximation of the Munsell renotations* [Illustration], by Michael Horvath. Wikimedia Commons. (https://commons.wikimedia.org/wiki/File:Munsell_1943_color_solid_cylindrical_coordinates.png). CC BY-SA 3.0

is organized in the form of a color tree, with hue (H) as the circular axis, value (V) as the vertical axis and chroma (C) as the radial axis.

The Munsell renotation data (Figure 2) is a set of numerical values that describe the Munsell color space in terms of the CIE XYZ color space. The renotation data consists of a table of Munsell color samples, where each sample is represented by its Munsell hue, value and chroma coordinates (HVC) along with its corresponding CIE XYZ tristimulus values. The renotation data are currently made publicly available by the Munsell Color Science Lab Educational Resources at http://www.rit-mcsl.org/MunsellRenotation/real.dat [6].

This study uses 2734 colors from the renotation data and 10 additional neutral values from black to white to quantize palettes from continuous color space in order to study the effect of quantization on the aesthetics of the palette.

K-means Clustering

The K-means algorithm is one of the most widely used methods for data clustering. Colors in continuous CIELAB space can be represented as a data set $X = \{x_1, \ldots, x_N\} \in \mathbb{R}^3$. K-means clustering partitions X into K exhaustive and mutually exclusive clusters $S = \{S_1, \ldots, S_K\}$ by minimizing the sum of squared errors $SSE = \sum_{k=1}^{K} \sum_{x_i \in S_k} \|x_i - c_k\|^2$ where $\|\ \|$ denotes the Euclidean (L_2) norm and c_k is the centroid of the cluster S_K calculated as the average of points that belong to this cluster [7].

In this study, 7152 palettes with 5 colors each were considered, so N = 7152×5 = 35760. K is taken to be 2744 for comparing with the quantization to Munsell color space described above. The algorithm is started with K arbitrary centers chosen uniformly at random from the data points. Each point is assigned to the nearest center and each center is recalculated as the mean of all points assigned to it.

User Validation

A set of 24 patterns with 5 colors each were selected. Each pattern was colored with a random palette, a version of the palette quantized to 2744 colors from the Munsell color space and a third version of the palette quantized to 2744 K-means clusters. An app was developed to present 150 of such images in random order interspersed with 350 other colored versions of the same 24 patterns to 20 respondents. The respondents were asked to like or dislike the colored patterns. To check the consistency of the responses, 50 check images were also introduced. The check images were the same as the original images. If the responses for check images were different than the response for the original image in 75% of the cases, the respondent's response was discarded.

RESULT AND DISCUSSION

The 35760 colors from the 7152 palettes, the 2744 discrete colors from Munsell color space and an equal number of K-means clusters were plotted in CIELAB color space. The results are shown in Figure 3. The colors from the palettes were quantized to the Munsell color space and to the K-means clusters. As expected, the quantization error was less in the case of the K-means clustering. The quantization error analysis is summarized in Table 1.

Table 1: Quantization Error Analysis

Quantization error while quantizing to	Mean	Median	SD
Munsell Colors	2.66	2.56	1.21
K-means Centroids	1.62	1.49	0.85

It is also possible to iteratively reduce the number of K-means centroids to find the number of centroids that result in the similar quantization error statistics as quantizing to the Munsell colors. This number was found to be 770 centroids.

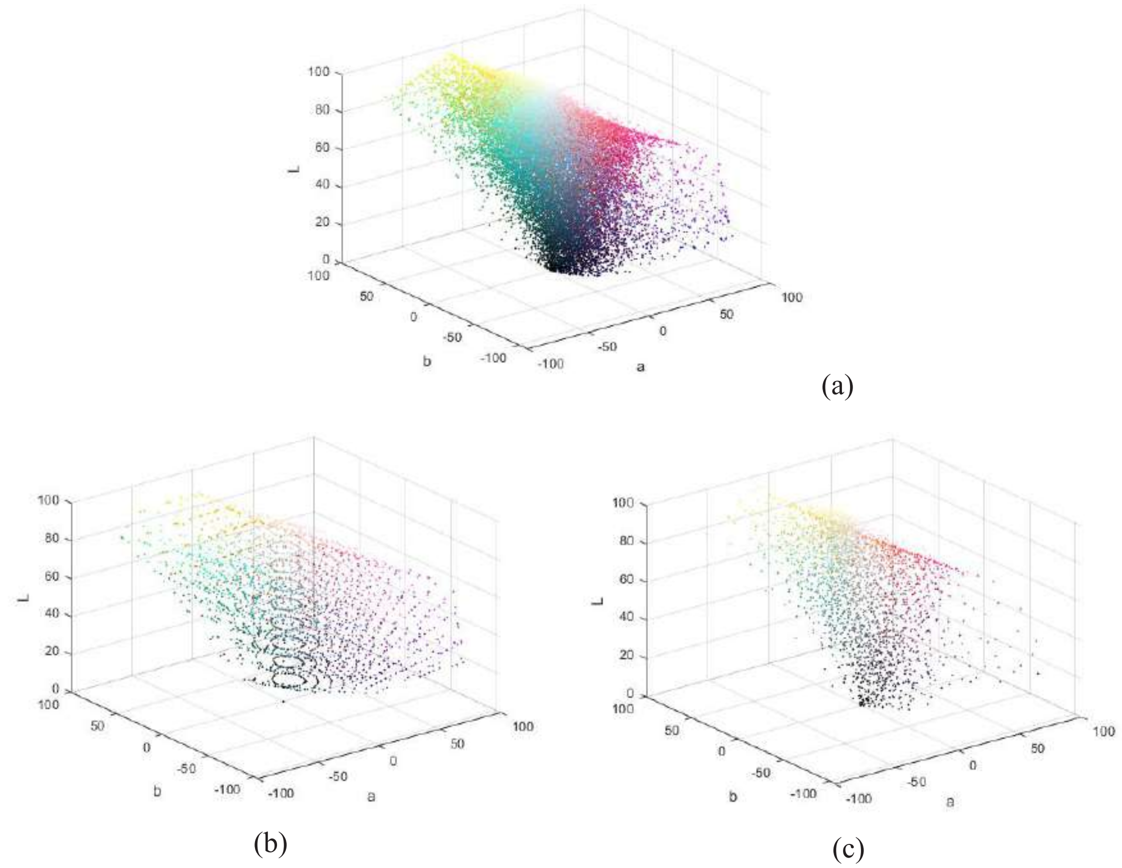

Figure 3: Colors plotted in CIELAB color space. (a) the 37560 colors from 7152 palettes, (b) the 2744 colors from Munsell renotation data and (c) 2744 K-means cluster centroids

While quantizing the colors, individual colors are perceptibly different, but the harmony perception of the color palettes is unaltered. This is illustrated in Figure 4.

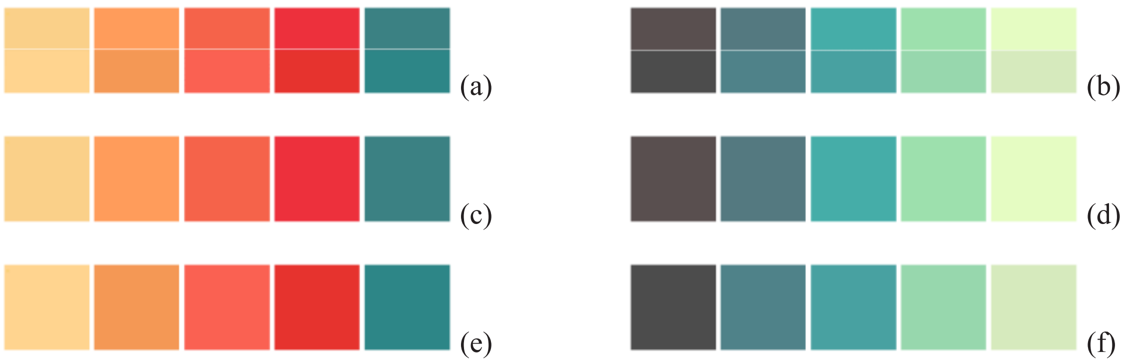

Figure 4: Two example color palettes with versions quantized to K-means clusters with average $\partial E = 1.22$ (left) and with average $\partial E = 2.17$ (right). In (a) and (b), the individual color differences are perceptible. In (c) original and (e) quantized, as well as (d) original and (f) quantized, the perception of color harmony remains unaltered.

A total of 20 respondents participated in the survey. The results of 3 respondents were discarded because the consistency of responses among original and check (repeating the original) images were not same in more than 75% of the cases. The responses of the remaining 17 participants are summarized in Table 2.

Table 2: Likelihood that the respondent likes/dislikes the original image and gives the same response for the quantized palette

Check palette (same as original palette)	Palette quantized to discrete Munsell color space	Palette quantized to K-means clusters
85.2%	82.7%	82.8%

It follows that in 97% of the cases that a respondent would like/dislike the original image, the user would give the same response for the quantized image too.

This establishes that quantizing colors to K-means clusters of the colors do not significantly affect the perception of harmony of a color palette. This may simplify further studies on color harmony. For instance, it would now be possible to test an n-Gram approach to creating new color combinations.

Each quantized palette with 5 colors would be a sentence composed with words from a dictionary of 2744 words. A palette of 5 colors has 120 permutations, so 7152 palettes would result in a corpus of 7152×120 = 858240 sentences. With this information, it is possible to compute the probabilities of all possible bigrams and trigrams. Using bigrams and trigrams, it is possible to construct new sentences, i.e., color combinations. This approach for creating harmonious color combinations would be difficult without quantizing the color palettes.

CONCLUSION

The subject of color quantization of images has been well studied but the quantization of harmonious color palettes, not so much. This study applied some of the color quantization methods to crowdsourced color palettes and demonstrated that the quantization of colors of a palette does not significantly affect the harmony perception of the color palette. This leads to simplification of analytical studies on color harmony.

REFERENCES

1. Chamaret, C. (2016). *Color harmony: experimental and computational modeling* (Doctoral dissertation, Université Rennes 1).
2. https://www.colourlovers.com/api/ retrieved on Feb 22, 2023.
3. O'Donovan, P., Agarwala, A., & Hertzmann, A. (2011). Color compatibility from large datasets. In *ACM SIGGRAPH 2011 papers* (pp. 1-12).
4. Burchett, K. E. (1991). Color harmony attributes. *Color Research & Appl.*, *16*(4), 275-278.
5. Celebi, M. E. (2023). Forty years of color quantization: a modern, algorithmic survey. *Artificial Intelligence Review*, 1-82.
6. https://www.rit.edu/science/munsell-color-science-lab-educational-resources retrieved on Aug 31, 2023.
7. Celebi, M. E. (2011). Improving the performance of K-means for color quantization. *Image and Vision Computing*, *29*(4), 260-271.

INFLUENCE OF COLOR APPEARANCE ON DICHROMATS' SUPERIORITY IN THE VISUAL SEARCH TASK WITH COLOR

Hector A. Palomo[1]*, Tsukasa Muraya[2], and Shoji Sunaga[3]

[1] Graduate School of Design, Kyushu University, Japan.
[2]Faculty of Contemporary Social Studies, Chikushi Jogakuen University, Japan.
[3]Faculty of Design, Kyushu University, Japan.

Corresponding author: Hector Palomo hpalomo1@gmail.com

ABSTRACT

In addressing the unexpectedly high prevalence of congenital red-green color blindness, an intriguing hypothesis has emerged, suggesting that individuals with dichromacy might possess a distinct advantage in detecting specific forms of color camouflage. The goal of the present study was to investigate why the performance of dichromats is superior to that of trichromats in the case of Hishikawa et al.'s experiments, from the viewpoint of the differences in dichromats color appearance. Our investigation comprised three experiments. Experiment 1 aimed to verify the existence of specific conditions indicating an advantage of dichromacy in the visual search task, using a target color and two distractor colors. In Experiment 2, the effect of prior knowledge about the target color was examined. Experiment 3 employed the elementary color-scale method to quantify the color appearance of the displayed colors, namely the target colors and distractor colors, assigning a total of 10 points to whiteness, blackness and chromaticness. If the points were assigned to chromaticness, an additional 10 points were allotted to the redness, yellowness, greenness, and blueness of the chromaticness. Results from Experiments 1 and 2 demonstrated that the deuteranopic participant could more-readily indicate the position of the target color faster than the trichromats in the visual search task. Experiment 3's results indicated that the differences in color appearances between the target colors and distractor colors were smaller in trichromats than in dichromats, revealing the advantages of dichromacy. These findings underscore the significant influence of color perception on the distinct advantage that dichromats possess in tasks related to a multi-colored environment.

Keywords: Color deficiency, visual search, color appearance, dichromat, S-cone stimulus value

INTRODUCTION

Typical dichromacy hampers the distinction of red-green colors due to the absence of function of specific photoreceptors (L or M cones), thus reducing color vision to two dimensions instead of trichromacy's three. Although trichromats generally outperform in everyday activities, due to the former's broader color perception, certain studies have demonstrated the advantages of the latter. Morgan et al. and Saito et al. found that dichromats detect red-green camouflaged patterns more effectively [1, 2]. Sharpe et al. noted lower M-cone contrast flicker-detection thresholds in protanopes [3]. Notably, the tasks in these studies involved pattern or flicker detection, which may imply mechanisms beyond color perception.

Hishikawa et al. discovered that dichromats can surpass trichromats under specific test conditions, where differences in S-cone stimulus values lead to distinct color perceptions [4]. Their visual search task solely relied on color information. Nonetheless, the reasons behind the task-performance advantage of dichromats remain unclear. This study aims to validate Hishikawa et al.'s findings (Experiments 1 and 2) and explore the reasons for dichromacy's superiority, considering differences in color appearance between dichromats and trichromats (Experiment 3).

METHODOLOGY

Participants

Three normal trichromats (one male and two females) and one male deuteranope took part in the experiments.

Apparatus

Color stimuli were presented on a 25-inch OLED monitor (with a resolution of 1920 × 1080 pixels and a refresh rate of 60 Hz, Sony PVM-A250 or PVM-2541), controlled by a computer (Apple Mac mini), within a dark room. The monitor was positioned at a viewing distance of 57 cm from the participant.

Stimuli

For Experiments 1 and 2, 13 colored disks were displayed against a gray background (D65 chromaticity, 15 cd/m²). These disks, each measuring 1 degree in diameter, were symmetrically placed at equal intervals around the circumference of an 8-degree diameter circle (Figure 1). Among the 13 disks, 1 disk was designated as the target, while the remaining 12 served as distractors. Two colors were utilized as distractor colors, with each color assigned to 6 of the 12 disks, the two colors of dots were aligned as 6 of one color opposite 6 of the other color around the ring with the target color in a random place. To specify both the target color and distractor colors, the MacLeod-Boynton cone excitation chromaticity diagram, based on Stockman and Sharpe's LMS cone fundamentals on the equal luminance plane, Sharpe et al.'s, was employed. The luminance of all disks was set at 10.2 cd/m². The target color and distractor colors only differed in terms of the S-cone stimulus value. Moreover, the S-cone value of the target color was positioned between those of the distractors. The luminance (Y) and chromaticity coordinates (l, s) of the disks were described using equations (1) through (3):

$$Y = 0.690L + 0.348M \quad (1)$$

$$l = 0.690L/Y \quad (2)$$

$$s = S/Y \quad (3)$$

Here, L, M, and S denote the L-, M-, and S-cone stimulus values, respectively. The background's D65 chromaticity (l, s) was set at (0.69, 0.5). The l-chromaticity of the target (l_{tar}) was adjusted within the range of 0.65 to 0.73, with an increment of 0.01. The s-chromaticity of the target (s_{tar})

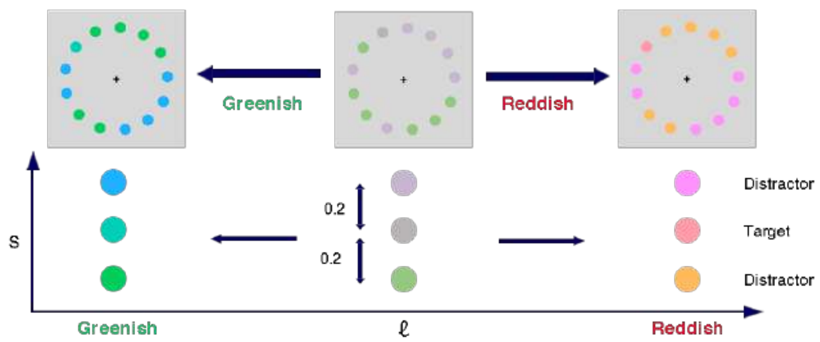

Figure 1. Stimuli: reddish colors to the right, greenish colors to the left along the ℓ-chromaticity axis.

varied from 0.3 to 0.7, with a step of 0.1. The chromaticity of the distractors differed from that of the target in terms of the s value, providing the S-cone stimulus value as the search cue. The *s*-chromaticity of the distractors (s_{dis}) was either +0.2 or −0.2 relative to s_{tar}.

In Experiment 3, a colored disk was displayed at the center of the monitor, maintaining the same background and disk size as used in Experiments 1 and 2. The chromaticity of the disk corresponded to one of the target colors or distractor colors utilized in Experiments 1 and 2.

Procedure

In Experiments 1 and 2, the method of constant stimuli was employed. Each session began after 2 minutes of dark adaptation, followed by an additional 2 minutes of background adaptation. One of 7 randomly selected stimulus durations— 33, 67, 133, 250, 500, 1000, 2000, and 4000 msec for the dichromat and 67, 133, 250, 500, 1000, 2000, 4000, and 8000 msec for trichromats— was utilized in each trial. To prevent color afterimages, a 400-msec mask stimulus, comprising achromatic random dots, was presented following the primary stimulus. Participants were tasked with indicating the target disk and the quadrant in which the target color was positioned (Figure 1) by pressing one of the buttons (7, 9, 1, or 3) of a keyboard depending on the quadrant of the target perception. Notably, the difference between the experiments was that the target color disk was exhibited to participants for 500 msec before the stimulus presentation in Experiment 2 but not 1 (Figure 2). A total of 280 combinations of target color and stimulus duration were presented once in each session, and 30 sessions were conducted for everyone in Experiments 1 and 2.

In Experiment 3, after the presentation of the disk, participants assessed the color appearance of the disk using the elementary color-scaling method. The participants allocated a cumulative total of 10 points to evaluate the disk's whiteness, blackness and chromaticness. Furthermore, if chromaticness was discernible, an additional 10 points were assigned for evaluating the redness, yellowness, greenness, and blueness of the chromaticness. The stimulus durations were 33, 67, 133, 250, 500, 1000, 2000, and 4000 msec for all participants. Individuals performed 10 sessions of 74 trials for each stimulus duration.

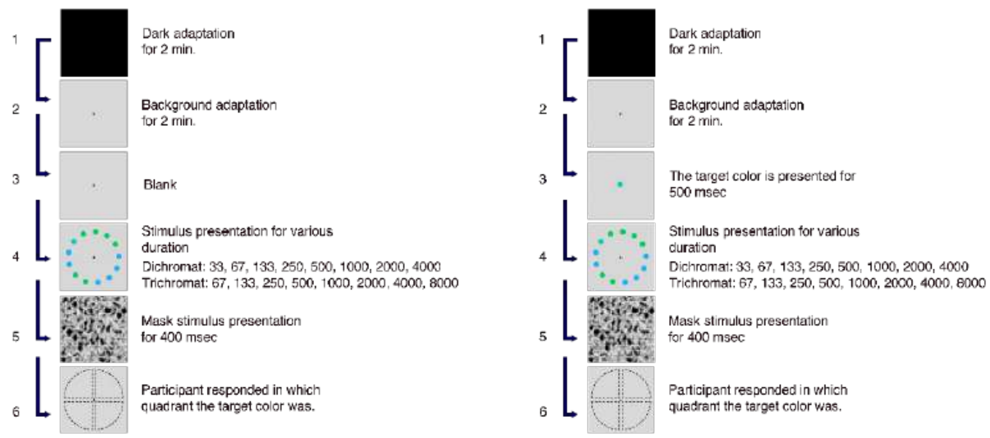

Figure 2. The stimulus presentations. The right side (Experiment 2) illustrates the sequence when the target is shown before displaying the stimulus; the left side (Experiment 1) shows the sequence when the target is not shown in advance.

RESULT AND DISCUSSION

The percentage of accurately reported target positions was calculated for each target color in Experiments 1 and 2, based on the stimulus duration. The duration thresholds were determined by fitting the Weibull function (Eq. 4) to the dataset. This function incorporated variables such as "t" for duration time, "m" for the slope of the function, and "η" for the thresholds indicating the duration required for target detection. In this analysis, the duration thresholds were set to a percentage of 72.4% correct. Figure 3 illustrates the duration thresholds for Participants A, B, and C (trichromats) as well as D (deuteranope) in Experiments 1 and 2. The horizontal axis represents the *l*-chromaticity of the target color (l_{tar}), while the vertical axis signifies the duration thresholds. Different symbols are used to denote variations in the s-chromaticity of the target color (s_{tar}).

$$P(t) = \left[1 - \exp\left\{-\left(\frac{\log(t)}{\eta}\right)^{m}\right\}\right] \times 0.75 + 0.25 \tag{4}$$

Whereas the duration thresholds of Deuteranope D depended on the *s*-chromaticity of the target color, the thresholds did not rely on the *l*-chromaticity of the target color. This outcome aligns with the expectation that dichromats struggle with distinguishing red-green chromatic information. Conversely, the duration thresholds of the trichromats were contingent on both the *l*-chromaticity and *s*-chromaticity of the target color. Interestingly, when the target color and the distractor colors shifted towards greenish or reddish simultaneously, the duration thresholds of the trichromat participants were longer than those of Deuteranope D. This confirms the findings of Hishikawa et al. Furthermore, the results of Experiment 2 closely resembled those of Experiment 1, indicating that prior knowledge of the target color had minimal impact on the duration threshold.

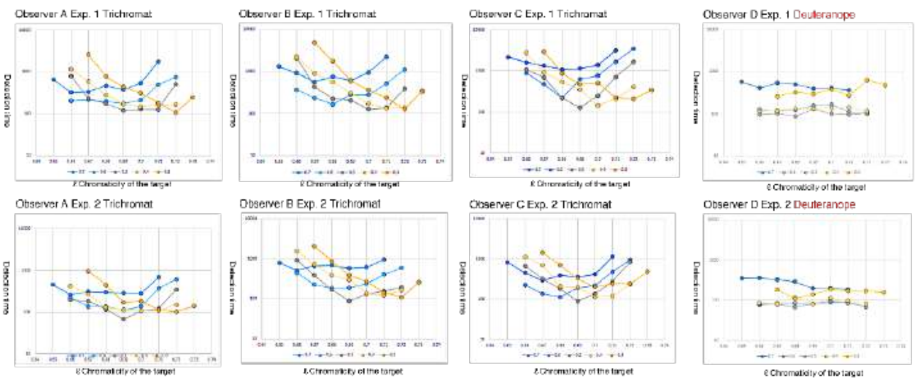

Figure 3. The results of Experiments 1 and 2

We undertook Experiment 3 with the assumption that the results of Experiments 1 and 2 could be elucidated through the color appearances of the target and distractor colors. Figures 4 and 5 illustrate some results from Experiment 3. The first example portrays the outcomes for the target color of (0.69, 0.5) and the distractor colors of (0.69, 0.3) and (0.69, 0.7), wherein the detection thresholds of the trichromats closely resembled those of the dichromat as shown Figure 3 (Figure 4). The second example presents the results for the target color of (0.66, 0.5) and the distractor colors of (0.66, 0.3) and (0.66, 0.7), wherein the detection thresholds of the trichromats were significantly longer than those of the dichromat (Figure 5).

Figure 4 compares the color appearances between the results obtained from Experiment 3 for Trichromat A and Deuteranope D. The color appearances between (0.69, 0.7), (0.69, 0.5), and (0.69, 0.3) were different for both participants Trichromat A and Deuteranope D. The colors of (0.69, 0.7), (0.69, 0.5), and (0.69, 0.3) were purple, gray, and green for Trichromat A, and were blue, blueish-green, and green for Deuteranope D, respectively even with a difference between the answer scores. This suggests that both the trichromats and the deuteranope were able to detect the target color within a relatively short duration.

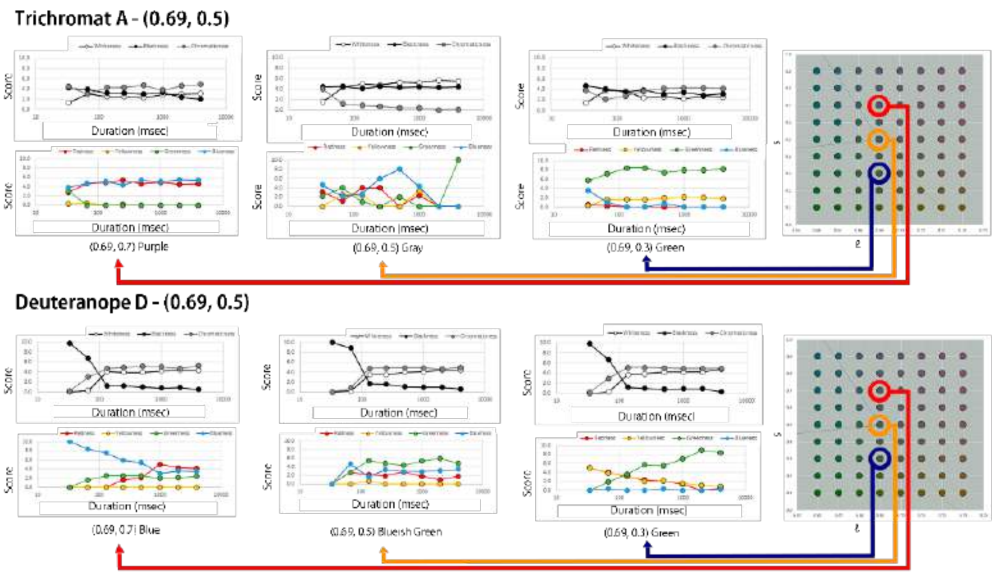

Figure 4. Comparison of the results from Experiment 3 between Trichromat A and Deuteranope D. The target color was (0.69, 0.5), with distractor colors of (0.69, 0.7) and (0.69, 0.3).

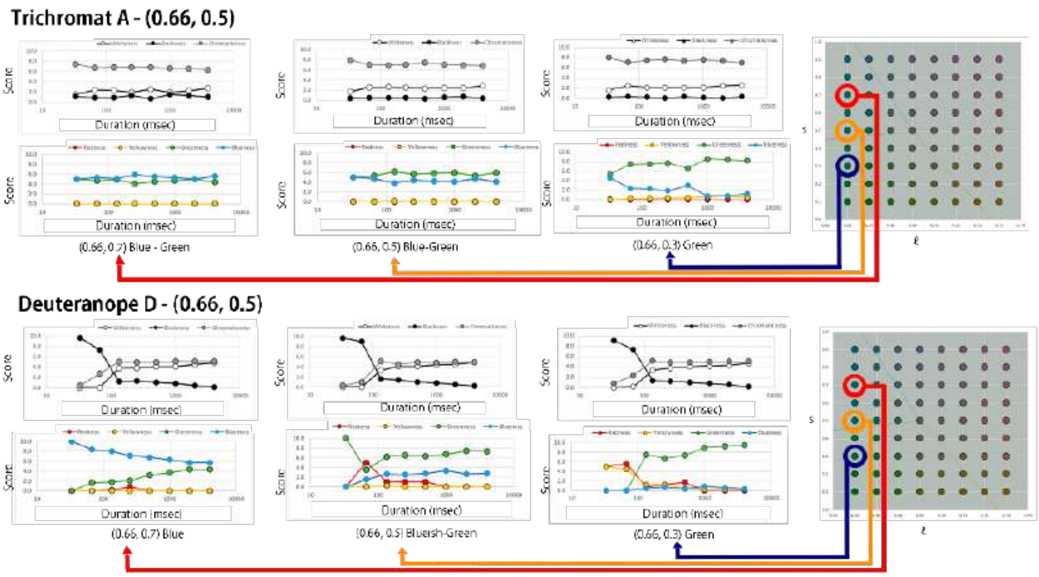

Figure 5. Comparison of the results from Experiment 3 between Trichromat A and Deuteranope D. The target color was (0.66, 0.5), with distractor colors of (0.66, 0.7) and (0.66, 0.3).

As shown in Figure 5, the color appearances of (0.66, 0.7), (0.66, 0.5), and (0.66, 0.3) for Trichromat A were blue, blueish-green and green, which were almost the same as those of the *l*-chromaticity of 0.69, in Deuteranope D. Conversely, the color appearances of (0.66, 0.7), (0.66, 0.5), and (0.66, 0.3) were blue-green, blue-green and blueish-green, respectively, for Trichromat A. This indicates that the difference in those color appearances in the condition with the target color of (0.66, 0.5) and distractor colors of (0.66, 0.7) and (0.66, 0.3) was smaller than in the condition with the target color of (0.69, 0.5) as shown in Figure 4. Therefore, trichromats need more time to detect the target color of (0.66, 0.5) surrounded by the distractor colors of (0.66, 0.7) and (0.66, 0.3).

CONCLUSION

We demonstrated the advantages of dichromacy in the visual search task within a multi-colored environment, utilizing the distinction in S-cone stimulus values as a cue. Additionally, we investigated whether this advantage in such an environment could be attributed to the relationship between the color appearances of the target color and the distractor colors. Our findings suggest the possibility that the benefits of dichromacy stem from the contrasting color appearances between trichromats and dichromats.

This study not only enhances our comprehension of the unexplored capabilities of dichromats but also provides insights for designing tasks and support strategies that cater to their unique visual abilities.

ACKNOWLEDGEMENT

This work was supported by JSPS KAKENHI Grant Number JP 21H04342. We thank Claire Barnes, PhD, from Edanz Group (https://en-author-services.edanz.com/ac) for editing a draft of this manuscript.

REFERENCES

1. Morgan, M. J., Adam, A. & Mollon, J.D. (1992). Dichromats detect colour-camouflaged objects that are not detected by trichromats. *Proceedings of the Royal Society of London. Series B: Biological Sciences, 248(1323), 291-295.*
2. Saito, A., Mikami A, Hosokawa T. & Hasegawa, T. (2006) Advantage of dichromats over trichromats in discrimination of color-camouflaged stimuli in humans. *Perceptual and motor skills, 102(1), 3-12.*
3. Sharpe, T. L., Luca, E., Hansen, T,. Jägle, H. & Gegenfurtner, K. R. (2006) Advantages and disadvantages of human dichromacy. *Journal of Vision*, *6*(3), 3-3.
4. Hishikawa, Y., Katsura, S. & Sunaga, S. (2016) Influence of the number of distractor colours on performance in the visual search task cued by S-cone stimulus value. *Proceedings of AIC 2018(1), 697-702.*

RESEARCHING OF COSTUME FEATURED IN THE K-MOVIE, <THE KING'S LETTERS(나랏말싸미 Naramalsami)>

Mihee Bae[1], Hyewon Park[2]*

1Doctoral Course, Major in Clothing & Textiles, Interdisciplinary Program in Senior Human Ecology, Changwon National University, South Korea
2Professor, Major in Clothing & Textiles, Interdisciplinary Program in Senior Human Ecology, Changwon National University, South. Korea

*Corresponding author: Hyewon Park, hwpark@changwon.ac.kr

ABSTRACT

The movie, <The King's Letters(나랏말싸미Naramalsami)>, deals with the details of the processes in creation of '<HunminJeongeum(한글, Korean alphabets that the general public can learn and use easily)>' by King Sejong in the early era of Joseon Dynasty during the 15th century. This study is aimed at the confirmation of the importance of movie costumes as mise-en-scéne by comparatively contemplating the uniqueness and aesthetic characteristics of colors used in the traditional Korean costumes of Korea along with the costume design characteristics in the movie, <The King's Letters>. As the study method, empirical research that examined the apparels and the traditional Korean costumes during the 15th century as mise-en-scéne through reviewing of literature and preceding studies, and comparatively analyzed the colors of movie costumes and traditional 5 cardinal colors of Korea featured in 58 still-images and 9 poster scenes of the movie was conducted. This particular era in Korean history displays characteristics of the costumes in the early stage of Joseon Dynasty. Designs of costumes won by the leading characters in the movie were examined with focus on their colors along with characteristics of silhouettes and details. Through this approach, it is possible to examine the changes in the colors in accordance with the temporospatial changes and development of stories of the movie. In the process, it was possible to discern the presence of characteristics that express the personality of characters wearing the corresponding movie costumes, and imply their psychological changes and development of stories thereof. It is deemed possible to have the value of Korean beauty and sentiments of Korea contained in the traditional colors of Korea be known more widely through confirmation of colors of costumes featured in this movie.

Keywords: The King's Letters(나랏말싸미Naramalsami), film costume colors, mise-en-scéne,

5 cardinal colors

INTRODUCTION

Mise-en-scène, in the past, referred to the overall plan, such as the position of an actor's location or the role in a play, stage background, equipment, lighting, and so on. Today, the meaning has been expanded, and now it refers to plans and elements related to visual effects, such as lighting for all images, actors' costumes and makeup, and background art. The mise-en-scène of a film plans and controls the visual elements of a video to keep the audience's attention on an important scene and effectively convey the information of the movie to the audience. The color and visual expression must be intended and designed along with the facial expression of the character[1]. In particular, because of the expressive role of the clothes, the costumes worn by the actors convey information about the times, places, psychology, and class even if they do not convey information in language. In many cases, the understanding of a movie depends not only on the primary understanding that depends on the plot of the scenario but also on the combined effect through mise-en-scène. In other words, the color of the costume in the movie plays a big part as a mise-en-scène.

Historical dramas are presented based on historical background and show the social aspects of the time. The costume primarily expresses the clothing of the period. Types of historical dramas include traditional historical dramas, popular historical dramas, and fusion historical dramas, and <The King’s Letters> examined in this study is a traditional historical drama. The costumes were reproduced through historical research covering the background of the times, lifestyle, character's inclination, and clothing. King Sejong, the fourth king of the early Joseon Dynasty (15th century), laid the foundation for culture, ideology, politics, and institutions. This film is set in the Joseon Dynasty, the last years of King Sejong's reign, when he created the Korean alphabet, <HunminJeongeum(한글)>, in the 28th year of King Sejong's reign (1446 A.D.). The creation of <HunminJeongeum(한글)> is the most brilliant achievement among the cultural heritage left by King Sejong. It is also the great cultural heritage of Korea.

Color is a visual phenomenon comprising light, object, and the observer's perception. The process until a color is perceived is as follows. When light hits an object, the light passing through the object enters the eye. This process is called color stimulation, and the light stimulates the retina of the eye and is transmitted to the optic nerve, resulting in creating a sense of color and finally, the color of an object is perceived. Ordinary color is more suitable for subjective inspection than a quantitative inspection of the color of an object that looks differently due to the difference in lighting environment or visual viewing conditions.[2]

This study aimed to examine the color and aesthetic characteristics of Korean traditional costumes, focusing on <The King’s Letters>, a film set in the era of King Sejong the Great in the early Joseon Dynasty (15th century) directed by Cho Cheol-hyeon. It intended to identify the color and its important role as the mise-en-scène of the film.

METHODOLOGY

As a research method, literature and content were examined. First, previous research and literature related to the color of the costume in the movie were reviewed. In addition, nine posters and 58 still cuts from the movie <The King's Letters> were collected. Among them, still cuts where the shape or color of the costume could not be distinguished, cuts of similar scenes or the same costumes, and repeated scenes were excluded, and finally, eight out of nine posters except one, 33 out of 58 still cuts, final 42 cuts were examined. This study aimed to examine the aesthetic characteristics of costumes in the early Joseon Dynasty (15th century) and the importance of mise-en-scène in the color of costumes in the film by referring to interviews with directors, producers, costume directors, and art directors, who participated in the production, and other directors who saw and reviewed the film.

RESULT AND DISCUSSION

Ryu Seong-hee, the art director of this film, said, “We focused on visualizing the design elements that were incorporated in the film until the birth of <HunminJeongeum(한글)> . Rather than the splendid and raw colors of existing historical dramas, the colors are dimmed down as much as possible so that the characters can stand out, and by appropriately combining historical facts with modern interpretations, such as geometric lines of palaces and temples in the Joseon Dynasty, we created the unique attractions of 'The King’s Letters.'”[3]

Costume Director Shim Hyeon-seop said, “I put emphasis on the harmony between art, costumes, and characters, and based on traditional patterns and historical research, I wanted to incorporate the emotions of the characters into the costumes in each scene and to embody a sense of the season in costumes that is not well expressed in historical films.”[4] It shows that this film invested much effort in the historical research of traditional costumes and utilized visual colors dominantly in expressing characters. The main characters of this film are King Sejong, Priest Sinmi, and Queen Soheon, who is King Sejong's wife. The results of examining the colors of the costumes for these characters are as follows;

Based on thorough research on a total of 2,000 costumes, from those of the king, the highest status, to those of the monks, the lowest status at the time, he created a traditional Korean style that melded the emotions of the characters. Specially, for King Sejong's royal robe was expressed the basic colors and shape of the clothes according to historical facts. The natural tones such as ocher to express his love for the people and created all 19 layers of clothes to complete the king's figure.[5] The royal robe for the king is called Gonryongpo and represents the king's status. Yellow bright red (7.5R 5/14) of the one the king wears daily when he deals with state business was applied as it is, and sometimes ocher was applied to express the kindness of the king who loves his people.

Priest Sinmi is the main character who appears stately in front of the king even when it was the time when Buddhist priests were depressed due to the policy of promoting Confucianism and suppressing Buddhism. Various feelings were expressed according to the atmosphere of the story by adjusting the brightness of gray for a simple but rough and wild feeling. Each priest's robe was hand dyed and to create different textures[6]. To emphasize the feeling of the priest, the priest's robes were made in a darker ink color than gray.[7]

For Queen Soheon's costume, pastel tones were used to express her neat and gentle image. However, in her scene teaching the court ladies Hangeul, contrasting colors and tones were used to give a sense of dignity and authority as a queen, a person of a high rank. The shade of blue was adjusted and flowers and lonely birds were embroidered to express the feeling of a woman who had her grief as a wife, a mother, and a daughter. Also, the design of the headdress and accessories were added to create a unique style for the queen.[5] For her winter clothes, a difference in texture was given by putting cotton inside silk and quilting it. Characters with wealth and power wore more colorful clothes within the range of red and blue, while people with integrity wore simple clothes.[7]

The colors appearing in the movie are mainly red, blue, gray, white, and ocher, and the psychology of the main character is expressed by differentiating the brightness of the color. In other words, when expressing her joy, the colors of Queen Soheon's costumes are bright and splendid, with red and blue, and when expressing her sadness and loneliness, her jacket appears close to white and her skirt is dark blue, describing the depression. Also, to express her authority, a contrast is used to add weight to the color.

<Table 1> Characteristics and Details of Costume Colors by Characters

Lead Character	Representative Costume			Color Characteristic	Role of Color as mise-en-scène
King Sejong				-Dark blue costume of the king during the rain ritual -Red costume the king as the official uniform (royal robe) -White and ocher for plain clothes	- Blue for wish and desire - Darker blue for heavier atmosphere - King's symbol
					

Priest Sinmi				-Dark gray in front of Japanese priests asking for the Tripitaka Koreana -Gray image in the time of agony for the creation of Hangeul - Dark gray clothes and red chanting robe, giving an organized feeling when having an audience with the king for the promulgation of Hangeul	-Conveying coercive feelings -With one color, gray, adjusted the brightness to the story
					
Queen Soheon				- Dark blue to express loneliness and sadness - Bright blue and red to express the daily life of the king and queen - Blue and red when giving an order as a queen - Red and blue for banquets	- The queen's dress is symbolized by blue and red -Conveying the meaning of the story with pastel pink and green
					

CONCLUSION

The purpose of this study was to confirm the academic development of film costumes and the importance of film costumes mise-en-scène. to this end, the historical background of <The King's Letters > and the shape and color characteristics of the main character's costume were examined, and the aesthetic characteristics were confirmed by interpreting the meaning.

This film is set in the Joseon Dynasty, the last years of King Sejong's reign, when he created the Korean alphabet, HunminJeongeum(한글), in his 28th year (1446. A.D.). The spatial background is the royal family of Joseon. The costumes of the king and the queen based on the Yin-Yang and the Five Elements of the time are historically correct. The red color in the film symbolizes the south among directions, summer among seasons, fire, sun, and blood in the Yin-Yang Five Element Theory.[8] It is a color of the gentle south where everything is abundant and of powerful yang. Since the direction represented by blue in Korea is east, it symbolizes sunrise, brightness, clarity, creation, new birth, and reproduction. In the theory of Yin-Yang and the Five Elements, blue represents east and spring and is rich in yang. It represents the light of the sky, the sea, and the water, and it takes a large part in the cosmology of Korean mythology, symbolizing the joy of recovery and birth. Since the sun rises and gives light, blue symbolizes full of energy and is recognized as something that ensures life and happiness and gives the greatest hope. In addition, blue symbolizes youth, hope, and freshness in that it also meant immaturity in the era when the custom of giving precedence to the elders was revered. Yellow is the color that symbolizes the king's garments and authority; its use by the general public was limited, as in China. However, because Buddhism was revered, only monks were exempted from this rule. In general, yellow is the center of five colors and directions and is related to all four seasons and directions, it corresponds to the center of the universe, is the brightest, most radiant, and is recognized as the noblest color. It was recognized as the color symbolizing the emperor and the color only the ruler could use. Yellow symbolizes the earth that embraces and harmonizes all things. It represents light, respect, faith, wealth, divinity, loyalty, generosity, wisdom, and peace, while it also symbolizes envy, resentment, evil, and injustice.[8]

Mise-en-scène, in the past, referred to the overall plan, such as the position of an actor or the role in a play, stage background, equipment, lighting, and so on. Today, the meaning has been expanded, and now it refers to plans and elements related to visual effects such as lighting for all images, actors' costumes and makeup, and background art. The colors of the costumes in this film are ascertained through historical research on mostly the royal court costumes of the 15th century Joseon Dynasty, and yet the emotions in the story are well expressed through the dynamics of colors and tones, including the king's psychology, the queen's character and sadness, and the monk's aspirations and concerns. Although the colors of the costumes have been strictly limited due to historical research, it seems clear that they are a visual medium that explains the psychological characteristics of the protagonist and an important element of mise-en-scène that sets the atmosphere of the film. Many diverse attempts are expected from cinematic costumes in the future.

REFERENCES

1. Kim, Y. (2009). Film costume design. Seoul: Communication Books
2. Moon. E. Color Systems. Book Publishing International 2002.06.15
3. Lee. J. (2019.July.24). Bong Joon-ho, Lee Jun-ik, Lim Soon-rye...The famous directors watched ‘naranmalssami‘. CBS No Cut News Retrieved from (2023.June.11.) https://m.nocutnews.co.kr/news/5187864.
4. Lee. Y.(2019.June.24). Director Cho Chul-hyun and high-end production team work together with strong power 'naranmalssami’. NEWSCULTURE Retrieved from (2023. June.11). http://www.newsculture.press/news/articleView.html?idxno=218708
5. *nunnaerineun ridoseu.(2020.06.23).* Interpretation of the ending of the storyline of the movie "naranmalssami". Nunnaerineunridoseu Retrieved from (2023.June.11) https://otherbada.tistory.com/267
6. Jang. Y. & Lim. S. (2019.07.25). <naranmalssami> Production machine - Art director Ryu Sung-hee, cinematographer Kim Tae-kyung, costume director Shim Hyun-seop, and producer Oh Seung-hyun speak. Magazine Retrieved from (2023. June.11). http://www.moazine.com/article/detail.asp?articleid=1344066
7. Jang. Y. & Lim. S. (2019.07.25). <naranmalssami> Production machine – Art director Ryu Sung-hee, cinematographer Kim Tae-kyung, costume director Shim Hyun-seop, and producer Oh Seung-hyun speak. Cine21 Retrieved from (2023.June.11). http://www.cine21.com/news/view/?mag_id=93503
8. Kim, J. (2009). A Comparison of Color Culture in Traditional Performance of Korea and China : focus on Obangsaek. *Journal of Korean Traditional Costume,* 12.(2), 5-16.

EFFECT OF NARROW-BAND PRIMARY COLORS ON OBSERVER METAMERISM OF ANOMALOUS TRICHROMATS

Taiju Inoshita[1]*, Tsukasa Muraya[2], and Shoji Sunaga[3]

[1] *Graduate School of Design, Kyushu University, Japan.*
[2] *Faculty of Contemporary Social Studies, Chikushi Jogakuen University, Japan.*
[3] *Faculty of Design, Kyushu University, Japan.*

*Corresponding author: Taiju Inoshita, inoshita.taiju.026@s.kyushu-u.ac.jp

ABSTRACT

Using a narrow-band spectral distribution for a primary color of a display often leads to failure of color matching because of observer metamerism. Especially, it has been reported that this problem is not negligible in anomalous trichromats. In this study, we investigated the relationship between the wavelengths of primary colors with a narrow-band spectral distribution and observer metamerism in anomalous trichromats through a color-matching experiment. Three trichromats and two deuteranomalous trichromats participated in the experiment. The additive mixture color field consisted of the RGB primary colors with the half bandwidths of 10nm and peak wavelengths of 630 nm, 533 nm, and 463 nm, respectively. In addition, the red primary was changed from 630 nm to 600 nm; or the green primary was changed 533 nm to 500 nm. The total number of primary colors sets was three. The participants conducted color matches between the color chips and the colors of the mixture field by adjusting the luminance and chromaticity of the mixture color. It was found that the matched colors obviously shifted along the confusion lines of the deuteranopia for deuteranomalous trichromats, whereas the color shifts were small for the trichromats. Whether color shifts diverged or converged to the centers of confusion lines, and the amount of divergence or convergence, depended on the primary color set and the degree of anomalous trichromacy. Moreover, we examined whether the shifts of matched colors could be accounted for by the shift in the wavelength sensitivity of the M cones in the deuteranomalous case. The predicted matching color based on the shift in the wavelength sensitivity of the M cones showed good agreement with the experimental results in the deuteranomalous case. However, we could not explain some matched point for stronger deuteranomalous trichromat. In conclusion, it is possible to control the effects of observer metamerism by changing the set of primary colors even when using narrow-band primary colors. However, the results also suggest that a change in the primary colors could decrease the color gamut of a display.

Keywords: observer metamerism, anomalous trichromats, color reproduction, wide gamut display

INTRODUCTION

Displays, which we use daily, perform colorimetric color reproduction that adjusts the intensities of the three primary colors so that the cone responses of a standard observer are equal. However, the cone responses do not completely match because of individual differences in color matching functions of observers. This phenomenon of color reproduction depending on the observer is called observer metamerism.

Recently, the bandwidth of the spectral distribution of primary colors has become narrow in response to increased demand for highly saturated colors. However, Ramanath reported that observer metamerism is more obvious in displays with such bandwidths [1]. Anomalous trichromats have a critical problem because the spectral absorbance peaks of their cone pigments are shifted, and their color-matching function is significantly different from that of the standard observer.

Sunaga et al. reported that anomalous trichromats perceived a large difference between the reference color and the colors reproduced by a laser display with narrow-band primary colors. It was also reported that the matching point on the laser display for anomalous trichromats deviated greatly from that of the reference color. In addition, they conducted a color matching simulation using the color appearance model of Yaguchi et al. to show that the experimental color matching results for deuteranomalous trichromats are caused by the peak shift of the M-cone fundamental [2][3].

In this study, we investigated how observer metamerism based on the difference in cone fundamentals is affected by changing the wavelength of the R or G primary with a narrow band.

METHODOLOGY

Observers

Three normal trichromats (NT1, NT2, NT3) and two deuteranomalous trichromats (DA1, DA2) participated in the experiments. Their color vision was classified by their performances on the Ishihara pseudoisochromatic plates, the Farnsworth–Munsell 100-hue test, the Panel D-15 test, and the Nagel anomaloscope (Anomaloscope OT-II, Neitz). DA2 failed in the Panel D-15 test, but his anomaloscope result indicated he is a deuteranomalous trichromat.

Apparatus

Figure 1 shows our experimental apparatus, which consisted of two viewing booths covered by N6.3 gray papers. A color chip was illuminated with a 6500K LED lamp (OD 261 225R, ODELIC) in the left booth. The right booth, which was illuminated with another 6500K LED lamp, had a window of the same size and the same position as the color chip. The observers could view the additive mixture color through the window. The illuminances on the floor surfaces of the booths were 300 lx.

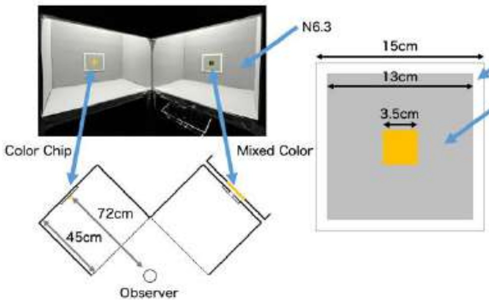

Figure 1. Apparatus

To present the color stimulus consisting of RGB primary, we used eight LED light sources (AS3000, AS ONE). Each spectral distribution of the emitted lights was narrowed by interference filters and transmitted and mixed using optical fibers and a diffusing screen. Of the eight LED sources, three were assigned to R, two to G, and three to B primary. The intensity of each primary color was controlled by a computer via a PWM generator (DACS-2500KD-RSV24-EV, DACS electronics).

Stimulus

We tested three sets of primary colors. The first was RGB monochromatic light with peak wavelengths of 630 nm (R1), 533 nm (G1), and 463 nm (B); the second was the red primary, which was changed from 630 nm to 600 nm (R2); and the third was the green primary color, which was changed from 533 nm to 500 nm (G2). The FWHM of all monochromatic spectra was 10 nm. The color gamut of each primary color set is shown in Figure 2.

We used 16 color chips as test colors. Their CIE (x_F, y_F) chromaticity coordinates are shown in Figure 2. Their spectral distributions are shown in Figure 3. The size of the color chip was 2.7°. The background of the test color was N6.1 medium grey surrounded by N9.2 white as shown in Figure 1.

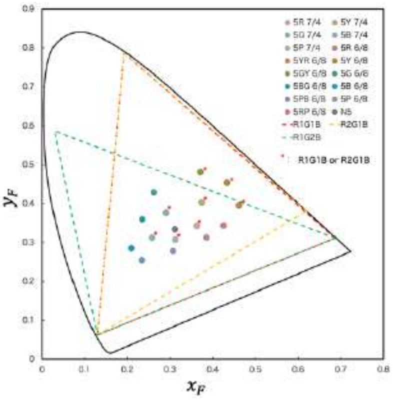

Figure 2. Chromaticity coordinates of 16 color chips and three primary sets

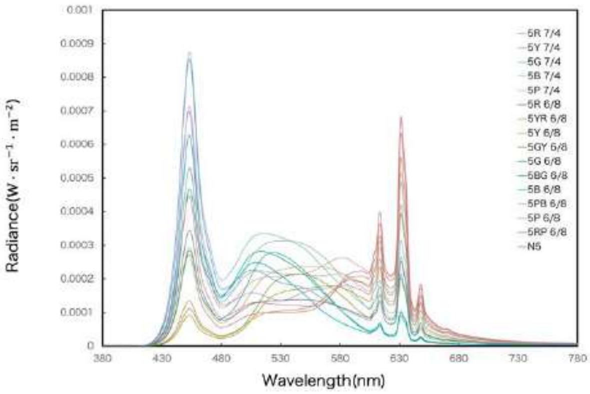

Figure 3. Spectral distributions of color chips

Procedure

The observer's task was to make a color match between the color in the right booth and the color chip in the left booth by adjusting the luminance and the chromaticity of the mixed-color stimulus. Each observer performed five matchings for each test color.

RESULT AND DISCUSSION

Figure 4 shows the results of the R1G1B primary sets for each participant. The chromaticity of all the matched colors shifted toward green along deuteranopic confusion lines for DA1, who is deuteranomalous and passed the Panel D-15 test. This means that the colors reproduced by the R1G1B primary sets become reddish for DA1. In DA2, who is deuteranomalous and failed the Panel D-15 test, many colors shifted to diverge from the centers of deuteranopic confusion lines, but some reddish colors shifted to converge to them. These results indicate that the reddish colors become greenish and the greenish colors become reddish. Specifically, the red–green saturation of the color on R1G1B decreased.

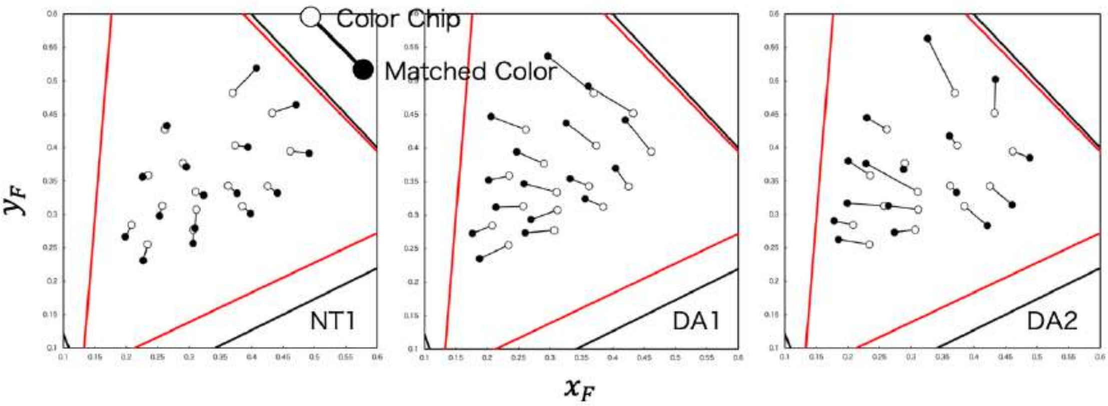

Figure 4. Results of color matching experiments on R1G1B

We investigated whether these results also occur when the primary color set is changed. Figure 5 shows the results of the R2G1B and R1G2B1 primary sets for the deuteranomalous trichromats. When the red primary was changed from 630 nm to 600 nm, both deuteranomalous observers matched red–green saturation of colors to be high. When we changed the green primary from 533 nm to 500 nm, the matched point for DA1 moved along with the deuteranopic confusion line in the direction of increasing greenness compared with R1G1B. However, for DA2, the shift amount and direction did not change much from that for R1G1B.

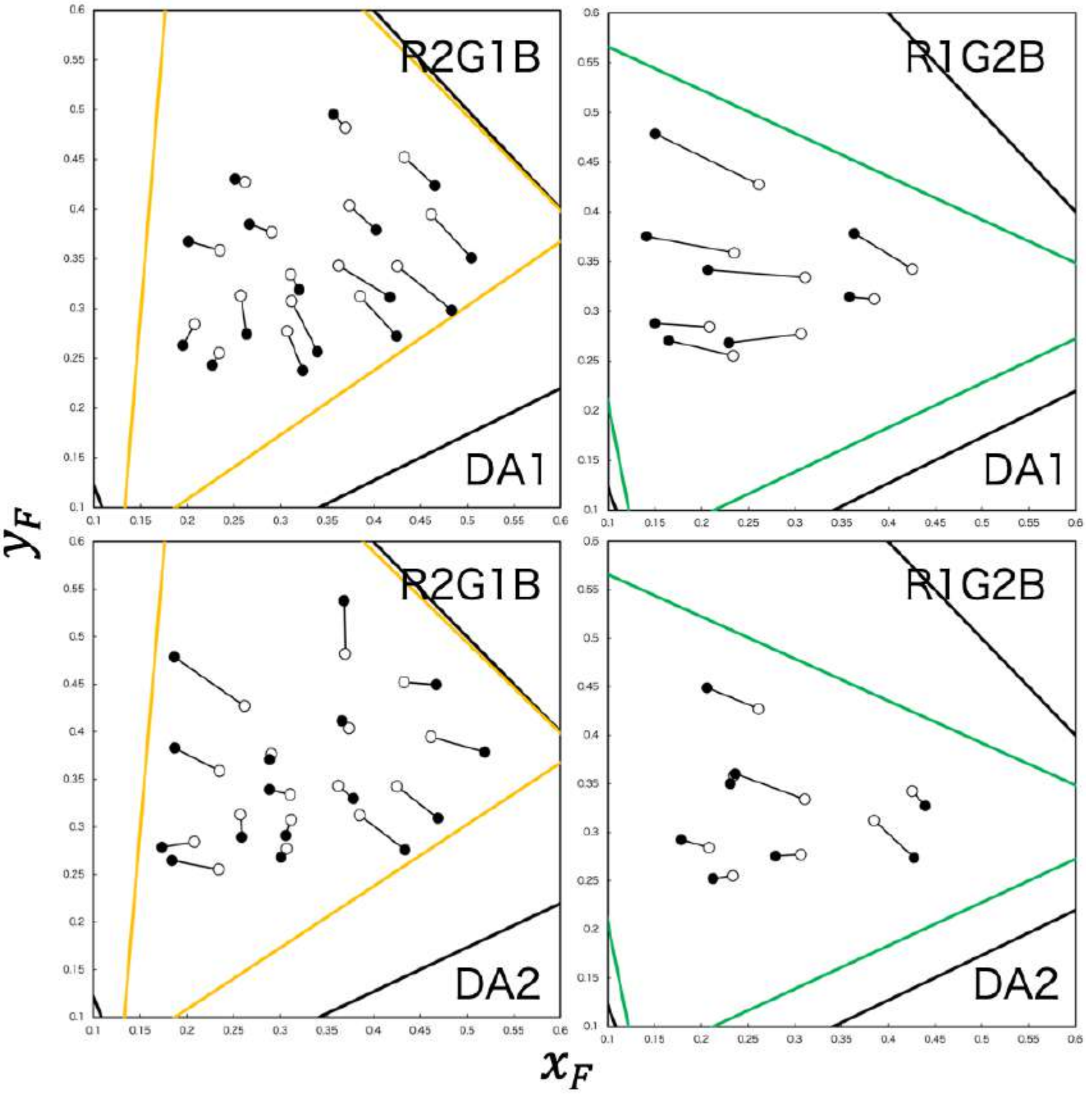

Figure 5. Results of color matching experiments on R2G1B and R1G2B for deuteranomalous trichromats

We calculated the color differences between the matched colors and the color chips to examine the effect of the wavelength of narrow band primaries. The results are shown in Figure 6. The color differences for the anomalous trichromats were larger than those for the normal trichromat. For DA1, the color difference increased considerably only when the green primary color was changed, while for DA2, the color difference did not change much even when the primary was changed.

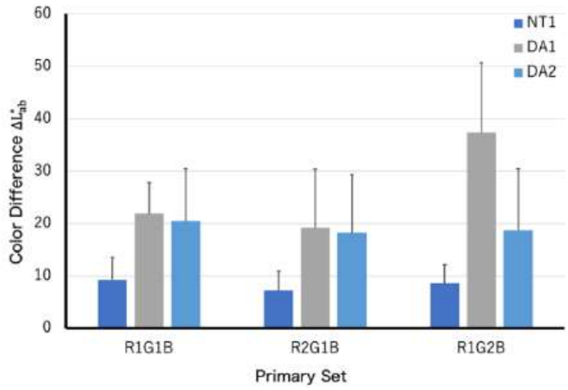

Figure 6. Differences between the color chips and the matched colors on each display.

We tried to explain these color shifts using a color appearance model for anomalous trichromats proposed by Yaguchi et al [2]. The model can account for the color shift of DA1 as shown in Figure 7. However, it cannot account for all color shifts of DA2. DA1 and DA2, who were the deuteranomalous trichromats, were different in whether they passed the Panel D-15 test. Although it is not known failing the panel D-15 test is directly related to the inability to predict color shifts for stronger deuteranomalous trichromats such as DA2, this result suggests that there are unknown factors in the color perception of anomalous trichromats.

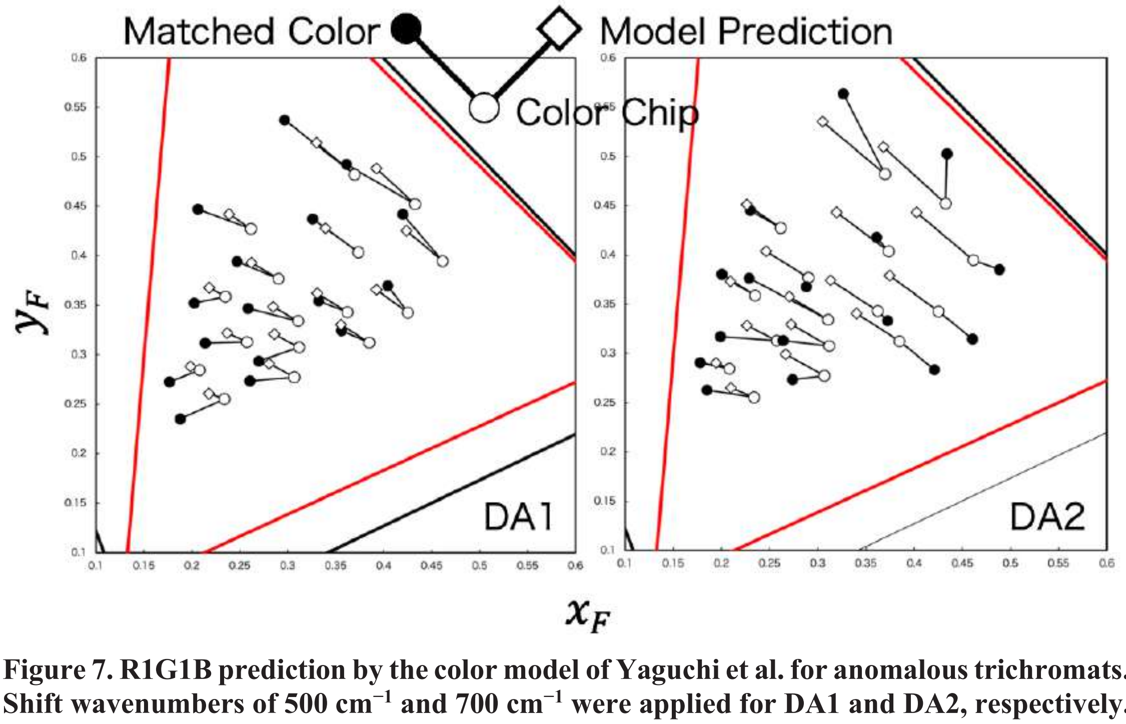

Figure 7. R1G1B prediction by the color model of Yaguchi et al. for anomalous trichromats. Shift wavenumbers of 500 cm^{-1} and 700 cm^{-1} were applied for DA1 and DA2, respectively.

CONCLUSION

In this study, we investigated the effect of narrow-band primary colors on observer metamerism by changing the peak wavelength of each primary color. We conclude that the degree of observer metamerism with a display using narrow-band primary colors depends on the peak wavelength of the primary color. This result suggests that changing the peaks of primary colors makes it possible to control the effects of observer metamerism even though narrow-band primary colors are used. We also found that the observer metamerism of anomalous trichromats cannot be completely explained by the color appearance model proposed by Yaguchi et al. To investigate what kind of primary color is used, it is necessary to increase variations of parameters such as the bandwidth and peak wavelength of the primary and the degree of anomalous trichromacy.

ACKNOWLEDGEMENT

This work was supported by JSPS KAKENHI Grant Number JP 21H04342. Mark R. Kurban from Edanz (https://www.jp.edanz.com/ac) edited a draft of this paper.

REFERENCES

1. R. Ramanath (2008). Minimizing Observer metamerism in display systems, *Color Res. Appl.*, 34, 5, 391-398
2. S. Sunaga, R. Suto, S. Katsura, and H. Yaguchi (2018). Observer metamerism in wide color gamut display for anomalous trichromats, *Proceedings of the 4th Conference of Asia Colour Association*, 236-240.
3. H. Yaguchi, J. Luo, M. Kato, and Y. Mizokami (2018). Computerized simulation of color appearance for anomalous trichromats using the multispectral image, *J. Opt. Soc. Am. A.*, 35, 4, B278- B286

AUTOMATIC COLOUR PALETTES FROM MOOD BOARDS

Sally Angharad* and Peihua Lai and Stephen Westland

Leeds Institute of Textiles and Colour, School of Design, University of Leeds, UK.

*Corresponding author: Sally Angharad, sdsab@leeds.ac.uk

ABSTRACT

Colour forecasting has been an important process for many manufacturing sectors for nearly a century. However, developments in technology and changes to the way that goods can be manufactured are giving birth to more rapid and agile manufacturing and supply chains. This is putting increasing pressure on the traditional colour forecasting industry (because companies require more rapid information about consumer trends) and recently there has been an increase in automated methods driven by machine learning and AI. In this manuscript methods to automatically extract colour palettes from mood boards are investigated. The main research question is whether the machine-derived palettes are different to those that humans would arrive at. To test this, 12 digital mood boards were generated and each of 10 participants (5 experts and 5 naïve) were asked to select 6 colours to represent each mood board. Several machine-learning methods (such as clustering) were implemented to automatically extract 6 colours from each mood board. Standard methods for comparing colour palettes were used to compare the colours generated by the algorithms with those generated by humans to ascertain whether the difference between the machine palettes and the human palettes was greater than the difference between human palettes. Further work will identify which machine-learning algorithms are most effective and which are best suited to be used to develop tools that can enhance colour forecasting. A broader research question will explore the potential of machine learning in the context of practical colour forecasting workflows; for example, what role does intuition play in the colour forecasting process? Are there limits to what machine-learning can achieve in this field?

Keywords: colour forecasting, trend forecasting, colour design, machine learning, psychophysics.

INTRODUCTION

The trend forecasting industry has continued to evolve since its creation over a century ago. Yet despite the changing landscape, colour remains central to the mood and aesthetic of the forecasting model [1].

The consumer-driven economy has been a significant driver for businesses to invest in trend forecasting. While a large emphasis is placed on tacit knowledge and the intuition of trend experts within the process, more accurate predictions and planning based on key factors such as consumer preferences, opinions and behaviours are becoming commonplace [2]. Data science provides insight into human behaviour with quantitative and qualitive research augmenting human-based expertise. This allows large volumes of information to be analysed through machine-learning. In doing so, there are two main opportunities that arise: firstly, that non-trained people can discover information that could be indistinguishable from those extracted by experts; secondly, that analysis of big data may enable expert designers and researchers to be more productive. This could potentially save a business time and money as well as improving the commercial success of its offerings.

An important environmental and economic issue for fashion and textile industries is overproduction and so a sustainable approach to colour trend forecasting is essential; aiming to improve the accuracy of predication thus reducing deadstock [3]. Research also indicates that design psychology such as colour associations can improve the connection between user and product to increase longevity in opposition to fast-fashion [4]. To date, studies have mostly focused on fashion forecasting; however, it is acknowledged that trend inspiration originates from a variety of disciplines with similar themes influencing aesthetics in multiple sectors from apparel to interiors [5]. This emphasises that trends for a specific product are part of a broader context, also taking into account social, cultural, political, environmental, economic and technological factors. Therefore, research that examines fashion forecasting has been used as a key indicator for the developments needed for the wider colour forecasting industry. The impact of colour within trend forecasting spans all design industries and is also recognised as a key marketing tool [6]. Colour attributes are discussed in relation to associations and mood to understand the influence of a colour palette on a trend theme. The importance of mood boards as a visual tool is highlighted as an important area of research, with opportunities for machine-learning methods to enhance the analytical process [7].

Later, this research will explore a hybrid model for colour trend insights using human-based and machine learning methods, to deliver more accurate forecasts.

The two objectives of the current study are:

1. To evaluate the performance of automatic colour extraction methods using images of mood boards.

2. To compare the colour palettes generated by expert and naïve participants.

METHODOLOGY

A set of 12 mood boards (see Figure 1) were created for this psychophysical experiment. A total of 10 human participants (5 experts with design experience and 5 naïve participants) were sent the 12 mood board images in a PowerPoint file and asked to select 6 colours that represent each board. The participants used the eye dropper GUI in PowerPoint to make their colour selections. When colour palettes had been selected for each of the 12 mood boards the participants returned the PowerPoint files and the RGB values of each of the colours were then extracted for analysis. For analysis it is assumed that the RGB values were sRGB values. However, each participant carried out the experiment on their own display.

Three algorithms were used to extract 6 colours from each of the images used in the study. The first method was a standard k-means approach. K-means is an unsupervised machine learning method that has been widely used in image processing for the last 40 years or more [8]. In Figure 2, the first row shows the image that was evaluated and the second row shows the 25 colours that were selected using the k-means algorithm (with k=25). The third row shows the 25 extracted colours sorted in terms of membership; colours that are associated with the most pixels in the image are on the left and those with that are associated with the least pixels are on the right. The standard k-means selects the 6 leftmost colours as being representative of the image.

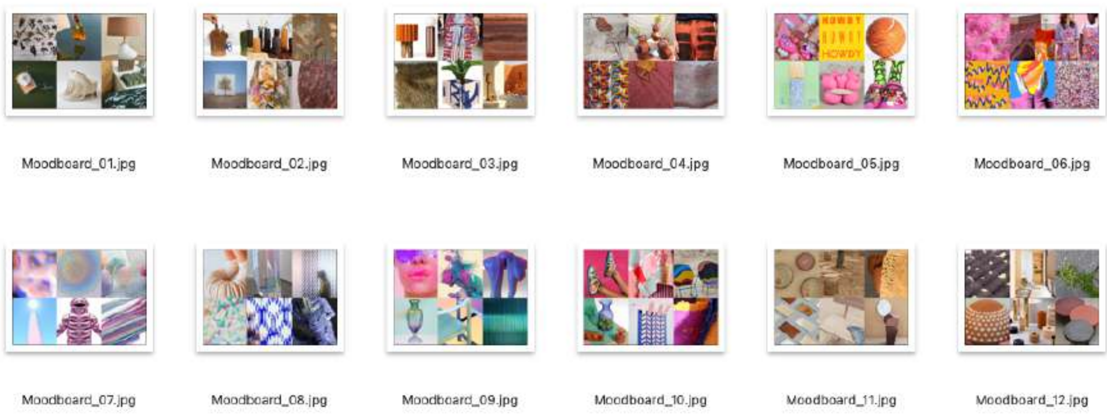

Figure 1: The 12 mood boards that were used in the study

Figure 2: An example analysis showing (from top to bottom) the mood board, the 25 extracted colours, the 25 extracted colours sorted by membership, the 6 most populous clusters (standard k-means) and then two methods (enhanced and maxminc) of selected 6 colours from the 25.

The last two rows of Figure 2 show two different ways of selecting 6 colours from the 25 that were found by k-means. Whereas the standard k-means method would take the 6 colours with the greatest membership (to some extent this is like selected the six most frequent colours from the image), the other two methods select colours to maximise their dissimilarity. The maxminc method has been previously published in a different context [8].

Colour differences between palettes generated for the same image were calculated using the palette difference metric DE_P [9] and using the CIEDE2000 colour difference equation.

RESULTS AND DISCUSSION

The initial analysis was to compare the colour palettes generated by the naïve and expert observers. Figure 3 shows a visual representation of the colour palettes that were generated by the two groups of observers for one of the mood boards (Mood Board 1 from Figure 1).

Figure 3: Comparison of the palettes generated by five naïve (left column) and five expert (right column) participants for Mood Board 1.

The average DE_P value between the naïve palettes and between the expert palettes in Figure 3 was 9.1 and 6.7 respectively. This suggests that the variability between the palettes selected by the expert observers was smaller than the variability between the palettes by the naïve observers. When the same analysis is done for all 12 mood boards and the colour differences are averaged over all mood boards the average variability of the naïve and expert observers respectively was 10.3 and 8.6. There is some evidence, therefore, that the experts are more self-consistent than the naive group ($p < 0.05$). Notice that the finding in this section doesn't say anything about whether the palettes selected by experts are different from those selected by naives; it simply says that the palettes selected by experts are more consistent with each other.

Table 1: Mean palette colour differences between the paletes generated by the three algorithms (standard, enhanced and maxminc) and those generate by the participants (naïve and expert) pooled over all mood boards.

	Standard	**Enhanced**	**Maxminc**
Naïves	10.8 ($p > 0.05$)	10.7 ($p > 0.05$)	11.7 ($p < 0.05$)
Experts	10.0 ($p < 0.05$)	9.8 ($p < 0.05$)	11.4 ($p < 0.05$)

Table 1 shows the average palette differences when the palettes generated by the algorithms are compared with those generated by naïve or expert participants. Although the differences between the algorithms are small, the data suggest that the enhanced method produces palettes that are more similar to those generated by either naïve or expert participants. It is evident that for both the standard and enhanced models the difference between the colour palettes and the human palettes was no different than the difference between the humans' palettes. In other words, these two models are effective at reproducing the palettes generated by this group of participants. This is not the case for the maxminc method which is the worst of the three methods tested.

A t-test analysis was conducted, and the p values can be seen in Table 1. There is a statistically significant difference between the palettes generated by the models and the palettes generated by expert observers. That is, the difference between the model palettes and the expert human palettes is statistically larger than the differences between the expert's palettes. In short, there is evidence that these models can adequately predict palettes as well as naïve observers but not as well as expert observers.

CONCLUSION

Colour is recognised as a significant factor within trend forecasting, influencing commercial success across industries. Research within this manuscript presented areas for development within the forecasting model. A particular focus highlighted opportunities in combining automated methods (through machine learning) with a human-based approach to gather and analyse trend research for colour analysis and prediction. The pilot study in this report explored methods to augment colour selection in the trend forecasting process. Further research is required into the probability of more accurate colour forecasting via automated methods in comparison to more traditional methods.

The methodologies for the experimental work were concerned with 2 particular aspects: firstly to evaluate the performance of automatic colour extraction methods using images of mood boards. The second aim was to compare the colour palettes generated by expert and naïve participants. The study found a statistically significant difference between the palettes generated by the automated models and the palettes generated by expert observers. That is, the difference between the automated palettes and the expert human palettes is statistically larger than the differences between the expert's palettes. There is evidence that these models can adequately predict palettes as well as naïve observers but not as well as expert observers. It could be argued that this supports the belief within the trend industry that expertise and creative intuition cannot be replaced by a machine. However, the difference between naïve and expert observers may not be apparent if a larger group size was used. The pilot study has identified future research aims and objectives.

REFERENCES

1. Cassidy, T.D. (2019). Colour forecasting. *Textile Progress*, **51** (1), 1-37.
2. Scully, & Cobb, D. J. (2012). Colour forecasting for fashion. Laurence King Publishing.

3. Lai, P. & Westland, S. (2020) Machine learning for colour palette extraction from fashion runway images. *International Journal of Fashion Design, Technology and Education*, **13** (3), 334-340.
4. Scully, & Cobb, D. J. (2012). Colour forecasting for fashion. Laurence King Publishing.
5. Kim, Fiore, A. M., Payne, A., & Kim, H. (2021). Fashion trends : analysis and forecasting (Second editon.). Bloomsbury Visual Arts. Ahmed. M., Seraj, R. & Islam, S.M. (2020). The k-means algorithm: A comprehensive survey and performance evaluation, *Electronics*, **9** (8), 1295.
6. Hidefi. (2017). 12 - Understanding and forecasting colour trends in design. In Colour Design (Second Edition, pp. 285–298). Elsevier Ltd. https://doi.org/10.1016/B978-0-08-101270-3.00012-6
7. Cassidy. (2013). Sustainable colour forecasting: The benefits of creating a better colour trend forecasting system for consumers, the fashion industry and the environment. In Sustainability in Fashion and Textiles (1st ed., pp. 111–124). Routledge. https://doi.org/10.4324/9781351277600-7
8. Cheung, V. & Westland. S. (2006). Optimal color selection methods, *Journal of Imaging Science and Technology*, **50** (5), 481-488.
9. Yang, J., Chen, Y., Xiao, K. & Westland, S. (2020). Predicting visual similarity between colour palettes, *Color Research and Application*, **45** (3), 401-408.

THE ENVIRONMENTAL COLOR IMAGERY SURVEY VIA VIRTUAL REALITY

Yuh-Chang Wei[1]*, Monica Kuo[2], Ya-Ping Kuo[2]

[1] Department of Information Communications, Faculty, Chinese Culture University, Taiwan R.O.C.
[2]Department of Landscape Architecture & Environmental Planning, Faculty, Chinese Culture University, Taiwan R.O.C.

*Corresponding author: Yuh-Chang Wei, ycwei@ulive.pccu.edu.tw

ABSTRACT

The objective of color planning is to maintain the balance between the color imagery of local environment and the heritage of local culture. In previous research, local color imagery was considered as one of the key factors influencing color scheme planning. The main focus of the environmental color imagery study is on the collection, induction and extraction of local colors to represent the color image of a regional environment, to illustrate the architectural color and local natural geographical environment (such as local materials), and to construct the relationship between the environment conditions and the human geography (local cultural traditions, customs, etc.). All the factors affecting the color imagery of the environment are included in the scope of investigation. An environmental color imagery survey conducted to collect regional colors information and to establish an environmental color database for further analysis. The investigation is through a systematic process using panoramic photography, sampling, color measurement, coding, and classification. A panoramic camera w/ UVA is used to capture 360-degree panoramic images in a series of photo shooting of regional environmental landscapes including mountains, sky, land, buildings, roads, etc. An immersive virtual reality of the regional landscape is created by a series of high-resolution panoramic images captured from different angles that makes observers feel like they are watching the scene at present. It is essential that the environmental color imagery survey via virtual reality would help to better understand the color image space of the regional environment and observer cognitive semantics of local environmental color space. The results of this study indicated that the distributions of certain color image data showed opposing image perception, and the mean value showed a mutual result, but in fact it is not a unanimous consensus. In-depth analysis of color image semantic scale needs to be further studied.

Keywords: Environmental color imagery survey, Virtual reality, Semantic differential (SD), Kobayashi color image scale

INTRODUCTION

The focus of environment color imagery survey, based on Jean-Philippe Lenclos' theory of color geography, is on the collection, induction and extraction of local chromatograms to represent the color composition of a region, to illustrate the architectural color and local natural geographical environment (such as local materials, and to construct the relationship between the environment conditions and the human geography (local cultural traditions, customs, etc.).

In previous research, an environmental color image analysis of Zheng-Bin Fishing Harbor was through a systematic process to develop a color database consisted of 269 color patches categorized into the domain color, secondary color and embellishment from the harbor landscape. A histogram color chart (Figure 1) was drawn to show the distributions of collected regional color samples via NCS five color categories.

Hue Range		Chromatogram	Color Tone	
Natural	N	14	B/W gray scale	Embellishment color
Color	Y-Y90R	91	Medium-Low Lightness Medium-High Chroma	
	R-R90B	58	Medium-High Lightness Medium-Low Chroma	Secondary color
	B-B90G	51	Medium-High Lightness Medium-Low Chroma	Domain color

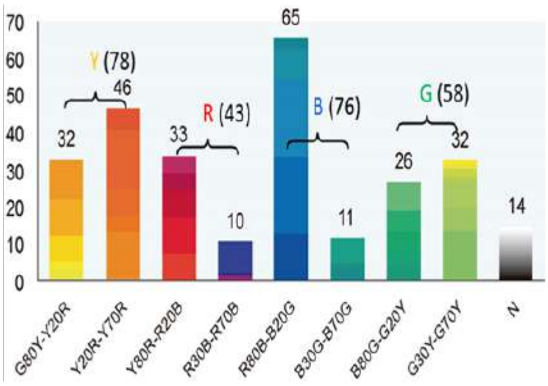

Figure 1. 269 regional colors collected by NCS environmental color survey tool and a histogram color chart showed the distributions of regional color samples.

Furthermore, an in-depth environmental color imagery survey conducted via virtual reality to provide a detailed environment image with comprehensive color information of region. It is expected that would help to better understand the color imagery space of the regional environment and observer's cognitive semantics of local environmental color space.

METHODOLOGY

The investigation is through a systematic process using photography, color measurement, sampling, coding, and classification. The collected color images are analyzed, classified, and presented by means of chart chromatography. A subjective environmental color imagery survey via virtual reality is conducted in order to collect observer's cognitive semantics of local environmental color imagery space.

Environmental Color Imagery Survey Tools

The use of environmental color survey tools began with landscape photography via panoramic digital camera and UAV. Adobe Color software is used to generate color palette for establishing a chromatogram chart measured by the image samples of Zheng-Bin Fishing Harbor regional colors. See Figure 2.

Figure 2. Tools used for the e*nvironmental color imagery survey*

Environmental Color Images and Chromatograms

Environment color image samples selected form both the macro (sky, sea, mountain, harbor, urban landscape, etc.) and micro (architecture, street, façade, etc.) levels based on the characteristics of regional landscape colors including main color, auxiliary color and embellishment color are respectively marked on the local cultural color image space (see Fig.3).

Figure 3. The Zhang-Bin Fishing Harbor environmental color images samples

Each of environment image samples is analyzed by Adobe color palette generator to create a chromatogram shown on Table 1.

Table 1: Chromatograms for Zhang-Bin Fishing Harbor Regional Colors

		Landscape elements site	Chromatogram	Photos of color sample
Natural environment color`	Sky			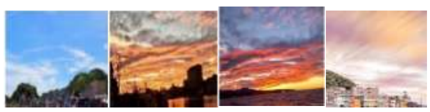
	Sea			
	Harbor			
	Mountain			

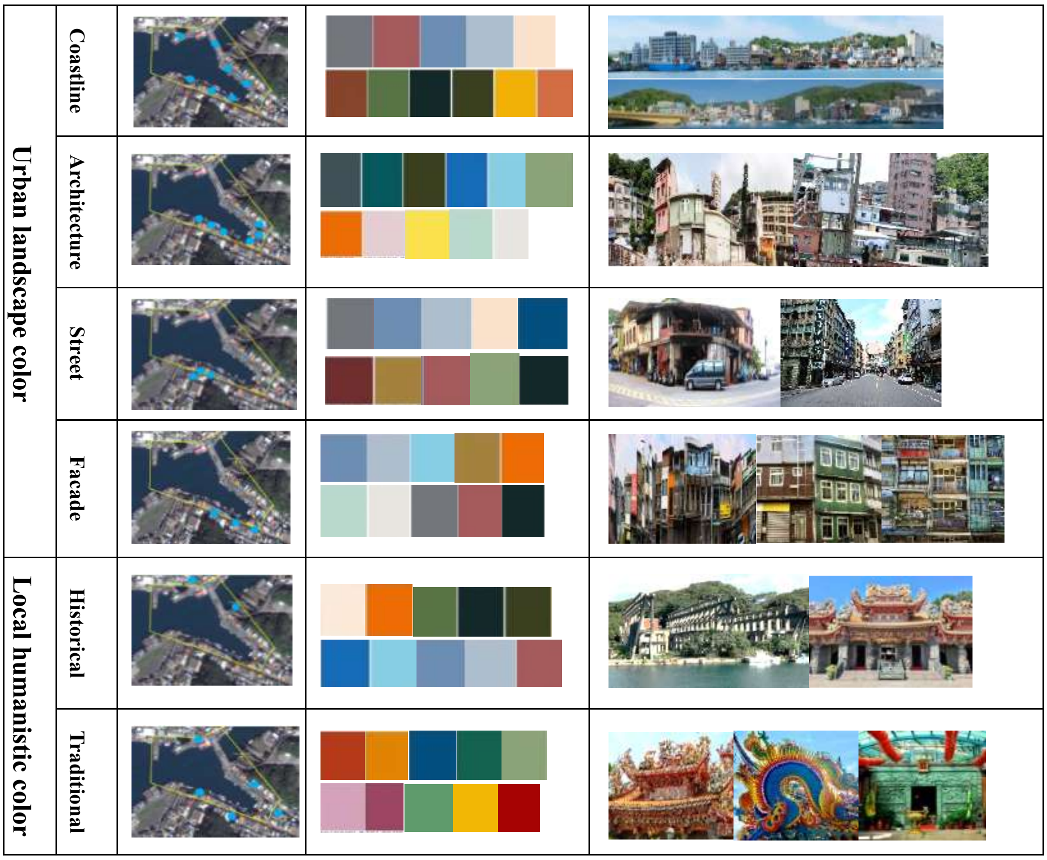

The Procedure of Environmental Color Imagery Survey

1. A semantic differential scale (SDS) was developed based on Kobayashi Color Image Scale to measure the color image of the observer's perception. The color imagery semantic words are selected to develop a SD questionnaire. The survey was conducted and analyzed.
2. A video guidance of the local environmental color image produced via virtual reality to provide the observers to establish a comprehensive color imagery of the region.
3. The color psychophysical experiment method is used to measure the semantic perception of each of the observers for the environmental color image. The experiment of environmental color imagery survey has shown on Figure 4. 15-20 volunteer research participants were recruited from the general public and local residents, a total of 30 people. Each participant did the experiment twice, a total of 60 trials data collected for the statistical analysis. The steps of the experiment are as follows:
   (1) First, the Farnsworth Munsell 100 Hue Test is used to evaluate the research participant's color recognition ability.
   (2) Observer wears a VR helmet to watch the guide video of the local environmental color landscape image.
   (3) Observer looks at the 2D local environment reference images on the computer screen to determine the semantic perception level between the local environmental color image in memory via SDS. According to the degree of cognitive strength, and the higher the scale value, the stronger the feeling, so as to obtain the psychophysical measurement value of the environmental color image.

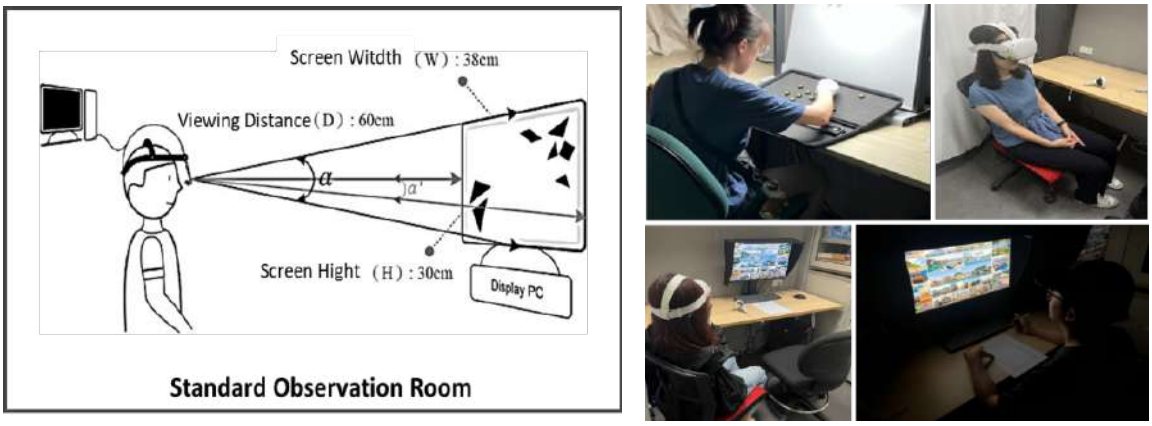

Figure 4. The experiment of environmental color imagery survey

RESULTS

Environmental Colors Imagery and Semantic Differential Analysis

After statistical analysis, the spatial distribution of the local color image is plotted via Kobayashi Color Image Scale coordinate plane. The scientific evaluation and analysis of relationship between the natural environment color image and observer's perception of environment color image was studied as follows:

1. The collected natural environment color image sample chromatograms were mapped to the Kobayashi color image coordinate plane. Semantic color image zones were created to present the natural environment landscape color image of Zhengbin Fishing Harbor. Four zones were plotted as: 1.Pretty–Romantic–Natural-Clear, 2.Casual-Dynamic, 3.Classic-Stylish-Rough, 4. Modern-Cool-Chic. See Figure 5.

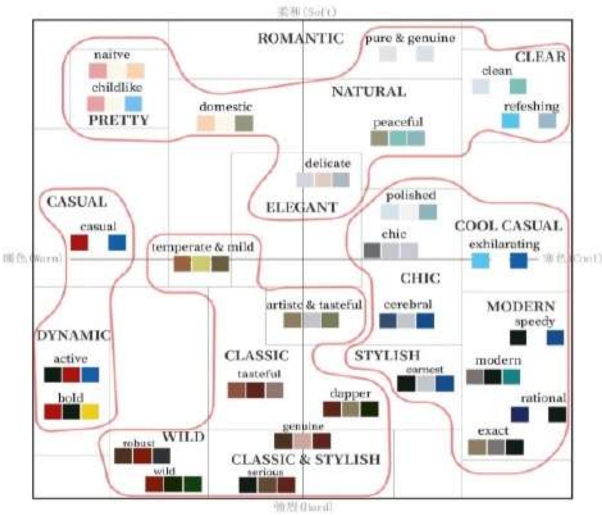

Figure 5. **Natural environment color image zones plotted on Kobayashi color image scale coordinate plane.**

2. The environmental landscape color image obtained through the SD evaluation experiment were mapped to the Kobayashi color image coordinate plane. Semantic color image zones were created to present the perceived landscape color image of Zhengbin Fishing Harbor. Four zones were plotted as: 1.Pretty-Romantic-Natural-Clear, 2.Casual-Elegant, 3.Dynamic, 4. Classic-Stylish-Rough, see Figure 6.

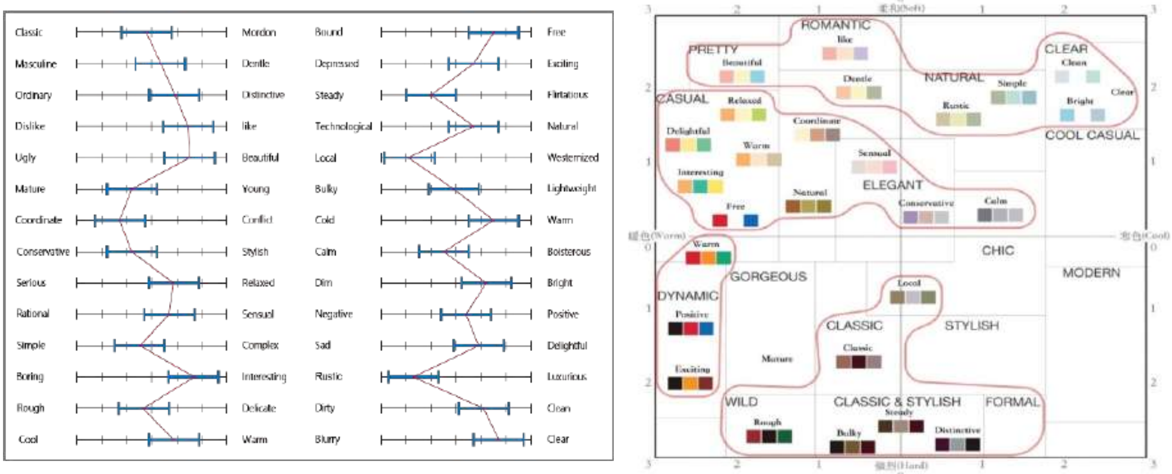

Figure 6. Color image SD evaluation results (left). Perceived semantic color image zones plotted on Kobayashi color image scale coordinate plane (right).

DISCUSSIONS

Issues regarding the environmental color image semantic differential analysis are discussed as follows:

1. The research results showed that the color image of the natural environment analyzed through scientific methods is different from the environmental color image subjectively perceived by the observers. Especially in terms of the perception of blue in this study, the color image did not reflect the meaning as predicted from the Kobayashi color image scale coordinate plane. The cognition related to "modernity" predicted by the statistical result of color semantic imagery reflected the difference of environmental imagery related to the historical sentiments of the region and the implementation of local renovation projects in recent years.
2. From the statistical data analysis, the distributions of certain color image data showed opposing imagery strengths, and the mean value showed a mutual result, but in fact it is not a unanimous consensus, such as blue. In-depth analysis of color image semantic scale needs to be further studied.
3. The use of virtual reality provides a comprehensive regional environmental color image space, which can effectively assist observers in establishing a comprehensive environment color space image to reduce potential judgment errors caused by rigid personal subjective cognition.

CONCLUSION

The results of the study indicated that color imagery has multiple meanings related to local cultural heritage and emotional experience. Therefore, in order to obtain universal color imagery, it is required a broader cross-cultural communication discipline, which will help continue to explore the integration research between color science and color psychology.

ACKNOWLEDGEMENT

The research project (MOST 111-2410-H-034-041) was funded by National Science and Technology Council. It is to express our sincere gratitude to NSTC in support of this research.

REFERENCES

1. Hård, A.; Sivik, L. & Tonnquist, G. (1996). "NCS Natural Color System - from Concepts to Research and Applications. Part I and II". *Color Research and Application*. Vol. 21, p.180–220. Toronto, Canada: John Wiley & Sons

2. Kobayashi, S. (1981). "The Aim and Method of the Color Image Scale", *Color Research & Application, 6,* 93-106. Toronto, Canada: John Wiley & Sons

3. Lee, L.S., Chien, C.C. & Lee, C.Y. (2012). 'The Harbor Environment Color Assessment and Planning Research", *Proceedings of the 34th Ocean Engineering Conference in Taiwan National Cheng Kung University.* P.625~630. Kaohsiung: Taiwan.

4. Lenclos, J. (1999) *Couleurs du monde*. Moniteur, Paris.

5. Lin, Y.T & Chuang, M.C. (2013). *Image of Color Combination in Different Types of Objects*, unpublished Thesis, National Chiao Tung University. Taipei: Taiwan

6. Qi, M.; Lu X. & Qian, Q. (2018) "Study on the Color Characteristics of Dalian City". *Proceedings of 9th International Conference on Urban Planning, Architecture, Civil and Environment Engineering*. P.18~22. Kyoto: Japan.

REDNESS PERCEPTION OF DICHROMATS FOR SHORT-WAVELENGTH LIGHTS

Suzuka Asakura[1]*, Taiju Inoshita[1], Tsukasa Muraya[2] and Shoji Sunaga[3]

[1] *Graduate School of Design, Kyushu University, Japan.*
[2] *Faculty of Contemporary Social Studies, Chikushi Jogakuen University, Japan.*
[3] *Faculty of Design, Kyushu University, Japan.*

*Corresponding author: Suzuka Asakura, asakura.suzuka.040@s.kyushu-u.ac.jp

ABSTRACT

The color perception of humans is based on differences in the activities of three types of cones in the retina. In trichromats, redness arises not only in the long-wavelength region from the L–M response but also in the short-wavelength region through the S cone response. In protanopes, there are no L cones, which makes red–green discrimination difficult. Similarly, deuteranopes lack M cones, making it difficult to distinguish red–green. However, it is known that they can respond to red and green under certain conditions and give color names similar to those given by trichromats. The cause of this phenomenon is not well understood in detail yet, and the contribution of S cones to redness perception in dichromats in the short-wavelength region has not been examined well. It is necessary to examine redness perception in dichromats for short-wavelength lights because they have S cones. In addition, in the dichromatic simulation proposed by Brettel et al. (1997), short-wavelength light could not be simulated [1]. In this study, the purpose was to investigate the redness perception of dichromats in the short-wavelength range. We used six short-wavelength light and two long-wavelength lights for comparison. There were two sets of conditions, luminances of 10 cd/m² and 30 cd/m² with a visual angle of 2°. Two protanopes, a deuteranope, and a trichromat participated in the experiment. Each participant's task was to estimate the color of each wavelength using a given color naming method and elementary color scaling method. The results established that dichromats perceive redness in both the long- and short-wavelength regions. However, because of individual differences and the small number of participants in the experiment, it is necessary to examine in detail the difference between the redness in the long-wavelength region and the redness in the short-wavelength region and to conduct this experiment with a larger number of participants.

Keywords: short-wavelength lights, redness, dichromacy, color naming, elementary color scaling

INTRODUCTION

Humans can perceive different colors depending on the responses of photoreceptors in the retina known as rods and cones. There are three types of cones: L cones, with a spectral sensitivity peak around long wavelengths (558 to 564 nm); M cones, with a spectral sensitivity peak around medium wavelengths (530 to 534 nm); and S cones, with a spectral sensitivity peak around short wavelengths (442nm) [2]. Color perception is roughly determined by the unique responses of these cones.

Dichromats, individuals with only two types of cones, are termed protanopes when lacking L cones, deuteranopes when lacking M cones, and tritanopes when lacking S cones. Because of having only two types of cones, protanopes and deuteranopes lack the red–green opponent channel and tritanopes lack the blue–yellow opponent channel. Despite this, it is reported that protanopes and deuteranopes responded "greenness" to medium-wavelength lights and "redness" to long-wavelength lights. However, consistent results related to the redness perception in protanopia and deuteranopia to short-wavelength lights have not been obtained. The protanopia participants in Bimler & Paramei's and Paramei et. al.'s studies gave no redness responses to short-wavelength lights, while those of Wachtler et. al.'s study reported redness perception to such lights as did trichromats [3] [4]. In trichromats, it is supposed that the S cone contributes to the redness perception at short wavelengths. If the redness perception from the S cone is independent of the L–M mechanism, protanopes and deuteranopes may perceive redness in short-wavelength lights.

In addition, there is a point concerning short-wavelength lights in dichromatic simulation that needs clarification. In the case of dichromats, all colors on a confusion line extending from the confusion point on the CIE chromaticity diagram appear to have the same color if their luminances are equal for dichromats. In other words, they cannot distinguish colors on the same confusion line. For colors that lie on the identical confusion color line, Brettel et. al. proposed protanopes and deuteranopes perceive colors at the points where the line intersects with another line from 475 nm to 575 nm through the achromatic point on the chromaticity diagram [1]. Capilla et. al. pointed out that short-wavelength lights below 475 nm do not have the simulated colors [5]. Thus, the perception of color at short wavelengths in individuals with dichromacy remains unknown.

In this study, we aimed to investigate whether individuals with protanopia and deuteranopia perceive redness in short-wavelength lights and, if so, how this perception occurs. We conducted experiments using color-name responses to shed light on this phenomenon.

METHODOLOGY

Apparatus and Stimuli

An optical system with a single channel was used in the experimental apparatus as shown in Figure 1. A 500 W xenon lamp was used as a light source, and monochromatic light was obtained using an interference filter within the optical path. The monochromatic light wavelengths were 400 (only for a luminance of 10 cd/m²), 420, 440, 460, 480, 500, 589, and 632 nm. The half-widths of the interference filters were 25 nm for the 400 nm wavelength and 10 nm for all the others. The luminance of the monochromatic light was 10 cd/m² or 30 cd/m², which was adjusted using a density wedge within the optical path and projected onto a rear projection screen. Participants observed the stimuli on the screen from a distance of 53 cm. The stimulus size was a visual angle of 2°.

Participants and Procedure

Two protanopes (KK, NH), one deuteranope (YR), and one trichromat (AS) participated in the experiment. The participants were initially dark-adapted, spending 2 minutes in a dark room. Subsequently, single monochromatic lights were randomly presented in turn. The participant had three tasks. The first was to respond to the color they perceived with any color name. The second task was to answer with a monolexical color name like "blue" or "red". Lastly, participants evaluated the color appearance of the monochromatic light using elementary color scaling. A

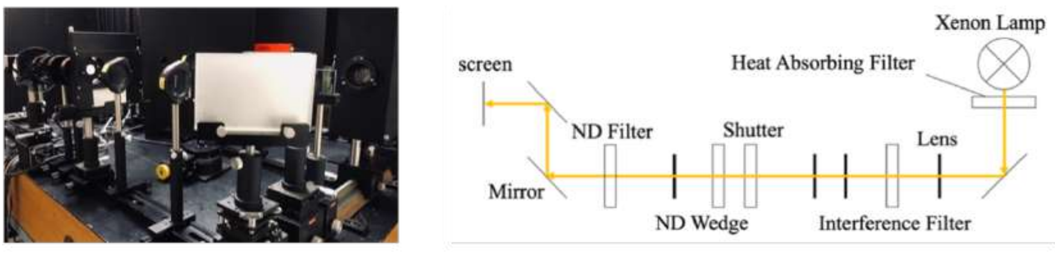

Figure 1. Apparatus

cumulative total of 10 points were assigned to the whiteness, blackness, and chromaticity of the color appearance of the monochromatic light. Additionally, if chromaticity was noted, an extra 10 points were assigned to the redness, yellowness, greenness, and blueness of the chromaticity. The stimulus was presented until the participant finished the tasks. This trial was conducted 15 times for each luminance and monochromatic light, except for KK, who performed the trial 10 times at the luminance of 30 cd/m².

RESULT AND DISCUSSION

Each participant's responses using elementary color scaling are shown in Figure 2. Individual difference was observed among the protanope participants. KK did not give responses indicating redness perception within the short-wavelength range, whereas NH responded with redness perception within this range. The deuteranope participant YR also revealed redness perception for the short-wavelength lights. However, for both NH and YR, the redness percentages were lower than those of the trichromatic participant AS. The dichromatic participants perceived redness at the long wavelength of 632 nm. In addition, green responses were obtained for the middle-wavelength lights. These results are consistent with those of the previous studies. That is, although dichromats hardly discriminate between red and green, they can respond to the redness and greenness of monochromatic lights.

The whiteness responses are also shown in Figure 2. The dichromatic participants assigned more points than the trichromat from 400 nm to 500 nm.

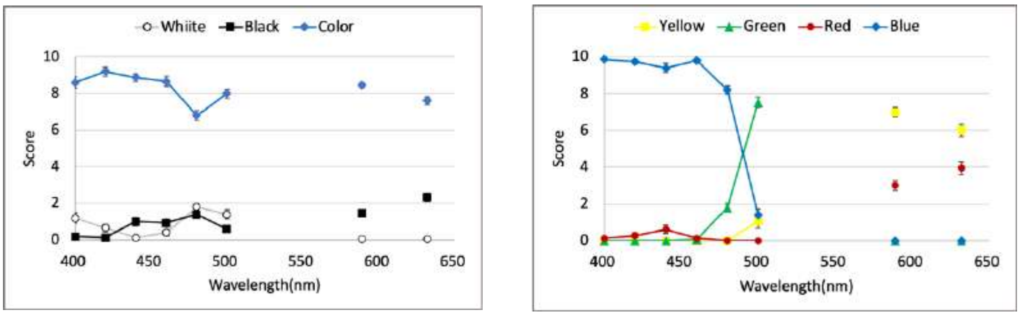

KK-P 10cd/m²

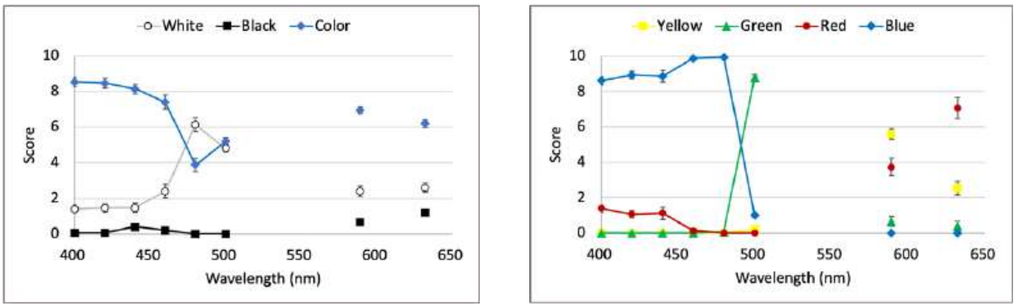

NH-P 10cd/m²

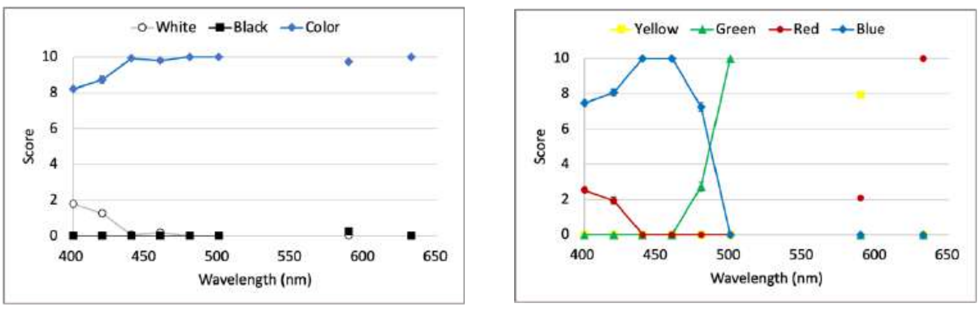

YR-D 10cd/m²

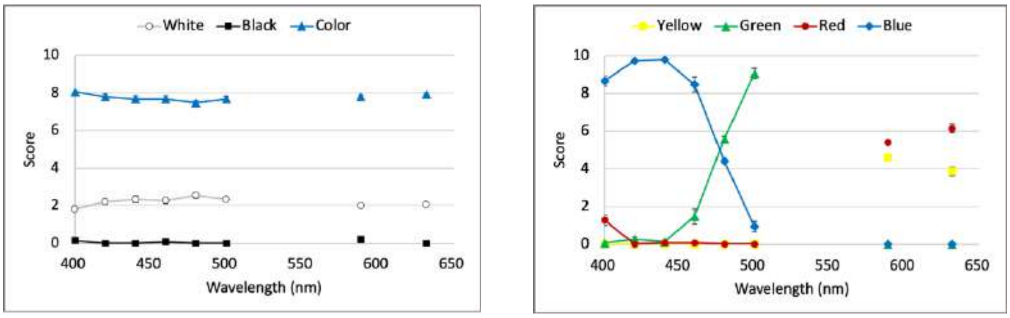

AS-N 10cd/m²

Figure 2. Results of color scaling for each participant.

Table 1 shows the color naming results with any color name and the monolexical color name. The dichromats described colors at 400 nm as “bright blue” or “blue,” whereas trichromats more frequently used terms like “bright purple” or “purple.” These results show that the magnitude of the redness perception in the dichromats to the short-wavelength lights may not be enough to affect the color name. For the longer wavelengths, the dichromat group often offered responses like “dark orange” or “light red,” whereas the trichromat group favored “bright orange” or “bright red.” Moreover, in contrast to the responses of the trichromats, the responses within the dichromat group exhibited variations dependent on the luminance. There was heightened variability particularly at 10 cd/m², leading to less consistent responses.

Table 1: Color naming results

KK-P 10cd/m²

Wavelength (nm)	Any color name	Single-word
400	Bright blue	Blue
420	Bright blue	Blue
440	Bright blue	Blue
460	Blue	Blue
480	Blue-green	Blue
500	Green	Green
589	Yellowish-orange	Orange
632	Dark orange	Orange

NH-P 10cd/m²

Wavelength (nm)	Any color name	Single-word
400	Blue	Blue
420	Blue	Blue
440	Blue	Blue
460	Blue	Blue
480	Light blue	Blue
500	Light green	Green
589	Reddish-yellow	Yellow
632	Light red	Red

YR-D 10cd/m²

Wavelength (nm)	Any color name	Single-word
400	Blue	Blue
420	Blue	Blue
440	Blue	Blue
460	Blue	Blue
480	Blue-green	Blue
500	Green	Green
589	Orange	Orange
632	Orange	Orange

AS-N 10cd/m²

Wavelength (nm)	Any color name	Single-word
400	Light purple	Purple
420	Light blue-purple	Purple
440	Bright blue	Blue
460	Bright blue	Blue
480	Bright light blue	Blue
500	Bright green	Green
589	Orange	Orange
632	Bright red	Red

This result confirmed that protanopes and deuteranopes did indeed perceive "red" and "green" at certain wavelengths. Some participants even responded with "redness" in the short-wavelength range, implying that dichromats perceive a form of "redness" when exposed to short-wavelength light. They also reported experiencing "redness" when encountering long-wavelength light. Further investigation is required to ascertain whether the redness perceived in short-wavelength light is equivalent to that in long-wavelength light. Should a relationship between rednesses in the long-wavelength and short-wavelength regions be established, it would suggest that factors beyond S cones contribute to redness perception. On the contrary, if no correlation is identified, then it is plausible that S cones are responsible for perceiving redness. However, given the substantial variation among subjects in this experiment, and considering the lesser vividness of redness compared with trichromatic perceptions in both the long-wavelength and short-wavelength regions, definitive conclusions about the contributing factors to redness perception remain elusive. The potential interconnection between rednesses in the long-wavelength and short-wavelength regions cannot be ruled out. However, its universality cannot be affirmed owing to the limited participant diversity involving one trichromat, two protanopes, and one deuteranope. For a comprehensive exploration of the redness perception, a more diverse participant pool is necessary for future experiments.

The outcomes of the dichromat experiment unveiled considerable overall variability, especially around longer wavelengths such as 589 nm and 632 nm. This suggests a potential lack of stability in color perception at these wavelengths.

The slight difference observed between the results at 10 cd/m² and 30 cd/m² indicates that the color perception of dichromats might be influenced by luminance. However, no significant alteration in overall color quality emerged between the two luminances, implying that the difference between 10 cd/m² and 30 cd/m² does not substantially impact color vision in either trichromats or dichromats.

In contrast to the outcomes of the color scaling experiments by Wachtler et al., "redness" starting from 420 nm in short-wavelength light has been reported for both dichromat and trichromat vision [4]. Although a direct comparison is challenging owing to differences in experimental luminance, previous studies have reported redness around 450 nm at luminances comparable to those used in this experiment. This aspect necessitates further investigation in the future.

CONCLUSION

This study revealed that dichromats indeed perceive redness within the short-wavelength range. However, the results also showed individual differences among the participants. Thus, it is necessary to conduct more experiments with more participants in the future.

ACKNOWLEDGEMENT

This work was supported by JSPS KAKENHI Grant Number JP21H04342. Mark R. Kurban from Edanz (https://www.jp.edanz.com/ac) edited a draft of this paper.

REFERENCES

1. Brettel, H., Viénot, F., & Mollon, J. D. (1997). Computerized simulation of color appearance for dichromats. *JOSA A*, *14*(10), 2647-2655.
2. Stockman, A., & Sharpe, L. T. (2000). The spectral sensitivities of the middle-and long-wavelength-sensitive cones derived from measurements in observers of known genotype. *Vision research, 40*(13), 1711-1737.
3. Bimler, D. L., & Paramei, G. V. (2005). Bezold–Brücke effect in normal trichromats and protanopes. *JOSA A, 22*(10), 2120-2136.

4. Wachtler, T., Dohrmann, U., & Hertel, R. (2004). Modeling color percepts of dichromats. *Vision Research, 44*(24), 2843-2855.
5. Capilla, P., Dıez-Ajenjo, M. A., Luque, M. J., & Malo, J. (2004). Corresponding-pair procedure: a new approach to simulation of dichromatic color perception. *JOSA A*, *21*(2), 176-186.

INFLUENCE OF LIGHTING SOURCE DIRECTION ON COLOR PERCEPTION AND TEXTURE IMPRESSION OF FABRICS

Shuilan He [1]*

(Tohoku Seikatsu Bunka University, 1-18-2 Nijinooka, Izumi Ku, Sendai Shi, Miyagi Ken)
[1] Fashion Culture Faculty, Department of Home Economics, Tohoku Seikatsu Bunka University, Japan..

* heshuilan@mishima.ac.jp

ABSTRACT

According to the author's recent research, the color appearance and texture impression of glossy fabrics can change significantly when the spectral distribution and illuminance of LED lighting are varied. Additionally, Ko et al. reported that the direction of the light source and display method can affect the perception of fabric texture, especially for glossy fabrics, which can exhibit significant changes in texture impression depending on the display method.
In this study, we simulated the lighting used in a fashion store and examined how the direction of the light source affected the color appearance and texture impression of glossy and matte fabrics using three types of LED lighting: LED-D65, 3000K, and High Ra. We also used three display methods (flat, hanging, and three-dimensional) to present the fabrics on tables, hangers, and mannequins. Red glossy fabric was used as the sample material, and the light source was varied in three directions: 0°, 45°, and 90°. Participants subjectively evaluated the color appearance and texture impression of the samples using the SD method (9-point scale). The results showed that subjective evaluations of texture impression varied depending on the angle of the light source, and different display methods and lighting types also had an impact on the perception of the samples.

Keywords: Lighting Source Direction, Color Perception, Texture Impression, Fabrics

INTRODUCTION

Ko et al. [1] conducted simulations of fashion store lighting and demonstrated that the impression evaluation of clothing varies depending on the display method and the type and direction of lighting. Previous studies by the authors [2,3] have revealed significant differences in the perception of fabric color and texture impressions under different illuminance and spectral distribution lighting conditions. Furthermore, it was revealed that the perception of fabric texture varies depending on the display method (tables, hangers, and mannequins).

This report investigates the differences in the appearance and texture impression of glossy and matte fabric colors when presented using different lighting directions (90°, 45°, 0°) and display methods (tables, hangers, and mannequins), assuming a fashion store environment.

METHODOLOGY

(1) Experimental Method

The experiment used a Semantic Differential (SD) method with 12 pairs of adjectives (as shown in Table 1) to evaluate the perception of color and texture impressions of fabric samples under lighting conditions with different color temperatures and color rendering properties.

Table 1: Adjective pairs

(-)		(+)
Muted	—	Vivid
Dry	—	Moist
Blur	—	Clear
Dark	—	Bright
Heavy	—	Light
Dull	—	Sharp
Polished	—	Unpolished
Matte	—	Glossy
Soft	—	Hard
Dense	—	Faint
Rough	—	Smooth
Thick	—	Thin

(2) Lighting Conditions

The experiment utilized an observation booth (Figure 1), with light sources placed at three locations: above (90°), lateral (45°), and left (0°) of the booth. Three types of commercial LED lamps were used as light sources: LDA12D-G-E26 (LED-D65), LDA12L-G-E26 (3000K), and DiCUNO ProOE (HighRa). The characteristics of each lighting condition used in the experiment are shown in Table 2. Subjects observed fabric stimuli through the aperture of a mask (non-chromatic, N6) installed in front of the booth to maintain a fixed observation angle.

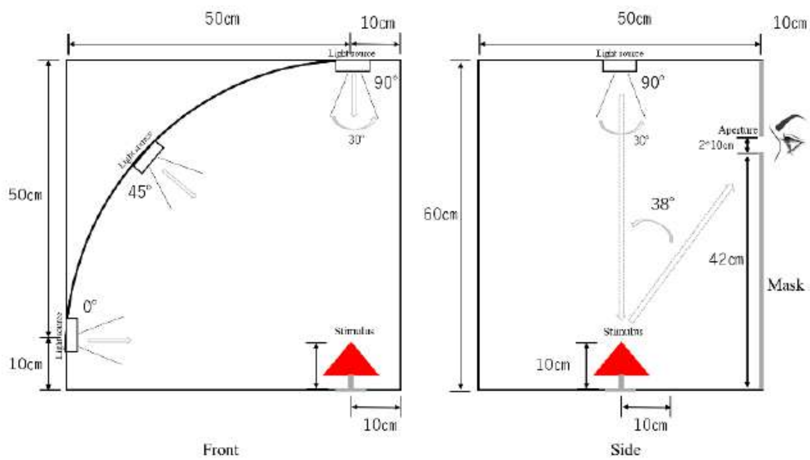

Figure 1. Evaluation booth

Table 2: Adjective pairs

	LED-D65	LED-HighRa	LED-3000
CCT	6470	5116	2912
duv	0.00818	0.00194	-0.00127
Ra	83.2	97.5	82.7
R9	5	85	6
R10	69	97	83
R11	84	97	82
R12	63	96	76

(3) Evaluation Samples

The evaluation samples (Figure 2) were as follows:

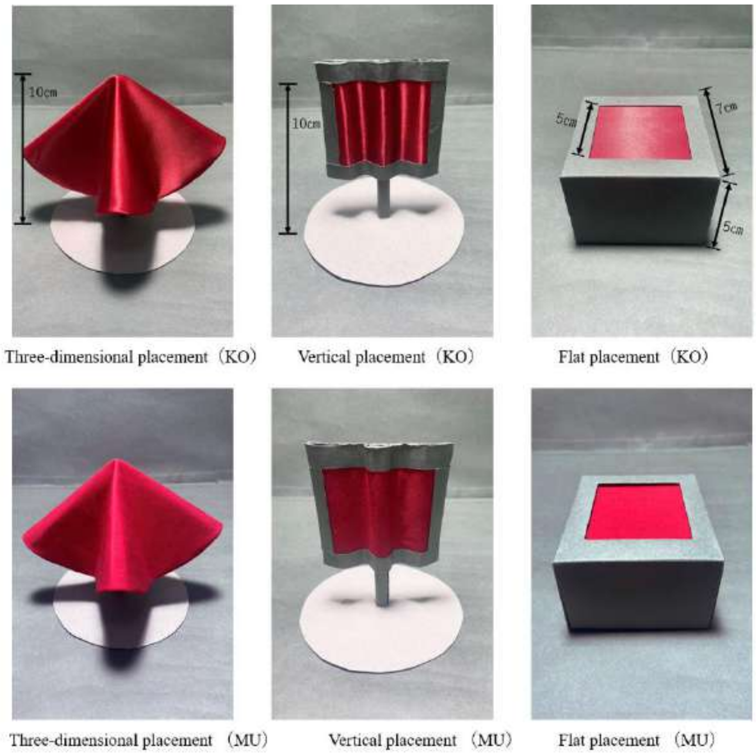

Figure 2. The evaluation samples

Fabric Types: Broadcloth (moonfarm, 100% cotton, 120g/m², thread count: CD40×CD40), Silk Satin (Toray, 100% polyester, 120g/m², thread count: CD80×CD80)

Color: Red

Surface Characteristics: Glossy (KO), Matte (MU)

Sample Shapes: Three-dimensional placement (mannequin), vertical placement (hanger), flat placement (table placement)

Sizes: Three-dimensional placement height 10 cm, fabric height 5 cm; vertical placement height 10 cm, fabric 5×5 cm; flat placement height 5 cm, fabric 5×5 cm; Surrounding: Non-chromatic mask (N5).

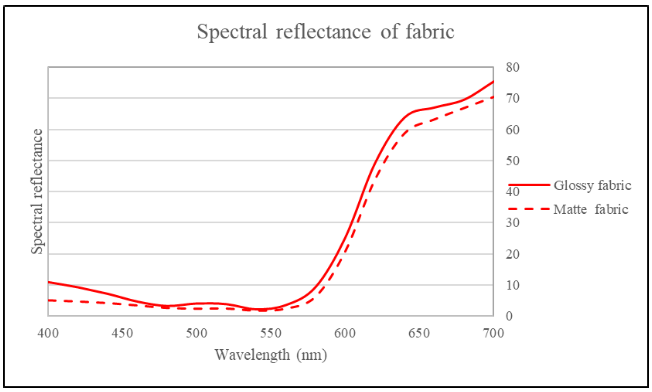

Figure 3. Spectral reflectance (SCE) of evaluation samples (Gloss: solid line, matte: dotted line)

(4) Experimental Procedure

Subjects underwent 3 minutes of dark adaptation before the experiment. They then observed fabric stimuli through the aperture of a mask installed in front of the booth and provided absolute ratings for color perception and texture impression. Evaluation was recorded by the subjects themselves on evaluation sheets.

(5) Subjects

Ten observers with normal color vision, aged between 19 and 38, including those with corrective eyewear or contact lenses, participated in the experiment.

RESULT AND DISCUSSION

(1) The result of Principal Component Analysis

The subjective evaluation results of all subjects under each lighting direction were analyzed using Principal Component Analysis (IBM SPSS). As shown in Table 3, the first principal component related to fabric surface impressions, and the second principal component related to weight impressions were extracted.

Table 3: The result of Principal Component Analysis

Evaluative adjective pairs \ Principal Component			(Ⅰ)Fabric surface impressions	(Ⅱ)Weight impressions	(Ⅲ)
Muted	—	Vivid	-0.94	-0.16	-0.08
Polished	—	Unpolished	-0.90	0.11	0.01
Matte	—	Glossy	-0.89	0.35	0.07
Rough	—	Smooth	-0.88	0.33	0.05
Dull	—	Sharp	-0.71	-0.19	-0.18
Dark	—	Bright	-0.67	-0.50	-0.20
Blur	—	Clear	0.79	-0.53	-0.36
Heavy	—	Light	-0.36	-0.83	0.26
Dry	—	Moist	-0.66	0.66	-0.03
Dense	—	Faint	0.35	-0.64	0.23
Thick	—	Thin	-0.53	-0.5391	0.43
Soft	—	Hard	0.54	-0.44	-0.53

(2) Subjective Evaluation Results

In the first principal component (surface impressions), the evaluation results included pairs of adjectives such as " Muted-Vivid," " Dark-Bright," " Dull -Sharp," " Polished-Unpolished," and " Rough-Smooth" Correspondences with subjective evaluation results were examined.

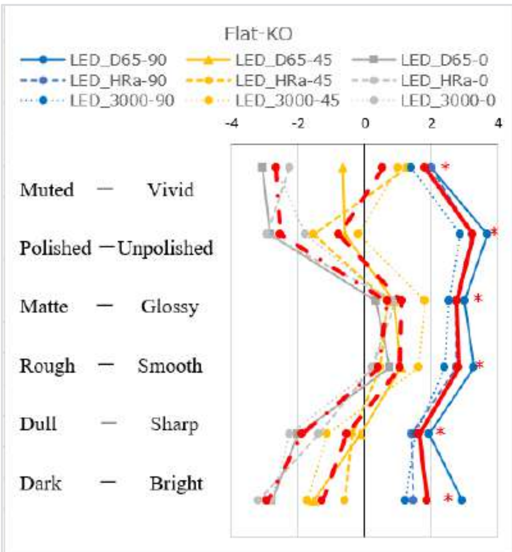

Figure 4. The relationship between Flat-KO's lighting angle and surface impression

In Figure 4, it was revealed that for flat glossy fabric samples, the results of subjective evaluations related to surface impressions, belonging to the first principal component, varied significantly depending on the angle of the light source. T-tests showed significant differences between subjective evaluations at 90° and 45° ($t(4) = 15.39$, $p < 0.001$), 45° and 0° ($t(4) = 15.39$, $p = 0.043$), and 90° and 0° ($t(4) = 7.74$, $p < 0.001$). As the angle of the light source decreased, subjective evaluation results were more likely to include terms such as "dull," "dark," "rough," and "non-glossy."

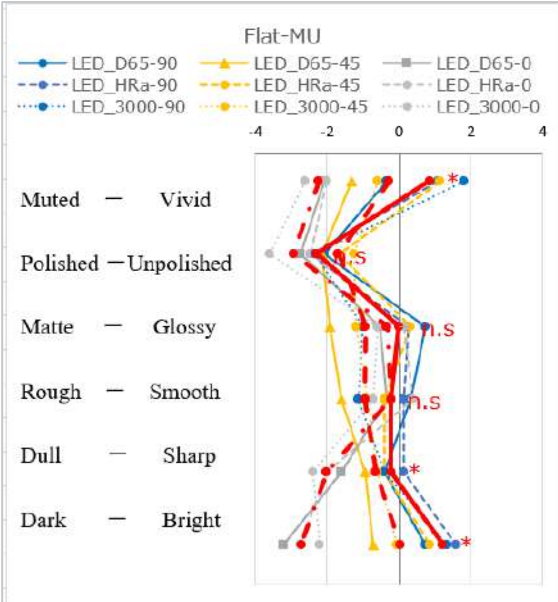

Figure 5. The relationship between Flat-MU's lighting angle and surface impression

In Figure 5, it was similarly demonstrated that for flat matte fabric samples, subjective evaluation results related to surface impressions, belonging to the first principal component, also varied depending on the angle of the light source. A significant difference was found between subjective evaluations at 90° and 0° ($t(4) = 2.54$, $p < 0.05$). Subjective evaluation results were more likely to include terms such as "dull," "dark," "rough," and "non-glossy" as the angle of the light source decreased.

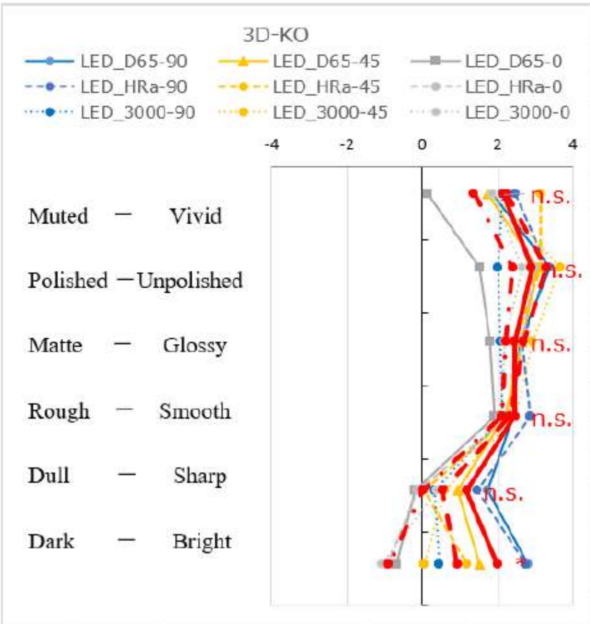

Figure 6. The relationship between 3D-KO's lighting angle and surface impression

In Figure 6, for three-dimensional glossy fabric samples, it was observed that the results of subjective evaluations related to surface impressions, belonging to the first principal component, remained relatively stable regardless of the lighting source direction. No significant difference was found in subjective evaluations between 90° and 0°.

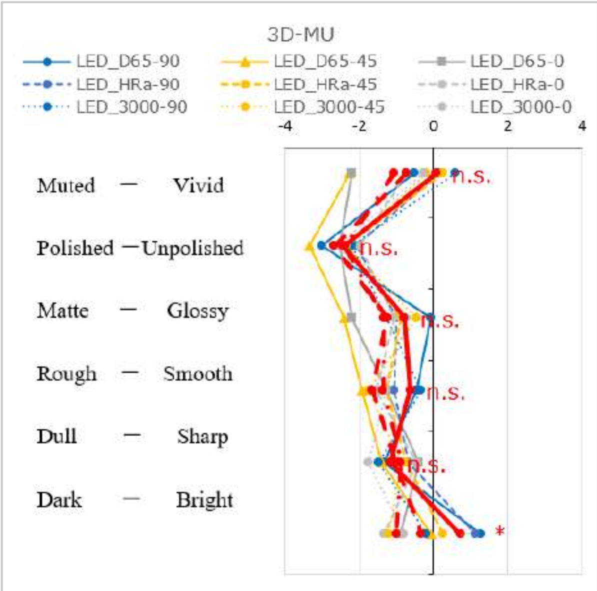

Figure 7. The relationship between 3D-MU's lighting angle and surface impression

In Figure 7, for three-dimensional matte fabric samples, it was also demonstrated that subjective evaluation results related to surface impressions did not vary significantly depending on the lighting source direction. No significant difference was found in subjective evaluations between 90° and 0°.

CONCLUSION

The following results were obtained from this study:

It became clear that the subjective evaluation results differed depending on the lighting source direction. It was shown that the three-dimensional display method is less affected by the lighting source direction. On the other hand, it has become clear that shiny fabrics are more easily affected by the lighting source direction than matte fabrics. It became clear that the flat display method, regardless of whether it is glossy or not, is greatly affected by the lighting source direction.

In summary, in fashion stores, it has become clear that three-dimensional display methods, whether glossy or not, are less affected by the lighting source direction, while flat display methods are significantly affected by the lighting source direction.

REFERENCES

1. T.K. Ko, et al. (2016). Simulation and perceptual evaluation of fashion shop lighting design with application of exhibition lighting techniques. SungBuilding Simulation. 9(6). pp.641–658. doi:10.1007/s12273-016-0312-5
2. He, S., & Nakajima, Y., (Eds.). (2020). Effect of Spectral Distribution of Illumination on Color Appearance and Texture Impression of the Fabric with Different Surface Properties. *J. Illum. Engng. Inst. Jpn. 104* (2020), pp. 3–10.doi.org/10.2150/jieij.190000586
3. He, S., & Nakajima, Y., (Eds.). (2019). The Influence of Spectral Distribution of Illumination on the Color and Texture Appearance of Glossy Fabric. *Journal of Japan Society of Kansei Engineering.* Vol.18No.5 pp.407-416. doi:10.5057/iiskeTJSKE-D-19-00005

STEADY STATE PUPIL RESPONSE ELICITED BY INDEPENDENT STIMULATION OF MELANOPSIN AND CONE PHOTORECEPTORS

T. Ito[1], M. Takikawa[2], A. Takasu[1], Y. Fujita[1] and S. Tsujimura[1*]

1 Graduate School of Design and Architecture, Nagoya City University, Nagoya, Japan
2 School of Design and Architecture, Nagoya City University, Nagoya, Japan

*Corresponding author: Sei-ichi Tsujimura, tsujimura@sda.nagoya-cu.ac.jp

ABSTRACT

A recently discovered photoreceptor, ipRGC (intrinsically photosensitive retinal ganglion cell, or melanopsin cell) contributes to the non-image forming pathway such as photoentrainment of circadian rhythms and pupillary light reflex. Although a large number of studies have been made on the investigation of the non-image forming pathway in rodents, little is known about humans. It is important what kind of attributes of ambient light, e.g. colour luminance and melanopsin stimulation, most influences the non-image forming pathway in humans. The melanopsin ganglion cells receive signals from all photoreceptors. Therefore, to investigate the influence of melanopsin ganglion cells on the non-imaging forming pathway, it is necessary to investigate how the signals from melanopsin and cone photoreceptors contribute to the non-image forming pathway. In the present study, we focused on the pupillary light reflex in the non-image forming pathway of brain function. The purpose of this study was to investigate how melanopsin and cone photoreceptors contribute to the pupillary light reflex and to determine a pupillary light reflex mechanism. We used a multi-primary stimulation system, which can stimulate each photoreceptor independently. The right eye was exposed to full-field stimuli and the steady pupillary response of the left eye was measured. Nine test stimuli were used which increased or decreased the stimulation of four types of photoreceptors, melanopsin, L-cone, M-cone, and S-cone photoreceptors. For example, the stimulus in which only the amount of stimulation to melanopsin was increased from the control (MelH), and similarly the amount of stimulation to melanopsin was decreased (MelL). These melanopsin stimuli were metameric stimuli with the same luminance and the colour as the control stimuli. The results showed that the steady-state pupil diameter in MelH stimulation was smaller than that in the MelL stimulation although they had the same luminance and colour. This result was consistent with those of previous studies. It was shown that the pupil diameter in LH stimulation was smaller than that in the LL stimulation and that the pupil diameter in ML stimulation was smaller than that in the MH stimulation although the luminance of ML stimulus was greater than MH. Based on the results, we proposed a model of the pupillary light reflex mechanism. The model can estimate the steady-state pupil diameter from the spectrum. In the model, the amount of stimulation of each photoreceptor is calculated from the spectrum of the light stimulus using the spectral sensitivity of melanopsin, L-cone, M-cone, and S-cone photoreceptors. It is assumed that the amount of stimulation from each photoreceptor is linearly combined and contributes to the steady-state pupil diameter. In other words, there are four unknown parameters that convert from each photoreceptor to the steady-state pupil diameter. The parameters were solved as an optimisation problem using the results from nine different test stimuli.

Keywords: pupillary light reflex, melanopsin, non-image forming pathway, cone photoreceptors, luminance

INTRODUCTION

Around 2000, a third photoreceptor, intrinsically photosensitive retinal ganglion cells (ipRGCs), was discovered in addition to cone and rod cells [1]. Here they are referred to simply as melanopsin cells. Melanopsin cells have been reported to be associated with non-imaging pathways [2]. The non-image forming pathway is related to physiological brain functions, including the pupillary reflex and circadian rhythms. However, studies on the contribution of melanopsin cells to the non-image forming pathway have been mainly animal studies, and their effects on humans are largely unknown. This study will focus on pupillary light reflex in human to verify the contribution of melanopsin cells to non-image forming pathway in humans.

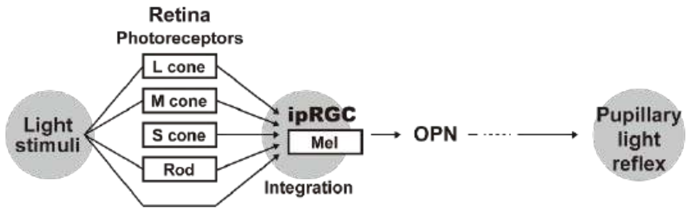

Figure 1. Retinal photoreceptions and pupillary light reflex

In order to examine the effect of melanopsin cells on the pupillary light reflex, it is necessary to consider the effect melanopsin cells as well as the three types of cone and rod photoreceptors on the pupillary light reflex. As shown in Figure 1, melanopsin cells (ipRGCs) receive signals not only from melanopsin in their own photoreceptors (Mel) but also from cone and rod photoreceptors [2].

The purpose of this study is to investigate how melanopsin cells and each cone photoreceptor contribute to the steady-state pupil diameter and to clarify the mechanism of the non-imaging forming pathway.

METHODS

Apparatus

We used a multi-primary stimulation system for our experiments [3]. This stimulation system can independently stimulate each photoreceptor using silent-substitution technique, based on the amount of stimulation to each photoreceptor. The stimulation system has four primary colours: red, yellow, green and blue, with peak wavelengths of 633 nm, 569 nm, 532 nm and 463 nm, respectively.

Test Stimuli

We used the test stimuli that stimulated each photoreceptor independently. The test stimuli were independently modulated of the control stimulus in the amount of stimulation to each photoreceptor.

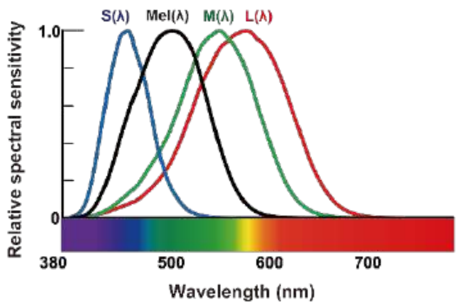

Figure 2. Relative sensitivities of cone and melanopsin photoreceptors

The amount of stimulation to each photoreceptor was calculated from the spectral radiance of the test stimuli and the spectral sensitivity of each photoreceptor. Figure 2 shows the spectral sensitivities of L, M, S cones, and melanopsin. The amount of stimulation for each photoreceptor

(*P*) is determined by the following Eq. (1); *I(λ)* is the spectral radiance of the test stimulus and *P(λ)* is the spectral sensitivity of the photoreceptor.

$$P = \int I(\lambda)P(\lambda)\, d\lambda \tag{1}$$

The control stimuli were white stimuli with photoreceptor stimulations of 206 cd m^{-2} for L cone, 76 cd m^{-2} for M cone, 132 cd m^{-2} for S cone, and 174 cd m^{-2} for melanopsin, respectively. We used the melanopsin-high stimulus, MelH and melanopsin-low stimulus, MelL, which only modulated the amount of melanopsin stimulation by ±20% from the control stimulus. Similarly, we modulated the amount of stimulation to L, M and S cones by ±20%. Those stimuli were LH, LL, MH, ML, SH and SL stimuli described in Figure 3.

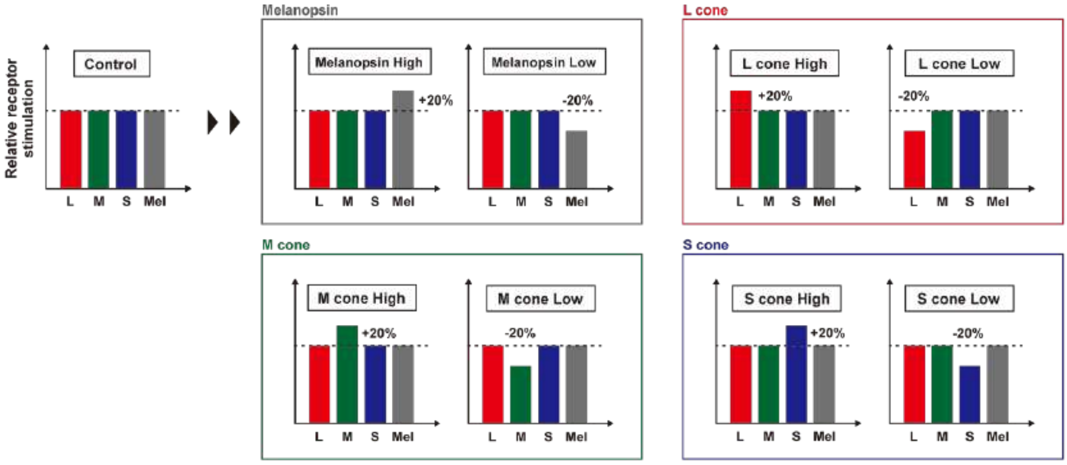

Figure 3. Modulation of stimulation from the control stimulus

The five test stimuli, Control, MelH, MelL, SH, and SL stimuli, have the same luminance at 282 cd m^{-2}. In particular, Control, MelH, and MelL stimulus were white and metameric to each other. We chose the steady background as test stimuli with high illuminance since we have shown that there was little/no influence of rod in the similar condition [4].

Procedure

The right eye was exposed to full-field stimuli and the pupillary response of the left eye was measured with an infrared camera. The observers adapted to the test stimulus for 5 minutes, then were exposed to the test stimulus for approximately 2 minutes. The order of a pair of the test stimuli were counterbalanced as shown in Figure 4. The eight observers participated in the experiment. They were 3 males and 5 females between the ages of 21 and 25, with a mean age of 22.1 years.

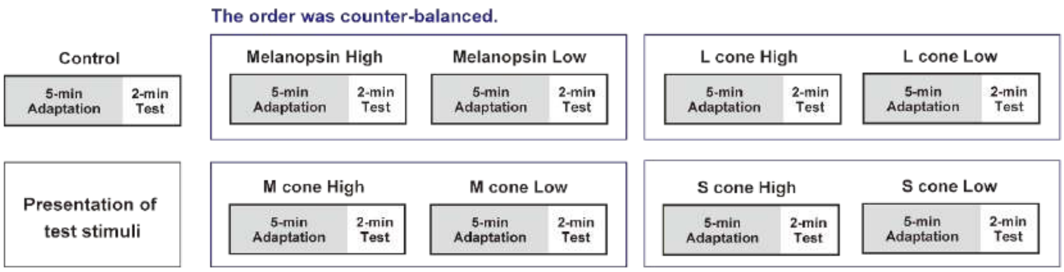

Figure 4. Presentation of the test stimuli

Analysis

A time series of pupil data for 100 seconds of the 2-minute period during which the observer was exposed to the test stimulus was used for analysis. The video was captured at 30 frames per second, resulting in 3000 frames of pupil images for each test stimulus. The pupil diameters during these 100 seconds period were averaged to obtain the steady-state pupil diameter for the test stimulus. The observers took a minimum of four measurements for each test stimulus.

RESULTS AND DISCUSSION

The averaged results for eight subjects were shown in Figure 5. Error bars were standard deviations. The results showed that the steady-state pupil diameter to MelH stimulus was smaller than that to MelL stimulus (p=.0074, paired t-test). The pupil diameter to LH stimulus was found to be smaller than that to LL stimulus (p=.0028, paired t-test). The pupil diameter to ML stimulus was found to be smaller than that to MH stimulus (p=.0329, paired t-test).

It was found that the stimulation of melanopsin cells affects steady-state pupil diameter, consistent with previous studies [5]. In addition, the results suggested that there was a contribution of L-M cone-opponent mechanism. In the previous studies have shown that the L-M cone opponent mechanism contributes to pupil response [6,7].

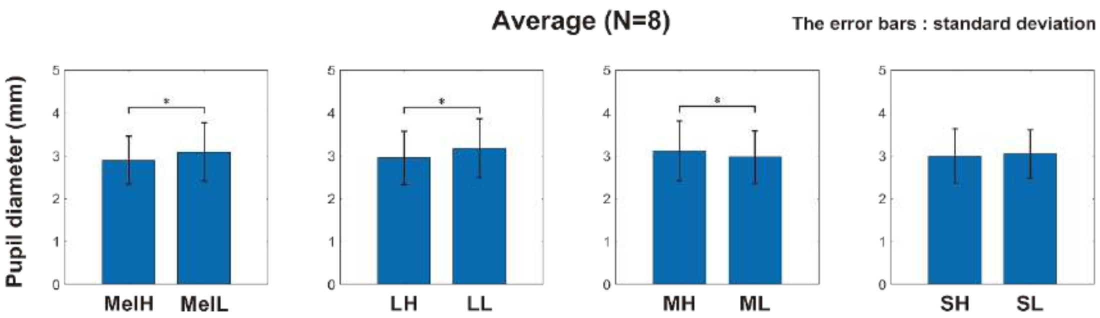

Figure 5. Average pupil diameters to the test stimuli

Model of the pupil driving mechanism

The amount of stimulation to each photoreceptor was determined from the spectral radiance and the spectral sensitivity of each photoreceptor (Eq. 1). Assuming that the steady-state pupil diameter was determined by the ipRGC output, the pupil driving mechanism linearly receives the amount of stimulation from each photoreceptor. We assumed that the mechanism was a linear combination of the amounts of stimulation to each photoreceptor contributing to the steady-state pupil diameter.

$$Vp = aL + bM + cS + dMel \tag{1}$$

where Vp represents the change in the steady-state pupil diameter; L, M, S and Mel represent the photoreceptor stimulation for each photoreceptor; a, b, c and d represent weights of each photoreceptor to the steady-state pupil diameter. The L, M, S, Mel and Vp varied with the spectral radiance of the input light and could be expressed as in the following Eq. (2).

$$Vp(\lambda) = aL(\lambda) + bM(\lambda) + cS(\lambda) + dMel(\lambda) \tag{2}$$

$$Vp = \int I(\lambda)Vp(\lambda)\, d\lambda \tag{3}$$

In other words, the pupil driving mechanism $Vp(\lambda)$, i.e. Eq. (2) could be estimated by combining the spectral sensitivity curves of each photoreceptor (Fig.2). We estimated this mechanism by calculating *a, b, c* and *d* using our experimental results. There are four unknown parameters, i.e. *a, b, c* and *d* that convert from each photoreceptor to the steady-state pupil diameter; the cost function *J* for the unknown parameters was defined as follows.

$$J(a, b.c.d) = \sum \{Ep_i - Cp_i\}^2 \tag{4}$$

$$Ep_i = \int I_i(\lambda) Vp(\lambda)\, d\lambda \tag{5}$$

$$Cp_i = Sp_i - Sp_{control} \tag{6}$$

$$i \in \{Control, MelH, MelL, LH, LL, MH, ML, SH, SL\}$$

$Sp_{control}$ represents the steady-state pupil diameter in the control stimulus; Sp_i represents the pupil diameter in the nine different stimulus conditions for each photoreceptor; Cp_i is the difference between them; Epi is the estimated change in pupil diameter from the model. Ep_i is the change in pupil diameter estimated from the model. The *a, b, c* and *d* represent parameters that minimize the difference between Cp_i and Ep_i calculated by an optimization problem. The solved parameters *a, b, c* and *d* are shown in Table 1.

Table 1: Weight for each photoreceptor

a:L	*b:M*	*c:S*	*d:Mel*
0.76	-1.77	-0.71	1.28

The model represents the relationship between the spectral radiance of the stimulus i.e. W sr^{-1} m^{-2} and the steady-state pupil diameter in mm. The model could estimate the steady-state pupil diameter from the spectral radiance at around the white. The weights of the model suggest that increased stimulation of melanopsin cells and L cone facilitate pupil constriction, whereas increased stimulation of M cone and S cone facilitate pupil dilation. These results were consistent with those in the previous studies [5-7].

CONCLUSION

In this study, we found how melanopsin cells and L, M and S cone photoreceptors contribute to steady-state pupil diameter. The steady-state pupil diameters in Mel, L, M stimulus were significantly different from those in the control condition. In addition, the results suggested that there was a contribution of L-M cone-opponent mechanism. We proposed a simple model which linearly receives signals from L, M, S cones and melanopsin.

ACKNOWLEDGEMENT

This research was supported by the Ministry of Education, Science, Sports and Culture of Japan, Grants-in-Aid for Scientific Research (A) 21H04426 (Kitaoka) and 20H00614 to ST, the Grant in Aid for Challenging Research (Exploratory) 22K19333 to ST.

REFERENCES

1. Provencio, I., Rodriguez, I. R., Jiang, G., Hayes, W. P., Moreira, E. F., & Rollag, M. D. (2000). A novel human opsin in the inner retina. *J Neurosci, 20*(2), 600-605. Retrieved from http://www.ncbi.nlm.nih.gov/pubmed/10632589
2. Lucas, R. J., Hattar, S., Takao, M., Berson, D. M., Foster, R. G., & Yau, K. W. (2003). Diminished pupillary light reflex at high irradiances in melanopsin-knockout mice. *Science, 299*(5604), 245-247. doi:DOI 10.1126/science.1077293

3. Tsujimura, S., & Matsumoto, A. Y., A. (2023, 24-26 May 2023). Intrinsic Phase Difference between Cone and Melanopsin Signals in the Pupillary Pathway. *Paper presented at the 2023 24th International Conference on Control Systems and Computer Science (CSCS)*.
4. Chien, S.-E., Yeh, S.-L., Yamashita, W., & Tsujimura, S.-i. (2023). Enhanced human contrast sensitivity with increased stimulation of melanopsin in intrinsically photosensitive retinal ganglion cells. *Vision Research, 209*, 108271. doi:https://doi.org/10.1016/j.visres.2023.108271
5. Tsujimura, S., Ukai, K., Ohama, D., Nuruki, A., & Yunokuchi, K. (2010). Contribution of human melanopsin retinal ganglion cells to steady-state pupil responses. *Proc Biol Sci, 277*(1693), 2485-2492. doi:10.1098/rspb.2010.0330
6. Tsujimura, S., Wolffsohn, J. S., & Gilmartin, B. (2001). A linear chromatic mechanism drives the pupillary response. *Proc Biol Sci, 268*(1482), 2203-2209. doi:10.1098/rspb.2001.1775
7. Kimura, E., Young, R. S. (2010). Sustained pupillary constrictions mediated by an L- and M-cone opponent process. *Vision Res 50,* 489-496.

CONTRIBUTION OF MELANOPSIN PHOTORECEPTORS TO BRIGHTNESS PERCEPTION BY STEADY LIGHT STIMULATION

Y. Fujita[1], A. Takasu[1], T. Ito[1] and S. Tsujimura[1]

Graduate School of Design and Architecture, Nagoya City University, Nagoya, Japan

*Corresponding author: Sei-ichi Tsujimura, tsujimura@sda.nagoya-cu.ac.jp

ABSTRACT

There are three types of photoreceptors, cone, rod and ipRGC (intrinsically photosensitive retinal ganglion cell or melanopsin cell) in the human retina. Melanopsin photoreceptors were discovered as the third photoreceptor around 2000. They contribute to brain functions in the non-image forming pathways, for example, brightness perception, circadian rhythms and the pupillary light reflex.

Luminance, an index of brightness perception in photometry, is calculated from the spectrum of a light source and luminous efficiency function. Luminous efficiency function is defined by the flicker photometry which uses high temporal frequency stimuli of ~15 Hz. Luminous efficiency function consists of the L- and M-cone sensitivity curves. It has been assumed that L and M cones can respond to high temporal frequency stimuli, whereas S-cones and melanopsin photoreceptors cannot respond to high temporal frequency stimuli. Several researchers have shown that the brightness perception of artificial illumination cannot be explained solely by the amount of stimulation of the L and M cones, i.e. luminance. The aim of the present study was to investigate the contribution of melanopsin photoreceptors to the brightness perception.

In general, it is difficult to investigate the contribution of melanopsin photoreceptors to the brightness perception since a light flux from the light source stimulates all photoreceptor classes. We used a multi-primary stimulation system which can stimulate L, M and S cones and melanopsin photoreceptors independently to investigate the contribution of melanopsin photoreceptors to brightness perception. Furthermore, it is important to investigate the contribution from each photoreceptor to brightness perception since it was shown that melanopsin photoreceptors receive signals from all photoreceptor classes.

We used a total of nine steady light stimuli: a white control stimulus and eight stimuli modulated along the L, M, S and melanopsin directions. The amount of modulation was ±20% and ±5% in each direction from the control stimuli. The results showed that the amount of brightness perception increased as melanopsin stimulation increased, which is consistent with previous studies.

Keywords: brightness perception, melanopsin, luminous efficiency function, photoreceptor stimulation

INTRODUCTION

It has been known that there are cone and rod photoreceptors on the human retina. In addition to these, melanopsin cells has been discovered around 2000 as the third photoreceptor[1]. Melanopsin cells receive light itself and also receive input from the cone and rod photoreceptors. Melanopsin cells contribute to non-imaging forming pathways such as the photoentrainment of circadian rhythms and the pupillary light reflex. Previous studies have shown that melanopsin cells contribute not only to non-imaging forming pathways, but also to imaging forming pathway. It has shown that melanopsin cells contribute to brightness perception [2-5] Luminance and illuminance, the units of intensity of light, were defined based on the assumption there are only cone and rod photoreceptors. Several studies have shown that the luminance alone is not sufficient to represent brightness perception. The purpose of this study was to investigate the contribution of melanopsin cells to brightness perception.

METHODS

In the experiment, we investigated the contribution of melanopsin cells to brightness perception. To this end, we measured brightness perception by varying the amount of stimulation to L, M, S cone and melanopsin photoreceptors independently. We used silent-substitution paradigm for the independent stimulations [6].

In the experiment, test stimuli were presented using a multi-primary illumination system [7]. The LEDs produced four primaries with the peak wavelength of 633 nm, 531 nm, 462 nm, 569 nm, respectively. The output lights from the LEDs were carefully controlled by a stimulus control unit using pulse width modulation.

Test stimuli

We used nine types of test stimuli which were modified from a control stimulus along L, M, S cone and melanopsin cells. The amount of stimulation to each photoreceptor was calculated from the spectral sensitivity of L, M, S cone and melanopsin cells (Figure 1) and the spectral radiance of the test stimulus.

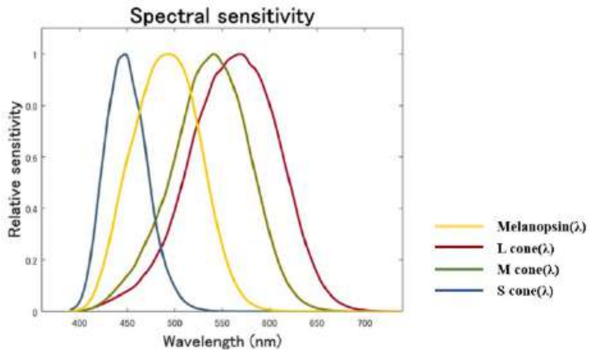

Figure 1. Normalized spectral sensitivities of L, M, S cone and melanopsin cells.

For example, Melanopsin high and Melanopsin low stimuli (Figure 2), which modulated the amount of stimulation to melanopsin cells by ±20% from the control stimulus. Similarly, stimuli with ±5% modulation of the amount of stimulation to L, M, S cones were used as L-cone high, L-cone low, M-cone high, M-cone low, S-cone high and S-cone low stimuli.

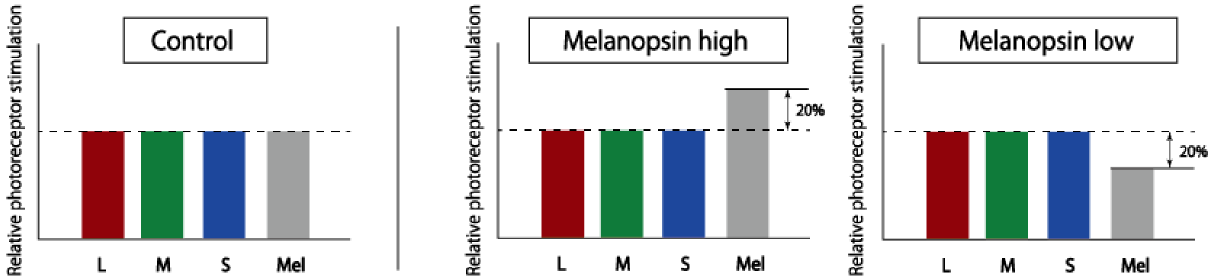

Figure2. Relative photoreceptor stimulation
Relative photoreceptor stimulations for L, M, S cones and melanopsin cells. The test stimuli were modulated from the control stimulus.

Table 1 shows the amount of stimulation to the L, M, and S cones and melanopsin cells and the chromaticity of these light stimuli.

Table 1. The Luminance and chromaticity of the light stimuli

	Luminace (cd/m^2)	L(cd/m^2)	M(cd/m^2)	S(cd/m^2)	Melanopsin (cd/m^2)	x	y
Melanopsin high	282	206	76	132	209	0.429	0.389
Melanopsin low	282	206	76	132	140	0.429	0.389
L-cone high	293	217	76	132	174	0.445	0.383
L-cone low	272	196	76	132	174	0.411	0.396
M-cone high	286	206	80	132	174	0.415	0.400
M-cone low	278	206	72	132	174	0.442	0.378
S-cone high	282	206	76	139	174	0.426	0.385
S-cone low	282	206	76	126	174	0.432	0.393
Control	282	206	76	132	174	0.429	0.389

Previous studies in the similar condition we have shown that rods have little or no effect at high illuminance [8]. Therefore, the effect of the rods was not considered in the present experiment.

In the experiments, we used light stimuli with a modulation rate of 5% in order to reduce the colour difference between the light stimuli. We conducted a preliminary experiment using light stimuli with a modulation rate of 20%. It was found that the brightness differences were the same regardless of the modulation rate. Figure 3 shows the results of the experiment using light stimuli with a modulation rate of 5% and 20%.

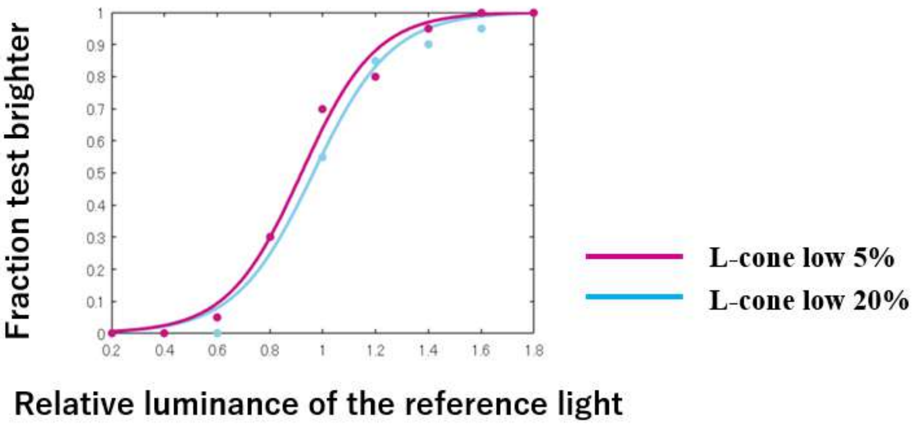

Figure 3. Comparison of the results using a modulation rate of 5% and 20%

Figure 3 shows the results of the experiment using L-cone low with a modulation rate of 5% and 20%.

Procedure

Constant method was used to measure the brightness perception of each light stimulus. A logistic function was used for the psychometric function, and the point with a probability of 0.5 was the subjective equivalence point for brightness perception induced. A two-intervals alternative-forced-choice method (2IAFC) was used in the experiment. The test stimulus and nine reference stimuli were compared 20 times each, i.e. a total of 180 comparisons were conducted. Counterbalance was taken into account with regard to the order of test stimulus presentation. Subjects had the initial adaption before the session for 5 minutes in a dark booth.

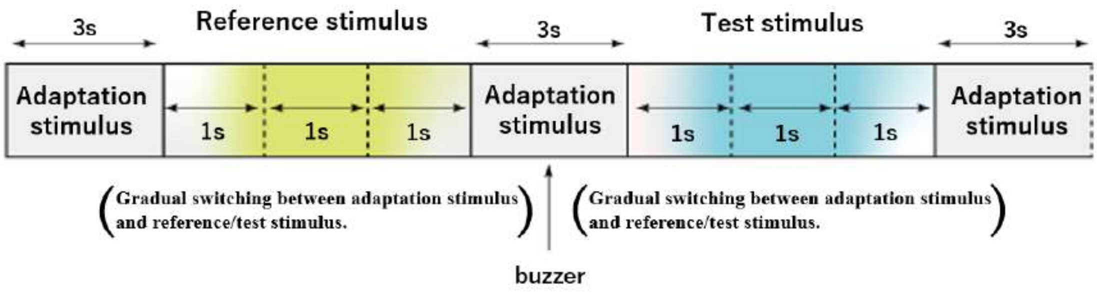

Figure 4. Presentation of stimuli

The test and reference stimuli were presented for 3 seconds with the adaptation stimulus in between. The test and reference stimuli were gradually varied to avoid artifacts caused by abrupt change.

A reference light and a test light were presented with an adapting light in between. as shown in Figure 4. The luminance of the reference stimulus ranged from -80% to +80% from the control stimulus.

RESULTS AND DISCUSSION

Three subjects participated in the experiment. They are females aged from 22 to 25 years old. The average age was 23 years old. Figure 5 showed the results of brightness perception for each subject.

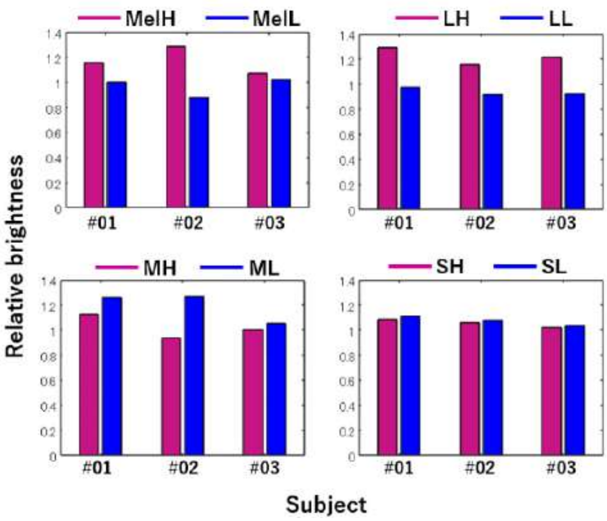

Figure5.   Relative brightness perception to the control stimulus

As shown in Figure 5, all three subjects had a similar tendency for all test stimuli. A large difference in brightness was found in the L, M-cone and melanopsin modulations, whereas little difference was found in S-cone modulation. The melanopsin-high stimulus, MelH, was perceived brighter than the melanopsin-low stimulus, MelL although MelH and MelL were metamers, i.e. had the same luminance and colour. Similarly, L-cone high stimulus, LH was perceived brighter than the L-cone low stimulus, LL. On the other hand, M-cone low stimulus, ML was perceived brighter than the M-cone high stimulus, MH although the luminance of the MH was higher than ML.

Our results showed that subjects perceived brighter as melanopsin stimulation increased although there was no difference in luminance and colour. The results were consistent with previous studies. Brown et al. showed that subjects perceived brighter in the entire field stimulation. Yamakawa et al showed the quantitative analysis for brightness. DeLawyer et al. showed the similar facilitation of brightness although the effect was little when colour and melanopsin stimulation varied simultaneously. The little effect they observed could be due to a suppression/inhibition between cone and melanopsin cells when they are integrated.

Perceived luminance varies depending on method of measurement. For example, luminance measured by flicker photometry is different from that measured by direct heterochromatic brightness matching. The luminous efficiency function is defined by the flicker photometry which uses high temporal frequency stimuli of ~15 Hz. The luminous efficiency function is a linear summation of the L- and M-cone sensitivity curves. On the other hand, luminous efficiency function measured by direct heterochromatic brightness matching provides a different shape of spectral sensitivity curve[9].

This difference could be explained by a difference in temporal property between cones and melanopsin cells. The flicker method uses high temporal frequencies more than ~15 Hz, whereas the direct heterochromatic brightness matching uses steady-state light stimulus. Since L and M cone can respond to high-temporal frequency stimulus and melanopsin cells cannot respond a test stimulus at high temporal frequency it is reasonable to assume that the difference in temporal property between cone and melanopsin cells could cause a difference in sensitivity curve.

In our experiment since we used test stimulus at low temporal frequency it is close to the direct heterochromatic brightness matching method. There were differences in brightness perception between MelH and MelL stimuli, even at the photometrically the same luminance.

CONCLUSION

In this experiment, we found that melanopsin cells contribute to brightness perception to steady-state light stimuli. We used test stimuli with small colour differences. The results showed that brightness perception varies depending on the photoreceptor stimulation.

ACKNOWLEDGEMENT

This research was supported by the Ministry of Education, Science, Sports and Culture of Japan, Grants-in-Aid for Scientific Research (A) 21H04426 (Kitaoka) and 20H00614 to ST, the Grant in Aid for Challenging Research (Exploratory) 22K19333 to ST.

REFERENCES

1. Brown, T. M., Tsujimura, S., Allen, A. E., Wynne, J., Bedford, R., Vickery, G., Vugler, A., & Lucas, R. J. (2012). Melanopsin-based brightness discrimination in mice and humans. Curr Biol, 22(12), 1134-1141. https://doi.org/10.1016/j.cub.2012.04.039

2. Chien, S.-E., Yeh, S.-L., Yamashita, W., & Tsujimura, S. (2023). Enhanced human contrast sensitivity with increased stimulation of melanopsin in intrinsically photosensitive retinal ganglion cells. *Vision Research*, *209*, 108271. https://doi.org/https://doi.org/10.1016/j.visres.2023.108271
3. DeLawyer, T., Tsujimura, S., & Shinomori, K. (2020). Relative contributions of melanopsin to brightness discrimination when hue and luminance also vary. J Opt Soc Am A Opt Image Sci Vis, 37(4), A81-A88. https://doi.org/10.1364/JOSAA.382349
4. Provencio, I., Rodriguez, I. R., Jiang, G., Hayes, W. P., Moreira, E. F., & Rollag, M. D. (2000). A novel human opsin in the inner retina. J Neurosci, 20(2), 600-605. http://www.ncbi.nlm.nih.gov/pubmed/10632589
5. Tsujimura, S., & Matsumoto, A. Y., A. (2023, 24-26 May 2023). Intrinsic Phase Difference between Cone and Melanopsin Signals in the Pupillary Pathway. 2023 24th International Conference on Control Systems and Computer Science (CSCS),
6. Tsujimura, S., Ukai, K., Ohama, D., Nuruki, A., & Yunokuchi, K. (2010). Contribution of human melanopsin retinal ganglion cells to steady-state pupil responses. Proc Biol Sci, 277(1693), 2485-2492. https://doi.org/10.1098/rspb.2010.0330
7. Yamakawa, M., Tsujimura, S., & Okajima, K. (2019). A quantitative analysis of the contribution of melanopsin to brightness perception. Scientific reports, 9(1), 1-8.
8. Zele, A. J., Feigl, B., Adhikari, P., Maynard, M. L., & Cao, D. (2018). Melanopsin photoreception contributes to human visual detection, temporal and colour processing. Sci Rep, 8(1), 3842. https://doi.org/10.1038/s41598-018-22197-w
9. l'Eclairage, C.I.d. and I.C.o. Illumination, *Light as a True Visual Quantity: Principles of Measurement*. 1994: CIE.

DYNAMIC AND RESPONSIVE COLOR IN FASHION DESIGN

Shuang He[1,3], Cuiqin Lan[2] and Jiajia Song[1,3]*

[1] *School of Fashion Accessory, Beijing Institute of Fashion Technology, Beijing, China.*
[2] *Graduate School, Beijing Institute of Fashion Technology, Beijing, China.*
[3] *Academy of Arts & Design, Tsinghua University, China.*

*Corresponding author: Jiajia Song, 20170097@bift.edu.cn

ABSTRACT

The mass production of industrial society has led to serious environmental pollution and product homogenization, including in the world of fashion. Despite the progressive changes in the dyeing technology of clothing fabrics, which alleviate many of the problems of water pollution and chemical dyes, technological advances have given more color expression to fashion designs. In this study, by using parametric generation software and voxelized printing technology, different color information is incorporated into each unit structure and combined and arranged to print the best dynamic color changing sequence directly on the garment fabric, forming a 3D dynamic garment color like chameleon skin. In addition, in the responsive color experiments, this study uses dynamic thermal ink, where the temperature change activates the dynamic color change of the ink. Based on the test data of human thermal imaging, this design is designed for layered arrangement of smart thermal control ink in the key thermal sensing area of human body, and with the help of special digital printing and screen-printing technology, different color coatings and smart thermal control ink are printed on the garment fabric in layers to achieve different color effects at different temperatures. Dynamic color breaks the traditional static color effect and color gamut limitations of garment dyeing. Responsive color can occur in response to external stimulus sources, such as UV and temperature, and dynamically activate the color change.

Although this research might not yet be conducive for mass production, it unequivocally pioneers the intersection of technology and artistry in the realm of fashion color design. Fashion stands to benefit from technological evolution, even as technology itself undergoes its iterative cycles. The dynamic color change can be expressed in the clothing, and with the temperature, motion state and the wearer's body posture to produce a gorgeous color effect. This study tries to combine dynamic color and reactive color and apply them to clothing design, hoping to digitize color design and add more possibilities to the color expression of clothing.

Keywords: Dynamic color, Color-changing, Responsive design

INTRODUCTION

The promotion of fashion has led to the overproduction and overconsumption of fashion products [1], and the processes of dyeing and washing in the production of fashion have had a serious impact on the environment on which we depend for our survival. In an era of rapid technological advancement and changing consumer expectations, 3D printing and eco-friendly reactive dyeing technologies have given fashion design more color expression and sustainability. Fashion design is no longer limited to the traditional paradigm of textures, silhouettes and static colors. The fusion of technology and fashion has brought about transformative capabilities that add new dimensions to the way clothing is perceived, experienced and interacted with. One of the most innovative breakthroughs is the concept of dynamic and responsive color, which is discussed in this paper to mean that beyond the static dimension, clothing color becomes an expression of the wearer's response to the environment, emotions, and self-personality.

Fashion as a manifestation of identity, culture, and emotion is energized by color. Dynamic color is the change of color in vision, color will change with external stimuli, such as light, temperature, and even the physiological state of the wearer, as well as internal structural reasons. Dynamic color breaks the limitations of traditional dyeing in fashion design and opens the door to a world of possibilities for enhanced personalization and interaction.

And what about responsive color? Responsive design was conceived as a concept within web design. As advancements in computer technology proliferated, a multitude of users began accessing the internet through a variety of mobile devices, such as tablets and smartphones. Clearly, the conventional approach to web design could no longer meet the diverse needs of these users. As a result, responsive design emerged, offering dynamic adaptations across all device platforms. In the realm of fashion, responsive design represents an innovative frontier. Examples include garments that adjust to environmental conditions, screens that react to hand gestures, and bracelets that resonate with a user's emotions, all made possible through cutting-edge technology and pioneering materials [2].

This paper examines the integration of dynamic and responsive color in apparel design, exploring its technical underpinnings and its potential to redefine the relationship between the individual and fashion design.

METHODOLOGY

This paper discusses the methods and results used in practice from two perspectives: dynamic color design, and responsive color design. They are both ultimately modeled and presented as garments.

Dynamic color for 3D voxelized printing

In this project, Grasshopper is used to incorporate different color information into each unit structure by imitating and learning the changing principle of biological colors. Also, with the aid of 3D voxelized printing technology (Figure 1), the model is directly printed on the fabric to form a skin design with color illusions, looking like the chameleon skin. The illusional fabric is combined with clothing design, so the color will change as the wearer moves or other people look at it from different angles.

Figure 1: Fashion fabrics in 3D voxelized printing. Source: Stratasys

The chameleon changes its skin color by adjusting the refraction of light through nanocrystalline structures. We used the principle of adjusting the refraction of the nanocrystal structure to change the color, and simulated the refraction angle in 3D Studio Max software, and obtained a set of color change data after calculation (Figure 2).

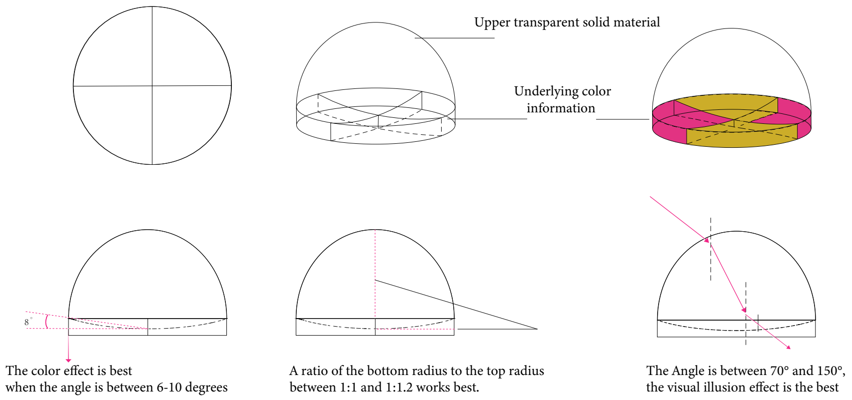

Figure 2: Illusional color and structure.

The crystal model is divided into two layers, the upper layer is the transparent solid material, and the lower layer is the color information we input according to the design, so far, we have made 2 color split structures. We found that the best color change effect is when the angle between the color layer and the transparent mask is 6 to 10 degrees, and the minimum diameter of a single crystal model is 8mm to 4cm. Second, the size of the radius of the bottom color information and the structure of the top transparent layer also need to maintain a certain ratio relationship. A ratio between 1:1 and 1:1.2 works best, while the rest of the range is not significant or has no optical color change effect.

Digital color offers us the possibility to create responsive garments with visually variable colors, and in this paper, we use a combination of art and technology to realize this vision. We have 3D voxelized printing our designs directly onto fabrics to reduce textile fabric waste while breaking the limitations of traditional garment dyeing and being able to print in a wider range of colors using RGB color modes.

Responsive design by dynamic-thermo ink

Responsive design can respond to temperature, light, pressure, etc. by changing color or form. We tried to create a jacket in winter that could absorb heat and balance temperature and change color. Dynamic-thermo ink is our best choice of material, which is a composite of thermally responsive scattering nanocrystalline spheres and graphene sheets, which can effectively reflect the ambient light source and radiate its own infrared heat to achieve cooling at high temperature; at low temperature, the ink shows black surface phase switching for strong light absorption and warmth, thus achieving human comfort in high and low temperature environments. Constant temperature control. The phase switching temperature of the ink can be freely customized to realize the intelligent human thermal regulation function in different seasons and environments.

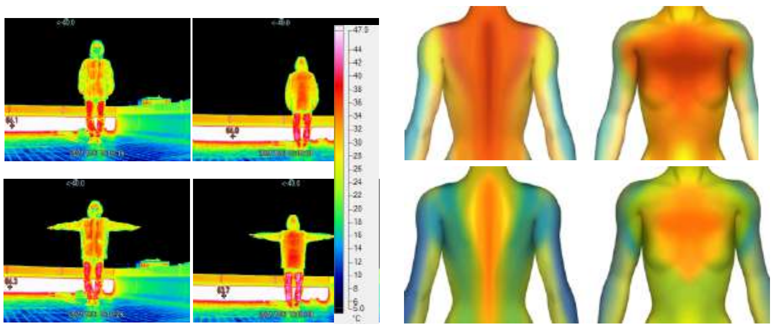

Figure 3: Thermal testing and localization

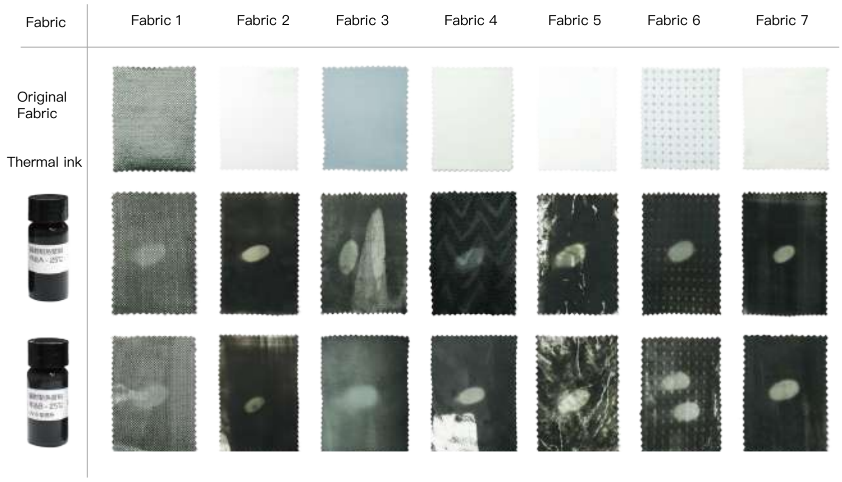

Figure 4: Dynamic-thermo ink testing on different fabrics

First, we measured the heat-sensitive areas of the human body with an infrared thermography camera during the noon time outdoors in winter and drew a model of the heat-sensitive temperature change of the human body to determine the location of the dynamic colors we would use: the back and the front chest area (Figure 3). Then we selected the most effective fabrics for the garment, Fabric 6 and Fabric 7, based on the effect of the temperature change of the ink tested on different fabrics (Figure 4).

Based on the data of human body thermal imaging, this project uses Grasshopper software to generate different graphic arrays and design the arrangement of intelligent thermal control inks by region to realize the function of temperature control of garments on demand.

RESULT AND DISCUSSION

This paper discusses the methods and results used in design practice from two perspectives: dynamic color design, and responsive color design. They are both ultimately presented as garments.

Dynamic color in fashion design

The fashion design work ‘Illusional Fashion in Motion’ is designed with inspiration from the color-changing mechanism of chameleons, i.e., the Nano-crystalline nature is adjusted to change the refraction of light and then to change the color of the skin. Dynamic digital color makes it possible for us to create environment-adaptable clothing colors and colors that can cause visual illusions. This vision can be realized through a combination of art and technology. This design work is directly 3D voxelized printing on the fabric, thus breaking through the limitation of color gamut in the traditional clothes, including static color effects and dyeing effects, while reducing fabric waste.

With the aid of high technology, ‘Illusional Fashion in Motion’, as shown in Figure 5, explores color changes in motion, aiming to digitize color design and make clothing colors dynamic so as to realize integration of technology with art to add more possibilities to the fashion industry. Visual effect and texture are one of the most important elements in fashion design, which directly affect the visual sense and touch of consumers. Fashion brands need to constantly innovate, while dynamic digital color-changing visual effects can create eye-catching designs and differentiated

Figure 5: Dynamic color in fashion design ‘Illusional Fashion in Motion’.

Responsive design in fashion design

With the help of special digital printing technology, different color layers are mixed with intelligent thermal control ink and printed on the garment fabric. Based on the design of outdoor breathability and sports comfort, the thermal control ink on the surface of the garment intelligently responds to the temperature change of the wearer in the outdoors and performs human heat regulation to meet different wearing scenarios and temperature requirements. Meanwhile, it always adheres to the design concept of "intelligent and sustainable" in the design and production process. In terms of material selection, we use environmentally friendly fabrics such as washable Dupont paper, and adopt a sustainable design approach of zero waste and removability in the design and cutting to achieve the goal of sustainable fashion (Figure 6).

Figure 6: The thermal responsive fashion design.

CONCLUSION

This paper showcases dynamic and responsive color designs in fashion using two distinct works as examples. Dynamic color garments display a variety of digital color effects, achieved through parametric design, digital color palettes, modular structure design, and 3D voxelized printing technology. On the other hand, responsive garments employ dynamic-thermo ink to intelligently adapt to external temperature variations. The resulting color change also serves as an indication of temperature regulation.

Through the design practices presented in this paper, it is hoped to offer expanded possibilities for the growth and innovation of the apparel industry. While upholding sustainable principles, this work seeks to introduce dynamic variations in garment coloration and foster an intelligent interaction between individuals and their attire.

ACKNOWLEDGEMENT

This work was supported by project ‘Digital Visionary Biomimetic Material Research’ of Beijing Institute of Fashion Technology (Project Number: NHFZ20230085).

REFERENCES

1. Xu, H. & Dong, F. (2017). On the Diversity of Environmental Protection Concept Promotion in Fashion Consumption. *Hunan Packaging* (01), 59-62.
2. He, Shuang. (2018). When fashion meets technology— responsive and personalized design for fashion bag. *Cumulus Conference Proceedings Wuxi 2018,* (pp. 21-30). Wuxi, China.
3. Kong, Y. & Li, J. (2022). Research progress on graphene/polymer flexible sensors for smart garments. *Shanghai Textile Science and Technology* (06), 56-60+64. doi:10.16549.
4. Ergoktas M Said, Bakan Gokhan, Steiner Pietro. & Kocabas Coskun.(2020).Graphene-Enabled Adaptive Infrared Textiles. *Nano letters* (7). doi:10.1021.

A STUDY ON ADDITIVITY OF PSYCHOLOGICAL STRESS BY MIXED COLOUR LIGHTING OF THREE PRIMARY COLOURS

Y. Oe[1,*], Y.Miura[2], M. Onai[2] and N.Yoshizawa[1]

[1] *Faculty of Science and Technology, Department of Architecture, Tokyo University of Science, Japan.*
[2] *Graduate school of Science and Technology, Department of Architecture, Tokyo University of Science, Japan.*

*Corresponding author: Yuki Oe, oe.y@shc.usp.ac.jp

ABSTRACT

The purpose of this study is to investigate the effects of stress when utilizing coloured lighting in everyday lighting environments by mixing light from three primary colours and to clarify the presence of additivity. Based on the results of experiments conducted in the experimental room assumed to be a living room with LED lighting, this paper presents findings related to psychological stress. The participants were 24 university students with normal colour vision. A total of 10 lighting conditions were used: 3 primary coloured light (R, G, and B), 1 white light, and 6 mixed-colour light using 3 primary colour lights. The participants evaluated the physical condition and lighting environment immediately after irradiation and one hour after irradiation for each condition. Regarding the elapsed time since irradiation, no trends based on hue or purity were observed in relation to stress. White light was generally significantly more positively evaluated than coloured light, with green light being associated with the lowest stress and blue light with the highest. An interaction between hue and purity was observed for stress, particularly notable in red and blue lights, where differences in evaluation based on purity were substantial, indicating that lower purity led to more positively evaluated responses. Furthermore, the possibility of additivity was suggested when evaluation of stress was considered as the dependent variable and stimulus purity as the independent variable.

Keywords: psychological effects, stress, additivity, chromatic light, LED lighting

INTRODUCTION

In recent years, with the widespread use of LEDs that can be freely dimmed and coloured, coloured lighting is beginning to be used not only for extraordinary dramatic lighting, but also in spaces close to everyday life, such as dialysis or delivery rooms. Such spaces should be stress-free both physically and mentally. The impact of coloured lighting on physiological and psychological stress has been investigated [1][2], with most studies utilizing single-colour lights in each experiment. The researches conducted by Chiang et al. and Lee et al. has explored mixed-colour light in workspace settings; however, the relationship between the proportions of mixed colours and psychological evaluations has not been fully determined [3][4]. The ultimate goal of this study is to elucidate the effects of various colours and intensities of coloured lighting on physiological and psychological stress, and enable the utilization of coloured lighting in real spaces without inducing stress.

The previous researches [5][6] has examined the additivity when mixing two primary coloured lights and indicated the potential for additivity under certain mixing colour conditions for both physiological and psychological aspects. For mixed colour lights that exhibit additivity, it is possible to predict the effects of coloured light located on the line connecting the chromaticities of the two primary coloured lights on a chromaticity diagram. Furthermore, If we can grasp the range within which additivity holds when mixing three primary coloured lights, it can be predicted that the effects of coloured lights composed of R, G, and B. Therefore, in this study, conditions with multiple purity levels were created by mixing three primary coloured lights, aiming to comprehend their stress effects and to investigate whether additivity holds when mixed. This paper focuses on psychological stress.

METHODOLOGY

Under the approval of the Ethics Committee at Tokyo University of Science, the experiments were conducted from October to December 2022, following explanations to the participants and obtaining their consent prior to the commencement of this experiment. The participants consisted of university students aged 20 to 25, totaling 24 individuals (8 males and 16 females), with an average age of 21.3 years. All participants had normal colour vision, as checked by the Ishihara Test. The experiment was conducted in a space simulating a living room at the Tokyo University of Science. As shown in Fig. 1, two sofas and a table were placed in the experimental space, and the sofa was arranged so that the two participants' lines of sight did not cross and they were fully exposed to light from the sample light source (LED lighting). The stand lights beside the sofas were switched on only when explaining the content of the experiment, which was conducted before the experiment. In this experiment, an LED panel (Colour Kinetics) with adjustable RGB output in the range 0~255 each was used.

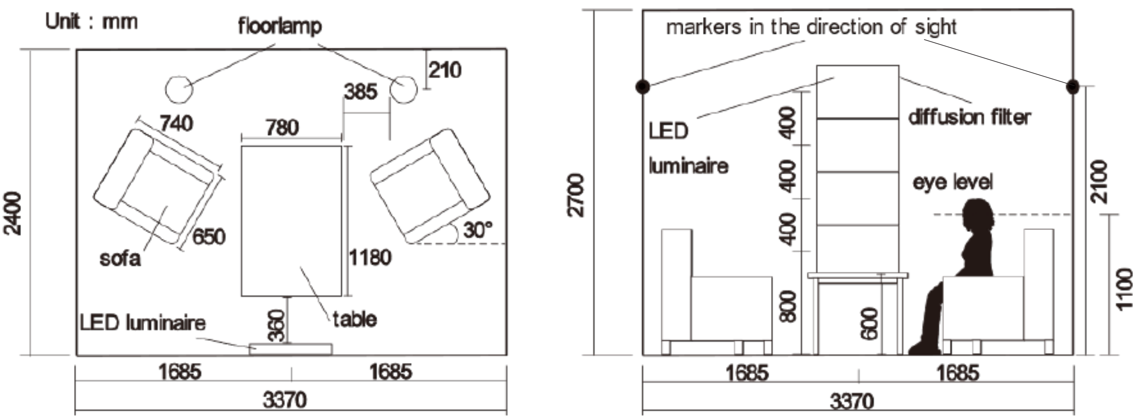

Figure 1. Experimental room (left: plan view; right: sectional view)

A total of ten lighting conditions were used: three primary colour light conditions (red, green and blue), one white light condition obtained by mixing the three primary colour lights, and six conditions (three hues x two levels of purity) with relatively low chromaticity for each primary colour light. As shown in Fig. 2, the chromaticity of white light was set at the origin of the isochromatic locus based on the Abney phenomenon on the xy chromaticity diagram (CIE 1931) [8]. For conditions with lower purity, the positions were adjusted on the u'v' chromaticity diagram (CIE 1976 UCS) to maintain approximately equal colour differences between each primary colour and white light. Furthermore, to eliminate the influence of differences in hue, adjustments were made to ensure that these lighting conditions aligned with the isochromatic locus on the xy chromaticity diagram. The names of primary and white lights are denoted by the first letter of the light colour in English (e.g. red: R). The colour mixing conditions were distinguished by the initial letter of the primary colour for higher purity and the initial letter of white for lower purity, followed by the initial letter of the light colour (relatively high purity red mixing condition: RR, relatively low purity red mixing condition: RW). The illuminance in front of the eye and irradiance for each lighting condition are shown in Table 1, the spectral characteristics are shown in Fig. 3 and the photographs taken when each lighting condition was switched on are shown in Fig. 4. The lighting conditions in the experiments were set at the participant's eye position using a spectroradiometer (Konica Minolta, CL-500A). The illuminance in front of the eye was 53 lx for all conditions.

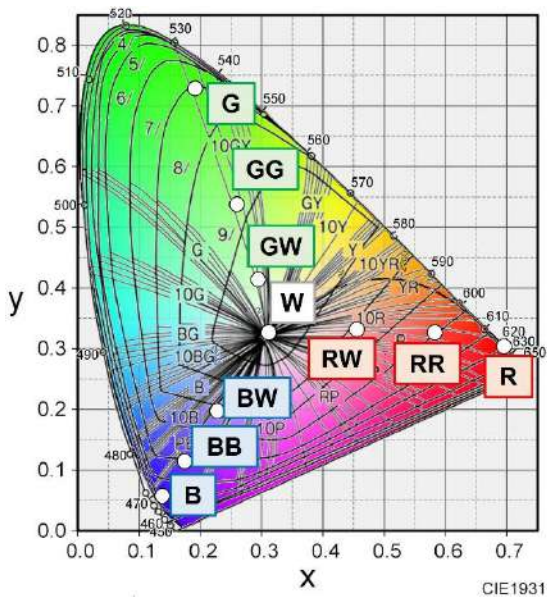

Figure 2. Isochromatic locus and chromaticity coordinates for lighting conditions

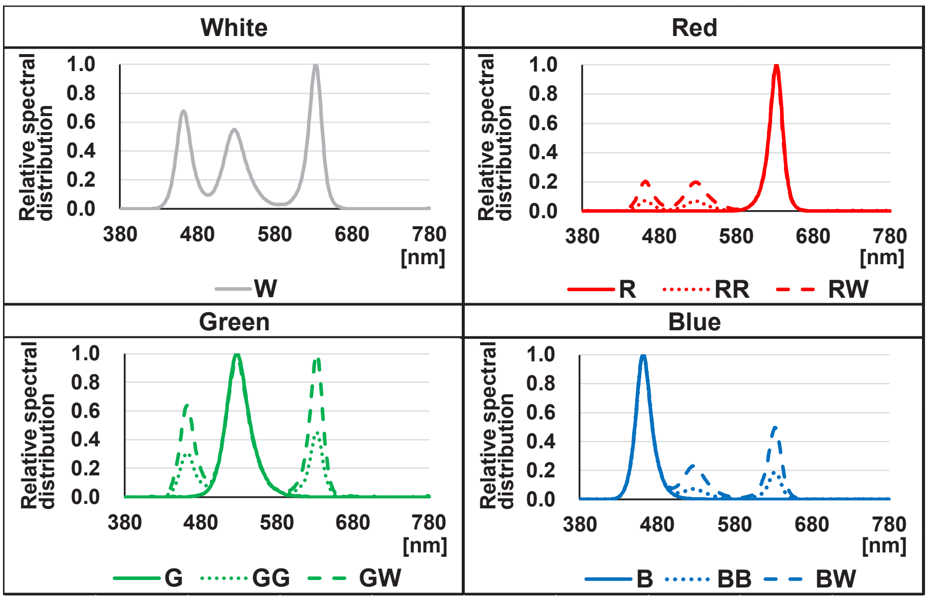

Figure 3. Spectral distributions

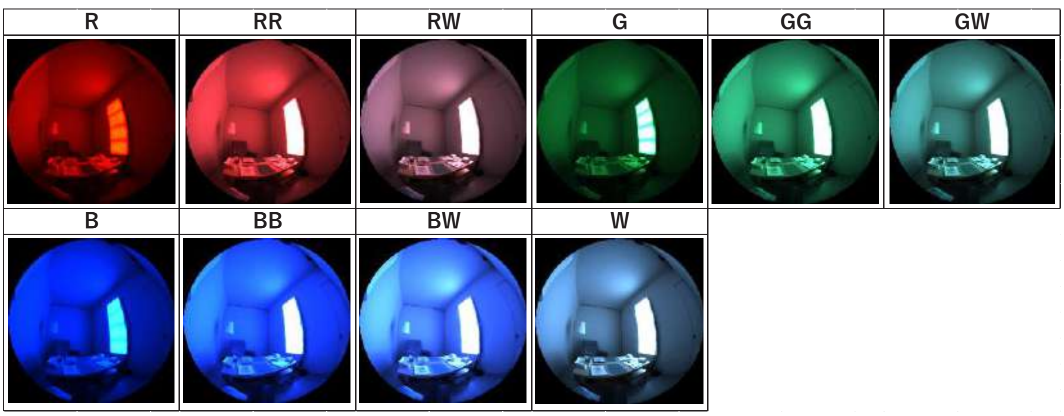

Figure 4. Images of each lighting condition

Fig. 5 shows the experimental procedure. In each experiment, two conditions were randomly presented to each participant. The experiment consisted of five phases: Phase 1: 6-minute period of rest in darkness; Phase 2: Participants engaged in tasks involving KAPLA (French building blocks), Sudoku, and sketching under the first lighting condition for 8 minutes each (After each task, there was a 6-minute rest period in darkness); Phase 3: 6-minute period of rest in darkness; Phase 4: Participants repeated the same tasks as in Phase 2 under the second lighting condition; Phase 5: 6-minute period of rest in darkness. For each lighting condition, psychological assessments related to the body's state and the lighting environment were conducted twice. These assessments were carried out immediately after the start of irradiation and again one hour after the start, referred to as Q1 and Q2, respectively. The questionnaire employed a 9-point Likert scale, inquiring about nine items: stress, pleasantness, visibility, eye strain, anxiety, drowsiness, motivation, comfort, and concentration.

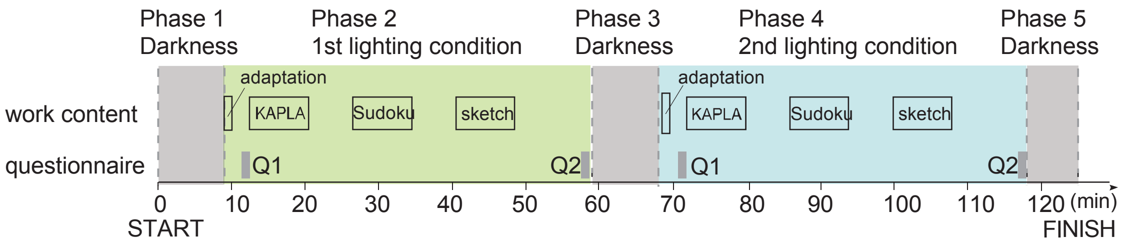

Figure 5. Experimental protocol

RESULT AND DISCUSSION

Regarding "stress," the results for Q1 compared to Q2 are shown in Fig. 6 for each lighting condition. While there were significant differences ($p < 0.05$) between Q1 and Q2 for certain conditions, no simple trends were observed based on hue or purity, and this result was similarly observed for other items. Subsequently, the results for Q1 are presented.

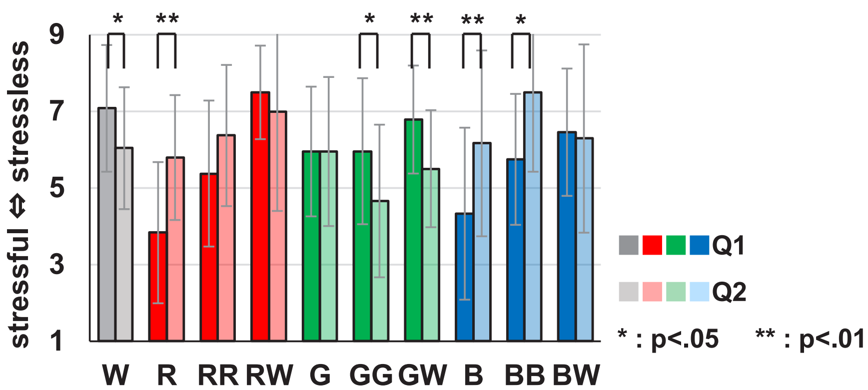

Figure 5. Evaluation of stress in Q1 and Q2

The results for Q1 are presented Fig.6 for some evaluation items. For "stress," "comfort," "pleasantness," and "concentration," no significant differences were observed for green light, but there was a tendency for positively evaluated with decreasing purity in the coloured lighting conditions. In addition, under conditions of high purity, green light was evaluated more positive than red and blue light. The white lights, overall, received significantly more positive evaluations compared to coloured lighting conditions.

To examine the main effects of hue and purity, as well as the interaction between hue and purity within the coloured lighting conditions, a two-way analysis of variance (ANOVA) was conducted. The results are presented in Table 1. The main effect of hue manifested in "stress" and "eye strain," with green light being most positively evaluated and blue light being the most negatively evaluated. The main effect of purity appeared in eight out of nine items, except for "drowsiness," where lower purity was associated with more positive evaluations. The interaction between hue and purity emerged in six items, including "stress," revealing significant differences. In the case of red and blue lights, the evaluation difference based on purity was substantial, indicating that lower purity led to more positively evaluated responses.

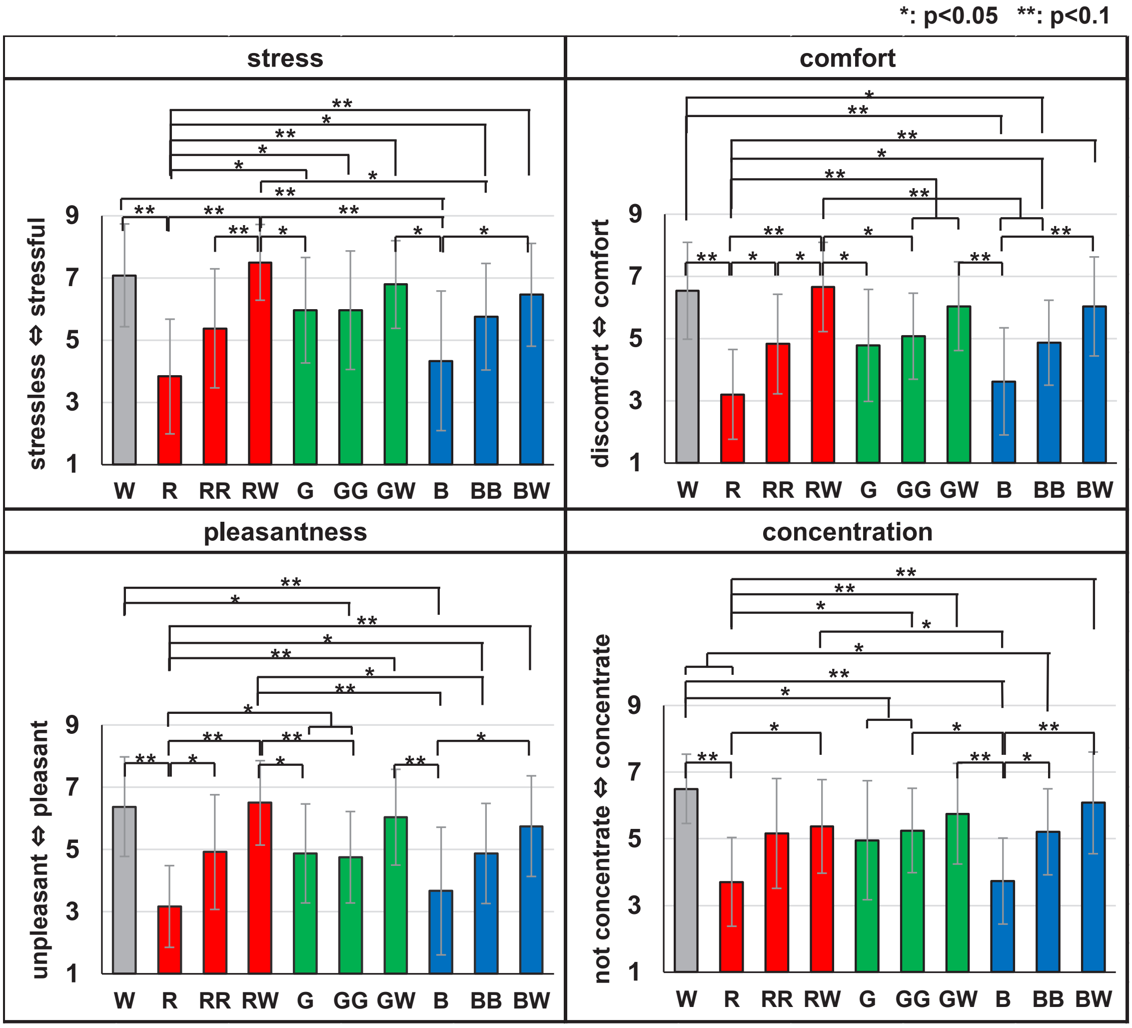

Figure 6. Differences in evaluations according to light colour (Q1)

Table 1. Two-way analysis of variance by hue and purity

	stress	eye strain	comfort	pleasantness	motivation
main effect of hue	*	**	—	—	—
main effect of purity	**	**	**	**	**
interaction of hue and purity	**	**	**	**	*

	concentration	visibility	anxiety	drowsiness
main effect of hue	—	—	—	—
main effect of purity	**	**	**	—
interaction of hue and purity	*	—	—	—

* : p<.05
** : p<.01
— : p>0.05

Next, the additivity of stress is examined. Fig. 7 shows the relationship between evaluation of stress and seven physical quantities (x, y, u', v', irradiance, dominant wavelength, stimulus purity). In a simple linear regression analysis with stress ratings as the dependent variable and stimulus purity as the independent variable, a strong linear relationship (R^2=0.72) suggested the possibility of additivity. Results of multiple regression analysis, where evaluations of stress were the dependent variable and combinations of each physical quantity were the independent variable. Even in the multiple regression analysis with irradiance and stimulus purity as independent variables, which showed high fitness (R^2=0.73), the effect of irradiance was not significant. This suggests that psychological stress can generally be explained by stimulus purity.

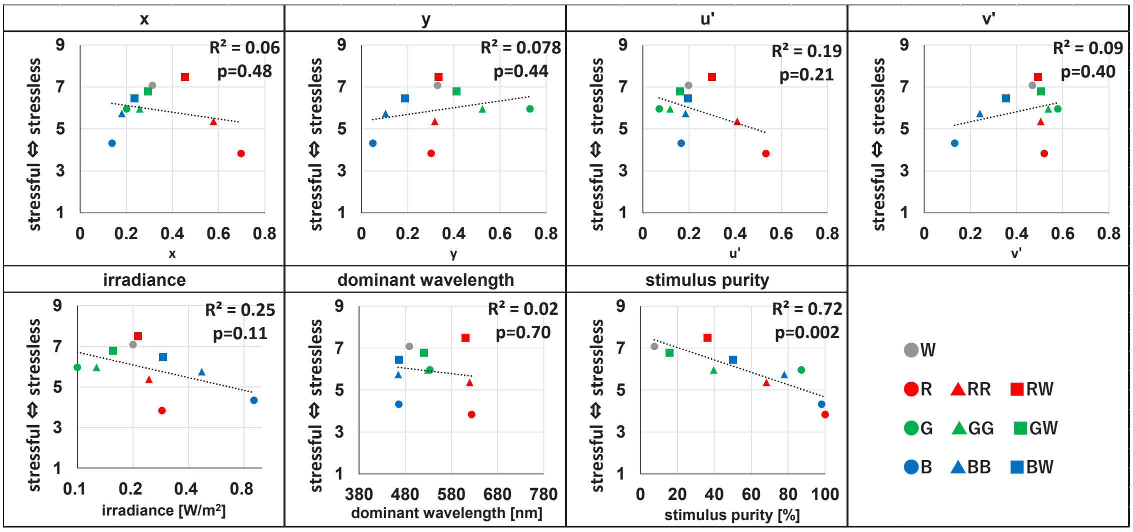

Figure 7. Relationship between stress assessment and physical quantity

CONCLUSION

The results of the experiment involving mixing coloured light from three primary colours indicated that green hue lights were perceived as causing the least stress, while blue hue lights were associated with the most stress. Particularly, both red and blue hue lights were found to induce less stress with lower purity. When stress was considered as the dependent variable, with stimulus purity as the independent variable, the possibility of additivity was suggested. In future, further investigations will be conducted to explore the relationship with physiological stress, aiming to propose coloured lighting that is free from physiological and psychological stress.

REFERENCES

1. Takahashi S. (2005). Psychological study of environmental colors (1): effects of color lighting on the performance of simple task. *Journal of Human Environment Studies (in Japanese), 3*(1), 41-46. doi: 10.4189/shes.3.1_41
2. Plitnick B et al. (2010). The effects of red and blue light on alertness and mood at night. *Lighting Research and Technology*, *42*(1), 449-458. doi: 10.1177/1477153509360887
3. Chiang H et al. (2010). A study on the psychological and physiological effects by LED lightings for workspace. *Journal of Environmental Engineering (in Japanese), 75*(654), 683-690. doi: 10.3130/aije.75.683
4. Lee D et al. (2011). Basic study on discomfort caused by LED lighting colors in working space. *AIJ Journal of Technology and Design. 17*(35), 201-204, doi: 10.3130/AIJT.17.201
5. Miura et al. (2021). Examination of Psychological Effects and the Additivity Assumption in the Stress Evaluation of Chromatic LED Lightings, *PROCEEDINGS of the Conference CIE 2021*, 73-79, doi: 10.25039/x48.2021.OP07
6. Miura et al. (2022). Psychological effects of white- and coloured-LED lighting for older people, *Proceedings of the International Color Association Conference 2022*, 687-690.

A COMPARATIVE STUDY ON IMPRESSIONS OF CLOTHES WITHHELD BRAND NAMES IN JAPAN, CHINA, AND THAILAND

Takashi Sakamoto[1]*, Nanako Hattri[2], Naoki Takahashi[2] and Toshikazu Kato[2]

[1]*Human Augmentation Research Center,*
National Institute of Advanced Industrial Science and Technology (AIST), Japan.
[2]*Faculty of Science and Engineering, Chuo University, Japan.*

*Corresponding author: Takashi Sakamoto, takashi-sakamoto@aist.go.jp

ABSTRACT

This research compared impressions of clothing provided by international apparel brands, such as GUCCI, Louis Vuitton, H&M, and UNIQLO. We conducted a survey on clothing impressions without disclosing brand names, using online questionnaires in three Asian countries: Japan, China (People's Republic of China), and Thailand. We selected 44 adjectives to assess these clothing impressions, and respondents quantified the degree of fit to these adjectives using the visual analog scaling (VAS) method. Through exploratory factor analysis, we identified three factors: a style factor, a diversity factor, and a utility factor. It is worth emphasizing that these three factors—style, diversity, and utility—are essential and significant aspects of clothing. The results of the questionnaire survey revealed that gender and cultural differences among these countries manifested in evaluations and attitudes toward the style, diversity, and utility of clothing, and perceived clothing images varied across genders and cultures in different countries.

Keywords: Brand images, Cultural diversity, Gender differences, Factor analysis, Adjectives.

INTRODUCTION

The survey targets of this study are the impressions of clothing marketed by international apparel brands, and we aim to clarify the influences of brand images, genders, cultural differences, and the countries of residence. These targets are closely related to product branding and sales strategy. Product branding strategies are essential when selling products in various countries and expanding the market. Related studies suggest that brand image varies by country or cultural sphere [1,2]. Therefore, it is necessary to understand the factors that influence the brand image of products and utilize them in the sales strategy.

This study aims to clarify the images of clothing distributed by international apparel brands in different countries and specify the factors that influence the differences in clothing images. Additionally, we aim to discover helpful information on product branding strategies to effectively expand international business. The research may contribute to international apparel brands in constructing their brand images and also reveal, from a cross-cultural perspective, what people expect from clothing and what kind of image they seek in clothing.

METHODS

Questionnaire survey: We conducted a questionnaire survey from November 21, 2020, to January 15, 2021, using web-based online questionnaires in three Asian countries: Japan, the People's Republic of China (abbreviated as China), and Thailand. We surveyed four well-known international apparel brands, including both luxury and popular brands. We selected GUCCI and Louis Vuitton as the luxury brands; H&M and UNIQLO as the popular brands. The total number of respondents was 206, and their breakdown was as follows:

- 15 females and 15 males from Japan.
- 120 females and 41 males from China.
- 15 females from Thailand.

Japanese and Chinese respondents consisted only of university students and graduate students, while the population of Thai respondents was not limited to them. Thai males' data were excluded from our survey due to a low number of respondents. The respondents were gathered within the possible limits of graduation research, so the survey was conducted without random sampling and did not use screening questions.

Evaluation items and rating method: We selected 44 adjectives and three modalities [1], such as functional, social, sensory, of brand image to respond to the impression of clothes (see Table 1).

Table 1. 44 Adjectives and 3 modalities

elegant	casual	formal	flashy	delicate	bright
luxury	chic	childlike	romantic	sporty	cute
sophisticated	classical	vulgar	youthful	modern	fusty
exciting	plain	understated	eccentric	rustic	gorgeous
cheesy	pretentious	harmonious	unbalanced	ethnic	active
mannish	bold	moderate	artificial	neat	decorative
sexy	feminine	avantgarde	mode	fashionable	refreshing
simple	cool		functional	social	sensory

The evaluated clothes were presented to the respondents using clothing photographic images available on each brand's web page. For each brand, four clothing images were selected, resulting in a total of 16 images for the evaluation items. The images were presented to the respondents randomly to eliminate order effects. We chose the four clothing images based on selling well or being promoted. Therefore, complete elimination of experimenter bias was not possible. The degree of impressions expressed by 44 adjectives and three modalities for the clothing images was quantified by the visual analog scaling (VAS) method (see Figure 1).

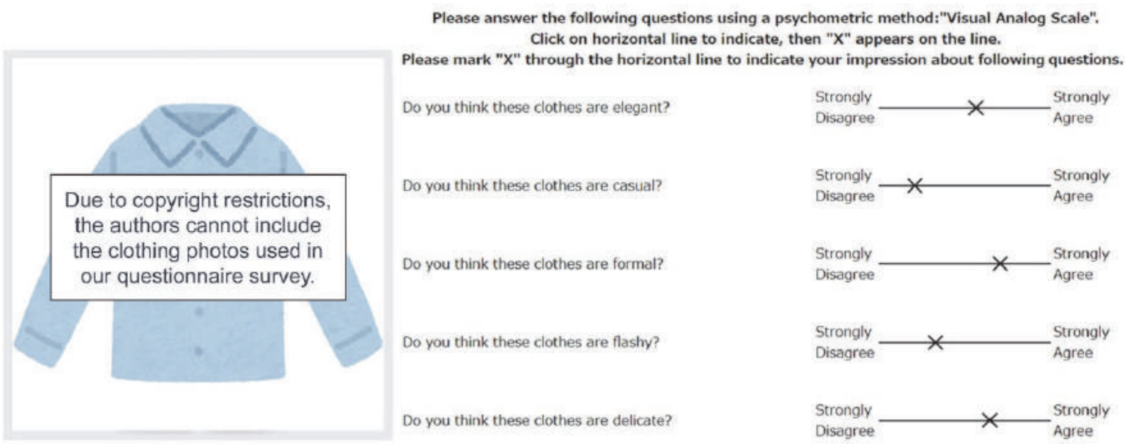

Figure 1. A sample of clothing image replaced with a copyright-free image and questionnaire items using visual analog scaling (VAS) method

RESULT AND DISCUSSION

The rated values for the 44 adjectives and three modalities were applied to an exploratory factor analysis. The results were summarized into three factors based on the scree plots of the factor analysis. Factor 1 indicates clothing style, encompassing characteristics such as stylishness, sociability, elegance and being fashionable. Therefore, factor 1 is considered a comprehensive expression of "style" or “stylishness.” Factor 2 relates to clothing individuality, uniqueness, assertiveness, and diversity. Therefore, factor 2 is considered a comprehensive expression of “diversity.” Factor 3 reflects aspects of mix and match, functionality, versatility, and the utility of clothing. Therefore, factor 3 is considered a comprehensive expression of “utility.” Based on these analyses, we named three factors as follows:

Factor 1: Style factor.
Factor 2: Diversity factor.
Factor 3: Utility factor.

All respondents were classified into five groups: Japanese females and males, Chinese females and males, and Thai females. The impression survey data for the 16 clothing images were compared among these five groups and analyzed using statistical tests: analysis of variance (ANOVA) and multiple comparisons.

Style factor: The results of statistical tests for the style factor suggest that Japanese and Thai females appreciate the stylishness of clothing by GUCCI, Louis Vuitton, and H&M. In contrast, Japanese females and males believe clothing by UNIQLO is less stylish.

Diversity factor: The results of statistical tests for the diversity factor suggest that both Japanese and Chinese males evaluate Louis Vuitton’s clothing as diversity-appreciated. However, Japanese females and males consider clothing by H&M and UNIQLO to lack diversity. Moreover, Thai females consider that clothing by all the four surveyed brands lacks diversity.

Utility factor: The results of statistical tests for the utility factor suggest that both females and males in the surveyed three countries consider Louis Vuitton’s clothing to lack utility. In contrast, they believe that clothing by UNIQLO is functional and usable. The statistical results also suggest that Japanese males highly evaluate the utility of clothing by H&M, while Japanese females rate the utility of GUCCI clothing as less.

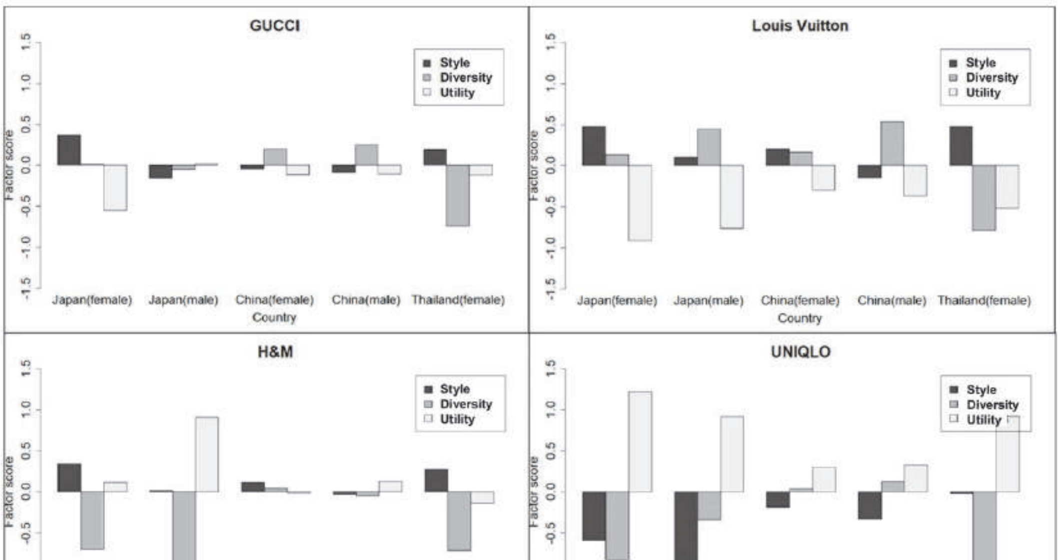

Figure 2. The results of statistical tests for the style, diversity, and utility factors

CONCLUSION

This study revealed that respondents might perceive unique brand images formed in each country despite hiding the brand names. We also found that evaluations and attitudes toward brand images and their clothes varied in gender and cultural differences among these countries, and they were summarized in style, diversity, and utility factors, which are essential and considerable functions of clothing. The results of this study may recommend that international apparel brands consider different strategies according to gender and cultural differences when constructing their brand images.

This study is not based on a large-scale survey with a clearly defined consumer target. Instead, this preliminary investigation was conducted as part of a university graduation research project. Therefore, there were issues with random sampling, and no screening survey was conducted. However, despite being a preliminary and limited survey, it provided valuable insights, and meaningful results were obtained, which can offer valuable feedback for our future larger-scale studies.

ACKNOWLEDGEMENT

We would like to express gratitude to Prof. Pei-Luen Patrick Rau (Tsinghua University, China), Prof. Kuohsing Chen (Fuzhou University of International Studies and Trade, China), Prof. Fen-Tzu Chiu (Fuzhou University of International Studies and Trade, China), and Dr. Chanprapha Phuangsuwan, director of Color Research Center (Rajamangala University of Technology Thanyaburi, Thailand) for their invaluable cooperation in conducting the international survey for this research. This research was partially supported by the Joint Research Institute of Science and Engineering at Chuo University, and the Research Cluster, Chuo University.

REFERENCES

1. Roth, M. S. (1995). The Effects of Culture and Socioeconomics on the Performance of Global Brand Image Strategies. *Journal of Marketing Research*, 32(2), 163-175. https://doi.org/10.1177/002224379503200204
2. Kawasumi, M., & Nishina, K. (2018). Comparative Analysis of Silver Color Preferences for Metallic Products between Japan and Thailand (in Japanese). *Transactions of Japan Society of Kansei Engineering,* 17(2), 267-274. https://doi.org/10.5057/jjske.TJSKE-D-17-00033

AN INVESTIGATION INTO THE VARIABILITY OF HAIR COLOUR MEASUREMENTS

Haoyu Wang* , Kaida Xiao, Michael Pointer and Chris Carr
School of Design, University of Leeds, UK
Steve Singleton Unilever

ABSTRACT

This study investigated the variability of hair colour measurements made using a commercial Konica Minolta CM700D spectrophotometer. The back, top and side positions of the hair of fifty subjects were analysed and different spectral parameters were used to establish spatial and colorimetric variability. Short-term repeatability was defined using the mean colour difference of the mean values. The results indicated that the spectrophotometer provided consistent hair colour values at different positions over a human head using a range of spectral parameters. In addition, little difference between hair colour values when measured with different settings, was observed.

Keywords: Hair colour measurement, spectrophotometer, repeatability

INTRODUCTION

It is recognised that the hair on a human head can significantly affect our perception of overall appearance and the expression of people's personalities. Although human body colour has been extensively studied for more than 4000 years [1], there are relatively few studies on hair colour and the genetic factors that influence colouring characteristics [2, 3].

With the advent of more sophisticated colour characterisation instrumentation, accurate hair colour measurement has become important in fields such as genetics [4], the cosmetics industry [5], and forensic science [6]. Across these disciplines different measurement approaches may be used for hair colour measurements, for example, in the cosmetics industry large-area analysis of hair colour is prevalent [7], while in the forensic field, the focus is generally on individual fibres [8]. However, while the importance of reliable hair colour measurements is recognised, little is known about the variability of these measurements and their dependence on acquisition parameters. Therefore, the main aim of this paper is to quantify the impact of these factors on the measurement reliability of hair. Identifying the instrumental conditions that produce the highest repeatability is vital for researchers involved in hair colour measurements and will enable comparative analysis of datasets obtained with different instruments.

METHODOLOGY

Subjects and samples measured

Forty-four Chinese and six Europeans, aged between 20 and 30 years, with healthy hair, including both dyed and undyed hair. The CIELAB parameters a^*, b^* and L^*, C_{ab}^* are shown plotted in Figure 1.

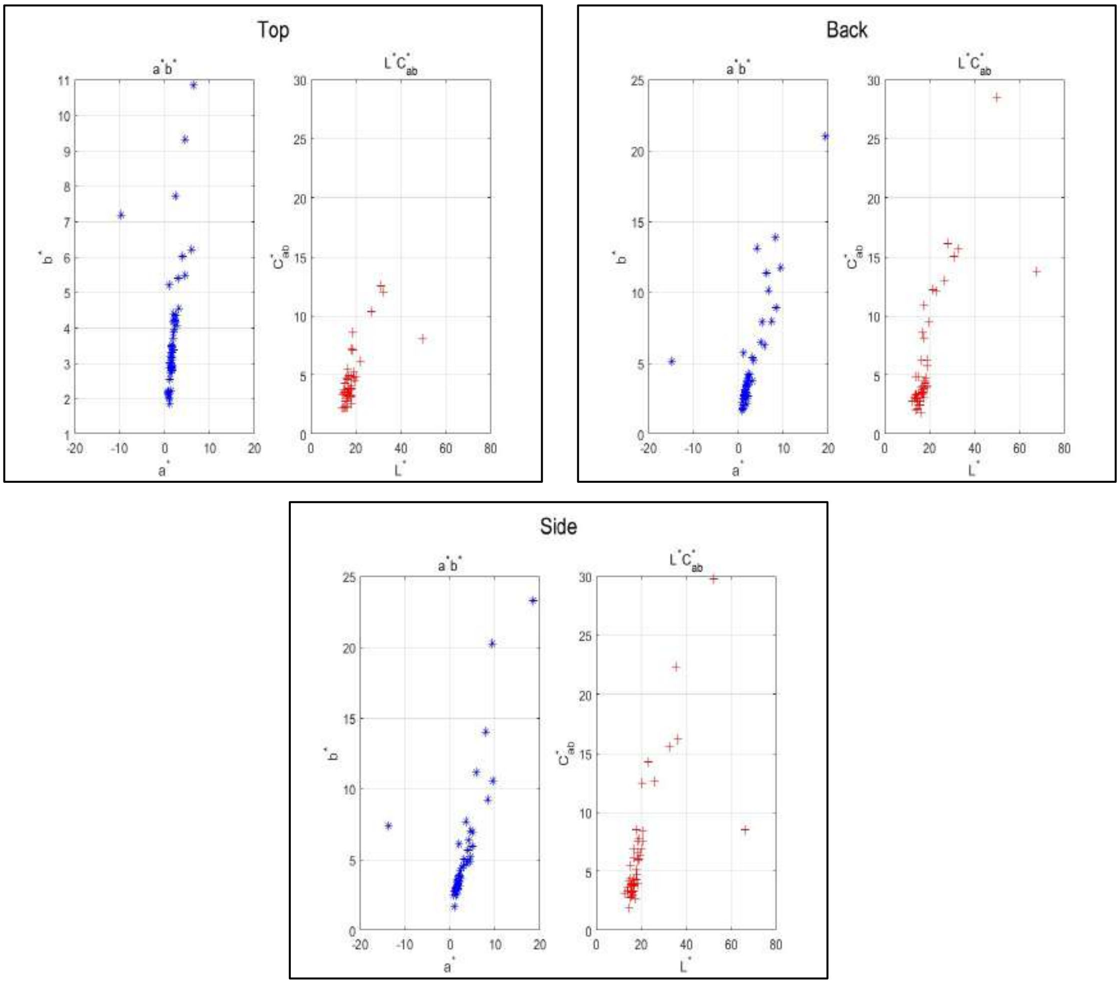

Figure 1. The CIELAB parameters a^*, b^* and L^*, C_{ab}^* of the 50 subjects

In order to investigate whether different hair measurement positions affect the variability of hair colour measurements, three positions on the hair (back, top, and side) were selected (as shown in Figure 2) and measured five times continuously at the same position using the spectrophotometer (SPM).

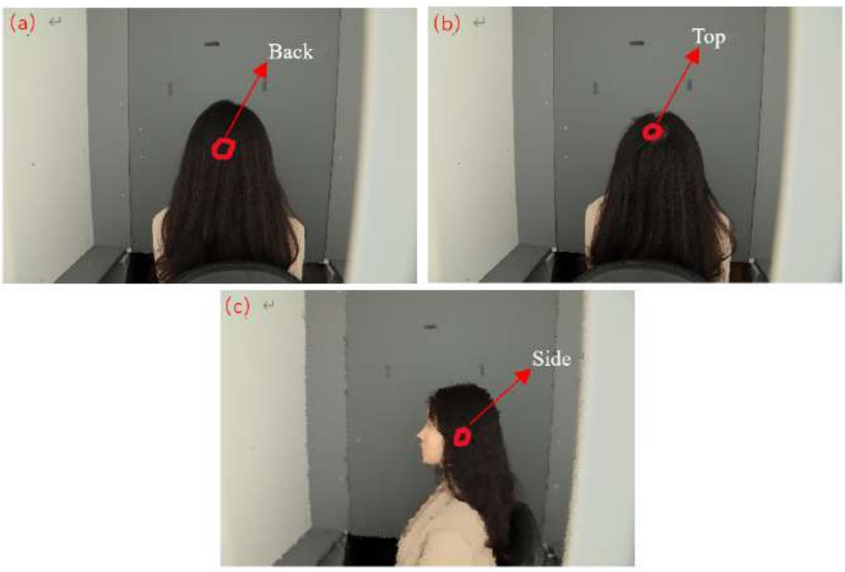

Figure 2. Measurement position of the hair (a) back, (b) top, (c) side

Spectrophotometer measurements
The spectrophotometer measures the ratio of the radiant flux reflected from the sample into the defining cone to the radiant flux similarly reflected from the perfect diffuser. The measurement is independent of the power of the spectral distribution of the light source used in the instrument, and the perfect diffuser is usually a ceramic or enamelled white tile.
SPM instruments require the aperture to be in contact with the surface during measurement so that environmental light does not affect the measurement as shown in Figure 3. The Konica Minolta CM700D was used in this experiment. It uses a pulsed xenon lamp with a UV cut-off filter and a very short measurement time which helps to minimize the possibility of movement during the measurement. In this research, the instrument measurements included the specular component of the reflected light.

Figure 3. The spectrophotometer location to obtain measurements on the back of the subject's head

In this study, four different aperture masks were used to vary the size of the measurement area as well as the pressure exerted on the hair surface (as shown in Figure 4): a direct medium aperture of 8 mm (*MAV*) and a small aperture of 3 mm in diameter (*SAV*). Two masks have a flexible, transparent plastic plate at the front, which can be used to reduce the pressure by enlarging the contact surface, the low-pressure medium aperture (*LPMAV*) and the low-pressure small aperture (*LPSAV*). The total number of measurements over the 50 subjects, each measured 5 times at 3 positions with 4 alternative masks, was a total of 3000 measurements. Measurements were displayed and saved in the CM-SA analysis software and were obtained in the 400-700 nm wavelength range, with a measurement interval of 10 nm.

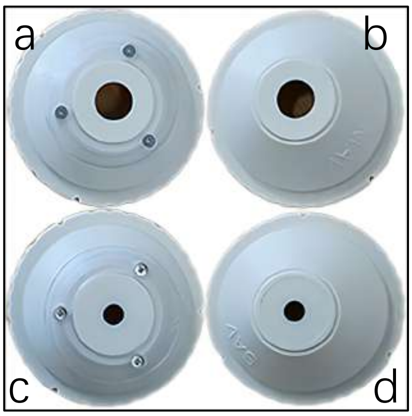

Figure 4. Four masks of the spectrophotometer (a) lpmav, (b) mav, (c) lpsav, (d) sav

Short-term repeatability

In order to assess the intra- and inter-instrument agreement, measurements were recorded as CIELAB coordinates using the CIE illuminate D65 and the CIE two-degree standard observer. From these coordinates, it was possible to calculate the mean value of the mean colour difference(MCDM) between the five repeated measurements, as defined in Equation 1: Larger MCDM values reflect poorer repeatability.

$$\mathrm{MCDM} = \frac{\sum_{i=1}^{n} \Delta E^{*}_{k1,\ 2}}{n} \tag{1}$$

$$\Delta E^{*}_{k1,\ 2} = \sqrt{(L_i^* - L_m^*)^2 + (a_i^* - a_m^*)^2 + (b_i^* - b_m^*)^2}$$

$$L_m^* = \frac{\sum_{i=1}^{n} \Delta L_i^*}{n}, a_m^* = \frac{\sum_{i=1}^{n} \Delta a_i^*}{n},\ b_m^* = \frac{\sum_{i=1}^{n} \Delta b_i^*}{n}$$

The number of repeat measurements in each group were taken a total of five times, thus $n = 5$. L_i^*,a_i^*,b_i^* are CIELAB of each measurements. L_m^*, a_m^*, b_m^* are the mean CIELAB of each group of measurements.

RESULT AND DISCUSSION

Short-term repeatability

The average MCDM for the fifty individual hair colour measurements using SPM is approximately 0.34$\triangle E_{ab}^*$. The maximum value is 0.87$\triangle E_{ab}^*$ and the minimum value is 0.16 $\triangle E_{ab}^*$.

Position

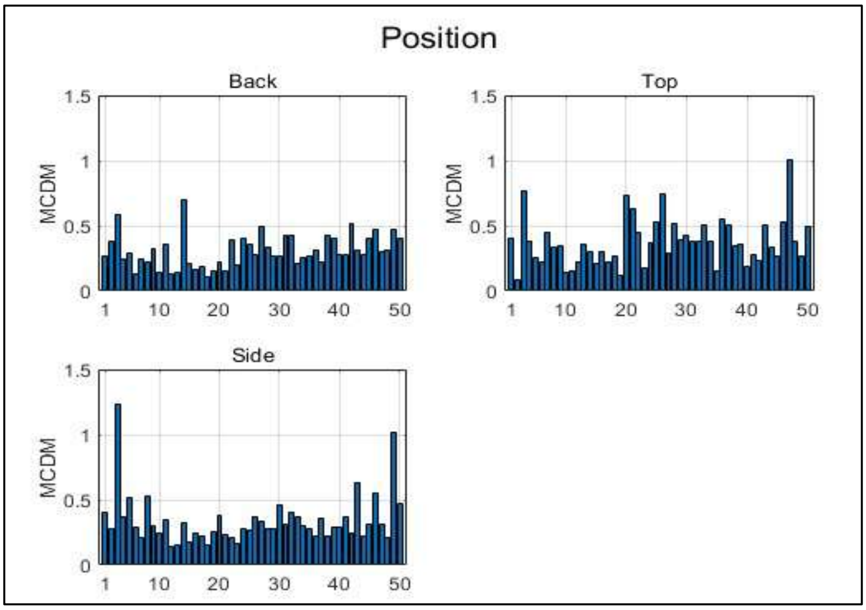

Figure 5. Comparison of the results for 50 observers and three measurement positions

Table 1. MCDM results for different positions of measurement

	Back	Top	Side
Mean	0.30	0.37	0.34
Max	0.70	1.00	1.23
Min	0.11	0.08	0.13

The MCDM results of different positions are shown in Figure 5 and Table 1. The average

MCDM for the back, top, and sides of the hair is 0.30$\triangle E_{ab}^{*}$, 0.37$\triangle E_{ab}^{*}$, and 0.34$\triangle E_{ab}^{*}$ respectively. The three values are very similar, suggesting that the change in position does not affect the repeatability of the instrument in measuring hair colour

Pressure & Aperture

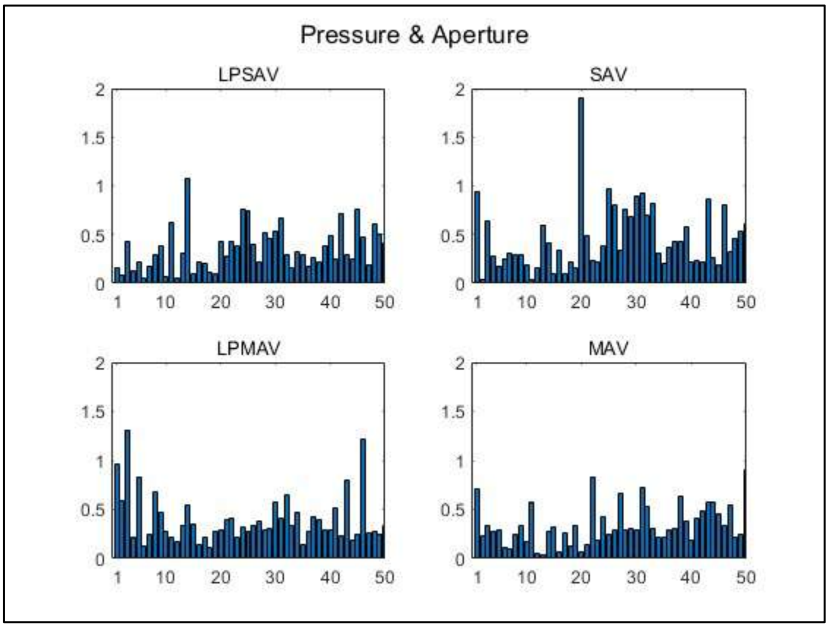

Figure 6. Different pressure and aperture results of spectrophotometer

Table 2. MCDM results of measurements using different pressures and apertures

Value	MCDM Values			
	LPSAV°	SAV*	LPMAV[a]	MAV[+]
Mean	0.35	0.45	0.39	0.34
Max	1.07	1.92	1.32	0.91
Min	0.03	0.04	0.04	0.06

* Medium aperture; [+] Medium aperture; ° Low-pressure small aperture; [a] Low-pressure medium aperture

The MCDM results of different pressures and apertures are shown in Figure 6 and Table 2. The average MCDM for the four different settings ranged from 0.34$\triangle E_{ab}^{*}$ to 0.45$\triangle E_{ab}^{*}$. There was not much difference between the four settings, with the largest difference being 0.09. This suggests that the repeatability of SPM measurements is not affected by changes in pressure or aperture.

Instrument agreement

Table 3. Values of colour differences, $\triangle E_{ab}^{*}$ obtained by different settings of SPM

Cross-comparisons	Mean Colour Difference, ($\triangle E_{ab}^{*}$)
MAV with different pressure: HP and LP	1.06
SAV with different pressure: HP and LP	1.30
LP with different aperture size: SAV and MAV	1.41
HP with different aperture size: SAV and MAV	1.51

The MCDM between different instrumental conditions on the SPM indicated the mean colour difference between HP and LP measurements was 1.06 and 1.30$\triangle E_{ab}^*$ for large and small apertures, respectively, Table 3. For different aperture sizes, the measured colour difference was 1.41 and 1.51$\triangle E_{ab}^*$ for low and high pressure respectively. This suggests that there was no significant effect on the results of the hair colour values when changing the pressure or the size of the measuring area.

CONCLUSION

In this study, a Konica Minolta CM700 spectrophotometer was used to characterise the colorimetric nature of head hair on the head of 50 subjects and to establish any potential and instrumental colour variability. Hair colour measurements were collected from fifty subjects at three head locations-, back, top and side, and different measurement parameters were used to determine any variability. It was observed, there was little change in repeatability related to head position using continuous measurements without removing the instrument from the subject's head. Further, there was no significant difference in repeatability after changing the measurement area and pressure size. In addition, when changing the different measurement settings, the hair colour values remained constant.

In conclusion, this analysis provides a useful guide to real human hair measurement and the potential creation of hair colour database. Future studies should compare the variability of the data sets obtained by different instruments.

REFERENCES

1. Westerhof, W. (2006). *The discovery of the human melanocyte*. Pigment Cell Research, 19(3), pp.183-193.
2. Sturm, R.A., Duffy, D.L., Box, N., Newton, R.A., Shepherd, A.G., Chen, W., Marks, L.H., Leonard, J.H. and Martin, N.G. (2003). *Genetic Association and Cellular Function of MC1R Variant Alleles in Human Pigmentation*. Annals of the NewYork Academy of Sciences, 994, pp.348-358.
3. Duffy, D.L., Box, N.F., Chen, W., Palmer, J.S., Montgomery, G.W., James, M.R., Hayward, N.K., Martin, N.G. and Sturm, R.A. (2004). *Interactive effects of MC1R and OCA2 on melanoma risk phenotypes*. Human Molecular Genetics, 13(4), pp.447-461.
4. Ancāns, J., Flanagan, N., Hoogduijn, M.J. and Thody, A.J. (2003). *P-Locus Is a Target for the Melanogenic Effects of MC-1R Signaling: possible control point for facultative pigmentation.* Annals of the New York Academy of Sciences., 994.
5. Corbett JF. (1976). *Hair dyes – their chemistry and toxicology.* Cosmetics & Toiletries, pp. 91:21-28.
6. Grimes, E.A., Noake, P., Dixon, L. and Urquhart, A. (2001). *Sequence polymorphism in the human melanocortin 1 receptor gene as an indicator of the red hair phenotype*. Forensic science international, 122 2-3, pp.124-129.
7. Madnani N, Khan K. (2013). *Hair cosmetics*. Indian J Dermatol Venereol Leprol, 79:654-667.
8. Bednarek, J. ~2004!. *An attempt to establish objective criteria for morphological examinations of hairs using the image analysis system*. Probl Forensic Science,56 (LVI),

pp.65–77.

Effect of modality on the efficacy of light exposure on mood

Mengyuan Chen*[1], Stephen Westland[1]

[1]School of Design, University of Leeds, UK

ABSTRACT

Light therapy is an established treatment for people suffering from seasonal affective disorder and has been shown to be effective. This study explores the possibility that exposure to light in the hours shortly after waking may also have a beneficial effect on healthy adults' subjective mood or wellbeing. Subjective wellbeing, as a multifaceted psychological attribute, remains challenging to measure directly. This study explores the effect of three light modes (front facing, backlit and transcranial) or delivery methods on subjective mood and alertness. The Positive and Negative Affect Schedule (PANAS) was used to concurrently gauge positive (PA) and negative (NA) emotions. Alertness was assessed via the Karolinska Sleepiness Scale (KSS). The forward-facing light condition increased PA and decreased KSS; however, results failed to reach statistical significance and this may be due to the relatively small number of participants in this study. An attempt was made to develop a wellbeing scale based on PA, NA and KSS. According to this metric neither illumination conditions nor temporal factors substantially influenced wellbeing scores in isolation. However, a salient interaction was discerned between illuminative conditions and temporal factors, predominantly under the backlit condition. More data is required from a larger population to substantiate these findings.

Keywords: Colour Temperature, Alertness, Mood, Transcranial Light

INTRODUCTION

Human physiological and behavioural processes are affected by the circadian cycle, which is controlled by many factors, the most important of which is the effect of light [1]. Human circadian rhythms are influenced by light exposure and significantly impact overall wellbeing. This non-imaging aspect of our visual systems means that light exposure (or lack of light exposure) can affect people's physiological and psychological condition [2]. Traditionally there were thought to be four photopigments in the human retina: rhodopsin in the rod cells and three photopsins in the cone cells. However, during the last couple of decades a fifth photopigment (melanopsin) has been identified [3]. The response of melanopsin is not thought to be involved with vision but rather plays a role in the regulation of the circadian clock, as it allows the pineal gland to sense changes in external light and adjust melatonin levels, for example, accordingly [4]. Melatonin is a hormone secreted by the pineal gland that peaks at night to help you fall asleep. There is growing evidence that exposure to light in the hours before bedtime suppresses melatonin secretion and shortens the duration of melatonin action, thereby affecting a person's circadian rhythm and quality of sleep [5]. Although retinal ganglion cells indirectly respond to light (when they are stimulated by rods and cones) intrinsically photosensitive retina ganglion cells (ipRGC) can respond to light independently of rod and cone responses due to the presence of melanopsin. Whereas rods and cones send signals that primarily terminate in the visual cortex, ipRGCs send signals to a central part of the brain called the hypothalamus which controls the release of various hormones and regulates body temperature. Light exposure is thus intimately tied to the human circadian rhythm and profoundly impacts an individual's mood and overall wellbeing. A healthy circadian system is entrained by limited exposure to light in the late evening and sufficient exposure to light in the hours after waking [6]. Adequate exposure to natural light throughout the day can augment alertness and positively influence emotional states. Light therapy has proven efficacious in mitigating a broad spectrum of depressive disorders.

The application of phototherapy for the treatment of Seasonal Affective Disorder (SAD) began in the early 1980s. SAD is a disorder that affects people's emotional state during winter or spring. Patients typically suffer from anxiety, depression, and fatigue, often accompanied by changes in appetite and sleep problems [7]. Phototherapy improves the emotional state of SAD patients by providing patients with appropriate light, stimulating the ipRGCs cells in the retina at the appropriate time, and regulating the body's biological clock. Light therapy is typically delivered using a light box or phototherapy glasses to expose patients to light for a certain amount of time at specific times each day. Light therapy, incorporating various wavelengths of light, has found applications in medicine as a form of physical treatment, yielding certain therapeutic benefits. However, its deployment necessitates careful consideration of specific diseases and patient conditions.

While the impact of light on the human body via eyes or skin has long intrigued researchers, a novel perspective has emerged in recent years: transcranial phototherapy. This nascent research field investigates the effects of light, particularly of specific wavelengths such as near-infrared, penetrating the scalp and skull to directly irradiate and influence the brain. Despite the promise this field holds, it remains in the early stages of research, with many of the initial findings requiring further validation. Unanswered questions also abound, concerning optimal parameters (such as light intensity, duration, and wavelength), and long-term safety and efficacy of transcranial phototherapy.

Although light therapies can positively impact mood, particularly for individuals with seasonal affective disorder or other forms of depression, their effects on the wellbeing of healthy individuals are less clear. Wellbeing is a combination of many aspects including personal history, stress levels, physical comfort and level of alertness or sleepiness. Furthermore, current methodologies for quantifying happiness are not without their flaws.

In this paper, healthy participants were exposed to three different lighting systems in the early morning to explore the effect of light on wellbeing. The lighting systems were (1) a forward-facing light box, (2) a light box behind the participants and (3) an in-ear transcranial device. Wellbeing was assessed in two ways: using a questionnaire called PANAS (Positive and Negative Affective Scale) and KSS (the Karolinska Sleepiness Scale). EEG recordings were also made in the study but are not reported in this paper.

METHODOLOGY

A total of 12 participants were selected for this experiment, with an equal number of males and females aged 24 ± 4 years. Recruitment criteria for participants included exclusion of individuals with excessive coffee or alcohol consumption habits, as well as individuals maintaining irregular circadian rhythms, to ensure that no participants exhibited significant abnormalities in physical or mental health. The University of Leeds Ethics Committee granted approval for the study, and all participants provided informed consent before their involvement. The experiment tested three distinct lighting conditions (see Figure 1).

Figure 1. The lighting conditions used in the study: (1) two forward-facing light boxes (5000k) (left); (2) two backlighting light boxes (5000k) (middle); (3) transcranial lighting condition using a commercially available in-ear device (right).

Illumination levels were quantified using an X-Rite I1 pro2 spectroradiometer, with the capability to measure spectral power distribution along with various chromaticity indices. Participants were instructed to report to the laboratory in the morning and were allocated to one of the three described lighting conditions. Subjects were first exposed to a 3500k, 200lux baseline light source for a period of 20 minutes for adaptation (the baseline condition), followed by data collection using the PANAS and KSS questionnaires. Note that PANAS allows for specific measurement of positive (PA) and negative (NA) scores. For KSS, the higher the KSS score, the higher the subjective sleepiness. Subsequently participants were exposed to their designated target lighting condition. After 40 minutes under this lighting, they completed the same set of questionnaires (see Figure 2 for experimental protocol).

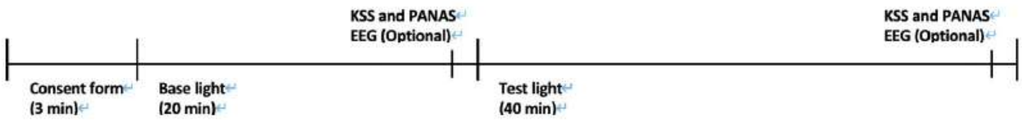

Figure 2. Experimental Protocol.

RESULT AND DISCUSSION

Figure 3 and 4 show the mean PA and NA scores respectively for the baseline condition and for the test lighting condition. A two-way repeated-measures ANOVA revealed a significant effect of time on PA ($F=6.707$, $p=.025$), indicating that PA scores for the test lights were different than for the baseline condition. However, there was no significant effect of lighting condition ($F=.215$, $p=.810$). Specifically, the change in PA values from the baseline condition to the test light condition (as shown in Figure 3) was not significant for any of the three lighting conditions (p=0.054, p=0.551 and p=0.438 for the Front light, Ear light and Back light respectively). Note, however, that for the Front light condition the effect was nearly significant; given the relatively small number of participants this suggests that a larger study may yield a significant effect. The change in NA values from the baseline condition to the test light condition (as shown in Figure 4) was not significant for any of the three lighting conditions (p=0.995, p=0.995 and p=0.995 for the Front light, Ear light and Back light respectively).

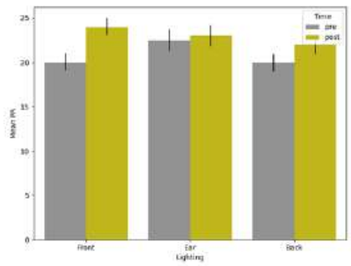

Figure 3. Mean and SEM of PA by Lighting and Time

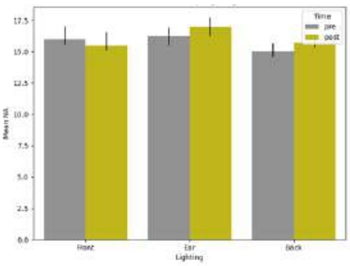

Figure 4. Mean and SEM of NA by Lighting and Time

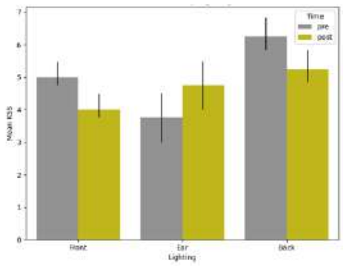

Figure 5. Mean and SEM of KSS by Lighting and Time

The mean KSS scores the three lighting conditions are illustrated in Figure 5. The KSS data were analysed using the same two-factor repeated measures analysis of variance method. The results indicated that neither individual light environments (p=0.927) nor time factors (p=0.417) significantly influenced the KSS scores. However, the interaction between light and time approached significance (p=0.071). Subsequent comparative analyses suggested that the relationship between time and the KSS score was not linear under specific lighting conditions, with the interaction effect between Quadratic and Linear achieving significance (p=0.018). This suggests that KSS scores might exhibit significant temporal changes under particular lighting conditions, offering a fresh angle for future investigations into the intricate interplay between lighting conditions, alertness, and fatigue.

Recent studies have revealed that subjective wellbeing is a complex psychological variable that is challenging to measure directly. In order to evaluate its indicators more accurately, a new method is proposed, which is estimated by integrating the two dimensions of vigilance and emotion. KSS measured alertness, while mood was measured using PANAS, resulting in positive affect (PA) and negative affect (NA). Based on these data, an equation was developed to calculate wellbeing W based on the PA, NA and KSS scores:

$$W = \frac{2.5(PA - 10) + 100 - \left(2.5(NA - 10)\right) + 100 - \left(12.5(KSS - 1)\right)}{3}$$

This equation is an attempt to construct a wellbeing index based on all three measurements (PA, NA and KSS); the coefficients in the equation are chosen to make sure that wellbeing W increases as PA increases and as NA and KSS decrease. The coefficients were also selected to balance the contributions of the three factors, at least in a numerical sense. However, clearly we do not know what the relative contributions of PA, NA and KSS towards wellbeing should be or even which of these factors makes a contribution. Further experiments will be needed to ascertain this and the data from these experiments could be used to modify the equation that has been introduced in this paper.

Nevertheless, the subjective wellbeing equation was analysed using the general linear model (GLM), and the results showed that neither lighting conditions nor time itself had a significant effect on the wellbeing score ($p = 0.985$ and 0.144, respectively see table 1). However, it is noticeable that there is a significant interaction effect between light conditions and time ($p=0.007$). Specifically, the change in wellbeing score from the first time point to the second time point was significant ($p = 0.049$) under the backlighting condition. However, this conclusion needs to be further verified on a larger sample.

Table 1. General Linear Model (GLM) Summary on wellbeing

Analysis Type	Main Effect/Interaction	Significance Level (Sig.)
General Linear Model		
Multivariate Tests	Lighting	0.985
	Time	0.144
	Lighting * Time	0.007

CONCLUSION

In the study, the effects of three lighting environments on mood, alertness, and subjective wellbeing were evaluated. Across all three lighting conditions there was a significant influence of the time factor on PA, yet negligible impact on NA and KSS alertness scores. This means that PA scores were higher under the three test conditions compared with the starting baseline lighting conditions. For the front light condition, there was a marked increase in PA (Figure 3), a marginal decrease in NA (Figure 4), and a heightened sense of alertness (Figure 5). These observations align with Hofmann et al. (2014) who postulated that intense light could elevate mood and energy levels [8]. The Back light condition led to an elevation in PA, with modest increases in both NA and alertness. This augmentation in alertness under backlighting parallels the findings of Jones et al. (2016), who observed that backlighting might enhance performance on select cognitive tasks, notably those associated with attention and alertness [9]. The Ear light conditions presented a nuanced scenario with a slight increase in PA while NA and drowsiness both rose. Such trends resonate with Lee and Kim (2017), suggesting that lateral lighting could attenuate alertness [10]. These patterns indicate that the influence of distinct lighting conditions on mood and alertness is intricate and mutable. Some lighting orientations might subtly deteriorate mood, and reports of minor ear discomfort following prolonged exposure to ear light highlight potential factors that could impinge on emotional or physical comfort.

Moreover, the subjective wellbeing estimation formula introduced in this study furnishes an innovative framework for ensuing investigations. This formula amalgamates positive and negative emotional states with alertness scores to deduce subjective wellbeing (see figure 7).

Analyses derived from this formula underscore a significant interaction between light conditions and time, heralding fresh avenues for future research.
Conclusively, it has posited that diverse lighting environments could influence different brain regions, subsequently modulating mood, and alertness. Several rationales might elucidate these fluctuations. Firstly, distinct lighting environments could activate various brain regions, consequently influencing mood and alertness. Secondly, the primordial states of mood and alertness varied across lighting conditions, potentially introducing an experimental bias. Lastly, individual discrepancies might play a pivotal role, given that responses to identical lighting environments can differ person-to-person. This research elucidates novel intersections between light, mood, and alertness, prompting further studies to delve deeper into the nuanced mechanisms connecting light conditions with mood and alertness, taking a broader array of variables and conditions into account.

REFERENCES

1. Roenneberg, T., Wirz-Justice, A., & Merrow, M. (2003). The human circadian clock entrainment by light and sleep. *Current Biology, 13*(5), 432-437.
2. Lockley, S. W., Brainard, G. C., & Czeisler, C. A. (2003). High sensitivity of the human circadian melatonin rhythm to resetting by short wavelength light. *The Journal of Clinical Endocrinology & Metabolism, 88*(9), 4502-4505.
3. Panda, S., Sato, T. K., Castrucci, A. M., Rollag, M. D., DeGrip, W. J., Hogenesch, J. B., ... & Kay, S. A. (2002). Melanopsin is required for non-image-forming photic responses in blind mice. Science, 297(5581), 525-527.
4. Reppert, S. M., & Weaver, D. R. (2002). Coordination of circadian timing in mammals. *Nature, 418*(6901), 935-941.
5. Aeschbach, D., Chang, A. M., Duffy, J. F., & Czeisler, C. A. (2015). Evening use of light-emitting eReaders negatively affects sleep, circadian timing, and next-morning alertness. Proceedings of the National Academy of Sciences, 112(4), 1232-1237.
6. Czeisler, C. A., Duffy, J. F., Shanahan, T. L., Brown, E. N., Mitchell, J. F., Rimmer, D. W., ... & Kronauer, R. E. (1981). Bright light induction of strong (type 0) resetting of the human circadian pacemaker. *Science, 244*(4910), 1328-1333.
7. Figueiro, M., Nagare, R., & Price, L. (2018). Non-visual effects of light: How to use light to promote circadian entrainment and elicit alertness. *Lighting Research & Technology, 50*(1), 38–62.
8. Hofmann, W., Vohs, K. D., & Baumeister, R. F. (2012). What people desire, feel conflicted about, and try to resist in everyday life. *Psychological science, 23*(6), 582–588. https://doi.org/10.1177/0956797612437426
9. Jones, L. T., Mullin, C., & Stone, B. D. (2016). The effects of ambient light direction on cognitive performance. *Applied Cognitive Psychology, 30*(4), 650-656.
10. Lee, T. Y., & Kim, Y. K. (2017). The role of lateral ambient light on emotional and cognitive response. Lighting Research & Technology, 49(2), 185-198.

AN IMAGE QUALITY EVALUATION DATASET FOR ATMOSPHERE QUALITY MODELING

Nanlin Xu[1], Yuechen Zhu, Ming Ronnier Luo[1]*

[1]*State Key Laboratory of Modern Optical Instrumentation, Zhejiang University, CHINA.*

*Corresponding author: Ming Ronnier Luo, m.r.luo@zju.edu.cn

ABSTRACT

With the popularization of digital devices, images are more accessible. However, how to judge the image quality of a picture is highly desired. Image quality evaluation model is becoming increasingly important and there appears abundant datasets. Nevertheless, there were few datasets include the rendering by color attributes. and assessed using atmosphere terms. Note the earlier works were based on preference. With this in mind, the present work includes to render 7 images including the contents restaurants, museums, sunset, blue moments after sunset, bars, KTVs and concerts.

Whole experiment was divided into two parts. In the first part, 7 scenes were selected according to captured image contents and each scene was represented with five images. 50 participants were asked to write down three to five terms to describe the atmosphere of the scene and also to choose one image from the 5 to represent the scene. Overall, a total of 1,704 atmosphere terms were accumulated. Finally, the most occurrence 3 atmosphere terms for each image were selected for the main experiment.

In the second part, the 7 images were first rendered in three ways: 1） to be rendered by 6 color rendering methods with 5 or 6 intensities, resulting in 217 images; 2) to invite 14 professional photographers to edit images with 3 top atmosphere terms for each scene together with the average image from all 14 professionals, resulting 315 images; 3)To carry on the image style analysis in CIE La*b* space to the photographer's edited images, obtaining 13 most consistent edited images. A total of 545 color rendered images were obtained for the formal experiment. In the formal experiment, 30 observers were asked to scale each image on a display 1) preference of the image and 2) the intensity of three atmosphere terms in terms of 6 rating levels to ensure accurate evaluation. Finally, 71,940 ratings were accumulated. The average value of $STRESS_{intra}$ was 13.72, and the average value of $STRESS_{inter}$ was 26.33, which proved that the results of the dataset were stable.

To predict the atmosphere and preference score of an image, an atmosphere quality model (AQM) was developed and produced good results when predicting atmosphere scores with mean R value of 0.70.

Keywords: Image dataset, atmosphere quality model, atmosphere reproduction.

INTRODUCTION

With the popularization of photo capture, task of visual score assessment arises much interest around diverse industries. Compared to traditional subjective scoring methods, visual score assessment models offer advantages of convenience and high accuracy.

Visual score assessment model can be divided into 3 types; namely, full reference (FR) [1], reduced reference (RR) [2, 3] and no-reference (NR) methods [4].

Among these methods, NR methods are the most popular on account of the independence. NR methods predict visual score only with features of the test image. Among these methods, because of the difficulty of obtaining reference image in the practical application scene, NR methods is the most widely used and urgently needed by the industry. Bianco trained a neural network model DeepBIQ with a migration learning approach [4]. Model was pre-trained on the public dataset Image-Net and then migrated to individual database for parameter tuning.

In addition, image evaluation can be divided into subjective evaluation and objective evaluation. Subjective evaluation means that conduct a psychophysical experiment in which final evaluation scores are obtained by combining statistical methods to synthesize the image quality scores of all observers. The objective evaluation is to fit the subjective evaluation data by analyzing the characteristics of the image which is the simulation of the subjective evaluation. Therefore, the establishment of subjective image evaluation datasets is significant to build an effective model. At present, several image datasets [5-10] are developed which are applied a lot in image quality modeling, such as the LIVE database of the University of Texas [5].

However, most image datasets mentioned above almost focus on image quality rather the atmosphere intensity of images which can bring much more attraction and reflect the emotional variance. Two experiment were conducted in this paper resulting 545 rendered experimental images. And the established dataset took the preference and intensity of atmosphere into consideration.

In addition, a no-reference atmosphere quality model was proposed consisting of 8 attributes which demonstrated a good result during prediction tasks.

METHODOLOGY

Whole experiment was divided into two parts including pre-experiment and formal experiment.

1. Pre-experimental design and results analysis

In the first part, 7 scenes were selected according to captured image contents and each scene was represented with five images. The first part experiment was conducted on an online website, and 50 participants were asked to write down three to five terms to describe the atmosphere of the scene and also to choose one image from the 5 to represent the scene. Overall, a total of 1,704 atmosphere terms were accumulated. Finally, the most occurrence 3 atmosphere terms for each image were selected for the main experiment as showed in Figure. 1 and Table 1.

Table 1: Top 3 atmosphere terms of 7 scenes.

Scene	Restaurant	Museum	Sunset	Blue moment	Bar	KTV	Concert
Atmo 1	cozy	quiet	quiet	quiet	lively	relaxing	enthusiastic
Atmo 2	relaxing	solemn	relaxing	sorrowful	relaxing	joyful	lively
Atmo 3	joyful	bright	romantic	lonely	joyful	lively	joyful

Figure 1. Images used in the 2ed experiment.

2. Image preparation for the formal experiment

The 7 images were rendered in three ways as showed in Table 2. Firstly, 7 images were rendered by 6 color rendering methods with 5-6 intensities, including chroma, vividness, depth, clarity as Eq. (1-4), correlate color temperature (CCT) change and hue change, resulting in 217 images.

Table 2: Formal experimental images composition.

Method	Attributes rendering	Photographer	Style image

Composition	Vividness (5 levels) Depth (5 levels) Clarity (5 levels) Chroma (5 levels) CCT (5 levels) Hue change (6levels)	Rendered image of 3 terms Average images	Restaurant (1) Museum (4) Sunset (1) Blue moment (2) Bar (1) KTV (0) Concert (4)
Num of images	7×5×5+7×6 = 217	(14×3+3) ×7 = 315	13
Total	545 images		

$$vividness = \sqrt{L^2 + a^2 + b^2} \tag{1}$$

$$depth = \sqrt{(L-100)^2 + a^2 + b^2} \tag{2}$$

$$clarity = \sqrt{(L-50)^2 + a^2 + b^2} \tag{3}$$

$$chroma = \sqrt{a^2 + b^2} \tag{4}$$

What' more, 14 professional photographers were invited to edit images only in color aspect with 3 top atmosphere terms for each scene, resulting 315 images together with the average image from all 14 professionals.

Moreover, image style analysis was carried out in CIE La*b* space to the photographer's edited images as followings:

1) 50 color centers were obtained by k-means clustering method of the original image under a certain atmosphere term of a scene. 2) Deflection vectors of the color centers between the original and rendered were calculated in a CIE LA*B*color space, which indicated a rendering style of the photographer as showed in Figure 2. 3) Between two photographers, the color centers with similar deflection directions were marked as 1 (△hue<=20°), otherwise marked as 0. 4) Color-style matching coefficient between the photographers then will be obtained using the weighted sum of color center weights and the marks. 5) The photographers will be judged whether the image style is similar, based on the color-style matching coefficient (threshold was set as 0.5). 6) It was considered that there literally existed a style under the atmosphere if there were more than 3 photographers in the same style. 7) At last, rendered images of photographers under the same style were averaged to generate one style image, obtaining 13 most consistent style images.

Finally, a total of 545 color rendered images were obtained for the formal experiment.

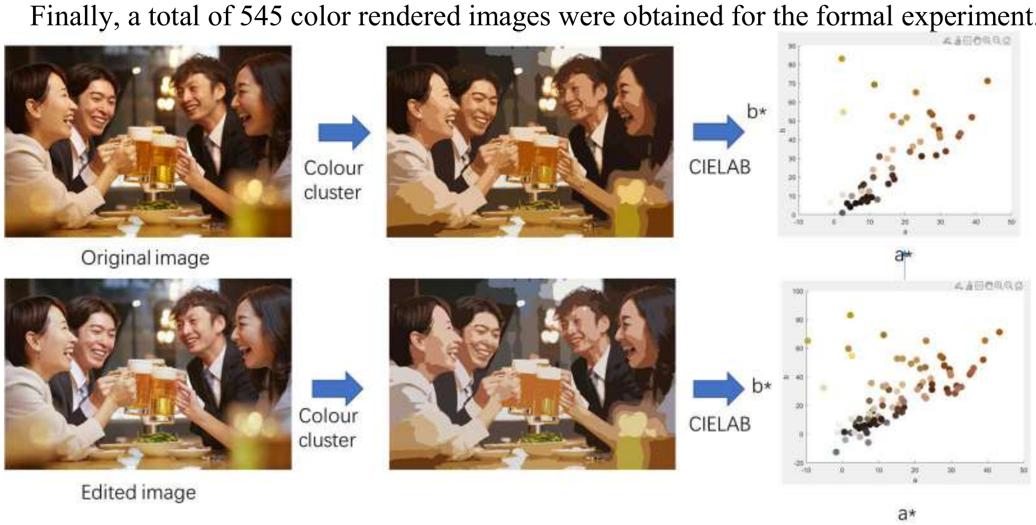

Figure 2. Color centers of original image and rendered image of photographer.

3. *Formal experiment setup*

In the formal experiment, to begin with, observers were asked to adapt to the dark experimental conditions for 60 seconds and then provided the evaluation of the image using the experiment software. Figure 3 shows the interface used to perform the experiment.

In the experiment, 10 percent of all images were randomly picked out as a repeated group for observers' performance evaluation. The whole formal experiment took about 180 mins to complete for each observer. 30 normal observers who performed the Ishihara color vision test participated in the formal experiment. At the end of the formal experiment, a total of 71,940 evaluations were accumulated.

Figure 3. User interface for the experiment.

4. Experimental results analysis

4.1 Raw data processing

All obtained evaluation data ranging from -3 to +3 were first converted to 1-6. Then the ratings of each image were average to obtain final visual score. The average scores (1-6) were then normalized to a 0-1 scale in which 0 corresponds to the lowest perceptual score and 1 corresponds to the highest perceptual score. The data were then used in subsequent process.

4.2 Observer variability

Intra- and inter- Standardized Residual Sum of Squares (STRESS) were calculated to represent the data consistency of observers using raw data as

$$STRESS = 100\sqrt{\frac{\sum_{i=1}^{n}(F_s p_i - v_i)^2}{\sum_{i=1}^{n} v_i^2}} \tag{5}$$

$$F_s = \frac{\sum_{i=1}^{n} v_i p_i}{\sum_{i=1}^{n} p_i^2} \tag{6}$$

Where p and v are the refence and batch data respectively. n is the number of images.

For a perfect agreement, STRESS should be 0. The mean values of intra-R and inter-R are 13.72 and 26.33 in formal experiment, which proved that the results of the dataset were stable.

5. No-reference atmosphere quality model

To predict atmosphere quality, the proposed AQM consists solely of 8 attributes listed in Eq. (7) which extracts the key information including chroma (C) of CIELAB color space, chroma contrast 5x5 (CC5), sharpness contrast 9x9 (CS9), chroma ratio (Cr), clarity ratio (Clr), global contrast (GC), local contrast (LC) and sharpness (S) attributes.

Chroma contrast (CC5) was employed to model the contrast changes in the images. The CC5 value was calculated by taking the average of standard deviations of local image regions of sizes 5 × 5, around all pixels of chroma (C) channels. For sharpness (CS9), edge detection was first applied on the lightness (L) channel using the Sobel operator. Then the standard deviations of local image regions were calculated around the detected edge pixels and averaged to obtain a single value for an entire image.

The chroma ratio and clarity ratio values were relative attributes based on the display gamut.

$$IQ = f(C, CC5, CS9, Cr, Clr, GC, LC, S) \tag{7}$$

$$Clr = \frac{1}{N}\sum\frac{Cl_t}{Cl_g} \tag{8}$$

$$Cr = \frac{1}{N}\sum\frac{C_t}{C_g} \tag{9}$$

For certain attributes, the computational procedure is to increase this attribute of the target pixel until it reaches the gamut boundary. Then the end point on the gamut could be regarded as a reference point showed in Figure 4. The ratio of the target pixel and the reference point attribute is considered the relative attribute value. The ratio value of an image for certain attributes was obtained by averaging the ratio values of all pixels as given by Eq. (7-9).

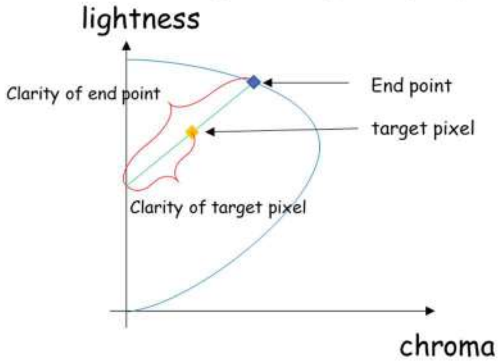

Figure 4. Calculation procedure of clarity ratio (Clr) value. The blue curve is the gamut boundary in the hue page of the target pixel.

In addition to the above-mentioned five attributes, three more image attributes were chosen to build the AQM, including global contrast (GC), local contrast (LC), and sharpness (S) [10].

RESULT AND DISCUSSION

Results of no-reference atmosphere quality model

Pearson correlation coefficient (R) was chosen as the evaluation criterion of prediction model results, which calculated as:

$$\mathrm{R}(\mathrm{x}, \mathrm{y}) = \frac{\mathrm{cov}(\mathrm{x},\mathrm{y})}{\mathrm{std}(\mathrm{x})\cdot\mathrm{std}(\mathrm{y})} \tag{10}$$

Where, cov is the co-variance, std is the standard deviation and n is the number of images.

Firstly, 28 (4x7) linear models trained from respective images were built, whose prediction results are listed in Table.4. the average R value of linear models obtained 0.7875, which demonstrated the reliability of attributes.

Table 4: Prediction results of linear models

R	Atmo 1	Atmo 2	Atmo 3	Preference
Restaurant	0.7483	0.5944	0.6406	0.6311
Museum	0.8571	0.8395	0.9359	0.8592
Sunset	0.7674	0.6817	0.8345	0.7330
Blue moment	0.6923	0.6717	0.6967	0.7837
Bar	0.9402	0.7617	0.9118	0.8403
KTV	0.7170	0.7703	0.9127	0.7531
Concert	0.8796	0.9100	0.8847	0.8008
Average	0.7875			

However, 28 models were too complex to apply. One preference SVR model was proposed to predict all visual scores, which was trained by all preference scores including 7 scenes with support vector machine (SVM) regression method.

Table 5: Prediction results of preference SVR model

R	Atmo 1	Atmo 2	Atmo 3	Preference
Restaurant	0.4896	0.7948	0.6684	0.8897
Museum	0.7379	0.7223	0.6948	0.9742
Sunset	0.5252	0.7707	0.7634	0.9074
Blue moment	0.1965	-0.1858	-0.2790	0.9594
Bar	0.7631	0.8103	0.8524	0.9676
KTV	0.8684	0.8067	0.6233	0.9695
Concert	0.7075	0.7162	0.7924	0.9151
Average	0.7041			

The prediction results of preference SVR model was listed in Table 5. Most of R values achieved good results. results of blue moment obtained low R values, which indicated that there was no strong positive correlation between the 3 atmosphere terms (quiet, sorrowful and lonely) and preference. Most of other terms symbolizing positivity, such as joyful, had a stronger correlation with preference. The results above are in line with our cognition and also revealed a possibility that only a few models cover all terms.

CONCLUSION

This study aimed to establish an image dataset for atmosphere quality model and atmosphere reproduction model. The mean R value between SVR model prediction and visual scores obtained 0.704, demonstrating the reliability of the image attributes.

ACKNOWLEDGEMENT

This research is supported by National Natural Science Foundation of China (61775190).

REFERENCES

1. Larson, Eric C. and Damon M. Chandler. “Most apparent distortion: full-reference image quality assessment and the role of strategy.” J. Electronic Imaging 19 (2010): 011006.
2. Rehman A, Zhou R. Reduced-reference image quality assessment by structural similarity estimation. IEEE Trans Image Process. 2012 Aug;21(8):3378-89. doi: 10.1109/TIP.2012.2197011. Epub 2012 May 1. PMID: 22562759.
3. H. Yeganeh, and Z. Wang, "Objective assessment of tone mapping algorithms," in 17th IEEE International Conference on Image Processing (ICIP 2010), pp. 2477–2480.
4. Bianco S, Celona L, Napoletano P,et al. On the use of deep learning for blind image quality assessment. SIViP 12, 355–362 (2018).
5. Sheikh H. Live image quality assessment database release 2[J/OL], 2005[2022-04-04].
6. Ponomarenko N, Lukin V, Zelensky A, et.al. TID2008 – A Database for Evaluation of Full-Reference Visual Quality Assessment Metrics[J]. 14
7. Ponomarenko N, Jin L, Ieremeiev O, et.al. Image database TID2013: Peculiarities, results and perspectives[J/OL]. Signal Processing: Image Communication, 2015, 30: 57-77.
8. Liu X, Pedersen M, Hardeberg J Y. CID:IQ – A New Image Quality Database[J]. 2010, 17(6): 503-510.
9. Lin H, Hosu V, Saupe D. KADID-10k: A Large-scale Artificially Distorted IQA Database[C/OL]//2019 Eleventh International Conference on Quality of Multimedia Experience (QoMEX). Berlin, Germany: IEEE, 2019: 1-3[2021-08-29].
10. Khan MU, Luo MR, Tian D. No-reference image quality metrics for color domain modified images. J Opt Soc Am A Opt Image Sci Vis. 2022 Jun 1;39(6):B65-B77. doi: 10.1364/JOSAA.450595. PMID: 36215544.

COLOR PREFERENCE OF THAI TEA PHOTO

C. Saksirikosol[1], K. Rattanakasamsuk[1]* and C. Hiramatsu[2]

[1]*Color Research Center, Rajamangala University of Technology Thanyaburi, Thailand.*
[2]*Graduate School of Design, Kyushu University, Japan.*

*Corresponding author: Kitirochna Rattanakasamsuk, e-mail kitirochna@rmutt.ac.th

ABSTRACT

Thai tea, also known as Thai iced tea, is a popular beverage made from black tea, condensed milk, fresh milk, and sugar. It has a unique orange color and aroma, which have made it popular among both Thais and foreigners. However, preferences for the color of Thai tea may vary depending on personal experiences. Therefore, this research aimed to investigate the relationship between Thai tea color and its preference. A set of Thai teas was created by varying the proportion of black tea to milk from 0% to 100%, resulting in a total of 15 recipes. A digital camera was used to take a photo of each cup, which was then randomly presented on an iPad screen. The subjects were 38 Japanese and 111 Thai students. They were asked to evaluate their overall satisfaction for each Thai tea color using a 9-point hedonic scale. The subjects also evaluated the color category, drink category, and perceived attribute. The results suggested that cultural differences influence the perception of Thai tea beverages. Thai subjects preferred Thai tea images with a wider tea solution concentration range than Japanese subjects. In contrast, Japanese subjects, who are not familiar with Thai tea, perceived the quality of This tea based on their perception of milk tea.

Keywords: Thai tea, Thai tea color, Cross culture difference

INTRODUCTION

A survey and ranking of the top 50 delicious beverages in the world by CNN Travel found that Thai tea was ranked 27th [Cheung, 2018]. This ranking has made Thai tea widely known and popular, both among Thais and foreigners as a Thailand's iconic drinks. We can see that besides coffee, Thai tea is one of the drinks that every cafe, coffee shop, or beverage shop always has on the menu. This shows that Thai tea is a beverage with a high market value in Thailand.

While Thai tea is renowned for its aromatic and sweetly rounded flavor, it is the distinctiveness of its orange color that distinguishes it from the milk tea in other countries, such as India and Taiwan. Normally, the milk tea's color in those countries is beige or lighter shades of brown. Notably, the variety shade of orange in Thai tea depends on several factors like tea leaves, brewing methods, and the proportions of condensed milk and sugar. [Jullaya and Wongpaisarnrit, 2015; Phensuk, T., 2017]. Saksirikosol et al. (2019) had investigated the boundary of Thai tea color by color adjusting method on a display. The result has shown that the boundary of Thai tea color was in the yellowish-orange region with the average color of L^* = 52.61, a^* = 19.36, b^* = 52.81. In 2021, Saksirikosol et al. also continually studied the color of Thai tea for advertising by using the Munsell Color System [Saksirikosol et al., 2021]. The color chips were selected as a representative color of Thai tea based on their field experience. The result showed that there were 8 colors representing Thai tea color: 3.75YR 6/12, 3.75YR 5/12, 5YR 5/12, 1.25YR 5/12, 5YR 6/10, 2.5YR 6/12, and 2.5YR 5/14.

While the desirable attributes of Thai tea are typically perceived through the sense of taste, but these attributes are primarily perceived visually by consumers. Therefore, Thai tea advertisements often focus on creating visually appealing images to stimulate consumers' desire to drink Thai tea without actually tasting it.

Therefore, the objective of this research is to investigate the relationship between the color of Thai tea and its perceived attributes such as "look delicious, greasy, creamy, and rich of taste.

The 9-point hedonic scale [Lim, J., 2011] was used to evaluate overall satisfaction. Color category and drinks category of the various Thai tea color are also examined. Cross culture difference on perception of Thai tea is also investigated by comparative result between Thai subjects who are familiar with Thai tea and Japanese subjects who are not familiar with Thai tea.

METHODOLOGY

Subjects

All subjects are university students aged between 17-23 years old. 111 Thai and 38 Japanese subjects were voluntarily recruited to participate in this experiment. The number of Japanese and Thai are unequal due to the limitation of time and recruiting process.

Stimuli

Thai tea beverages were created by mixing tea solution and milk, with the tea solution concentration varying from 0% to 100%. Photographs of these beverages were captured using a Canon EOS 5D Mark III DSLR camera. The photographs were presented on an iPad at its highest brightness setting. A Konica Minolta CS-160 chroma meter was used to measure the color of the presented images. The xy chromaticity of these colors was plotted on an xy chromaticity diagram. Some colors were not evenly distributed, so we decided to discard the superimposed color values. Therefore, the stimuli were 15 images of tea solution concentrations in the following percentages: 2%, 6%, 12%, 20%, 28%, 36%, 44%, 60%, 68%, 76%, 84%, 88%, 92%, 96%, and 100%. Figure 1 shows the xy chromaticity of these Thai tea images.

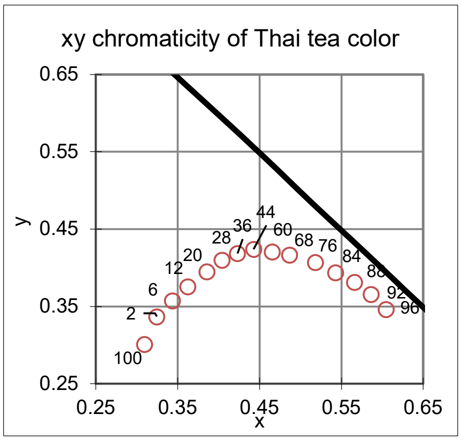

Figure 1. xy chromaticity of Thai tea images. Number represented the tea solution concentration.

Procedure

The experiment was conducted as an online survey using a website. Subjects will be presented with a Thai tea image on an iPad in a random order. After each image appeared, subjects must evaluate it by answering the following questions:

Overall satisfaction: Subject used a 9-point Hedonic Scale to rate their overall satisfaction, with 1 being "extremely dislike" and 9 being "extremely like."

Color category: Subject selected a color name from the following list: white, beige, orange, brown, or red.

Drinks category: Subject selected one of the following options: tea, milk tea, Thai tea, milk, or other.

Perceived attributes: Subject selected multiple adjectives from the following list: rich of taste, creamy, greasy, bitter, look delicious.

All questions and answers were provided in Thai, English, and Japanese. Each subject must evaluate all 15 Thai tea images to complete their task.

RESULT AND DISCUSSION

Table 1. shows the comparative result of the cross-cultural perception of Thai tea beverages. Thai and Japanese subjects evaluated Thai tea images of varying tea solution concentrations on Hedonic scale scores, Color category, drinks category and perceived attribute.

Overall satisfaction

The Hedonic Scale assessment revealed that Thai participants preferred Thai tea images with 12% tea solution concentration, with a mean score of 6.2. Thai tea images with 20% and 92% tea solution concentration also received high scores, averaging 6.1. Notably, the range of the average score is rather narrow, only between 5.2 and 6.2.

Japanese participants preferred Thai tea images with a 12% tea solution concentration, with an average score of 6.3. Their average scores ranged from 3.9 to 6.3, which was wider than the range for Thai participants. When the tea solution concentration was greater than 12%, the evaluation score decreased.

Color category

Both Thai and Japanese participants tended to select the same color categories when naming Thai tea images. As tea solution concentration increased, the images were categorized from white to beige, orange, brown, and finally red.

Thai participants associated orange with Thai tea images when the tea solution concentration ranged from 44% to 96%. In contrast, Japanese participants only associated orange with tea images within the range of 60% to 96%. A significant difference was observed in the identification of beige; Japanese participants identified beige in a wider tea solution concentration range, from 12% to 84%, while Thai participants only associated beige with concentrations of 28% and 36%.

Drinks category

When asked to name the beverages depicted in Thai tea images, Thai participants consistently referred to them as "Thai tea" when the tea solution concentration ranged from 60% to 96%. Japanese participants, unfamiliar with Thai tea, referred to the beverage as "milk tea" when the tea solution concentration ranged from 12% to 76%. For tea solution concentrations greater than 76%, the beverage was categorized as an unknown type.

Perceived attribute

Regarding the perception of taste and quality, Thai participants found Thai tea images appealing across a wide tea solution concentration range, from 2% to 96%. In contrast, Japanese participants exhibited a different trend. When the tea solution concentration exceeded 84%, the perceived deliciousness of Thai tea decreased. Furthermore, when the tea solution concentration exceeded 84%, most Japanese participants began to perceive the beverage as having a stronger flavor.

Table 1. Comparative result of Thai and Japanese subject in Thai tea images evaluation. *(W = white, Be = beige, O = orange, R = red)*

Quality	Thai														
	Concentration of Tea Solution (%wt/wt)														
	2	6	12	20	28	36	44	60	68	76	84	88	92	96	100
Hedonic Scale	5.6	5.9	6.2	6.1	5.8	5.9	5.7	5.8	5.9	5.9	5.9	6.0	6.1	5.5	5.2
Color	**W**	**W**	**W**	**W**	**Be**	**Be**	**O**	**O**	**O**	**O**	**O**	**O**	**O**	**O**	**R**
Perceived Drinks															
Milk Tea	1	11	23	49	61	56	42	28	23	23	19	8	10	8	10
Milk	90	83	60	34	14	23	3	1	2	1	0	0	0	0	1
Thai Tea	3	3	9	8	14	10	43	57	60	59	67	73	79	73	62
Tea	0	0	1	5	7	4	5	9	10	14	9	14	9	11	18
Other	6	4	6	4	3	7	6	5	5	4	5	5	2	8	9
Perceived attribute															
Look Delicious	74	85	91	91	90	88	77	81	85	89	91	87	90	79	53
Rich of Taste	16	14	33	52	53	70	32	37	39	45	51	60	77	87	95

Quality	Japanese														
	Concentration of tea (%wt/wt)														
	2	6	12	20	28	36	44	60	68	76	84	88	92	96	100
Hedonic Scale	6.1	6.0	6.3	6.1	5.7	5.7	5.8	5.7	5.8	5.6	5.2	4.9	4.6	4.3	3.9
Color	**W**	**W**	**Be**	**Be**	**Be**	**Be**	**Be**	**O**	**O**	**O**	**O**	**O**	**O**	**O**	**R**
Perceived Drinks															
Milk Tea	3	21	74	74	58	58	58	66	61	53	37	34	13	3	3
Milk	92	76	8	3	3	0	3	0	0	0	0	0	0	0	0
Thai Tea	5	3	11	8	13	11	11	16	21	29	37	24	24	16	13
Tea	0	0	0	0	0	0	3	3	3	3	0	3	8	13	8
Other	0	0	8	16	26	32	26	16	16	16	26	39	55	68	76
Perceived attribute															
Look Delicious	76	84	89	87	82	74	61	76	74	66	63	50	39	24	8
Rich of Taste	11	8	5	8	13	13	18	18	21	32	45	58	76	89	92

General discussion

The research suggest that cultural differences influence the perception of Thai tea beverages. Thai subjects preferred Thai tea images with a wider tea solution concentration range than Japanese subjects. However, due to the Japanese's limited familiarity with Thai tea, they tended to categorize Thai tea images as "milk tea" rather than "Thai tea." This categorization aligned with the color of the image, as beige images were consistently categorized as "milk tea". Japanese subjects perceived Thai tea images with higher tea solution concentration which are orange as being of lower quality milk tea. This suggests that Japanese subjects prefer milk tea with a milder flavor. This finding is consistent with previous research on cross-cultural differences in taste perception. For example, a study by Wan et al. (2014) found that East Asians generally prefer less intense flavors than Westerners. And Japanese cuisine is known for its emphasis on delicate flavors and textures. This suggests that people from different cultures may have different preferences for the richness of taste.

The findings of this study have implications for food and beverage companies that are marketing Thai tea products in different markets. Food and beverage companies should consider the cultural preferences of their target market when developing and marketing Thai tea products. Food and beverage companies that are marketing Thai tea products in Japan may want to focus on developing products with a milder flavor profile, less vivid orange.

CONCLUSION

This research provides insights into the cross-cultural perception of Thai tea beverages. The ideal color for advertising Thai tea to a Thai customer is an image with a 92% tea solution concentration, as it received the highest hedonic scores. And it was perceived as a highly delicious Thai tea. For a Japanese customer, the ideal image may be one with a 60% tea solution concentration, as it received the most look delicious drink with orange color which is the color of Thai teal.

ACKNOWLEDGEMENT

We would like to thank Associate Professor Chihiro Hiramatsu for collecting the data in this research.

REFERENCES

1. Cheung, T. (2018). *World's 50 Most Delicious Drinks*. https://edition.cnn.com/travel/article/most-delicious-drinks-world.
2. W. Jullaya and R. Wongpaisarnrit: 105 Recipe of Coffee and Tea, (2015), pp.57.
3. Phensuk, T. (2017). *Factors Affecting Consumer Decisions about Cha Tra Mue Brand Thai Tea Mix* (An Independent Study Submitted in Partial Fulfillment of the Requirements for the Degree of Master of Business Administration). Bangkok: Thammasat University.
4. Saksirikosol, C., Rattanakasamsuk, K., Jarernros,J. and Phuangsuwan, C. (2019). Color of Thai Iced Tea. Journal of the Color Science Association of Japan, Vol.44, No.3 Supplement, Kyoto, June 27-28, pp.180-181.
5. Saksirikosol, C., Jarernros, J., and Rattanakasamsuk, K. (2021). The Investigate Color of Thai Iced Tea for Advertising. Proceedings of the 6th Asia Color Association Conference, 2-3 November 2021, Yogyakarta, Indonesia, 76-80.
6. Lim, J. (2011). Hedonic scaling: *A review of methods and theory*. Food quality and preference, 22(8), 733-747. https://doi.org/10.1016/j.foodqual.2011.05.008
7. Wan, X., Woods, A. T., van den Bosch, J. J., McKenzie, K. J., Velasco, C., & Spence, C. (2014). Cross-cultural differences in crossmodal correspondences between basic tastes and visual features. *Frontiers in Psychology*, 5. https://doi.org/10.3389/fpsyg.2014.01365

RED AND BLUE – ABSTRACT AND CULTURAL ISSUES

Akira Asano[1]*, Chie Muraki Asano[2], Genki Ogura[1], and Emi Chida[2]

[1]*Faculty of Informatics, Kansai University, Japan.*
[2]*Sapporo Campus, Hokkaido University of Education, Japan.*

*Corresponding author: Akira Asano, a.asano@kansai-u.ac.jp

ABSTRACT

Red and blue are fundamental and typical color categories. We investigated the effect of these fundamental colors from the viewpoints of abstract and cultural issues and conducted two research works. 1) Abstract issue: It is often said that red suggests activeness and blue quietness. However, geometrical shapes of color samples have similar effects; for example, the rectangular shape implies more sharpness than the rounded shape. Color swatches are often used in experiments to present color samples, and they usually consist of simple geometrical shapes such as rectangles or disks. Geometrical shapes of presented color swatches and surrounding geometrical shapes may influence the impressions of colors. We combined color swatches with surrounding geometrical shapes and investigated whether there was a difference between the impressions obtained from the color swatches alone and those obtained from the combination. We presented to the respondents red and blue color swatches of disk and rectangle shapes and those surrounded by circles, triangles, rectangles, etc., and asked for their impressions. We used two adjective pairs, "passionate-calm" and "dynamic-static," and measured the impressions using a five-step scale. The results showed that, in some cases, there were significant differences in impressions when color samples were presented alone and when geometrical shapes surrounded them. The strength of the impression of the color tended to be suppressed when the color was presented together with surrounding shapes. 2) Cultural issue: Red and blue are often used as dominant colors of clothes. We presented to respondents in Hokkaido, the northernmost part of Japan, illustrations of a woman and a man wearing kimonos in many variants of red and blue. We asked about their preferences and suitability for kimonos. The results showed that people in Hokkaido prefer deep tones with low brightness and chroma. It contrasts well with our previous survey of Japanese people in the southern part; they preferred brilliant red for kimonos.

Keywords: red, blue, geometrical effects, kimono, traditional costumes in Japan

INTRODUCTION

Red and blue are fundamental and typical color categories. We investigated the effect of these fundamental colors from the viewpoints of abstract and cultural issues and conducted two research works on the issues.

Abstract issue

Firstly, we show an abstract aspect of the impression of red and blue under the combinations of the impression of geometrical shapes. It is often said that red suggests activeness and blue quietness. However, geometrical shapes of color samples have similar effects; for example, the rectangular shape implies more sharpness than the rounded shape. Color swatches are often used in experiments to present color samples, and they usually consist of simple geometrical shapes such as rectangles or disks. Geometrical shapes of presented color swatches and surrounding geometrical shapes may influence the impressions of colors. The mutual interaction between the impressions caused by colors and those by shapes has been investigated [1].

We combined color swatches with surrounding geometrical shapes and investigated whether there was a difference between the impressions obtained from the color swatches alone and those obtained from the combination. We presented to the respondents red and blue color swatches of disk and rectangle shapes and those surrounded by circles, triangles, rectangles, etc., and asked for their impressions. We used two adjective pairs, "passionate-calm" and "dynamic-static," and measured the impressions using a five-step scale. The results indicate that, in some cases, there were significant differences in impressions when color samples were presented alone and when geometrical shapes surrounded them. The strength of the impression of the color tended to be suppressed when the color was presented together with surrounding shapes.

Cultural issue

Secondly, we show a cultural aspect of the impression of red and blue clothes. Red and blue are often used as dominant colors of clothes, as well as the traditional costume in Japan. We have investigated the differences in the preferences of red in traditional costumes in several regions of Japan and found significant differences among the Northern region, Western region, and Okinawa [2].

We extend that research to the impression of red and blue. We present to respondents in Hokkaido, the northernmost part of Japan, illustrations of a woman and a man wearing kimonos in many variants of red and blue and ask about their preferences and suitability to kimonos. The results show that people in Hokkaido prefer deep tones with low brightness and chroma. It contrasts well with our previous survey of Japanese people in the southern part; they preferred brilliant red for kimonos [2].

ABSTRACT ISSUE

Method of Survey

The survey was conducted remotely using Google Forms in Japanese language. Figure 1 shows the color samples presented in the survey. These color swatches were presented one at a time in random order, and respondents were asked to answer their impression of each color on a 5-point scale using the adjective pair "passionate-calm." The same set of 16 color samples in random order was then presented again, and the respondents were asked to rate their impressions on a 5-point scale using the adjective pair "dynamic-static." Because the survey was conducted remotely, the size and the exact color of the color swatches did not match, depending on the terminal used by the respondents.

Results

Thirty-eight respondents participated in the experiment. Tables 1 and 2 show the percentage of respondents who chose each adjective pair for each color sample for the adjective pairs "passionate - calm" and "dynamic - static," respectively. In the "passionate - calm" category, blue tended to be perceived as

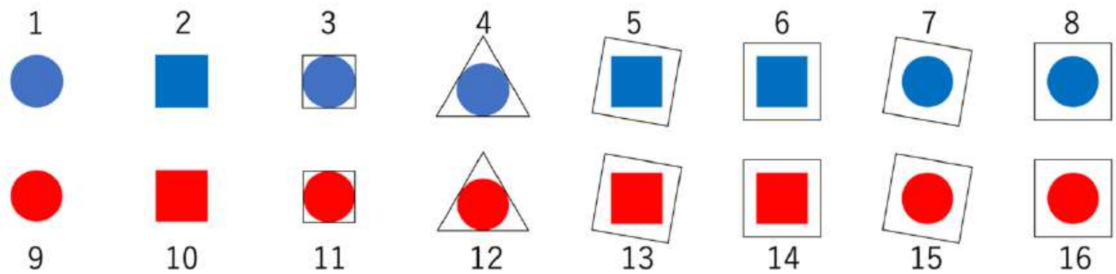

Figure 1. Color swatches presented in the experiment.

Table 1. Evaluations for "passionate - calm" impressions (%).

	1	2	3	4	5	6	7	8
1. Very passionate	0.0	2.6	0.0	0.0	0.0	0.0	0.0	0.0
2. Rather passionate	2.6	5.3	7.9	7.9	2.6	2.6	5.3	2.6
3. Neither	26.3	15.8	31.6	26.3	28.9	13.2	42.1	18.4
4. Rather calm	52.6	36.8	50.0	55.3	55.3	44.7	50.0	57.9
5. Very calm	18.4	39.5	10.5	10.5	13.2	39.5	2.6	21.1

	9	10	11	12	13	14	15	16
1. Very passionate	39.5	23.7	26.3	15.8	15.8	10.5	10.5	13.2
2. Rather passionate	47.4	47.4	44.7	55.3	50.0	50.0	50.0	44.7
3. Neither	10.5	26.3	28.9	23.7	34.2	31.6	36.8	31.6
4. Rather calm	2.6	2.6	0.0	5.3	0.0	7.9	2.6	10.5
5. Very calm	0.0	0.0	0.0	0.0	0.0	0.0	0.0	0.0

Table 2. Evaluations for "dynamic - static" impressions (%).

	1	2	3	4	5	6	7	8
1. Very dynamic	0.0	0.0	0.0	0.0	7.9	0.0	0.0	0.0
2. Rather dynamic	2.6	0.0	5.3	13.2	31.6	0.0	21.1	2.6
3. Neither	26.3	15.8	28.9	26.3	18.4	10.5	39.5	13.2
4. Rather static	36.8	34.2	47.4	47.4	39.5	42.1	34.2	65.8
5. Very static	34.2	50.0	18.4	13.2	2.6	47.4	5.3	18.4

	9	10	11	12	13	14	15	16
1. Very dynamic	21.1	13.2	5.3	13.2	26.3	7.9	26.3	13.2
2. Rather dynamic	36.8	36.8	36.8	42.1	57.9	47.4	50.0	36.8
3. Neither	36.8	36.8	36.8	23.7	13.2	26.3	23.7	34.2
4. Rather static	5.3	10.5	15.8	15.8	2.6	13.2	0.0	15.8
5. Very static	0.0	2.6	5.3	5.3	0.0	5.3	0.0	0.0

calm, and red as passionate. However, for the color swatches surrounded by tilted squares (Nos. 5, 7, 13, and 15), "neither" was selected more often than for those not surrounded by squares (Nos. 1, 2, 9, and 10). It indicates that the impression of the colors was suppressed by surrounding tilted squares. The "dynamic-static" category shows that blue tends to be perceived as static and red as dynamic. However, the percentages of "very static" for blue and "very dynamic" for red in the disk-shape swatch surrounded by upright squares (Nos. 8 and 16) are smaller than those in the swatches not surrounded by shapes. It indicates that the surrounding figure also suppresses the impression of the colors.

Tables 1 and 2 show the percentage of respondents who chose each option. Friedman's test was employed to examine whether there was a significant change in responses in the overall respondents between the cases of color samples alone and those enclosed in tilted squares. The results show that for the blue color swatches, for both “passionate - calm” and “dynamic - static” pairs, the responses are significantly different at the 5% significance level for both the disk (No. 1 - No. 7) and square (No. 2 - No. 5) cases. On the other hand, for the red color swatches, significant differences are found only in the “passionate - calm” case for the disk case (No. 9– No. 15) and the “dynamic - static” case for the square case (No. 10 – No. 13). It is supposed that for the blue swatches, the influence of the tilted square is considerable because the calm impression given by the blue color conflicts with the unstable impression of the tilted square. On the contrary, the influence is smaller for the red swatches because the red color has a passionate impression and thus does not conflict with the unstable impression of the tilted square.

In the study of the abstract issue, we combined color swatches with simple shapes and surrounding shapes to investigate how the impression of color is affected by the impression of shapes. We investigated whether there is a difference between the impression of color swatches alone and the impression when combined with shapes. The results show that the strength of the impression of the color tends to be suppressed when the color samples are presented together with the surrounding figures. Further research is expected to be conducted to study the interaction between color and graphic images in different situations.

CULTURAL ISSUE

Method of Survey

The respondents were 80 university students, 31 males and 49 females, living and studying in Hokkaido. The survey was conducted remotely using Google Forms in Japanese language. The illustrations of a man and a woman in Japanese traditional costumes of 18 variations of red and 18 variations of blue were presented in the form. The variations contain traditional Japanese colors. The respondents were requested to select the three most preferred colors for the presented four gender-color combinations, i. e. woman – reds, woman – blues, man – reds, man – blues. The color parameters of the variations of red and blue are shown in Table 3. Figure 1 shows the illustrations presented to the respondents. Note that the colors are not identical on each respondent's terminal since the survey was conducted remotely.

Table 3. Parameters of the presented colors. Japanese traditional color names are *italicized.* (a) reds. (b) blues.

(a)

No.	Name	L*	a*	b*
1	Agate	35	35	13
2	Turkey red	41	42	14
3	*Enji*（臙脂）	36	38	10
4	Wine red	35	36	10
5	Copper red	42	41	25
6	Percian red	32	28	12
7	*Akaneiro*（茜色）	43	43	17
8	*Benihi*（紅緋）	54	44	30
9	Cardinal	44	44	14
10	*Beniiro*（紅色）	42	53	15
11	Carmine	42	53	17
12	*Shuiro*（朱色）	54	48	30
13	*Shojohi*（猩々緋）	45	53	24
14	*Shinshu*（真朱）	57	39	13
15	*Niiro*（丹色）	50	42	36
16	*Bingata*（紅型）*-1*	45	54	29
17	*Bingata*（紅型）*-2*	45	56	20
18	*Bingata*（紅型）*-3*	45	55	23

(b)

No.	Name	L*	a*	b*
1	*Aiiro*（藍色）	30	-4	-22
2	*Ruriiro*（瑠璃色）	36	10	-46
3	*Byakugun*（白群）	71	-5	-22
4	*Kamenozoki*（瓶覗き）	71	-14	-11
5	*Hanadairo*（縹色）	41	-3	-31
6	*Tetsunando*（鉄納戸）	34	-9	-14
7	Sky blue	76	-12	-19
8	*Gunjoiro*（群青色）	36	18	-45
9	Turquoise blue	61	-25	-26
10	Cobalt blue	41	-4	-41
11	*koiai*（濃藍）	20	-2	-15
12	*Asagiiro*（浅葱色）	51	-30	-22
13	*Tsuyukusairo*（露草色）	51	-5	-44
14	Marine blue	30	-20	-25
15	Saxe blue	51	-6	-17
16	Iron blue	30	1	-19
17	Baby blue	76	-6	-10
18	Hyacinth	56	1	-24

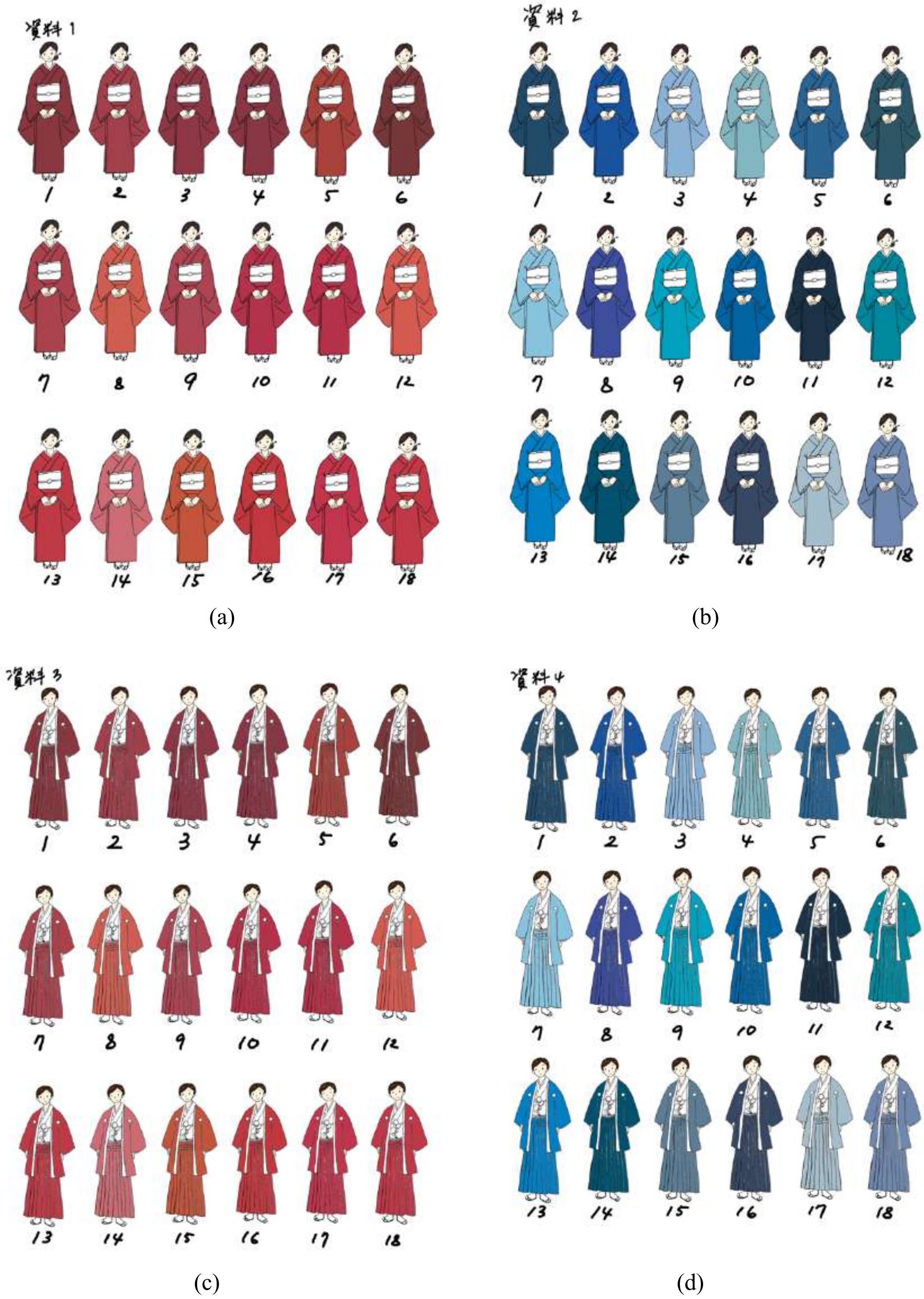

Fig 1. The illustrations presented to the respondents. The number below each illustration corresponds to the number in Table 3. (a) woman – reds. (b) woman blues. (c) man – reds. (d) man – blues.

Results

The most preferred color variations by all / female / male respondents are shown in Table 4. The results show that the overall preference in Hokkaido tends to be for calm tones of low chroma and brightness. This result contrasts with the preference for the woman – reds combination in

Table 4. The most preferred color variations by all / female / male respondents for the four gender-color combinations.

	Illustrations			
Respondents	woman - reds	woman - blues	man - reds	man - blues
All	*Shinshu* (No. 14)	*Aiiro* (No. 1) *Tetsunando* (No. 6)	Agate (No. 1)	*Koiai* (No. 11)
women	*Shinshu* (No. 14)	*Tetsunando* (No. 6)	Agate (No. 1)	Iron blue (No. 16)
men	*Shuiro* (No. 11)	*Byakugun* (No. 3) *Asagiiro* (No. 12)	Agate (No. 1) Persian red (No. 6)	*Koiai* (No. 11)

Okinawa, the South-West islands in Japan, which we investigated in [2]. In that survey, color variations of higher chroma and higher brightness were preferred in Okinawa.

CONCLUSIONS

This paper shows our research on two issues on the basic colors, red and blue. One is on the abstract aspect and investigates visual impressions on red and blue color swatches surrounded by geometrical figures. The results show that impressions of colors can be affected by the shapes of surrounding figures. The other work is on the cultural aspect and investigates preferences of variations of red and blue in Hokkaido region in Japan. The result shows that calm tones of low chroma and brightness are preferred in Hokkaido. The result contrasts our previous research that surveyed preferences in Okinawa, where high chroma and high brightness were preferred.

ACKNOWLEDGEMENT

This work was partially financially supported by JSPS KAKENHI Grant Nos. JP19K12692, JP22K03202, and JP23K11751, and Kansai University Secondary Fund for Research, 2023.

REFERENCES

1. Sato, K. and Oda, M. (2013). Effect of Color and Shape on Aesthetic Evaluations of Colored Shapes, *The 22nd IEEE International Symposium on Robot and Human Interactive Communication (IEEE ROMAN)*, 478-483.
2. C. Muraki Asano, A. Nishino, A. Asano, and K. Okajima (2014). Regional characteristics on preferences of ceremonial red color in Japan, *The 2nd Conference of Asia Color Association (ACA2014),* 112-116.

QUALIA CHANGE PHENOMENON RELATED TO COLOR VISION DIVERSITY

C. Hiramatsu[1]*, A. Yamada[1], M. Ishii[1], and Y. Baba[2,3]

[1]*Graduate School of Design, Kyushu University, Japan.*
2Graduate School of Information Sciences, Tohoku University, Japan.
3Japan Society for the Promotion of Science (JSPS), Japan.

*Corresponding author: Chihiro Hiramatsu, e-mail: chihiro@design.kyushu-u.ac.jp

ABSTRACT

There is no inevitable relationship between the physical properties of light, such as wavelength, and color qualia (the subjective experience of sensory awareness). Further, it is difficult to prove whether others perceive the same quality of sensation for the same light wavelength. However, in human society, where people communicate using color terms, there is intersubjectivity, the belief that others perceive the same qualia, though it is often questioned whether the color qualia of people with dichromatic or anomalous trichromatic vision, color vision minorities, is homogeneous with the color qualia of people sharing common trichromatic vision, color vision majorities. However, color vision minorities might form color vision impressions similar to those of the common trichromatic majorities and have homogeneous qualia as they become accustomed to the color language system used by common trichromats. In this presentation, we report the preliminary results of a study conducted to challenge the hard problem of color qualia generation by focusing on the diversity of color vision. Specifically, we investigated the phenomenon of qualia change in which the visibility of colors and letters composed of colors changes in a few dozen seconds, especially in color vision minority individuals. In the experiment, we asked people with anomalous trichromacy and common trichromacy to report introspective changes in their vision when viewing the same physical stimuli using color vision testing instruments such as anomaloscopes and pseudochromatic plates. The preliminary results show that there are conditions under which visibility change is more likely in people with anomalous trichromacy. In addition, the observation of stimuli produced by an anomaloscope resulted in a phenomenon where different color names were reported and qualia changes were more likely to appear under the same physical stimulus as when the ambiguous light wavelength for anomalous trichromacy is compared. These findings suggest that when the visual input of wavelength information is ambiguous, a qualia alternation similar to the perceptual alternation for ambiguous figures will occur.

Keywords: Color vision diversity, Color qualia, Perceptual alternation

INTRODUCTION

Many people use light wavelength information to perceive color; however, the question remains as to whether the subjective experience of color (color qualia) is common to other people. No inevitable correspondence exists between light wavelength information and color qualia, and people may have different qualia for the same wavelength information. In particular, the qualia of people with minor color vision types (a few percent of the population) is often thought to be quite different from that of people with common trichromatic vision, although it is difficult to prove the truth of this assumption. Investigating the subjective experiences of people with various color vision types might reveal unknown aspects of qualia in humans.

This study was inspired by a previous report on the phenomenon of flickering numbers on pseudochromatic color vision test plates experienced by author Y. B., whose color vision is of a minor type [1]. The report of this phenomenon raised the possibility that such unstable perception is likely to occur when people with minor color vision types are observing ambiguous stimuli, similar to the phenomenon of perceptual alternation with the famous example of a Necker cube [2,3]. In this paper, we report the preliminary results of an investigation of the qualia change phenomenon in people with various color vision types using conventional color vision test apparatus, pseudochromatic plates, and an anomaloscope.

METHODOLOGY

Participants

Three male undergraduate students (age 21.3 ± 1.2) whose color vision types were determined in previous experiments were recruited to participate in the investigation. The color vision type of the participants had been determined comprehensively based on the results of Ishihara pseudochromatic plates (38-plate, 2nd edition; hereafter Ishihara plates), anomaloscope HMC Anomaloskop MR (Oculus GmbH), and Colour Assessment Diagnosis (CAD) test (City Occupational Ltd) [4]. Participants 1 and 2 have deuteranomalous trichromatic vision (a form of anomalous trichromatic vision) in which the wavelength sensitivity of the M cone is shifted toward that of the L cone [5]; their red-green thresholds in the CAD unit were 19.35 and 9.07, respectively. Participant 3 was confirmed to have common trichromatic vision, and his red-green threshold in the CAD unit was 0.96. This study was approved by the Ethics Committee for Human Experiments (Approval No. 506) of Kyushu University Faculty of Design. Written informed consent was obtained from all participants prior to the investigation.

Procedure

To phenomenologically investigate the subjective change in color qualia, we utilized the conventional color vision test apparatuses, that is, Ishihara plates and an anomaloscope. Several Ishihara plates were observed approximately an arm's length apart under the D65 LED illumination (Sanken Electric Co., Ltd.) for 5 minutes each under three illuminance levels: low (~15 lx), middle (~150 lx), and high (~5400 lx). The stimuli for Rayleigh matches using an anomaloscope, comprising mixing light of 549 and 666 nm at the upper hemifield and reference light of 589 nm at the lower hemifield, were presented in two degrees of foveal vision (Figure 1a). We used 9 mixing light ratios [0 (549 nm only), 10, 20, 30, 40, 50, 60, 70, and 73 (666 nm only)] and 3 reference light intensities (0, 15, and 45) and presented 27 combinations (Figure 1b) of the mixing and reference lights in random order. The participants observed each combination for 30 seconds.

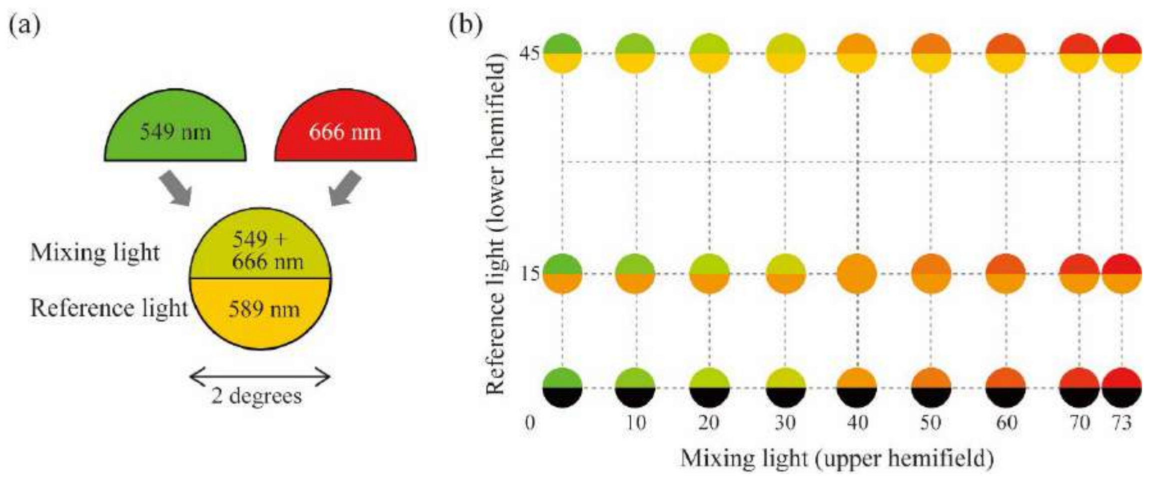

Figure 1. Schematic diagram of stimuli by using anomaloscope

No neutral adaptation step (white blank) was inserted during the 30-second observation to prevent the interruption of qualia change. The participants were asked to report the appearance (qualia) of the test stimuli if their appearance had changed. We recorded the participants' introspective verbal reports, while they were observing the test stimuli. The experimenter (author A.Y.) asked the participants for details of their appearance accordingly to record additional information on phenomenological changes. To examine the consistency of the phenomenological changes during the observation of the anomaloscope stimuli, the same procedure was repeated on a different day.

Analysis

The recorded verbal reports for each stimulus were transcribed for each participant. For the Ishihara plates, the flickering (alternation) of numbers and other phenomenal changes in visibility were analyzed under various illuminant levels. For the anomaloscope stimuli, reports on color names were analyzed primarily in the upper and lower hemifields. Specifically, we examined the consistency of color names for physically identical stimuli, for different combinations of mixing and reference lights, and for the consistency of reporting on different experimental dates.

RESULT AND DISCUSSION

Appearance of pseudochromatic plates

For the Ishihara plates, all participants reported the expected appearance of the number for the color vision type of each participant at the beginning of the observation. They also reported that the spots that made up the numbers were assimilated with the background as they continued to look at the stimulus. An unstable appearance of numbers was observed for Participants 1 and 2 on several plates under various illuminant conditions (Table 1). The interval between the changes in appearance ranged from a few seconds to a few dozen seconds. Participant 1 reported that changes in appearance were repeated during the observation period, while different appearances were not present simultaneously. Participant 2 reported perceptual uncertainty. Participant 3 reported various depth perceptions, while the numbers appeared to be the same. No consistency was found between participants and stimuli in the illuminance at which changes in visibility were likely to manifest.

Table 1: Appearance of numbers on Ishihara plates

Plate		Participant 1	Participant 2	Participant 3
ID	Photo			
2		**3**	**3** ↔ 8 (15, 5400 lx) **3** ↔ 8, 9 (150 xl)	**8**
3		**70** ↔ 10 (150, 5400 lx)	**70** ↔ 79 (150 xl, 5400 lx)	**29**
5		**2** ↔ 8 (5400 xl)	**2** ↔ 8 (15, 150, 5400 lx)	**5**
8		**21** ↔ 81 (15 xl)	**21** ↔ 24 (150, 5400 lx)	**74**

Table 1 shows the list of Ishihara plates with reported unstable appearances of numbers. In each cell, the bold number on the left indicates the expected visibility for each participant and is the number reported at the start of the observation. The number on the right is the number that appeared to each participant during the observation under the specific lighting conditions shown in parentheses.

Appearance of anomaloscope stimuli

The reported color appearances of the anomaloscope are summarized in Figure 2. Although the physical composition of the light was identical along the columns for the mixing light and along the rows for the reference light, the reported color appearance varied with the combination of mixing and reference lights for all participants. Particularly, Participant 1 frequently reported an unstable appearance when the intensity of the reference light was 15, which is the matching condition in common trichromatic vision when the mixing light is 40. Participant 2 sometimes reported the names of the colors as inferred. Participant 3 reported subtle differences in the color appearance.

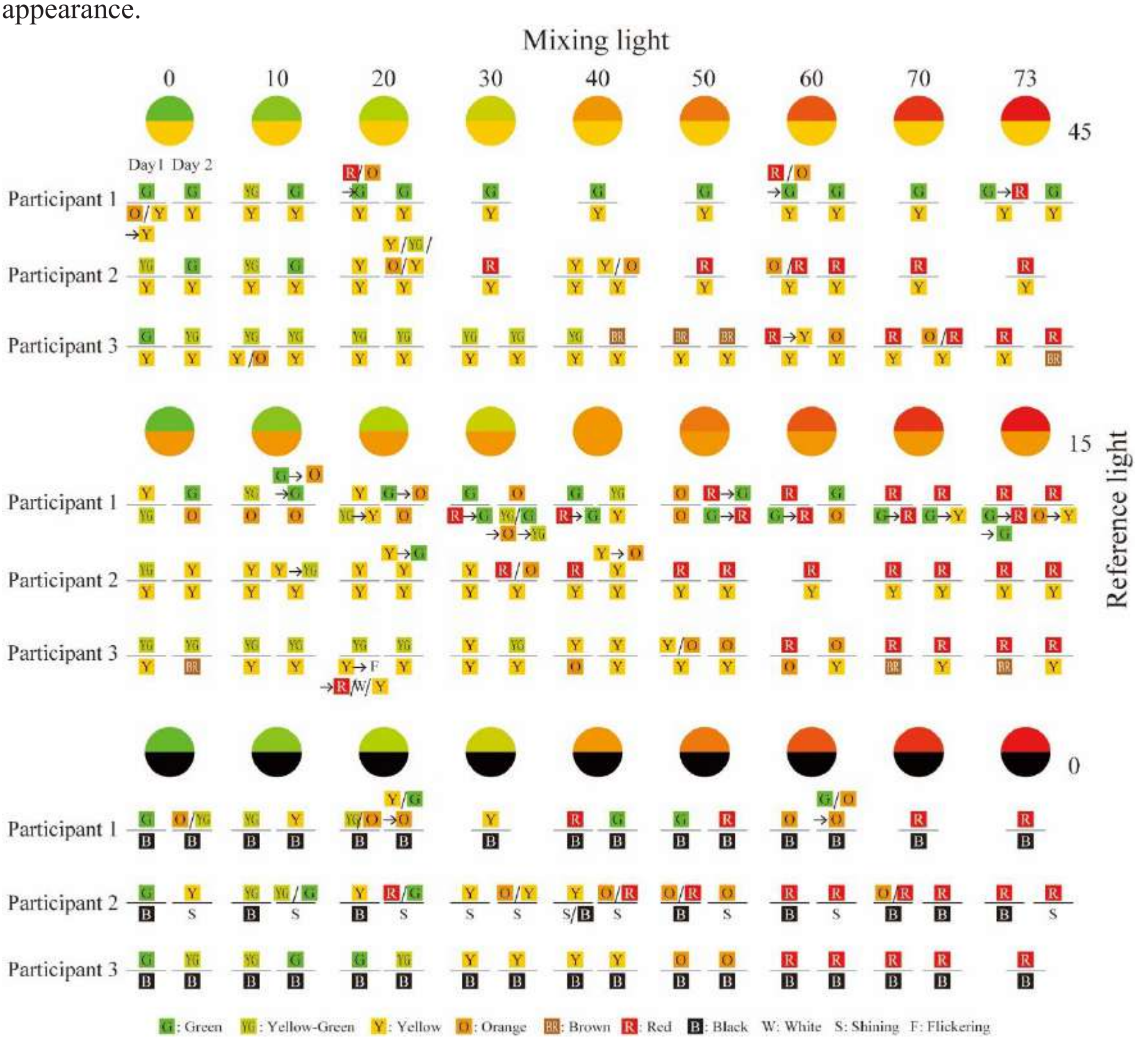

Figure 2. Appearance of anomaloscope stimuli

The alphabetic abbreviations represent the reported mixing light (top) and reference light (bottom) appearances for each stimulus on Days 1 (left) and 2 (right). If the reported appearances were identical, the reports for both days were merged. If the reported visibility showed slight differences between the two days, they were shown separately using the same letter. The arrows represent the change in appearance reported during the 30-second observation period.

Scientific significance of this study

We demonstrated that stable and unstable subjective appearances occur somewhat systematically in people with various types of color vision. This may indicate that even during the inconsistent reporting of color names in a color vision test, the participants are subjectively experiencing the qualia they report rather than just guessing. Whether the phenomenon of qualia change is due to adaptation by continuing to see the same stimuli needs to be investigated in the future. However, the retinal image continued to change under the conditions of observing the Ishihara plates; thus, it is likely that the alternation of numbers is similar to perceptual alternation [2,3]. We believe that further investigation of the phenomenon of change in appearance and its neural correlates in people with diverse color vision may help us understand how subjective experience is generated.

Sociological perspectives of this study

From a sociological point of view, the landmark of this study lies in the use of color vision test apparatuses. The color vision test eliminates color names from testing, and the anomaloscope and pseudochromatic plates are at the apex of this process. This process also deprives colorblind people (those with minor color vision types) of their color names. Color names uttered by colorblind people have lost their credibility as "incorrect" representations of real colors. However, in this study, we adopted the approach of using an anomaloscope to encourage colorblind people to say color names, thereby, unintentionally restoring their ability to say color names again.

A frequent objection to this kind of research is that "colorblind people are just guessing at color names." However, the criticism itself reveals that this is not a problem of physiology or psychology but rather a problem of social power. We need to consider the reasons why color names uttered by colorblind people seem to be "guesswork."

The concept of "interpretive labor," which refers to the effort of the inferior to infer the feelings of the superior in power-asymmetrical human relationships, as proposed by cultural anthropologist David Graeber [6], seems to accurately describe the situation in which colorblind people find themselves in with respect to color names. Colorblind people are forced to perform such "interpretive labor" when confronted with others with major color vision and are constantly forced to imagine how the other group, which is superior in power relations, would use color names ("correct" color name usage). They are not just "guessing" but are expending a lot of intellectual effort in their interpretation. Both ignoring this fact and unilaterally declaring it as "guesswork" seem presumptuous.

Furthermore, it should be noted that behind the phrase "They're just guessing," there exists the power to define color names. How can one confidently assert that color names uttered by colorblind people are "guesswork" when no one-to-one correspondence exists between color names and colors? This is because this critic has the power to define such correspondence names (or the one standing on the side of the majority who need not question the definition of color names), and one believes that color names and colors should have a one-to-one correspondence.

This study serves to witness the existence of the color experience of colorblind people by using their existing color names in opposition to the system that has deprived such people of their color names and enforced "a color name" = "color" match.

CONCLUSION

By phenomenologically examining the subjectivity of vision using color vision testing tools in a manner different from their original purpose, the commonality and diversity of vision among people with different color visions were highlighted. The previously reported phenomenon of flickering on pseudochromatic plates was reproduced in this study. A certain regularity existed in the change in the appearance of the anomaloscope stimuli. These findings indicate that phenomena similar to perceptual alternation may occur when color stimuli are ambiguous to the observer.

ACKNOWLEDGEMENT

We thank all three participants for their cooperation. This work was supported by JSPS KAKENHI (grant number 23K17643 to C. H.).

REFERENCES

1. Baba Y. (2020). *'Colorblindness' and modernity: the reorganization of the color order in the nineteenth century*. Tokyo: Seikyusha (in Japanese).

2. Klink PC, Van Wezel RJA, Van Ee R. (2012). United we sense, divided we fail: context-driven perception of ambiguous visual stimuli. *Phil. Trans. R. Soc. B* 367, 932–941. doi:10.1098/rstb.2011.0358

3. Maksimenko V, Kuc A, Frolov N, Kurkin S, Hramov A. (2021). Effect of repetition on the behavioral and neuronal responses to ambiguous Necker cube images. *Sci Rep* 11, 3454. doi:10.1038/s41598-021-82688-1

4. Barbur JL, Rodriguez-Carmona M, Evans BEW. (2021). Color vision assessment-3. An efficient, two-step, color assessment protocol. *Color Res. Appl.* 46, 33–45. doi:10.1002/col.22599

5. Deeb S. (2005). The molecular basis of variation in human color vision. *Clin. Genet.* 67, 369–377. doi:10.1111/j.1399-0004.2004.00343.x

6. Graeber D. (2012). Dead zones of the imagination: On violence, bureaucracy, and interpretive labor: The Malinowski Memorial Lecture, 2006. *HAU: Journal of Ethnographic Theory* 2, 105–128. doi:10.14318/hau2.2.007

WORLDWIDE SURVEY OF THE ASSOCIATION BETWEEN COLOR AND TEMPERATURE

N. M. Sow[1]*, C. Saksirikosol[2], M. Shamohammadi[1], K. Rattanakasamsuk[2], C. Phuangsuwan[2], and C. Hiramatsu[1]

[1]Graduate School of Design, Kyushu University, Japan.
[2]Color Research Center, Rajamangala University of Technology Thanyaburi, Thailand.

*Corresponding author: Meissa Ndeye Sow, e-mail: sow.ndeye.meissa.042@s.kyushu-u.ac.jp

ABSTRACT

There are times when two or more concepts are linked and given a specific meaning or application. As with categorizing objects or animals, it helps to associate a particular shape or sound with a concept to help describe and recognize it. It can result from a process of learning or cognitive behavior, which we gradually use as an intellectual mechanism to help us find our bearings and better understand our complex world. People also tend to associate color with temperature, and colors are often categorized as warm or cold. However, the reason for this correspondence is unknown, and it is considered that color and temperature are not initially sensory-related. Previous studies have suggested that the change in room temperature can impact our perception of color, and children tend to develop a similar color-temperature association with adults as they grow up, regardless of congenital color vision differences. All these insightful discoveries raised several questions about this cross-modal correspondence. Why do people associate color and temperature? Is this a culturally shared association or are there some cultural differences? Is the association more susceptible to developmental processes? To uncover the answers to these questions, we created an online experiment for the worldwide survey on the color-temperature association. The experiment included 70 trials of two-alternative forced choices. In each trial, participants had to choose between which of the two colors felt warmer to them. The 20 stimulus colors, four tones (vivid, light, soft, and dark), and five hues (red, yellow, green, blue, and purple) were used for the experiment. So far, we have collected data from several cultures in Asia, Africa, and Europe. We analyzed the color-temperature association pattern of each participant and calculated the mean pattern of each culture. Then we conducted correlation analyses to investigate the similarity of patterns. Our results suggested that the association patterns are similar in many cultures, although there are some variations. Overall, people tend to associate red and yellow with warmth and blue with coldness. We will present more detailed analyses focusing on possible biases and developmental influences in each culture.

Keywords: Temperature, Cross-modal correspondence, Culture, Development

INTRODUCTION

The tendency to associate color with temperature is an ancient and intriguing cross-modal correspondence in humans [1]. It is commonly known that hues ranging from red to yellow are perceived as warmer, and bluish hues as cooler. Classical psychological approaches of the past several decades have yielded results supporting this trend [2, 3], and modern approaches have attempted to obtain new insights into this correspondence [4, 5]. However, the reasons for this correspondence remain unclear; since this phenomenon has been studied primarily in the context of Western culture, some may question whether it is a universal cross-cultural human tendency [6].

Studies focusing on the development of this correspondence have shown that young participants tend to make unconventional associations [7, 8]. These studies suggest that cultural norms may lead to customary associations between color and temperature; however, the existence of intrinsic perceptual biases is also argued [1, 5].

Since there is relatively little evidence for the existence of this correspondence in non-Western cultures, we conducted a global online survey experiment to collect data from various regions. We also focused on the developmental aspects of this phenomenon to obtain further insight into how this correspondence is created in individuals. In this paper, we present the preliminary results for cultures for which we have obtained a substantial amount of data thus far.

METHODOLOGY

Participants

This study was approved by the Ethics Committee for Human Experiments (Approval No. 523) of Kyushu University, Faculty of Design. Participants of various ages (over the age of 7 years) were recruited from various regions worldwide. Informed consent (over the age of 16 years) or assent for minors (under the age of 16 years) were obtained online prior to the experiment. Parental consent was also obtained from participants under the age of 18 years.

Stimuli

Twenty color stimuli consisting of five hues (red, yellow, green, blue, and purple) and four tones (vivid, bright, soft, and dark), similar to the stimuli in previous research using colored papers [8], were selected for the online experiment. The red/green/blue (RGB) values that most closely represent these colors in standard red/green/blue (sRGB) display mode were used (Table 1). The colors were presented as square spots (0.6 relative spatial units in height and width) on the screen. Two spots with different colors were placed side by side on the screen on a neutral gray background (RGB = 128,128,128). To reduce the number of trials, the two colors were combined into the same hue or tone, resulting in 70 combinations.

Table 1: Stimulus colors used in the online experiment

		Hues				
		Red	Yellow	Green	Blue	Purple
Tones	Vivid	5R 4/14 (188,25,51)	2.5Y 8/12 (248,192,17)	10GY 5/10 (41,140,48)	5PB 4/10 (32,98,163)	5P 4/10 (124,76,146)
	Light	5R 6.5/10 (238,128,124)	2.5Y 8.5/10 (255,207,79)	10GY 7/8 (120,190,112)	5PB 6/8 (111,149,202)	5P 6/8 (168,134,189)
	Soft	5R 6.5/6 (209,143,139)	2.5Y 7.5/6 (216,183,111)	10GY 6.5/5 (128,172,123)	5PB 6.5/5 (140,162,193)	5P 6.5/5 (173,153,186)
	Dark	5R 2.5/6 (102,40,47)	2.5Y 4/6 (121,92,27)	10GY 2.5/5 (28,68,35)	5PB 2.5/5 (37,61,94)	5P 2.5/5 (75,50,86)

Upper values: Hue lightness/saturation values in the Munsell Color System; Lower values (in parentheses): R, G, and B values used to present the upper Munsell colors in sRGB display mode.

Procedure

An online experiment was conducted using the Pavlovia/PsychoPy [9] platform (www.pavlovia.org). The instructions were translated into 14 languages to recruit participants from all over the world. The experiment consisted of 70 trials with different color combinations. Each color appeared seven times during the experiment. The order of presentation of each combination, and the left and right sides on which each color was presented in each pair, were randomized across individuals. In each trial, the participants were required to make a choice by clicking on the spot of a color that appeared warmer than the other color (two-alternative forced choice). There was no time limit for this choice. The inter-trial interval was 1.5 seconds.

Analysis

For each color, the proportion of trials in which the color was selected as the warm color out of seven trials was calculated. First, the analysis was conducted for each individual. Then, averages were calculated for each culture, and the proportion of warmth was represented in a heat map. For cultures with more than 20 participants in each age group (minors: under the age of 18 years; young adults: 19–30 years; senior adults: over the age of 31 years), a group analysis was conducted for each age group. Pearson correlation coefficients were calculated using the proportions of warmth for 20 colors, and similarities in color–temperature correspondence between cultures were examined for each age group.

RESULT AND DISCUSSION

A total of 463 responses were collected from 15 countries. This paper presents results for groups with more than 20 participants, namely, Japan (n = 204, age 21.5 ± 10.1), Thailand (n = 91, age 32.2 ± 21.0), Senegal (n = 35, age 16.9 ± 1.1), and Croatia (n = 32, age 25.6 ± 6.0). Figure 1 shows the heatmaps of the averages of all participants in each group. In all cultures, red and yellow hues tended to be felt as warmer, whereas green, blue, and purple were felt to be colder.

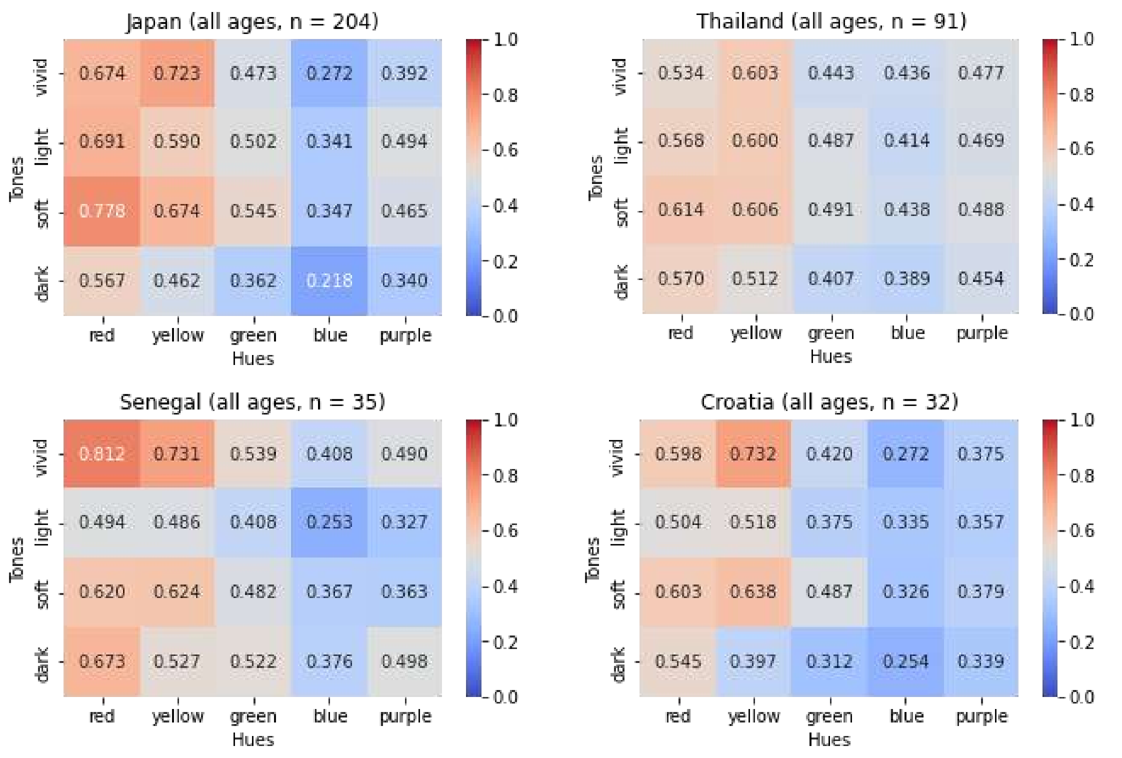

Figure 1. Average heatmap of all participants in Japan, Thailand, Senegal, and Croatia. Color bars represent the proportion of warmth.

Correlation analyses between two cultures revealed a high correlation between any two cultures, as indicated in Table 2.

Table 2: Correlation coefficients between two cultures

	Japan	Thailand	Senegal	Croatia
Japan				
Thailand	0.90			
Senegal	0.64	0.65		
Croatia	0.94	0.90	0.76	

The relatively low correlations between Senegal and other cultures may be because most participants in Senegal were minors.

Since more than 20 individuals in each age group participated in Japan and Thailand, the correlation results between the two cultures for each age group were obtained (Figure 2).

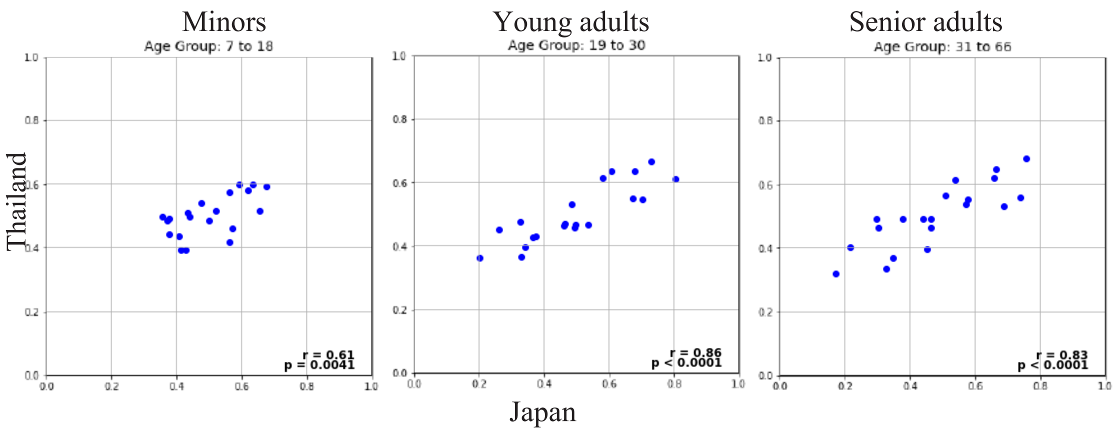

Figure 2. Scatter plots of the proportion of warmth for 20 colors between two cultures (Japan and Thailand) in different age groups

There were significant positive correlations between participants in Japan and Thailand in each age range (minors: $r = 0.61$, $p < 0.01$; young adults: $r = 0.86$, $p < 0.0001$; senior adults: $r = 0.83$, $p < 0.0001$), suggesting that the apparent warmth of color was likely similar between the two cultural backgrounds at any age range. The increase in correlations in adult groups between cultures supports previous findings that strong associations are created through the development of individuals [7, 8]. All age groups of both the Japanese and Thai participants showed a tendency to associate red and yellow hues with warmth. There was an extreme distribution of proportions (red and yellow hues had higher values, while blue had lower values) in the Japanese adult groups compared to the Thai adult groups. This may indicate a strong association between color and temperature in Japanese individuals. However, there may have been bias in the Japanese young adult group, since many of the participants were students from a design school who tend to have an interest in colors.

This study has some limitations. The nature of online surveys with color displays on a digital device makes it difficult to present the same colors to each participant. Furthermore, since each participant is undeniably exposed to contemporary global industrial culture, these factors will inevitably influence the results, and it will be difficult to obtain data from cultures that are less susceptible to Western culture using this method. However, expanding this global survey would provide a better understanding of the correspondence between color and temperature in human life.

CONCLUSION

By examining the association between color and temperature in various cultures and age groups, we revealed ubiquitous trends and some variations among cultures. Variations can be derived from the social environment, which creates a stronger correspondence with age.

ACKNOWLEDGEMENT

We thank Kazuhiko Shibuta, Davor Posavec, and Jean Luc Brunette for their help in recruiting the participants. This work was supported by JSPS KAKENHI (grant number 18K18694) and the NTT-Kyushu University Collaborative Research Program for Fundamental Sciences (to C.H.).

REFERENCES

1. Spence, C. (2020). Temperature-based crossmodal correspondences: Causes and consequences. *Multisensory Research*, *33*(6), 645-682. https://doi.org/10.1163/22134808-20191494.
2. Newhall, S. M. (1941). Warmth and coolness of colors. *The Psychological Record*, *4*(15), 198-212. https://doi.org/10.1007/BF03393246.
3. Wright, B. (1962). The influence of hue, lightness, and saturation on apparent warmth and weight. *The American Journal of Psychology*, *75*(2), 232-241. https://doi.org/10.2307/1419606.
4. Ho, H.-N. (2015). Color-temperature correspondence: Its nature and its impact on object temperature perception. *NTT Technical Review*, *13*.
5. Luo, W., Kramer, R., Kompier, M., Smolders, K., de Kort, Y., & van Marken Lichtenbelt, W. (2023). Effects of correlated color temperature of light on thermal comfort, thermophysiology, and cognitive performance. *Building and Environment*, *231*, 109944. https://doi.org/10.1016/j.buildenv.2022.109944.
6. Tomaselli, K. G. (2001). Blue is hot, red is cold: Doing reverse cultural studies in Africa. Cultural Studies? *Critical Methodologies*, *1*(3), 283-318. https://doi.org/10.1177/153270860100100301.
7. Morgan, G. A., Goodson, F. E., & Jones, T. (1975). Age differences in the associations between felt temperatures and color choices. *The American Journal of Psychology*, *88*(1), 125-130. https://doi.org/10.2307/1421671.
8. Mori Y. & Hiramatsu C. (2019). Color-temperature association in children and adults with various color vision types. *Proceedings of the 5th Asia Color Association Conference*, 313-316.
9. Peirce, J., Gray, J. R., Simpson, S., MacAskill, M., Höchenberger, R., Sogo, H., Kastman, E., & Lindeløv, J. K. (2019). PsychoPy2: Experiments in behavior made easy. *Behavior Research Methods*, *51*(1), 195-203. https://doi.org/10.3758/s13428-018-01193-y.

IMPACT OF COLOUR ON RECOGNITION OF CULTURAL LANDSCAPE IMAGES

Yulia A. Griber[1]* and Galina V. Paramei[2]

[1]*Color Lab, Smolensk State University, Russia.*
[2] *Department of Psychology, Liverpool Hope University, United Kingdom.*

*Corresponding author: Yulia A. Griber, e-mail: y.griber@gmail.com

ABSTRACT

We explored whether colour affects recognition of cultural landscape images. For this, 72 images were used in a matched-to-sample task, whereby the image colour, original or black-and-white, was manipulated in both learning and recognition phases of the task. A total of 154 participants (45 males), aged between 18–66 years (mean = 24.88, SD = 9.28) participated in the experiment. All had normal or corrected-to-normal visual acuity, and none was colour-blind. The images were sourced from the *McGill Calibrated Colour Image Database* and other open access databases. Employed were images of different categories of cultural landscapes: (1) landscape designed and created intentionally by people (garden and parkland landscapes constructed for aesthetic reasons, modern urban and residential areas, industrial landscapes); (2) organically evolved landscapes (cultivated fields, rice terraces, midland and northern villages, historic city panoramas, and historic centres); (3) associative cultural landscapes (sites of memory, places of creativity, sacred sites, and battlefields). The experiment consisted of two phases – the learning and the test. In the learning phase, participants were briefly shown 36 images in a random order. Each of the images was presented for a duration of either 64 ms, or 128 ms, or 300 ms, or 2,000 ms, with a 7-s interval between successive image presentations. Half of the images were presented in colour, the other half in black-and-white. In the test phase that followed directly after the learning phase, presented were the same 36 target images but these were randomly interleaved with 36 distractor images. The participant's task was to indicate whether s/he had seen each image in the learning phase. The test phase was self-paced: each image was exposed until response ("yes" or "no" input using a button). This study used a 2 x 2 design. Half of the images, originally presented in colour, were tested in black-and-white (CB condition), the other half was presented, as originally, in colour (CC). Conversely, half of the images presented in black-and-white in the learning phase, in the test phase were rendered in colour (BC), while the other half was presented, as originally, in black-and-white (BB). Image recognition rate was assessed for each of the four colour mode conditions. As expected, regardless of the landscape category, the recognition rate increased with the duration of the presentation in the learning phase, and even with the shortest exposure (64 ms) the number of correctly recognised target images was quite high. The main finding is that the learning phase image colour facilitated recognition of cultural landscapes in the test phase (conditions CC and CB). Furthermore, the extent of the colour impact depended on the category of the cultural landscape: colour affected greater recognition of images of designed landscapes, but less recognition of organically evolved landscapes. We also found that recognition of images presented in black-and-white in the learning phase was notably lower when these images were rendered in colour in the testing phase (condition BC).

Keywords: colour vision, recognition, memory, cultural landscape, matched-to-sample task

INTRODUCTION

Recent studies demonstrated that colour enhances visual memory for natural scenes [1, 2]. First, it impacts memory by conferring an advantage during encoding and by strengthening the encoding-specificity effect [3]. Colour also has an advantage in retrieval, presumably as the result of an enhanced image representation in memory due to the additional attribute [4]. However, specific role of colour in memory for and recognition of anthropogenic landscapes remains controversial.

In the present study we explored whether and how colour affects recognition of cultural landscape images. According to UNESCO *World Heritage Convention*, cultural landscapes present the "combined works of nature and of man" [5, p. 22]. Cultural landscapes are the result of the evolution of human societies and settlements over time, influenced by physical constraints and opportunities stipulated by the natural environment, as well as by successive social, economic and cultural forces.

Cultural landscapes fall into three main categories, namely [5, p. 22–23]:

(1) landscapes designed and created intentionally by people (garden and parkland landscapes constructed for aesthetic reasons, modern urban and residential areas, industrial landscapes);

(2) organically evolved landscapes, resulting from an initial social, economic or administrative imperative (cultivated fields, rice terraces, midland and northern villages, historic city panoramas, and historic centres);

(3) associative cultural landscapes (sites of memory, places of creativity, sacred sites, and battlefields).

We hypothesised that the impact of colour on recognition of cultural landscapes would be different from that on recognition of natural scenes. Further, we hypothesised that the effect of colour on recognition may differ depending on the type of cultural landscape, as defined in (1)-(3). To test our hypotheses, we conducted an experimental study.

METHODOLOGY

Participants

A total of 154 participants (45 males), aged between 18–66 years (mean = 24.88, SD = 9.28) participated in the experiment. All had normal or corrected-to-normal visual acuity, and none was colour-blind.

Stimuli

We used 72 images in a matched-to-sample task, whereby the image colour, original or black-and-white, was manipulated in both learning and recognition phases of the task. The images were sourced from the *McGill Calibrated Colour Image Database* [6] and other open access databases.

Employed were images of different categories of cultural landscapes: (1) designed, (2) organically evolved, and (3) associative (Fig. 1).

The images were down-sampled to a resolution of 1024 x 768 pixels. For image presentation, a 32-inch Dell S3221QS monitor at 60-Hz vertical refresh rate was used. Participants were seated 80 cm from the monitor.

(1) (2) (3)

Figure 1. Exemplary images from the three different categories of cultural landscapes: (1) designed, (2) organically evolved, and (3) associative

Experimental procedure and design

The experiment consisted of two phases – the learning and the test phases. In the learning phase, participants were briefly shown 36 images in a random order. Each of the images was presented for a duration of either 64 ms, or 128 ms, or 300 ms, or 2,000 ms, with a 7-s interval between successive image presentations. Half of the images were presented in colour (C), the other half in black-and-white (B).

In the test phase that followed directly after the learning phase, presented were the same 36 target images but these were randomly interleaved with 36 distractor images. The participant's task was to indicate whether s/he had seen each image in the learning phase. The test phase was self-paced: each image was exposed until response ("yes" or "no" input using a button).

This study had a 2 (C or B in the learning phase) x 2 (C or B in the test phase) design. Half of the images, originally presented in colour, were tested in black-and-white (CB condition), the other half was presented, as originally, in colour (CC). Conversely, half of the images presented in black-and-white in the learning phase, in the test phase were rendered in colour (BC), while the other half was presented, as originally, in black-and-white (BB) (Fig. 2). Image recognition rate was assessed for each of the four colour mode conditions.

CC

BB

CB

BC

Figure 2. Four colour mode conditions of image presentation: CC (learning and testing in colour), BB (learning and testing in black-and-white), CB (learning in colour and testing in black-and-white), and BC (learning in black-and-white and testing in colour)

RESULTS AND DISCUSSION

Results showed, unsurprisingly, that, regardless of the landscape category, the recognition rate increased with the presentation duration, and even with the shortest exposure (64 ms) the number of correctly recognised target images was quite high. For each of the cultural landscape types (1)-(3), we identified specific recognition pattern; it appeared to be consistent across the exposure durations (Fig. 3).

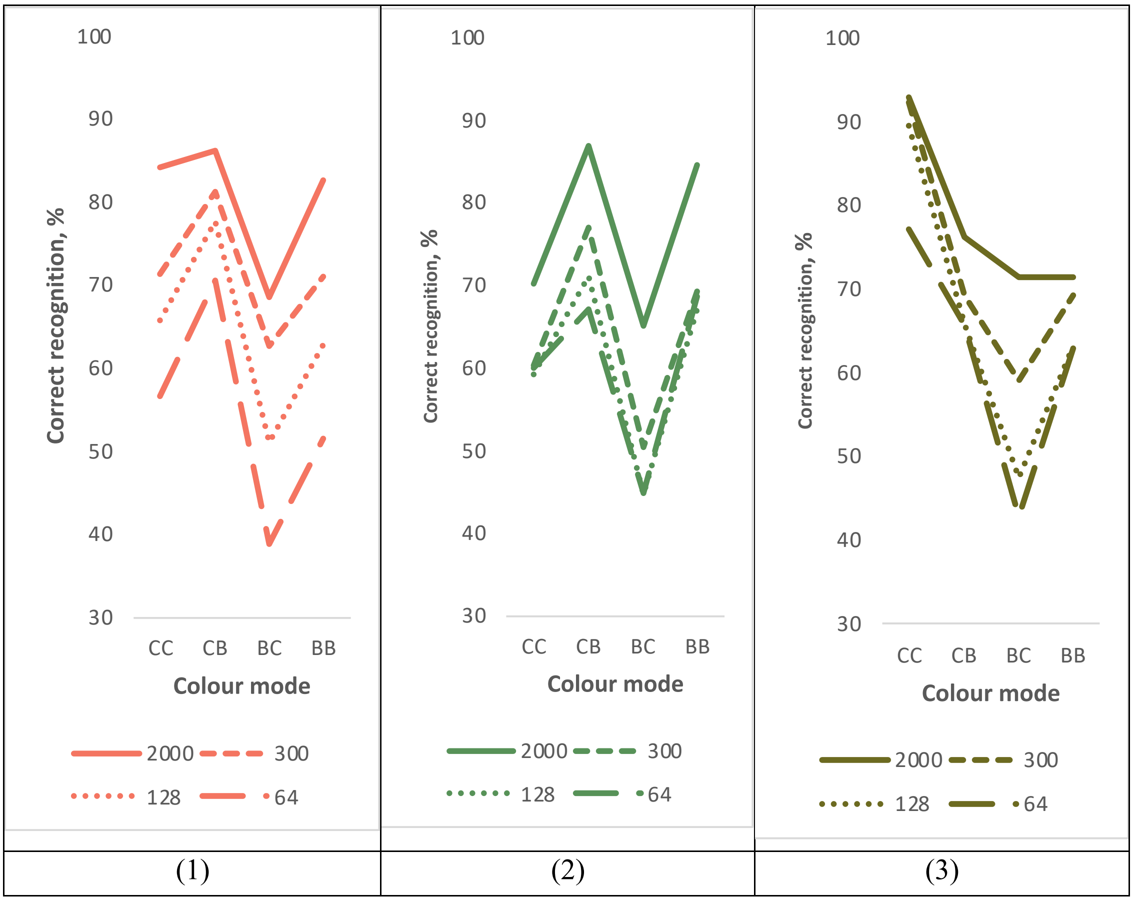

Figure 3. Mean recognition rate (%) for three different categories of cultural landscapes: (1) designed, (2) organically evolved, and (3) associative. Presentation colour mode: CC = learning and testing in colour, BB =learning and testing in black-and-white, CB = learning in colour and testing in black-and-white, and BC = learning in black-and-white and testing in colour

Colour was found to exert the strongest support for recognition of the designed landscapes, when rendered in the learning phase (conditions CC and CB). Colour impact was lesser for recognition of the organically evolved landscapes (conditions CC and CB). For the associative landscapes, the positive impact of colour was observed, in addition, when images presented in black-and-white in the learning phase were rendered in colour in the recognition phase (conditions CC, CB and BC), however only at the longest presentation duration (2000 ms).

Following Gegenfurtner and Rieger [4], we anticipated that a “sensory” advantage of image colour at the encoding stage, in the learning phase, would be manifested by higher recognition rate in the CB compared to the BB condition. Crucially, we also expected a “cognitive” facilitation of colour at the retrieval stage, i.e. higher recognition rate in the CC compared to the CB condition, since colour information, used for encoding in the learning phase (CC condition) cannot be utilised for recognition in the CB condition. Surprisingly, for the designed and organically involved landscapes the recognition rate was higher in the CB condition compared to the CC and BC conditions suggesting that at the retrieval stage rather than having a facilitative effect, colour may impede the process of matching the image representation and the test stimulus.

CONCLUSION

We examined whether the presentation colour mode of cultural landscape images, in colour (C) or black-and-white (B) affects image recognition. Employed were images of three categories of cultural landscapes: designed, ecologically evolved and associative. The presentation colour mode was orthogonally manipulated in the learning and testing phases, constituting four testing conditions: CC, BB, CB, and BC. In addition, in the learning phase image presentation duration was varied: 64 ms, or 128 ms, or 300 ms, or 2,000 ms. In the recognition phase, target images were interleaved with the equal number of distractor images. Recognition rate was assessed for each landscape category / condition.

As expected, regardless of the landscape category, recognition rate increased with the duration of the image presentation; and even with the shortest exposure (64 ms) the number of correctly recognised target images was quite high. One of the main findings is the "colour encoding effect": rendering images in colour in the learning phase (conditions CC and CB) facilitated recognition of cultural landscapes in the test phase, compared to conditions BC or BB. Furthermore, the extent of the colour impact depended on the category of the cultural landscape: colour affected greater recognition of images of designed landscapes and less recognition of organically evolved landscapes. An unexpected finding was that recognition of images presented in black-and-white in the learning phase was notably lower when these images were rendered in colour in the testing phase (condition BC) hinting that at the retrieval stage colour may impede the process of matching the image representation and the test stimulus.

ACKNOWLEDGEMENTS

The authors would like to thank Alexey Delov for developing the online platform of the experiment. Support of Karina Zygankova, Alena Nankiewicz, and Grigory Elkind in data collection is gratefully appreciated. The project was supported by the Russian Science Foundation (grant No. 22-18-00407; https://rscf.ru/en/project/22-18-00407/).

REFERENCES

1. Suzuki, K., & Takahashi, R. (1997). Effectiveness of color in picture recognition memory. *Japanese Psychological Research, 39*(1), 25–32. https://doi.org/10.1111/1468-5884.00033
2. Wichmann, F. A., Sharpe, L. T., & Gegenfurtner, K. R. (2002). The contributions of color to recognition memory for natural scenes. *Journal of Experimental Psychology: Learning, Memory, and Cognition*, *28*(3), 509–520. https://doi.org/10.1037/0278-7393.28.3.509
3. Spence, I., Wong, P., Rusan, M., & Rastegar, N. (2006). How color enhances visual memory for natural scenes. *Psychological Science, 17*(1), 1–6. https://doi.org/10.1111/j.1467-9280.2005.01656.x
4. Gegenfurtner, K. R., & Rieger, J. (2000). Sensory and cognitive contributions of color to the recognition of natural scenes. *Current Biology, 10*(13), 805–808. https://doi.org/10.1016/S0960-9822(00)00563-7
5. *Operational Guidelines for the Implementation of the World Heritage Convention* (2021). Paris: UNESCO. https://whc.unesco.org/document/190976
6. Olmos, A., & Kingdom, F. A. A. (2004). *McGill Calibrated Colour Image Database*. Retrieved from http://tabby.vision.mcgill.ca

APPEARANCE OF FLUORENCE IN ARCHITECTURAL SPACES: QUANTIFICATION OF THE INFLUENCE OF SIZE AND LUMINANCE GRADIENT

Hidetoshi Noguchi[1]* and Nozomu Yoshizawa[1]

[1]*Faculty of Science and Technology, Department of Architecture, Tokyo University of Science, Japan.*

*Corresponding author: Hidetoshi Noguchi, hidetoshi480124@gmail.com

ABSTRACT

Light occasionally appears as a phenomenon in architectural spaces and it can change the impression of space dramatically. Although many of these phenomena can be defined and characterized by the modes of colour appearance classified by Katz (1935) [1], some ambiguous phenomena have not yet been fully quantified. This study deals with one such phenomenon, fluorence, which was defined by Evans (1959) as "the colors appear brighter than the white surround "and "colors before the surface mode of color perception changed to the illuminant mode" [2]. Such phenomena are sometimes used as a spatial design technique, but currently it depends largely on the designer's ability. By quantifying factors related to fluorence, it is possible to deliberately manifest the phenomenon in space. This study examined the effects of the size and luminance gradient of the surface on representation. Images of different sizes, luminance gradients, and maximum luminances of the target were displayed, each of them has three, four, and eight levels, respectively. Participants were asked to evaluate the impression of the target in the process of changing modes of colour by increasing or decreasing the target luminance, keeping the luminance gradient and the size constant. The evaluations were conducted when participants perceived changes in mode and when the average luminance of the target surface was at its lowest and highest. The results showed that the smaller the luminance gradient and the gentler and more fluid the edges appeared, the more easily fluorence appeared. It was also observed that the larger the target was, the more easily it appeared to be flourence. Participants got an ambiguous impression from the fluorence mode. In future, we will continue to clarify the effect the size of the target for the flourence appearance under more various circumstances, and the applicability of these results in real space will be explored.

Keywords: fluorence, the mode of colour appearance, luminance gradient, area

INTRODUCTION

Light occasionally emerges as a phenomenon in architectural spaces. Although most phenomena can be defined and characterized by the modes of colour appearance classified by Katz (1935), many phenomena have not yet been fully quantified. This study focused on the phenomena: Fluorence, which was defined by Evans (1959) as "the colors appear brighter than the white surround "and "colors before the surface mode of color perception changed to the illuminant mode". One of the remarkable examples of fluorence in architecture is the bare concrete ceiling of the Kimbell Art Museum, which appears as though it shines in silver and gives a warm and soft impression to the galleries as shown in Figure 1. Clarifying the mechanism of this phenomenon would enables architects and lighting designers to reproduce such kind of marvellous spaces more easily and intentionally. In previous studies, Gilchrist discovered that fluorence emerges when the luminance of the target surface is 1.7 times higher than that of the surface perceived as white [3]. In this study, this luminance ratio is referred to as the "luminance ratio G". It can be calculated by the formula expressed in Equation 1, based on the anchoring theory of lightness perception [4]. Fluorence basically emerges during the transition from surface colour mode to luminosity mode (self-luminous appearance). Nakamura et al. listed four factors related to the appearance of luminosity: brightness of the surroundings, size of the object, edges around the object, and texture and material of the object [5]. This study aims to quantify the expression of fluorence by examining it from two perspectives: the size of the visual object and its edges (hereafter referred to as "luminance gradient").

$$=\text{Luminance ratio G} = \frac{Luminance\ of\ the\ target\ surface}{Luminance\ of\ the\ background\ surface} \times \frac{Perceived\ reflectance\ of\ the\ background}{90(\%)} \quad (1)$$

Figure 1. The appearance of fluorence on the ceiling

Source : https://commons.wikimedia.org/wiki/File:Kimbell_Art_Museum_January_2017_2.jpg

METHODOLOGY

The size of the experimental space was 2300 mm in dpeth × 2300 mm in width × 2000 mm in height, and it was covered with a blackout curtain. The images were presented using the Apple Pro Display XDR, which had a resolution of 6016 × 3384 pixels. The observation position was set at three levels: 500, 1000, and 2000 mm from the display surface, with a viewpoint height of 1300 mm. The plan and cross-sectional views of the experimental space are shown in Figure 2.

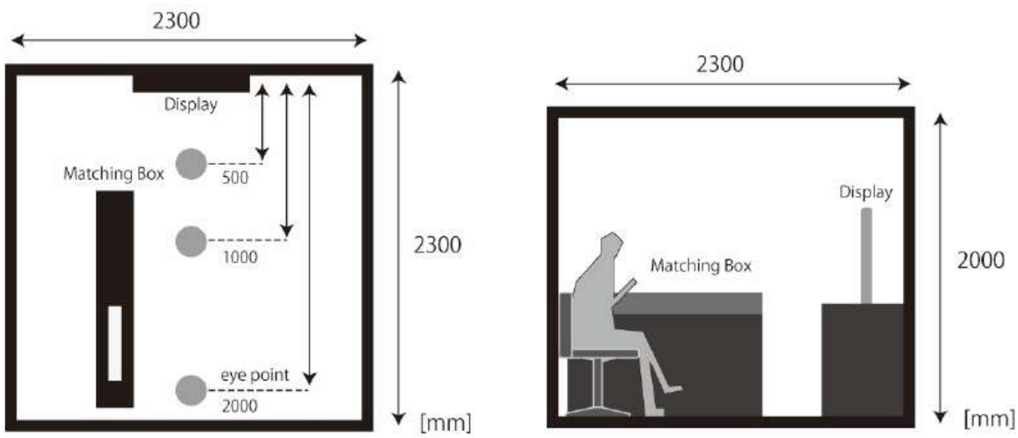

Figure 2. The plan and cross-sectional view of the experimental setup

The image of the object to be observed was created using MATLAB, with four luminance gradient levels and three size levels, for a total of 12 levels as shown in Table 1. Each image had eight maximum luminance levels: 29, 49, 93, 190, 340, 650, 899, and 1242 [cd/m^2]. All background luminance values were set to 3.8 [cd/m^2]. Based on the actual measured diameter defined by the inflection points, three levels of observation distance and three levels of target area yielded a solid angle of nine levels (Table 2).

Table 1: Examples of experimental images

	Size 1	Size 2	Size 3
Luminance gradient 1	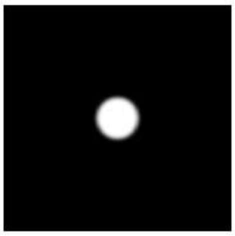		
Luminance gradient 2			
Luminance gradient 3	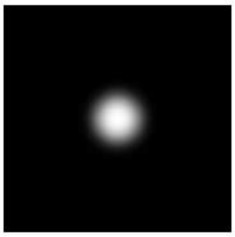		
Luminance gradient 4			
Distance between inflection points	615 pixel	1229 pixel	1845 pixel

Table 2: Levels of solid angle

		Observation distance to the target		
		500 mm	1000 mm	2000 mm
Area of the target	3959 mm^2	0.0158 sr	0.0026 sr	0.0004 sr
	16061 mm^2	0.0466 sr	0.0168 sr	0.0038 sr
	35968 mm^2	0.0678 sr	0.0369 sr	0.0089 sr

Method

A participant adapted to the lighting environment in a dark room for 10 min. Figure 3 presents the flow of the evaluation. After the adaptation, the target with the lowest luminance (surface colour mode) was displayed and evaluated. Subsequently, the target luminance was increased step by step. When the participant perceived change in the mode of colour appearance to fluorence, he/she signaled to the experimenter, and evaluated the target. Next, the image was changed to the highest luminance condition (luminosity mode) and the participant evaluated the target again. Then the target luminance was decreased step by step, and the participant were asked to evaluate it when he/she perceived change in the mode of colour appearance to fluorence. There were four evaluations in total under one condition. Three evaluation items were size perception, impression, and lightness matching. The magnitude estimation (ME) method was used to evaluate the size perception. A reference image with the highest luminance and the same distance between the inflection points was presented, and the participant evaluated the perceived size of the target in positive integer compared with this reference. The impression of the target surface was assessed on seven-point scales. For lightness matching, the participant was asked to evaluate the lightness (whiteness - blackness) of the background surface compared with the grayscale of Munsell chips mounted onto a white board in a matching box. The participants were asked to evaluate 36 conditions at three observation distances.

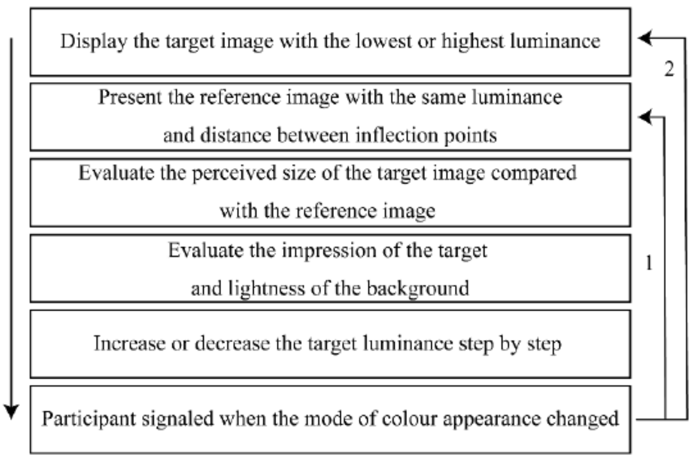

Figure 3: Evaluation Flow

RESULT AND DISCUSSION

Figure 4 shows a line through the centre of the target surface on the measured luminance image. Two inflection points on the line were selected, and the distance between them was taken as the

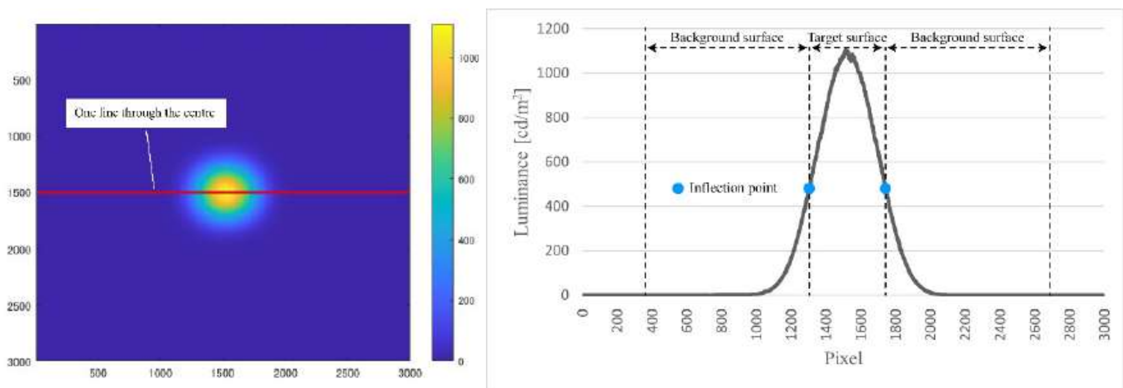

Figure 4. The way to separate the target and background

inflection point distance. In the image, the interior of the circle, whose diameter is the distance between the inflection points, is the target surface and the exterior of the circle is the background surface.

The gradient at the inflection point was considered as the luminance gradient of the condition, and the luminance gradient per viewing angle was calculated. To calculate the luminance ratio G, the luminance averages at each surface were used as the target surface luminance and background surface luminance. The result of lightness matching was converted into the perceived reflectance of the background surface. Figure 5 shows the results of the regression analysis of the luminance ratio G and the luminance gradient, with the partial regression coefficient expressed as RC and the standard error as SE. The luminance ratio G tends to be smaller under conditions with small gradients. This means that fluorence is likely to be expressed under conditions in which the edge around the object is weak and the boundary is ambiguous.

Next, image sizes were examined. First, the size of the target surface was represented by a solid angle. The effect on luminance ratio G was examined using the solid angle and luminance gradient as explanatory variables. The results showed that the effect of the solid angle was statistically insignificant as shown in Figure 6. In Figure 7, the area and luminance gradient of the target surface were used as explanatory variables and the luminance ratio G as the objective variable. The results showed that the luminance ratio G was influenced by the area, and that the luminance ratio G tended to be smaller for images with a larger area.

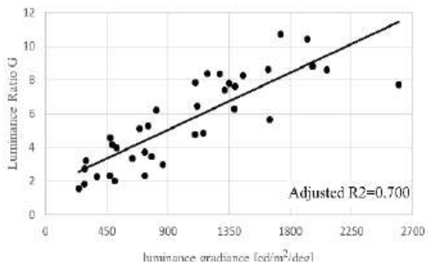

	RC	SE	t - value	p - value
Intercept	1.63	0.493	3.31	0.0022
Luminance gradient	0.000378	0.000416	9.090	<0.0001

Figure 5. Simple regression analysis

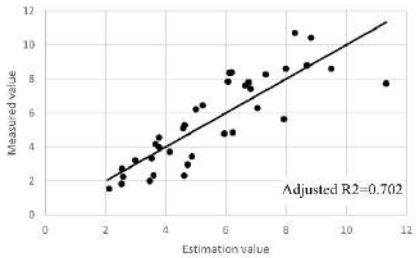

	RC	SE	t - value	p - value
Intercept	2.12	0.656	3.23	0.0028
Luminance gradient	0.00360	0.0004447	8.04	<0.0001
Solid angle	-13.0	11.7	-1.11	0.276

Figure 6. Multiple regression analysis : Solid angle

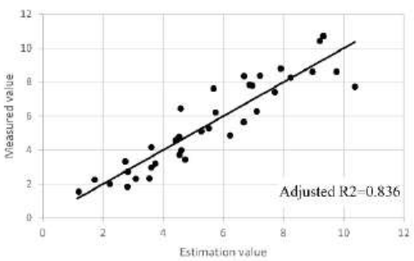

	RC	SE	t - value	p - value
Intercept	2.87	0.430	6.66	<0.0001
Luminance gradient	0.00390	0.0004447	12.7	<0.0001
Area	-7.27e^{-5}	1.35e^{-5}	-5.40	<0.0001

Figure 7. Multiple regression analysis : Area

In the impression evaluation, the participants were asked to evaluate the image on a seven-point scale regarding softness and fluidity. The evaluation results are graphed in order of the mode of colour appearance to see what impression each mode gives. Surface colour and luminosity are abbreviated to S and IL respectively, and fluorence evaluated when the target luminance was increased is FL(S) and the one when the luminance was decreased is FL(IL). According to Figure 8 and 9, surface colour brought harder and stabler impression. On the other hand, luminosity gave us soft and fluid impression. Fluorence appears in the transition process between these two modes of colour appearance, and gave us an impression that was just between surface colour and luminosity. The impression of the fluorence was distributed around more intermediate numbers on the evaluation axes, indicating that fluorence has more ambiguous appearances.

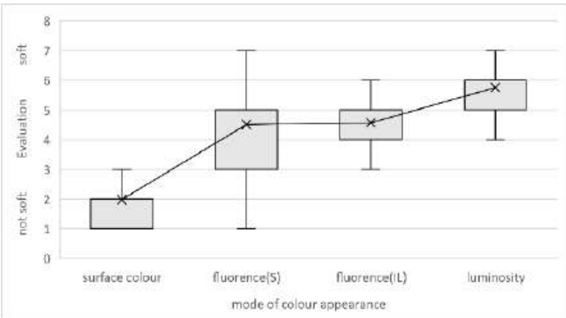

Figure 8. Softness evaluation

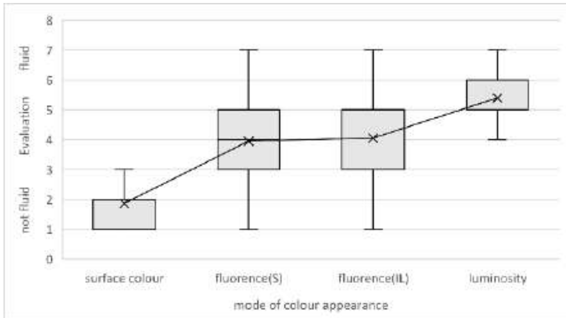

Figure 9. Fluidity evaluation

CONCLUSION

In this study, the quantitative factors of the fluorence appearance were examined in terms of the luminance gradient and size of the target. The results showed that the luminance gradient was significantly related to fluorence. As to the size of the target, its area, not the solid angle, had an influence on the appearance of fluorence mode. The larger the target size is, the more easily the fluorence mode appears. One of the assumed causes is the constant size of the background in this experiment, and there would be the possibility that the participants judged the area of the target compared with this constant background. In the impression evaluation, the gentler the luminance gradient was, the softer and more fluid the impression of the target was. In addition, the answer to the questionnaire tended to be closer to 'neither' or 'ambiguous' when the participants evaluated the fluorence mode. In future, we will continue to clarify the effect the size of the target for the flourence appearance under more various circumstances.

ACKNOWLEDGEMENT

I express my appreciation to Okamura Akane and Nisihanra Shoki for their cooperation.

REFERENCES

1. Katz, D. (1935). Oxford Taylor & Francis Group. *the World of Colour*
2. RALPH M. EVANS (1959) JOURNAL OF THE OPTICAL SOCIETY OF AMERICA. *Fluorescence and Gray Content of Surface Colors, VOLUME 49, NUMBER 11.* doi 10.1364/JOSA.49.001049
3. Gilchrist, A. L. & Bonato, F. (1994) Perception*. The perception of luminosity on different background and in different illumination, 23, 991-1006*. doi:10.1068/p230991.
4. Gilchrist, A. L. & Kossyfidis, C. (1999). Psychological Review. *An Anchoring Theory of Lightness Perception, 106 (4), 795-834*. doi:10.1037//0033-295X.106.4.795.
5. Sugano, S. and Nakamura, Y. (2008). Summaries of technical papers of Annual Meeting Architectural Institute of Japan. D, Environmental engineering: *Analysis of Visual Images Held by Architects: Part2.*

TINTED INTERIOR SPACES WITH THE DAYLIGHT REFLECTING OFF THE OUTSIDE GREENERY

Kaoruko Kitamura[1]*, Kanoko Makino[2], Yuki Oe[2] and Nozomu Yoshizawa[2]

[1]*Dept. of Human Environmental Sciences, Fac. of Human Environmental Sciences, Mukogawa Women's University, Japan.*
[2]*Graduate school of Science and Technology, Faculty of Science and Technology, Tokyo University of Science, Japan.*

*Corresponding author: Kaoruko Kitamura, kitamura@mukogawa-u.ac.jp

ABSTRACT

Faint tints and tones are sometimes perceived in an interior space when the daylight reflected off outside greenery enters via window. Our previous study (2021) suggested that these tints tend to be perceived in the boundaries between the illuminated bright area and the ambient dark area. We hypothesized that this phenomenon is perceived in the process of the Bezold-Brücke shift. This shift is a phenomenon in which the perceived hue changes according to the luminance. Vos (1986) reported that this occurs as a response of cone photoreceptors, suggesting that increasing luminance saturates cone sensitivity and diminishes the perceived colours. We verified this hypothesis to clarify the perception of colour-tinted at various luminance in interior spaces reflecting off the outside greenery.

Colours can be categorized into three types: psychophysical colour, which is the colour under standard illuminant, colour under actual lighting, which is affected by the surrounding lighting, and perceived colour, which is the colour that people see due to the effects of adaptation and contrast. We conducted subjective experiments using a model combined an interior space with an outside space. The interior space was an achromatic cube of 360 mm square with a reflectance of eighty six percent. A window was installed in six conditions: upper wall, middle wall, and lower wall, and its aperture ratio of ten percent and three percent. The outside space was a hemispherical dome with a reflectance of ninety four percent, in which the diffused light from D65 was set under two conditions: the average luminance of 830 cd/m2 and 415 cd/m2. To examine the effect of greenery, green turf or a black board was laid on the floor in the outside space. These conditions were presented to observers, and the colour-tinted in the interior space was evaluated. The observer adapted to 10 lx for 10 minutes, then observed the interior space through the peephole for 1 minute and recorded the tinted areas and the perceived colours. Fourteen observers with normal colour vision were randomly conditioned. The adapted colours of each observer were measured during the evaluation.

As a result, in the 154 evaluations, 125 tinted areas were selected, and its perceived colour ranged of u': 0.1650 - 0.2064 and v': 0.4505 - 0.5061. Forty three percent of areas perceived as strongly tinted were in bright areas directly illuminated through a window and twenty eight percent were in the areas where the luminance gradually decreased. To understand the perception of colour-tinted varied with luminance, the Euclidean distance between the perceived colour and the adapted colour on the u'v' chromaticity diagram (CIE1976UCS) was calculated. The average value of all observers for each condition was defined as Δ Epp. The smaller Δ Epp indicates that the colour-tinted was perceived more faintly. In the conditions with green turf and high average luminance, Δ Epp was small in interior spaces with a window at lower or middle on the wall. That is, even in the areas directly illuminated by light reflected off the outside greenery, tinted colour was decreasingly perceived.

Keywords: Colour Appearance, Colour-tinted, Interior space, Daylight, Greenery

INTRODUCTION

In an interior space with natural light reflected from outdoor greenery through the window, a part of the space may appear coloured. Makino et al. suggested that this coloration is easily perceived at the boundary between the bright area exposed to incident light and the dark area of ambient light in the space [1]. The following three hypotheses can be proposed as the cause of this. The first is the perception of boundary coloration based on the same principle as the Mach bands, the second is the colour perception at a certain angle due to the reflective properties of its interior finish, and the third is the colour perception in a certain luminance range in the process of the Bezold-Brücke phenomenon.

We first tested the first hypothesis. Tsofe et al. suggest that in the Mach band effect on chromatic colors, the color perceived in the boundary changes in the direction of the complementary colour of the stimulus. However, in experiments conducted under the same conditions as in this report, subjects did not perceive a reddish color in response to green-tinted light, thus rejecting that it was a color perception based on this hypothesis [2] [3].

Next, we tested the second hypothesis. In general, light reflected off the surface of a material is divided into an epidermal reflection component and an in-layer reflection component. The epidermal reflecting component is reflected with the same spectral distribution as the light source according to the material surface, and the in-layer reflective component is reflected with the spectral distribution of the material colour. In this hypothesis, when epidermal reflective components are diffusely reflected by unevenness on the material surface, the colour is perceived as whitish than the material colour. Measurements of the reflective directional properties of interior finishes have shown that the epidermal reflective components only affect the intensity of the reflected light and does not cause or reduce colour. Therefore, this hypothesis was also rejected.

Based on the third hypothesis, this study aims to clarify perception mechanism of tinted colour in interior spaces lit through windows from the viewpoint of changes in luminance. The Bezold-Brücke phenomenon is known as a phenomenon in which the perceived hue changes with luminance, and Vos suggests that this phenomenon occurs at the cone level, with an increase in luminance saturating the cone sensitivity and making it perceived whitish [4].

METHODOLOGY

Colours in architectural spaces are classified into three types: psychophysical colour, colour under standard illuminant, and perceived colour [3]. In order, these are the colour of the material surface under a standard illuminant, the colour illuminated by the surrounding light, and the color perceived by humans. In this study, these three colours are used to quantify the perceived colour.

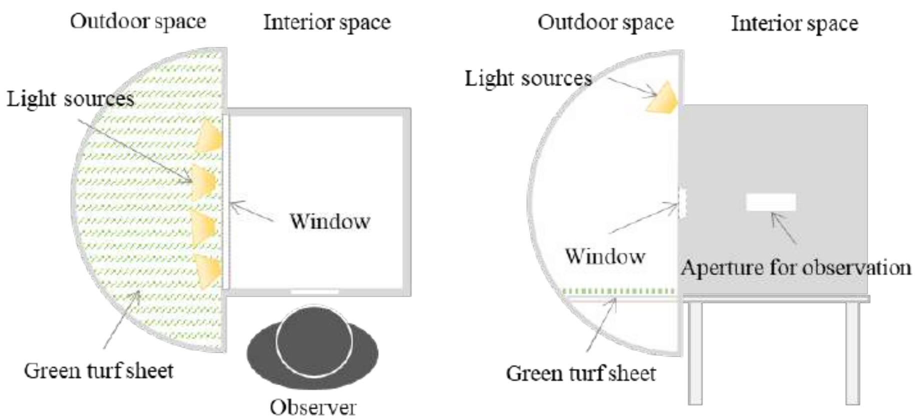

Figure 1. Model used for evaluation (left: plan view, right: cross-section view)

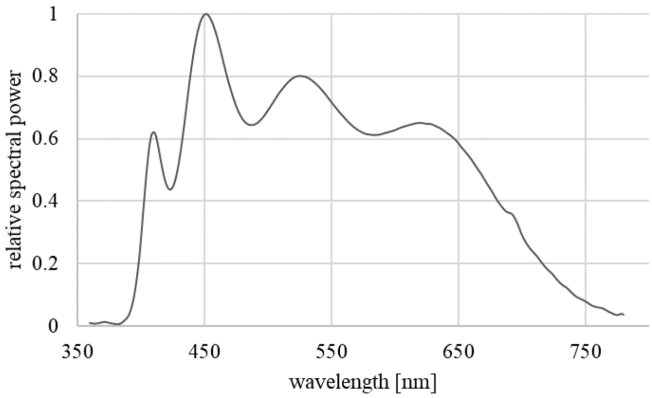

Figure2. Spectral distribution of the light source

To evaluate perceived colour, a model consisting of an interior space (86% reflectance) and an outdoor space (94% reflectance) with an achromatic matte finish was used. The model is shown in Figure 1. The interior space was a cube with an inner dimension of 360 mm, and the outdoor space was a hemisphere, where light from a standard D65 light source installed in the outdoor space was diffused in the hemisphere to simulate skylight, and incident into the interior space through an opening as a window between the two spaces. Figure 2 shows the spectral distribution of the light source.

Table 1 shows the window conditions and the average luminance measured of the interior space under each condition. The position of the window was set under three conditions: the lower part of the wall, the middle of the wall, and the upper part of the wall, and the opening ratio was 3%, 10%, and 100%. The luminance of the outdoor space was approximately 415 cd/m2 and approximately 830 cd/m2, respectively, under two conditions, low and high. To compare the presence or absence of tinted colour, the floor of the outdoor space was changed to green artificial turf or black board under the condition that the window was in the middle of the wall and the opening ratio was 10%. The u'v' chromaticity of light reflected from the green artificial turf was (0.192, 0.482), and the reflectance of the black board was approximately 3.4%. A total of eleven conditions combining these conditions were evaluated the tinted colour that appeared in the interior space.

Table 1. Experimental condition

Outdoor space		Window condition and interior average luminance [cd/m2]				
Floor colour	Luminance level	center	lower	middle	upper	whole
		3%	10%	10%	10%	100%
		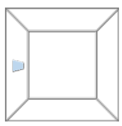	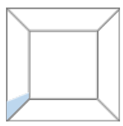	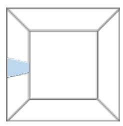	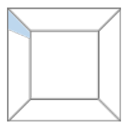	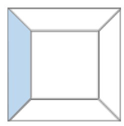
green	low	9.49	14.57	26.42	31.63	-
	high	19.20	30.01	54.40	66.08	426.35
black	low	-	-	24.93	-	-
	high	-	-	51.02	-	-

After adapting to the 10 lx, the observer observed the interior space through a small observation aperture for 1 minute, and recorded the area where the tinted colour was appeared and its perceived colour in multiple answers. The coloured areas were drawn on the answer sheet and the perceived colours were recorded by adjusting the colour scale displayed on a tablet device [3]. The observers were 14 students with normal colour vision, and the order of conditions was random. A spectrophotometer (CL-500A) was used to measure the light in front of the observer's eyes at the time of evaluation, which was determined as the adapted colour. The experiment was conducted on November 24 to December 7, 2022. All responses took a total of two hours per person.

RESULT AND DISCUSSION

As a result of the evaluation, out of a total of 154 evaluations, tinted colour was perceived in 125 cases, with the perceived colours in the range u': 0.1650 - 0.2064 and v': 0.4505 - 0.5061. Figure 3 shows a comparison of the perceived colour in the interior space due to the difference of the floor colour in the outdoor space. The perceived colour is slightly distributed in green, including around white, which is the psychophysical color of the indoor space surface, and the tendency is more so on green artificial grass than on black boards. Therefore, the evaluation method used in this experiment is valid, and the following is discussed.

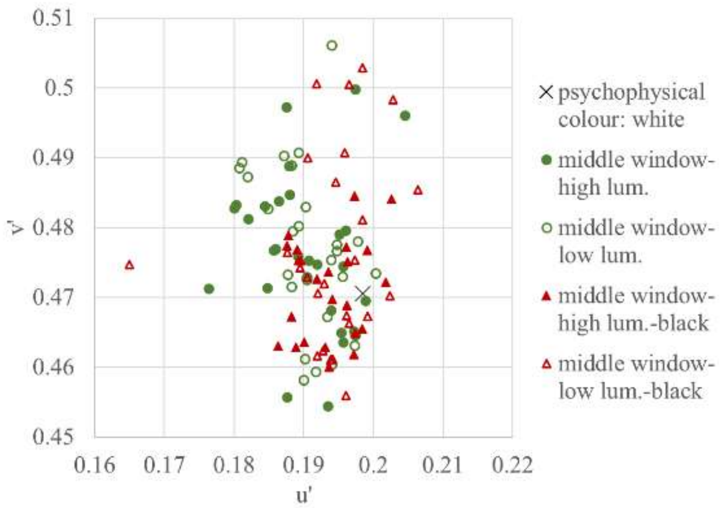

Figure 3. Distribution of perceived colour due to different floor colours in outdoor spaces

Since the perceived colour varies with the environment to which one is adapted at that time, the degree of perceived colour is indicated by the difference between the perceived colour and the adapted colour. The Euclidean distance on the u'v' chromaticity diagram (CIE1976UCS) of the two was determined as the amount of colour perception Δ Epp. The higher this value, the stronger the perception of the tinted colour.

First, Δ Epp was used to determine the adaptation status of observers. The indoor space was divided into areas with relatively high luminance, areas with varying luminance, and areas with low luminance, and the Δ Epp where the strongest colour was perceived, it was smaller in the low luminance area than in the high luminance area under almost all window conditions. In other words, the observers were adapted to the relatively dark ambient light in the interior space as they perceived weaker tinted colour in the low luminance area. In addition, tinted colours were perceived, forty three percent were in areas of high luminance and twenty eight percent in areas of varying luminance. Therefore, it was suggested that tinted colours are more likely to be perceived when adapting to dark ambient light in a interior space and more likely to be perceived when looking at high luminance areas or varying luminance areas.

The relationship between the average luminance in the interior space and the perceived colour. Figure 4 shows the distribution of the perceived colours by window height. Compared to the case where the window was at the lower part of the wall, the perceived color spread in greenish when the window was higher on the wall. This tendency was particularly pronounced when the interior average luminance was high.

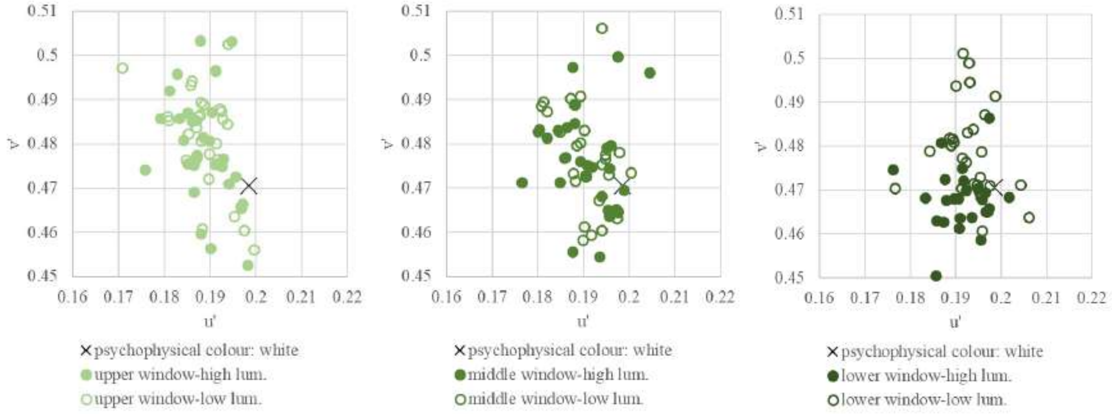

Figure 4. Relationship between window height and the perceived colour

Furthermore, the degree of these colour perception is discussed using Δ Epp, a colour perception quantity that takes adaptation into account. Figure 5 is an arithmetic average of Δ Epp by extracting answers with perceived colours at the same area and comparing the difference in interior average luminance for each window position. Although there was no significant difference, Δ Epp tended to be smaller at higher average luminance for the same window height. In addition, Δ Epp increased with as the window position increased. In other words, it can be said that the intensity of tinted colour perception weakens as the interior average luminance increases, resulting in a whitish perception.

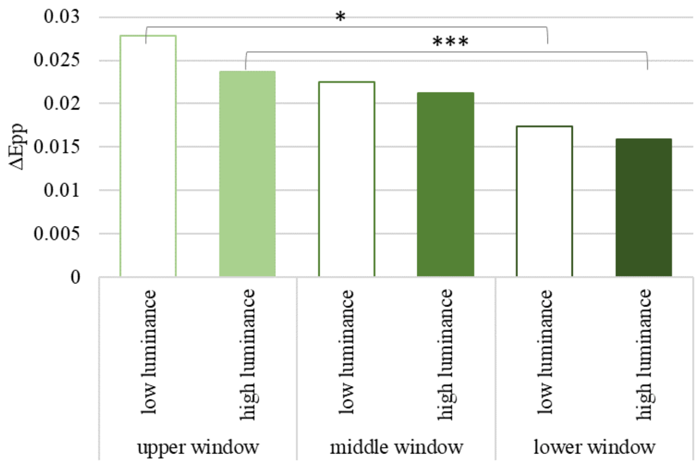

Figure 5. Relationship between interior average luminance and Δ Epp

These results are compared with the Vos graph in Figure 6. It can be seen that as the window position increases, the perceived colour moves away from the whitish range and slightly toward green. As this tendency is observed regardless of interior average luminance, it is difficult to say that the perceived colour becomes weaker and closer to white as the luminance increases. This is consistent with Vos's suggestion that at higher luminance, colour perception saturates and the perceived colour tends towards whitish colour. However, the luminance of the interior space in this study may have been lower than the luminance of the stimulus used by Vos, and it has not been verified that the cone sensitivity is saturated, so further verification is required.

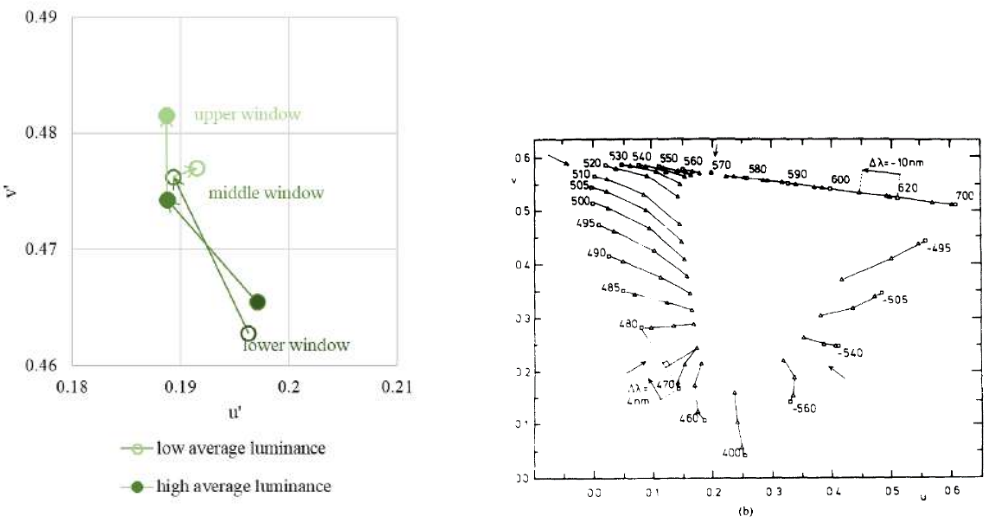

Figure 6. Perceived colour change in this study (left) and Vos's result (right)

CONCLUSION

The phenomenon in which a part of a space with natural light reflected from outdoor greenery is perceived as coloured was investigated from the viewpoint of changes in luminance. Using a model combining outdoor and interior spaces was used to evaluate the tinted colours appearing in the interior space by varying conditions of the window and the interior average luminance, and the results showed that the colour was perceived in areas of relatively high luminance and areas with varying luminance. In addition, in the interior space with the same window position, the tinted colour tended to be perceived slightly weaker when the interior average luminance increased. Future work is needed to analyze and examine in detail the luminance in the areas where tinted colours are perceived in relation to changes in the perception of luminance and perceived colour based on the Bezold-Brücke phenomenon.

REFERENCES

1. Makino, K., Kitamura, K., Tsuda, H., Oe, Y., and Yoshizawa, N. (2021). Colour appearance of a white space with greenish daylight. *Proceedings of the International Colour Association Conference 2021*.
2. Tsofe, A., Spitzer, H., and Einav, S. (2009). Does the chromatic Mach bands effect exist?. *Journal of Vision, 9(6):20*, 1–29.
3. Tsuda, H, Takei, A., Oe, Y., Kitamura, K., and Yoshizawa, N. (2021). An evaluative study on perceived colour measurement method in architecture using tablet devices. *Journal of the International Colour Association, 26*, 49-58.
4. Vos, J. J. (1986) Are unique and invariant hues coupled?. *Vision Res., 26(2)*, 337-342.

APPEARANCE OF OBJECTS SEEN THROUGH COLOURED LOW-E GLASSES: APPLICATION OF AN EDGE DETECTION ALGORITHM FOR VISIBILITY JUDGMENT

Akane Okamura[1]*, Nozomu Yoshizawa[1]*, Yukie Kitadani[2], and Hirotaka Suzuki[3]

[1] *Faculty of Science and Technology, Department of Architecture, Tokyo University of Science, Japan.*
[2] *Building Research Department, Hokkaido Research Organization, Japan.*
[3]*Hokkaido Research Organization, Japan.*

*Corresponding author: Akane Okamura, akane.okamura.222@gmail.com

ABSTRACT

In recent years, the use of low-E glasses in windows has become increasingly popular in terms of the thermal environment. However, their effects on the visibility of outside view (hereafter referred to as "clarity") have not been fully examined yet. The purpose of this study is to investigate the visual clarity of objects through coloured low-E glasses using a neurophysiology-based edge detection algorithm that reproduces human visual information processing. By applying this algorithm to luminance distribution images, we can calculate the intensity of edge perception and predict clarity. We prepared a scale model of indoor space with one window, placed coloured objects on the outside, and captured the luminance distribution of these objects through various coloured low-E glasses using a CCD camera. The model was approximately 300 mm in width and depth, and 200 mm in height, with the opening of the camera lens on the opposite wall of the window. The interior reflectance of the model was set to 70% on the ceiling, 50% on the walls, and 20% on the floor, whereas the outdoor ground reflectance was set to 20%. Two fluorescent lamps (correlated-colour temperature: 6,500 K) were installed above the outdoor space. Seventeen types of double glazing were used as window glasses. They were composed of a combination of two types of glass (3 mm clear single pane and 3 mm low-E glass), with colour tones of green, silver, blue, or bronze. For outdoor objects, we used a Macbeth Colour Checker consisting of 24 colours. They were installed in an outdoor space approximately 1000 mm away from the window. There were patches where the values of ΔC^*, which was the colour difference (CIE 1976 L*a*b* colour space) for each colour patch between the a*b* value without a glass and the one with the double-glazed window with a low-E glass, were more than 10 when blue and bronze glass were used. In particular, we observed a large saturation difference between the reddish colour chart for blue glass and the bluish colour chart for bronze glass. Edge detection algorithms can predict visibility based on luminance, but cannot take chromaticity into account. Therefore, we conclude that the current algorithm can predict visibility based on luminance when using clear, green, and silver glass which do not cause saturation differences in the colour of objects but cannot predict it when using blue and bronze glass which cause large saturation differences.

Keywords: coloured low-E glass, edge detection, window, visibility

INTRODUCTION

In recent years, the use of coloured low-E glasses in windows in living and working spaces has become more popular in terms of the thermal environment. However, their effects on the visibility of the outside view have not yet been fully examined. Based on the recognition that visibility is determined by the luminance and chromaticity of an object, image-processing algorithms that reproduce human visual information processing have been developed in previous studies, making it possible to predict visibility based on luminance information, as shown in Figure 1[1]. However, the current algorithm considers only luminance information and cannot adequately capture the effect of colouration on visibility. It would be an effective method for predicting visibility through glass that does not change the colouration of the object and may be inadequate for predicting visibility through glass that changes the colouration of the object because the effect of chromaticity on visibility also needs to be fully considered. In this study, we first examined the effects of various types of coloured low-E glasses on the colouration of objects through the glass. Based on this information, we aimed to identify the types of tinted low-E glasses for which visibility can be predicted using current clarity prediction algorithms.

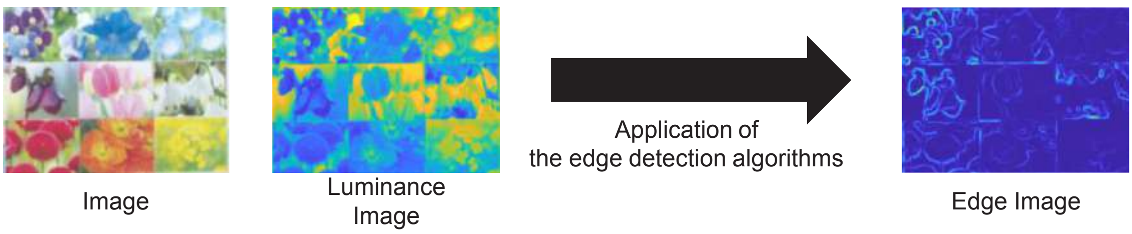

Figure 1. Edge Detection

METHODOLOGY

We prepared a scale model of an indoor space with a window, placed coloured objects outside, and captured the luminance distribution of these objects through various coloured low-E glasses using a CCD camera. The model was approximately 300 mm in width and depth, and 200 mm in height, with the opening of the camera lens on the opposite wall of the window, as shown in Figure 2.

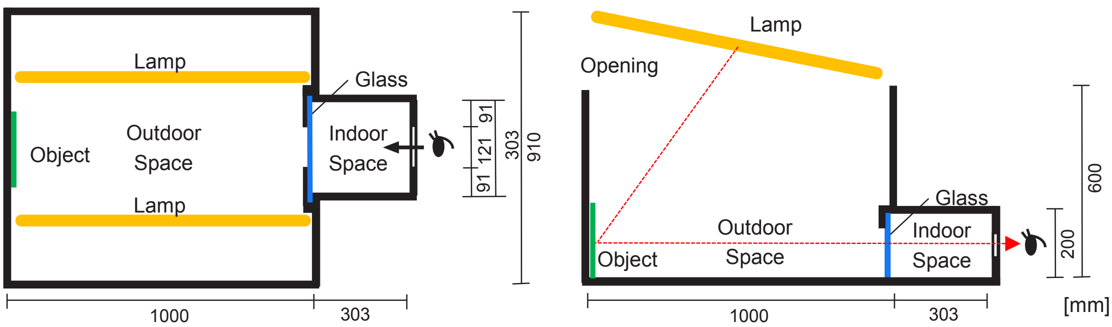

Figure 2. Plan and section of the space

The interior reflectance of the model was set to 70% on the ceiling, 50% on the walls, and 20% on the floor, whereas the outdoor ground reflectance was set to 20%. Two fluorescent lamps (correlated-colour temperature:6,500 K) were installed above the outdoor space. Seventeen types of double glazing were used as window glasses. They were composed of a combination of two types of glass (3 mm clear single pane and 3 mm low-E glass), with colour tones of clear, green, silver, blue, or bronze, as shown in Table 1. The spectral transmittance of each glass sample was measured (Figure 3). A Macbeth Colour Checker consisting of 24 colours was used as the outdoor object and was installed in an outdoor space approximately 1000 mm away from the window.

Table 1: Coloured Low-E Glasses

No.	Glass	Colour	Glass Configuration			Solar Heat Gain Rate	Visible Transmittance	Visible Reflectance	
			Outdoor Glass	Air Layer	Indoor Glass			Inside	Outside
1	Clear1	Clear	Clear 3 mm	6 mm	Clear 3 mm	0.80	82.2%	14.8%	14.8%
2	Clear2		Clear 3 mm	12 mm	Low-E 3 mm	0.59	78.9%	13.3%	12.4%
3	Clear3		Clear 3 mm	12 mm	Low-E 3 mm	0.60	78.7%	13.6%	12.9%
4	Clear4		Low-E 3 mm	12 mm	Clear 3 mm	0.67	75.5%	17.3%	15.9%
5	Clear5		Clear 3 mm	6 mm	Clear 3 mm	0.80	82.4%	15.0%	15.0%
6	Clear6		Low-E 3 mm	6 mm	Clear 3 mm	0.60	77.5%	12.6%	12.1%
7	Clear7		Clear 3 mm	12 mm	Low-E 3 mm	0.62	77.4%	11.1%	11.1%
6	Green1	Green	Low-E 3 mm	12 mm	Clear 3 mm	0.38	72.4%	15.2%	14.3%
7	Green2		Low-E 3 mm	12 mm	Clear 3 mm	0.38	70.6%	13.2%	12.3%
8	Green3		Clear 3 mm	12 mm	Low-E 3 mm	0.47	70.6%	12.3%	13.2%
9	Green4		Low-E 3 mm	6 mm	Clear 3 mm	0.38	68.9%	14.0%	15.6%
10	Silver1	Silver	Clear 3 mm	12 mm	Low-E 3 mm	0.63	72.9%	18.8%	15.8%
11	Silver2		Low-E 3 mm	6 mm	Clear 3 mm	0.54	70.6%	20.3%	16.6%
12	Bronze1	Bronze	Clear 3 mm	12 mm	Low-E 3 mm	0.44	64.9%	22.5%	22.5%
13	Bronze2		Clear	12 mm	Low-E	0.44	64.9%	-	-
14	Blue1	Blue	Low-E 3 mm	12 mm	Clear 3 mm	0.40	61.7%	29.5%	29.5$
15	Blue2		Clear 3 mm	12 mm	Low-E 3 mm	0.45	61.7%	22.2%	22.2%

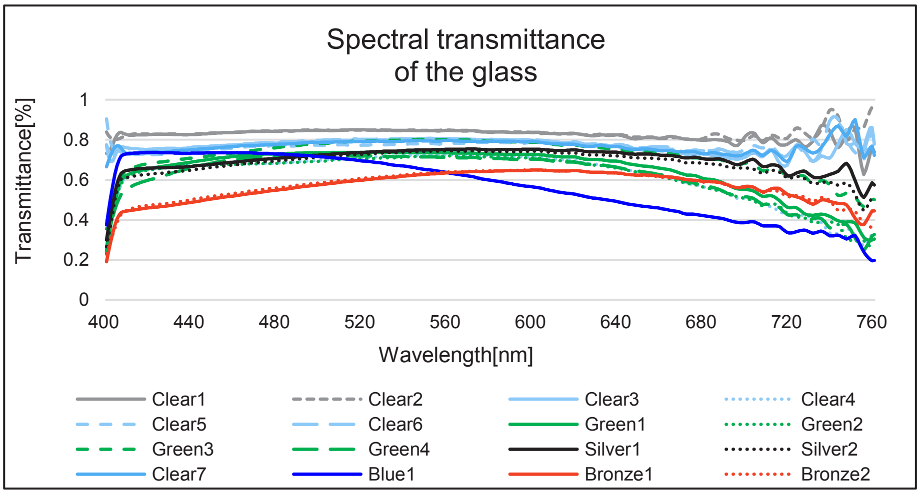

Figure 3. Spectral transmittance data for each glass

RESULT AND DISCUSSION

Chromaticity analysis: Comparing the obtained values for the conditions with and without glass, we calculated the colour difference (ΔE^*_{ab}) and chromaticity difference (ΔC^*) for each colour patch when using each glass (Figure 4). In addition, to represent the difference in chromaticity, we plotted the chromaticity of the patch without glass as black dots and that of the patch with glass as blue dots on the a*b* coordinates (Figure 5). While ΔC^* in all the patches were less than 10 for clear, green, and silver glasses, they were more than 10 in reddish and yellowish patches for blue glasses, and more than 10 in bluish patches for bronze glasses.

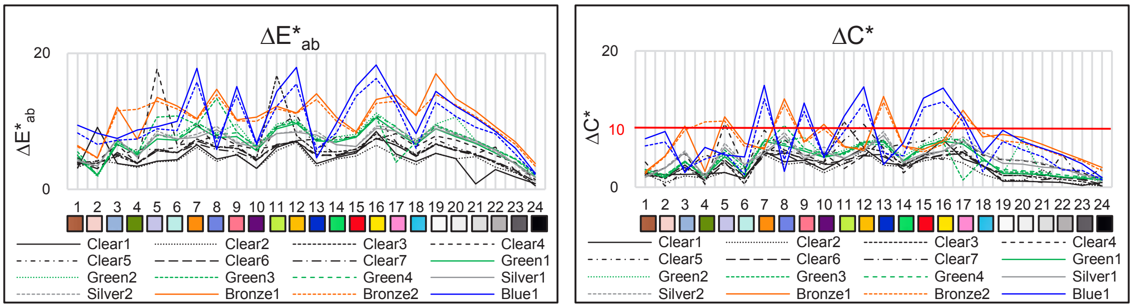

Figure 4. ΔE*a*b and ΔC* for each patch

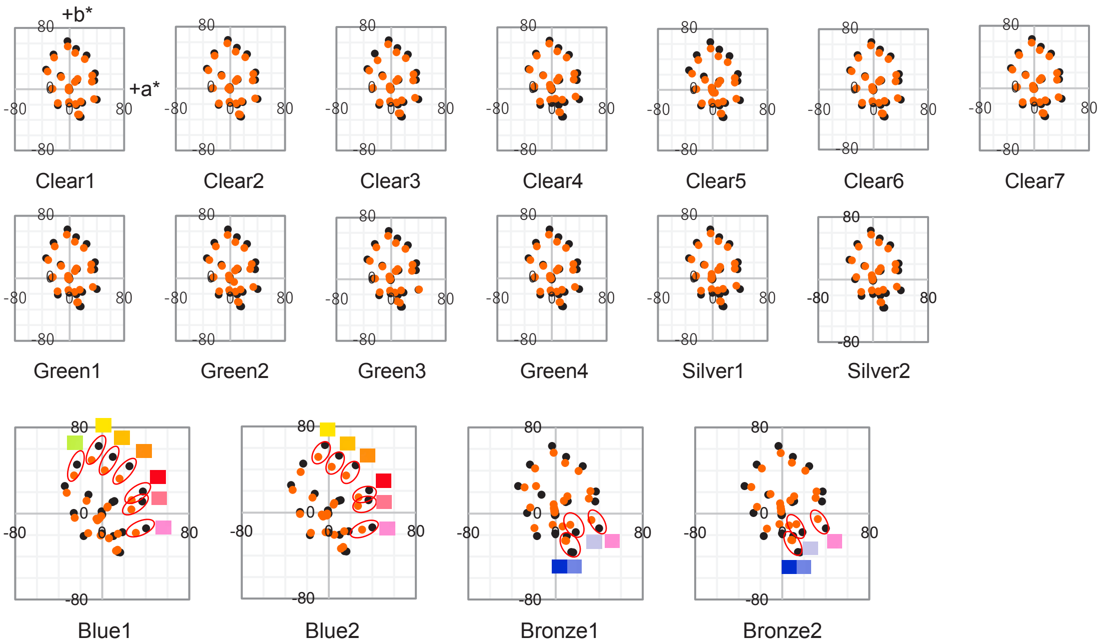

Figure 5. ΔE*a*b and ΔC* for each patch

This result can be explained by the fact that the visibility of a visual object through glass is obtained by multiplying (1) the spectral characteristics of the light source, (2) the spectral reflectance of the object, and (3) the spectral transmittance of the glass. We present an example of a purplish-blue patch with a large saturation difference when bronze glass was used (Figure 6). The figure shows that the saturation of the patches was reduced by using bronze glass. It is considered that this is due to the combination of the blue patch which contains many low-wavelength components, and the bronze glass, which has a low transmittance of low-wavelength components.

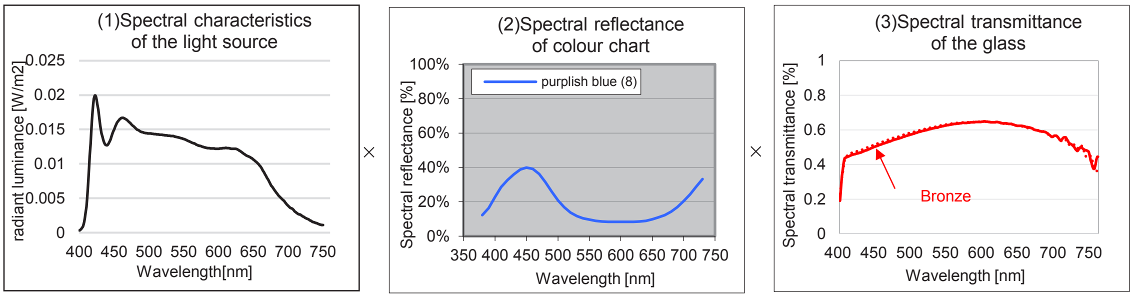

Figure 6. Colour chart of Purplish Blue when using bronze glass

Edge detection analysis: Edge detection is an image processing algorithm that reproduces the flow of human visual information processing [1]. In human vision, the input information is first smoothed in the retina, passes through the lateral geniculate nucleus (LGN), and then, the edge is detected in the primary visual cortex (V1). This algorithm reproduces the flow of processing from the retina to V1 via the LGN and makes it possible to predict visibility based on luminance information by producing edge images from the luminance images (Figure 7).

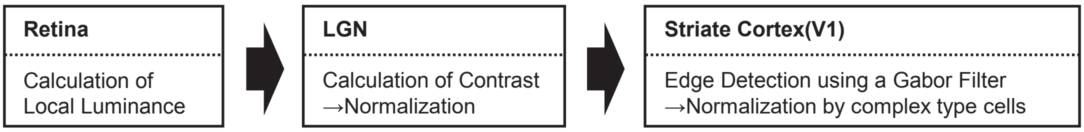

Figure 7. Edge detection algorithm

In this case, as shown in Figure 8, the background of the colour chart is black, and there is a luminance difference between each patch and the background. Therefore, we used an edge detection algorithm and detected the edges created by the luminance difference.

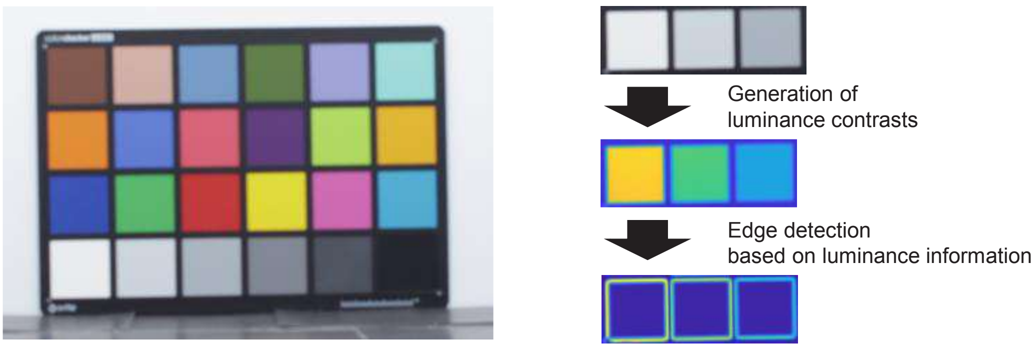

Figure 8. Colour chart of Purplish Blue when using bronze glass

However, since this algorithm does not consider chromaticity information, a current problem with this algorithm is that the calculated edge values cannot account for the impact of chromaticity on visibility. Therefore, we conclude that the current algorithm can predict visibility based on clarity when using clear, green, and silver glasses, which does not cause saturation differences in the colour of objects. However, when using blue and bronze glasses, which cause large saturation differences, it is necessary to consider both clarity and chromaticity, and the current algorithm, which does not consider chromaticity, cannot adequately predict visibility (Figure 9).

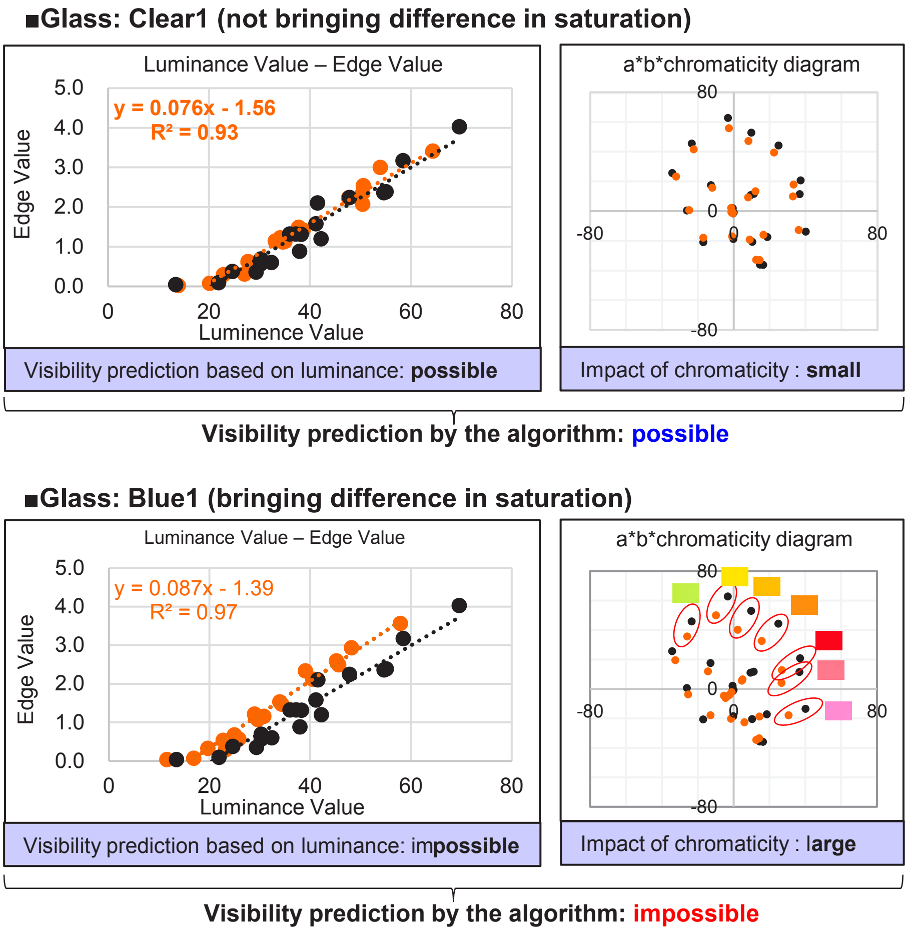

Figure 9. Colour chart of Purplish Blue when using bronze glass

CONCLUSION

In this study, based on the assumption that object visibility is determined by luminance and colour, we confirmed the effect of glass colour on the colour of objects viewed through different coloured glasses and found that visibility could be predicted using the current edge-detection algorithm when using glass that produces a small saturation difference of less than 10. In future studies, we will further verify the effect of colour on visibility through subjective experiments and improve the algorithm.

ACKNOWLEDGEMENT

We conducted this experiment as part of the activities of "General Incorporated Association HEAT20 Society of Hyper- Enhanced insulation and Advanced Technology houses for the next 20 years". Glass samples used in the experiment were kindly provided by Flat glass manufactures association of Japan, YKK AP Inc., and EXCEL SHANON Corporation. We would like to show our greatest appreciation to them.

REFERENCES

1. N Yoshizawa, H Shida, A Neurophysiology-Based Model to Estimate Visibility in Actual Lighting Environment, Proceedings of CIE Conference 2021.

VISUALIZING HEALTH STATUS USING FACE COLOR ANALYSIS AND ITS APPLICATION TO SMART MIRRORS

Tsuyoshi Moriyama[1]* and Nobuhiro Tsunashima[2]

[1]*Dept. of Eng., Tokyo Polytechnic University, 5-45-1 Iiyama-minami, Atsugi, Kanagawa 243-0297 Japan*
[2]*TB-eye Ltd., Kyobashi Edogrand 28F 2-2-1 Kyobashi, Chuo, Tokyo 104-0031, Japan*

*Corresponding author: Tsuyoshi Moriyama, moriyama@t-kougei.ac.jp

ABSTRACT

Economic growth tends to accompany aging problems that require unignorable medical expense on young generation in the society. Such circumstances need preventive medicine in which only the primary prevention that prevents illness from occurring is feasible. Further, preventive care is needed for those who are not interested in maintaining their health or do not want to admit they are in danger in their health even when they are completely ill. Accordingly, non-contact, non-invasive, easy, cheap, and available methods that residents can live as usual even without noticing the existence are mandatory. Face skin color reflects specific wave lengths of illumination depending on the balance of both amounts of blood flowing in artery and vein. That means measuring face color can clarify the heart-beat and also nerve activity that change the balance between artery and vein. Image analysis research on measuring face skin color using ordinary web camera has been prevalent so far, but using PC does not suite the context of preventive medicine because you wouldn't like to start PC for measuring your face every morning. These days, use of smart mirrors (half mirrors) has been proposed for that purpose where the mirror is settled where the residents always go in front of. This paper describes the experimental results of implementation of such image analysis algorithm that can visualize the health status of a person. The input camera images are analyzed to find the location of face and facial components using a statistical image model called the Constrained Local Models (CLM), and the cheek region where the face color is picked is located based on the key points of the facial components. The mean values of face color (red, green, and blue) over time in the cheek region are decomposed into independent components using independent component analysis that consist of the component correlated with flowing-blood of interest and the other image noise. From the fixed range of frequency band of the power spectrum density function of the extracted independent component, a peak correspondent with heart-beat rate is detected. An experiment on the comparison between two conditions of being rested and having an exercise demonstrated the implemented algorithm successfully visualized the difference between those two conditions.

Keywords: AIC2023, Chiang Rai, Thailand (Keywords or brief phrases are appropriate for indexing the article in the following terms: Time news roman, size 10, maximum 5 keywords, separated by commas)

INTRODUCTION

Daily practice of monitoring one's health condition is easy for a very limited population who are extremely industrious and active, otherwise too difficult no matter how well they understand the necessity and the value. In order to make those lazy people take care of their own health, it should never require to do something additionally to daily routine, i.e., cheap, easy, non-contact, non-invasive, non-restraint, and as natural as they do not feel any load. One of the past research activities has suggested to take face images by computer-mounted camera for analyzing skin color changes to detect heart-beat rate [1]. But it requires to turn on the computer every morning that never works for real. A recent trend of using half mirror with sensors such as camera and microphone behind it, which is called "smart mirror", on the other hand, do not force people to do anything special for system startup but to be able to monitor health condition for a mid- or a long-term in life. Such device can also incorporate other information such as temperature, humidity, and news articles, and display the result of analyzing health condition together with headline news on the device. This paper describes the result of a preliminary experiment on analyzing face images captured through a smart mirror to detect heart-beat rate.

OBSERVATION OF HEALTH CONDITION

Camera images are captured through a smart mirror. The skin of a face has multiple layers, i.e., epidermis, dermis, and subcutaneous tissue, and the skin color of a camera image (RGB values) reflects the absorption characteristics of both melanin pigment and hemoglobin pigment that exist in the epidermis under a given condition of illumination and image noise. Heart-beat rate that changes the quantity of hemoglobin pigment periodically is known to reflect blood pressure and breath, emotion in the intensity of each correspondent frequency band. Past research has investigated such methods that analyzes color changes of face image sequence and extracts the signal component which is originated from the quantity changes of hemoglobin pigment using independent component analysis [2][3].

One of other non-intrusive sensors that has been recently drawn public attention than image analysis is a doppler sensor that uses 25GHz band millimeter wave, which is one of active sensors that applied doppler effect. The surface of human chest has both expansion and contraction by both heart-beat and body movement and taking a specific frequency band of the reflection of irradiated 25GHz band millimeter wave can extract only the component of heart-beat. Since it can pass through clothes and bedding due to the characteristics of millimeter wave, it can extract heart-beat under conditions of usual life.

METHODOLOGY WITH AN EXPERIMENTAL RESULT

Figure 1 describes the proposed method of heart-beat rate detection by analyzing face color. A camera attached to the back of a half-mirror, which is called "smart-mirror" in the sense that it is a mirror with a sensor system, captures the face of a person to get face images. As far as a face appears in an image, the position of the face and the contour points of the facial components such as eyes are detected in the image. A cheek region that is defined by surrounding face points gives a set of mean values of RGB channels in each frame of the face image sequence and the temporal series is analyzed by independent component analysis to get the power spectral density

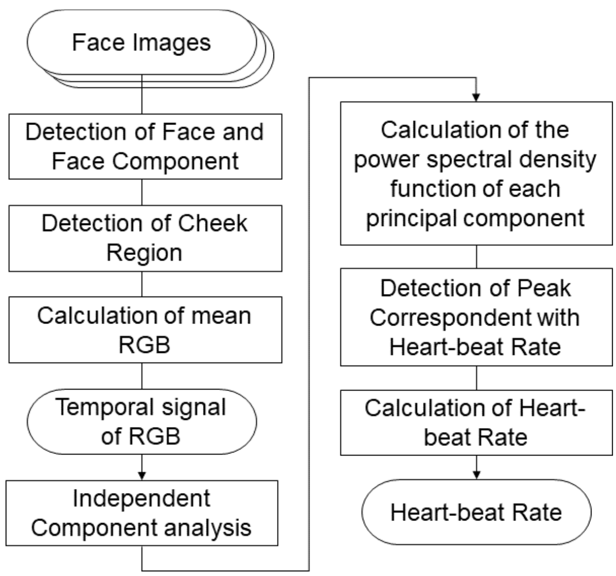

Figure 1. Heart-beat rate detection by analyzing face color

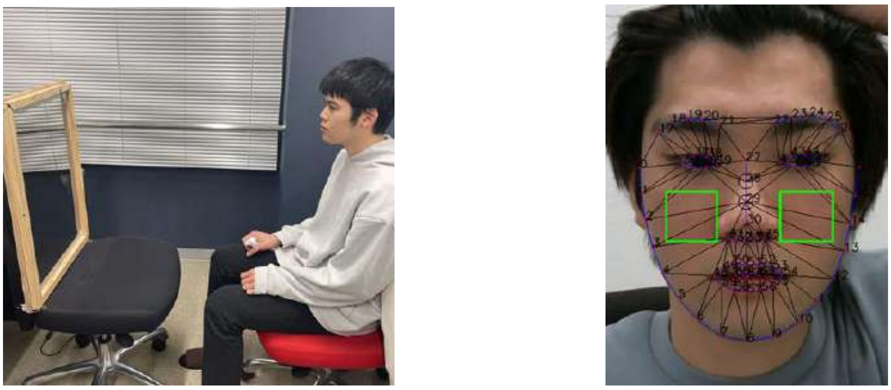

(a) Smart mirror with a camera behind it. (b) Cheek region detection using the coordicates of key points detected on a face image.

Figure 2. An example result of cheek area detection with a smart mirror.

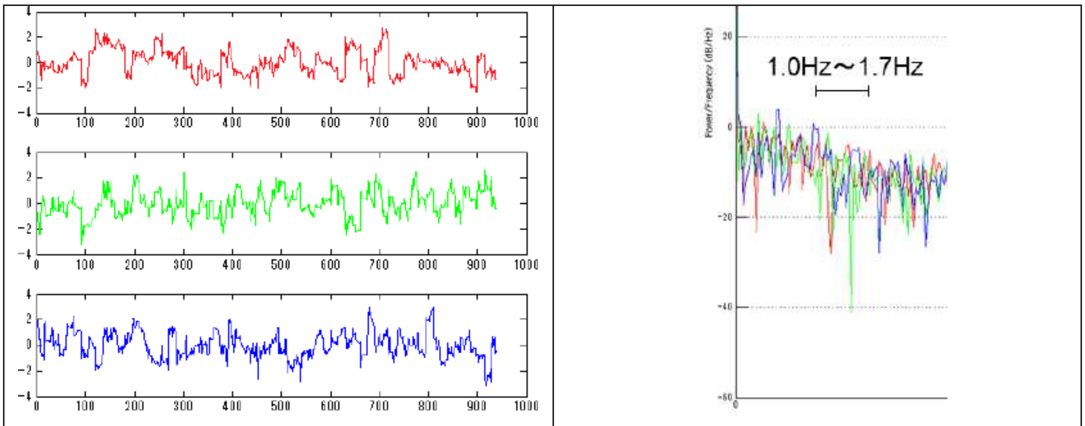

(a) An example of calculated independent components (1st, 2nd, and 3rd from the top).	**(b) An example of power spectral density function and the search interval of peak detection.**

Figure 3. An example result of independent component analysis and peak detection.

function of each principal component. Finally, the spectral peak correspondent with heart-beat rate is detected.

Figure 2(a) shows the scene of a smart mirror with a person in front of it. Figure 2(b) shows an example result of cheek region detection by the method explained in Figure 1. The green rectangles show the cheek regions where mean RGB values are calculated. The temporal sequences of RGB values are individually analyzed by independent component analysis (see the example result in Figure 3(a)). From the power spectral density function of those temporal sequences, feasible peaks are detected in the frequency interval that is correspondent with heart-beat rate (Figure 3(b)). Healthy adults have heart-beat rate at about 60 to 100 times per minute, that is equal to 1.0 to 1.7 Hz in frequency. The third independent component gives the nearest heart-beat rate to the ground truth given by OMRON HCR 7106.

RESULT AND DISCUSSION

Six university students were asked to ride a road bike at 80 rpm for three minutes and to face at a smart mirror for 20 seconds for capturing their face images. The proposed method analyzed the face images to get the third independent component that best fit the ground truth and the correlation coefficient between them reached 0.44.

In addition to face color, a doppler sensor (Calea's non-intrusive vital sensor) shown in Figure 4 detected heart-beat rate at the same time. The absolute values of detected heart-beat

Figure 4. A doppler sensor attached to a road bike that measures heart-beat rate.

rate were not reliable enough, nevertheless the result of measurement showed stepwise increase from the state of rest to that of riding the pedal.

CONCLUSION

We proposed a method of extracting heart-beat rate by analyzing face color that is supposed to be able to install in a scene of usual lives. Future work includes an experiment in living home.

REFERENCES

1. Ming-Zher Poh, Daniel J. McDuff, & Rosalind W. Picard. (2011). Advancements in Noncontact, Multiparameter Physiological Measurements Using a Webcam, *IEEE Transactions on Biomedical Engineering*, *58(1)*.
2. S. L. Fernandes, V. P. Gurupur, N. R. Sunder, N. Arunkumar, & S. Kadry. (2020). A Novel Nonintrusive Decision Support Approach for Heart Rate Measurement. *Pattern Recognition Letters, 139,* 148–156.
3. Z. Guo, Z. J. Wang, & Z. Shen. (2014). Physiological Parameter Monitoring of Drivers Based on Video Data and Independent Vector Analysis. *2014 IEEE International Conference on Acoustics, Speech and Signal Processing (ICASSP)*, 4374-4378, doi: 10.1109/ICASSP.2014.6854428.

THE APPEARANCE CHARACTERISTICS OF THE TEXTILE MATERIAL AND COLOR TINT OF THE *AINU* COSTUME – THE DIFFERENCES BETWEEN THE *ATTUS* OF SAKHALIN AND HOKKAIDO

Chie Muraki Asano*

Sapporo Campus, Hokkaido University of Education, Japan.

*Corresponding author: Chie Muraki Asano, asano.chie@s.hokkyodai.ac.jp

ABSTRACT

The clothing's characteristics were influenced by social, cultural, scientific, and technological factors during its design and production period. Recently, I have been conducting research to analyze the characteristics of costumes worn by the *Ainu* people in the 19th and early 20th centuries. The *Ainu* are an indigenous ethnic minority living in Hokkaido and the Tohoku region of the northern island of Honshu, as well as the Kuril Islands and Sakhalin, which are now part of Russia. Many clothes worn by the *Ainu* people in different regions and periods are now preserved in museum collections, providing significant insight into the basic patterns and designs of *Ainu* costumes, the characteristics of *Attus* woven from fibers of Ulmus laciniata (lobed elm) or lime trees, sometimes mixed with nettle or hemp fibers, the abstracts of textile materials used for clothes, and the methods and roots of acquisition, which have been researched and preserved. Therefore, I have been participating in a research project since 2021 that investigates the historical situation of the northern trading area inhabited by the *Ainu* people and Japanese people in Hokkaido, Tohoku, and Sakhalin. The project references pertinent records and analyses conducted during those time periods. Additionally, a comparative analysis of the costumes worn by the Sakhalin *Ainu*, northern minorities, and Hokkaido *Ainu* has been carried out using costumes preserved in museums in Hokkaido.

In the past, much research has been conducted on the meaning of the unique *Ainu* appliqué and embroidered figure patterns, which are the most distinctive features of *Ainu* costumes, and on the characteristics of embroidery techniques, but in this project I am further classifying and analyzing these systems and relating them to the regions where they were made and the culture of the period that formed the background of their creation. The project is also working on the following. In most cases, when traditional costumes are restored, priority is given to the original forms and images of the costumes. However, it has often been necessary to consider whether the sewing techniques and textile materials used to restore the costume were the same as those used to make the original and whether the same materials were still available at the period. In addition, the item may be so damaged, deformed, or discolored that it is difficult to repair. In other words, the restoration period may include various conditions that existed during the period. This paper is a report mainly focused on the characteristics of material and color tint from the study of detailed observation and analysis of the characteristics of the minute parts, which seem to be restored particularly frequently, of those *Ainu* costumes.

Keywords: Sakhalin *Ainu*, *Ainu* costume, *Attus*, Textile material, Color tint

INTRODUCTION

The clothing's characteristics were influenced by social, cultural, scientific, and technological factors during its design and production period. I have been conducting research to analyze the characteristics of costumes worn by the *Ainu* people in the 19th and early 20th centuries. The *Ainu* are an indigenous ethnic minority living in Hokkaido and the Tohoku region of the northern island of Honshu, as well as the Kuril Islands and Sakhalin, which are now part of Russia. Figure 1 shows the map of each *Ainu* ethnic group's neighborhood and cultural exchange/trading areas. Many of the garments worn by the *Ainu* people in various regions and periods are now housed in museums, where abstracts of the textile materials used for the garments, the methods of acquisition, and the roots of the garments are studied and preserved. Among them are various garments worn by the *Ainu* people, ranging from undergarments to jackets and overgarments. The garments that have been the main subject of research and study as characteristic traditional *Ainu* garments are outer garments with a unique design of embroidered symbolic patterns over sewn appliqué. A few examples are shown in Figure 2. As the figures show, the structure of the garment is constructed linear structure, similar to the kimono of the Japanese, but the garment is unlined garment regardless of season, basically with tubular or mojiri-style sleeves, no Okumi, and a collar with cloth added only around the neck, etc. The name of the garment varies according to the main material of the woven fabric from which it is made. The Hokkaido *Ainu* call the outer garment made mainly of tree bark, such as Ulmus laciniata (lobed elm) and lime tree, *Attus*, while the outer garment made mainly of grass skin, such as stinging nettle and hemp fiber, is usually called Tetarape. The outer garments of the Sakhalin *Ainu* have often been combined with these fibers, and they seem to have been regarded as "garments made of fibers," which is also the meaning of the *Ainu* word "*Attus*. These previous studies have provided important insights into the cultural study of *Ainu* clothing [1][2].

Since 2021, I have been participating in a research project on the historical situation of the *Ainu* people who lived in Hokkaido, Tohoku, and Sakhalin in terms of their relationship with Japanese culture in the northern trading areas. The project will refer to relevant records and analyses conducted during these periods. In addition, a comparative analysis of the costumes of the Sakhalin *Ainu*, the Northern Minorities, and the Hokkaido *Ainu* has been conducted using items of clothing preserved in various museums in Hokkaido.

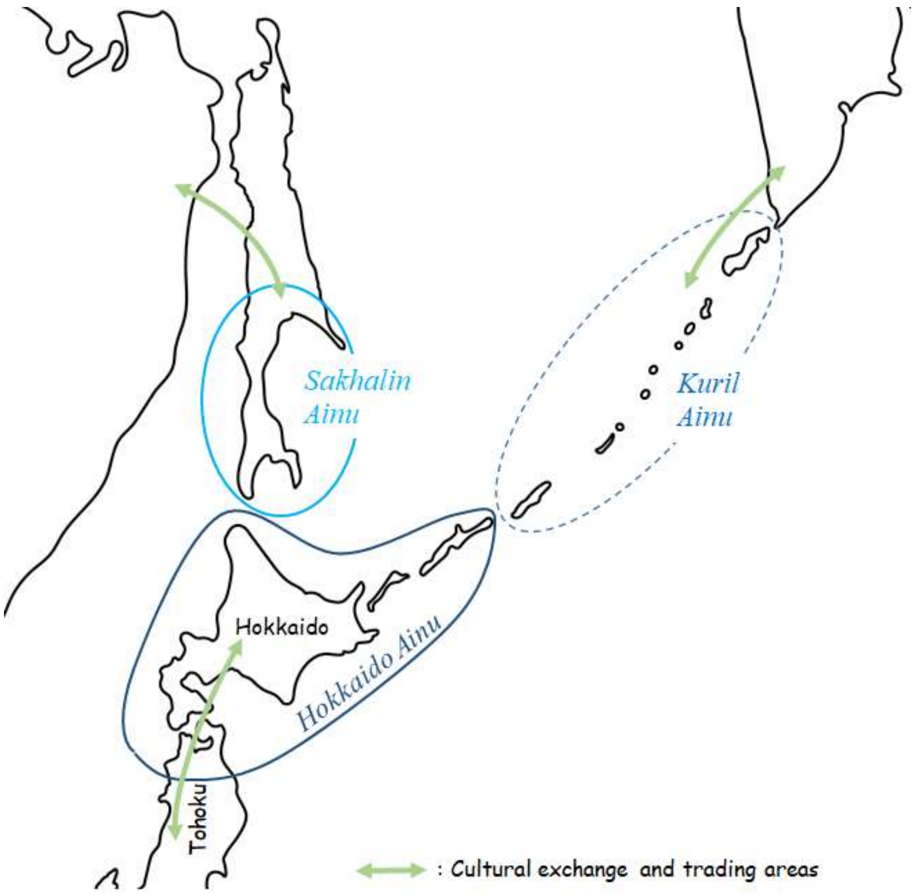

Figure 1: Neighborhood of each *Ainu* ethnic group and cultural exchange/trading areas.

As mentioned above, many studies have been conducted on the meaning of the unique *Ainu* appliqué and embroidery patterns and the characteristics of the embroidery techniques that are the most distinctive features of *Ainu* costumes[3]. In this project, these techniques and design systems are going to be further classified and analyzed within historical time and geographical space axes, and related to the regions where they were produced and the culture of the period that served as the background for their production. Currently, the following analyses have been also carried out.

In most cases, when restoring traditional costumes, the form and image of the original costume are given priority. However, it is often necessary to consider whether the sewing techniques and textile materials used to restore the costume were the same as those used for the original, and whether the same materials were available at the time. In other cases, the item may be so damaged, deformed, or discolored that it is difficult to restore. In other words, the time of restoration may include various circumstances that existed at the time, such as changes in the textile materials available or the introduction of new sewing techniques. This paper reports on a study of such *Ainu* costumes, focusing mainly on the characteristics of materials and color tones, based on detailed observation and analysis of the characteristics of minute parts of such costumes that are thought to have been restored most frequently.

Figure 2: Examples of "*Attus*."
- Left: Sakhalin *Ainu* clothing, Right: Hokkaido *Ainu* clothing

METHOD - INVESTIGATION AND ANALYSIS

In most cases, when traditional garments are restored, priority is given to the original shape and image of the garment. However, it is often difficult to determine whether the sewing techniques and materials used to create the garment can be made exactly the same as the original, due to various factors such as whether the materials are still available today and whether the garment has been damaged, deformed, or discolored to such an extent that it is difficult to restore. In museums and other facilities that require official storage, these changes are stored as part of the history, or restored with as little damage as possible to the original image. However, restorations and repairs made during the period of private storage, transmission, and transmission before being stored in such facilities are considered to reflect the geographical, temporal, and technological background of the time, as well as the purpose of the use of the restored garment. Moreover, since the garment tradition does not necessarily retain the original form of the garment when it was first produced, it can be considered to reflect the background of the period in which the garment was continuously worn, preserved, and passed down.

For this reason, the following procedures were used in this observational survey, which led from a general survey to a detailed survey.

(1) Photograph the entire garment (Figure 2) and analyze the outline of color distribution.

(2) After dividing and enlarging the photographed images, take close-up photographs (Figure 3) of areas requiring detailed observation and analysis, and use the photographs as data for comparing color changes and other aspects.

(3) From the close-up photographs, observe and analyze the parts of the cloth, materials, sewing parts, etc. where changes or alterations are observed, and search for parts that require further detailed observation with a microscope.

(4) Microscopic observation and photography using a digital microscope are conducted on the focused areas (Figure 4).

Figure 3: Examples of close-up photographs of embroidery parts
- Left: Sakhalin *Ainu* clothing, Right: Hokkaido *Ainu* clothing

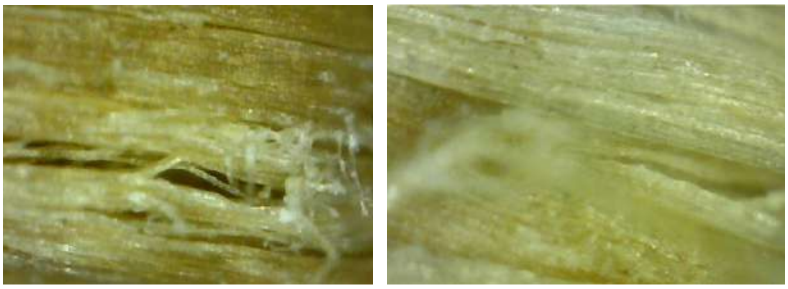

Tree bark fiber Grass skin fiber

Cotton fiber Silk fiber Chemical Fiber

Figure 4: Examples of digital microscope photographs of fibers

(5) For areas that show obvious changes or features, carry out detailed observation and analysis by changing the magnification (Figure 5).

In order to provide further scientific evidence, it is necessary not only to use optical microscopy but also electron microscopy and elemental analysis. However, at the present stage, it is almost impossible to bring such equipment to a museum or other places where costumes are stored. Therefore, in this report, a digital camera with as high a photographic accuracy and resolution as possible was used for close-up photographs, and a digital microscope that can be carried to a museum and yet can capture images with as high a magnification and resolution as possible was used for microscopic observation.

(6) After estimating the fiber type, the color information in the close-up images was corrected, in order to remove the effect of diffuse reflection of light inside the chemical fiber when photographing.

(7) The color distribution of characteristic design areas of Ainu clothing is analyzed using image processing techniques.

Figure 5: Examples of detailed observation and analysis by changing the magnification

RESULT AND DISCUSSION

Microscopic observation revealed that nettle fibers were used in the weaving of the fine parts of the garments and that hemp fibers were also used in the joining threads of the fabric, even though the museum records only indicated the use of halibut fibers. This was done to create a vertical weave pattern by using colored yarns of different fiber types for the body part, which had the effect of changing the color and texture of the garment. This feature was rarely seen in Hokkaido Ainu costumes of the same period.

The original fabric used for the appliquéd parts was a cotton fabric with a high thread density, and cotton fabric was also used for the back collar and sleeve ends, which were probably added after the restoration. Such a combination can be seen in recent Hokkaido Ainu collections, but it is still a somewhat new garment.

Furthermore, the embroidery threads used in the embroidered patterns of the Sakhalin Ainu costumes were silk threads whose colors were brighter than those of cotton threads due to dyeing and whose colors held up better. Therefore, embroidery was done with multi-colored silk threads. In the restored parts of the embroidery, there were some relatively new parts where embroidery threads were added using chemical fibers. However, the embroidery of the Hokkaido Ainu costume was mainly dark indigo-colored cotton thread.

In light of these characteristics, we analyzed the color distribution of a close-up photograph of the collar area (Figure 6), where it is easy to see the balance between the body fabric, the cut-up area, and the embroidered area, by plotting the color distribution on a CIE 1931 xy chromaticity diagram (Figure 7). The results show that the Sakhalin Ainu costume differs from the Hokkaido Ainu costume in terms of coloration and that there are similarities with the costumes of northern ethnic minorities, particularly in the fiber and coloration of the embroidery threads.

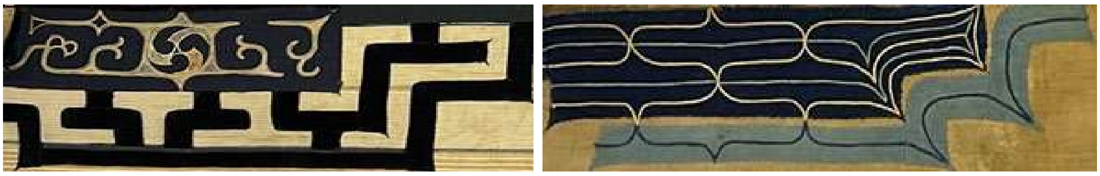

Figure6: Examples of close-up photograph of the collar side area of embroidery parts - Left: Sakhalin *Ainu* clothing, Right: Hokkaido *Ainu* Clothing

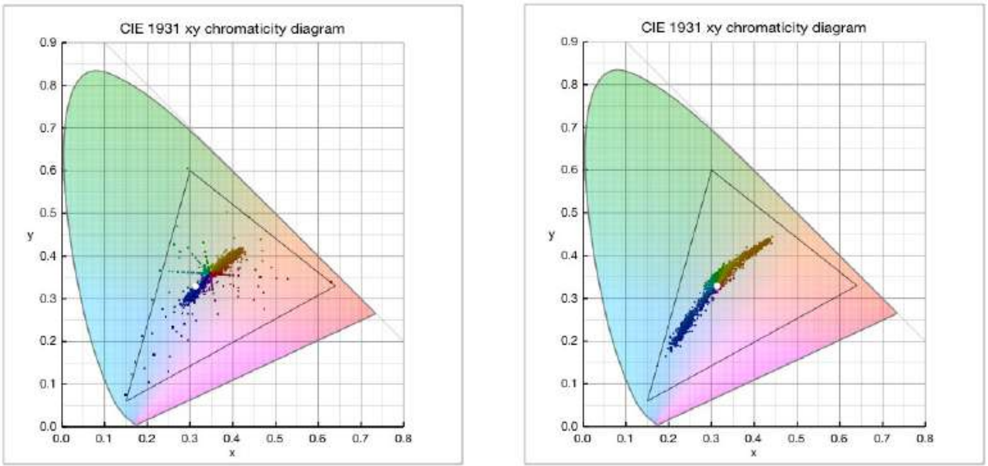

Figure 7: Examples of the color distribution of embroidery parts on the CIE 1931 *xy* chromaticity diagrams
Left: Sakhalin *Ainu* clothing, Right: Hokkaido *Ainu* Clothing

CONCLUSIONS

Cultural anthropology argues that the Sakhalin Ainu, the same Ainu people, have long been in the northern trading area, have more in common with northern minority cultures, and already in the 18th century had characteristics that differed from those of the Hokkaido Ainu. This study was able to demonstrate and argue, using the methods of textile science and clothing science, the elements of the arguing points, even though they are characteristics of minute details. At the same time, I believe that I was able to show that clothing plays an important role in supporting such a theory and how it can be analyzed from the viewpoint of clothing science.

ACKNOWLEDGEMENT

This work was partially financially supported by JSPS KAKENHI Grant Nos. JP19H01386. The authors would like to thank the cooperation of The Asahikawa City Museum, Hakodate City Museum of Northern Ethnology, Ishikari Sand Dunes Museum, and Yoichi Regional Fisheries Museum.

REFERENCES

1. Sato, M. (2018). The Tree Bark Clothing and the Grass Skin Clothing of Ainu, Journal of Chiba University Eurasian Society, Vol.20, 203-227.
2. Miyazawa, T. and Ito, N. (2010). An Overview of the Ainu Clothing Materials, the Bulletin of the Faculty of Home Economics, Kyoritsu Women's University, Vol.56, 33-39.
3. Tsuda, M. (2004) "Patterns and Changes in Ainu Clothing" Journal of the Japan Research Association for Textile End-Use, Vol.45, No.12, 893-898.

COLOR NAMING AND CONSTANCY OF 3D TRANSLUCENT OBJECTS

Davit Gigilashvili[1]* and Ana Amirkhanashvili[2]

[1]*Colourlab, Department of Computer Science, NTNU, Norway*
[2]*Literary Georgia, Georgia*

*Corresponding author: Davit Gigilashvili, davit.gigilashvili@ntnu.no

ABSTRACT

A large body of research on color constancy and naming of colors is based on flat homogeneous patches. Even though recent studies highlight the importance of studying color in context of 3D objects and scenes, they usually address opaque objects only, whereas many objects that we interact with in the real world on a daily basis, such as wax, plastic, or various foodstuff, are translucent. Different amounts of light re-emerge from different parts of the translucent object due to thickness and other geometrical variations, which leads to high spatial variation of color in translucent objects. Little is known about how humans name colors of translucent objects and how constant color is when perceived translucency changes due to illumination direction. In this work, we generated images of chromatic translucent objects with a complex 3D shape and conducted color naming and color matching experiments. Color naming was conducted in two unrelated languages - English and Georgian. We found that the color of the translucent object substantially varies across illumination conditions, and the mean color of the object is a poor predictor of the matched color. Observers usually pick lighter and more chromatic colors than the global average. They prioritize specific spatial regions, whose exact manner remains poorly understood. If the background is highly chromatic, it may affect the hue of the translucent object. The change in illumination conditions did not cause a flip in basic categories in color naming, but we observed several curious exceptions when the background was chromatic. Future works should offer more rigorous quantitative modeling of how optical material properties and shape of the translucent object affect its color variation across the shapes and illumination conditions.

Keywords: color naming, color constancy, translucency, material appearance, perception

INTRODUCTION

Color impacts the perception of translucency [1,2], but little is known about whether the opposite is true. Translucency affects color preferences proposedly because translucent stimuli are associated with ripe fruit and sugar [3]. Certain colorimetric and geometric regularities between the part of the background seen in a plain view and through an overlay are necessary to perceive transparency. This has given rise to color transparency research, which is relatively well-studied [4]. However, highly scattering translucent objects that we encounter daily completely occlude the background [5]. While a substantial part of color science is based on flat homogeneous patches, recent studies show that 3D shape information and interaction with gloss and texture improve color constancy [6,7]. Different authors highlight the importance of studying colors not as isolated points but in context of real-world scenes, objects and materials [8,9]. Giesel and Gegenfurtner [10] studied color matching for real objects and found that humans are good at matching hues, chroma gets affected by lightness, and lightness depends on the brightest areas except specular highlights.

Another important research question is color naming, boundaries among color categories and the linguistic communication of colors [11]. The naming differences among languages [12], persons

[13], and their development over time [14] is an active topic of research. However, the research has also mostly been focused on flat homogeneous patches, such as Munsell Sheets of Color [15]. A notable exception is a work by Tanaka *et al.* [16] - however, the work used opaque objects.

Despite advances, the knowledge gaps remain that motivate our research: first, how humans assign representative colors to 3D translucent objects; and second, how constant the color of a translucent object is across different illuminations. Color alone is not enough to convey how objects look, and previous studies show that humans also use gloss- and translucency-related terminology to communicate appearance [17]. High spatial variation of color in translucent objects makes it difficult to quantify it with spot measurements and raises questions about the description of its color [18]. Little is known whether humans can account for shading variations due to the translucency of the object when describing its color (e.g. what would be the color of the objects shown in Figure 1?). Besides, translucency constancy is limited, and illumination geometry significantly affects perceived translucency [5, 19], which on its part may affect color.

To address these questions, we conducted psychophysical experiments. In the first experiment, observers named the color of the overall translucent object; in the second experiment, observers matched the color between a 3D translucent object and a flat homogeneous patch. The objects varied in hue, chromaticity, and degree of translucency, and were placed in different illumination conditions. The objectives of the experiments were to explore: first, how observers assign color names to translucent objects, whether this depends on the degree of translucency and varies across illumination conditions; second, how observers pick the most representative color for the translucent object and whether it can be predicted from global color statistics; third, how constant color of a translucent object is when illumination and geometry change. To the best of our knowledge, this is the first study that investigates color constancy and color naming specifically for 3D translucent objects. Finally, due to the peculiarities of color naming in Georgian and its differences from English [20,21], we decided to conduct naming in two unrelated languages – English (Indo-European) and Georgian (Kartvelian), to analyze the differences between them.

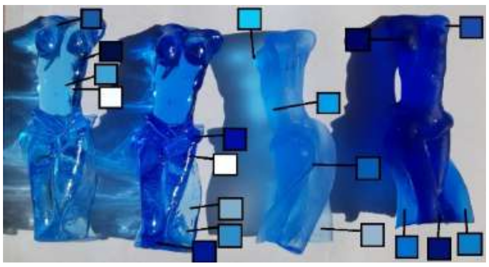

Figure 1. Translucency makes it difficult to measure and describe the color of an object. For instance, which of these point colors best represent the color of the translucent material? The image is reproduced from [22].

METHODOLOGY

Experimental Protocol

We conducted three experiments: Experiment 1 – Color Naming in English, Experiment 1B – Color Naming in Georgian, and Experiment 2 – Color Matching. 48 images of translucent objects were shown one by one. In Experiments 1 and 1B, the observers had to provide a color term in the respective language (English and Georgian). In Experiment 2, both the image and a color picker (implemented with MATLAB's *uisetcolor()*) were displayed. The observers' task was to match a color between the 3D translucent object and a flat homogeneous patch. They were instructed to use the color picker to navigate through the color space and pick one color that best represented the translucent material that the object was made of. They were given unlimited time.

Once they were satisfied with the match, they proceeded to the next image. Experiments 1 and 2 were conducted in the same session with the same observers. Color naming in Georgian was conducted independently from the other two experiments.

Stimuli

We used 48 images of translucent objects that varied in hue, degree of translucency, and illumination. We selected a complex 3D shape – a bust figurine from the *Plastique* [23] collection. It includes both thick and thin parts, has both flat and uneven surfaces, and exhibits a broad range of visual cues to translucency. We used 24 synthetic images rendered with Mitsuba Renderer [24] and 24 photographs of real objects from the *Plastique* [23] collection. We rendered materials in 3 hues (red, green, and magenta) with 2 levels of extinction coefficient in 4 different environments. We used Paul Debevec's [25] *The Grace Cathedral* and *The Uffizi Gallery* light probes for a chromatic background and diffuse natural lighting, respectively, and Bernhard Vogl's [26] light probe *At the Window* rotated to two different angles to produce back-lit and front-lit objects. We selected 6 physical objects: blue, yellow-orange, and white-cream, each with 2 levels of translucency, and photographed them four times: front-lit on white and red backgrounds; under dim diffuse lighting; and back-lit with a strong directional light.

Experimental Conditions

Experiments 1 and 2 were conducted on a calibrated display under controlled conditions in a dark room. The 15.8-inch LCD display with a resolution of 3840×2400 was calibrated using a colorimeter to: white point – D65 (x=0.313; y=0.329); Gamma – 2.2; Luminance – 80 cd/m^2. The distance to the display was 50cm. Color naming in Georgian (1B) was conducted online.

Observers

14 observers, 8 male and 6 female, participated in Experiments 1 and 2 with average age of 33.9. All had normal color vision and visual acuity. They were graduate-level students and faculty members with prior knowledge of color science but were naïve to the purpose of the study. All the observers had a good command of English (only 1 was a native speaker). 17 native Georgian speakers took part in Experiment 1B. The majority had no knowledge related to color science and were naïve to the purpose of the study. Their demographic information was not recorded.

Analysis

For color naming, we conducted frequency analysis to identify how color terms vary across illuminations and materials. For the color matching, we are interested in: (1) how the matched color for a given object changes across illumination conditions – for this purpose, we calculate the mean matched color for each condition; (2) which parts of the 3D translucent object the observers rely on when making the match – for this, we calculated the color difference between the mean matched color and each pixel of the object and illustrated as a heatmap. RGB data was converted to CIELAB (D65 white point), and all calculations were performed in CIELAB.

RESULT AND DISCUSSION

Color Naming

Even though color terms in English reflected changes in lightness of basic terms (e.g. "dark red" versus "red"; 1-2 (A-D) in Figure 4), changes in illumination did not usually lead to crossing the categorical boundaries, except for several specific cases. 6A and 6D (Figure 4) were considered purple, but pink in back-lit conditions (6B, 6C). The boundaries of the basic color categories were crossed when a translucent object was placed on a chromatic red background. The object that was consistently labeled as blue (1E, 1F, 1H), became black on a red background (1G). Similarly, the object in 2E, 2F, and 2H was cyan, and was judged inconsistently on the red background (2G) (described as dark gray, black, blue, dark blue, dark green, petrol, and brown by different observers). The objects in 3-4 (E, F, and H) were labeled as yellow and orange by almost half of the observers each. When they were placed on a red background, the majority considered it orange. The objects shown in 5-6 (E-H) were opaquer and less dependent on the conditions. The trends were similar for Georgian too. The confusing object 2G was also described as black, gray, dark green, dark blue, and brown. However, Georgian observers used a broader vocabulary and more non-basic, composite polylexemic color terms. One noticeable difference between English and Georgian was the abundance of reference to commonly translucent objects and materials, such as wax, candle, milk, condensed milk, honey, caramel, amber, ivory, etc.

Color Matching

The first hypothesis was that observers simply spatially average the color of the entire object. Figure 2 illustrates the average color of the object and the average matched color picked by observers (see all images in Figure 4). The observers systematically overestimate lightness and oftentimes chromaticity (e.g. 1C, 2B, 2C, 6B, 6C etc.) – especially for transmissive back-lit (columns B, C, and F) objects. Figure 3 illustrates that the mean difference among matched colors for a given material across lighting conditions is substantial. The illumination condition has more impact on the color of less opaque objects, which is intuitive (cf. 3-4 (A-D), 3-4 (E-H)). There are several instances where change in hue was also observed: e.g., refer to 1G and 2G. In this case, a translucent object, which appears blue in most conditions, is placed on a red background. The blue object absorbs all the spectrum incident from the red background and appears black.

If the observers do not take the average color, it is interesting to investigate which regions they base their judgments on. In Figure 5 we see all images, respective matched colors, and the heatmaps that illustrate the color difference (ΔE CIE76) between the mean matched color and each individual pixel. Even though the shape was identical, the spatial regions that are closer to observers' judgments vary across materials and illumination conditions. In diffuse natural light (column A), the color differences are more evenly distributed but are smallest for vivid highlights of subsurface scattering (A4, A6). When the object is back-lit, the observers interestingly match thin parts of the dress or a flat torso part instead of a thicker and more geometrically complex waist, which appears darker (B, C, F). When the object is lit from front (D and H), observers are able to discount and ignore specular reflections, which is consistent with the previous research [10]. Under dim light observers mostly match the brightest and thin parts (E2) and avoid shadows that are produced if the object is opaque enough (e.g. waist in E1, stomach in E5-6). Black-looking objects placed on a red background appear more homogeneous, while for others, the matched color is closest to the flat chest area, which is lit directly and has no shadows.

Figure 2. The top row shows the average color of the entire object, while the bottom row shows the matched colors (average). Alphanumeric labels are for reference purposes and will be used throughout the paper.

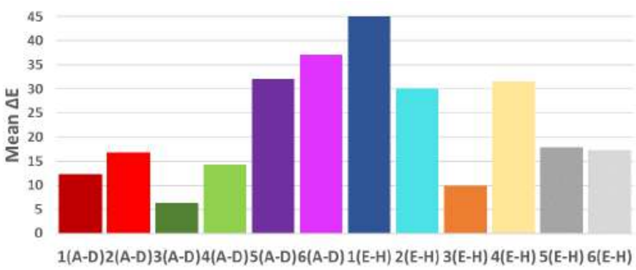

Figure 3. ΔE among matched colors among all conditions for each material.

Discussion

We observed that change in illumination conditions affects the lightness-related label of the color term, but rarely the hue. However, when the background is chromatic, it may still cause to flip hue and cross categorical boundaries – such as, blue becoming black and yellow becoming orange on a red background. This was observed both for English as well as Georgian speakers; however, in Georgian, the reference to translucent objects and materials was abundant. This is

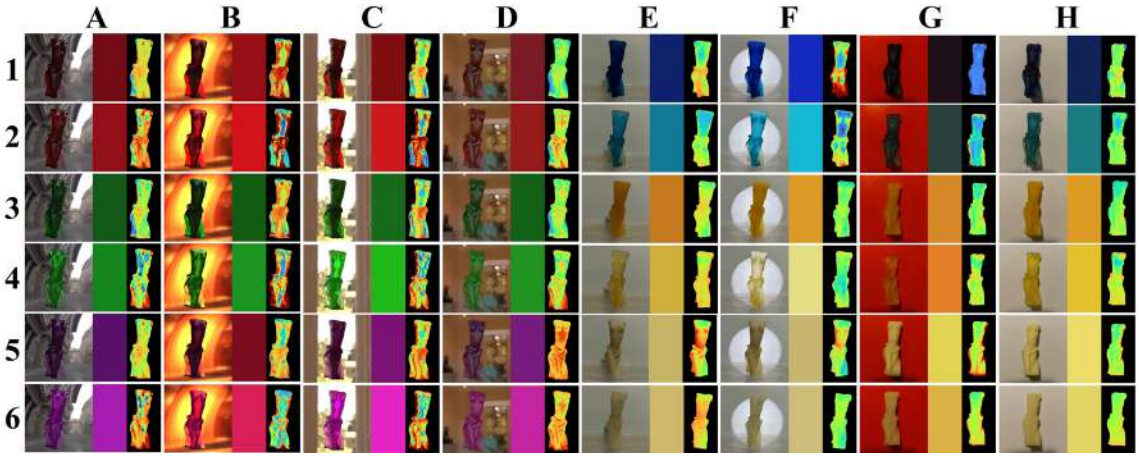

Figure 4. The images with respective matched color and a heatmap, which illustrates differences between matched color and individual pixels (ΔE CIE76). Blue shades correspond to lower color difference, redder shades – to the larger.

an indication that unlike flat homogeneous patches, 3D translucent objects bring material recognition into the color communication. Another explanation is a peculiarity of generating color terms in the Georgian language. Polylexemic composite color terms are broadly used in Georgian. It is very common to produce an intelligible color term by simply putting a noun in the genitive case and adding the suffix *-peri* (lit. "color" in Georgian). Hence, the vocabulary included terms like *tsvilisperi* (color of wax), *rdzisperi* (color of milk) etc. It is also worth mentioning that, unlike English, in the Georgian experiment all participants were native speakers. Future works should include a broader range of colors to measure categorical boundaries among colors, which may be different for translucent objects. Besides, the association between translucent material recognition and color terms certainly merits a future study.

The color constancy of translucent objects seems to be far from perfect. The matched color varies substantially across the conditions, and human observers seemingly do not attempt to discount the effect of light transmission. In comparison with the object's mean color, observers seem to overestimate the lightness and chromaticity. In post-experiment interviews, multiple observers pointed out that thicker parts look "too dark" and are avoided, and that they prefer flat areas. Coincidently, the thickest area near the waist is also geometrically most complex, which produces sharp shadows if the object is opaque enough. Discounting shadows could be an additional explanation of why observers overestimate lightness. Hue shift can be striking where the background is highly chromatic. Future works should provide more rigorous modeling to predict color inconstancy by object's shape and subsurface scattering properties, as well as the illuminant's spectral power distribution and geometry. Our object included areas that were thin enough for the light to shine through. The effect could be smaller for thicker compact objects, such as spheres. Finally, using images inherently limits the realism, which may undermine the color constancy. Future works should use physical objects in real scenes.

CONCLUSION

We conducted color naming and color matching experiments to investigate how translucency affects color. We observed that translucency may affect color terminology if the background is chromatic. We found indications that translucency limits color constancy, human observers do not discount the transmitted light and backlit translucent observers are usually considered lighter. Furthermore, the mean color of the object did not turn out a good predictor of the matched color. Instead of taking a global average, human observers prioritize specific parts of the object. Future works should investigate more robust modeling of how an object's properties impact color constancy and inconstancy thereof.

REFERENCES

1. Liao, C., Sawayama, M., & Xiao, B. (2022). Crystal or jelly? Effect of color on the perception of translucent materials with photographs of real-world objects. *J. Vis.*, 22(2):6, 1-23.
2. Hassan, A., Gigilashvili, D. (2023), Perceived Translucency of Familiar and Unfamiliar Objects in Color and Grayscale Images, Accepted for presentation at *CIC31*, 6 pages.
3. Hwang, Y. J., & Cho, T. Y. (2022). The role of transparency in color preferences: Sweetness expectation and preference for translucency. *Psychol. Aesthet. Creat. Arts.*, pp. 1-9.
4. D'Zmura, M., Colantoni, P., Knoblauch, K. and Laget, B. (1997). Color transparency. *Perception*, 26(4), pp.471-492.
5. Gigilashvili, D., Thomas, J.B., Hardeberg, J.Y. and Pedersen, M. (2021). Translucency perception: A review. *J. of Vis.*, 21(8):4, pp.1-41.
6. Hedrich, M., Bloj, M. and Ruppertsberg, A.I. (2009). Color constancy improves for real 3D objects. *J. Vis.*, 9(4):16, pp.1-16.
7. Granzier, J.J., Vergne, R. and Gegenfurtner, K.R. (2014). The effects of surface gloss and roughness on color constancy for real 3-D objects. *J. Vis.*, 14(2):16, pp.1-20.
8. Witzel, C., & Gegenfurtner, K. R. (2018). Color perception: Objects, constancy, and categories. *Annu. Rev. Vis. Sci.*, 4, 475-499.
9. Xiao, B., Hurst, B., MacIntyre, L., & Brainard, D. H. (2012). The color constancy of three-dimensional objects. *J. Vis.*, 12(4):6, 1-15.
10. Giesel, M., & Gegenfurtner, K. R. (2010). Color appearance of real objects varying in material, hue, and shape. *J. Vis.*, 10(9):10, 1-21.
11. Berlin, B. and Kay, P. (1991). Basic Color Terms: Their Universality and Evolution. Univ. of California Press.
12. The World Color Survey (Accessed on 15/09/2023), http://www1.icsi.berkeley.edu/wcs/
13. Mylonas, D., Paramei, G. V., & MacDonald, L. (2014). Gender differences in colour naming. Colour studies: A broad spectrum, pp. 225-239.
14. Mylonas, D., Caparos, S., & Davidoff, J. (2022). Augmenting a colour lexicon. *Humanit. Soc. Sci*, 9(1), pp. 1-12.
15. Beretta, G. B., & Moroney, N. M. (2010). Color naming: color scientists use Munsell Sheets of Color. In: *IS&T/SPIE Electronic Imaging, Color Imaging XV*. 27 pages.
16. Tanaka, M., Horiuchi, T. and Tominaga, S. (2015). Color naming experiments using 2D and 3D rendered samples. *Color Res. Appl.*, 40(3), pp. 270-280.
17. Gigilashvili, D., Thomas, J.B., Pedersen, M. and Hardeberg, J.Y. (2021). On the appearance of objects and materials: Qualitative analysis of experimental observations. *Journal of the International Colour Association (JAIC)*, vol. 27, pp. 26–55
18. Gigilashvili, D., Thomas, J.B., (n.d.), Appearance beyond colour: Gloss and Translucency Perception. Colour Engineering: Fundamentals and Applications (Phil Green Ed.), In Press.

19. Xiao, B., Walter, B., Gkioulekas, I., Zickler, T., Adelson, E. and Bala, K. (2014). Looking against the light: How perception of translucency depends on lighting direction. *J. Vis.*, 14(3):17, pp.1-22.
20. Amirkhanashvili, A. and Gigilashvili, D. (2020). Color Naming and Communication of Color Appearance: Is it Different for Native Georgian Speakers?, In *Proceedings of the CVCS2020, CEUR Workshop Proceedings*, 2688, pp. 1-15.
21. Khomeriki, M., Kezeli, A., & Lomashvili, N. (2009). The revealing of color categorical boundaries among Georgian speakers. *Bull. Georg. Natl. Acad. Sci*, 3(3), 135-140.
22. Gigilashvili, D., Thomas, J. B., Hardeberg, J. Y., & Pedersen, M. (2020). On the nature of perceptual translucency. In *Proceedings of the MAM2020.* EG Digital Library, pp. 17–20.
23. Thomas, J. B., Deniel, A., & Hardeberg, J. Y. (2018). The plastique collection: A set of resin objects for material appearance research. In *XIV Conferenza del Colore*, 12 pages.
24. Wenzel, J. (2010). Mitsuba Renderer. http://www.mitsuba-renderer.org.
25. Debevec, P., Light Probe Image Gallery. https://www.pauldebevec.com/Probes/
26. Vogl, B., Light Probes, Retrieved from: http://dativ.at/lightprobes/ on 15/09/23.

Effect of lip colours on colour appearance and preference of facial skin

Shino Okuda[1]*, Riho Jonai[1] and Katsunori Okajima [2]

[1]*Faculty of Human Life and Science, Doshisha Women's College of Liberal Arts, Japan.*
[2]*Faculty of Environment and Information Sciences, Yokohama National University, Japan.*

*Corresponding author: Shino Okuda, sokuda@dwc.doshisha.ac.jp

ABSTRACT

Lip colours have a significant impact on skin tone and facial impression. This study aims to clarify the effect of lip colours on the colour appearance and preference of facial skin using image stimuli. First, we measured the chromaticity values of a female face using a 2D spectroradiometer under a standard illuminant D65. These measured values were transformed into RGB values using the calibration data of an LC-display, and the digital image of the woman's face with true colours was generated. We modified the colour of the lips out of 36 quantitatively different colours, and created 37 different images in total. A subjective evaluation experiment was conducted using the digital images. In the experiment, participants observed a woman's face with the nude lip which was the reference image, and a face with a different lip colour which was a test target. They evaluated for 'bright - dark', 'yellowish - reddish', 'high-contrast - low-contrast', and rated 'naturalness', 'activity', 'sophistication' and 'preference' with a numerical scale from -10 (bad) to +10 (good) for each visual image. The twenty participants were all female in their twenties, and all had normal colour vision. As a result, the facial skin looked brighter and more reddish with increasing the C^* value of lip colour. In addition, the more yellowish the lip color, the more yellowish the facial skin tended to appear. It was also shown that the higher the L^* value of the lip color, the lower the contrast. When the hue angle of the lip color was around 30 degrees, medium saturation and high lightness, the facial skin was evaluated as natural and sophisticated. In any hue condition, the higher the C^* value of the lip color, the higher the skin's activity rating. Skin tone was preferred under the medium saturation and high lightness conditions at a hue angle of 20 degrees, and under the medium saturation and high lightness conditions at a hue angle of 30 degrees. These results indicate that hue assimilation occurs between lip colour and skin colour, and the chroma of lip colour affects the appearance and preference of facial skin.

Keywords: Colour emotion, Facial skin colour, Lip colour, Hue assimilation, Preference

INTRODUCTION

The appearance of the skin is important for women and various products aim at improving the skin condition. However, the appearance of the facial skin depends on the cosmetics being applied. Indeed, cosmetics can alter the perceived color of the skin which affects the visual evaluation.

The previous study reported that red lip colour makes reddish faces more reddish whreas orange lip colour makes yellowish faces yellower. Although the lip colour also changes the perceptual lightness of complexion, such colour effects are neither assimilation nor contrast, and the physical lightness of lipsticks do not correlate with perceptual lightness of faces [1]. On the other hand, another study examining the colour appearance of facial skin using illustrations of women's faces surrounded by scarves of various hues reported that changes in skin colour appearance are caused by contrast rather than assimilation [2]. Moreover, our previous study shows that differences due to face recognition and object recognition affect the appearance of skin colour, based on the results that hue assimilation occurrs in the case of facial images and illustrations, while no assimilation were observed in the case of colour charts [3].

According to these previous researches, the present study aims to examine the influence of hue, lightness and saturation of lip colour on the appearance and preference of facial skin colour, using Mongoloid female facial images as the visual targets.

METHOD

First, a 22 years old woman was selected as the target model, and her face with nude lip and the face with a lip colour were measured using a two-dimensional spectroradiometer [SR-5000/ TOPCON] under the illuminant D65 with a vertical face illuminance of 500 lx. The facial skin (lower cheek) colour was L^*= 65.8, a^*=10.4 and b^*=13.6. We generated the digital image of her face using these measured spectral reflectance values and calibration data of an LC-display [ColorEdge, CG248-4K/ EIZO] used in the visual experiment. We modified the lip colour of the face using Adobe Photoshop 2021, aiming lip colours with h = 0°, 10°, 20° and 30°, C*=30, 40 and 50 and L*=25, 35 and 45. In total, 36 lip colour conditions were prepared. Figure 1 shows the measured chromaticity values of lip colour displayed on a monitor.

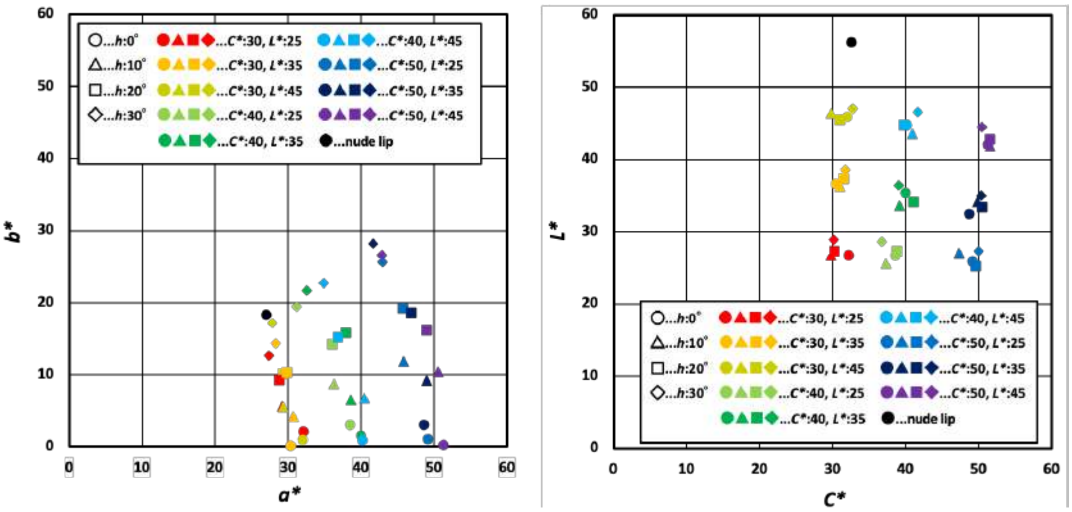

Figure 1. Chromaticity values of lip colours of the face images

In the experiment, the image of the face with the nude lip was juxtaposed on the left side and a test image of the face with lip colour on the right side in the monitor screen. Observers were asked to evaluate the lower cheeks of the face with lip colour of each test image compared with the reference image. They evaluated for 'bright - dark', 'yellowish - reddish', 'high-contrast - low-contrast', and rated 'naturalness', 'activity', 'sophistication' and 'preference' with a numerical scale from -10 (bad) to +10 (good) for each test image. They were 20 Japanese women in their twenties and with normal colour vision.

RESULTS AND DISCUSSION

Figure 2 shows the evaluation results for "brightness" and for "yellowish - reddish" as the mean values of responses from the 20 observers. In the results of "brightness", the hue, lightness and saturation of the lip colour affected the evaluations (P<.005). It was shown that the higher the saturation of the lip colour, the brighter the facial skin colour significantly looked. It was therefore cleared that in the brightness evaluation, the saturation had an impact on the evaluation. In the results of "yellowish – reddish", the hue and saturation of the lip colour affected the evaluations (P<.005). It was shown that the larger the hue angle of the lip colour, the more yellowish the skin colour appeared. It could also be seen that under the same hue conditions, the higher the saturation, the more yellowish the skin colour appeared. On the other hand, the lightness of the lip colour had no effect on the reddish-yellowish evaluations of facial skin colour.

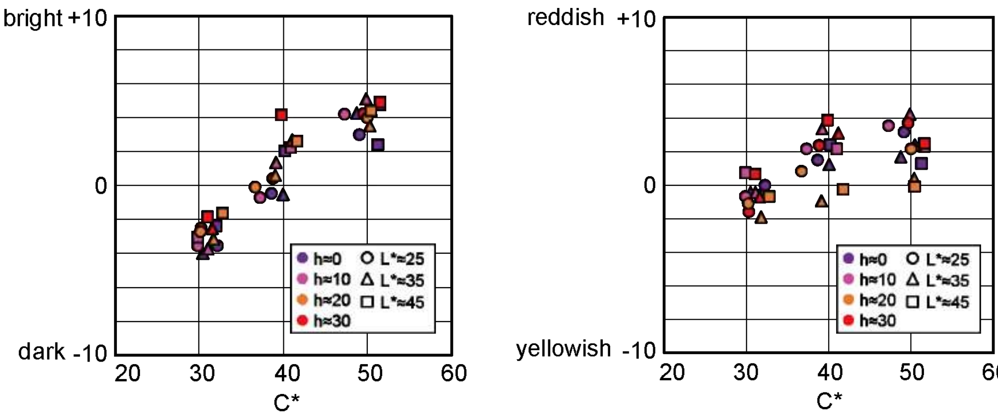

a) "dark – bright"— b) "yellowish - reddish"—

Figure 2. Results of the appearance of facial skin colour.

Figure 3 shows the evaluation results for "naturalness", "sophistication", "activity" and "preference" as the mean values of responses from the 20 observers. In the results of "naturalness", the hue, lightness and saturation of the lip colour affected the evaluations (P<.005). It was shown that the "naturalness" evaluations were low when the hue angle of lip colour was small while the "naturalness" were high when the hue angle was 20° or 30°. Also, it was shown that the higher lightness, the more natural the facial skin looks, in the same hue conditions of lip colour, which is more pronounced when the hue angle of lip colour is 20° or 30°. Moreover, it was seen that the facial skin was felt more natural when the saturation value of lip colour was between 30° and 40°, under the same conditions of hue and lightness of the lip colour.

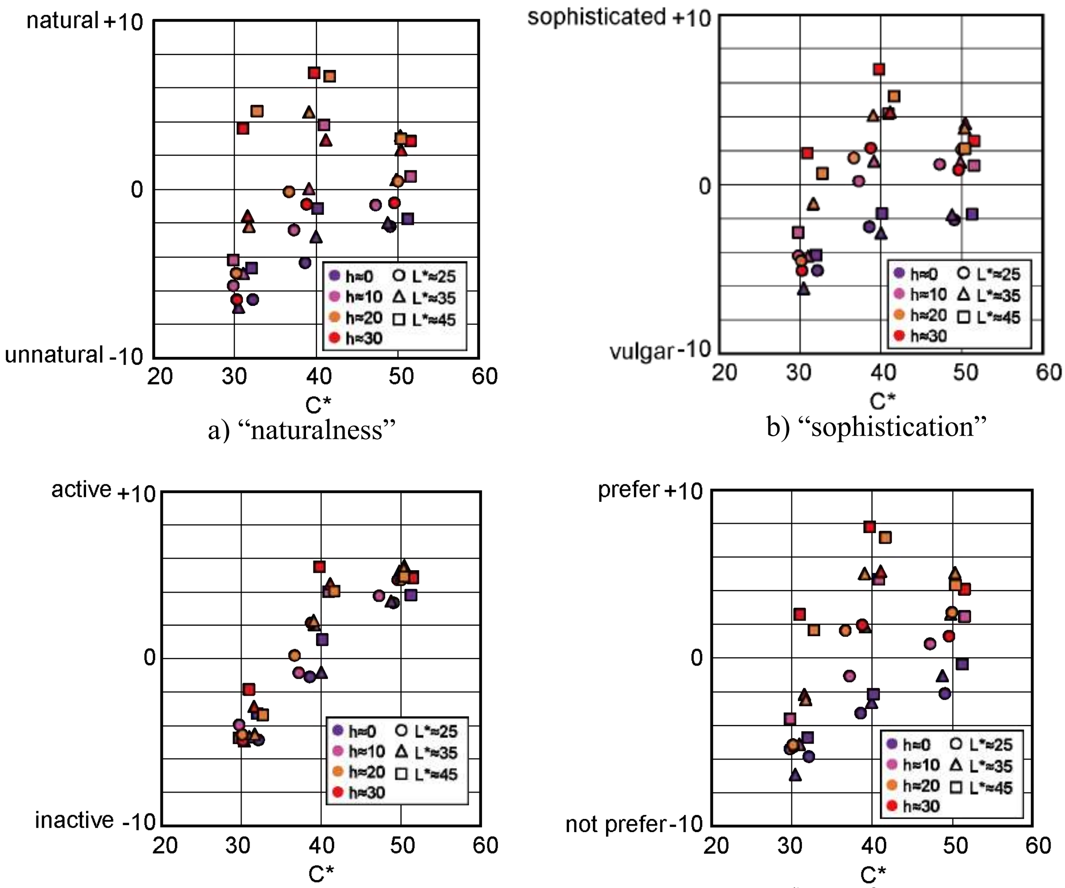

a) "naturalness" b) "sophistication"

c) "activity" d) "preference"

Figure 3. Results of "naturalness", "sophistication", "activity" and "preference".

In the results of "sophistication", the hue, lightness and saturation of the lip colour affected the evaluations (*P*<.005). It was shown that the facial skin looked vulgar in the case of lip colours with the hue angle of 0° whereas the facial skin looked sophisticated in the case of lip colours with the hue angle of 20° and 30°. Also, it was shown that the facial skin was perceived more sophisticated when *C** was 40.

In the results of "activity", the hue, lightness and saturation of the lip colour affected the evaluations (*P*<.005). It was shown that the higher the saturation of the lip colour, the more active the facial skin was significantly perceived. Moreover, it is revealed that the brightness of the facial skin colour was strongly correlated to the activity of facial skin (*R*=0.97).

In the results of "preference", the hue, lightness and saturation of the lip colour affected the evaluations (*P*<.005). It was shown that the facial skin was not so preferred in the case of lip colours with the hue angle of 0° and 10°, and that the facial skin was more preferred as the saturation of the lip colour was higher. On the other hand, it was shown that the facial skin was preferred under the lip colours with the hue angle of 20° and 30°, and that the facial skin was more preferred when *C** was 40.

According to the results, the facial skin looks brighter and more reddish with increasing the C* value of lip colour, and the more yellowish the lip color, the more yellowish the facial skin tends to appear. When the hue angle of the lip color is around 30 degrees, medium saturation and high lightness, the facial skin is evaluated as natural and sophisticated. In any hue condition, the higher the C* value of the lip color, the higher the skin's activity rating. Skin tone is preferred under the medium saturation and high lightness conditions at a hue angle of 20 degrees, and under the medium saturation and high lightness conditions at a hue angle of 30 degrees.

CONCLUSIONS

The lip colour affects the colour appearance of facial skin. Especially, these results indicate that the brightness of the facial skin is influenced by the saturation of the lip colour, and the reddish and high saturated lip colours make the facial skin more reddish. These results indicates that hue assimilation occurs between facial skin colour and lip colour. Also, the facial skin is preferred with the lip colours which is felt natural.

ACKNOWLEDGEMENTS

This study was supported by JSPS KAKENHI Grant Number JP22H03896. We would like to thank Masahito Nagata for his help in generating digital images of the female model. Also, we would like to thank the student who participated as a visual target model in our experiment.

REFERENCES

1. Kiritani, Y., Okazaki, A., Motoyoshi, K., Takano, R., Ookubo N., (2017). Color illusion on complexion by lipsticks and its impression, *The Japanese Journal of PsychonomicScience*, Vol. 36, No. 1, 4–16, DOI: http://doi.org/10.14947/psychono.36.2
2. Nakajima, Y., He, S., Fuchida, T., (2018). Influence of colors of clothe to skin color impression, *Journal of the Color Science Association of Japan*, 42 (3) Supplement, 201-204. (*In Japanese*)
3. Komai, K., Kako, M., Okuda, S., Okajima, K., Effects of lip color on appearance of facial Sskin -Depending on visual targets-. (2022). *Proceedings of the 53th Annual Meeting of the Color Science Association of Japan*, 123-124. (*In Japanese*)

INDIVIDUAL COLOUR PREFERENCE CHANGE OVER TIME : A THREE-MONTH STUDY

Soojin Lee*[1], Stephen Westland[1] and Stan Rodski[2]

[1]*Leeds Institute of Textiles and Colour, University of Leeds, U.K.*
[2]*Cernova, Melbourne, Australia*

*Corresponding author: Soojin Lee, Email: s.j.lee@leeds.ac.uk

ABSTRACT

This paper explores the abstract aesthetic choices individuals make in relation to colour. Drawing upon a historical background of colour preference studies since the late 19th century, we seek to unravel the paradox of why people exhibit varying colour preferences. While prior research has unveiled a general inclination towards cool colours and some cultural consistency in colour preferences, individual differences remain an intriguing puzzle. One key inquiry in this domain is whether an individual's colour preferences change over time. In this study, employing a repeated-measures design, we collected data from 51 participants across two distinct time periods, approximately three months apart: Study 1 (S1) and Study 2 (S2). Participants were tasked with ranking 16 colours from most to least preferred. 'Light blue' consistently emerged as the favoured colour in both S1 and S2, yet participants showed fluctuations in their colour choices. 'White' persistently ranked as the least preferred colour across time periods. Notably, 'brown' and 'grey' remained consistently unpopular choices. By employing cross-tabulation techniques, we further examined the relationships between colours and how participants' choices changed, and it revealed a degree of consistency in choices. However, only 17.6% selected the same colour as their first choice and 13.7% chose the same colour as their last choice. Nevertheless, the Wilcoxon Signed-Rank Test showed no significant difference in first and last colour choices between S1 and S2, suggesting a consistent pattern in colour preferences over a three-month span. While our findings suggest lasting patterns in the most and least preferred colours, further investigations are warranted to scrutinise colour preferences over longer periods and to explore sequential colour choice patterns. The specific colours highlighted in this paper would provide a promising foundation for deeper exploration of colour preference dynamics.

Keywords: colour preference, most and least preferred colours, individual differences, repeated-measures design

INTRODUCTION

Colour preference has been studied since the late 19th Century. By colour preference here we refer to a person's aesthetic preference for one colour over another in an abstract sense, free of context. A person may prefer blues to yellows in general though of course might exhibit all sorts of other colour preferences in the context of things that are coloured such as cars, clothes and cosmetics. There were at least 50 published studies about colour preference between Cohn's seminal article in 1894 and a paper by Eysenck in 1941 [1]. Cohn was unconvinced that there were any systematic effects of colour preference (i.e. that people on average might prefer some colours more than others) whereas Eysenck argued that this was mainly because of methodological problems with early experiments. Eysenck produced some data which started to suggest that there might be a systematic preference in the population for some colours. This was confirmed in 1959 when Guildford and Smith established the idea that in general preferences of some colours are systematically higher than for others [2]. Over the last 60 years there have been many similar studies of colour preference in this abstract sense. Research has also been carried out about colour preferences for products in the context of consumer studies [e.g. 3]. Studies of abstract colour preference have consistently found that on average participants prefer blue colours and dislike yellow colours. Often this effect is phrased such that cool colours (blue, cyan and green) are generally preferred to warm colours (red, orange and yellow). A recent review of the literature also confirmed that people (especially Western observers) tend to prefer lighter and more chromatic colours, that some gender differences exist, and that although there is broad agreement in colour preferences across cultures (people tend to like blue and dislike yellow) this is not sufficient to conclude that colour preferences are universal across cultures [4]. For example, in one study was found that blue was a least-preferred hue in Kuwait [5].

Despite the general trend that on average people tend to prefer lighter, more chromatic and cooler colours it has long been evident that individuals vary in their colour preferences. Why should these differences exist? Indeed, why do people have colour preferences at all? Several ideas have been put forward. For example, Hurlbert and Ling proposed an explanation based on an analysis of cone responses that explained differences between male and female colour preferences [6]. This can be thought of as a physiological explanation. Perhaps differences in cone populations between individuals could explain individual colour preferences? On the other hand, Palmer and Schloss have put forward an explanation that is more cognitive [4]. According to this explanation people like colours because of the emotional associations for those colours; people like colours that remind them of things that they like. In terms of evolution, organisms may benefit by approaching objects whose colours they like and avoiding objects whose colours they dislike; this has been called the Ecological Valence Theory of colour preference. This explanation does seem to provide a rationale for why people might have colour preferences and why there is some consistency across cultures. As has been noted by Palmer and Schloss, 'clear sky and clean water are universally blue, whereas biological wastes and rotting food are universally dark yellow' [4]. The variation in colour preferences for individuals over time has been less well studied and is the focus of this paper.

METHODOLOGY

Repeated-measures design was used with multiple measures of the same variables on matched participants over two time periods. In the first phase (Study 1: S1), 99 participants (students and staff) were recruited on campus at the University of Leeds. They were invited to visit the psychophysical lab twice on different days. On day 1, each of the participants was provided with a wearable heart monitor watch to use for about seven days (at least 48 hours) and completed the 'Resilience Scale for Adults' (RSA) questionnaire [17]. On day 2 (about seven days later), they took the 'Connor-Davidson Resilience Scale' (CD RISC-25) questionnaires [18] and a colour preference test which asks to choose colours from 16 different colour options in an order of colours that they are most drawn to until all the colours are gone. In the second phase (Study 2: S2), about three months later, about 97 participants took part in the repeat of Study 1. Of these 97 participants, 67 took part in both studies. However, after a data cleaning exercise, data for 51 participants who participated in both S1 and S2 were obtained. Figure 1 shows the colours that were presented during the colour preference task. These colours are derived from a commercial colour test (Cernova).

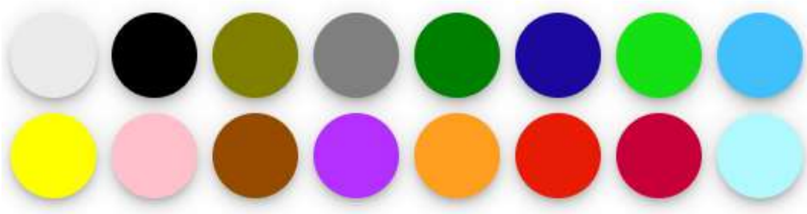

Figure 1. The colours used in the colour preference task.

The colours in the colour preference test (Figure 1) are referred to as white, black, dark green, grey, green, dark blue, light green, light blue, yellow, pink, brown, purple, orange, red, strong red and light

●

cyan (from left to right, top row first). This paper focuses solely on analysing the first and last colour choices made by participants across both S1 and S2.

●

RESULT AND DISCUSSION

A total of 51 participants (35 female and 16 male) were involved in both S1 and S2 and their colour rank data were analysed. In this analysis, we calculated the frequency with which each colour was selected as the most favourite (first rank) and least favourite (last rank).

Comparison of Colour Preference Rankings in S1 and S2: First and Last Choices

Figure 2 illustrates the per cent of participants who selected each colour as their first preference choice in S1 and S2. Notably, 'brown' and 'grey' were never chosen as the first choice by any participant in either study, and 'black' and 'orange' were infrequently selected. 'Light blue' emerged as the most preferred colour in both studies, accounting for 13.7% (7 out of 51 participants) in S1 and 19.6% (10 out of 51 participant) in S2. 'Pink' and 'purple' were also strongly preferred (but note that there were about twice as many females as males in the population).

To investigate the relationships between colours and how participants made their choices (i.e. the interactions between the two categorical colour variables), we employed cross-tabulation techniques. The results of this analysis are presented in Table 2. Among the consistently chosen colours across both S1 and S2 were 'dark green', 'dark blue', 'light blue', 'yellow', 'red', and 'light cyan' (highlighted in dark grey). For instance, 'light blue' was the first preference choice for 3 participants in both S1 and S2. While Figure 2 highlights some differences between the two studies, it is important to note that only 9 out of 51 participants (18%) selected the same colour as their first choice in both S1 and S2.

Turning our focus on the last choice of colour, we calculated the per cent of cases in which each colour was chosen as the last preference in both S1 and S2. These findings are visually represented in Figure 3. Significantly, 'white' emerged as the last preference in both studies, chosen by 17.6% (9 out of 51 participants) in each study. While the figure indicates some variations in preferences between the studies, such as 'black' and 'purple' being more frequently selected in S2, these differences were relatively minor. However, it is worth noting that colours like 'dark green' and 'light green' exhibited more pronounced variations. For example, 'dark green' were chosen more often in the S2, while 'light green' was less frequently selected in S2. To assess the relationships between the last colour preference in both S1 and S2, we also applied cross-tabulation techniques, and the results are presented in Table 3. The colours consistently chosen as the least favourite across both S1 and S2 were 'white', 'black', 'light green', 'yellow', 'brown', and 'purple' (highlighted in dark grey). However, only 7 out of 51 participants (13.7%) selected the same colour as their last choice in both studies.

●

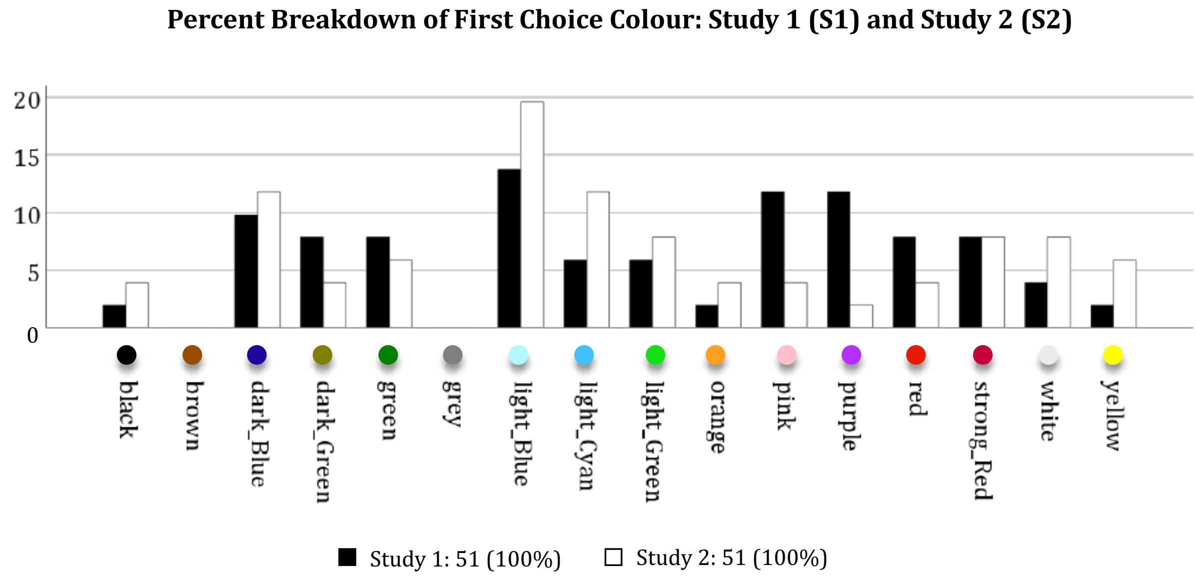

Figure 3. Per cent of times each colour was selected first for S1 (black bars) and S2 (grey bars).

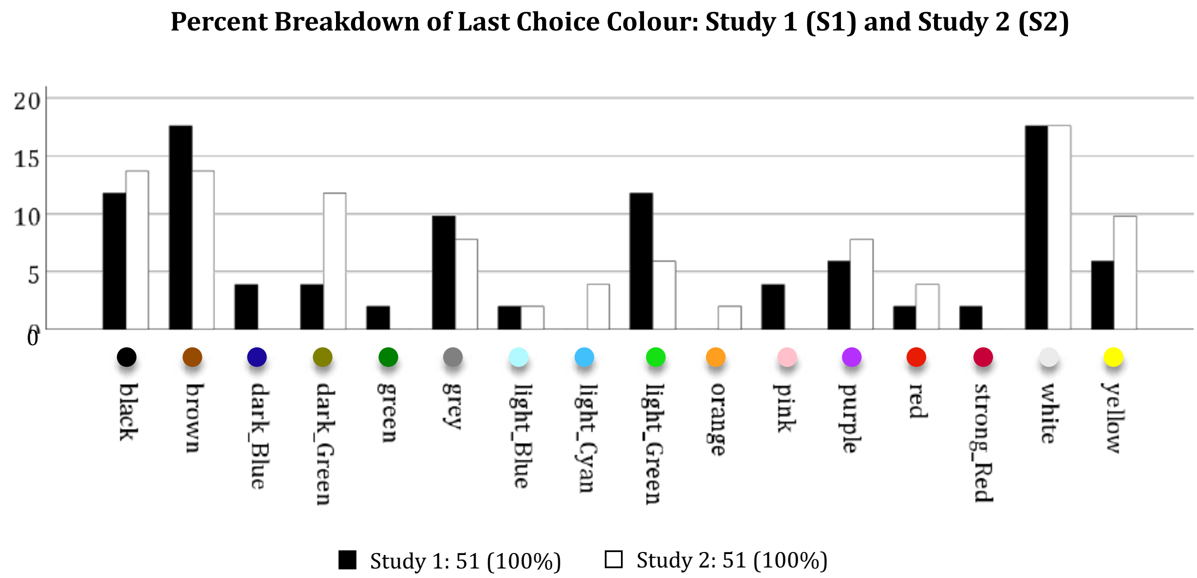

Figure 2. Per cent of times each colour was selected last for S1 (black bars) and S2 (grey bars).

●

●

Analysing Statistical Significance in Colour Preference Changes Over Time●

We conducted a series of statistical tests to evaluate the consistency in colour preferences among participants across two distinct studies (S1 and S2) separated by a 3-month interval. We sought to determine whether there were statistically significant differences in the rank order of colour preferences, both in terms of first and last choices, and to explore individual variations within this broader context in a four-step approach.

Step 1: Initially, we examined the frequency which each colour was selected as the first preference in both S1 and S2. To assess statistical significance, we conducted the Wilcoxon Signed-Rank Tests (referred to as the Rank Test below) on these two sets of data. The test revealed no statistically significant difference in the ranks ($Z = -.186$, $p = 0.860$).

Step 2: Subsequently, we investigated the number of times each colour was chosen as the last preference in both studies. Once again, we conducted the Rank Test on these data sets and found no significant difference in the ranks ($Z = -.160$, $p = 0.873$)

Step 3: Furthermore, we calculated the average rank for each colour across all positions, not limited to just first and last preferences. Subsequently, we performed the Rank Test on these data sets and found no significant difference in the ranks between the two studies ($Z = -.140$, $p = 0.889$)

Step 4: While these initial findings indicated no overall statistical difference between the two studies, it was crucial to explore potential individual differences. To achieve this, lastly, we conducted significance tests comparing the rank order of colours in S1 with the rank order in S2 for each participant separately. In all 51 cases, we found no significant difference in the rank order between S1 and S2 (average for 51 cases, $p = 0.873$).

Note that the colour preference ranking data for first and last choices in S1 and S2, as well as the average rank positions for each colour in each study relating to Steps 1 to 3, are shown in Table 1. This comprehensive analysis underscores the consistency in colour preferences among participants over the 3-month period. It highlights the stability of individual colour preferences, as evidenced by the absence of statistically significant variations both in the aggregate data and at the individual level. However, it is vital to acknowledge the potential for longer-term investigations to further elucidate this phenomenon, such as extending the study duration to six months or one year.

Table 1: Colour preference ranking data for first and last choices in S1 and S2, and average rank positions for each colour in each study.

Step 1			Step 2			Step 3		
	S1	**S2**		**S1**	**S2**		**S1**	**S2**
white	2	4	white	9	9	white	10.5	10.5
black	1	2	black	6	7	black	9.9	9.8
dark green	4	2	dark green	2	6	dark green	9.8	10.7
gray	0	0	gray	5	4	gray	11.6	11.5
green	4	3	green	1	0	green	7.6	7.2
dark blue	5	6	dark blue	2	0	dark blue	8.0	7.2
light green	3	4	light green	6	3	light green	9.0	8.4
light blue	7	10	light blue	1	1	light blue	6.2	5.8
yellow	1	3	yellow	3	5	yellow	8.1	8.1
pink	6	2	pink	2	0	pink	8.2	8.3
brown	0	0	brown	9	7	brown	11.5	11.5
purple	6	1	purple	3	4	purple	7.1	8.1
orange	1	2	orange	0	1	orange	8.0	7.5
red	4	2	red	1	2	red	6.4	7.3
strong red	4	4	strong red	1	0	strong red	6.8	7.6
light cyan	3	6	light cyan	0	2	light cyan	7.2	6.6
Note. This is the number of times each colour appears in the first rank in each study.			*Note. This is the number of times each colour appears in the last rank in each study*			*Note. This is the average rank position for each colour in each study*		

							dark_ Blue		light_ Blue								light_ Cyan		
Study 1 (S1) _First Choice Colour	white	0	0	0	0	0	1	0	0	0	0	0	0	0	0	1	0	2	3.9%
	yellow	0	0	0	0	0	0	0	0	1	0	0	0	0	0	0	0	1	2.0%
Total (percent)		7.8%	3.9%	3.9%	0.0%	5.9%	11.8%	7.8%	19.6%	5.9%	3.9%	0.0%	2.0%	3.9%	3.9%	7.8%	11.8%	100%	

		Study 2 (S2)_Last Choice Colour																	
							dark_ Blue		light_ Blue								light_ Cyan		
_Last Choice Colour	dark_Blue	1	0	0	1	0	0	0	0	0	0	0	0	0	0	0	0	2	3.9%
	strong_Red	0	1	0	0	0	0	0	0	0	0	0	0	0	0	0	0	1	2.0%

Three noteworthy findings emerged from our study:

- First, we found a remarkable degree of consistency in participants' colour choices. Despite the presence of a diverse palette of 16 different colours, our analysis revealed that the rank order of both first and last colour preferences exhibited no statistically significant differences over the 3-month period. It may suggest that individuals tend to stick to their colour preference over time. However, further investigation is needed with a longer duration, such as six months or one year, to fully explore this phenomenon.
- Second, our findings also revealed a group of colours that were consistently preferred across both S1 and S2. These colours—green, dark blue, light blue, strong red, and light cyan—stood out as the most favoured choices among participants. The stability of these preferences suggests that certain colours may possess universal or enduring appeal.
- Third, while overall stability was evident in our results, some interesting variations in colour preferences between S1 and S2 emerged. For instance, 'black' and 'purple' were chosen more frequently in S2 as last preferences. Additionally, colours like 'dark green' and 'light green' exhibited more distinct variations, indicating that individual preferences for these shades may be more susceptible to change.

Future research could delve deeper by focusing on the sequential order rather than solely initial choices. The present findings in this paper provide a strong foundation for further analysis of the sequential choice of 16 colours in the near future.

CONCLUSION

In this study, we set out to explore how individuals make choices and rank colours, considering both their most and least favorite options, and sought to understand whether these choices maintain consistency over a three-month time. We highlighted stability of colour preference, consistently preferred colours, and variations in colour preferences.

REFERENCES

1. Eysenck HJ. (1941). A critical and experimental study of colour preferences. *The American Journal of Psychology*. Jul 1;54(3):385-94.
2. Guilford JP, Smith PC. (1959). A system of color-preferences. *The American Journal of Psychology*. Dec 1;72(4):487-502.
3. Yu L, Westland S, Li Z, Pan Q, Shin MJ, Won S. (2018). The role of individual colour preferences in consumer purchase decisions. *Color Research & Application*. Apr;43(2):258-67.
4. Palmer SE, Schloss KB, Sammartino J. (2013). Visual aesthetics and human preference. *Annual review of psychology*. Jan 3;64:77-107.
5. Choungourian A. (1968). Color preferences and cultural variation. *Perceptual and Motor Skills*. Jun;26(3_suppl):1203-6.
6. Hurlbert AC, Ling Y. (2007). Biological components of sex differences in color preference. *Current biology*. Aug 21;17(16):R623-5.

COLOUR DESIGN AND SPATIAL QUALITY- A CRITICAL ANALYSIS OF THE MOSAIC COLOURS IN HONG KONG MASS TRANSIT RAILWAY STATIONS

Jiaxin Liang[1], Raine Marie Chang[2], Wanting Wang[1] and Changying Xiang[1]*

[1]Division of Integrative Systems and Design, School of Engineering, the Hong Kong University of Science and Technology, China.
2 Department of Civil and Environmental Engineering, the Hong Kong University of Science and Technology, China.

*Corresponding author: Changying Xiang, changyingx@ust.hk

Abstract

Colour design plays a pivotal role in shaping spatial identity and attractiveness, especially in urban transit systems. The Mass Transit Railway (MTR) in Hong Kong exemplifies this with its vibrant mosaic designs featured across its stations. This study explored the relationship between these color designs and the spatial quality of the stations, concentrating on four key factors: identification, attractiveness, openness, and brightness. The initial phase of the research involved the analysis of color themes in ten busy MTR stations. This was achieved using perspective RGB photos and NCS colour scanners. Following this, an online survey was conducted to gather feedback from both residents and tourists on these colour designs. The survey sought suggestions for improvements to the colour design in MTR stations and asked participants to rate the designs on a 5-scale semantic differential scaling. The survey results showed that 69.7% participants identified subway stations based on the different colors within the station. There was a prevailing sentiment among respondents that refurbishing colour designs could enhance the stations' space identities and improve the perceived spatial quality. Another fundamental insight drawn from the survey was that the satisfaction level has a strong association with the colour design in MTR stations, where colour schemes of the top-rated stations were perceived as both pleasing and spacious. The study showed a necessity to improve the spatial quality of many MTR stations in Hong Kong, and that colour design within these stations should aim for a higher level of distinctiveness and regional representation.

Keywords: Colour design, Spatial identity, Railway station, Architecture, Mosaic

INTRODUCTION

Colour is a powerful design element that can influence our emotions and behavior [1]. In public transportation systems, where people need to navigate in complex spaces and interact with others, colour design becomes even more important [2]. Hong Kong, a city with rich cultural diversity, is also characterized by a vibrant range of colour identities in its environment [3]. This distinct colour palette is noticeable in the façades of its buildings, urban infrastructure like pedestrian bridges and rest kiosks, and, not least, its Mass Transit Railway (MTR) stations.

Transit around 4 million passengers per day, the MTR stations play an essential role of the city. The MTR stations' interior spaces are recognized for their vibrant and intricate mosaic designs, which incorporate a range of colours [4]. These mosaics are not only visually appealing but also have potential to serve as wayfinding elements that help passengers navigate the stations. The MTR stations' mosaic designs are a product of a unique cultural and historical context. Mosaic tiles began to appear on the buildings of Hong Kong in the 1950s and 1960s, often used as a form of decoration and protection against harsh weather. The use of these colorful, small tiles added a unique and vibrant aesthetic to the cityscape [3]. The mosaic tiles were used on both the exteriors and interiors of residential, commercial, and public buildings. The usage of colour in the mosaics

was particularly attractive for designer at that time. The designers used a wide range of colours, including bright and bold hues, to create a visually stunning environment.
The impact of colour on spatial perception is well-acknowledged. Colours can create an illusion of depth, alter the perceived size of a space, and affect our mood and behavior [1][5]. The process of space recognition is a complex phenomenon that involves not just the detection and appearance of surroundings, but also factors from the viewers' individual background. Aspects such as memory, personal experiences, mood, age, sex and thousand others may significantly impact this process [6]. From Gerhard Meerwein [2], in his book 'Colour — Communication in Architectural Space,' he conducted a "spatial colour experience scheme" model to illustrate six factors to influence people's colour experience, they are biological reactions, the collective unconscious, symbols and associations, fashion and style, cultural factors and personal factors. All of them interplay in the model and some of them interact with each other. Our eyes are the receptor of colour; people can feel completely different about different colours, cause the colour will change the environment atmosphere, and colouration will arouse our feelings about various things; even these feelings could involve smell, hearing, taste, and touch, those will relate to personal factors in the model.
Several studies demonstrated the links between colour and human perceptions. Pyykkö [7] utilized a colour walk methodology to examine the role of colour on two levels: architectural and urban design. This exploration of neighborhood chromatic experiences led to the revelation of seven key elements shaping the experience: (1) Material; (2) Light; (3) Views within, from, and into the area; (4) Atmosphere; (5) Identity; (6) Landscape/Nature/Landscape Architecture; and (7) Architecture. Kuller [8] undertook a series of studies to explore whether interior colour influences people's mood. He employed psychological and physiological detection devices, such as EEG and EKG, to gather data while subjects were exposed to different colour conditions in a room. The results suggested that interior colour can indeed affect emotions, drastically evoking certain emotional responses while suppressing others.

RESEARCH QUESTIONS

Although many researchers conducted studies on colour theoretically, striving to establish a link between colour in built environments and people's perceptions. However, few have explored human experience based on actual scenes [9], particularly within the context of public transportation space. The topic of colour effects on public spatial recognition or spatial image is rarely investigated academically. Therefore, this study examines the colour design of Hong Kong's MTR stations, offering insights into the strategic use of colour in public transportation design and its influence on spatial quality with topics of passenger's environmental perception and spatial recognition. The research questions this study are: 1. Can the mosaic colour design enhance spatial identification of MTR spaces? 2. How do people feel the mosaic colour design of the MTR stations by different colour combination and design methods?

METHODOLOGY

A two-stage research method is employed in this study. Initially, we selected ten high-traffic MTR stations as our case studies to gather objective colour data from each station. Following this, we conducted a large-scale online survey for the second stage. We invited both local citizens and tourists to participate, requesting their subjective evaluations of the MTR's interior environment. This approach aimed to explore the impact of mosaic colour design on people's experiences across various stations.

Site Selection

10 MTR stations locate at different districts of Hong Kong were selected for the case study: Causeway Bay, Kennedy Town, Central, Admiralty, Tsim Sha Tsui, Mong Kok, Yau Ma Tei, Diamond Hill, Prince Edward and Hung Hom, with the mosaic tiles inside of the stations and its

interior environment as shown in Figure 4. These stations were chosen for several reasons that enhance the validity of this study. Firstly, these stations are characterized by high daily passenger traffic. This not only enhances the generalizability of this study's findings, but it also allows us to capture a diverse array of experiences and perceptions. This diversity is informed by the local population's prior experiences with the MTR system. Secondly, these stations serve as major traffic nodes within the city, playing a significant role in the daily lives of many residents. Therefore, understanding the perceptual responses to colour in these settings could have profound implications for future urban and transport design strategies. This understanding could contribute to the development of public spaces that are more identifiable and emotionally engaging.

Colour Collection

The representative colours data of the interior of 10 MTR stations was collected. In this study, the nominal colours were registered via portable NCS colour devices [10], while photos of the corresponding environment were also taken as the visual presentation material for the further online evaluation survey. An example of a station photo used is depicted in Figure 1.

The NCS - Natural Color System is a colour system that entirely grounded in visual perception, rather than in colour mixing [11]. It is a globally recognized system used for describing, communicating, and studying environmental colours. This system uses six fundamental colours - yellow, red, blue, green, black, and white - which represent the pure colours as perceived by humans [12].

Every colour in the NCS is defined by two main attributes: hue and nuance. The hue of a particular colour is determined by its relative similarity to two of the chromatic elementary colours - blue (B), green (G), red (R), and yellow (Y) [10]. In contrast, the nuance of a colour is characterized by its blackness (its resemblance to black or white) and its chromaticness (its relationship to the most saturated level that bears no similarity to either white or black) [13].

The NCS Colourpin II was employed [14] as a detection tool to gather nominal colours present in the MTR stations, as depicted in Figure 2. This tool is best used in conjunction with the NCS+ colour app [15] to accurately capture onsite colour data.

Figure 1 (Left). Pillars are decorated with mosaic tiles in the MTR station (Diamond Hill Station)

Figure 2 (Right). The method for determination of nominal colour with NCS Colourpin II

Online survey

In the second stage, an anonymous online survey was conducted to collect data on public sentiment and attitudes towards the colour design of MTR stations in Hong Kong. The primary goal was to gather subjective perceptions about the spatial quality of the stations, with a focus on the impact of colour design on station identification and station spatial perception. The survey welcomed participants from all backgrounds, genders, and ages. The survey, which was developed using the Microsoft Forms online platform, was made available in both English and Chinese. It was divided into three main sections: 1. Collection of basic personal information from the participants and a general perceptual evaluation of the spatial quality of Hong Kong's MTR stations. 2. Individual assessments of ten selected MTR stations by the participants, focusing on four aspects: identifiability, attractiveness, openness, and brightness. A five-levels semantic differential scale was used, ranging from “Very Good” to “Very Poor” (Figure 3). 3. The final section was designed to gather overall participant preferences concerning the environmental conditions of MTR stations. This included their personal favorite stations and the reasons for their choices, provided as open-ended responses. Additionally, this section aimed to collect suggestions for spatial improvements and to understand participants' perspectives on the spatial design of MTR stations.

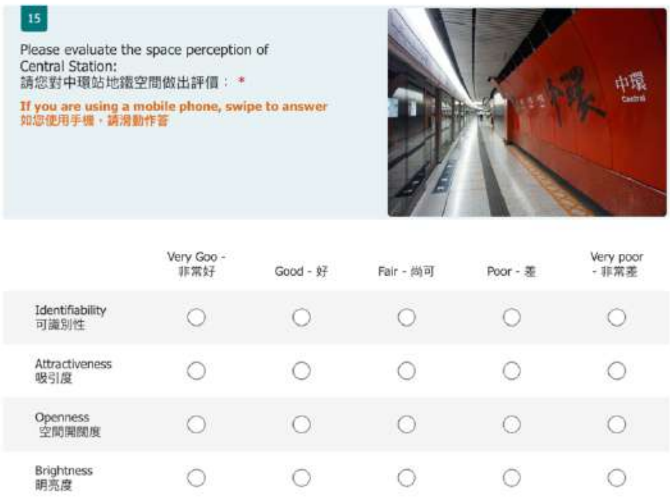

Figure 3. Interface of the online survey evaluating identifiability, attractiveness, openness, and brightness in MTR stations.

RESULT AND DISCUSSION

The survey utilized a 5-scale semantic differential scaling, allowing participants to evaluate the spatial quality of MTR stations based on images showcasing the stations' interior colour design and environmental conditions. A total of 148 participants from Hong Kong and beyond engaged in the online survey. Responses from individuals who indicated they had never visited MTR stations (those who chose "Never" for question no.7 as invalid data) were excluded. This filtration resulted in a final valid sample of 145 responses for analysis. Descriptive statistics derived from these responses were coded and computed using SPSS (v26) and Microsoft Excel for further analysis.

Table 1: Descriptive statistics of respondents' personal characteristics (n = 145)

Attribute	Categories	Count	Percentage
Work in MTR company	Yes	17	11.70%
	No	128	88.30%
Age	Under 18	1	0.70%
	18 - 30	103	71.00%
	30 - 60	39	26.90%
	Over 60	2	1.40%
Gender	Female	58	40.00%
	Male	87	60.00%
Residency	Hong Kong	130	89.70%
	Outside Hong Kong	15	10.30%
Occupation	Architect/designer/urban planner/artist or a student	22	15.20%
	Layperson	123	84.80%
Can speak Chinese / Cantonese	Yes	133	91.70%
	No	12	8.30%
Frequency of taking MTR	1-3 times per month	20	13.80%
	1-3 times per week	53	36.60%
	On weekdays	31	21.40%
	Every day	41	28.30%
Think MTR stations is Distinctive	Strongly agree	13	9.00%
	Agree	79	54.50%
	Neither agree nor disagree	32	22.10%
	Disagree	19	13.10%
	Strongly disagree	2	1.40%
Notify colour design in MTR stations	Yes	136	93.80%
	No	9	6.20%
Use interior colour to identify stations	Yes	101	69.70%
	No	44	30.30%
MTR Satisfaction	Very Good	9	6.20%
	Good	69	47.60%
	Fair	55	37.90%
	Poor	10	6.90%
	Very Poor	2	1.40%

Respondent details

The first section of the online survey collected basic personal information from the participants and their general evaluations of their experiences with MTR station spaces. As illustrated in Table 1, the demographic results revealed that male respondents constituted a larger portion (60%) of the survey participants compared to females (40%). The majority of respondents (71%) were

aged between 18 to 30. In terms of occupational background, 15.2% of the participants were architects, designers, urban planners, artists, or students in related fields The remaining participants were 'laypersons' with no background related to these fields. By analysing the survey results, it is concluded that the factor of professional background does not have a significant impact on the overall spatial evaluation of MTR stations.
The survey results revealed that 89.7% of respondents reside in Hong Kong, and nearly half of the participants (49.7%) use the MTR on weekdays or even daily. Notably, while 93.8% of participants acknowledged noticing colour differentiation within MTR stations, only 69.7% reported using colour as a reminder of specific stations. These findings warrant further consideration. 53.8% of the survey participants expressed satisfaction with their experience at MTR stations, yet 8.2% of respondents reported having a poor experience with the MTR stations.

Personal subjective evaluation of 10 MTR stations

The second section of this survey aimed to capture participants' subjective evaluations of 10 selected MTR stations. To avoid any potential number preference bias, numerical ratings were not provided in the survey itself. Instead, these were assigned during data analysis, using a scale where 1 equates to 'Very Poor' and 5 to 'Very Good'. The numerical results of this section are illustrated in Table 2. Evaluations were made based on four criteria: identification, attractiveness, openness, and brightness.
Kennedy Town station (Figure 4.i) and **Admiralty station** (Figure 4.d) were particularly noteworthy. Kennedy Town achieved the highest scores in attractiveness (mean = 3.76) and openness (mean = 3.91), and also secured a respectable second place in the brightness category, with a mean score of 4.17. Admiralty station, on the other hand, was rated highest in the identification (mean = 4.09) and brightness (mean = 4.2) categories. Admiralty also performed well in the other categories, ranking second with mean values of 3.74 for attractiveness and 3.86 for openness.
A mosaic colour scheme was also compiled, capturing the primary identification colours used at different stations. The primary identification colours of Kennedy Town station and Admiralty station were identified as S2030-B40G and S2065-B, respectively, according to the NCS colour system. A visual representation of these colours can be found in Figure 6.
In contrast, **Tsim Sha Tsui station** (Figure 4.a) performed the worst in two evaluation factors - identification (mean = 3.4) and brightness (mean = 3.34). Moreover, it was second to last in the evaluations for attractiveness (mean = 3.16) and openness (mean = 3.12). Concurrently, **Causeway Bay station** (Figure 4.h) was observed to have the least favorable scores in the categories of attractiveness and openness, both receiving a mean value of 3.06. With regards to the colour schemes, Tsim Sha Tsui station is characterized by the colour S0575-G90Y in the NCS colour system. Causeway Bay station exhibits a mosaic of two primary colours, namely S2020-R and S4020-R40B, shaping the station's visual identity.

Figure 4. 10 selected MTR stations (a. Tsim Sha Tsu; b. Hung Hom; c. Central; d. Admiralty; e. Diamond Hill; f. Mong Kok; g. Yao Ma Tei; h. Causeway Bay; i. Kennedy Town; j. Prince Edward).

Table 2. Analysis of participants' space perception evaluation of stations (n=145)

Factor	Identification		Attractiveness		Openness		Brightness	
Station Name	M	SD	M	SD	M	SD	M	SD
Tsim Sha Tsu	3.4	0.931	3.06	0.818	3.12	0.932	3.34	0.861
Hung Hom	3.83	0.817	3.59	0.778	3.86	0.76	4.09	0.686
Central	4.02	0.795	3.59	0.894	3.31	1.024	3.77	0.745
Admiralty	4.09	0.807	3.74	0.888	3.86	1.014	4.2	0.673
Diamond Hill	3.88	0.881	3.49	0.867	3.75	0.812	3.43	0.814
Mong Kok	3.69	0.862	3.34	0.828	3.45	0.865	3.89	0.708
Yao Ma Tei	3.54	0.799	3.23	0.806	3.17	0.825	3.61	0.783
Causeway Bay	3.87	0.81	3.46	0.85	3.06	0.915	3.59	0.777
Kennedy Town	3.76	0.784	3.76	0.784	3.91	0.772	4.17	0.687
Prince Edward	3.43	0.848	3.16	0.761	3.4	0.869	3.37	0.874

In the final section of the online survey, participants were asked to select their favorite station from among the 10 options and provide their reasons. It's noteworthy that Admiralty station emerged as the most favored, chosen by 41 out of 145 participants. This station also received high ratings in the second section of the survey. Participants cited various reasons for their preference, including the station's colour design. Comments included *"nice bright colours"* (P113*), "It's nicely designed, and the colour is very recognizable"* (P51), and *"Spacious, bright, the blue chosen is bright"* (P15). Many participants also noted the bright lighting conditions within the station, which contributed to a sense of depth, and praised its modern, clean appearance following reconstruction. Some participants expressed their preference for Admiralty station due to the convenience of transfers at this location.

The data yielded intriguing insights regarding the relationship between NCS colour attributes and passenger preference. Common features were observed among the top four stations – the most favored colour predominantly featured bluish, bluish-greenish, or reddish hues. Station with a pure, highly chromatic blue were preferred over the with a less chromatic bluish-greenish (S2065-B VS. S2030-B40G). Meanwhile, the MTR station utilizing three variants of red were more favored than the station only displaying two red shades.

The final section of the survey sought to gather participants' attitudes towards the importance of colour design. 94% of participants believed that colour contributes to enhancing spatial experience, and 76% felt there is a need to improve spatial design in Hong Kong's MTR stations (Figure 7). In response to the closing question – "Do you have any suggestions or comments on the colour and space design of MTR stations?", several noteworthy points were raised. Some participants suggested that colour design should be more distinguishable across different stations and *"could be utilized to define different space functions, such as the waiting area"* (P81). There were also suggestions to use colour to change the atmosphere of the MTR stations to *"improve the emotional connection between the station and passengers"* (P53), as the current colours were described as *"very depressive"* (P106). Interestingly, some participants recommended using colours to represent regional cultural identities, suggesting that each station should have its own visual identity.

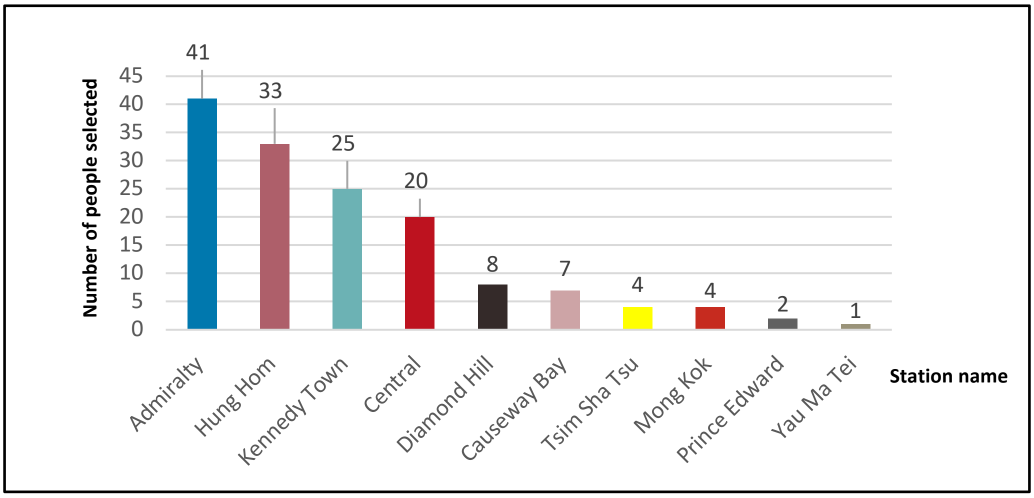

Figure 5. Participants' favorite station rank (n=145)

Station Name	NCS notation
Admiralty	S2065-B
Hung Hom	S3040-R10B, S5040-Y80R, S1070-R
Kennedy Town	S2030-B40G
Central	S1580-Y90R, S2570-Y90R
Diamond Hill	S8502-R, S5005-R20B
Causeway Bay	S2020-R, S4020-R40B
Tsim Sha Tsui	S0575-G90Y
Mong Kok	S1580-Y80R, S3005-G80Y
Prince Edward	54010-R10B
Yau Ma Tei	S4010-G90Y, S2005-G60Y

Figure 6. The NCS colour notation of the primary colours of mosaic tile in MTR stations

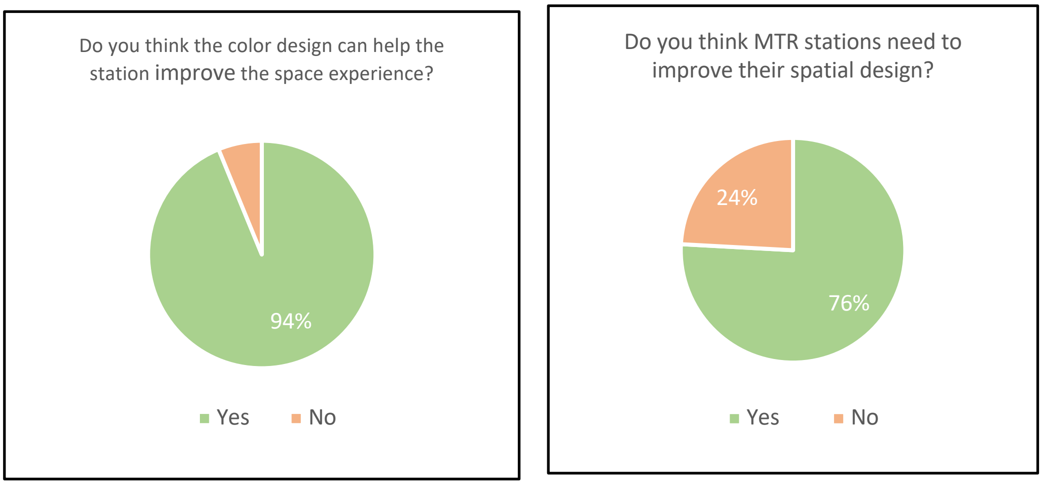

Figure 7. Participants attitudes towards Hong Kong MTR stations

CONCLUSION

The online survey revealed that the majority of passengers recognized diverse mosaic colour designs across the Hong Kong MTR stations, with 69.7% participants using these colour designs to distinguish between different stations. Additionally, the study explored participants' subjective spatial experiences based on four criteria. Notably, the ranking of scores mirrored the ranking of participants' favorite stations, as identified in the final section of the survey.

A significant number of participants indicated that the interior colour design of the stations was a crucial factor in determining environmental quality, suggesting that effective colour design can enhance spatial experience while providing a more identifiable and functional environment.

The findings of this study offer valuable insights into colour design within urban transport spaces and can inform future design recommendations for spatial designers and colour experts. For future research, investigators could concentrate on specific parameters of colour within the NCS colour system to explore how different colour design options influences people's perceptions, thereby providing more foundational suggestions for urban transportation space design.

APPENDIX

The questions in the first section of the online survey:

(1) Do you work for the MTR company? (Yes; No)

(2) What is your age? (Under 18; 18-30; 30-60; Over 60)

(3) What is your gender? (Female; Male)

(4) Do you live in Hong Kong? (Yes; No)

(5) Do you speak Cantonese / Chinese? (Yes; No)

(6) Are you an architect/designer/urban planner/artist or a student in a related field? (Yes; No)

(7) Please rate the frequency with which you use the MTR as your transportation mode: (Never; 1-3 times per month; 1-3 times per week; On weekdays; Every day)

(8) Do you think the space of Hong Kong MTR stations is distinctive? (Strongly agree; Agree; Neither agree nor disagree; Disagree; Strongly disagree)

(9) Have you noticed the different colour design in MTR stations? (Yes; No)

(10) Do you use the indoor colour scheme of MTR stations to identify them? (Yes; No)

(11) Based on your experience, what is your overall satisfaction level with the spatial quality in MTR subway stations? (Very good; Good; Fair; Poor; Very poor)

The questions in the third section of the online survey:

(1) Of all the MTR stations below, your personal favorite is: (Tsim Sha Tsu; Hung Hom; Central; Admiralty; Diamond Hill; Mong Kok; Yau Ma Tei; Causeway Bay; Kennedy Town; Prince Edward)

(2) Why do you like this MTR station most?

(3) Do you think the colour design can help the station improve the space experience?

(4) Do you have any suggestions or comments on the colour and space design of MTR stations?

REFERENCES

1. Cha, S. H., Zhang, S., & Kim, T. W. (2020). Effects of Interior Color Schemes on Emotion, Task Performance, and Heart Rate in Immersive Virtual Environments. *Journal of Interior Design*, *45*(4), 51–65. https://doi.org/10.1111/joid.12179
2. Meerwein, G., Rodeck, B., & Mahnke, F. H. (2007). *Color—Communication in Architectural Space*. DE GRUYTER.
3. Wong, M. (2011). Another look at Hong Kong's mosaic tiled buildings. *Checkerboard Hill*. https://www.checkerboardhill.com/2011/07/hong-kong-building-walls-mosaic-tile/
4. Xue, C., Ma, L., & Hui, K. (2012). Indoor 'Public' Space: A study of atria in mass transit railway (MTR) complexes of Hong Kong. *Urban Design International*, *17*. https://doi.org/10.1057/udi.2012.6
5. Manav, B. (2017). Color-emotion associations, designing color schemes for urban environment-architectural settings. *Color Research & Application*, *42*(5), 631–640. https://doi.org/10.1002/col.22123
6. Zennaro, P. (2017). Strategies in colour choice for architectural built environment. *Journal of the International Colour Association*, *19*, 15–22.
7. Pyykkö, S. (2023). Conceptualizing the chromatic experience of environment: Two case studies using the Color Walk method. *Color Research & Application*, *48*(5), 585–598. https://doi.org/10.1002/col.22878
8. Küller, R., Mikellides, B., & Janssens, J. (2009). Color, arousal, and performance—A comparison of three experiments. *Color Research & Application*, *34*(2), 141–152. https://doi.org/10.1002/col.20476
9. Wang, J., Zhang, L., & Gou, A. (2020). Study on the preference of city color image selection based on the logistic model: A case study of Shanghai. *Color Research & Application*, *45*(3), 542–557. https://doi.org/10.1002/col.22487
10. Anter, K. F. (2000). *What colour is the red house?*
11. Angelo, K., & Booker, A. (2016). *Perceived Colour and Colour Perception.*
12. Sochocka, A., & Anter, K. F. (2017). Perceived façade colours in different daylight situations: Survey in the Old Town of Warsaw. *Journal of the International Colour Association, 17, 92-119.*
13. Berns, R. S. (2019). *Billmeyer and Saltzman's Principles of Color Technology* (4th ed.). Wiley. https://doi.org/10.1002/9781119367314
14. *Colourpin II*. (n.d.). NCS Colour. https://ncscolour.com/colourpin-ii/
15. *NCS+ App*. (n.d.). NCS Colour. https://ncscolour.com/ncs-app/

Effect of Wall Color on Comfort of Indoor Space

Yoshihiko Azuma[1]* and Zhang Dongai[2]

(Tokyo Polytechnic University, 5-45-1 Iiyamaminami)
[1]Department of Engineering, Faculty of Engineering, Tokyo Polytechnic University, Japan.
[2]Graduate School of Engineering, Tokyo Polytechnic University, Japan.

*Corresponding author: Yoshihiko Azuma, azuma@t-kougei.ac.jp

ABSTRACT

In this study, we conducted two experiments to reveal the essential conditions of wall colors that are important for designing comfortable and cozy indoor spaces. In the experiments, we used a VR headset (VIVE COSMOS) for stimulus presentation. In the first experiment, 12 participants evaluated the visual impressions of 10 sample colors (vivid and pale tones of red, yellow, green, and blue, as well as white and gray) selected from the PCCS color system. For each sample color, psychological evaluation was performed using a 7-point Semantic Differential Scale and the average scores for each evaluation criterion were calculated. The results indicated that vivid tones of red and yellow were dominant in impressions such as "animated", "warm", "bright", and "loud". Pale tones consistently gained high ratings for "calming" regardless of hue. White and gray were associated with high ratings of "cold" and "calming", and white also conveyed impressions of "light" and "bright". In the second experiment, 3D CG images of single-room interiors were generated using the 10 sample wall colors, employing the software MAYA. Participants observed these images through the VR headset, during which their brainwaves were measured. The occurrence rate of alpha waves, known to reflect a relaxed state of the brain, was obtained from these measurements. Since there are individual differences in the occurrence rate of alpha waves, we found that many participants tended to have a high occurrence rate for pale tone of green, vivid tone of blue, and gray, and a low occurrence rate for white and red. In comparison of the results of the two experiments, it was suggested that pale tone of green, vivid tone of blue, and gray wall, which have a calm psychological impression, induce alpha waves, and have a high relaxing effect, while red and yellow are not suitable for indoor spaces where comfort is desired.

Keywords: comfort of indoor space, wall color, visual impression, alpha wave occurrence rate, relaxing effect

INTRODUCTION

In indoor spaces, the color of the walls is considered a crucial element in shaping the overall impression of the space and is believed to have various psychological effects on individuals who occupy it. These effects can range from creating a sense of tension or relaxation to inducing excitement or calmness, and they vary depending on the colors of the walls. These psychological effects of wall colors have primarily been evaluated through subjective assessments using the Semantic Differential (SD) method in experimental settings that utilized different colored wallpapers and similar materials to simulate indoor spaces [1]. Additionally, attempts have been made to measure physiological responses such as blood pressure, heart rate, and brainwave patterns as indicators for evaluation [2]. In these studies, experimental laboratories simulating indoor spaces or partitions were often used instead of actual indoor environments. Using partitions can create a significantly different impression from the actual interior space, making it difficult to say that it is an appropriate method. Furthermore, preparing a laboratory where wall colors can be changed in various ways is not an easy task. Therefore, we explored a method that would allow us to achieve effects equivalent to those of actual indoor experiments while easily changing the wall colors.

In recent years, with the improvement in the quality of 3D computer-generated (CG) images and the immersive experience offered by Virtual Reality (VR), it has become possible for individuals to feel as though they are truly within indoor spaces. Therefore, this study employs VR images to simulate indoor environments and assess the colors of the walls. The objective is to find the wall color conditions that create a comfortable and cozy indoor space, specifically aiming to reveal colors that induce a sense of relaxation. Additionally, the study investigates these conditions not only from a psychological perspective but also from a physiological standpoint.

METHODOLOGY

In this study, computer-generated (CG) one-room interior images were created, and the room's walls were presented in 10 different colors to examine the psychological and physiological effects they have on individuals. For the psychological effects, the Semantic Differential (SD) method was employed, while for the physiological effects, the occurrence rate of alpha waves, known to be associated with the body's relaxation state among brainwave patterns, was investigated.

Sample colors

As sample colors for the experiment, a total of 10 colors were selected from the Practical Color Co-ordinate System (PCCS) color chart, including vivid and pale tones of red, yellow, green, blue, as well as neutral white and gray colors. These colors were approximately reproduced on a display using the hexadecimal color codes listed in Table 1.

Table 1: Hexadecimal Color Codes of the Sample Colors

color name	vivid red	vivid yellow	vivid green	vivid blue	pale red	pale yellow	pale green	pale blue	white	light gray
reproduction example										
hex color code	#EE0026	#FFE600	#33A23D	#0F218B	#FBB4C4	#FFFFB3	#CCEBC5	#B3D7DD	#FFFFFF	#B5B5B5

Apparatus

To present and observe the sample colors and images in virtual reality (VR), an HTC VIVE COSMOS ELITE headset, as shown in Figure 1, was used. The display of the headset features dual 3.4-inch screens with a resolution of 1440 x 1700 pixels per eye and a refresh rate of 90 Hz. For control purposes, a Thirdwave Lightning AH5 PC was used, equipped with a Ryzen 5 3500 CPU, 8GB of memory, 256GB SSD storage, and an NVIDIA GeForce GTX 1650 graphics card. To maintain the participants' posture consistently, the headset was secured to the chinstrap.

Figure 1. VR headset used for observation

Participants

Twelve university students aged 21 to 26 with normal color vision participated in two separate experiments, as described below. The participants included 3 Japanese males, 3 Japanese females, 3 Chinese males, and 3 Chinese females.

Experiment 1: Impression Evaluation of Sample Colors

To investigate the psychological effects of the sample colors, an impression evaluation was conducted using the Semantic Differential (SD) method. To facilitate the evaluation, 10 pairs of adjectives suitable for the purpose of this study were selected through a preliminary experiment from the evaluation words commonly used in previous research. A response sheet, as shown in Figure 2 (originally in Japanese), was prepared. Participants observed the sample colors through the headset for 5 seconds each and evaluated their impressions on a 7-point scale for each pair of adjectives, recording the results on the response sheet. The presentation order of colors was white, vivid red, vivid yellow, vivid green, vivid blue, gray, pale red, pale yellow, pale green, and pale blue. The experimental setup is shown in Figure 3.

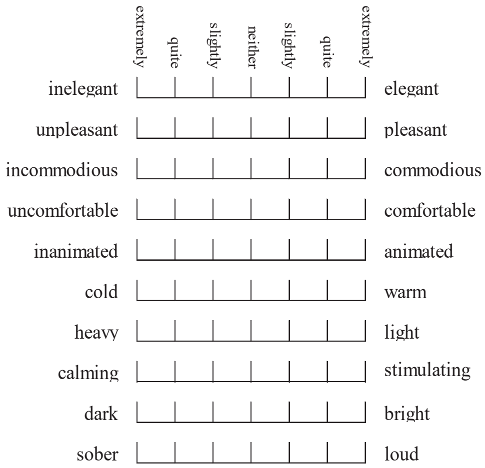

Figure 2. Response sheet for 7-point Semantic Differential Scale

Figure 3. A participant observing sample colors

Experiment 2: Evaluation of VR Indoor Images

Using the CG software MAYA, we set up daylight white lighting conditions and created indoor image data of a one-room setting as depicted in Figure 4. Based on this image, we prepared evaluation images with the walls colored in the 10 sample colors. These evaluation images are shown in Figure 5.

Figure 4. An interior image created with MAYA

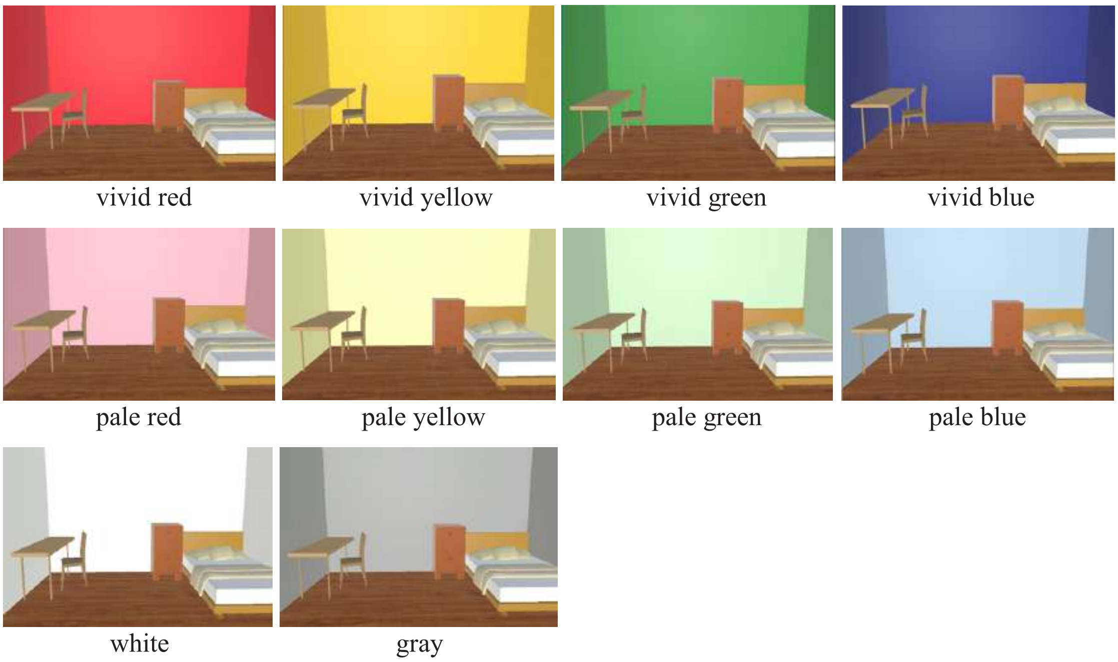

Figure 5. Interior images with walls in sample colors

Participants observed the evaluation images as VR images through the headset, and we examined how the relaxation state varied based on the wall color. First, one evaluation image was presented for 45 seconds, followed by a uniform gray image displayed for 15 seconds. Then, a different wall color evaluation image was presented for 45 seconds, followed by another presentation of the uniform gray image. In this procedure, images of all wall colors were presented, and the participants observed the images presented sequentially.

To assess the relaxation state of the participants, we measured alpha (α) waves using a simplified brainwave measurement device (Muse Brain System). Alpha waves are closely related to relaxation and comfort. We calculated the alpha wave occurrence rate, which serves as an indicator of the participant's relaxation state, using the following formula.

$$Alpha\ wave\ occurrence\ rate = (Q(\alpha))/(Q(\theta) + Q(\alpha) + Q(\beta)) \quad (1)$$

$Q(\theta)$, $Q(\alpha)$, and $Q(\beta)$ represent the occurrence quantities of Theta waves, Alpha waves, and Beta waves, respectively. The alpha wave occurrence rate calculated using Eq. (1) was determined for each second, and the average value over the measurement period was used.

RESULT AND DISCUSSION

Impression Evaluation of Sample Colors

Figure 6 shows the evaluation results using the SD method in the form of an image profile. Differences in evaluations based on the hue of the samples can be observed, but overall, vivid tones show more pronounced variations in evaluations based on hue compared to pale tones. Vivid red and yellow are predominantly associated with "animated", "warm", "bright", and "loud", while for pale tones, "calming" is consistently high regardless of the hue. White and gray gained high ratings for "cold" and "calm," while white also conveyed impressions of "light" and "bright."

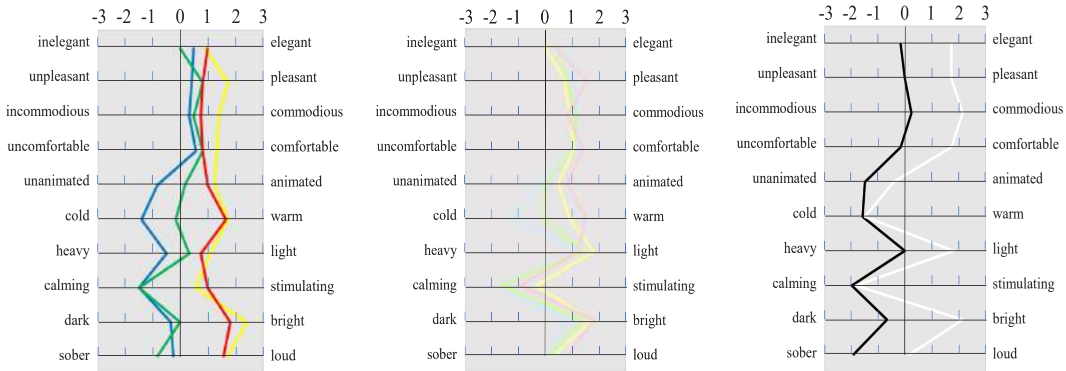

Figure 6. Evaluation results based on the SD method as illustrated in image profiles

Evaluation of VR Indoor Images

Figure 7 shows the results of calculating the average alpha wave occurrence rates during the observation of simulated indoor images (VR images) for the 12 participants. Error bars represent the standard deviation. It is evident that there is little difference observed based on wall colors. Figure 8 presents the results averaged separately for Japanese and Chinese participants. In the case of Japanese participants, there is some variation in the alpha wave occurrence rates based on wall colors. The rates are slightly higher for "vivid blue," "pale red," "pale yellow," "pale green," and "gray." However, for Chinese participants, there is little difference observed based on wall colors.

Furthermore, when examining Japanese participants separately by gender and comparing the results, as shown in Figure 9, there is not much difference for Japanese males. However, for Japanese females, the previously mentioned trend observed in the Japanese average becomes more pronounced. Although the number of male and female participants is only three each, making it difficult to draw definitive conclusions, it can be suggested that Japanese females have higher alpha wave occurrence rates, indicating greater relaxation, for "vivid blue," "pale red," "pale yellow," "pale green," and "gray" compared to other colors.

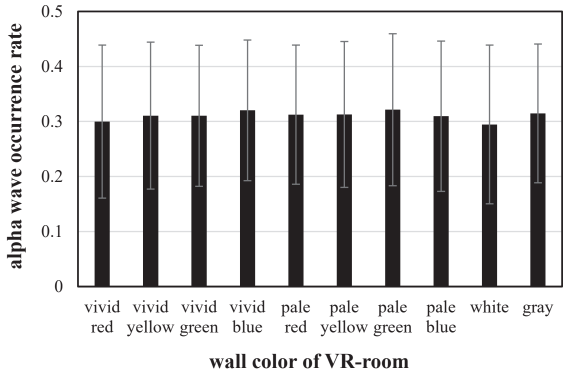

Figure 7. Averaged value of alpha wave occurrence rate for all participants

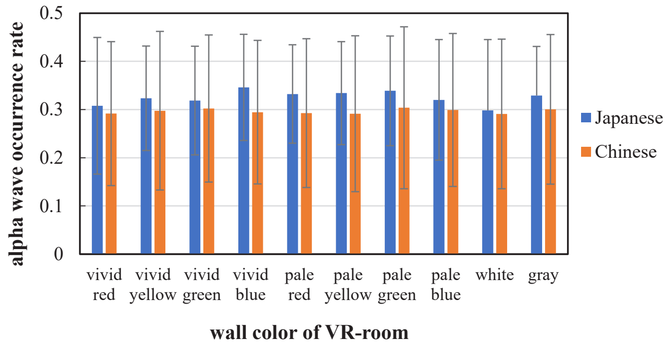

Figure 8. Comparison of alpha wave occurrence rate between Japanese and Chinese participants

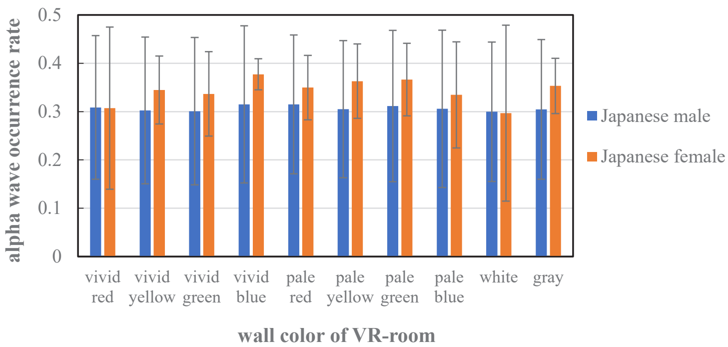

Figure 9. Comparison of alpha wave occurrence rate between Japanese male and female participants

relationship between impressions of sample colors and alpha wave occurrence rates

From the pairs of adjectives used in the impression evaluation of sample colors, specifically the "calming" - "stimulating" adjective pair, we obtained evaluation scores. These scores were then analyzed in relation to alpha wave occurrence rates, focusing on the average scores for all participants and the average scores for Japanese females who exhibited differences in alpha wave occurrence rates based on wall colors. The results are shown in Figure 10. For all participants, there was little correlation between the evaluation scores and alpha wave occurrence rates.

However, for Japanese females, a negative correlation was observed with a correlation coefficient of R = -0.485, indicating that colors rated as having a stronger calming psychological effect were associated with higher alpha wave occurrence rates. Therefore, it suggests that colors perceived as psychologically calming may also lead to higher alpha wave occurrence rates.

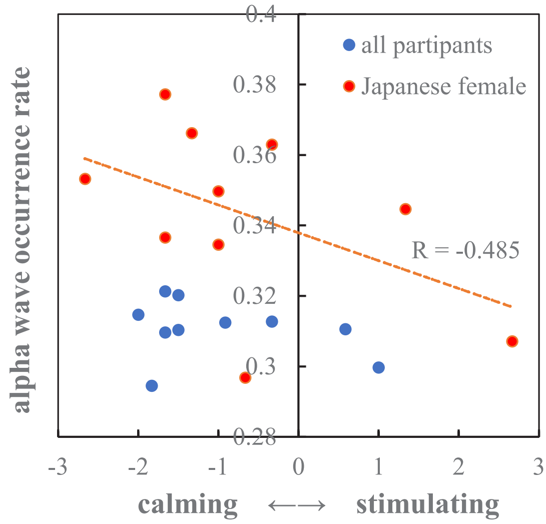

Figure 10. Relationship between psychological effect and alpha wave occurrence rate

CONCLUSION

The results of investigating the brain's relaxation state using alpha wave occurrence rates as an indicator suggest that vivid tones such as red, yellow, and white impose a higher cognitive load on the brain, indicating that they may not be suitable as wall colors for indoor spaces where comfort is desired. On the contrary, pale tones of green, vivid tones of blue, and light gray were found to have a relaxing effect on the brain, making them suitable choices for wall colors in such spaces.

ACKNOWLEDGEMENT

This work was supported by JSPS Core-to-Core Program（grant number: JPJSCCB20220006）.

REFERENCES

1. Nami, U., Hiroko, T. & Takuko, Y. (1990). An experimental study on the effects of the colour of furniture contiguous to the wall on the room-atmosphere. *The Japanese journal of ergonomics*, *26*(2), 67-73. doi: https://doi.org/10.5100/jje.26.67
2. Kazuko, I., Keiko, M. & Miho, S. (2008). Affective and Physiological Effects of Different Wall Color. *Color Science Association of Japan*, *32*(SUPPLEMENT), 98-99.

IMPROVING ABANDONED PET DETECTION IN NATURAL SPACES THROUGH ADAPTIVE SINGLE-COLOURED IMAGE AUGMENTATION TECHNIQUES

Oluwakemi Akinwehinmi[1]* and Pedro Arnau del Amo[2]

(CIMNE - Edifici C1 Campus Nord UPC C/ Gran Capità, S/N 08034 Barcelona,)
[1]*Information Technology, Engineering, University of Lleda, Spain.*
[2]*Information Technology, Engineering, UPC, Spain.*

*Corresponding author: Francesc Xavier Solsona Tehas, University of Lleda, Spain

ABSTRACT

Image data augmentation is a widely used technique in computer vision to enhance the performance of deep learning models by increasing the size and diversity of labeled datasets. However, traditional augmentation methods can be computationally expensive and may introduce biases or distortions in the data. In this research paper, we propose a novel approach to address these challenges in the domain of detecting abandoned pets in natural spaces.

Our paper explores the use of adaptive and automated image augmentation techniques specifically tailored to single-color signals in RGB, HSV and HSL. By applying single-channel image augmentation, we aim to overcome challenges related to illumination contrasts, occlusion, and scaling, thereby improving model performance. Second, we provide a detailed implementation methodology that effectively addresses the limitations of small image datasets in computer vision tasks. Our methodology employs state-of-the-art techniques for augmenting the dataset and demonstrates its effectiveness through graphical displays of performance. The results showed a significant improvement of approximately 4% in precision and recall when compared to the original RGB images. This finding supports our hypothesis that a larger and more diverse augmented dataset can enhance the performance of deep learning models on limited-sized datasets.

Our research study contributes to the field of animal detection in natural spaces by providing a practical solution for improving model performance through adaptive and automated single-color-channel image augmentation. Researchers to augment their image datasets, thereby reducing the need for extensive data collection and labeling, can utilize the proposed approach

Keywords: Dropout, Overfitting, CNNs, Image data augmentation, Biases, Color channel, robustness, Neural networks, Computer vision, Large Scale Visual Recognition Challenge.

INTRODUCTION

Image data augmentation is a widely used technique in computer vision that aims to increase the size and diversity of labeled training or testing sets. Augmentation has shown to improve the convergence, generalization, and robustness of deep learning models on out-of-distribution tests. However, collecting a large and diverse dataset can be difficult, expensive, and time-consuming, particularly in practical applications like detecting abandoned pets in the wild. Deep learning models can suffer from poor generalization due to insufficient labeled datasets, resulting in overfitting and reduced performance on new data. While image data augmentation has numerous benefits, there are also some potential drawbacks to consider. One disadvantage of image data augmentation is that it can increase the computational requirements and training time for deep learning models. Generating and processing each augmented image can be time-consuming and resource-intensive. Additionally, certain augmentations may not be appropriate for all types of datasets or applications, and improper use of augmentations can potentially introduce bias or distort the underlying patterns in the data. Finally, illumination contrasts, occlusion, and scaling issues arise with some augmentation practices.

To address this challenge, especially in the domain of stray animals in natural spaces, this research paper finds that using adaptive and automated image augmentation technique on single-color signals could potentially improve model performances. Our main contributions are:

- We address the recommendation by Connor and Taghi in their article "A Survey on Image Data Augmentation for Deep Learning" to explore performance benchmarks across color space augmentations across datasets in image recognition tasks. Our study has addressed this recommendation by using single-channel image augmentation techniques to enhance limited datasets for abandoned pets in natural spaces, as well as regularizing networks resulting in improved performance.

- This study provides a detailed implementation methodology that could potentially address data size limitations in computer vision tasks. The methodology employs state-of-the-art techniques to augment a small image dataset and demonstrates the effectiveness of the proposed approach through graphical displays of performance.

LITERATURE REVIEW

Undoubtedly, state-of-the-art research investigations and findings in deep learning have contributed significantly to advancements and increased accessibility of algorithms, hardware, and large labeled datasets. In the field of computer vision, the concept of augmenting images started with the ImageNet database and the Large Scale Visual Recognition Challenge, which became a primary benchmarking platform for advanced deep learning models for image classification after the breakthrough performance of AlexNet in 2012. Prior to this, fundamental image augmentations had been recognized as an essential technique for training neural networks for visual recognition [14], and AlexNet extended the usage to include random crops, translations, flips, and modification of the power of RGB channels, resulting in improved results.

In recent years, various novel state-of-the-art approaches to increasing input image datasets have been proposed and utilized, such as Set Pattern [6], Mixup [22], their derivatives [8], and combinations [21]. However, some of these approaches have been criticized for being too aggressive, resulting in decreased model accuracy and introducing biases in the dataset [7, 15]. For instance, while image rotation is an effective image data augmentation technique on CIFAR-10, it can adversely affect the model's ability to distinguish between handwritten digits 6 and 9 on MNIST [16].

Researchers have proposed new strategies, such as reducing the number of augmentations in the final epochs of data training to decrease the gap between clean and augmented data and improve model performance [11]. Additionally, AutoAugment [4] and Fast AutoAugment [17] use reinforcement learning to discover the ideal image data augmentation techniques through a discrete search space of transform operations. Population-Based Augmentation [12] focuses on generating augmentation strategy plans rather than fixed augmentation formulas. However, even these advanced augmentation techniques still lead to performance inconsistency on well-examined performance benchmarks. Thus, we can still improve by expanding the pool of utilized image augmentations to enhance the performance of deep learning models.

METHODOLOGY

In stray animal detection in natural spaces, having a large and diverse dataset is crucial for training machine learning models that can accurately identify and track animals. However, collecting and labeling a significant number of images can be challenging, costly, and may even cause harm to the animals. To overcome these challenges, image dataset augmentation is a popular approach to increase the size and diversity of these pet-focused datasets. This technique involves modifying the initial images by applying various transformations such as flipping, scaling, and cropping, among others. However, image data augmentation has a potential drawback of overfitting, where the model becomes excessively specialized on the training data and exhibits poor performance on new and unseen data. Therefore, it is essential to strike a balance between augmentation and regularization to ensure the model's robustness and accuracy.

Single-Color-Channel Image Augmentation: Single-color-channel image augmentation is a technique that applies to color channel spaces. It involves isolating each color channel in an image dataset to individual color channels. In a standard RGB image, there are three-color channels: Red, Blue, and Green, as shown in Figure 1. The RGB image color space is converted to Blue-Green-Red (BGR), or switches to another color format such as Hue-Saturation-Value (HSV), Hue-Saturation-Lightness (HSL), Cyan Yellow Magenta Key (CYMK), and more. We believe that using this technique will bring regularization to CNNs, and overcome challenges such as illumination contrasts, occlusion, and scaling.

Fig 1: Diagrammatic View of Color Channels in RGB, HSV and HSL formats

Creating Datasets with Declarative Parameters Definition

This research study follows the best practices of object-oriented design in Convolutional Neural Network (CNN) by defining a class with clear and well-documented structure for image augmentation operations. To create a large training dataset, a class named TrainingData is instantiated to accommodate the distinct categories of the manually labeled image datasets for image identification. We declare and create the path to save the training datasets in the designated folder.

```
def create_training_data():
    for category in CATEGORIES:
        path = os.path.join(DATADIR, category)
        class_num = CATEGORIES.index(category)
        for img in tqdm(os.listdir(path)):
            img_array = cv2.imread(os.path.join(path,img))
            new_array = cv2.resize(img_array, (IMG_SIZE, IMG_SIZE))
            training_data.append([new_array, class_num])
```

The research study involved processing image datasets for abandoned pet detection using various techniques, including CNN-based resizing and color channel splitting for image augmentation. The study iterated through each dataset in every category, located them using indexing in an accumulated folder, and converted them from BGR to RGB for proper processing by the CNN features. We employed the technique of color channel splitting to split an RGB or BGR color channel into a single-color-channel dataset. To ensure each augmented dataset has a unique identifier, we attached a value channel to the separated color channels. We shuffled the training data to prevent overfitting and promote generalization, reducing variance and improving the learning effectiveness of the model.

Creating the Testing Data: To ensure diverse and extensive test data, this research study employs image augmentation enhancement. The initial step involves specifying the location of the datasets and the number of categories they were manually divided. To create the paths to all the image datasets in each category in the dataset folder, we define a class and use a for-loop.

```
def enhancer(factor):
    for category in CATEGORIES:
        count = 1
        path = os.path.join(DATADIR, category)
        for image in os.listdir(path):
            img = os.path.join(path, image)
            im = Image.open(img)
            enhancer = ImageEnhance.Brightness(im)
            factor = factor
            im_output = enhancer.enhance(factor)
            enc = path + '_en'
            print(enc)
            os.chdir(enc)
            im_output.save(category + '_enhanced' + str(count) + str(factor) + '.jpg
            os.chdir(DATADIR)
            count += 1
```

Afterwards, we carry out the image enhancement technique on the datasets in this research study by iterating over each image dataset per category in the image augmentation task. We implement the image enhancement technique using the code snippet above, which enhances the brightness of the image dataset. We save the augmented dataset to a new directory with a unique identifier. Overall, this enhancement technique enables us to create large and diverse test data in this research study, which is crucial for building a robust and accurate model.

RESULT AND DISCUSSION

We hypothesized that a larger and more diverse augmented dataset can improve the performance of deep learning models on limited-sized datasets. To test this hypothesis, we collected animal image datasets from Kaggle and used our proposed single-channel image augmentation technique to create an augmented training dataset. The original training dataset contained 17,500 animal images, and the proposed technique created a new augmented training dataset consisting of 5000 single-channel images per class, resulting in 35,000 training images. We trained and evaluated a deep learning model on both the original RGB images and the single-channel augmented data. The model achieved roughly a 4% increase in precision and recall with the augmented data, confirming our hypothesis. Researchers to augment their image datasets and improve model performance can use a significant contribution to the field of animal detection in natural spaces, as the proposed technique.

Image Dataset	Precision Initial Datasets	Precision Augmented Dataset	Image Dataset	Recall Performance on Initial Datasets	Recall Performance on Augmented Dataset
Animal 1	0.83	0.94	Animal 1	0.87	0.78
Animal 2	0.73	0.55	Animal 2	0.87	0.94

Animal 3	0.96	0.83	Animal 3	0.77	0.91
Animal 4	1.00	0.99	Animal 4	0.83	0.87
Animal 5	0.63	0.94	Animal 5	0.79	0.79
Animal 6	0.69	0.91	Animal 6	0.88	0.76
Animal 7	1.00	0.96	Animal 7	0.57	0.80
Accuracy					
Macro Average	**0.83**	**0.87**		**0.80**	**0.83**
Weighted Average	**0.83**	**0.88**		**0.80**	**0.84**

Table 1: Performance Comparison of Precision and Recall for Initial and Augmented Image Datasets

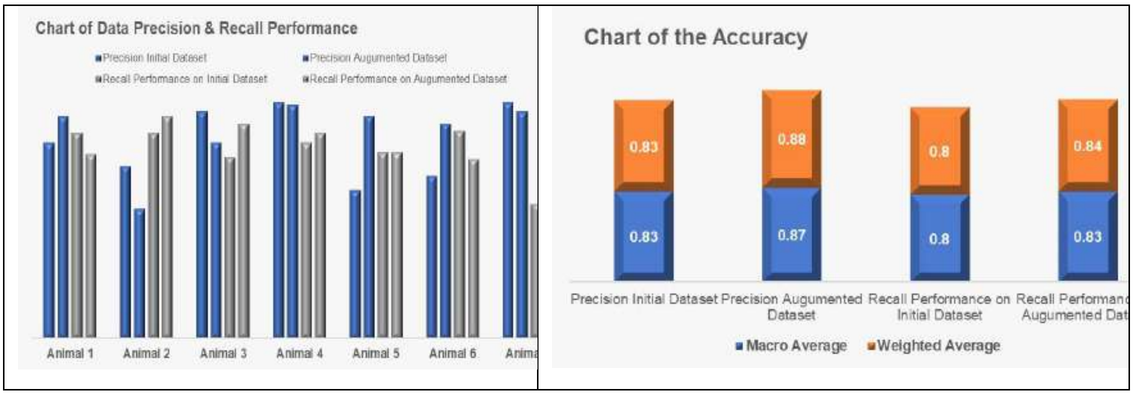

Figure 2: Graphical Comparison of Precision and Recall for Initial and Augmented Sets.

DISCUSSION

This research study demonstrates a 4% improvement in classification precision when using single color space image datasets in comparison to default RGB, HSV or HSL image datasets, using CNN. This finding challenges the presumption that color changes can dispose of vital color data, making it an unreliable augmentation technique. Some authors have found that single color space augmentation can result in a 3% drop in classification precision, making it difficult for the model to recognize objects in the picture. However, this research study overcame this challenge by using an image enhancement feature in CNN for label reservation and properties conservation, which helped to identify, recognize, and classify each category of creature within the datasets.

SUMMARY

The approach proposed in this study for single color space augmentation using CNN incorporates translational invariances into datasets, leveraging an augmentor and image enhancer to overcome issues with lighting, scale, and impediment. Lighting biases are a common challenge in image recognition problems, and the real-world application of single-color space augmentation can help solve issues with overfitting datasets in varying lighting conditions.

While we have proposed an image augmentation technique for creating large and diverse test data in our domain, we believe that there is potential for further refinement and exploration of its effectiveness on a wider range of datasets and tasks. Future research could investigate the impact of different color spaces and image enhancement techniques on model performance, including alternative color spaces like YUV, CMYK, or LAB. Additionally, different types of color space augmentation techniques could be compared to determine their effectiveness in various contexts.

Furthermore, there is potential to extend image augmentation techniques to other domains, such as natural language processing or speech recognition. Developing data augmentation techniques for text corpora or audio recordings could increase their size and diversity, potentially enhancing the quality of results obtained through these systems.

INTERESTS

The research paper authors declare that they have no competing interests.

REFERENCES

1. Aranzazu J, Miguel P, Mikel G, Carlos L-M, & Daniel P. *A comparison study of different color spaces in clustering based image segmentation. IPMU; 2010.*
2. Bengio, Y, Bastien, F, Bergeron, A, Boulanger-Lewandowski, N, Breuel, T, Chherawala, Y, Cisse, M, Côté, M, Erhan, D, & Eustache, J et al. *Deep learners benefit more from out-of-distribution examples. In Proceedings of the Fourteenth International Conference on Artificial Intelligence and Statistics. Ft. Lauderdale, FL, USA, 164–172.*
3. Bruno, A, Ardizzone, E, Vitabile, S, & Midiri, M. *A novel solution based on scale invariant feature transform descriptors and deep learning for the detection of suspicious regions in mammogram images. J. Med. Signals Sens. 2020, 10, 158.*
4. Cubuk, E.D, Zoph, B, Mane, D, Vasudevan, V, & Le, Q.V. *AutoAugment: Learning Augmentation Policies from Data. arXiv 2018, arXiv:1805.09501.*
5. Deng, J, Dong, W, Socher, R, Li, L.J, Li, K, & Fei-Fei, L. *Imagenet: A large-scale hierarchical image database. In Proceedings of the IEEE Conference on Computer Vision and Pattern Recognition (CVPR 2009), Miami, FL, USA, 248–255.*
6. DeVries, T, & Taylor, G.W. *Improved regularization of convolutional neural networks with cutout. arXiv 2017, arXiv:1708.04552.*
7. Graham, B. *Fractional max-pooling. arXiv 2014, arXiv:1412.6071.*
8. Guo, H, Mao, Y, & Zhang, R. *Mixup as locally linear out-of-manifold regularization. In Proceedings of the AAAI Conference on Artificial Intelligence, Honolulu, HI, USA, 33, 3714–3722.*
9. Hendrycks, D, Mu, N, Cubuk, E.D, Zoph, B, Gilmer, J, & Lakshminarayanan, B. *AugMix: A Simple Data Processing Method to Improve Robustness and Uncertainty. In Proceedings of the International Conference on Learning Representations (ICLR), Millennium Hall, Addis Ababa, Ethiopia*.
10. Hernández-García, A, & König, P. *Further advantages of data augmentation on convolutional neural networks. In Proceedings of the International Conference on Artificial Neural Networks, Rhodes, Greece, 95–103.*
11. He, Z, Xie, L, Chen, X, Zhang, Y, Wang, Y, & Tian, Q. *Data Augmentation Revisited: Rethinking the Distribution Gap between Clean and Augmented Data. arXiv 2019, arXiv:1909.09148.*
12. Ho, D, Liang, E, Chen, X, Stoica, I, & Abbeel, P. *Population Based Augmentation: Efficient Learning of Augmentation Policy Schedules. In Proceedings of the International Conference on Machine Learning, Boca Raton, FL, USA, 2731–2741*.
13. Ken C, Karen S, Andrea V, & Andrew Z. *Return of the devil in the details: delving deep into convolutional nets. In: Proceedings of BMVC. 2014*.
14. LeCun, Y, Bottou, L, Bengio, Y, & Haffner, P. *Gradient-based learning applied to document recognition. Proc. IEEE 1998, 86, 2278–2324.*
15. Lee, H, Hwang, S.J, & Shin, J. *Rethinking Data Augmentation: Self-Supervision and Self-Distillation. arXiv 2019, arXiv:1910.05872*.
16. Lemley, J, Bazrafkan, S, & Corcoran, P. *Smart Augmentation Learning an Optimal Data Augmentation Strategy. IEEE Access 2017, 5, 5858–5869*.

17. Lim, S, Kim, I, Kim, T, Kim, C, & Kim, S. *Fast AutoAugment. In Proceedings of the Advances in Neural Information Processing Systems (NeurIPS), Vancouver, BC, Canada, 6665–6675.*
18. Liu S, Papailiopoulos, D, & Achlioptas, D. *Bad Global Minima Exist and SGD Can Reach Them. arXiv, 2019. arXiv:1906.02613.*
19. Oza, P, Shah, Y, & Vegda, M. *A Comprehensive Study of Mammogram Classification Techniques In Tracking and Preventing Diseases with Artificial Intelligence. Springer, Cham, Switzerland, 2022, 217–238.*
20. Shorten, C, & Khoshgoftaar, T.M. (2019). *A survey on image data augmentation for deep learning. J. Big Data, 6, 60.*
21. Yun, S, Han, D, Oh, S.J, Chun, S, Choe, J, & Yoo, Y. *Cutmix: Regularization strategy to train strong classifiers with localizable features. In Proceedings of the International Conference on Computer Vision (ICCV), Seoul, Korea.*
22. Zhang, H, Cisse, M, Dauphin, Y.N, & Lopez-Paz, D. *Mixup: Beyond empirical risk minimization. In Proceedings of the International Conference on Learning Representations (ICLR), Vancouver, BC, Canada.*

A METHODOLOGICAL APPROACH TO COLOUR CONSTRUCTION FOR ISLAND FISHING VILLAGE COMMUNITY BASED ON "SOCIAL LIFESTYLE"

Xue. Mao[1]*

(China Academy of Art, Liangzhu Campus, Liangzhu, Hangzhou)
[1] Foundation Studies, China Academy of Art, China.

Corresponding author: Xue Mao,502950699@qq.com*

ABSTRACT

This study takes the theoretical model of rural "social lifestyle" as the top-level theory, and focuses on the self-sustaining living conditions of rural residents. Taking the island-type fishing village as the research object, and using the community color creation as a means, this paper explores the methodology of community color creation based on "social lifestyle". Starting from the "three rural issues" in fishing villages, a community color creation methodology based on the "soft environment" of social life, the "hard environment" of physical space, and the "three-in-one" co-construction of the main villagers is formed. Taking Dachen Island in Taizhou City, Zhejiang Province, China as an experimental field, the "Island Colour" workshop was launched, which emphasized that community colour construction was a mild and flexible endogenous force, paid attention to the capitalization of local colour resources in rural areas, and improved residents'awareness and ability of colour construction from the perspective of "bottom-up" sustainable construction. In order to verify that the colour creation based on "social lifestyle " is a tool of social innovation and change with the participation of multiple subjects.

Keywords: Social lifestyle, Island-type fishing village, Community colour development method.

INTRODUCTION

This project is the overall color construction project of Dachen Island in Taizhou, which was appointed by the Dachen Island Development and Construction Management Committee of Taizhou by the Color Research Institute of China Academy of Art. The goal of the project is to improve the landscape environment of the island by focusing on the color resources of Dachen Island. While inheriting and protecting the traditional living conditions of fishing villages, tourism should be renewed and developed to achieve the transformation of fishing villages and sustainable value-added benefits. Moreover, it can activate local residents and tourists to participate in the action of community color creation.

As an isolated village far away from the mainland and surrounded by the sea, island fishing villages have a unique island-style "social lifestyle". There are a large number of island fishing villages in China, especially the islands in eastern Zhejiang that have the largest number of islands in China. However, due to inconvenient transportation, aging population, labor shortage, over-development and other reasons, there have been problems such as low quality landscape and loss of regional ecological characteristics. Both local residents and government managers lack attention to the local rural lifestyle. Therefore, how to highlight the characteristics of residents' daily life, activate the vitality of regional charm, and enhance the enthusiasm of community residents to spontaneously construct their own living environment? As a tourist island, there is an urgent need to explore and reshape its own "lifestyle" landscape through colour creation.

The project lasted four years starting in 2018 and went through three phases. The first stage is the overall landscape colour planning and guideline preparation of Dachen Island; the second stage is community colour design, that is, through micro-update colour design for the soft and hard environment to improve the style and environment of Dachen Island; the third stage , community colour design management, holding periodic community color creation workshops for residents. We hope to use a progressive and participatory workshop format to enhance residents' interest in and ability to participate in community color creation awareness, and realize a community colour creation model from government-led to community-led, so as to improve local environmental aesthetics and increase community Neighborhood activities enhance residents' sense of regional cultural identity.

METHODOLOGY

In this paper, the methods of interdisciplinary literature research, the combination of qualitative and quantitative research, visual research, comparative case study and practical research are used to conduct in-depth research through the cross-process of theory, investigation, interview, collation, construction, practice, feedback, inspection and improvement.

(1) Interdisciplinary literature research: The disciplinary framework of this paper is a trinity of interdisciplinary knowledge framework with humanities and social sciences as the logical starting point, urban and rural planning and design as the field, and colour discipline as the perspective. This paper makes an interdisciplinary study of the existing literature on life landscape, urban and rural color planning, community construction and other related fields at home and abroad.

（2）Case comparative study: The author visited more than 10 islands of different types at home and abroad, and conducted comparative research from the perspectives of natural colour, humanistic colour, architectural colour and life colour.

(3) Quantitative research-questionnaire survey: The author takes Dachen Island in Taizhou as the research object of the design survey, through the questionnaire survey of different groups in the community, collects the evaluation of local residents, tourists, operators and other different groups on the local environmental colour and the acceptance of community building activities, and summarizes the building path and methods from the data.

(4) Visual research method: Through the visual analysis method of colour atlas and chromatogram, the color resources of fishing villages extracted by field shooting, visiting, colorimetric, sampling and other methods are visualized, so as to analyze the color resource data, form the color database of island-type fishing villages, and lay the foundation for the construction of digital color management of fishing villages.

(5) Practical research: This paper applies the methodology of theoretical construction to Xiadachen Island, Taizhou, Zhejiang Province, and constantly revises and improves the methodology of community colour construction through periodic community color construction and regular return visits and feedback research.

RESULT AND DISCUSSION

The theory of "social lifestyle" comes from the theory of "lifescape", which Haruhiko Goto (2006) defines as: "a landscape with a strong sense of life. It does not refer specifically to government officials, experts, and intellectuals, but through unknown local people. A self-generated living environment cultivated by the social management of sei-katsu-sha and craftsmen." Haruhiko Goto (2007) also proposed: "Excellent 'living scenery' as a community landscape is nurtured through daily maintenance and management under residents' autonomy. .'Lifescape' and 'resident autonomy' are closely related."

Community color creation can be understood as the effective extraction, design, and management of color elements based on regional color resources, with "social lifestyle " as the core, and regional development as the goal. By empowering residents and using participatory color creation with a diverse group of people, it gives the community life pleasure, activates the community's endogenous power, and jointly builds a comprehensive creation of community cohesion.

Based on the theory of "social lifestyle" and the characteristics of community color creation, this article proposes a community color design method based on "social lifestyle" and uses Dachen Island as an experimental field for practice.

Method 1, a community colour design method based on the "hard environment" of physical space;

The "hard environment" of material space refers to the tangible physical space environment surrounding regional settlement space, place space, and building units. "Hard environment" colours will form intuitive color images due to their larger scale. Based on the three aspects of the "hard environment" of physical space, the author proposes "three methods" to enhance the color of the "hard environment" of community physical space. (1) Macro dimension: colour design of community settlement space based on landforms. (2) Meso dimension: spatial colour design of community places with functional zoning. (3) Micro dimension: community building colour design with material superposition.

The colour creation of individual micro-buildings in Dachen Island starts from the "prototype" of the building type and follows the "face" theory proposed by Semper. Retaining the characteristics of the island stone house architecture, using the "stone +" method, using the "same colour and heterogeneous" or "same color and heterogeneous" method, using stone as the basic material, adding imitation wood materials, transparent glass curtain walls, and granite , concrete, carbon steel plates and other modern composite materials are superimposed to enhance the brightness and chroma of the stone house architectural colours and enhance the richness of people's visual colours. (Figure 1)

Figure 1. Stone house architectural color micro-update

Method two, community colour design based on the “soft environment” of social life.

The "soft environment" of social lifestyle refers to regional culture, folk festivals, public facilities and other small-scale living artifacts and activities in non-macro spaces. Community colour design methods based on the "soft environment" of social lifestyle include (1) experiential community public facility colour design methods; (2) full-time colour design methods for regional cultural activities. Compared with the colour creation of the "hard environment" of physical space, the "soft environment" focuses more on community activities and the connection between community objects and people.

In the "soft environment" community color creation of Dachen Island, the author focuses on the color creation of community public facilities and cultural activities. The playground in Dachen Town is adjacent to Dachen Qingken Plaza and the township government. It is an important community activity venue in Dachen Island. It not only hosts villagers, community and neighborhood activities, but also is an important place for tourism and a transportation hub. The author uses colour as an element to connect groups of people, choosing blue and purple colors that are complementary to the yellow architectural colours of Dachen Island, and using gradient red to add fashion and vitality to the original playground, creating neighborhood activities and leisure A sports check-in place (Figure 2).

Figure 2. Playground color creation

Method three, community colour design based on the joint construction of villagers.

Community residents are the main body of community color creation. Only when community residents truly identify and love the community landscape colour and care for and maintain the landscape environment color in their daily lives can a good community colour state and form of sustainable development be formed. The author proposes four stages of community colour design jointly built by villagers, namely color awareness, colour visualization, colour resource utilization, and color autonomy.

The first step is a resident empathy research workshop, which aims to make community residents aware of the importance of color resources. Qualitative research fieldwork, in-depth interviews and quantitative research questionnaires were used to conduct empathic surveys with residents to collect first-hand information on residents' awareness of Dachen Island's style and color resources and their true willingness for public participation in community color creation. (Figure 3) .

Figure 3. Resident empathy research workshop

The second step is the " Island Colour " workshop activity. The purpose of this activity is to allow participating residents to record the island's natural colors, architectural colors and folk custom colors through photos, and to discover and visualize the island's colours. The expert team sorted out the interesting landscape photos taken by residents through classification and color genealogy to form Dachen Island's "Colour Landscape Card", which became a local cultural and creative product and improved the diverse people's understanding of regional culture and colour creation .

Unlike most previous color creations that only focused on the colour of physical space, the author hopes to explore community colour creation methods that empower residents' autonomy from the relationship between people and communities. Realize the dynamic shift from the "big government" power model of urban and rural construction to the "big society" of community construction. It also explores how community residents can go from discovering colour resources, to sharing color resources, to translating color resources, and finally to protecting colour resources through a sustainable process, realizing color design to unite the power of the community.

Figure 4. Dachen Island's "Colour Landscape Card"

CONCLUSION

The methodology constructed in this article is based on the existing problems of cultural identity, common interests, and lack of construction capabilities in urban and rural environments. It proposes solutions and methods by combining theory and practice. At the theoretical level, first of all, in order to make up for the current urban and rural color planning that ignores the construction power of residents and the colour problem of soft public facilities, cultural activities and neighborhood activities, community colour creation is proposed as a comprehensive creation that empowers the people. It includes the colour creation of the "hard environment" of the physical space in the "social lifestyle", as well as the color creation of the "soft environment" of social life. It also includes the comprehensive creation of relevant color organizations and colour activities with residents as the main body.

ACKNOWLEDGEMENT

Thanks to the Dachen Island residents, tourists, government personnel, etc. who participated in the Dachen Island empathy survey and island walking workshop for providing first-hand research information. Thanks to the students from the Colour Institute of China Academy of Art for participating in a series of shadow activities such as colour research, colour visualization, colour design, and colour education.

REFERENCES

1. Haruhiko Goto.（2006）. An expansive view of life. *Japan Society of Architectural Engineers Conference Energy Discussion Fee*,(09):26-32.
2. Architectural Institute of Japan.（2009）. Discovering the value of landscapes and urban development that are familiar to daily life. San Francisco, Tokyo: Xueyun Publishing House.
3. Gottfried Semper.（1989）. The Four Elements of Architecture and Other Writings. Trans. Harry F. Mallgrave and Wolfgang Herrmann (Cambridge).

EMOTIONAL RESPONSES TO IMAGES OF THE SAME SCENE WITH DIFFERENT COLOURS

Suchitra Sueeprasan* and Tananan Khantee

Department of Imaging and Printing Technology, Faculty of Science, Chulalongkorn University, Thailand.

*Corresponding author: Suchitra Sueeprasan, suchitra.s@chula.ac.th

ABSTRACT

The relationship between colour and human emotions has long been a subject of fascination and study within the field of psychology. Colour is a powerful tool that can evoke a wide range of emotional responses, making it a crucial element in various domains, including design, marketing, and psychology. This study delved into the intriguing interplay between colour and emotional response by exploring the impact of colour on individuals' reactions to images with identical content. The aim was to investigate whether colour could divert emotional responses to coloured images with the same content. Four pictorial images with different contents were included in the experiments: Sunrise, Beach, Festival, and Hope. The four image scenes had different emotional impacts. The original colours of each image were altered to obtain five reproduction images with different dominant tones: red, green, yellow, blue, and purple. Thus, there were six experimental images (five tones and one original) for each scene. The six images for each scene were printed with an inkjet printer on an A4 page of 120-gramme art paper. Fifty observers rated their emotional responses to each image according to four opposite-word pairs: fear/safe, tense/relaxed, sadness/joy, and boring/interesting, with each pair forming a 7-point scale (ranging from -3 to 3, where negative numbers represent negative emotions and vice versa). It was found that by casting a dominant colour over an entire image, the emotional responses to the images of the same scene changed. However, the effects of colour depended on image content. For an image with strongly positive content, colouring the image in one tone yielded a negative effect.

Keywords: Colour emotion, colour psychology, tone, image content

INTRODUCTION

The use of colour to convey emotions and elicit specific responses has been extensively explored in the realms of design, branding, and marketing. It is well-established that color can significantly influence human emotions, affecting our mood, behavior, and decision-making processes [1]. Colour psychology suggests that certain colours can evoke specific emotions and have a psychological impact on people, depending on their individual experiences and cultural associations. Designers use colour to create desired associations with products or services, such as blue for calmness and trust, and red for passion and excitement [2,3]. Numerous studies have investigated the psychological and physiological effects of colour, such as the concept of color symbolism [4] and color associations [5], the study of emotional responses to visual stimuli [6] and the role of color in eliciting affective reactions [7]. Nevertheless, there are several factors, besides colour, that can affect human emotions. While colour can arouse particular emotions and moods, image content can have a more direct and immediate impact on the viewer. Overall, both image content and colour can have a significant impact on design, and designers need to carefully consider both when creating visuals that communicate their intended message effectively. Understanding the relationships between colour and emotions is advantageous when considering its impact in the context of images with identical content.

This study investigated the effects of colour on emotional responses to coloured images with respect to image content. The aim was to examine whether different colours could lead to distinct emotional responses when the underlying image content remains constant.

METHODOLOGY

Four pictorial images with different contents were included in the experiments. Figure 1 shows the experimental images in their original colours. The first scene, "Sunrise", depicted the rising sun in a sea with an island. "Beach" featured a large expanse of white sand set against a bright blue sky. "Festival" was a picture of people gathered at a night-time event. The fourth scene, "Hope," was a portrait of a lady making a hopeful gesture.

Sunrise **Beach** **Festival** **Hope**

Figure 1. Original images.

The original colours of each image were altered using the Photo Filter tool in Adobe Photoshop by applying an 80% density of red, green, yellow, blue, and purple to generate five images with different tones. Thus, there were six experimental images (five tones and one original) for each scene. The six images were arranged into two columns on an A4 page and printed with an ink jet printer on 120-gramme art paper. Therefore, in visual assessments, observers saw all six images with identical content but different in dominant hues together in one page. The example of experimental prints is shown in Figure 2.

Figure 2. Experimental images for Sunrise.

Fifty observers (21 males and 29 females), 18–25 years of age, participated in the visual assessments. For each scene, they rated their emotional responses to all six different coloured images (including the original) according to four opposite-word pairs: fear/safe, tense/relaxed, sadness/joy, and boring/interesting, with each pair forming a 7-point scale (ranging from -3 to 3, where negative numbers represent negative emotions and vice versa). Each observer completed all four sets of image content. The emotional scores of each image were calculated by averaging the results of all observers.

RESULT AND DISCUSSION

Figures 3-6 show the results for Sunrise, Beach, Festival, and Hope, respectively. The negative values describe the intensities of the unfavourable emotions of fear, tension, sadness, and boredom. On the other hand, the positive values of the associated paired emotions represent the intensities of the positive feelings of safety, relaxation, joy, and interest, respectively. Overall, the emotional responses to different coloured images with identical content were found to shift when a dominating hue was applied to the entire image.

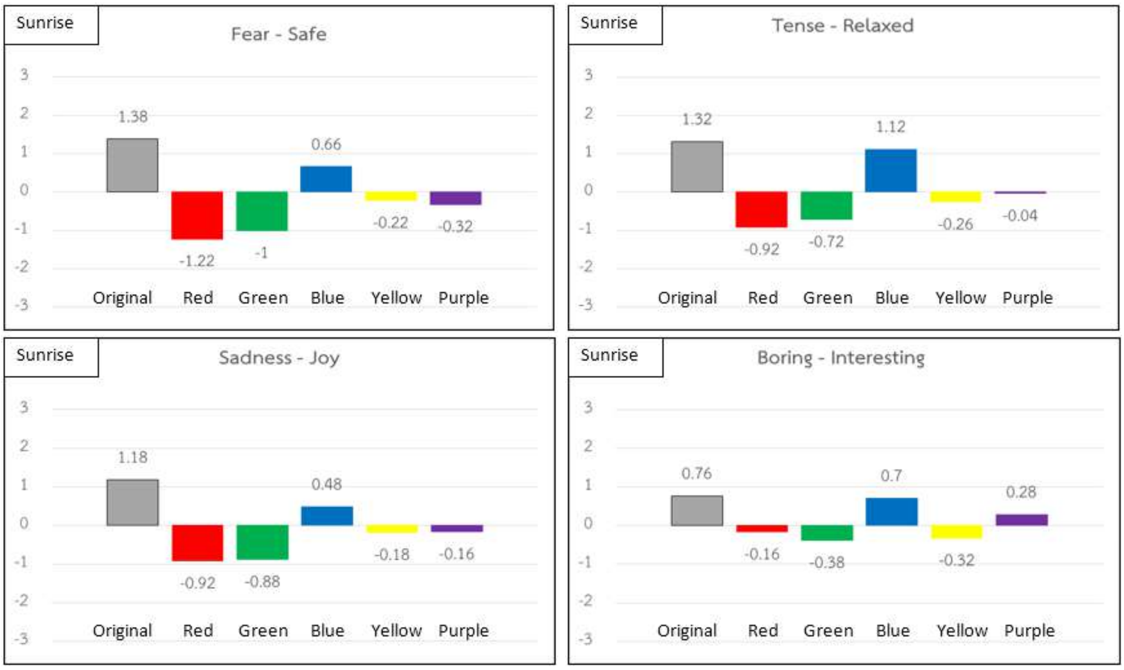

Figure 3. Results for Sunrise.

Red yielded unfavourable feelings with varying degrees depending on the emotions as well as image content. The emotion of fear was affected by red more strongly than the other hues, with Beach showing the highest shift from the response to the original coloured image. This is possibly because Beach depicts natural scene with calm and peaceful sea. The colour red broke the tranquility and infused danger into the image. People instinctively relate the colour red to the idea of rage, given that many people experience increased blood flow to the face when they are furious [8]. In the case of boredom, red gave a lower intensity than the other emotions, with Sunrise produced somewhat neutral response. It could be that the red sky is reasonably common for sunrise and sunset, so people are neither bored nor interested.

Blue created positive reactions in most cases. However, images with one predominating hue, albeit favourable one, reduced the positive degrees from the original colourful images. Blue turned all positive feelings into negative ones in the case of Hope, which had a powerfully optimistic message. Comparing with the other hues that also yielded unpleasant feelings to Hope, blue produced the least unfavourable effect. This suggests that portraying the entire image in a single dominant hue would provoke adverse reactions regardless of hue for an image with a highly optimistic message.

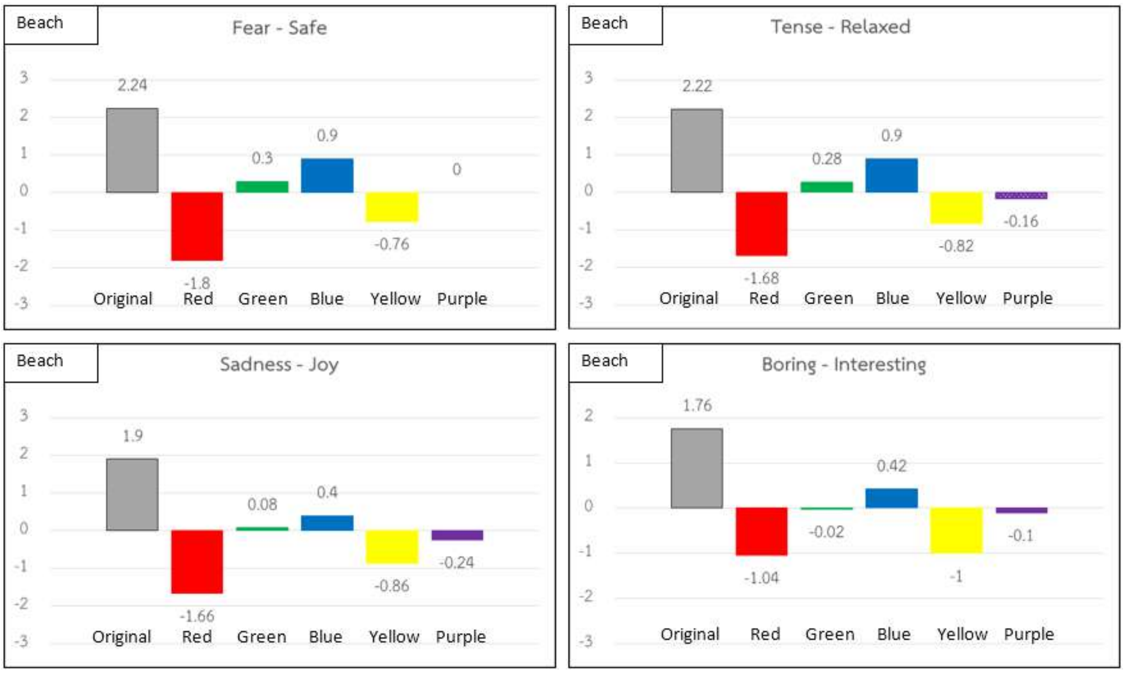

Figure 4. Results for Beach.

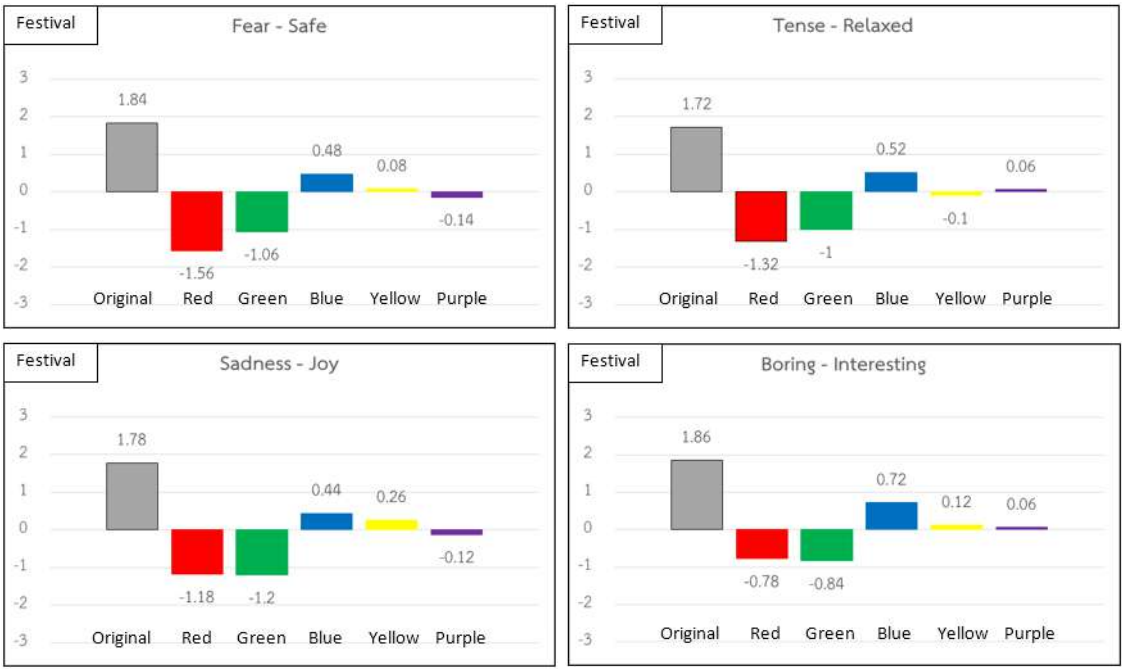

Figure 5. Results for Festival.

In most cases, purple neutralized all types of emotional responses to the original images. It was found that it was only for Hope that purple evoked somewhat unpleasant reactions. The probable cause for this case has been discussed above. As for other cases, since red often produced negative effects while blue positive ones, it is possible that purple, which is the combination of red and blue, eliminates all kinds of emotional reactions, as red and blue are opposed to each other.

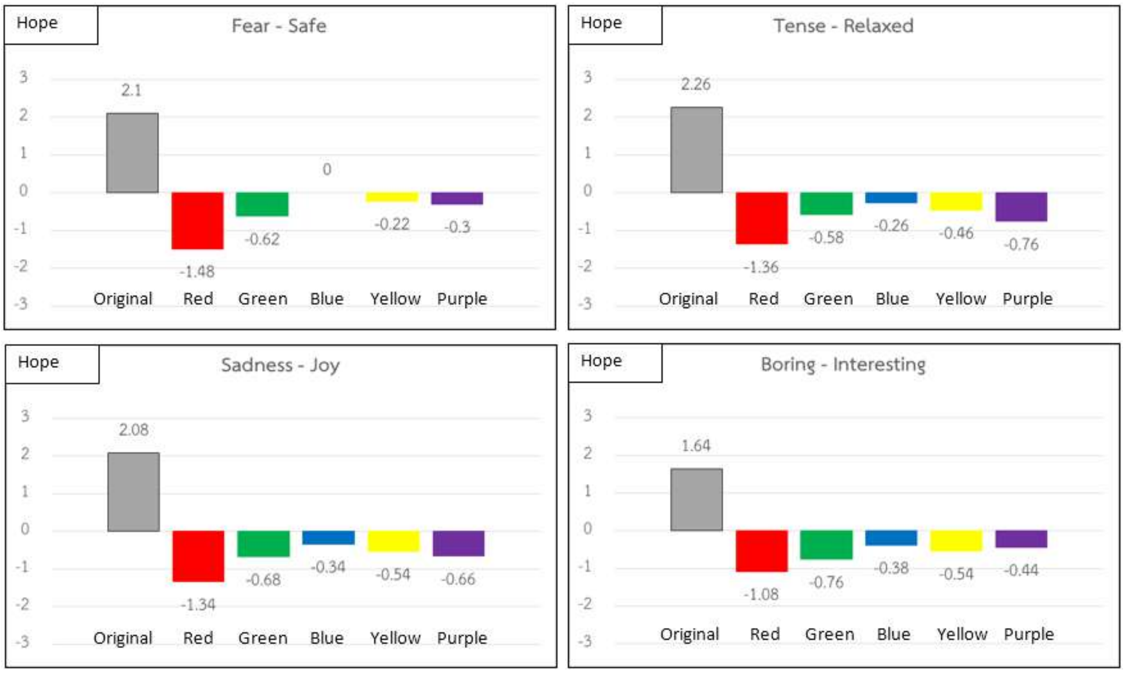

Figure 6. Results for Hope.

Yellow and green had varied degrees of impact on the emotional reactions to the images, ranging from somewhat pleasurable to noticeably unfavourable emotions, depending on the visual content. For Sunrise and Festival, the casting of green made the scene unnatural, resulting in unpleasant effects. For the nature scene as Beach, green could produce slightly favourable emotions. On the other hand, yellow evoked unpleasant reactions to Beach. It is possible that the casting of yellow illustrated too strong sunlight, which is unfavourable to be in such situation.

All in all, red and blue provoked more emotional effects than the other hues. Portraying an image with a single dominant hue could change the emotional responses to the image. The degrees of colour impact varied with image content.

CONCLUSION

The interplay between colour and human emotions is a multifaceted and captivating area of study. This study seeks to contribute to our understanding of this relationship by investigating how colour can impact emotional responses to images with the same content. Four different image contents with different emotional impacts, from neutral to positive, were included in the study. The colours of the original images were changed in such a way that the entire image had a dominant colour cast. The results showed that changing the prevailing hue of an image affected how observers reacted emotionally to images of the same scene. However, the effect of hue was influenced by the content of the image. Red induced negative emotions regardless of the image content. Blue elicited favourable reactions in most cases. Purple tended to give neutral responses to all emotions. In the case of yellow and green, the effects highly depended on image content. A negative result was produced when a picture with a strong positive message was coloured in one tone.

ACKNOWLEDGEMENT

The authors wish to acknowledge the financial support from the Faculty of Science, Chulalongkorn University. Thanks also go to all observers who took part in the visual experiments.

REFERENCES

1. Kurt, S., & Osueke, K. K. (2014). The effects of color on the moods of college students. *sage Open*, 4(1), 2158244014525423.
2. Kwallek, N., Lewis, C. M., & Robbins, A. S. (1988). Effects of office interior color on workers' mood and productivity. *Perceptual and Motor Skills*, 66(1), 123-128.
3. Elliot, A. J., & Maier, M. A. (2014). Color psychology: Effects of perceiving color on psychological functioning in humans. *Annual review of psychology*, 65, 95-120.
4. Ou, L. C., Luo, M. R., Woodcock, A., & Wright, A. (2004). A study of colour emotion and colour preference. Part I: Colour emotions for single colours. *Color Research & Application*, 29(3), 232-240.
5. Palmer, S. E., & Schloss, K. B. (2010). An ecological valence theory of human color preference. *Proceedings of the National Academy of Sciences*, 107(19), 8877-8882.
6. Lang, P. J. (1995). The emotion probe: Studies of motivation and attention. *American Psychologist*, 50(5), 372-385.
7. Valdez, P., & Mehrabian, A. (1994). Effects of color on emotions. *Journal of Experimental Psychology: General*, 123(4), 394-409.
8. Peromaa, T., & Olkkonen, M. (2019). Red color facilitates the detection of facial anger—But how much?. *PloS one*, 14(4), e0215610.

CONCENTRATION DEPENDENCY ON THE IDENTIFICATION OF PIGMENT

S. Khampaeng[1], P. Katemake[1*] and N. Tse[2]

[1] *Department of Imaging and Printing Technology, Faculty of Science, Chulalongkorn University, Thailand.*
[2]*Grimwade Centre for Cultural Materials Conservation, University of Melbourne, Australia*

*Corresponding author: Pichayada Katemake, pichayada.k@chula.ac.th

ABSTRACT

The multispectral imaging technique is used to capture images in various wavelengths, which can provide detailed information on the characteristics and texture of an object. This technique is widely used in multiple applications, such as art conservation. Specifically, this technique is one of the methods used to identify pigments in a painting before the restoration process. By analysing the reflectance of light reflected on the painting's surface using many wavelengths, multispectral imaging can assist in visualising the coloured paint in a captured image, which depends on the thickness, the opacity/transparency of its pigment, the concentration of pigment mixed with its binder, and the radiation/pigment interaction. This study proposes a method of identifying pigments using fifteen channels of wavelengths ranging from 365 nm to 706 nm with three pass filters: visible, UV and IR. This makes up forty-five channels in total. The procedure is threefold. Firstly, the making of the database: three hundred fifty-six Kremer pigments were activated by individual channels of 15 LEDs and captured the total reflectance through three filters. Secondly, a series of known samples comprising seven coloured pigments: cadmium red, alizarin red, indigo, lapis lazuli, Egyptian blue, yellow ochre and Naples yellow. They were mixed with acacia gum binder into six concentrations. These samples were representatives of artists' paintings having various lightness of paint. Subsequently, they were captured using the same technique as the database. Finally, the number of channels was optimised using the principle component analysis, and the accuracy of pigment identification based on the sum of colour difference between forty-five channels of the database and that of samples was demonstrated. The results show that the number of optimised channels could be reduced from forty-five to twenty-three. The percentage of accuracy of identification of some pigments is 100 in the first ten predicted pigments out of three hundred fifty-six. The advantage of combining reflected visible light, UV and IR channels and applying colour differences as a criterion of identifying could be used to narrow down the number of pigments in the predicted group. Furthermore, the various concentrations of Egyptian blue can be identified accurately. The reflected UV and IR images of these two pigments are unique. It implies that the pigment with unique characteristics is concentration independence. On the contrary, pigments without unique characteristics show high accuracy in a limited range of concentrations. The opacity/transparency of painted layers of non-unique features pigment influences the accuracy because the increased transparency gave a larger limited range of concentration.

Keywords: Pigment Identification, Multispectral Imaging, Color difference, PCA, single pigment

ACKNOWLEDGEMENT

This research received partial support from the Graduate Research Development Program, Faculty of Science, Chulalongkorn University.

THE QUESTION OF COLOR / THE COLOR IN QUESTION: CATHEDRAL OF PORTALEGRE, PORTUGAL

Rui Duarte[1]* and Ana Paula Pinheiro[2]

[1] *CIAUD, Research Centre for Architecture, Urbanism and Design, Lisbon School of Architecture, Universidade de Lisboa, Portugal.*
[2]*RBD.APP – Arquitectos, Lda, Portugal.*

*Corresponding author: Rui Barreiros Duarte, rbdapp@gmail.com

ABSTRACT

This paper refers to the Restoration of the Cathedral of Portalegre (16th century), a Portuguese National Monument since 1910, where color was key. The photographic information collected shows various uses of color, with the entire space decorated with paintings that covered the vaults, the plastered walls, as well as granite pillars. These paintings were removed in the 40s, by Estado Novo, an authoritarian regime that intended to annul the decorative painting to give an austere character to the space. The state of constructive degradation and works of art required a multidisciplinary team consisting of archaeologists, architects, restorers, and builders to work on the monument. The aim was to carry out a coordinated intervention, bearing in mind the material and symbolic authenticity, whose final resolution highlighted the chromatic qualities of the interventions. The General Directorate of Cultural Heritage supervised the intervention methodologies, having previously carried out Previous Reports on Immovable Heritage and Movable and Integrated Heritage. A survey of the architectural elements and a historical investigation into the materiality and color of the monument were carried out previously. Among the various works to be carried out, there was a need to restore the Mannerist altarpieces, unique in Portugal; glazed tile paneling had to be restored and corrected; it was necessary to restore the glazed tiles of the Old Sacristy; to cover the spires with glazed tiles; restore very dirty and degraded decorative elements; choose the color of the cloister. In the new support area, green roofs with flowers were created, responding to sustainability issues, while diluting their presence and letting go of heritage buildings. The lighting design and natural light highlight the beauty and color of the entire set. The results obtained met the expectations set out in the program, registering a global work of great rigor, with colors being used following historical investigations. Therefore, the architecture, paintings, and liturgical furniture harmony and authenticity of the set were achieved.

Keywords: Color, Authenticity, Glazed Tile, Restoration, Cathedral of Portalegre

INTRODUCTION

The project won 1st prize in a competition by invitation, a component of the 2014 *Rota das Catedrais*. [1]

The aim was: to restore the Cathedral of Portalegre, a 16th-century building and National Monument since 1910, which had fallen into major disrepair due to a lack of maintenance since the 1940s, and to provide the Cathedral with a program, spaces, and requisite infrastructure to make the complex as economically sustainable as possible. The Cathedral would become a religious and cultural center, bringing together events and offering a museum where the Cathedral's rich heritage would be exhibited: vestments, objects of worship, reliquaries, sculptures, and paintings.

"These Treasures had been collected since the 14th and 15th centuries, they are of unparalleled value due to the diversity of the pieces, their quality and artistic interest, along with the rarity of the collections." [2].

The approach was grounded in exhaustive historical and technical research, leading to the formulation of a Preliminary Report that served as the basis for the subsequent Project and Work. The work carried out shows the intentionality behind the decision-making process and the intervention methodology, in which color played a decisive role, guaranteeing the authenticity of this monument through the techniques, materials, and colors used.

DRCALEN and the DGPC were both integral to the Project, leading on archaeology and restoration. These heritage institutions oversaw the work as it progressed and approved the works.

This Framework underpinned the principles, techniques, and methods developed to create harmony, framing the architecture, paintings, and liturgical furniture with a view to ensuring their material and symbolic authenticity.

The technical, cultural, social, and economic objectives were formulated in an organic process in step with where and how to add value. This ensured that the Cathedral and the additional program of works were in keeping with regional integrity and collective memory.

Color is a determining factor in the overall process, as it expresses the material, textural, luminous, and chromatic qualities that appear when illuminated, in all its changing qualities.

It is critical to highlight the chromatic aspect in painted altarpieces, tile coverings, stone applications, plaster paintings, mortars, and veneer, and the connections these materials create with one another (Figure 1, left).

The restricted economic scope of the project demanded that the chromatic interventions were managed, opting for the solution in which the frescoes that were discovered during the work, remained hidden under whitewash, waiting for future restoration. Thus, for viewing these frescoes, apertures were opened in the plaster to hint at existing paintings, regardless of their current state of conservation (Figure 1, center-left).

The painting of the granite pillars that existed before the 1940s, and which showed continuity with the painting of the plasterwork of the vaults, according to records from the time (Figure center-right, Photo: SIPA), has definitively disappeared, as there were no longer any traces of it.

Figure 1. Photos: RBD.APP, 2023, and SIPA (center-right), 1941

The Chapel of Santiago was the only architectural space that retained the color given by the frescoes that were already visible (Figure 1, right), despite a high degree of degradation.

The existing structure next to the "Porta do Sol", made up of extensions, was demolished and a new area was erected to house technical facilities and toilets. The roof of this area has been landscaped in an extensive multi-colored system, using plant species that need minimal irrigation and maintenance. Climbing plants from the roof will grow in front of the glazed southern area, acting as natural shade (passive sustainability), making the works less conspicuous.

METHODOLOGY

The state of degradation of the building and the works of art required a multidisciplinary team of architects, archaeologists, restorers, and a builder to work on the monument.

All kinds of existing problems were considered, following this the architectural elements were surveyed, and a historical investigation was undertaken to consider the materials and color of the monument.

The Mannerist panels, which are unique in Portugal, needed to be restored; the tile panels, which had been altered and damaged, needed to be corrected; the decorative elements, already adulterated, had to be restored, returned to their original materials and color; and a new color was chosen for the cloister, previously changed by careless upkeep.

The methodology used resulted in a combination of techniques, materials, colors, and lighting to restore the original colors, materials, and the links between these.

The restoration of the altarpieces, the paintings on the mortar, and the apertures opened to reveal the underlying paintings, was carried out by qualified specialists using the appropriate techniques, to restore the colors after they had been carefully cleaned of the dirt that had accumulated over many decades.

Azulejos

The glazed tiles—*azulejos*—were located on the walls of the old Sacristy (Figure 2, left), on the wainscoting inside the Cathedral (Figure 2, center) on the staircase leading up to the Cloister terrace (Figure 2, right), and acted as a high plinth on three sides of the Cloister. According to Patrão "*On the baseboards of the cloister structure, they had haphazardly placed several azulejos taken from the cathedral chapels*." [3]

Figure 2. Photos: RBD.APP, 2023

The tile is a glazed and more reflective material, so it forms surfaces that preserve a good finish over time, providing the tile has a good quality topcoat with a thickness of around 10mm, and if it is fixed with lime mortar, so it bonds well with the substrate, which is necessary with mortar to allow good adhesion. Portland cement mortars should be avoided, as they do not maintain good adhesion over time, creating peeling surfaces and loose tiles. Glaze degradation, from broken pieces and omissions, needs upkeep repair, as the tile is susceptible to water damage and biological incursions that lead to vein cracks. These issues require good maintenance and careful cleaning over time, paying close attention to the peeling of surfaces, edges or seepage ingress. [4]

Glazed tiles were added to the whole complex in order to correct deficiencies in existing layouts and patterns. To do this, a preliminary survey was made of the glazed tiles available in storage and their quality, to these, tiles removed from the skirting boards on three of the cloister walls were also added, as there were already a great number of tiles loosened from their original fixture, many of them broken.

Mortars

In the composition of the mortars, the coloring process restored the existing colors as well as the veneers.

The ochre color was removed from the cloisters' plasterwork after discussions about its authenticity, as it didn't fit in with its architectural features, which were intended to be homogeneous, grounded in white marble columns on the north façade.

The grayish-white color chosen for the Cloister—Rialto IS13 paint by CIN—blends into the whole, bringing together the traces of architectural elements with the length of the galleries (Figure 3, left).

Figure 3. Photos: RBD.APP, 2023

Plastering

For the interior plastering of the Cathedral, we kept the existing finishing, based on lime water.

The exterior plastering was finished with CIN's Cinoxano Mineral white paint, which looks similar to lime but is more weather-resistant and requires less maintenance. In the remaining interior spaces, the plaster was also finished with CIN's Cinoxano Mineral white paint.

Marble

White marble is used as a 1.5m high wainscot to standardize the inner walls of the galleries and to mark a transition between more expensive materials and the plaster (Figure 3, center).

The interior floors are laid in white Estremoz marble. The large stone blocks create greater clarity and homogeneity in the spaces.

Granite

The brown of the granite on the exterior sidewalk and façade is another dominant color in the cathedral. The granite was cleaned of dirt and the joints were filled with adherent mortar in a color designed to blend in with its surroundings.

Wood

On the first floor, the colors of the exterior doors and wooden elements, such as the antechambers at the entrance to the Cathedral, which were painted a shiny dark brown, are now the traditional reddish color. This color was traditionally made with linseed oil, gold dust (highly toxic lead protoxide), and iron oxide (Fe_2O_3). It has now been replaced, after several experiments, with a satin finish paint, including priming, according to the manufacturer's recommendations, with CIN's Oxidrot color, RAL 3009.

On the upper floors, the wooden openings were painted white, RAL 9016, with acrylic water enamel paint, a satin finish.

For the wooden floors, we chose a light color, so the white pine wood selected was used (Figure 3, right). Beech was used for the wooden liturgical furniture, with a satin varnish.

Metals

A dark grey, anti-corrosive gel enamel paint for ferrous metals, Forge color Y764, was used to identify the material.

Tiles and green roof

The roofs are principally made up of fluted tiles on the coping and Roman tiles on the channel, of the same red clay color.

The green roof built in the new area was designed to create a natural transition with the adjacent cloister, enhancing interaction between colors and materials.

RESULT AND DISCUSSION

Spire (s)

The spires—8m tall octagonal pyramid towers—were very dilapidated and finished with plaster.

According to Patrão, the Cathedral’s historian, the towers were built “*with glazed tiles purchased in Lisbon to cover the spires and copper spheres*”. [5]

Patrão goes on: “*In the past, these shrines were covered in monochrome glazed tiles that time has destroyed, giving color to the towers, which Diogo Sotto Maior describes as 'exquisite', with balls on the top, gilded by the painter Flores*” [6]

As to how the tiles are laid “*earlier references describe the Cathedral's two towers ´with spires decorated with expensive azulejo tiles´, which could have been, as usual, checkered or contrasting squares, very much in use at the end of the 16th century*”. [7]

In the project, the spires were covered with a 14x14 cm white tile, hand-glazed with red paste, with an exact thickness and controlled manufacture. The composition of the glaze to obtain the color was made up of a base of White Matte. To obtain the color tone, Burnt Yellow and Brown Ochre dyes were used, guaranteeing its authenticity and the variation of the whites in relation to the façade plasters. The checkered design with edges reinforced by protruding pieces creates a chromatic element that sparkles in the sunlight (Figure 4, left, and center).

Figure 4. Photos: RBD.APP, 2023

Cloister

The cloister was covered on three sides by a 45-cm-high tile plinth, which was in poor condition: loose, broken glazed tiles, areas that were visible due to a lack of glaze, and random applications with no patterns. The north façade—with no glazed tiles—had large patches of rising dampness.

The design choice was to apply 1.5m—high wainscoting on the staircase leading to the terrace—white Estremoz marble wainscot with no veins on the four façades of the cloister, in order to give uniformity to the space and to prevent it from deteriorating ahead of time. In this way, it matches the color of the marble pillars of the Cloister on the north façade and continues the white plaster of the background walls. The marble ennobles the space and transitions the geometry of the finishes.

The tiles removed were used as stock to fill in the gaps in the Cathedral's wainscoting patterns. Despite the care taken to remove them, most of the tiles were in a very poor state of repair, although the intention was always to restore them whenever necessary.

This made it possible to repair the existing patterns on the interior paneling.

The possibility of covering the antechamber of the Porta do Sol in the Cloister with tile patterns was considered, but there were only a few surplus tiles and they were quite dilapidated. The decision was therefore made to install a wainscot with white tiles left over from the spires, with a similarly tiled checkered layout.

The paintwork on the cloister walls (greyish white) was chosen to emphasize the incomplete link to the white marble pillars, and the ochre paintwork that clashed with the architecture was removed; for better color integration, colored mortars were applied instead of painting the architectural elements; the stone joints were filled with colored mortars relative to the paving stones and the stones of the cloister's marble pillars and the granite stones of the building's exterior walls.

CONCLUSION

Color has always played a decisive role in the choices made in the restoration of the monument, whether in the mortars, veneers, painting of the Cloister, restoration of the tile patterns, flooring materials—wood and marble—granite and paintings of the space and altarpieces.

A lack of funding meant we had to cover some of the old paintings—leaving only a few apertures open—but this does not impede future restoration activities.

The documentation of existing paintings preceding the modifications made in the 1940s—which whitewashed the interior to in alignment with the austerity of the Regime—was factored into our research into the authenticity of the interior decoration.

Custom-made white tiles were applied to the spires, with a color scheme matching old samples in storage. Special care was taken to finish the edges, using rounded pieces with a prominent geometric expression to highlight the contrasts, designed and manufactured specifically to adorn the spires.

The irregular surfaces lend themselves to a vibrant chromatic and luminous arrangement, a "diamond point" that ennobles the whole, standing out from the white color of the façades.

The overall work was of high quality and the expectations set out in the program were met. The colors were used in accordance with historical research, and there was harmony and authenticity in the ensemble of architecture, paintings, and liturgical furnishings.

ACKNOWLEDGEMENT

This work is financed by national funds through FCT - Fundação para a Ciência e a Tecnologia, I.P., under the Strategic Project with the references UIDB/04008/2020 and UIDP/04008/2020.

We also thank RBD.APP-Architects for the availability of the photographs.

REFERENCES

1. Pinheiro, A. P. and Duarte, R. (2020). *Reabilitação arquitetónica e Património: Catedral de Portalegre. Architectural Rehabilitation and Heritage: Cathedral of Portalegre. al.madan*, (2nd series | November 2020). pp. 96-105.
2. Duarte, R. and Pinheiro, A. P. (2016). *Relatório prévio - Reabilitação da Sé Catedral de Portalegre, claustros e espaços anexos. Architectural report for the General Directorate of Cultural Heritage (DGPC), Portugal*. Portalegre: Diocese de Portalegre e Castelo Branco. p. 281.
3. Patrão, J. (2002). *Portalegre, Fundação da Cidade e do Bispado Levantamento e Progresso da Catedral. Portalegre, Foundation of the City and Bishopric Survey and Progress of the Cathedral.* Editor: Fernando Mão de Ferro, Lisboa. p. 290.
4. Pereira, S. (2021). *Problemas e Opções no Restauro de Paramentos Azulejares de Edifícios. Problems and Options in the Restoration of Tile Facings of Buildings* In: VIII Seminário de Reabilitação Urbana, L.N.E.C., 11 de março de 2021.
5. Patrão, J. (2002). *Portalegre, Fundação da Cidade e do Bispado, Levantamento e Progresso da Catedral. Portalegre, Foundation of the City and Bishopric, Survey and Progress of the Cathedral.* Editor: Fernando Mão de Ferro, Lisboa. p.101.
6. Patrão, J. (2013). *Catedral de Portalegre: Guia de Visitação. Cathedral of Portalegre: Visitation Guide.* Editor: Fernando Mão de Ferro, 2.ª Edição, Lisboa. p. 24.
7. *A Cidade: Revista Cultural de Portalegre* (1992). Estudos sobre o Séc. XVIII. Studies on the 18th Century. p. 132.

PETROLOGICAL CHARACTERISTICS OF NATURAL PIGMENTS FROM RAYONG, EASTERN THAILAND

J. Meethum[1], A. Fanka[1,2]*, S. Hattagee[3], P. Katemake[3], P. Ngamukot[3], S. Noppakundilograt[3], and T. Assawincharoenkij[1,2]

[1] *Department of Geology, Faculty of Science, Chulalongkorn University, Bangkok 10330, Thailand.*
[2] *Applied Mineral and Petrology Research Unit (AMP RU), Department of Geology, Faculty of Science, Chulalongkorn University, Bangkok, 10330 Thailand*
[3] *Department of Imaging and Printing Technology, Faculty of Science, Chulalongkorn University, Bangkok 10330, Thailand.*

*Corresponding author: Alongkot Fanka, Alongkot.f@chula.ac.th

ABSTRACT

Geological materials, including minerals and rocks, have been widely used as natural pigments for numerous purposes, including artistic ones. In the Khao Nong Taling area, Rayong Province, Eastern Thailand, geological materials with various colours are commonly found. These materials were studied for the petrological characteristics of the natural pigments by combination methods, including field investigation, petrography, and mineralogy, together with colour identification. Fifteen mineral pigments found can be classified into primary and secondary deposits regarding petrological characteristics. The primary deposit of the pigment materials includes carbonaceous shale, siltstone (group I), and basaltic dike (group II). In contrast, the secondary deposit of the mineral pigment is composed of laterite and Fe-oxides (group III). Group I, containing nine pigments, shows the different grain sizes ranging from clay to silt sizes and varied proportions of clay minerals (kaolinite, montmorillonite, illite) and quartz together with pyrite and organic carbon. Consequently, these materials in the pigment form of group I present white, neutral grey, pinkish grey, brown, and black shades. The colour appearance of this group in powder form and paint form is different to a certain degree. The pigments mixed with gum arabic and applied on a watercolour substrate using the applicator with a 37-micrometre thickness match Munsell N2.75, N3, N4.75, N6.25, 2.5YR 7/4, 10YR 9/1, 2.5Y 9/1 and 10Y 8.5/1. Most of them are highly transparent, except for the opaque black pigments. Group II, containing two pigments, comprises mainly plagioclase, pyroxene, and chlorite, characterised by greenish grey. Their paints match 5Y4/4 and 5Y4/2 with medium transparency. Group III, containing four pigments, is characterised by brown dominated by Fe-oxide minerals (goethite, limonite, hematite), clay minerals (montmorillonite), and quartz in compositions. Their paints match 7.5R 4/6, 2.5YR 4/4, 7.5YR 5/8 with low to medium transparency, and 7.5YR 4/2 with opaque. The lightfastness property of all paints is investigated. The optical properties of these pigments and paints are related to their components and compounds.

Keywords: Pigment, Petrology, Colour, Mineral, Paint, Thailand

INTRODUCTION

Natural pigments have been used for painting, coating, textile, and other applications for a long time [1–4]. Several kinds of rocks and minerals have been reported as natural pigments, e.g., Fe-oxides (goethite, limonite, hematite), cinnabar, orpiment, malachite, azurite, kaolinite [1, 5–6]. In Khao Nong Taling area, Rayong Province, Eastern Thailand (Fig. 1), several rock units widely exposed, including the Triassic to Permian Khao Wang Chik Formation, characterised by various rocks of mudstone (light grey, siliceous, thinly bedded, interbedded with ribbon chert), carbonaceous shale, sandstone (dark brown, medium grained, thick bedded, on top of sequence), and basaltic dike [7]. Moreover, these rocks can be clearly found in an open-pit quarry of construction materials in the Khao Nong Taling. Although these rocks clearly show various colours in different petrological characters (Fig. 2), a detailed study on the petrological characters related to the colour of the natural pigments from these rocks and related minerals has not been done. Therefore, this research aims to characterise the petrological characters related to their colour from the natural pigments from the Khao Nong Taling area, Rayong Province, Eastern Thailand, that can lead to the proper applications of the natural pigments.

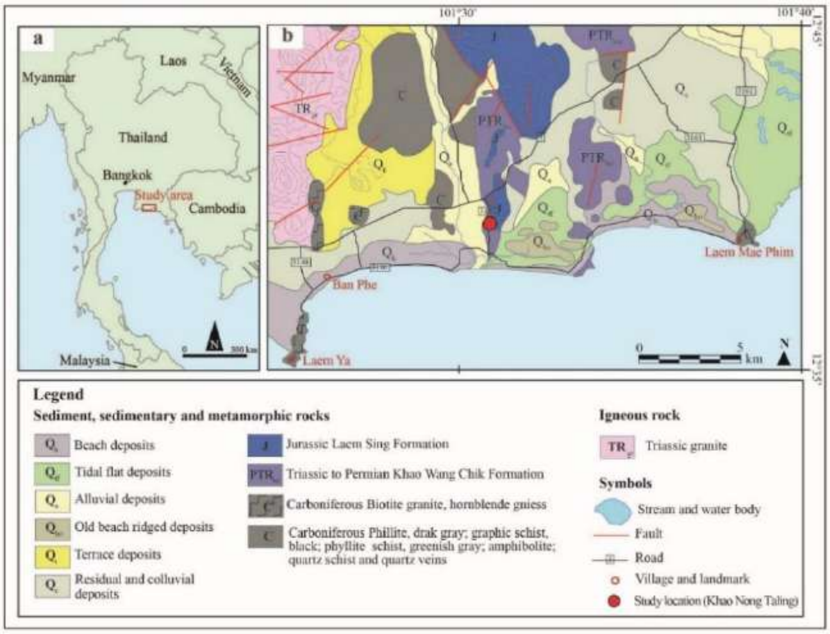

Figure 1. Geological map of Khao Nong Taling area, Rayong Province, Eastern Thailand [7].

METHODOLOGY

The fifteen representative natural pigment samples were collected from Khao Nong Taling, Rayong Province, Eastern Thailand (Fig. 1), where the various rock types and colours are clearly exposed. The collected samples include ten samples of sedimentary rocks (carbonaceous shale, white shale, pink shale, red siltstone, and grey siltstone), two samples of basaltic dikes, and three samples of laterites and samples of white shale coupled with Fe-oxide and limonite. The rock samples were prepared as thin sections by grinding powder no. 600, 1000, 2000, and 3000 for petrographic study using a NIKON polarising microscope at the Department of Geology, Faculty of Science, Chulalongkorn University, Thailand. Powdered samples were prepared by disc mill, and drying the powder at 105°C for 2 hours to eliminate humidity. The powdered samples' mineral compositions were identified using an X-ray diffraction (XRD) model BRUKER D8 Advance, based at the Department of Geology, Faculty of Science, Chulalongkorn University. The resultant powdered pigments were measured with Konica Minolta 700d, illuminant/observer: D65/2 and thoughtfully matched with Munsell patches to capture their characteristics. These pigments were mixed with gum Arabic, applied on a watercolour substrate using a precision applicator, ensuring a uniform 37-micrometre thickness, measured their colour and matched with the Munsell patches.

RESULT AND DISCUSSION

Field investigation and Sample description

Khao Nong Taling area is located at 12°39'17.0"N 101°30'55.3", Rayong Province, Eastern Thailand. The rocks in this location are composed mainly of three groups: Group I: sedimentary rocks, Group II: basaltic dike, and Group III: secondary minerals.

The rocks in Group I include the various types of clastic sedimentary rocks, including carbonaceous shale or black shale, pinkish shale, grey shale, white shale, grey siltstone and brown siltstone (Fig.2). These rocks are generally presented as thin beds (2-10 cm) and always present the folding and joints in the outcrops (Fig.2b-2c). These rocks can be clearly observed in different colours in the field (Fig.2b-2c).

Group II is characterised by basaltic dike cut into those rocks of Group I. The basaltic dike is exposed at the ground level of the quarry (5 m wide). The rocks in this group show greenish grey to dark grey in the outcrop (Fig. 2d) with the fractures.

Based on the specimen characteristics, the rocks' colours come from both primary compositions of rocks (e.g., mineral compositions, organic carbon materials (coal liked), rock cementing) and secondary products from the primary rock (e.g., Fe-oxides) that can be observed by the iron stain in the rock surface and the laterite depositing in downstream of the study area.

For Group III, this group is characterised by the secondary iron-oxides, including limonite showing yellowish powder covering the dried stream surface and laterite showing a thick layer (5-10 m) in downstream.

Group I and Group II can be classified into the primary deposits of pigment minerals, whereas Group II is the secondary deposits of pigment minerals generated by the weathering of Fe-bearing minerals (e.g., pyrite, hematite, pyroxene) of the Group I and II as the chemical weathering products [8–10].

Figure 2. (a) Outcrop exposure of the natural pigments in Khao Nong Taling, Rayong, Eastern Thailand; (b) black shale and (c) mixed colour shale, mudstone, and siltstone (Group I); (d) basalt (group II); (e) laterite (Group III).

Petrographic characters and mineralogy

Group I is characterised by clastic sedimentary rocks containing different grain sizes varying from clay to silt size (Fig.3) in the shale and siltstone. The samples in this group can be classified into carbonaceous shale, pink shale, white shale, grey siltstone, and red siltstone based on their colour, composition, and rock type. Carbonaceous shale is composed mainly of organic carbon together with clay minerals (kaolinite, montmorillonite, illite) and quartz with some opaque minerals (pyrite) (Fig. 3a, Table 1). The organic carbon in the main composition could act as the course of the black colour of this pigment material [11]. Pink shale and white shale are composed of clay minerals (kaolinite, montmorillonite, illite) and quartz with different amounts of opaque minerals (pyrite and Fe-oxides) (Fig.3b–3c, Table 1). The pink shale shows higher concentrations of Fe-oxides than the white shale, which might be generated by the oxidation or weathering of pyrite [12–14]. The low content of Fe-oxides mixing with the high content of quartz and clay minerals can make the pink colour in this pigment material [5]. Moreover, white shale with a high content of clay minerals and quartz with less opaque minerals (pyrite and Fe-oxides) can show a white shade [15].

Siltstone shows two main colours, including grey siltstone and brown siltstone. Although major mineral compositions of both grey siltstone and brown siltstone are quartz and clay minerals (montmorillonite, illite, kaolinite) with different content opaque minerals (pyrite) (Fig.3d–3e, Table 1), Fe-oxides (hematite and goethite) are mainly presented in only brown siltstone (Fig.3d, Table 1). Therefore, the brown colour in the brown siltstone should be affected by Fe-oxides in composition [16–18].

Group II is characterised by basaltic dike composed mainly of plagioclase, pyroxene, opaque minerals, and chlorite (Fig.3, Table 1). The mixed mineral compositions of plagioclase (grey), pyroxene (black), and chlorite (green) might be the cause of the greenish gray colour of this pigment material.

Group III comprises laterite (mixed sediments and Fe-oxides) and Fe-oxides (hydroxides). This group contains several phases of Fe-oxides, including hematite, goethite, and limonite, with some mineral sediments of quartz and clay minerals (montmorillonite). The main compositions of Fe-oxides are the main cause of the brown colour of these pigment materials [1, 5, 16-18].

Colour characteristics

The pigments in Group I can be effectively divided into two distinct categories: 1) those ranging from black to grey and 2) those exhibiting reddish to orange hues. These pigments fall within the C^*_{ab} range of 9 to 43 and L^* values from 46 to 86. They contain varied proportions of clay minerals (kaolinite, montmorillonite, illite), quartz, pyrite, and organic carbon in the shales and siltstones (Table 1). The pigments mixed with gum arabic and applied on a watercolour substrate using the applicator with a 37-micrometre thickness match Munsell N2.75, N3, N4.75, N6.25, 2.5YR 7/4, 10YR 9/1, 2.5Y 9/1 and 10Y 8.5/1. Most of them are highly transparent, except for the opaque black pigments.

The black shade could be caused by the dominant organic carbon in composition [11], while the white, grey, pinkish grey and brown shades could be influenced by the dominant compositions of clay minerals and quartz [15], mixed clay mineral and pyrite [19], low Fe-oxide content [16-18], and high Fe-oxide content [16-18], respectively.

Group II comprises mainly plagioclase (grey), pyroxene (black), and chlorite (green), characterised visually by greenish grey [20]. However, their red-green (a^*) values fall within the range of 0.5 to 1.9, while the yellow-blue (b^*) values range from 17 to 22. These attributes, coupled with an L^* value of approximately 47, characterise them as possessing yellowish powder. Their paints correspond to 5Y4/4 and 5Y4/2 Munsell colour codes. They are medium transparency.

Group III stands out with its distinctive dark to medium brown shades, characterised by L* values ranging from 35 to 40 and C* values spanning from 17 to 33. The composition of these pigments predominantly includes Fe-oxide minerals (like goethite, limonite, and hematite), clay minerals (particularly montmorillonite), and quartz.

Their paints match the Munsell colour codes 7.5R 4/6, 2.5YR 4/4, 7.5YR 5/8 with low to medium transparency, and 7.5YR 4/2 with opaque properties. This colour shade should be resulted from the dominant Fe-oxides in composition [16-18].

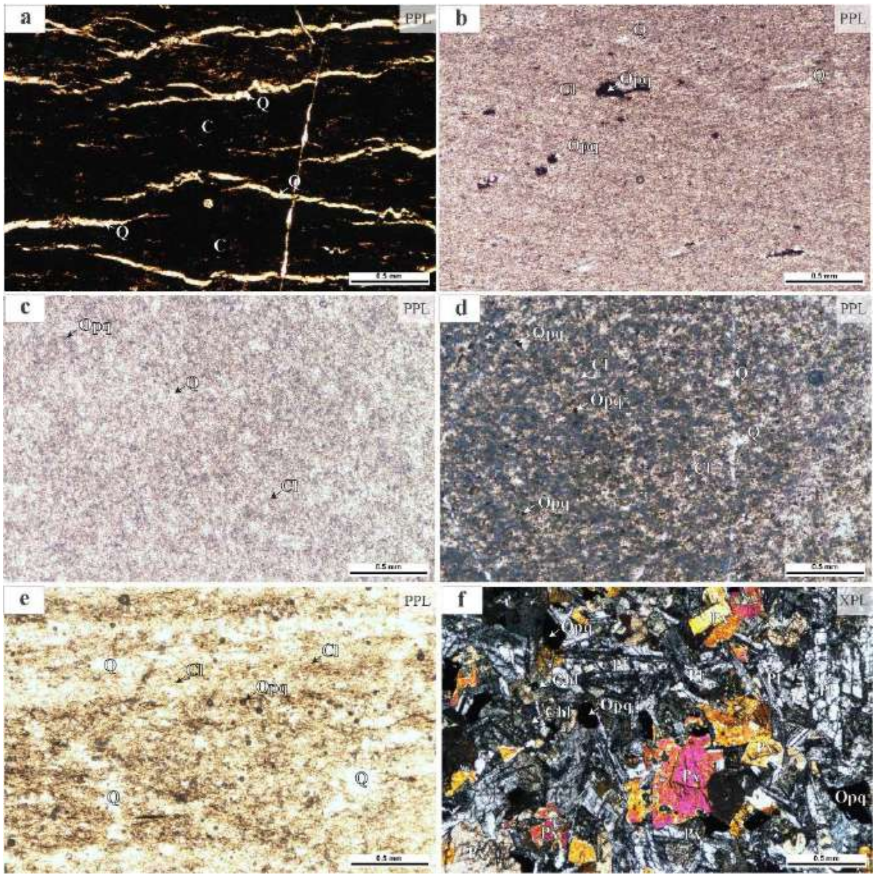

Figure 3. Photomicrograph of the mineral compositions in the natural pigments from Khao Nong Taling, Rayong Province, Eastern Thailand. (a) carbonaceous shale; (b) pink shale; (c) white shale; (d) brown siltstone; (e) grey siltstone; (f) basaltic dike. Abbreviations: C (organic carbon); Cl (clay minerals); Q (quartz); Opq (opaque minerals); Pl (Plagioclase); Px (pyroxene); Chl (chlorite); PPL (plane polarized light); XPL (cross polarized light)

Table 1: The major mineral compositions of pigments from Rayong, Eastern Thailand.

Pigment group	Rock type	Sample no.	Mineral assemblages	Pigment colour	
Group I (Sedimentary rocks)	Brown siltstone	RY6	Quartz, Montmorillonite, Pyrite, Hematite, Goethite	Brown	
	Pink shale	RY7	Quartz, Kaolinite, Montmorillonite, Illite, Pyrite	Pinkish grey	

Pigment group	**Rock type**	**Sample no.**	**Mineral assemblages**	**Pigment colour**	
	Pink shale	RY9	Quartz, Montmorillonite, Kaolinite, Pyrite	Pinkish grey	
	Grey siltstone	RY3	Quartz, Kaolinite, Illite, Pyrite, Chlorite	Grey	
	Grey siltstone	RY5	Quartz, Montmorillonite, Kaolinite, Pyrite	Grey	
	Carbonaceous shale	RY1	Quartz, Illite, Kaolinite, Montmorillonite, Pyrite	Black	
	Carbonaceous shale	RY2	Quartz, Illite, Kaolinite, Montmorillonite	Black	
	Carbonaceous one	RY4	Quartz, Illite, Kaolinite, Montmorillonite, Pyrite	Black	
	White shale	RY8	Quartz, Montmorillonite, Kaolinite, Pyrite	White	
	White shale	RY10	Quartz, Illite, Kaolinite, Montmorillonite, Pyrite	White	
Group II (Basaltic dike)	Basaltic dike	RY11	Plagioclase, Pyroxene, Chlorite	Greenish grey	
	Basalt dike	RY12	Plagioclase, Pyroxene, Chlorite	Greenish grey	
Group III (Secondary minerals)	Fe-oxides	RY13	Fe-oxides (limonite), Goethite, Hematite, Montmorillonite, Quartz	Brown	
	Laterite	RY14	Goethite, Hematite, Fe-oxides (limonite), Montmorillonite, Chlorite, Quartz	Brown	
	Fe-oxides	RY15	Goethite, Hematite, Fe-oxides (limonite), Montmorillonite, Quartz	Brown	

CONCLUSION

Natural pigments from Khao Nong Taling area, Rayong Province, Eastern Thailand, can be characterised into three categories of pigment materials based on the petrological characteristics and their colours, including Group I: sedimentary rocks (shale and siltstone) with colour shades of white, grey, pinkish grey, brown, and black shades, Group II: basaltic dike with greenish grey colour shade, and Group III: secondary Fe-oxides and laterite with the brown colour shades. These colour shades of all pigments are related to their compositions.

ACKNOWLEDGEMENT

The authors would like to thank the Department of Geology and the Department of Imaging and Printing Technology, Faculty of Science, Chulalongkorn University, for supporting all facilities to obtain the research data.

REFERENCES

1. Barnett, J.R., Miller, S., & Pearce, E. (2006). Colour and art: A brief history of pigments. *Optics & Laser Technology*, 38, 445–453

2. Umale, S., & Mahanwar, P. (2012). Characterization and Application of Naturally Occurring Mineral Based Pigment in Surface Coating. *Journal of Minerals and Materials Characterization and Engineering*, 11, 1101–1107.
3. Siddall, R. (2018). Mineral Pigmemts in Archaeology: Their Analysis and the Range of Available Materials. *Minerals*, 8(201).
4. Tomasini, E., Costantini, I., Careaga, V., Landa, C.R., Castro, K., Madariaga, J.M., Maier, M., & Siracusano, G. (2023). Identification of pigments and binders of a 17th century mural painting (Bolivia). New report on pigments associated with Andean minerals. *Journal of Cultural Heritage*, 62. 206–216.
5. Reiche, I. (2019). Mineral pigments: the colourful palette of nature. *EMU Notes in Mineralogy*, 20 (7), 283–322.
6. Matarrese, A., Prado, V.D., & Poiré, D.G., (2011). Petrologic analysis of mineral pigments from hunter-gatherers archaeological contexts (Southeastern Pampean region, Argentina). *Quaternary International*, 245, 2–12.
7. Department of Mineral Resources (2008). Geological Map of Changwat Rayong. Scale 1:250,000.
8. Bonnissel-Gissinger, P., Alnot, M., Ehrhardt, J., & Behra, P. (1998). Surface Oxidation of Pyrite as a Function of pH. *Environmental Science & Technology*, 32(19), 2839–2845.
9. Moses, C., Nordstrom, D.K., Herman, J.S., & Mills, A.L. (1987). Aqueous pyrite oxidation by dissolved oxygen and by ferric iron. *Geochimica et Cosmochimica Acta*, 51, 1561–1571.
10. Rimstidt, J.D., & Vaughan, D.J. (2003). Pyrite oxidation: A state-of-the-art assessment of the reaction mechanism. *Geochimica et Cosmochimica Acta*, 67(5), 873–880.
11. Zinke, L. (2020). The colours of carbon. *Nature Reviews Earth & Environment*, 1, 141.
12. Mahoney, C., März, C., Buckman, J., Wagner, T., & Blanco-Velandia, V. (2019). Pyrite oxidation in shales: Implications for palaeo-redox proxies based on geochemical and SEM-EDX evidence. *Sedimentary Geology*, 389, 186–199.
13. Chen, Q., Kang, Y., You, L., Yang, P., Zhang, X., & Cheng, Q. (2017). Change in composition and pore structure of Longmaxi black shale during oxidative dissolution. *International Journal of Coal Geology*, 172, 95–111.
14. Tuttle, M.L.W., & Breit, G.N., (2009). Weathering of the New Albany Shale, Kentucky, USA: I. Weathering zones defined by mineralogy and major-element composition. *Applied Geochemistry*, 24, 1549–1564.
15. Gamiz, E., Melgosa, M., Sanchez-Maranon, M., Martin-Garcia, J.M., & Delgado, R., (2005). Relationships between chemico-mineralogical composition and color properties in selected natural and calcined Spanish kaolins. *Applied Clay Science*, 28, 269–282.
16. U.S. Geological Survey (2022). Iron oxide pigments. *Mineral Commodity Summaries*, 87.
17. Nicola, M., Mastrippolito, C., & Masic, A., (2016). Iron Oxide-Based Pigments and Their Use in History. *Iron Oxides: From Nature to Applications*, 545–565.
18. Gareev, K.G., (2023). Diversity of Iron Oxides: Mechanisms of Formation, Physical Properties and Applications. *Magnetochemistry*, 9(119).
19. Herrmann, J.R., Maas, R., Rey,P.F., & Best, S.P., (2019). The nature and origin of pigments in black opal from Lightning Ridge, New South Wales, Australia. *Australian Journal of Earth Sciences*, 66(7), 1027–1039.
20. Ghazal, M.M., Al-Juboury, A.I., & Jalal, S.M., (2019). Mineral Chemistry of Chalki Basalts in Northern Iraq and Their Petrological Significance. *Mineralogy Significance and Applications*, 1–20.

INFLUENCE OF ILLUMINATION SPECTRUM ON VISUAL COMFORT

He Liu[1] and Hiroyuki Shinoda[2]

(Graduate School of Ritsumeikan University)
[1] Graduate School of Information Science and Engineering, Ritsumeikan University, Japan.
[2] College of Information Science and Engineering, Ritsumeikan University, Japan.

*Corresponding author: He Liu, gr0369sr@ed.ritsumei.ac.jp

ABSTRACT

In past studies, lighting was often described by derivative index such as correlation color temperature (CCT), color rendering index (CRI) or chromaticity. Although some lightings produce the same color temperature and illumination, the spectrum of these lightings may be different. In recent years, a lot of studies have proved the influence of lighting spectrum on individuals. Many of the research have proved the influence of spectrum on people through non-visual pathway (ipRGCs). There were few studies through visual pathway like brightness and color constancy. In this study, we focused on visual effects, examined the influence of lighting spectrum on visual comfort. Four types of lightings with different spectrum were compared: low-CCT (3000K) with multipeak spectrum, low-CCT (3000K) with broad-band spectrum, high-CCT (5000K) with multipeak spectrum and high-CCT (5000K) with broad-band spectrum. Three different illuminance levels are set for each type of lighting. The experiment was divided into 12 sessions based on different lighting conditions. Critical flicker frequency (CFF) tests were performed before and after each session. In a session, subjects did receipt processing twice under each lighting conditions in a test room that mimics a general room. Between the receipt processing they had 5 minutes for rest. After these tasks, the subjects were asked to fill out a questionnaire for subjective judgements. The work under each kind of lighting last about 35-40 minutes and was completed on separate days. As a result, in the Absolute Category Rating assessment of subjective evaluations, such as item1 (dark-bright), item5 (discomfort-comfort), item6 (inattention-concentration), item12 (depressing-refreshing) showed a strong correlation to the shape of spectrum and CCT of illuminant. The lighting with broad-band spectrum got higher scores than the lighting with multipeak spectrum even when the color temperature and illumination were the same. In addition, the above items of subjective evaluation showed a tendency that as the illuminance decreases, the decrease of scores of lightings with high-CCT is significantly higher than the lightings with low-CCT. Combined with the evaluation content of item 1, it can be considered that the perceived spatial brightness affects the results of other items. The difference of CFF before and after the experiment had no significant correlation with the shape of spectrum. As for the receipt processing, by the time illuminance and color temperature were the same, the average processing time of each receipt under lighting with multipeak spectrum was longer than that under lighting with broad-band spectrum, and the standard deviation of data under lighting with broad-band spectrum was smaller than that under lighting with multipeak spectrum. It means subjects had higher attention working under broad-band spectrum lighting. The result was consistent with item 6 in subjective judgements.

Keywords: lighting spectrum, color temperature, illuminance, visual comfort, subjective evaluation

INTRODUCTION

With the amount of time people spend indoors increasing dramatically in modern society, healthy and comfortable indoor lighting has become an important requirement for human activity. In indoor lighting, the spectrum of the light source is a very important feature. In previous studies on lighting and human vision, researchers have typically used derivative index such as correlation color temperature (CCT), color rendering index (CRI) or chromaticity to describe indoor lighting. [1] [2] While these indices are very convenient during experimental analysis, there is a possibility that they may not capture essential spectrum features. some lightings produce the same color temperature and illuminance, the spectrum of these lightings may be different. It is necessary to treat the lighting spectrum itself as a variable to explore the influence of illumination on visual comfort.

Over the past decades, researchers have demonstrated the influence of spectrum on people through non-visual pathway (ipRGCs). The spectrum acts on ipRGCs to regulate the suppression level of melatonin, thereby affecting human physiological activities. [3-6] In recent years, some researchers have proposed exploring the effects of spectrum on people through the visual pathway like brightness and color constancy. Wout van Bommel [7] indicates that the spectrum of lighting is the major aspects that affect one's overall impression of spatial brightness. Hokudo & Shinoda [8][9] investigate color constancy between LED illuminants with different chromaticities and spectrum distribution shapes.

As far as the authors are aware, the spectrum of lighting has shown influences on both non-visual pathway and visual pathway in the human body. However, research on the visual pathway is limited to the perceived spatial brightness and color appearance. The effects of spectrum on visual comfort and work efficiency through the visual pathway have not been studied yet. In this study, an examination was conducted to assess the impact of lighting spectrum on visual comfort and work efficiency through the visual pathway. Illuminants were devised with both broad-band continuous spectrum (BB) and multi-peaks spectrum (MP) at color temperatures of 3000 K and 5000K. A series of experiments, encompassing visual tasks, visual fatigue assessments, and subjective evaluations, were carried out under three distinct illuminance conditions. The experimental outcomes facilitated the establishment of correlations between spectrum characteristics and both visual comfort and task efficiency.

METHODOLOGY

Experiment setup: The experiment was carried out in a windowless room 1.8 m long, 1.5 m wide and 2.0 m high. The walls and ceiling were uniformly covered with white foam panels. To prevent interference from external light, the entrance of the room was covered with black curtains. Two LED cubes (THOUSLITE) were installed at the top of the room to provide the required illumination for the experiment. A desk with a height of 70 centimeters and a chair were arranged inside the room. A monitor (EIZO ColorEdge CS230) with mouse and keyboard were placed on the desk. In order to simulate a real office, colorful items such as a desk clock and potted plants were also placed on the desk. The participants sat in the room to complete the entire experimental procedure.

Lighting source: The lighting sources were set to 12 combinations, with 2 color temperatures, 2 spectrum distribution shapes, and 3 illuminance levels each. In order to simulate the lighting conditions in real-life living environments, we set two types of illuminants with color temperatures of 3000K and 5000K along the blackbody radiation locus. The illuminance on the surface of the desk was set to three levels: 24lx, 80lx, and 240lx.

Table 1: CIE xy Chromaticity and Correlated Color Temperature

correlated color temperature 3000K					correlated color temperature 5000K				
spectrum	Illuminance(lx)	x	y	CCT(K)	spectrum	Illuminance(lx)	x	y	CCT(K)
MP	24	0.430	0.406	3064	MP	24	0.343	0.356	5108
	80	0.436	0.405	3024		80	0.346	0.352	4969
	240	0.436	0.409	3054		240	0.342	0.353	5121
BB	24	0.434	0.403	3031	BB	24	0.344	0.347	5044
	80	0.430	0.397	3073		80	0.343	0.356	5080
	240	0.438	0.401	2953		240	0.345	0.357	5007

The spectrum distribution of the lighting was set to two types: Broad Band spectrum (BB) and Multi Peaks spectrum (MP). For the settings, we selected all 11 types of LEDs embedded in the LED Cube for BB, and for MP, we chose 4 types with different dominant wavelengths. The intensities of the LEDs were adjusted to approximate the settings of illuminance and color temperature shown in Table 1. The spectrum for all 12 lighting conditions is shown in Figures 1. The settings and measured CIE xy chromaticity coordinates, as well as correlated color temperature (CCT) of the lighting sources are presented in Table 1.

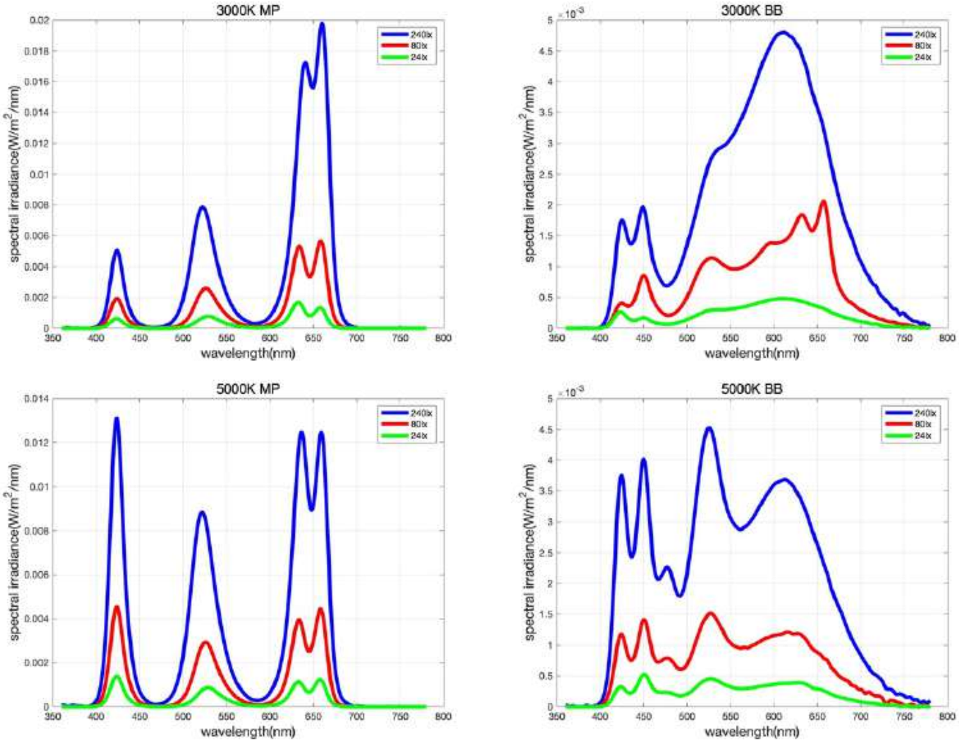

Figure 1: Spectrum irradiance

Experiment and evaluation methods: Critical Flicker Fusion (CFF) test has been used to assess the visual fatigue of the participants in the experiment. The Critical Flicker Frequency (CFF) test is an examination method that indicates the discrimination threshold of perceiving intermittent light as continuous light or as flickering light in terms of the frequency (Hz) of the interruptions.

Receipt processing was used for conducting the task efficiency experiment. [10] The template of the receipts is shown in Figure 2. During the experiment, we prepared 30 receipts, and the participants collected the three pieces of data information within the red circles. Then clicked on the overlapping portion on the display screen as shown in Figure 3. The time taken for each response was recorded.

Figure 2: Receipt sample

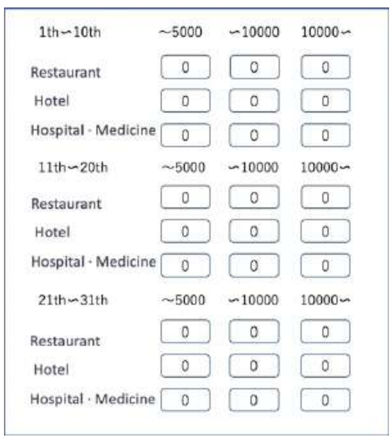

Figure 3: Input interface

A 9-point rating scale is employed to assess each lighting environment. The scale with 13 pairs of adjective phrases related to impression and mood at both ends of the linear scale was made for this purpose. The 13 pairs of adjective phrases were categorized into three groups. The first group assessed the overall illumination environment, including dark-bright, hot-cool, feel bad-good, hard-easy to see, and discomfort-comfort. The second group evaluated the illumination environment during tasks, covering inattention-concentration, easy to get tired-not easy to get tired, lack of motivation-motivation, and sleepy-not sleepy. The third group gauged the lighting environment during mid-experiment breaks, addressing untranquil-feel at ease, anxious-clam down, depressing-refreshing, and difficulty falling asleep-feeling sleepy. At the end of task and relax, subjects were asked to mark positions on the scales from 1 to 9, depending on their subjective feelings.

Procedure and Participants: The experiment is divided into 12 sessions, each corresponding to a specific lighting condition. In each session, participants first underwent a Critical Flicker Frequency (CFF) test in dark room. Subsequently, they were exposed to the corresponding lighting condition for two rounds of receipt processing tasks, with each round involving the processing of 30 receipts. A 5-minute break was simulated between the two rounds, during which participants freely viewed two sets of color landscape photographs under the same lighting condition. After completing the two rounds of tasks and the simulated break, participants filled out a subjective evaluation form under the same lighting condition. Following the completion of the form, the lights were turned off for the second CFF test.
The participants consisted of 10 undergraduate and graduate students with normal vision aged between 20 and 30 years (5 males and 5 females). Each participant completed 4 sessions per day, and the entire 12 sessions of the experiment were conducted over a span of three days. As the participants consisted of 5 Japanese and 5 Chinese individuals fluent in Japanese, the paper receipts and evaluation forms for this experiment were written in Japanese, while the input interface on the display screen was in English, which all participants could understand.

RESULT AND DISCUSSION

Critical Flicker Frequency (CFF) test: The difference in CFF before and after the task are depicted in Figure 4. In this experiment, due to variations in the initial states of the participants, CFF pre-task is varied between 40.2 and 42.5. The evaluation of the influence of different light sources on the subjects' level of visual fatigue was based on the difference in CFF values before and after the task (ΔCFF). The calculation is as shown in Equation 1.

$$\Delta CFF = CFF_{pretask} - CFF_{posttask} \qquad (1)$$

From an overall perspective, ΔCFF decreases with increasing illuminance. When the illuminance is 24lx and 240lx, there is not much difference in ΔCFF between 3000K illumination and 5000K illumination. However, when the illuminance is 80lx, the ΔCFF for 5000K illumination is notably lower than for 3000K illumination. When the color temperature is 3000K, ΔCFF between MP spectrum lighting and BB spectrum lighting is almost the same. However, at a color temperature of 5000K, ΔCFF between MP and BB spectrum lighting varies. For lower illumination levels (24lx, 80lx), MP spectrum lighting has a lower impact on visual fatigue than BB spectrum lighting, while for moderate illumination levels (240lx), the reverse is observed. This indicates that as illuminance levels increase, the degree of visual fatigue induced by tasks tends to decrease. With the rising illuminance levels, 5000K color temperature lighting is affected earlier compared to 3000K color temperature lighting. When the color temperature is 3000K, the spectrum type of lighting has a limited effect on visual fatigue during tasks. However, at a color temperature of 5000K, the impact of MP spectrum lighting on visual fatigue is lower in low illuminance conditions, while BB spectrum lighting is more favorable for reducing visual fatigue in moderate illuminance conditions.

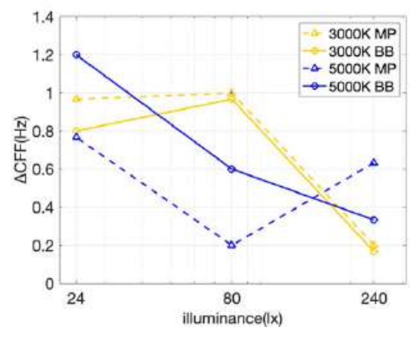

Figure 4: ΔCFF (pre-post)

Subjective evaluation: Figure 5 illustrates the scores of the subjective evaluation, where we have chosen four representative items for display. In the evaluation of the overall room illumination environment and the evaluation of the working illumination environment, overall, except for the item2(hot-cool), all other items exhibited a trend towards an upward and rightward shift. when the color temperature is 5000K, item 1(dark-bright) received higher subjective evaluation scores under BB spectrum lighting compared to MP spectrum lighting at all levels of illuminance (24lx,80lx and 240lx). However, when the color temperature is 3000K, the impact of lighting spectrum shape on the evaluation scores is less pronounced. The results for items 3(feel bad-feel good), 4(hard to see-easy to see), 5(discomfort-comfort), 6(inattention-concentration), 7(easy to get tired-not easy to get tired), 8(lack of motivation- motivation), and 9(sleepy-not sleepy) also exhibit similar trends as item 1.

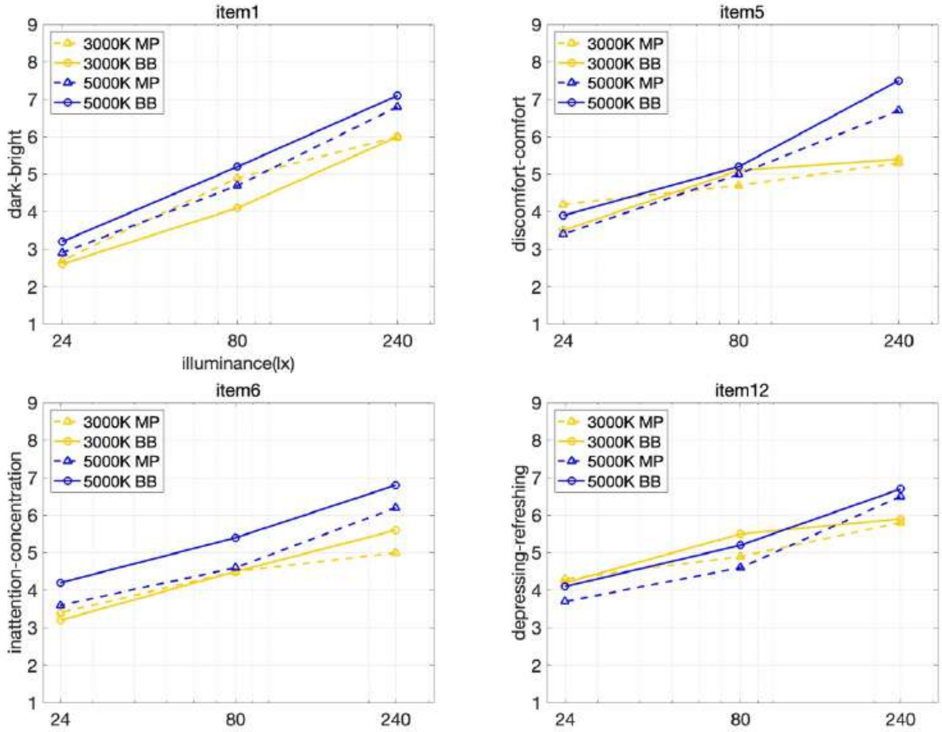

Figure 5: scores of the subjective evaluation

Among the four items in illumination environment evaluation during rest, only item 12(depressing-refreshing) showed significantly higher evaluation scores for the BB lighting spectrum compared to the MP lighting spectrum when the color temperature was 5000K. When the color temperature was 3000K, the lighting spectrum shape had minimal influence on the evaluation scores. In this evaluation group, the other items exhibited consistent responses to spectrum shape across various color temperature conditions.

Based on the results of subjective evaluations, in subjective evaluations related to factors such as brightness, comfort, and attention, participants tend to provide higher ratings as the illuminance increases. Under the same illuminance conditions at 5000K, lighting with the BB spectrum exhibits superior performance in terms of perceived brightness, visibility, and comfort compared to lighting with the MP spectrum. Moreover, the BB spectrum lighting also demonstrates advantages in enhancing attention, reducing fatigue, and alleviating drowsiness when compared to the MP spectrum lighting.

Work Efficiency Test: The results of the task efficiency test are shown in Figure 6. Overall, there is no clear trend in the average processing time of receipts with changing illuminance. When the color temperature is 5000K, the average processing time for a receipt under BB spectrum illumination is noticeably lower compared to that under MP spectrum illumination. In contrast, at a color temperature of 3000K, there is no substantial difference in the average processing time between the two spectrum illuminations.

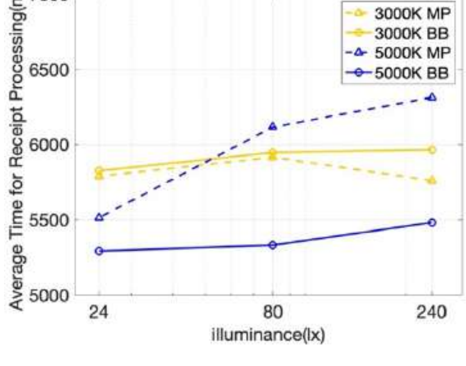

Figure 6: result of work efficiency

This indicates that when the color temperature is 5000K, BB spectrum illumination notably enhances participants' work efficiency across all illuminances levels when compared to MP spectrum illumination. The monitor's brightness remains constant regardless of the illuminance conditions, so when the illuminance is high, the perceived brightness of the monitor is darker, whereas under low illuminance conditions, the monitor appears relatively brighter. Due to the combination of paper-based and computer-based work in this task, the relatively higher screen brightness under low illuminance conditions and the relatively lower screen brightness under high illuminance conditions are considered to be the main reasons for the nearly unchanged task efficiency (average receipt processing time) as illuminance increases."

CONCLUSION

This study explored the impact of lighting spectrum on visual comfort and work efficiency, shedding light on a relatively unexplored area of research. The results highlight the influence of lighting spectrum and color temperature on subjective evaluations, revealing that broad-band spectrum (BB) lighting generally received higher ratings, particularly at higher illuminance levels, emphasizing its superior performance in terms of brightness, visibility, comfort, attention, and reduced fatigue. Additionally, BB spectrum lighting significantly improved work efficiency, particularly under 5000K color temperature conditions, compared to multi-peak spectrum (MP) lighting.

From the perspective of CFF (Critical Flicker Fusion) testing, the experimental results demonstrate that different light sources have a significant impact on participants' levels of visual fatigue, especially under different illuminance and color temperature conditions. This underscores the importance of spectrum selection for managing visual fatigue.

While illuminance appeared to have a relatively limited impact on task time due to the combined nature of paper-based and computer-based work, the pronounced effects of spectrum and color temperature on visual comfort and efficiency are evident. These findings emphasize the importance of considering lighting spectrum as a key variable in indoor lighting design to enhance overall well-being and productivity.

REFERENCES

1. Fotios, S. A., & Cheal, C. (2011). *Brightness matching with visual fields of different types. Lighting Research & Technology*, 43(1), 73-85.
2. Veitch, J. A., Fotios, S. A., & Houser, K. W. (2019). *Judging the scientific quality of applied lighting research. Leukos,* 15(2-3), 97-114.
3. Lewy, A. J., Wehr, T. A., Goodwin, F. K., Newsome, D. A., & Markey, S. P. (1980). *Light suppresses melatonin secretion in humans. Science*, *210*(4475), 1267-1269.
4. Berson, D. M., Dunn, F. A., & Takao, M. (2002). *Phototransduction by retinal ganglion cells that set the circadian clock. Science*, *295*(5557), 1070-1073.
5. Aaen-Stockdale, C. (2015). *Human factors in lighting.*
6. Dai, Q., Cai, W., Shi, W., Hao, L., & Wei, M. (2017). *A proposed lighting-design space: circadian effect versus visual illuminance. Building and Environment*, *122*, 287-293.
7. Wout van Bommel (2019), *Interior Lighting: Fundamentals, Technology and Application.*
8. Hokudo, A., & Shinoda, H. (2021). *Color constancy of LED lighting with different spectral distribution and chromaticity. Journal of Color Science Association of Japan*, 45(3),153-156.
9. Hokudo, A., & Shinoda, H. (2022). *Color constancy under LED lighting with different spectral distribution and chromaticity. proceedings of The 53rd Annual Meeting of the Color Science Association of Japan,*181-184.
10. Ishii, H., Kanagawa, H., Shimamura, Y., Uchiyama, K., Miyagi, K., Obayashi, F., & Shimoda, H. (2018). *Intellectual productivity under task ambient lighting. Lighting Research & Technology*, *50*(2), 237-252.

PIGMENT ANALYSIS IN THREE PAINTINGS (1966-1967) BY PRATUANG EMJAROEN BY PORTABLE MICRO-X-RAY FLUORESCENCE

N. Kaew-on* and T. Kaewkong

Restaurateurs Sans Frontières, Studio for art conservation and restoration,
6 Soi Kasemsan 2, Rama I Road, Wangmai,
Phayathai, Bangkok 10330 Thailand

*Corresponding author: Nawarat Kaew-on, rsfasie_nawarat@hotmail.com

ABSTRACT

Pratuang Emjaroen is a well-known Thai visual artist who has a successful international career. He is an artist whose self-taught learning and has played an important role in the development of his creative work through the ages. He has been praised for the 2005 National Artist of Thailand in Visual Arts. His works have its own style of optimism and believing in virtue. It is said that the colors used in Pratuang works are inspired by the sun, which is the source of light, resulting in the creation of works of art with bright colors. This great artist created many works throughout his career. Due to the opportunity to receive three paintings painted in 1966 to 1967 from the art collectors, the pigments used in these paintings, were therefore studied. Nondestructive techniques that included the UV light examination and portable micro-X-Ray fluorescence (XRF) were employed to obtain information on pigments applied and possible later intervention. The XRF is an analytical technique used to identify chemical elements that has been found widespread use in the cultural heritage sector to characterize artists' materials including the pigments in paintings. XRF has been well known and recommended for characterization of the inorganic pigments, while the UV light was commonly used to identify if the pigments were the original ones, or applied later during the restoration. The single point measurement was carried out in this analysis. Four colors; white, red, orange, and yellow were mainly focused and presented in this paper. The results reported the use of zinc white (ZnO), lead white ($2PbCO_3.Pb(OH)_2$), cadmium red (CdS+CdSe), chrome orange ($PbO.PbCrO_4$) and lemon yellow ($BaCrO_4$). Another organic yellow that was not identified by XRF was also found in the pallet.

Keywords: Pratuang Emjaroen, Pigments characterization; X-Ray fluorescence; Thai contemporary artist

INTRODUCTION

Pratuang Emjaroen (1935-2022) is the most famous self-taught artist and one of the most famous figures in Thai contemporary art. He was praised the 2005 National Artist of Thailand in Visual Arts [1, 2]. His works are driven by his concerns about the vicissitudes of life, social problems, nature and Buddhism. He created a large variety of works throughout his career. Pratuang Emjaroen began his career by working as a painter of cinema billboards and movie posters. He was inspired by the biographic film Lust for Life (1956), about Vincent Van Gogh. Pratuang developed his interest in becoming a visual artist and began studying painting independently [2]. He has recently passed away in early of 2022 [3]. In late 2022 and early of 2023, three paintings that were painted by this artist during 1966-1967 in the collections of private collectors, were given to the author for scientific analysis. These analyzed data have been aimed to be used as references in future. Identification of inorganic pigments in the artist's pallet was therefore carried out. The XRF (X-ray fluorescence) spectroscopic as nondestructive technique was employed. XRF is helpful to evaluate the cultural assets, neither touching it nor damaging it at all. The analysis by XRF is a qualitative and quantitative method based on the measurement of the characteristic X-ray intensities emitted by the elements that constitute a sample. X-rays emitted by X-ray tubes excite the elements present in the sample, so they emit spectral lines in characteristic energies [4]. Inorganic pigments on the painting or mural paintings can be analysed by this technique without even any micro sample taken [5-7]. Although XRF is an excellent technique for painting analysis and it is widely used in literature, it does have some limitations related to the insufficient sensitivity for low Z elements, is the inability to identify organic pigments [4,8].

This article presents the results of the analyses carried out on three paintings, painted in 1966-1967 (Figure 1). Particular attention has been paid on four colors including white, red, orange and yellow by mean of XRF technique.

METHODOLOGY

Figure 1 presents three paintings and the XRF inspected locations. The “Abstract Scenery” (Figure 1a) is oil painting on canvas of 75x70 cm. It was painted in 1966. Figure 1b shows “The birth of the golden sea”. It is oil painting on canvas of 100x120 cm. It was painted in 1967. The large painting in blue color “untitled” (Figure 1c) is oil painting on canvas, of 195 x 614 cm. It was painted in 1966.

UV Examination

In this study, to ensure that the investigation proceeded with the original pigments painted on the the paintings, the paintings were observed under UV light to get more precise information about later intervention and retouches [9, 10]. For this, one pair of the UV lamp were placed on each side of each painting to obtain the most homogeneous illumination of the surface (the bulbs are UV LED radiation power: 14250 mW, UV max spectral emission: 365 nm).

X-Ray Fluorescence

Base on the UV examination results, locations of different colors on each painting were selected and analyzed by X-Ray fluorescence technique. Main colors including white, red, orange, yellow, green, brown, and blue, were investigated but not all of them were discussed in this article, only four colors; white, red, orange, and yellow, were taken to discuss and summarize. The equipment used for this work was the Bruker- Elio micro X-Ray fluorescence. Throughout the analysis, the points of interest were constantly analyzed at 50 kV and 80 mA for 60 seconds acquisition time. Tube target material was Rh, and sample to detector material was Air. The diameter of the radiated spot is 1 mm. In the painting, the pigments were recognized on the basis of the characteristic chemical composition from the XRF spectra of the analyzed locations. The selected spots where XRF measurements were performed on the paintings, were shown in Figure 1. In the results section, the characteristic elements for different pigments were given in bracelets where they were mentioned (Table 1).

Figure 1. The points analyzed by the X-Ray fluorescence of the painting titled; (a) "Abstract Scenery", (b) "The birth of the golden sea", and (c) "Untitled".

RESULT AND DISCUSSION

Visual exam and UV Light

Following usual practice, the paintings were first observed under UV light. The examination with UV light (Figure 2) showed that the painting *"The birth of the golden sea"* (Figure 2b) and *"Untitled"* (Figure 2c) have none of retouched areas or later interventions. For the *"Abstract Scenery"* painting, the exam with UV light showed later interventions. The owner of the painting informed that the restoration was done by the artist himself but no mentioning of the date. Even with the naked eye, it was clear that this painting had been repaired. The painting was patched onto another piece of canvas and the paints were applied to blend with the original painting. Under UV light, the difference was clearly visible. And some areas of the painting were also retouched. (In white circles and rectangular, as shown in Figure 2a). Images obtained under UV light helped at the selection of the points analyzed by X-Ray fluorescence.

Figure 2. The paintings under UV light illumination; (a) Abstract Scenery, (b) The birth of the golden sea, and (c) Untitled.

X-Ray Fluorescence

The Table 1 presents all detected elements found in different three paintings, related to possible pigments applied with its chemical composition. Not all XRF spectra of all colors were shown here, only whites and yellows that presented differently in the same painting were presented.

Abstract Scenery Painting: Total 19 locations across painting surface were investigated, all the XRF spectra obtained during the study showed the presence of Zn, Pb, Ca, and Ba peaks (8 locations of 4 colors were listed in the table 1). These results indicated that the painting was possibly made over preparatory layer of a zinc white, and/or Ca-base substrate, most likely chalk ($CaCO_3$) and/or gypsum ($CaSO_4.2H_2O$). Lead white ($2PbCO_3.Pb(OH)_2$) and lithopone ($ZnS + BaSO_4$) were also possibly used [4].

White; it was clearly seen as zinc white (ZnO) that characterized by high Zn peaks in the white area.

Orange; the characteristic chemical elements obtained from the location number O1-1 and O1-2 were Zn, Pb, Cr, Ca, Ba, and trace of Cl and Fe. The identification of Pb and Cr revealed the use of chrome orange ($PbO.PbCrO_4$) [4].

Yellow; presenting of strong Zn and trace of Pb, Ba, S, and Sr showed that this yellow pigment was likely unidentified by the XRF. The Zn was the main constituent of zinc white or probably the lithopone white of the preparation or mixture. Red was not presented in this painting.

The birth of the golden sea Painting: Eighteen locations on the paintings were investigated. The whole set of spectra acquired during the analysis of the painting showed the Pb, Zn, Ca, and Ba peaks. These results suggested that these paintings were possibly made over preparatory layer of a zinc white, and/or Ca-base substrate, most likely chalk ($CaCO_3$) and/or gypsum ($CaSO_4.2H_2O$), with lead white ($2PbCO_3.Pb(OH)_2$) and lithopone ($ZnS + BaSO_4$) [4].

White; white areas of the painting were carried out as a mixture of zinc white (ZnO) and lead white ($2PbCO_3.Pb(OH)_2$) characterized by strong signals of Pb [4] and Zn in the same locations; number w2-1, w2-2.

Orange; the XRF spectra indicated the Zn, Pb, Se, Ba, as dominant component while Ca, Cd, S, and Cr were less intense. Presenting of Se, Cd, and S suggested the use of cadmium orange (Cd(S,Se)) or cadmium red (Cd(S,Se)) mixed with organic yellow.

Red; the XRF spectra of the area number r2-1 presented the predominance of Zn, Ba, Se, and Pb together with the less intense of Cd, Ca, Cr, and Fe suggested the use of cadmium red.

Yellow; regarding the yellow areas, thanks to UV examination that showed two yellows differently though they presented the same hue under visible light. Thus, the possibility of using two pigments in the pallet was hinted. The location of y2-1 and y2-2 presented spectra of Pb and Zn as dominant elements while Ca, Ba, S, and Sr were traced element, these results were unidentified by XRF. The location of y2-3, and y2-4 presented strong peaks of Pb, Zn, Ba, and Cr. This presenting led to investigate that the lemon yellow (barium chromate ($BaCrO_4$.)) was used. Figure 3a-3b presented XRF spectra of yellows.

Untitled Painting

Fourteen locations on the paintings were investigated. The whole set of spectra acquired during the analysis of the painting showed the Pb, Zn, Ca, and Ba peaks. These results suggested that these paintings were possibly made over preparatory layer of a zinc white, and/or Ca-base substrate, most likely chalk ($CaCO_3$) and/or gypsum ($CaSO_4.2H_2O$), with lead white ($2PbCO_3.Pb(OH)_2$) and lithopone ($ZnS + BaSO_4$) [4].

Table 1: The table presents the detected elements found in different colors on three paintings, related to possible pigments applied (with its chemical composition).

painting	color	location no.	detected elements *major; **minor; (tr) trace	possible pigments applied	chemical composition
Abstract Scenery	white	W1-1	*Zn; (tr) Pb, Ca, Ba, Sr	zinc white (Zn)	ZnO
		W1-2	*Zn; (tr) Ba, Pb, Ca, Sr	zinc white (Zn)	ZnO
	orange	O1-1	*Zn, Pb, Cr, Ca; **Ba, (tr) Cl, Fe	Chrome Orange (Pb, Cr)	$PbO.PbCrO_4$
		O1-2	*Zn, Pb, Cr; **Ca, Ba; (tr) Fe, Cl	Chrome Orange (Pb, Cr)	$PbO.PbCrO_4$
	red	not present			
	yellow	Y1-1	*Zn; (tr) Pb, Ba, Ca, Cr, Fe	Unidentified by XRF	
		Y1-2	*Zn; (tr) Pb, Ba, Ca, Cr, Fe	Unidentified by XRF	
The birth of the golden sea	white	W2-1	*Pb, Zn; (tr) S, Ca, Sr, Cl	lead white (Pb)/zinc white (Zn)	$2\ PbCO_3{\cdot}Pb(OH)_2$ / ZnO
		W2-2	*Pb, Zn; (tr) S, Ca, Sr, Cl	lead white (Pb)/zinc white (Zn)	$2\ PbCO_3{\cdot}Pb(OH)_2$ / ZnO
		W2-3	*Pb, Zn; (tr) S, Ca, Sr, Cl	lead white (Pb)/zinc white (Zn)	$3\ PbCO_3{\cdot}Pb(OH)_2$ / ZnO
	orange	O2-1	*Zn, Pb, Se; **Ba, Cd, S; (tr) Ca, Cr, Fe, Sr	cadmium orange (Se, Cd), or cadmium red mixed with yellow?	Cd(Se,S)
		O2-2	*Zn, Pb; **Se, Ba, (tr) Ca, Cd, S, Fe,Sr	cadmium orange (Se, Cd), or cadmium red mixed with organic yellow.	Cd(Se,S)
	red	R2-1	*Zn, Pb, Se; **Ba, Cd, Ca; (tr) S, Cr, Fe	Cadmium red (Se, Cd)	Cd(Se,S)
	yellow	Y2-1	*Pb, Zn; (tr) Ca, Ba, Sr	Unidentify by XRF	
		Y2-2	*Pb, Zn; (tr) Ba, Ca, Cl, Sr	Unidentify by XRF	
		Y2-3	*Pb, Zn; **Ba, Cr; (tr) (Ca, Sr, S, Cl, Fe)	Lemon yellow (Ba, Cr)	$BaCrO_4$
		Y2-4	*Zn, Pb, Ba; **Cr; (tr) Ca, S, Sr, Cl, Fe)	Lemon yellow (Ba, Cr)	$BaCrO_5$
Untitled	white	W3-1	*Zn, Ba; (tr) Pb, Ca white1	Lead white (Pb),Zince white (Zn),Lithopone white (Zn, Ba)	$2PbCO_3{\cdot}Pb(OH)_2$,ZnO, BaSO4.ZnS,
		W3-2	*Ba, Zn; (tr) Pb, Ca, Sr, Fe white2	Zinc white (Zn)	ZnO/,$BaSO_4$.ZnS,
		W3-3	*Zn, Ba; (tr) Pb, Ca, Cr white3	Zinc white (Zn)	ZnO/,$BaSO_4$.ZnS,
		W3-4	*Zn; **Ba, Pb; (tr)Ca, Fe, Sr white4	Zinc white (Zn)	$2PbCO_3{\cdot}Pb(OH)_2$,ZnO, $BaSO_4$.ZnS,
		W3-5	*Zn; (tr) Ba, Pb, Cr, Fe white5	Zinc white (Zn)	ZnO
		W3-6	*Zn; (tr) Ba, Pb, Cr, Fe white6	Zinc white (Zn)	ZnO
	orange	O3-1	*Zn; (tr) Ba, Se, Cd, S, Pb, Cl, Ca,	Cadmium orange (Cd), or cadmium red mixed with yellow	Cd(S,Se)
		O3-2	*Zn; (tr) Ba, Ca, Pb	not conclusive	
	red	R3-1	*Zn; **Ba, Pb; (tr) Se,Ca, Cr, Cd	not clear but possible to have Cadmium red (trace of Cd, Se)??	Cd(S,Se)??
	yellow	Y3-1	*Zn; ** Ba; (tr) Pb, Cl, Se, Ca, Cr, Sr	Cadmium yellow Trace of selenium but not clear to identify. Not conclusion	Trace of selenium but not clear to identify. Not conclusive
		Y3-2	*Zn; **Ba; (tr) Pb, Ca	Unidentified by XRF	

White; the XRF spectra of white colors were showed in Figure 3c-3f. Although at a visual observation the white paints appeared to have similar hue, thanks to large number of point measurements collected across the painting surface, two to three different possible whites have been pinpointed. On some of the white paints, XRF measured strong signal of zinc and barium (Figure 3c, 3d), while other points of white, XRF showed only strong peak of zinc (Figure 3f). Lead presented as trace element in almost all measurement points but it significantly presented at some points (Figure 3e). Thus, indicating the possible use of zinc white (ZnO), lithopone white ($ZnS + BaSO_4$) and perhaps lead white ($2PbCO_3.Pb(OH)_2$)[4].

Orange; Orange presented strong zinc with trace elements of S, Se and Cd. These results were not able to highly identified as cadmium orange or cadmium red mixed with yellow. However, it was possible to have trace of these pigments in the pallet.

Red; For the red, the XRF spectra corresponding to the area of the red location number r3-1 that showed the predominance of Zn, Ba, Se, and Pb together with the less intense of Cd, Ca, Cr, and Fe. Though presenting of Se, S, and Cd was not very clear but it could possibly indicate the use of cadmium red (Cd(S, Se)).

Yellow; Signals of yellow of the Untitled painting were not sufficient to identify by XRF method.

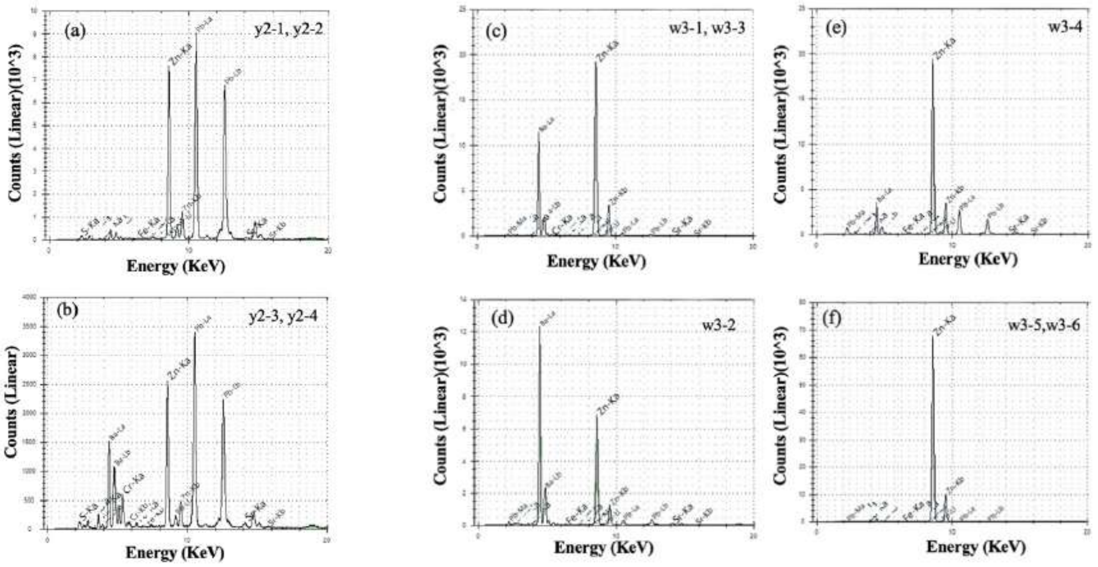

Figure 3. XRF spectra of yellow of the birth of the golden sea (a) and (b), and white of the untitled painting at different locations(c), (d), (e), and (f).

CONCLUSION

Three paintings by Pratuang Emjaroen, one of the most famous figures in Thai contemporary art, were analyzed by portable micro-XRF. XRF provided substantial information about the materials present in the paintings. Four colors in the paintings; white, red, orange, and yellow were mainly focused and presented in this paper. The results reported the use of zinc white (ZnO), lead white ($2PbCO_3.Pb(OH)_2$), chrome orange ($PbO.PbCrO_4$), cadmium red (CdS+CdSe), lemon yellow ($BaCrO_4$), and another organic yellow that was not identified by XRF. It is expected that the results discussed here may help the art historians and conservators to understand the artist's method of work, as well as his creative process. It's also expected that these artworks can be further analyzed by other techniques, such as Raman spectroscopy, and/or IR spectroscopy, etc., in order to complement the information obtained by this XRF, contributing more to the reconstruction of the history of these artworks. These results presented can facilitate and guide for further analysis by other methodologies.

ACKNOWLEDGEMENT

The authors gratefully acknowledge the private art collectors, Piriya Watchjitpan, Director of The Art Auction Center (TAAC) and the Co- founder of Thai Art Collector Association (TACA) and Kittiporn Jalichandra, the founder of Thai Art Collector Association (TACA) who gave permission for the analyses of these paintings. The authors would also like to thank the Robert Bougrain, director of Restaurateurs Sans Frontières Laboratory, Studio for art conservation and restoration for his all support, and Luigi Fieni the restorer/photographer for his helpful photography of the paintings presented in this article.

REFERENCES

1. Thailand's Contemporary Art on the Web. (n.d.). Thai artist- Pratuang Emjaroen. Rama IX Art Museum Foundation. http://www.rama9art.org/pratuang/

2. Thanom, C. (9 May 2016). Pratuang Emjaroen 1935. The Routledge Encyclopedia of Modernism. doi:10.4324/9781135000356-REM803-1.

3. ThaiPBSworld. (March 7, 2022) Thai national artist Pratuang Emjaroen dies of COVID-19 at 87. ThaiPBSWorld. https://www.thaipbsworld.com/thai-national-artist-pratuang-emjaroen-dies-of-covid-19-at-87/.

4. Molari, R., & Roberto, A. (2021). Pigment analysis in four paintings by Vincent van Gogh by portable X-ray fluorescence (XRF). *Radiation Physics and Chemistry*, 181 109336.

5. Kriznar, A., Muñoz, M.V., F, de la Paz., Respaldiza, M. A., & Vega, M. (2008). Non-Destructive XRF Analysis of Pigments in a 15th Century Panel Painting. 9th Int. *Conference on NDT of Art 2008.* Jerusalem, Israel, May 2008. https://www.ndt.net/?id=6125 p25.

6. Vornicu, N., Geba, M., & Bibire, C. (2009). Non-destructive analysis in a study of the religious art objects. *Journal of Physics: Conference Series, 182, PROCESSES IN ISOTOPES AND MOLEKULS 24-26 September, 2009, Cluj-Napoca, Romania.* **doi:** 10.1088/1742-6596/182/1/012044.

7. Ha, J. W., & Lee, S. J. (2015). Identification of natural inorganic pigments used on 18th century Korean traditional mural paintings by using a portable X-ray fluorescence. *Journal of Industrial and Engineering Chemistry,* 28, 328–333. doi:10.1016/j.jiec.2015.03.011.

8. Merkaj, E. and Civici, N. (2019) Micro-XRF Investigation of Decoration Materials and Painting Techniques in Three 18th-19th Century Mosques in Berat, Albania. *Journal of Materials Science and Chemical Engineering*, **7**, 1-15. doi: 10.4236/msce.2019.75001.

9. Serafima, S., Duliu, O.G., Manea, M.M., Niculescu, G. (2016). FTIR, XRF and optical microscopy analysis of the painting layer of an early 19th century icon. *Romanian Reports in Physics, 68 (1), 191–202, 2016.*

10. Kriznar, A., Maria del Valme Muñoz, Respaldiza, M.A., and Vega, M. (2012) Materials applied in Bernardo Martorell's painting analysed by portable XRF**.** *ArcheoSciences.36.*37-46. https://doi.org/10.4000/archeosciences.3712.

INFLUENCE OF ILLUMINATION COLOR ON PERSON TRACKING BASED ON DEEP LEARNING AND ITS COMPENSATION

Motonori Doi[1]*, Yoshiki Ishikawa[2], Shogo Nishi[3] and Akira Kimachi[3]

[1]*Faculty of Information and Communication Engineering, Department of Telecommunications and Computer Networks, Osaka Electro-Communication University, Japan.*
[2] *Graduate School of Engineering, Osaka Electro-Communication University, Japan.*
[3] *Faculty of Information and Communication Engineering, Department of Engineering Informatics, Osaka Electro-Communication University, Japan.*

*Corresponding author: Motonori Doi, doi@oecu.jp

ABSTRACT

Person tracking in video is important in many applications, such as video surveillance and marketing strategies. Nowadays, image processing for person tracking is mostly based on deep learning techniques. In particular, the combination of the YOLO algorithm and the DeepSORT algorithm shows good accuracy in object tracking. The YOLO is an object detection method that uses convolutional neural networks (CNN), and the DeepSORT is an object tracking method that utilize the SORT algorithm based on the Kalman filter method and a re-identification (Re-ID) model using CNN. The degree of similarity between the detected person and the person being tracked is evaluated by the cosine distance of detected features by the CNN in the Re-ID model. The cosine distance ranges from 0 to 2. The cosine distance of 0 indicates the highest similarity. Person tracking sometimes fails due to changes of lighting environment. Investigating the influence of changes in illumination color on person tracking is required. This study aims to improve the accuracy of person tracking under various lighting conditions. First, we investigated the influence of the illumination color on person tracking performance. In our experiments, we varied the color temperatures of the illumination from 2000 K to 8000 K in 1000 K intervals using a programmable light source and captured videos of indoor scenes with a person walking along the same path. Images illuminated at 5000K were used as references. The cosine distance increased as the illumination color varied away from 5000 K, exceeding 0.5 at 8000 K. It becomes difficult to track person accurately at this cosine distance. Next, we attempted to compensate for the illumination color. For this compensation, we calculated the averages of the R, G, and B values for the reference image and each frame of the target video to be compensated, and derived the ratio of these averages. These R, G, and B ratios were multiplied by the value of all pixels in the image to be compensated, resulting in an image that closely matched the color of the reference image. In our experiments, we confirmed that the color correction reduced the cosine distance when the illumination changed. We also investigated cases involving two-color light sources. We attempted partial illumination compensation, and the result implicates the effectiveness of this compensation.

Keywords: Illumination color compensation, Person tracking, Deep learning

INTRODUCTION

Person tracking in video is important in many applications, such as video surveillance and marketing strategies. Nowadays, image processing for person tracking is mostly based on deep learning techniques. In particular, the combination of the YOLO algorithm and the DeepSORT algorithm shows good accuracy in object tracking [1-3]. This deep-learning-based method is robust to fluctuations in video.

However, person tracking using this method sometimes fails due to changes of lighting environment. Most cameras have auto white balance (AWB) function. However, AWB doesn't work well in some lighting situations [4]. Investigating the influence of changes in illumination color on person tracking is required.

This study aims to improve the accuracy of person tracking under various lighting conditions. First, we investigated the influence of changes in illumination color on person tracking performance. Next, we attempted to compensate for the illumination color and confirmed the improvement in tracking performance.

PERSON TRACKING AND COLOR COMPENSATION

Person tracking method

In this study, we employed the combination of the YOLO algorithm and the DeepSORT algorithm as the person tracking method. The YOLO algorithm is an object detection method that uses convolutional neural networks (CNN), and the DeepSORT algorithm is an object tracking method that utilize the SORT algorithm based on the Kalman filter method and a re-identification (Re-ID) model using CNN. The Re-ID model was trained using a large-scale person re-identification dataset of MARS [5]. In our implementation, we used the YOLOv4 and the DeepSORT modified to track only people were used.

The degree of similarity between the detected person and the person being tracked is evaluated using the cosine distance of the detected features by the CNN in the Re-Id model. The cosine distance is defined as Eq. (1),

$$(cosine\ distance) = 1 - \frac{\mathbf{D} \cdot \mathbf{T}}{\|\mathbf{D}\|\|\mathbf{T}\|} \quad (1)$$

where $\mathbf{D}$ is a feature vector of detected person, and $\mathbf{T}$ is a feature vector of person being tracked. The dimension of each feature vector was 128. The cosine distance ranges from 0 to 2. A cosine distance of 0 indicates the highest similarity between the detected person and the tracked one.

Compensation of illumination color

There are several methods for illumination color compensation. In this study, we employed a simple method using average values for each R, G, and B color values. The color compensation by averaging color values is based on the gray-world assumption. Under this assumption, if the average color in the vision is considered a neutral gray, the effect of illumination is cancelled, and objects' colors are perceived as their natural colors.

In the compensation, RGB values of the input image sequence are transformed using the ratio of the average color for each R, G, and B value in the scene and the reference. The compensated color values in the current k-th frame of the image sequence (R_k',G_k', B_k') are defined as Eq. (2),

$$R_k' = \frac{R_a}{R_{ak}} R_k,\ G_k' = \frac{G_a}{G_{ak}} G_k,\ B_k' = \frac{B_a}{B_{ak}} B_k \quad (2)$$

where (R_a,G_a,B_a) are the averaged RGB values over all pixels in the reference image, (R_k,G_k,B_k) are the RGB values in the current k-th frame and (R_{ak} , G_{ak} , B_{ak}) denotes averaged RGB value over all pixels in the k-th frame.

INVESTIGATING INFLUENCE OF ILLUMINATION COLOR

Dataset

To investigate the influence of illumination color, we created an original small dataset. The dataset includes videos of indoor scenes with a walking person under illumination with color temperatures ranging from 2000 K to 8000 K in 1000 K intervals. The color temperatures were adjusted using a programmable light source (Ledmotive Technologies, Spectra Tune 7!). The scenes were captured using a common USB camera (Logicool HD Pro Webcam C920) with auto gain control and without AWB. The tracked person wore white, black and red clothing on the upper body. In the scenes, the person walks to the left and exits the field of view under the reference illumination of 5000K, then re-enters the field of view from the left and walks to the right under illumination of each color temperature.

Influence of illumination color to person tracking

The influence of lighting conditions on tracking performance was investigated. A scene under 5000K illumination was used as reference. The cosine distance between the person in the reference scene and the detected person under each illumination color was recorded.

Figure 1 shows samples of frames from our dataset. The tracked person wore white, black and red clothing. This figure shows examples of illumination color temperatures of 2000, 5000, and 8000K. Figure 2 shows graphs of cosine distance under each illumination color for each clothing color. The cosine distance increased as the illumination color varied away from 5000 K. In particular, the distance exceeded 0.5 at 8000 K with white and black clothes. It becomes difficult to track person accurately at this cosine distance.

Compensation of illumination color

The cosine distances under illumination color compensations using the averages of RGB values were also investigated in the same manner as the investigating influence of illumination color. Figure 3 shows graphs of cosine distances with illumination color compensation for our dataset. In comparison with Figure 2, all results show that color compensation reduced the cosine distance. The compensation method was simple, but it was effective.

Partial illumination compensation

In many cases, the illumination is not uniform. Therefore, we attempted partial compensation. We captured image sequences under two illuminations: blue and white, and green and white combinations. The illumination color for reference was blue. We compared cosine distances with compensations by average values of the entire image and partial compensation by average values of separated parts. In this attempt, the separation was done by dividing the image equally into the left and right sections.

A scene under two illuminations is shown in Figure 4(a) for blue and white and Figure 4(b) for green and white. The compensated image using the average values of the entire image is shown in Figure 4 (c), and the partial compensated image using the average values of separated parts is shown in Figure 4(d). The cosine distance without compensation was 0.661. With compensation, cosine distances were reduced to 0.274 and 0.225 in the cases of compensation by the average values of the entire image and separated parts, respectively.

Discussions

Our examinations revealed that illumination variations have influences on the common deep-learning-based person tracking method. The compensation of illumination color using the average values of R, G, and B values in the image was effective in our examinations. In many real scenes, the illumination conditions are complex with several light sources. The results for the two illumination scenes implicate the effectiveness of partial illumination compensation. Future work includes compensation for multi-illuminations, automatic separation of compensation areas, and precise evaluations.

CONCLUSION

This study investigated the influence of illumination color on person tracking using deep-learning-based method. The combination of the YOLOv4 and the DeepSORT was employed as the person tracking method. Our examinations revealed that illumination variations have influences on the common deep-learning-based person tracking method. The evaluations in our dataset demonstrated the effectiveness of illumination color compensation using the average values of each R, G, and B value in the image. We also implicated the effectiveness of the partial illumination compensation.

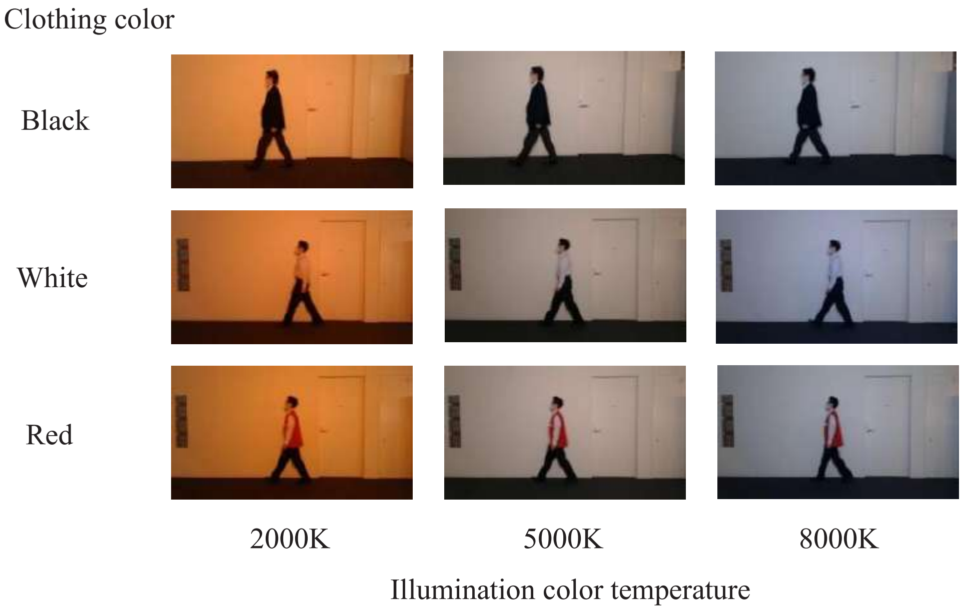

Figure 1. Samples of frames from our dataset

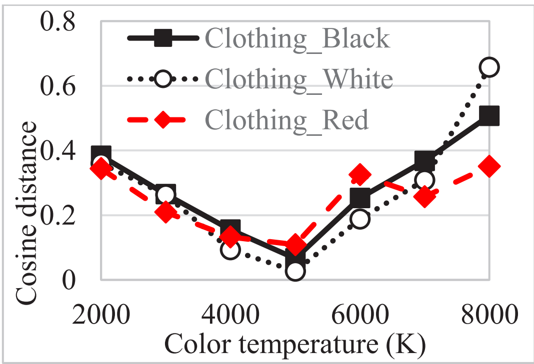

Figure 2. Cosine distance for each clothing color under illumination color changes.

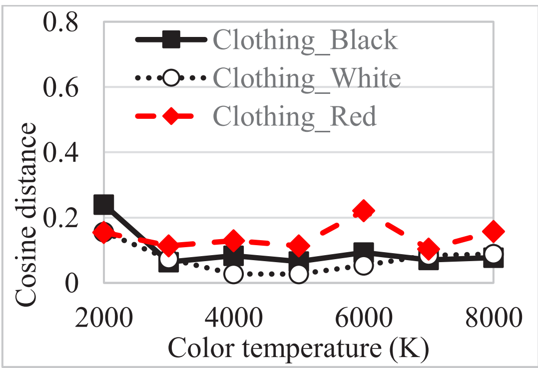

Figure 3. Cosine distance with illumination color compensation for each clothing color under illumination color changes.

(a) Two illuminations scene for reference.

(b) Input scene.

(c) Color compensation using entire image.

(d) Color compensation using separated parts.

Figure 4. Scenes under two illumination colors and compensated images.

REFERENCES

1. Wojke, N., Bewley, A., & Paulus, D. (2017). Simple Online and Realtime Tracking with a Deep Association Metric. *Proceedings of IEEE International Conference on Image Processing*, 3645-3649. doi: 10.1109/ICIP.2017.8296962.
2. Bochkovskiy, A., Wang, G. Y., & Liao, H. Y. M. (2020). YOLOv4: Optimal Speed and Accuracy of Object Detection. *Computing Research Repository*, abs/2004.10934
3. Bewley, A., Ge, Z., Ott, L., Ramos, F., & Upcroft, B. (2016). Simple Online and Realtime Tracking. *Proceedings of IEEE International Conference on Image Processing*, 3464-3468. doi: 10.1109/ICIP.2016.7533003.
4. Doi, M., Tsujimoto, A., Kimachi, A., Nishi, S., & Ikoma, N. (2018). Color based Person Tracking with Illumination Compensation by using Multiple Statistics of Scene, *Proceedings of SCIS-ISIS2018*, 427-430.
5. Zheng, L., Bie, Z., Sun, Y., Wang, J., Su, C., Wang, S., & Tian, Q. (2016). MARS: A Video Benchmark for Large-scale Person Re-identification, *Proceedings of ECCV 2016*.

EFFECT OF COLOR ON GENDER IDENTIFICATION IN THAILAND AND JAPAN

K. Rattanakasamsuk and C. Saksirikosol*

Color Research Center, Rajamangala University of Technology Thanyaburiน Thailand.

*Corresponding author: Chanida Saksirikosol, Chanida_S@rmutt.ac.th

ABSTRACT

Color code is almost standardized for gender identification in some cultures. In Japan, most female toilet signs are red or pink, whereas male toilet signs are blue. As a result, it is not necessary to recognize the sign's details. The color of the toilet sign alone can help you identify the type of toilet. In this study, we compared the impact of color on gender identification. The subjects were 15 Japanese and 15 Thai university students, ages 18 to 22 years old. To confirm their normal color vision, all subjects must pass the Ishihara Test. The stimuli consisted of four different patterns of female and male symbols. Each pattern was created with seven different colors: blue, navy blue, red, pink, purple, gray, and black. As a result, the stimuli included two genders, four patterns, and seven colors, totaling 56 symbols. The stimuli were 10 degrees of visual angle in size. The stimuli were presented on an LED monitor. There were two tasks for each subject. In the first task, the subject assessed the details of the symbol to determine whether they were male or female. In the second task, the subjects were asked to determine whether the color of the symbol was associated with male or female. In each assessment, a symbol was randomly presented for one second and separated by at least three seconds' blank screen. The subjects pressed keypad 1 if they assessed that it was male and keypad 3 if they assessed that it was female. If the subject did not finish their assessment within three seconds of the blank screen, the blank screen would appear until each assessment was finished. For both tasks, the subject's reaction time was recorded.

The findings revealed that there was a clear association between color and gender in both Thai and Japanese culture. Majority of the subjects associated black, grey, navy blue, and blue with males, whereas pink, red, and purple are associated with females. These color-gender associations in Japanese culture were strong enough to influence symbol interpretation. When the symbol's meaning contradicted the color-gender association, for instance, a navy blue female or pink male symbol, the correct response of symbol interpretation of Japanese subjects was lower, and their reaction time was distinctly longer than the navy blue male or pink female, i.e., the non-contradiction between the symbol's meaning and the color-gender association. On the contrary, there is no influence of color on the female symbol interpretation in Thai subjects. Their correct response and their reaction time were quite similar, regardless of the color of the female symbols. This tendency was also observed in almost all male symbols except the pink male symbols. The correct response of the pink male symbols was lower than other color male symbols. Based on our results, we concluded that symbol interpretation could be influenced by color, especially in gender identification.

Keywords: Color and gender, reaction time, gender identification

ACKNOWLEDGEMENT

We would like to thank Prof. Yoko Mizokami and all members of the Vision Science Laboratory for their support to collect data in Japan. This research was supported by JSPS Core-to-Core Program, (grant number: JPJSCCB20220006.).

THE INFLUENCE OF COLOR ON SHORT-TERM MEMORY

U. Tangkijivwat*, M. Meenorn and P. Yamprasai

Color Research Center, Rajamangala University of Technology Thanyaburi, Thailand.

*Corresponding author: uravis_t@rmutt.ac.th

Keywords: short-term memory

Short-term memory (STM) refers to the retention of a small amount of information for a short period of time, such as remembering the names and faces of new friends or a new telephone number. It is essential for daily functioning, allowing us to immediately recall anything we are learned. In this type of memory, information is held temporarily while it is being rehearsed, elaborated upon, recoded, related to past knowledge, and so on, before it is transferred to long-term memory or is forgotten. STM can be improved by repeatedly rehearsing an information. An interesting issue in memory research is on ways to enhance memory performance and information retention. This study, hence, aims to investigate the relationship between color and STM ability. Thirty-one undergraduate students participated in a STM experiment, using a serial-recall set up. The series for serial recall included random numbers, random words, and abstract images. The foreground and background colors of the series varied among six colors: black, white, red, yellow, green, and blue. The subjects were presented with a series of items and immediately asked to recall them in the correct order. In a series of random numbers, the highest STM score was found with black numbers on a white background, with a mean score of 19.0, while the lowest STM score was observed with yellow numbers on a white background, with a mean score of 11.9. In the series of random words, the best STM score was achieved with blue random words on a black background, with mean score of 14.9, while the lowest score was found with yellow random words on white background, with mean score of 11.8. In the case of abstract images, white abstract images on a black background yielded the highest STM score, with a mean score of 18.7, whereas black abstract images on a white background resulted in the lowest STM score, with a mean score of 6.7. The results of ANOVA test revealed a significant difference among various foreground and background color combinations in abstract images at 0.01 level, but this difference was not observed in random numbers and random words series.

DATA ANALYSIS OF REGIONAL AESTHETIC FACTORS ON "COLOR-SCAPE" IN JAPAN

Ryoma Yamashita[1*], Shoma Nagaya[1], Takashi Hanari[2], and Mikiko Kawasumi[1]

[1]*Graduate School of Science and Technology, Meijo University, Japan*
[2]*School of Culture-Information Studies, Sugiyama Jogakuen University, Japan*

*Corresponding author: Ryoma Yamashita, 233426019@ccmailg.meijo-u.ac.jp

ABSTRACT

This study aims to clarify the differences in regional aesthetic factors of the 'colorscape' and to apply them to develop color townscape guidelines based on regional characteristics. The 'Beautiful Colorscape in Japan' project started in 2020 in the context of the COVID-19 pandemic. Over four hundred beautiful townscapes were nominated by the regular members of the Color Science Association of Japan (CSAJ) for two years[1], and a data library was built that can be browsed and searched according to place, time, and eleven basic color terms[2]. In this study, we first examined aesthetic factors of the regional features of photo images of three towns in Aichi prefecture, *Ichinomiya, Tokoname,* and *Arimatsu*, using the CSAJ's data library. Twenty-eight CSAJ members reported their visual impressions of each photo image using Japanese adjectives such as 'vivid', 'calm', 'dynamic', and 'high contrast'. The semantic differential (SD) method was used to quantify the observers' visual impressions, and principal component analysis was used to visualise the structure of the impressions of each townscape. The factors affecting aesthetic appeal were shown to differ among the towns, and industrial and cultural traditions were reflected in the results. For instance, 'high contrast' is important for the textile industry town *Ichinomiya*, while 'orderly' is the effective aesthetic factor in the ceramic industry town *Tokoname*. Secondly, the symbolic colors of each photo image were visualised to examine the effect of color on the aesthetic factors in townscapes. The RGB values of all pixels on the photo image were converted to L*a*b* values, and the ratio of colors in each photo image was calculated using k-means clustering. As a result, the townscapes that contain more cold than warm colors tend to be closer to 'beautiful', and the townscape with a simple color composition might be effective for aesthetic impression. For future research, we will use various approaches for full analysis including text mining and statistics, because the 'Beautiful Colorscape in Japan' data library contains much information such as memorial stories by the poster, the reason for the aesthetic elements, and eleven basic color terms. In the near future, we plan to expand the project to the 'Beautiful Colorscape in the World' in English.

Keywords: Townscape, Regional factors, Photo image, SD method, Principal component analysis

INTRODUCTION

The 'Beautiful Colorscape in Japan' project was established in 2020 during the COVID-19 pandemic by interested members of the Color Science Association of Japan (CSAJ). In this project, CSAJ members nominate images of diverse beauty in their own familiar daily environments for inclusion in an online library. This library can be browsed and searched according to place, time, and eleven basic color terms. Although the project website already contains more than four hundred items[1] from over a two-year period, we continue to collect more, and we plan to apply a similar process to future human resource development in various fields and value education for children. The purpose of this study is to identify differences in regional aesthetic elements of townscapes from a color perspective.

The next sections will show the results of structural analysis of townscapes from three towns and discuss the effects of color on aesthetic factors.

STRUCTURAL ANALYSIS OF TOWNSCAPES

Six photo images of *Ichinomiya*, *Arimatsu*, and *Tokoname* were selected from the 'Beautiful Colorscape in Japan' website, as shown in Figure 1. These three towns in Aichi prefecture are famous for their textile industry, pottery, and dyeing and have a long history and tradition. The semantic differential (SD) method was used to quantify the visual impression of the photo images. Twenty pairs of antonym adjectives, including 'vivid'–'dull', 'calm'–'excited', 'dynamic'–'static', and 'high contrast'–'low contrast', were prepared in Japanese and applied to five-point rating scales. Twenty-eight CSAJ members responded on these scales about the visual impression observed in each photo image. The SD data were analysed using principal component analysis (PCA) to visualise the structure of the impression.

Table 1 shows the results of PCA summarizing principal components with a contribution rate of 10% or more, and Figure 2 describes the positioning of eighteen photo images on the PCA score diagrams. Factors affecting aesthetic appeal clearly differed among the towns, and industrial and cultural traditions were reflected in the results. For instance, 'high contrast' is important for the textile industry town *Ichinomiya*, while 'orderly' is effective as the aesthetic factor in the ceramic industry town *Tokoname*, and 'calm' and 'static' are located near 'beautiful' in the dyeing cultural town *Arimatsu*.

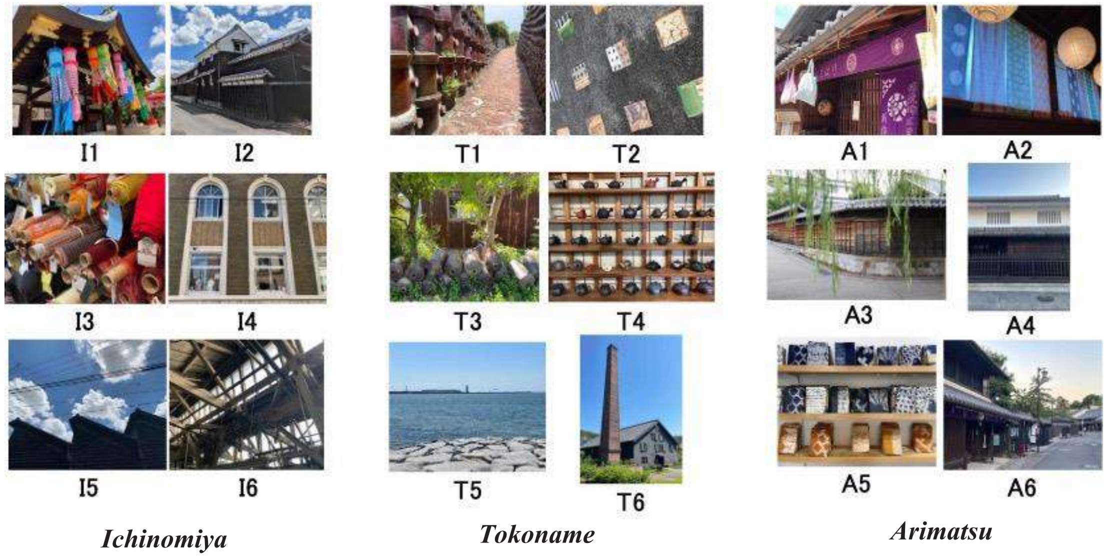

Figure 1: Photo images of townscape

Table 1: Results of PCA

Ichinomiya

Variable name	PC1	PC2
Eigenvalue	13.016	3.461
Contribution rate	0.651	0.173
Cumulative contribution rate	0.651	0.824
bright	0.926	0.333
vivid	0.794	0.522
high-contrast	-0.226	0.81
rough	-0.763	-0.233
stately	-0.939	-0.283
complex	0.7	-0.207
hard	-0.955	-0.162
warm	0.705	-0.469
quiet	-0.979	-0.142
static	-0.956	-0.204
strong	-0.857	-0.11
free	0.981	-0.101
calm	-0.95	-0.219
orderly	-0.84	0.297
new	0.937	0.291
unique	0.97	-0.057
traditional	-0.716	0.545
artificial	0.541	-0.251
beautiful	-0.372	0.804
favorite	-0.415	0.827

Tokoname

Variable name	PC1	PC2	PC3	PC4
Eigenvalue	7.014	4.654	4.382	2.708
Contribution rate	0.351	0.233	0.219	0.135
Cumulative contribution rate	0.351	0.583	0.802	0.938
bright	0.77	0.422	-0.326	0.338
vivid	0.656	0.598	-0.269	0.363
high-contrast	-0.325	0.168	0.605	0.347
rough	0.286	-0.27	0.127	0.899
stately	-0.859	0.456	-0.142	0.182
complex	-0.883	-0.338	0.046	-0.089
hard	-0.85	0.374	0.248	0.201
warm	-0.844	0.151	0.401	0.036
quiet	0.177	0.339	-0.848	0.221
static	-0.319	-0.03	-0.932	0.085
strong	-0.457	0.625	-0.17	0.609
free	0.712	-0.631	0.228	0.189
calm	-0.122	-0.278	-0.869	-0.323
orderly	-0.026	0.819	0.052	-0.569
new	0.891	0.173	0.131	-0.381
unique	0.296	0.175	0.877	0.33
traditional	-0.992	0.027	-0.067	-0.093
artificial	0.185	0.247	0.595	-0.527
beautiful	0.263	0.946	0.006	-0.094
favorite	0.145	0.928	0.062	-0.104

Arimatsu

Variable name	PC1	PC2	PC3
Eigenvalue	11.864	4.219	2.034
Contribution rate	0.593	0.211	0.102
Cumulative contribution rate	0.593	0.804	0.906
bright	0.377	0.877	0.173
vivid	0.657	0.691	0.091
high-contrast	-0.123	0.613	0.756
rough	-0.001	0.481	-0.65
stately	-0.891	0.325	-0.093
complex	0.797	-0.364	0.125
hard	-0.918	0.362	-0.064
warm	-0.311	0.518	-0.302
quiet	-0.915	-0.235	-0.263
static	-0.901	-0.378	-0.096
strong	-0.756	0.507	0.286
free	0.989	-0.077	0.05
calm	-0.827	-0.53	-0.179
orderly	-0.979	0.017	0.184
new	0.829	-0.411	0.256
unique	0.97	-0.086	0.192
traditional	-0.939	-0.077	0.193
artificial	-0.788	0.571	0.12
beautiful	-0.716	-0.607	0.275
favorite	-0.649	-0.327	0.651

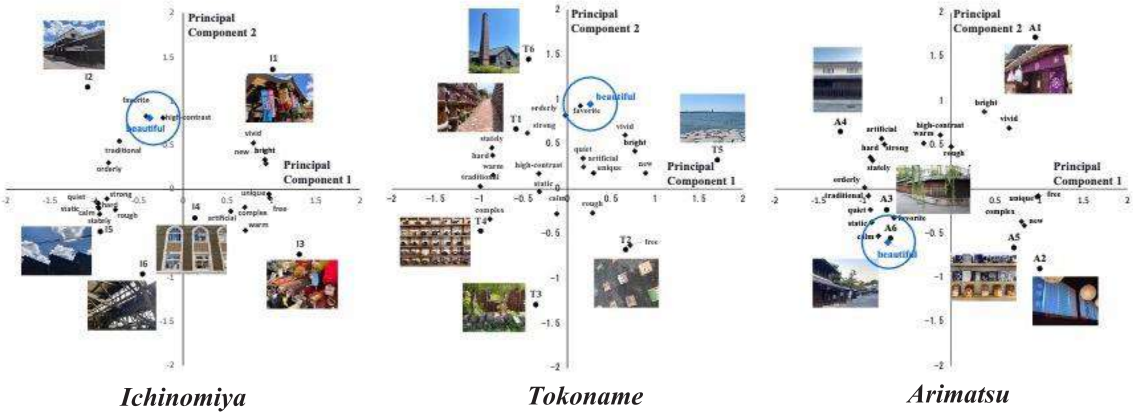

Figure 2: Positioning of eighteen photo images on the PCA score diagrams

EFFECTS OF COLOR ON AESTHETIC FACTORS

The symbolic colors of each photo image are visualised in the procedure shown in Figure 3 to examine the effect of color on aesthetic factors in townscapes. As the first step, the RGB values of all pixels on the photo image are converted to L*a*b* values and considered in three-dimensional space, as in the figure. Second, the three-dimensional data are clustered using k-means. For townscapes such as the one shown in Figure 1, ten clusters are sufficient, although twenty may be necessary for colorful images. In the last step, the ratio of the number of pixels in the same cluster is represented as a band graph in descending order. In the following, this will be represented as a color palette.

A color palette was generated for each photo image using the procedure described above and pasted into the scatter plot of the principal component scores, as shown in Figure 4. The townscapes that contain more cold than warm colors tend to be rated more closely to 'beautiful', especially those with a high ratio of monotone colors, such as black, white, and grey. In addition, color palettes with many colors tend to be rated as far from 'beautiful'. A small number of colors may mean that symbolic colors are emphasised. Based on these findings, a townscape with a simple color composition may be effective in creating an aesthetic impression.

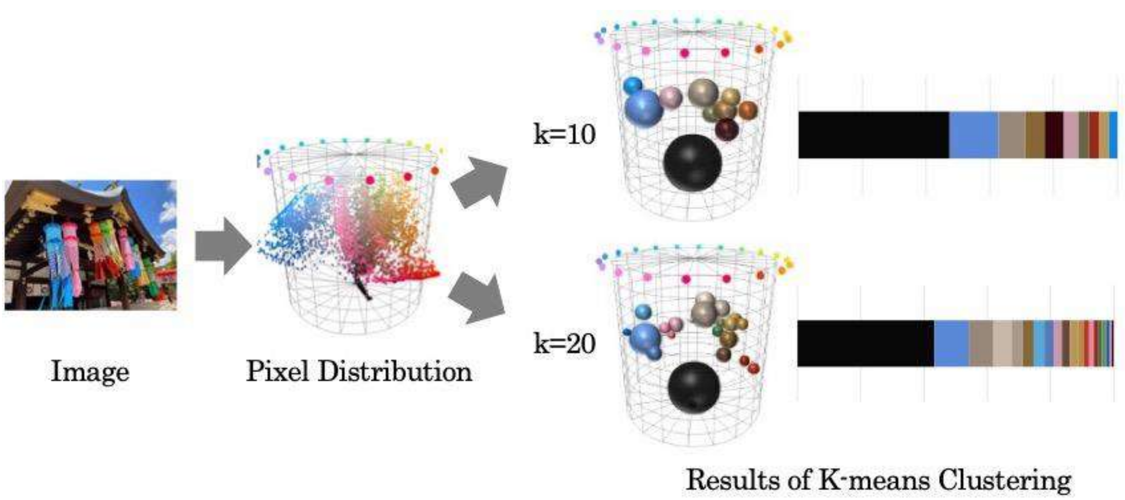

Figure 3: Method to derive symbolic colors from each photo image

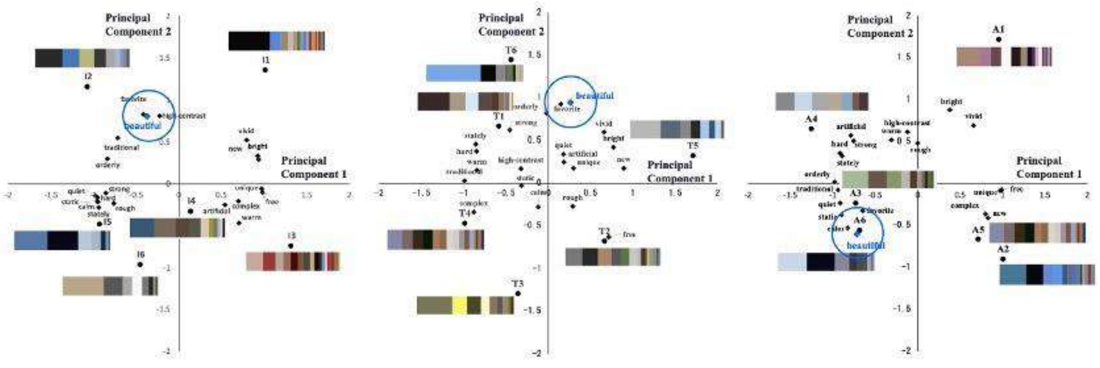

Ichinomiya ***Tokoname*** ***Arimatsu***

Figure 4: Positioning of eighteen color pallets on the PCA score diagrams

CONCLUSION

The differences in regional aesthetic elements of townscapes in three towns were compared using structural analysis by PCA and color pallets, and it became clear that the psychological factors and color characteristics affecting aesthetic appeal differed among the towns. Future research should use various approaches for complete analysis including text mining and statistics, because the 'Beautiful Colorscape in Japan' data library contains much other information, such as memorial stories of the poster, the reasons for the aesthetic elements, and eleven basic color terms. Additionally, townscapes change depending on the season and time and differ on special days such as festivals. Future research should focus on breaking down the components into universal or variable factors. In the future, we plan to extend the project to a 'Beautiful Colorscape in the World' in English.

ACKNOWLEDGEMENT

This work was supported by Ichihara International Scholarship Foundation, Shikishima Academic and Cultural Promotion Foundation.

REFERENCES

[1] The Color Science Association of Japan. (2020). *Beautiful Colorscape in Japan.* Retrieved September 7, 2023, from https://color-science.jp/colorscape/

[2] Berlin, B. and Kay, P. (1969). *Basic Color Terms: Their Universality and Evolution.* Studies in English Literature, 1972, p.170–184

COLOR INDEX DEVELOPMENT OF NAGOYA COCHIN EGGSHELL

Shoma Nagaya [1*], Ryoma Yamashita[1], Mika Akao[2], Hiromitsu Miyakawa [2], Akihiro Nakamura[2], Toshihiko Tsukada[3], and Mikiko Kawasumi[1]

[1]*Graduate School of Science and Technology, Meijo University, Japan*
[2]*, Aichi Agricultural Research Center, Japan*
[3]*Faculty of Information Science, Aichi Institute of Technology, Japan*

*Corresponding author: Shoma Nagaya, 233426013@ccmailg.meijo-u.ac.jp

ABSTRACT

The eggshell surface of a hen named the Nagoya breed (commonly known as Nagoya Cochin) has a unique color, which is one of the reasons for its attractiveness. The purpose of this study was to survey an attractive color range and develop a color visualisation system for eggshells of Nagoya Cochin to manage their visual quality. These results will be useful for agricultural producers to maintain traditional breeds and improve their commercial value. As the first experiment to determine the appropriate color range of Nagoya Cochin eggs, the eggshell color of 60 eggs was measured, and the visual quality of each egg was evaluated using the eggshell photo image by 14 visual inspection experts of the Aichi Agricultural Research Center. They scored the attractiveness of Nagoya Cochin's eggshell color on a five-point Likert scale in five steps, and the relationship between colorimetric data and color attractiveness score was determined in the color space. Second, color variations of eggshells were generated based on the actual image of the egg, and the visual qualities of 315 egg images were scored quantitatively by seven experts. Although the actual eggs differed individually in size and shape, in this experiment, they were standardised and only the visual quality of color was examined. From the results of the two experiments, the color range of the attractive eggshells of Nagoya Cochin was determined using the Hunter LAB color space. Finally, a prototype system to visualise the quality of eggshell color was developed, and the color quality was confirmed as reddish or yellowish using colorimetric data from the CM-700d spectrophotometer (Konica Minolta). After testing the system in the field, several functions that required improvement were identified, and the graphical user interface was modified. This system is expected to be a useful and practical tool for agricultural producers to continue traditional breeding to obtain regional products.

Keywords: Eggshell, Nagoya Cochin, Color attractiveness, Visualization, Prototype system

INTRODUCTION

The Nagoya breed (commonly known as Nagoya Cochin) is one of the most famous chicken breeds and was the first domestic commercial chicken in Japan. It is a traditional breed with a long history since 1868 that cannot be mass-produced. Chicken meat and eggs of Nagoya Cochin are more expensive than those of other popular breeds. The eggshell surface of the Nagoya Cochin has a unique visual characteristic called "Sakura Fubuki" because of its cherry blossom colored body with white speckles (Figure 1), which helps maintain its brand power. However, numerical management methods for eggshell color have not yet been developed and Aichi Agricultural Research Center does not have an accurate color index for quality control [1]. This study aims to determine a practical color index and develop a color visualisation system that is easy to use for managing job sites.

In the next chapter, the appropriate range of attractive color for Nagoya Cochin eggs using Hunter LAB color system will be confirmed. Then, the development of the prototype system to measure and manage the eggshell color is described.

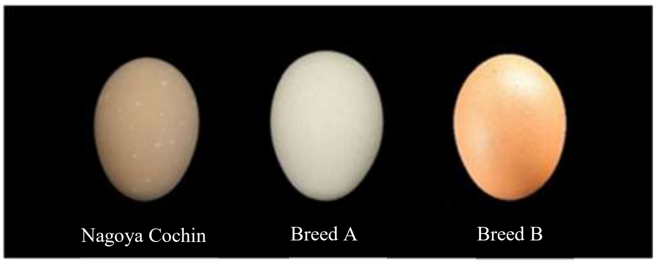

Figure 1: Appearance of eggs of three types

COLOR RANGE SURVEY

Photographs of 60 Nagoya Cochin eggs that were randomly selected are shown on the left side of Figure 2. Colors ranging from yellowish pink to reddish pink were observed. Colorimetric data and visual evaluation scores for the 60 eggs are summarised on the right side of Figure 2. Colorimetric data of the Hunter LAB color system were measured using a colorimeter TC-8600A (Tokyo Denshoku). In addition, a visual evaluation experiment was conducted to score the color attractiveness of "Sakura Fubuki" in Nagoya Cochin eggs. The 14 inspectors who had experience in the visual evaluation of eggshells of Nagoya Cochin at the Aichi Agricultural Research Center rated the "attractiveness of the Nagoya Cochin's eggshell color" on a Likert scale in five steps. These scores and their relationship to colorimetric data of the Hunter LAB color space were then described. Figure 2 confirms the range of egg colors with an attractiveness score of 3.5 or higher. The attractive color range was determined as follows: lightness (L), 60–65; chromaticity (C),10–20; hue angle (h), 40–56.

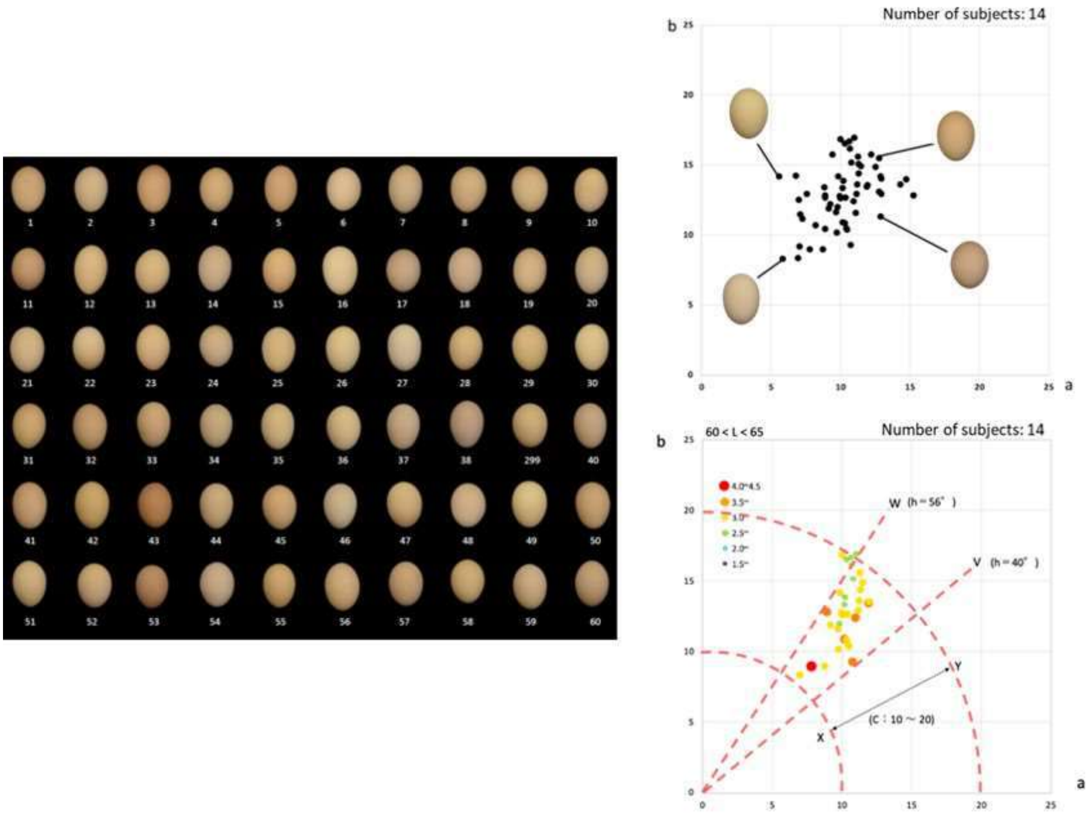

Figure 2: Results of colorimetric data of sixty eggs and their color evaluation scores

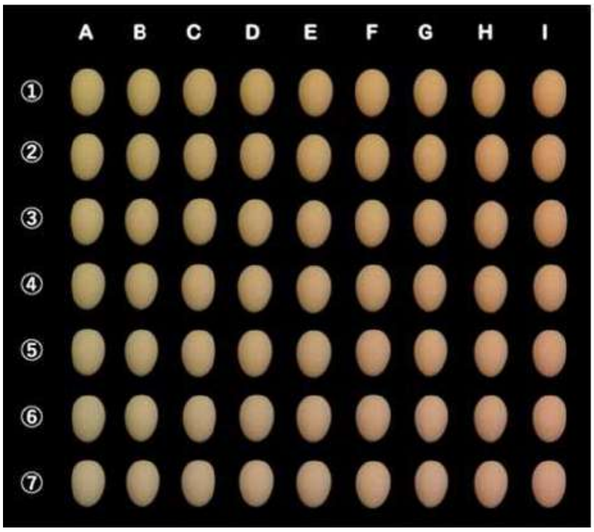

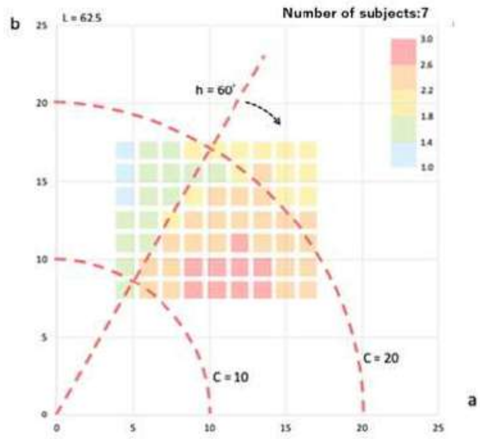

Figure 3: Color variations of eggshells on the screen and colour attractiveness scores

Second, the color variations of eggshells were generated based on the real egg's photo image using Adobe Photoshop, and the "attractiveness of the Nagoya Cochin's eggshell color" of 315 egg images was scored on a 3-point scale by seven experts. Although the eggs differed individually in size and shape, they were standardised, and only the effect of color was examined in this experiment. For the first time, the color simulation experiment enabled us to understand the color range of attractiveness in the form of contour lines and clarify the effect of the hue angle and positioning of the three-dimensional color space.

The results of the above two experiments showed that the appropriate L range was between 60 and 65 for Nagoya Cochin's attractive eggshells. For L = 62.5°, C was between 10 and 20°, with higher scores for hue angles closer to the axis [2].

DEVELOPMENT OF THE COLOR VISUALIZATION SYSTEM

A prototype system for visualising the color quality of an eggshell was developed using the color range survey described above. In this system, the color quality can be confirmed as reddish or yellowish, for instance, using colorimetric data from the CM-700d spectrophotometer (Konica Minolta). The system consists of a spectrophotometer, laptop computer, and external input device (Figure 4) and is implemented in two types of graphical user interfaces (GUI) that measure and visualise color (Figure 5). The software development kit (SDK) provided by Konica Minolta was used to control the colorimeter through the computer [3]. MATLAB (MathWorks) was used for the implementation of GUI. The user can command the initialisation and calibration of the colorimeter and measure egg color from an external input device. The user can also check colorimetric data in real time on the screen and record special notes on the egg surface directly from the GUI. For example, after many measurements are completed, the user can search for eggs with the same mother and confirm the color positioning of the same egg group and its changes based on past data on a single graph. Furthermore, the attractiveness range of colors for Nagoya Cochin eggs is also indicated on the graph, such that the user can immediately understand if the color is outside the proper range.

After testing this prototype system on many actual eggs in the field, several functions that require improvement can be identified and modified. This prototype system is expected to be a useful and practical tool for agricultural producers in managing and maintaining traditional breeds to obtain regional products.

Figure 4: Prototype of the color visualization system for egg color

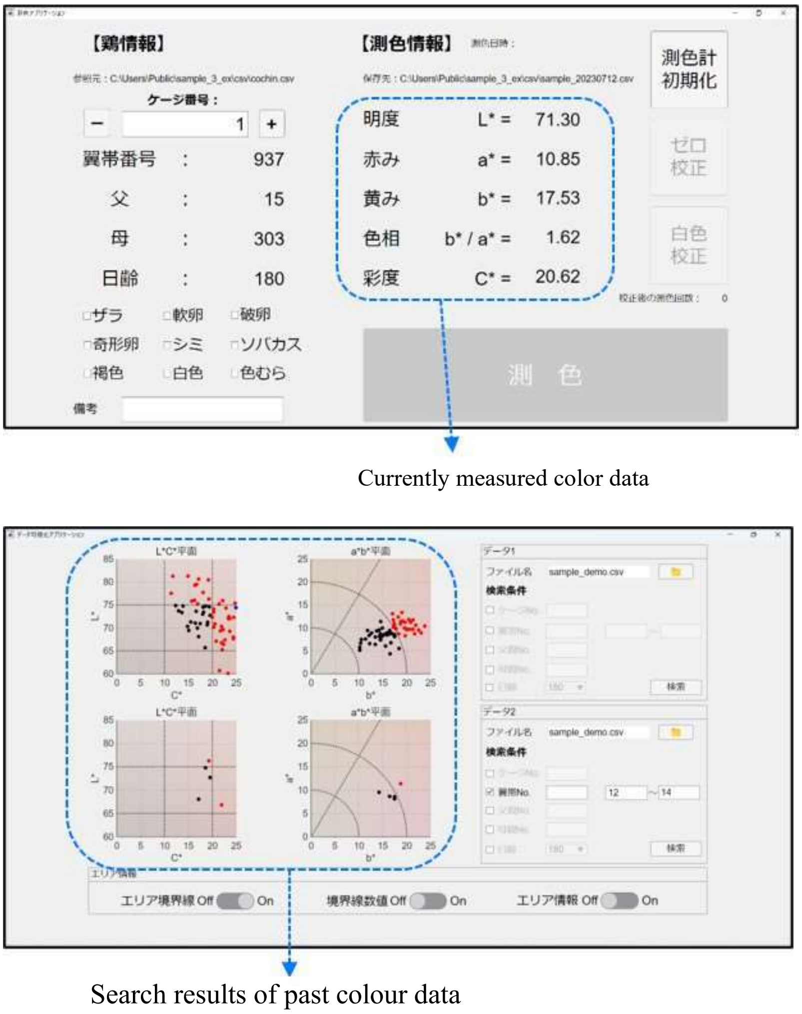

Figure 5: Example of GUI on the prototype system

CONCLUSION

A prototype system that measures the color of eggshells of Nagoya Cochin and indicates their position in real time was developed. The prototype system was successfully debugged. This system will operate on trial in an actual colorimetry scenario in October. After the demonstration of the feasibility of the system, we plan to organise the results of interviews with on-site staff and resolve issues, including user operation errors.

In the near future, we will focus on white spots on the surface of Nagoya Cochin eggs and analyse their distribution patterns to enable automatic visual quality judgment in combination with color management.

REFERENCES

[1] Aichi Agricultural Research Center. (2014). *Feed Management Manual for Layer – Type Nagoya Cochin (revised edition)*. Retrieved September 5, 2023, from https://www.pref.aichi.jp/nososi/jouhou/kenkyuushitsudayori/nagoyakouchinmanyuaru2014.pdf
[2] Kawasumi, M., Tsukada, T., Akao, M., & Miyakawa, H. (2021). *Color Index Development of Nagoya Cochin Eggshell*. Japan Society of Kansei Engineering, 20(3), p. 277–284. doi:org/10.5057/jjske.TJSKE-D-20-00067
[3] Konica Minolta. (n.d.). *CM-700d Spectrophotometer Instruction Manual*. Retrieved September 5, 2023, from https://sensing.konicaminolta.us/wp-content/uploads/cm-700d_instruction_eng-54pn5p743t.pdf

RED BACKGROUND ENHANCES DOMINANCE JUDGEMENT OF GEOMETRIC SHAPES

Yidie Yang[1*], Na Chen[2], Maiko Kobayashi[1,3], Koyo Nakamura[1,3,4], and Katsumi Watanabe[1]

1. Faculty of Science and Engineering, Waseda University, Japan
2. The Gonda Multidisciplinary Brain Research Center, Bar-Ilan University, Israel
3. Japan Society for the Promotion of Science (JSPS), Japan
4. Faculty of Psychology, Department of Cognition, Emotion, Methods in Psychology, University of Vienna, Austria.

*Corresponding author: Yidie Yang, ginayang@ruri.waseda.jp

ABSTRACT

The colour red is thought to signal dominance in both animals and humans. In our previous study, we found that a red background enhanced the perception of dominance in human faces. However, little is known about whether the effect of red background on dominance is specific to human faces. In the present study, we investigated the effect of red background on the dominance judgments of geometric shapes. In addition, we tested whether the effect of red on dominance judgments would be perceptual or conceptual. Ten simple geometric shapes were presented against three different background colours (red, green, and gray; Experiment 1) and flanked by two Japanese words representing colours (Experiment 2). Participants were asked to rate the dominance of each shape stimulus using a seven-point Likert scale. The results showed that dominance judgments of simple geometric shapes increased when presented against the red background compared to the green and gray backgrounds. However, when presented with Japanese words representing colours, there was no difference in dominance judgments. These results suggest that the colour red enhances dominance judgments of geometric shapes and the effects are specific to the perception of red.

Keywords: dominance, red effect, morphed face, geometric shape, background colour

INTRODUCTION

People perceive, use, and are affected by colour in their daily lives. In addition of being an important visual property of objects, colour is often used to describe emotions. Studies have shown that colours carry meaningful information that can affect people's emotions (Kaya & Epps, 2004), cognition (Xia et al., 2016), and behavior (Cuthill et al., 1997; Pryke, 2009, Elliot & Maier, 2014). The colour red has been studied the most. Many studies suggest that red is associated with dominance, aggression, anger, danger, arousal, and sexual attractiveness, and the red effect could have corresponding behavioral consequences (Elliot & Niesta, 2008; Fetterman et al, 2012; Elliot & Maier, 2012, 2014; Mentzel et al, 2017; Pravossoudovitch et al, 2014; Wiedemann et al, 2015).

Red has been suggested to serve as a testosterone-based indicator of dominance (Archer, 2006; Changizi et al., 2006; Hackney, 2006; Hill & Barton, 2005). A red visual cue (e.g., red clothing or red background) is perceived as more dominant, dangerous, and aggressive (Attrill et al., 2008; Hill & Barton, 2015; Wiedemann et al., 2015). Hill and Barton (2015) found that competitors who were randomly assigned to wear red rather than blue sportswear were more likely to win in martial arts at the 2004 Olympics. Attrill et al. (2008) analyzed more than 50 years of archival data from elite English soccer leagues and found a performance advantage for teams wearing red relative to other colours. In the contextual perspective, not only in English, in Japanese, the word red is also associated with fire, serious injury, prohibition, earnestness and invasion even without contexts (Harashima, 2016).

In our previous study (Chen et al., under review), we examined the effect of red background colour on dominance judgments of morphed human faces. The face stimuli were computer-generated East Asian female and male faces whose dominance impression was quantitatively morphed from submissive to dominant. The face stimulus was presented with one of three background colours (i.e., red, green, and gray). Participants were instructed to categorize the face stimulus as dominant or obedient. The results showed that the participants judged the face stimulus as more dominant when it was presented against the red background than against the green and gray backgrounds, for both female and male faces. These results suggest that the red background enhances the perception of dominance in human faces.

Based on this previous study, we aimed to further investigate whether the effect of red background on enhancing dominance perception would be specific to human faces. Using two online questionnaires, we investigated the effect of red on the dominance perception of geometric shapes. Ten simple geometric shapes were presented with three backgrounds (red, green, and gray) that were visually presented as background colours (Experiment 1) and with three flanking Japanese words representing colours (Experiment 2). Participants were instructed to rate the dominance perception of each shape stimulus using a 7-point Likert scale. It has been shown that even abstract shapes coloured red are rated as more dominant (Little & Hill, 2007). Therefore, we hypothesized that the red background colour could influence the dominance judgments of shapes and that it was specific to the perceptual red.

METHODOLOGY

Experiment 1 Effect of Background Colour on Geometric Shape Dominance

Participants

Sixty-one Japanese undergraduate students (Mage = 19.38, SD = 1.18) participated. The sample size was set a priori at 32 participants, based on a target power of 0.8 with a medium effect size by power analysis (Cohen's d = 0.6). We collected more participants in case of missing data.

Stimuli

Ten geometric shapes (square, triangle, inverted triangle, circle, oval, pentagon, hexagon, rectangle, parallelogram, and square diamond; see Figure 1a) were created as visual stimuli. The shape stimuli were presented against three background colours of red, green, and gray (see an example of a visual stimulus in Figure 1b). The choice of colours was consistent with Chen et al. (under review).

Procedure

An online questionnaire on the Qualtrics platform was used to collect the data. Participants were suggested to use a computer or laptop instead of a smartphone to complete all the questions and were unaware of the purpose of the questionnaire. Participants were informed beforehand that it might take 5-8 minutes to complete the questionnaire.

These 3 colour stimuli (red, green, and gray) were displayed uniformly in the background in combination with 10 geometric shapes (square, triangle, inverted triangle, circle, oval, pentagon, hexagon, rectangle, parallelogram, and squared diamond), resulting in a total of 30 questions. The questions were randomized for each participant. In each question, participants were instructed to rate the dominance of each shape stimulus on a seven-point Likert scale, ranging from not dominant at all to extremely dominant.

Experiment 2 Effect of Word of Colour on Geometric Shape Dominance

Participants

Sixty-seven newly recruited Japanese students and researchers (Mage = 26.39, SD = 6.7) participated.

Stimuli

The same collection of geometric shapes was used as in Experiment 1. The background cues were 3 words representing the colours red, green, and gray in Japanese ("あか" for red, "みどり" for green, "はいいろ" for gray), cueing one of the colours, positioned above and below each of the 10 geometric shapes (see Figure 1c for an example).

Procedure

The procedure was identical to Experiment 1.

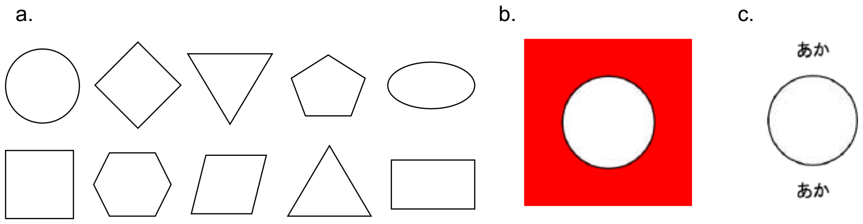

Figure 1. a). Shape stimuli used in the questionnaire survey; b). An example of questionnaire survey 1 with a circle in red background colour; c). An example of questionnaire survey 2 with a circle presented with the words of red (あか).

RESULT

Experiment 1 Effect of Background Colour on Geometric Shape Dominance

The mean dominance rating of all the shapes was calculated in the perspective of each background colour, and a comparison on these three background colours by ANOVA was applied. The result showed that there was a significant difference on the dominance judgments of shapes between the three background colours (Figure 2a), $F(2, 180) = 35.15$, $p < .001$, $\eta^2 = 0.28$. The dominance rating of shapes on the red background colour ($M = 4.47$, $SD = 1.61$) was significantly higher than those on the green background colour ($M = 3.05$, $SD = 1.47$), $t(60) = 9.81$, Bonferroni corrected $p < .001$, and the gray background colour ($M = 3.26$, $SD = 1.55$), $t(60) = 8.71$, Bonferroni corrected $p < .001$. There was no significant difference between the green and gray background colours, $t(60) = 2.01$, Bonferroni corrected $p = .15$.

Experiment 2 Effect of Word of Colour on Geometric Shape Dominance

Using the same analysis method as in Experiment 1, no significance was found for the dominance ratings of geometric shapes between the three colour-background words (Figure 2b; red: $M = 3.88$, $SD = 2.03$; green: $M = 3.74$, $SD = 1.81$; gray: $M = 3.84$, $SD = 1.84$), $F(2, 198) = 0.41$, $p = .67$, $\eta^2 = 0.0052$.

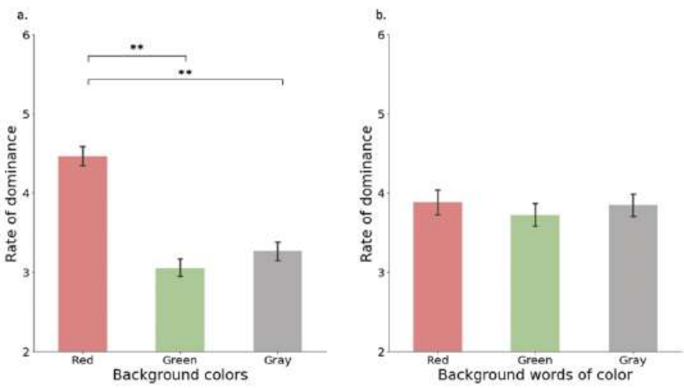

Figure 2. a). Mean dominance ratings of geometric shapes for three-colour backgrounds; b). Mean dominance ratings of geometric shapes for three-word colour cues. Error bar represents the error of the mean. Asterisks indicate significant differences after Bonferroni correction (**p < .01).

DISCUSSION

The present study investigated the effect of colour on the dominance judgments of geometric shapes, where colour was either visually cued by background colours (Experiment 1) or conceptually cued by colour words (Experiment 2). The results showed that a geometric shape presented in a red background colour was rated higher in dominance compared to green and gray background colours, while the word cue of red did not show the same effect. These results suggest that the effect of red on increasing the dominance judgment of geometric shapes is not caused by the concept of redness, but by the visual perception of the red colour. These results are consistent with previous studies in which red enhanced the perception of dominance in different contexts and using different methods (Hill & Barton, 2005; Setchell & Dixson, 2001; Stephen et al., 2012; Wiedemann et al., 2015; Young, et al., 2013). Thus, red backgrounds may enhance dominance perception for both human faces (Chen et al., under review) and geometric shapes. Furthermore, this effect of red on dominance was specific to the perceptual colour rather than the conceptual meaning of red.

Studies have demonstrated that red is associated with dominance and aggression in a large group of animal species, including anthropoid primates (Khan et al., 2011; Rhodes et al., 1997; Setchell & Wickings, 2005), fish (Dijkstra et al., 2005), birds (Pryke, 2009), reptiles (Healey et al., 2007), and humans (Hill & Barton, 2005). In primates, it has been suggested that trichromatic colour vision (L, M, and S), in addition to dichromatic colour vision (L and S), is optimal for detecting changes in skin redness, thereby facilitating the assessment of social and emotional states in conspecifics (Changizi et al., 2006). In animals, red skin colour signals dominance, aggression, and fighting ability due to oxygenated blood perfusion (Hill & Barton, 2005; Khan et al., 2011; Rhodes et al., 1997; Setchell & Wickings, 2005). In humans, an opponent's red face signals anger, dominance, and aggressiveness, whereas pallor signals fear (Archer, 2006; Changizi et al., 2006; Drummond, 1997; Hackney, 2006; Montoya et al., 2005; Young et al., 2013). Furthermore, visual cues of red, such as red clothing or a red background, are perceived as more dominant, dangerous, angry, aggressive, and more likely to win a competition (Attrill et al., 2008; Dreiskaemper et al, 2013; Elliot et al., 2010; Fetterman et al., 2011, 2012; Hill & Barton, 2005; Hagemann et al., 2008; Peromaa & Olkkonen, 2019; Piatti et al., 2012; Re et al., 2011; Sorokowski et al., 2014; Young et al. 2013). Individuals wearing red are perceived by themselves and others as more dominant and aggressive than those wearing blue (Feltman & Elliot, 2011; Wiedemann et al., 2015). Even abstract shapes coloured red are rated as more dominant and more likely to "win a fight" than those coloured blue (Little & Hill, 2007). Thus, the observed effect of red background colour on dominance might be biologically rooted.

Future studies are needed to elucidate the mechanism underlying the formation of red-dominance associations, such as examining red-dominance/status associations in infants/children to show the development of these associations. It might also be interesting to examine the perceptual colour dimensions (e.g., hue/lightness/saturation) that determine the red-dominance association, in order to distinguish the effect of colour dimensions that influence the perception of dominance, anger, health, and attractiveness.

REFERENCES

1. Archer, J. (2006). Testosterone and human aggression: an evaluation of the challenge hypothesis. *Neuroscience & Biobehavioral Reviews, 30*(3), 319–345.
2. Attrill, M. J., Gresty, K. A., Hill, R. A., & Barton, R. A. (2008). Red shirt colour is associated with long-term team success in English football. *Journal of Sports Sciences, 26*(6), 577–582.

3. Changizi, M. A., Zhang, Q., & Shimojo, S. (2006). Bare skin, blood and the evolution of primate colour vision. *Biology Letters, 2*(2), 217–221.
4. Chen, N., Yang, Y., Kobayashi, M., Nakamura, K., & Watanabe, K. (under review). Red background colour enhances face dominance perception.
5. Cuthill, I. C., Hunt, S., Cleary, C., & Clark, C. (1997). Colour bands, dominance, and body mass regulation in male zebra finches (Taeniopygia guttata). *Proceedings of the Royal Society of London. Series B: Biological Sciences*, *264*(1384), 1093–1099.
6. Dreiskaemper, D., Strauss, B., Hagemann, N., & Büsch, D. (2013). Influence of red jersey color on physical parameters in combat sports. *Journal of Sport and Exercise Psychology*, *35*(1), 44–49.
7. Drummond, P. D. (1997). The effect of adrenergic blockade on blushing and facial flushing. *Psychophysiology, 34*(2), 163–168.
8. Elliot, A. J., Kayser, D. N., Greitemeyer, T., Lichtenfeld, S., Gramzow, R. H., Maier, M. A., & Liu, H. (2010). Red, rank, and romance in women viewing men. *Journal of Experimental Psychology: General*, *139*(3), 399–417.
9. Elliot, A. J., & Niesta, D. (2008). Romantic red: red enhances men's attraction to women. *Journal of Personality and Social Psychology*, *95*(5), 1150–1164.
10. Elliot, A. J., Maier, M. A., Binser, M. J., Friedman, R., & Pekrun, R. (2009). The effect of red on avoidance behavior in achievement contexts. *Personality & Social Psychology Bulletin*, *35*(3), 365–375.
11. Elliot, A. J., & Maier, M. A. (2012). Colour-in-context theory In: Advances in experimental social psychology. *Advances in Experimental Social Psychology*, *45*, 65–125.
12. Elliot, A. J., & Maier, M. A. (2014). Colour psychology: Effects of perceiving colour on psychological functioning in humans. *Annual Review of Psychology*, *65*, 95–120.
13. Fetterman, A. K., Robinson, M. D., Gordon, R. D., & Elliot, A. J. (2011). Anger as seeing red: Perceptual sources of evidence. *Social Psychological and Personality Science*, *2*(3), 311–316.
14. Fetterman, A. K., Robinson, M. D., & Meier, B. P. (2012). Anger as "seeing red": Evidence for a perceptual association. *Cognition & Emotion, 26*(8), 1445–1458.
15. Feltman, R., & Elliot, A. J. (2011). The influence of red on perceptions of relative dominance and threat in a competitive context. *Journal of Sport and Exercise Psychology*, *33*(2), 308–314.
16. Hackney, A. C. (2006). Testosterone and human performance: influence of the colour red. *European Journal of Applied Physiology, 96*(3), 330–333.
17. Harashima, J. (2016). Japanese word-color associations with and without contexts. In Proceedings of the 10th International Conference on Language Resources and Evaluation (LREC'16) (pp. 2119–2123).
18. Hill, R. A., & Barton, R. A. (2005). Red enhances human performance in contests. *Nature*, *435*(7040), 293–293.
19. Kaya, N., & Epps, H. H. (2004). Relationship between colour and emotion: A study of college students. *College Student Journal*, *38*(3), 396–2405.
20. Little, A. C., & Hill, R. A. (2007). Attribution to red suggests special role in dominance signalling. *Journal of Evolutionary Psychology*, *5*(1), 161–168.
21. Mentzel, S., Schücker, L., Hagemann, N., & Strauss, B. (2017). Emotionality of colors: An implicit link between red and dominance*. Frontiers in Psychology, 8,* 317.
22. Montoya, P., Campos, J. J., & Schandry, R. (2005). See red? Turn pale? Unveiling emotions through cardiovascular and hemodynamic changes. *Spanish Journal of Psychology, 8*(1), 79–85.
23. Peromaa, T., & Olkkonen, M. (2019). Red color facilitates the detection of facial anger—But how much? *PloS one*, *14*(4), e0215610.
24. Piatti, M., Savage, D. A., & Torgler, B. (2012). The red mist? Red shirts, success and team sports. *Sport in Society*, *15*(9), 1209–1227.
25. Pravossoudovitch, K., Cury, F., Young, S. G., & Elliot, A. J. (2014). Is red the colour of danger? Testing an implicit red–danger association. *Ergonomics*, *57*(4), 503–510.

26. Pryke, S. R., Astheimer, L. B., Buttemer, W. A., and Griffith, S. C. (2007). Frequency-dependent physiological trade-offs between competing colour morphs. *Biology Letter, 3*, 494–497.
27. Pryke, S. R. (2009). Is red an innate or learned signal of aggression and intimidation? *Animal Behaviour,* 78, 393–398.
28. Setchell, J. M., & Dixson, A. F. (2001). Changes in the secondary sexual adornments of male mandrills (Mandrillus sphinx) are associated with gain and loss of alpha status. *Hormones and Behaviour*, *39*(3), 177–184.
29. Setchell, J. M., & Jean Wickings, E. (2005). Dominance, status signals and coloration in male mandrills (Mandrillus sphinx). *Ethology*, *111*(1), 25–50.
30. Sorokowski, P., Szmajke, A., Hamamura, T., Jiang, F., & Sorokowska, A. (2014). "Red wins","black wins" and "blue loses" effects are in the eye of beholder, but they are culturally universal: A cross-cultural analysis of the influence of outfit colours on sports performance. *Polish Psychological Bulletin*, *45*(3), 318–325.
31. Stephen, I. D., Oldham, F. H., Perrett, D. I., & Barton, R. A. (2012). Redness enhances perceived aggression, dominance and attractiveness in men's faces. *Evolutionary Psychology, 10*(3), 562–572.
32. Wiedemann, D., Burt, D. M., Hill, R. A., & Barton, R. A. (2015). Red clothing increases perceived dominance, aggression and anger. *Biology letters*, *11*(5), 20150166.
33. Xia, T., Song, L., Wang, T., Tan, L., & Mo, L. (2016). Exploring the effect of red and blue on cognitive task performances. *Frontiers in Psychology, 7*, 784.
34. Young, S. G., Elliot, A. J., Feltman, R., & Ambady, N. (2013). Red enhances the processing of facial expressions of anger. *Emotion, 13*(3), 380–384.

A Study on Improving Efficiency of Color matching Function Measurement Using Selection Techniques

A. Okuda*, Y. Kamimura, Y. Kawashima, K. Okubo, and Y. Yamauchi

Graduate School of Science and Engineering, Yamagata University, JAPAN.

*Corresponding author: A. Okuda, okuda2akito1@gmail.com

ABSTRACT

It is well known that colorimetric matching of colors on different media does not ensure that their appearance is the same for everyone. One of the reasons is that there are variations in the color matching functions (CMFs) among observers. If CMFs can be measured easily for each observer, it would be possible to attain customized color management. Traditional method (maximum saturation method) requires an adjustment of the intensities of three primary lights (R, G, B) , which is not easy for naïve observers. Also, it takes longer time to adjust the color as there are three degrees of freedom for the change of the intensities. We proposed a method in which multiple sets of the combination of different color intensities were prepared in advance for each reference light and the subject were instructed to select one of the preset colors closest to the reference light (the matching color). The purpose of this study is to explore more accurate and less time-consuming methods of color matching experiment and to verify their validity. Based on the problems obtained from our preliminary experiment, two modifications were introduced: the store function and the two-step procedure. The store function allows the subject to temporarily "store" a setting for matching and the setting can be recalled at any time during the matching procedure. The two-step procedure consists of 1) the first step to find a rough matching region, and 2) the second step to make a final choice in the region. A wide color interval for the prepared colors is used in the first step and the smaller color region and interval are used in the second step. The experiments were conducted for six subjects whose CMFs were obtained with the traditional method. The matching accuracy and time required to complete the experiments were compared with those obtained in the traditional method. The results showed that the deviations of the CMFs from the adjustment method were smaller for both methods, especially for the two-step procedure. Our new method took a little longer time than the previous one, but it was much shorter than that of the traditional method. In conclusion, it is shown that the two-step procedure has a potential to be used as a color matching experiment method that concurrently satisfies the accuracy and time-efficiency.

Keywords: color matching functions, experiment time, accuracy, store function, two-step procedure

INTRODUCTION

Currently, in several media such as displays, magazines, and advertisements, there has been reported a problem that the colors of the identical colorimetric value appear differently when they are displayed in different types of media [1][2]. One of the reasons for this issue is that the CIE 1931 standard observer CMFs used to calculate colorimetric values does not represent the actual observer's CMFs [3]. The CIE 1931 CMFs is the average of the CMFs of 17 subjects.

This color mismatch could be improved by using the observer's CMFs to calculate colorimetric values. Conventional measurement of CMFs requires a large-scale equipment and the procedure to obtain CMFs is time-consuming, so various studies have been conducted to develop simple equipment and methods [4][5]. However, the main measurement method is to manipulate RGB stimuli independently (hereinafter referred to as the "conventional method"), which requires complex operations and long measurement time, and it offers a high degree of freedom.

Yamauchi et al. [6] proposed a method in which subjects are asked to select the color closest to the reference stimulus from the candidate color stimuli, which composed a three-dimensional grid, prepared in advance in the color space for each reference stimulus. Although the experiment time was shortened, the accuracy of matching could not be improved because the candidate stimuli were located on the discrete grids, and subjects were forced to select one from them.

To improve color matching accuracy using the selection method described above, two issues need to be considered. Firstly, the stimuli selected from the grid of color stimuli in the previous study could not be freely selected, and had to be gradually changed along the one of the RGB direction. Therefore, if there were multiple candidate color matching stimuli, the colors had to be stored in memory in order to compare them, which may have resulted in poor accuracy. Secondly, because the candidate stimulus colors were predetermined and distributed discretely on a grid, it was not possible to present color differences more precisely than the grid spacing. In this study, we proposed a new method to improve these problems, and conducted experiments to verify its effectiveness in terms of color matching accuracy and experimental time.

METHODOLOGY

Experimental apparatus

In this study, a simple color matching function measurement device using LED light sources was used in the experiments. Figure 1 shows the appearance and schematic diagram of the device.

The integrating sphere at the rear of the apparatus contains LEDs for the original RGB stimulus and the reference stimulus, and which LED in which light path of the bifocal field of view is turned on is controlled in synchronization with the movement of the chopper, which rotates at approximately 100 Hz. Although the test and reference stimuli actually blinked at high speed, they were perceived as steady light by the subjects because of their high frequency. It was possible to arbitrarily choose any combinations of the LEDs to be presented both to the test and to the reference stimulus area. The experimental booth was enclosed with a blackout curtain to shut the light from outside. The experiment was started after 3 minutes of dark adaptation.

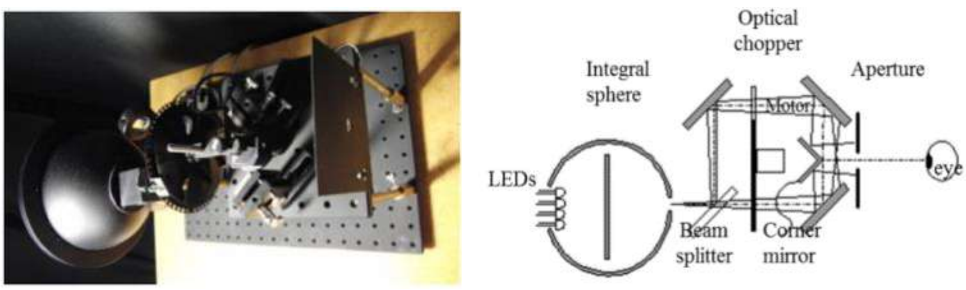

Figure 1. Appearance (left) and schematic diagram (right) of the simple color matching experiment apparatus

Procedure

Three sessions were conducted for each subject. One session was consisted of color matching to the reference stimulus *L(λ)* of 20 different wavelengths.

The spectral distribution of the reference stimulus is shown in Figure 2. The spectral distributions of the reference stimulus, which are normalized so that the intensity at the peak wavelength is equal to 1, are shown in Figure 2. The test stimulus was composed of the mixture of three primaries: red (627nm), green (523nm) and blue (471nm).

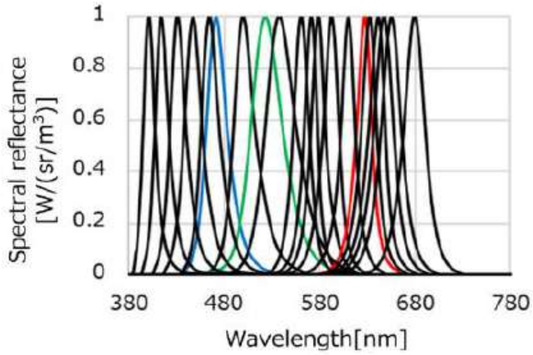

Figure 2. Spectral distribution of reference stimulus

In each trial, the subjects used a controller to move from one of the grid points in the RGB direction to another to change the color of the test stimuli in the bipartite test until they felt the color of the test stimulus to match that of the reference stimulus. The trial was repeated for another reference stimulus until all of the reference stimuli were matched. Figure 3 shows an image of the grid of stimulus. The reference value, Ave, is the average of the results of the preliminary experiment conducted by 14 subjects using the conventional method. The standard deviation (SD) was calculated from these results, and a grid was created with the SD to be the interval of the grid. As a result, the values for the grid were: Ave, Ave ± SD and Ave ± 2SD.

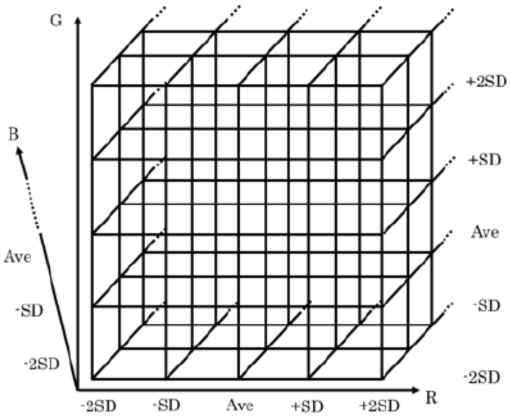

Figure 3. Color space relationship of candidate colors

This experiment used two different methods and compared the results with those obtained by the same method used in the previous study [6] (hereafter referred to as “the simple method”). The new method proposed in this research is denoted as “the store function” and “the two-step procedure”.

In the store function method, the candidate color, whose color was close to the reference color, could be temporarily stored and the subject could recall that setting (color) at any timing. This makes it possible to compare multiple color stimuli to find the best matched color.

In the two-step procedure, the operation was the same as the simple method, but once a candidate color stimulus is selected, the selection was repeated with the maximum and minimum values reduced to ±0.5 SD at ±0.25 SD intervals within the selectable range based on that color. This allowed the color matching experiments to be performed with finer grid.

Calculation of Color matching Functions

The color matching function is obtained using the following equation (Eq.1), where L(λ) is the radiance of the reference stimulus and R, G, and B are the radiance of the matching original stimulus, respectively.

$$\bar{r} = \frac{R(\lambda)}{L(\lambda)},\ \bar{g} = \frac{G(\lambda)}{L(\lambda)},\ \bar{b} = \frac{B(\lambda)}{L(\lambda)} \tag{1}$$

This was obtained for the 20 wavelengths used in the experiment, and the tristimulus values $\overline{r}$(λ), $\bar{g}$(λ), and $\bar{b}$(λ) were calculated.

Participants

The participants were composed of five men and one woman in their 20s with normal color vision. Four subjects had experienced color matching experiments, but not for the selection method (simple method) so as not to be affected by their prior experience.

Data by conventional method

Since two of the subjects in this study were naïve, who had no previous experience of color matching experiments, they performed the experiment with the conventional adjustment method before this experiment, and measured the time required for the experiment with the conventional method. In the conventional method, the subjects freely adjusted the intensity of the RGB. For other four participants, the experimental time was not measured as their CMFs had already been measured.

RESULTS

Deviation from conventional method

We defined the value of "deviation from conventional method" as an index of the degree to which the results of the three methods differed from those of the conventional method. The formula is shown in (Eq.2), which is calculated for each subject by accumulating the squares of the Euclidean distances between the setting of the test method and that of the conventional method for all the 20 wavelengths of the reference stimuli: RGB denote the tristimulus values obtained by the conventional method, while R'G'B' denote those obtained by the test method.

$$\sqrt{\sum_{i=1}^{20}\left(R'(\lambda_i) - R(\lambda_i)\right)^2 + \sum_{i=1}^{20}\left(G'(\lambda_i) - G(\lambda_i)\right)^2 + \sum_{i=1}^{20}\left(B'(\lambda_i) - B(\lambda_i)\right)^2} \tag{2}$$

The average deviation from the conventional method for each method is shown in Figure 4. Error bars represent standard errors.

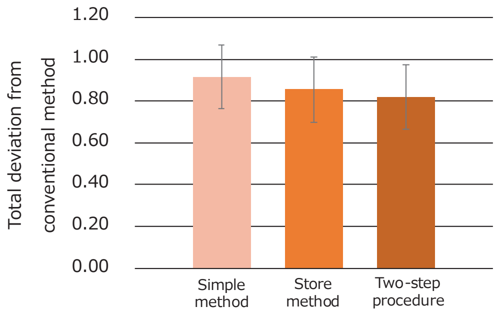

Figure 4. Deviation from conventional methods in each method

The results indicate that the deviation from the conventional method is 0.92, 0.86 and 0.82 for the simple method, the store method, and for the two-step procedure, respectively.

Experiment Time Aggregation

The experiment times for each method are shown in Figure 5. Error bars represent standard errors.

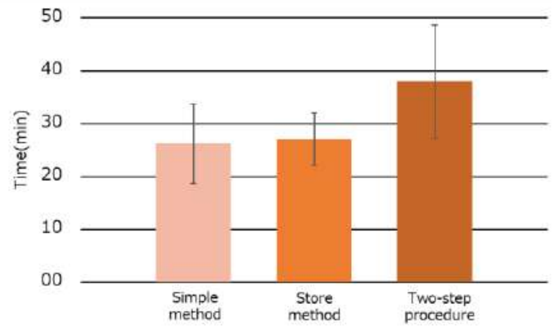

Figure 5. Experiment time in each method

Analysis of Variance

A one-way analysis of variance was performed for the discrepancy from the conventional method to verify whether there was a significant difference in accuracy among the three types of experiments ($p < 0.05$). The result was $p = 0.92 > 0.05$, which indicates no significant difference.

Time compared with the conventional method

The results of this experiment showed that the experimental time for the two-step procedure increased by approximately 10 minutes. To verify whether this increase in experimental time was acceptable, we compared the average experimental time for the conventional method and the two-step procedure for two subjects whose experimental time for the conventional method were measured. The experimental times are shown in Figure 6. The experiment time for the two-step procedure decreased by approximately 40% compared to the conventional method. Therefore, the time is sufficiently short.

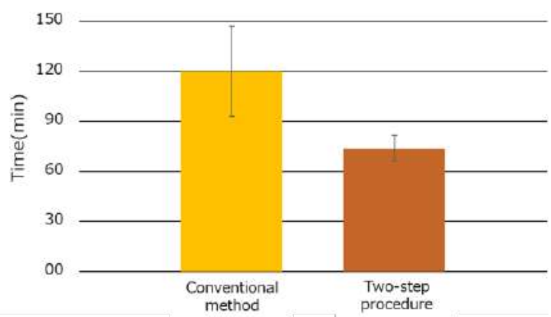

Figure 6. Experiment time for conventional method and two-step procedure

DISCUSSION

Correlation

Figure 7 shows the correlation between color matching accuracy and experimental time for the three methods.

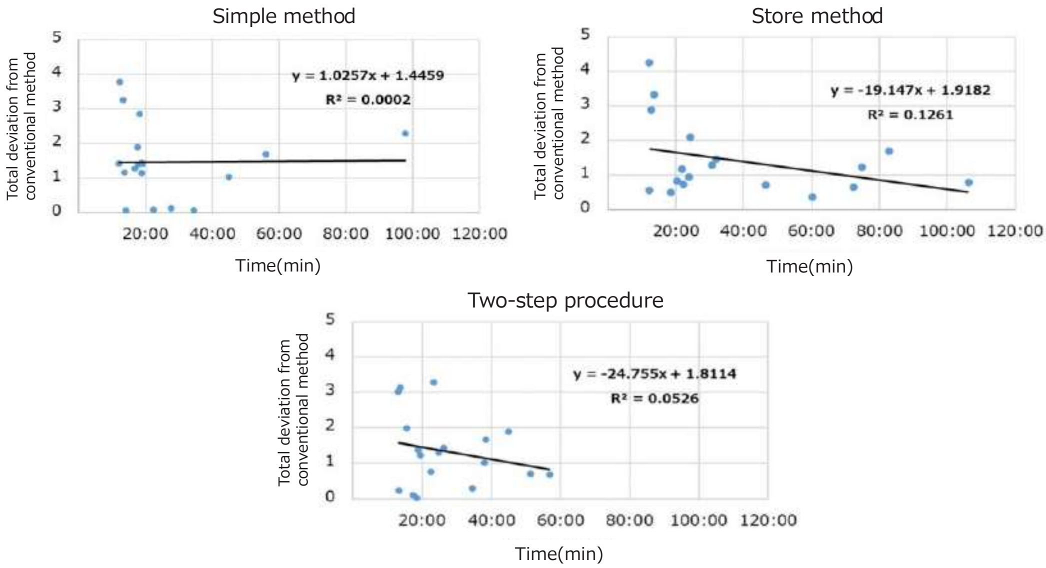

Figure 7. Correlation of experimental time with deviation from conventional methods

The correlation coefficients were 0.014 for the simple method, -0.22 for the store method, and -0.3 for the two-step procedure, indicating a weak negative correlation for all three methods except the simple method. These results suggest that the both of the methods proposed in this study are effective in terms of color matching accuracy and experimental time.

Accuracy

In this experiment, the two-step procedure is more accurate. It is because the differences between detailed stimuli were small and as close as possible to the individual's matching point. Also, the deviation tended to be smaller for the store method as well. By combining our two methods, it might be possible to get further improvement in accuracy.

CONCLUSION

In this study, we examined how color matching accuracy and experimental time would change if experiments were conducted using a new selection method. The results suggest that the two-step procedure is the color matching experimental method with the lowest error compared with the conventional method, and that it is the method with the best balance between color matching accuracy and experimental time.

REFERENCES

1. Oicherman, B. et al. (2008). Effect of observer metamerism on colour matching of display and surface colours. *COLOR research and application*, *33(5)*, 346-359. doi:10.1002/col.20429
2. Yamauchi Y. et al. (2006). Metameric color matching conditions under heterogeneous illumination with perceptual matching established. *VSJ2006,* Tokyo
3. Stiles, W. S., & Burch, J. M. (1959). N.P.L. Colour-matching Investigation: Final Report (1958). *Optica Acta*, *6*, 1-26. doi:10.1080/713826267
4. Suzuki, M. et al. (2012). A novel method to measures color-matching functions. *AIC2012*, Taipei
5. Morishima M. et al. (2014). Effects of the bandwidth of the spectrum on the color matching function. *ACA2014*, Taipei
6. Yamauchi Y. et al. (2022). A Simple Method for the Measurement of the Color Matching Functions. *Optica Fall Vision Meeting*, New York

Effect of Lighting on Wristwatch for Advertising Photography

J. Jarernros*, P.Srisuro, W. Kanuengsupapon, A.Chanphengphen and P.Bumrungphuet.

Department of Advertising and Public Relations Technology, Faculty of Mass Communication Technology, Rajamangala University of Technology Thanyaburi, Thailand.

*Corresponding author: Jarunee Jarernros, e-mail : jarunee_j@rmutt.ac.th

ABSTRACT

This research aimed to study the characteristics of light that affect wristwatch photography for advertising purposes. The research methodology involved photographing wristwatches with different types of materials for straps, namely stainless steel, leather, rubber, and fabric. Two types of lighting conditions were used: soft light and hard light. The researchers evaluated the photos by providing the photos to the experimental group who were 53 students from Rajamangala University of Technology Thanyaburi wearing wristwatches. They assessed the suitability of the lighting conditions for wristwatch advertising photography.
The result found that, hard light is suitable for photographing stainless steel, fabric and leather watch straps because hard light has high contrast, bright, show details on the watch straps and shows texture of the materials clearly. Soft light is suitable for photographing rubber watch straps because soft light has low-contrast and produces a more even color tone. It also show details on the watch straps clearly and highlights the characteristics of the materials more clearly than hard light.

Keywords: Lighting, Advertising Photography, Wristwatch, Soft light, Hard light

INTRODUCTION

Wristwatches are commonly utilized as fashionable accessories. In the contemporary day, the market for timepieces is seeing significant growth, seen in the diverse range of brands, models, price points, and materials employed in the production of watch straps, including leather, stainless steel, fabric, and rubber. Hence, it is imperative for business proprietors to employ promotional strategies in order to generate attention and establish product difference, ultimately fostering a lasting impression. Advertising images are crucial in influencing consumers' purchasing decisions. Therefore, advertising images must have good qualities in terms of realism, beauty, and be effective in capturing consumer attention, generating awareness, impression, and purchase decisions.
The consideration of lighting is crucial for photographers when capturing advertising photos. The selection of appropriate lighting is crucial as it should align with the surface features of the product, considering that various sources of light might provide distinct visual impacts. As an example, the utilization of soft light yields a subdued and dispersed aesthetic characterized by minimal disparity between illuminated and shaded areas. Conversely, the implementation of hard light creates a more pronounced visual effect distinguished by a substantial discrepancy between illuminated and shaded regions. Furthermore, it is worth noting that various forms of light exhibit distinct impacts on the reflection properties of surfaces. Hence, the goal of this research project is to examine the specific attributes of light that have an impact on the photographic representation of wristwatches, particularly in the context of advertising.

METHODOLOGY

In the conducted experiment, the researchers subjected four distinct watch strap materials, namely stainless steel, leather, rubber, and fabric, to shooting settings employing both soft and hard illumination. Subsequently, the researchers assessed the outcomes by administering the sample group with photographic material and employing a questionnaire to assess the appropriateness of the lighting settings for wristwatch advertising photography. The methods are as follows:

1. There are four distinct categories of wristwatch straps often found in the wristwatch market: Stainless steel, Leather, Rubber, and Fabric. These categories are based on the different materials used in the construction of wristwatch straps.

Figure 1. Example of watch straps

2. The lighting equipment setup consists of soft light using a mono flash, a standard reflector, and a diffuser, as well as hard light using a mono flash and a standard reflector.

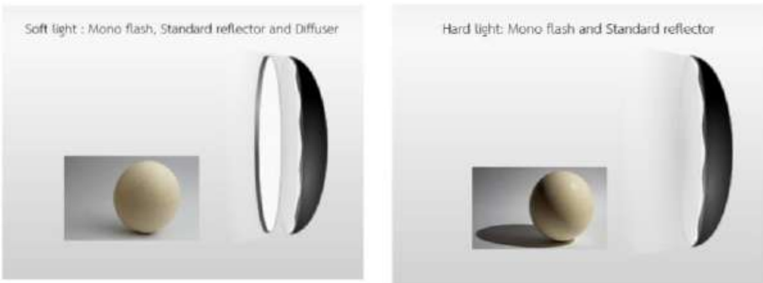

Figure 2. Example of Soft light and hard light

3. The camera settings : Aperture f/11, Shutter speed 1/200, ISO 100
4. Set the focal length of the lens to 50 mm.
5. Direct of lighting in the three quarter back (1H 10V)

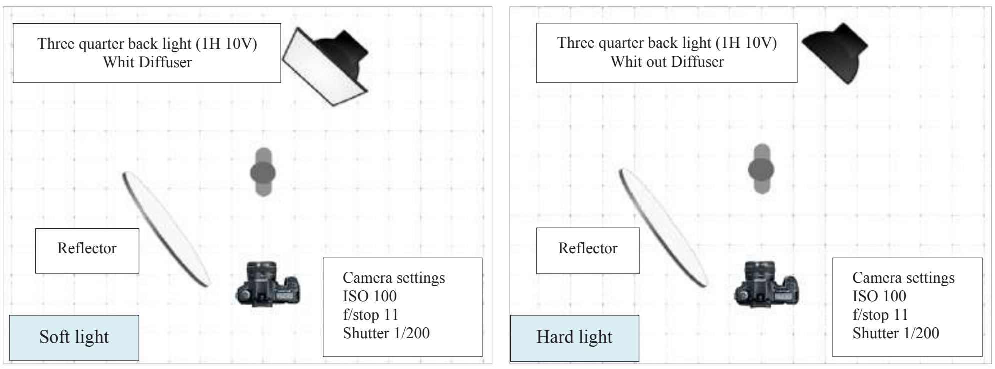

Figure 3. Example of Lighting diagram

6. Take photos of all four types of wristwatch straps by changing the characteristics of the light as specified.

Figure 4. Example of the wristwatch Photo Used in the Study

7. The images were presented to a sample of 53 participants who were students registered at Rajamangala University of Technology Thanyaburi and were seen to be wearing wristwatches. The objective of this analysis is to evaluate the appropriateness of the lighting conditions employed in the photographing of wristwatches. The participants observed the photographs on a 10.9-inch Apple iPad Air display under conditions of white light illumination, and afterwards responded to the questionnaire by following the prescribed procedure.
   7.1 The wristwatch photos captured under varying lighting circumstances, namely soft and hard lighting, will be sequentially presented to the subject. The subject will be requested to identify the corresponding wristwatch strap type from the provided alternatives, which include Stainless Steel, Leather, Rubber, and Fabric, as show in figure 5.

Figure 5. Scenario of the data collection method

   7.2 Providing sample photographs of the same wristwatch model captured under both soft light and hard light conditions. The subjects are tasked with selecting the image that most effectively showcases the intricate features of the watch strap and emphasizes the defining attributes of the wristwatch band with utmost clarity, as show in figure 6.

Figure 6. Scenario of the data collection method

RESULT AND DISCUSSION

The result of the study of the effect of lighting on wristwatch for advertising photography was as the following.

1. The study presented the findings about the accuracy of wristwatch straps, with the classification based on variations in light, as shown in Chart 1.

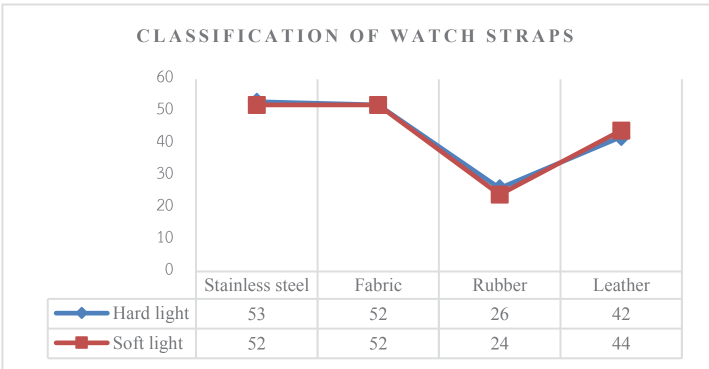

Chart 1. Shows results the classification of watch straps, classified by difference light.

Based on the provided chart, the classification accuracy of various watch strap types under hard light conditions is as follows: stainless steel watch straps were correctly classified by 53 individuals, representing a 100 percent accuracy rate. This was followed by fabric watch straps, which were accurately classified by 52 individuals, accounting for 98.11 percent. Leather watch straps were correctly classified by 44 individuals, representing an accuracy rate of 83.02 percent. Lastly, rubber watch straps were accurately classified by 26 individuals, accounting for 49.06 percent. In terms of accurately classifying watch strap types under soft lighting conditions, the findings indicate that stainless steel watch straps were correctly classified by 52 individuals, accounting for 98.11 percent. This was followed by fabric watch straps, which were also correctly classified by 52 individuals, accounting for 98.11 percent. Leather watch straps were correctly classified by 42 individuals, accounting for 79.25 percent, while rubber watch straps were correctly classified by 24 individuals, accounting for 45.28 percent.

2. The findings of the clarity study, specifically regarding the level of detail in watch straps, are shown in Chart 2.

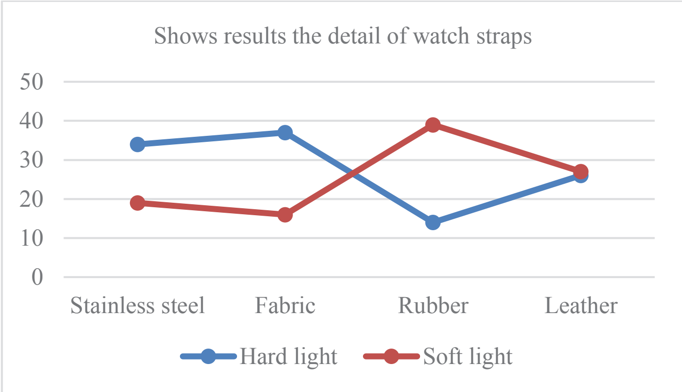

Chart 2. Shows results the detail of watch straps

Based on the presented chart illustrating the characteristics of watch straps, it is evident that hard light offers the highest level of clarity when observing details on fabric wristwatches, achieving an accuracy rate of 69.81 percent. The subsequent category consists of stainless steel wristwatches, accounting for 64.15 percent, followed by leather wristwatches at 49.06 percent, and rubber wristwatches at 26.42 percent. In contrast, it can be observed that soft light provides the highest level of clarity in discerning intricate features on rubber wristwatches, with a visibility rate of 73.58 percent. Subsequently, leather wristwatches exhibit a visibility rate of 50.94 percent, followed by stainless steel wristwatches at 35.85 percent, and fabric wristwatches at 30.19 percent.

3. The findings of the clarity study, especially with respect to the various types of watch straps, are shown in Chart 3.

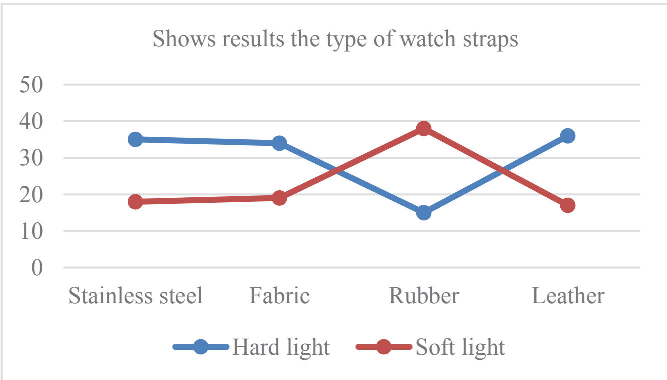

Chart 3. Shows results the type of watch straps

Based on the provided chart, it can be observed that the utilization of harsh light yields the highest level of clarity in showcasing the surface characteristics of leather watch straps, exhibiting an accuracy rate of 67.92 percent. The subsequent category with the highest percentage is stainless steel wristwatches, accounting for 66.04 percent, followed by fabric wristwatches at 64.15 percent, and rubber wristwatches at 28.30 percent. In terms of the visibility of surface characteristics, soft light demonstrates the most pronounced effect on rubber watch straps, with a percentage of 71.70. This is succeeded by fabric wristwatches at 35.85 percent, stainless steel wristwatches at 33.96 percent, and leather wristwatches at 32.08 percent, in sequential order.

CONCLUSION

The study found that variations in lighting attributes did not yield a statistically significant influence on the classification of wristwatch strap types. The subject demonstrated a higher level of accuracy in categorizing stainless steel wristwatches, potentially due to the distinctive attributes exhibited by this material, such as its lustrous appearance and reflective properties. These unique characteristics enabled the participant to easily discern the features of stainless steel wristwatches and effectively classify them with precision. On the contrary, the subject exhibited the least precision in classifying rubber wristwatches, potentially due to the inherent nature of rubber as a material, which possesses less discernible attributes, a more uniform texture, and light reflection capabilities similar to stainless steel although lacking its luster. The potential for confusion may have arisen in the process of classifying the many sorts of materials within the subject.

The investigation revealed that the attributes of light have an impact on wristwatch advertising photography. It was determined that hard light is well-suited for capturing images of stainless steel, fabric, and leather wristwatches. The utilization of harsh light is advantageous due to its ability to enhance contrast, clarity, and vividness. Consequently, this facilitates the clear visibility of complex information on watch straps as well as the surface properties of the materials used.

The utilization of soft light is considered appropriate for capturing images of rubber wristwatches. Soft light is characterized by its low contrast, subtle color transitions, and ability to eliminate highlights and reflections. The utilization of soft light enhances the visibility of patterns on rubber watch straps, hence facilitating a clearer perception of these patterns. Additionally, soft light enables a more pronounced representation of the material's distinctive qualities, as opposed to the utilization of hard light. Nevertheless, it is important to acknowledge that intense illumination can result in the occurrence of reflections and highlights on watch straps, so generating a visual impression of luster that resembles that of stainless steel. The aforementioned resemblance has the potential to induce perplexity among consumers in their differentiation of various material categories.

An effective advertising photograph should correctly depict the key attributes of the product, so facilitating consumer comprehension and having influence over their purchasing choices. Hence, it is important for advertising photographers to employ methodologies that effectively capture the distinct attributes of the product. Lighting plays a crucial role in photography as it serves to enhance the image by introducing elements such as dimension, aesthetic appeal, mood, and ambiance. Additionally, lighting serves the purpose of accentuating the distinctive qualities of the photographed subject. Photographers must possess a comprehensive understanding of lighting and its various qualities and properties in order to make informed decisions on its selection and use for a certain product.

ACKNOWLEDGEMENT

We would like to thank the Faculty of Mass Communication Technology and the Department of Advertising and Public Relations Technology for the opportunity to conduct this research. As well as 53 subjects and other parties who are not mentioned here who helped with this research.

REFERENCES

1. Earnest, A. (2019). *The New Lighting for Product Photography: The Digital Photographer's Step-bye-Step Guide to Sculpting with Light*. New York, NY: Amherst Media.
2. Freeman, M. (2006). *The Complete Guide to Light & Lighting in Digital Photography.* Utah, UT: Lark Book.
3. Jarearnros, J., Saksirikosol, C., Srisuro, P. (2021). *Effect of lighting on lipstick texture for advertising photography*. Proceeding of The 6th Asia Color Association Conference 2021: Color and Culture. (pp.150-156). Yogyakarta, Indonesia.2-3 November 2021.

THE ANALYSIS OF EYE-CATCHING ON THAI MOVIE POSTERS

P. Srisuro*, P. Sriwattana, S. Tianthitiwuth and A. Suwan

Department of Advertising and Public Relations Technology, Rajamangala University of Technology Thanyaburi Thailand

*Corresponding author: Ploy Srisuro, srisuro@rmutt.ac.th

ABSTRACT

Print media is the earliest form of information delivery. Posters fall into four categories: (1) huge outdoor posters like billboards outside the building. (2) mobile posters like those on trains and buses, (3) indoor posters like movie posters or department shop posters, and (4) amusing 3D posters. Print media—especially posters—consists of graphics and text. The movie industry still uses posters to attract viewers, thus if these two elements are missing, the poster will fail to attract attention. Thus, researchers are studying Thai movie posters' headlines, body copy, and illustrations to find their most eye-catching elements. These elements are essential for design, marketing, and advertising and can increase consumer attention. This study collects experimental data from 100 Bangkok and neighboring inhabitants utilizing Taro Yamane's sample size table at a 95 percent confidence level. Researchers selected 53 movie posters from 2017 since it had the most movie posters before the COVID-19 pandemic. The statistics showed 57 percent male and 43 percent female respondents. The sample found the headline with sub-components of color, size, visual emotional expression, element placement, famous person, light, and shape/form most eye-catching, followed by the headline. The sample selected color, size, element placement, and typeface as headline sub-elements. The least appealing part is the body copy, which includes color, shape/form, placement, and type style. Color components are among the samples' reasons for choosing eye-catching points, demonstrating that movie poster design's use of color affects their choice. Thus, to create an appealing movie poster, focus on visual composition and color contrast.

Keywords: eye-catching, Thai movie posters, color and culture

INTRODUCTION

The print media is widely regarded as the most ancient and conventional medium employed for the dissemination of information to diverse audiences. Posters can be categorized into four distinct sorts of publications, including huge outdoor posters, such as billboards, which are typically positioned outside of buildings. There are four main types of posters: (1) static posters, which are commonly seen on walls or bulletin boards, (2) mobile posters, typically found on trains or buses, (3) indoor posters, such as movie posters or those displayed in department stores, and (4) 3D posters that feature a playful design and convey a specific meaning [1].

Thai filmmakers use posters to communicate. Thailand started advertising movies using posters in 1958. Movie posters initially only conveyed the film's title, actors, and production data together with promotional elements. Modern manufacturers use posters for advertising and PR. Many aspects are used in movie posters to improve their aesthetic appeal and grab attention. Movie poster design requires the creation of aesthetically appealing focal points to attract clients and boost cinematic interest [2].

If a movie poster design lacks visual appeal, it will fail to effectively catch the attention of customers through the production of print media and posters. It does not induce a transformation in cognitive processes and perceptual patterns. Furthermore, it has an impact on the revenue generated by the film. The significance of customer viewing behavior and purchasing decisions lies in their substantial impact on the overall revenue generated by a movie. The increasing number of watching alternatives in the market can be attributed to heightened competition. Consequently, the film production team must create visually captivating movie posters as a means of advertising and public relations in order to raise consumer awareness and achieve the objectives set forth by the team [3].

Hence, the researchers are keenly interested in investigating and analyzing the aesthetic attraction of Thai movie posters. The primary emphasis is on the design principles pertaining to three key aspects: headline, body copy, and illustrations. The characteristics mentioned above hold significant importance in the realm of design principles, marketing, and advertising since they serve the purpose of generating awareness and fostering consumer interest. The findings of this research will be beneficial for both the company and the graphic designer.

METHODOLOGY

This research study is an analysis of the eye-catching on Thai movie posters that consists of 3 elements which were headline, body copy, and illustrations and is presented in the following areas.

Population and Samples

According to the National Statistical Office's 2021 data, the population residing in Bangkok and surrounding areas amounts to 10,872,100 individuals who possess unimpaired vision or have undergone corrective measures for visual impairments. The researchers employed convenience sampling to choose the sample from the population in Thailand. The sample was determined using Taro Yamane's formula, which accounts for a confidence level of 95 percent, a sample size error of 10 percent, and a population size of 10,872,100 persons. Consequently, the sample size was determined to be 100 individuals.

Criteria for Selecting Movie Posters

The movie posters were chosen from a pool of 53 films that were released in Thailand during the year 2017, which marked the period with the highest number of movie posters prior to the outbreak of the COVID-19 pandemic. The poster exhibits a resolution of 72 dpi or above, adhering to a scale of 4:6.

Research Tool

In this study, researchers interviewed movie poster viewers and carefully recorded their data. The researchers used an open-ended questionnaire to let individuals freely express their thoughts, remarks, and words. The questionnaire had two parts: Part 1 asked demographic questions, whereas Part 2 asked sample opinions. The samples were asked to pick the most outstanding part of 53 movie posters. Two questions were asked: "What do you perceive as the primary eye-catching point in this particular poster?" and "What was the rationale behind selecting this particular point as the initial eye-catching of your attention?"

Data Collection

The researchers conducted data gathering from a sample group through a systematic process consisting of six steps, which are outlined as follows:

Step 1: In the initial stage, a total of 53 movie posters were selected for participation in the experiment.

Step 2: Use PowerPoint to create five movie posters for the experiment. Randomize movie poster placement to avoid bias from extensive exposure to a single poster, which can cause eye fatigue during data analysis.

Step 3: Sampling procedure. Using random sampling, the researchers selected 100 people without prior publicity. After the sample group consented, researchers assessed its characteristics. Participants must have unimpaired vision or have had vision correction.

Step 4: Participants are interviewed, and the researcher carefully documents the data. As demonstrated in Figure 1, lab monitors help regulate and manipulate sample visual characteristics. Samples were advised to sit in front of a 24-inch display. From the screen center, participants were 110 cm away. In a 300 Lux room, this is the normal monitor viewing distance.

Figure 1. The model of the room utilized for data collecting

Step 5: Instruct the sample to identify the most striking characteristics of 53 movie posters. Movie posters on a dark background will be used in a PowerPoint survey. Movie posters were alternated with black slides to reduce visual distractions and eye fatigue from screen use.

Step 6: Before showing participants the movie posters, researchers asked two questions.

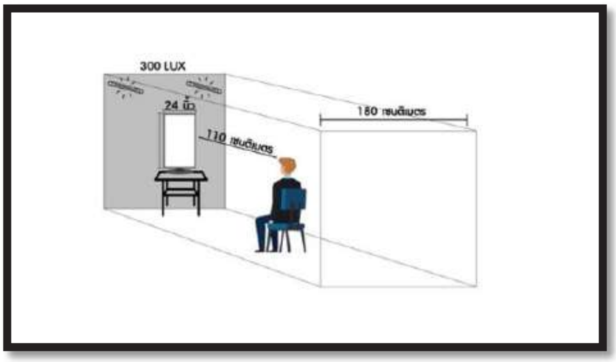

Question 1: What draws your attention to this poster's first visual element? After the initial enquiry, researchers asked the next question. Why did you notice the initial focal point? Samples were free to share their thoughts. After gathering the data, the researchers created a complete database. This database was used to generate statistical data, which was then displayed clearly. This statistical data was provided for analysis and conclusions.

RESULT AND DISCUSSION

The research findings revealed the following subjects based on data collected from a sample.

Demographic characteristics of the sample

The study revealed that the sample of 100 individuals can be categorized into 57 men, representing 57 percent, and 43 females, representing 43 percent. Based on the analysis of data, it was determined that eye-catching features in movie posters may be categorized into three primary components, as seen in Figure 2.

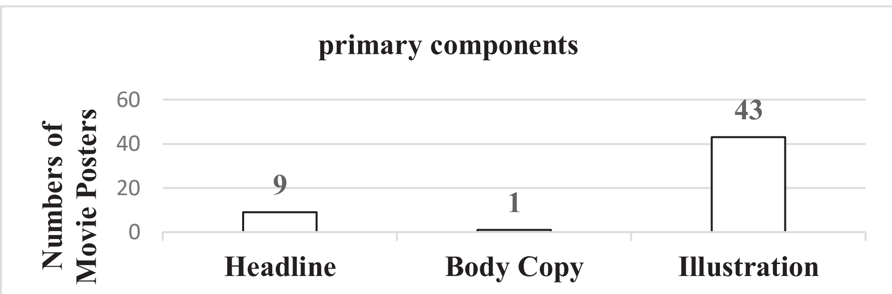

Figure 2. The primary components of movie posters

According to the findings presented in Figure 2, it was observed that pictures were the most visually captivating elements, comprising a total of 43 times. Following illustrations, headlines ranked second with a count of 9 times. The Body Copy was chosen as the final component for one time.

Analysis of Eye-catching in Headline Elements

The study revealed that the headline element has sub-elements that influence its selection as the eye-catching point, as shown in Figure 3.

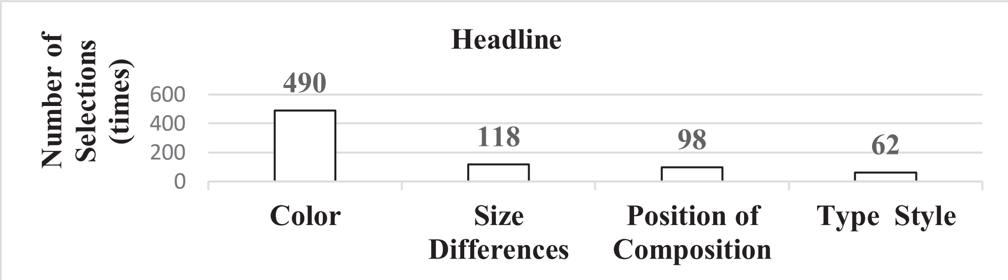

Figure 3. Eye-catching Movie Posters: Headline

According to the findings presented in Figure 3, the color element was identified as the most visually striking attribute in 490 times. The size differences was picked 118 times, while the position of composition were selected 98 times. Lastly, the type style was judged to be the most eye-catching 62 times. The study of the color used in the headline revealed that the color components were classified into three different groups: 1) contrast between light and dark shades, 2) contrast in color values, and 3) simultaneous contrast, as shown in Figure 4 from left to right respectively.

Figure 4. Movie posters with eye-catching headline in color components

Analysis of Eye-catching in Body Copy Elements

The study revealed that the body copy element has sub-elements that influence its selection as the eye-catching point, as shown in Figure 5.

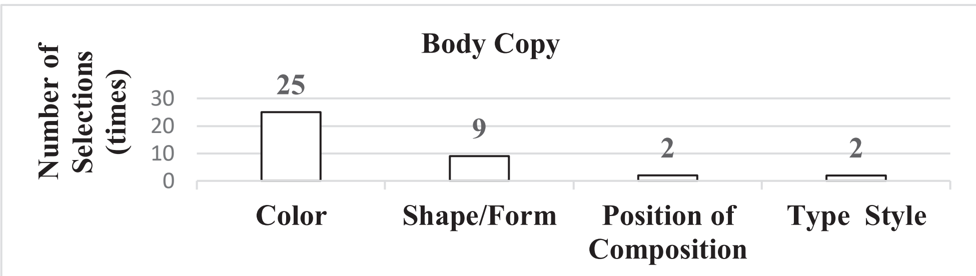

Figure 5. Eye-catching Movie Posters: Body Copy

According to the findings presented in Figure 5, the color element was identified as the most visually striking attribute in 25 times. The shape/form was selected 9 times, while the position of composition and type style were selected 2 times. The study of the color used in the body copy was simultaneous contrast, as shown in Figure 6.

Figure 6. A movie poster with eye-catching body copy in color components

Analysis of Eye-catching in Illustration Elements

The study revealed that the illustration element has sub-elements that influence its selection as the eye-catching point, as shown in Figure 7.

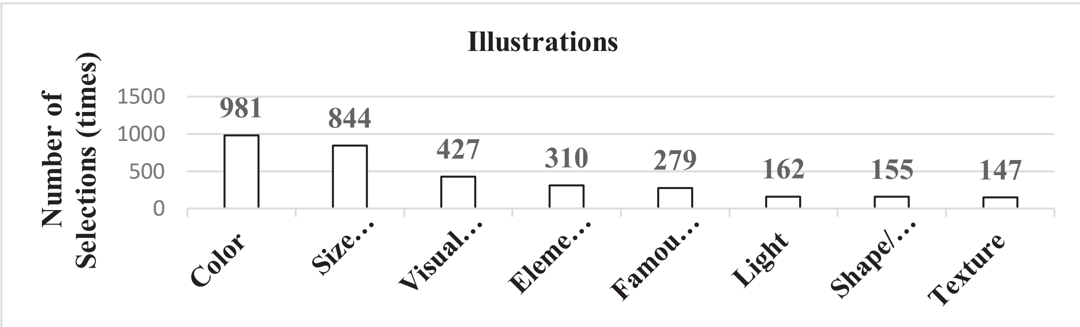

Figure 7. Eye-catching Movie Posters: Illustrations

Figure 7 shows that 981 times, color was the most noticeable attribute. Size differences 844 times, visual emotional expression 427 times, element placement 310 times, famous person 279 times, light 162 times, shape/form 155 times, and texture 147 times. The illustrations' color components were divided into four groups: Figure 8 shows simultaneous contrast, cold-warm contrast, extension contrast, and background contrast from left to right.

Figure 8. Movie posters with eye-catching illustration in color components

CONCLUSION

In relation to the component elements of movie posters, namely the headline, body copy, and illustration, the findings of the study indicate that color plays a significant role across all three components due to its ability to capture the viewer's attention effectively. In order to produce an appealing movie poster, it is essential to prioritize the elements of visual composition and color contrast. When designing the headline, it is advisable to employ the utilization of contrasting light and dark shades, as well as color values or the idea of simultaneous contrast. When choosing, designing, or creating the illustration for the movie poster, it is recommended to consider the principles of simultaneous contrast, cold-warm contrast, extension contrast, and background contrast.

ACKNOWLEDGEMENT

We express our gratitude for the help received from colleagues at RMUTT, friends and families.

REFERENCES

1. *The various types of posters and their respective applications* (n.d.). wynnsoftstudio.com. https://www.wynnsoftstudio.com
2. Nongapat Romsukwanasan. (2016, January 27). *Handwritten film posters: From concrete to vague memories.* Sarakadee. https://www.sarakadee.com/2016/01/27/ใบปิดหนังเขียนมือ/
3. Smuchanan Ekapanyakul. (2020). *The use of effective verbal and visual components in Thai out of home advertising design: poster*. Thesis. Thammasat University, Thailand (in Thai).

CONGENITAL RED-GREEN COLOUR DEFICIENCY: STUDY OF THE EFFICACY OF COMMERCIAL COLOR FILTERS

R. Huertas *, M. Jiménez, C. Martínez, M.A. López, A. Martín, E.M. Valero, L. Gómez-Robledo, M.A. Martínez-Domingo, J. Hernández-Andrés

Color Imaging Lab, Department of Optics, Faculty of Sciences, University of Granada, Spain.

*Corresponding author: Rafael Huertas, rhuertas@ugr.es

ABSTRACT

This study focuses on the effectiveness of passive aids, particularly colored filters. Although companies have toned down their claims in the face of mounting scientific evidence, they still stand by the effectiveness of their products. This study evaluates the long-term adaptation of EnChroma, Pilestone and Colorlite filters in different CVD subjects using multiple color vision tests. The results indicate that these filters alter color discrimination, with a trade-off between red-green and yellow-blue discrimination. The primary inference of this inquiry aligns with established scientific data: colored filters provide minimal contrast enhancement for certain color stimuli, but with a likely downside of diminished information for other color stimuli. Although companies claim that long-term chromatic adaptation is crucial for the filter's effectiveness, this study concludes that such filters do not offer a solution for individuals with CVD seeking normal color vision.

Keywords: Color Vision Deficiencies (CVD), commercial filters, color perception

INTRODUCTION

Around 8% of Caucasian males and 0.5% of females have congenital red-green color vision deficiency (CVD) [1]. People with CVD typically possess weaker color discrimination abilities compared to those with normal color vision [2, 3], which can lead to trouble executing daily activities and preclude them from specific professions [4]. This led to extensive research into aids for CVD [5]. Passive aids, such as color filters, and active aids, such as smart glasses or recoloring algorithms, are broad categories of such aids.

In this paper, we examine the effectiveness of passive aids in improving color contrast for CVD. Various companies, including EnChroma, VINO, Pilestone, Colorlite, and others, have introduced colored filters in spectacles or contact lenses as a means to address this issue. However, it should be noted that a considerable portion of the improvement can be attributed to adjustments in luminance contrast [6]. This phenomenon explains why passive aids can in some cases enable people with dichromatic vision to successfully complete the Ishihara test or to discriminate between two colors in a scene that they would perceive as identical without the aid of a filter. However, there is considerable evidence that these aids do not in any way make the vision of people with CVD more like normal color vision. Furthermore, they do not universally improve the observer's ability to discriminate between colors [7-11]. Some passive aids aim to be more individualised, allowing the user to choose from a range of color filters the one they prefer or the one that gives better results on certain CVD screening tests [12].

According to abundant and compelling scientific evidence [13-16], using a colored filter cannot make the vision of individuals with CVD equivalent to that of normal trichromatic individuals. Additionally, applying a spectrally selective external filter that is similar to altering the illuminant cannot expand the color gamut. In particular, selective narrow-band or cutoff filters that increase chromatic and/or luminance contrast in some wavebands must take away even more contrast in other wavebands. Furthermore, although these filters are capable of altering the overall relative sensitivities of cone types, they are unable to modify their spectral responsivity shapes. As a result, CVD observers cannot attain typical trichromatic vision using these devices.

Some companies have moderated their claims in recent years due to numerous scientific papers assessing the effectiveness through various experiments. Most of them have stopped asserting the provision of normal color vision for CVD subjects, as they did initially. Instead, they now assert the ability to enhance CVD's color vision to some extent. However, they persist in their refusal to accept the widely accepted scientific consensus that the studies carried out by scientists are accurate, well-designed, and properly assess the claimed enhancement of color vision. They further assert that the efficacy of the filters needs to be evaluated after long-term usage to account for prolonged chromatic adaptation [17-18].

METHODOLOGY

Our evaluation considered the subjects wearing the glasses continuously for two weeks. During this period, we measured color perception every two days using two color vision tests: Farnworth-Munsell 100 [19] and the Color Assessment and Diagnosis (CAD) [20]. Prior to participating in the study, all subjects provided informed consent. The study was conducted in conformity with the Declaration of Helsinki, and the Ethics Committee of the University of Granada approved the protocol (2604/CEIH/2021). CVD participants were classified based on their discrimination outcomes attained via an OCULUS anomaloscope. The results obtained from the CVD participants were compared to those obtained from a control group with normal color vision.

Different models of coloured filters, whose spectral transmittances are shown in Figure 1, from three different companies - EnChroma, Pilestone and Colorlite - were used in this study. The EnChroma models evaluated were the Cx1 and Cx1 DT, with a total of seven subjects, consisting of three protanopes and four deuteranopes. The Pilestone filters tested were TP-002, TP-025 and TP-037, with six subjects including one deuteranomalous, two protanomalous and three protanopes. Finally, the Colorlite models included D15, D30, P15 and P30 and were tested on 13 subjects including 4 deuteranopes, 1 deuteranomalous, 3 protanomalous and 5 protanopes.

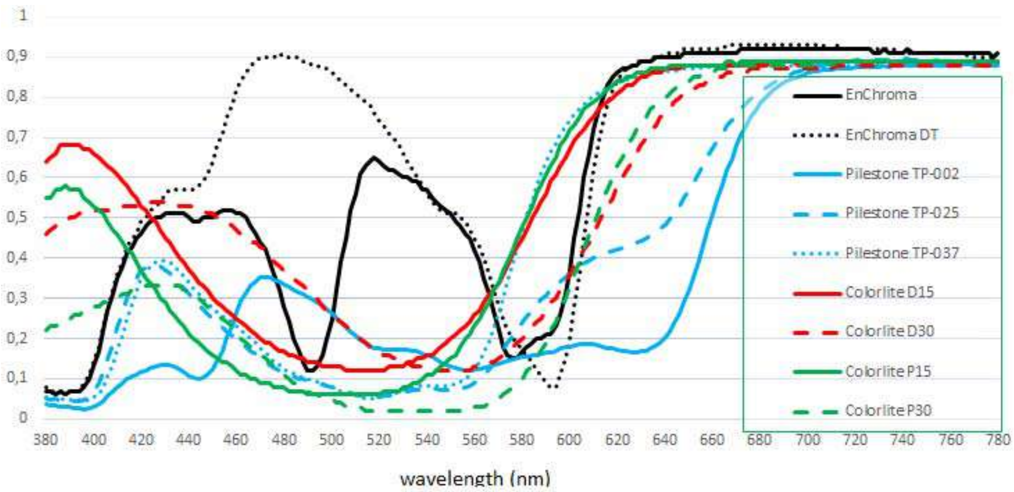

Figure 1. Spectral transmittance in the visible range of all the colored filters analyzed in this study

RESULTS

The Pilestone filters had mixed effects on color discrimination. The TP-037 filter showed a slight improvement in red-green discrimination but caused confusion in yellow-blue colors. On the other hand, the TP-002 filter worsened discrimination for all colors, and the TP-025 filter also reduced the ability to differentiate most colors, although less severely than TP-002. These findings suggest that Pilestone filters may be more effective for mild deficiencies than severe ones. Additionally, our study supported previous research [6-8] showing that wearing colored filters shifted the confusion axis for protanopes in a clockwise direction and for deutans in a counterclockwise direction. Notably, none of the participants wearing Pilestone filters passed the Ishihara test, and their FM 100 results did not reach the Total Error Score of individuals with normal vision.

The Colorlite filters lead to a decrease in FM-100 test scores for all individuals, regardless of their CVD type and filter model. With regard to CAD, a slight reduction in the size of the discrimination ellipse is seen for anomalous trichromats. Additionally, a shift of the ellipse for protanopes from protan to deutan is also observed.

For EnChroma filters, it has been noted that during an FM-100 test, protan individuals make more mistakes without spectacles than with them. The opposite holds for deutan individuals. The CAD test results for protan individuals indicate a gradual enlargement in discrimination ellipse. On the other hand, deutan participants displayed a reduction in the semi-major axis of their discrimination ellipse, accompanied by rotation and an increase in the Y-B threshold.

In summary, the CAD test showed that some filters provided a minor improvement in distinguishing red-green colors, while simultaneously causing confusion in previously unaffected yellow-blue colors. Additionally, other filters resulted in a slight alteration of the orientation of ellipses. Specifically, the ellipses shifted from a protan to deutan orientation, which predominantly affected dichromats, namely protanopes. Any slight improvement in the FM-100 test, as compared to the initial day of filter use, might be credited to mere repetition-based learning as opposed to chromatic adaptation. The participants provided subjective feedback that corresponded with the crucial moments of the study, which occurred when they put on or took off the glasses, as these were the periods in which they experienced the greatest variation during the numerous examinations. Several participants have reported experiencing difficulties and discomfort, especially at home, because the color of many everyday household objects they were already familiar with has changed.

CONCLUSIONS

The filter companies we analyzed assert that long-term chromatic adaptation must be considered for a fair assessment, which our research accomplished. Our findings indicate that the filters alter contrast levels which may be advantageous or disadvantageous depending on the specific task at hand. The key finding, aligning with overwhelming scientific evidence, is that colored filters can be valuable in generating partial increases in contrast for certain stimuli, while sacrificing information for differing color stimuli. The specific outcomes are also contingent upon the type and severity of the observer's CVD.

ACKNOWLEDGEMENT

This research was supported by grant PID2022-139056NB-I00 funded by the Spanish Ministry of Science and Innovation.

REFERENCES

1. Birch J. (2012). Worldwide prevalence of red-green color deficiency. *Journal of the Optical Society of America A, 29*(3), 313-320. https://doi.org/10.1364/JOSAA.29.000313
2. Linhares J.M., Pinto P.D., Nascimento S.M. (2008). The number of discernible colors perceived by dichromats in natural scenes and the effects of colored lenses. *Visual Neuroscience 25*(3), 493–499. https://doi.org/10.1017/S0952523808080620
3. Pastilha R.C., Linhares J.M., Gomes A.E., Santos J.L.A., de Almeida V.M.N., Nascimento S.M. (2019). The colors of natural scenes benefit dichromats. *Vision Research 158*, 40–48. https://doi.org/10.1016/j.visres.2019.02.003
4. Cole B.L. (2004). The handicap of abnormal colour vision, *Clinical and Experimental Optometry 87(4-5)*, 258–275. https://doi.org/10.1111/j.1444-0938.2004.tb05056.x

5. Valero, E. M., Neitz, J., & Drum, B. (2022). Aids for color vision deficiency: introduction to the feature issue. *Optics Express, 30*(26), 46560-46563. https://doi.org/10.1364/OE.480473
6. Patterson, E. J., Mastey, R. R., Kuchenbecker, J. A., Rowlan, J., Neitz, J., Neitz, M., & Carroll, J. (2022). Effects of color-enhancing glasses on color vision in congenital red-green color deficiencies. *Optics Express 30(17)*, 31182-31194. https://doi.org/10.1364/OE.451295
7. Martínez-Domingo M.A., Gómez-Robledo L., Valero E.M, Huertas R., Hernández-Andrés J., Ezpeleta S, Hita E. (2019). Assessment of VINO filters for correcting red-green Color Vision Deficiency. *Optics Express 27(13)*, 17954–17967. https://doi.org/10.1364/OE.27.017954
8. Gómez-Robledo L., Valero E.M., Huertas R., Martínez-Domingo M.A., Hernández-Andrés J. (2018). Do EnChroma glasses improve color vision for color blind subjects? *Optics Express 26(22)*, 28693–28703. https://doi.org/10.1364/OE.26.028693
9. Swarbrick H.A., Nguyen P., Nguyen T., Pham P. (2001), The ChromaGen contact lens system: colour vision test results and subjective responses, *Ophthalmic and Physiological Optics 21(3)*, 182–196. https://doi.org/10.1046/j.1475-1313.2001.00583.x
10. Mastey R., Patterson E.J., Summerfelt P., Luther J., Neitz J., Neitz J.,M., Carroll J. (2016). Effect of "color-correcting glasses" on chromatic discrimination in subjects with congenital color vision deficiency, *Investigative Ophthalmology and Visual Science 57*, 192.
11. Patterson E.J. (2017). Glasses for the color blind: their effect on chromatic discrimination in subjects with congenital red-green color vision deficiency, *in International Conference on Computer Vision Systems (ICVS)*, 18–22.
12. Wenzeland K., Urbin A. (2014). Improving colour vision, *in Lumen V4 Conference,* 427–438.
13. Valero, E. M., Huertas, R., Martínez-Domingo, M. Á., Gómez-Robledo, L., Hernández-Andrés, J., Nieves, J. L., & Romero, J. (2021). Is it really possible to compensate for colour blindness with a filter?. *Coloration Technology, 137*(1), 64-67. https://doi.org/10.1111/cote.12505
14. Marques D.N., Gomes A.E., Linhares J.M.M., Nascimento S.M.C. (2023). Discrimination of natural colors in anomalous trichromacy and the effects of EnChroma and Vino filters, Optics Express 31(11), 18075-18087. https://doi.org/10.1364/OE.451326
15. Nascimento, S. M., & Foster, D. H. (2022). Information gains from commercial spectral filters in anomalous trichromacy. *Optics Express 30(10)*, 16883-16895. https://doi.org/10.1364/OE.451407
16. Pattie, C., Aston, S., & Jordan, G. (2022). Do EnChroma glasses improve performance on clinical tests for red-green color deficiencies?. *Optics Express, 30(18),* 31872-31888. https://doi.org/10.1364/OE.456426
17. Werner, J. S., Marsh-Armstrong, B., & Knoblauch, K. (2020). Adaptive changes in color vision from long-term filter usage in anomalous but not normal trichromacy. *Current Biology, 30*(15), 3011-3015. https://doi.org/10.1016/j.cub.2020.05.054
18. Wenzel, K. (2020). Regular Wear of Coloured Glasses Improved the Symptoms of Colour Vision Deficiency. *International Journal of Innovative Studies in Sciences and Engineering Technology 6(5).*46-49.
19. Vingrys, A. J., & King-Smith, P. E. (1988). A quantitative scoring technique for panel tests of color vision. *Investigative Ophthalmology & Visual Science, 29(1)*, 50-63.
20. Rodriguez-Carmona, M., O'Neill-Biba, M., & Barbur, J. L. (2012). Assessing the severity of color vision loss with implications for aviation and other occupational environments. *Aviation, Space, and Environmental Medicine, 83(1)*, 19-29. https://doi.org/10.3357/ASEM.3111.2012

DATA SCIENTIFIC COLOUR COMPARISON AMONG FIVE ETHNIC TOWNSCAPES IN SINGAPORE

Natsuko Kawasumi[1*], Chanprapha Phuangsuwan[2], and Mikiko Kawasumi[3]

[1] *ACS (International), Singapore*
[2] *Rajamangala University of Technology Thanyaburi, Thailand*
[3] *Meijo University, Japan*

*Corresponding author: Natsuko Kawasumi, natsukok2014@gmail.com

ABSTRACT

This study aims to analyse the colour characteristics of unique townscapes in Singapore, to create a colour palette that distinguishes each cultural difference, and to apply this palette to souvenirs production and public relations design for foreign tourism. Singapore is known as a multicultural country that comprises various ethnic groups, including Chinese, Malay, Tamil, Western and so on. Foreigners can experience the cultural atmosphere of certain ethnic groups in various places through the colours. In this research, we decided to particularly focus on five towns; Chinatown, Kampong Glam, Little India, Katong and Colonial District, to visualise the different regional characteristics of colours in Singapore. Firstly, many photos of the townscapes were collected in the five selected towns, five symbolic photos were chosen for each town. The characteristic nine colours for each region were extracted from those photos. The RGB data of the nine colours were picked and converted to the HSV data, and the characteristics for each town were observed on the colour space. Consequently, it was found that Chinatown exhibited warm colours, and Colonial District had low-saturation colours such as black and white as expected. Though Little India, Kampong Glam and Katong were hard to distinguish due to shared colour characteristics, they varied in saturation, with Little India having the highest saturation and Katong the lowest. After the analysis, we tried to produce the actual packaging of gifts and brochures by using the colour palettes to verify its practical effectiveness for people who have different cultural backgrounds in Singapore. We will be conducting further experiments investigating the effects of colours of products' packaging on their sales. This research could be applied for tourists to understand and enjoy colour townscape formed by Singapore's unique historical and cultural background. Additionally, these outcomes could be useful to add extra value to products created by Made with Passion[1], a national initiative jointly led by Singapore Tourism Board and Enterprise Singapore in the future.

Keywords: Townscape, Culture, Regional colour, Data science

INTRODUCTION

Currently, I live in Singapore which is known as a multicultural country that comprises various ethnic groups, including Chinese, Malay, Tamil, Western and so on. Foreigners can experience the cultural atmosphere of certain ethnic groups in various places through the colours. For example, red Chinese temples can be found in Chinatown, Kampong Glam is known as a colourful historical Malay enclave, and Little India has vivid Indian shops and temples. Additionally, Katong has pastel-coloured Peranakan houses, and white and black colonial-style buildings can be seen around the banks of the Singapore River. Urbanisation and tourism development have been carried out while complying with the conservation guidelines implemented by the Urban Redevelopment Authority[2].

The purpose of this study is to create a colour palette that identifies cultural differences based on an analysis of the colour characteristics of Singapore's symbolic townscape, and to apply this palette in the production of souvenirs and the design of public relations materials for foreign tourism. In this research, five famous towns for tourists in Singapore; Chinatown, Little India, Kampong Glam, Katong and Colonial District, were selected to showcase the different characteristics of colours. First, the methodology employed to investigate the colours of each townscape will be explained. Subsequently, the analysis results of colour characteristics will be compared and discussed. Finally, efforts will be made to connect these findings to propose colour designs for tea packaging.

METHODOLOGY

The symbolic colours of five cultural towns in Singapore; Chinatown, Little India, Kampong Glam, Kalang and Colonial Distinct were visualised following the steps shown in Figure 1.

As the first step, many photo images of the townscapes of the five selected towns were captured in real life by an author using an iPhone 12 mini camera. All the photos were taken on sunny days to minimise the effect of shadows. Afterwards, five photos of road scenery that show the characteristics and incorporate symbols were selected for each town, resulting in 25 photo images used for our investigation in total. These photos were chosen to distinguish the colour characteristics of five towns. All photos mainly focused on architectural elements but included trees, streetlights, roads and sky as well.

As the second step, to isolate the essential colours in each townscape, post-processing of the photo images was conducted. Specifically, the colours of roads and sky were transformed to transparency since those are not typically considered memorable colours and not recognised as symbolic elements of each townscape by the human eye.

As the third step, nine symbolic colours were identified for each photo image using a software called Pick Color From Image[3]. A total of ten options ranging from five to ten colours were considered, and it was found that nine colours were better to showcase the uniqueness of each townscape. Subsequently, the RGB values data of the nine colours were picked and converted to the HSV values. This conversion was carried out to enable a more intuitive understanding of the colour differences, aligning with human perception.

Figure 1. Procedure for deriving symbolic colours

RESULT AND DISCUSSION

The derived symbolic nine-colours bands are placed below 25 original townscape photos in Figure 2. The colourful characteristics of the historic buildings can be seen expressed in the colour bars. It is observed that there are many reddish colour chips in Chinatown, Little India, and Kampong Glam, and that there are many monotone colour chips in Colonial District.

Next, the HSV data was presented through two different 2D diagrams as shown in Figure 3. The upper diagram describes the polar coordinates, which corresponds to the Munsell hue circle. The angle from the positive of the horizontal axis means H (hue), and the distance from the origin demonstrates S (saturation). In the lower diagram, the horizontal axis shows S (saturation), and the vertical axis indicates V (value). There are nine symbolic colours for each photo image, and every town has five photo images, so a total of 45 points are plotted within a single diagram. Figure 4 shows the mean and the standard deviation of each town. In the left graph, the vertical axis represents S (saturation), while in the right graph, it represents V (value).

The upper diagram of Chinatown in Figure 3 shows a concentration of points near warm colours, indicating that warm hues such as red and orange are unique colours of its townscape. Conversely, in the upper diagram representing Colonial Distinct, most of the points are situated close to the origin, showing low saturation. The lower diagram of Colonial Distinct further illustrates that the majority of points have saturations lower than 50%. Moreover, as demonstrated in the left graph of Colonial Distinct in Figure 4, the mean of S is notably low as approximately half of that of others. This demonstrates that low-saturation colours such as black and white are more dominant compared to highly saturated vivid colours within Colonial Distinct. In terms of V, Colonial Distinct significantly differs from other towns, with the lowest mean of V at 52%, meaning that colours of Colonial Distinct are relatively darker compared to other towns. On the other hand, the upper diagrams of Little India, Kampong Glam and Katong are similar in a way that points are generally scattered and clustered predominantly around two directions; the red colour zone and the blue colour zone. This means that these three towns are hard to distinguish colours since they exhibit similar characteristics. However, Figure 4 reveals characteristic differences among these three townscapes. The left graph in Figure 4 shows that Little India has the higher mean of S at 38%, while Katong has the lower mean of S at 31% among these three towns. This implies that the symbolic colours of Little India tend to be more vivid and those of Katong are paler in comparison. Unlike the left graph, the right graph in Figure 4 shows no significant difference among the five towns in the right graph, although they all exhibit wide diversions, showing that road sceneries in these towns encompass both dark and bright elements.

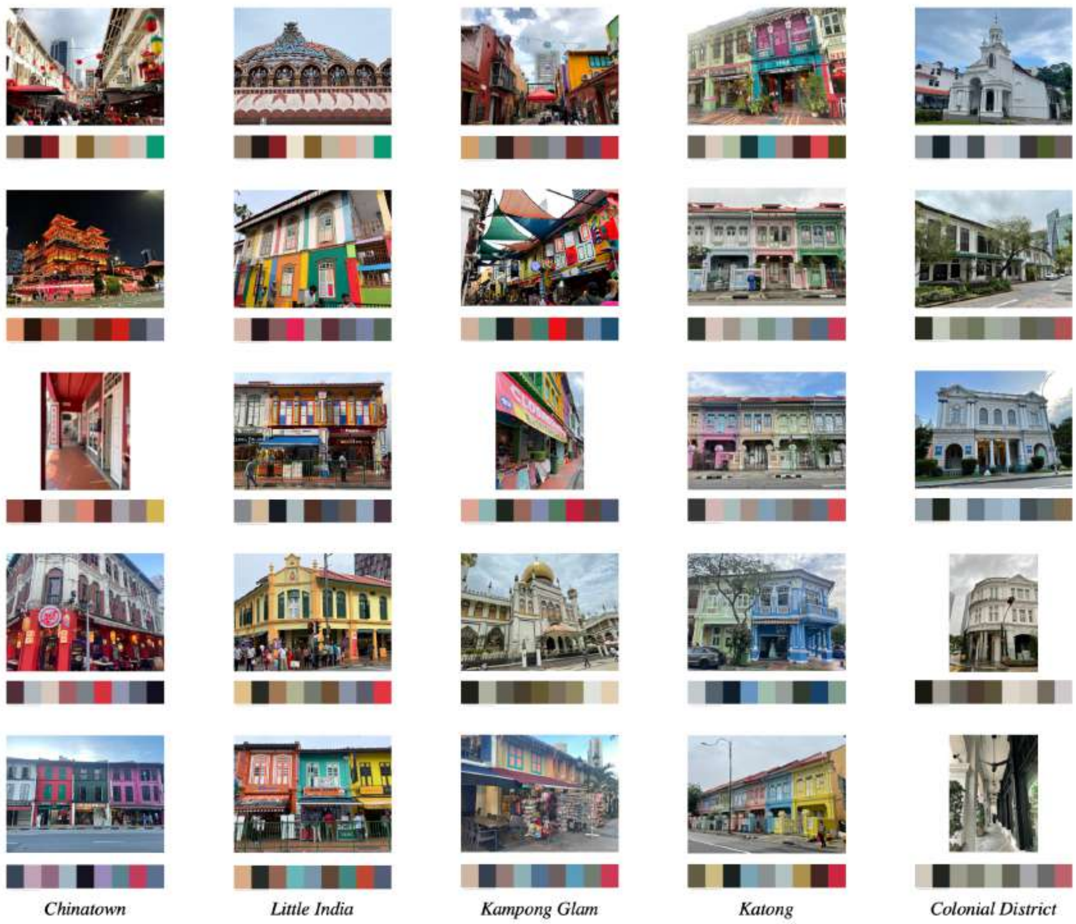

Figure 2. Original townscape photos and symbolic nine colours

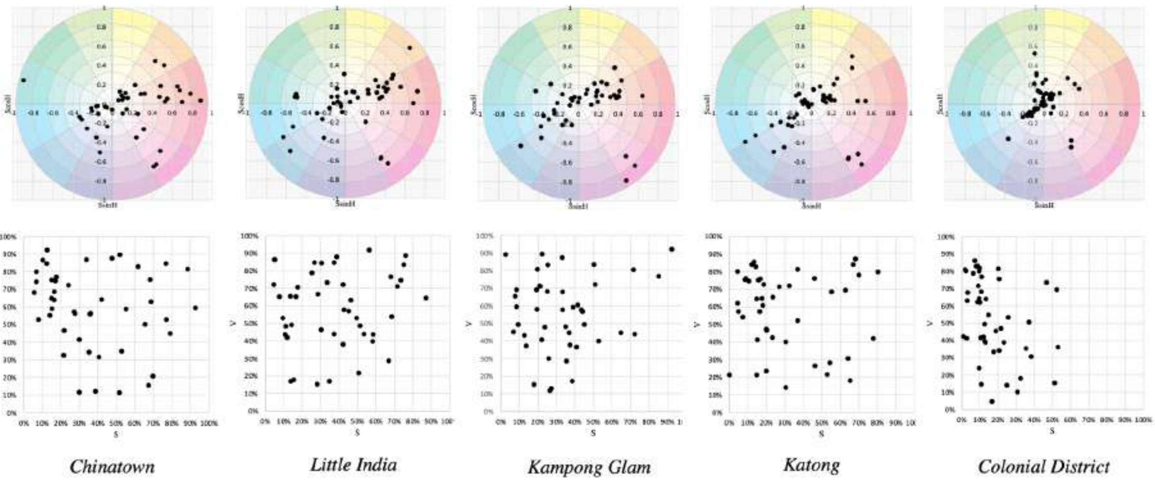

Figure 3. Comparison of HSV data for five townscapes

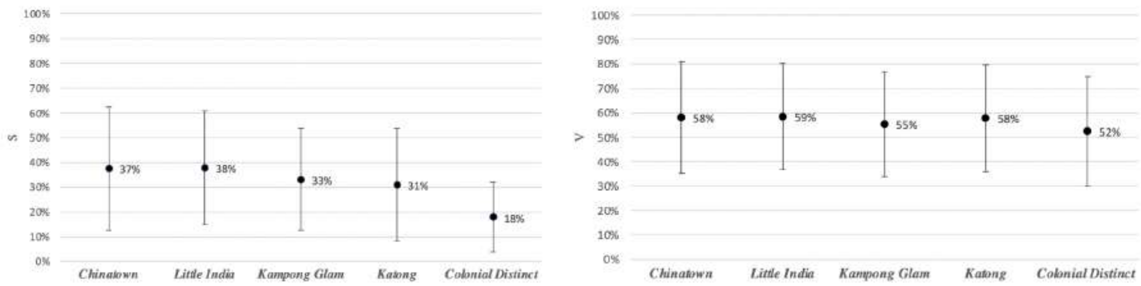

Figure 4. Comparison of S (saturation) and V (value) for five townscapes

CONCLUSION

The colours characteristics of distinct five towns in Singapore were compared and discussed using data science. However, several limitations were encountered in this research. Firstly, the selection of nine symbolic colours for each town relied on existing software where the process of selection is unknown. Using scientific methods such as k-means clustering could potentially enhance the accuracy of colour extraction. Secondly, colours can be easily influenced by various factors beyond cultural difference among towns, including lighting conditions and camera angles. Moreover, it was found that the dominant area of a colour may not directly correlate with its psychological impact. It was challenging to capture the contextual nuances of the original photos in the colours extraction process since memorable colours do not exactly match scientifically measured physical colours. Additionally, even if memorable colours were scientifically measurable, they could vary depending on an individual's cultural background, past experiences, and changes in visual sensitivity due to ageing.

In the future, it is recommended to employ k-means clustering carried out to select four symbolic colours for each town to create tea packaging design, as shown in Figure 5. Further investigations on the effects of colours of products' packaging on their sales should also be conducted. This would enable a more comprehensive understanding of how colours of towns affect individuals' behaviours and preferences.

Figure 5. Examples of colour package design for five townscapes

REFERENCE

[1] Singapore Tourism Board. *Passion Made Possible.* Retrieved September 12 2023, from https://www.visitsingapore.com/madewithpassion/
[2] Urban Redevelopment Authority. *Urban Design.* Retrieved September 14 2023, from https://www.ura.gov.sg/Corporate/Guidelines/Urban-Design
[3] imagecolorpicker.com. *Pick Color From Image.* Retrieved September 12 2023, from https://imagecolorpicker.com/

UNVEILING EMOTIONS AND MEANING THROUGH COLOUR SIGNIFICANT EXPERIENCES

Verónica Conte[1]*

[1] *CIAUD, Research Centre for Architecture, Urbanism and Design, Lisbon School of Architecture, Universidade de Lisboa, Rua Sá Nogueira, Polo Universitário do Alto da Ajuda, 1349-063 Lisboa, Portugal.*

*Corresponding author:Verónica Conte, e-mail conte.verónica@gmail.com

ABSTRACT

Immersed in a world of natural and artificial colours, we focus on the study of how we import colour into our inner world and give it back. We worked with autobiographical testimonies, and followed a research design based on Grounded Theory (Charmaz, 2006)[1],a methodology whose application to the subject in question is unknown). We sought to determine whether significant experiences with colour arise, and if so in what contexts and how they are prolonged over time. Thus, memories were collected from 61 participants from western culture. All were adults (23 to 84 years old), with higher education, many with a degree or interest in Arts and Humanities and sensitive to the subject. We used methods familiar to Grounded Theory, and integrated others from Thematic Analysis (Braun & Clarke, 2019)[2], Structural Existential Analysis (van Deurzen, E., 2014)[3], and Holistic Content Analysis (Leiblich et al, 1998)[4], to analyse the data and reach conclusions. The colour significant experiences collected a) appear throughout all stages of the protagonists' lives, with a greater emphasis on childhood and adulthood; b) are mainly associated with temporal contexts of travel, personal habits and family gatherings; and c) are linked to spatial contexts of landscape view or aesthetic elements, family homes and hand-scale objects such as clothes. The colours and emotions identified appear across the entire chromatic and emotional spectrum (Plutchik)[5], with the exception of emotions associated with anger. Within the caveats of qualitative analysis, we note the predominant role of pleasant emotions, especially those associated with surprise and joy, and of the colour blue. All the testimonies produced strong memories, but 45 were considered more significant, because of the emotional intensity, their permanence over time, or because they introduced a relevant reflection or change in the protagonist's life. The effect over time manifests itself through: the maintenance of the experience in daily life (for example through contemplation and meditation); by a change of worldview or of professional approach. Possible biases were identified in the sample (especially the lack of experiences associated with the emotions of anger, disgust and fear), so increasing the sample could make the conclusions more reliable. Although preliminary, the results of the research are considered useful both from a theoretical point of view, in terms of the psychology of colour, or for anthropological studies, and for the practice of professionals who work with the human environment, in particular architecture and design.

Keywords: meaningful experiences, emotions, colour, biographic memories

INTRODUCTION

70% of the information we receive is visual and 40% of that information is chromatic (Küppers, 1978)[6]. To be able to distinguish the colour of things played a survival role in the early history of mankind. This ability evolved with human evolution, as we began to colour objects and places, weakening the biological response to colour, but endowing it with meaning (Humphrey, 1976)[7]. Thus, the perception of colour is a complex activity, which embraces an object's physical elements, cultural contexts, knowledge and individual experiences. In a phenomenological approach, more than a mental perception (Maund, 2012)[8], colour is the echo of the body through the visualization of things (Merleau-Ponty, 1964)[9], an expression of the world and understanding of the being who sees it; or a characteristic that "enters our eyes" and becomes a matter of existence itself (Lakoff & Johnson, 1999)[10]. This interrelation of colour with the being that sees it expresses itself in neuroscience at the level of the emotions implied in its perception. Among others, Prinz (2004)[11], Damásio (2020)[12], defines emotions as mechanisms that generate sense and adaptation/ regulation of homeostasis, since they are "simultaneously bodily and cognitive-evaluative: they convey meaning and personal significance as bodily meaning and significance" (Colombetti & Thompson, 2008)[13]. Therefore, the perception of colour is a source of emotion, and may give rise to significance and feelings to its perceiver. The aim of this ongoing research is to contribute 1) to evince meaningful moments from colour experiences, 2) to a better understanding of its contexts, as well as the emotions involved, and 3) how those moments have a lasting impact on participants' lives.

METHODOLOGY

Colour perception, colour preferences, and colour-derived emotions, have received significant attention in many domains and certainly in psychology studies, especially through research exploring reactions to chromatic stimuli. In the proposal herein, the intention is to reverse the starting point, not naming or showing any colour, but instead collecting personal narratives of significant experiences (Damásio, 2020, 2017; Csikszentmihalyi & Rochberg, 1981)[12, 14, 15] or meaningful moments (van de Goor, et al., 2020)[16], driven by colour. To summarise, according to van de Goor et al (2020) [16] meaningful experiences can occur during short moments out of the ordinary, where something disruptive, positive or negative, happens accidentally, or they can be created deliberately through an everyday routine. They are usually felt and processed in depth and involve a mixture of positive and negative emotions, thereby relating to wonder and awe. They are enlightening and transforming experiences. The research design is based on the Grounded Theory methodology (Charmaz, 2006)[1], as it suited the aim of this study, i.e. the intention is not to test theories or perspectives, but to deepen knowledge through the participants' responses. The current study began in 2016 and remains open-ended.

Participants: sixty-one participants (36 female and 25 male) contributed with personal narratives - almost all share a western cultural perspective (they come from 7 European countries, 3 American countries and 1 Asian country), most have higher education, many of them with a degree or interest in Arts and Humanities, and are aged between 23 and 84 years old.

Data collection: Most participants were introduced to the research project during an initial informal talk and were invited to think about significant emotional experiences from their life relating to colour. The remainder only received an email invitation, when contact was established through the snowball strategy (Miles & Huberman, 1994 *apud* Velho, 2016)[17]. The initial informal talk is important because it allows the researcher to find people who are willing and able to write about their experience. To help with their responses, improve data coherence and the research focus, all participants were asked (by email) to choose and write down one or two testimonies of around 300 words which could answer the following questions: *a) "If colour in the world ceased to exist tomorrow, and you could only keep the colour of one thing (object, moment, place…). What would it be?" Visualize it. Tell me the story of this thing. b) "Is there any relevant thing or event in your life that is important to you or has become important, (object, moment, place…) which you strongly relate with colour? Visualize it. Tell me this story*. These questions were first tested and fine-tuned in order to obtain answers that were truly meaningful to the participants, and from which meaning could be produced in their lives. After receiving the testimonies by email-answer, a semi-structured interview was conducted with most of the participants to complement / elicit meaning from the chosen memory. The open questions explored aspects related to the emergence of meaning according to van de Goor, et al. (2020)[16]: feelings; meaning; context; impact, and the nature of impact – without addressing them directly. In some cases participants were invited to complement their writing or to review the researcher's editing after the interview. According to Velho (2016)[17], the importance of this part of the process is that "the use of writing as a means of communication not only allows for some distance, enhancing reflection, but the use of written language as a form of expression requires an increased effort to clarify ideas", thus achieving the necessary depth in the answers. Participants were also asked to send a photo of the "thing" described, but the images have not yet been considered or analysed in this study. It should be noted that all participants were asked to consent to the study, editing and publication of their memories, which could also be anonymised or pseudonymised as desired. Other personal data collected for the study has been protected.

Analysis: Grounded Theory methods were used to analyse the data, integrating Thematic Analysis methods (Braun & Clarke, 2021)[2], Structural Existential Analysis (van Deurzen, E., 2014)[3], and Holistic Content Analysis (Leiblich et al, 1998)[4]. Thus, the testimonies have been read and reread by the researcher (immersion in the data), allowing for constant comparison and identification of patterns and themes emerging from the observation of similarities and differences and theory-related material. Plutchik's emotion wheels have been used for coding emotions. Colour coding has followed an *invivo* transcription of the narratives. The rest of the data has been subject to a semantic code followed by a latent code, interpreted from the testimonies. It is important to note that for the data analysed here, a mixture of manual procedures and the use of an excel spreadsheet were used. Although the qualitative methods were applied, a quantitative characterisation helped a) to systematise the coding, b) to understand the missing data in order to saturate it and follow the study.

RESULTS AND DISCUSSION

Ninety-two different testimonies were extracted from the email answers. As an example of the type of testimonies collected, I present excerpts from two, chosen for their expressiveness in relation to the dimensions of meaning identified below:

"(…) If I could only preserve one colour, I would choose the colour of the sea, a colour that contains many colours and that would save the world from monotony and melancholy. (...) I choose the colours of the sea because I live by the sea, my atelier is by the sea, it is by the sea that many good memories spent with the family surface, bike rides with the children, the sun and our city, Espinho, in constant romance with the sea, fishing, nets and boats, Xávega art and a whole tradition of very characteristic colours and smells. Maybe that's also why I carry many of these colours into my painting. (...) I end with a deeply intimate and unforgettable experience related to the colours of the sea and the emotion they provoke in me: further away from home, in the beautiful southwest of Alentejo, I saw Cabo Sardão for the first time. I was with my husband and pregnant with my first daughter, who is now ten years old. The moment was breathtakingly beautiful: the contemplation of the power of nature, the deafening silence of the sea, the beautiful places in our country, a perspective of the future. Exactly ten years later, we took our daughter there, to the colours of the sea. If only one colour of this world could be preserved, it would be the colour of the sea." (Ana Pais Oliveira)

"The colour I would like to preserve would be the yellow of a sunflower, a strong and deep nuance of yellow but warm, not screaming but rather golden and soul-warming. It's a colour I often see in my meditation as some little balls or bubbles dancing in front of my closed eyes, or some undefined but bright forms of anything/something. I tried to capture the tone of yellow I'm speaking about in the pictures attached. After having reflected quite a lot about this question, I always return to the image of the first sun rays at dawn that I can see when entering the kitchen at a particular time in the morning, or from my room where the sun rays are reflected back from the opposite house. I also have these moments when riding my bike early in

the morning and catching the first sun rays. It's this tone of yellow that I associate with moments of tranquillity, maybe also with peace and a sort of happiness. Maybe it's also light after darkness, the new after what's gone, a sign that the world has not ended." (Antje Disterheft)

The following themes emerged from the data analysis: a) colours, b) emotions, c) the spatial contexts of the experience; d) the temporal contexts of the experience and e) the impact of the experience in the present. Some of the testimonies were very complex (as we would expect from significant experiences), which was reflected in the presence of various colours and emotions, some in polarised tension.

Colours: the colours described in the testimonies (correspond to those commonly used in developed languages (Lyons, 1995)[18]: *Brown, Ochre, Yellow, Orange, Red, Green, Turquoise, Blue, Purple, Pink, Gray, Black, White, Gold, All colours.* Although not responding to a specific colour, *Light* also emerged as a category (when participants chose memories related to sunlight and unspecific types of light). It should be noted that the main colour mentioned was *blue* (the colour preferred by most people, Pastoureau, 1997)[19], followed by *"all colours"* (in line with testimonies where the object described was the rainbow). These two categories were followed by *red, green and yellow.* It should also be noted that there were only three occasional occurrences of the colour pairs *White-blue, Brown-white, Green-blue.*

Emotions: all of Plutchik's basic emotions and their expressions (apart from anger) are present in the testimonies a) *Sadness: grief, pensiveness, melancholy, discouragement; b) Disgust: hate, repulsion, boredom; c) Anticipation: interest, excitement, awareness, expectant; d) Joy: happiness, joy, pleasure, satisfaction, pride, serenity; e) Fear: terror, fear, anxiety; Surprise: amazement, wonder, amusement, speechlessness; f) Trust: safety, comfortable, relaxed*.

Spatial context: the following categories among the objects of the experiences were identified a) *Environment: family house, landscape, ocean/sky/water, rainbow, stars/sunlight/light, urban*; b) *Objects: art, cloth, cultural, hand scale objects, plant, toy*; c) *Person*; d) *Pet*. We know that sky, ocean and rainbow are all types of aesthetic components of the landscape, but we opted for a more detailed categorization because it is more expressive.

Temporal context: the following categories among the objects of the experiences were identified a) *One-off* (for different types of single, short and unique experiences) *Travelling* (for unique experiences during a trip, a subcategory from the first was created because it is very frequent in the testimonies) b) *Habits*: *personal, family gathering* (differs from the social habits because the reference to family is very frequent), *social*, *cultural*; *life period* (when the testimonies relate to a repeated event during a period of life that has already ended) c) *ideal* (when the sense of the responses is underlined by an ideal of the participant). It is also important to note that the testimonies refer to all stages of life (*childhood, adolescence, young adulthood, adulthood, late adulthood*). Although the most frequently mentioned were childhood and adulthood, no relationship between the ages of the memories and the ages of the participants was identified.

Impact of the experience in the present: most experiences resulted in memories or strong memories. Forty-five testimonies evinced a lasting impact over time identified as: a) *Experiences that influenced an adult decision*; b) *Experiences still repeated/ occurring in the present* (with special attention to moments of contemplation and meditation); c) *Experiences that strengthened family ties*; d) *Experiences which were taught to children;* e) *Reflection that changed their worldview/ way of being* or; f) *Reflection that changed / influenced their work;* g) just one experience was referred to a *Trauma*.

By relating the colour theme to emotions (with the exception of emotions with negative associations) the results resonate to the culturally based study carried out by Jonauskaite, D., & all. (2020)[20]. We can postulate the presence of a bias through this comparison, resulting from the way the data were collected. The few protagonists of life stories with negative associations did not respond to the email invitation, although these memories surfaced in the first informal conversations. They were unable to write them down, with the exception of the one referring to an (already resolved) trauma. In the future, these data should be exclusively collected through interviews. It could also be hypothesised that the strong presence of memories relating to the ocean/sea/water is due to the fact that most of the participants belong to countries with coastlines.

CONCLUSION

In answer to the first research question, we can say that there are significant events involving experiences of colour. From the analysis of the data, these experiences involve the whole spectrum of colours and emotions (except anger), the most frequent being blue, amazement and serenity, respectively. Spatial contexts include experiences that refer to the colour of: the landscape, and its aesthetic elements, sky, sea, water or rainbows; the clothes worn in a particular period in their life; and the childhood home or the home of the family's children. These are experiences that occur at all stages of life, in short moments of time that leave strong memories (often when travelling), or that are habits repeated throughout life such as contemplation, meditation or family gatherings. In addition to the repetition, the impact of these events has been described as involving decisions in adult life or reflections on the protagonists' view of life and the world, and sometimes they give rise to a desire for self-transcendence through passing this habit on to their children.

In recalling the differentiating role of colour, it seems that it continues to be used through the manifestation of surprise and pleasure, between a previous and a present reality that at a certain moment enters our eyes, dazzles us and/ or elevates us. Before closing with a question, we will add a few more observations. It is curious to note that more than half of the events brought out by the testimonies arose from natural rather than man-made colours. At this point, I invite the reader to following the outline of the data through the adult's memories of childhood memories, and to revisit the colours of the landscape, its aesthetic elements whose admiration from childhood we wish to perpetuate in habits that span generations. With this in mind, can we today attribute to the colour of our affections an aura of unknown, wonder and transcendence? And isn't this colour, the same "color" compared by "Isidore of Seville, the savant's savant" to "calor" through the same matter that is the sunlight, the one that makes colour vision "less a retinal and more a total bodily activity common to fairy tales, in that we may pass into the image while we are looking at it" Taussig (2006)[21], and that, by doing so, it brings us "a little closer to the 'heart of things'" Merleau-Ponty (1964)[9]?

Future studies, with a larger number of participants (correcting male/female bias and positive/negative expression of emotions) and educational and geographical scope will allow us to draw more solid conclusions and compare results with cultural studies on colour, emotions and meaning. I believe that through these contributions, in addition to knowledge in the theoretical fields of colour psychology and anthropology, research questions can be formulated for professionals working with the design of objects and the human environment, in order to achieve greater comfort, usability and lifespan of products, establishing a stronger emotional connection between the object and its user.

ACKNOWLEDGEMENT

I would like to express my gratitude to all who participated with their biographic material. Also to Isabel Gonçalves, Cláudia Costa and Sara Hagá for their bibliographic references and discussion; to Luís Antunes for his help in the data processing. Thank you all.

REFERENCES

1. Charmaz, K. (2006). *Constructing grounded theory: A practical guide through qualitative analysis.* London: Sage
2. Braun, V. & Clarke, V. (2019). *Reflecting on reflexive thematic analysis, Qualitative Research in Sport, Exercise and Health*, 11:4, 589-597, DOI:10.1080/2159676X.2019.1628806
3. van Deurzen, E. (2014). Invited Paper Structural Existential Analysis (SEA): A phenomenological research method for counselling psychology. *Counselling Psychology Review Vol 29 Issue 2*. DOI: https://doi.org/10.53841/bpscpr.2014.29.2.54
4. Lieblich, A., Tuval-Mashiach, R., & Zilber, T. (1998). *Narrative analysis: Reading, analysis, and interpretation.* New Delhi, India: Sage Publications
5. Plutchik, R. (1991).*The Emotions.* EUA: University Press of America
6. Küppers, H. (1978). *Fundamentos de la teoría de los colores*. Barcelona: Gustavo Gili.
7. Humphrey N.K. (1976). The social function of intellect. in: Bateson P.P.G, Hinde R.A, (Eds). *Growing points in ethology.* UK: Cambridge University Press.
8. Maund, B. (2012). "Color", In *The Stanford Encyclopedia of Philosophy* (Winter 2012 Edition), Edward N. Zalta (ed.) (online)
9. Merleau-Ponty, M. (1964). *L'Oeil et L'Esprit.* Paris: Gallimard
10. Lakoff, G., & Johnson, M. (1999). *Philosophy in the Flesh: The Embodied Mind and Its Challenge to Western Thought.* New York: Basic Books.
11. Prinz, J. (2004). *Gut reactions - A perceptual theory of emotion.* Oxford: Oxford University Press
12. Damásio, A. (2020) *Sentir & Saber. A Caminho da Consciência*. Lisboa: Circulo Leitores.
13. Colombetti, G., & Thompson, E. (2008). The Feeling Body: Toward an inactive approach to emotion. in W. F. Overton, V. Muella, & J. Newman (eds.), *Body in Mind, Mind in Body*. Lawrence Erlbaum Associates
14. Damásio, A. (2017). *A estranha ordem das coisas.* Lisboa: Círculo de Leitores.
15. Csikszentmihalyi, M. & Rochberg, E. (1981). *The Meaning of Things: Domestic Symbols and the Self.* Cambridge: Cambridge University Press
16. van de Goor, J., Sools, A. M., & Westerhof, G. J. (2020). The Emergence of Meaning From Meaningful Moments in Life. *Journal of Humanistic Psychology*, https://doi.org/10.1177/0022167820967779
17. Velho, C. (2016). *Bem-estar, regulação de necessidades psicológicas e processo psicoterapêutico: integrando a perspetiva dos pacientes (tese de doutoramento em psicologa).* Lisboa: Universidade de Lisboa, Faculdade de Psicologia.
18. Lyons, J. (1995) Colour and Language. in Lamb, T, Bourriau, J. (Eds). *Colour: Art and Science.* Cambridge: Cambridge University Press. pp.194-224.
19. Pastoureau, M (1997). *Dicionário das cores do nosso tempo. Simbólica e sociedade*. Lisboa: Editorial Estampa.
20. Jonauskaite, D., & all. (2020). Universal Patterns in Color-Emotion Associations Are Further Shaped by Linguistic and Geographic Proximity. in *Psychological Science, 31*(10), 1245–1260.https://doi.org/10.1177/0956797620948810
21. Taussig, M. (2006) What Colour is Sacred? in *Critical Inquiry 33*(1), 28–51. Chicago: University of Chicago Press. https://doi.org/10.1086/509745

OPTIMISED WAVELENGTHS FOR DISPLAYING COLOURED MATERIALS WITH CINNABAR AND RED CORAL PIGMENTS

A. Ariyavarapong[1], K. Leewatchararoongjaroen[1], S. Noppakundilograt[1], A. Fanka[2,3] and P. Katemake[1*]

[1]Department of Imaging and Printing Technology, Faculty of Science, Chulalongkorn University, Bangkok 10330, Thailand.
[2]Department of Geology, Faculty of Science, Chulalongkorn University, Pathumwan, Bangkok 10330, Thailand.
[3]Applied Mineral and Petrology Special Task Force for Activating Research (AMP STAR), Department of Geology, Faculty of Science, Chulalongkorn University, Bangkok, 10330 Thailand

*Corresponding author: Pichayada Katemake, pichayada.k@chula.ac.th

ABSTRACT

Displaying coloured materials under a particular light source for some time can lead to a deterioration in terms of discolouration and structure change. The discolouration is caused mainly by visible light, while the change of structure is caused by ultraviolet (UV) to a great degree. The coloured materials selectively absorb visible light and scatter some light. Factors affecting the absorption and scattering efficiencies include particle size, wavelength, the refractive index of a particle and the medium in which the particle is dispersed. Furthermore, types of colourants and materials contribute to the deterioration rate. This research aims to identify the wavelengths having peaks from 367.1 nm to 740.2 nm, categorised into UV, blue, green, yellow, orange and red, that bring less damage to paints made from cinnabar and Japanese red coral pigments (natural Koikuchi sangomatsu). The causes of the colour of these two samples are a band gap energy and a crystal field energy as an impurity, respectively. The deterioration of paints was investigated under sixteen narrow-band wavelengths of LED. The cinnabar and red coral pigments having eight different sizes varying from the largest one (#7) to the smallest one as a fine powder (#14) were mixed in gum arabic and coated on a watercolour paper before exposing them to sixteen narrow-band wavelength LEDs. The largest, medium, and smallest particle size of both pigments have also exposed three selected blue, green and red LEDs. The spectral reflectance, colour difference and chemical compound were compared regularly after 790 and 1500 hours of coloured light exposure. The optical microscope results show that the particle size distributions of the cinnabar #7 to #13 are so large that the colour changes among samples of various sizes are not significantly different. Moreover, their sizes are greater than the wavelength, and the absorption efficiency is equal. Therefore, the colour change is caused mainly by the energy of individual wavelengths. In the case of cinnabar, the maximum colour difference, dE^*_{ab}, of 9.8 is at 445-460 nm and drops to 0.00 at 585-592 nm. This could be explained by the nature of cinnabar, which absorbs energy less than the energy gap of 591.7 nm and appears red; the energy greater than 591.7 turns it into a semiconductor. The increase and decrease of dE^*_{ab} are clearly corresponding to the radiance of individual wavelengths. This pattern is declining with the increase of reflectance of the coloured objects. This is also valid for Japanese red coral pigments. Finally, we could suggest narrow-band LEDs in blue, green, yellow and red that give minimum colour difference after being exposed for some time.

Keywords: mineral pigment, cinnabar, deterioration, discolouration, narrow band LEDs

TONE MAPPING OPERATOR BASED ON JUST NOTICEABLE DIFFERENCE OF LUMINANCE

Kasidet Kanthong* and Jakkarin Singnoo

Department of Imaging and Printing Technology, Faculty of Science, Chulalongkorn University, Thailand.

*Corresponding author: Kasidet Kanthong, Kasidet.kt.1998@gmail.com

ABSTRACT

Tone Mapping Operator (TMO) is required to display High dynamic range (HDR) images on conventional displays. Many TMOs have been proposed, and the results are satisfactory with different processing. One of the methods that is interesting is the tone-mapping operator which processes and mimics the human visual system (HVS). In this work, the proposed operator uses quantization technique combined with a concept of Just Noticeable Differences (JND) which is used to explain the ability to perceive brightness differences of the HVS. The performance of the proposed algorithm is evaluated by comparing it with five state-of-the-art TMOs. To evaluate the proposed operator, a paired-comparison psychophysical experiment is conducted. The result shows that in terms of naturalness, the proposed algorithm produces more naturalness tone when comparison with ATT, which uses histogram adjustment based on HVS.

Keywords: high dynamic range, tone mapping, just noticeable difference, human visual system, quantization

INTRODUCTION

The dynamic range (ratio between maximum and minimum luminance intensities) in real-world scenes can be up to ten orders of magnitude which far greater than the dynamic range - we refer to this as Low Dynamic Range or (LDR) – that conventional imaging devices can cope with. High dynamic range (HDR) imaging techniques have been presented to capture such range. However, the display devices can display images with a much lower dynamic range. HDR images cannot be displayed properly on lower dynamic range devices. Thus, tone mapping methods have been presented to compress HDR luminance into a range that is displayable on LDR devices.

Over the past decades, many TMOs have been proposed [1], [2], [3], [4] and [5]. Variant tone mapping operators may use different methods, but they have the same essentially, mapping luminance HDR images to be displayable on LDR devices.

Larson et al. [1] proposed TMO that compresses real-world luminance to LDR luminance with histogram adjustments algorithm. Histogram adjustments will plot histogram based on luminance of real-world scene and modify a luminance histogram with naïve equalization and refined with a linear contrast ceiling. Later, further improvements were refined with human contrast sensitivity data. However, histogram adjustment causes issues of extreme contrast enhancement of highly populated bins (luminance levels), affecting the quality of results [5].

Adaptive logarithm TMO proposed by Drago et al. [2], a fast process tone-mapping operator to display HDR images on devices, which uses adaptive logarithmic method to mimic the human response to light. Adaptively vary logarithmic based is done by a bias power function, which enables fast non-linear tone-mapping without image artifacts. The usage of this TMO is automatic and the user can also adjust parameters to vary the output image as appropriate.

Kim and Kautz [4] proposed a photographic curve TMO, which conducts with characteristic curve of photographic with non-linear dynamic scaling method. Results from this TMO achieve consistent results with a fixed set of parameters for a widely variety of images.

Reinhard et al. [3] proposed a TMO, that was inspired from photographic technique called Zone-System. Zone-System was originally first address by Adam [6], which uses for measured information in the field to improve the chances of producing a good final print [3]. This TMO will define zone, which uses to specify luminance in real-world scene and use to define luminance compress levels. In compress luminance procedure will compress luminance zone. The resulting algorithm is satisfactory and produce artifact free image for wide variety of images.

Adaptive TVI-TMO (ATT) proposed by Khan et al. [5], that uses histogram-based TMO by Larson et al. [1] combined with concept of human visual system to compress luminance of the scene. The preference of working on a histogram adjustment method arises from the fact that it is fully automatic and independent of user-defined parameters or image-based dependencies [5]. However, the histogram adjustment method used in the operator often results in poor output images. Thus, to address this problem, a function of visual adaptation is incorporated to construct histogram.

In this paper, the proposed tone-mapping operator is based on the HVS similar to ATT, the proposed operator uses quantization method which is quicker to process [7] compared to the histogram adjustment used in ATT. Quantization is a process that is widely known and mostly used to convert analog signals into digital signals. The principle of quantization is to map continuous infinite values into a smaller set of discrete finite values [8], which is also used to develop tone-mapping operators to compress luminance of HDR images into LDR range. Tone-mapping with quantization method is also like histogram adjustment.

METHODOLOGY

The design of the proposed algorithm was guided by two criterions. It should produce natural-looking LDR images with preserved detail and simple to process. From these criterions, the proposed TMO mimics the JND of the HVS similar to the algorithm found in ATT by Khan et al. [5]. However, here we use a much simpler quantization technique instead of the histogram adjustment.

The proposed TMOs operates in the luminance domain of image. The luminance of HDR image HDR_L can be calculated from its RGB channels as found in Eq. (1).

$$HDR_L = 0.2126R + 0.7152G + 0.0722B \tag{1}$$

The distribution of luminance levels is not perceived to be uniform by HVS. The Threshold vs. Intensity (TVI) function can be written as a piecewise non-linear equation as found in [5], and is given in Eq. (2).

$$log_{10}(\delta L_a) = \begin{cases} -3.81, \quad if \ log_{10}(L_a) < -3.94, \\ (0.405log_{10}(L_a) + 1.6)^{2.18} - 3.81, \quad if -3.94 \le log_{10}(L_a) < -1.44, \\ log_{10}(L_a) - 1.345, \quad if -1.44 \le log_{10}(L_a) < -0.0184, \\ (0.249log_{10}(L_a) + 0.65)^{2.7} - 1.67, \quad if -0.0184 \le log_{10}(L_a) < 1.9, \\ log_{10}(L_a) - 2.205, \quad if \ log_{10}(L_a) \ge 1.9, \end{cases} \tag{2}$$

Where $\delta L_a$is the threshold value that is perceived as a JND by human eye adapts to the background luminance L_a. Unit of both δL_a and L_a is cd/m^2 [5]. From Eq. (2), the TVI curve can be plotted as shown in Figure 1.

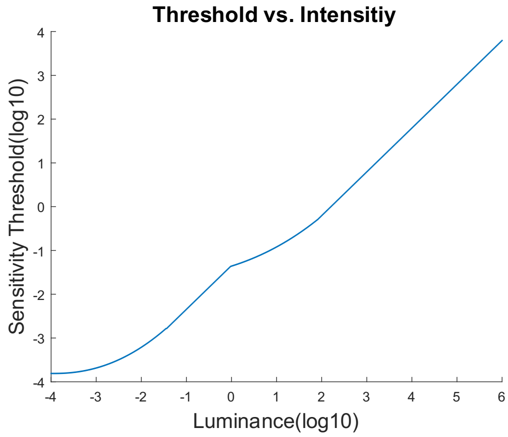

Figure 1. TVI curve giving sensitivity of the human visual system with different adaptation levels of luminance.

As can be seen from Figure 1, when luminance increases, the Sensitivity Threshold also increases. This relationship is referred as JND. This indicates that the quantization should be done in the non-linear fashion followed the shape of the TVI curve.

Before quantization begins, the minimum luminance and maximum luminance of HDR are first calculated. They are used to define a starting point and the ending point of the iterative process of the quantization. The minimum luminance is used to define the first levels of intensities of the quantization, which have value equal to distance from previous levels as JND step. The iterative process can be written as Eq. (3). This process will repeat until maximum luminance of HDR is reached.

$$L_{i+1} = L_i + n * \delta L_i \tag{3}$$

L_i is the starting luminance of the current intensities level of the current iteration. L_{i+1} is the starting position of the luminance of the next iteration. Width of intensities level is depended on JND steps that are determined as δL_i in Eq. (2). In the case of conventional 8-bit LDR, the iteration occurs 256 times.

After the iteration is finished, the quantization is performed as shown in Eq. (4).

$$LDR_{Li} = \begin{cases} i-1 \ \ if \ \ HDR_L(i) \geq L_{i-1} \ and \ HDR_L(i) < L_i \\ 255 \ \ if \ \ HDR_L(i) \geq L_i \end{cases} \tag{4}$$

Where Luminance of input HDR image $HDR_L$is calculated from Eq. (1) and L_i are from Eq. (3). In this step, grouping each HDR luminance in to LDR luminance that followed the JND is calculated.

After compressing HDR to LDR, the normalization is done by dividing the LDR_L with the maximum value of LDR_L.

$$LDR_{Lnormalized} = \frac{LDR_L}{\max{(LDR_L)}} \tag{5}$$

Finally, color reconstruction uses to bring back color data to LDR image.

$$LDR_{R,G,B} = \left(\frac{HDR_{R,G,B}}{HDR_L}\right)^s \cdot LDR_{Lnormalized} \tag{6}$$

From Eq. (6), where $HDR_{R,G,B}$ is original HDR image, HDR_L from Eq. (1), LDR_L from Eq. (5) and s is saturation factor. Saturation factor value does not exceed 1, because this value multiplies all pixel in image, which can beyond the range of the LDR image to be displayed. In this work uses $s = 0.67$ follow author of ATT [5].

Figure 2. HDR image Fribourggate [9] tone-mapped with Larson et al. [1] (top left), Drago et al. [2] (top middle), Reinhard et al. [3] (top right), Kim and Kautz [4] (bottom left), ATT [5] (bottom middle), and proposed algorithms (bottom right).

The design and development of proposed operators compresses HDR luminance into a displayable dynamic range of devices. Meanwhile, it can produce natural tones like how the human eye would see. Different HDR scenes with a variety of luminance conditions have been tested to prove that the proposed operator can produce visually pleasing results. Figure 2 shows different tone-mapped images of FribourgGate scene. As can be seen, although the overall look of the tone-mapped images is very similar (except the tone-mapped from Larson et al.), the details of the building are well preserved in both dark and bright regions by the proposed operator.

Figure 3. HDR images Bristolbridge [9] (left column), Crowfootglacier [9] (middle column), and Montrealstore [9] (right column) are tone-mapped with ATT algorithm (top row) and proposed algorithms (bottom row).

Figure 3 shows the chosen tone-mapped images results from the proposed operator and ATT operator, which is noticeable difference. In the forest area of the Bristolbridge and Crowfootglacier scenes, the tone-mapped image by proposed operator produced flatter images than ATT, resulting in a more naturalness look. Also, Montrealstore scene, the proposed operator produces more preserves detail in the highlight areas, which can be notice from the store interior.

RESULT AND DISCUSSION

In this section, a pair-comparison psychophysical experiment [10] has been conducted to test the preference of the proposed operator in terms of naturalness and beauty. Nine HDR scenes with different dynamic range are used. The scenes are obtained from [9]. These scenes are widely used in many TMO publications. Five state-of-the-art TMOs are used in the experiment. The operator are listed as follows: histogram processing by Larson et al. [1], adaptive logarithmic methods by Drago et al. [2], photographic operator by Reinhard et al. [3], photographic curve method by Kim and Kautz [4], and ATT by Khan et al. [5]. The source codes of these operators were obtained from the original sources. Thus, the comparison occurs 15 times per scene. The whole experiment involves 270 comparisons (15 comparisons per scene, 9 scenes, and 2 preference criteria). The experiment was conducted with 30 observers in a darkroom environment, all observers have normal vision.

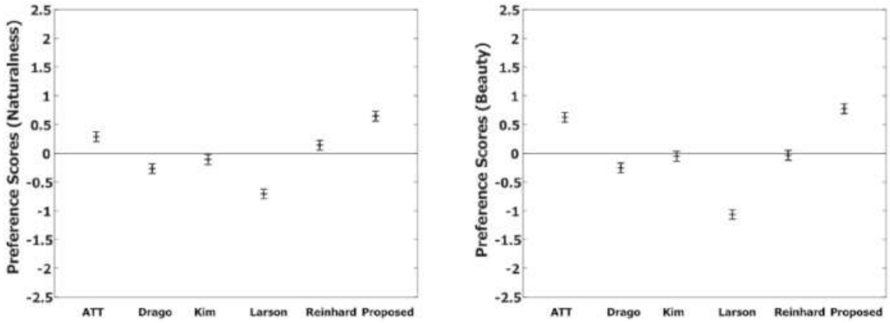

Figure 4. Overall preference score of 6 TMOs in term of Naturalness (left), Overall preference score of 6 TMOs in term of Beauty (right)

The results of average preference scores for six TMOs are shows in Figure 4. The error bar represents the 95 percent confidence interval for 30 Observers. It is clear that the proposed operator is the most preferable in terms of naturalness. In terms of beauty, the proposed operator also outperforms other tested operators, but does not significant difference compared to the ATT operator since the error bars of the two operators are overlap.

CONCLUSION

In this paper, we have proposed a tone-mapping operator that can compress dynamic range of the scene into the range that can be displayed on typical imaging devices. The operator uses quantization technique that mimics the JND of the HVS to compress HDR luminance. Thus, the tone-mapped images are natural-looking and visually pleasing. The tones are well preserved especially in the bright areas. Two Pair-comparison psychophysical experiments was conducted to evaluate the quality of the proposed operator compared with five state-of-the-art TMOs. The preference scores indicates that the proposed tone-mapping is more preferred in terms of naturalness. However, in terms of beauty the operator is also more preferred, but the score is equivalent to the ATT operator. In the future, we would like to evaluate our operator using the Tone-Mapping Quality Index (TMQI) method. Furthermore, evaluating the performance of operator with graphic processing unit (GPU) implementation is an interesting approach.

REFERENCES

1. Larson, G.W., H. Rushmeier, and C. Piatko, *A visibility matching tone reproduction operator for high dynamic range scenes.* IEEE Transactions on Visualization and Computer Graphics, 1997. **3**(4): p. 291-306.
2. Drago, F., et al. *Adaptive logarithmic mapping for displaying high contrast scenes*. in *Computer graphics forum*. 2003. Wiley Online Library.
3. Reinhard, E., et al. *Photographic tone reproduction for digital images*. in *Proceedings of the 29th annual conference on Computer graphics and interactive techniques*. 2002.
4. Kim, M.H. and J. Kautz. *Consistent tone reproduction*. in *Proceedings of the Tenth IASTED International Conference on Computer Graphics and Imaging*. 2008. ACTA Press Anaheim.
5. Khan, I.R., et al., *A tone-mapping technique based on histogram using a sensitivity model of the human visual system.* IEEE Transactions on Industrial Electronics, 2017. **65**(4): p. 3469-3479.
6. Latour, I.H., *Ansel Adams, the zone system and the California School of Fine Arts.* History of Photography, 1998. **22**(2): p. 147-154.
7. Schlick, C., *Quantization techniques for visualization of high dynamic range pictures*, in *Photorealistic rendering techniques*. 1995, Springer. p. 7-20.
8. Gonzalez, R.C., R.E. Woods, and S.L. Eddins, *Digital image processing using MATLAB*. 2004: Pearson Education India.
9. Reinhard, E., et al., *High dynamic range imaging: acquisition, display, and image-based lighting*. 2010: Morgan Kaufmann.
10. Engeldrum, P.G., *Psychometric scaling: a toolkit for imaging systems development*. 2000: Imcotek press.

Poster Paper

BAGIS Session

THE COMPARISON OF THE LIGHT DISTRIBUTION CHARACTERISTICS OF EXTERNAL FLASH ACCESSORIES

Suwat Puenpa[1]* Benjamas Sasungnern[1] Kanyarat Sirisoingern[1] and Kitirochna Rattanakasamsuk[2]

[1] Photography and Cinematography Technology, Faculty of Mass Communication Technology, Rajamangala University of Technology Thanyaburi, Thailand.
[2]Color Research Center, Rajamangala University of Technology Thanyaburi, Thailand.

**Corresponding author: Suwat Puenpa, suwat_p@rmutt.ac.th*

ABSTRACT

Advertising photography is often conducted in a studio using studio speed lights or a set of studio flashlights. However, these equipment options tend to be expensive and are only available in some professional studios. Nevertheless, using standard equipment can help general photographers or beginners achieve photography quality like that of advertisements. Therefore, this research focuses on comparing the light distribution characteristics on a model's face produced by four types of external flash accessories: flash bounce reflector white, flash bounce reflector silver, flash diffuser soft box, and soft flash diffuser, all used in conjunction with continuous ring light. In this experiment, the camera-to-model distance was controlled at 50 centimeters, and the lighting direction was set at 0 degrees (6H, 3V; directly in front of the model's face). A Canon EOS 70D digital single-lens reflex camera with a Tamron 18-200mm lens was used to capture the images. The ISO was set at 400, the aperture at f/5.6, and the shutter speed at 1/250. The results showed that each external flash accessory exhibited different light distribution characteristics on the model's face. The flash diffuser soft box produced the best lighting for contact lens advertising photography. From a professional photographer evaluator's perspective, the quality of the obtained image was acceptable and comparable to images taken with studio flash equipment.

Keywords: light distribution, external flash accessories, comparison, characteristics.

INTRODUCTION

Photography for advertising is often done using studio flash kits or studio speedlights. Studio flash is a powerful lighting equipment that allows photographers to control light intensity, creating various lighting effects. It helps photographers control light intensity, and shadows, and reduce unwanted reflections. However, studio flash equipment can be expensive and may not be accessible to everyone. For beginners or photographers with budget constraints, there are alternative options such as using natural light or continuous light sources like LED panels, tungsten lights, or external flashes that can be attached to smaller and more affordable equipment. Therefore, the objective of this research was to compare the light distribution characteristics on the model's face of four types of external flash accessories; flash bounce reflector white, flash bounce reflector silver, flash diffuser soft box, and soft flash diffuser, combined with a continuous ring light.

METHODOLOGY

An apparatus of external electronic flash, front cover accessories, including Flash bounce (white), Flash Bounce (silver), Softbox (pico Softbox), and cloth Softbox, together with circular continuous lights (ring light) for contact lens product photography. And a Canon EOS model 70D (APS-C 22.5x15.0mm), Tamron 18-200 f/3.5-6.3 lens.

The operation method has 3 steps: 1. Experimental planning and design process. 2. Experimental photography by controlling the exposure value of the camera and setting a close-up image size, the distance between the camera and the subject was determined at 50 centimeters. The lighting direction was at a 0-degree position (6H, 3V; direct and perpendicular to the model face) Set the exposure value on the DSLR camera to take photos at a fixed aperture of f/stop 5.6, a shutter speed of 1/250, and sensitivity (ISO) of 400. In this experiment, we will take one picture at a time and change the equipment for each type, including Flash Bounce (white), Flash Bounce (silver), Softbox (pico Softbox), and Cloth Softbox, together with a continuous circle light (ring light) and without a continuous circle light (ring light).

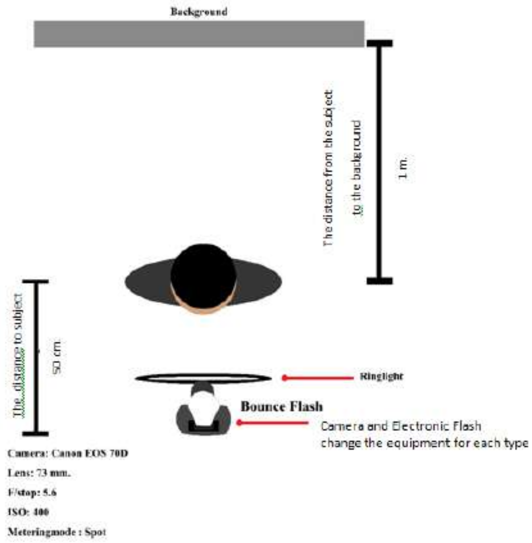

Fig. 1 shooting diagram

Change the equipment for each type. 3. The evaluation of this study was done using a questionnaire and in-depth interviews with a group of three photography experts, consisting of a contact lens photography expert and a photographer expert. Each expert will not know what equipment was used to take each picture (Blind Testing). Then rank their interest in the photographic works (Ranking Test). Along with a simple analysis of differences.

RESULT AND DISCUSSION

The results of the light distribution from the equipment for each type of external flash attachment. It was found that the light distribution in all 4 photos was different. (Fig.2)

Fig. 2 image from 4 types of external flash accessories.

This can be seen from the brightest areas on the model's face. When evaluating the shadows and dimensions on the model's face, it was considered perfect but still unable to make the contact lenses stand out.

The results of sequencing were found to be different between Photography experts who are most interested in the fourth photo because the eyes stand out more than the rest and the skin color in the photo is the closest to human skin color. The colors of the cosmetics make the eyes stand out with contrast and the light is just right, not too bright, and most suitable for photographing contact lens advertisements.

In addition, the analysis results found that in each image Start with the picture. 1 The matter of slightly distorted skin tones, highlights, or light that falls on some spots is too bright. This makes the overall area around the eyes not stand out as much as it should. Picture 2: Picture of the forehead area. The eyes are bright. The picture is cloudy until the details are unclear. The picture taken has Overexposure. The makeup elements around the eyes blend with the skin color, making it not stand out. And in the third picture, the highlight on the side of the nose jumps out. But the light in the picture is just right. There is some yellowing, but not as much as in the previous pictures. The setting of the picture is still not sharp, which makes the picture not sharp.

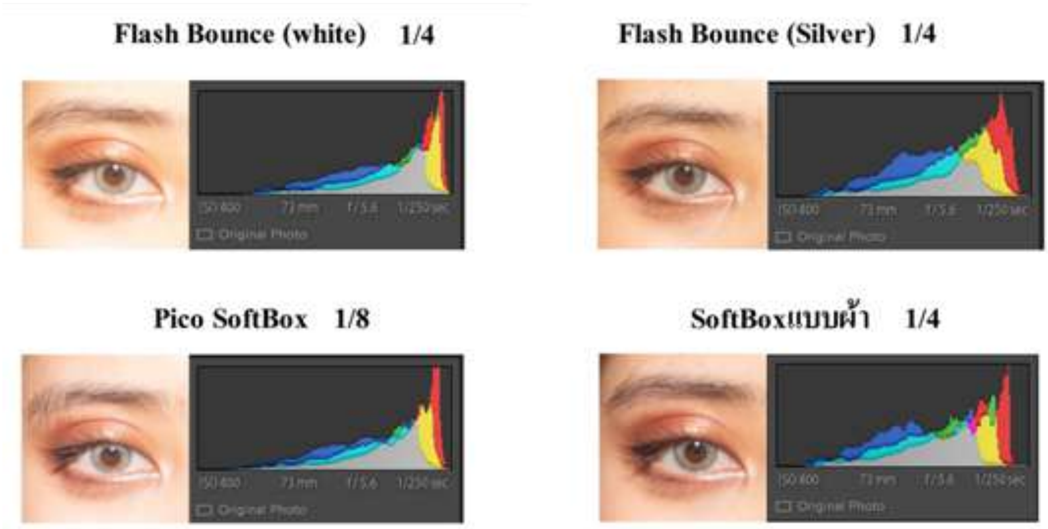

Fig. 3 compare the light diffusion ability of each type of device.

From Figure 3, it can be said that all 3 types of external flash headgear have similar light distribution efficiency except A pico Softbox which can provide maximum light distribution in a similar image size and similar brightness level.

CONCLUSION

The results of the study can be described as the best results in comparing the light distribution of internal flash electronic headgear. It is an electronic flashlight of the Pico Softbox type or Softbox type, combined with a continuous circular light (ring light) with the same image size, illuminating from 1/4, aperture value f/5.6, light sensitivity (iso) at 400, the shutter speed value (shutter speed) at 1/250 can be used for most advertising shoots because the light is just right in both the highlight and shadow areas, making the skin shades come out similar to humans. Overall, it is considered to have the most complete dimensions if compared to the Flash bounce (white), Flash bounce (silver), and cloth Softbox devices. It is also an affordable device and an accessory that is generally available in the market.

ACKNOWLEDGEMENT

The author would thank Faculty of Mass Communication Technology, Rajamangala University of Technology Thanyaburi, Thailand for supporting to doing this research.

REFERENCES

1) Patchaya Wutthiprasit. (1991). Magazines and the use of advertising images: a study in communication psychology. (Master of Journalism). Faculty of Journalism Thammasat University, Thailand.
2) Phongchet Wiriyakraikul. (2002). Effects of advertising images and product types that are related to consumers' attitudes and purchase intentions. (Master of Communication Arts). Faculty of Communication Arts Chulalongkorn University, Thailand.
3) Pramaiwat Kengngan. (2016). The influence of the lighting ratio in food photography on the feelings of consumers. (Master of Science). Faculty of Mass Communication Technology Rajamangala University of Technology Thanyaburi, Thailand.

VISUAL PERCEPTION EXPERIMENT AND ANALYSIS OF METAMORPHOSIS FOR OBJECT APPEARANCE BY CHANGE-DETECTION TASK

K. Iwase[1]*, M. Matsufuji[2], M. Tanaka[3] and T. Horiuchi[1]

[1]*Graduate School of Science and Engineering, Chiba University, JAPAN*
[2]*Faculty of Engineering, Chiba University, JAPAN*
[3]*Graduate School of Global and Transdisciplinary Studies, Chiba University, JAPAN*

*Corresponding author: Kota Iwase, 1vvs-iwase@chiba-u.jp

ABSTRACT

Conventional studies of object appearance have assumed the conscious and active acquisition of object appearance, such as "evaluating glossiness". In our daily lives, we often passively perceive an object's appearance using visual information. This study aims to experimentally investigate the extent to which humans passively perceive object appearance without paying attention and to analyse the image indices that influence perception. In this study, we conducted a visual perception experiment using a change-detection task in which five types of clues were partially metamorphosed and analysed the results. The five types of clues for metamorphosed areas were (A) colour, (B) shape, size, and direction, (C) location, appearance, and disappearance, (D) semantics, and (E) gloss and texture. The responses to 15 pairs of test images were obtained from 112 participants using crowdsourcing. The results indicated that the order of noticeability of the clues was (D) semantics; (A) colour; (C) location, appearance, and disappearance; (B) shape, size, and direction; and (E) gloss and texture. We then analysed the image statistics as an index of the ease of noticing clues. The results showed that when the structural similarity index measure (SSIM) or CIE1976 ΔE colour difference was held constant, the ease of noticing was found to have a rank correlation with the amount of mutual information in the metamorphosis area.

Keywords: Passive perception, change-detection, object appearance, visual experiment

INTRODUCTION

In recent years, studies on the measurement, reproduction, and perception of human-perceived surface quality have been actively conducted in various fields; however, most of these studies have assumed conscious and active acquisition of object appearance [1], [2]. In our daily lives, we often act by passively perceiving object appearance, such as "The road looks icy, so let's walk carefully". from the visual information. However, few studies have been conducted on the passive acquisition of surface quality. In studies on visual information that passively acquires surface quality, there have been studies on feature binding in visual short-term memory for colour, location, and shape. However, these studies did not focus on surface quality [3]. There have also been studies on information access in visual working memory [4], but they have focused on "colour and location" and not on surface quality.

In this study, we aim to experimentally investigate the extent to which humans passively perceive object appearance without paying attention to it, and to analyse the image indices that influence perception. In the experiment, we prepared images A and B, in which the five types of clues of (A) colour, (B) shape, size, and direction, (C) location, appearance, and disappearance, (D) semantics, (E) gloss, and texture were partially metamorphosed, and analysed a visual perception experiment using a change-detection task. By analysing the obtained results, we examined the image features that represent the ease of noticing changes in the surface quality.

METHODOLOGY

Discriminative clues

The five discrimination clues investigated in this experiment were (A) colour; (B) shape, size, and direction; (C) location, appearance, and disappearance; (D) semantics, which are mainly used in tests for visuospatial cognitive impairment; and (E) gloss and texture, which are the subject of this study (hereinafter abbreviated as (B) shape and (C) location). Although there are various types of surface qualities, we treated gloss and texture as representative surface qualities in this study. Because the human memory capacity is reported to be limited to approximately four clues in general [5], we included one of these clues in each image in our experiment, and all five clues were metamorphosed for all experimental stimuli. This allowed us to examine the extent to which surface quality was perceived passively and remembered correctly compared with other clues.

Experimental stimuli

Figure 1 shows the stimuli created and used in the experiment. Various objects, including people and objects, were used in the images without being biased toward any category. As source images for the experimental stimuli, we obtained free images from the Internet and downsampled them to a resolution of 400 × 300. Then, by using the tools in Adobe Photoshop, an image editing software, we created images in which each of the five clues was metamorphosed one by one.

An enlarged example of one of these stimuli is shown in Figure 2. Figure 2(a) shows the experimental stimulus before the change, and Figure 2(b) shows an example of the experimental stimulus in the original image after the change. In each experiment, the post-processed image was used as the image before the change and the pre-processed image was used as the image after the change to avoid the perception of artefact-based unnaturalness.

A reset image was used to reset the image structure and afterimage when presenting the pre-to post-change images. The reset image is created by tiling and randomly rearranging the block images before and after the change.

Figure 1. Full set of experimental stimuli

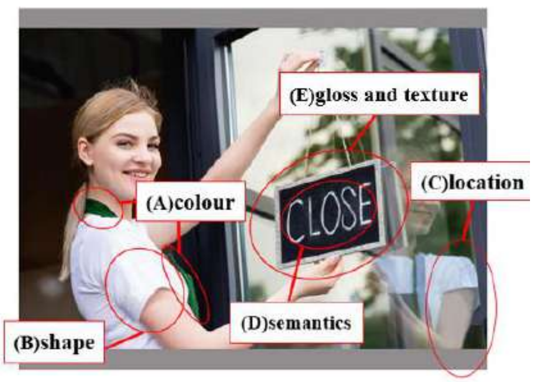

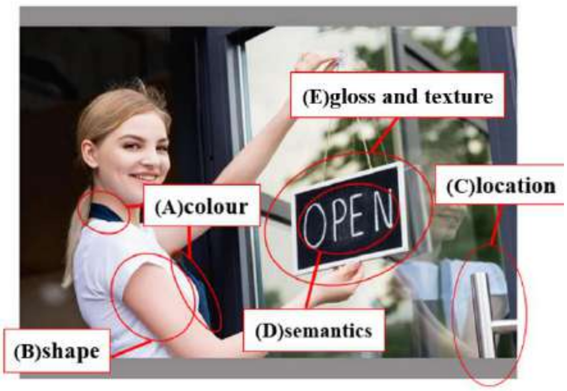

(a) Before metamorphosis **(b) After metamorphosis**

Figure 2. An Example of experimental stimuli

Experimental condition

The experiment was conducted on a cloud using the participants' personal PCs and browsers. As the experiment was conducted online, there were no detailed environmental restrictions such as viewing distance or room brightness, and the experimental conditions differed for each participant. However, to ensure an environment for checking details, the specifications prohibited the use of smartphones and tablets. The experiment was implemented using PsyToolkit software [6], [7].

Experimental method

First, the participants were shown the image before the change. Twenty seconds later, a reset image was shown to reset the image structure and afterimage. We did not inform the participants of the number of locations that had metamorphosed in each experimental stimulus, so that they could respond only to the metamorphosed locations that they noticed spontaneously. When the participant judged that there were no more changes, he or she moved on to the next image, which was presented with 15 different experimental stimuli. Next, because the strength of the clues may differ depending on the type of discrimination, we juxtaposed the images before and after the change, and asked the participants to compare the left and right images to determine whether the differences were discriminable. The experiment was terminated after 15 different stimuli had been administered.

RESULT

The participants for whom correct data were obtained were 112 Japanese men and women between 20 and 60 years old. The Smirnoff-Grubbs test was conducted on the number of responses from each participant to eliminate outlier data. Data from 94 participants whose responses statistically followed a normal distribution were used for the analyses. Figure 3 shows the participants' mean (True Positive: TP) percentage of correct responses. In Figure 3, the vertical axis represents the mean percentage of correct responses, the horizontal axis represents the results when the experimental stimuli were presented in a time series, and TP2 represents the results when two images were presented side by side. TP3 represents the mean of the time series of the correct response rate when the clue strength was normalised by denominating only the parts that were discriminated by juxtaposition for each participant. In other words, TP3 refers to the number of metamorphoses noticed by juxtaposition, as indicated by the time-series presentation. Because items that were not noticed when presented in juxtaposition can be judged as indistinguishable in the first place, we will focus on the results of TP3 in this experiment. The results of the t-test of the paired samples for TP3 are shown in Figure 3. In Figure 3, the results are indicated as "*" if significant at the 5% significance level, "**" if significant at the 1% significance level, "***" if significant at the 0.5% significance level, and "****" if significant at the 0.1% level.

Figure 3 shows that the order of noticeability of the clues is (D) semantics, (A) colour, (C) location, (B) shape, and (E) gloss and texture. When tested at 5% significance, (E) gloss and texture were not significantly different from (B) shape but were significantly harder to notice than the other clues. The reason (D) semantics was more significant than order clues is that it can be associated with meaning rather than being stored as an image, as is the case with other clues, and is therefore easier to recall at will, similar to semantic memory, which is positioned as a manifest memory of long-term memory.

The surface quality indicators used in this experiment can be further classified into two types: gloss and texture. A comparison of the ease of noticing these two types of clues showed that glossiness tended to be noticed more easily, but the difference was not statistically significant.

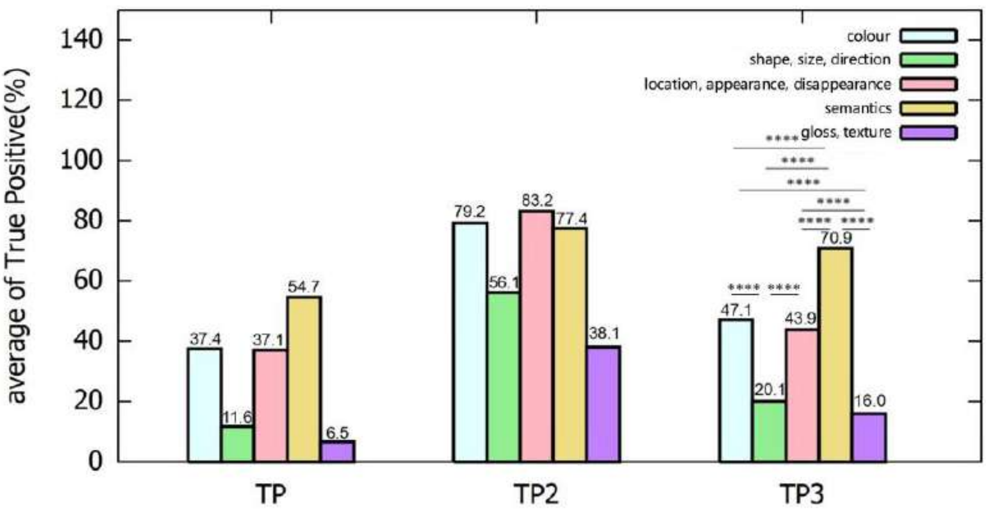

Figure 3. Average of correct responses

A comparison of the experimental results according to sex (E) gloss and texture were harder to notice than the other clues, except for (B) shape, for both men and women. Men showed significant differences in the ease of noticing (B) shape and (E) gloss and texture, whereas women showed significant differences in (A) colour and (C) location. Thus, the results showed that the ease of noticing differed by sex, with men being better at identifying "shape" and "location" and women being better at identifying "colour" and "surface quality". This may be due, in part, to the fact that men require slightly longer wavelengths to perceive the same colours as women [8], and that women are considered to be better at discriminating fine colours. However, overall, both sexes shared difficulty in noticing metamorphosis in surface quality. There were no differences in the perceptions of gloss and texture by sex.

Next, when compared by age, (E) gloss and texture were significantly different for (A) colour, (C) location, and (D) semantics in all age groups, but not for (B) shape. This indicates that, regardless of age, (E) gloss and texture are more difficult to notice than (A) colour, (C) location, and (D) semantics, but are not significantly different from (B) shape. In addition, there were no differences in the perceptions of gloss or texture according to age.

DISCUSSION

In general, noticeability is not simply related to the type of cue but also to the area of the altered cue and the intensity of metamorphosis. The area and intensity change of the altered area were calculated at each altered location, and a different image was used to represent the image and intensity of metamorphosis. The difference image was created by outputting the absolute value of the difference in the RGB values for each pixel in the two images. The image represents the number of pixels in the area that appeared in the difference image, and the intensity of metamorphosis was calculated as the average of the RGB values in the area that appeared in the difference image. The results showed that in both experiments, there was little correlation between the area and the number of people who noticed the metamorphosis, suggesting that discrimination was based on a mechanism different from memory, based simply on the detection of differences.

Therefore, we analysed the relationship between the ease of noticing clues rather than the area or intensity of metamorphosis using a general image quality evaluation index. In this study, the peak signal-to-noise ratio (PSNR), the structural similarity index measure (SSIM) [9], and CIE1976 colour difference ΔE, which are typically used, were used as image quality evaluation indices. The analysis showed that neither PSNR, SSIM, nor colour difference had a significant relationship with the ease of noticing clues. Therefore, we analysed the image features related to entropy as features related to the ease of noticing clues when these conventional indices are fixed. We used three types of feature values for analysis: mutual information, relative entropy, and entropy ratio. The results showed that the descending order of mutual information content and ease of noticing clues coincided in many pairs when SSIM and colour difference were held constant, indicating a relationship between the two. As for the relative entropy and entropy ratio, there was no relationship between the relative entropy and ease of noticing clues because the values of both these characteristics varied in many of the pairs.

CONCLUSION

To investigate the extent to which surface quality is acquired passively, we set up a change-detection task and conducted a discrimination experiment using five clues: (A) colour, (B) shape, (C) location, (D) semantics, and (E) gloss and texture. In the experiment, 112 participants responded to a crowdsourced questionnaire. The results showed that (E) gloss and texture were more difficult to notice than the other clues and were not significantly different from (B) shape; however, there were significant differences between (A) colour, (C) location, and (D) semantics. Furthermore, when the SSIM and colour difference were held constant, the ease of noticing the clues correlated in rank order with the descending order of the mutual information content. Future research will include an analysis of the effects of different experimental environments on noticeability.

ACKNOWLEDGEMENT

This work was supported by JSPS KAKENHI (Grant Number 20H05958) and JSPS Core-to-Core Program (Grant Number JPJSCCB20220006).

REFERENCES

1. Amari, S., Horiuchi, T., & Tanaka, M. (2021). Modeling of perceptual Gloss by Physical Measurement of Flat Surface. *Proc. CIE Midterm Meeting.*
2. H. Ishiyama., Horiuchi, T., & Tanaka, M. (2020). Colour Contribution in Spontaneous Identification of Copper Materials, *Proc. CIE 5th CIE Expert Symposium on Colour and Visual Appearance*.
3. Logie, R. H., & Brockmole, J. R. a. J. S. (2011). Feature binding in visual short-term memory is unaffected by task-irrelevant change of location, shape, and color. *Memory & Cognition*. 39, 24-36
4. Raisic, J. & Wilson, D. E. (2014). Asymmetrical access to solor and location in visual working memory. *Attention, Perception, & Psychophysics*, 76, 1902-1913
5. Bays, P. M., & Husain, M. (2008). Dynamic Shifts of Limited Working Memory Resources in Human Vision. *Science*, 321(5890), 851-854
6. Stoet, G. (2010). Psytoolkit – A software package for programming psychological experiments using Linux. *Behavior Research Method*, 42(1), 1096-1104
7. Stoet, G. (2017). Psytoolkit: A novel wev-based method for running online questionnaires and reaction-time experiments. *Teaching of Psychology*, 44(1), 24-31
8. Abramov, I., Gordon, J., Feldman, O., & Chavarga, A. (2012). Sex and vision II: color appearance of monochromatic lights, *Biol Sex Differ 3*, 21
9. Wang, Z., Bovik, A. C., Sheikh, H. R. & Simoncelli, E. P. (2004). Image Quality Assessment: From Error Visibility to Structural Similarity. *IEEE Trans. Image Processing*, 13(4), 600-612. doi:10.1109/TIP.2003.819861

PERCEPTUAL COLLATION METHOD FOR COLOUR HALFTONE IMAGES BASED ON VISUAL SALIENCY

T. Baba[1]*, M. Tanaka[2], S. Imaizumi[1], T. Horiuchi[1]

[1] *Graduate School of Science and Engineering, Chiba University, JAPAN*
[2] *Graduate School of Global and Transdisciplinary Studies, Chiba University, JAPAN*

*Corresponding author: Taiga. Baba, taiga0618bb@chiba-u.jp

ABSTRACT

When printing a digital colour image using a printing device, 24-bit RGB data are typically converted into CMYK halftone data via printer driver processing. The converted halftone pattern may change depending on the version of the operating system (OS) or printer driver. In this case, because it is costly to correct all differences, only the visible differences are corrected. This study aims to investigate a method of automatic perceptual collation instead of visual inspection. In this paper, we propose a perceptual collation method using visual saliency features. In the proposed method, a saliency map is first computed from the grayscale difference image output of a comparative image pair. The grayscale difference image is weighted using a saliency map to produce a weighted difference image. This weighted difference image is used to determine whether the differences are acceptable, and is used as the collation result. Collation experiments were performed on 508 comparative image pairs provided by the company that were converted using different OS or printer drivers. The experimental results showed that the proposed method with the saliency map improved the correct answer rate compared to the conventional method.

Keywords: Perceptual matching, halftone image, visual saliency, visual characteristics

INTRODUCTION

When printing digital colour images using a printing device, obtaining the same printing results from the input image is extremely important for manufacturer of the printing device. However, even when the same image is input, differences in printing results are common. General inkjet printers do not print 24-bit RGB image data, but convert it to CMYK halftones before printing. In this conversion process, differences in the conversion results may occur, depending on the computer's operating system (OS) and printer driver. Figure 1 shows two examples of halftone images (each enlarged) of the same input image converted using different operating systems. Figure 1 (a) is converted using Windows 7 32-bit and Figure 1 (b) is converted using Windows 7 64-bit. As shown in the figure, a difference exists in the way the black areas are represented. Figure 1 (a) shows a single black colour, whereas Figure 1 (b) shows black represented by the four CMYK colours. Such differences in the conversion results can cause discrepancies in the printing results, which can result in customer complaints. Therefore, companies that manufacture printed devices must account for these differences. However, in recent years, regular updating of OS and printer drivers has become a common practice, resulting in a large number of differences. Correcting for these large differences would be costly. Therefore, companies are adopting measures, such as tolerating differences that cannot be visually perceived by humans and correcting only those differences that can be perceived. Thus, a collation that tolerates differences that cannot be perceived by humans and only considers those that can be perceived is called perceptual collation. Because visual perceptual collation by inspectors poses problems in terms of cost and skill, perceptual collation system that can replace visual collation is required.

This study aims to develop a method for automatic perceptual collation instead of visual collation by inspectors. A previous study [1] proposed a perceptual collation method using colour differences in S-CIELAB [2], which is a perceptual colour space. However, visual collation evaluations occasionally differed, even for the same colour difference, and sufficient accuracy could not be obtained. When inspectors perform visual collation, their level of attention may vary depending on the content within the same image. For example, differences can be easily noticed when collating text areas than other areas because of the unique act of "reading", and differences are difficult to notice when collating landscape images because the entire image is observed over a wide area. The idea was to emphasise the differences in regions in the image that are easy to focus on and to suppress the differences in regions that are difficult to focus on, enabling the collation evaluation by the system to be made more similar to the collation evaluation by visual inspection.

In this paper, we attempt to improve the collation accuracy by constructing a perceptual collation method that introduces visual saliency [3] as a new visual property.

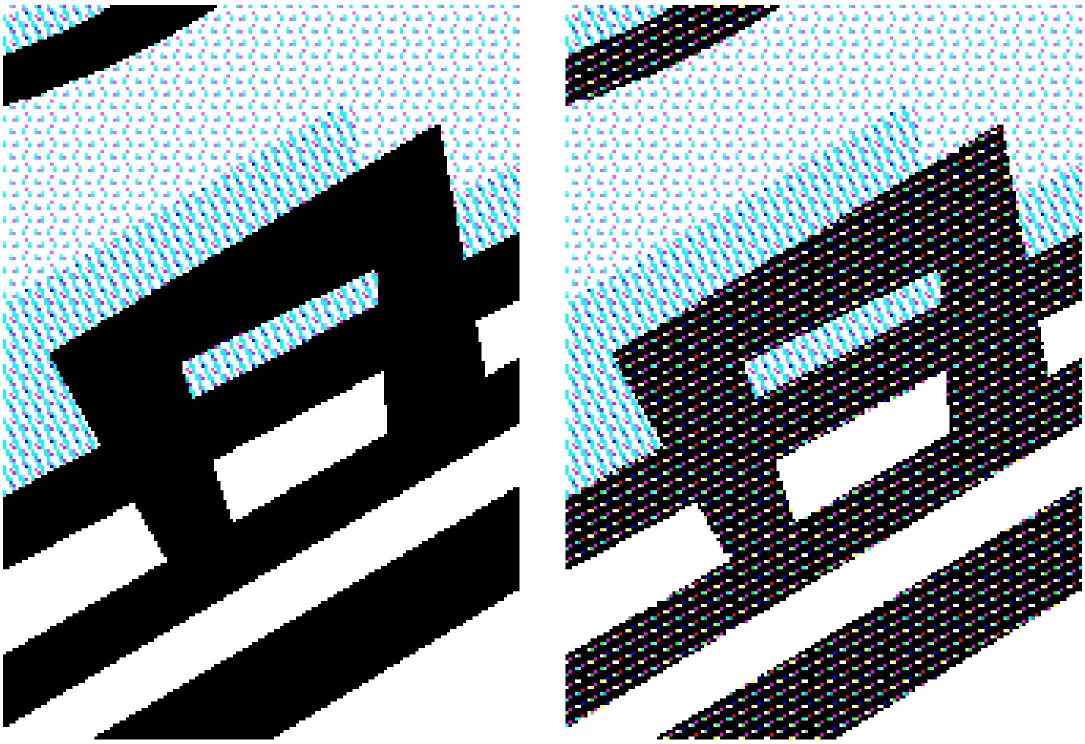

(a) Windows 7 32bit (b) Windows 7 64bit

Figure 1. Examples of halftone images converted by different operating systems. Representation of black area is different.

METHODOLOGY

Saliency Map

As shown in the left image in Figure 2, we can observe that attention is easily directed toward the yellow stimulus because its colour and orientation are different from those of the surrounding stimuli. This passive attraction of attention to stimuli is called bottom-up attention, and the property by which stimuli induce bottom-up attention is called saliency. The saliency strength of each region of the input image is expressed as the luminance, and the image is called a saliency map. The saliency map for the left image in Figure 2 is shown on the right image in Figure 2. A mechanism for obtaining saliency maps from image features was proposed by Koch et al. [3], and an actual computational model was constructed by Itti et al. [4].

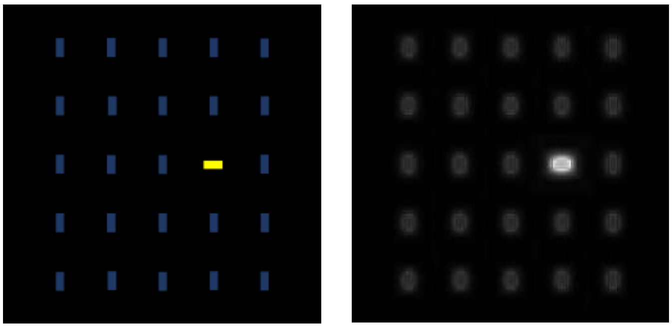

Figure 2. Example of bottom-up attention and its saliency map

Processing Step

The processing steps of the proposed method for perceptual collation using saliency are illustrated in Figure 3. The inputs were two types of digital halftone image outputs from different OSs. The difference image was calculated from the two input images. Next, a saliency map was constructed for the calculated difference image. The weighted difference image was calculated by weighting the difference image pixel-by-pixel using this saliency value. The weighted difference image refers to a difference image that considers the degree of attention. Because the weighting method was arbitrary, the following three methods were considered in this study.

Let $E(x, y)$ be the difference image pixel value at a pixel (x, y) and $S(x, y)$ be the saliency map pixel value. The weighted difference image pixel value $K(x, y)$ is calculated as follows:

(Method 1) linearly weighted

$$K(x, y) = E(x, y) \times S(x, y) \tag{1}$$

(Method 2) log weighted

$$K(x, y) = E(x, y) \times \log_e\{S(x, y) + 1\} \tag{2}$$

(Method 3) power weighting

$$K(x, y) = E(x, y) \times S(x, y)^{\frac{1}{3}} \tag{3}$$

An output-weighted difference image is used to determine whether the difference between the two input images is perceived by humans. Specifically, the weighted difference image is divided into $N \times N$ tiled blocks. If the average value of the weighted differences within a block exceeds a predetermined decision threshold, it is an NG block where differences are perceived, and if it does not exceed the threshold T, it is an OK block. If there is even one NG block in the image, the image is considered as NG; if there is none, the image is considered as OK.

EXPERIMENT AND DISCUSSION

The experimental images comprised 508 pairs of two comparison images converted by different OSs and printer drivers provided by printer manufacturers. For each image pair, the results of the perceptual collation by the company's visual inspectors were labelled, and these were used as correct answers to evaluate the collation accuracy of the proposed method. The saliency map used in this experiment was implemented using the computational model proposed by Montabone et al. [5], which was implemented in the OpenCV library. In this paper, the number of blocks used for matching was set to $N = 100$.

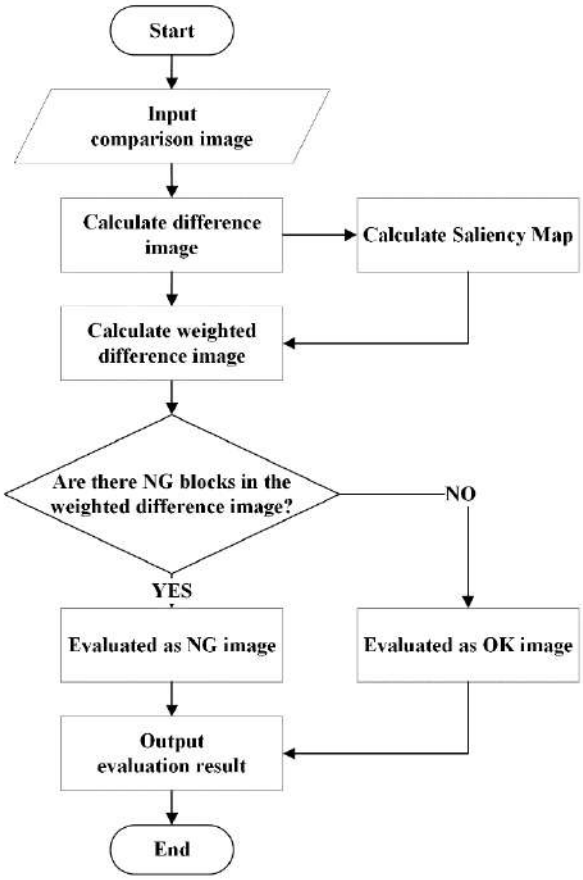

Figure 3. Processing steps of the proposed method

Table 1 lists the miss rate, over-detection rate, and correct answer rate when comparing the matching results of the proposed methods (Methods 1‐3) and conventional method [1] with the visual collation results. Misdetection is a case in which the method determines the difference to be OK, which is acceptable, but the visual inspector determines the difference to be NG. Over-detection is a case in which the method determines the difference to be NG, but the visual inspector determines it to be OK because the difference is not sufficiently visible to be NG. The correct answer is when the evaluations of the method and the visual inspector agree. The miss, over-detection, and correct answer rates are defined by Equations (4), (5), and (6), respectively.

$$Misdetection\ rate = \frac{Number\ of\ miss\ images}{Number\ of\ experimental\ images} \tag{4}$$

$$Over - detection\ rate = \frac{Number\ of\ over\ detection\ images}{Number\ of\ experimental\ images} \tag{5}$$

$$Correct\ answer\ rate = \frac{Number\ of\ over\ correct\ answer\ images}{Number\ of\ experimental\ images} \tag{6}$$

The accuracy of the proposed method was the result of the highest correct answers rate when the threshold T was varied: $T = 10$ for Method 1, $T = 20$ for Method 2, and $T = 18$ for Method 3. For comparison, we present the results obtained by applying the conventional method [1] to 508 pairs of experimental images.

The experimental results showed that all the weighting methods of the proposed method improved the miss rate, over-detection rate, and correct answer rate of the conventional method. Comparing the accuracy of the three weighting methods, Methods 1 and 2 yielded the highest percentage of correct answers. Although the percentage of correct answers was the same, Method 2 was more effective than Method 3 because it missed fewer items. However, for both methods, the miss rate is higher than the over-detection rate. By contrast, Method 3 was superior in that it had the lowest miss rate and the miss rate was lower than the over-detection rate, although the correct answer rate was lower than that of Methods 1 and 2.

Figure 4 shows an example of the way Method 2 of the proposed method improves the collation results of the conventional method. Figure 4(a) shows the results of the ambiguity collation by the visual inspector; red is the area where the differences were determined to be unacceptable. The conventional method shown in Figure 4(b) could not determine the character areas where the differences occurred as NG. However, when a saliency map is calculated for the difference image, as shown in Figure 4(c), differences in character areas are more likely to be focused than illustrations differences. Using this as a weighting factor, this method can determine the NG without missing any text areas, as shown in Figure 4(d).

Figure 5 shows an example of over-detection in Method 2 of the proposed method. Many over-detections in our method were caused by the small number of NG blocks. We believe that it is necessary to consider an algorithm that suppresses over-detection owing to small blocks without increasing the number of misses.

Table 1: Experimental accuracy

	Proposed Method			Conventional Method [1]
	Method 1	Method 2	Method 3	
miss rate	9.1%	8.3%	7.5%	8.5%
over-detection rate	6.5%	7.3%	8.5%	16.1%
correct answers rate	84.4%	84.4%	84.0%	75.4%

(a) Ground-truth **(b) Conventional Method** **(c) Saliency Map** **(d) Proposed Method**

Figure 4. Example of improvement of matching results of conventional method by the proposed method

Figure 5. Example of over-detection image (Red squares are the detected area)

CONCLUSION

In this paper, we proposed a perceptual collation method, in which differences in the transformation results that occur in the process of image printing are tolerated, and those that are not perceivable to humans are tolerated. By introducing saliency, we were able to improve the miss rate, over-detection rate, and correct answer rate compared to conventional methods.

Further investigation is required to test the output method of the saliency map and other weighting methods to determine whether they are effective in improving the collation accuracy. Examining algorithms to suppress over-detection owing to the small number of NG blocks is crucial.

ACKNOWLEDGEMENT

This work was supported by JSPS Core-to-Core Program (Grant Number JPJSCCB20220006). We thank our co-researcher Ren Nakamura for providing the program and guidance.

REFERENCES

1. Nakamura, R., Horiuchi, T., Tanaka, M., Imaizumi, S., & Takanashi. T. (2020). Perceptual Collation Method for Multi-Level Color Halftone Image based on visual Characteristics. *CEUR Workshop Proc. CVCS 2020*, *2688*, paper 1, 13 pages.
2. Zhang, X., & Wandell, A. B. (1997). Spatial Extension of CIELAB for Digital Color-Image Reproduction. *Journal of the Society for Information Display, 5* (1), 61-63.
3. Koch, C., & Ullman, S. (1985). Shifts in Selective Visual Attention: Towards the Underlying Neural Circuitry. *Human Neurobiology, 4*(4), 219-227.
4. Itti, L., Koch, C., & Neibur, E. (1998). A Model of Saliency-based Visual Attention for Rapid Scene Analysis. *IEEE Transactions on Pattern Analysis and Machine Intelligence, 20*(11), 1254-1259.
5. Montabone, S., & Sato, A. (2010). Human Detection using a Mobile Platform and Novel Features Derived from a Visual Saliency Mechanism. *Image and Vision Computing, 8*(3), 391-401.

ANALYSIS OF HARMONY BETWEEN COLOURED LIGHT AND FRAGRANCE BY THE REACTION OF THE LEFT-RIGHT ORBITOFRONTAL AREA

T. Oba[1]*, M. Tanaka[2] and T. Horiuchi[1]

[1]Graduate School of Science and Engineering, Chiba University, JAPAN
[2]Graduate School of Global and Transdisciplinary Studies, Chiba University, JAPAN

*Corresponding author: Toshinori Oba, toshinori_oba@chiba-u.jp

ABSTRACT

In our daily lives, we select actions by obtaining information from the five senses (sight, hearing, smell, taste, and touch). In recent years, studies have been conducted on integrating information from multisensory modalities, known as the cross-modal perception. Our previous study focused on the cross-modal perception between sight and smell, and analysed the harmony of colour and fragrance in a coloured light environment based on the orbitofrontal cortex (OFC) response. In this study, we analysed harmony by considering the influence of different lighting environments on the OFC response and the functional differences between the left and right OFC. In the experiment, observers evaluated the degree of harmony between the fragrance selected from a preliminary survey and the coloured light. The evaluation was conducted using two methods: a cross-modal method, in which observers evaluated the degree of harmony while smelling the fragrance, and a single-modal method, in which observers evaluated the degree of harmony based on fragrance names without smelling them. Based on the evaluation results, three types of coloured light were selected: harmonious, disharmonious, and neutral (neither harmonious nor disharmonious). Therefore, we presented combinations of each coloured light and fragrance and measured left and right OFC responses. The results showed that the combinations selected through cross-modal integration activated the OFC more than single-modal combinations, and this effect was more pronounced in the left OFC than in the right OFC. Furthermore, the OFC tends to be more activated in lighting environments that are closer to our daily lives. Additionally, in an experiment using neutral-coloured light, a correlation between the degree of harmony evaluation and the level of OFC activation was confirmed.

Keywords: cross-modal, orbitofrontal cortex, near-infrared spectroscopy, oxy-Hb

INTRODUCTION

Humans use their five senses (e.g., sight, hearing, and smell) to acquire various types of information. It is believed that moments of individually perceiving these pieces of information are relatively rare, and in daily life, we often simultaneously perceive multiple senses. Therefore, it may be assumed that we integrate information from our five senses to make comprehensive judgements and choices regarding our actions. Consequently, in recent years, studies integrating information from multisensory modalities, known as cross-modal or multi-modal perception, have been actively conducted [1]. Focusing on cross-modal studies between sight and smell, Gilbert et al. [2] confirmed significant colour-based characterisation for 20 different test fragrances. Moreover, when the same experiment was conducted several years later, a consistent correspondence between colour and fragrance was demonstrated, suggesting a strong association between sight and smell. Additionally, Osterbauer et al. [3] showed that when colour stimuli and fragrances were simultaneously presented, the more combinations matched, the more the brain was activated, indicating a correlation between sight and smell. Miura & Saito [4] conducted experiments using colour panels to investigate the effect of colour and fragrance harmony on stress reduction. The results showed that stress was alleviated when colour and fragrance were in harmony compared to when they were not in harmony. However, in these conventional studies on the cross-modal effects of colour and fragrance, visual stimuli were limited to a narrow field of view, such as coloured liquids [5], coloured chips [1,4], and monitor colour [6], which only examined planar visual stimuli. Additionally, the analysis of colour and fragrance harmony relies on subjective evaluations by observers, resulting in an analysis based on subjective data. Furthermore, the selection of harmonious colours based on the names of fragrances often relies on a single-modal method in which observers do not smell the fragrance. This method may have been influenced by preconceptions affecting the analysis.

In a previous study, we analysed the harmony between colour and fragrance in a coloured light environment using physiological indicators [7]. Using coloured light as a visual stimulus, we conducted spatial verification and performed an objective analysis by measuring the physiological response to the stimuli. The measurements were focused on the orbitofrontal cortex (OFC), which is located on the ventral surface of the prefrontal cortex. Additionally, we incorporated a cross-modal method in which observers evaluated the degree of colour harmony while smelling the fragrance and analysed the differences in OFC responses between this cross-modal method and a single-modal method in which observers evaluated colour harmony based on fragrance names without smelling them. However, the lighting environment in the study of Ref. [7] was limited to a localised space, and the OFC response used for the analysis was limited to a narrow range of brain reactions. Furthermore, the evaluation only considered combinations with harmonious or disharmonious colours, and the verification of other combinations remains a challenge.

In this study, an analysis of colour and fragrance harmony in a coloured light environment was conducted using the following three approaches. (1) In addition to the lighting environment used in a previous study, a new real-life environment closer to our daily lives was introduced to investigate whether spatial differences influenced the OFC response. (2) Functional differences were analysed by expanding the range of OFC response measurements. (3) The OFC response was measured when presenting a coloured light perceived as neutral (neither harmonious nor disharmonious).

EXPERIMENT

Functions of OFC and Measurement Method of Its Response

The OFC is located on the ventral surface of the prefrontal cortex and is associated with the integration of sensory and memory information and decision-making [8]. Additionally, the OFC is related to the reward system of emotions, such as pleasure experienced when presented with visual or smell stimuli [9], and studies have shown that this area is activated during emotional recollection [4,8]. Furthermore, the left OFC is associated with positive emotions, whereas the right OFC is associated with negative emotions [10]. A previous study [7] focused primarily on the response of the left OFC when conducting harmony analysis. Therefore, in this study, we analysed the response of the right OFC and conducted a harmony analysis focusing on functional differences. Stimuli were presented to the observers, and the concentration of oxygenated haemoglobin (oxy-Hb) in the blood near the OFC was measured non-invasively using near-infrared spectroscopy (NIRS). A Brain Activity Monitor (Hb133, ASTEM Corp.) was used in this experiment. The measurements were conducted using two channels on the left and right sides. Channel 1 (ch1) measured the area near the left OFC, whereas Channel 2 (ch2) measured the area near the right OFC. By calculating the change in peak values (Δoxy-Hb) between pre-stimulus presentation and presentation during stimuli, it was possible to quantitatively show the OFC response to the stimuli.

Generation of Experimental Stimuli

First, we generated visual stimuli using coloured light. We referred to the practical colour coordinate system (PCCS), which offers a two-dimensional system based on hue and tone and is suitable for considering colour harmony. Among the PCCS, we used a vivid tone, which represented the highest chroma, and selected 12 hues at equal intervals from the 24 colours available in the vivid tone. Additionally, considering that pure colour alone may not harmonise well with fragrance, we prepared additional colour variations by reducing the chroma to two-thirds or one-third based on white light (x = 0.33, y = 0.33). Consequently, we generated 36 coloured lights consisting of 12 hues with 3 levels of chroma. Next, we describe the generation of smell stimuli. In this study, we used essential oils that are presumed to have relaxing effects in humans and are likely to elicit physiological responses. For the smell stimuli, we used five essential oils that are relatively familiar in daily life: vanilla, mint, lime, grapefruit, and hinoki. Smell stimuli were presented by impregnating a 1 cm^2 of defatted cotton with the essential oils and placing it in a 20 ml brown light-shielding bottle. This setup made it difficult for observers to judge the colour of the essential oils. Moreover, the brown light-shielding bottle is lightweight and easy to handle, allowing observers to bring it close to their nose with ease and reduce body movement, which helps minimise noise during NIRS measurements. We adjusted the intensity of the fragrance near the opening of the brown light-shielding bottle to achieve an approximate value of 100 on the odour meter (OMX-SRM, SAKATA INX Corp.).

Preliminary Survey

We conducted a preliminary survey to select different visual and smell stimuli for each observer from the generated 36 coloured light and the 5 types of fragrances. First, observers were asked to choose one fragrance that they found most ‘pleasant’ among the five essential oils. Subsequently, they evaluated the harmony between the chosen fragrance and each of the 36 coloured lights. The evaluation was conducted using two methods: a cross-modal method (Method A), in which observers smelled the fragrance while assessing harmony, and a single-modal method (Method B) in which observers assessed harmony based on the name and imagined representation of the fragrance without smelling it. Based on the evaluation results, each observer selected three types of coloured light: harmonious, disharmonious, and neutral (neither harmonious nor disharmonious) using both evaluation methods. Therefore, six visual stimuli and one smelling stimulus were selected for each observer, considering the two evaluation methods.

Experimental Environment

In this study, we conducted experiments in two different lighting environments to investigate whether the OFC response was affected by different lighting environments. Figure 1 shows the appearance of each environment. Lighting Environment 1 was the same as that used in a previous study [7]. It consisted of a simple dark room with a lighting observation box measuring 45 cm in width and 55 cm in height, placed in front of the observer. Both the observation box and the observer are covered with blackout curtains, creating a localised space. Lighting Environment 2, however, is a larger real setting, approximately the size of a 5.5 m^2 room. It features dimmable and colour-adjustable LED lighting installed on the ceiling. The room's walls, floor, and furniture were all unified in grey to avoid any influence of object colour. Additionally, all coloured lights in both environments were set to a uniform intensity of 50 lx, and we ensured that they had the same chromaticity coordinates.

Procedure

We used six coloured lights and one fragrance selected through a preliminary survey of each of the six observers. We presented six combinations of stimuli and measured OFC responses. In each experiment, we allowed approximately 60 seconds before presenting the stimuli to ensure the stability of the measurement equipment. Once the stability of the brainwaves was confirmed, we presented the stimuli to the observers for 30 seconds. This duration was chosen based on a previous study [7], which indicated that stimulus-related responses were not observed in short durations of approximately 10 seconds, and too long a duration might affect the observers' concentration and brain activity. After the stimuli presentation, we asked the observers to remain calm and quiet for approximately 60 seconds to thoroughly observe the progression of their responses.

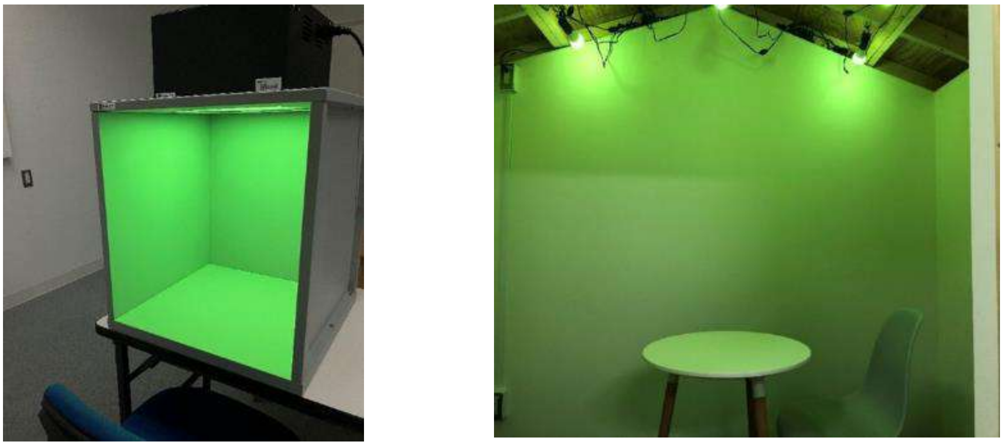

(a) Lighting Environment 1 **(b) Lighting Environment 2**

Figure. 1 Experimental Environment

RESULTS AND DISCUSSION

The experimental results are shown in Figures 2 and 3. The vertical axis of each graph represents the average oxy-Hb change caused by stimulus presentation, and the error bars indicate the standard deviation among the observers. Figure 2 shows the oxy-Hb changes in the left OFC, specifically in Channel 1, in the two lighting environments. The results for the oxy-Hb change in the harmonious colour confirmed that the OFC was more activated with the colour-fragrance combinations selected for Method A than with Method B. However, for disharmonious colours, no significant differences were observed in either environment. This result is consistent with those of a previous study [7]. Additionally, in Method A, the oxy-Hb change was greater in Lighting Environment 2 than in Lighting Environment 1. This suggests that observers could relax more in Lighting Environment 2, which resembles their daily living space, and potentially feel more pleasure when the colours and fragrances are harmonious.

Figure 3 shows the oxy-Hb changes in the left and right OFC under Lighting Environment 2. In Method A, the oxy-Hb changes were greater in the left OFC than in the right OFC. This result indicates that due to the pleasant fragrance used in the experiment, activation was observed more in the left OFC, which is associated with positive emotions. Therefore, this experiment accurately measured functional differences between the left and right OFC. Figure 4 shows that the results of the experiment in coloured light were perceived as neutral (neither harmonious nor disharmonious). For Method A, the oxy-Hb change was greater in combinations with harmonious colour than with neutral-coloured light. In contrast, for Method B, there was no significant difference in oxy-Hb changes between harmonious and neutral colours. Therefore, in the cross-modal evaluation, in which observers assessed harmony while smelling fragrances, a correlation existed between the harmony rating and the activation level of the OFC. In all the experiments, Method A yielded clearer results, which can be attributed to its cross-modal method. When evaluating the harmony between the coloured light and fragrance using Method A, the observers were unaware of the fragrance's name, potentially enabling the analysis of sensory harmony without being influenced by preconceptions.

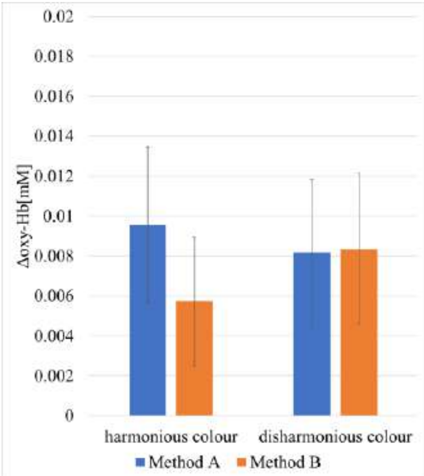

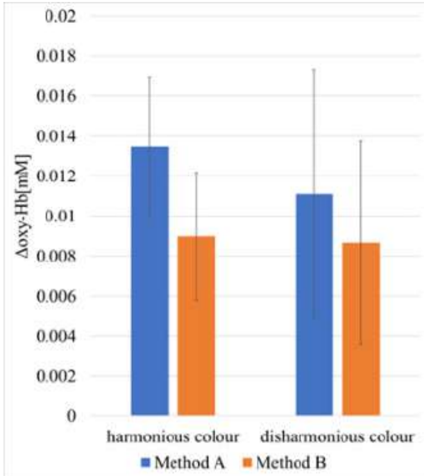

(a) Lighting Environment 1 **(b) Lighting Environment 2**

Figure 2. Analysis focusing on differences in lighting environments

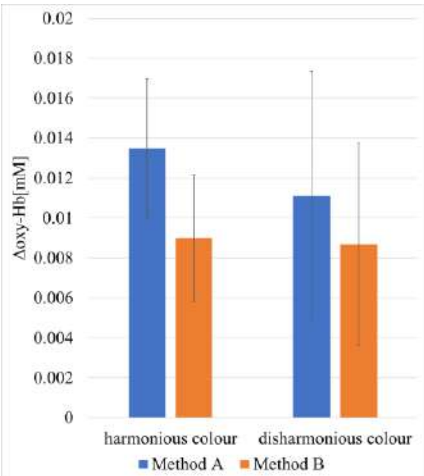

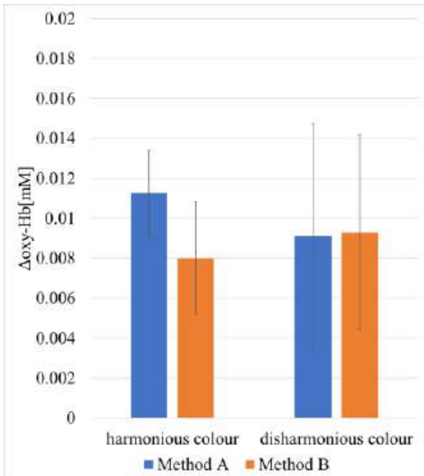

(a) Left OFC **(b) Right OFC**

Figure 3. Analysis focusing on functional differences between the left and right OFC

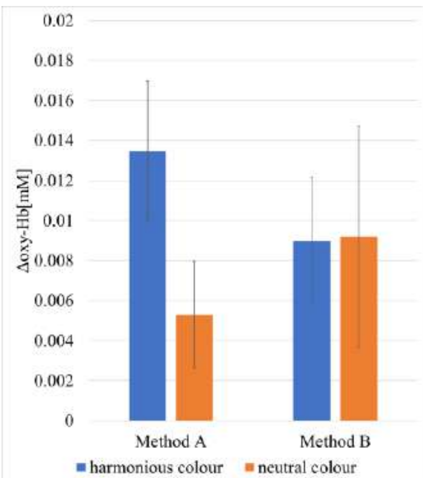

Figure 4. Analysis of experiments in neutral-coloured light

CONCLUSION

In this study, we analysed the harmony between coloured light and fragrance in lighting environments based on OFC responses. To solve the problems in the previous study [7], experiments were conducted using the following three approaches. (1) We prepared a new lighting environment in a real setting to investigate whether differences in the environment could affect the OFC response. (2) We expanded the area of measurement to consider functional differences between the left and right OFC. (3) We investigated the OFC response to coloured light perceived as neutral (neither harmonious nor disharmonious). Therefore, we suggest that differences in lighting environments can potentially influence the OFC response. Moreover, the use of pleasant fragrances led to the activation of the left OFC, which is associated with positive emotions, supporting the notion that we have successfully measured the functional difference between the left and right OFC. Additionally, under some conditions, when we presented combinations of neutral-coloured light, we confirmed that harmonious colour showed greater oxy-Hb changes, and a correlation existed between the harmony rating and the OFC response.

For this experiment, we used only fragrances that the observers perceived as pleasant. In future studies, we plan to compare these results with the use of unpleasant fragrances to further analyse the reward system's emotional response in cross-modal perception.

ACKNOWLEDGEMENT

This work was supported by JSPS KAKENHI (Grant Number 20H05958) and JSPS Core-to-Core Program (Grant Number JPJSCCB20220006).

REFERENCES

1. Spence, C. (2020). Olfactory-colour crossmodal correspondences in art, science, and design. *Cognitive Research: Principles and Implications, 5(52).*
2. Gilbert, A. N.,Martin, R., & Kemp, S. E. (1996). Cross-modal correspondence between vision and olfaction: The color of smells. *The American J Psycho, 109(3)*, 335–351.
3. Osterbauer, R. A., et al. (2005). Color of scents: Chromatic stimuli modulate odor responses in the human brain. *Journal of Neurophysiology.*
4. Miura, K., & Saito, M. (2012). Harmonious color model with fragrances. *Color Research & Application, 37(3)*, 219–232.
5. Zellner, D. A., & Whitten, L. A. (1999). The effect of color intensity and appropriateness on color-induced odor enhancement. *The American Journal of Psychology, 112(4)*, 585–604.
6. Danja, K., et al. (2019). Multisensory enhancement of odor object processing in primary olfactory Cortex. *Neuroscience, 418*, 254–265.
7. Yamashita, G. Tanaka, M., & Horiuchi, T. (2022). Analysis of Harmony between Color and Fragrance in Lighting Environments by the Reaction of the Orbitofrontal Area. *i-Perception, 13(3)*, 1–13.
8. Kringelbach, M. L. (2005). The human orbitofrontal cortex: linking reward to hedonic experience. *Nature Reviews Neuroscience, 6*, 691-702.
9. Rolls, E. T. (2004). The functions of the orbitofrontal cortex. *Brain and Cognition. 55(1)*, 11-29.
10. Noriuchi, M., Kikuchi, Y & Senoo, A. (2008). The Functional Neuroanatomy of Maternal Love: Mother's Response to Infant's Attachment Behaviors. *Biological Psychiatry, 63(4)*, 415–423.

RELATIONSHIP BETWEEN THE OBSERVER METAMERISM OF COLOR VISION DIVERSITY AND THE SPECTRAL BANDWIDTH OF PRIMARY COLOR SPECTRUM

Rei Nakayama[1]*, Hiromi Y. Sato[2], Yoko Mizokami[2]

[1] *Graduate School of Science and Engineering, Chiba University, Japan.*
[2] *Graduate School of Engineering, Chiba University, Japan.*

*Corresponding author: Rei Nakayama, ray0203@chiba-u.jp

ABSTRACT

The advent of organic light-emitting diode (OLED) technology has expanded display capabilities, resulting in a more extensive color gamut and the representation of highly vivid and saturated colors. These displays often use primaries with narrower spectral bandwidths compared to traditional liquid crystal displays (LCDs). Observer metamerism refers to the variation between the intended and realized color reproduction caused by differences in individual spectral sensitivity. The issue of observer metamerism, where perceived colors differ from intended colors due to individual variations in spectral sensitivity, has become more pronounced with wide-gamut displays. Furthermore, it has been reported that individuals with anomalous trichromacy show substantial variations in their perception of light composed of narrowband spectra. However, this phenomenon has predominantly been investigated through comparisons involving extremely narrowband laser light and exceedingly broadband color charts. Thus, the mechanisms underlying observer metamerism when the spectral bandwidth varies continuously have remained unclear. Our study aimed to address this issue by generating five primary spectra characterized by gradually varying spectral bandwidths, all achieved through a spectrally tunable light source. We conducted a color discrimination experiment using the broadest primary spectrum as a reference stimulus and the other four primary spectra as test stimuli. We selected eight sets of stimuli with varying chromaticity coordinates from a color checker. During the experiment, an observer viewed a white plate with a 2-degree visual angle in a black box, illuminated by either the test or reference spectra. The reference and test stimuli were presented consecutively, and the observer judged whether they appeared as the same or different colors. Our results indicate that only individuals with anomalous trichromacy exhibited significant individual differences in their perception of stimuli with the second narrowest bandwidth compared to those with broader bandwidths. In contrast, individuals with normal color vision displayed substantial individual differences for stimuli with the narrowest spectral bandwidth. These results suggest that observer metamerism can manifest in anomalous trichromacy under spectral bandwidth conditions similar to the primary color spectrum in OLED displays. Consequently, achieving metameric color reproduction for individuals with color vision variations like anomalous trichromacy in displays employing narrowband primaries may be challenging.

Keywords: Spectral bandwidth, anomalous trichromacy, Observer metamerism

INTRODUCTION

Approximately 5% of Japanese males and 0.2% of Japanese females are estimated to have color deficiency. Previous research conducted by Sunaga et al. has indicated the occurrence of observer metamerism in wide-gamut displays and color charts through visual simulations and evaluations of color deficiency [1]. These experiments were based on spectral information and a spectral sensitivity shift model [2]. This metamerism could be attributed to the difference between the narrow bandwidth of spectral distribution in wide-gamut displays and the broadband reflectance characteristics observed in actual color charts. However, the direct relationship between spectral bandwidth and metamerism hasn't been rigorously examined. Therefore, it is crucial to elucidate the connection between spectral distribution bandwidth and visibility simulation. In our study, we investigate the visibility of multiple metameric colors with varying spectral bandwidths using the visual sensitivity simulation method proposed by Yaguchi et al. [2].

METHODOLOGY

Experimental Environment

The experiment setup involved an observation box in a dark room, as illustrated in Figure 1. At the top of the box, a spectral tunable light source (LEDcube, THOUSLITE) was positioned. To present color stimuli, a standard white plate (X-lite, ColorChecker) was situated on the side of the box, reflecting the stimulus light emitted by a spectral tunable light source. The observation window had dimensions of 2 cm in length and width and was 55 cm from the observer's eyes. This configuration ensured that the visual angle size of the stimuli was 2°.

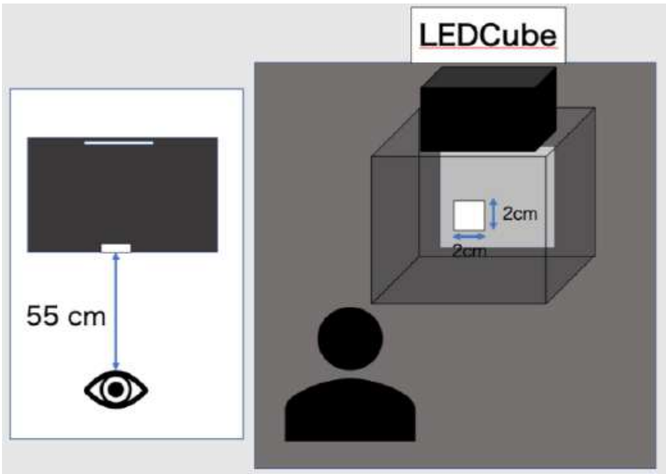

Figure 1. Experimental environment

Experimental Stimuli

We generated five primary color sets, denoted as Primary Sets 1 through 5, by combining different full width at half maximum (FWHM) values of spectral bases from the 13 available spectral basis combinations of the spectral tunable light source. These primary color sets consisted of combinations of five R and G bases along with one B basis. Primary Set 1 had the widest FWHM, followed by Primary Set 2, 3, 4, and 5 in decreasing order of FWHM. Figure 2 illustrates the spectral distributions of these primary sets, with spectral information measured using an illuminance spectrophotometer (CL-500A, Konica Minolta).

We selected eight colors from the Color Checker (X-rite) for our experimental stimuli, as shown in Figure 3. We generated metameric colors from each primary color set to match the xy chromaticity coordinates of the Color Checker under an approximate D65 light source. The luminance of these stimuli was approximately 50 cd/m^2. The metameric colors derived from Primary Sets 1 through 5 were labeled Stimuli 1, 2, 3, 4, and 5, with Stimuli 5 as the reference stimulus. These metameric colors were grouped into eight sets, denoted as CG 1-8, each containing a single metameric color group.

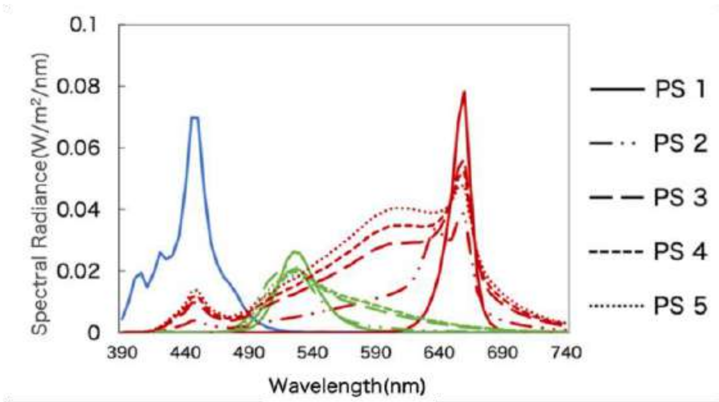

Figure 2. Spectral distribution of the primary set

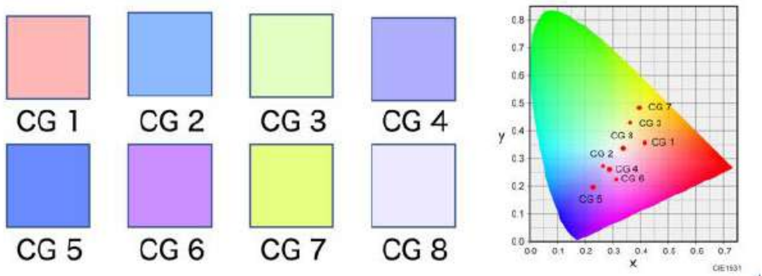

Figure 3. Eight stimulus colors selected from ColorChecker (X-rite)

Procedure

The experimental procedure began with light-adapting the observers to D65 illumination for 1 minute. Subsequently, a sequence of dummy stimuli was presented sequentially, followed by a set of metameric stimuli (test stimuli). These test stimuli were generated using RGB bases with varying FWHM values compared to the reference stimuli. The observers were tasked with identifying which set, the dummy or the test stimuli, exhibited more noticeable differences. Each set of trials was replicated five times for all four types of metameric stimuli, constituting one session for all color groups. In total, three sessions were conducted as part of the experiment.

RESULT AND DISCUSSION

Figure 4 illustrates the results of the color difference evaluation. Subfigure (a) presents the results for individuals with normal color vision, while subfigure (b) displays the results for individuals with color deficiency. The vertical axis represents the response rate, indicating that the color difference of the test stimulus set is perceived as greater than that of the dummy stimulus set. The horizontal axis corresponds to the type of stimulus used in the experiment. The error bar indicates the standard deviation. The chance level, which signifies the point at which color differences are invisible, is set at 0.5. In the case of normal color vision, significant differences were observed between Stimuli 1 and the other stimuli ($p < .001$). However, for individuals with deuteranomalous color vision, the chance level was significantly higher than 0.5 for both Stimuli 1 and 2, indicating that metamerism occurred even for stimuli with a broader bandwidth than those perceived by individuals with normal color vision. On the other hand, for individuals with deutan color vision, metamerism was close to the chance level for all stimuli. Also, as no significant differences were observed, it was suggested that observer metamerism did not occur in the current settings.

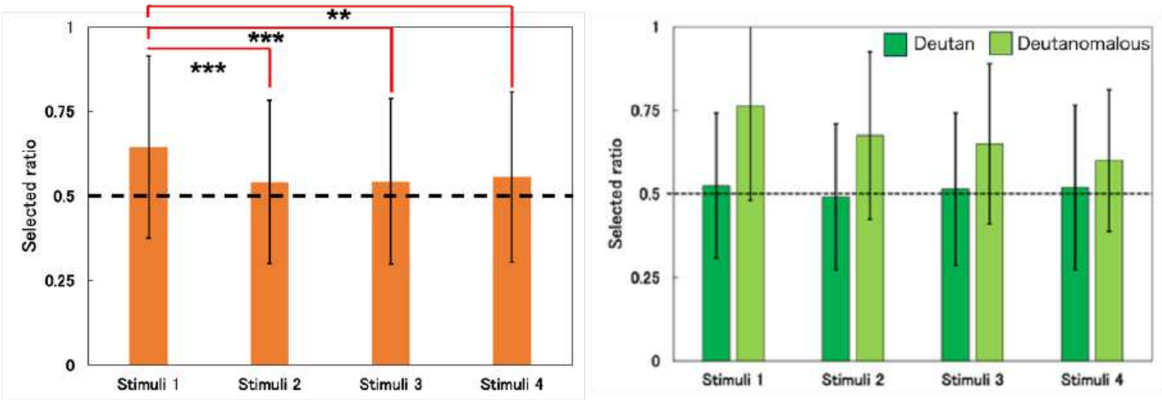

(a) Normal color vision **(b) Color deficiency**

Figure 4. Evaluation results of the color difference experiment. The vertical axis represents the response rate, indicating that the color difference of the test stimulus set is perceived as greater than that of the dummy stimulus set. The horizontal axis corresponds to the type of stimulus used in the experiment. (****p* < .001)**

The prediction of color differences based on Asano's simulation model [3], which accounts for individual variations in spectral sensitivity, aligns with the experimental findings, indicating that metamerism occurs for Stimuli 1. These results also align with the findings of Ramanath [4], who reported that observer metamerism can manifest for narrowband spectral distributions even in individuals with normal color vision. Yaguchi's simulation model [2], designed for deuteranomalous color vision, predicted substantial metamerism only for Stimuli 1. However, the experimental results demonstrated that metamerism also occurred for Stimuli 2, suggesting that metamerism may arise with a slightly narrower range of stimuli than initially predicted by the simulation model.

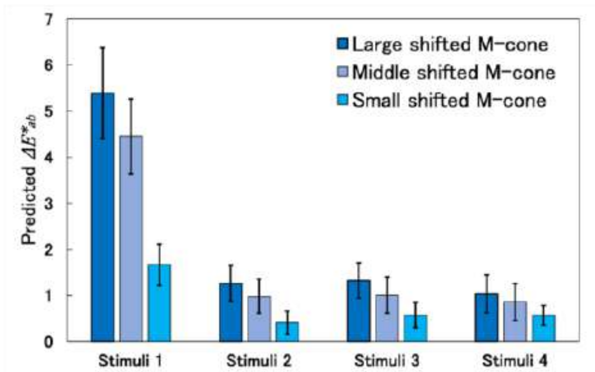

Figure 5. The color difference prediction based on the simulation model of Asano et al. [3]

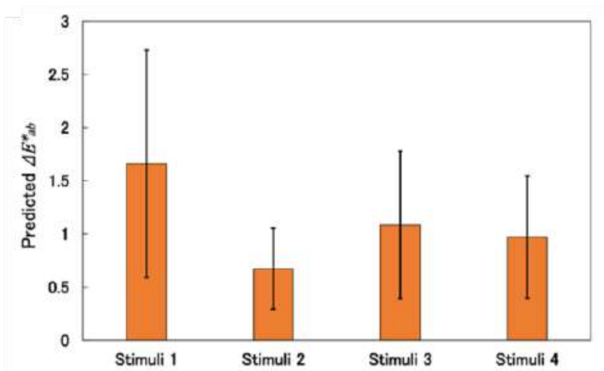

Figure 6. The color difference prediction for deuteranomalous individuals based on the simulation model of Yaguchi et al. [2]

CONCLUSION

Our study aimed to address the occurrence of observer metamerism by generating five primary spectra with gradually varying spectral bandwidths using a spectrally tunable light source. We conducted a color discrimination experiment using the broadest primary spectrum as a reference stimulus and the other four primary spectra as test stimuli. Our results revealed that metamerism was more pronounced as the spectral distribution narrowed, primarily due to individual differences in color vision. Interestingly, in the case of deuteranomalous observers, metamerism occurred for stimuli with a broader spectral bandwidth than initially predicted by the simulation model. This suggests that the simulation may have underestimated the occurrence of metamerism in deuteranomalous individuals. Furthermore, it became evident that the narrow spectral distribution had a more significant impact on the occurrence of observer metamerism in comparison to normal color vision.

ACKNOWLEDGEMENT

This study was supported by JSPS Core-to-Core Program (JPJSCCB20220006) and JSPS KAKENHI (JP19H04196, JP21K 05805, and 23H04332).

REFERENCES

1. Sunaga, S., Katsura, S., & Yaguchi, H. (2018). Color appearance of abnormal trichromatic vision in wide gamut displays. *Journal of the Color Science Society of Japan*, 42(3), 224-227. (in Japanese)
2. Yaguchi, H., Luo, J., Kato, M., & Mizokami, Y. (2018). Computerized simulation of color appearance for anomalous trichromats using the multispectral image. *Journal of the Optical Society of America A, 35, B27*8 – B286.
3. Asano, Y., Fairchild, M. D., & Blondé, L. (2016). Individual colorimetric observer model. *PloS one*, *11*(2), e0145671.
4. Ramanath, R. (2009). Minimizing Observer Metamerism in Display Systems. *Color Research & Application,* 34(5), 391-398.

The linear scale between Chromaticness and lightness axis

Phubet Chitapanya[1]*, Chanprapha Phuangsuwan [2] and Mitsuo Ikeda [2]

[1] *Color science and Human vision, Mass Communication Technology, Rajamangala University of Technology Thanyaburi, Thailand.*
[2] *Color Research Center (CRC), Rajamangala University of Technology Thanyaburi, Thailand.*

*Corresponding author: Phubet Chitapanya, phubet_c@mail.rmutt.ac.th

ABSTRACT

Many studies have utilized the polar diagram, which is a circular color space with a radius of 100, to visualize results based on the elementary color naming method. The horizontal axis of the polar diagram represents the relationship between greenness and redness, while the vertical axis represents the relationship between yellowness and blueness. A central question in this field is whether the relationship between chromaticness and lightness remains consistent, especially when compared to a standardized color system like CIEL*a*b*. In our experiment, five participants were tasked with a color-matching exercise. They referenced the Munsell hue book and concentrated on four unique colors: red, yellow, green, and blue. We maintained uniform test conditions, with lightness values ranging from 20 to 80 percent for whiteness and the reverse scale for blackness. Chromaticness was examined at intervals ranging from 10 to 70 percent. After the participants made their selections, a Konica Minolta FD-7 device was used to measure the exact values of the chosen colors. This allowed us to determine the difference or distance between each color selection, focusing on the gaps between chromaticness and lightness. Our results revealed unique patterns for each of the primary colors. In the red condition, the relationship between chromaticness and lightness was affected by changes in whiteness or blackness levels. The yellow condition consistently displayed a larger gap in chromaticness compared to lightness, while the blue condition showed the opposite trend. In conclusion, this research underscores that the differences between chromaticness and lightness in the elementary color naming method are not static. These differences vary based on the chromaticness level and the specific color being observed, indicating a complex relationship between chromaticness and lightness in human color perception.

Keywords: Elementary color naming, linear scale, uniformity, color matching, chromaticness

INTRODUCTION

Investigating human vision, particularly our perception of color, presents significant challenges. This difficulty arises because color perception is not just biologically determined at the retinal level but also processed and interpreted at the cerebral level. One widely employed method to study this intricate subject is psychophysics. It offers a robust methodology for researchers delving into the realm of visual perception.

One popular technique within this domain is 'color naming'. It provides a direct gauge of a participant's perception by asking them to assign a name or descriptor to a specific color. The elementary color naming' approach [1-3] is a two-phase task. In the initial phase, participants are asked to evaluate and assign percentages to three qualities of a color stimulus: chromaticness, whiteness, and blackness. If a participant assigns any percentage to chromaticness, it indicates that they discern a hue within the stimulus. This recognition then necessitates the second phase, where the participant is required to assign another percentage, this time based on the opponent color theory. The hues used for this judgment are red, yellow, green, and blue. Notably, according to the theory, red and green cannot be perceived or judged simultaneously and vice versa.

In a previous study [4], the elementary color naming technique was applied to examine the color appearance of color chips under various LED illuminations. Concurrently, the color constancy index was also analyzed using the polar diagram integral to the elementary color naming methodology. Although the theoretical framework and original design of the polar diagram, as employed in the elementary color naming method, proposes linearity from 0 to 100 for each hue axis, no research to date has authenticated the linearity between lightness and chromaticness within this method. A specific query arises: does the interval between chromaticness values of 10 to 20 mirror the distance between lightness values of 10 to 20?

The primary objective of this study is to validate whether the relationships between chromaticness and lightness (represented as blackness and whiteness) maintain consistent uniformity relative to one another, especially when juxtaposed against a uniformly established color space like CIEL*a*b*

METHODOLOGY

In this experiment, five participants engaged in a color-matching task, using a given color sample as a reference shown in Table 1.and choosing the closest matching color from the Munsell hue book to match the color in their imagination corresponding to the reference. Participants were given the flexibility to interpolate if they believed the best match was situated between two samples. This procedure was reiterated five times for each participant to ensure thoroughness.

All experimental conditions maintained a consistent step interval of 20 percent. The levels of lightness tested were 20, 40, 60, and 80 percent for whiteness, with a corresponding inverse range for blackness. Chromaticness was varied at intervals of 10, 30, 50, and 70 percent. Within these chromaticness tests, two distinct scenarios were established: the first with a fixed whiteness at 10 percent, adjusting blackness levels accordingly, and the second with a constant blackness at 10 percent, varying the levels of whiteness. Notably, the chromaticness trials also involved testing four primary colors at their peak intensities: 100 percent red, yellow, green, and blue as shown in Table 1.

To derive objective data on the participants' selections, the chosen samples underwent measurement using a Konica Minolta FD-7 instrument to ascertain their CIE L*a*b* values. This data enabled the determination of the 'Euclidean distance' across each color axis. Specifically, the 'Lightness Distance' (LD) was computed based on the difference between the L* values of sequential lightness samples, as outlined in (Eq. 1). In a similar vein, the 'Chromaticness Distance' (CD) emanated from the variances between the a*b* values of back-to-back chromaticness samples, as referenced in (Eq. 2). The culmination of this analysis was the derivation of a ratio, captured in (Eq. 3), where the chromaticness distance was divided by the lightness distance.

$$\text{Lightness distance} = \sqrt{(\mathrm{L}_1 - \mathrm{L}_2)^2} \tag{1}$$

$$\text{Chromaticness distance} = \sqrt{(\mathrm{a}_1 - \mathrm{a}_2)^2 + (\mathrm{b}_1 - \mathrm{b}_2)^2} \tag{2}$$

$$\text{Ratio} = \frac{\text{Chromaticness distance}}{\text{Lightness distance}} \tag{3}$$

Table 1 The naming condition of the preliminary experiment

Lightness		Color condition: Red 100%, Yellow 100%, Green 100 %, and Blue 100%					
		Fixed whiteness			Fixed blackness		
Wh%	Bl%	Chr%	Wh%	Bl%	Chr%	Wh%	Bl%
20	80	10	10	80	70	20	10
40	60	30	10	60	50	40	10
60	80	50	10	40	30	60	10
80	20	70	10	20	10	80	10

RESULT AND DISCUSSION

Results for the ratio calculations are presented in Figures 1 through 4, each corresponding to one of the primary colors: red, yellow, green, and blue. In these figures, the x-axis (abscissa) represents chromaticness, while the y-axis (ordinate) illustrates the ratio determined from Equation 3.

Observing Figure 1, which averages the results of five subjects for the unique red condition, specific trends emerge. Under the fixed black condition, the ratio exceeded what one would expect when chromaticness distance and lightness distance are equivalent, given that both axes have the same interval distance. In such a scenario, this ratio would ideally be 1. However, as chromaticness values expanded along the x-axis, the ratio under the fixed black condition began to decrease. This trend contrasts with the fixed white scenario specific to the red condition. Here, the ratio started at values less than 1 and subsequently rose as chromaticness increased. This behavior suggests that the variance in the ratio between chromaticness and lightness is contingent upon changes in either whiteness or blackness.

In Figures 2 and 3, results are presented for the unique yellow and green conditions, respectively. The data reveals that, under the fixed black condition, the ratio remains constant as chromaticness varies. However, under the fixed white condition, the ratio behaves similarly to that of the red condition. In contrast, the unique blue condition, depicted in Figure 4, mirrors the red condition but exhibits a more subtle slope change in the ratio as chromaticness fluctuates. Notably, the ratio for the yellow condition consistently surpasses 1, indicating that the chromaticness distance is greater than the lightness distance. Inversely, the blue condition's ratio is predominantly below 1.

The findings by Xie and Fairchild [5] postulated luminance and chromaticity as independent scales. However, our current results suggest a nuanced relationship: the scales of chromaticness and lightness are not isolated from one another but exhibit interconnected behaviors influenced by both the chromaticness value and the distinct color being observed.

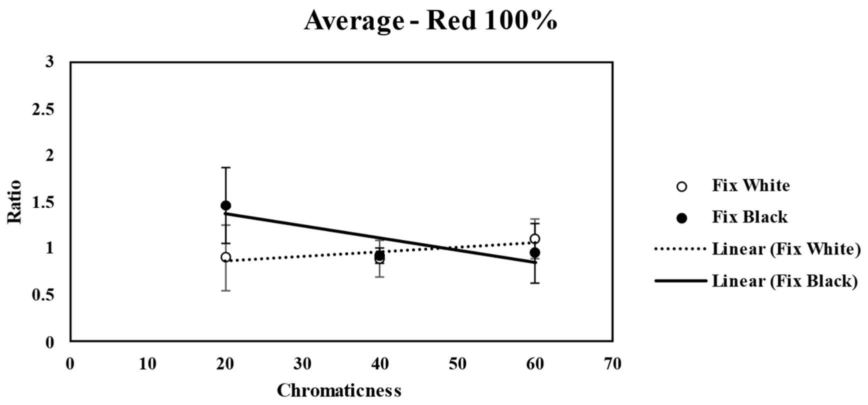

Figure 1 The relation of chromaticness and the weight ratio of red at 100 %.

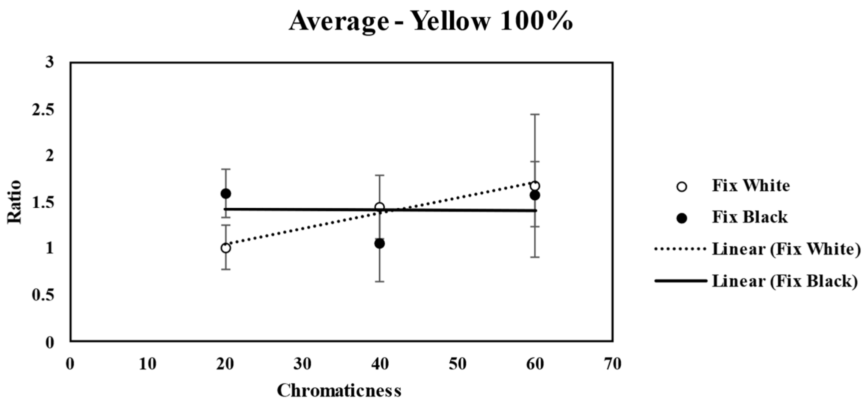

Figure 2 The relation of chromaticness and the weight ratio of yellow at 100 %.

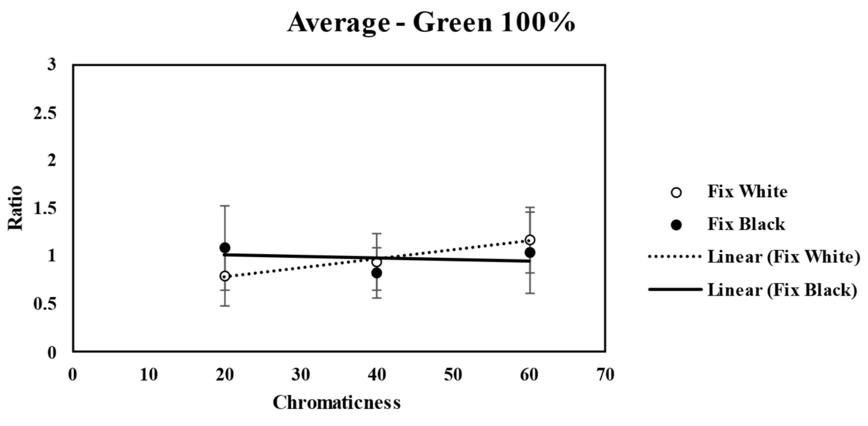

Figure 3 The relation of chromaticness and the weight ratio of green at 100 %.

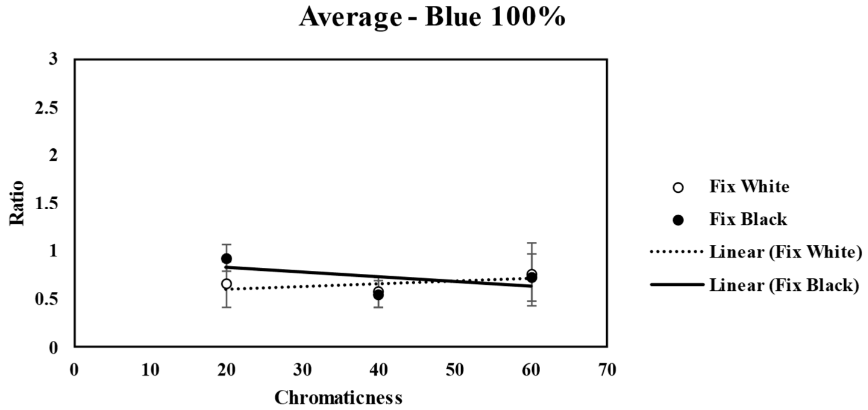

Figure 4 The relation of chromaticness and the weight ratio of blue at 100 %.

CONCLUSION

The results indicate that each unique color condition possesses distinct characteristics concerning the distance differences between chromaticness and lightness, as reflected by the gradual changes in their ratios. For most conditions under fixed black, the results remain consistent regardless of changes in chromaticness. However, exceptions arise in the red and green conditions, with the latter nearly maintaining a ratio equal to 1 throughout the changes in chromaticness. Additionally, the findings underscore that, in the elementary color naming method on the polar diagram, chromaticness and lightness are interdependent, with the difference in ratio being influenced by both chromaticness value and the specific color in focus.

ACKNOWLEDGEMENT

This research was funded by the JSPS Core-to-Core Program (grant number: JPJSCCB20220006). I am grateful to Professor Yasuki Yamauchi, who inspired this research with his questions, and to all of my participants for their vital contributions.

REFERENCES

1. Phuangsuwan, C., & Ikeda, M. (2017). Chromatic adaptation to illumination investigated with adapting and adapted color. *Color Research & Application*, *42*(5), 571-579.
2. Ikeda, M., & Phuangsuwan, C. (2019). Strong effect of the simultaneous color contrast in an afterimage. *Color Research & Application*, *44*(1), 50-53.
3. Ikeda, M., & Phuangsuwan, C. (2020). The effect of tissue paper on the color appearance of colored papers. *JOSA A*, *37*(4), A114-A121.
4. Chitapanya, P., Phuangsuwan, C., & Ikeda, M. (2022). Color appearance of color chips under light-emitting diode lamps. *Color Research & Application*, *47*(3), 585-604.
5. Xie, H., & Fairchild, M. D. (2023). Representing color as multiple independent scales: brightness versus saturation. *JOSA A*, *40*(3), 452-461.

QUANTIFYING THE HUE COMPONENTS OF FA AND BLUE USING THE ELEMENTARY COLOR NAMING METHOD

C. Phuangsuwan[1]*, M. Ikeda[1], K. Likitpunyawat[2], Y. Mizokami[3], and R. Tokunaga[4]

[1]*Color Research Center, Rajamangala University of Technology Thanyaburi, Thailand*
[2]*Faculty of Mass Communication Technology, Department of Printing Technology and Mass Communication, RMUTT, Thailand*
[3]*Graduate School of Science and Engineering, Department of Imaging Sciences, Chiba University, Japan*
[4]*Graduate school of Global and Transdisciplinary Studies College of Liberal Arts and Sciences, Chiba University, Japan*

*Corresponding author: Chanprapha Phuangsuwan, phuangsuwan@rmutt.ac.th

ABSTRACT

The 12 basic color terms (BCTs) from Thai speakers were proposed by Panitanang et al in 2022. It is composed of; Red, Green, Yellow, Orange, Brown, Pink, Purple, Blue, Gray, White, Black, and Fa. It is still unknown how Thai speakers distinguish between Blue and Fa using the category color naming approach. We selected the Munsell color chips at the border of Fa, and we got 50 color chips. The illumination in the booth was CCT of 5900 K and an illuminance of 2500 lx. The observer's task was to judge the color appearance of each color chip presented one by one to the observer using the elementary color naming method. The restriction of the elementary color naming method is that colors of opponent hues will not be named together, such as red vs. green or yellow vs. blue. Another judgment was to name the color term using the 12 BCTs proposed by Panitanang. The results at 50% consent for Fa were chromaticness = 30%, whiteness = 60%, and blackness =10%, while blue was chromaticness = 54%, whiteness = 17%, and blackness = 29%. The chromaticness of Fa was lower than Blue with a ratio of 1.8; for whiteness was higher than Blue at 0.28, and for blackness was lower than blue at 2.9. About the color component between Fa and Blue, there were two hue components, which were blue and green. Furthermore, we can see that Fa had a larger maximum portion of green than Blue.

Keywords: Fa, Blue, Elementary color naming method, Basic color terms, Munsell color chips

INTRODUCTION

The well-known basic color terms were proposed by Berlin and Kay (B&K) in 1969. A basic color term (BCT) is a color word that is relevant to a spacious class of objects, is monolexemic, and is reliably used by most native speakers. The surveying of B&K was conducted in 7 stages, and it was found that 11 BCTs were used the same in many languages: I stage found white and black, II stage found red, III and IV found green and yellow, blue found in stage V, brown found in stage VI, and pink, purple, orange, and gray found in stage VII.[1)] Later on, they extended to the World Color Survey (WCS), which included the results from many researchers using 330 color chips from the Munsell color system.[2)] In 2022, Panitanang et al. proposed 12 BCTs for Thai speakers: red, yellow, green, blue, pink, orange, brown, purple, white, grey, black, and fa.[3)] Fa means (blue sky). Similar to mizu (watercolor) found in Japanese speakers[4)] and goluboj (light blue) found in Russian speakers.[5)] In Thailand fa and blue is different color name and meaning. Blue is called nam-ngoen in Thai language and the meaning is silver liquid. Fa means blue sky or light blue. It is clearly seen the difference in color appearance and color name used in fa and blue. It would be useful to know how Thai people make the decision of using fa and blue color. In this paper, we emphasized the difference between fa and blue. The elementary color naming method was used to quantify the hue components of fa and blue. The result will be very important for communicating about color among the graphic art and printer in printing industry.

METHODOLOGY

We selected the Munsell color chips at the border of Fa which is shown in Fig. 1, and we got 50 color chips. The color chips were sized 2 × 2 cm and they were mounted on gray cardboard of about N5 and a cardboard size of 7 × 7 cm. The experiment was conducted in a booth that was 150 cm wide, 180 cm high, and 60 cm deep as shown in Fig. 2 (a). Fluorescent lamps were used to illuminate the booth, with a CCT of 5900 K and an illuminance of 2500 lx. The observer's task was to judge the color appearance of color chip using the elementary color naming method, which consisted of chromaticness, whiteness, and blackness totally 100%, then the observer had to judge the apparent hue from red, yellow, green, and blue, again totally 100%. The restriction of the elementary color naming method is that colors of opponent hues will not be named together, such as red vs. green or yellow vs. blue. Another judgment was to name the color term using the 12 BCTs; red, yellow, green, blue, pink, orange, brown, purple, white, grey, black, and fa. The distance between observer to the color chip was about 70 cm giving visual angle of color chip at 1.63° ×1.63° as you can see in Fig. 2 (b).

There were 30 observers; females (18) and males (12) participated in the experiment. Their ages were 21–45 years old. All observers passed the color defect check using the Ishihara test.

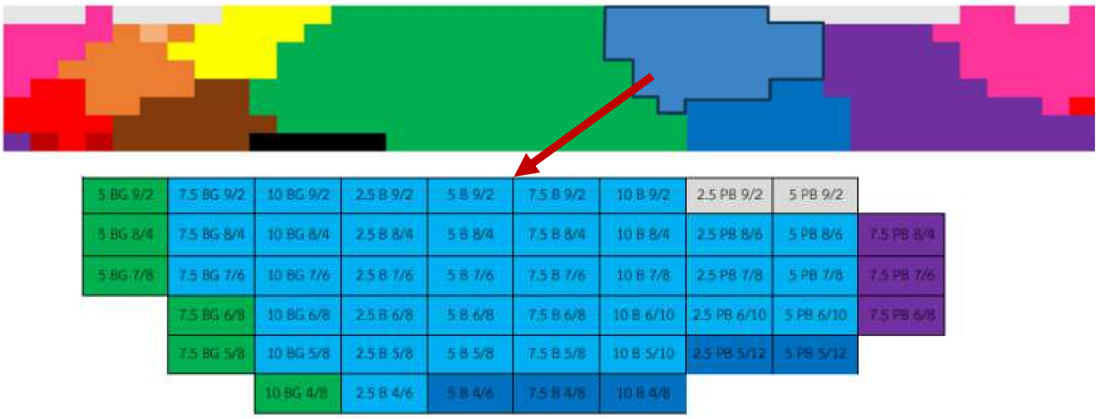

Figure 1. The color name pattern obtained from Thai speakers showing in 330 color chips of WCS from Panitanang et al.[3)] The black line on the picture indicated the border of fa color name.

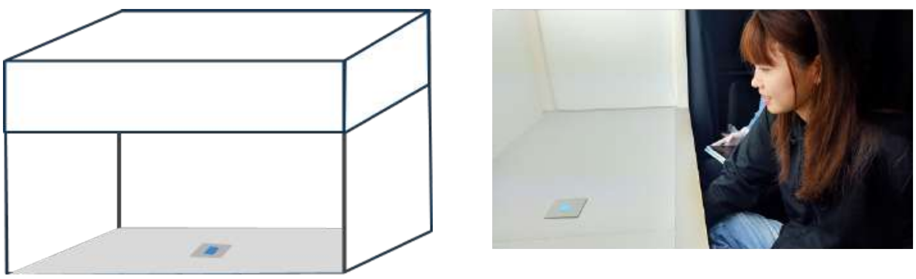

(a) (b)

Figure 2. (a) Experimental booth

(b) The observer assessed the color component of the color chip.

RESULT AND DISCUSSION

Result of 12BCTs

Firstly, the result of color names from 12 BCTs is shown in Fig. 3 in percentage of frequency. The colored bar graphs represent the color name. Our results showed that six color names—green, fa, blue, purple, grey, and white—were used in 50 color chips picked up from the border of the fa and fa areas in the WCS patterns, as shown in Fig 1. Here we emphasized the results of fa and blue; henceforth, from Fig. 4, we would draw only fa and blue. Figure 4 (a) shows the frequency of fa and blue from all color chips. To see clearly the 50% of frequency of responses (N=90) was shown in Fig. 4 (b) and found that 23 color chips were called fa, and 6 color chips were called blue. By looking at the Munsell color notation it was found that at 50% of frequency of response of fa appeared at 7.5BG, 10BG, 2.5B, 5B, 10B, 7.5B, 10B, 2.5PB, and 5PB. In the case of blue showed at the same hue 5B, 7.5B, 10B, 2.5PB, and 5PB but the difference was at value (lightness) of blue was mostly lower than fa. Furthermore, in chroma (saturation) blue showed highest at 12 but fa showed highest at 10.

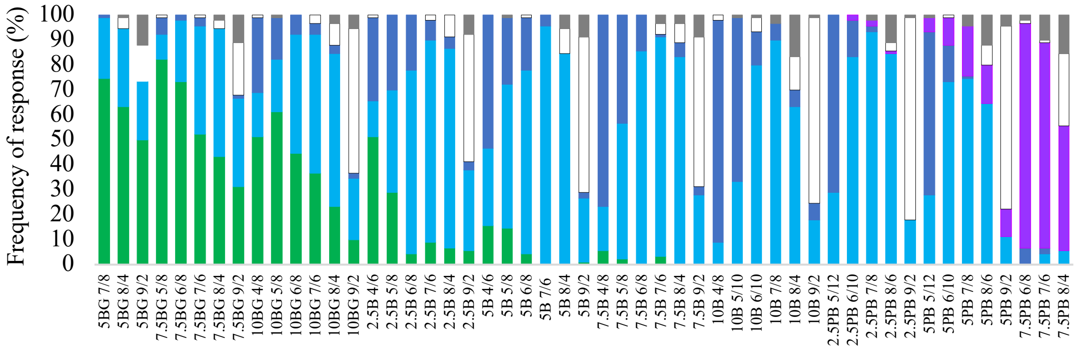

Figure 3. The color name from 12BCTs.

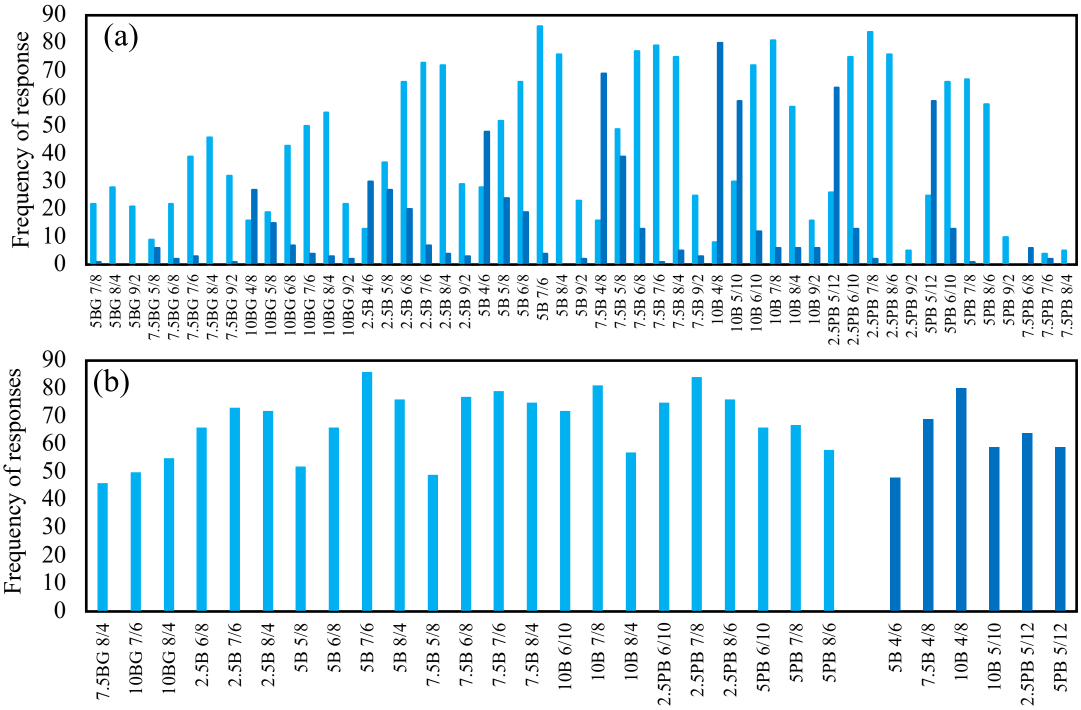

Figure 4. (a) The frequency of response for fa and blue.
(b) The frequency of response for fa and blue at 50% (from 45 to 90).

Result of elementary color naming

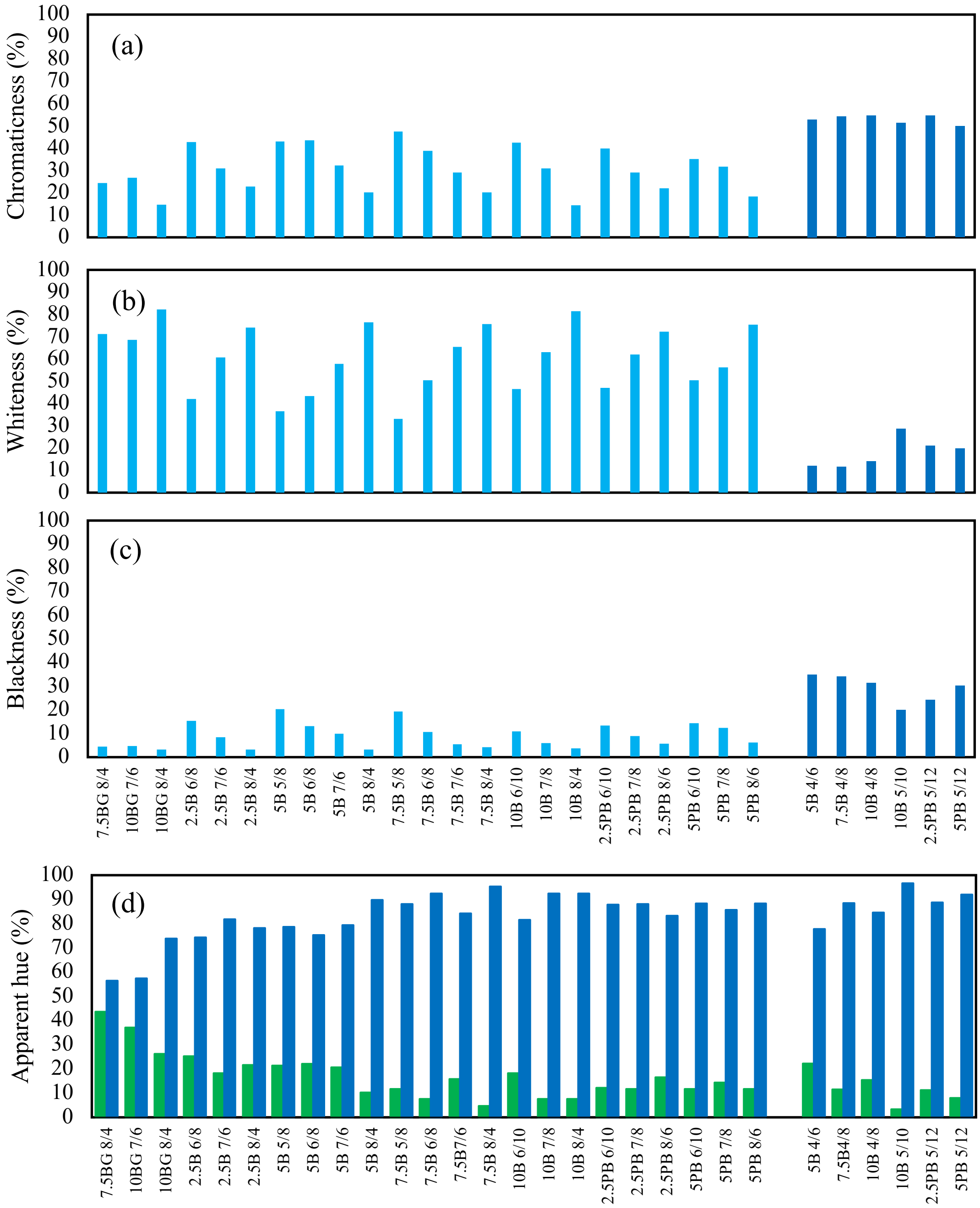

Figure 5. The elementary color naming results of fa and blue at the frequency of reaponse 50%; (a) chromaticness, (b) whiteness, (c) blackness, and (d) apparent hues. The apparent hue from 7.5BG 8/4 to 5PB 8/6 represents fa and on the most right 5B 4/6 to 5PB 5/12 represents blue.

The results of the elementary color naming of fa and blue at a frequency of 50% response are shown in Fig. 5. The chromaticity of fa ranged from 14% to 47%, and blue ranged from 50% to 55%. It seems that blue showed higher chromaticness than fa. In the case of whitness, it showed 33% to 82% at fa, and for blue, it showed quite low whiteness, from 12% to 29%. The blue color showed a high range of blackness, from 20% to 35%, while fa showed quite low blackness, from 3% to 20% at its maximum. Interestingly, there were the same apparent hues of green and blue between the fa and blue color names. The apparent hue "blue" ranged from 56% to 95% for fa and 78% to 97% for blue color names. For the apparent hue, "green" ranged from 5% to 44% in fa and 3% to 22% in blue. It seems that the proportion of apparent green and blue is slightly different between FA and blue. By thinking of apparent hues in fa and blue, it might be that when the proportion of apparent "green" is higher than 44%, the observer might call that color chip by its green name.

The average method was applied to the results of elementary color naming to see the overall characteristics of fa and blue. The mean chromaticness of fa was 31% and blue was 53%; blue appeared more vivid than fa color. Contrary to the means of whiteness, fa was 61% and blue was 18%. The fa color appeared clearly brighter than blue. The blackness of the fa color showed at 8% and blue at 29%. The means of apparent hue, fa color, were hue green 18% and hue blue 82%. In the case of blue, the means of apparent hue showed hue green at 12% and hue blue at 88%.

Therefore, when the color chip appeared "light blue," the observer used fa to name it, but when the color chip appeared "dark blue," the color name blue was used.

The limitation of the experiment was that the number of observers was a bit small. And the elementary color naming method needs to be trained, but it was still giving the criteria among observers quite large. The advantage of the elementary color naming method is that the absolute judgment is direct to the color of the chip that appears to us.

CONCLUSION

The conclusion of these results is that the hue component of fa and blue showed the same apparent hue in green and blue. It is clearly seen that whiteness of fa is much higher than blue about 3.4 times which is cause to blue be about 3.6 times more blackness than fa. The vividness of blue is higher than fa about 1.7 times than fa.

ACKNOWLEDGEMENT

We would like to thank the thirty observers who participated in the experiment with very kind patience. Also, we appreciated our colleagues in the Color Research Center, CRC; they always supported us in many things until the experiment was completed.

REFERENCES

1. Berlin, B., Kay, P. (1996). *Basic Color Terms*. Berkeley, University of California Press.
2. Kay, P., Berlin, B., Maffi, L., Merrifield, W.R., Cook, R. (2009). *The World Color Survey*. Stanford, CSLI Publications.
3. Panitanang, N., Phuangsuwan, P. and Ikeda, M. (2022). Basic color terms in Thai. *Color Res and Appl, 47*(6), 1402-1425.
4. Uchikawa K, Boynton RM. (1987). Categorical color perception of Japanese observers: comparison with that of Americans. *Vision Res. 27*(10), 1825-1833.
5. Paramei GV, Griber YA, Mylonas D. (2018). An online color naming experiment in Russian using Munsell color samples. *Color Res Appl. 43*(3), 358-374.

INFLUENCE OF SKIN COLOR CHANGE ON FACIAL EXPRESSION RECOGNITION AMONG ASIAN OBSERVERS

Yuanyuan He[1]*, Ryo Michishita[1], Hiromi Y. Sato[2] and Yoko Mizokami[2]

[1]Graduate School of Science and Engineering, Chiba University, Japan.
[2]Department of Imaging Sciences, Graduate School of Engineering, Chiba University, Japan.

**Corresponding author: Yuanyuan He, heyuanyuan@chiba-u.jp*

ABSTRACT

The universality of facial expression recognition has been a subject of debate. Previous research has indicated that skin color can influence the recognition of facial expressions, with reddish skin tones promoting the recognition of angry expressions. However, it remains unclear whether this effect holds across different ethnic groups and how it influences facial expression recognition. In this study, we aimed to investigate the impact of skin color changes on facial expression recognition among Japanese, Thai, and Chinese observers. We achieved this by simulating variations in hemoglobin levels to modulate skin color. We used morphing software to create average male faces displaying neutral, angry, and happy facial expressions to conduct our experiments. These expressions were then morphed to different intensity levels, ranging from neutral to fully angry (or happy). Specifically, we defined the average neutral face as having an angry (or happy) rate of 0%, while the average angry face had an angry (or happy) rate of 100%. We generated seven angry (or happy) rates, including 18%, 30%, 42%, 54%, 66%, 78%, and 90%. We simulated two skin color conditions for each facial expression: hemoglobin decrease (H-) and hemoglobin increase (H+). Therefore, we used a total of 28 stimuli, which included male faces, two skin color types, two expression conditions, and seven expression rate levels. During the experiment, one stimulus image was randomly presented to the observers in various expression conditions. The observers answered whether the presented face appeared angry (or happy) or not angry (not happy). Our findings revealed that angry facial expressions were recognized at a lower threshold in high hemoglobin skin color conditions than in low hemoglobin skin color conditions. This indicates that skin color affects the perception of angry facial expressions, with reddish skin tones enhancing sensitivity to anger. Asian observers generally exhibited a similar trend in their responses, although the strength of the effect varied slightly in some conditions. This suggests that while the impact of skin color on facial expression recognition may be consistent across these ethnic groups, the extent of the effect may differ. These results emphasize the importance of considering the influence of skin color on facial expression recognition, particularly in cross-cultural communication contexts.

Keywords: Skin color, Facial expression recognition, Perception

INTRODUCTION

Facial color is known to play a role in enhancing the perception of emotional expressions. Previous research has suggested that reddish facial tones can amplify the perception of anger [1]. Additionally, studies conducted by Kato et al. [2] have demonstrated that modifications in natural facial color resulting from variations in hemoglobin and melanin levels can influence the recognition of facial expressions. However, it remains unclear whether individuals from diverse cultural backgrounds are affected by these factors to a similar extent. In this study, we aimed to investigate the impact of alterations in skin color on facial expression recognition, specifically among Japanese, Thai, and Chinese observers. These alterations were achieved by simulating changes in hemoglobin levels to modulate skin color.

METHODOLOGY

Experimental environment

The experiment was conducted using an LCD monitor in a dark room. The observers were positioned at a fixed viewing distance of 60 cm using a chinrest. Observer responses were recorded using a response keyboard.

Observers

The observer group consisted of seven Japanese, 19 Thai, and four Chinese participants, all of whom had normal or corrected-to-normal vision and normal color vision. Among the Thai observers, nine took part in all conditions, five were involved only in the happy condition, and another five were exclusively in the angry condition. The experiment strictly adhered to the principles of the Declaration of Helsinki (Code of Ethics of the World Medical Association) and followed research ethics standards at Chiba University. Informed consent was obtained from all the observers. A few observers did not exhibit clear boundaries in their perceived changes in expression. For instance, one observer consistently identified all expression stimuli as happy, even when the actual happy rate was only 20%. Consequently, the analysis relied on data from seven observers in the angry condition and six observers in the happy condition for the Japanese group, 11 observers in the angry condition and 12 observers in the happy condition for the Thai group.

Stimulus

The stimulus in the experiment was a face image sized at 216 × 272 pixels, which subtended a visual angle of 17.0 × 13.0 degrees. These images were presented at the center of a neutral gray background corresponding to Munsell N5. Two facial expressions, angry and happy, were used in the study, and the source images were obtained from the ATR Facial Expression Image Database (DB99) (ATR-Promotions, Kyoto). To create the stimuli, we utilized morphing software (FantaMorph Deluxe5, Abrosoft) to generate average male faces based on six male Japanese images for each angry and happy expression. An example of a morph continuum featuring two different facial color conditions employed in this research is illustrated in Figure 1.

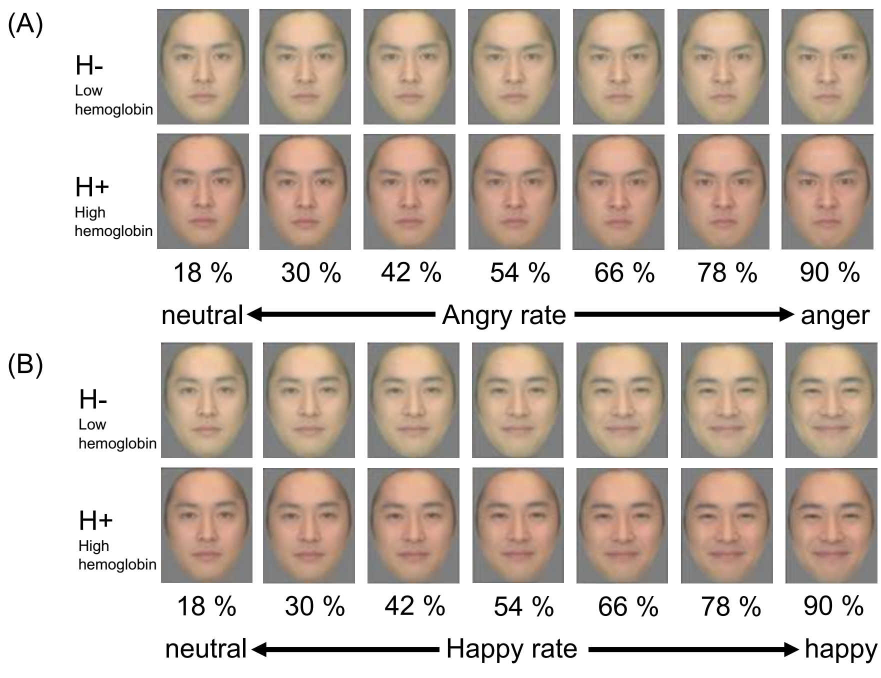

Figure 1. Morph continua illustrating variations in skin color. (A) Angry condition, (B) Happy condition. The top row represents the low hemoglobin skin color type, and the bottom row represents the high hemoglobin skin color type.

The standard skin color used in this study was calibrated to match the average under D65 lighting condition, as previously employed by Hamada et al. [3]. This calibration was based on spectral reflectance data collected from 694 Japanese women aged 20 to 78, as documented by Kikuchi et al. [4].

To create skin color conditions with varying hemoglobin and melanin concentrations, we used Monte Carlo simulation based on the absorption coefficient of the skin layer [5]. The absorption coefficient values were selected to ensure that the distance from the average color in both the positive and negative directions matched specific values: 0.1 and 1.9 for the hemoglobin absorption coefficient. In the CIELAB color space, the entire facial area's color distribution was shifted to align the average color with the hemoglobin or melanin-modulated average $L^*a^*b^*$ values, as reported by Hamada et al. [3]. This means that the color of each pixel within the facial area was adjusted by the same amount as the shift in the average color while maintaining the overall color distribution of the face. Table 1 provides details of the hemoglobin and melanin absorption coefficients and the $L^*a^*b^*$ values for each skin color condition.

Table 1: Absorption coefficient and colorimetric data of two face color conditions.

Skin color type		H-	H+
Absorption coefficient	Hemoglobin	0.1	1.9
	Melanin	1.0	1.0
	L^*	68.941	63.243
	a^*	5.477	11.626
	b^*	17.985	16.788

In the context of angry conditions, we defined the average neutral face as having an anger rate of 0%, while the average angry face had an anger rate of 100%. We employed morphing techniques to generate a continuum of expressions ranging from neutral to angry, resulting in seven distinct anger rates: 18, 30, 42, 54, 66, 78, and 90%. Similarly, we followed the same procedure for the happy condition, creating a morph sequence that transitioned from a neutral expression to a happy one under each skin color condition. In total, there were 28 stimuli, comprising one male face, two skin color types, and seven different levels of expression rates, used in the experiment.

Procedure

We employed the constant stimuli method to determine the boundary between the neutral expression and each facial expression (anger and happiness). The experimental procedure began with 30 seconds of dark adaptation, followed by 30 seconds of light adaptation to the white display and another 30 seconds to the neutral background. A fixation point was then presented for a duration of 5000 ms. Subsequently, the first facial stimulus was displayed for 1000 ms, and the fixation point reappeared. Observers were tasked with assessing the facial expression of the stimulus using a keyboard, indicating whether the face appeared "angry" ("happy") or "not angry" ("not happy") for each specific condition via forced-choice responses. The following facial stimulus was presented 1000 ms after submitting the answer. Each session exclusively featured one facial expression condition, and the fourteen stimuli within each condition were randomly presented in a single block. A session consisted of five blocks, and each observer completed three sessions, yielding 15 responses for each stimulus.

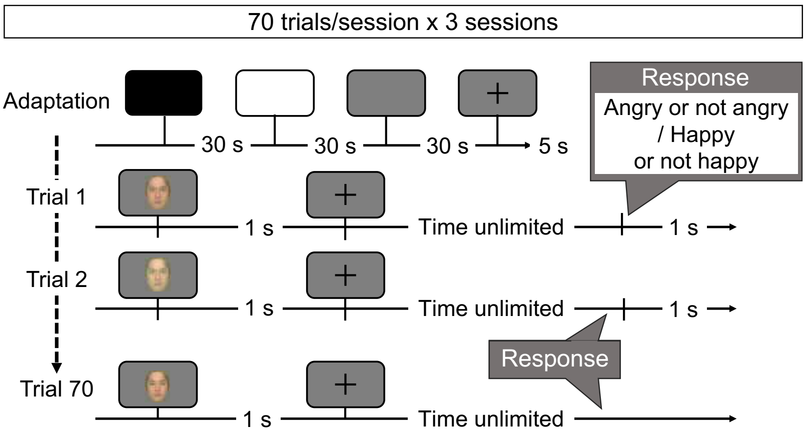

Figure 2. Experimental procedure.

RESULT AND DISCUSSION

The likelihood of an "anger" (or "happiness") response for each facial stimulus was computed for every observer. Subsequently, each observer's anger (or happiness) response rate was subjected to a psychometric function fitting procedure using Python. From the resulting psychometric function, we determined the boundary at which the probability of responding as "angry" (or "happy") reached 50%.

Figure 3 presents the average results from Japanese, Thai, and Chinese observers in the angry condition. The graph on the left displays the results of Japanese observers, while the middle and right graphs show the outcomes for Thai and Chinese observers, respectively. The horizontal axis represents the response rate to the stimuli, while the vertical axis represents the response rate of anger. The data indicates that an increased hemoglobin concentration in the skin, as opposed to decreased hemoglobin, enhances the perception of anger. This trend was consistent across all three observer groups.

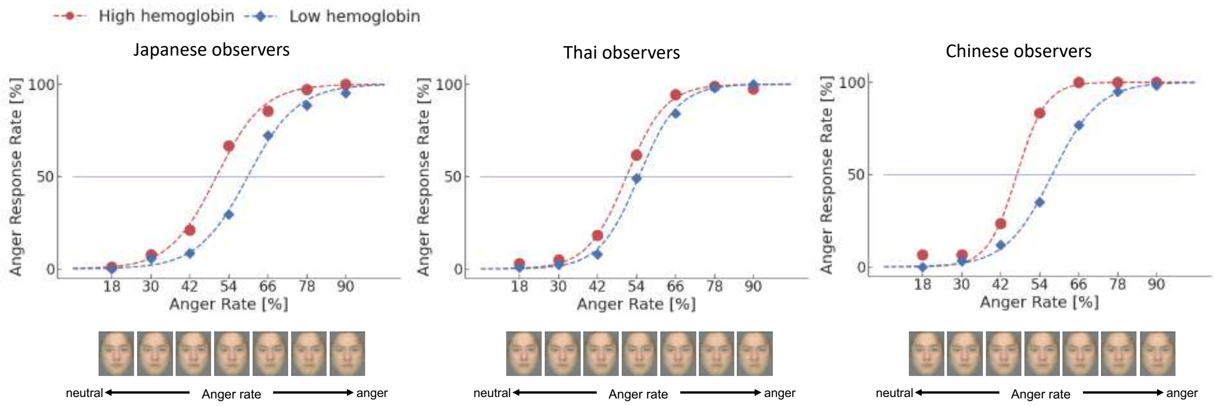

Figure 3. Psychometric function of observers and boundaries for angry expressions.

Figure 4 shows the average results of Japanese, Thai, and Chinese observers for the happy condition. The left, middle, and right graphs are the results for Japanese, Thai, and Chinese observers. The graph illustrates that the influence of skin color change on the perceived boundaries of happy expressions doesn't appear to be as pronounced. This trend was consistent among Japanese and Thai observers. However, the Chinese observer's results seem to deviate slightly, although this may be attributed to the smaller sample size in this group.

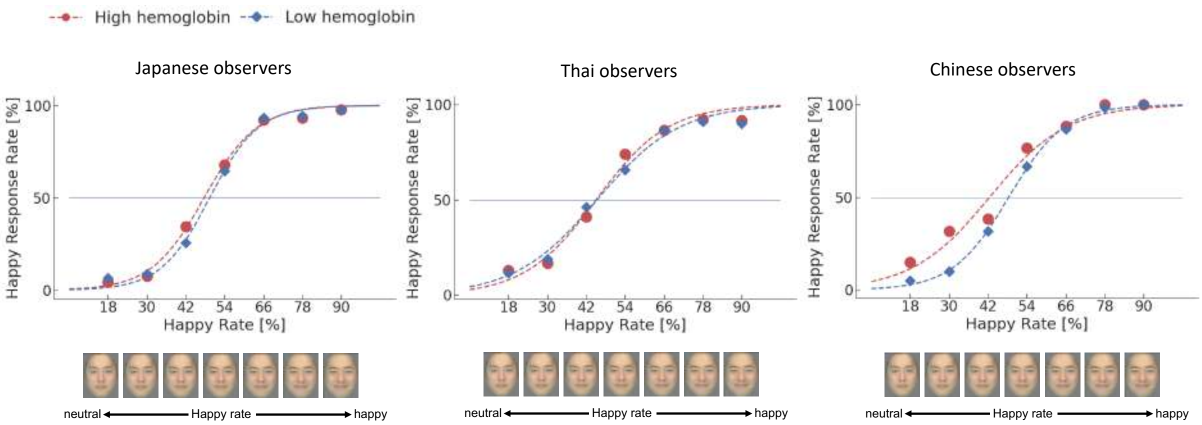

Figure 4. Psychometric function of observers and boundaries for happy expressions.

The boundaries of perceived facial expressions were measured in response to changes in facial color, specifically related to the perception of anger. The results indicated that increased hemoglobin levels, which altered skin color, enhanced the perception of anger in facial expressions. This effect was consistent across three observer groups, although the intensity of the effect varied among them. These findings align with research demonstrating enhanced anger perception with increased a^* values in facial color modulation [1].

Figure 5(a) displays the average boundary for all observers in the angry condition, with the vertical axis representing the anger rate at the boundary. Each bar represents the average boundary for each skin color condition, and the error bars indicate the standard deviation (SD). A lower boundary value indicates that, under this condition, observers judged the expression as angry when the anger rate was lower.

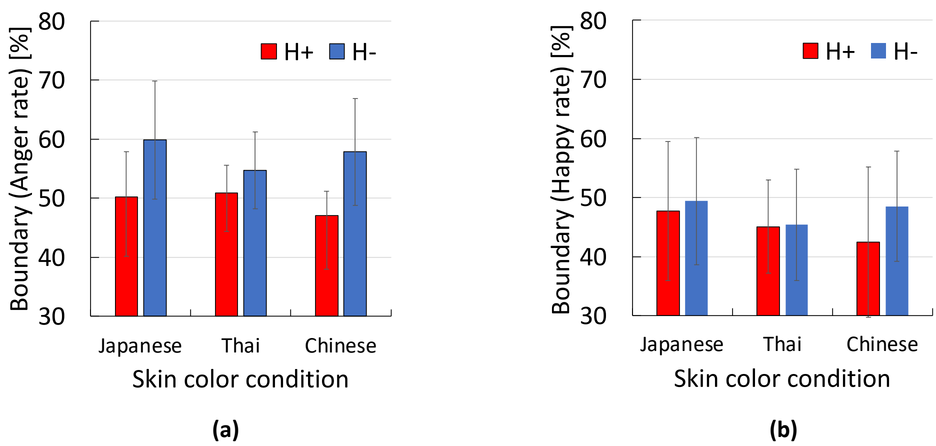

Figure 5. The boundary of anger in each skin color.
(a) Angry condition. (b) Happy condition

Figure 5(b) illustrates the average boundary for all observers in each skin color condition for the happy condition. Similar to Figure 5(a), the vertical axis represents the anger rate at the boundary, and each bar displays the average boundary for each skin color condition, with error bars denoting the SD. These visualizations provide insights into how variations in skin color influence the perception of anger and happiness in facial expressions. In the happy condition, changes in skin color appeared to have subtle effects on the perception of happiness. There could be several reasons for this observation. One possibility is that the interpretation of changes in expression intensity may vary among different cultures, especially in the context of the happy condition. Some observers may have interpreted even the lowest happy rate as indicating happiness. To further investigate this, it might be necessary to use more finely subdivided rates or explore other factors that could influence the perception of happiness across different cultural groups.

The increase in hemoglobin concentration resulted in reddish skin, which, in turn, heightened the perception of angry expressions. This finding is consistent with prior research and was further supported by our study. Interestingly, He et al. [6] demonstrated that reddish skin appears brighter than yellowish, which seems specific to Japanese observers. Observers from Thai, Korean, Chinese, and other backgrounds exhibited the opposite or inconsistent trend. Our results suggest that the Japanese may be more sensitive to perceiving skin redness as a cue for emotional expression. The results of Chinese observers demonstrated a clear trend similar to Japanese observers. However, a larger sample size of Chinese observers would be necessary for a more in-depth investigation and comparison.

CONCLUSION

We explored the influence of skin color variations on the recognition of facial expressions among Japanese, Thai, and a limited number of Chinese observers by simulating changes in hemoglobin levels to modify skin color. Our findings indicated that the perception of angry facial expressions occurred at lower thresholds in conditions with higher hemoglobin levels, resulting in reddish skin tones. This suggests that skin color plays a role in influencing the perception of angry expressions, with redder skin tones leading to a more sensitive recognition of anger. While all three observer groups generally exhibited a similar trend, the effect was more pronounced in Japanese and Chinese observers. This implies that skin color's impact on facial expression recognition may be consistent across these ethnic groups, but the degree of influence may vary. Further data collection involving participants from diverse cultural backgrounds is would be necessary. These results underscore the significance of considering the role of skin color in cross-cultural communication contexts when interpreting facial expressions.

ACKNOWLEDGEMENT

This work was supported by JSPS Core-to-Core Program (JPJSCCB20220006) and JSPS KAKENHI (JP18H04183, JP21H05805, and 23H04332).

REFERENCES

1. Nakajima, K., Minami, T., & Nakauchi, S. (2017). Interaction between facial expression and color. *Scientific reports*, *7*(1), 41019. https://doi.org/10.1038/srep41019
2. Kato, M., Sato, H., & Mizokami, Y. (2022). Effect of skin colors due to hemoglobin or melanin modulation on facial expression recognition. *Vision Research*, 196, 108048. doi: 10.1016/j.visres.2022.108048
3. Hamada, K., Mizokami, Y., Kikuchi, K., Yaguchi, H., & Aizu, Y. (2018). Discrimination threshold of skin color in skin image. *Journal of the Color Science Association of Japan*, 42(2), 50. doi:10.15048/jcsaj.42.2_50 [In Japanese].
4. Kikuchi, K., Katagiri, C., Yoshikawa, H., Mizokami, Y., & Yaguchi, H. (2016). A correction method for skin reflectance obtained with different spectrophotometers and its application: changes in the skin color of Japanese women for 25 years. *Journal of the Color Science Association of Japan*, 40(6), 195-205. doi:10.15048/jcsaj.40.6_195 [In Japanese]
5. Maeda, T., Arakawa, N., Takahashi, M., & Aizu, Y. (2010). Monte Carlo Simulation of Spectral Reflectance Using a Multilayered Skin Tissue Model. *Optical Review*, 17(3), 223-229. Retrieved from https://ci.nii.ac.jp/naid/10026357879
6. He, Y., Mikami, T., Tanaka, S., Kikuchi, K., & Mizokami, Y. (2021). Comparisons in perception of facial skin brightness, as influenced by differences in skin color: Asian observers. *Color Research & Application*, 46(4), 808-820. doi:10.1002/col.22622

Author Index

Abebe, Mekides Assefa 310
Aebischer, Cyrill 585
Ahn, Kyuhee 654
Akao, Mika 978
Akinwehinmi, Oluwakemi 920
Al-Rasheed, Abdulrahman S. 431
Amirkhanashvili, Ana 886
Angharad, Sally 758
Ariyavarapong, Airin 1022
Artioli, Gilberto 130
Asaga, Sota 705
Asakura, Suzuka S 771
Asano, Akira 835, 880
Asano, Chie Muraki 310
Asghari, Sahara Smith 946
Assawincharoenkij, Thitiphan 292, 304
Ayama, Miyoshi 914
Azuma, Yoshihiko 236
Azzahra, Laily Rahmadina 1039
Baba, Taiga 841
Baba, Yasuhito 470
Bäckström, Eva-Lena 399
Baniani, Mahshid 585
Basic, Nina 496
Bieske, Karin 112
Bini, Lorenzo 735
Bista, Rabindra 585
Blattner, Peter 431
Bogushevskaya, Victoria 360
Bonnardel, Valerie 230
Cahyono, Hadi 412
Cappitelli, Francesca 550
Caramelo Gomes, Cristina 550
Chan, David, Kw 538
Chang, Kaiping 437
Chang, Raine Marie 904
Chen, Mengyuan 818
Chen, Na 983
Chen, Yifei 722
Cheng, Qian 177
Cheng, Wen-Hsin 342
Cheung, Vien 687
Chevallier, Aurélie 360
Chida, Emi 835
Chitapanya, Phubet 1056
Choi, Gyoungsil 654, 729
Choi, Youngmi Christina 518
Cholilie, Irvan Adhin 230
Colantoni, Philippe 676
Conte, Veronica 1016
Cordero Jahr, Elisa 431
Cortes Jaramillo, Felipe 676
Damodaraswamy, Sudhakar 485
De Lucas Tron, Alfonso 638
Dedrick, Donald 443
Dethsuphar, Duantemdoung 191
Diaz-Ramos, Isolina 130
Dinet, Eric 329
Doi, Motonori 966
Duarte, Rui B 940
Dubey, Nijoo 485
Durão, Maria João 517
Emmel, Patrick 131
Eskew, Rhea T. 425
Fanka, Alongkot 946, 1022
Francesc, Xavier Solsona Tehas 920
Fu, Ming Chuan 452
Fujita, Yuno 783, 789
Galindo, Jose Luis 323
Gasparini, Katia 170
Gigilashvili, Davit 886
Gomez-Robledo, Luis 1007

Gong, Shi Min 634
Gong, Zhe 392
Gouaich, Yacine 431
Griber, Yulia A. 431, 852
Hafslund, Bente 310
Ham, Dakyeong 649
Han, Xu 354
Hanari, Takashi 973
Harada, Masayuki 544
Hardeberg, Jon Yngve 310
Hattagee, S. 946
Hattri, Nanako 807
He, Shuang 366, 795
He, Shuilan 777
He, Yuanyuan 1066
Hee, Bae Mi 747
Hemingray, Caroline 184
Henry, Phil 177
Henry, Philip 392
Hernandez-Andres, Javier 323, 1007
Hiramatsu, Chihiro 841, 847
Hongrattanavichit, Intatch 190
Horiuchi, Takahiko 1034, 1039, 1045
Hsu, Chi-Ying 557, 624
Huang, Qian 385
Huang, Yiming 127
Huertas, Rafael 323, 1007
Hutchings, John 437
Ichihara, Yasuyo G. 532
Ikeda, Mitsuo 224, 1056
Ikonen, Erkki 611
Imaizumi, Shoko 1039
Ingoldsby, Joseph E. 199
Inoshita, Taiju 752, 771
Ishii, Mochine 841
Ishikawa, Tomoharu 292, 304
Ishikawa, Yoshiki 966
Ito, Tomoe 783, 789
Iwasaki, Takuma 563
Iwase, Kota 1034
Jackson, Kel 518
Jarernros, Jarunee 995
Jimenez Molina, María 1007
Jonai, Riho 893
Kaew-On, Nawarat 404, 664, 959
Kaewkong, Thanaporn 404, 664, 959
Kamegawa, Shohei 218
Kamolrat, Kannikar 298
Kanthong, Kasidet 1023
Katemake, Pichayada 190, 191, 329, 425, 939, 946, 1022
Kato, Toshikazu 807
Kawamata, Takumi 292
Kawasumi, Mikiko 973, 978, 1011
Kawasumi, Natsuko 1011
Khampaeng , Sureeporn 939
Kim, Se Jin 694
Kimachi, Akira 966
Kitadani, Yukie 870
Kitamura, Kaoruko 864
Kobayashi, Maiko 983
Koliousis, Alexandros 425
Kuo, Monica 764
Kuo, Ya-Ping 764
Kurniati, Yuni 230
Kwon, Minseo 694
Ladson, Jack A 118
Lai, Peihua 184, 758
Lamarra, Julie K 348
Lan, Cuiqin 795
Lategano, Charles 118
Lee, Gyeonghwa 687
Lee, Soojin 392, 897
Lee, Wen-Yuan 557, 624, 630, 634, 1022
Leewatchararoongjaroen, Kasama 729
Lhi, Wona 729
Li, Anni 385

Li, Hesong 587
Li, Liting 354, 366
Li, Molin 464
Li, Qinyuan 437
Li, Siqi 280
Li, Yuemin 127
Liang, Jiaxin 904
Likitpunyawat, Kusuma 1061
Lin, Jinyi 578
Lingyan, Wang 593
Liu, He 953
Liu, Xiaoxuan 601
Liu, Yue 280, 317
Lopez-Jabalera, Maria De Los Angeles 1007
Lorey, Thierry 360
Lu, Yi-Chan 630
Luo, Ming Ronnier 137, 274, 437, 458, 464, 491, 578, 601, 824
Ma, Shining 280, 317
Machado, Pedro 323
Maehara, Takashi 292
Maham, Kinza 611
Makino, Kanoko 864
Manteith, James 431
Mao, Ningtao 354
Mao, Xue 927
Mardhiyyah, Yunita Siti 230, 236
Martin-Sevilla, Arturo 1007
Martinez-Domingo, Miguel Angel 1007
Martinez-Navarro, Carlos 1007
Masson, Gilles 360
Matsufuji, Momoka 1034
Meenorn, Methawee 972
Meethum, Jinnawat 946
Meeusah, Natchaphak 206, 212
Mefoh, Philip 431
Mepean, Janejira 224
Michishita, Ryo 1066
Miura, Yukie 801
Miyakawa, Hiromitsu 978
Mizokami, Yoko 218, 563, 1051, 1061, 1066
Moreira Da Silva, Ana M S 267
Moreira Da Silva, Fernando J C 286
Moriyama, Tsuyoshi 876
Motoyoshi, Isamu 218, 607
Mukaiguchi, Takeshi 544
Murakami, Shiho 304
Muraya, Tsukasa 532, 741, 752, 771
Murdoch, Michael 260
Muselet, Damien 676
Mylonas, Dimitris 425
Nagaya, Shoma 973, 978
Nakamura, Akihiro 978
Nakamura, Koyo 983
Nakamura, Shinji 618
Nakayama, Rei 1051
Ndeye Meissa Koura Sow, Sow 847
Ng, Woon Lam 538
Ngai, Carey 538
Ngamukot, Passapol 946
Nilmanee, Somporn 716
Nilsson, Anders 502
Nishi, Shogo 671, 966
Noguchi, Hidetoshi 858
Noppakundilograt, Supaporn 946, 1022
Noury, Larissa 248
Noviasri, Rizky 230
Nugraheni, Roostikasari 230
O'Connor, Natalie A 136
Oba, Toshinori 1045
Odetti, Jimena Vanina 431
Oe, Yuki 801, 864
Ogura, Genki 835
Ohtera, Ryo 671
Okajima, Katsunori 512, 893
Okamura, Akane 870
Okuda, Akito 989

Okuda, Shino 304, 512, 893
Onai, Miku 801
Ono, Tomoka 544
Osumi, Masayuki 418
Ou, Li-Chen 342
Palomo, Héctor A 741
Pan, Qianqian 184
Paramei, Galina 852
Park, Hyewon 643, 649, 681, 747
Park, Yungkyung 574, 659
Pedro, Arnau Del Amo 920
Peng, Ching-Wei 452
Phongsuphap, Sukanya 298
Phuangsuwan, Chanprapha 224, 1011, 1056, 1061
Pinheiro, Ana Paula 940
Plerksophon, Ektawat 329
Politi, Gloria 431
Pouzalgues, Nathalie 360
Premier, Alessandro 242
Puenpa, Suwat 1030
Qingmei, Huang 593
Queiroz, Francisco 177, 392
Rahmat, Anni 230
Rattanakasamsuk, Kitirochna 830, 971, 1030
Rennie, Julian 242
Rezazadeh, Yasaman 611
Rider, Andy 274
Rizzi, Alessandro 112, 412
Rodski, Stan 897
Rong, Liang 593
Rossi, Maurizio 254
Safdar, Muhammad 131
Sakamoto, Takashi 807
Saksirikosol, Chanida 820, 847, 971
Sakurai, Masato 375
Samoilova, Tatiana 431
Sari, Lisa Risfana 230
Sarti, Beatrice 412
Sato, Hiromi 218, 563, 1051, 1066
Schierz, Christoph 496
Schindler, Verena M. 253
Serra, Juan 260
Seymour, John 502
Shamey, Renzo 143, 699
Shamohammadi, Mina 847
Sharma, Shreeniwas 735
Shen, Zhang 593
Shi, Keyu 274
Shi, Xinye 137
Shibata, Wakana 335
Shinoda, Hiroyuki 710, 953
Shrader, Stephen 164
Shukla, Anshika 643
Siangyai, Rattachai 190
Singnoo, Jakkarin 1023
Sivova, Tatiana 431
Song, Jiajia 795
Song, Weitao 280, 317
Souza, Pedro Felipe P 380
Srisuro, Ploy 995, 1001
Stockman, Andrew 274, 425
Stutters, Jonathan 425
Sueeprasan, Suchitra 569, 933
Sun, Lijia 317
Sun, Pei 366
Sun, Vincent 452
Sun, Wenjun 587
Sunaga, Shoji 532, 741, 752, 771
Suzuki, Hirotaka 870
Taguchi, Satoko 512
Takahashi, Hiroshi 705
Takahashi, Naoki 807
Takasu, Aoi 783, 789
Takeda, Ena 375
Takikawa, Mizuki 783
Tanaka, Midori 1034, 1039, 1045

Tandukar, Jyoti 735
Tangkijviwat, Uravis 206, 972
Taniguchi, Yunoka 532
Terashima, Toshiharu 544
Tokunaga, Rumi 335, 1061
Tominaga, Shoji 671
Torsabsinchai, Kamonthip 206, 212
Tremeau, Alain 329, 676
Trentini, Andrea 112
Tse, Nicole 939
Tsuchida, Kento 705
Tsujimura, Sei-Ichi 335, 783, 789
Tsukada, Toshihiko 978
Tsunashima, Nobuhiro 876
Ume Farwa, Syeda 681
Valero, Eva M 323, 1007
Villa, Federica 412
Wang, Haoyu 811
Wang, Liqing 601
Wang, Wanting 476, 904
Wang, Yongtian 280, 317
Watanabe, Katsumi 983
Wei, Robert Y.C. 764
Westland, Stephen 177, 184, 191, 758, 818, 897
Wu, Jiaying 143
Xia, Guobin 177, 354, 392
Xiang, Changying 476, 904
Xiao, Kaida 354, 587, 722, 811
Xiong, Nian 699
Xu, Haisong 106, 127
Xu, Kaiyan 476
Xu, Nanlin 824
Xu, Peng 106
Yamada, Anna 841
Yamada, Yuko 164
Yamashita, Ryoma 973, 978
Yamauchi, Yasuki 989
Yamprasai, Porntip 972
Yanagida, Yoshiko 292
Yang, Jie 177
Yang, Junghee 643
Yang, Minhang 127
Yang, Yang 587
Yang, Yidie 983
Ye, Yuxin 437
Yeo, Jiwon 659
Yoshimura, Kohji 164
Yoshizawa, Nozomu 801, 858, 864, 870
Yu, Jinsang 681
Yu, Luwen 177, 354
Yue, Longxin 366
Zapata, Lucia 323
Zhang, Yan 607
Zhang, Yuhang 710
Zhou, Fanyi 587
Zhou, Sicong 587
Zhu, Yuechen 137, 458, 601, 824
Ziyuan, Wei 593

Appendix
CADE Award research paper

THE *"COLOR FEVER"* CHROMA SURVEY 1973

Clino Trini Castelli[1]*
*Castelli Design; memo@castellidesign.it

ABSTRACT

Fifty years have passed since the author, observing a series of developments related to the evolution of color culture in the early 1970s, realized that major historical events often coincided with epochal changes capable of giving rise to new global color languages. In those years the selection of a color was based not so much on the subjective choice of hues, as on the objective vivacity of the color's saturation (chroma). Each color was thus selected at its maximum intensity, further accentuated by the monochromatic scheme inherited from the historical trend of the 1960s. That decade had been characterized by increasingly saturated primary colors, which precisely in 1973 led to a chromatic outburst whose maximum peak was reached in a sort of "color fever". As we know, a fever is not itself an illness, but a symptom that reveals the presence of a pathology. In this case the peak of saturation, already detected in the field in 1973 and then measured and depicted in 1979 with the tracing of a new diagram: the *"Color Fever" Chroma Survey* (Figure 1). The peak registered the symptom of a crisis in the by-then obsolete quantitative dynamics that still regulated the choice of colors in use according to a rigid linear progression, lacking in other possible evolutions. These dynamics were no longer sustainable on a *qualistic* plane, and above all they proved to be unsuitable to grasp the signs of the appearance of a new "sentiment of color."

Keywords: AIC2023 Chiang Rai Thailand, CMF Design Forecasting, 1973 Oil Shock, 1973 "Color Fever", Advent of Ecology Concept, Conceptual Inversion, Emotional Experience, Umbrella Diagram, Qualistic, World-wide "Sentiment of Color", Fragments.

INTRODUCTION [1]

[…] Since the beginning of the 1970s, the color offering (*color presence*) of some new industrial products began to show obvious anomalies in the forecasting models. In fact, although still very primitive, they were changing under the influence of historical upheavals triggered by epochal events (such as in 1973, with the Arab-Israeli *Yom Kippur War*), which would lead us to experience the "oil shock": a sudden energy crisis that led to significant shortages throughout the western countries. For a rapidly growing society like ours, founded however on limited fossil energy resources and even more problematic nuclear alternatives, it was a heavy blow. The crisis and the resulting austerity led to a quadrupling of fuel costs and other grave limitations which, however, lasted only one season, from the winter of 1973 to the spring of 1974. We had experienced a historic event that would radically change our future, even if we did not realize the energy dependence to which we were exposed and the influence on the patterns of our material culture. For example, until then the growth of color saturation on industrial products had followed a linear increase, with a rise in saturation already underway in the late 1960s. This was a *quantitative* effect connected to the demand for color typical of chromatic languages which did not suggest changes in a *qualitative* sense, such as the choice of new color shades (hue). What really mattered then was in fact only the strength of the color itself (chroma), i.e., its saturation (Figure 2). The real mutation would then be triggered spontaneously, precisely with the shock caused by the effects of that distant conflict which almost immediately led to the sudden collapse of the color saturation of most of the products on the markets. Thus, a surprising effect was created, a sudden "conceptual inversion" which brought confusion between the colors and emotional languages which until that moment seemed to be completely stable and consolidated. […]

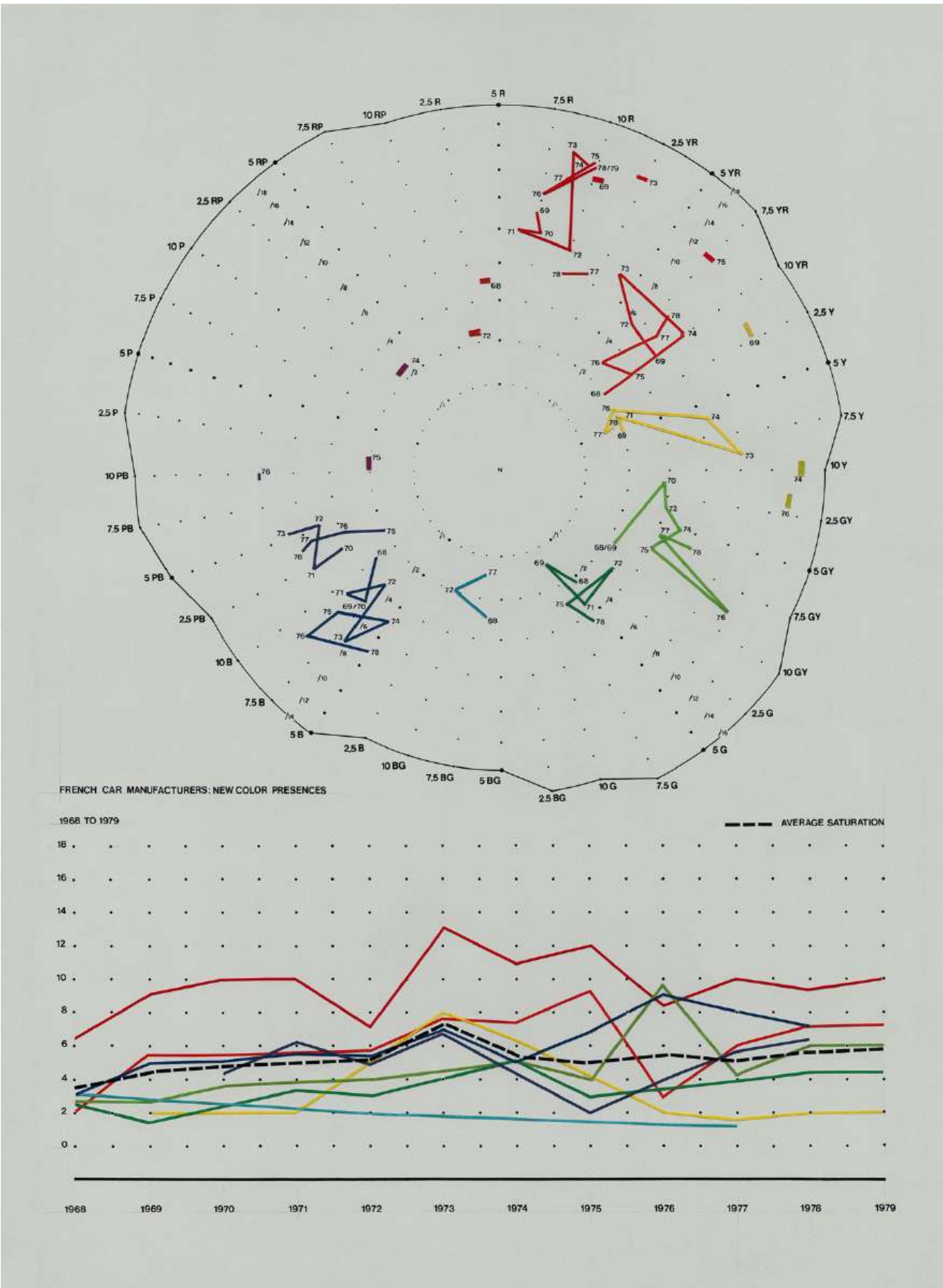

Figure 1. The original *"Color Fever" Chroma Survey 1973*

In 1973 the "Color Fever" Chroma Survey *diagram revealed a sudden peak on the line that indicated the average saturation of colors of automotive paints on the French market. France was chosen for the study because of the number of auto brands already active in that country. This peak, already detected through the first observations in the field, was shown on the saturation diagram of 1979, on the basis of data gathered from 1968 to 1979.*

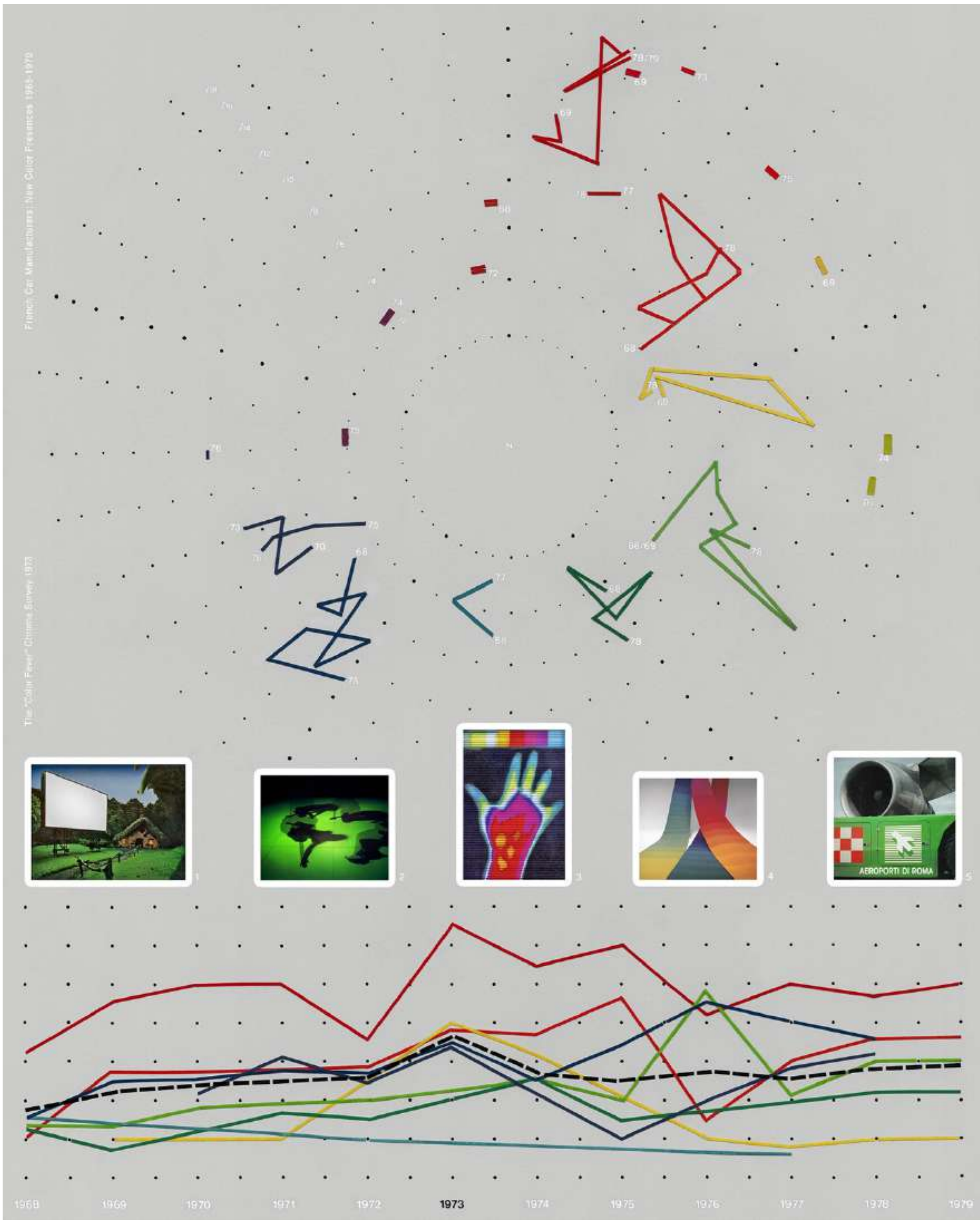

Figure 2. The *"Color Fever"* Peaks and the Early 1970s Project Scenarios

The "Color Fever 1973" *diagram combined with images of several project scenarios made by Trini Castelli in the first half of the 1970s. In those projects, the high levels of saturation of the start of the decade are still evident, shortly before the rise of the new* color presence *with the appearance on the market of color schemes having nuances typically found in nature (the new 70s* natural colors*, which in fact would replace the previous 60s* primary colors*). In 1976 we can also notice the progressive growth of the peak of a medium blue, and the sudden surge of the peak of a saturated green, which then became a fleeting fashion trend on the automotive market in that moment.*

THE CHROMA SURVEY FOCUS [2]

[…] In the early 1970s the end of the growth of saturation in paints seemed improbable, especially in a sector like that of automobiles, which amazingly enough was still operating with the color offerings of the previous decade. I should point out, however, that the 1960s had immediately stood out for the unprecedented use of a single highly saturated *primary color* (but also totally *neutral* tones like white, gray and black) which was applied to the entire body of the product, making it typically *monochromatic* (*color distribution*). An eloquent example of this historical trend was the Olivetti *Valentine,* the typewriter designed by Ettore Sottsass in 1968, entirely in red ABS (one of the first products on which I was to work). Among the typical color presences of that decade, besides red and orange there were also yellow and blue. These colors were only used individually, and their brightness was always balanced by the juxtaposition with *generic colors* (neutral finishes in white, gray, black or chrome) applied to the generic parts of the products themselves, such as the legs of chairs or the bumpers of cars (Figure 3). […]

Figure 3. *Leart* Safety Lamp, 1965

The Leart *safety lamp for garages was the first industrial product entirely designed by Trini Castelli in 1964. It was without metal parts (except for the electrical gear) and was made entirely in polypropylene, in N7 gray (apart from the functional details in red). This lamp is also a good example of the* historical trend *of the 1960s, which favored a* monochromatic color presence *that was typically very saturated or - as in this case - totally neutral. That revolutionary polymer* (Moplen) *- created by the Nobel laureates for chemistry in 1963, Giulio Natta and Karl Ziegler - was the same resin utilized by Montedison to produce the new polypropylene fiber* Meraklon*, a material at the base of the prize-winning chromatic system of textile flooring* Fibermatching 25 *(Figure 4).*

Figure 4. The Meraklon *Fibermatching 25* System, 1975

In the early 1970s, with Massimo Morozzi and Andrea Branzi, Clino Trini Castelli founded the Centro Design Montefibre *of Gruppo Montedison, which was to mark the beginning of "*Design Primario"*, comprising innovative ideas and systematic projects for new materials and processes in the "chemical-textile" sector. One of them was the* Fibermatching 25 *system, a new method of color formulation based on the inner mixture of* Meraklon *polypropylene fibers,* "mass-dyed" *or colored in full depth. That idea, based on the* "partitive synthesis" *of a limited series of special base colors, made it possible to create wide chromatic ranges with an* eco-sustainable *method, avoiding the pollution caused by the dyeing process. The* physical synthesis *of particles in the form of filaments of suitable chromaticity exploited the capacity for "visual discrimination" of the human eye, and had never been applied until then on an industrial scale. That method, having become an industrial process, was then re-applied twenty years later by Trini Castelli in Japan, this time utilizing nylon fibers, again batch-dyed, to produce other millions of square meters of textile flooring, which thus prevented any pollution from water used in the dyeing operation. In practice, starting with a limited number of fibers with very vivid based colors, these were simply de-saturated, mixing them closely with a range of other neutral-base gray fibers, in paler or darker blends. The project won the* Compasso d'Oro ADI *award in 1979.*

THE NEW "SENTIMENT OF COLOR" [3]

[…] The trend towards a progressive increase of color saturation of products in the industrial sector continued, in any case, with the introduction of new categories of super-saturated pigments. Nevertheless, precisely with the overall retreat from high saturation in 1973, new schemes of *color presence* spread on the market with neutral tones, whose identity could be associated with forms of *proto-ecology*. The intensity of the *primary colors*, seen until this point as the reflection of energy optimism, was increasingly rejected by the emerging environmentalist sensibility. The colors of materials and coatings utilized in various sectors thus became more imitative of nuances that could be found in nature (the 1970s *natural colors* would replace the 1960s *primary colors*). That drastic change also triggered a crisis in the various sectors of the automotive chain of design and production. It was a true debacle for major investors in the sector, which had focused only on quantitative programs of forecasting. This painful lesson would lead the entire sector into new forms of "design awareness" and to the passage from a linear perception of the flow of time towards a cyclical and evolutionary vision.

While in fashion changes in tastes and emotional languages seemed to mutate spontaneously, adapting to the new realities already at the start of the 1970s, the big chemicals industry had stubbornly clung to its saturated tones, although they had been rendered obsolete by a new "sentiment of color". In the end, that industrial sector squandered at least 10 years of massive investments for the production of new and very costly pigments, which due to their long development processes would systematically reach the market with major lag times with respect to current trends.

The exaggerated chromatic choices, no longer suited to the new emotional demands of the market, were immediately and totally rejected, in spite of last-minute attempts to enact shrewd marketing strategies, always with scant results. One of the first came from the insurance companies, which offered large discounts to car buyers who opted for high-visibility paint jobs that would be effective even in dense fog. I too, in 1976, in a corporate identity project for Aeroporti di Roma, had applied an apple green paint, almost fluorescent, for the entire fleet of ground support equipment: a choice dictated by the need for an image, but also by concerns of safety (Figure 5).

Figure 5. The *"Green Peak"*, 1976

The super-saturated colors developed at the start of the decade found new applications, dictated by necessities of image and safety, as in the case of the "green peak" *of 1976 shown in the diagram, which sees the super-saturated signal-green applied to the bodywork of the ground support vehicles of* Aeroporti di Roma*. The same green was then used only for the bumpers and other generic parts of the* Fiat Racing 131*, combined instead with totally neutral bodywork.*

[…] Many sizeable investments went up in smoke, in fact, simply because no one wanted the new colors that were being produced. This was the outcome of the above-mentioned "conceptual inversion" that was rapidly becoming very obvious: people no longer wanted the super-saturation of "emergency" colors; everyone wanted only natural, intimate, non-assertive tones: nothing poisonous, nothing like the hues of the heavy metals. For the first time, the industry that stubbornly insisted on those old paints was automatically associated with the emerging problematic issues of environmental pollution.

I should point out, however, that already in 1964, when I began working for Olivetti in the Milan studio of Ettore Sottsass, at the headquarters in Ivrea the new CEO of Olivetti, Aurelio Peccei, made his appearance. Like him, I too came from the FIAT group in Turin, and like him I would remain with Olivetti only for the three subsequent years. Peccei, who did not appear to be particularly operative in the company, however, was one of the founders of the historic *Club of Rome* in 1968 (the non-governmental association created with the mission of catalyzing global changes). Aurelio Peccei, thanks to his early vision, is now considered one of the originators of the idea of *ecology* itself. In 1972 he was to write the famous preface to the MIT report on *The Limits to Growth* [1], influencing international public opinion by foreseeing the issues and consequences of the first worldwide oil crisis of 1973. His position also helped to raise awareness among Italian companies of the importance of the environmental question.

Shortly thereafter, in May 1974, came the initiative of the historic magazine *Domus*, presenting the exhibition *Environment '74* [2] precisely in Turin. I participated with the entire section *Eco'74* (Figure 6), where I presented the themes of "*Design Primario*", with *Le Superfici Reattive* (Reactive Surfaces) [3] and *Camera Riverberante* (Reverberating Room): works and installations entirely made with *Lumiphos,* a luminescent HPL laminate from Abet Print. This was one of the very first international expositions in Europe on the new theme of ecology and environmental qualities. […]

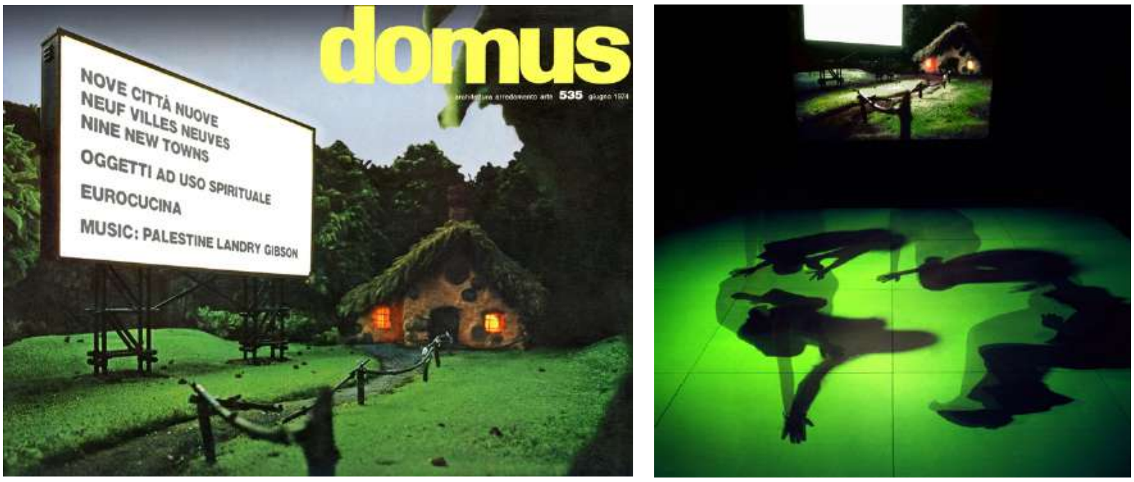

Figure 6. *Eco '74. La Radura Pubblicitaria* e *Le Superfici Reattive*, 1974

Lumiphos*, in 1971, was the first true design of a new material developed in the form of a semi-finished product. It consisted of large totally photoluminescent HPL panels, which were then produced for over forty years by Abet Print. The choice of working on the design of materials instead of forms was already the start of a meta-design intention, oriented towards dematerialization of products and spaces. The idea was to design while remaining outside the traditional figurative culture, which took the "compositional aspects" of form as its ideal referent.*

THE INTERNATIONAL SCENARIOS [3]

[…] The surprising diagram of the *"Color Fever" Chroma Survey* is the most illustrative result of wide-ranging research on saturation in the paints made for the European automotive market. Begun in the early 1970s, that effort - conducted at first only in the field - had to do with the evolution of colors of the entire decade and stemmed from local observations made during my first trips in Europe and the United States. Actually it all began in July 1967, when at an early age I had the unmissable opportunity to travel to New York with my authoritative colleague Flavio Lucchini, who had just been appointed as art director of *Vogue Italia*, on his first visit to the editorial offices of *Vogue America*. Grace Mirabella was the editor at the time, and she introduced us to some of the most outstanding celebrities in New York, including Andy Warhol at his *Factory*, and visits to the studios of great Vogue photographers, from Richard Avedon to Hiro and Bert Stern. For me, the encounters with Irving Penn and Diane Arbus were unforgettable. Finally, we were invited to the opening of the *Electric Circus*, an amazing occasion that confirmed, from my viewpoint, the new format of international club culture, which I had already explored one year earlier at the *Piper Club* in Turin [4], with art events and design programs that became legendary in that historic context.

My second trip to the United States came two years later, in 1969, when I went to Berkeley by way of San Francisco, and was able to observe firsthand the protest movements of the students in California, which met with extensive media coverage. That trip continued with the discovery of the icons and colors of the Beat Generation and the "Flower Children," thanks to the local contacts of Fernanda Pivano, a writer and the translator of the leading American authors. "Nanda" had already introduced me, from the early 1960s, to those new literary genres and the captivating psychedelic imagery of the new underground magazines of California. Finally, with a detour to the Astrodome in Houston - courtesy of NASA - I was able to celebrate the return of the astronauts from the moon, after which I returned to Italy, passing through New York. That metropolis would soon become the true center of the world, and it was no coincidence that the most lucid interpretation of the events of the start of the decade came from the futurologist from New York, Alvin Toffler, who with his book *Future Shock* in 1970 [5] pertinently described the condition of impermanence and the prospects of that whole decade, foreseeing the crisis of technocracies and already envisioning the abandonment of the still dominant techno-centric culture. We need only recall the unexpected developments of the oil shock of 1973 to understand just how precise and farsighted Toffler's forecasts were at the time.

With the arrival of the new decade there were multiple signals of change. Fashion was the first field to be involved in the phenomenon that was then to trigger the collapse of saturation of colors in other sectors. In London, in fact, we had passed from the minimalist vivacity of Mary Quant to the languid and dreamy intimism of Sarah Moon, and to the seductive scenarios of Biba, with the transgressive mini department stores of Barbara Hulanicki on Kensington High Street. In cinema, Stanley Kubrick would pass, instead, from the lysergic imagery of *2001: A Space Odyssey* (1968) to the nascent youthful deviations of *A Clockwork Orange* (1971). The new decade began with more frequent trips, on my part, between the Olivetti offices in Milan and London, where I was developing my ambitious project on the *Red Books* (Figure 7), the institutional identity manuals of Olivetti. London, besides being the city where my children were born, from 1970 to 1972, had become the worldwide capital of many of the events that were to influence the history of music and entertainment, as well as the production of new glamour merchandise for young tastes, at the two centers of Kings Road and Carnaby Street. […]

Figure 7. Olivetti *Red Books*, 1969-1974

The Corporate Identity manuals of Olivetti, known as the Red Books*, were the first operative manuals developed in a meta-design form by Trini Castelli. They are therefore true "cookbooks" capable of guiding other designers in the combination and measurement of the identifying ingredients of Olivetti. These were manuals prepared in an extensive and propositional way, full of "open" operative solutions, quite different from the intensive "menu-manuals" of Paul Rand for IBM. The latter imposed only choices between "closed" design solutions, which though they were extraordinary in quality were also limited to a few preset options. The new concepts would make the formula of operating manuals a true novelty in the sector.*

CMF DESIGN & FORECASTING [4]

[…] In the meantime, Milan was preparing to become an international focal point for fashion, as well as for industrial design and the emerging *CMF Design (Color, Materials, Finishes).* This activity was indicated with the acronym, which since 1981 I would use to define the projects on "*soft redesign*" of systemic products, such as those of Herman Miller for the office. With that company, at the XV Neocon in Chicago in 1983, I received the *Best in the Mart* award for the installation of the *Cathedral Office* (Figure 8). John Naisbitt immediately grasped the innovation of that project-setting created for Neocon. In his book *Megatrends. Ten New Directions Transforming Our Lives* [6], Naisbitt suggested a vision of the future which he defined as "High Touch", in keeping with my principle of "emotionally touching," aimed at the humanization of technology through the deep touch of qualistics. In this way, the transcendent image of the Cathedral Office was released from the current of technicism of the time, entering a sort of celebration of nature that was better suited to the new rituals of work in the office, as opposed to the accent on "High Tech" performance. […]

Figure 8. The *Cathedral Office*, Dark and Light Versions, 1983

Details of the installation of the Cathedral Office *of Herman Miller for the Chicago Merchandise Mart at Neocon 15, 1983. Awarded as the showroom* Best in the Mart*, the large installation by Trini Castelli - through the theatrical and transcendent use of the components of the office furnishing system - visualized the aspects of the new composite* High Touch *language. This was based on the novel principle of a profound touch of emotions, aimed at the humanization of technology. In this way, the transcendent image of the* Cathedral Office *was shifted away from the technicism of the time, instead entering a sort of celebrative nature, better suited to the rituals of a new idea of office work.*

[…] Returning from Chicago to Milan, leafing through *Color & Human Response* [7], a book by Faber Birren on color in psychedelic culture, I found an image that left me speechless: it showed a young couple dancing on a cube at the Electric Circus in New York, a woman in a long lace gown, and a man in a two-tone jacket. The book, headed for the nascent library of the *ColorTerminal*, had been published in 1978, the same year in which I had invited Birren to Milan for the *Seminari Colordinamo* (Figure 8). Birren, who was known as a true guru of modern chromatic culture, had chosen that image for the colors of the jacket, though it was then published in black and white. It was an incredible coincidence, because I was the young man with the blue and apple green jacket in the image. When I pointed this strange fact out to Faber Birren, he hinted at a sort of predestination: in his entire book there were only about a dozen recognizable people, at a time when the population of the world was already four billion! […]

Figure 9. ***Operazione Colordinamo*****, 1975-1977**

The Operazione Colordinamo *(Colordinamo Operation), which took place mostly from 1975 to 1978, is one of the first examples in Italy of research and development of color culture in the environmental field. Initiated with the* Centro Design Montefibre*, the* Operazione Colordinamo *operation gave rise to seminars, exhibitions and the well-known manuals for professional use, which were the first tool of orientation in the field of color design in Italy, published from 1975 to 1977. The first* Colordinamo *manual, in 1975, from which the poster is taken, was entirely devoted to the color of energy and the advent of RGB additive synthesis.*

[…] All the research conducted in the context of these *Chroma Surveys* had the main aim of identifying the "driving" chromatic languages of historical trends, which from the 1920s onward could be connected to their respective decades. The analysis of the variations of those chromatic trends, detected from their earliest manifestations, had already permitted me to observe how the color presences changed in the passage from one decade to the next, offering an effective way of understanding the origin and evolving nature of color languages as they emerge. This research would then lead to the development of the *Umbrella Diagram* [9], a tool owned by Castelli Design that was introduced at the start of the 1980s, which has enabled me to predict - far in advance - the changes that would take place regarding the identity of colors, new materials and emerging finishes.

The research has also had the aim of orienting designers in the assignment of colors to products, according to proper criteria of sustainability, in both industrial design and space design. This is also a response to the large quantities of discarded products, caused by errors in the strictly subjective chromatic choices in areas of consumption that are sometimes lacking in sufficient awareness. In 1986 all this led to the formulation of *Qualistics* (initially defined as an "ecology of emotional consumption"), which has effectively proven to be useful to orient unresolved project themes, addressed by new qualifying practices which today we would define as "eco-sustainable".

From the mid-1970s to the end of the 1990s, the world of design - not just in Italy - was faced by the need to define new qualitative standards (today we would say “qualistic”) for products whose identity had to be increasingly articulated in a subjective sense. The challenge, as always, was to remain within the “design culture”, adopting CMF design strategies, such as the introduction of the *Color Matrix*, appropriately modulated according to the inclusive strength of the meta-project (Figure 10). […]

Figure 10. Herman Miller *Color Library* (based on the *Color Matrix*), 1981

The Color-Matrix *was introduced by Trini Castelli in 1978 and applied for the first time to the* Lancia Color System*, a CMF design project entirely based on this innovative meta-project tool. The Color Matrix is also the basis of the Herman Miller* Color Library*, the first major CMF project created for the entire production of Herman Miller furniture and systems (1981-1984). It allowed multiple alternative color combinations aimed at satisfying the different aesthetic preferences of users. A paradigmatic change, which has allowed us to exploit coded color families to create alternative combinations in a systemic way, overcoming the old "intensive" concept of the color chart to adhere to the new "extensive" vision of the* Color Matrix*, fully logical and practicable only through the* meta-project*. The colors of the matrices were finally conceived as immanent entities, as independent color notations that could adhere to any shape and whose application remained open and well-coordinated.*

CHROMA SURVEY - MODES AND METHODS [5]

[…] From those years, it is worth recalling two authoritative viewpoints in the debate on how to approach the practice of design: for Ettore Sottsass it was important to steer clear of the "underpinning" of the *methodology*, with its corollary of previously established rules. For Alessandro Mendini, on the other hand, it was necessary to "deconstruct" the concept of *modality*. He consolidated this position in 1977 with the founding of the design magazine *Modo*, through the idea of looking more closely at the "making", the direct experience of reality, a property that upon closer examination was already intrinsic precisely to the themes of color design [10]. This research began, in fact, with the observation of a clear variance between the figurative languages of fashion and those of design, which tended to diverge more and more. A theme to investigate more deeply, on a professional level, through a simple but effective format, capable of permitting the carrying out of activities in keeping with conventional modes, such as research "in the field," elaboration "in the studio," and development "in the laboratory."

The activities in the field, conducted in alternating phases and across very wide time spans, were fundamental to make this survey, which began with the above-mentioned travels in the United States, which enabled an intense activity of collection of design data and materials. After this, from 1970 to 1973, all the activities in the field and those in the studio continued, for the most part, in Milan and London. The development in the studio of the *"Color Fever" Chroma Survey* was instead completed in just one year, 1978, with the gathering of data and the related documentation. In 1979, there was also added the incredible experience of my mission in China [11] for the chemical corporation Montedison. This was at the beginning of the opening of China's borders to foreigners, and in an area of the trade fair of Wuhan, a series of pilot plants were launched for the molding of small and large articles in plastic, the first objects of that type produced in the thousands of years of Chinese history.

From 1978, the observations of the initial *Chroma Survey* of the early 1970s were reapplied in relation only to the colors of automotive paints, visualized through the "*Color Fever" Chroma Survey* diagram. This had the aim of detecting the levels of saturation of paint in the cars available on the French market from 1968 to 1979, a choice based mainly on the variety and number of automotive brands still active in that country at the time. Finally, the development in the laboratory was instead a totally new activity, begun in 1978 with the creation of the *ColorTerminal* and the use of the *Graphicolor* tool, which made it possible to exploit the digital processing of RGB color synthesis, applied in a nascent state. […]

CHROMA SURVEY CONCLUSION [6]

[…] In the 1960s, with the advent of color television, and in the 1970s, with the further spread of new electronic media, we passed from the exclusive use of subtractive color synthesis to the widespread application of RGB additive synthesis, a way of generating color that had never previously been utilized. Rarer in nature, additive synthesis revealed its efficacy as a new mode of chromatic interaction. This was an event that was to impact the history of art and design with substantial changes, also on an anthropological level. With the use of additive synthesis, color forcefully entered the kingdom of darkness, also saturating the hours of the night with autogenous chromatic shadings never seen before. […]

ACKNOWLEDGEMENT

My heartfelt thanks to AIC President Leslie Harrington and - for my candidacy for the AIC 2023 CADE Award - to GdC-AIC President Marcello Picollo. Furthermore, I thank both Verena M. Schindler for welcoming me as an honorary member of the AIC SG ECD, and Alessandro Rizzi for the citation in the conference proceedings.

A special thanks in memory of my assistant Antonio Petrillo, who developed the original collection and reporting of the data from the Automotive Chroma Survey in 1979.

I would also like to thank Esperanza Nunez and Daniela Domina, who at different times contributed to the completion of the history of this research, and to Stephen Piccolo for his English translations of all my texts over the decades.

REFERENCES

1. Meadows, H. D.; Meadows, L. D.; Randers, J.; Behrens III, W. W., (1972). *The Limits to Growth. A Report for THE CLUB OF ROME'S Project on the Predicament of Mankind*, New York: Universe Books.
2. Casati, C. (1974). *Environment '74: An Exhibition*, Domus 536: 21-25.
3. Trini Castelli, C. (1972). *Reactive surface,* Japan Interior Design 165: 31.
4. Trini, T. (1968). *Divertimentifici*, Domus 458: 16-23.
5. Toffler, A. (1970). *Future Shock*, New York: Random House.
6. Naisbitt, J. (1982). *Megatrends. Ten New Direction Transforming Our Life*, New York: Warner Books.
7. Birren, F. (1978). *Color & human response: Aspects of Light and Color Bearing on the Reactions of Living Things and the Welfare of Human Beings*, New York: Van Nostrand Reinhold.
8. Trini Castelli, C.; Morozzi, M.; Branzi, A., (1975). *Il Colore dell'Energia. Colordinamo 1975 - Manuale per uso professionale*, Milano: Centro Design Montefibre.
9. Trini Castelli, C. (1983). *Dal cucchiaio alla qualità (Editorial)*, Modo 63: 27.
10. Trini Castelli, C. (2021). *Umbrella Diagram: 1981-2021, five decades of forecasts and CMF design*, Color Culture and Science Journal v.13 n.2: 84-90.
11. Trini Castelli, C. (2019). *No-form 2020. 10 racconti oltre il design*, Mantova: Corraini Edizioni.

Sponsered by

IMAGING & PRINTING
CHULALONGKORN
UNIVERSITY

TCEB
THAILAND CONVENTION
& EXHIBITION BUREAU